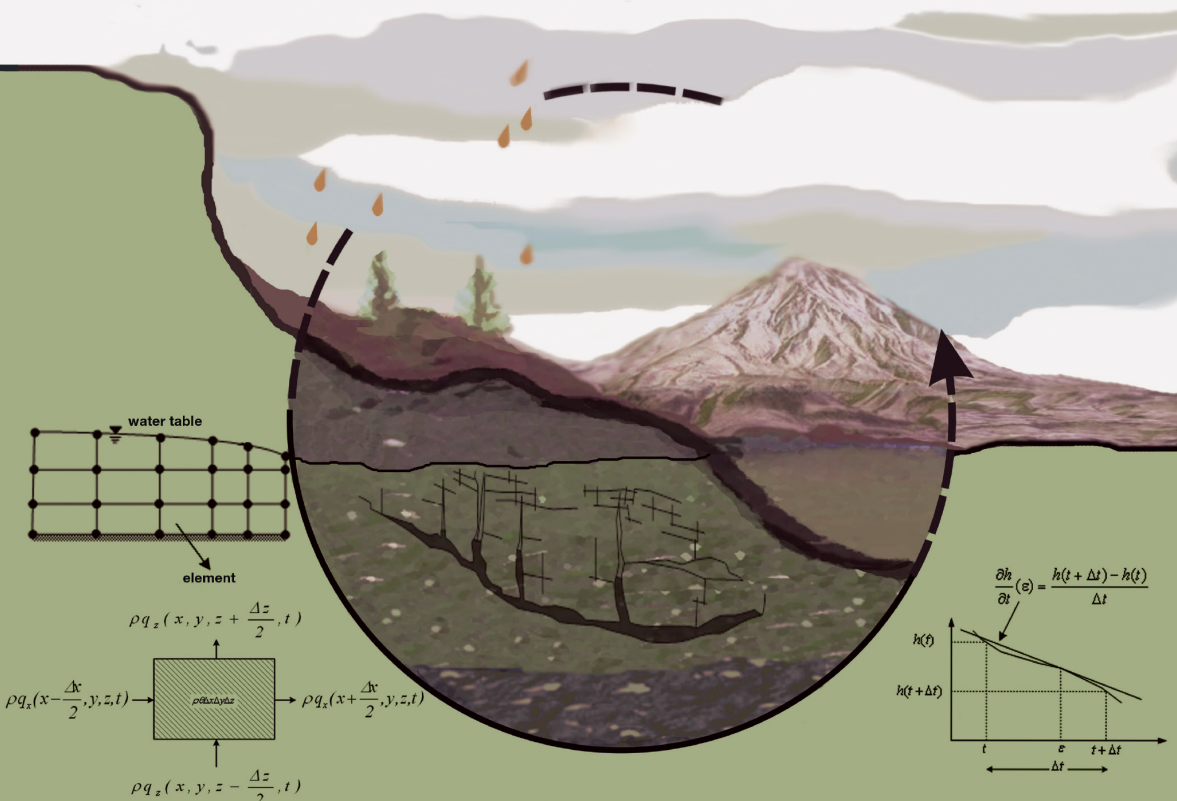


SECOND EDITION

GROUNDWATER HYDROLOGY

Engineering, Planning, and Management



Mohammad Karamouz • Azadeh Ahmadi • Masih Akhbari

Groundwater Hydrology



Taylor & Francis

Taylor & Francis Group

<http://taylorandfrancis.com>

Groundwater Hydrology

Engineering, Planning, and Management

Second Edition

Mohammad Karamouz

Azadeh Ahmadi

Masih Akhbari



CRC Press
Taylor & Francis Group
Boca Raton London New York

CRC Press is an imprint of the
Taylor & Francis Group, an **informa** business

CRC Press
Taylor & Francis Group
6000 Broken Sound Parkway NW, Suite 300
Boca Raton, FL 33487-2742

© 2020 by Taylor & Francis Group, LLC
CRC Press is an imprint of Taylor & Francis Group, an Informa business

No claim to original U.S. Government works

International Standard Book Number-13: 978-0-367-21147-9 (Hardback)

This book contains information obtained from authentic and highly regarded sources. Reasonable efforts have been made to publish reliable data and information, but the author and publisher cannot assume responsibility for the validity of all materials or the consequences of their use. The authors and publishers have attempted to trace the copyright holders of all material reproduced in this publication and apologize to copyright holders if permission to publish in this form has not been obtained. If any copyright material has not been acknowledged please write and let us know so we may rectify in any future reprint.

Except as permitted under U.S. Copyright Law, no part of this book may be reprinted, reproduced, transmitted, or utilized in any form by any electronic, mechanical, or other means, now known or hereafter invented, including photocopying, microfilming, and recording, or in any information storage or retrieval system, without written permission from the publishers.

For permission to photocopy or use material electronically from this work, please access www.copyright.com (<http://www.copyright.com/>) or contact the Copyright Clearance Center, Inc. (CCC), 222 Rosewood Drive, Danvers, MA 01923, 978-750-8400. CCC is a not-for-profit organization that provides licenses and registration for a variety of users. For organizations that have been granted a photocopy license by the CCC, a separate system of payment has been arranged.

Trademark Notice: Product or corporate names may be trademarks or registered trademarks, and are used only for identification and explanation without intent to infringe.

Library of Congress Cataloging-in-Publication Data

Names: Karamouz, Mohammad, author. | Ahmadi, Azadeh, author. | Akhbari, Masih, author.
Title: Groundwater hydrology : engineering, planning, and management / Mohammad Karamouz, Azadeh Ahmadi, Masih Akhbari.
Description: Second edition. | Boca Raton, FL : CRC Press, Taylor & Francis Group, [2020] | Includes bibliographical references and index.
Identifiers: LCCN 2019052922 (print) | LCCN 2019052923 (ebook) | ISBN 9780367211479 (hardback) | ISBN 9780429265693 (ebook)
Subjects: LCSH: Groundwater--Management. | Groundwater flow.
Classification: LCC TC176 .K365 2020 (print) | LCC TC176 (ebook) | DDC 628.1/14--dc23
LC record available at <https://lccn.loc.gov/2019052922>
LC ebook record available at <https://lccn.loc.gov/2019052923>

Visit the Taylor & Francis Web site at
<http://www.taylorandfrancis.com>

and the CRC Press Web site at
<http://www.crcpress.com>

*To millions of people around the world
with no access to safe drinking water*

Mohammad Karamouz

Azadeh Ahmadi

Masih Akhbari



Taylor & Francis

Taylor & Francis Group

<http://taylorandfrancis.com>

Contents

| | |
|--|-----------|
| Preface..... | xxi |
| Acknowledgments..... | xxv |
| Authors..... | xvii |
| | |
| Chapter 1 Introduction | 1 |
| 1.1 Introduction | 1 |
| 1.2 Water Availability..... | 2 |
| 1.2.1 Groundwater Availability | 4 |
| 1.3 Groundwater Systems | 5 |
| 1.4 Science and Engineering of Groundwater..... | 6 |
| 1.5 Planning and Management of Groundwater | 8 |
| 1.5.1 Integrated Water Resources Management..... | 10 |
| 1.5.2 Conflict Issues in Groundwater..... | 10 |
| 1.5.3 Economics of Water | 11 |
| 1.5.4 Groundwater Sustainability..... | 13 |
| 1.5.5 Supply and Demand Side Management | 15 |
| 1.6 Tools and Techniques | 17 |
| 1.7 People's Perception: Public Awareness..... | 19 |
| 1.8 Groundwater Protection: Concerns and Acts | 20 |
| 1.8.1 Clean Water Act..... | 21 |
| 1.8.2 Groundwater Protection | 21 |
| 1.8.3 USEPA Groundwater Rule | 22 |
| 1.8.4 California's Sustainable Groundwater Management Act | 23 |
| 1.9 Overall Organization of This Book | 24 |
| Problems..... | 25 |
| References | 25 |
| | |
| Chapter 2 Groundwater Properties..... | 29 |
| 2.1 Introduction | 29 |
| 2.2 Vertical Distribution of Subsurface Water..... | 31 |
| 2.3 Aquifers, Aquitards, and Aquiclude | 33 |
| 2.4 Types of Aquifers | 33 |
| 2.4.1 Unconfined Aquifer..... | 33 |
| 2.4.2 Confined Aquifers | 34 |
| 2.4.3 Aquitard (Leaky) Aquifer..... | 34 |
| 2.5 Groundwater Balance..... | 35 |
| 2.5.1 Water Balance in Confined Aquifers..... | 36 |
| 2.5.2 Water Balance in Unconfined Aquifers | 37 |
| 2.5.3 Water Balance in Unsaturated Zone..... | 37 |

| | | |
|------------------|--|-----------|
| 2.6 | Compressibility and Effective Stress..... | 38 |
| 2.6.1 | Compressibility of Water..... | 38 |
| 2.6.2 | Effective Stress | 38 |
| 2.6.3 | Compressibility of a Porous Medium..... | 40 |
| 2.6.4 | Effective Stress in the Unsaturated Zone | 42 |
| 2.7 | Aquifer Compressibility | 42 |
| 2.8 | Aquifer Characteristics..... | 43 |
| 2.8.1 | Porosity and Void Ratio..... | 44 |
| 2.8.2 | Specific Yield in Unconfined Aquifers | 46 |
| 2.8.3 | Specific Retention..... | 47 |
| 2.8.4 | Storage Coefficient and Specific Storage | 48 |
| 2.8.5 | Safe Yield of Aquifers | 52 |
| 2.9 | Storage in the Unsaturated Zone | 52 |
| 2.10 | Water-Level Fluctuations..... | 55 |
| 2.11 | Groundwater in Karst | 55 |
| 2.11.1 | Karst Aquifer | 55 |
| 2.11.2 | Types of Karst..... | 56 |
| 2.11.3 | Fluctuation of Karst Aquifer..... | 56 |
| 2.11.4 | Recharge of Karst Aquifer..... | 57 |
| 2.11.5 | Groundwater Tracing in Karst..... | 58 |
| 2.11.6 | Water Resources Problems in Karst | 58 |
| | Problems..... | 59 |
| | References | 61 |
| Chapter 3 | Groundwater Hydrology..... | 63 |
| 3.1 | Introduction | 63 |
| 3.2 | Groundwater Movement..... | 63 |
| 3.2.1 | Darcy's Law..... | 63 |
| 3.2.1.1 | Validity of Darcy's Law..... | 68 |
| 3.2.2 | Hydraulic Head..... | 68 |
| 3.2.3 | Hydraulic Conductivity | 69 |
| 3.2.3.1 | Hydraulic Conductivity in Saturated Media..... | 69 |
| 3.2.3.2 | Hydraulic Conductivity in Unsaturated Media..... | 70 |
| 3.2.3.3 | Laboratory Measurement of Hydraulic Conductivity | 72 |
| 3.2.3.4 | Field Measurement of Hydraulic Conductivity | 74 |
| 3.3 | Homogeneous and Isotropic Systems..... | 75 |
| 3.3.1 | Hydraulic Conductivity in Multilayer Structures | 76 |
| 3.4 | Transmissivity | 80 |
| 3.5 | Dupuit–Forchheimer Theory of Free-Surface Flow | 81 |
| 3.6 | Groundwater Flow in Unsaturated Zone | 83 |

| | | |
|------------------|---|-----|
| 3.7 | Flownets..... | 88 |
| 3.7.1 | Isotropic and Homogeneous Media | 88 |
| 3.7.2 | Heterogeneous Media | 92 |
| 3.7.3 | Anisotropic Media | 93 |
| 3.8 | Statistical Methods in Groundwater Hydrology | 95 |
| 3.8.1 | Normal Distribution..... | 95 |
| 3.8.2 | Lognormal Distribution | 97 |
| 3.8.3 | <i>t</i> -Distribution..... | 98 |
| 3.8.4 | Chi-Square (χ^2) Distribution..... | 100 |
| 3.8.5 | Errors | 100 |
| 3.8.5.1 | Sampling Error..... | 100 |
| 3.8.5.2 | Standard Errors | 100 |
| 3.8.6 | Estimating Quantiles (Percentiles) | 101 |
| 3.8.7 | Probability/Frequency/Recurrence Interval..... | 102 |
| 3.9 | Time Series Analysis | 103 |
| 3.9.1 | Nonstationary Hydrologic Variables..... | 103 |
| 3.9.2 | Hydrologic Time Series Modeling..... | 104 |
| 3.9.3 | Data Preparation | 105 |
| 3.9.4 | Parameter Estimation..... | 108 |
| 3.9.4.1 | Method of Moments | 108 |
| 3.9.4.2 | Method of L-Moments..... | 109 |
| 3.9.4.3 | Method of Least Squares | 110 |
| 3.9.4.4 | Method of Maximum Likelihood | 111 |
| 3.9.5 | Goodness of Fit Tests..... | 113 |
| 3.9.5.1 | Chi-Square Goodness of Fit Test | 113 |
| 3.9.5.2 | Tests of Normality | 115 |
| 3.9.6 | Akaike's Information Criterion..... | 117 |
| 3.9.7 | Autoregressive Modeling..... | 117 |
| 3.9.8 | Moving Average Process..... | 121 |
| 3.9.9 | Autoregressive Moving Average Modeling | 122 |
| 3.9.9.1 | Generation and Forecasting Using ARMA Models | 122 |
| 3.9.10 | Autoregressive Integrated Moving Average Modeling..... | 123 |
| 3.9.10.1 | Time Series Forecasting Using ARIMA Models..... | 124 |
| | Problems..... | 130 |
| | Appendix | 132 |
| | References | 135 |
| Chapter 4 | Hydraulics of Groundwater | 139 |
| 4.1 | Introduction | 139 |
| 4.2 | Continuity Equation..... | 139 |
| 4.3 | Equation of Motion in Groundwater | 142 |
| 4.3.1 | Groundwater Flow Equation..... | 144 |

| | | |
|------------------|--|------------|
| 4.4 | Wells | 153 |
| 4.4.1 | Steady Flow into a Well..... | 155 |
| 4.4.1.1 | Confined Flow..... | 155 |
| 4.4.1.2 | Unconfined Flow..... | 158 |
| 4.4.2 | Unsteady State in a Confined Aquifer | 161 |
| 4.4.2.1 | Aquifer Test Application..... | 165 |
| 4.4.2.2 | Theis Method of Solution | 166 |
| 4.4.2.3 | Cooper–Jacob Method of Solution | 168 |
| 4.4.2.4 | Variable Pumping Test..... | 172 |
| 4.4.3 | Unsteady State for Unconfined Aquifer | 175 |
| 4.5 | Multiple-well Systems..... | 181 |
| 4.6 | Effective Conditions on Time-Drawdown Data | 182 |
| 4.6.1 | Recharge Boundary | 182 |
| 4.6.2 | Impermeable Boundary | 184 |
| 4.6.3 | Partially Penetrating Wells..... | 186 |
| 4.7 | Design of Wells..... | 188 |
| 4.8 | Well Construction | 191 |
| 4.8.1 | Cable-Tool Drilling..... | 191 |
| 4.8.2 | Rotary Drilling Method | 191 |
| 4.8.2.1 | Well Development | 192 |
| | Problems..... | 193 |
| | References | 197 |
| Chapter 5 | Groundwater Quality | 199 |
| 5.1 | Introduction | 199 |
| 5.2 | Groundwater Constituents and Contaminants | 199 |
| 5.2.1 | Inorganic Contaminants..... | 199 |
| 5.2.2 | Organic Contaminants | 200 |
| 5.2.3 | Dissolved Gasses | 200 |
| 5.2.4 | Particles | 202 |
| 5.3 | Water Quality Standards | 203 |
| 5.4 | Groundwater Solubility | 209 |
| 5.5 | Disequilibrium and Saturation Index..... | 212 |
| 5.6 | Sources of Groundwater Contamination | 214 |
| 5.6.1 | Disposal of Solid Wastes | 214 |
| 5.6.2 | Underground Petroleum Tank Leakage | 214 |
| 5.6.3 | Disposal of Liquid Wastes | 215 |
| 5.6.4 | Sewage Disposal on Land..... | 215 |
| 5.6.5 | Agricultural Activities | 216 |
| 5.6.6 | Other Sources of Contamination | 216 |
| 5.7 | Mass Transport of Dissolved Contaminants..... | 217 |
| 5.7.1 | Diffusion..... | 218 |
| 5.7.2 | Advection..... | 220 |
| 5.7.3 | Mechanical Dispersion | 221 |
| 5.7.4 | Hydrodynamic Dispersion..... | 224 |

| | | |
|------------------|---|------------|
| 5.7.5 | Derivation of the Advection–Dispersion Equation | 225 |
| 5.7.6 | Solute Transport Equation | 233 |
| 5.7.7 | Capture-Zone Curves..... | 234 |
| 5.8 | Modeling Contaminant Release | 240 |
| 5.8.1 | Modeling Instantaneous Release of Contaminants..... | 240 |
| 5.8.1.1 | Fourier Analysis in Solute Transport..... | 240 |
| 5.8.1.2 | Point Spill Model..... | 241 |
| 5.8.1.3 | Vertically Mixed Spill Model | 241 |
| 5.8.1.4 | Vertical Mixing Region | 242 |
| 5.8.2 | Modeling Continuous Release of Contaminants | 244 |
| 5.8.2.1 | Development of Contaminant Plume Models | 244 |
| 5.8.2.2 | Simple Plume Model | 244 |
| 5.8.2.3 | Point-Source Plume Model..... | 245 |
| 5.8.2.4 | Gaussian-Source Plume Model..... | 245 |
| | Problems..... | 248 |
| | References | 250 |
| Chapter 6 | Groundwater Modeling | 251 |
| 6.1 | Introduction | 251 |
| 6.2 | Process of Modeling..... | 251 |
| 6.3 | Mathematical Modeling..... | 252 |
| 6.3.1 | Analytical Modeling..... | 253 |
| 6.3.2 | Numerical Modeling..... | 254 |
| 6.4 | Finite-Difference Method | 254 |
| 6.4.1 | Forward Difference Equation | 257 |
| 6.4.2 | Backward Difference Equation..... | 261 |
| 6.4.3 | Alternating Direction Implicit Method..... | 262 |
| 6.4.4 | Crank–Nicolson Difference Equation | 281 |
| 6.5 | Finite Element Method | 284 |
| 6.5.1 | Discretize the Problem Domain..... | 284 |
| 6.5.2 | Derive the Approximating Equations | 290 |
| 6.5.3 | Transient Saturated Flow Equation | 303 |
| 6.5.4 | Solute Transport Equation | 311 |
| 6.6 | Finite Volume Method | 319 |
| 6.6.1 | Steady-State One-Dimensional Flow Equation | 319 |
| 6.6.2 | Unsteady-State, One-Dimensional Flow Equation..... | 323 |
| 6.6.3 | Two-Dimensional Flow Equation..... | 324 |
| 6.6.4 | Orthogonals Coordinate System..... | 333 |
| 6.7 | Simulation of Groundwater Flow Using the Discrete Kernel Approach..... | 336 |
| 6.8 | Saturated-Unsaturated Transport (SUTRA) Code..... | 346 |
| 6.9 | MODFLOW..... | 347 |
| | Problems..... | 364 |
| | References | 366 |

| | | |
|------------------|---|-----|
| Chapter 7 | Groundwater Planning and Management | 369 |
| 7.1 | Introduction | 369 |
| 7.2 | Data Collection..... | 370 |
| 7.3 | Simulation Techniques | 371 |
| 7.3.1 | Model Calibration | 372 |
| 7.3.2 | Model Verification..... | 372 |
| 7.3.3 | Model Predictions | 373 |
| 7.3.3.1 | Artificial Neural Networks | 374 |
| 7.3.3.2 | Fuzzy Sets and Parameter Imprecision..... | 389 |
| 7.3.3.3 | System Dynamics | 395 |
| 7.3.3.4 | Agent-Based Modeling..... | 405 |
| 7.4 | Optimization Models for Groundwater Management | 409 |
| 7.4.1 | Optimization Model for Groundwater Operation..... | 410 |
| 7.4.2 | Optimization Model for Capacity Expansion..... | 413 |
| 7.4.3 | Optimization Model for Water Allocation..... | 417 |
| 7.4.4 | Optimization Model for Conjunctive Water Use..... | 420 |
| 7.4.5 | Optimal Groundwater Quality Management Model ... | 421 |
| 7.4.6 | Optimization Model for Parameters of Groundwater Model | 422 |
| 7.5 | Optimization Techniques..... | 423 |
| 7.5.1 | Single-Criterion Optimization..... | 424 |
| 7.5.2 | Multi-criteria Optimization | 426 |
| 7.5.2.1 | Sequential Optimization..... | 427 |
| 7.5.2.2 | The ϵ -Constraint Method..... | 427 |
| 7.5.2.3 | The Weighting Method..... | 428 |
| 7.5.2.4 | Interactive Fuzzy Approach..... | 430 |
| 7.5.3 | Special Methods for Groundwater Optimization | 432 |
| 7.5.3.1 | Dynamic Programming | 432 |
| 7.5.3.2 | Genetic Algorithm | 434 |
| 7.5.3.3 | Simulation Annealing | 438 |
| 7.6 | Conflict Resolution..... | 440 |
| 7.6.1 | Stakeholder Involvement | 446 |
| 7.6.1.1 | Effective Meeting Facilitation | 447 |
| 7.6.1.2 | Conflict Handling | 447 |
| 7.6.1.3 | Quantifying Meeting Outcomes | 448 |
| 7.6.2 | Application of Game Theory in Multi-objective Groundwater Management | 449 |
| 7.6.2.1 | Non-cooperative Stability Definitions | 452 |
| 7.7 | Groundwater Systems Economics..... | 452 |
| 7.7.1 | Economic Analysis of Multiple Alternatives..... | 457 |
| 7.7.2 | Economic Evaluation of Projects Using Benefit–Cost Ratio Method | 459 |

| | | |
|------------------|---|------------|
| 7.8 | Case Studies | 460 |
| 7.8.1 | Case 1: Development of a System Dynamics Model for Water Transfer | 460 |
| 7.8.1.1 | Area Characteristics | 461 |
| 7.8.1.2 | Conflict Resolution Model for Land Resources Allocation in Each Zone..... | 461 |
| 7.8.1.3 | Results of the Conflict Resolution Model | 463 |
| 7.8.1.4 | Optimal Groundwater Withdrawal in Each Zone..... | 464 |
| 7.8.1.5 | Sizing Channel Capacity | 464 |
| 7.8.1.6 | Conclusion—Making Technologies Work ... | 465 |
| 7.8.2 | Case 2: Conflict Resolution in Water Pollution Control for an Aquifer..... | 466 |
| 7.8.2.1 | Water Resources Characteristics in the Study Area | 466 |
| 7.8.2.2 | Conflict Resolution Model | 468 |
| 7.8.2.3 | Results and Discussion..... | 471 |
| 7.8.3 | Case 3: An Agent-Based Modeling Application in Groundwater..... | 472 |
| 7.8.3.1 | Case Study Characteristics | 472 |
| 7.8.3.2 | Model Characteristics..... | 473 |
| 7.8.3.3 | Model Calibration and Verification | 475 |
| 7.8.3.4 | Results of Agent-Based Modeling..... | 475 |
| 7.8.4 | Case 4: Development of a Noncooperative Game in Groundwater Management..... | 476 |
| 7.8.4.1 | Area Characteristics | 476 |
| 7.8.4.2 | Simulation-Multi-objective Optimization Model | 477 |
| | Problems..... | 482 |
| | References | 486 |
| Chapter 8 | Surface Water and Groundwater Interaction | 491 |
| 8.1 | Introduction | 491 |
| 8.2 | Interaction between Surface and Groundwater | 491 |
| 8.2.1 | Infiltration..... | 492 |
| 8.2.2 | Concepts of Interaction between Surface Water and Groundwater..... | 492 |
| 8.2.3 | Bank Storage and Baseflow Recession | 495 |
| 8.2.3.1 | Master-Depletion Curve Method..... | 496 |
| 8.2.3.2 | Seasonal Recession Method (Meyboom Method) | 497 |
| 8.2.3.3 | Constant-Discharge Baseflow Separation ... | 498 |
| 8.2.3.4 | Constant-Slope Baseflow Separation | 498 |
| 8.2.3.5 | Concave-Baseflow Separation..... | 499 |
| 8.2.4 | Groundwater and Lakes..... | 500 |

| | | |
|------------------|--|------------|
| 8.3 | Conjunctive Use of Surface and Groundwater | 502 |
| 8.3.1 | Advantages of Conjunctive Use | 503 |
| 8.3.2 | Impediments of Conjunctive Use | 504 |
| 8.3.3 | Case Study 1: Conjunctive Use of Surface and Groundwater in Lakhota Canal Uttar Pradesh, India | 504 |
| 8.3.4 | Surface and Groundwater Conjunctive Use Modeling | 507 |
| 8.3.5 | Multi-objective Conjunctive Use Optimization | 515 |
| 8.3.5.1 | Groundwater Resource Sustainability Limits | 516 |
| 8.3.6 | Case Study 2: Application of Genetic Algorithms and Artificial Neural Networks in Conjunctive Use of Surface and Groundwater Resources | 517 |
| 8.3.6.1 | Simulation Model | 517 |
| 8.3.6.2 | Optimization Model Framework | 521 |
| 8.3.6.3 | Results and Discussion | 523 |
| 8.3.7 | Case Study 3: Water Allocation from the Aquifer-River System Using a Conflict Resolution Model | 524 |
| 8.3.7.1 | Optimization Model Framework | 528 |
| 8.3.7.2 | Results and Discussion | 530 |
| 8.3.8 | Case Study 4: Conjunctive Use and Crop Pattern Management | 532 |
| 8.3.8.1 | Optimization Model Structure | 534 |
| 8.3.8.2 | Results and Discussion | 537 |
| 8.4 | Operation of Groundwater Resources in Semiarid Region | 538 |
| | Problems | 540 |
| | References | 541 |
| Chapter 9 | Aquifer Restoration and Monitoring | 543 |
| 9.1 | Introduction | 543 |
| 9.2 | Partitioning Process | 544 |
| 9.3 | Retardation | 546 |
| 9.4 | Natural Losses of Contaminants | 547 |
| 9.4.1 | Volatilization | 548 |
| 9.4.2 | Biological Degradation | 548 |
| 9.4.3 | Plant Uptake | 549 |
| 9.5 | Groundwater Pollution Control | 550 |
| 9.5.1 | Institutional Tools | 550 |
| 9.5.1.1 | Regional Groundwater Management | 550 |
| 9.5.1.2 | Land Zoning | 550 |
| 9.5.1.3 | Effluent Charges/Credits | 550 |
| 9.5.1.4 | Guidelines | 551 |
| 9.5.1.5 | Aquifer Standards and Criteria | 551 |

| | | |
|---------|--|-----|
| 9.5.2 | Source Control Strategies..... | 551 |
| 9.5.3 | Stabilization/Solidification Strategies | 552 |
| 9.5.4 | Well Systems | 554 |
| 9.5.5 | Interceptor Systems..... | 554 |
| 9.5.6 | Surface Water Control, Capping, and Liners..... | 555 |
| 9.5.7 | Sheet Piling | 556 |
| 9.5.8 | Grouting | 557 |
| 9.5.9 | Slurry Walls | 557 |
| 9.6 | Treatment of Groundwater | 559 |
| 9.6.1 | Air Sparging | 559 |
| 9.6.2 | Carbon Adsorption | 560 |
| 9.6.3 | Adding Chemicals and In Situ Chemical Oxidation ... | 561 |
| 9.6.4 | Thermal Technologies | 562 |
| 9.6.5 | Bioremediation Techniques..... | 563 |
| 9.6.6 | Dissolved Phase (Plume) Remediation | 564 |
| 9.6.6.1 | Pump and Treat | 564 |
| 9.6.6.2 | Permeable Reactive Barriers | 564 |
| 9.7 | Aquifer Restoration—Overdraft Issues..... | 566 |
| 9.7.1 | Case Study: The National Restoration and Remediation of Groundwater Resources in Iran | 567 |
| 9.7.1.1 | General Purpose | 567 |
| 9.7.1.2 | Projects..... | 567 |
| 9.7.1.3 | Operational Program (Action Plans) | 568 |
| 9.7.1.4 | Time Table..... | 569 |
| 9.8 | Monitoring Subsurface Water..... | 569 |
| 9.8.1 | Vadose-Zone Monitoring..... | 570 |
| 9.8.2 | Groundwater Monitoring..... | 571 |
| 9.8.3 | Water Quality Variable Selection | 572 |
| 9.8.4 | Geostatistical Tools for Water Quality-Monitoring Networks | 573 |
| 9.8.4.1 | Kriging | 574 |
| 9.8.5 | Location of Water Quality Monitoring Stations | 577 |
| 9.8.5.1 | Definition and Discretization of the Model Domain | 578 |
| 9.8.5.2 | Calculation of Weights for Candidate Monitoring Sites..... | 579 |
| 9.8.5.3 | Optimal Configuration of a Monitoring Well Network | 580 |
| 9.8.5.4 | Kriging Method in Designing an Optimal Monitoring Well Network | 581 |
| 9.8.5.5 | Genetic Algorithms in Designing an Optimal Monitoring Well Network | 582 |
| 9.8.6 | Sampling Frequency..... | 584 |
| 9.8.6.1 | Methods of Selecting Sampling Frequencies.... | 584 |
| 9.8.6.2 | Single Station and Single Water Quality Variable | 585 |

| | | |
|-------------------|--|------------|
| 9.8.6.3 | Single Station and Multiple Water Quality Variables | 586 |
| 9.8.6.4 | Multiple Stations and a Single Water Quality Variable | 587 |
| 9.8.6.5 | Multiple Stations and Multiple Water Quality Variables | 588 |
| 9.8.7 | Entropy Theory in a Water Quality-Monitoring Network | 588 |
| 9.8.7.1 | Entropy Theory | 589 |
| 9.9 | Managed Aquifer Recharge | 591 |
| 9.9.1 | Principal Consideration | 591 |
| 9.9.1.1 | Sources of Recharge Water and Its Quality Considerations | 593 |
| 9.9.1.2 | Hydrogeological Settings and Controls on Recharge | 594 |
| 9.9.1.3 | MAR Methods | 595 |
| 9.9.2 | MAR in Support of Groundwater Sustainability | 600 |
| 9.9.2.1 | MAR in Urban Settings | 600 |
| 9.9.2.2 | MAR in Agricultural Settings | 602 |
| 9.9.2.3 | MAR in Coastal Areas | 606 |
| 9.9.3 | The United Nations MAR Portal | 607 |
| 9.10 | Summary | 607 |
| | Problems | 607 |
| | References | 609 |
| Chapter 10 | Groundwater Risk and Disaster Management | 615 |
| 10.1 | Introduction | 615 |
| 10.2 | Groundwater Risk Assessment | 616 |
| 10.2.1 | Elements of Risk Assessment | 616 |
| 10.2.2 | Assessment of Dose-Response | 618 |
| 10.2.3 | Risk Assessment Methods and Tools | 619 |
| 10.2.3.1 | Potency Factor for Cancer-Causing Substances | 620 |
| 10.2.4 | Environmental Risk Analysis | 624 |
| 10.3 | Groundwater Risk Management | 625 |
| 10.3.1 | Groundwater Risk Mitigation | 626 |
| 10.4 | Groundwater Disaster | 627 |
| 10.4.1 | Requirements for Institutional and Technical Capacities | 627 |
| 10.4.2 | Prevention and Mitigation of Natural and Man-Induced Disasters | 628 |
| 10.4.3 | Disaster Management Phases | 629 |

| | | |
|-------------------|--|------------|
| 10.5 | Disaster Indices | 630 |
| 10.5.1 | Reliability | 630 |
| 10.5.2 | Resiliency | 636 |
| 10.5.3 | Vulnerability | 636 |
| 10.6 | Groundwater Vulnerability | 637 |
| 10.6.1 | Drought..... | 638 |
| 10.6.1.1 | Drought Indicators..... | 641 |
| 10.6.1.2 | Drought Triggers..... | 641 |
| 10.6.1.3 | Drought Management Strategy Plan..... | 643 |
| 10.6.1.4 | Drought Vulnerability Maps | 643 |
| 10.6.1.5 | Drought Early Warning Systems | 644 |
| 10.6.1.6 | Case Study | 644 |
| 10.6.1.7 | Qanats | 645 |
| 10.6.2 | Flood..... | 647 |
| 10.6.2.1 | Maps of Groundwater Flood Hazard | 648 |
| 10.6.3 | Land Subsidence..... | 650 |
| 10.6.3.1 | Subsidence Calculation..... | 651 |
| 10.6.3.2 | Monitoring Land Subsidence..... | 652 |
| 10.6.3.3 | Reducing Future Subsidence | 652 |
| 10.6.3.4 | Examples of Subsidence | 653 |
| 10.6.4 | Widespread Contamination | 653 |
| 10.6.4.1 | Vulnerability Assessment in Groundwater Pollution..... | 657 |
| 10.6.4.2 | DRASTIC Method..... | 659 |
| 10.6.5 | Case Study: Development of Vulnerability Maps for a Drought | 664 |
| 10.6.5.1 | Summary..... | 668 |
| | Problems..... | 669 |
| | References | 671 |
| Chapter 11 | Climate Change Impacts on Groundwater | 675 |
| 11.1 | Introduction | 675 |
| 11.2 | Climate Change | 676 |
| 11.3 | Climate Change Impacts on Hydrological Cycle | 677 |
| 11.3.1 | Floods and Droughts..... | 678 |
| 11.3.2 | Agricultural Droughts..... | 679 |
| 11.3.3 | Water Use | 679 |
| 11.3.4 | Water Quality..... | 680 |
| 11.3.5 | Habitat | 680 |
| 11.3.6 | Hydroelectric Power | 680 |
| 11.3.7 | Snowpack..... | 681 |
| 11.3.8 | River Flow | 681 |

| | | |
|----------|---|-----|
| 11.4 | General Climate Change Impacts on Groundwater | 681 |
| 11.4.1 | Hydrological Components Affecting the Groundwater | 683 |
| 11.4.1.1 | Temperature and Evaporation | 683 |
| 11.4.1.2 | Precipitation | 683 |
| 11.4.1.3 | Soil Moisture | 685 |
| 11.4.2 | Direct Impacts of Climate Change on Groundwater | 686 |
| 11.4.2.1 | Groundwater Recharge | 687 |
| 11.4.2.2 | Recharge Estimation Methods | 688 |
| 11.4.2.3 | Aquifers Recharging | 689 |
| 11.4.2.4 | Hydraulic Conductivity | 689 |
| 11.4.3 | Indirect Impacts of Climate Change on Groundwater | 690 |
| 11.4.3.1 | Sea-Level Rise | 690 |
| 11.4.3.2 | Saltwater Intrusion in Coastal Aquifers | 691 |
| 11.4.3.3 | Storm Surge and Saltwater Intrusion | 693 |
| 11.4.3.4 | Ghyben–Herzberg Relation between Freshwater and Saline Waters | 694 |
| 11.4.3.5 | Island Freshwater Lens | 695 |
| 11.4.3.6 | Land Use and Land Cover | 698 |
| 11.5 | Groundwater Quantity and Quality Concerns | 698 |
| 11.5.1 | Depletion of Groundwater Table | 698 |
| 11.5.2 | Deterioration of Groundwater Quality | 699 |
| 11.5.2.1 | Increasing Groundwater Contamination | 699 |
| 11.5.2.2 | Salinization of Groundwater by Sea-Level Rise | 699 |
| 11.6 | Adaptation to Climate Change | 700 |
| 11.6.1 | Artificial Recharge | 701 |
| 11.6.2 | Modification of Groundwater Extraction Pattern | 701 |
| 11.6.3 | Injection Barrier | 702 |
| 11.6.4 | Subsurface Barrier | 702 |
| 11.6.5 | Tidal Regulators | 702 |
| 11.7 | IPCC Assessment Report | 702 |
| 11.8 | Climate Change Simulation | 704 |
| 11.8.1 | Spatial Variability | 705 |
| 11.8.1.1 | Recent Communities' Scenarios Development | 705 |
| 11.8.1.2 | Downscaling | 707 |
| 11.8.1.3 | Regional Models | 708 |
| 11.8.2 | Statistical Downscaling | 709 |
| 11.9 | Downscaling Models | 712 |
| 11.9.1 | Statistical Downscaling Model | 712 |
| 11.9.2 | LARS-WG Model | 715 |

| | | |
|-------------------|--|------------|
| 11.10 | New Insights—Risks and Vulnerabilities | 724 |
| 11.11 | Climate Change Impacts on Water Availability in an Aquifer..... | 725 |
| 11.12 | Conclusion..... | 732 |
| | Problems..... | 732 |
| | References | 734 |
| Index..... | | 739 |

Preface

The demand for fresh water is increasing as the world's population continues to grow and expects higher standards of living. Water conservation, better systems' operation, higher end use, and water allocation efficiencies have not been able to offset the growing demand. Many societies are struggling to bring supply and demand to a sustainable level. Although water is abundant on earth, fresh water accounts only for about 2.5% of global water reserves. Out of this amount, approximately 30% is stored as groundwater, and the same amount is on the surface as rivers and lakes; the remaining reserves are held in glaciers, ice caps, soil moisture, and atmospheric water vapor. Groundwater is a source of vital natural flow. In arid and semi-arid areas, groundwater may represent 80% or more of the total water resources. The public has a perception of groundwater as a reliable, clean, and virtually unlimited source of water supply. Even though there could be exceptions, it is a dependable source almost everywhere in the world.

The term "groundwater" is usually used for subsurface water that is located below the water table in saturated soils and geological formations. Groundwater is an important element of the environment; it is a part of the hydrologic cycle, and an understanding of its role in this cycle is necessary if integrated analyses ought to be promoted. Aquifers and watershed resources are two inseparable media for the regional assessment of water and contamination movement, as well as the soil–water interaction.

Water enters the formation of the earth from the ground surface by natural or artificial recharge. Within the subsurface, the water moves slowly downward through unsaturated zones under the force of gravity and in saturated zones in the direction determined by the hydraulic gradient. It is discharged naturally to the streams and lakes, as a spring, or by transpiration from plants. It can also be discharged by pumping from wells. Storage of the groundwater could be significantly beneficial as compared to surface storage, which may require massive infrastructure and is subject to considerable evaporation.

In this book, a compilation of the state-of-the-art subjects and techniques in the education and practice of groundwater is presented. The materials are described in a systematic and integrated fashion that is useful for undergraduate and graduate students and practitioners.

[Chapter 1](#) provides an introduction to different aspects of groundwater science, engineering, planning, and management. It discusses the concepts of integration, sustainability, and public participation with an emphasis on laws and regulations governing groundwater operation and management.

[Chapter 2](#) presents an overview of the general concepts on the occurrence of groundwater as a part of the hydrologic cycle. The basic definitions of subsurface water and aquifers are discussed in this chapter. The occurrence of groundwater in karst areas and karst aquifers is also explained.

Chapter 3 discusses groundwater hydrology and the basic laws of groundwater movement. It describes some characteristics of aquifers and soil formations that govern the movement of groundwater, such as hydraulic conductivity, transmissivity, homogeneity, and the isotropy of soil layers. It then discusses flownets simply as procedures to solve flow equations. Statistics and probabilistic methods in hydrogeology are also explained. Finally, the analysis of time series and the methods of generating synthetic time series and forecasting data are introduced.

Chapter 4 presents the technical aspects of developing and solving governing groundwater flow equations. It provides a mathematical description of groundwater flow based on the continuity equation and the equation of motion. The utilization of groundwater by pumping from wells leads to a decline in the water level. The chapter takes a detailed look at the theoretical analyses of the aquifer system's response based on the physics of flow toward a well in both confined and unconfined aquifers for steady and unsteady states. It also describes the pumping test to estimate the aquifers' parameters, as well as the methods of well design and well construction.

Chapter 5 describes environmental water quality issues related to groundwater systems. It describes the factors that can affect groundwater solubility as well as the evaluation of the non-equilibrium status of groundwater; this is followed by a short discussion on different types of contaminants in groundwater. The pollution of groundwater is caused by many activities, including leaching from municipal and chemical landfills and abandoned dump sites, accidental spills of chemicals or waste materials, improper underground injection of liquid wastes, and placement of septic tanks. Finally, the chapter covers the principles of reactive and non-reactive transport of contaminants in both saturated and unsaturated zones.

Chapter 6 provides details of the specific information about groundwater flow modeling. In the application of numerical methods, partial differential equations of groundwater are transformed into a set of ordinary differential or algebraic equations. State variables at discrete nodal points are determined by solving the equations. Three major classes of numerical methods have been presented for solving groundwater problems including finite difference method (FDM), finite element method (FEM), and finite volume method (FVM).

Chapter 7 introduces conceptual models to simulate groundwater systems. The management problem can be viewed and determined in an appropriate type, location, and setting for the control of desirable system outputs. This chapter provides a comprehensive description of planning tools and important issues related to groundwater management in order to optimize groundwater resources and allocation schemes. Optimization methods are powerful tools that could maximize water utilization, minimize the costs of groundwater operation, and minimize the adverse impacts of the overexploitation of groundwater. This chapter presents a set of analytical tools, based on coupling groundwater simulation and optimization models, to assist the analyst in solving complex management problems. It also provides examples and case studies to illustrate the application of the topics presented.

Chapter 8 presents basic information about the conjunctive use of surface and groundwater. It describes the interactions between groundwater and different types of surface water with an emphasis on planning issues. It also discusses certain advantages of conjunctive use planning especially in semi-arid regions and presents case studies.

[Chapter 9](#) discusses aquifer restoration in the context of different groundwater pollution control issues and the utilization of groundwater treatment. First, it describes the processes affecting the amount of contaminants, as well as the natural and mechanical means of reducing the contaminants concentration. It then explains the importance of groundwater monitoring and the corresponding processes.

[Chapter 10](#) discusses different groundwater disasters and the vulnerability of aquifers to natural hazards and human impacts, such as drought, flood, widespread contamination, and land subsidence. It presents risk as an overlay of hazard and a system's vulnerability, as well as methods for risk analysis. It also discusses the planning processes for groundwater disaster management, including the development of contingency plans.

[Chapter 11](#) presents the impact of climate change on the hydrological cycle. It evaluates the direct impacts of climate change on the groundwater as affected by changes in precipitation, temperature, evaporation, and soil moisture. It also presents different downscaling models to adjust to the resolution of data for climate change impact studies and assesses indirect impacts, such as saltwater intrusion, sea level rise, and changes in land use. Finally, methods to cope with climate change with some applications to adapt to the impacts of climate change on groundwater resources are discussed.

In this 2nd edition, about 100 pages are added with many new illustrations, examples, state-of-the-art new materials, and citations. All and any typing errors and inconsistencies have been corrected. The book incorporates student feedback from those who used it for the eight consecutive years it was taught by the 1st author. Here, the main chapters are listed. In [Chapter 3](#), the groundwater flow in an unsaturated zone has been further discussed and the methods of parameter estimation have been updated. In [Chapter 4](#), an aquifer's parameters and drawdown have been generalized for variable pumping and illustrated through a field example. In [Chapter 6](#), the use of the kernel discretization method to numerically solve the groundwater problems for long-term management planning is described. The application of the alternative direction implicit (ADI) method in groundwater modeling and its numerical code have also been added to this chapter. In [Chapter 7](#), agent-based modeling, game theory, and stakeholder involvement are added in the context of social aspects in groundwater planning and management. These models are utilized to simulate social interactions and probable conflicts included in groundwater management. In [Chapter 8](#), the conjunctive use of surface and groundwater is further discussed and a case study is added. In [Chapter 9](#), the issue of excessive drawdown, well permit revocation, and unauthorized use of groundwater are added with a case study. In [Chapter 10](#), a case study is added. In [Chapter 11](#), the impact of climate change on risk and resilience are added and the new Intergovernmental Panel on Climate Change (IPCC) directives on climate change scenarios are discussed.

This book can serve water communities around the world and add significant value to engineering and the application of systems analysis techniques for groundwater engineering, planning, and management. It can be used as a textbook by students in civil engineering, geology, soil science, urban and regional planning, geography, and environmental science, and in courses dealing with the hydrologic cycle. It also

introduces basic tools and techniques for engineers and policy—and decision-makers who plan future groundwater development activities toward regional sustainability.

It is our hope that this book can add significant value to the application of engineering and system analysis techniques for groundwater studies around the world.

Mohammad Karamouz

Azadeh Ahmadi

Masih Akhbari

Acknowledgments

Many individuals have contributed to the preparation of this book and its 2nd edition. The initial impetus for the book was provided by Professor Milton E. Harr through his class notes when he taught at Purdue University. Professor Jacques W. Delleur has been a role model for Mohammad Karamouz as his PhD co-adviser and, as an inspiring professor, published two outstanding books entitled *Time Series Analysis* and *Handbook of Groundwater Engineering*. The authors acknowledge the significant contribution of Mehri Dolatshahi, a PhD student at the University of Tehran, in the preparation of the 2nd edition, and Dr. Navideh Noori in the preparation of **Chapter 11** of the 1st edition.

Many graduate students at the University of Tehran, including D. Mahmoodzadeh (PhD candidate), and the Polytechnic Institute of New York, who attended the first author's groundwater course, were a driving force for the completion of the class notes that formed the basis for this book and the significant revision and improvements of the 2nd edition. Their valuable input is hereby acknowledged.

The authors would also like to thank Drs. A. Moridi, L. Foglia, H. Safavi, S. Nazif, Z. Zahmatkesh, M. Taherion, and A.M. Olyaie; the PhD students A. Ansari, E. Ebrahimi Sarindizaj, M. Nazari, and A. Zeynolabedin; and the MS students H. Meydani, S. Mahmoodi, F. Fooladi Mahani, A.H. Adibfar, R. Saleh Alipoor, A. Ghomlaghi, H. Barkhordari, J. Teymoori, M.R. Zare, S. Nazari, S. Semsar, B. Ahmadi, A. Abolpour, M. Fallahi, B. Rohanizade, S. Ahmadinia, F. Emami, S. Safaie, and M. Sherafat. Special thanks to Mehrdad Karamouz, Mona Lotfi, Mina Akhbari, and Omid Ebrahimi for preparing the cover page, figures, and artwork for the 1st edition. The artwork for the 2nd edition was done by the graduate students listed above.



Taylor & Francis

Taylor & Francis Group

<http://taylorandfrancis.com>

Authors

Mohammad Karamouz is a professor at the University of Tehran. He is an internationally known water resources engineer and consultant. He is licensed as a PE in the state of New York since 1985. Dr. Karamouz is the former dean of engineering at Pratt Institute in Brooklyn, New York. He is also a fellow of the American Society of Civil Engineers (ASCE) and a diplomat of the American Academy of Water Resources Engineers.

Dr. Karamouz received his BS in civil engineering from Shiraz University, his MS in water resources and environmental engineering from George Washington University, and his PhD in hydraulic and systems engineering from Purdue University. He served as a member of the task committee on urban water cycle in UNESCO-IHP VI and was a member of the planning committee for the development of a 5-year plan (2008–2013) for UNESCO's International Hydrology Program (IHP VII).

Among many professional positions and achievements, he also serves on a number of task committees for the ASCE. In his academic career spanning 35 years, he has held positions as a tenured professor at Pratt Institute (Schools of Engineering and Architecture in Brooklyn) and at Polytechnic University (Tehran, Iran). He was a visiting professor in the Department of Hydrology and Water Resources at the University of Arizona, Tucson, 2000–2003 and a research professor at NYU, 2009–2014. He was also the founder and former president of Arch Construction and Consulting Co. Inc. in New York City.

His teaching and research interests include integrated water resources planning and management, flood resilient cities, groundwater hydrology and pollution, drought analysis and management, water quality modeling and water pollution, decision support systems, climate forecasting, and the conjunctive use of surface and groundwater. He has more than 350 research and scientific publications, books, and book chapters to his credit, including three books: *Urban Water Engineering and Management and Hydrology & Hydroclimatology* published by CRC Press in 2010, and 2012, respectively, *Water Resources System Analysis* published by Lewis Publishers in 2003, and a coauthored book entitled *Urban Water Cycle Processes and Interactions* published by Taylor & Francis Group in 2007.

Professor Karamouz serves internationally as a consultant to both private and governmental agencies, such as UNESCO and the World Bank. Dr. Karamouz is the recipient of the 2013 ASCE Service to the Profession and 2018 ASCE Hydraulic Engineering Awards.

Azadeh Ahmadi is an associate professor in the Department of Civil Engineering at Isfahan University of Technology (IUT). She received her BS in civil engineering and her MS in water resources engineering from IUT, and her PhD in water resources management from the University of Tehran. She was a research associate in the Department of Civil and Environmental Engineering at the University of Bristol through a UK fellowship in 2008 and at the Eawag Institute of ETH University in 2017. Dr. Ahmadi is an international expert and consultant in the application of

systems engineering in the planning of aquifer-river-reservoir systems. Her teaching and research interests include groundwater modeling, water engineering and management, systems analysis, the conjunctive use of surface and groundwater, conflict resolution, climate change impacts studies, analysis of risk and uncertainty, and development of decision support systems.

Masih Akhbari is the founder of Global Water Resources Inc., where he develops interdisciplinary models and provides consultant services for water resources management and offers expert witness services on cases with disputes over the management of water resources systems. He is also a project engineer at Larry Walker Associates, where he supports development of groundwater sustainability plans under California's Sustainable Groundwater Management Act. Prior to these positions, he served as a senior water resources engineer at Riverside Technology Inc., a cutting-edge company that provides innovative IT-based solutions to develop decision support systems for water resources.

Dr. Akhbari obtained his PhD from Colorado State University (CSU), followed by two years of postdoctoral research at the University of California, Davis to investigate the effects of climate change on streamflow, stream temperature, and cold-water habitats for the California Energy Commission, and at CSU to assess the United States perspective on the water-energy-food nexus for the Department of State and U.S. Army Corps of Engineers. His journey to apply increasingly complex tools of analysis to thorny problems around the world has already led to the development of interdisciplinary decision-support tools to increase the security of water, energy, and food systems. He has employed hydrologic, engineering, systems analysis, and social science concepts to develop frameworks and tools that support informed decision-making for improved management of water resources.

Through his academic background, along with his professional experience outside of academia, he has gained a unique blend of research experience and knowledge of the broader impacts of the technological advances to deal with the most urgent global water issues. He has built a rigorous perspective on how scientific, engineering, and systems analysis techniques can be implemented to support resources planning and management. Dr. Akhbari has also served as a review panelist for the National Science Foundation's Graduate Research Fellowship Program, as a discussion panelist at the American Water Resources Associations Annual Conference, as a reviewer for multiple scientific journals, as a session chair and convener at the American Geophysical Union Fall Meetings, and as a coadvisor on multiple masters and PhD theses.

1 Introduction

1.1 INTRODUCTION

Increasing demand for water, higher standards of living, depletion of resources of acceptable quality, and excessive water pollution due to urban, agricultural, and industrial expansions have caused intensive environmental, social, and political predicaments. In the last century, the population of the world has tripled, nonrenewable energy consumption has increased by a factor of 30, and the industrial production has multiplied by 50 times. Continuously, we are seeking a balance between our physical being, ability to manage our water resources, and the limitations imposed by the environment. Although progress has improved the quality of life, it has caused significant environmental destruction in such a magnitude that could not be predicted. Now “the environment” is fighting back. The impacts of climate change on natural water resources have been devastating in many regimes around the world. More frequent and intensive floods and droughts have changed the ability of the man-made system to operate and provide services to the public. Also, it has changed the way we have planned and managed our surface and groundwater resources.

A question that should be answered is whether development in the next decades could be done in a way that is economically and ecologically sustainable. We cannot answer this question unless we have a vision of the future and our planning schemes are environmentally responsible and sensitive toward the major elements of our physical environment, namely, air, water, and soil. Water among these elements is of special importance. Excessive use of surface and groundwater, and misusing and polluting these vital resources by residential, agricultural, and industrial wastewater have threatened our well-being. Groundwater is more vulnerable to pollution because it is invisible to monitor and regulatory issues related to groundwater misuse, and laws against contaminating groundwater are not easy to enforce.

Planning for sustainable development of water resources means water conservation, waste and leakage prevention, improved efficiency of water systems, improved water quality, water withdrawal and usage within the limits of the system, water pollution within the carrying capacity of the streams, and water discharge from groundwater within the safe yield of the system. It is not easy to determine and monitor the safe yield of the aquifers. Aquifer safe yields cannot be enforced for many technical, operational, and political resources. So, the aquifers are subject to conditions of over expectation in many parts of the world, especially in arid and semiarid regions, where groundwater is widely used for irrigation.

Water is a sustainable resource and the need for integrated water resources management (IWRM) is in every state and national agenda. Water, as a key element in the formation and conservation of the environment, is receiving global

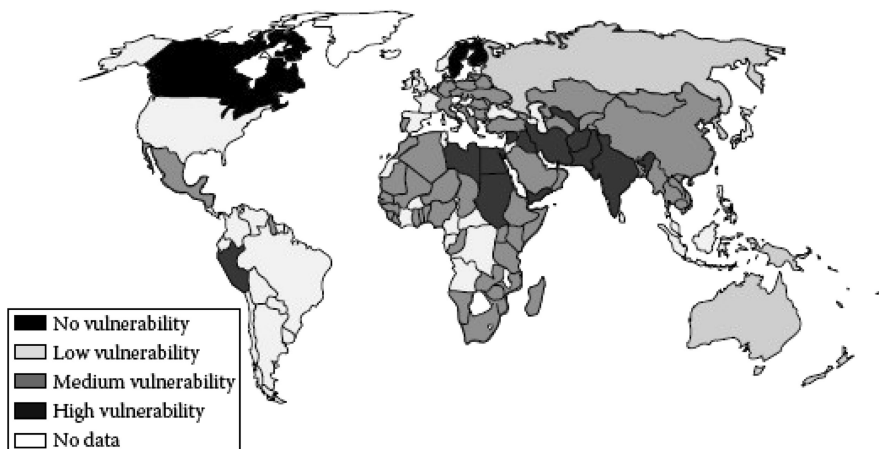


FIGURE 1.1 Nations' vulnerability to water scarcity. (From WRI World Resources Institute, *World Resources, 1998–1999: A Guide to the Global Environment*, Oxford University Press, New York, 384, 1998.)

attention more than ever. Water security and water disaster preparedness are the subjects of many global concerns. Figure 1.1 shows a global map of nations' vulnerability to water scarcity using a composite index based on available water resources and current use, reliability of water supply, and the national incomes (World Resources, 1998).

Approximately 45% of the total irrigated lands in the United States are irrigated by groundwater. In Asia and Africa, more than 60% of land mass is irrigated by groundwater. Libya's irrigated farming is primarily from low-quality groundwater resources, several kilometers deep.

1.2 WATER AVAILABILITY

Groundwater is one of the main components of the environment that is relatively less affected by short-term climate and hydrologic variability. According to a global model of irrigation requirements, Water Global Assessment and Prognosis (WaterGAP) (Doll, 2002), 36% of the total river runoff is formed by groundwater. Therefore, separating groundwater shares from surface water resources is not easy to assess. The primary input for estimating the volume of water naturally available to a given nation is an information database (AQUASTAT) that has been developed and maintained by the Food and Agriculture Organization of the United Nations (FAO, 2007). It is based on a water balance approach for each country and the quantity of available water resources (FAO, 2003). This database has become a common reference tool used to estimate each nation's renewable water resources. The FAO has compiled an index called Total Actual Renewable Water Resources (TARWR). This index is a measure of the water resources availability for development from all sources within a region. It is a total-volume figure expressed in km^3/year ; divided

by the total population. The index estimates the total available water resources per person in each country, considering a number of individual resources as follows:

- Adding all internally generated surface and groundwater from precipitation falling within a country's boundaries
- Adding flow entering from other countries, both surface and groundwater
- Subtracting any potential shared resource from surface and groundwater system interactions
- Subtracting the water that leaves the country through surface and groundwater resources, required by an existing treaty and/or a set by international guidelines.

TARWR gives the maximum amount of water that could actually be available for a country on a per capita basis. From 1989, this method has been used to assess water scarcity and water stress. It is important to note that the FAO considers what is shared in surface and groundwater resources. However, as discussed by the United Nations Educational Scientific and Cultural Organization (UNESCO, 2006), these volumes do not consider the socioeconomic criteria that are applied to societies, nations, or regions that are developing those resources. Water pricing and net costs can vary when developing surface and groundwater sources. Therefore, the reported renewable volume of water will be less available for a variety of economic and technical reasons. Simply, a lot of water is not used because of the circumstances that control the supply and the demand. The following factors should be considered when using the TARWR index (UNESCO, 2006):

- Roughly 27% of the surface water runoff is floods, and this share of water is not considered as a usable resource. Despite that, floods are counted in the nations' TARWR as part of the available, renewable annual water resource.
- Seasonal variation in precipitation, runoff, and recharge, is not well reflected in annual figures. However, it is important in the assessment of supply and demand spatial and temporal distribution for basin-scale decision-making and strategy setting.
- Many sizable countries have different climatic zones as well as scattered population, and the TARWR does not reflect the ranges of these factors that can vary in different regions in that country.
- TARWR has no data to identify the volume of water that sustains ecosystems, namely, the volume that provides water for forests, direct rain fed agriculture, grazing, grass areas, and environmental demand.

It is also documented that not all of the renewable freshwater resources can be used and controlled by the population of a country. It is estimated that only about one-third of the renewable freshwater resources can potentially be controlled even with the most technical, structural, nonstructural, social, environmental, and economic means. The global potentially useable water resources of the renewable freshwater resources are estimated to be around 9000–14,000 km³ (Secker, 1993; UN, 1999). A part of the primary water supply (PWS) is evaporated, other parts return to rivers,

streams, and aquifers and in many instances withdrawn again for different uses. This is known as the recycled portion of the PWS. The PWS and the recycled water supply adds up to 3300 km³ that constitute the water used in different sectors such as agriculture, industry, public, and water supply.

1.2.1 GROUNDWATER AVAILABILITY

Groundwater is by far the most abundant source of freshwater on continents outside polar regions, followed by ice caps, lakes, wetlands, reservoirs, and rivers. In 2012, UNESCO reported that about 2.5 billion people depended solely on groundwater for their drinking water supply (WRI, 1998). It is estimated that about 20% of global water withdrawals come from groundwater (WMO, 1997).

According to the United Nations Environment Programme, annual global freshwater withdrawal has grown from 3790 km³ in 1995 to about 4430 km³ in 2000. The annual global water withdrawal is expected to increase with a rate of 10%–20% every 10 years, reaching approximately 5240 km³ in 2025. The share of groundwater is expected to increase at a slower rate due to already over drafted aquifers in many points of the world.

There are many advantages in storage of groundwater compared to the surface storage:

1. Minimum evaporation losses—it is limited to
 - a. Groundwater close to the surface by capillary fringes.
 - b. “Phreatophytes”—plants feed on capillary fringe.
2. Quality may benefit from filtering action (however, may be too high in dissolved solids). There is general improvement of water quality because of the porous media filtration of airborne and surface runoff contaminants and pathogens.
3. Outflow is gradual (good regulation in underground reservoir).
4. No other massive structure such as dams is needed (however, may involve high pumping costs).
5. Land use above the groundwater resources can be continued without change (there is no submergence of houses, abstraction to infrastructure, and property development and agricultural development).

Groundwater quality is under continuous threats. Unless protected, groundwater quality deteriorates from saline intrusion, pollution from agricultural and urban activities, uncontrolled wastewater, as well as solid and hazardous waste disposal. The following activities should be undertaken:

- Improve the understanding of groundwater contribution to the hydrologic cycle and evaluate changes to groundwater storage and water table fluctuations.
- Raise the awareness of decision-makers, water users, and public on the importance of groundwater in order to encourage protection and sustainable use.

- Assess the impacts of economic development on groundwater resources and support international collaboration for nations and regional needs.
- Quantify climate change impacts on groundwater resources including sea levels rise and intrusion of saltwater.

1.3 GROUNDWATER SYSTEMS

The groundwater system is a part of the hydrologic cycle and should be studied on a watershed scale. Combination of many elements and factors affect groundwater, requiring a holistic view to groundwater challenges within a hydrologic cycle.

Groundwater systems are traditionally developed as sources of water for different uses of domestic, industrial, or agricultural purposes. The generally good quality of the water and its accessibility in many regions of the world, where surface water is nonexistent or extremely costly to develop, have been important factors in stimulating the development of this relatively low-cost, reliable water resource. An example of groundwater system representation is shown in [Figure 1.2](#). See Willis and Yeh (1987) for more details.

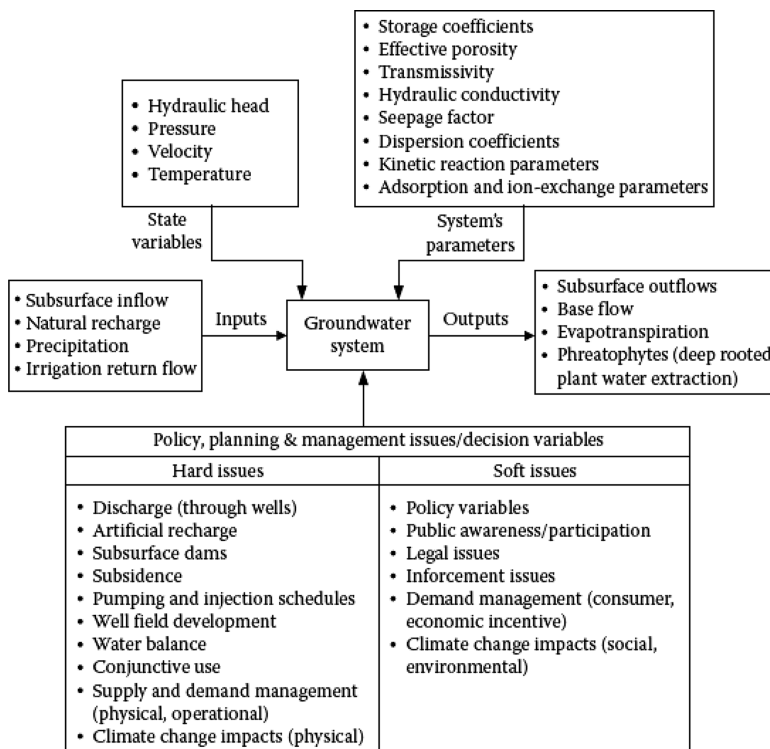


FIGURE 1.2 Groundwater system.

A groundwater system is defined as a system that can be isolated from upstream and downstream aquifers for the computation of its water balance and pollution characteristics:

1. Inputs to the system that are partially or completely controlled include precipitation, subsurface inflows, natural and artificial recharge, and irrigation return flows, interaction with streams.
2. Outputs include subsurface outflows to adjacent aquifers, discharges to surface waters, naturally occurring springs, and evapotranspiration losses.
3. Parameters of the groundwater system help define flow, quality, and thermal properties of the aquifer system. These parameters are hydraulic conductivity, transmissivity, storativity, storage coefficient, and dispersion/advection parameters.
4. Control or decision variables within the context of policy, planning, and management that detail the pumping, injection, and artificial recharge variables of the ground and surface water system. The decision variables are bounded by policy, legal, physical, and operational constraints.
5. State variables characterize the condition of the system, such as the hydraulic head, pressure, velocity, or temperature distribution or the concentrations of pollutants in the groundwater system.

Groundwater systems are often treated as a lump system, but in reality, they have distributed parameters. For temporal variation of the parameters, the lump system can be justified, but most of the aquifers have spatial variation in their parameters that cannot be ignored. They are often referred to as nonhomogeneous properties that need to be tested and determined in many locations across aquifers. For engineering applications, the system can be simplified with constant dispersion and diffusion characteristics in any time and space element. Simplification of groundwater system should be done to the extent that the overall characteristic of the system could be preserved.

1.4 SCIENCE AND ENGINEERING OF GROUNDWATER

In hydrogeology, the groundwater flow equation is the mathematical expression that describes the flow of groundwater. The flow between two states of equilibrium (transient flow) in groundwater can be expressed by the diffusion equation. This is similar to heat transfer that describes the heat flow through a solid. The Laplace equation describes the steady-state flow of groundwater which is a form of potential flow and has analogs in numerous fields.

The flow equation is derived for a small representative elemental volume. Within the representative elemental volume, properties of the medium are considered to be constant. The continuity of water flowing in and out of the representative elemental volume is expressed in terms of an equation called Darcy's law.

[Figures 1.3](#) and [1.4](#) show different aspects of groundwater science and engineering. A driving force, states, and responses framework is used in these figures to define the hydrogeology (science of groundwater) and hydrological and hydraulic design in groundwater.

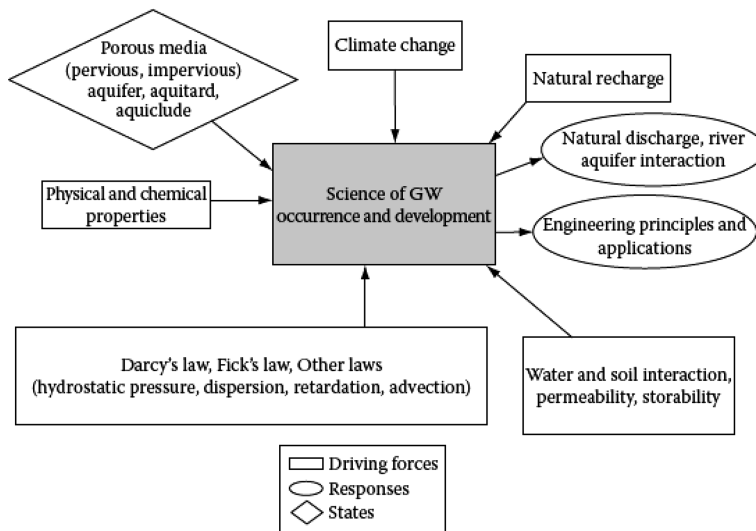


FIGURE 1.3 Science framework of groundwater (GW) occurrence (hydrogeology).

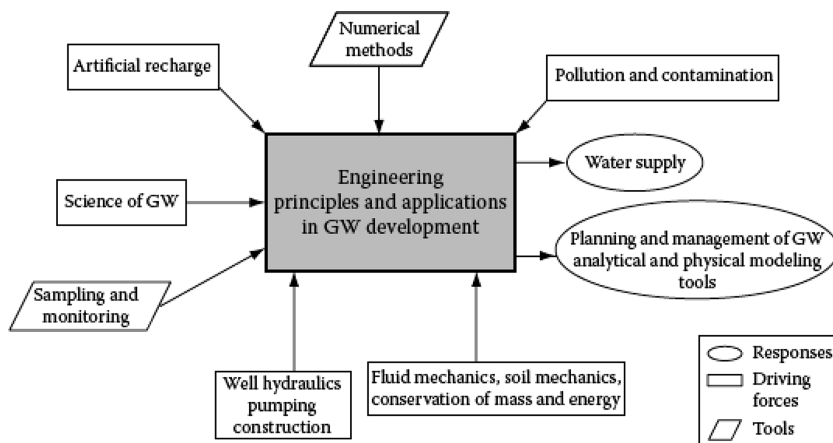


FIGURE 1.4 Basic engineering principles and applications in groundwater (hydrological and hydraulic design).

Figure 1.3 shows certain components of groundwater science in understanding its occurrence and development. Some principles including Darcy's law for hydraulic head/pressure simulation and Fick's law for water quality simulation, the physical/chemical properties of the aquifer, and porous media are transformed to the equations for clarifying the groundwater occurrence. The state of the system consists of changes due to certain driving forces such as climate change, natural disasters, interaction of surface and groundwater, and groundwater recharge that need to be predicted through system modeling using basic groundwater engineering principles and applications.

Simply stated, water enters the formation of the earth from the ground surface by natural or artificial recharge. Within the ground, water moves slowly downward through an unsaturated zone under gravity force and in the saturated zone in the direction determined by the hydraulic gradient. It is discharged naturally to the streams and lakes or as a spring or by transpiration from plants. It can also be discharged by pumping from wells. The main differences between surface and groundwater are as follows:

1. Surface and groundwater movement. Surface waters flow in a channel with a given cross section, while groundwater flows in soil and the pores between soil particles of various shapes. In general, groundwater moves significantly slower than surface water. Flow is fully laminar in most of the groundwater systems (Reynolds number, $Re \approx 1$).
2. Slow movement of contaminants. If groundwater becomes polluted, its natural treatment is a difficult process. Occasionally, the only alternative process for treatment of groundwater is to discharge, treat, and recharge it back.
3. Filtration process: Considering groundwater flows through the soil layers, biological contaminants will be treated through these natural layers.
4. Sampling and monitoring of groundwater is difficult and must be done by drilling and installing observation wells.

1.5 PLANNING AND MANAGEMENT OF GROUNDWATER

Groundwater management is broadly concerned with the evaluation of the environmental, hydrologic, and economic impacts and trade-offs associated with the development and allocation of groundwater supply and quality to competing water users. The planning and management of groundwater problems are done based on a system's representation of the underlying physical, chemical, and hydraulic transport processes occurring within the groundwater basin.

The inputs, boundary conditions, initial conditions, and possibly the parameters of the groundwater system may be considered as random variables. These state variables of the system are also random. For example, if the annual groundwater recharge is a random event, then water levels fluctuation in wells will follow a stochastic process.

In the analysis of groundwater systems, it is also useful to consider three classes of management problems: the detection problem, the parameter estimation or the inverse problem, and the prediction or simulation problem. In the detection problem, the set of inputs to the system is unknown. The identification of the recharge or leakage in semiconfined or unconfined aquifers, from the response properties of the aquifer system, is an example of the instrumentation/detection problems. Parameter estimation is the key to groundwater simulation and modeling. Laboratory or field data could be combined with theoretical assessment to estimate parameters (Willis and Yeh, 1987).

In prediction problems, usually water table/piezometric surface fluctuation is predicted. Several monitoring wells and piezometers should be installed to calibrate the prediction models. At least three monitoring wells are needed to find the groundwater direction and to perform any meaningful field monitoring.

The water resources including groundwater and surface water should be managed considering the issue of sustainability. It can be addressed if we focus on the availability of resources for key services and their economical values. The consequence of losing access to such services that should be borne by the stakeholders should be equitably assessed. For example, if the water table of an aquifer drops significantly, it imposes a high equity impact on a region that could be measured only if we look at the broad spectrum of social, economic, and environmental impacts over a long-term horizon.

Many farmers in the developing world can only afford low yield and shallow wells. As water level drops, these farmers cannot afford the costs of well deepening and new pumps. As a result, the food production and economic development can be affected, and the benefit of access to groundwater may be lost. The drop in the water table could also increase the probability of water pollution migration and adverse impacts.

Figure 1.5 shows certain components of planning and management of groundwater systems. The groundwater system can be classified by considering the driving forces, responses, and tools. The driving forces include socioeconomic issues, environmental issues, laws, standards, regulation, conflicts, and climate change. Management tools should be developed and implemented in order to develop the policies related to conflict resolution, water allocation, disaster management, conjunctive use, aquifer remediation and restoration, and modifying and improving standards as the system responses.

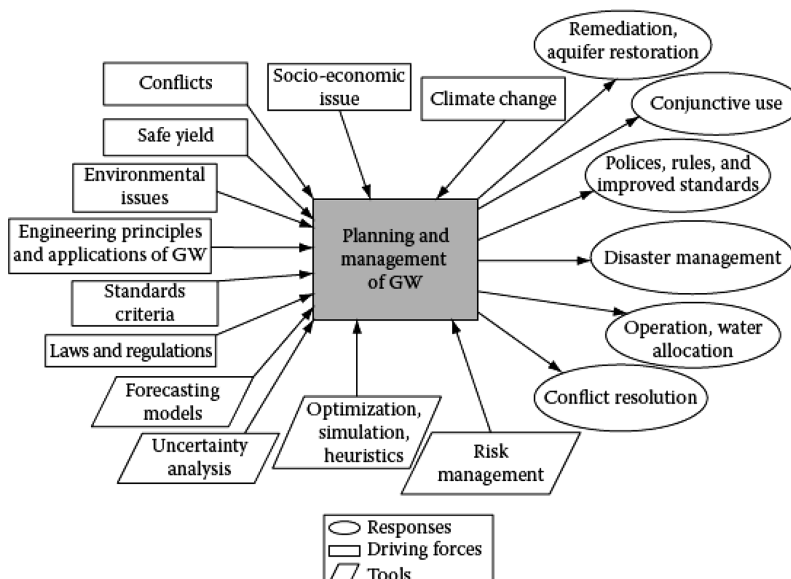


FIGURE 1.5 Basic principles of planning and management in groundwater (GW).

Optimization and simulation, forecasting, uncertainty analysis, and risk assessment models are useful tools for resource allocation, monitoring, assessment, and dealing with probability and randomness in groundwater systems.

1.5.1 INTEGRATED WATER RESOURCES MANAGEMENT

According to Rogers and Hall (2003), in the IWRM schemes, politics, and the traditional fragmented and sectorized approach to water, is made between resource management and the water service delivery functions. It should be noted that the IWRM is a political process, because it deals with reallocating water, the allocation of financial resources, and the implementation of environmental goals. For an effective water governance structure, much more work has to be done.

There is a general agreement that IWRM is the only passage to sustainable management use of water, even though there is extended debate on the process and there is no generally accepted framework. For example, the IWRM is put into practice in the Orange County Water District in California. It includes the use of groundwater recharge, alternative sources, conservation management, and construction of levees in the river channel to increase infiltration and injection of treated recycled water to form a seawater intrusion barrier.

In the IWRM, there are two incompatibilities: the needs of ecosystems and the needs of a growing population. The shared dependence on water for both needs makes it quite natural to give ecosystems full attention within the IWRM. At the same time, the millennium goals of 2000, set by the United Nations, call for safe drinking water and sanitation for all population suffering from poverty by year 2015 (Falkenmark, 2003).

The fundamental objective of IWRM is to sustain humans and the planet's life support systems, and it should be done on a watershed scale. The following goals are suggested by Falkenmark (2003):

- Satisfy societal water consumption needs while minimizing the pollution load
- Meet environmental flow requirements of rivers and aquifers with acceptable water quality
- Secure "hydro-solidarity" between upstream and downstream stakeholders and ecological needs

The IWRM is sometimes referred to as integrated water cycle management such as in Australia, where water supply and management, in general, are the two top priorities for all levels of the government, all water-related agencies, water utilities, and everybody else. This is understandable since Australia is the driest continent and in the middle of experiencing a 1000-year drought (Kresic, 2009).

1.5.2 CONFLICT ISSUES IN GROUNDWATER

There are many conflicts over groundwater allocation and over exploitation of groundwater on a regional scale. There are also conflicts over shared aquifers between



FIGURE 1.6 Transboundary aquifers and major groundwater basins of the world. (From International Groundwater Resources Assessment Center, Transboundary aquifers of the World Map 2015, Retrieved from http://www.un-igrac.org/sites/default/files/resources/files/TBAmap_2015.pdf, 2015.).

politically divided regions. Transboundary aquifers and major groundwater basins of the world are shown in Figure 1.6. Transboundary river basins are in most cases well defined, and there are agreements/treaties for sharing surface water resources. But transboundary aquifers are not well defined and managed by decision-makers and authorities on both sides of the borders. International agreements about shared aquifers have limited practical implications and do not address the groundwater and its spatial distribution as well as how the limited resources should be allocated and discharged.

The International Association of Hydrogeologists established a commission to investigate the issue of transboundary groundwater in 1999. It is a program supported by the UNESCO, FAO, and UNECE (United Nations Economic Commission for Europe). One of the main objectives of the program is to support cooperation among countries in order to develop technical knowledge and conceptual understanding to alleviate potential conflicts. It is intended to train, educate, inform, and provide input to decision and policy makers (Puri, 2001).

1.5.3 ECONOMICS OF WATER

Considering water as an economic good was first initiated at the Earth Summit of 1992 in Rio de Janeiro, Brazil. It was discussed during the Dublin conference on Water and the Environment (ICWE, 1992) and became one of the four Dublin Principles as having an economic value for its competing uses, which must be recognized as an economic good. Within this principle, it is vital to recognize first the basic right of all human beings to have access to clean water and sanitation at an affordable price. Past failures to recognize the economic value of water have led to

wasteful and environmentally damaging uses of this vital resource. Managing water as an economic good is an important way of achieving efficient and equitable use by encouraging conservation and protection of water resources.

Van der Zaag and Savenije (2006) explained the overall concerns over the true meaning of “water as an economic good” based on two schools of thought. The first school is the pure market driven price. Its economic value would arise spontaneously from the actions of willing buyers and willing sellers. This would ensure that water is allocated to users based on its highest value. The second school interprets the process of allocation of scarce resources in an integrated fashion which may not involve financial transactions (McNeill, 1998).

A unique property of water is that it belongs to a system, its use always affects the other users, and any change in upstream water use will affect the entire system downstream. Groundwater and surface water interchange their resources on a continuous basis so groundwater could be found in surface water at some other point and vice versa.

Temporal and spatial variability of water resources is also constantly changing due to short- and long-term climate and land-use changes. Water could have negative economic value in case of floods. All of these make it difficult to establish the value of external impacts on water use.

The price of water could be defined as the price that water users are paying per unit volume of water delivered in a unit of time (e.g., cubic meters/month). In most cases, neither the water users nor the providers pay the full price (value) of water, which should be equal to the real value of water and should include:

- Capital costs of water withdrawal and distribution system including well installation and well field development, pumps, reservoirs, and water transfer facilities
- Costs of operation and maintenance of the system including water treatment, water infrastructure maintenance, staff, and administrative costs
- Investments for augmenting the existing system
- Source protection costs reflecting its intrinsic value (water quality, reliability) including wellhead protection
- Environmental costs
- Sustainability costs

Kresic (2009) described the full price and value of water as shown in [Figure 1.7](#). It is very difficult to assess the environmental and sustainability costs. They are quite related, and a good assessment of tangible and nontangible environmental costs in shorter terms will help us to assess a longer time cost that should be paid to assure sustainability.

Groundwater use typically should be based on the current and future functions of groundwater as well as its expected values/costs. Groundwater use can generally be divided into drinking water, ecological, agricultural, industrial/commercial, and recreational uses. Drinking water use includes both public supply and individual (household or domestic) water systems. Ecological use commonly refers to groundwater functions, such as providing base flow to surface water to support wildlife and

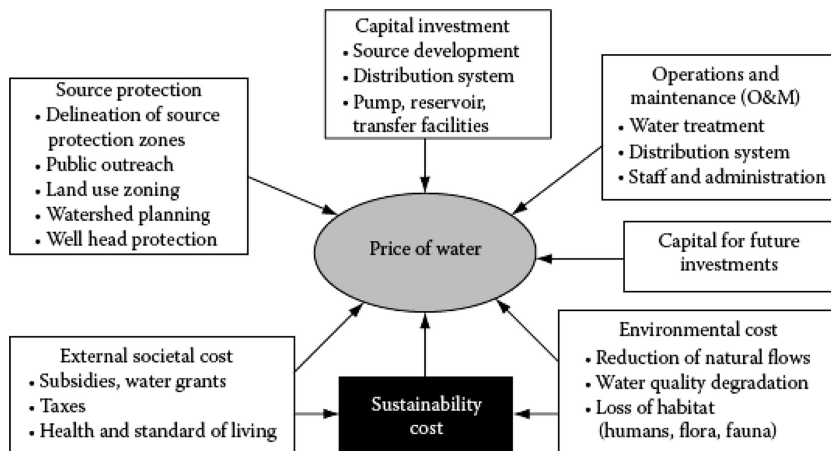


FIGURE 1.7 Components of full water price equal to full water value. (From Kresic, N., *Groundwater Resources: Sustainability, Management, and Restoration*, McGraw-Hill, New York, 852 p., 2009.)

water species. Agricultural use generally refers to crop irrigation and livestock water demand. Industrial/commercial use refers to water need in industrial processes, especially for cooling purposes in manufacturing or commercial uses. Recreational use of groundwater generally refers to its impacts on surface water; however, groundwater in karst aquifers may be used for recreational, such as cave observation purposes. These are considered “beneficial uses” of groundwater. Furthermore, within a range of reasonably expected uses and functions, the most beneficial groundwater use refers to the use or function that warrants the least stringent groundwater cleanup or remediation.

Groundwater value typically considers its current and future uses as well as its intrinsic value. Current use value depends on need. Groundwater is more valuable where it is the sole source of water, or less costly than treating and utilizing surface water. Current use value can also consider the “costs” associated with impacts from contaminated groundwater on the surrounding area (e.g., drinking supply wells and adjacent surface water). Future values refer to the value people place on groundwater to be used in the future. Society places an intrinsic value on groundwater; just knowing that clean groundwater exists and will be available, irrespective of current or expected uses, and it is a vital recourse to the preservation of the ecosystem. While the real value of groundwater is difficult to quantify, it will certainly increase with the increase in the expense of surface water treatment costs and with continuing development and increasing demand.

1.5.4 GROUNDWATER SUSTAINABILITY

The term “sustainable development” was popularized by the World Commission on Environment and Development (Commission) in its 1987 report entitled

“Our Common Future.” The objective of the Commission was to address the environmental and developmental problems in an integrated fashion. The Commission had three general objectives:

- Examine the critical environmental and developmental issues and how to deal with them
- Formulate new forms of international cooperation that will influence policies in the direction of many changes needed
- Raise the level of understanding and commitment to action of all adversaries including institutions and governments

Commissioners from 21 countries analyzed the report, with the final report accepted by the United Nations General Assembly in 1987 (UNESCO, 2002). In various publications, the findings of the Commission and the final resolution of the United Nations General Assembly were summarized as a single sentence describing sustainable development as “meeting the needs of the present without compromising the ability of future generations to meet their own needs.” This sentence was criticized for failing to address the natural environment.

Educating the public, considered by default as “stakeholders,” about various choices is the crucial path toward sustainable development. Groundwater is a perfect example of many misunderstandings, by both the public and policy makers, about the meaning of sustainability. Because there is a strange connotation about groundwater: as soon as groundwater reaches the surface, it can no longer be seen as groundwater, which makes it hard to convince the public when certain groundwater policies are announced.

The development of groundwater often provides an affordable and rapid way to alleviate poverty and ensure food security in the underdeveloped and developing countries. Furthermore, the conjunctive use of groundwater and surface water, thoroughly IWRM strategies, can serve to foster efficient use and sustainability and enhance the longevity of water supply by improving the allocation and end user efficiencies.

Instances of poorly managed groundwater development and the inadvertent impact of land-use practices have produced adverse effects on water quality, impairment of aquatic ecosystems, lowered groundwater levels, and, consequently, caused land subsidence and the drying of wetlands. As it is less costly and more effective to protect groundwater resources from degradation than to restore them, improved water management will diminish such problems and save money.

To make the notion of groundwater as a sustainable resource requires the responsible use, management, and governance of groundwater. In particular, actions need to be taken by water users, who sustain their well-being through groundwater abstraction; decision-makers, both elected and none elected; civil society groups and associations; and scientists who must advocate for the use of sound science and engineering in support of better management.

The international panel on climate change (IPCC, 2007) shows a broader perspective of sustainable development as shown in [Figure 1.8](#). They have combined the impacts of socioeconomic development paths with technology, population, and governance through adaptation by human and natural systems.

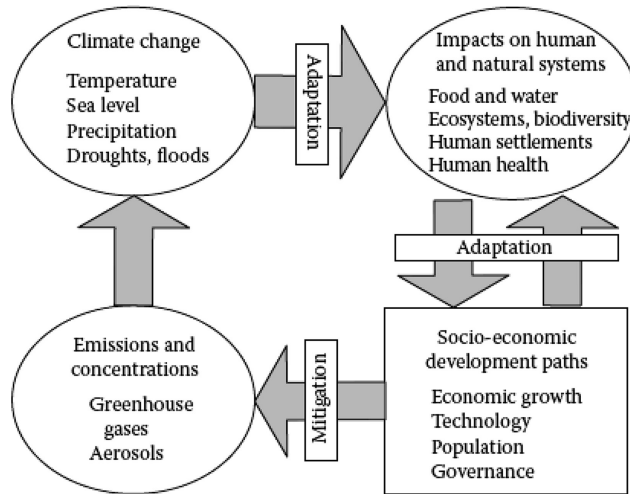


FIGURE 1.8 Sustainable development, adaptation, and migration interactions. (From IPCC, *Fourth Assessment Report, Intergovernmental Panel on Climate Change (IPCC)*, 2007, <http://www.ipcc.ch>).

The objective is to sustain food, water, ecosystems, biodiversity, and human health and prevent migration. At the same time, human and natural systems should adapt to climate change impacts, such as more frequent droughts and floods. The emission of greenhouse gases is the direct by-product of socioeconomic development that should be mitigated. This general framework could be adopted to foster groundwater sustainability on a more regional and global scale.

1.5.5 SUPPLY AND DEMAND SIDE MANAGEMENT

In the last three decades, the “ecological” or “holistic” paradigm comes to the forefront of dealing and solving man-made problems. This new way of thinking began out of new discoveries and theories in science, such as Einstein’s theory of relativity, Heisenberg’s uncertainty principle, and chaos theory contrary to Newton’s mechanistic universe. These theories have taken away the foundation of the opposing paradigm, the Cartesian (Newtonian) model (Karamouz et al., 2010). The world has tried to “control the environment” for many centuries through the mechanistic way of thinking. The new way of thinking calls for “live with the environment,” which is the essence of horizontal and creative thinking in this paradigm shift. It also demands a change in the way we perceive and understand our connecting world.

Water resources management is not an exception in this dramatic shift of paradigm throughout the history of water resources management, many methodologies have reflected some aspects of ecological thinking and have been shaping a water vision of the new paradigm.

For creating an opportunity for action, a paradigm shift in water management, away from the entrenched supply-side focus toward a comprehensive demand-side

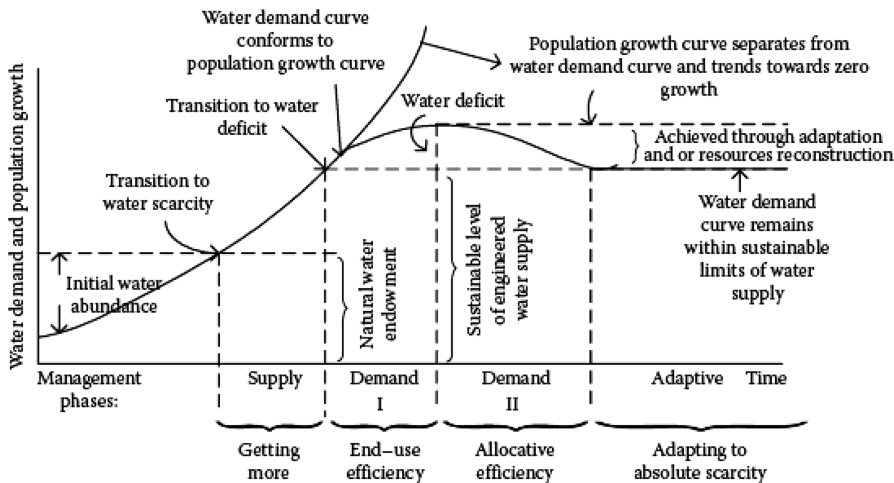


FIGURE 1.9 Schematic representation growth of water demand and supply. (From Ashton, P.J. and Haasbroek, B., Water demand management and social adaptive capacity: A South African case study, in *Hydropolitics in the Developing World: A Southern African Perspective*, eds. Turton, A.R. and Henwood, R., African Water Issues Research Unit, Pretoria, South Africa, 21 p., 2001.)

management. For instance, the recent National Round Table on the Environment and the Economy report, “Environmental Quality in Canadian Cities: The Federal Role,” could easily be extended to explicitly include urban groundwater management. A schematic as shown in Figure 1.9 was proposed by Ashton and Haasbroek (2001) for representation of the growth in water demand and management. Two periods of demand I and demand II are defined to bring the normal growth of demand, as a result of population growth, to the level of sustainable limits of water supply.

Developing water-saving technologies should be considered in developing water demand management strategies. These methods cover a wide range of solutions, such as dual-flush toilets, flow restrictors on showers and automatic flush controllers for public urinals, automatic timers on fixed garden sprinklers, moisture sensors in public gardens, and improved leakage control in domestic and municipal distribution systems. All these measures are practical, but regulations and incentives are needed for their implementation.

The water loss rate in many water distribution systems may vary from 10% to 60% of the supplied water and higher values are reported for the developing countries. To achieve the desired level of efficiency in water use, more attention should be given to decrease the amount of water losses and nonrevenue water which generally includes:

- Leakage pipes, valves, tanks, meters, and other components of water supply and distribution systems
- Water used in the treatment process (backwash, cooling, pumping, etc.) or for flushing pipes and reservoirs (see Karamouz et al., 2010, for more details)

The cost of water supplying services and technologies have a major influence on the level of water demand, especially in developing countries. In rural areas, the distance from households to the standpipes or the number of persons served by a single tap or well are the main factors that control the water demand.

1.6 TOOLS AND TECHNIQUES

Simulation and optimization models of groundwater quantity or quality can be formulated with a mathematical expression of the groundwater system. The model-building process consists of several interrelated stages as outlined in [Figure 1.10](#). Groundwater hydrology is broad, complex, and due to the invisible nature of its media, many tools are needed to plan and manage groundwater resources, protection, mitigation, and development. [Figure 1.10](#) shows a framework for a combination of tools and methods needed for groundwater resources planning.

Models are based on the available hydrologic and hydrogeologic information. In the first phase of the modeling process, well logs, pumping test data, groundwater contour maps, water levels, precipitation, stream flow, and recharge information are compiled and statistically analyzed to determine the probable aquifer parameters, recharge conditions, initial and boundary conditions, and current

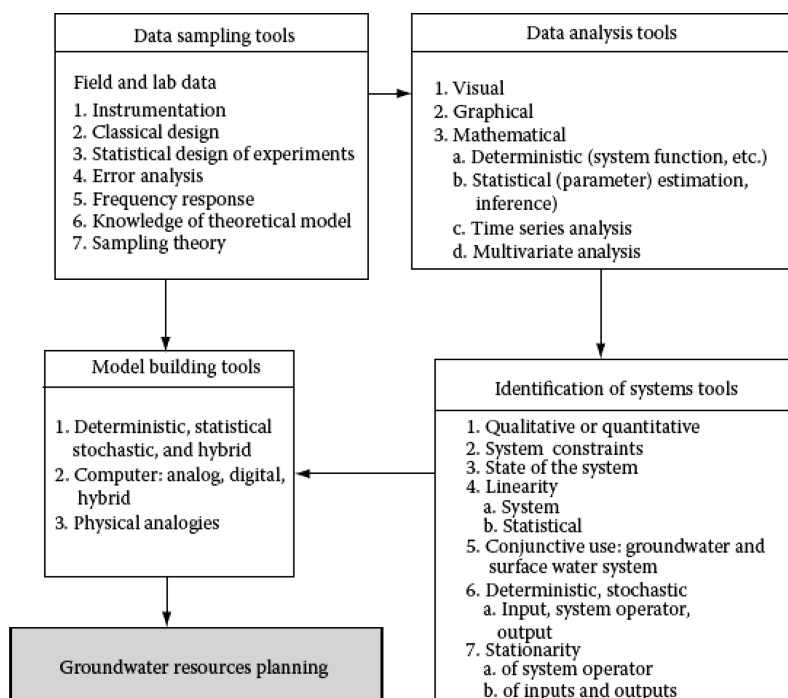


FIGURE 1.10 Framework of tools needed for groundwater resources planning. (From Kisiel, C.C., and Duckstein, L., *Water Resour. Bull.*, 6(6), 857, 1970.

groundwater pumping schedule. On the basis of the statistical reliability of this information, a choice has to be made regarding the most appropriate and realistic type of mathematical model. The model choice problem, the second phase of the process, is characterized by a hierarchy of mathematical models (Willis and Yeh, 1987). For example, in the case of limited or imprecise information regarding the underlying physical processes occurring in the aquifer system, a statistical or time series approach may be warranted. The analysis of trends, periodicities, and the correlation structure of the historical records may further define the mechanisms responsible for groundwater movement and water quality variations.

From a planning perspective, however, mathematical models of the groundwater flow or mass transport will consist of:

1. Mathematical expressions in term of algebraic, integral, or differential equations characterize the flow or transport processes in groundwater. These equations relate variables such as hydraulic head or mass concentration to the policy or decision variables such as pumping or injection rates that provide control over the variables. The process is also bounded by the parameters that define the flow, properties, and quality of the system such as storage coefficients, hydraulic conductivity, and dispersion coefficients.
2. Initial conditions that show the state of the system prior to development or operation of the aquifer system.
3. Inputs to the system such as recharge, precipitation, and subsurface inflows (recharge), and outputs such as discharges to surface waters or evapotranspiration.

The next phase in building models is the calibration and validation. Model calibration compares the model's response or predictions with the actual collected groundwater data. The differences between predicted and historical groundwater levels can be used to judge the predictive capability of the model. It should be brought to a minimum by changing the estimated parameters and the initial/boundary conditions. The underlying assumptions of the model should be re-examined to determine their appropriateness in the context of the validation results. This feedback element of the calibration and validation process is developed through and is facilitated by the iteration nature of the model-building process.

The validation process usually predicts groundwater levels or water quality concentrations with a new set of historical or generated surface and groundwater data. Again, the model's performance is evaluated on the basis of how well, in a statistical sense, the model predictions match the observed data.

Following the calibration-validation process, the mathematical model can be used for the prediction (simulation) and/or optimization of the groundwater resources of the aquifer system. In a simulation approach, a set of planning, design, or operational policies can be analyzed by examining the simulated response of the aquifer system to the proposed management alternatives. Costs and benefits can be determined and sensitive hydrologic or environmental areas of the groundwater systems can be identified. From this information, the "best" management practices can be found. It should be emphasized, however, that the

policy is optimal only in relation to the other simulated policies. Furthermore, simulation analysis provides only localized or limited information regarding the response properties of the system and the possible hydrologic and environmental trade-offs of the groundwater system.

1.7 PEOPLE'S PERCEPTION: PUBLIC AWARENESS

“There could be no Great Society if the water, air and soil are dirty” as stated by Goldman (1967). He reiterated that “there is a reason to believe that only the very wealthy countries are able to afford the luxury of clean water and air, which can make a fuss about it.” It can be argued that until recently having clean water was a “luxury” as often cited by the delegates of developing countries at the United Nations.

In most of the developed countries, legislation for pollution control was introduced in the 1960s and 1970s. In the United States, the Environmental Protection Agency was created in 1970 to administer environmental programs. It was an encouraging effort, but many details were left undefended. The United Nations focused Conference on the Human Environment in 1972 in Stockholm was a starting global effort. Many other United Nations conferences followed dealing with population, food, women’s rights, desertification, and human settlements continued to emphasize on environmental issues.

Eckholm (1982) describes the enormous task faced by the developing countries to provide reasonable clean water, disposal facilities, and the enforcement of sanitary standards. He estimated that half of the people in the developing countries do not have reasonable access to safe water supplies and only one-fourth have access to adequate waste disposal facilities.

It will take extraordinary statesmanship and wisdom at national and international levels to balance the economic development with the amount of sustainable water resources and the assimilative capacity of rivers and aquifers to withstand any quality degradation.

A high priority for environmental improvement will be difficult to impose when the social costs of welfare and unemployment have caused huge financial deficits for governments of the developed world and have brought many developing and underdeveloped countries to the brink of financial disaster.

Groundwater plays an important role in the life of many especially in the developing countries. The quantity of water is the major concern. The economic development has imposed considerable pressure on the water resources especially on groundwater. People’s perception generally is that groundwater is an unlimited, reliable, and safe source of water to drink. The impact of climate change has affected the groundwater recharge and the frequency of droughts. That has changed the safe yield of aquifers and has caused considerable drawdown in many aquifers around the world.

In developed countries, groundwater quality issues are the governing factor and the major public concern. There have been many United Nations and other international agencies as well as nongovernmental organizations initiatives to promote public awareness on groundwater quality and quantity as well as health issues among infants and children exposed to groundwater contamination.

1.8 GROUNDWATER PROTECTION: CONCERNS AND ACTS

A groundwater and food security investigation by the international food and agriculture organization (FAO, 2003), confirms that it is not possible to assess the extent to which global food production could be at risk from over abstraction and exploitation of groundwater resources. Indeed, the search for reliable groundwater levels and abstraction data to determine depletion rates is very difficult to obtain with consistency, reliability, and adequate coverage.

The impacts of over exploitation and water level declines have been reported widely. Over abstraction of groundwater can lead to a wide range of social and economic problems and environmental predicaments including:

- Declines in base flows of the rivers and wetlands with significant damage to ecosystems and downstream users
- Increased pumping costs and energy consumption
- Land subsidence and damage to surface infrastructure
- Changes in patterns of groundwater flow exchange with the adjacent aquifer systems
- Less water for drinking, irrigation, and other uses, particularly for the low-income people
- Increases in agriculture vulnerability (food security) and vulnerability of other water user sectors to climate change and/or natural climatic fluctuations.

Warnings of a groundwater disaster (declining groundwater tables and/or polluted aquifers) have led to calls for urgent social, governmental, and management responses. There is a need to evaluate all of the indications including documented records and facts and figures that call for an occurrence of a disaster and to identify the types of management responses and adaptive measures that could actually work.

Hötzl (1996) discussed the need to distinguish between resource and source protection. Even though both concepts are related, it is not practical to utilize a source without protecting the resource. For example, in European countries, groundwater is considered a vital resource that must be protected. Activities endangering groundwater quality are forbidden by different members of the European Union including Germany through their regulation of Wasserhaushaltsgesetz (WHG 1996). The European Water Framework Directive (The European Parliament and the Council of the European Union, 2000) calls for treating and protecting water like no other commercial product.

In the United States, many communities use groundwater as the sole source of water supply despite a relatively high annual precipitation rate. For example, in Long Island, just outside of New York City, most of the water supply is provided by groundwater resources. There have been many social, state, and federal concerns about groundwater protection almost everywhere in the United States that have resulted in many regulatory acts as explained in the next section.

In many parts of arid and semiarid areas in Asia and Africa, groundwater is vital to the economic stability, social preservation, and development plan of different regions and nations. All of these concerns have brought many actions for the use,

protection, and development of groundwater resources. But, the increasing demand for water in all of these societies (developing or less developing countries) resulted in over exploitation of water resources as discussed earlier. There is a need for well-defined transparent laws and regulations that are enforceable, tailored to local and regional level of resources, treatments, and vulnerabilities of groundwater.

1.8.1 CLEAN WATER ACT

Increasing public awareness and concern for control of surface and groundwater pollution led to enactment of the Federal Water Pollution Control Act Amendments of 1972. It was amended in 1977, and this law became commonly known as the Clean Water Act (CWA), the basis for many other statutes and regulations that followed, especially related to groundwater that were not explicitly spelled out in CWA. The act established the basic structure for regulating discharges of pollutants into the surface waters and groundwater resources of the United States. It gave the United States Environmental Protection Agency (USEPA) the authority to implement pollution control programs such as setting wastewater standards for industrial use and discharge to groundwater.

The CWA set water quality standards directed toward all contaminants primarily in surface waters, but with applicability to groundwater. The CWA made it unlawful for any person to discharge any pollutant from a point source into navigable waters and other natural water resources including groundwater unless a permit is obtained under its provisions. It also funded the construction of wastewater treatment plants and recognized the critical problems posed by nonpoint source pollution.

The key elements of the CWA are establishment of water quality standards, their monitoring, and developing strategies for meeting water quality standards. Drinking water regulations set enforceable maximum contaminant levels for particular contaminants in drinking water or required ways to treat water to remove contaminants. Maximum contaminant levels are legally enforceable, which means that both USEPA and states can take enforcement actions against water supply systems not meeting the standards. USEPA and states may issue administrative orders, take legal actions, or fine water utilities. Additionally, the National Secondary Drinking Water Standards are recommended, but they are not enforceable. However, states may choose to adopt them as enforceable standards or may relax the National Secondary Drinking Water Standards.

1.8.2 GROUNDWATER PROTECTION

Protection of groundwater has limited enforceable regional and national acts and regulations. On a local (state or city) scale, the groundwater management acts could protect the right of local groundwater users as long as they are not in conflict with other local and national laws and regulations. The highest priority is to protect groundwater for drinking water supplies (USEPA, 2005). The water districts have been established to conserve and protect the groundwater resources, to maintain its economic value, and to prevent its deterioration. There are many opportunities for the water districts as a result of the authorities that are given to them.

In the United States, groundwater as a resource is addressed at the federal level as well as through the Safe Drinking Water Act. As a part of the USEPA's cleanup programs in 2002, the Ground Water Task Force was established to improve the quality of the USEPA cleanup program. This program deals with brownfields, federal facilities, leaking underground storage tanks, and the Resource Conservation and Recovery Act Corrective Action and Superfund. It also provides a discussion on the importance of groundwater resources and their vulnerability (GWT, 2007).

The USEPA defines a sole or principal source aquifer as one which supplies at least 50% of the drinking water consumed in the area overlying the aquifer. Such area cannot have an alternative drinking water source(s) which could physically, legally, and economically supply all those who depend upon the aquifer for drinking water.

The Sole Source Aquifer (SSA) program within the Safe Drinking Water Act is aimed at promoting the importance of these aquifers. Although USEPA has statutory authority to initiate SSA designations, it has a long-standing policy of only responding to petitions. Any individual, corporation, company, association, partnership, state, municipality, or federal agency may apply for SSA designation. A petitioner is responsible for providing USEPA with hydrogeologic and drinking water usage data, and other technical and administrative information required for assessing the designated criteria.

If an SSA designation is approved, proposed federally funded projects which have the potential to contaminate the aquifer are subject to USEPA review. Proposed projects that are funded entirely by state, local, or private concerns are not subject to USEPA review. Examples of federally funded projects that have been reviewed by USEPA under the SSA protection program include public water supply wells and transmission lines, wastewater treatment facilities, and construction projects that involve disposal of storm water (Kresic, 2009).

In the European Union, the European Groundwater Directive of 2006 extends the concept of overall resource protection including groundwater in detail (The European Parliament and the Council of the European Union, 2006).

1.8.3 USEPA GROUNDWATER RULE

The USEPA is promulgating a National Primary Drinking Water Regulation, the Groundwater Rule, to provide for increased protection against microbial pathogens in public water systems that use groundwater sources (USEPA, 2006). This regulation is in accordance with the Safe Drinking Water Act as amended. The Department of Water Resources requires disinfection as a treatment technique for all public water systems, including surface water systems and, as necessary, groundwater systems.

The groundwater rule establishes a risk-targeted approach to target groundwater systems that are susceptible to fecal contamination. The occurrence of fecal indicators in a drinking water supply is an indication of the potential presence of microbial pathogens that may pose a threat to public health. This rule requires groundwater systems that are at risk of fecal contamination to take corrective action to reduce cases of illnesses and deaths due to exposure to microbial pathogens.

In the 1999 Ground Water Report to Congress, the USEPA emphasized the need for more effective coordination of groundwater protection programs at the federal, state, and local levels. While the Clean Water Action Plan and states' watershed protection programs address groundwater, true coordination of groundwater management efforts has not been achieved in most states (USEPA, 1999). However, the agency also indicated that at the time, 47 states have approved wellhead protection programs, which mandate delineation of wellhead protection areas for public water supplies. The wellhead protection area is a designated surface and subsurface area surrounding a well or well field for a public water supply and through which contaminants or pollutants are likely to pass and eventually reach the aquifer that supplies the well or well field. The purpose of designating the area is to provide protection from the potential contamination of the water supply. These areas are designated in accordance with laws, regulations, and plans that protect public drinking water supplies.

1.8.4 CALIFORNIA'S SUSTAINABLE GROUNDWATER MANAGEMENT ACT

Approximately 40% of California's annual water supply relies on groundwater resources. This rate could increase to above 60% in dry years. Regardless of the water year type, some communities are always completely reliant on groundwater. Advancements in pumping technology has made it possible to extract groundwater from deeper levels, resulting in groundwater overdraft and, in consequence, land subsidence, creating a crisis of shared supply. These issues along with the idea that "groundwater management is best accomplished locally" led to the enactment of new regulations to control groundwater extraction and use in California (Water Education Foundation, 2015).

On September 16, 2014, California's Sustainable Groundwater Management Act (SGMA) was signed into law as a three-bill legislative package (California Department of Water Resources, 2018). SGMA supports the sustainable management of groundwater through the formation of locally organized groundwater sustainability agencies (GSAs) that pursue development and implementation of groundwater sustainability plans (GSPs) (California Department of Water Resources, 2016). A GSA consists of one or more local agencies that implement the provisions of SGMA, which requires local governments and water agencies of high and medium priority basins to stop groundwater overdraft and create a balance between pumping and recharge within groundwater basins. California Department of Water Resources prioritizes the basins and subbasins by applying datasets and information in a consistent, statewide fashion in accordance with the provisions in California Water Code Section 10933(b), outlined below:

- The population overlying the basin or subbasin as well as the rate of current and projected growth of that population
- The number of public supply wells extracting from the basin or subbasin
- The total number of wells extracting from the basin or subbasin
- The irrigated area overlying the basin or subbasin
- The degree to which people within the basin or subbasin rely on groundwater as their primary source of water

- Documented impacts on the groundwater within the basin or subbasin, such as overdraft, subsidence, saline intrusion, and other water quality degradation
- Adverse impacts on local habitat and local streamflows
- Other information determined to be relevant by the department.

According to the act, sustainable groundwater management is defined as the “management and use of groundwater in a manner that can be maintained during the planning and implementation horizon without causing undesirable results.” SGMA identifies six undesirable results:

- Chronic lowering groundwater levels, excluding a decline in groundwater levels during a drought
- Significant and unreasonable reduction of groundwater storage volumes
- Significant and unreasonable seawater intrusion
- Significant and unreasonable water quality degradation
- Significant and unreasonable land subsidence
- Depletion of surface waters resulting in significant and unreasonable adverse impacts on beneficial uses.

Under SGMA, the high and medium priority basins should form GSA(s) to manage basins sustainably and collaborate to develop and finalize their GSP by 2022, which clearly overlays an implementation plan to reach sustainability within 20 years. The deadline to reach sustainability will be 2040 for critically overdrafted basins that have to finalize their GSP by 2020, and 2042 for the remaining high and medium priority basins (California Department of Water Resources, 2018). A GSP must include measurable objectives and milestones in increments of five years (Water Code § 10727.2(b)(1)).

During this process, the Department of Water Resources provides ongoing support to GSAs through financial and technical assistance to implement the act and develop best management practices, which are designed to achieve sustainable groundwater management and have been determined to be technologically and economically effective, practicable, and based on the best available science.

1.9 OVERALL ORGANIZATION OF THIS BOOK

In the following chapters, an attempt has been made to develop a system view of groundwater fundamentals and model-making techniques through the application of science, engineering, planning, and management principles. In [Chapters 2 through 4](#), the classical issues in groundwater hydrology and hydraulics are discussed followed by quality aspects in [Chapter 5](#). In these chapters, the process of analyzing data, identification, and parameter estimation are presented. In [Chapters 6 through 8](#), tools and model-building techniques and conjunctive use of surface and groundwater are described, followed by aquifer restoration, remediation, and monitoring techniques, as well as analysis of risk in [Chapter 9](#). [Chapter 10](#) is an introduction to groundwater risk and disaster management. Finally, in [Chapter 11](#), the impact of climate change on

groundwater, the needed tools and methods for analysis of future data realization, and downscaling of large-scale low-resolution data to local watershed and aquifer scale for impact studies are discussed.

PROBLEMS

- 1.1 Make an assessment of groundwater resources around the world and compare them with the United States share of total groundwater.
Hint: use UNESCO, Cambridge/Oxford L.C. World Resources, World Bank, European Union Switch program, FAO, USGS, sites, and publications.
- 1.2 In Problem 1.1, assess groundwater quality figures around the world.
- 1.3 Identify the federal and national agencies involved in management and protection of groundwater, at least one in each part of the globe.
- 1.4 Compare the driving forces dealing with groundwater science and engineering with those affecting groundwater planning and management.
- 1.5 Identify and compare the “response” issues in Problem 1.4, concentrating on improvement of standards and quality of life as well as economic, environmental, and legal issues.
- 1.6 Explain IWRM for aquifers in the context of public awareness/participation and consideration of social impacts.
- 1.7 What is the estimated water cost for residential customers in east (New York City) and west (city of Los angles of the United States)? Compare it with the price of water in five other major cities around the world. Is the price of groundwater in selected areas different from surface water resources?
- 1.8 Briefly discuss a case of transboundary conflict over shared aquifer.
Hint: Example of Kura aquifer in the Caucasus region (Puri, 2001) can be used.
- 1.9 Briefly explain available approaches (or tools) used to resolve conflicts over shared aquifers.
- 1.10 Identify and briefly explain factors affecting groundwater sustainability.
- 1.11 In demand side management, explain the two periods of demand I and demand II in **Figure 1.9**.
- 1.12 Identify three local (city or county) agencies in the United States or in other countries with the charter of protecting and enforcement issues related to quality and quantity (discharge) of groundwater.

REFERENCES

- Ashton, P.J. and Haasbroek, B. 2001. Water demand management and social adaptive capacity: A South African case study, in *Hydropolitics in the Developing World: A Southern African Perspective*, A.R. Turton and R. Henwood, eds., African Water Issues Research Unit (AWIRU) and International Water Management Institute (IWMI), Pretoria, South Africa, 21 p.
- California Department of Water Resources. 2016. *Bulletin 118 Interim Update 2016: California's Groundwater Working Toward Sustainability*. https://water.ca.gov/-/media/DWR-Website/Web-Pages/Programs/Groundwater-Management/Bulletin-118/Files/Statewide-Reports/Bulletin_118_Interim_Update_2016.pdf.

- California Department of Water Resources. 2018. "SGMA Groundwater Management." <https://water.ca.gov/Programs/Groundwater-Management/SGMA-Groundwater-Management> (December 12, 2018).
- Doll, P. 2002. Impact of climate change and variability on irrigation requirements: A global perspective. *Climatic Change*, 54, 269–293.
- Eckholm, E. 1982. *Down to Earth: Environment and Human Needs*. Pluto Press, London, UK, 173 p.
- Falkenmark, M. 2003. *Water Management and Ecosystems: Living with Change*, Global Water Partnership Technical Committee. Global Water Partnership, Stockholm, Sweden, 50 p.
- FAO (Food and Agriculture Organization of the United Nations). 2003. *Review of World Water Resources by Country*, Water Reports 23, FAO, Rome, 110 p. www.fao.org/ag/aglw/docs/wr23e.pdf.
- FAO-AQUASTAT, 2007. *AQUASTAT Main Country Database*. www.fao.org/ag/aglw/aquastat/main.
- Goldman, M.I. 1967. *Controlling Pollution, the Economics of a Cleaner America*. Prentice Hall, Englewood Cliffs, NJ.
- GWTF (Groundwater Task Force). 2007. Recommendations from the EPA Groundwater Task Force; Attachment B: Groundwater use, value, and vulnerability as factors in setting cleanup goals. EPA 500-R-07-001, Office of Solid Waste and Emergency Response, pp. B1–B14.
- Hötzl, H. 1996. Grundwasserschutz in Karstgebieten. *Grundwater*, 1(1), 5–11.
- ICWE. 1992. *Dublin Statement and Report of the Conference*, January 26–31, 1992, Dublin, Ireland.
- International Groundwater Resources Assessment Centre. (2015). Transboundary aquifers of the World Map 2015. Retrieved from http://www.un-igrac.org/sites/default/files/resources/files/TBAmapping_2015.pdf.
- IPCC (Intergovernmental Panel on Climate Change). 2007. Summary for policymakers of the Synthesis Report of the IPCC Fourth Assessment Report; 23 p. Available at: <http://www.ipcc.ch/>.
- Karamouz, M., Moridi, M., Nazif, N. 2010. *Urban Water Engineering and Management*. CRC Press, Boca Raton, FL, 602 p.
- Kisiel, C.C. and Duckstein, L. 1970. Operation research study of water resources—Part II: Case study of the Tucson Basin (Arizona). *Water Resources Bulletin*, 6(6), 857–867.
- Kresic, N. 2009. *Groundwater Resources: Sustainability, Management, and Restoration*. McGraw-Hill, New York, 852 p.
- McNeill, D. 1998. Water as an economic good. *Natural Resources Forum*, 22(4), 253–261.
- Puri, S. 2001. Internationally shared (transboundary) aquifer resources, management, their significance and sustainable management. A framework document International Hydrological program, IHP-VI, IHP Non Serial Publications in Hydrology, UNESCO, Paris, 71 p.
- Rogers, P. and Hall, A.W. 2003. Effective water governance. TEC Background Papers No. 7, Global Water Partnership Technical Committee (TEC), Global Water Partnership, Stockholm, Sweden, 44 p.
- Secker, D. 1993. *Designing Water Resources Strategies for the Twenty-First Century*. Discussion Paper 16, Water Resources and Irrigation Division, Winrock International, Arlington, VA.
- The European Parliament and the Council of the European Union. 2000. Directive 2000/6/EC of the European Parliament and the Council of October 23, 2000, establishing a framework for Community action in the field of water policy, *Official Journal of the European Union*, December 22, 2000, L 327/1.
- The European Parliament and the Council of the European Union. 2006. Directive 2006/118/EC of the protection of groundwater against pollution and deterioration, *Official Journal of the European Union*, December 27, 2006, L 372/19-31

- UN (United Nations). 1999. *World Population Prospect*, 1998 Revision. UN Department of Policy Coordination and Sustainable Development, New York.
- UNESCO (United Nations Educational Scientific and Cultural Organization). 2006. *Water, a Shared Responsibility*. The United Nations World Water Development Report 2.
- UNESCO. World Water Assessment Program (WAPP), Paris, and Berghahn Books, New York, 584 p.
- UNESCO. 2002. Manual of the General Conference, including texts and amendments adopted by the General Conference at Its 31st Session, Paris.
- USEPA. 1999. *Compendium of ERT Groundwater Sampling Procedures*. EPA 540/P-91/007. Environmental Protection Agency, Washington, DC.
- USEPA. 2005. *Guidance for Developing Ecological Soil Screening Levels (Eco-SSL): Exposure Factors and Bioaccumulation Models for Derivation of Wildlife Eco-SSL*. Environmental Protection Agency, Washington, DC.
- USEPA. 2006. *Final Groundwater Rule, Fact Sheet*. EPA 815-F-06-003. United States Environmental Agency, Office of Water, Washington, DC, 2 p.
- Van der Zaag P.V. and Savenije, H.H.G. 2006. Water as an economic good: The value of pricing and the failure of the markets. *Value of Water Research Report Series* No. 19. UNESCO-IHE Institute for Water Education, Delft, the Netherlands, 28 p.
- Water Education Foundation. 2015. *The 2014 Sustainable Groundwater Management Act: A Handbook to Understanding and Implementing the Law*. Sacramento, CA. <http://groundwater.ucdavis.edu/files/208021.pdf>.
- WHG. 1996. *Gesetz zur Ordnung des Wasserhaushalts*, BGBI, Bonn, Germany.
- Willis, R. and Yeh, W.W.-G. 1987. *Groundwater Systems Planning and Management*. Prentice Hall, Englewood Cliffs, NJ.
- WMO (World Meteorological Organization). 1997. *Comprehensive Assessment of the Freshwater Resources of the World*. WMO, Geneva, Switzerland, p. 9.
- WRI (World Resources Institute). 1998. *World Resources, 1998–1999: A Guide to the Global Environment*. Oxford University Press, New York, 384 p.



Taylor & Francis

Taylor & Francis Group

<http://taylorandfrancis.com>

2 Groundwater Properties

2.1 INTRODUCTION

Water in nature is in solid, liquid, and vapor form. It exists in different places like atmosphere (atmospheric water), surface of the ground (surface water), and subsurface of the ground (groundwater and unsaturated zone water). The source of surface and subsurface water is snow and rain precipitation. A portion of the precipitation flows on the land (surface runoff), a portion of that goes back to the atmosphere because of evapotranspiration from surface water and the surface of plants, and the remaining portion infiltrates into the land (subsurface flow). The movement process of water in nature is called the *hydrologic cycle*. A schematic of the hydrologic cycle is shown in [Figure 2.1](#).

Groundwater constitutes only about 0.62% of the entire amount of water on the globe ([Table 2.1](#)). Although it is a small portion of the world's total water resources, it is considered as an important resource to supply water demands due to the population increase and, in consequence, increasing needs for water supply.

In this chapter, the fundamental aspects of subsurface water are explained. It should be noted that all of the subsurface water is not considered as groundwater. Groundwater is a part of the subsurface water that totally saturates the soil pores and flows with a pressure more than atmospheric pressure. The difference between pressure in groundwater and atmospheric pressure is called *gage pressure*. At the groundwater table, the gage pressure is zero. Depending on the location, the depth of the groundwater varies. The zone between the land surface and the surface of groundwater is called *unsaturated* or *vadose zone*. The water is under the influence of capillary and adhesion forces (surface tension) between soil and water molecules. [Figure 2.2](#) shows the classifications of the subsurface water which are explained with some details in this chapter. As it is shown, the hydraulic head at point A in the saturated zone is equal to the pressure head ψ and elevation head z .

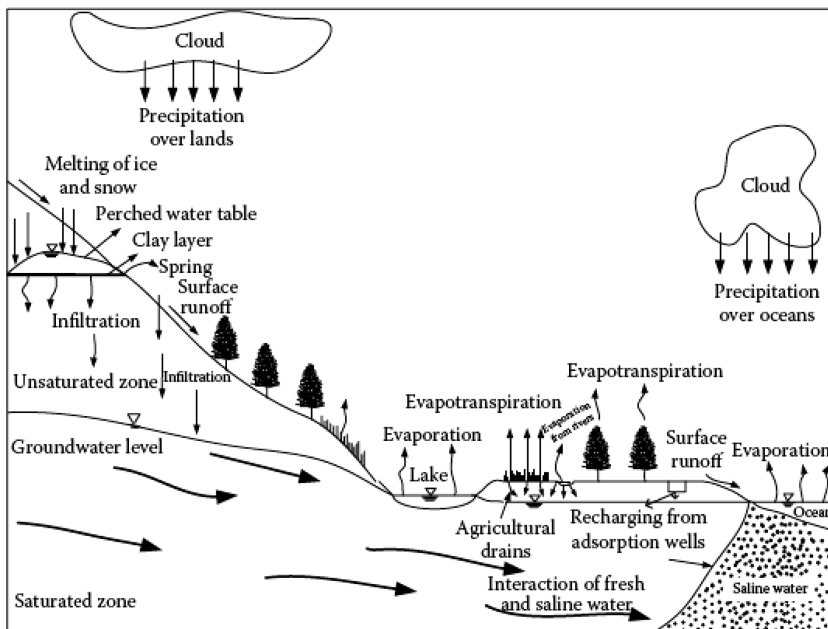


FIGURE 2.1 Schematic representation of the hydrologic cycle.

TABLE 2.1
Water Resources in the World

| Water Resources | Volume (1000 km ³) | Percentage |
|---|--------------------------------|------------|
| Atmospheric water | 13 | 0.001 |
| Surface water | | |
| Oceans saline water | 1,320,000 | 97.2 |
| Seas saline water | 104 | 0.008 |
| Lakes fresh water | 125 | 0.009 |
| Rivers fresh water | 1.25 | 0.0001 |
| Biosphere fresh water | 29,000 | 2.15 |
| Glacial water | 50 | 0.004 |
| Groundwater | | |
| Water in vadose zone | 67 | 0.005 |
| Groundwater in the depth less than 0.8 km | 4,200 | 0.31 |
| Groundwater in the depth more than 0.8 km | 4,200 | 0.31 |
| Total | 1,360,000 | 100 |

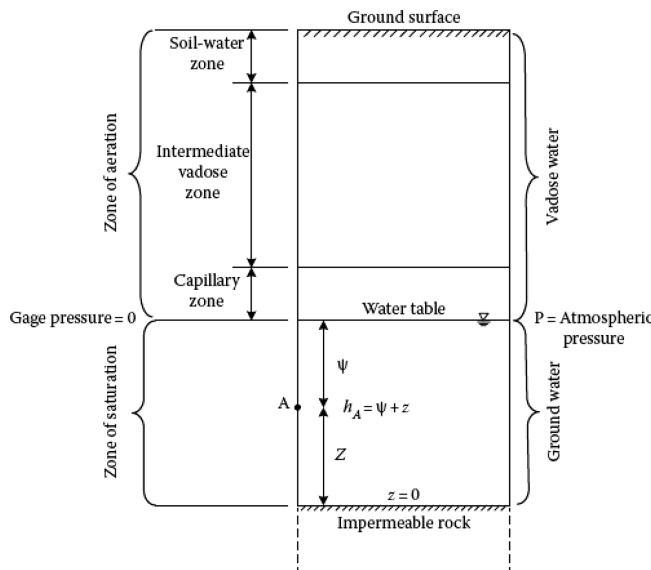


FIGURE 2.2 Classification of subsurface waters in a hypothetical section.

2.2 VERTICAL DISTRIBUTION OF SUBSURFACE WATER

Subsurface water flows below the ground surface. The water behavior in these areas and the characteristics of these zones are as follows:

1. *Soil-water zone*: The main characteristics of this zone are
 - a. Water content is usually less than saturation.
 - b. It might be saturated during rainfall or irrigation.
 - c. Thickness depends upon the type of soil and vegetation.
 - d. It consists of hydroscopic water, which sticks to soil and is unavailable to plants; capillary water, which is held by surface tension and is available to plants; and gravitational water (excess and drain through soil).
 - e. Field capacity is the water held after gravity water drains away. In other words, field capacity is the water content of the soil when a thoroughly wetted soil has drained for approximately 2 days.
 - f. Water in the root zone (after gravity water drains) varies between field capacity and “wilting point.” Wilting point is the near dry condition, which, if prolonged, causes plants to wilt beyond recovery. It is also defined as the water content of soil when plants, growing in the soil, wilt and do not recover.
 - g. The amount of water held in the soil between field capacity and wilting point is considered to be the water available for plant extraction.
2. *Intermediate zone*: Water must move through this zone to reach groundwater. In this zone, excess water moves downward due to gravity force.

But part of the intermediate zone has pellicular water, which is nonmoving water and consists of hydroscopic and capillary water.

3. **Capillary zone:** The capillary zone (or capillary fringe) extends from the water table up to the limit of the capillary rise of water. The water table is defined as the depth at which the water pressure equals atmospheric pressure. If a pore space could be idealized to represent a capillary tube, the capillary rise h_{cap} (Figure 2.3) can be derived from an equilibrium between the surface tension of water and the weight of water raised:

$$h_{cap} = \frac{2\tau}{r\gamma} \cos\lambda \quad (2.1)$$

where:

τ is the surface tension (N/m)

γ is the specific weight of water (N/m³)

r is the tube radius (m)

λ is the angle of contact between the meniscus and the wall of the tube.

For pure water in a clean glass, $\lambda = 0$, and $\tau = 0.074 \text{ kg/s}^2$ at 20°C, so that the capillary rise approximates:

$$h_{cap} = \frac{0.15}{r} \quad (2.2)$$

h_{cap} is less than 2.5 cm for gravel, about 200 cm for silt, and several meters for clay.

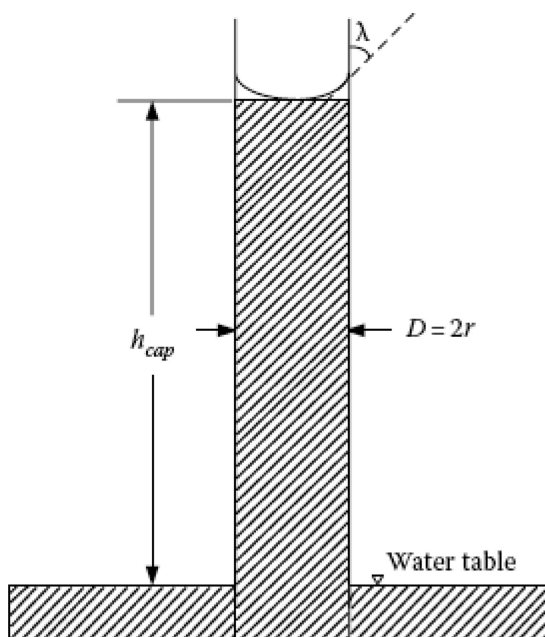


FIGURE 2.3 A schematic of capillary rise.

4. *Saturated zone*: It is the source of the water supply. In the zone of saturation, groundwater fills all of the pores; therefore, the (effective) porosity shows a direct measure of the water contained per unit volume. Available water depends upon various factors such as porosity, specific yield, and specific retention.

All of these layers are shown in [Figure 2.2](#).

2.3 AQUIFERS, AQUITARDS, AND AQUIINCLUDES

Dingman (1994) defined an *aquifer* as “a geologic unit that can store enough water and transmit it at a rate fast enough to be hydrologically significant.” If significant quantities of water cannot be transmitted under ordinary hydraulic gradients in a saturated geologic formation, this formation is called an *aquiclude*. In general, it can be claimed that an aquifer is permeable enough to be economically exploited, while it is not economic to withdraw water from aquiclude.

Less-permeable geologic formations are termed as *aquitards*. Significant quantities of water might be transmitted through these media; however, their permeability is not sufficient to exploit water through wells within them. Very few geological formations have the characteristics of an aquiclude, and most of the geologic strata are considered as either aquifers or aquitards.

Unconsolidated sand and gravel, permeable sedimentary rocks such as sandstone and limestone, and heavily fractured volcanic and crystalline rocks are most common aquifers. The most common aquitards are clay, shale, and dense crystalline rocks (Todd, 1980).

However, it is hard to specify whether a formation with given constituents is aquifer or aquitard. In other words, there is vagueness in the definition of aquifers and aquitards. For instance, in an interlayered sand-silt formation, the silt layer may be considered an aquitard; while if the formation is a silt-clay system, the silt may be considered aquifer. In general, aquifer has different meanings to different people, and it might even have various meanings to the same person at different times.

2.4 TYPES OF AQUIFERS

Most aquifers are underground storage reservoirs made up of water-bearing permeable rock or unconsolidated materials. Water penetrates downward through the pores by gravitational forces until it reaches the saturated area. The water level, which is termed water table, is not always at the same depth below the land surface. Depending on the presence or absence of a water table, aquifers are classified as unconfined or confined, while a leaky aquifer is considered as a semiconfined aquifer, which has the characteristics of both types of the aquifers.

2.4.1 UNCONFINED AQUIFER

In an unconfined aquifer, the top of the aquifer is defined by the water table which varies in fluctuation form and in slope. The water table fluctuation depends on changes in volume of water storage resulting from recharge and discharge, pumping from wells,

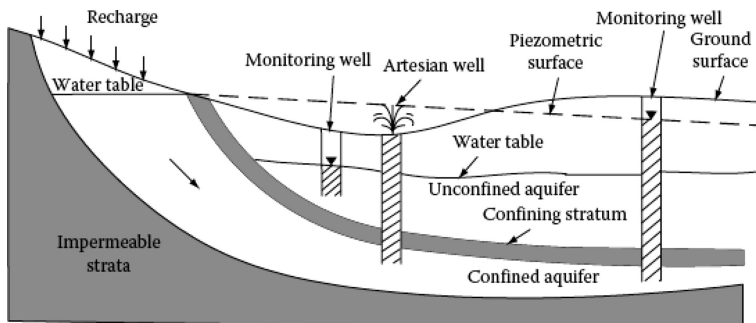


FIGURE 2.4 Schematic cross section illustrating unconfined and confined aquifers.

and permeability. In Figure 2.4, the upper aquifer represents an unconfined aquifer. Using the water elevations in wells, the contour maps and profiles of the water table are prepared. Typically, the shallowest aquifer at a given location does not have a confining layer between it and the surface, and it is considered as an unconfined aquifer.

The perched water body is the groundwater accumulating above an impermeable stratum such as a clay layer. This term is a special case of an unconfined aquifer, which refers to a small local area with an elevation higher than a regionally extensive aquifer. Clay lenses in sedimentary deposits often have shallow perched water bodies overlying them.

2.4.2 CONFINED AQUIFERS

Confined aquifers are restricted on the top by impermeable materials. Water in a confined aquifer is normally under pressure greater than atmospheric pressure. This pressure in a well can cause the water level to rise above the ground surface, which is designated a flowing artesian well as shown in Figure 2.4. An area where water flows into the earth to resupply a water body or an aquifer is known as a recharge area. Water fluctuations in wells discharging water from confined aquifers lead to variations in pressure rather than in storage volumes. Therefore, small changes in storage volume will occur in confined aquifers that carry water from recharge areas to locations of natural or artificial discharge.

Figure 2.4 shows the potentiometric surfaces, which are known as isopotential levels and piezometric surfaces. This surface represents the static head of groundwater and is defined by the level to which water will rise. In general, the piezometric surface at a point in a well, penetrating a confined aquifer, is shown by the water level at that point in the well. If the potential level of piezometric surface is higher than the land surface, it results in overflow of the well. When the piezometric surface is lower than the bottom of the upper confining bed, a confined aquifer becomes an unconfined aquifer.

2.4.3 AQUITARD (LEAKY) AQUIFER

Aquitards are zones within the earth that limit the groundwater flow from one aquifer to another. They are beds of low permeability along an aquifer. In general,

the existence of leaky or *semiconfined* aquifers is more expected than confined or unconfined aquifers. This is because it is hard to find an aquifer that is completely confined or unconfined. Such characteristics are common in alluvial valleys, plains, or former lake basins.

2.5 GROUNDWATER BALANCE

For a particular area, the groundwater balance study is accomplished for the following purposes:

- To check if all flow components in the system are quantitatively accounted for and what components have the greatest bearing
- To calculate one unknown component of the groundwater balance equation, if the values of all other components are known with an acceptable accuracy
- To model the hydrological processes in the study area.

To be able to estimate groundwater balance of a region, all individual inflows to or outflows from a groundwater system as well as changes in groundwater storage over a given time period must be quantified. The general form of water balance over a period of time is

$$\text{Input to the system} - \text{outflow from the system} = \text{Change in storage of the system} \quad (2.3)$$

To compute the groundwater balance of a system, the significant components are identified first. After that, the quantifying individual components are evaluated. Now, these quantified components can be presented in the form of a water balance equation.

Considering the various inflow and outflow components in a given study area, the groundwater balance equation can be written as:

$$\Delta S = R_r + R_s + R_i + R_t + S_i + I_g - E_t - T_p - B_f - O_g \quad (2.4)$$

where:

ΔS is the change in groundwater storage

R_r is the recharge from rainfall

R_s is the recharge from canal seepage

R_i is the recharge from field irrigation

R_t is the recharge from tanks

S_i is the influent seepage from rivers

I_g is the inflow from other basins

E_t is the evapotranspiration from groundwater

T_p is the draft from groundwater

B_f is the baseflow, the part of the groundwater inflows to rivers

O_g is the outflow to other basins.

The following data are required to accomplish a groundwater balance study in an area over a given time period:

- Rainfall data
- Land use data and cropping patterns
- River stage and discharge data
- River cross sections
- Canals discharge and distributaries data, and the possible seepage from canals
- Tanks depth, capacity, area, and seepage data
- Water table data
- Groundwater draft (the number of each type of well operating in the area, their corresponding running hours each month, and their discharge)
- Aquifer parameters

Example 2.1

Assume that there is 900 mm/year rainfall in an area. The irrigation rate and evapotranspiration are 180 and 420 mm/year, respectively. Also, 330 mm/year of the rainfall flows over land. The rate of outflow to the other basins is 200 mm/year and 150 mm/year flows to rivers.

Calculate the influent from the rainfall seepage.

Assuming groundwater inflow and outflow remain unchanged, calculate the baseflow in the region if 80 mm/year water is pumped from the region.

SOLUTION

- a. When it rains, a portion of the precipitation, P , is evaporated, E_r , a portion flows over the land surface, O_r , and the rest of that recharges the groundwater, R_r . Therefore,

$$P + R_r = E_r + O_r + R_r \Rightarrow 900 + 180 = 420 + 330 + R_r$$

$$R_r = 330 \text{ mm/year}$$

$$I_g + R_r = O_g + R_f \Rightarrow I_g = 200 + 150 - 330 = 20 \text{ mm/year}$$

- b. In this case, the inflow to groundwater and recharge from rainfall are the *inflows* and baseflow and the discharge from pumping are the *outflows* from the system:

$$I_g + R_r = O_g + B_f + Q_p \Rightarrow 20 + 330 = 200 + B_f + 80$$

$$\Rightarrow B_f = 70 \text{ mm/year}$$

2.5.1 WATER BALANCE IN CONFINED AQUIFERS

In the water balance for the confined aquifer, the recharge and evaporation can be neglected in a short period (i.e., a day). Therefore, the daily water balance can be written as:

$$W_{sc,i} = W_{sc,i-1} + W_{per} - W_{pc} \quad (2.4a)$$

where:

- $W_{sc,i}$ is the amount of water stored in the confined aquifer on day i (mm)
- $W_{sc,i-1}$ is the amount of water stored in the confined aquifer on day $i-1$ (mm)
- W_{per} is the amount of water percolating from the unconfined aquifer into the confined aquifer on day i (mm)
- W_{pu} is the amount of water removed from the confined aquifer by pumping on day i (mm).

2.5.2 WATER BALANCE IN UNCONFINED AQUIFERS

Due to short-term input of recharge in unconfined aquifer and the interaction between surface and groundwater flow (base flow), the water balance for unconfined aquifers can be written as:

$$W_{su,i} = W_{su,i-1} + R_r - B_f - W_{sd} - W_{per} - W_{pu} \quad (2.4b)$$

where:

- $W_{su,i}$ is the amount of water stored in the unconfined aquifer on day i (mm)
- $W_{su,i-1}$ is the amount of water stored in the unconfined aquifer on day $i-1$ (mm)
- R_r is the amount of recharge entering the aquifer on day i (mm)
- B_f is the base flow to the main channel on day i (mm)
- W_{sd} is the amount of water moving into the soil zone in response to water deficiencies on day i (mm)
- W_{per} is the amount of water percolating from the unconfined aquifer into the confined aquifer on day i (mm)
- W_{pu} is the amount of water removed from the unconfined aquifer by pumping on day i (mm).

2.5.3 WATER BALANCE IN UNSATURATED ZONE

The incoming terms of the unsaturated zone are infiltration, capillary rise from the saturated zone, and lateral inflow. The outgoing terms consist of evapotranspiration, baseflow, and percolation to the saturated zone. The water balance setup for a selected time interval is:

$$\Delta S_{unsat} = W_{inf} + W_{cap} + I_g - W_{per} - E_t - B_f \quad (2.4c)$$

where:

- ΔS_{unsat} is the storage change in unsaturated zone for the reflected time interval (mm)
- W_{inf} is the amount of recharge entering the zone by infiltration (mm)
- W_{cap} is the amount of recharge entering the zone by capillary rise (mm)

The other terms were described before.

2.6 COMPRESSIBILITY AND EFFECTIVE STRESS

The change in volume or strain, induced in a material under an applied stress, can be described by compressibility. It is the inverse of the modulus of elasticity, which is the ratio of the change in stress, $d\sigma$, to the resulting change in strain, $d\epsilon$. Therefore, compressibility can be defined as $d\epsilon/d\sigma$. In aquifer systems, compressibility is considered for both the water and the porous media, which are explained in the following.

2.6.1 COMPRESSIBILITY OF WATER

If water is subjected to an increase in pressure, dp , a decrease in the volume of water, V_w , occurs. The compressibility of water, β , can then be expressed as:

$$\beta = \frac{-dV_w / V_w}{dp} \quad (2.5)$$

The negative sign guarantees obtaining a positive number for the compressibility of water. This equation expresses a linear elastic relationship between the volumetric strain, dV_w/V_w , and the stress caused by the change in fluid pressure. In groundwater hydrology, the ratio shown in Equation 2.5 does not change over the range of fluid pressures. On the other hand, the impact of temperature on β is so small that it can be ignored. Hence, β is considered as a constant in groundwater hydrology. Equation 2.5 can also be rewritten as:

$$\beta = \frac{d\rho / \rho}{dp} \quad (2.6)$$

where ρ is the water density. The equation of state for water can then be obtained by integrating Equation 2.6, which gives:

$$\rho = \rho_0 \exp[\beta(p - p_0)] \quad (2.7)$$

where:

ρ_0 is the water density at the datum pressure, p_0 . If p_0 is considered equal to the atmospheric pressure, Equation 2.7 can be written as:

$$\rho = \rho_0 e^{\beta p} \quad (2.8)$$

For a given fluid, if $\beta = 0$ and $\rho = \rho_0 = \text{constant}$, the fluid is considered incompressible.

2.6.2 EFFECTIVE STRESS

If a unit mass of saturated sand is subjected to a stress, three mechanisms may cause a reduction in the volume of this saturated sand. These mechanisms are:

1. Compression of the water in the pores
2. Compression of the sand grains
3. Rearrangement of the sand grains and formation of a more closely packed configuration.

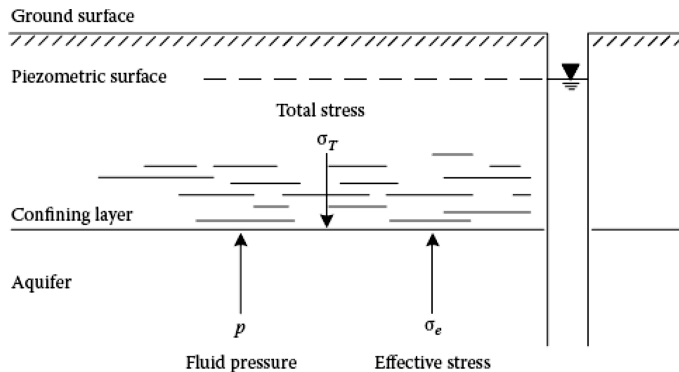


FIGURE 2.5 Total stress, effective stress, and fluid pressure on an arbitrary plane through a saturated porous medium.

The water compressibility controls the first mechanism and the second mechanism is almost negligible. Therefore, the third mechanism needs to be defined to obtain a compressibility term that reflects it. In this regard, the principle of effective stress, proposed by Terzaghi (1925), is required to be delineated first.

In Figure 2.5, consider the stress equilibrium on the confining layer. σ_T is the total stress, due to the weight of overlying rock and water, being imposed downward to the confining layer. This stress is held up by the soil grains and water pressure in the porous medium. Effective stress, σ_e , refers to that portion of the total stress that is held by the granular skeleton, i.e., the grains of the porous medium. The relation between the total and effective stresses is:

$$\sigma_T = \sigma_e + p \quad (2.9)$$

or

$$d\sigma_T = d\sigma_e + dp \quad (2.10)$$

According to the fact that the weight of rock and water overlying each point in an aquifer system often remains constant through time, there is usually no change in total stress, $d\sigma_T = 0$. Therefore,

$$d\sigma_e = -dp \quad (2.11)$$

Equation 2.11 implies that an increase in the water pressure causes an equal amount of decrease in the effective stress and vice versa. Therefore, if the total stress remains constant, the effective stress and, in consequence, the resulting volumetric deformations are controlled by the water pressure. If z is the elevation head and h is the hydraulic head, $p = \rho g \psi$ and the pressure head, ψ , is $\psi = h - z$. Hence, the hydraulic head controls the changes in the effective stress at a point of interest:

$$d\sigma_e = -\rho g d\psi = -\rho g d\hbar \quad (2.12)$$

Example 2.2

Determine the total stress acting on the top of the aquifer underlying a clayey aquitard, which is 30 m thick, and calculate the effective stress in the aquifer. Assume the bulk density of the aquitard is 2500 kg/m³ and there is an average of 40 m pressure head in it. If pumping causes a reduction of 1.5 m in the hydraulic head in the aquifer, what will be the resulting changes in the water pressure and effective stress. Consider the density of water equal to 1000 kg/m³.

SOLUTION

$$\sigma_T = \rho_b g b = 2,500 \times 9.806 \times 30 = 735,450 \text{ N/m}^2$$

$$\sigma_e = \sigma_T - p \quad \text{and} \quad p = \rho_w g h.$$

Therefore,

$$\sigma_e = 735,450 - (1,000 \times 9.806 \times 40) = 343,210 \text{ N/m}^2$$

The corresponding change in water pressure and effective stress due to the reduction of the hydraulic head in the aquifer by 1.5 m will be

$$\Delta p = \rho_w g \Delta h = 1,000 \times 9.806 \times (-1.5) = -14,709 \text{ N/m}^2$$

$$\Delta \sigma_T = \Delta \sigma_e + \Delta p \Rightarrow 0 = \Delta \sigma_e + (-14,709) \Rightarrow \Delta \sigma_e = 14,709 \text{ N/m}^2$$

2.6.3 COMPRESSIBILITY OF A POROUS MEDIUM

The compressibility of a porous medium can be expressed as:

$$\alpha = \frac{-dV_T / V_T}{d\sigma_e} \quad (2.13)$$

where:

V_T is the total volume of a soil mass ($V_T = V_s + V_v$)

V_s is the volume of the solids

V_v is the volume of voids.

An increase in effective stress, $d\sigma_e$, causes a reduction in the total volume of the soil mass. In general, $dV_T = dV_s + dV_v$; however, the change in the volume of the grains is usually negligible, i.e., $dV_s = 0$, and therefore, $dV_T = dV_v$.

For determination of soil compressibility, consider a sample of saturated soil as depicted in [Figure 2.6a](#). Imagine a total stress $\sigma_T = \text{Load}/A$ is applied to the sample through the pistons; while the sample is laterally confined by the cell walls. Water can escape through vents in the pistons to an external pool, which has a constant given pressure. While *Load* is increased step by step, the reduction of the volume of the soil sample is measured. In the initial steps, the increased total stress, $d\sigma_T$, is

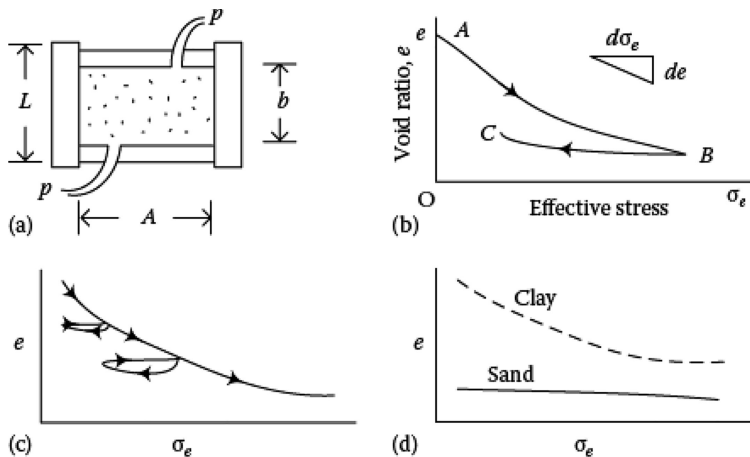


FIGURE 2.6 (a) Laboratory loading cell for the determination of soil compressibility. (b) Change of effective stress relative to void ratio. (c) Impact of repeated loading and unloading on effective stress. (d) Schematic curves of void ratio versus effective stress for clay and sand. (From Freeze, R. and Cherry, J., *Groundwater*, Prentice-Hall, Englewood Cliffs, NJ, 1979.)

held by the water under increased pressures. However, since water is drained from the sample, the stress will be transferred from the water to the soil grains. This transient process is termed consolidation. As consolidation is achieved, $dp = 0$ within the sample. In this condition, according to Equation 2.10, $d\sigma_e = d\sigma_T = d\text{Load}/A$. Assuming that $dV_T = dV_v$, if the soil sample has an initial void ratio e_0 ($e = V_v/V_s$) and height b , Equation 2.13 can be rewritten as:

$$\alpha = \frac{-db/b}{d\sigma_e} = \frac{-de/(1+e_0)}{d\sigma_e} \quad (2.14)$$

To determine the compressibility, α , a strain–stress plot is created in the form of e versus σ_e and the slope of this plot specifies α . In Figure 2.6b, the curve AB represents loading (increasing σ_e) and the curve BC corresponds to unloading (decreasing σ_e). The strain–stress relation is not linear or elastic. As shown in Figure 2.6c, for repeated loadings and unloadings, many fine-grained soils have hysteretic properties. Unlike the fluid compressibility, β , the soil compressibility, α , is not a constant and is a function of the applied stress. Moreover, the previous loading history influences the soil compressibility as well.

A schematic comparison of the strain–stress curves for clay and sand has been expressed in Figure 2.6d. Since sand has a smaller α , the corresponding curve has a lesser slope. Furthermore, its linearity means that its value remains constant over a wide range of σ_e . Table 2.2 presents compressibility values for various types of geologic materials (Domenico and Mifflin, 1965; Johnson et al., 1968). In this table, values are expressed in SI units of m^2/N or Pa^{-1} . As presented in this table, there is the same order of magnitude for the compressibility of water and the compressibility of the less-compressible geologic materials.

TABLE 2.2
Values of Compressibility for Different Soil Types

| Soil Type | Compressibility, a (m^2/N or Pa^{-1}) |
|--------------|--|
| Clay | $10^{-6}\text{--}10^{-8}$ |
| Sand | $10^{-7}\text{--}10^{-9}$ |
| Gravel | $10^{-8}\text{--}10^{-10}$ |
| Jointed rock | $10^{-8}\text{--}10^{-10}$ |
| Sound rock | $10^{-9}\text{--}10^{-11}$ |

It can be concluded that the compressibility of some soils in expansion is much less than in compression (Figure 2.6b and c). The ratio of the soil compressibility in loading and unloading conditions for clays is usually in the order of 10:1; while it approaches 1:1 for uniform sands. If the compressibility value is significantly less in expansion than compression for a soil, volumetric deformations corresponding to increasing effective stress will be irreversible. In other words, this soil will not be recovered when effective stresses consequently decrease. For example, if large compactions occur in a clay aquitard, it will not be recovered; but the small deformations in the sand aquifers are considerably recoverable.

2.6.4 EFFECTIVE STRESS IN THE UNSATURATED ZONE

From the Equation 2.12, it can be inferred that there is a linear relationship between the effective stress, σ_e , and the pressure head, ψ . However, this relation can be applied only in the saturated zone and not in the unsaturated zone (Narasimhan, 1975). Bishop and Blight (1963) suggest that in the unsaturated zone, Equation 2.12 should be modified as:

$$d\sigma_e = -\rho g \chi d\psi \quad (2.15)$$

where the parameter χ depends on the degree of saturation, the soil structure, and the wetting-drying history of the soil. If $\psi > 0$, $\chi = 1$, and if $\psi < 0$, $\chi \leq 1$. For $\psi \ll 0$, $\chi = 0$. However, Narasimhan (1975) claimed that for $\psi < 0$, $\chi = 0$, $d\sigma_e = d\sigma_r$, and changes in pressure head in the unsaturated zone will not cause changes in effective stress. Equation 2.13 is yet useful to define the compressibility of a porous medium in the unsaturated zone.

2.7 AQUIFER COMPRESSIBILITY

Equation 2.14 and Figures 2.5 and 2.6 define compressibility in one dimension, which means it has been assumed that the vertical direction is the only direction that the soils and rocks are stressed. Equation 2.14 can be applied to an actual aquifer problem, if b is considered as the aquifer thickness rather than a sample height. In this condition, the parameter α expresses the vertical compressibility. α can be

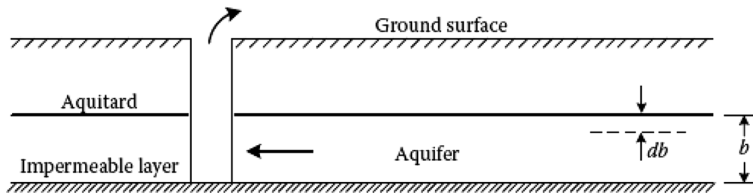


FIGURE 2.7 Land subsidence caused by groundwater pumping.

measured in a laboratory device (like the one in [Figure 2.6a](#)), while the soil cores are arranged to be vertical, and loading is applied at right angles to any horizontal bedding. However, α usually varies from point to point in a horizontal direction within an aquifer, since it is unlikely to find a completely homogeneous aquifer. The concepts of homogeneity and heterogeneity will be discussed in [Chapter 3](#). However, since the changes of horizontal stresses are very small and negligible, the aquifer compressibility is usually considered as an isotropic parameter, which means that it does not change in all directions. It should be noted that the only direction that large changes in effective stress are expected is the vertical direction.

Consider the aquifer shown in [Figure 2.7](#) has the thickness b . If the hydraulic head in the aquifer is reduced by an amount $(-dh)$, while the weight of overlying material remains constant, the increase in effective stress $(d\sigma_e)$ can be obtained by Equation 2.12 as $\rho g dh$. The aquifer compaction can then be calculated as:

$$db = -abd\sigma_e = ab\rho g dh \quad (2.16)$$

In this equation, the negative sign shows that the decrease in head results in a reduction in the thickness b .

If groundwater is pumped out from an aquifer, the hydraulic head will be decreased. In other words, pumping stimulates horizontal hydraulic gradients toward the well in the aquifer. Therefore, the hydraulic head is reduced at the points close to the well and in consequence, there will be an increase in effective stress at those points which will result in the compaction of the aquifer. In contrast, there will be an increase in the hydraulic head, a decrease in effective stress, and, in consequence, aquifer expansion due to an aquifer recharge (pumping water into an aquifer). If the compaction of an aquifer-aquitard system is expanded to the ground surface, it will lead to land subsidence. Therefore, in the operation of well systems, the amount of discharge from an aquifer needs to be carefully determined to avoid undesired consequences.

2.8 AQUIFER CHARACTERISTICS

Some important characteristics of aquifers are porosity and void ratio, specific retention, specific yield, storage coefficient, specific storage coefficient, and safe yield. Specific yield is usually used in unconfined aquifer, and specific storage is used in confined aquifers. These parameters are explained as follows.

2.8.1 POROSITY AND VOID RATIO

The total volume of a porous medium, V_T , involves the volume of the solid portion, V_s , and the volume of the voids, V_v . The ratio of the volume of voids over the total volume gives the porosity, n , of the medium ($n = V_v/V_T$), which parameter is in the form of a decimal fraction or percentage.

The porosity of the medium in different rock and soil textures are shown in [Figure 2.8](#). Well-graded sedimentary deposit with porous pebbles that has high porosity is depicted in [Figure 2.8a](#). Poorly graded sedimentary deposit is shown in [Figure 2.8b](#). [Figure 2.8c](#) shows a well-graded sedimentary deposit containing mineral filling that has a very low porosity. [Figure 2.8d](#) shows rock rendered porous by solution and fracturing with high porosity.

Consider a cylinder full of gravel and its cross section at the elevation z . The porosity at elevation z , $n(z)$, in this cylinder can be calculated as:

$$n(z) = \frac{A_p}{A} \quad (2.17)$$

where:

A_p is the cross section of the porous medium (the area of the pores)

A is the area of the cylinder.

Therefore, the porosity in the whole cylinder can be obtained as

$$n = \frac{1}{h} \int_0^h n(z) dz = \frac{1}{Ah} \int_0^h A_p(z) dz = \frac{1}{V_T} \int_0^h A_p(z) dz = \frac{V_v}{V_T} \quad (2.18)$$

and then,

$$n = 100 \frac{V_v}{V_T} = 100 \left(\frac{V_T - V_s}{V_T} \right) = 100 \left(1 - \frac{V_s}{V_T} \right) \quad (2.19)$$

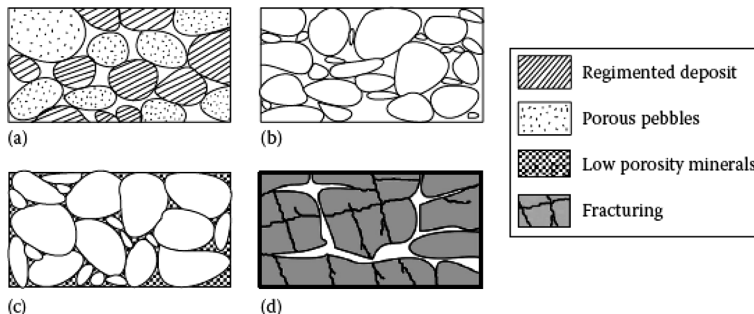


FIGURE 2.8 (a) Well-graded sedimentary deposit, with porous pebbles. (b) Poorly graded sedimentary deposit. (c) Well-graded sedimentary deposit with mineral filling. (d) Rock rendered porous by solution and fracturing.

$$n = 100 \left[1 - \frac{\rho_b}{\rho_d} \right] \quad (2.20)$$

where:

V_v is the volume of pores

V_T is the volume of cylinder

V_s is the volume of solids

ρ_b is the dry bulk density (about 1400–1900 kg/m³)

ρ_d is the particle density (about 2650 kg/m³).

Table 2.3 presents the porosity ranges for various geologic materials (Davis, 1969). According to this table, gravels, sands, and silts, which are formed by angular and rounded particles, have lower porosities than soils made up of platy clay minerals.

Example 2.3

Given a porosity of 0.22 and a dry bulk density of 1.95 g/cm³, what is the particle density?

SOLUTION

$$\rho_d = \frac{\rho_b}{(1-n)} = \frac{1.95}{1-0.22} = 2.50 \text{ g/cm}^3$$

Example 2.4

Consider the wet bulk density, ρ_{bw} which includes the mass of water, or $\rho_{bw} = m/V = m_s + m_w/V$, where m is the total mass, including the mass of water, m_w and the mass of solid, m_s , and V is the total, or bulk, volume. Given a wet bulk density, ρ_{bw} of 2.25 g/cm³ and a dry bulk density, ρ_d , of 1.95 g/cm³, and assuming the material as completely saturated with water, what is the porosity?

TABLE 2.3
Porosity of Different Geologic Materials (%)

| Unconsolidated Deposits | Porosity | Effective Porosity |
|----------------------------|----------|--------------------|
| Gravel | 25–40 | 13–44 |
| Sand | 25–40 | 10–46 |
| Silt | 35–50 | 10–39 |
| Clay | 40–70 | 10–18 |
| Fractured basalt | 5–50 | — |
| Karst limestone | 5–50 | — |
| Sandstone | 5–30 | 2–41 |
| Limestone, dolomite | 0–20 | 10–24 |
| Shale | 0–10 | — |
| Fractured crystalline rock | 0–10 | — |
| Dense crystalline rock | 0–5 | — |

SOLUTION

$$\rho_{bw} = \frac{m_s + m_w}{V} = \frac{m_s}{V} + \frac{m_w}{V} = \rho_d + \frac{m_w}{V}$$

$$m_w = \rho_w V_w$$

$$\text{Assuming } V_v = V_w \Rightarrow \frac{m_w}{V} = \frac{\rho_w V_v}{V} = \rho_w n$$

$$\text{Therefore, } \rho_{bw} = \rho_d + n \rho_w \Rightarrow$$

$$n = \frac{\rho_{bw} - \rho_d}{\rho_w} = \frac{2.25 - 1.95}{0.998} = 0.3 \quad (\rho_w = 0.998 \text{ g/cm}^3 \text{ at } 20^\circ\text{C})$$

In studying porosity of a medium, another term, widely used in soil mechanics, is void ratio, e , which is closely related to porosity. The void ratio can be defined as $e = V_v/V_s$, and usually ranges from 0 to 3. The relation between e and n can be expressed as:

$$e = \frac{n}{1-n} \quad \text{or} \quad n = \frac{e}{1+e} \quad (2.21)$$

Effective porosity (\hat{n}) is another concept of porosity that can be defined as the volume of the continuously connected path for water movement through the soil. In other words, it is the ratio of the continuous fissures over total volume of the medium:

$$\hat{n} = \frac{V_{wm}}{V_T} \quad (2.22)$$

where V_{wm} is the volume of the path of water movement.

2.8.2 SPECIFIC YIELD IN UNCONFINED AQUIFERS

Specific yield is the volume of water that is released from storage in an unconfined aquifer per unit surface area of the aquifer per unit decline in the water table. To determine this coefficient, a given volume of the aquifer is extracted and put on a mesh surface. The ratio of the volume of water discharged from the sample, considering the gravity, over total volume of the sample is its specific yield.

$$S_y = \frac{dV}{Adh} \quad (2.23)$$

where:

S_y is the specific yield

dV is the volume of withdrawn water

h is the level of water in the aquifer

A is the aquifer area.

2.8.3 SPECIFIC RETENTION

Specific retention is described as

$$S_r = n - \hat{n} \quad (2.24)$$

where:

S_r is the specific retention

n is the porosity

\hat{n} is the effective porosity, which is the same as the specific yield for all practical purposes.

Different soil particles have different yields and retentions. For example, clay has a good retention and low yield.

Therefore, the summation of the specific yield and specific retention of an aquifer gives the porosity of this aquifer:

$$n = S_y + S_r \quad (2.25)$$

Example 2.5

An aquifer with an area of 7 km^2 experiences a head drop of 0.85 m after 8 years of pumping. If the pumping rate is $5.5 \text{ m}^3/\text{day}$, determine the specific yield of the aquifer:

SOLUTION

$$S_y = \frac{V_w}{A\Delta h} = \frac{Q\Delta t}{A\Delta h} = \frac{5.5 \text{ m}^3/\text{day} \times 8 \text{ year} \times 365 \text{ day/year}}{7.5 \text{ km}^2 \times 10^6 \text{ m}^2/\text{km}^2 \times 0.85 \text{ m}} = \frac{20,440}{5.525 \times 10^6} = 2.7 \times 10^{-3}$$

Example 2.6

A soil sample has a volume of 180 cm^3 . The volume of voids in the sample is estimated equal to 67 cm^3 . Out of the volume of voids, water can move through only 45 cm^3 . Determine the porosity, effective porosity, specific retention, and specific yield of the soil. What is the area of the aquifer, which the sample was taken from, if pumping at rate $6.0 \text{ m}^3/\text{day}$ causes 1.0 m head drop in the aquifer in 5 years?

SOLUTION

$$n = \frac{V_V}{V_T} = \frac{67}{180} = 0.37$$

$$\hat{n} = \frac{V_{wm}}{V_T} = \frac{45}{180} = 0.25$$

$$S_r = n - \hat{n} = 0.37 - 0.25 = 0.12$$

$$S_y = n - S_r = 0.37 - 0.12 = 0.25$$

$$A = \frac{V_w}{S_y \Delta h} = \frac{Q \Delta t}{A \Delta h} = \frac{6.0 \text{ m}^2/\text{day} \times 5 \text{ year} \times 365 \text{ day/year}}{0.25 \times 1.00 \text{ m}} = \frac{10,950 \text{ m}^3}{0.25 \text{ m}} = 43,800 \text{ m}^2$$

2.8.4 STORAGE COEFFICIENT AND SPECIFIC STORAGE

By discharging water from, or recharging water to, an aquifer, the storage volume within the aquifer will be changed. This storage volume can be determined for unconfined aquifers as the product of the volume of aquifer, between the beginning and the end of a certain period of time, and the average specific yield of the aquifer. Nonetheless, changes in pressure produce only small changes in storage volume in confined aquifers. When the water is pumped out from an aquifer through a well, the hydrostatic pressure will be reduced and subsequently increases the aquifer load, which causes compression of the aquifer. Besides, lowering of the pressure results in a small expansion and, in consequence, release of water. The storage coefficient can be used to express the water-yielding capacity of an aquifer.

A storage coefficient, which is also called storativity, is defined as the volume of water released from, or taken into storage of, an aquifer per unit surface area of aquifer over the unit change in the head normal to that surface. Given the value of the storage coefficient, specific storage can be determined by dividing it by the unit thickness of the aquifer. [Figure 2.9a](#) shows a vertical column of unit area extending through a confined aquifer. The storage coefficient, S , in this aquifer is equal to the volume of water released from the aquifer if the piezometric surface drops a unit distance. This coefficient is dimensionless and expresses the volume of water per

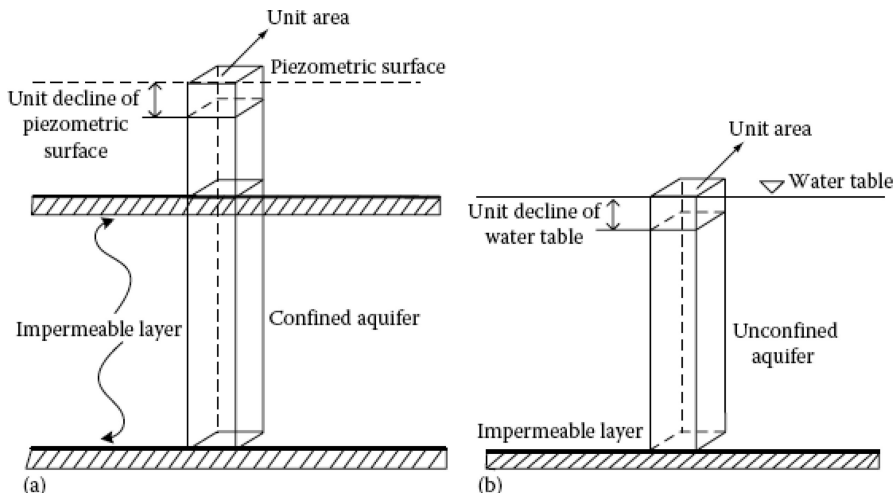


FIGURE 2.9 A schematic for defining storage coefficients of (a) confined and (b) unconfined aquifers.

volume of aquifer. The common range of the storage coefficient in confined aquifers is from 0.00005 to 0.005. Due to this wide range, it can be inferred that there must be large pressure changes over extensive areas to create substantial water yields.

To determine storage coefficients, pumping tests of wells are usually applied. The relationship between the storage, S , and the saturated aquifer thickness, b , can be expressed as

$$S = 3 \times 10^{-6} b \quad (2.26)$$

where b is in meters.

In an unconfined aquifer, the storage coefficient corresponds to the aquifer's specific yield (Figure 2.9b). Jacob (1940) defined this coefficient as:

$$S = \gamma_w b (\alpha + n\beta) \quad (2.27)$$

where:

S is the storage coefficient

γ_w is the specific weight of water (Table 2.4 presents the specific weight of water in different temperatures)

b is the thickness of the layer

α is the compressibility of the bed particles (inverse of the soil particles elasticity module, $\alpha = 1/E_s$)

β is the compressibility of water (inverse of water elasticity module, $\beta = 1/E_w$)

n is the porosity of the medium.

Table 2.5 presents the elasticity modules of some soils. The water elasticity module is about 2.1×10^9 N/m².

TABLE 2.4
Density and Specific Weight of Water in Different Temperatures

| Temperature (°C) | Density, ρ (kg/m ³) | Specific Weight, γ_w (kN/m ³) |
|------------------|--------------------------------------|--|
| 0 | 999.9 | 9.806 |
| 5 | 1000 | 9.807 |
| 10 | 999.7 | 9.804 |
| 20 | 998.2 | 9.789 |
| 30 | 995.7 | 9.765 |
| 40 | 992.2 | 9.731 |
| 50 | 988.1 | 9.690 |
| 60 | 983.2 | 9.642 |
| 70 | 977.8 | 9.589 |
| 80 | 971.8 | 9.530 |
| 90 | 965.3 | 9.467 |
| 100 | 958.4 | 9.399 |

TABLE 2.5
Elasticity Modules of Some Soils

| Soil Type | E_s (N/m ²) $\times 10^4$ |
|-----------|---|
| Peat | 10–50 |
| Clay | 50–1470 |
| Sand | 980–7850 |
| Gravel | 9806–19,620 |
| Rock | 14,710–294,200 |

Example 2.7

The thickness of the unsaturated layer in a field is 8.2 m. The porosity of the soil was measured equal to 0.28. The soil type is clay with an elasticity module of 5.3×10^7 . Determine the corresponding storage coefficient for this layer. Assume the temperature is 20°C.

SOLUTION

First, compressibility of water and the soil layer are calculated as:

$$\beta = \frac{1}{E_w} = \frac{1}{2.1 \times 10^9} = 4.76 \times 10^{-10} \text{ m}^2/\text{N}$$

$$\alpha = \frac{1}{E_s} = \frac{1}{5.3 \times 10^7} = 1.89 \times 10^{-8} \text{ m}^2/\text{N}$$

$$S = \gamma_w b(\alpha + n\beta) = 9789 \text{ N/m}^3 \times 8.2 \text{ m} \times \left[1.89 \times 10^{-8} \text{ m}^2/\text{N} + 0.28 \times 4.76 \times 10^{-10} \text{ m}^2/\text{N} \right]$$

$$\Rightarrow S = 1.53 \times 10^{-3}$$

It should be noted that there is a difference between storage coefficient, S , and specific storage, S_s . The difference is that S is the storage coefficient per unit thickness of a confined aquifer; while the specific storage, S_s , of a saturated aquifer is the volume of water that a unit volume of aquifer releases from storage due to a unit drop in hydraulic head. Recall that a decrease in hydraulic head h implies a decrease in fluid pressure, p , and an increase in effective stress, σ_e . There are two mechanisms that cause the release of water from storage due to the decrease of hydraulic head. These mechanisms are:

1. Increasing σ_e , which results in the compaction of the aquifer. This mechanism is controlled by the aquifer compressibility, α .
2. Decreasing p , which causes the expansion of the water. This mechanism is controlled by the fluid compressibility β .

In the case of the compaction of the aquifer, the volume of water released from the unit volume of the aquifer during compaction and the reduction in the unit

volume of the aquifer will be equal. The volumetric reduction, dV_T , will be negative, while the amount of water produced, dV_w , will be positive. Therefore, from Equation 2.13:

$$dV_w = -dV_T = \alpha V_T d\sigma_e \quad (2.28)$$

For a unit volume, $V_T = 1$, if a unit drop in hydraulic head, $dh = -1$, occurs, considering Equation 2.12, $d\sigma_e = -\rho g dh$,

$$dV_w = \alpha \rho g \quad (2.29)$$

From Equation 2.5, the volume of water produced by the expansion of the water is:

$$dV_w = -\beta V_w dp \quad (2.30)$$

The product of the porosity and the total volume (nV_T) gives the volume of water, V_w . If $V_T = 1$, $dh = -1$, and $dp = \rho g d\psi = \rho g d(h - z) = \rho g dh$, Equation 2.30 can be rewritten as:

$$dV_w = \beta n \rho g \quad (2.31)$$

The specific storage, S_s , can then be calculated by summing up the two terms obtained by Equations 2.29 and 2.31:

$$S_s = \rho g (\alpha + n\beta) \quad (2.32)$$

Another way to calculate the specific storage coefficient, presented by De Wiest (1965), is:

$$S_s = \gamma_w [(1-n)\alpha + n\beta] \quad (2.33)$$

The dimension of S_s is $[L]^{-1}$. Given the value of S_s , the storage coefficient for confined aquifers can be calculated as:

$$S = bS_s \quad (2.34)$$

For unconfined aquifers, the concept of specific yield could be expressed as the difference between storage coefficient and specific storage times the aquifer thickness. In an unconfined aquifer, the storage will be reduced by ΔbS_s or S_y ; therefore, S and $S_s b$ are not the same:

$$S = S_y + bS_s \quad (2.35)$$

Comparing Equation 2.35 with 2.34, it is perceived that specific yield is so small in confined aquifers that it can be considered negligible. The storage coefficient for confined aquifers is usually equal to or less than 0.005. This value for unconfined aquifers is almost between 0.2 and 0.3.

Example 2.8

The porosity of a confined aquifer is 42%. The thickness of this aquifer is 78 m. The compressibility of water and the granular matrix are 4.76×10^{-10} and 6.3×10^{-8} , respectively. Estimate the specific storage and storativity of the aquifer. Also, calculate how much water is released if there is a total head drop of 100 m and the area is 1200 km^2 .

SOLUTION

$$S_s = \rho g(\alpha + \eta\beta) = (998.2 \text{ kg/m}^3) \times (9.81 \text{ m/s}^2) \times \left[(4.76 \times 10^{-10} \text{ m}^2/\text{N}) \right] + 0.42 \times (6.3 \times 10^{-8} \text{ m}^2/\text{N})$$

$$S_s = 2.64 \times 10^{-4} \text{ (1/m)}$$

$$S = b \cdot S_s = 100 \text{ (m)} \times 2.64 \times 10^{-4} \text{ (1/m)} = 2.64 \times 10^{-2}$$

The volume of water withdrawn from the area due to the head drop in hydraulic head is

$$V = S \Delta h A = 2.64 \times 10^{-2} \times 100 \text{ m} \times 1200 \text{ km}^2 \times 10^6 \text{ m}^2/\text{km}^2 = 3.168 \times 10^9 \text{ m}^3$$

2.8.5 SAFE YIELD OF AQUIFERS

The yield of an aquifer is defined as the rate at which water can be withdrawn without depleting the supply to such an extent that withdrawing at a rate higher than that is no longer economically feasible. This concept is applied to the entire aquifer. In other words, the safe yield is the limit to the quantity of water which can be regulatory withdrawn without depletion of aquifer storage reserve.

2.9 STORAGE IN THE UNSATURATED ZONE

In the unsaturated zone, downward (recharge) and upward (evaporation and transpiration) vertical flow, movement and transportation of pollutants from ground surface, and horizontal flow in the capillary zone between the water table and ground surface are important. The amount of water held in partially saturated media is termed as the volumetric water. [Figure 2.10a](#) represents a typical distribution of water content above a water table. The capillary zone will be shifted downward by lowering the water table. The volume of water drained from above the water table is shown by the hatched area in [Figure 2.10a](#). Vertical percolation causes this water to be released

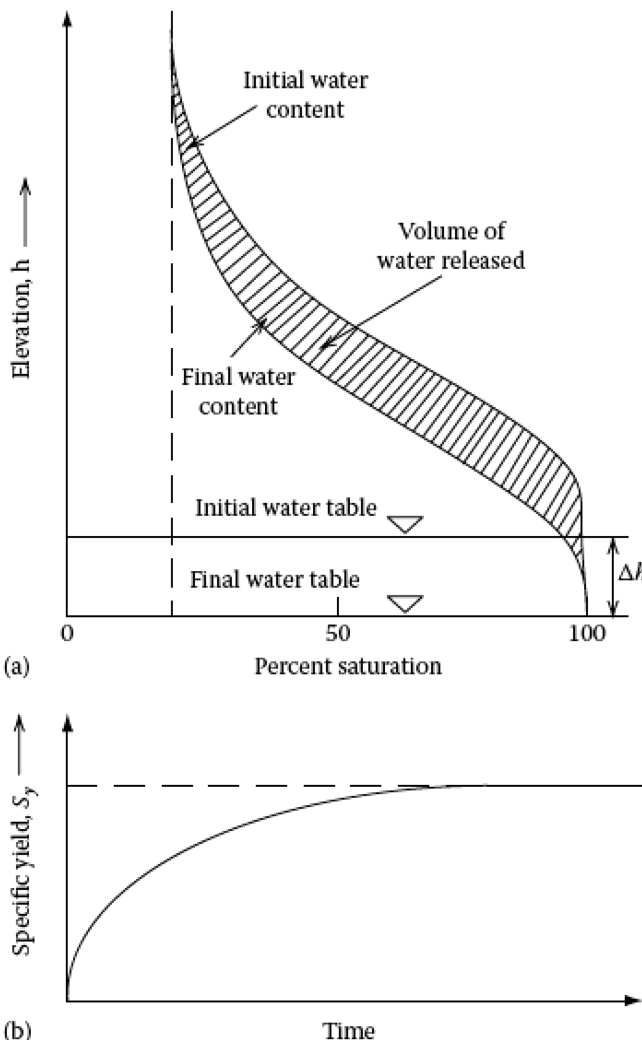


FIGURE 2.10 Movement of water in the zone of aeration by lowering the water table. (a) Water content above the water table. (b) Specific yield as a function of the time of drainage. (From Todd, D.K. and Mays, L.M., *Groundwater Hydrology*, John Wiley & Sons, New York, 2005.)

and, in consequence, the specific yield becomes an asymptotic function of time (Figure 2.10b). The volumetric water content, θ , which is one of the main properties of unsaturated media, can be calculated as:

$$\theta = \frac{V_w}{V_T} \quad (2.36)$$

To measure this parameter in the laboratory, first the soil is placed and capped tight in a can, to avoid evaporation, and is weighed. Then, it is dried in a forced draft oven for 10 h or in a convection oven for 24 h. After drying the soil, it is put into a desiccating jar, with desiccant, until the soil cools. The dried and cooled sample is weighed again and the water content, θ_w , is calculated as (Wierenga et al., 1993):

$$\theta_w = \frac{W_{wet-soil}}{W_{dry-soil}} - 1 \quad (2.37)$$

where $W_{wet-soil}$ and $W_{dry-soil}$ are the wet and dry weights of the soil sample, respectively. The volumetric water content, θ , can then be defined as:

$$\theta = \theta_w \frac{\rho_b}{\rho_w} \quad (2.38)$$

where:

ρ_b is the bulk density of the soil

ρ_w is the density of water.

In the unsaturated zone, the water saturation, S_w , is a function of the volume of voids:

$$S_w = \frac{V_w}{V_{void}} \quad (2.39)$$

where V_{void} is the volume of the void space in the sample volume V_T

In the unsaturated zone, the water content of the sample is usually less than the volume of void space, i.e., in unsaturated condition, θ is less than porosity ($0 < \theta < n$), and the water saturation is less than 1 ($0 < S_w < 1$). The water saturation is generally the ratio of porosity over water content:

$$S_w = \frac{\theta}{n} \quad (2.40)$$

Example 2.9

The total volume of a soil sample is 280 cm³. The volume of water and volume of voids were measured equal to 65 and 115 cm³, respectively. Determine the porosity, water content, and water saturation of this sample.

SOLUTION

$$n = \frac{V_V}{V_T} = \frac{115}{280} = 0.41 = 41\%$$

$$\theta = \frac{V_w}{V_T} = \frac{65}{280} = 0.23 = 23\%$$

$$S_w = \frac{0.23}{0.41} = 0.56 = 56\%$$

The pressure head, $\psi = h - z$, is negative in the unsaturated zone, positive in the saturated zone, and it is zero right at the water table. The reason that water contained in partially saturated soils cannot flow into a borehole is the negative pressure head in the unsaturated zone.

Since air and water fluid phases are present together in the unsaturated zone, flow in this zone is complicated. Both the volumetric moisture content and the unsaturated hydraulic conductivity depend on the pressure head, or the capillary pressure. The pressure head–moisture content relationship describes how a sample reflects to the addition or removal of water. There is a relationship between hydraulic conductivity and pressure head in the unsaturated zone. As a soil dries out, an increasingly large negative pressure head means that the mostly air-filled system has a large resistance to flow passage.

The relationship between the capillary pressure and water content in the unsaturated zone for a particular soil is provided by the soil water characteristic curve. There are three soil water characteristic curves:

- *Water retention or θ_ψ curves*: show the relationship between soil water content and soil water pressure potential
- *Relative hydraulic conductivity or K_ψ curves*: depict the relationship between relative hydraulic conductivity and soil water pressure potential
- *Moisture capacity or C_ψ curves*: illustrate the relationship between soil moisture capacity and soil water pressure potential. Soil moisture capacity is defined as the change in moisture content divided by the change in pressure head

For more details, please see Schwartz and Zhang (2003).

2.10 WATER-LEVEL FLUCTUATIONS

Changes in groundwater storage due to pumping and recharge result in changes in the water table and the piezometric surface elevations. Besides pumping, other factors such as barometric pressure changes, ocean tides, and use of groundwater by plants also influence water levels. The details of water table fluctuations due to pumping and recharge are explained in [Chapter 4](#). For other water table fluctuation factors, refer to McWhorter and Sunada (1977).

2.11 GROUNDWATER IN KARST

2.11.1 KARST AQUIFER

“The term *karst* represents terranes with complex geological features and specific hydrogeological characteristics. The karst terranes are composed of soluble rocks,

including limestone, dolomite, gypsum, halite, and conglomerates" (Milanovic, 2004); i.e., carbonate rocks (limestone and dolomite) and all their varieties and conglomerates with carbonate matrix represent karst.

Limestones are mostly composed of the mineral calcium carbonate (CaCO_3). Dolomites are composed of the mineral dolomite, which is a dual carbonate salt of calcium and magnesium. The chemical composition of dolomite is expressed as $\text{CaMg}(\text{CO}_3)_2$.

Karstification occurs by the chemical, and sometimes mechanical, action of water in a region of limestone, dolomite, or gypsum bedrock. Therefore, in loess (a sediment formed by the accumulation of wind-blown silt and some sand and clay), clay, lava deposits, and effusive rocks, the voids developed by erosive action of water instead of solution processes cannot be considered as karst.

A nonhomogeneous underground reservoir containing networks of interconnected cracks, caverns, and channels collecting water is called a karst aquifer.

2.11.2 TYPES OF KARST

There are different classifications of karst according to its morphological features, structural factors, geographical position, and depositional environment of carbonate rocks, etc. One of the first classifications of karst was introduced by Cvijic (1926) based on the morphological features. He considered three types of karst as:

1. *Holokarst* (complete karst) is developed in areas included entirely of soluble carbonate rocks. It is characterized by the vast, bare, and rocky land, without arable land and with or without the presence of vegetation.
2. *Merokarst* (incomplete karst) has many properties of nonkarst regions. The karst phenomena in these regions are infrequent and karstification occurs in lower depths. Carbonate sediments are covered with arable soil and with vegetation. Merokarsts are also called covered karsts.
3. *The transitional type*: The degree of karstification in this type of karst is between holokarst and merokarst. The transitional type is usually formed in limestone isolated by impermeable and less soluble sediments.

Quinlan (1972) classified karsts based on the soils or sediments covering them. Different types of karst based on this classification are:

1. *Subsoil karst*: covered with residual soil
2. *Mantled karmic*: covered with a thin layer of post-karst sediments
3. *Buried karst*: are also called paleokarst and covered by a relatively thick layer of post-karst sediments
4. *Interstratal karst*: covered by pre-karst rocks or sediment.

2.11.3 FLUCTUATION OF KARST AQUIFER

One of the distinctive features of karst aquifers is their capability of being filled and emptied by water very fast. This ability is because of the large dimensions of

karst channels, their good interconnections, high water-level gradients, and the high permeability of surface zones. In other words, aquifers are formed and drained very fast in karsts. The aquifer reacts quickly to high precipitation in the rainy season. The difference between maximum and minimum levels of a water table can be great in wet seasons.

Milanovic (2004) considered two distinguished periods with different characteristics of fluctuation for karst terrains:

- *The wet season:* with continuous vertical changes in the aquifers water table.
- *The dry season:* with constant lowering of the aquifers water table. This season is also called the recession or depletion period of the aquifer.

2.11.4 RECHARGE OF KARST AQUIFER

There are different categories for karst aquifer recharge. If the karst area recharges itself, it is called autogenic recharge. Allogenic recharge occurs when the adjacent nonkarst areas recharge the karst aquifer. Infiltration into shallow holes is called point recharge. The water may also be diffused into fissures in the rock through overlaying soils. Allogenic recharge sometimes infiltrates via shallow holes, while autogenic recharge is often more diffusive. Point recharge via shallow holes is a major pathway for contaminants (Goldsheider and Drew, 2007). Figure 2.11 shows a schematic of karst aquifers and the allogenic and autogenic recharge areas.

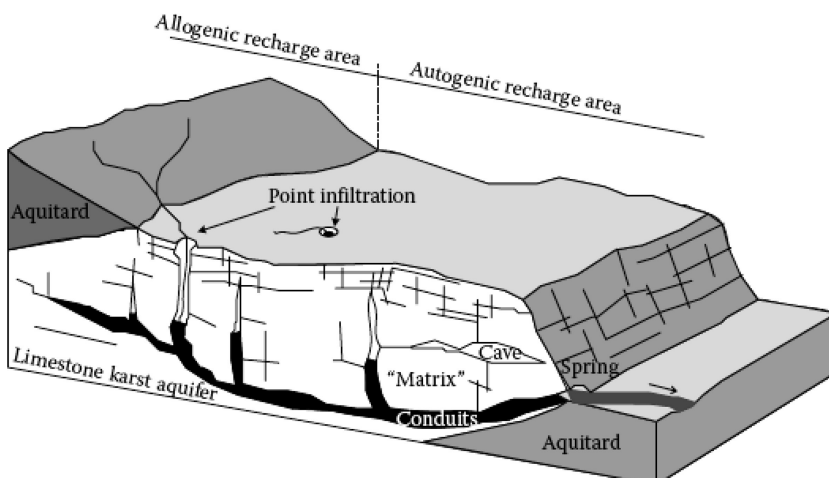


FIGURE 2.11 Heterogeneous karst aquifer system. (From Goldsheider, N. and Drew, D., *Methods in Karst Hydrology*, Taylor & Francis Group, London, UK., 2007; Hansch, C. and Leo, A., *Substitute Constants for Correlation Analysis in Chemistry and Biology*, John Wiley & Sons, New York, 1979.)

2.11.5 GROUNDWATER TRACING IN KARST

Tracers are referred to as substances that are added to water to specify its spatial and temporal distribution. They might be soluble or insoluble in water. The most important characteristic of tracers is their sensitivity to accurate concentration detection. Some common tracing technologies are:

Dye tracer: which is the most common technique for investigation of underground links in karst. Na-fluorescein, rhodamine B, rhodamine WT, eozine FE, and salt (NaCl) are some common dye tracers.

Radioactive isotopes: The best advantage of these tracers is that they can be simply detected in a very diluted solution. The most common isotopes for investigation of groundwater in karsts are Bromine-82, Iodine-131, Chromium-51, and Tritium.

Proactive isotopes: In this technique, the inorganic salts are used as tracers. Since the contamination by these isotopes is negligible, this technique is recommended for water flows that are used as the source of potable water.

Smoke and gaseous tracers: These tracers are used to evaluate the porosity characteristics of the aeration zone above the aquifer. In this method, smoke is injected into the void above the aquifer, and by tracing it; the interconnected karst voids are specified.

For more details of these methods, Milanovic (2004) is recommended.

2.11.6 WATER RESOURCES PROBLEMS IN KARST

The main water resources problems in karst zones can be summarized to:

Water supply in karst: In karst zones, rapid infiltration causes absence or deficit of surface water to meet supplying demands. Generally, two main ways of supplying water in karst zones are from wells and/or springs. In supplying water from wells, the most important issue is to select the location of wells. Fractured limestone and dolomite aquifers provide the most acceptable water quality. However, it should be noted that wells must be drilled on fracture intersections. In supplying water from karst springs, usually, a good quality of water can be obtained from the springs draining fracture systems. The main quality issue in supplying water from karst aquifers is hardness.

Flood flows in karst: During a flooding event, because of the rapid response of open conduit systems, flooding in caves has almost the same characteristics as flooding in drainage basins. As a result, high discharges happen in conduits. Therefore, sinkhole terrains can be flooded by either water ponded in closed depressions or groundwater rise. The flooded sinkhole terrains are filled by water injected from below. Since these terrains are not usually expected to be flooded, they might be urbanized and subjected to development. Therefore, significant damage may be imposed due to the flooding of these terrains.

Water pollution in karst: Since water movement through open conduits in karst zones is almost the same as surface water flows, its filtering by soil layers is negligible. Therefore, the pollution of water in open conduits is as susceptible as surface waters. In addition, the calcium, magnesium, and bicarbonate ions existing in karst aquifers, due to the solution of rocks, increase the hardness and alkalinity of water in these aquifers. Fecal material from septic tanks, leachate from landfills, agricultural chemicals, pesticides, herbicides, etc. are some major pollutants that reach groundwater in karst fields without any significant dilution by filtering through soil layers.

Water-quality monitoring in karst: As is discussed in [Chapter 9](#), monitoring networks must be installed under or adjacent to main sources of pollution, such as landfills, to detect pollutants before they spread into the underlying aquifer or move off-site. The monitoring network may be designed for unsaturated or saturated zones or both of them. Because of the heterogeneous distribution of permeability in karst aquifers as well as rapid movement of contaminants through these conduits, there might not be any trace of contaminants in monitoring wells. Therefore, monitoring systems in karst aquifers differ from regular aquifers. The strategy is to excavate trenches to bedrock and inject tracers into them with water flush. Meanwhile, the spring(s) to which the aquifer is drained are determined and these springs are monitored. The monitoring is especially important after flood events.

PROBLEMS

- 2.1 The porosity and volumetric water content of a sample are 0.40 and 0.18, respectively. Calculate the water saturation of the sample.
- 2.2 An undisturbed core sample is obtained from an unsaturated aquifer 1.0 m above the water table. The sample is 0.150 m high and 0.1 m in diameter. A dry sample of the aquifer has a specific gravity of 2.65 g/cm^3 . The weight of the sample is 630 g before drying and 570 g after drying. Calculate the porosity, volumetric water content, and bulk density of the aquifer. Assume that the volume of voids is 450 cm^3 .
- 2.3 An unconfined aquifer with a specific yield of 0.20 is used as a water supply for the irrigation of farmlands. The groundwater is pumped out of this aquifer at the rate of $4.2 \text{ m}^3/\text{day}$. The area of the aquifer is 1500 m^2 . How long does it take to have a one meter drop in the water table in this aquifer?
- 2.4 How much water can be removed from an unconfined aquifer with a specific yield of 0.18 when the water table is lowered 1.0 m? How much water can be removed from a confined aquifer with a storage coefficient of 0.0005 when the piezometric surface is lowered 1.0 m? Express your answers in m^3/km^2 .
- 2.5 Determine the total stress acting on the top on an aquifer, which is underlying a 20 m thick aquitard. The bulk density of the aquitard is 2100 kg/m^3 . What is the effective stress in the aquifer if the pressure head is 25 m?

- 2.6** A sample of silty sand has a volume of 215 cm^3 . It has a weight of 514.7 g . After saturating, the sample weighs 594.2 g . The sample is then drained by gravity until it reaches a constant weight of 483.4 g . Finally, the sample is dried in an oven for ten hours, and it reaches the weight 452.1 g . Assuming the density of water is 1 g/cm^3 , compute the following:
- Water content of the sample
 - Volumetric water content of the sample
 - Saturation ratio of the sample
 - Porosity
 - Specific yield
 - Specific retention
 - Dry bulk density
- 2.7** The porosity of the unsaturated zone in a field is 0.35. The elasticity module of the medium is 9.5×10^6 . Determine the storage coefficient for this layer if the thickness of the unsaturated layer is 10 m.
- 2.8** What is the specific yield of a soil sample that has the total volume of 250 cm^3 , void volume of 150 cm^3 , and flow volume of 100 cm^3 ?
- 2.9** The average water table elevation has dropped 1.5 m due to the removal of 85 million cubic meters from an unconfined aquifer over an area of 200 km^2 . Determine the specific yield for the aquifer. What is the specific retention of the aquifer if its porosity is 0.42?
- 2.10** Resolve Example 2.8 for an unconfined aquifer. Assume that the specific yield is 2.5%.
- 2.11** Records of the average rate of precipitation over an area show 680 mm/year rainfall, out of which, 250 mm/year flows overland. The evaluation of the time series of the data shows that 300 mm/year is evapotranspirated. The area is irrigated at the rate of 250 mm/year . In this area, 170 mm/year flows through rivers and the rate of outflow to the other basins is 250 mm/year . Determine the influence from seepage. Also, calculate the rate of baseflow. Assume groundwater inflow and outflow remain unchanged and the groundwater is not pumped out.
- 2.12** Calculate the density of a soil sample if its porosity and a dry bulk density are 0.28 and 1.65 g/cm^3 , respectively.
- 2.13** Between bulk density (ρ_b) and particle density (ρ_d), which would be expected to be greater in magnitude? Prove your answer?
- 2.14** The dry and wet bulk densities of a soil sample are measured equal to 1.65 and 1.98 g/cm^3 , respectively. Calculate the porosity of the sample. Assume the sample is completely saturated with water.
- 2.15** Determine the specific yield of an aquifer. The water is pumped at the rate of $6.75 \text{ m}^3/\text{day}$. There is a 1.2 m drop in the water table after 7 years, and the area of the aquifer is $8.2 \times 10^6 \text{ ha}$ ($10,000 \text{ m}^2$).

REFERENCES

- Bishop, A.W. and Blight, G.E. 1963. Some aspects of effective stress in saturated and partly saturated soils. *Geotechnique*, 13, 177–197.
- Cvijic, J. 1926. *Geomorfologija (Morfologie Terrestre)*. Tome Secondo, Beograd, Yugoslavia.
- Davis, S. N. 1969. Porosity and permeability of natural materials, in *Flow Through Porous Media*, ed. R.J.M. De Wiest, Academic Press, New York, pp. 54–89.
- De Wiest, R.J.M. 1965. *Geohydrology*. John Wiley & Sons, New York.
- Dingman, S.L. 1994. *Physical Hydrology*. Prentice-Hall, Englewood Cliffs, NJ.
- Domenico, P.A. and Mifflin, M.D. 1965. Water from low-permeability sediments and land subsidence. *Water Resources Research*, 1, 563–576.
- Goldsheider, N. and Drew, D. 2007. *Methods in Karst Hydrology*. Taylor & Francis Group, London, UK.
- Hansch, C. and Leo, A. 1979. *Substitute Constants for Correlation Analysis in Chemistry and Biology*. John Wiley & Sons, New York.
- Jacob, C.E. 1940. On the flow of water in an elastic artesian aquifer. *Transaction. American Geophysical Union*, 2, 574–586.
- Johnson, A.I., Moston, R.P., and Morris, D.A. 1968. *Physical and Hydrologic Properties of Water Bearing Deposits in Subsiding Areas in Central California*, U.S. Geological Survey, Professional Paper 497A.
- McWhorter, D.B. and Sunada, D.K. 1977. *Ground-Water Hydrology and Hydraulics*. Water Resources Publications, Littleton, CO, p. 290.
- Milanovic, P.T. 2004. *Water Resources Engineering in Karst*. CRC Press LLC, Boca Raton, FL.
- Narasimhan, T.N. 1975. A unified numerical model for saturated-unsaturated groundwater flow, PhD dissertation, University of California, Berkeley, CA.
- Quinlan, J.F. 1972. Karst related mineral deposits and possible criteria for recognition of paleokarst: A review of preservable characteristics of Holocene and older karst terranes, *24th IGC*, Section 6, Montreal, Canada.
- Schwartz, F.W. and Zhang, H. 2003. *Fundamentals of Groundwater*. John Wiley & Sons, New York.
- Terzaghi, K. 1925. *Erdbaumechanic auf bodenphysikalischer grundlage*. Franz Deuticke, Vienna, Austria.
- Todd, D.K. 1980. *Groundwater Hydrology*. John Wiley & Sons, New York.
- Todd, D.K. and Mays, L.W. 2005. *Groundwater Hydrology*. John Wiley & Sons, New York.
- Wierenga, P.J., Young, M.H., Gee, G.W., Hills, R.G., Kincaid, C.T., Nicholson, T.J., and Cady, R.E. 1993. *Soil Characterization Methods for Unsaturated Low Level Waste Sites*, U.S. Nuclear Regulatory Commission, NUREG/CR-5988 (PNL-8480).



Taylor & Francis

Taylor & Francis Group

<http://taylorandfrancis.com>

3 Groundwater Hydrology

3.1 INTRODUCTION

Hydrology is the study of water and addresses the occurrence, distribution, and movement of water on the earth. The science of occurrence, distribution, and movement of water under the ground surface is referred to as groundwater hydrology. The hydrologic cycle was introduced in the previous chapter. Within the hydrologic cycle, groundwater has an extensive role and has been the subject of research for many researchers. It became more important especially during and after the hydraulic mission, the second half of the nineteenth century, due to an exponential increase in industrial activities. Industrial improvement created many pollution problems in surface water that caused some of the surface water resources to become unsuitable for certain purposes such as drinking and irrigation. Moreover, population increase and, in consequence, augmentation in need for food production has led to a significant increase in demands for water. Therefore, groundwater is now considered as a supplementary source to supply increasing demands of water.

3.2 GROUNDWATER MOVEMENT

The subject of groundwater movement is quite complex. The movement of groundwater will be discussed in this chapter in its simplest forms to illustrate the principles involved. More complex groundwater models will be discussed in the next chapters.

3.2.1 DARCY'S LAW

Darcy's law is the basic empirical relationship governing the movement of groundwater through a porous medium (Bouwer, 1978; De Wiest, 1965; Freeze and Cherry, 1979; Todd, 1980). Imagine water flowing at a rate Q through a cylinder of cross-sectional area A packed with sand and having piezometers at a distance L apart, as shown in [Figure 3.1](#). Henry Darcy in 1856 determined the velocity of water flowing through this cylinder as:

$$v = -K \frac{h_2 - h_1}{\Delta l} = Ki \quad (3.1)$$

where:

v is the superficial flow velocity, m/s

K is the hydraulic conductivity, m/s

i is the hydraulic gradient, $-dh/dl$, m/m

h_1 is the height of water in the upper piezometer, m

h_2 is the height of water in the lower piezometer, m

Δl is the distance between piezometers, m.

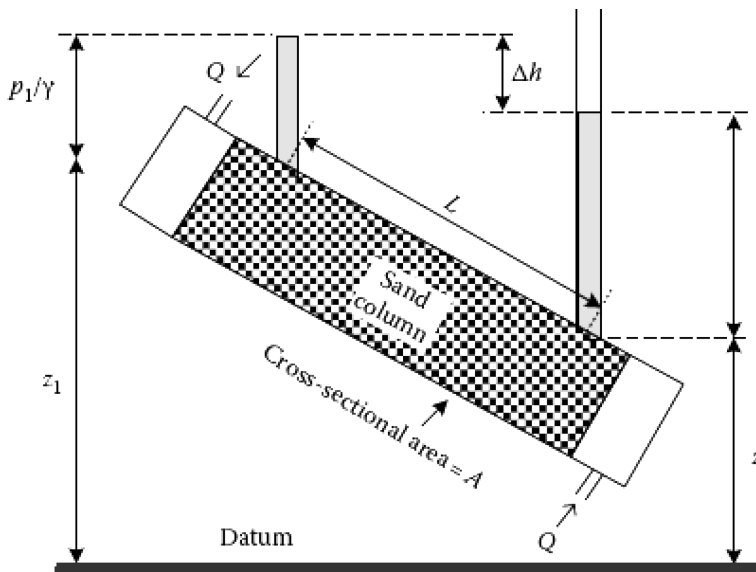


FIGURE 3.1 Pressure distribution and head loss in flow through a sand column.

The negative sign in Darcy's law arises from the fact that the head loss is negative. The discharge through a cross-sectional area of an aquifer is given by:

$$\frac{Q}{A} = Ki \Rightarrow Q = KiA \quad (3.2a)$$

or

$$q = Kib \quad (3.2b)$$

where:

Q is the hydraulic discharge, m^3/s

A is the cross-sectional area, m^2

q is the discharge in unit width of the aquifer, m^2/s

b is the thickness of the aquifer, m .

The application of Equation 3.2 is based on the assumption that the porous medium is homogenous and is saturated with water. Example 3.1 illustrates the application of this equation.

Porosity n influences hydraulic conductivity K . In well sorted sand or fractured rock formations, samples with higher n generally have higher K . For example, clay-rich soils usually have higher porosities than sandy or gravelly soils, but lower hydraulic conductivities.

Using the porosity of the medium and Darcy's law ($Q = Av$), the real velocity of water in a porous medium can be calculated. Regarding the fact that the water moves through the pores in the medium, this equation should be modified to $Q = A_p v_{\text{real}}$. A_p is the area of pores, and v_{real} is the average velocity of water through the pores. Therefore, the average velocity of water through the soil and the average velocity of water through the pores have a direct relation with each other:

$$\begin{aligned} Q &= Av \\ Q &= A_p v_{\text{real}} \end{aligned} \Rightarrow v = \frac{A_p}{A} v_{\text{real}} \Rightarrow v = nv_{\text{real}} \quad (3.3)$$

The above relation implies that velocity in the Darcy's law has lower value than the real velocity of water through the soil.

The pure velocity of groundwater is obtained from dividing the superficial flow velocity by the porosity of the porous medium.

Example 3.1

In [Figure 3.2](#), determine the superficial and real pore velocities of flow through the porous medium as well as the time of flow from the upper to the lower reservoir. Assume the following data are applicable:

Cross-sectional area $A = 100 \text{ m}^2$

Head loss $\Delta h = 35 \text{ m}$

Length of flow path $\Delta L = 1500 \text{ m}$

Hydraulic conductivity $K = 7.5 \times 10^{-4} \text{ m/s}$

Porosity of porous medium $n = 0.45$.

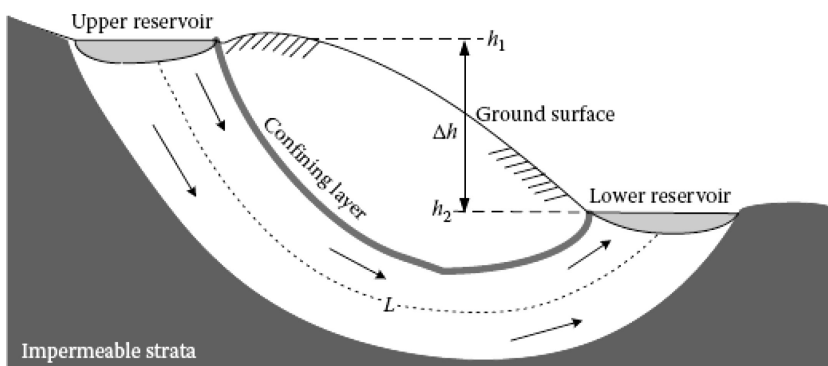


FIGURE 3.2 Two hypothetical reservoirs connected by a permeable subsurface stratum.

SOLUTION

a. Superficial velocity

$$v = -K \frac{dh}{dl} = - (7.5 \times 10^{-4} \text{ m/s}) \frac{-35 \text{ m}}{1500 \text{ m}} = 1.75 \times 10^{-5} \text{ m/s}$$

b. Pore velocity

$$V_p = V/n = 1.75 \times 10^{-5} / 0.45 = 3.89 \times 10^{-5} \text{ m/s}$$

c. Time of travel

$$t = \frac{1500 \text{ m}}{3.89 \times 10^{-5} \text{ m/s}} = 3.86 \times 10^7 \text{ s} = 446.4 \text{ days}$$

Example 3.2

Figure 3.3 shows a contour representation of the potentiometric surface for a confined aquifer being discharged into a river. Hydraulic heads in different locations were measured at 15 monitoring wells. Table 3.1 presents these measurements. The aquifer is considered homogeneous and isotropic and has an average thickness of 18 m, with a porosity of 0.34 and hydraulic conductivity of 2.6×10^{-4} m/s.

Assuming steady-state conditions, estimate the average hydraulic gradient in the aquifer.

Calculate the rate of water discharge from the aquifer to the stream.

Determine the time it would take for a hypothetical tracer injected in well #11 to reach the river.

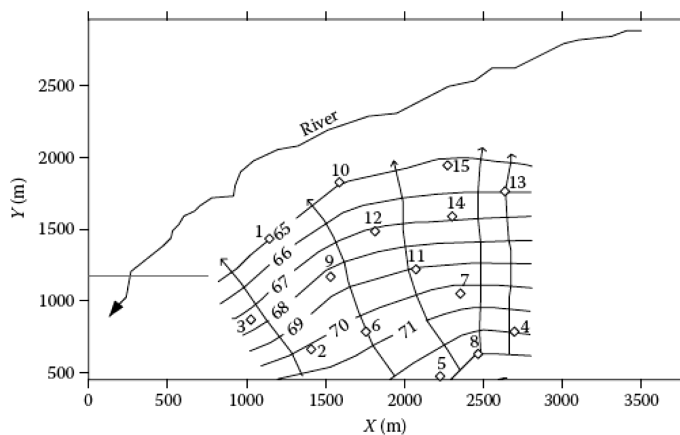


FIGURE 3.3 Contour representation of the potentiometric surface for a confined aquifer being discharged into a river.

TABLE 3.1
Hydraulic Heads at Five Streamlines

| Streamline | I (m) | Δh (m) |
|------------|---------|----------------|
| 1 | 900 | -4 |
| 2 | 1000 | -4 |
| 3 | 1150 | -6 |
| 4 | 1300 | -7 |
| 5 | 1200 | -8 |

SOLUTION

a. The hydraulic gradient at each streamline is:

| Streamline | I (m) | Δh (m) | $\Delta h/I$ |
|------------|---------|----------------|------------------------|
| 1 | 900 | -4 | -4.44×10^{-3} |
| 2 | 1000 | -4 | -4.00×10^{-3} |
| 3 | 1150 | -6 | -5.22×10^{-3} |
| 4 | 1300 | -7 | -5.38×10^{-3} |
| 5 | 1200 | -8 | -6.67×10^{-3} |

The average gradient is therefore: $i = 5.14 \times 10^{-3}$.

b. The rate of water discharge from the aquifer to the stream is:

$$q = bKi = 18 \text{ m} \times 2.6 \times 10^{-4} \text{ m/s} \times 5.14 \times 10^{-3} \text{ m/m}$$

$$= 2.41 \times 10^{-5} \frac{\text{m}^3/\text{s}}{\text{m}} = 2.08 \frac{\text{m}^3/\text{day}}{\text{m}}$$

c. Well #11 is located on line 69. The tracer must pass lines 65, 66, 67, and 68 to reach the river. Therefore, the hydraulic gradient through these lines must be calculated. Based on [Figure 3.3](#), coordinates of well #11 are approximately (2050, 1150) and coordinates of the point that the flowline intersects with line 65 are almost (1950, 1900). Thus, the distance between these two lines is 757 m. Average pore velocity along the flowline intersecting well # 11 can then be calculated as:

$$V_p = -\frac{K}{n} \cdot \frac{\Delta h}{\Delta I} = \frac{2.6 \times 10^{-4}}{0.34} \times \frac{4}{757} = 4.04 \times 10^{-6} \text{ m/s}$$

To reach the river, the tracer should travel the distance between well #11 (2050, 1150) and the intersection point of the flowline and river (1950, 2300). This distance is approximately 1154 m ($\sqrt{(1950-2050)^2 + (2300-1150)^2}$). The travel time can thus be calculated as:

$$t_{tr} = \frac{d}{V} = \frac{1154 \text{ m}}{4.04 \times 10^{-6} \text{ m/s}} \cong 2.86 \times 10^8 \text{ s} \cong 9.07 \text{ years}$$

3.2.1.1 Validity of Darcy's Law

In a laminar flow, velocity is proportional to the first power of hydraulic gradient. Hence, it is acceptable to believe that Darcy's law can be applied to laminar flow in porous media. A reasonable criterion to determine whether the flow is laminar or turbulent is the Reynolds number. Therefore, this number can be considered as a factor to establish the limits of flow described by Darcy's law. Reynolds number is expressed as:

$$N_R = \frac{\rho v D}{\mu} \quad (3.4)$$

where:

ρ is the fluid density

v is the velocity

D is the diameter (of pipe)

μ is the viscosity of the fluid.

It can be inferred that the above equation has been adopted for flow in pipes. To be able to apply this equation to a porous medium, Darcy's velocity and an effective grain size d_{10} are substituted from v and D , respectively.

It has been proven experimentally that Darcy's law is valid for $N_R < 1$, and it is not that far away for up to $N_R = 10$ (Ahmed and Sunada 1969). Considering that natural groundwater flow mostly occurs when the Reynolds number is less than 1, Darcy's law is applicable to groundwater movement.

3.2.2 HYDRAULIC HEAD

In a groundwater system in a saturated zone, hydraulic head at a specific point (Figure 3.4) can be expressed as:

$$h = z + \frac{p}{\rho g} \quad (3.5)$$

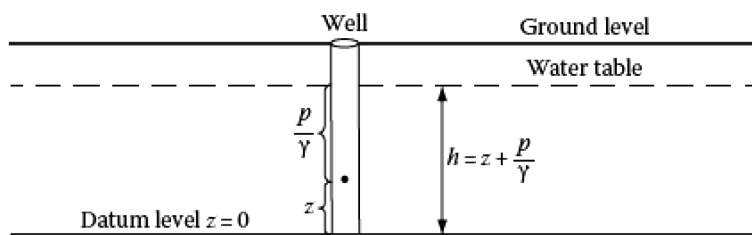


FIGURE 3.4 Illustration of hydraulic head.

where:

- z is the elevation head above a datum plane (m)
- p is the fluid pressure at the point applied by the column of water above the point (Pa)
- ρ is the water density (kg/m^3)
- g is the gravity constant (m/s^2)
- ρg expresses the specific weight of water (γ).

In groundwater studies, fluid potential and hydraulic head are equivalent; however, hydraulic head is most commonly used. Water can flow from a region of lower pressure to a region of higher pressure if the total head at the starting point is greater than that at the ending point.

In the field of petroleum and natural gas engineering, pressure is generally used in place of head because pressures at great depths are normally so great and elevation heads are often insignificant.

3.2.3 HYDRAULIC CONDUCTIVITY

Hydraulic conductivity is defined in two separate parts considering the saturation or unsaturation status of the media.

3.2.3.1 Hydraulic Conductivity in Saturated Media

Hydraulic conductivity, K , contains properties of both the medium and fluid. It can be used for evaluating water transmissivity in a porous medium. Hydraulic conductivity of a saturated media is defined as:

$$K_s = k \frac{\gamma}{\mu} \quad (3.6)$$

where:

- K_s is the saturated hydraulic conductivity, cm/s or ft/day
- $k = Cd^2$ is the specific or intrinsic permeability
- C is the constant of proportionality, unitless
- d is the grain size of porous medium, m
- γ is the specific weight of water, kN/m^3
- μ is the dynamic viscosity of water, $\text{N s}/\text{m}^2$.

The physical meaning of hydraulic conductivity is stated as “the volume of liquid flowing perpendicular to a unit area of porous medium per unit time under the influence of a hydraulic gradient of unity.” Earlier literature described this phenomenon as the field coefficient of permeability with units of gallons per day per square feet. This definition is now rarely used. [Table 3.2](#) lists hydraulic conductivities of several lithologies. It can be also obtained by [Table 3.3](#).

TABLE 3.2
Important Physical Properties of Soil and Rock

| Lithology | Hydraulic Conductivity (cm/s) | Compressibility, α (m^2/N or Pa^{-1}) |
|----------------------------|-------------------------------|---|
| Unconsolidated | | |
| Gravel | 10^{-2} – 10^2 | 10^{-8} – 10^{-10} |
| Sand | 10^{-4} – 1.0 | 10^{-7} – 10^{-9} |
| Sat | 10^{-7} – 10^{-3} | No data |
| Clay | 10^{-10} – 10^{-7} | 10^{-6} – 10^{-8} |
| Glacial till | 10^{-10} – 10^{-4} | 10^{-6} – 10^{-8} |
| Indurated fractured basalt | 10^{-5} – 1.0 | 10^{-8} – 10^{-10} |
| Karst limestone | 10^{-4} – 10.0 | Not applicable |
| Sandstone | 10^{-8} – 10^{-4} | 10^{-11} – 10^{-10} |
| Limestone, dolomite | 10^{-7} – 10^{-4} | $<10^{-10}$ |
| Shale | 10^{-11} – 10^{-7} | 10^{-7} – 10^{-8} |
| Fractured crystalline rock | 10^{-7} – 10^{-2} | 10.0^{-10} |
| Dense crystalline rock | 10^{-12} – 10^{-8} | 10^{-9} – 10^{-11} |

Source: Domenico, P.A. and Schwartz, F.W., *Physical and Chemical Hydrogeology*, John Wiley & Sons, New York, 1990; Freeze, R.A. and Cherry, J.A., *Groundwater*, Prentice Hall, Englewood Cliffs, NJ, 1979; Fetler, C.W. *Applied Hydrogeology*, 3rd ed., Macmillan College Publishing Co., New York, 1994; and Narasimhan, T.N. and Goyal, K.E., Subsidence due to geothermal fluid withdrawal, in *Man-Induced Land Subsidence, Reviews in Engineering Geology*, Geological Society of America, pp. 35–66, 1984.

Example 3.3

The saturated hydraulic conductivity of a coarse sand measured in a laboratory at 20°C is 2.74×10^{-4} m/s. What is the intrinsic permeability?

$$\text{At } 20^\circ\text{C: } \rho_w = 998.29 \text{ kg/m}^3, \mu_w = 1.003 \times 10^{-3} \text{ kg/ms}$$

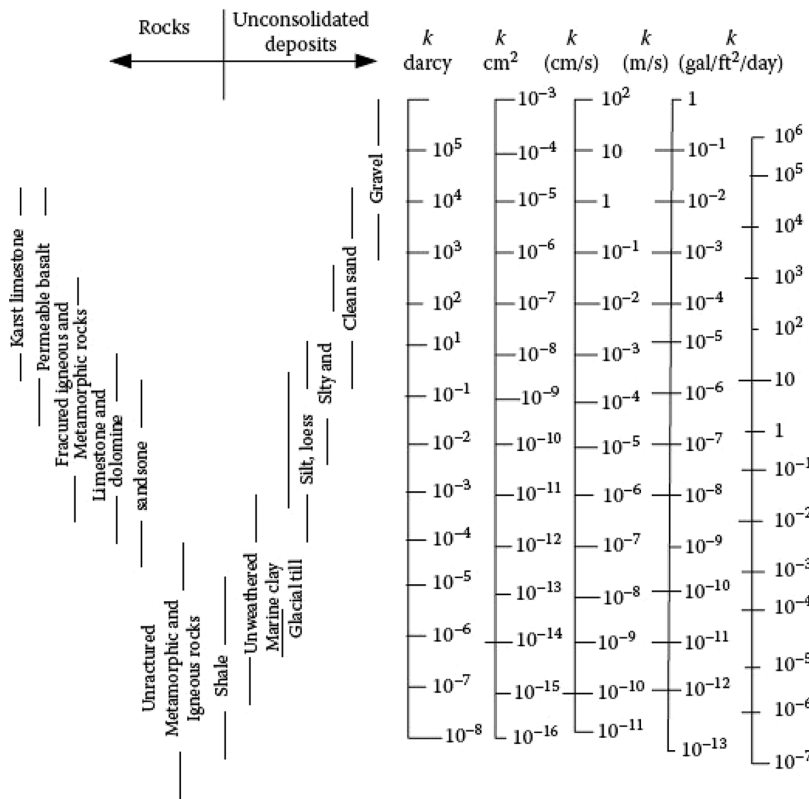
$$\begin{aligned} k &= \frac{\mu_w}{\rho_w g} K_s = \frac{1.003 \times 10^{-3} \text{ kg/ms}}{998.29 \text{ kg/m}^3 \times 9.81 \text{ m/s}^2} \times 2.74 \times 10^{-4} \text{ m/s} \\ &= 2.81 \times 10^{-11} \text{ m}^2 = 2.81 \times 10^{-7} \text{ cm}^2 \end{aligned}$$

3.2.3.2 Hydraulic Conductivity in Unsaturated Media

In unsaturated media, the hydraulic gradient, molecular attraction, and surface tension influence water flow. Therefore, unsaturated hydraulic conductivity is a function of the pressure head, Ψ (always negative in unsaturated media). Unsaturated hydraulic conductivity is shown as $K(\Psi)$.

Unsaturated hydraulic conductivity is at its maximum when infiltration reaches its capacity. In dry conditions, water will not flow any significant distance unless the

TABLE 3.3
Range of Values of Hydraulic Conductivity and Permeability



Source: Freeze, R. and Cherry, J., *Groundwater*, Prentice Hall, Englewood Cliffs, NJ, 604 p, 1979.

water content in the soil is sufficient and the pressure head becomes less negative. Then, the specific discharge is:

$$q = -K(\Psi)h \frac{\partial h}{\partial l} \quad (3.7)$$

or

$$q = -K(\theta)h \frac{\partial h}{\partial l} \quad (3.8)$$

where θ is the water content of the soil. There are three methods for computing unsaturated hydraulic conductivity as a function of water content. These methods have been summarized in Rawls et al. (1993). The three methods are based on dimensionless equations, which makes them applicable to any set of units.

Hydraulic conductivity in an unsaturated zone can be estimated by the formula introduced by Brooks and Corey (1964) as:

$$\frac{K(\theta)}{K_s} = \left[\frac{(\theta - \theta_r)}{n - \theta_r} \right]^m \quad (3.9)$$

where:

K_s is the saturated hydraulic conductivity

θ_r is the residual water content

n is the porosity,

and

$$m = 2 + 3\lambda \quad (3.10)$$

where λ is the pore-size index (Brooks and Corey 1964). Equation 3.9 is valid when $(n - \theta_r) > (\theta - \theta_r)$. If $(n - \theta_r) \leq (\theta - \theta_r)$, $K(\theta)/K_s = 1$.

Campbell (1974) presents the following formula for hydraulic conductivity in an unsaturated zone:

$$\frac{K(\theta)}{K_s} = \left(\frac{\theta}{n} \right)^m \quad (3.11)$$

and the following formula was presented by Van Genuchten (1980) for hydraulic conductivity in an unsaturated zone:

$$\frac{K(\theta)}{K_s} = \left[\frac{(\theta - \theta_r)}{(n - \theta_r)} \right]^{1/2} \left\{ 1 - \left[1 - \left(\frac{(\theta - \theta_r)}{(n - \theta_r)} \right)^{1/m} \right]^m \right\}^2 \quad (3.12)$$

where:

$$m = \frac{\lambda}{(\lambda + 1)} \quad (3.13)$$

The reader is recommended to check Schwartz and Zhang (2003) for more details.

3.2.3.3 Laboratory Measurement of Hydraulic Conductivity

To measure hydraulic conductivity in a laboratory, samples must be taken from the aquifer and transferred to the laboratory in an undisturbed condition, which is, in general, possible for consolidated materials, but usually not for unconsolidated materials. It is also rarely possible for fissured aquifers. Cylinders or cubes with diameter and length of 25–50 mm are typically used for consolidated aquifer samples. To determine permeability in three directions, cubic samples are used.

Since the samples need to be representative of the aquifer, they can be obtained where the stratum of the aquifer is horizontal. They can be collected from bore holes

that intersect several strata. The samples can also be taken from cliffs or quarry faces. If the stratum is inclined, the samples are taken from bore holes or the outcrop. However, bore hole samples are more desirable, since the outcrop material is likely to be weathered and unrepresentative of the aquifer.

In a laboratory, a permeameter is used to determine the hydraulic conductivity with application of Darcy's law. There are two types of permeameter: the constant head permeameter (Figure 3.5a) and the falling head permeameter (Figure 3.5b). The constant head permeameter is used for noncohesive soils (e.g., sands and gravels). The falling head permeameter is used for materials which have lower hydraulic conductivity.

In the permeameter test, groundwater from the same aquifer must be used. This is because some materials are sensitive to changes in water chemistry, such as clays that may swell or shrink, but this water is in a chemical equilibrium with the aquifer material.

To obtain the hydraulic conductivity for the constant head permeameter (Figure 3.5a):

Q_{of} is the rate of overflow. From Darcy's law we have:

$$Q = -KA \frac{h_2 - h_1}{L}$$

Therefore:

$$K = \frac{QL}{Ah} \quad (3.14)$$

where:

Q is the flow rate

A is the cross-sectional area

L is the length of the sample

h is the constant head.

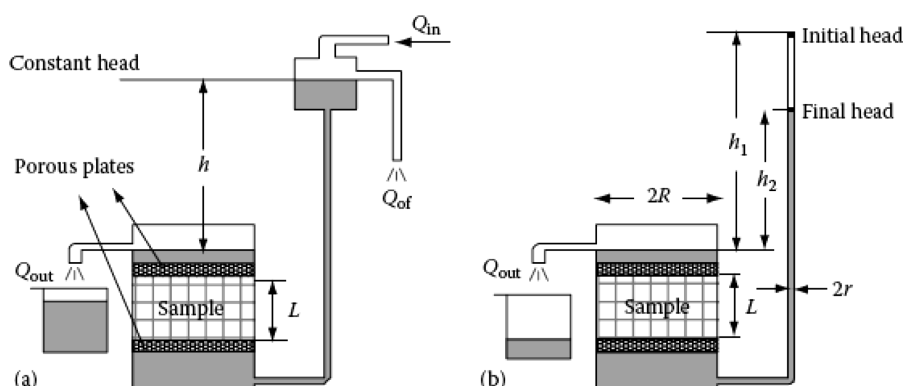


FIGURE 3.5 Permeameters for measuring hydraulic conductivity under: (a) constant head and (b) falling head.

For the falling head permeameter, the hydraulic conductivity is obtained as following:

$$Q_{\text{in}} = -A_t \frac{dh}{dt}$$

$$Q_{\text{out}} = KA_c \frac{h}{l}$$

where A_t and A_c are the cross-sectional area of the tube and the container, respectively. In steady-state condition, $Q_{\text{in}} = Q_{\text{out}}$:

$$\begin{aligned} -A_t \frac{dh}{dt} &= KA_c \frac{h}{l} \\ \int_{h_1}^{h_2} \frac{dh}{h} &= \frac{-K}{L} \frac{A_c}{A_t} \int_{t_1}^{t_2} dt \\ [\ln h]_{h_1}^{h_2} &= \frac{-K}{L} \frac{A_c}{A_t} (t_2 - t_1) \\ \ln \frac{h_2}{h_1} &= \frac{-K}{L} \frac{A_c}{A_t} (t_2 - t_1) \\ K &= \frac{A_t L}{A_c (t_2 - t_1)} \ln \frac{h_1}{h_2} \end{aligned} \quad (3.15)$$

where:

L is the length of the sample

h_1 and h_2 are the heads at the beginning, t_1 and at time t_2 later.

3.2.3.4 Field Measurement of Hydraulic Conductivity

Pumping tests are common ways for measuring hydraulic conductivity at a field. Hydraulic conductivity is estimated from observations of water levels near the pumping wells. The data of hydraulic conductivity obtained from pumping tests are not as accurate as the punctual information from laboratory tests. However, pumping tests have the advantage that the aquifer is not disturbed. The pumping tests are described in detail in [Chapter 4](#).

Tracer tests can be another alternative for hydraulic conductivity measurements at a field. In tracer tests, a dye such as fluorescent or a salt such as calcium chloride can be used. If there is a drop in the water table, h , between the injection well and the observation bore hole that are L meters apart from each other, the pore velocity obtained by Darcy's law can be equated to that obtained by dividing the distance by the travel time between the two bore holes. Rearranging the relationship gives:

$$K = \frac{nL^2}{ht} \quad (3.16)$$

where:

n is the porosity

t is the travel time between the two bore holes.

Since there might be some uncertainties about the flow direction in actual conditions, this test is hard to accomplish in practice. Besides, if the distance between the bore holes is long, the travel time becomes too long, which makes the test unreasonable.

There are some other commonly used tests for the determination of hydraulic conductivity. These tests are the slug test, the auger-hole test, and the piezometer test. In these tests, the rate of water level rise in a bore hole is measured after the water level has been lowered by the removal of water with a bailer or bucket, and the hydraulic conductivity is determined based on this rate. Although these tests give more localized values for the hydraulic conductivity, they are less expensive to conduct. More detail about these tests can be found in Bouwer (1978).

3.3 HOMOGENEOUS AND ISOTROPIC SYSTEMS

A homogeneous formation has uniform hydraulic conductivity at all points in the aquifer. In contrast, if the hydraulic conductivity varies with location, the formation is called heterogeneous. [Figure 3.6](#) shows three different ways that hydraulic conductivity changes in heterogeneous formations.

In a geologic formation, if at a given point the hydraulic conductivity is not changed in all directions, the formation is isotropic. In anisotropic formations, the hydraulic conductivity varies with direction. The system depicted in [Figure 3.7a](#) has the same consolidation in different directions and shows an isotropic formation. In [Figure 3.7](#), system (b) is more consolidated in the vertical direction. This system shows an anisotropic formation.

If the coefficient of permeability is independent of the direction of velocity, the soil is said to be an isotropic flow medium. If the soil has the same coefficient of permeability at all points within the flow region, the soil is said to be homogeneous and isotropic. If the coefficient of permeability is dependent on the direction of velocity, and if this directional dependence is the same at all points of the flow region, the soil

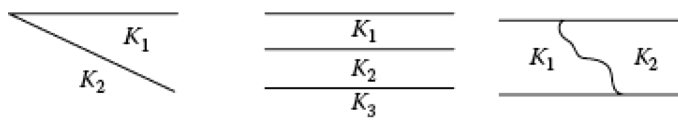


FIGURE 3.6 Hydraulic conductivity formations in three types of heterogeneous systems.

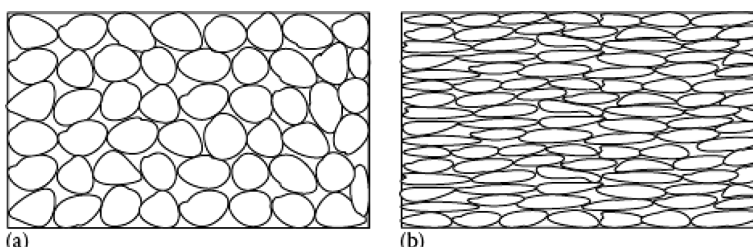


FIGURE 3.7 (a) Isotropic and (b) anisotropic sediment deposits.

is said to be homogeneous and anisotropic. In homogeneous and anisotropic soils, the coefficient of permeability is dependent on the direction of velocity, but independent of the space coordinates.

Most soils are anisotropic to some degrees. Sedimentary soils often exhibit thin alternating layers. In general, in homogeneous natural deposits, the coefficient of permeability in the horizontal direction is greater than that in the vertical direction (Snow, 1969).

Although idealized aquifers that are homogeneous and isotropic do not exist, for mathematical calculations of groundwater storage and flow, the aquifers are assumed to be homogeneous and isotropic. These assumptions give acceptable quantitative approximations, particularly in large-scale studies.

3.3.1 HYDRAULIC CONDUCTIVITY IN MULTILAYER STRUCTURES

In geology, if a structure has various characteristics (soil type, permeability, compressibility, etc.) in different depths, it is called a multilayer structure. The hydraulic conductivity of this type of structure differs in vertical and horizontal directions and is obtained as follows:

- Average horizontal hydraulic conductivity: In this status, the hydraulic gradient is equal in all layers and total discharge is the summation of the discharge of all the layers.

$$i = i_1 = i_2 = \dots = i_n$$

$$Q = Q_1 + Q_2 + \dots + Q_n$$

$$K_H i A = K_1 i_1 A_1 + K_2 i_2 A_2 + \dots + K_n i_n A_n$$

$$K_H i b = K_1 i_1 b_1 + K_2 i_2 b_2 + \dots + K_n i_n b_n$$

$$K_H = \frac{\sum_{i=1}^n K_i b_i}{\sum_{i=1}^n b_i} \quad (3.17)$$

where:

K_H is the horizontal hydraulic conductivity

i_i is the hydraulic gradient of the layer

Q_i is the discharge of the layer

A_i is the area of the layer

b_i is the thickness of the layer

- Average vertical hydraulic conductivity: The rate of discharge in all layers is equal in this status, but total head loss is obtained from the summation of the head losses of all layers:

$$dh = dh_1 + dh_2 + \dots + dh_n$$

$$Q = Q_1 = Q_2 = \dots = Q_n$$

$$\frac{b}{K} Q = \frac{b_1}{K_1} Q_1 + \frac{b_2}{K_2} Q_2 + \dots + \frac{b_n}{K_n} Q_n$$

$$K_V = \frac{\sum_{i=1}^n b_i}{\sum_{i=1}^n b_i / K_i} \quad (3.18)$$

The horizontal hydraulic conductivity in alluvium is normally greater than that in the vertical direction:

$$K_H > K_V \quad (3.19)$$

Imagine a two-layer case. The above status can be proven as:

$$\frac{K_1 b_1 + K_2 b_2}{b_1 + b_2} > \frac{b_1 + b_2}{b_1 / K_1 + b_2 / K_2} \quad (3.20)$$

which can be simplified to:

$$\frac{b_1}{b_2} (K_1 - K_2)^2 > 0 \quad (3.21)$$

Because the left side is always positive, Equation 3.19 is confirmed.

Ratios of K_H/K_V , usually fall in the range of 2–10 for alluvium, but values up to 100 or more occur where clay layers are present. For consolidated geologic materials, anisotropic conditions are governed by the orientation of strata, fractures, solution openings, or other structural conditions, which do not necessarily possess a horizontal alignment.

In applying Darcy's law to a two-dimensional flow in an anisotropic media, the appropriate value of K must be selected for the direction of flow. For diagonal directions, the K value can be obtained from:

$$\frac{1}{K_\beta} = \frac{\cos^2 \beta}{K_H} + \frac{\sin^2 \beta}{K_V} \quad (3.22)$$

where K_β is the hydraulic conductivity in the direction making an angle β with the horizontal direction.

This equation relates the principal conductivity components in horizontal and vertical directions to the resultant K_β in the angular direction β . Assuming $H = r \cos \beta$ and $V = r \sin \beta$, we can rewrite Equation 3.22 as:

$$\frac{1}{K_\beta} = \frac{H^2}{K_H} + \frac{V^2}{K_V} \quad (3.23)$$

For cases where flow is at an angle to a geological boundary between layers (Figure 3.8), the tangent refraction law affects the groundwater flow. The extent of refraction of the flowlines will depend on the hydraulic

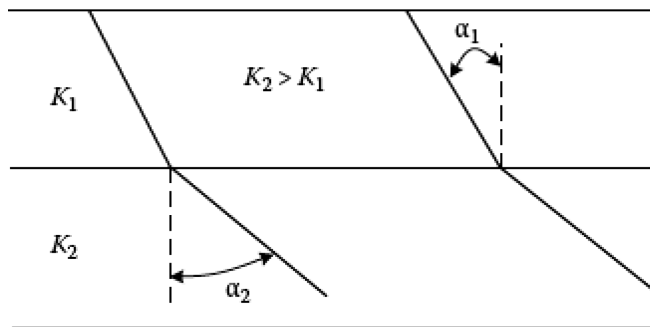


FIGURE 3.8 Diagram of flowline refraction at the boundary between two layers with different permeability.

conductivity ratio of the two layers. This ratio is equal to the ratio of tangents of the angles that the flowlines make with the normal to the boundary, or:

$$\frac{K_1}{K_2} = \frac{\tan(\alpha_1)}{\tan(\alpha_2)} \quad (3.24)$$

where:

K_1 and K_2 are the hydraulic conductivity of layers 1 and 2, respectively
 α is the refraction angle.

Example 3.4

A constant head permeameter has a cross-sectional area of 150 cm^2 . At a head of 20 cm , the permeameter discharges 57 cm^3 in 6 min through a sample of 40 cm length. Calculate the hydraulic conductivity in cm/s . From the hydraulic conductivity value, identify the soil type. Compute the intrinsic permeability if the test was carried out at 15°C ?

SOLUTION

$$K = \frac{VL}{Ath} = \frac{57 \text{ cm}^3 \times 40 \text{ cm}}{150 \text{ cm}^2 \times 360 \text{ s} \times 20 \text{ cm}} = 2.11 \times 10^{-3} \text{ cm/s}$$

$K = 2.11 \times 10^{-3} \text{ cm/s} \Rightarrow$ using Table 3.3, the soil must be silty sand or clean sand.

$$\text{at } 15^\circ\text{C: } \rho_w = 999.19 \text{ kg/m}^3, \mu_w = 1.139 \times 10^{-3} \text{ kg/ms}$$

$$k = \frac{\mu_w}{\rho_w g} K = \frac{1.139 \times 10^{-3} \text{ kg/ms}}{999.19 \text{ kg/m}^3 \times 9.81 \text{ m/s}^2} \times 2.11 \times 10^{-5} \text{ m/s} = 2.45 \times 10^{-12} \text{ m}^2$$

$$k = 2.45 \times 10^{-8} \text{ cm}^2$$

Example 3.5

In a falling head test, the initial head at $t = 0$ is 72 cm. At $t = 30$ min, the head is 66 cm. The diameters of the standpipe and the specimen are 1.5 and 25 cm, respectively. The length of the specimen is 25 cm. Calculate the hydraulic conductivity and intrinsic permeability of the specimen.

$$A_t = \frac{\pi \times 1.5^2}{4} = 1.77 \text{ cm}^2$$

$$A_c = \frac{\pi \times 25^2}{4} = 490.86 \text{ cm}^2$$

$$h_0 = h(t = 0) = 72 \text{ cm}$$

$$h_t = h(t = 30 \text{ min}) = 66 \text{ cm}$$

$$K = \frac{A_t}{A_c} \frac{L}{t} \ln \left[\frac{h_0}{h_t} \right] = \frac{1.77 \text{ cm}^2}{490.86 \text{ cm}^2} \times \frac{25 \text{ cm}}{30 \text{ min}} \times \ln \left(\frac{72 \text{ cm}}{66 \text{ cm}} \right)$$

$$= 2.61 \times 10^{-4} \text{ cm/min} = 4.35 \times 10^{-6} \text{ cm/s} = 4.35 \times 10^{-8} \text{ m/s}$$

Assuming the experiment was conducted was at 20°C:

$$\rho_w = 998.29 \text{ kg/m}^3, \mu_w = 1.003 \times 10^{-3} \text{ kg/ms}$$

$$k = \frac{\mu_w}{\rho_w g} K = \frac{1.003 \times 10^{-3} \text{ kg/ms}}{998.29 \text{ kg/m}^3 \times 9.81 \text{ m/s}^2} \times 4.35 \times 10^{-8} \text{ m/s} = 4.46 \times 10^{-15} \text{ m}^2$$

Example 3.6

Five horizontal formations with an equal thickness of 1 m for each of them exist in a hydrogeological system. Hydraulic conductivities of the formations are 40, 20, 30, 100, and 10 cm/day. Calculate equivalent horizontal and vertical hydraulic conductivities. Also, if flow in the uppermost layer is at an angle of 30° away from the horizontal direction relative to the boundary, calculate flow directions in all of the formations.

$$d_i = d = 1 \text{ m}, i = 1 \dots 5$$

$$K_h = \frac{\sum_{i=1}^5 K_i d}{\sum_{i=1}^5 d} = \frac{\sum_{i=1}^5 K_i}{5} = \frac{40 + 20 + 30 + 100 + 10}{5} = 40.0 \text{ cm/day}$$

$$K_V = \frac{\sum_{i=1}^5 d}{\sum_{i=1}^5 d/K_i} = \frac{5}{\sum_{i=1}^5 1/K_i} = \frac{5}{(1/40) + (1/20) + (1/30) + (1/100) + (1/10)} = 22.9 \text{ cm/day}$$

Angle of incidence: α_1 Angle of refraction: α_2

$$\frac{k_i}{k_r} = \frac{\tan \alpha_i}{\tan \alpha_r} \Rightarrow \alpha_i = \tan^{-1} \left(\frac{K_i}{K_r} \tan \alpha_r \right)$$

The angle of refraction in one layer constitutes the angle of incidence to the next one:

$$\frac{20}{40} = \frac{\tan \alpha_i}{\tan(30)} \Rightarrow \alpha_i = \tan^{-1} \left(\frac{20}{40} \tan(30) \right) = 16.1^\circ$$

and considering the above relationship, the direction of all formations are:

$$\alpha_1 = 30^\circ, \alpha_2 = 16.1^\circ, \alpha_3 = 23.41^\circ, \alpha_4 = 55.28^\circ, \alpha_5 = 8.21$$

3.4 TRANSMISSIVITY

Transmissivity is the amount of water that moves horizontally through a unit width of a saturated aquifer as a result of a unit change in gradient.

$$T = Kb \quad (3.25)$$

where:

K is the hydraulic conductivity

b is the depth of the saturated aquifer.

This dimensional characteristic derives from the definition of transmissivity as the flow rate of water passing through a unit width of aquifer perpendicular to flow direction over the entire thickness of the aquifer (Figure 3.9).

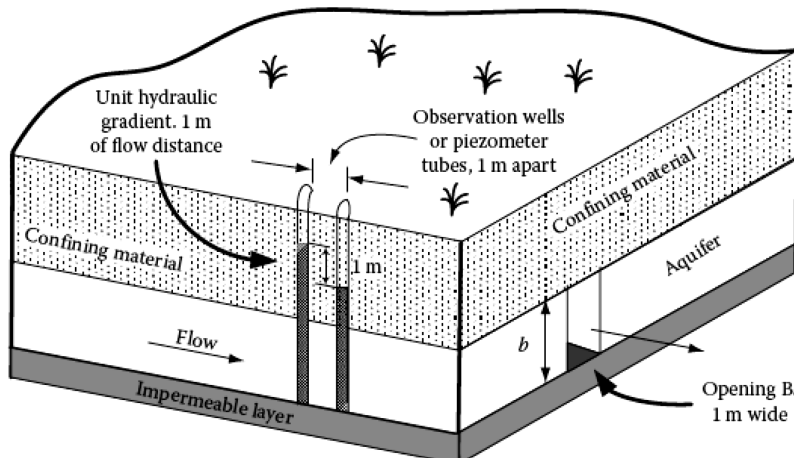


FIGURE 3.9 A schematic for defining transmissivity. (Adapted from Ferris, J.G. et al., *Theory of Aquifer Tests*, U.S. Geological Survey, Water-Supply Paper 1536E, 174 p, 1962. With permission.)

Transmissivity is usually reported in units of square feet per day or square meters per day. The total rate of flow (Q) through any area (A) of the aquifer perpendicular to the flow direction under the gradient (i) is then given as:

$$Q = WTi \quad (3.26)$$

where:

W is the width of aquifer

i is the hydraulic gradient

T is transmissivity in (m^2/s)

Q is the discharge rate in (m^3/s).

For multilayer aquifers, the transmissivity is calculated as follows:

$$T = \sum_{i=1}^n T_i \quad (3.27)$$

By multiplying the pertinent K values of hydraulic conductivity from [Table 3.2](#) by the range of reasonable aquifer thicknesses, say 5–100 m, a range of values of T can be calculated. Transmissivities greater than $0.015 \text{ m}^2/\text{s}$ (or $0.16 \text{ ft}^2/\text{s}$ or $100,000 \text{ gal/day/ft}$) represent good aquifers for water well exploitation.

In an unconfined aquifer, transmissivity is not as well defined as in a confined aquifer. However, Equation 3.25 can still be used for unconfined aquifers. In this case, b is now the saturated thickness of the aquifer or the height of the water table above the top of the underlying aquitard that bounds the aquifer.

3.5 DUPUIT–FORCHHEIMER THEORY OF FREE-SURFACE FLOW

The movement of groundwater in unconfined systems bounded by a free surface is usually treated as a steady-state flow problem and a simple Dupuit–Forchheimer analysis is often used. The Dupuit–Forchheimer analysis is based on the assumption that streamlines are virtually horizontal (potential lines are vertical), and that the slope of the hydraulic grade line is the same as the free-surface slope (Bouwer, 1978; De Wiest, 1965; Hansch and Leo, 1979; Todd, 1980). Although the model is for unconfined aquifers, with suitable assumptions, it can be extended to confined aquifers.

Example 3.7

In [Figure 3.10](#), irrigation water is being infiltrated with uniform intensity into the ground. If the intensity of infiltration is f , suggest a relationship for calculating the highest level of the water table.

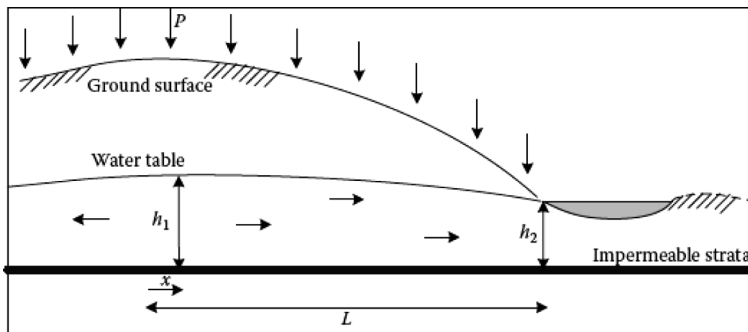


FIGURE 3.10 Definition sketch for Example 3.7.

SOLUTION

Using the Dupuit–Forchheimer assumptions and Darcy's law, velocity of water in x -direction at the highest point of the water table is:

$$V_x = -K \frac{dh}{dx}$$

dh/dx shows the slope of the water table. The rate of discharge in unit width at distance x is:

$$q_x = -Kh \frac{dh}{dx}$$

On the other hand, the rate of discharge due to infiltration, f_x , is:

$$f_x = -Kh \frac{dh}{dx} \Rightarrow -f_x dx = Kh dh$$

Integrating the above equation from the point of peak (P) to the stream flow,

$$K(h_1^2 - h_2^2) = PL^2$$

So,

$$h_1 = \sqrt{h_2^2 + \frac{PL^2}{K}}$$

Example 3.8

A wastewater treatment plant is supposed to release its effluent overland. This wastewater should be infiltrated into the land to avoid overland flow. The slope is 1%, and the soil type is sandy clay with hydraulic conductivity of 4.2 m/day. The depth of the permeable layer is 10 m (Figure 3.11). If the effluent rate is 3 cm/day, determine the length at which the effluent must be released to avoid overland flow?

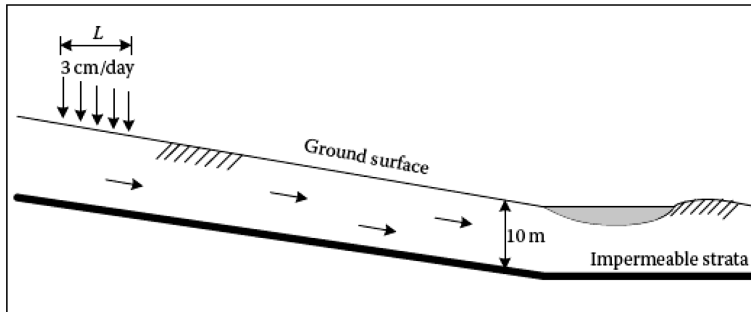


FIGURE 3.11 Definition sketch for Example 3.8.

SOLUTION

The maximum rate of groundwater flow occurs when the soil layer between the permeable strata and ground surface is totally saturated. In this condition, using the Dupuit-Forchheimer assumptions and Darcy's law, the rate of discharge in unit width is:

$$q = Kh \frac{dh}{dx} = 4.2 \times 10 \times 0.01 = 0.42 \text{ m}^2/\text{day}$$

The effluent rate is 3 cm/day, which is released over the land in length L . Hence, the rate of discharge in unit width, q , is $0.03 L$ (m^2/day). The length required to release the wastewater and avoid overland flow is:

$$0.03L = 0.42 \Rightarrow L = \frac{0.42}{0.03} = 14 \text{ m}$$

3.6 GROUNDWATER FLOW IN UNSATURATED ZONE

Groundwater flow in the unsaturated zone is described by the Richards equation, which can be derived from the continuity equation and the Darcy equation. For one-dimensional vertical flow, the continuity equation takes the following form:

$$\frac{\partial \theta}{\partial t} = -\frac{\partial q}{\partial z} - \xi \quad (3.28)$$

where:

θ is the water content [L^3L^{-3}]

q is the soil water flux [LT^{-1}]

z is the vertical space coordinate in the downward direction from the soil surface [L]

t is the time [T]

ξ is a sink term defined as soil water extraction rate [$\text{L}^3\text{L}^{-3}\text{T}^{-1}$].

Combined with the Darcy equation in the unsaturated zone as follows:

$$q = -K(\psi) \frac{\partial h}{\partial z} \quad (3.29)$$

the Richards equation (Richards, 1931) can be written as:

$$\frac{\partial \theta}{\partial t} = \frac{\partial}{\partial z} \left[K(\psi) \left(\frac{\partial \psi}{\partial z} - 1 \right) \right] - \xi \quad (3.30)$$

where:

$h = \psi - z$ is the hydraulic head [L]

ψ is the pressure head [L]

$K(\psi)$ is the unsaturated hydraulic conductivity [LT^{-1}].

The pressure head is negative in the unsaturated zone. This reflects the fact that water is held in the soil pores of the unsaturated zone under the surface tension forces. Regarding this mechanism, the negative pressure head is also called the suction head, as referred to in infiltration analysis.

As discussed earlier in [Chapter 2](#) and [Section 3.2.3.2](#), in the unsaturated zone, both the water content and unsaturated hydraulic conductivity depend on the pressure head ($\theta = \theta(\psi)$ and $K = K(\psi)$). Hence, it is also true that $K = K(\theta)$, and the water retention and unsaturated hydraulic conductivity functions represent the unsaturated soil hydraulic properties. Solution of the Richards equation requires data on the water retention and unsaturated hydraulic conductivity functions (relationships among θ , ψ , and K). Several models are proposed for this purpose. The van Genuchten-Mualem model (Mualem, 1976; Van Genuchten, 1980) is the most widely used. According to this model and considering Equation 3.13, Equation 3.12 for the unsaturated hydraulic conductivity function can be rewritten as:

$$K(\psi) = K_s \left[\frac{\theta(\psi) - \theta_r}{n - \theta_r} \right]^{0.5} \left\{ 1 - \left[1 - \left(\frac{\theta(\psi) - \theta_r}{n - \theta_r} \right)^{\frac{\lambda+1}{\lambda}} \right]^{\frac{\lambda}{\lambda+1}} \right\}^2 \quad (3.31)$$

and the water retention function can be written as:

$$\theta(\psi) = \theta_r + \frac{n - \theta_r}{\left(1 + |\alpha \psi|^{\frac{\lambda}{\lambda+1}} \right)^{\frac{\lambda}{\lambda+1}}} \quad (3.32)$$

where:

n is the porosity

θ_r is the residual water content

K_s is the saturated hydraulic conductivity

α is an air-entry parameter

λ is the pore-size index.

TABLE 3.4
Average Values of K_s , n , θ_r , α , and λ for 12 Soil Textural Classifications

| Soil Texture | K_s (cm/h) | n | θ_r | α (cm ⁻¹) | λ |
|-----------------|--------------|------|------------|------------------------------|-----------|
| Clay | 0.20 | 0.38 | 0.068 | 0.008 | 0.09 |
| Clay loam | 0.26 | 0.41 | 0.095 | 0.019 | 0.31 |
| Loam | 1.04 | 0.43 | 0.078 | 0.036 | 0.56 |
| Loamy sand | 14.59 | 0.41 | 0.057 | 0.124 | 1.28 |
| Silt | 0.25 | 0.46 | 0.034 | 0.016 | 0.37 |
| Silt loam | 0.45 | 0.45 | 0.067 | 0.020 | 0.41 |
| Silty clay | 0.02 | 0.36 | 0.070 | 0.005 | 0.09 |
| Silty clay loam | 0.07 | 0.43 | 0.089 | 0.010 | 0.23 |
| Sand | 29.70 | 0.43 | 0.045 | 0.145 | 1.68 |
| Sandy clay | 0.12 | 0.38 | 0.100 | 0.027 | 0.23 |
| Sandy clay loam | 1.31 | 0.39 | 0.100 | 0.059 | 0.48 |
| Sandy loam | 4.42 | 0.41 | 0.065 | 0.075 | 0.89 |

Source: Carsel, R.F. and Parrish, R.S., *Water Resour. Res.*, 24, 755–769, 1988.

The van Genuchten-Mualem model contains five independent parameters (n , θ_r , K_s , α , λ), which should be determined for the unsaturated zone flow model. The average values of these hydraulic parameters are given in **Table 3.4**.

Direct measurements of the hydraulic parameters are difficult. A common alternative is to parameterize hydraulic functions indirectly, using pedotransfer functions, which employ empirical correlations between the hydraulic parameters and easily obtainable soil properties such as soil texture and bulk density. There are uncertainties associated with pedotransfer functions that should be paid attention to. Refer to Wang et al. (2016) for more details. A newly proposed approach is inverse modeling, which calibrates the hydraulic parameters against flow data, such as observed water content and/or pressure head.

Example 3.9

Water is flowing at a rate of $q/K_s = -0.05$ in a 3 m long vertical unsaturated soil column under a steady-state flow situation. The water table is at the bottom of the soil column, and the unsaturated hydraulic conductivity function is given by $K(\psi) = K_s e^{\beta\psi}$, where $\beta = 5 \text{ m}^{-1}$. Calculate and plot the vertical distribution of pressure head for this column. Assume that the vertical space coordinate, z , is positive upward from the soil surface. Hence, the negative sign of q/K_s refers to the downward flux.

SOLUTION

We can write the Darcy equation for the steady-state flow as:

$$q = -K(\psi) \left[\frac{dh}{dz} \right] = -K(\psi) \left[\frac{d(\psi + z)}{dz} \right] = -K(\psi) \left[\frac{d\psi}{dz} + 1 \right] \Rightarrow \frac{d\psi}{1 + \frac{q}{K(\psi)}} = -dz$$

By integration, we have:

$$\int_{\psi_1}^{\psi_2} \frac{d\psi}{1 + \frac{q}{K(\psi)}} = - \int_{z_1}^{z_2} dz$$

So,

$$\int_{\psi(z)}^{\psi(-L)} \frac{d\psi}{1 + \frac{q}{K_s} e^{-\beta\psi}} = - \int_z^{-L} dz = L + z$$

where L is the water table depth ($\psi(-L) = 0$). We know that:

$$\int \frac{dx}{p + qe^{ax}} = \frac{x}{p} + \frac{1}{ap} \ln[p + qe^{ax}] + C$$

Therefore, with applying the appropriate boundary conditions, we have:

$$z + L = \psi(z) - \frac{1}{\beta} \ln \left[1 + \frac{q}{K_s} e^{-\beta\psi(z)} \right] + \frac{1}{\beta} \ln \left[1 + \frac{q}{K_s} \right]$$

Rearranging and log-transforming produces:

$$\psi(z) = \frac{1}{\beta} \ln \left[-\frac{q}{K_s} + e^{-\beta(L+z)} + \frac{q}{K_s} e^{-\beta(L+z)} \right]$$

Using the derived relationship and the given data, the vertical distribution of pressure head is calculated and presented in [Table 3.5](#) and [Figure 3.12](#).

Linear groundwater velocity in the unsaturated zone is related to the soil water flux by:

$$v = \frac{q}{\theta} = \frac{q}{S_w n} \quad (3.33)$$

where:

v is the linear groundwater velocity or groundwater pore velocity vector
 S_w is the degree of saturation.

TABLE 3.5
Vertical Distribution of the
Pressure Head

| $z(m)$ | $\psi(z)(m)$ |
|--------|--------------|
| 0.00 | -0.5991 |
| -0.25 | -0.5991 |
| -0.50 | -0.5991 |
| -0.75 | -0.5991 |
| -1.00 | -0.5990 |
| -1.25 | -0.5985 |
| -1.50 | -0.5971 |
| -1.75 | -0.5919 |
| -2.00 | -0.5751 |
| -2.25 | -0.5253 |
| -2.50 | -0.4112 |
| -2.75 | -0.2265 |
| -3.00 | 0.0000 |

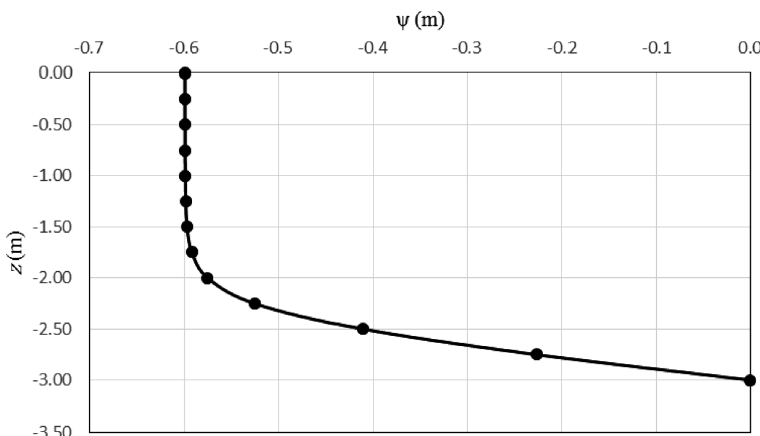


FIGURE 3.12 Vertical distribution of the pressure head.

Example 3.10

Under steady-state infiltration conditions, the degree of saturation of soil is 0.80 in an aquifer having a porosity of 0.42. The soil water flux in the unsaturated zone is 3.75 cm/h. If the thickness of the unsaturated zone is 18 m, calculate the time required for a drop of water at the ground surface to travel to the water table.

SOLUTION

$$v = \frac{3.75 \text{ cm/h}}{(0.42)(0.80)} = 11.16 \text{ cm/h}$$

$$t = \frac{1800 \text{ cm}}{11.16 \text{ cm/h}} = 161.29 \text{ h} = 6.72 \text{ days}$$

3.7 FLOWNETS

One of the simplest procedures to solve a flow equation is a graphical approach. In a graphical approach, a unique set of streamlines and equipotential lines that describe flow within a domain are sketched. The streamlines (or flowlines) indicate the path through which water moves in the aquifer. The equipotential lines represent the contours of equal head in the aquifer intersecting the streamlines. In this section, flownets in isotropic and homogeneous media as well as heterogeneous and anisotropic media are discussed and evaluated.

3.7.1 ISOTROPIC AND HOMOGENEOUS MEDIA

For steady-state conditions, the two-dimensional groundwater flow equation for an isotropic and homogeneous media is described by the Laplace equation as:

$$\frac{\partial^2 h}{\partial x^2} + \frac{\partial^2 h}{\partial y^2} = 0 \quad (3.34)$$

The Laplace equation will be discussed in detail in [Chapter 4](#). A flownet is a graphical solution to the above equation. It depicts a selected number of flowline and equipotential lines in the flow system. A quantitative and graphical solution to the groundwater flow problem is obtained from the flownet. A flownet may give the distribution of heads, discharges, areas of high (or low) velocities, and the general flow pattern. The flow channel between adjacent streamlines is called a streamtube. The equipotential lines are perpendicular to the streamtubes ([Figure 3.13](#)). The discharge in the streamtube per unit width perpendicular to the plane of the figure is:

$$\Delta Q = \alpha_2 - \alpha_1 = \Delta \alpha \quad (3.35)$$

$$q = \frac{\Delta Q}{\Delta W} = \frac{\Delta \alpha}{\Delta W} \quad (3.36)$$

Darcy's law gives:

$$q = -\frac{K \Delta h}{\Delta L} = \frac{\beta_2 - \beta_1}{\Delta L} = \frac{\Delta \beta}{\Delta L} \quad (3.37)$$

Also, taking the continuity into account:

$$q = \frac{\Delta \alpha}{\Delta W} = \frac{\Delta \beta}{\Delta L} \quad (3.38)$$

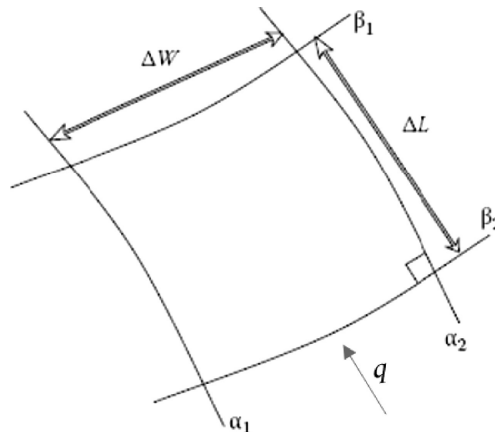


FIGURE 3.13 A flownet element of two-dimensional flow.

In the solution of a flow problem by flownet construction, the first step is to draw the two-dimensional flow domain in a way that all boundary locations, wells, etc. are considered relative to one another. A trial and error procedure is used to sketch a flownet.

To construct a flownet for an isotropic and homogeneous system, we need to sketch the streamlines and equipotential lines. Equipotential lines express the hydraulic head in the domain. These lines are perpendicular to the streamlines. The same hydraulic head drops between the equipotential lines form curvilinear squares that are formed by the streamlines and equipotential lines. These squares are described as the curved side squares that are tangent to an inscribed circle (Figure 3.14).

Assuming no inflow to/outflow from the region in the internal part of the net, the same quantity of groundwater flows between adjacent pairs of flowlines. In addition, the hydraulic head drop between two adjacent equipotential lines is the same.

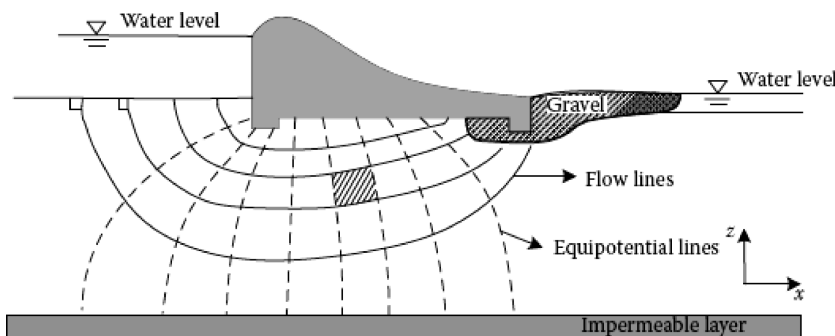


FIGURE 3.14 A flownet showing seepage under a dam.

[Figure 3.14](#) shows a flownet depicting seepage under a dam in an $x-z$ plane. In this figure, the solid lines show streamlines and dashed lines express the equipotential lines. Flow occurs because the hydraulic head of water in the pool above the dam is higher than in the pool below the dam. The flownet is a theoretical representation of flow beneath the dam. The bottom surface of the reservoir is considered as an equipotential line, which has a constant head boundary across which the flow is directed downward.

The base of the dam is a flowline. The pool below the dam receives discharge and provides another constant head boundary or another equipotential line. Because the system is isotropic and homogeneous, flowlines and equipotential lines intersect to form curvilinear squares.

Some strategies for sketching a flownet suggested by Bennett (1962) are as follows:

1. Use only four or five flow channels in a first attempt at sketching.
2. Observe the appearance of the entire flownet; do not try to adjust details until the entire net is approximately correct.
3. Take it into account that frequently parts of a flownet consist of straight and parallel lines, which result in uniformly sized true squares.
4. In a flow system that has symmetry, only a section of the net needs to be constructed because the other parts are images of that section.
5. During the sketching of the net, consider that the size of the rectangle changes gradually; all transitions are smooth, and where the paths are curved, they are of elliptical or parabolic shape.

It is very useful to keep several simple flow cases in mind before you begin studying complex flow systems. In preparing a flownet, the following rules must be taken into account:

1. A no-flow boundary is a streamline.
2. If there is no recharge or evapotranspiration, the water table is a streamline. When there is recharge, the water table is neither a flowline nor an equipotential line.
3. Streamlines end at extraction wells, drains, and gaining streams, and they start from injection wells and losing streams.
4. Streamlines divide a flow system into two symmetric parts.
5. Streamlines begin and end at the water table in areas of groundwater recharge and discharge, respectively.

Using Darcy's equation for a flow channel in a two-dimensional space,

$$\Delta Q = T \Delta h \frac{\Delta W}{\Delta L} \quad (3.39)$$

where:

ΔQ is the flow through a streamtube

T is the transmissivity of the aquifer

Δh is the hydraulic head drop between two equipotential lines

ΔW is the distance between two streamlines

ΔL is the distance between two equipotential lines ([Figure 3.13](#)).

In sketching a flownet, we always try to provide a mesh of squares. Therefore, ΔW is equal to ΔL and $\Delta W/\Delta L$ is equal to 1. If there are a total number of n_f flow channels and n_d hydraulic head drops (i.e., equipotential lines), Darcy's equation is written as:

$$Q = \frac{n_f}{n_d} T \Delta H \quad (3.40)$$

or

$$q = \frac{n_f}{n_d} K \Delta H \quad (3.41)$$

where:

Q is the total flow rate and is equal to $n_f \Delta Q$

ΔH is the total hydraulic head drop and is equal to $n_d \Delta h$

Example 3.11

The groundwater is withdrawn from an aquifer with a rate of 20,000 m³/day. Due to this withdrawal, hydraulic head drops at four equipotential lines. After sketching the flownet for this formation, it is determined that the groundwater is flowing through eight tubes. Assuming the transmissivity is 700 m²/day, determine the total hydraulic head drops.

SOLUTION

$$\Delta H = \frac{n_d Q}{T n_f} = \frac{(4)(20,000 \text{ m}^3/\text{day})}{(700 \text{ m}^2/\text{day})(8)} = 14.28 \text{ m}$$

Example 3.12

Estimate the discharge under the sheet piling shown in [Figure 3.15](#) using the flownet method. Assume that the sheet piling penetrates to 1/2 of the aquifer thickness $K = 3.2 \times 10^{-2}$ cm/s.

SOLUTION

The flownet construction is started with a vertical equipotential line, directly below the sheet piling. The upper streamline is located right in the vicinity of the sheet piling. Since it is assumed that the Darcy velocity will decrease with depth, the spacing between the streamlines is increased with depth. The equipotential line immediately adjacent to the vertical one is sketched next. In drawing these equipotential lines, the condition of orthogonality as well as the condition that each element forms a square must be taken into account. The process of drawing streamlines and equipotential lines is continued until we get to the vicinity of the terminal point. Since sketching a flownet is based on trial and error, some readjustments of both the streamlines and the equipotential lines are usually required.

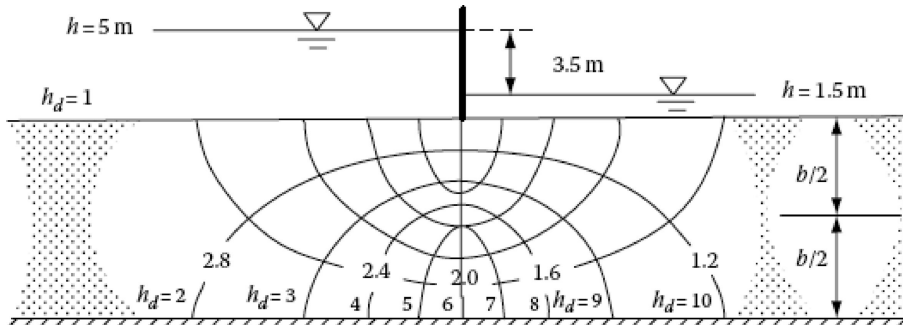


FIGURE 3.15 Flownet of seepage under a sheet pile.

From Figure 3.15, the number of streamtubes is five and the number of equipotential drops is ten. Thus, the discharge per meter of sheet pile length is:

$$Q = K \frac{n_f}{n_d} \Delta H = \frac{5}{10} 3.2 \times 10^{-4} \text{ m/day} \times 3.5 \text{ m} = 5.6 \times 10^{-4} \text{ m}^2 \text{ s}$$

3.7.2 HETEROGENEOUS MEDIA

In a heterogeneous media, the equipotential lines and the flowlines do not necessarily intersect to form squares. A constant discharge in a streamtube for two adjacent media with differing hydraulic conductivity is estimated as:

$$\Delta Q = T_1 \Delta h_1 \frac{\Delta W_1}{\Delta L_1} = T_2 \Delta h_2 \frac{\Delta W_2}{\Delta L_2} \quad (3.42)$$

If $\Delta h_1 = \Delta h_2$:

$$\frac{T_1}{T_2} = \frac{\Delta L_1 \Delta W_2}{\Delta L_2 \Delta W_1} \quad (3.43)$$

Example 3.13

Calculate the flow rate and length L_2 for the heterogeneous aquifer shown in Figure 3.16:

Assume that $\Delta W_1 = \Delta W_2 = 8 \text{ m}$, $\Delta L_1 = 10 \text{ m}$, and that the thickness of the aquifer is 150 m.

SOLUTION

$$\Delta Q = T_1 \Delta h_1 \frac{\Delta W_1}{\Delta L_1} = (85 \text{ m/day})(150 \text{ m})(1 \text{ m}) \frac{8 \text{ m}}{10 \text{ m}} = 10,200 \text{ m}^3/\text{day}$$

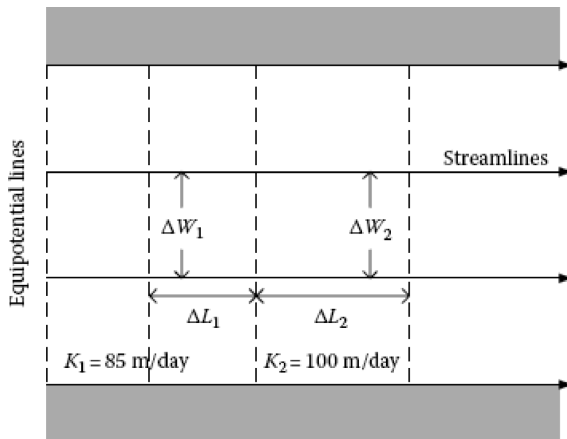


FIGURE 3.16 Definition sketch for Example 3.13.

The segment length ΔL_2 is:

$$\Delta L_2 = \frac{T_2}{T_1} \Delta L_1 = \frac{(100 \text{ m/day})(150 \text{ m})}{(85 \text{ m})(10 \text{ m})} (10 \text{ m}) = (11.76 \text{ m})$$

3.7.3 ANISOTROPIC MEDIA

In anisotropic media, there are not right angles at the interception of streamlines and equipotential lines except when flow is aligned with one of the principal directions of hydraulic conductivity or transitivity. Therefore, in an anisotropy medium, the flownet may be sketched by transforming the flow field. This procedure can be summarized as follows (Schwartz and Zhang, 2003):

1. Determine the direction of maximum transmissivity in the x -direction and the direction of minimum transmissivity in y -direction.
2. Multiply the dimension in x -direction by a factor of $(K_y/K_x)^{1/2}$. Sketch the flownet in the transformed flow domain.
3. Project the flownet back to the original dimension by dividing the x -coordinates of flownet by a factor of $(K_y/K_x)^{1/2}$.

Figure 3.17 shows a flownet in the original and transformed coordinate systems. As depicted in this figure, in the transformed system, the flownet consists of squares, while in the original system, it consists of rectangles. Flownets for seepage from one side of a channel through two different anisotropic two-layer systems are depicted in Figure 3.18.

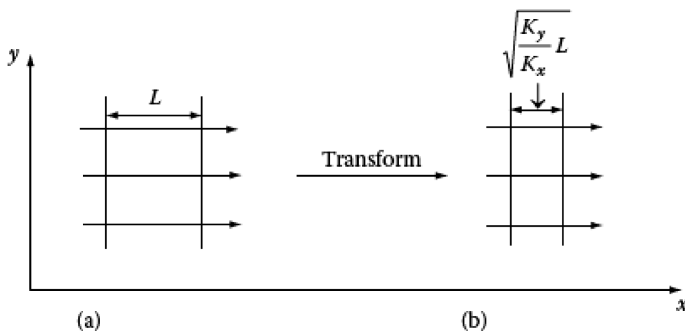


FIGURE 3.17 Flownet in anisotropic media (a) original cross section and (b) transformed cross section.

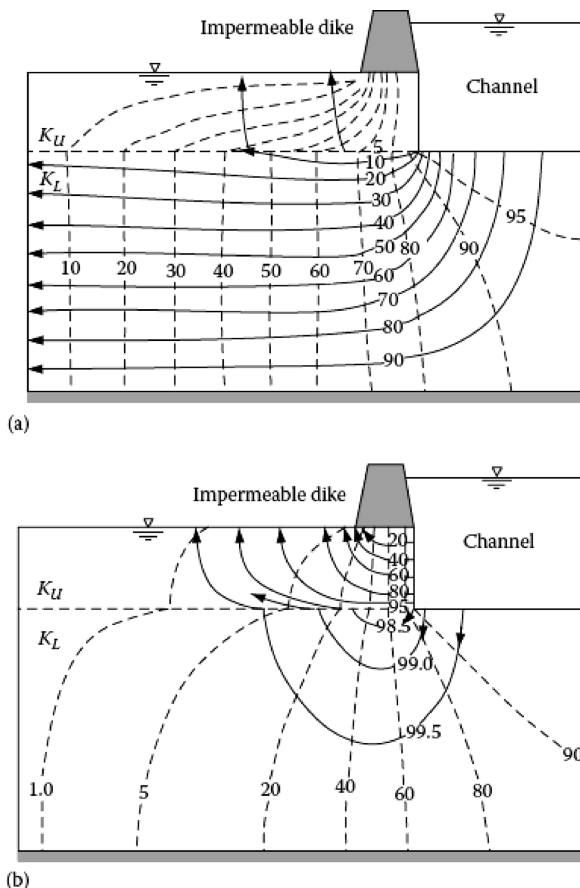


FIGURE 3.18 Flownets for seepage through two different anisotropic two-layer systems: (a) $K_v/K_L = 1/50$ and (b) $K_v/K_L = 50$. (From Todd, D. K. and Mays, L.M., *Groundwater Hydrology*, John Wiley & Sons, New York, 2005.)

3.8 STATISTICAL METHODS IN GROUNDWATER HYDROLOGY

Groundwater flows, the rate of discharges from and recharges to aquifers, and groundwater quality parameters are probabilistic time series that must be analyzed and interpreted by statistical time series analyses. A time series contains a sequence of measurements (e.g., daily water withdrawal from a well). A statistical sample contains measurements that were taken at irregular time intervals. For example, the sample may only contain data for a summer season. The simplest analyses assume that there is no correlation between individual members of the time series. In this case, it does not matter whether the data collected are a sample or a time series. All measurements that constitute a time series or a sample of a measured parameter are fitted to a probability distribution function. The most simple probability distribution function is the normal distribution, which defines the symmetric distribution of the individual members of the time series around the series mean value.

Normal distribution includes negative values, whereas the great majority of real-time series of statistical samples contain only positive numbers as well as zeros. In other words, the probability function is defined from 0 to ∞ and not from $-\infty$ to $+\infty$. Some series are skewed and not symmetrical. This is especially true for water quality and hydrologic data. Therefore, the time series data are transformed to their logarithmic values, $x = \log X$, which will yield the log-normal distribution. This transformation results in obtaining a probability distribution from zero to infinity and also resolves the problem of skewness of the data. There are some other asymmetrical probability distributions for analyzing the hydrologic data such as log-Pearson type III distribution and Gumbel distribution. Normal and lognormal distributions are explained later in this section.

3.8.1 NORMAL DISTRIBUTION

The normal distribution is a bell-shaped, symmetric distribution. It is described mathematically by its probability density function:

$$f(x) = \frac{1}{\sigma\sqrt{2\pi}} \exp\left[-\frac{(x-\mu)^2}{2\sigma^2}\right], -\infty < x < \infty, -\infty < \mu < \infty, \sigma > 0 \quad (3.44)$$

where $f(x)$ is the height (ordinate) of the curve at the value x . The density function is completely specified by two parameters, μ and σ^2 , which are the mean and variance, respectively, of the distribution. The notation $N(\mu, \sigma^2)$ is used to denote a normal probability density function (in short, normal distribution) with mean μ and variance σ^2 . The series mean is defined as:

$$\mu = \sum_1^N \frac{X_i}{N} \quad (3.45)$$

where:

X_i is an individual measurement of the time series

N is the number of members in the time series or in the sample data.

The variance is then defined as:

$$\sigma^2 = \sum_1^N \frac{(X_i - \mu)^2}{(N-1)} \quad (3.46)$$

The standard deviation is the square root of the variance, $s = \sqrt{\sigma^2}$.

Figure 3.19 shows two normal distributions. The solid curve is $N(0,1)$, and the dashed curve is $N(2,1.5)$. There is a different normal distribution for each combination of μ and σ^2 . However, they can all be transformed to the $N(0,1)$ distribution by the transformation:

$$Z = \frac{X - \mu}{\sigma} \quad (3.47)$$

Z is called a standard normal deviate.

The density function $f(x)$ and the cumulative distribution function for $aN(\mu, \sigma^2)$ distribution are depicted in Figure 3.20. The cumulative distribution function is the probability that the random variable X will take on a value less than or equal to a specified value x and is denoted by $F(x)$:

$$F(x) = \text{Prob}[X \leq x] \quad (3.48)$$

In other words, $F(x)$ gives the cumulative percentage of the normal density function that lies between $-\infty$ and the point x on the abscissa (Gilbert, 1987).

As shown in Figure 3.20, 2.15% of the density function lies above/under $\mu \pm 2\sigma$. Also, 95.44% of the density function lies between $\mu - 2\sigma$ and $\mu + 2\sigma$.

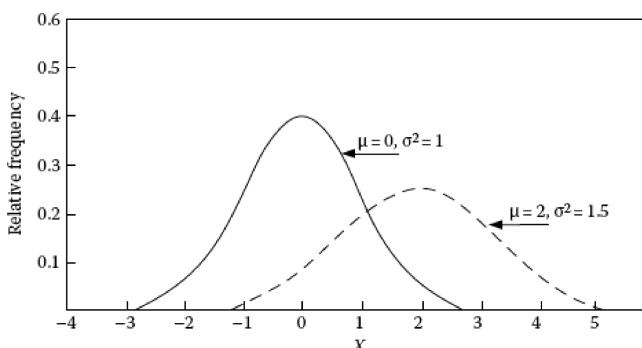


FIGURE 3.19 Two normal distributions: $N(0,1)$ and $N(2,1.5)$.

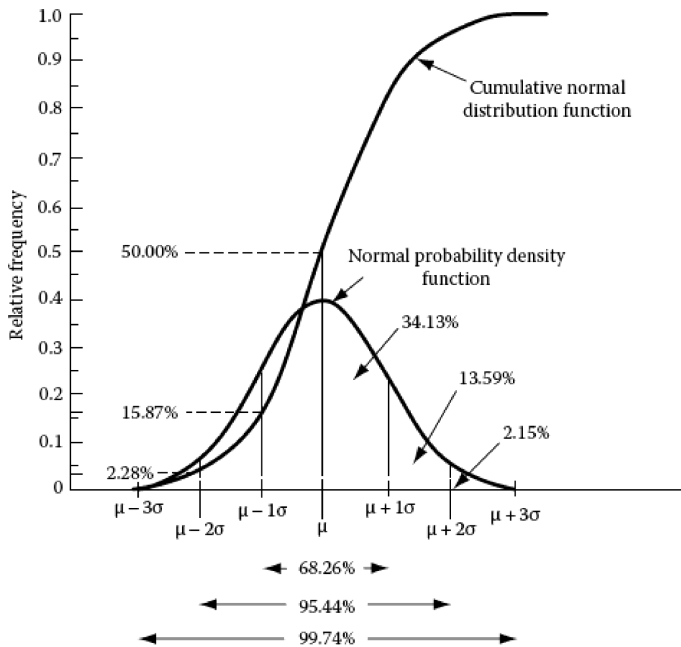


FIGURE 3.20 Areas under the normal probability density function and the cumulative normal distribution function. (From Sokal, R.R. and Rohlf, R. J., *Biometry*, W.H. Freeman, San Francisco, CA, 133 p, 1981.)

3.8.2 LOGNORMAL DISTRIBUTION

The lognormal distribution is used to model many kinds of hydrological and environmental data. Two-, three-, and four-parameter lognormal distributions can be defined. The two-parameter lognormal distribution is discussed in this section. For other lognormal distributions, please refer to statistics references. The two-parameter lognormal density function is:

$$f(x) = \frac{1}{x\sigma_y\sqrt{2\pi}} \exp\left[-\frac{1}{2\sigma_y^2}(\ln x - \mu_y)^2\right], x > 0, -\infty < \mu_y < \infty, \sigma_y > 0 \quad (3.49)$$

where μ and σ_y^2 , the two parameters of the distribution, are the true mean and variance, respectively, of the transformed random variable Y , which is equal to $\ln X$. A two-parameter lognormal distribution with parameters μ and σ^2 is expressed as $\Lambda(\mu_y, \sigma_y^2)$. Figure 3.21 shows some two-parameter lognormal distributions.

One of the most preferred methods to estimate the parameters μ and σ^2 is maximum likelihood. This method uses the following estimators:

$$\bar{y} = \frac{1}{n} \sum_{i=1}^n y_i \quad (3.50)$$

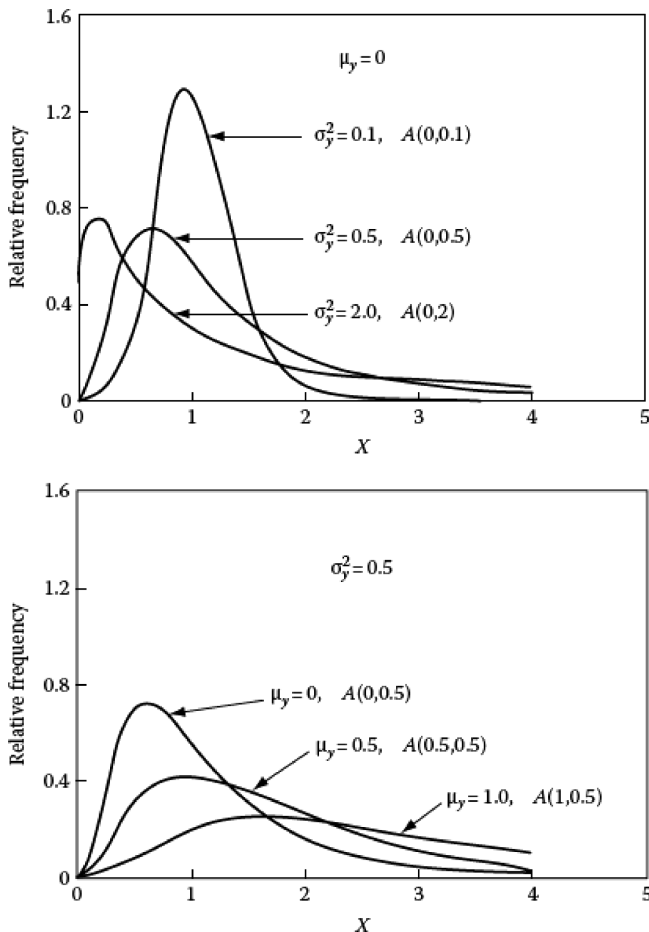


FIGURE 3.21 Lognormal distributions for different values of the parameters μ_y and σ_y^2 . (From Aitchison, J. and Brown, J.A.C., *The Lognormal Distribution*, Cambridge University Press, Cambridge, UK, 176 p, 1969.)

and

$$s_y^2 = \frac{1}{n} \sum_{i=1}^n (y_i - \bar{y})^2 \quad (3.51)$$

where $y_i = \ln x_i$. The standard deviation is then, $s_y = \sqrt{s_y^2}$.

3.8.3 *t*-DISTRIBUTION

The form of *t*-distribution is determined by a quantity called the degrees of freedom (DF), which can be calculated from the sample size, N , as $DF = N - 1$.

If the parent distribution of X is normal, the following quantity has a t -distribution with $DF = N - 1$:

$$T = \frac{N^{1/2} [m_X - \mu_X]}{S_X} \quad (3.52)$$

The t -distribution is symmetrical about its mean value, $\mu_T = 0$, and it has a variance $\sigma_T^2 = DF/DF - 2$. The quintiles of the distribution can be calculated if DF is given. **Table 3.6** gives the values for $t_{1-\alpha/2, N-1}$ for various DF . $t_{1-\alpha/2, N-1}$ is $(1 - \alpha/2)$ quantile of the t -distribution with $N - 1$ degrees of freedom.

As DF gets larger, the t -distribution approaches the standard normal distribution. If N is equal to or greater than 30, t -distribution is a good approximation even for skewed parent distributions, although T follows the t -distribution only when the parent distribution is normal (Barrette and Goldsmith, 1976).

TABLE 3.6
0.025 and 0.975 Quantiles of
 t -Distribution and χ^2 Distribution for
Different Values of Degrees of Freedom

| DF | t -Distribution | | χ^2 Distribution | |
|-----|-------------------|-----------------|-----------------------|----------------------|
| | $t_{0.025, DF}$ | $t_{0.975, DF}$ | $\chi^2_{0.025, DF}$ | $\chi^2_{0.975, DF}$ |
| 10 | -2.23 | 2.23 | 3.25 | 20.5 |
| 11 | -2.20 | 2.20 | 3.82 | 21.9 |
| 12 | -2.18 | 2.18 | 4.40 | 23.3 |
| 13 | -2.16 | 2.16 | 5.01 | 24.7 |
| 14 | -2.14 | 2.14 | 5.63 | 26.1 |
| 15 | -2.13 | 2.13 | 6.26 | 27.5 |
| 16 | -2.12 | 2.12 | 6.91 | 28.8 |
| 17 | -2.11 | 2.11 | 7.56 | 30.2 |
| 18 | -2.10 | 2.10 | 8.23 | 31.5 |
| 19 | -2.09 | 2.09 | 8.91 | 32.9 |
| 20 | -2.09 | 2.09 | 9.59 | 34.2 |
| 21 | -2.08 | 2.08 | 10.3 | 35.5 |
| 22 | -2.07 | 2.07 | 11.0 | 36.8 |
| 23 | -2.07 | 2.07 | 11.7 | 38.1 |
| 24 | -2.06 | 2.06 | 12.4 | 39.4 |
| 25 | -2.06 | 2.06 | 13.1 | 40.6 |
| 30 | -2.04 | 2.04 | 16.8 | 47.0 |
| 40 | -2.02 | 2.02 | 24.4 | 59.3 |
| 50 | -2.01 | 2.01 | 32.4 | 71.4 |
| 60 | -2.00 | 2.00 | 40.5 | 83.3 |
| 100 | -1.98 | 1.98 | 74.2 | 129.6 |

3.8.4 CHI-SQUARE (χ^2) DISTRIBUTION

The form of the χ^2 distribution also depends on the degrees of freedom. If the parent distribution of X is normal, the following quantity has a χ^2 distribution with $DF = N - 1$.

$$x^2 = \frac{(N-1)s_X^2}{\sigma_X^2} \quad (3.53)$$

The mean of the distribution is $\mu_X^2 = DF$, and its variance is $\sigma_{X^2}^2 = 2DF$. This distribution is asymmetrical. As N gets larger, the χ^2 distribution approaches the normal distribution (Yevjevich, 1972). The values of $\chi_{1-\alpha/2, N-1}^2$ for various DF are presented in [Table 3.6](#).

3.8.5 ERRORS

In general, the true values of the quintiles of hydrologic quantity populations and correlation coefficients between them are unknown. However, the true values can be estimated by taking samples from the populations and calculating the sample quintiles and correlation coefficients.

3.8.5.1 Sampling Error

Sampling error is the uncertainty inherent in these sample estimates of population quantities. It refers to the uncertainty in estimates of the population value based on the sample of finite size.

Assume that an infinite number of samples of size N are taken from a population, and the desired statistics for each sample are calculated. The value of each statistic results from functions of random variables and thus can be considered populations of random variables. Random variables are the random measured values in the sample. Each such population has a probability distribution, with its own quintiles and other statistics. These distributions, which are derived by sampling, are known as sampling distributions. Parent distribution is the underlying population from which the sample values are taken.

3.8.5.2 Standard Errors

The standard deviations of sampling distributions are called standard errors of the sample estimates. If the form of the sampling distribution is known, this information, along with the standard error, can be used to compute absolute measures of uncertainty in the form of confidence intervals.

If the parent distribution is normal, formulas for computing standard errors can be developed from a statistical theory. The theoretical standard errors are functions of the population and are inversely related to the sample size.

If the population of the sample mean, \bar{x} , has a standard deviation, S_x , the standard error of the mean is calculated as:

$$S_x = \frac{S}{N^{1/2}} \quad (3.54)$$

If the data are approximately normally distributed, the standard error of the sample standard deviation, S_s , can be calculated as (Yevjevich, 1972):

$$S_s = \frac{S}{(2N)^{1/2}} \quad (3.55)$$

3.8.6 ESTIMATING QUANTILES (PERCENTILES)

Quintiles of distributions are estimated to determine whether hydrologic data or environmental pollution levels exceed specified limits. For instance, a regulation may require that the true 0.98 quintile of the maximum discharge from a well, $x_{0.98}$, must not exceed 2 m³/day. In practice, x_p must be estimated from data. There are two methods for estimating x_p when a normal or lognormal distribution is underlying the data. These methods are the probability plotting method and the parametric method. For the procedure of the probability plotting method, the reader is referred to statistical methods books such as Gilbert (1987), Price et al. (1981), etc. We discuss the parametric and nonparametric methods in this section.

In the nonparametric method, there is no need for an underlying distribution. The data are first ranked from the smallest to the largest. The rank of $(100p)$ th percentile is then:

$$M = p(N + 1) \quad (3.56)$$

where:

M is the ascending order of magnitude

N is the number of data points

p is the fraction of the population below percentile of interest.

In other words, p is the nonexceedance probability, p can then be calculated as:

$$p(\%) = M(N + 1) \quad (3.57)$$

The median corresponds to 50% value.

Example 3.14

What is the rank of the 90th percentile of 10 observations? What is the 95th percentile of these observations?

SOLUTION

For the 90th percentile, $p = 0.9$, $M = (0.9)(10 + 1) = 9.9$. The 90th percentile is then calculated by interpolation between the 9th and 10th largest observations.

For the 95th percentile, $p = 0.95$, $M = (0.95)(10 + 1) = 10.45$!!!

We cannot estimate the 95th percentile with only 10 observations using these estimators. For extreme percentiles, we need to have a sufficiently large sample size.

An alternative estimator is $M = pN$; but it will not provide estimates as good as those from the other estimator.

Quantiles of a normal distribution, \hat{x}_p , can be estimated by using the sample mean, \bar{x} , and standard deviation, s , as:

$$\hat{x}_p = \bar{x} + Z_p s \quad (3.58)$$

where Z_p is the p th quintile of the standard normal distribution. In [Appendix Table 3.A1](#) gives values of p that correspond to Z_p .

Quantiles of a two-parameter lognormal distribution are also computed by:

$$\hat{x}_p = \exp(\bar{y} + Z_p s_y) \quad (3.59)$$

where \bar{y} and s_y are the estimates of μ_y and σ_y , respectively.

Example 3.15

In an aquifer, the mean of the logs of the annual rate of base flow from the aquifer through a surface stream is 0.25 (log of m^3/day). The standard deviation of the logs is 0.075 (log of m^3/day). Calculate the 90th percentile if a lognormal distribution is underlying the data.

SOLUTION

From [Table 3.A1](#), $Z_{0.90} = 1.282$:

$$Q_{90\%} = \exp(0.25 + 1.282 \times 0.075) = 1.41 \text{ m}^3/\text{day}$$

Example 3.16

The daily water withdrawal from a well is presented in the second column of the following table. Calculate the arithmetic and logarithmic mean of the data. Also, determine a value that would have a 95% probability of not being exceeded ($p[X \leq X_n] = 0.95$).

SOLUTION

In the following table, columns (1) and (2) are given. We calculate columns (3) through (5).

Using [Table 3.A1](#), $Z_{0.95} = 1.645$. The 95% probability of not being exceeded is then calculated as:

$$X_{0.95} = 10^{\mu_y + Z_p s_y} = 10^{0.2516 + 1.645 \times 0.269} = 4.94 \text{ m}^3/\text{day}$$

3.8.7 PROBABILITY/FREQUENCY/RECURRENCE INTERVAL

Hydrologic and water quality analysis reports express the extreme values in terms of probabilities of excellence, frequency of occurrence, and recurrence interval/return

period. All three terms have the same meaning. Since we deal with a time series, the probability can be converted to an average time between two occurrences of the extreme value, called the recurrence interval (Novotny, 2003).

Assume that we have a 10-year time series of a hydrologic parameter, which is measured based on a monthly basis. The total number of data is therefore $10 \times 12 = 120$.

Analyses show that the mean and standard deviation of the data are 150 and 48, respectively. A value of the series that would have a probability of 5% of being exceeded (95% of cumulative probability of being less than or equal to) is then:

$$X(p[X \geq X_n] = 5\%) = \mu + Z_p \sigma = 150 + 1.64 \times 48 = 228.7$$

The recurrence interval between two occurrences of measurements that would equal or exceed 228.7 is then a reciprocal of the probability multiplied by the sampling interval:

$$T_r = \frac{100}{p(\%)} (\Delta t) = \frac{100}{5} (1 \text{ month}) = 20 \text{ months}$$

The frequency is then simply a reciprocal of the recurrence interval—the measurements that would equal or exceed 228.7 will occur approximately once in 10 months

3.9 TIME SERIES ANALYSIS

To develop appropriate operation policies for water resources systems that are applicable to real-time decision-making, forecasting the future state of the resources is necessary. For instance, consider a well field, which supplies water for agricultural and domestic needs in an area. The amount of scheduled withdrawal depends on the probable range of inflow to the aquifer. Considering the fact that there is a sound lack of adequate knowledge about physical processes in the hydrologic cycle, the application of statistical models in forecasting and generating synthetic data have been expanded by researchers.

In this section, basic principles of hydrologic time series modeling and different types of statistical models are discussed. More details on statistical modeling can be found in Salas et al. (1988) and Brockwell and Davis (1987).

3.9.1 NONSTATIONARY HYDROLOGIC VARIABLES

Due to variations that are the result of natural and human activities, the hydrologic variables are mostly nonstationary. These variations in hydrologic modeling are classified as follows (Karamouz et al., 2003):

1. *Trend* is a gradual change (increasing or decreasing) in the average value of the variable. Trend is unidirectional and is mainly caused by anthropogenic changes in nature (changes in nature as a result of human activities).

A trend, T , is represented by a continuous and differentiable function of time. It can be modeled by different linear and polynomial functions such as:

- Linear function: $T_t = a + bt$
- Polynomial function: $T_t = a + bt + ct^2 + \dots + dt^m$
- Power functions: $T_t = a - br^t$ ($0 < r < 1$) and $T_t = 1/(a + br^t)$ ($0 < r < 1$)

2. *Jump* is a sudden change in the observed values that can be positive or negative. The main reasons for jumps in a hydrologic series are natural disruptions and human activities.
3. *Periodicity* can be defined as the cyclic variations in the hydrologic time series. These variations are usually repeated over the same intervals of time.
4. *Randomness* is the variation due to uncertainties of natural processes. The random component of the hydrologic time series is classified as autoregressive or purely random.

In statistical modeling of a time series, it is assumed that the time series is purely random. Therefore, all trends, jumps, and periodicities must be removed from the time series.

3.9.2 HYDROLOGIC TIME SERIES MODELING

The following steps are involved in a systematic approach to hydrologic time series modeling (Salas et al., 1988):

- *Data preparation*: Removing trends, periodicity, outlying observations, and fitting the data to a proper distribution.
- *Identification of model composition*: Different compositions for model selection are univariate model, multivariate model, and a combination of each of these models with disaggregation models. Based on the characteristics of the water resources system and existing information, it is identified that which composition is better to be used.
- *Identification of model type*: Different types of models mostly used in hydrologic studies are autoregressive (AR), autoregressive moving average (ARMA), and autoregressive integrated moving average (ARIMA). These models will be discussed in detail later in this chapter. The appropriate type of model is selected due to statistical characteristics of the time series and the modeler input and knowledge about different types of models.
- *Identification of model form*: The statistical characteristics of the time series determine the form of the selected model. The periodicity of the data and how it can be considered in the model is the main issue in this step.
- *Estimation of model parameters*: There are different methods for parameter estimation, such as method of moments and method of maximum likelihood. These methods will be discussed later in this chapter.

- *Testing the goodness of fit of the model:* In this step, different assumptions such as independence and normality of residuals should be checked.
- *Evaluation of uncertainties:* The uncertainties in the model and its parameters as well as natural uncertainties in measured data should be evaluated separately.

3.9.3 DATA PREPARATION

As mentioned before, data preparation involves removing trend, removing outlying observations, removing periodicity, and fitting the data to a proper distribution. In using statistical models for a hydrologic time series, considering the variable as a pure random variable is the principal assumption. Therefore, if the series contains unnatural components such as synthetic recharge of an aquifer, they should be first removed. The time sequence plot of the series is usually used to detect trend and seasonality. For instance, consider a nonseasonal series, x_t , which contains trend component as follows:

$$x_t = T_t + z_t \quad (3.60)$$

where T and z_t are the trend and random components, respectively. The trend components are defined as a function of time as:

$$T_t = f(t, \dots, t^m, \beta_1, \dots, \beta_m) \quad (3.61)$$

where β_1, \dots, β_m are the parameters to be estimated. These parameters can be estimated based on the least square method by minimizing the following sum:

$$\sum_t (x_t - T_t)^2 \quad (3.62)$$

To estimate β_1, \dots, β_m , the partial derivatives of the above sum with respect to each unknown parameter, β_1, \dots, β_m , are equated to zero. The random series is then generated using Equation 3.60.

Example 3.17

A series of annual water withdrawal from a well to supply agricultural demands for a period of 10 years is shown in [Table 3.7](#). Estimate a linear trend function and generate the random series of water withdrawals by removing the trend.

SOLUTION

The linear trend function is:

$$T_t = \alpha t + \beta \quad (3.63)$$

In least square method the following sum should be minimized:

$$\sum_{t=1}^{10} (x_t - T_t)^2 = \sum_{t=1}^{10} (x_t - \alpha t - \beta)^2$$

TABLE 3.7
Annual Water Withdrawals in a City
in Example 3.17

| Year | Water Withdrawals (MCM/Year) |
|------|------------------------------|
| 1 | 44 |
| 2 | 56 |
| 3 | 52 |
| 4 | 48 |
| 5 | 61 |
| 6 | 55 |
| 7 | 65 |
| 8 | 43 |
| 9 | 63 |
| 10 | 49 |

TABLE 3.8
Random Components of Annual Water Withdrawals—Example 3.17

| Year | Water Withdrawals (MCM/Year) | Trend Component | Random Component |
|------|------------------------------|-----------------|--------------------|
| 1 | 44 | 51.04 | 44 – 51.04 = –7.04 |
| 2 | 56 | 51.61 | 4.39 |
| 3 | 52 | 52.18 | –0.18 |
| 4 | 48 | 52.75 | –4.75 |
| 5 | 61 | 53.32 | 7.68 |
| 6 | 55 | 53.88 | 1.12 |
| 7 | 65 | 54.45 | 10.55 |
| 8 | 43 | 55.02 | –12.02 |
| 9 | 63 | 55.59 | 7.41 |
| 10 | 49 | 56.16 | –7.16 |

α and β can be calculated as:

$$\alpha = \frac{10 \sum_{t=1}^{10} t x_t - \sum_{t=1}^{10} t \sum_{t=1}^{10} x_t}{10 \sum_{t=1}^{10} t^2 - \left(\sum_{t=1}^{10} t \right)^2} = 0.57$$

$$\beta = \bar{x} - \bar{t}\bar{x} = 50.47$$

The random component after removing the trend is shown in [Table 3.8](#).

The above method is called the classical decomposition of the series into a trend component, a seasonal component, and a random component. There is another method for removing the trend and seasonality, which is widely used in modeling of

a hydrologic time series. This method is called differencing method. In this method, the first differencing operator, ∇ , is:

$$\nabla(x_t) = x_t - x_{t-1} = (1 - B)x_t \quad (3.64)$$

where B is the backward shift operator and is defined as:

$$B(x_t) = x_{t-1} \quad (3.65)$$

Higher orders of the operators B and ∇ can be defined as:

$$B^j(x_t) = x_{t-j} \quad \text{and} \quad \nabla^j(x_t) = \nabla(\nabla^{j-1}(x_t)), j \geq 1 \quad (3.66)$$

Applying the first-order difference operator to the linear trend function gives the constant function $\nabla(T_t) = \alpha$. Similarly, any polynomial trend of degree k can be reduced to a constant by application of the operator ∇^k . Hence, if a hydrologic time series has a polynomial trend such as:

$$T_t = \sum_{i=0}^m a_i t^i \quad (3.67)$$

and its operator can be written as:

$$\nabla^m(x_t) = m! a_m + \nabla^m z_t \quad (3.68)$$

In most of the parameter estimation methods, it is assumed that the time series fits a normal distribution. But in many cases, the hydrologic time series do not follow normal distribution, and so it is necessary to transform those variables to normal or lognormal before statistical modeling. The mostly used variable transformation is the two-parameter transformation developed by Box and Cox (1964). This transformation is:

$$z_t = \frac{(x_t + \lambda_2)^{\lambda_1} - 1}{\lambda_{1g}^{(\lambda_1-1)}}, \lambda_1 > 0 \quad (3.69)$$

and

$$z_t = g \ln(x_t + \lambda_2), \lambda_1 = 0 \quad (3.70)$$

where:

λ_1 and λ_2 are the model parameters

g is the geometric mean of $x_t + \lambda_2$

x_t and z_t are the original and transformed series, respectively.

The parameter λ_1 controls the strength of the transformation. $\lambda_1 = 1$ corresponds to the original data, and $\lambda_1 = 0$ to a logarithm. Since the values are scaled by the geometric mean to keep the variance constant in this transformation, mean squared errors between two different transformations can be compared.

Hashino and Delleur (1981) developed another transformation similar to Box and Cox as:

$$z_t^{(\lambda)} = \frac{(x_t + c) - 1}{\lambda}, \lambda \neq 0 \quad (3.71)$$

and

$$z_t^{(\lambda)} = \ln(x_t + c), \lambda = 0 \quad (3.72)$$

where λ and c are similar to λ_1 and λ_2 in the Box–Cox transformation. In this transformation, the values are not scaled and therefore are not allowing for the direct comparison of mean squared errors between two different transformations.

3.9.4 PARAMETER ESTIMATION

The basic methods for estimating model parameters are methods of moments, L-Moments, least squares, and maximum likelihood. These methods are discussed in the following.

3.9.4.1 Method of Moments

Consider a sample x_1, \dots, x_N . The n th sample moment is defined as follows:

$$M_n = \left(\frac{1}{N} \right) \sum_{i=1}^N x_i^n \quad (3.73)$$

When a model is fitted to a sample of data as Equation 3.74, the moment parameter estimation can be obtained by equating sample moments and population moments.

$$\hat{x}_i = f(x_{i-1}, x_{i-2}, \dots, \alpha_1, \alpha_2, \dots, \alpha_m) + \varepsilon_i \quad (3.74)$$

where ε_i is the model residual and $\alpha_1, \alpha_2, \dots, \alpha_m$ are the model parameters. Then the moments method performs as follows:

$$M_n = \left(\frac{1}{N} \right) \sum_{i=1}^N (x_i - c)^n = \left(\frac{1}{N} \right) \sum_{i=1}^N (f(x_{i-1}, x_{i-2}, \dots, \hat{\alpha}_1, \hat{\alpha}_2, \dots, \hat{\alpha}_m) - c)^n \quad (3.75)$$

$$\forall n = 1, \dots, m,$$

where m is the number of model parameters.

Example 3.18

Assume that the following model is fitted to the sample x_1, \dots, x_N :

$$x_t = \alpha z_t + \beta$$

where:

z_t is an independent random variable with mean zero and variance one
 α and β are the model parameters.

Estimate the model parameters with the method of moments.

SOLUTION

The first and second sample moments can be estimated as:

$$M_1 = \left(\frac{1}{N} \right) \sum_{i=1}^N x_i \quad \text{and} \quad M_2 = \left(\frac{1}{N} \right) \sum_{i=1}^N x_i^2$$

The first two population moments of the model are:

$$M_1 = \left(\frac{1}{N} \right) \sum_{i=1}^N x_i = \frac{1}{N} \sum_{i=1}^N ((\alpha z_i + \beta)) = \frac{\alpha}{N} \left(\sum_{i=1}^N z_i \right) + \frac{1}{N} \sum_{i=1}^N \beta = \alpha \times \mu_z (= 0) + \frac{N\beta}{N} = \beta$$

and

$$\begin{aligned} M_2 &= \left(\frac{1}{N} \right) \sum_{i=1}^N x_i^2 = \frac{1}{N} \sum_{i=1}^N (\alpha z_i + \beta)^2 = \frac{1}{N} \left(\sum_{i=1}^N \alpha^2 z_i^2 + 2\alpha\beta z_i + \beta^2 \right) \\ &= \alpha^2 \times \sigma_z (= 1) + 2\alpha\beta\mu_z (= 0) + \beta^2 = \alpha^2 + \beta^2 \end{aligned}$$

By equating the first population and sample moments:

$$\hat{\beta} = \left(\frac{1}{N} \right) \sum_{i=1}^N x_i$$

which is an estimate of the parameter β . And the estimate of parameter α is obtained by equating the second moment as:

$$\hat{\alpha} = \sqrt{\frac{1}{N} \sum_{i=1}^N x_i^2 - \hat{\beta}^2}$$

3.9.4.2 Method of L-Moments

L-moments are a sequence of statistics used to summarize theoretical probability distributions and observed samples. They are linear combinations of order statistics (L-statistics) analogous to ordinary moments, which are able to calculate quantities of standard deviation, skewness, and kurtosis. L-moment computes these quantities from the linear combinations of ordered values in the terms of L-scale,

L-skewness, and L-kurtosis, respectively. The advantages of the L-moment method are as follows (Central Water Commission, 2010):

- Wider range of probability distributions could be characterized.
- Less sensitive to outlier data points.
- Less sensitive to sample sizes and populations.
- Better approximation of asymptotic normal distribution.

The method of L-moments are particularly useful in providing accurate quantile estimates of hydrological data in developing countries, where small sample sizes typically exist.

According to Hosking (1990), for a random variable X, the $(r + 1)$ th L-moment is defined as:

$$l_{r+1} = \sum_{k=0}^r \frac{(-1)^{r-k} (r+k)!}{(K!)^2 (r-K)!} b_k \quad (3.76)$$

where l_{r+1} is the $(r + 1)$ th sample moment and b_k is an unbiased estimator with:

$$b_k = N^{-1} \sum_{i=k+1}^N \frac{(i-1)(i-2)\dots(i-K)}{(N-1)(N-2)\dots(N-K)} Q_{iN} \quad (3.77)$$

where Q_{iN} is a conceptual random sample of size N in which $Q_{iN} \leq Q_{2N} \leq \dots \leq Q_{NN}$.

3.9.4.3 Method of Least Squares

Consider that the following model is fitted to the sample x_1, \dots, x_N :

$$\hat{x}_t = f(x_{t-1}, x_{t-2}, \dots, \alpha_1, \alpha_2, \dots, \alpha_m) + \varepsilon_t \quad (3.78)$$

where:

ε_t is the model residual

$\alpha_1, \alpha_2, \dots$, and α_m are the model parameters

In the least square method, the following must be minimized:

$$\sum_{t=1}^N (x_t - \hat{x}_t)^2 = \sum_{t=1}^N \left(x_t - f(x_{t-1}, x_{t-2}, \dots, \hat{\alpha}_1, \hat{\alpha}_2, \dots, \hat{\alpha}_m) \right)^2 \quad (3.79)$$

In this method, all partial derivatives with respect to the estimated values of the parameters, $\hat{\alpha}_1, \hat{\alpha}_2, \dots, \hat{\alpha}_m$, should be equated to zero. Therefore,

$$\frac{\partial \sum_{t=1}^N (x_t - \hat{x}_t)^2}{\partial \hat{\alpha}_1} = 0, \dots, \frac{\partial \sum_{t=1}^N (x_t - \hat{x}_t)^2}{\partial \hat{\alpha}_m} = 0 \quad (3.80)$$

These equations are solved simultaneously to estimate the model parameters, $\hat{\alpha}_1, \hat{\alpha}_2, \dots, \hat{\alpha}_m$.

Example 3.19

Find the model parameter, α , using the least square method for the following model which is used for the sample x_1, \dots, x_N :

$$x_t = \alpha x_{t-1} + \varepsilon_t$$

SOLUTION

The square of errors is:

$$\sum \varepsilon_t^2 = \sum (x_t - \alpha x_{t-1})^2$$

The partial derivatives of the sum with respect to α is:

$$\frac{\partial \sum (x_t - \alpha x_{t-1})^2}{\partial \alpha} = \sum 2(x_{t-1}(\alpha x_{t-1} - x_t))$$

Therefore, the parameter is estimated as:

$$\alpha = \frac{\sum x_t x_{t-1}}{\sum x_{t-1}^2}$$

3.9.4.4 Method of Maximum Likelihood

The likelihood function is expressed as:

$$L(\varepsilon) = \prod_{t=1}^N f(\varepsilon_t, \alpha_1, \dots, \alpha_m) \quad (3.81)$$

To simplify the calculations, it is desirable to transform the multiplication operation to an addition operation. In this method, log of the function is taken to convert the operations. The log-likelihood function will then be maximized. By maximizing the function $L(\varepsilon)$, the maximum likelihood of the parameters, α_1, \dots , and α_m , is obtained:

$$\log(L(\varepsilon)) - \ln \prod_{t=1}^N f(\varepsilon_t, \alpha_1, \dots, \alpha_m) = \sum_{t=1}^N \ln [f(\varepsilon_t, \alpha_1, \dots, \alpha_m)] \quad (3.82)$$

Partial derivatives with respect to the parameters, α_1, \dots , and α_m , will then be equated to zero to maximize the above sum:

$$\frac{\partial \log(L(\varepsilon))}{\partial \alpha_1} = 0, \dots, \frac{\partial \log(L(\varepsilon))}{\partial \alpha_m} = 0 \quad (3.83)$$

The maximum likelihood estimate of the parameters can be obtained by simultaneously solving the above equations.

Example 3.20

Assume that the following model is fitted to the sample x_1, \dots , and x_N :

$$x_t = \beta z_t + \alpha$$

where:

z_t is an independent random variable with mean zero and variance one
 α and β are the model parameters.

Estimate the model parameters with the maximum likelihood method.

SOLUTION

When using the maximum likelihood method, it is assumed that the x time series follows the normal probability distribution as follows:

$$f(x_i | z_i) = \frac{1}{\sigma \sqrt{2\pi}} \times e^{-\frac{[x_i - (\alpha + \beta z_i)]^2}{2\sigma^2}}$$

where z_i is the independent variable. Thus, the maximum likelihood function would be equal to:

$$\log L = -n \times \log \sigma - \frac{n}{2} \times \log 2\pi - \frac{1}{2\sigma^2} \times \sum_{i=1}^n [x_i - (\alpha + \beta z_i)]^2$$

The parameters α , β , and σ are obtained based on taking the partial derivatives of the above equation with respect to these parameters:

$$\frac{\partial \log L}{\partial \alpha} = \frac{1}{\sigma^2} \times \sum_{i=1}^n [x_i - (\alpha + \beta z_i)] = 0$$

$$\frac{\partial \log L}{\partial \beta} = \frac{1}{\sigma^2} \times \sum_{i=1}^n z_i [x_i - (\alpha + \beta z_i)] = 0$$

$$\frac{\partial \log L}{\partial \sigma} = -\frac{n}{\sigma} + \frac{1}{\sigma^3} \times \sum_{i=1}^n [x_i - (\alpha + \beta z_i)]^2 = 0$$

which results in the following parameters:

$$\hat{\alpha} = \frac{\left(\sum_{i=1}^n z_i^2 \right) \left(\sum_{i=1}^n x_i \right) - \left(\sum_{i=1}^n z_i \right) \left(\sum_{i=1}^n x_i z_i \right)}{n \left(\sum_{i=1}^n z_i^2 \right) - \left(\sum_{i=1}^n z_i \right)^2}$$

$$\hat{\beta} = \frac{n \left(\sum_{i=1}^n x_i z_i \right) - \left(\sum_{i=1}^n x_i \right) \left(\sum_{i=1}^n z_i \right)}{n \left(\sum_{i=1}^n z_i^2 \right) - \left(\sum_{i=1}^n z_i \right)^2}$$

3.9.5 GOODNESS OF FIT TESTS

Two of the most common test statistics for the goodness of fit are the chi-square, χ^2 , test for testing the hypothesis of goodness of fit of a given distribution, and the Smirnov-Kolmogorov statistic for estimating maximum absolute difference between the cumulative frequency curve of the sample data and the fitted distribution function. The chi-square test is explained here, and the reader is encouraged to check Salas et al. (1988) for the other test.

Lapin (1990) suggested the following steps for hypothesis testing:

1. Formulate the null hypothesis, H_0 , which usually is that the data represent a specific distribution.
2. Select the test procedure, such as chi-square, and test statistic.
3. Select the significance/acceptance level.
4. Compute the value of the test statistic for the sample data.
5. Find the corresponding critical value for χ^2 from the χ^2 distribution table.
6. Compare the obtained value of χ^2 with the critical value. If the former is smaller than the latter one, the null hypothesis of fitness of the selected distribution is accepted. Otherwise, it is rejected.

3.9.5.1 Chi-Square Goodness of Fit Test

This test is based on the comparison of two sets of frequencies. To accomplish this test, the data are first divided into a number of categories. Then the actual frequencies (f_i) in each category (class) is compared with the expected frequencies, (\hat{f}_i), which are estimated based on the fitted distribution. The test statistic is estimated as:

$$\chi^2 = \sum_{i=1}^{NC} \frac{(f_i - \hat{f}_i)^2}{\hat{f}_i} \quad (3.84)$$

where:

i is the number of classes

NC is the total number of categories.

This estimation is close enough for testing the goodness of fit whenever the expected frequency in any category is equal to or greater than 5. χ^2 is the chi-square distributed with $NC - NP - 1$ degrees of freedom, where NP is the number of parameters to be estimated.

Example 3.21

A well field is used as a supplementary source of water to supply the water demands of an urban area in dry periods, i.e., when there is the deficit of surface water. The classified monthly withdrawal data, which are divided into nine categories is presented in [Table 3.9](#). Previous studies show that the withdrawal data

TABLE 3.9
Withdrawal Data in Example 3.21

| Interval (i) | Withdrawal Data Classes (MCM) | Actual Frequency (f _i) |
|--------------|-------------------------------|------------------------------------|
| 1 | $0 \leq D_w < 5$ | 38 |
| 2 | $5 \leq D_w < 10$ | 26 |
| 3 | $10 \leq D_w < 15$ | 12 |
| 4 | $15 \leq D_w < 20$ | 10 |
| 5 | $20 \leq D_w < 25$ | 8 |
| 6 | $25 \leq D_w < 30$ | 3 |
| 7 | $30 \leq D_w < 35$ | 2 |
| 8 | $35 \leq D_w < 40$ | 1 |
| 9 | $40 \leq D_w$ | 0 |

in this well field are exponentially distributed. Therefore, the probability of the monthly withdrawal, D_w , is equal to or below x and is expressed as:

$$\text{Prob}[D_w \leq x] = 1 - e^{-\lambda x}$$

where λ is estimated to be equal to 0.105. Use the chi-square test with 5% significance level to test whether the selected distribution fits the sample data.

SOLUTION

Using the given exponential distribution, the expected frequencies are computed and presented in the third column of [Table 3.10](#). For example, for the first class of the data, the probability of withdrawing less than 5 million cubic meteres (MCM) water from the well is:

$$\text{Prob}[D_w < 5] = 1 - e^{-0.105 \times 5} = 0.41$$

This value is then multiplied by 100 for the first interval. The resulting value is presented in the fourth column of [Table 3.10](#). From the second interval on, the expected frequencies are estimated based on the difference between cumulative probabilities multiplied by 100. For example, for the second interval,

$$\text{Expected frequency} = (0.65 - 0.41) \times 100 = 24$$

The actual frequency for the intervals six to nine in [Table 3.10](#) is less than 5. Therefore, these classes can be grouped together. The chi-square statistic is then estimated as 2.73. The degree of freedom for the test is $6 - 1 - 1 = 4$. From [Appendix Table 3.A2](#), for 5% significance level and four degrees of freedom, the critical value is $\chi^2_{0.05(4)} = 9.488$. Since, the estimated value of the test statistics, 2.73, is smaller than the critical value, 9.488, the null hypothesis that the monthly precipitation is exponentially distributed is accepted.

TABLE 3.10
Estimated Expected Frequencies and Chi-Square Statistic for the Withdrawal Data—Example 3.21

| Interval (i) | Actual Frequency (f_i) | Exponential Cumulative Probability at Upper Limit | Expected Frequencies (\hat{f}_i) | Actual Frequency (f_i) | $f_i - \hat{f}_i$ | χ^2 |
|------------------|----------------------------|---|--------------------------------------|----------------------------|-------------------|----------|
| 1 | 38 | 0.41 | 41 | 38 | -3 | 0.22 |
| 2 | 26 | 0.65 | 24 | 26 | 2 | 0.17 |
| 3 | 12 | 0.79 | 14 | 12 | -2 | 0.29 |
| 4 | 10 | 0.88 | 9 | 10 | 1 | 0.11 |
| 5 | 8 | 0.93 | 5 | 8 | 3 | 1.8 |
| 6 | 3 | 0.96 | 3 | 3 | -1 | 0.14 |
| 7 | 2 | 0.97 | 1 | 2 | | |
| 8 | 1 | 0.99 | 2 | 1 | | |
| 9 | 0 | 1 | 1 | 0 | | |
| Sum | 100 | 1 | 100 | | | 2.73 |

3.9.5.2 Tests of Normality

There are different ways to test the normality of a time series. The graphical test is the most widely used test to check the hypothesis that the time series of interest is normal. In this test, the empirical distribution of the series is plotted on a normal probability paper. Then it is checked if the plotted points fit a straight line. The chi-square test is another widely used method for testing the normality of data. Another common normality test is the skewness test. The skewness coefficient of a time series x_t is estimated as follows:

$$\hat{\gamma} = \frac{1/N \sum_{t=1}^N (x_t - \bar{x})^3}{\left[1/N \sum_{t=1}^N (x_t - \bar{x})^2 \right]^{3/2}} \quad (3.85)$$

where:

$\hat{\gamma}$ is the skewness coefficient

N is the total number of sample data

\bar{x} is the sample mean.

This test is based on the fact that the skewness coefficient of a normal variable is zero. If the series is normally distributed, the mean and variance of the skewness coefficient are zero and $6/N$, respectively (Snedecor and Cochran, 1967). $(1 - \alpha)$ probability limits on γ could be defined as:

$$\left[-Z_{1-\alpha/2} \sqrt{\frac{6}{N}}, Z_{1-\alpha/2} \sqrt{\frac{6}{N}} \right] \quad (3.86)$$

TABLE 3.11
Values of Skewness Coefficient
for Normality for Sample Sizes
Less than 150

| N | $\alpha = 0.02$ | $\alpha = 0.01$ |
|-----|-----------------|-----------------|
| 25 | 1.061 | 0.711 |
| 30 | 0.986 | 0.662 |
| 35 | 0.923 | 0.621 |
| 40 | 0.870 | 0.587 |
| 45 | 0.825 | 0.558 |
| 50 | 0.787 | 0.534 |
| 60 | 0.723 | 0.492 |
| 70 | 0.673 | 0.459 |
| 80 | 0.631 | 0.432 |
| 90 | 0.596 | 0.409 |
| 100 | 0.567 | 0.389 |
| 125 | 0.508 | 0.350 |
| 150 | 0.464 | 0.321 |
| 175 | 0.430 | 0.298 |

Source: Snedecor, G.W. and Cochran, W.G.,
Statistical Methods, Iowa State
 University Press, Ames, IA, 1967.

where $z_{1-\alpha/2}$ is the $1 - \alpha/2$ quantile of the standard normal distribution. Therefore, if $\hat{\gamma}$ falls within the limits of Equation 3.86, the hypothesis of normality is accepted. Otherwise, it is rejected. This procedure is recommended for the sample sizes greater than 150. For smaller sample sizes, the computed coefficient of skewness is compared with the tabulated values of the skewness coefficient, $\gamma_\alpha(N)$, presented in Table 3.11. If $|\hat{\gamma}| < \gamma_\alpha(N)$, the hypothesis of normality is accepted.

Example 3.22

The following logarithmic transformation is applied to the monthly rates of recharge of an aquifer:

$$y_t = \log_{10}(X_t)$$

where x_t and y_t are the original and the transformed rate of recharge in month t , respectively. The skewness coefficient of a transformed series is estimated to be 0.8. Use the skewness test to check on the normality of the transformed data. Consider a 5% significance level for this test. The number of data in the time series is 1020.

SOLUTION

Using Equation 3.86, the 95% probability limits on the skewness coefficient is:

$$\left[-Z_{0.975} \sqrt{\frac{6}{N}}, Z_{0.975} \sqrt{\frac{6}{N}} \right] = \left[-1.96 \sqrt{\frac{6}{1020}}, 1.96 \sqrt{\frac{6}{1020}} \right] = \left[-0.15, 0.15 \right]$$

The value of $Z_{0.975}$ can be read from the table of normal distribution in [Appendix](#). Because 0.8 does not fall within the above limits, the series is not normally distributed.

3.9.6 AKAIKE'S INFORMATION CRITERION

Akaike's information criterion (AIC), which was first proposed by Akaike (1974), is usually used as the primary criterion for model selection. It considers the parsimony in model building. Akaike defined the AIC among competing ARMA (p, q) models as follows:

$$AIC(p, q) = N \ln\left(\hat{\sigma}^2(\varepsilon)\right) + 2(p + q) \quad (3.87)$$

where:

N is the sample size

$\hat{\sigma}^2(\varepsilon)$ is the maximum likelihood estimate of the residual variance.

The model with minimum AIC is selected.

The goodness of fit tests should be applied to the model with minimum AIC to make sure the residuals are consistent with their expected behavior. If the model residuals do not pass the test, the models with higher values of AIC should be checked.

3.9.7 AUTOREGRESSIVE MODELING

AR models are effective tools for modeling a hydrologic time series such as streamflow in low flow season, which is mainly supplied from groundwater and has low variations (Salas et al., 1980). These models incorporate the correlation between the time sequences of variables. They have been widely used in hydrologic time series modeling. AR models are classified into the following subsets:

- AR models with constant parameters, which can be used to model an annual series
- AR models with timely variable parameters, which can be used to model a seasonal (periodic) series

The basic form of the AR model of order p , AR(p), with constant parameters is:

$$z_t = \sum_{i=1}^p \varphi_i z_{t-i} + \varepsilon_t \quad (3.88)$$

where:

z_t is the time-dependent normal and standardized series $\{N(0,1)\}$

φ_i is the autoregressive coefficient

ε_t is the time-independent variable (white noise)

p is the order of autoregressive model

Equation 3.88 can be applied to a standardized series. To obtain a standardized series, the following equation is used:

$$z_t = \frac{x_t - \mu}{\sigma} \quad (3.89)$$

where μ and σ are, respectively, the mean and standard deviation of the series x_t . The parameter set of the model is:

$$\{\mu, \sigma, \varphi_1, \dots, \varphi_p, \sigma^2(\varepsilon)\} \quad (3.90)$$

where $\sigma^2(\varepsilon)$ is the variance of a time-independent series. The Yule–Walker linear equations are solved simultaneously to estimate the model parameters. These equations can be expressed as:

$$r_i = \hat{\varphi}_1 r_{i-1} + \hat{\varphi}_2 r_{i-2} + \dots + \hat{\varphi}_p r_{i-p} \quad (i > 0) \quad (3.91)$$

where r_i is the sample correlation coefficients of lag i . The parameter $\sigma^2(\varepsilon)$ is estimated as:

$$\hat{\sigma}^2(\varepsilon) = \frac{N \hat{\sigma}^2}{(N - p)} \left(1 - \sum_{i=1}^p \hat{\varphi}_i r_i \right) \quad (3.92)$$

where:

N is the number of the data

$\hat{\sigma}^2$ is the sample variance.

To meet a stationary condition by the model parameters, the roots of the following equation should lie inside the unit circle (Yevjevich, 1972):

$$u^p - \hat{\varphi}_1 u^{p-1} - \hat{\varphi}_2 u^{p-2} - \dots - \hat{\varphi}_p = 0 \quad (3.93)$$

In other words, $|u_i| < 1$. To forecast or generate annual AR models, the following relation is used:

$$\hat{z}_t = \hat{\phi}_1 \hat{z}_{t-1} + \cdots + \hat{\phi}_p \hat{z}_{t-p} + \hat{\sigma}(\varepsilon) \zeta_t \quad (3.94)$$

where ζ_t is the standardized normal variable.

Example 3.23

For an AR (2) model, the parameters have been estimated as $\varphi_1 = 0.5$ and $\varphi_2 = 0.3$. Check the parameters stationary condition.

SOLUTION

Using Equation 3.93,

$$u^2 - 0.5u - 0.3 = 0 \Rightarrow \begin{cases} u_1 = 0.85 \\ u_2 = -0.35 \end{cases}$$

The roots lie within the unit circle; therefore, the parameters pass the stationary condition.

Example 3.24

An AR (2) model is selected for 20-year normal and standardized annual quality data of an aquifer. The first and second correlation coefficients are estimated as $r_1 = 0.6$ and $r_2 = 0.35$. Estimate the model parameters if the variance of a normal and standardized inflow series is estimated as 1.5.

SOLUTION

Using Equation 3.91, we have:

$$\begin{cases} r_1 = \varphi_1 + \varphi_2 r_1 \\ r_2 = \varphi_2 + \varphi_1 r_1 \end{cases}$$

By solving the above equations,

$$\varphi_1 = \frac{r_1(1-r_2)}{1-r_1^2} \text{ and } \varphi_2 = \frac{r_2-r_1^2}{1-r_1^2}$$

Therefore,

$$\varphi_1 = 0.61 \quad \text{and} \quad \varphi_2 = -0.02$$

The variance of model residuals is now estimated using Equation 3.92:

$$\hat{\sigma}^2(\varepsilon) = \frac{20 \times 1.5}{20-2} (1 - 0.6 \times 0.61 + 0.35 \times 0.02) = 1.173$$

In order to check whether an AR(p) is an appropriate model for a specific time series, the behavior of the partial autocorrelation function (PACF) of the series is estimated and investigated. PACF shows the time-dependence structure of the series in a different way. The partial autocorrelation lag k represents the correlation between z_1 and z_{k+1} , adjusted for the intervening observations z_2, \dots, z_k . For an AR(p) process, the partial autocorrelation function is the last autoregressive coefficient of the model, $\phi_k(k)$, which is estimated by rewriting Equation 3.91 as following and successively solving it:

$$r_i = \hat{\phi}_1(k)r_{i-1} + \hat{\phi}_2(k)r_{i-2} + \dots + \hat{\phi}_k(k)r_{i-k} \quad (3.95)$$

A set of linear equations are then resulted from the above equation. These equations are:

$$\hat{\phi}_1(k)r_0 + \hat{\phi}_2(k)r_1 + \dots + \hat{\phi}_k(k)r_{k-1} = r_1$$

$$\hat{\phi}_1(k)r_1 + \hat{\phi}_2(k)r_0 + \dots + \hat{\phi}_k(k)r_{k-1} = r_2$$

$$\vdots$$

$$\hat{\phi}_1(k)r_{k-1} + \hat{\phi}_2(k)r_{k-2} + \dots + \hat{\phi}_k(k)r_0 = r_k$$

The above equations can be written as:

$$\begin{bmatrix} 1 & r_1 & r_2 & \dots & r_{k-1} \\ r_1 & 1 & r_1 & \dots & r_{k-2} \\ r_2 & r_1 & 1 & \dots & r_{k-3} \\ \vdots & \vdots & \vdots & \ddots & \vdots \\ r_{k-1} & r_{k-2} & r_{k-3} & & 1 \end{bmatrix} \begin{bmatrix} \phi_1(k) \\ \phi_2(k) \\ \phi_3(k) \\ \vdots \\ \phi_k(k) \end{bmatrix} = \begin{bmatrix} r_1 \\ r_2 \\ r_3 \\ \vdots \\ r_k \end{bmatrix} \quad (3.96)$$

The partial autocorrelation function, $\phi_k(k)$, can be determined by successively applying the above relations. The partial correlogram of an autoregressive process of order p has peaks at lags 1 through p and then cuts off. Hence, the partial autocorrelation function is used to identify the p of an AR(p) model.

The basic form of the AR model with periodic parameters is:

$$z_{v,\tau} = \sum_{i=1}^p \varphi_{i,\tau} z_{v,\tau-i} + \sigma_\tau(\varepsilon) \zeta_{v,\tau} \quad (3.97)$$

where:

$z_{v,\tau}$ is the normal and standardized value in year v and season τ

$\varphi_{i,\tau}$ is the periodic autoregressive coefficients

$\sigma_\tau(\varepsilon)$ is the periodic standard deviation of residuals.

$z_{v,\tau}$ is estimated using seasonal mean and variance as:

$$z_{v,\tau} = \frac{x_{v,\tau} - \mu_\tau}{\sigma_\tau} \quad (3.98)$$

where μ_τ and σ_τ are the mean and standard deviation of x in season τ . The parameter set of the model can be summarized as:

$$\{\mu_\tau, \sigma_\tau, \varphi_{1,\tau}, \dots, \varphi_{P,\tau}, \sigma_\tau^2(\varepsilon), \tau = 1, \dots, \eta\} \quad (3.99)$$

where η is the total number of seasons. Equation 3.91 can be repeatedly used for each season. Therefore,

$$r_k = \sum_{i=1}^P \hat{\varphi}_{i,\tau} r_{[k-i],\tau-\min(k,i)} \quad (k > 0) \quad (3.100)$$

The residual variance can be estimated using the following relation:

$$\hat{\sigma}_\tau^2(\varepsilon) = 1 - \sum_{j=1}^P \hat{\varphi}_{j,\tau} \hat{r}_{j,\tau} \quad (3.101)$$

3.9.8 MOVING AVERAGE PROCESS

If the series, z_t , is dependent only on a finite number of previous values of a random variable, ε_t , then the process can be called a moving average process. The moving average model of order q , MA(q) can be expressed as:

$$z_t = \varepsilon_t - \theta_1 \varepsilon_{t-1} - \theta_2 \varepsilon_{t-2} - \theta_3 \varepsilon_{t-3} - \dots - \theta_q \varepsilon_{t-q} \quad (3.102)$$

or

$$z_t = - \sum_{j=0}^q \theta_j E_{t-j} \quad (\theta_0 = -1) \quad (3.103)$$

where θ_1, \dots , and θ_q are q orders of MA(q) model parameters. The parameter set of the model is summarized as:

$$\{\mu, \theta_1, \dots, \theta_q, \sigma^2(\varepsilon)\} \quad (3.104)$$

The parameters of the model should satisfy the invertibility condition. For this purpose, the roots of the following polynomial should lie inside the unit circle:

$$u^q - \hat{\theta}_1 u^{q-1} - \hat{\theta}_2 u^{q-2} - \dots - \hat{\theta}_q = 0 \quad (3.105)$$

Example 3.25

For an MA-(2) model, the parameters have been estimated as $\theta_1 = 0.65$ and $\theta_2 = 0.3$. Check whether the parameters pass the invertibility condition.

SOLUTION

Using Equation 3.105,

$$u^2 - 0.65u - 0.3 = 0 \Rightarrow \begin{cases} u_1 = 0.96 \\ u_2 = -0.31 \end{cases}$$

The roots lie within the unit circle; therefore, the parameters pass the stationary condition.

3.9.9 AUTOREGRESSIVE MOVING AVERAGE MODELING

The ARMA model of order (p, q) can be defined by combining an autoregressive model of order p and a moving average model of order q as follows:

$$z_t - \varphi_1 z_{t-1} - \cdots - \varphi_p z_{t-p} = \varepsilon_t + \theta_1 \varepsilon_{t-1} + \cdots + \theta_q \varepsilon_{t-q} \quad (3.106)$$

The ARMA(p, q) model is expressed as:

$$\varphi(B)z_t = \theta(B)\varepsilon_t \quad (3.107)$$

where $\varphi(z)$ and $\theta(z)$ are the p th and q th degree polynomials:

$$\varphi(z) = 1 - \varphi_1 z - \cdots - \varphi_p z^p \quad (3.108)$$

$$\theta(z) = 1 + \theta_1 z + \cdots + \theta_q z^q \quad (3.109)$$

The parameter set of the ARMA(p, q) model is $\{\mu, \theta_1, \dots, \theta_q, \varphi_1, \dots, \varphi_p, \sigma^2(\varepsilon)\}$. These parameters should satisfy both the conditions of invertibility and stationarity.

3.9.9.1 Generation and Forecasting Using ARMA Models

Two major uses of the time series modeling are generating synthetic values and forecasting future events. The generation of a synthetic time series often consists of the generation of the independent normal variables in a series, which is defined as random process.

Once the ARMA model is fitted to a time series, the following procedures are accomplished to generate or forecast the values of that time series. For the generation of the values of the times series using the ARMA (p, q) model (Equation 3.106), it is necessary to give p initial Z values to the model. The Equation 3.106 may be used recursively to generate the desired numbers of Z_t . By generating an adequately long series and deleting 50 or 100 initial terms, the transient effect of the initial values is negligible (Salas et al., 1988). The synthetically generated values conserve the statistical properties of the historical data.

To use ARMA (p, q) for forecasting Z values in a lead time L , the following equations are used if $Z_t(L)$ denotes the value of Z_t at lead time L :

$$Z_t(L) = \varphi_1 Z_{t+L-1} + \varphi_2 Z_{t+L-2} + \cdots + \varphi_p Z_{t+L-p} - \theta_1 \varepsilon_{t+L-1} - \cdots - \theta_q \varepsilon_{t+L-q} \text{ for } L \leq q \quad (3.110)$$

$$Z_t(L) = \varphi_1 Z_{t+L-1} + \varphi_2 Z_{t+L-2} + \cdots + \varphi_p Z_{t+L-p} \text{ for } L > q \quad (3.111)$$

3.9.10 AUTOREGRESSIVE INTEGRATED MOVING AVERAGE MODELING

A time series should have the following characteristics to be eligible for applying the ARMA models to it:

- There is no apparent deviation from stationarity in the series.
- Autocorrelation function is rapidly decreasing.

Considering the fact that a time series does not necessarily meet these conditions, a proper transformation is usually performed to generate the time series with the two above conditions. This has been usually achieved by differencing, which is necessary for ARIMA models, which is very powerful for describing a stationary and nonstationary time series, and the process is called an autoregressive integrated moving average process. The nonseasonal form of ARIMA models of order (p, d, q) is expressed as:

$$\varphi(B)(1-B)^d z_t = \theta(B) \varepsilon_t \quad (3.112)$$

where $\varphi(B)$ and $\theta(B)$ are polynomials of degree p and q , respectively:

$$\varphi(B) = 1 - \varphi_1 B - \varphi_2 B^2 - \cdots - \varphi_p B^p \quad (3.113)$$

$$\theta(B) = 1 - \theta_1 B - \theta_2 B^2 - \cdots - \theta_q B^q \quad (3.114)$$

The model has $p + q + 1$ parameters, which are $\{\varphi_1, \dots, \varphi_p, \theta_1, \dots, \theta_q, \sigma^2(\varepsilon)\}$.

The seasonal form of ARIMA models of nonseasonal order (p, d, q) , and of seasonal order (P, D, Q_w) with seasonality w , has also been developed to model the seasonal hydrologic time series. The general form of multiplicative ARIMA $(p, d, q)(P, D, Q_w)$ is:

$$(1 - \Phi_1 B^w - \Phi_2 B^{2w} - \cdots - f_p B^{Pw}) (1 - \varphi_1 B - \varphi_2 B^2 - \cdots - \varphi_p B^p) (1 - B^w)^D (1 - B)^d z_t \quad (3.115)$$

$$= (1 - \Theta_1 B^w - \Theta_2 B^{2w} - \cdots - \Theta_Q B^{Qw}) (1 - \theta_1 B - \theta_2 B^2 - \cdots - \theta_q B^q) \varepsilon_t$$

where:

ε_t is the independently distributed random variable

B is the backward operator as $B(z_t) = z_{t-1}$

$(1 - B^w)^D$ is the D th seasonal difference of season w

$(1 - B)^d$ is the d th nonseasonal difference

- p is the order of nonseasonal autoregressive model
 q is the order of nonseasonal moving average model
 P is the order of seasonal autoregressive model
 q is the order of seasonal moving average model
 Φ is the seasonal autoregressive parameter
 Θ is the seasonal moving average parameter
 ϕ is the nonseasonal autoregressive parameter
 θ is the nonseasonal moving average parameter.

Equation 3.115 can also be written as:

$$\Phi(B^w)\phi(B)(1-B^w)^D(1-B)^d z_t = \Theta(B^w)\theta(B)\varepsilon_t \quad (3.116)$$

Example 3.26

Formulate the model ARIMA(1,0,1)(1,0,1)₁₂.

SOLUTION

Using Equation 3.115, we have:

$$(1-\Phi_1 B^w)(1-\phi_1 B)z_t = (1-\Theta_1 B^w)(1-\theta_1 B)\varepsilon_t$$

or

$$z_t - \phi_1 z_{t-1} - \Phi_1 z_{t-12} + \phi_1 \Phi_1 z_{t-13} = \varepsilon_t - \theta_1 \varepsilon_{t-1} - \Theta_1 \varepsilon_{t-12} - \theta_1 \Theta_1 \varepsilon_{t-13}$$

Therefore, the model has nonlinear parameters because of the terms $\theta\Theta$ and $\phi\Phi$.

3.9.10.1 Time Series Forecasting Using ARIMA Models

The ARIMA models are nonstationary. Therefore, it is not reasonable to use them for synthetic generation of a stationary time series. However, they can be useful for forecasting. The equations of ARIMA models, mentioned before in this section, could be used for data forecasting. As an example, the forecasting equations for ARIMA (1, 0, 1) (1, 0, 1)₁₂ could be represented as follows:

$$\begin{aligned} z_t(L) &= \phi_1 z_{t-1+L} + \Phi_1 z_{t-12+L} - \phi_1 \Phi_1 z_{t-13+L} - \theta_1 \varepsilon_{t-1+L} \\ &\quad - \Theta_1 \varepsilon_{t-12+L} - \theta_1 \Theta_1 \varepsilon_{t-13+L} \quad \text{for } L \leq 12 \end{aligned} \quad (3.117)$$

$$z_t(L) = \phi_1 z_{t-1+L} + \Phi_1 z_{t-12+L} - \phi_1 \Phi_1 z_{t-13+L} \quad \text{for } L > 12 \quad (3.118)$$

Example 3.27

Table 3.12 presents a 16-year monthly time series of rates of recharge to an aquifer. Determine the best autoregressive model for these data and forecast the rate of recharge for the first half of water year 2007.

TABLE 3.12
Monthly Time Series of Rates of Recharge to an Aquifer (in./Month)

| | October | November | December | January | February | March | April | May | June | July | August | September |
|------|---------|----------|----------|---------|----------|-------|-------|-------|------|------|--------|-----------|
| 1991 | 1.71 | 1.72 | 1.45 | 1.41 | 1.66 | 8.74 | 8.09 | 4.73 | 0.67 | 0.11 | 0.01 | 0.86 |
| 1992 | 2.68 | 2.28 | 2.68 | 2.42 | 3.16 | 3.67 | 9.87 | 6.07 | 3.20 | 0.72 | 0.05 | 0.52 |
| 1993 | 1.26 | 1.93 | 1.86 | 1.61 | 1.87 | 2.46 | 6.07 | 4.83 | 0.38 | 0.02 | 0.13 | 0.32 |
| 1994 | 1.06 | 1.95 | 1.87 | 1.53 | 1.90 | 5.03 | 7.98 | 8.41 | 4.25 | 1.38 | 1.14 | 0.88 |
| 1995 | 1.13 | 1.63 | 1.82 | 1.85 | 2.66 | 3.44 | 4.89 | 0.92 | 0.22 | 0.05 | 0.03 | 0.20 |
| 1996 | 0.92 | 2.05 | 1.72 | 1.46 | 1.92 | 3.25 | 10.81 | 8.33 | 0.65 | 0.02 | 0.00 | 0.67 |
| 1997 | 0.92 | 1.37 | 1.78 | 2.23 | 2.02 | 2.38 | 5.84 | 1.82 | 1.39 | 0.62 | 0.03 | 0.38 |
| 1998 | 0.82 | 1.38 | 1.49 | 1.57 | 1.36 | 2.45 | 6.17 | 8.14 | 2.72 | 0.70 | 0.13 | 0.23 |
| 1999 | 0.90 | 1.56 | 1.36 | 1.48 | 1.90 | 2.31 | 14.14 | 13.27 | 5.18 | 0.83 | 0.45 | 0.49 |
| 2000 | 1.25 | 1.45 | 1.89 | 2.05 | 2.48 | 4.50 | 12.89 | 10.02 | 3.41 | 1.22 | 0.45 | 0.79 |
| 2001 | 2.10 | 2.10 | 2.69 | 2.71 | 3.34 | 4.24 | 5.74 | 3.78 | 1.99 | 0.94 | 0.07 | 0.84 |
| 2002 | 1.08 | 1.55 | 1.36 | 1.27 | 1.28 | 1.35 | 9.15 | 9.76 | 1.29 | 0.86 | 0.00 | 0.98 |
| 2003 | 1.07 | 1.35 | 1.38 | 1.57 | 2.88 | 2.55 | 4.72 | 3.31 | 2.05 | 0.02 | 0.42 | 0.01 |
| 2004 | 0.30 | 0.61 | 0.66 | 0.90 | 1.06 | 1.94 | 8.39 | 6.85 | 3.20 | 0.57 | 0.07 | 0.18 |
| 2005 | 0.78 | 1.05 | 1.10 | 1.32 | 4.11 | 3.07 | 3.35 | 5.79 | 1.85 | 0.59 | 1.37 | 1.87 |
| 2006 | 0.52 | 1.05 | 1.14 | 1.42 | 1.65 | 2.35 | 2.73 | 2.61 | 0.70 | 0.04 | 0.03 | 0.03 |

Solution

In data preparation for forecasting, first the stationary condition of the time series must be checked. In other words, the time series must meet the stationary condition in order to forecast newer data. Otherwise, the forecasted data are not accurate.

In this example, evaluation of the time series shows that there are no trends, outlying observations, and periodicity in the data. The data are plotted on a semi-logarithmic graph (Figure 3.22). As demonstrated in this figure, the data do not fit the normal distribution. Therefore, the data are normalized and standardized. Figure 3.23 depicts the normalized and standardized data.

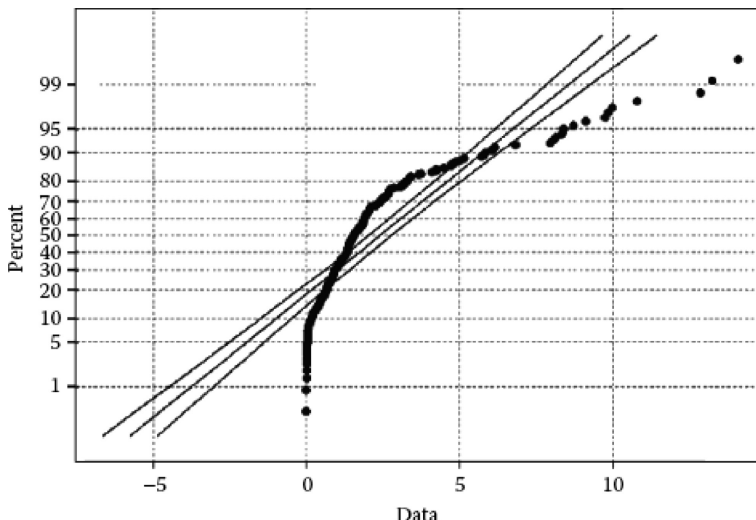


FIGURE 3.22 The time series plotted on a semilogarithmic graph.

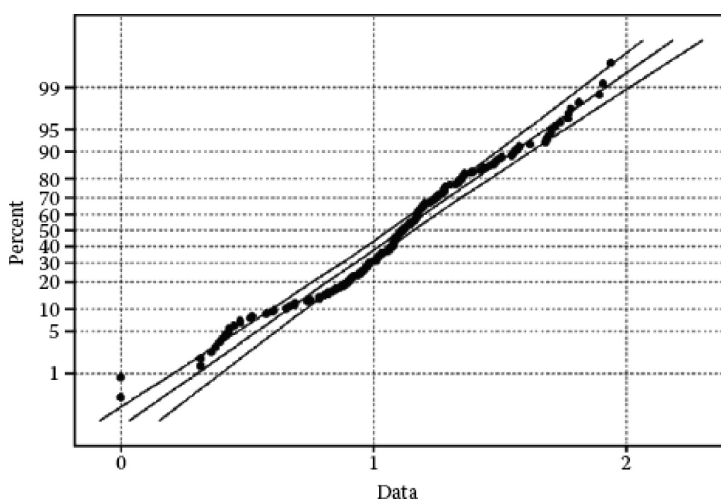


FIGURE 3.23 Normalized and standardized data plotted on a semilogarithmic graph.

To determine the parameters of an ARIMA model, an ACF graph and PACF graph can be used. An ACF graph evaluates the correlation between the data of a time series, and a PACF graph shows the correlation between autoregressive coefficients in different time lags. For each of these graphs, a confidence limit is set. Only if all of the correlation values are within this limit, can the model be selected and the forecasting is acceptable. Using ACF and PACF graphs of normalized data, the values of parameters p and q of the ARIMA model are determined.

The time lags that violate the confidence limits of ACF and PACF graphs represent the values of parameters p and q , respectively.

In this example, after normalizing and standardizing the data, their corresponding ACF and PACF graphs are plotted. [Figures 3.24](#) and [3.25](#) show these graphs. A 95% confidence limit is considered for these graphs. Using ACF and PACF graphs, the parameters p and q are approximated. According to these figures, values of both p and q are less than or equal to 1.

The final structure of the forecasting model is determined by trial and error. Then, an Akaike test is used to compare different ARIMA (p, q) models and select the best one. For this purpose we have:

$$AIC(p, q) = N \ln(\sigma_e^2) + 2(p + q)$$

The model with the least AIC is selected as the best one. [Table 3.13](#) presents the results for different ARIMA models. According to this table, the model ARIMA(1,1,1) (1,1,1) has the least AIC and is selected for our forecasting purpose.

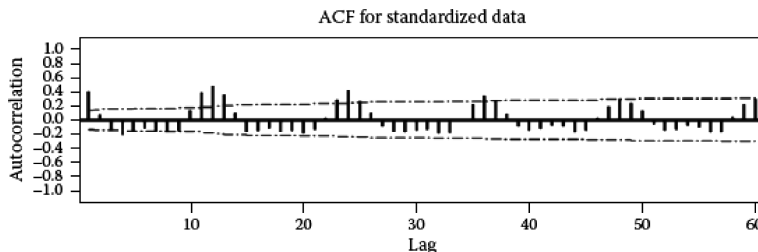


FIGURE 3.24 ACF graph for different lags.

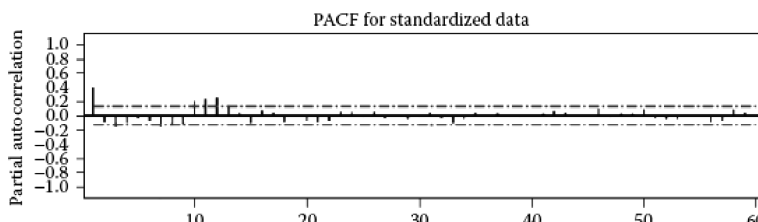


FIGURE 3.25 PACF graph for different lags.

TABLE 3.13
Values of AIC for Different ARIMA Models

| ARIMA Model | AIC | Residual Error |
|----------------|------|----------------|
| (1,0,0)(1,0,1) | -125 | 0.2975 |
| (1,1,1)(1,1,1) | -131 | 0.2886 |
| (1,0,0)(1,0,1) | -129 | 0.2868 |

Figures 3.26 and 3.27 show the ACF and PACF graphs for the residuals. These figures illustrate that the values of errors in both of the graphs are within the confidence limit. Therefore, the selected forecasting model, ARIMA (1,1,1)(1,1,1), is confirmed.

The goodness of fit tests are usually used to evaluate the performance of forecasting models. However, this can be evaluated more efficiently by developing

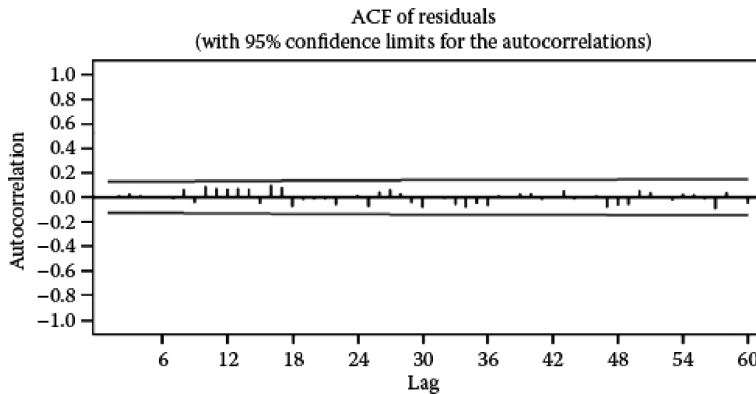


FIGURE 3.26 ACF graph for residuals of the data.

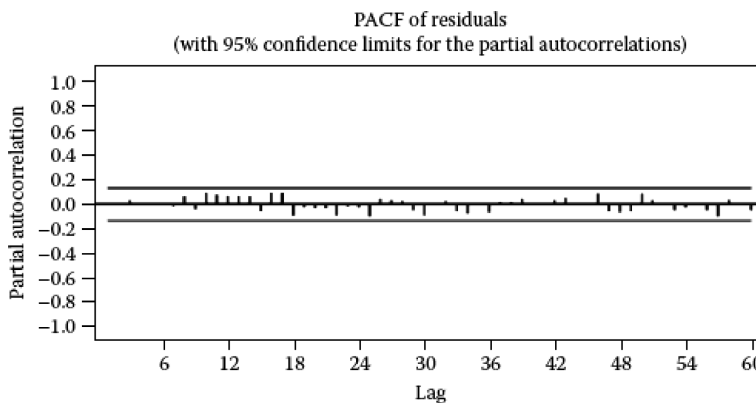


FIGURE 3.27 PACF graph for residuals of the data.

(forecasting) a long-term time series of the data and comparing this series with the corresponding historical time series. For this purpose, the first 36–48 months are usually used to estimate the parameters of forecasting model. Then, the forecasting process is done for the rest of the historical time series. In this process, after forecasting the value of each month, the actual value of the time series is substituted with the forecasted value to forecast the next month. This process continues until the last month of the time series.

In this example, the first 92 months of the recharge rate time series were used to train the forecasting model. Then, the remaining 100 months were forecasted. **Figure 3.28** expresses the actual and forecasted values.

This figure illustrates the acceptable performance of the selected forecasting model. Therefore, this model is used to generate six months of recharge rates for the first half of 2007. Since the generated values are standardized and normalized, the forecasted values must be converted to the regular format. It should be noted that if the main time series has a trend, this trend must also be added to the forecasted values. **Table 3.14** presents the forecasted values for rates of recharge to the aquifer.

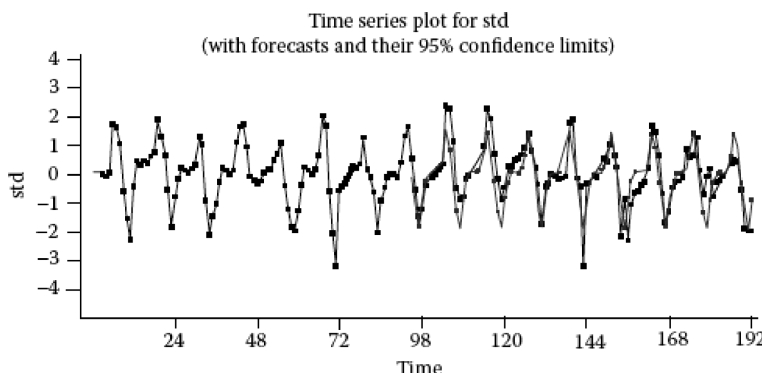


FIGURE 3.28 Comparison of observed and forecasted values for rates of recharge to the aquifer using an ARIMA(1, 1, 1)(1, 1, 1) model.

TABLE 3.14
Forecasted Values for Rates of Recharge to
the Aquifer for the First Half of Water Year 2007

| Month | 1 | 2 | 3 | 4 | 5 | 6 |
|---------------|------|------|------|------|------|------|
| Recharge rate | 0.39 | 0.70 | 0.78 | 0.85 | 1.31 | 1.73 |

PROBLEMS

- 3.1** Which property is a better measure of the productivity of an aquifer: porosity or hydraulic conductivity? Explain why.
- 3.2** A confined aquifer has a transitivity of 100 m²/day. If the slope of the piezometric surface is 0.0005, compute the flow rate of water through the aquifer per km of width.
- 3.3** An aquifer has a hydraulic conductivity of 10.0 m/day. Compute the velocity of water through the aquifer if the slope of the water table is 0.002 and the porosity is 0.2. How far will the groundwater travel in 1.0 year?
- 3.4** Two piezometers were installed at two wells 1 km apart. Well's information is listed below. If the intrinsic permeability of the aquitard is 0.005 m², determine the Darcy's velocity.

| Observation Well | | |
|-------------------------|-------|-------|
| | A | B |
| Depth to bottom of well | 114.7 | 125.8 |
| Depth of water surface | 48.4 | 51.2 |

- 3.5** Piezometers A and B are installed in a confined aquifer with an estimated hydraulic conductivity of 12 m/day and a porosity of 0.25 and 1 km apart. Piezometer A is at the true north, and piezometer B is located at an angle of 45° clockwise from A. The water level at B is 15 cm below A. What is the Darcy velocity along line AB? Explain why this is not the actual seepage velocity in the aquifer. Piezometer C is also located in the aquifer 0.5 km from A at an angle of 90° clockwise from it. The water level at C is 10 cm below A. Calculate the Darcy velocity and real seepage velocity in the aquifer.
- 3.6** An aquifer formation has a hydraulic conductivity of 18 m/day when the aquifer is at a temperature of 25°C. Determine the intrinsic permeability of the aquifer. If the fluid in the aquifer consists of spilled tetrachloroethylene, then determine the hydraulic conductivity of tetrachloroethylene movement. Under the same piezometric gradient, which fluid moves faster?
- 3.7** An anisotropic aquifer system has horizontally parallel layers with hydraulic conductivities of $K_n = 15$ m/day, $K_{22} = 5$ m/day. The thicknesses of the first and second layers are 2 m and 4 m, respectively. If the water table drops 1.2 m in 800 m in the aquifer, how much will the seepage velocity be? Compare this velocity with the seepage velocity when the aquifer is homogeneous with a hydraulic conductivity equal to the average of those two layers.
- 3.8** In an aquifer, $K_{xx} = 100$ m/day, $K_{yy} = 10$ m/day, and K_{xy} can be ignored, where the x and y axes are along the east/west and north/south directions, receptivity. Groundwater flows toward the east direction in this aquifer. The development of a new well field will cause the mean head gradient to shift from the east to the southeast. Compare the specific discharge in the direction of the head gradient for a gradient of 0.01 in the east direction with the specific discharge in the direction of the head gradient of 0.01 in the

TABLE 3.15
The Rates of Recharge to an Aquifer in Problem 3.10

| Time Sequences | Rate of Recharge (m ³ /hr) | Time Sequences | Rate of Recharge (m ³ /hr) |
|----------------|--|----------------|--|
| 1 | 200 | 11 | 172 |
| 2 | 212 | 12 | 180 |
| 3 | 302 | 13 | 185 |
| 4 | 212 | 14 | 190 |
| 5 | 192 | 15 | 302 |
| 6 | 186 | 16 | 215 |
| 7 | 148 | 17 | 218 |
| 8 | 312 | 18 | 158 |
| 9 | 220 | 19 | 142 |
| 10 | 195 | 20 | 175 |

southeast direction. In either of these cases, does the groundwater flow have the direction of the head gradient?

- 3.9** Four horizontal, homogeneous, isotropic geologic formations, each of them 5 m thick, overlie one another. If the hydraulic conductivities are 10^{-4} , 10^{-6} , 10^{-4} , and 10^{-6} m/s, respectively, calculate the horizontal and vertical components of hydraulic conductivity.
- 3.10** Table 3.15 shows the rates of recharge to an aquifer. Test the stationarity of the time series in its mean. Define a trend model and the residuals of the series.
- 3.11** The monthly discharges for 80 months from an aquifer are divided into eight categories as shown in the Table 3.16. Previous studies show that the precipitation data in this station are normally distributed. If the mean and standard deviation for the data are 20.48 (mm) and 11.84 (mm), respectively, use the chi-square test with 5% significance level and comment on the selected distribution for the sample data.

TABLE 3.16
The Monthly Discharges from an Aquifer in Problem 3.11

| Interval (i) | Discharges from the Aquifer (m ³ /d) | Actual Frequency (f _i) |
|--------------|---|------------------------------------|
| 1 | $0 \leq P < 5$ | 9 |
| 2 | $5 \leq P < 10$ | 13 |
| 3 | $10 \leq P < 15$ | 5 |
| 4 | $15 \leq P < 20$ | 10 |
| 5 | $20 \leq P < 25$ | 11 |
| 6 | $25 \leq P < 30$ | 12 |
| 7 | $30 \leq P < 35$ | 8 |
| 8 | $35 \leq P < 40$ | 12 |

TABLE 3.17**The Monthly Discharges from an Aquifer in Problem 3.12**

| Interval (<i>i</i>) | Discharges from the Aquifer (m ³ /d) | Actual Frequency (<i>f_i</i>) |
|-----------------------|---|---|
| 1 | 0 ≤ <i>P</i> < 5 | 27 |
| 2 | 5 ≤ <i>P</i> < 10 | 24 |
| 3 | 10 ≤ <i>P</i> < 15 | 9 |
| 4 | 15 ≤ <i>P</i> < 20 | 8 |
| 5 | 20 ≤ <i>P</i> < 25 | 5 |
| 6 | 25 ≤ <i>P</i> < 30 | 4 |
| 7 | 30 ≤ <i>P</i> < 35 | 2 |
| 8 | 35 ≤ <i>P</i> < 40 | 1 |

- 3.12** The classified monthly discharges from an aquifer are divided into eight categories as shown in the [Table 3.17](#). Previous studies show that the precipitation data in this station are normally distributed. Use the chi-square test with 5% significance level and comment on the selected distribution for the sample data.
- 3.13** The time series of inflow to an aquifer could be shown in the form of the following equation. Categorize this model as a multiplicative ARIMA model.

$$(1 - B^{10})Z_t = (1 + 0.4B)(1 - 0.7B^{10})\varepsilon_t$$

- 3.14** Write the mathematical expression of order 1 and order 2 nonseasonal ARIMA. Why is the seasonal differencing done? Write the mathematical expression for the second-order seasonal differencing for a monthly time series. (Assume 12 for the number of seasons.)
- 3.15** ARMA(1,1) model is fitted to the time series of groundwater quality data in an aquifer with parameters $\varphi = -0.6$ and $\theta = -0.4$. Plot the auto correlation functions of the time series from lag-1 to lag-5.

APPENDIX

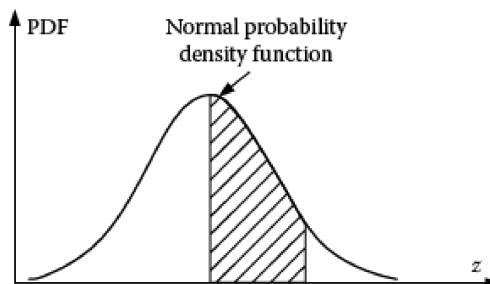
TABLE 3.A1
Normal Distribution

| <i>z</i> | 0 | 0.01 | 0.02 | 0.03 | 0.04 | 0.05 | 0.06 | 0.07 | 0.08 | 0.09 |
|-----------------|----------|-------------|-------------|-------------|-------------|-------------|-------------|-------------|-------------|-------------|
| 0 | 0.0000 | 0.0040 | 0.0080 | 0.0120 | 0.0160 | 0.0199 | 0.0239 | 0.0279 | 0.0319 | 0.0359 |
| 0.1 | 0.0398 | 0.0438 | 0.0478 | 0.0517 | 0.0557 | 0.0596 | 0.0636 | 0.0675 | 0.0714 | 0.0753 |
| 0.2 | 0.0793 | 0.0832 | 0.0871 | 0.0910 | 0.0948 | 0.0987 | 0.1026 | 0.1064 | 0.1103 | 0.1141 |
| 0.3 | 0.1179 | 0.1217 | 0.1255 | 0.1293 | 0.1331 | 0.1368 | 0.1406 | 0.1443 | 0.1480 | 0.1517 |
| 0.4 | 0.1554 | 0.1591 | 0.1628 | 0.1664 | 0.1700 | 0.1736 | 0.1772 | 0.1808 | 0.1844 | 0.1879 |
| 0.5 | 0.1915 | 0.1950 | 0.1985 | 0.2019 | 0.2054 | 0.2088 | 0.2123 | 0.2157 | 0.2190 | 0.2224 |

(Continued)

TABLE 3.A1 (Continued)**Normal Distribution**

| <i>z</i> | 0 | 0.01 | 0.02 | 0.03 | 0.04 | 0.05 | 0.06 | 0.07 | 0.08 | 0.09 |
|-----------------|----------|-------------|-------------|-------------|-------------|-------------|-------------|-------------|-------------|-------------|
| 0.6 | 0.2257 | 0.2291 | 0.2324 | 0.2357 | 0.2389 | 0.2422 | 0.2454 | 0.2486 | 0.2517 | 0.2549 |
| 0.7 | 0.2580 | 0.2611 | 0.2642 | 0.2673 | 0.2704 | 0.2734 | 0.2764 | 0.2794 | 0.2823 | 0.2852 |
| 0.8 | 0.2881 | 0.2910 | 0.2939 | 0.2967 | 0.2995 | 0.3023 | 0.3051 | 0.3078 | 0.3106 | 0.3133 |
| 0.9 | 0.3159 | 0.3186 | 0.3212 | 0.3238 | 0.3264 | 0.3289 | 0.3315 | 0.3340 | 0.3365 | 0.3389 |
| 1 | 0.3413 | 0.3438 | 0.3461 | 0.3485 | 0.3508 | 0.3531 | 0.3554 | 0.3577 | 0.3599 | 0.3621 |
| 1.1 | 0.3643 | 0.3665 | 0.3686 | 0.3708 | 0.3729 | 0.3749 | 0.3770 | 0.3790 | 0.3810 | 0.3830 |
| 1.2 | 0.3849 | 0.3869 | 0.3888 | 0.3907 | 0.3925 | 0.3944 | 0.3962 | 0.3980 | 0.3997 | 0.4015 |
| 1.3 | 0.4032 | 0.4049 | 0.4066 | 0.4082 | 0.4099 | 0.4115 | 0.4131 | 0.4147 | 0.4162 | 0.4177 |
| 1.4 | 0.4192 | 0.4207 | 0.4222 | 0.4236 | 0.4251 | 0.4265 | 0.4279 | 0.4292 | 0.4306 | 0.4319 |
| 1.5 | 0.4332 | 0.4345 | 0.4357 | 0.4370 | 0.4382 | 0.4394 | 0.4406 | 0.4418 | 0.4429 | 0.4441 |
| 1.6 | 0.4452 | 0.4463 | 0.4474 | 0.4484 | 0.4495 | 0.4505 | 0.4515 | 0.4525 | 0.4535 | 0.4545 |
| 1.7 | 0.4554 | 0.4564 | 0.4573 | 0.4582 | 0.4591 | 0.4599 | 0.4608 | 0.4616 | 0.4625 | 0.4633 |
| 1.8 | 0.4641 | 0.4649 | 0.4656 | 0.4664 | 0.4671 | 0.4678 | 0.4686 | 0.4693 | 0.4699 | 0.4706 |
| 1.9 | 0.4713 | 0.4719 | 0.4726 | 0.4732 | 0.4738 | 0.4744 | 0.4750 | 0.4756 | 0.4761 | 0.4767 |
| 2 | 0.4772 | 0.4778 | 0.4783 | 0.4788 | 0.4793 | 0.4798 | 0.4803 | 0.4808 | 0.4812 | 0.4817 |
| 2.1 | 0.4821 | 0.4826 | 0.4830 | 0.4834 | 0.4838 | 0.4842 | 0.4846 | 0.4850 | 0.4854 | 0.4857 |
| 2.2 | 0.4861 | 0.4864 | 0.4868 | 0.4871 | 0.4875 | 0.4878 | 0.4881 | 0.4884 | 0.4887 | 0.4890 |
| 2.3 | 0.4893 | 0.4896 | 0.4898 | 0.4901 | 0.4904 | 0.4906 | 0.4909 | 0.4911 | 0.4913 | 0.4916 |
| 2.4 | 0.4918 | 0.4920 | 0.4922 | 0.4925 | 0.4927 | 0.4929 | 0.4931 | 0.4932 | 0.4934 | 0.4936 |
| 2.5 | 0.4938 | 0.4940 | 0.4941 | 0.4943 | 0.4945 | 0.4946 | 0.4948 | 0.4949 | 0.4951 | 0.4952 |
| 2.6 | 0.4953 | 0.4955 | 0.4956 | 0.4957 | 0.4959 | 0.4960 | 0.4961 | 0.4962 | 0.4963 | 0.4964 |
| 2.7 | 0.4965 | 0.4966 | 0.4967 | 0.4968 | 0.4969 | 0.4970 | 0.4971 | 0.4972 | 0.4973 | 0.4974 |
| 2.8 | 0.4974 | 0.4975 | 0.4976 | 0.4977 | 0.4977 | 0.4978 | 0.4979 | 0.4979 | 0.4980 | 0.4981 |
| 2.9 | 0.4981 | 0.4982 | 0.4982 | 0.4983 | 0.4984 | 0.4984 | 0.4985 | 0.4985 | 0.4986 | 0.4986 |
| 3 | 0.4987 | 0.4987 | 0.4987 | 0.4988 | 0.4988 | 0.4989 | 0.4989 | 0.4989 | 0.4990 | 0.4990 |



For example, in order to calculate $Z_{0.9}$, the Z value corresponding to $(0.9 - 0.5) = 0.4$ should be find in the Normal Distribution table. $Z_{0.9} = 1.282$.

TABLE 3.A2
Chi-Square Distribution

| Degrees of Freedom | Upper-Tail Area α | | | | | | |
|--------------------|--------------------------|----------|---------|--------|--------|--------|--------|
| | 0.99 | 0.98 | 0.95 | 0.90 | 0.80 | 0.70 | 0.50 |
| 1 | 0.000157 | 0.000628 | 0.00393 | 0.0158 | 0.0642 | 0.148 | 0.455 |
| 2 | 0.0201 | 0.0404 | 0.103 | 0.211 | 0.446 | 0.713 | 1.386 |
| 3 | 0.115 | 0.185 | 0.352 | 0.584 | 1.005 | 1.424 | 2.366 |
| 4 | 0.297 | 0.429 | 0.711 | 1.064 | 1.649 | 2.195 | 3.357 |
| 5 | 0.554 | 0.752 | 1.145 | 1.610 | 2.343 | 3.000 | 4.351 |
| 6 | 0.872 | 1.134 | 1.635 | 2.204 | 3.070 | 3.828 | 5.348 |
| 7 | 1.239 | 1.564 | 2.167 | 2.833 | 3.822 | 4.671 | 6.346 |
| 8 | 1.646 | 2.032 | 2.733 | 3.490 | 4.594 | 5.527 | 7.344 |
| 9 | 2.088 | 2.532 | 3.325 | 4.168 | 5.380 | 6.393 | 8.343 |
| 10 | 2.558 | 3.059 | 3.940 | 4.865 | 6.179 | 7.267 | 9.342 |
| 11 | 3.053 | 3.609 | 4.575 | 5.578 | 6.989 | 8.148 | 10.341 |
| 12 | 3.571 | 4.178 | 5.226 | 6.304 | 7.807 | 9.034 | 11.340 |
| 13 | 4.107 | 4.765 | 5.892 | 7.042 | 8.634 | 9.926 | 12.340 |
| 14 | 4.660 | 5.368 | 6.571 | 7.790 | 9.467 | 10.821 | 13.339 |
| 15 | 5.229 | 5.985 | 7.261 | 8.547 | 10.307 | 11.721 | 14.339 |
| 16 | 5.812 | 6.614 | 7.962 | 9.312 | 11.152 | 12.624 | 15.338 |
| 17 | 6.408 | 7.255 | 8.672 | 10.085 | 12.002 | 13.531 | 16.338 |
| 18 | 7.015 | 7.906 | 9.390 | 10.865 | 12.857 | 14.440 | 17.338 |
| 19 | 7.633 | 8.567 | 10.117 | 11.651 | 13.716 | 15.352 | 18.338 |
| 20 | 8.260 | 9.237 | 10.851 | 12.443 | 14.578 | 16.266 | 19.337 |
| 21 | 8.897 | 9.915 | 11.591 | 13.240 | 15.445 | 17.182 | 20.337 |
| 22 | 9.542 | 10.600 | 12.338 | 14.041 | 16.314 | 18.101 | 21.337 |
| 23 | 10.196 | 11.293 | 13.091 | 14.848 | 17.187 | 19.021 | 22.337 |
| 24 | 10.856 | 11.992 | 13.848 | 15.659 | 18.062 | 19.943 | 23.337 |
| 25 | 11.524 | 12.697 | 14.611 | 16.473 | 18.940 | 20.867 | 24.337 |
| 26 | 12.189 | 13.409 | 15.379 | 17.292 | 19.820 | 21.792 | 25.336 |
| 27 | 12.879 | 14.125 | 16.151 | 18.114 | 20.703 | 22.719 | 26.336 |
| 28 | 13.565 | 14.847 | 16.928 | 18.939 | 21.588 | 23.647 | 27.336 |
| 29 | 14.256 | 15.574 | 17.708 | 19.768 | 22.475 | 24.577 | 28.336 |
| 30 | 14.953 | 16.306 | 18.493 | 20.599 | 23.364 | 25.508 | 26.336 |

| Degrees of Freedom | Upper-Tail Area αX | | | | | | |
|--------------------|----------------------------|-------|--------|--------|--------|--------|--------|
| | 0.30 | 0.20 | 0.10 | 0.05 | 0.02 | 0.01 | 0.001 |
| 1 | 1.074 | 1.642 | 2.706 | 3.841 | 5.412 | 6.635 | 10.827 |
| 2 | 2.408 | 3.219 | 4.605 | 5.991 | 7.824 | 9.210 | 13.815 |
| 3 | 3.665 | 4.642 | 6.251 | 7.815 | 9.837 | 11.345 | 16.268 |
| 4 | 4.878 | 5.989 | 7.779 | 9.488 | 11.668 | 13.277 | 18.465 |
| 5 | 6.064 | 7.289 | 9.236 | 11.070 | 13.388 | 15.086 | 20.517 |
| 6 | 7.231 | 8.558 | 10.645 | 12.592 | 15.033 | 16.812 | 22.457 |

(Continued)

TABLE 3.A1 (Continued)
Chi-Square Distribution

| Degrees of Freedom | Upper-Tail Area αX | | | | | | |
|--------------------|----------------------------|-------------|-------------|-------------|-------------|-------------|--------------|
| | 0.30 | 0.20 | 0.10 | 0.05 | 0.02 | 0.01 | 0.001 |
| 7 | 8.383 | 9.803 | 12.017 | 14.067 | 16.622 | 18.475 | 24.322 |
| 8 | 9.524 | 11.030 | 13.362 | 15.507 | 18.168 | 20.090 | 26.125 |
| 9 | 10.656 | 12.242 | 14.684 | 16.919 | 19.679 | 21.666 | 27.877 |
| 10 | 11.781 | 13.442 | 15.987 | 18.307 | 21.161 | 23.209 | 29.588 |
| 11 | 12.899 | 14.631 | 17.275 | 19.675 | 22.618 | 24.725 | 31.264 |
| 12 | 14.011 | 15.812 | 18.549 | 21.026 | 24.054 | 26.217 | 32.909 |
| 13 | 15.119 | 16.985 | 19.812 | 22.362 | 25.472 | 27.688 | 34.528 |
| 14 | 16.222 | 18.151 | 21.064 | 23.685 | 26.873 | 29.141 | 36.123 |
| 15 | 17.322 | 19.311 | 22.307 | 24.996 | 28.259 | 30.578 | 37.697 |
| 16 | 18.418 | 20.465 | 23.542 | 26.296 | 29.633 | 32.000 | 39.252 |
| 17 | 19.511 | 21.615 | 24.769 | 27.587 | 30.995 | 33.409 | 40.790 |
| 18 | 20.601 | 22.760 | 25.989 | 28.869 | 32.346 | 34.805 | 42.312 |
| 19 | 21.689 | 23.900 | 27.204 | 30.144 | 33.687 | 36.191 | 43.820 |
| 20 | 22.775 | 25.038 | 28.412 | 31.410 | 35.020 | 37.566 | 45.315 |
| 21 | 23.858 | 26.171 | 29.615 | 32.671 | 36.343 | 38.932 | 46.797 |
| 22 | 24.939 | 27.301 | 30.813 | 33.924 | 37.659 | 40.289 | 48.268 |
| 23 | 26.018 | 28.429 | 32.007 | 35.172 | 38.968 | 41.638 | 49.728 |
| 24 | 27.096 | 29.553 | 33.196 | 36.415 | 40.270 | 42.980 | 51.179 |
| 25 | 28.172 | 30.675 | 34.382 | 37.652 | 41.566 | 44.314 | 52.620 |
| 26 | 29.246 | 31.795 | 35.563 | 38.885 | 42.856 | 45.642 | 54.052 |
| 27 | 30.319 | 32.912 | 36.741 | 40.113 | 44.140 | 46.963 | 55.476 |
| 28 | 31.391 | 34.027 | 37.916 | 41.337 | 45.419 | 48.278 | 56.893 |
| 29 | 32.461 | 35.139 | 39.087 | 42.557 | 46.693 | 49.588 | 58.302 |
| 30 | 33.530 | 36.250 | 40.256 | 43.773 | 47.962 | 50.892 | 59.703 |

Note: The following table provides the values of χ^2_α . That correspond to a given upper-tail area α and a specified number of degrees of freedom.

REFERENCES

- Ahmed, N. and Sunada, D.K. 1969. Nonlinear flow in porous media. *Journal of Hydraulics Division, ASCE*, 95(HY6), 1847–1857.
- Aitchison, J. and Brown, J.A.C. 1969. *The Lognormal Distribution*. Cambridge University Press, Cambridge, UK, 176 p.
- Akaike, H. 1974. A new look at the statistical model identification. *IEEE Transactions on Automatic Control*, 19(6), 716–723.
- Barrette, J.P. and Goldsmith, L. 1976. When is n large enough? *The American Statistician*, 30, 67–71.
- Bennett, R.R. 1962. Flow net analysis, in *Theory of Aquifer Tests*. J.G. Ferris, D.B. Knowlers, R.H. Brown, and R.W. Stallman, eds., US Geological Survey Prof. Paper 708, 70 p.

- Bouwer, H. 1978. *Groundwater Hydrology*. McGraw-Hill Book Company, New York, 480 p.
- Box, G.E.P. and Cox, D.R. 1964. An analysis of transformation. *Journal of the Royal Statistical Society, B26*, 211–252.
- Brockwell, P.J. and Davis, R.A. 1987. *Time Series Theory and Methods*. Library of Congress Cataloging in Publication Data.
- Brooks, R.H. and Corey, A.T. 1964. *Hydraulics Properties of Porous Media*. Hydrology Paper 3, Colorado State University, Fort Collins, CO, 71 p.
- Campbell, G.S. 1974. A simple method for determining unsaturated conductivity from moisture retention data. *Soil Science*, 117, 311–314.
- Carsel, R.F. and Parrish, R.S. 1988. Developing joint probability distributions of soil water retention characteristics. *Water Resources Research*, 24(5), 755–769.
- Central Water Commission. 2010. Development of hydrological design aids (surface water) under hydrology project II: State of the art report. Consulting Engineering Services (India) in Association with HR Wallingford. New Delhi, India.
- De Wiest, R.J.M. 1965. *Geohydrology*. John Wiley & Sons, New York, 463 p.
- Domenico, P.A. and Schwartz, F.W. 1990. *Physical and Chemical Hydrogeology*. John Wiley & Sons, New York.
- Ferris, J.G., Knowles, D.B., Browne, R.H., and Stallman, R.W. 1962. *Theory of Aquifer Tests*, U.S. Geological Survey, Water-Supply Paper 1536E, 174 p.
- Fetler, C.W. 1994. *Applied Hydrogeology*, 3rd ed. Macmillan College Publishing Co., New York.
- Freeze, R. and Cherry, J. 1979. *Groundwater*. Prentice Hall, Englewood Cliffs, NJ, 604 p.
- Gilbert, R.O. 1987. *Statistical Methods for Environmental Pollution Monitoring*. John Wiley & Sons, New York.
- Hansch, C. and Leo, A. 1979. *Substitute Constants for Correlation Analysis in Chemistry and Biology*. John Wiley & Sons, New York, pp. 841–847.
- Hashino, M. and Delleur, J.W. 1981. *Investigation of the Hurst Coefficient and Optimization of ARMA Models for Annual River Flow*. Report CE-HSE-81-1, Civil Engineering, Purdue University, West Lafayette, IN.
- Hosking, J.R.M. 1990. L-moments: Analysis and estimation of distributions using linear combinations of order statistics. *Royal Statistical Society (Series B)*, 52, 105–124.
- Karamouz, M., Szidarovszky, F., and Zahraie, B. 2003. *Water Resources Systems Analysis*. Lewis Publishers, CRC Press, Boca Raton, FL, 590 p.
- Lapin, L.L. 1990. *Probability and Statistics for Modern Engineering*. PWS-KENT Publishing Company, Boston, MA, 810 p.
- Mualem, Y. 1976. A new model for predicting the hydraulic conductivity of unsaturated porous media. *Water Resources Research*, 12(3), 513–522.
- Narasimhan, T.N. and Goyal, K.E. 1984. Subsidence due to geothermal fluid withdrawal, in *Man-Induced Land Subsidence, Reviews in Engineering Geology*, Geological Society of America, pp. 35–66.
- Novotny, V.N. 2003. *Water Quality—Diffuse Pollution and Watershed Management*, 2nd edn. John Wiley & Sons, Hoboken, NJ.
- Price, K.R., Gilbert, R.O., and Gano, K.A. 1981. *Americium-241 in Surface Soil Associated with the Hanford Site and Vicinity*. Pacific Northwest Laboratory, Richland, WA.
- Rawls, W.J., Ahuja, L.R., Brakensiek, D.L., and Shirmohammadi, A. 1993. Infiltration and soil water movement, in *Handbook of Hydrology*, D.R. Maidment, ed., McGraw-Hill, New York, pp. 5.1–5.51.
- Richards, L.A. 1931. Capillary conduction of liquids through porous mediums. *Physics*, 1(5), 318–333.

- Salas, J.D., Delleur, J.W., Yevjevich, V., and Lane, W.L. 1988. *Applied Modeling of Hydrological Time Series*. Water Resources Publications, Littleton, CO, 484 p.
- Schwartz, F.W. and Zhang, H. 2003. *Fundamentals of Groundwater*. John Wiley & Sons, New York, 583 p.
- Snedecor, G.W. and Cochran, W.G. 1967. *Statistical Methods*, 6th edn. Iowa State University Press, Ames, IA.
- Snow, D.T. 1969. Anisotropic permeability of fractured media. *Water Resources Research*, 5, 1273–1289.
- Sokal, R.R. and Rohlf, F.J. 1981. *Biometry*, 2nd edn. W. H. Freeman, San Francisco, CA, 133 p.
- Todd, D.K. 1980. *Groundwater Hydrology*. John Wiley & Sons, New York, 621 p.
- Todd, D.K. and Mays, L.M., 2005. *Groundwater Hydrology*. John Wiley & Sons, New York.
- Van Genuchten, M.T. 1980. A closed form equation for predicting the hydraulic conductivity of unsaturated soils. *Soil Society of America Journal*, 44, 892–898.
- Wang, T., Franz, T.E., Yue, W., Szilagyi, J., Zlotnik, V.A., You, J., Chen, X., Shulski, M.D., and Young, A. 2016. Feasibility analysis of using inverse modeling for estimating natural groundwater recharge from a large-scale soil moisture monitoring network. *Journal of Hydrology*, 533, 250–265.
- Yevjevich, V. 1972. *Probability and Statistics in Hydrology*. Water Resources Publications, Fort Collins, CO, 302 p.



Taylor & Francis

Taylor & Francis Group

<http://taylorandfrancis.com>

4 Hydraulics of Groundwater

4.1 INTRODUCTION

Groundwater in its natural state moves due to hydraulic forces. Because hydraulic head represents the energy of water, groundwater flows from locations of higher head, usually upland areas, to locations of lower head, such as lowland areas, marshes, springs, and rivers. This is a principle to use water-level data obtained from wells, springs, and surface water features to determine the horizontal and vertical direction of groundwater movement and to estimate the rate of groundwater flow. In the subsurface, water occurs in four phases: water vapor from transpiration by plants and direct evaporation from the water table, condensed water absorbed by dry soil particles, water held around soil particles by molecular attraction, and water under the influence of gravity.

In the saturated zone, groundwater flows through interconnected voids in response to the difference in fluid pressure and elevation. The change in hydraulic head over a specified distance in a given direction is called the hydraulic gradient. The quantity of groundwater moving through a volume of rock can be estimated using Darcy's law, which is a function of the hydraulic gradient. Darcy's law determines the rate of groundwater flow through an area.

The groundwater flow equation is used in hydrogeology. It is a mathematical relationship representing groundwater flow through an aquifer. The mathematical description of groundwater flow is based on the principles of conservation of mass, energy, and momentum. In this chapter, groundwater flow equations are developed using these principles in confined and unconfined aquifers for steady- and unsteady-state conditions. Groundwater flow equations in an aquifer subjected to the impacts of a pumping well are also discussed in this chapter. Generally, groundwater flow equations are expressed in terms of partial differential equations with spatial coordinates and time as independent variables. In addition, different methods for artificial recharge, as a tool to store surplus surface water underground, are explained in this chapter.

4.2 CONTINUITY EQUATION

The conservation of mass states that for a given increment of time, the difference between the mass flowing in across the boundaries, the mass flowing out across the boundaries, and the sources within the volume is the change in storage.

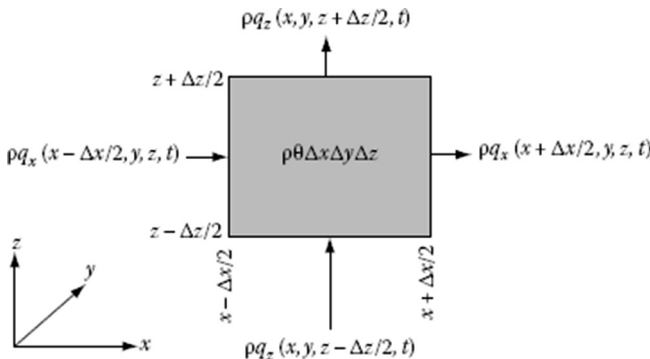


FIGURE 4.1 Mass conservation in elementary control volume.

The continuity equation, as a fundamental law of groundwater flow, expresses the principle of mass conservation as follows:

$$\text{Mass inflow rate} - \text{mass outflow rate} = \text{Rate of change of mass storage with time} \quad (4.1)$$

Considering an elementary control volume of soil (Figure 4.1), which has the volume of $(\Delta x \Delta y \Delta z)$, the mass of groundwater, M , in this control volume is:

$$M = \rho \theta \Delta x \Delta y \Delta z \quad (4.2)$$

where θ is the moisture content of the porous medium. The Equation 4.1 can be written as follows:

$$\frac{\partial M}{\partial t} = \text{inflow} - \text{outflow} \quad (4.3)$$

The inflow and outflow can be calculated for each side of the element. For example, the mass of groundwater inflow to the left side is:

$$\rho q_x \left(\frac{x - \Delta x}{2, y, z, t} \right) \Delta y \Delta z \approx \left(\rho q_x - \frac{\Delta x}{2} \frac{\partial \rho q_x}{\partial x} \right) \Delta y \Delta z \quad (4.4)$$

A similar equation can be derived for other sides. Considering these equations, the total inflow minus outflow can be derived as follows:

$$\frac{\partial M}{\partial t} = - \left(\frac{\partial \rho q_x}{\partial x} + \frac{\partial \rho q_y}{\partial y} + \frac{\partial \rho q_z}{\partial z} \right) \Delta x \Delta y \Delta z \quad (4.5)$$

Based on Equation 4.3, the change in storage is calculated by:

$$\frac{\partial M}{\partial t} = \frac{\partial}{\partial t} (\rho \theta \Delta x \Delta y \Delta z) = \rho \left(\theta \frac{\partial \rho}{\partial t} + \frac{\partial \theta}{\partial t} + \frac{\theta}{\Delta z} \frac{\partial \Delta z}{\partial t} \right) \Delta x \Delta y \Delta z \quad (4.6)$$

Compression of a porous medium and water can be considered using the following equations, respectively:

$$\frac{1}{\Delta z} \frac{\partial \Delta z}{\partial t} = \alpha \frac{\partial p}{\partial t} \quad (4.7)$$

$$\frac{1}{\Delta z} \frac{\partial \Delta p}{\partial t} = \beta \frac{\partial p}{\partial t} \quad (4.8)$$

where:

α is the elastic compressibility coefficient of a porous medium

p is the water pressure

β is the compressibility coefficient of water.

Substitution of these equations in Equation 4.6 gives:

$$\frac{\partial M}{\partial t} = \rho \left(\theta(\alpha + \beta) \frac{\partial p}{\partial t} + \frac{\partial \theta}{\partial t} \right) \Delta x \Delta y \Delta z \quad (4.9)$$

Therefore, using Equations 4.2 and 4.5, the continuity equation can be derived as:

$$\rho \left(\theta(\alpha + \beta) \frac{\partial p}{\partial t} + \frac{\partial \theta}{\partial t} \right) = - \left(\frac{\partial pq_x}{\partial x} + \frac{\partial pq_y}{\partial y} + \frac{\partial pq_z}{\partial z} \right) \quad (4.10)$$

The left side of this equation describes the change in the volume of water in a porous medium due to the change in water content or compression of the water and the medium. Considering ρ is constant and there is no change in moisture content, Equation 4.10 can be summarized two-dimensionally as expressed in Example 4.1.

Example 4.1

Derive the steady-state flow equation in an aquifer in terms of hydraulic head h with the following hydraulic conductivity function:

$$K = K_0 (a + b e^{cx} + d e^{fy})$$

where a , b , c , d , and f are the system's parameters.

SOLUTION

The continuity equation (Equation 4.10) in steady-state conditions can be simplified as follows:

$$\frac{\partial q_x}{\partial x} + \frac{\partial q_y}{\partial y} = 0$$

Applying Darcy's law, we have:

$$\frac{\partial}{\partial x} \left(K \frac{\partial h}{\partial x} \right) + \frac{\partial}{\partial y} \left(K \frac{\partial h}{\partial y} \right) = 0$$

or,

$$\frac{\partial}{\partial x} \left(K_0 (a + be^{cx} + de^{fy}) \frac{\partial h}{\partial x} \right) + \frac{\partial}{\partial y} \left(K_0 (a + be^{cx} + de^{fy}) \frac{\partial h}{\partial y} \right) = 0$$

Finally,

$$(a + be^{cx} + de^{fy}) \frac{\partial^2 h}{\partial x^2} + cbe^{cx} \frac{\partial^2 h}{\partial x^2} + (a + be^{cx} + de^{fy}) \frac{\partial^2 h}{\partial y^2} + fde^{fy} \frac{\partial^2 h}{\partial y^2} = 0$$

4.3 EQUATION OF MOTION IN GROUNDWATER

The equation of motion can be derived using conservation of momentum. Considering the elementary control volume (Figure 4.1), the forces that usually act on the water in the control volume are:

- Pressure forces
- Gravity forces
- Reaction forces of solids

For example, the pressure force on the left-hand side of the control volume in Figure 4.1 is as follows:

$$\theta p \left(\frac{x - \Delta x}{2, y, z, t} \right) \Delta y \Delta z \quad (4.11)$$

The left-hand side also has the same force, but in the opposite direction. Therefore, the resulting pressure force component in the x direction is as follows (Delleur, 1999):

$$-\frac{\partial \theta p}{\partial x} \Delta x \Delta y \Delta z \quad (4.12)$$

The other components of pressure force on the control volume in y and z directions can be obtained using a similar method.

The gravity force, which is equal to the total weight of water in the control volume and acts in the negative side of z direction, is:

$$-\rho g \theta \Delta x \Delta y \Delta z \quad (4.13)$$

where g is the gravity constant. The reaction forces are usually defined as average body forces per water volume. It consists of the friction forces due to water movement and the forces that act against the water pressure. The friction and reaction

forces are denoted as $r = (r_x, r_y, r_z)$ and $f = (f_x, f_y, f_z)$, respectively. The x component of these forces is as follows:

$$(r_x + f_x)\theta\Delta x\Delta y\Delta z \quad (4.14)$$

It can have similar components in y and z directions.

Using the operator $\nabla = \left(\frac{\partial}{\partial x}, \frac{\partial}{\partial y}, \frac{\partial}{\partial z}\right)$, the effects of all forces can be combined in one vector as follows:

$$[-\nabla(\theta p) - \rho g \nabla z + (r + f)\theta] \Delta x \Delta y \Delta z \quad (4.15)$$

Considering that when the fluid is at rest, the friction f is zero and the water pressure is hydrostatic, the overall reaction force can be evaluated as follows (Delleur, 1999):

$$r = \frac{p}{\theta} \nabla \theta \quad (4.16)$$

In the case of groundwater motion, the sum of forces is equal to the changes of fluid momentum and the friction force is not zero. As the groundwater flow is generally very slow, the changes in momentum are negligible and, therefore, the forces that act on the fluid in the control volume are approximately in equilibrium.

$$-\nabla p - \rho g \nabla z + f \approx 0 \quad (4.17)$$

The friction force can be represented as:

$$f = -\frac{\mu}{k} q \quad (4.18)$$

where:

μ is the dynamic viscosity of fluid

k is the intrinsic permeability

q is the groundwater flux.

The equation of motion can be expressed using Equations 4.12 and 4.13 as follows:

$$q = -\frac{k}{\mu} (\nabla p + \rho g \nabla z) \quad (4.19)$$

Neglecting the gradients of density, the motion equation can be simplified as:

$$q = -\frac{k \rho g}{\mu} (\nabla \psi + z) = -K \nabla h \quad (4.20)$$

where $\psi = \int \frac{dp}{\rho g}$ is the pressure potential, and the other variables have been defined in previous sections. The above equation clarifies the principles and assumptions that result in Darcy's law. One of the most important assumptions of Darcy's law is that

the flow of water in a porous medium is slow and the large values of frictional forces balance the driving forces. In the anisotropic porous media, Darcy's law in Cartesian coordinates can be written as:

$$q_x = -K_x \frac{\partial h}{\partial x} \quad (4.21)$$

$$q_y = -K_y \frac{\partial h}{\partial y} \quad (4.22)$$

$$q_z = -K_z \frac{\partial h}{\partial z} \quad (4.23)$$

4.3.1 GROUNDWATER FLOW EQUATION

The groundwater equation can be derived by a combination of the continuity equation and the equation of motion as expressed in Equations 4.10 and 4.20, as follows:

$$\theta(\alpha + \beta) \frac{\partial p}{\partial t} + \frac{\partial \theta}{\partial t} = \nabla \left[\frac{k}{\mu} (\nabla p + \rho g \nabla z) \right] \quad (4.24)$$

This equation can be rewritten as follows:

$$S \frac{\partial p}{\partial t} = \nabla \left[\frac{k}{\mu} (\nabla p + \rho g \nabla z) \right] \quad (4.25)$$

where S is the storage coefficient and is equal to:

$$S = \theta(\alpha + \beta) + \frac{\partial \theta}{\partial p} \quad (4.26)$$

S is related to water and soil characteristics such as saturated and unsaturated conditions of soil, and the water pressure in a confined aquifer. Therefore, the three-dimensional equation of groundwater movement as a function of water pressure (not as a function of groundwater potential) can be derived as follows:

$$S \frac{\partial p}{\partial t} = \frac{\partial}{\partial x} \left(\frac{k_x}{\mu} \frac{\partial p}{\partial x} \right) + \frac{\partial}{\partial y} \left(\frac{k_y}{\mu} \frac{\partial p}{\partial y} \right) + \frac{\partial}{\partial z} \left(\frac{k_z}{\mu} \frac{\partial p}{\partial z} \right) \quad (4.27)$$

The general form of the equation of groundwater flow is usually simplified in practice. Ignoring density effects, Equation 4.24 can be simplified as follows:

$$\theta(\alpha + \beta) \frac{\partial p}{\partial t} + \frac{\partial \theta}{\partial t} = \nabla (K \nabla h) \quad (4.28)$$

In groundwater, the density is usually considered to be constant; therefore, the temporal variation of water pressure and groundwater potential can be related as:

$$\frac{\partial p}{\partial t} = \rho g \frac{\partial h}{\partial t} \quad (4.29)$$

Therefore, the following basic groundwater flow equation can be derived:

$$\rho g \theta (\alpha + \beta) \frac{\partial h}{\partial t} + \frac{\partial \theta}{\partial t} = S_s \frac{\partial h}{\partial t} \nabla (K \nabla h) \quad (4.30)$$

where S_s is the specific storage coefficient. Written in the Cartesian coordinates, the equation of saturated groundwater flow becomes:

$$S_s \frac{\partial h}{\partial t} = \frac{\partial}{\partial x} \left(K_x \frac{\partial h}{\partial x} \right) + \frac{\partial}{\partial y} \left(K_y \frac{\partial h}{\partial y} \right) + \frac{\partial}{\partial z} \left(K_z \frac{\partial h}{\partial z} \right) \quad (4.31)$$

In steady-state conditions, Equation 4.31 can be simplified as:

$$\frac{\partial}{\partial x} \left(K_x \frac{\partial h}{\partial x} \right) + \frac{\partial}{\partial y} \left(K_y \frac{\partial h}{\partial y} \right) + \frac{\partial}{\partial z} \left(K_z \frac{\partial h}{\partial z} \right) = 0 \quad (4.32)$$

This equation shows that the difference in groundwater potential causes the movement of water in porous media and fluxes depend upon the hydraulic conductivity of the medium in different directions (Karamouz et al., 2003).

Example 4.2

Develop groundwater flow equations for the confined aquifer shown in Figure 4.2. Assume the aquifer is homogeneous with isotropic and steady-flow conditions. If the hydraulic gradient between two wells that are 250 m apart is equal to 0.45, find the flow velocity and aquifer discharge. Assume $k = 5 \times 10^{-6}$ m/s and $b = 30$ m.

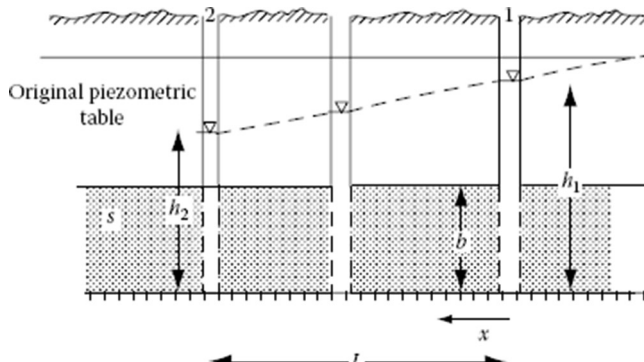


FIGURE 4.2 A confined aquifer with steady-flow conditions.

SOLUTION

For the one-dimensional confined aquifer system, the governing equation is given by the following equation:

$$\frac{d}{dx} \left(\frac{dh}{dx} \right) = 0$$

or,

$$\frac{dh}{dx} = C_1$$

Applying Darcy's law, we have:

$$\frac{dh}{dx} = -\frac{V}{K}$$

So,

$$h = -\frac{V}{K}x + C_2$$

With the boundary conditions,

$$h(0) = h_1, h(L) = h_2$$

$$V = -\frac{K}{L}(h_2 - h_1) \text{ and } q = -\frac{Kb}{L}(h_2 - h_1)$$

$$V = -K \frac{(h_2 - h_1)}{L} = 5 \times 10^{-6} \times 0.45 = 2.25 \times 10^{-6} \text{ m/s}$$

$$q = Vb = 2.25 \times 10^{-6} \times 30 = 6.75 \times 10^{-5} \text{ m}^2/\text{s}$$

Example 4.3

Develop the groundwater flow equations for a two-dimensional horizontal semi-confined or leaky aquifer, which has the thickness $b(x, y)$ at each point (x, y) .

SOLUTION

The average value of the hydraulic head at each point is as follows:

$$\bar{h} = \frac{1}{b} \int_0^b h dz$$

Using Equation 4.31 and considering $T = kb$, the flow equation is:

$$S_s b \frac{\partial \bar{h}}{\partial t} = \frac{\partial}{\partial x} \left(T_x \frac{\partial \bar{h}}{\partial x} \right) + \frac{\partial}{\partial y} \left(T_y \frac{\partial \bar{h}}{\partial y} \right) + q_z(b)$$

where $q_z(b)$ is the vertical recharge or discharge such as leakage, pumping, or injection. The vertical leakage from the upper semiconfining layer can be calculated using Darcy's law as follows:

$$q_z(b) = \frac{K_a(H_a - \bar{h})}{b_a}$$

where:

K_a is the hydraulic conductivity of the upper confining layer

H_a is the head in the upper boundary of confining layer

b_a is the thickness of the semiconfined layer.

Considering the point injection and pumping wells in the system, the flow equation can be written as follows (Hantush and Jacob, 1955; Willis and Yeh, 1987):

$$s_s b \frac{\partial \bar{h}}{\partial t} = \frac{\partial}{\partial x} \left(T_x \frac{\partial \bar{h}}{\partial x} \right) + \frac{\partial}{\partial y} \left(T_y \frac{\partial \bar{h}}{\partial y} \right) + \frac{K_a(H_a - \bar{h})}{b_a} \pm \sum_{w \in W} Q_w \delta_w$$

where:

$-Q_w$ is the discharge ($+Q_w$ is the recharge) from the pumping (injection) well w

δ_w is a zero-one integer variable. This variable is equal to one if there is pumping or injection at well site w .

Example 4.4

Determine the general form of hydraulic head distribution in the homogeneous and isotropic confined aquifer shown in the steady-flow conditions shown in Figure 4.3. Then, consider two channels with water depth at 80 and 70 m in two sides of the confined aquifer with varied thickness from 50 to 10 m. Find the hydraulic head in $L/2$ and $L/3$ from the datum.

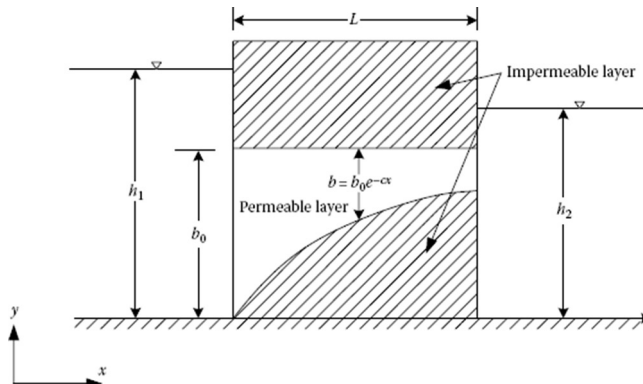


FIGURE 4.3 A confined aquifer between two impermeable layers. (From Willis, R. and Yeh, W.W.-G., *Groundwater Systems Planning and Management*, Prentice Hall, Englewood Cliffs, NJ, 1987.)

SOLUTION

For the one-dimensional aquifer system, the Equation 4.32 can be written as:

$$\frac{d}{dx} \left(kb \frac{dh}{dx} \right) = 0$$

with the boundary conditions,

$$h(0) = h_1, h(L) = h_2$$

and

$$b = b_0 e^{-cx}$$

Simplifying the equation,

$$Kb \frac{d^2h}{dx^2} + K \frac{db}{dx} \frac{dh}{dx} = 0$$

or

$$\frac{d^2h}{dx^2} - C \frac{dh}{dx} = 0$$

The solution of this second-order, linear ordinary differential equation is:

$$h = C_1 e^{cx} + C_2$$

where C_1 and C_2 are constants of integration. Using the boundary conditions to evaluate these constants, the steady-state head distribution is described by the equation (Willis and Yeh, 1987):

$$h = h_1 - \left[\frac{(h_1 - h_2)(e^{cx} - 1)}{(e^{cL} - 1)} \right]$$

$$b = b_0 e^{-cx} \quad 50 = 10 e^{-c \times 150} \quad c = -0.011$$

$$L/2 = 75 \text{ m} \quad h = 80 - \left[\frac{(80 - 70)(e^{-0.011 \times 75} - 1)}{e^{-0.011 \times 150} - 1} \right] = 73.06 \text{ m}$$

$$L/3 = 50 \text{ m} \quad h = 80 - \left[\frac{(80 - 70)(e^{-0.011 \times 50} - 1)}{e^{-0.011 \times 150} - 1} \right] = 74.77 \text{ m}$$

Example 4.5

Develop groundwater flow equations for a homogeneous and isotropic unconfined aquifer in steady-flow conditions as shown in Figure 4.4. If the water table in wells 1 and 2 is equal to 60 and 43 m, respectively, find the water table in the observation well in the middle. With the assumption of a linear variation of water table between two wells, find the water table in the observation well.

SOLUTION

Applying Darcy's law, we have:

$$q = -KA \frac{dh}{dx}$$

and

$$A = h \times 1$$

With the boundary conditions,

$$h(0) = h_1, h(L) = h_2$$

Direct integration of the equation produces:

$$\int_0^L q dx = -K \int_{h_1}^{h_2} h dh$$

$$\text{So, } q = -\frac{K}{2L} (h_2^2 - h_1^2) \text{ and } h = \sqrt{h_1^2 - (h_1^2 - h_2^2) \frac{x}{L}}$$

$$h = \sqrt{h_1^2 - (h_1^2 - h_2^2) \frac{x}{L}} = \sqrt{60^2 - (60^2 - 43^2) \times \frac{L/2}{L}} = 52.2 \text{ m}$$

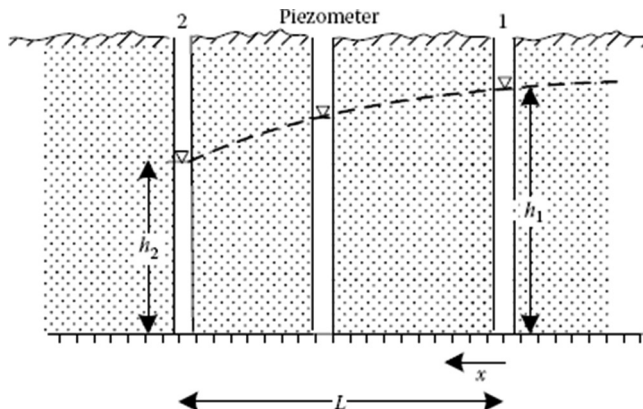


FIGURE 4.4 An unconfined aquifer with steady-flow conditions.

With the assumption of a linear variation of a water table:

$$h = 60 - \frac{(60-43)}{2} = 51.5 \text{ m}$$

It shows with a parabolic water table assumption, a water table is observed more than linear variation.

Example 4.6

Determine the hydraulic head for the homogeneous and isotropic unconfined aquifer in steady-flow conditions as shown in [Figure 4.5](#). Assume the aquifer has a uniform recharge rate, R (L/T).

SOLUTION

For the one-dimensional aquifer system, the governing equation can be written as:

$$\frac{d}{dx} \left[Kh \frac{dh}{dx} \right] + R = 0$$

and the boundary conditions:

$$h(-L/2) = h_0$$

$$\left. \frac{dh}{dx} \right|_{x=0} = 0$$

Direct integration of the equation produces:

$$h^2 = -\frac{Rx^2}{K} + C_1x + C_2$$

where C_1 and C_2 are the constants of integration. Evaluating these constants from the known boundary condition information, the steady-state head distribution is described by the ellipse equation, or

$$h^2 = h_0^2 - \frac{R}{K} \left[x^2 - \left(\frac{L}{2} \right)^2 \right]$$

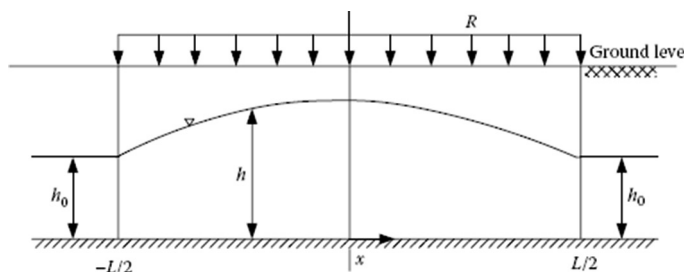


FIGURE 4.5 An unconfined flow with uniform recharge rate in Example 4.6.

Example 4.7

Artificial recharge of groundwater with spreading basins is used to mitigate or control saltwater intrusion into coastal aquifers. For the recharge system shown in [Figure 4.6](#), determine the steady-state head distribution. Assume that the aquifer is homogeneous and isotropic, and that for $x > x_e$ (the effective radius) $h = d$, the initial head in the system.

SOLUTION

For the one-dimensional aquifer system, the governing equation can be written as:

$$\frac{d}{dx} \left[Kh \frac{dh}{dx} \right] + f(x) = 0$$

where $f(x)$ is the source term that is defined as:

$$f(x) = \begin{cases} R, & |x| \leq L \\ 0, & |x| > L \end{cases}$$

The boundary conditions of the problem require that:

$$h(x_e) = d, \frac{dh}{dx} \Big|_{x=0} = 0$$

and that there will be continuity of the head and the velocity at the boundary, $x = L$, or

$$h|_{L^-} = h|_{L^+}, \frac{dh}{dx} \Big|_{L^-} = \frac{dh}{dx} \Big|_{L^+}$$

For the flow region, $|h| \leq L$, the governing equation is:

$$\frac{d}{dx} \left[h \frac{dh}{dx} \right] + \frac{R}{K} = 0$$

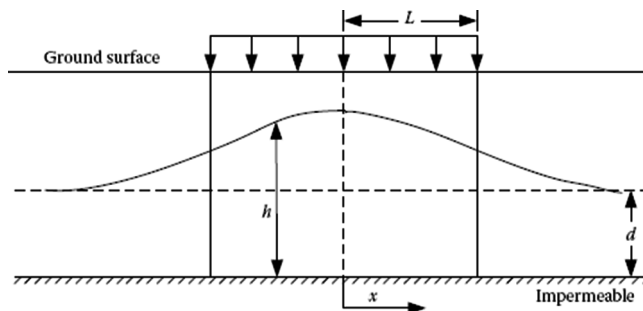


FIGURE 4.6 An unconfined aquifer system with uniform recharge rate in Example 4.7.

Direct integration of the equation produces:

$$h^2 = -\frac{R}{K}x^2 + C_2$$

where C_2 is a constant of integration, and we have used the gradient condition at $x = 0$ to evaluate the first constant of integration, $C_1 = 0$. For the flow domain, $|x| > L$, the governing equation is simply,

$$\frac{d}{dx} \left[h \frac{dh}{dx} \right] = 0$$

The solution is given as:

$$h^2 = C_3x + C_4$$

where C_3 and C_4 are constants of integration. We evaluate these constants from the given boundary conditions. For example, continuity of h and dh/dx at $x = L$ requires that:

$$2h \frac{dh}{dx} \Big|_{L^-} = -\frac{2RL}{K} = 2h \frac{dh}{dx} \Big|_{L^+} = C_3$$

and

$$C_3 = -\frac{2RL}{K}$$

At the effective distance, x_e , we also have:

$$h(x_e) = d \Rightarrow d^2 = \frac{2(-RL)}{K}x_e + C_4$$

or

$$C_4 = d^2 + \frac{2RLx_e}{K}$$

Additionally, at $x = L$,

$$h^2 = \frac{-RL^2}{K} + C_2 = \frac{2(-RL)}{K}L + d^2 + \frac{2RL}{K}x_e$$

or

$$C_2 = \frac{-RL^2}{K} + d^2 + \frac{2RL}{K}x_e$$

The head distribution in the aquifer system is then given by the equations (Willis and Yeh, 1987):

$$h^2 = \frac{-R}{K}x^2 - \frac{RL^2}{K} + d^2 + \frac{2RLx_e}{K}, |x| \leq L$$

$$h^2 = \frac{-rRL}{K} x + d^2 + \frac{2RLx_e}{K}, \quad L < |x| \leq x_e$$

$$h = d, \quad |x| \geq x_e$$

4.4 WELLS

Well drilling aids groundwater exploration with an objective to discover aquifers in different hydrogeological conditions and determination of hydraulic parameters. Groundwater exploitation from the well leads to decline in the water level that limits the yield of the basin. Water is removed from the aquifer surrounding the well during water pumping and the piezometric surface decreases. Instead of moving toward the natural discharge area, the groundwater within the influence of the pump flows toward the well from every direction. Drawdown occurs within the distance to which the piezometric surface is lowered. Hence, prediction of hydraulic-head drawdowns in aquifers under proposed pumping schemes is one of the goals of groundwater resource studies.

The pumping well creates an artificial discharge area by drawing down (lowering) the water table around the well.

The conical-shaped depression of the water table around a pumping well is caused by the withdrawal of water; a valley in the water table. This area of drawdown is called the cone of depression. [Figure 4.7](#) shows the creation stages of a cone of depression immediately surrounding the well when water is pumped out. At the initial stage in pumping an unconfined aquifer, water begins to flow toward the well screen. Most water follows a path with a high vertical component from the water table to the screen. ([Figure 4.7a](#)). At the intermediate stage in pumping an unconfined aquifer, although dewatering of the aquifer materials near the well bore continues, the radial component of the flow becomes more pronounced ([Figure 4.7b](#)). At the approximate steady-state stage in pumping an unconfined aquifer, the profile of the cone of depression is established. Nearly all water originates near the outer edge of the area of influence, and a stable, mainly radial flow pattern is established as shown in [Figure 4.7c](#).

If pumping continues, more water must be derived from the aquifer storage at greater distances from the bore of the well and the following are observed:

1. The cone of depression is expanded.
2. The radius of influence of the well increases due to the expansion of the cone.
3. The drawdown is incremented at any point with the increase in the depth of the cone to provide the additional head required to move the water from a greater distance.
4. The cone expands and deepens more slowly with time since an increasing volume of stored water is available with the horizontal expansion of the cone.

The expansion of the cone of depression during equal intervals of time is much like that shown in [Figure 4.8](#). Calculations of the volume of each cone would show that cone 2

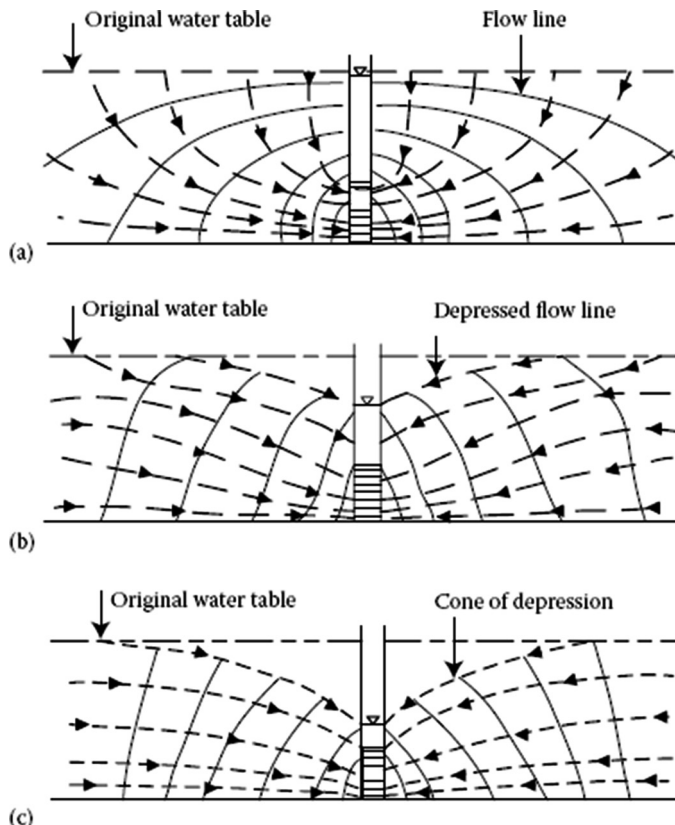


FIGURE 4.7 Development of flow distribution around a discharging well in an unconfined aquifer: (a) initial stage, (b) intermediate stage, and (c) steady-state stage. (From U.S. Bureau of Reclamation, *Groundwater Manual*, U.S. Government Printing Office, Denver, CO, 1981.)

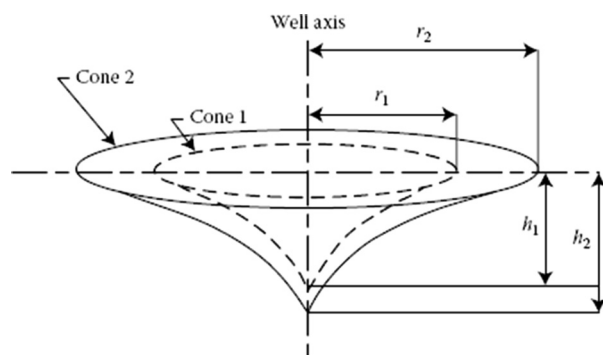


FIGURE 4.8 Changes in radius and depth of cone of depression.

has twice the volume as that of cone 1, and cone 3 has three times the volume as that of cone 1. It is because a constant pumping rate discharges the same volume of water from the well. Thus, if the aquifer is homogeneous and the well is being pumped at a constant rate, the increase in the volume of the cone of depression is constant over time. A water table, shaped now in the form of a cone, is steepest where it meets the well. Farther away from the well, the surface is flatter, and beyond a certain distance, called the radius of influence, the surface of the cone is almost as flat as the original water table.

After some time, deepening or expansion of the cone during short intervals of pumping is barely visible, and it becomes stabilized. This often misleads observers to conclude that the cone will not expand or deepen as pumping continues. The cone of depression continues to enlarge, until the flow in the aquifer with the source of surface water, vertical recharge from precipitation is intercepted to equal the pumping rate and the leakage that occurs through overlying or underlying formations.

Equilibrium occurs when continued pumping results in no further drawdown and the cone stops expanding. It might occur within a few hours after pumping begins; or never occurs even though the pumping period is extended for years. Well discharge to drawdown can be related by deriving a radial flow equation.

4.4.1 STEADY FLOW INTO A WELL

Steady-state groundwater problems are relatively simpler. Expression for steady-state radial flow into a well, under both confined and unconfined aquifer conditions, is presented in the next section.

4.4.1.1 Confined Flow

As discussed before, discharge from a completely confined aquifer by water pumping causes drawdowns of the potentiometric surface. Water is released from storage, and the fluid pressure decreases by the expulsion of water due to aquifer compaction under increased effective stress. A confined aquifer with steady-state radial flow to the fully penetrating well being pumped is shown in [Figure 4.9](#). The discharge from any well within the radial distance r from the pumping well is equal, but by increasing the radial distance from the well, the area of discharge increases. Thus, farther away from the well, the flow velocity decreases, the surface is flatter, and piezometric surface is almost static.

For a homogeneous, isotropic aquifer shown in [Figure 4.10](#), the well discharge at any radial distance r from the pumped well is:

$$\sum_{CS} \rho V dA = Q = 2\pi K r b \frac{dh}{dr} \quad (4.33)$$

Equation 4.33 can be presented for boundary conditions of $h = h_1$, at $r = r_1$, and $h = h_2$, at $r = r_2$:

$$\int_{h_1}^{h_2} dh = \frac{Q}{2\pi K b} \int_{r_1}^{r_2} \frac{dr}{r} \quad (4.34)$$

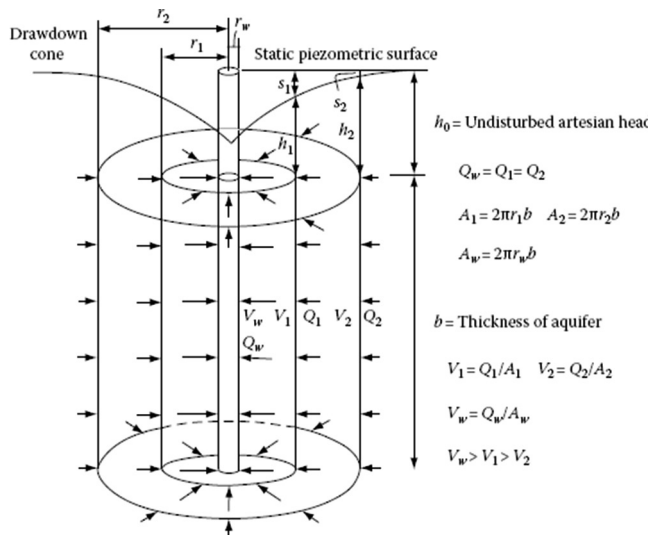


FIGURE 4.9 Flow distribution to a discharging well in a confined aquifer. (From U.S. Bureau of Reclamation, *Groundwater Manual*, U.S. Government Printing Office, Denver, CO, 1981.)

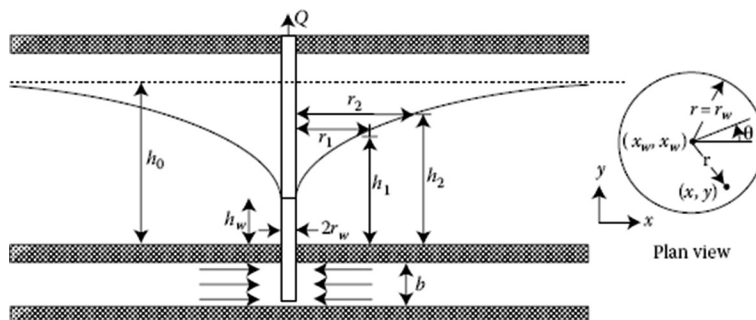


FIGURE 4.10 Well hydraulics for a confined aquifer.

$$h_2 - h_1 = \frac{Q}{2\pi K b} \ln \frac{r_2}{r_1} \quad (4.35)$$

Solving Equation 4.35 for Q gives:

$$Q = 2\pi K b \left[\frac{h_2 - h_1}{\ln(r_2 / r_1)} \right] \quad (4.36)$$

The general form of Equation 4.36 at any radial distance r from the pumped well is:

$$Q = 2\pi K b \left[\frac{h - h_i}{\ln(r/n)} \right] \quad (4.37)$$

The equation is known as the equilibrium or Theim equation (Theim, 1906).

Example 4.8

An extensive *homogeneous* and isotropic leaky aquifer of thickness b is overlain by a bed of glacial till shown in Figure 4.11. The thickness of the semiconfining stratum is m_a , and the hydraulic conductivity is K_a . The head in the aquifer overlying the aquitard is H_a and is assumed to be unaffected by pumping in the aquifer. Determine the steady-state response equation for a fully penetrating well in the aquifer system. As it is shown in the figure, the interior well area is sealed in the upper layer. (Why?)

SOLUTION

Assuming that the pumping well is located at the center of the aquifer system since groundwater flow is an essential radial, the confined flow equation may be expressed in radial coordinates. The flow equation in radial coordinates and applying Darcy's law for estimating the vertical leakage from the upper semiconfining layer is:

$$\frac{\partial^2 h}{\partial r^2} + \frac{1}{r} \frac{\partial h}{\partial r} = \frac{Q_w}{T}$$

or

$$\frac{T}{r} \frac{d}{dr} \left(r \frac{dh}{dr} \right) + \frac{K_a (H_a - h)}{m_a} = 0$$

Further, assuming that the well diameter is infinitesimally small, the boundary condition at the well is given by Darcy's law, or

$$\lim_{r \rightarrow 0} r \frac{dh}{dr} = \frac{Q}{2\pi T}$$

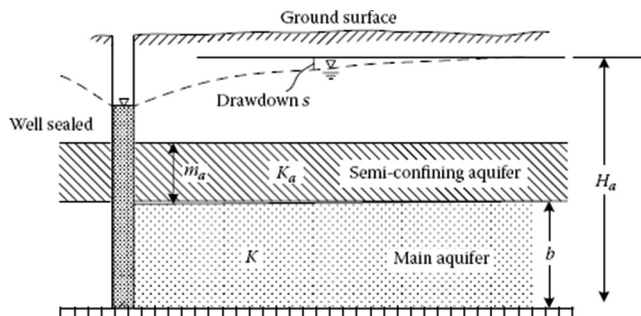


FIGURE 4.11 Leakage into aquifer for Example 4.8.

Defining the new dependent variable, y as:

$$y = H_a - h$$

the differential equation may be written as:

$$\frac{d^2y}{dr^2} + \frac{1}{r} \frac{dy}{dr} - \frac{K_a}{m_a} y = 0$$

Introducing the new independent variable, ρ ,

$$\rho = r \left(\frac{K_a}{m_a T} \right)^{1/2}$$

the differential equation becomes:

$$\frac{d^2y}{d\rho^2} + \frac{1}{\rho} \frac{dy}{d\rho} - y = 0$$

which is a modified form of the Bessel equation. The general solution of the equation is (Willis and Yeh, 1987):

$$y = A I_0(\rho) + B K_0(\rho)$$

where:

A and B are the constants of integration

I_0 and K_0 are the modified Bessel functions of the first and second kind of order zero

Requiring y to be finite as $\rho \rightarrow \infty$, A is 0 and the solution may be expressed as:

$$y = B K_0(\rho)$$

Using Darcy's law to evaluate the constant of integration and recover the original variables, the steady-state response equation is:

$$h = \frac{Q}{2\pi T} K_0 \left[r \left(\frac{K_a}{m_a T} \right)^{1/2} \right]$$

For a system of pumping and injection wells, the solutions may be superimposed again to obtain the total hydraulic response of the aquifer system. The solutions are valid for finite diameter wells as shown by Marino and Luthin (1982).

4.4.1.2 Unconfined Flow

In unconfined groundwater systems, water in the saturated zone is in open contact with atmospheric pressures. Groundwater release from storage occurs along permeable zones under the force of gravity as the aquifer responds to pumping. The streamline at the free surface of the aquifer is curved, and at the bottom of the aquifer it is horizontally lined, converging to the well.

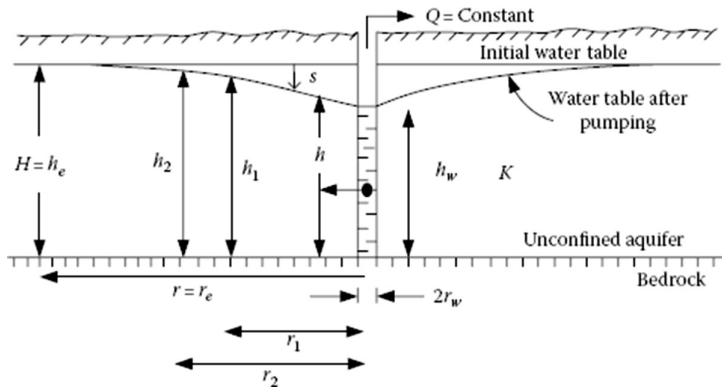


FIGURE 4.12 Radial flow in an unconfined aquifer.

Assuming that the aquifer is homogeneous and isotropic, develop the steady-state response equation relating the velocities (q_r , q_θ) and the groundwater extraction rate(s), Q as shown in Figure 4.12.

In radial coordinates, the Boussinesq equation may be expressed as:

$$\frac{1}{r} \frac{d}{dr} \left[r h \frac{dh}{dr} \right] = 0 \quad (4.38)$$

with the Darcy boundary condition,

$$\lim_{r \rightarrow 0} \left[r h \frac{dh}{dr} \right] = \frac{Q}{2\pi K} \quad (4.39)$$

The solution of the differential equation is:

$$h^2 = \frac{Q}{\pi K} \ln r + C$$

$$h^2 = \frac{Q}{2\pi K} \ln \left[(x - x_w)^2 + (y - y_w)^2 \right] + C \quad (4.40)$$

where:

C is the constant of integration

(x_w, y_w) are the coordinates of the pumping well.

For w pumping or injection ($-Q$) wells in the basin, the system response equation is found from superposition of the individual well responses, or:

$$h^2 = \sum_w \frac{Q_i}{2\pi K} \ln \left[(x - x_w)^2 + (y - y_w)^2 \right] + C \quad (4.41)$$

The velocity field is given by Darcy's law, or:

$$q_r = -K \frac{\partial h}{\partial r}, q_\theta = \frac{K}{r} \frac{\partial h}{\partial \theta} \quad (4.42)$$

Evaluating the partial derivatives, the velocities are (Willis and Yeh, 1987):

$$q_r = -\frac{K}{\pi} \sum_w Q_i \left\{ \frac{(r \cos \theta - x_w) \cos \theta + (r \sin \theta - y_w) \sin \theta}{(r \cos \theta - x_w)^2 + (r \sin \theta - y_w)^2} \right\} \Big/ (2h) \quad (4.43)$$

$$q_\theta = \frac{K}{\pi} \sum_w Q_i \left\{ \frac{(r \cos \theta - x_w)(-r \sin \theta) + (r \sin \theta - y_w)r \cos \theta}{(r \cos \theta - x_w)^2 + (r \sin \theta - y_w)^2} \right\} \Big/ (2rh) \quad (4.44)$$

The velocities, in this case, are nonlinear functions of the pumping or injection rates.

By rearranging Equation 4.39,

$$h dh = \frac{Q}{2\pi K} \frac{r}{dr} \quad (4.45)$$

Integrating between lines r_1 and r_2 where the water table depths are h_1 and h_2 , respectively, and rearranging,

$$Q = \frac{\pi K (h_2^2 - h_1^2)}{\ln(r_2 / r_1)} \quad (4.46)$$

There are large vertical-flow components near the well, so that this equation fails to describe accurately the drawdown curve near the well, but it can be defined for any two distances away from the pumped well. At the edge of the zone of influence with radius r_e , H_e = saturated thickness of the aquifer, Equation 4.46 can be rewritten as:

$$Q = \frac{\pi K (H_e^2 - h_w^2)}{\ln(r_e / r_w)} \quad (4.47)$$

In addition, Equation 4.36 for a confined groundwater system can be derived from Equation 4.46 as follows,

$$Q = \frac{\pi K (h_2^2 - h_1^2)}{\ln(r_2 / r_1)} = \frac{\pi K (h_2 - h_1)(h_2 + h_1)}{\ln(r_2 / r_1)} = \frac{2\pi K b (h_2 - h_1)}{\ln(r_2 / r_1)} \quad (4.48)$$

Example 4.9

A well penetrates an unconfined aquifer. Before pumping, the water table is at $h_0 = 25$ m. After a long period of pumping at a constant rate of $0.5 \text{ m}^3/\text{s}$, the drawdowns 50 m away from the well were observed to be 3 m. If $K = 7.26 \times 10^{-2} \text{ m/s}$, find the drawdowns at the distance of 150 m from the well.

SOLUTION

Applying Equation 4.46,

$$h_2^2 - h_1^2 = \frac{Q}{k\pi} \ln\left(\frac{r_2}{r_1}\right)$$

$$(25 - s)^2 - (25 - 3)^2 = \frac{0.5 \ln(150/50)}{\pi \times 7.26 \times 10^{-2}} \Rightarrow s = 2.46 \text{ m}$$

4.4.2 UNSTEADY STATE IN A CONFINED AQUIFER

When a fully penetrated well is pumped in a confined aquifer at a constant rate Q , water is released from storage by the expansion of the water as pressure in the aquifer is reduced and by expulsion as the pore space is reduced as the aquifer compacts. During pumping, the cone of depression is formed and expanded outward from the well, and pumping affects a relatively large area of the aquifer. Further, if no recharge occurs, the area of drawdown of the potentiometric surface will expand indefinitely, and the rate of decline of the head continuously decreases as the cone of depression spreads.

The confined flow equation in radial coordinates can be expressed as:

$$\frac{\partial^2 s}{\partial r^2} + \frac{1}{r} \frac{\partial s}{\partial r} = \frac{S}{T} \frac{\partial s}{\partial t} \quad (4.49)$$

where:

s is the drawdown ($s = h_0 - h$)

h_0 is the initial piezometric head.

The basic assumption can be expressed mathematically as initial and boundary conditions. The initial condition of a horizontal potentiometric surface is:

$$s(r, 0) = 0 \text{ for all } r \quad (4.50)$$

The boundary condition signifying an infinite horizontal extent with no drawdown at any time:

$$s(\infty, t) = 0 \text{ for all } r \quad (4.51)$$

$$\lim_{r \rightarrow 0} r \frac{\partial s}{\partial r} = -\frac{Q}{2\pi T} \quad (4.52)$$

The solution that Theis found for Equation 4.49 under the initial and boundary conditions is known as the Theis or nonequilibrium equation (Theis, 1935). In this method, the Boltzmann transformation is used for transforming the confined flow equation, a second-order linear diffusion equation, into an ordinary differential equation as follows:

$$u = \frac{r^2 S}{4Tt} \quad (4.53)$$

Substituting this variable in Equation 4.49, the flow equation in radial coordinates can be expressed as:

$$\frac{d^2 s}{du^2} + \left(1 + \frac{1}{u}\right) \frac{ds}{du} = 0 \quad (4.54)$$

Then, the initial and boundary conditions are transformed into:

$$S(\infty) = 0 \quad (4.55a)$$

$$\lim_{u \rightarrow 0} u \frac{ds}{du} = -\frac{Q}{4\pi T} \quad (4.55b)$$

Using the substitution, ds/du , a first integration of the equation yields:

$$u \frac{ds}{du} = C_1 e^{-u} \quad (4.56)$$

where C_1 is the constant of integration. Using the second boundary condition, the equation simplifies to:

$$\frac{ds}{du} = \frac{Q}{4\pi T} \times \frac{e^{-u}}{u} \quad (4.57)$$

Performing the final integration considering the first boundary condition, the drawdown equation is:

$$s = \frac{Q}{4\pi T} \int_u^{\infty} \frac{e^{-a}}{a} da \quad (4.58)$$

The integral in Equation 4.58 is well known in mathematics. It is called the exponential integral. It can be approximately presented by an infinite series so that the Theis equation becomes:

$$s = \frac{Q}{4\pi T} \left[-0.5772 - \ln u + u - \frac{u^2}{2 \times 2!} + \frac{u^3}{3 \times 3!} - \frac{u^4}{4 \times 4!} + \dots \right] \quad (4.59)$$

where $W(u)$ is called the dimensionless well function for nonleaky, isotropic, artesian aquifers, fully penetrated by wells having constant discharge conditions. Values of the well function corresponding to different values of u are listed in [Table 4.1](#). The well function is also expressed in the form of a type curve, as shown in [Figure 4.13](#). Both u and $W(u)$ are dimensionless.

This model can also be utilized to incorporate a variable groundwater pumping schedule. Assume the aquifer is pumped at a variable extraction rate for n planning periods. The drawdown for any period can be found from the superposition of the well responses because the response equations are linear functions of the extraction rates. The mathematical form of the equation for any period can be written as follows:

$$s = \frac{Q_1}{4\pi T} W\left(\frac{r^2 S}{4Tt}\right), \quad 0 \leq t \leq t_1 \quad (4.60a)$$

TABLE 4.1**Values of $W(u)$ for Various Values of u**

| | 1.0 | 2.0 | 3.0 | 4.0 | 5.0 | 6.0 | 7.0 | 8.0 | 9.0 |
|---------------------|-------|-------|-------|--------|--------|---------|---------|----------|----------|
| $\times 1$ | 0.219 | 0.049 | 0.013 | 0.0038 | 0.0011 | 0.00036 | 0.00012 | 0.000038 | 0.000012 |
| 1×10^{-1} | 1.82 | 1.22 | 0.91 | 0.70 | 0.56 | 0.45 | 0.37 | 0.31 | 0.26 |
| 1×10^{-2} | 4.04 | 3.35 | 2.96 | 2.68 | 2.47 | 2.30 | 2.15 | 2.03 | 1.92 |
| 1×10^{-3} | 6.33 | 5.64 | 5.23 | 4.95 | 4.73 | 4.54 | 4.39 | 4.26 | 4.14 |
| 1×10^{-4} | 8.63 | 7.94 | 7.53 | 7.25 | 7.02 | 6.84 | 6.69 | 6.55 | 6.44 |
| 1×10^{-5} | 10.94 | 10.24 | 9.84 | 9.55 | 9.33 | 9.14 | 8.99 | 8.86 | 8.74 |
| 1×10^{-6} | 13.24 | 12.55 | 12.14 | 11.85 | 11.63 | 11.45 | 11.29 | 11.16 | 11.04 |
| 1×10^{-7} | 15.54 | 14.85 | 14.44 | 14.15 | 13.93 | 13.75 | 13.60 | 13.46 | 13.34 |
| 1×10^{-8} | 17.84 | 17.15 | 16.74 | 16.46 | 16.23 | 16.05 | 15.90 | 15.76 | 15.65 |
| 1×10^{-9} | 20.15 | 19.45 | 19.05 | 18.76 | 18.54 | 18.35 | 18.20 | 18.07 | 17.95 |
| 1×10^{-10} | 22.45 | 21.76 | 21.35 | 21.06 | 20.84 | 20.66 | 20.50 | 20.37 | 20.25 |
| 1×10^{-11} | 24.75 | 24.06 | 23.65 | 23.36 | 23.14 | 22.96 | 22.81 | 22.67 | 22.55 |
| 1×10^{-12} | 27.05 | 26.36 | 25.96 | 25.67 | 25.44 | 25.26 | 25.11 | 24.97 | 24.86 |
| 1×10^{-13} | 29.36 | 28.66 | 28.26 | 27.97 | 27.75 | 27.56 | 27.41 | 27.28 | 27.16 |
| 1×10^{-14} | 31.66 | 30.97 | 30.56 | 30.27 | 30.05 | 29.87 | 29.71 | 29.58 | 29.46 |
| 1×10^{-15} | 33.96 | 33.27 | 32.86 | 32.58 | 32.35 | 32.17 | 32.02 | 31.88 | 31.76 |

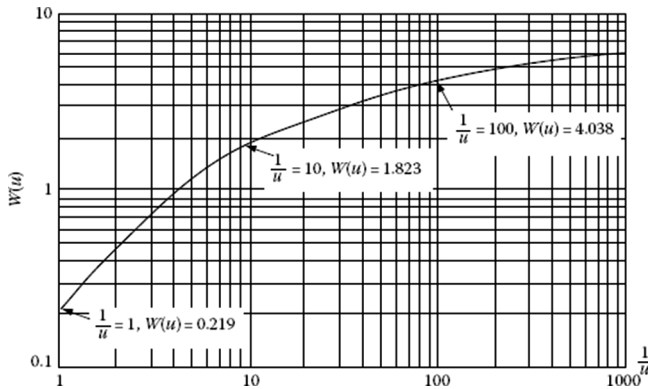


FIGURE 4.13 Values of $W(u)$ (well function of u) corresponding to values of $1/u$.

$$s = \frac{Q_1}{4\pi T} W\left(\frac{r^2 S}{4Tt}\right) + \left(\frac{Q_2 - Q_1}{4\pi T}\right) W\left(\frac{r^2 S}{4T(t-t_1)}\right), t_1 \leq t \leq t_2 \quad (4.60b)$$

$$s = \frac{Q_1}{4\pi T} W\left(\frac{r^2 S}{4Tt}\right) + \left(\frac{Q_2 - Q_1}{4\pi T}\right) W\left(\frac{r^2 S}{4T(t-t_1)}\right) + \dots$$

$$+ \left(\frac{Q_n - Q_{n-1}}{4\pi T}\right) W\left(\frac{r^2 S}{4T(t-t_{n-1})}\right), t \geq t_{n-1} \quad (4.60c)$$

where Q_k is the extraction rate for planning period k .

The drawdown commonly referred to as the nonequilibrium well pumping equation is expressed as:

$$s = \frac{Q}{4\pi T} W(u) \quad (4.61)$$

Equations 4.53 and 4.61 can be expressed in United States customary units where s is in ft, Q is in ft^3/d , T is in ft^2/d , r is in ft, and t is in days,

$$s = \frac{114.6Q}{T} W(u) \quad (4.62)$$

and

$$u = \frac{1.87r^2 S}{Tt} \quad (4.63)$$

or, for t in minutes,

$$u = \frac{2693r^2S}{Tt} \quad (4.64)$$

Example 4.10

A well is located in a 25-m confined aquifer with hydraulic conductivity of 30 m/day and a storage coefficient 0.005. If the well is being pumped at the rate of 1500 m³/day, calculate the drawdown at a distance of 100 m from the well after 20 h of pumping.

SOLUTION

$$T = KB = \frac{30}{86,400} \times 25 = 8.68 \times 10^{-3} \text{ m}^2/\text{s}$$

$$u = \frac{r^2S}{4Tt} = \frac{100^2 \times 0.005}{4 \times 8.68 \times 10^{-3} \times 20 \times 3600} = 0.02$$

Using the Theis method and calculating $W(u)$ to four significant digits,

$$W(u) = -0.5772 - \ln(0.02) + (0.02) - \frac{(0.02)^2}{2 \times 2!} + \frac{(0.02)^3}{3 \times 3!} = 3.3547$$

$$s = \frac{Q}{4\pi T} W(u) = \frac{1500 \times 3.3547}{4 \times \pi \times 8.68 \times 10^{-3} \times 24 \times 3600} = 0.53 \text{ m}$$

4.4.2.1 Aquifer Test Application

An aquifer test (or a pumping test) is performed to evaluate an aquifer by observing the aquifer's drawdown at observation wells. One or more monitoring wells or piezometers are used for aquifer testing as the observation/monitoring wells. Water is not being pumped from the observation well, instead, its drawdown is monitored. While water is being pumped from one well at a steady rate, the water tables are monitored in the observation wells. Typically, monitoring and pumping wells are screened across the same aquifers. Aquifer testing is based on the data processing to yield valuable qualitative and quantitative features about the subsurface geological composition of the aquifer domain. The test data processing is achieved by matching the data with an appropriate type curve. An analytical or numerical model of aquifer flow is used to match the data observed in the real world, assuming that the parameters from the idealized model apply to the real-world aquifer.

Most aquifer tests evaluate the aquifer characteristics including:

- Hydraulic conductivity or transmissivity, which shows how permeable the aquifer is and the ability of an aquifer to transmit water.
- Specific storage/specific yield or storativity, which is the measure of the amount of water an aquifer will release for a certain change in head.
- Boundary determination, which determines the type of boundaries that release water to the aquifer, providing additional water to reduce drawdown or no-flow boundaries.

Design, field observations, and data analysis are used for the aquifer tests to identify the ultimate objectives of quantifying the hydraulic properties, boundary determination, identification of the general type of aquifer, and hypothesis testing. In aquifer tests, in addition to knowing the geology of the site and construction of the wells (width, depth, materials used, and development), measuring devices for time, discharge, and water level should be calibrated and verified. Then, the observed data are plotted, and the best curve is fitted to the data. Finally, the aquifer characteristics are determined based on the fitted curve.

Graphical or computer estimation of parameter values using observed drawdown and well-produced rate records can be utilized as the method of analysis of the aquifer test data. For confined aquifers, there are two graphical methods including the log-log plot of drawdown versus time for the Theis method and the semilog plot for the Cooper–Jacob method.

4.4.2.2 Theis Method of Solution

The following equation was adopted by Theis (1935) and is used to determine T and S by expressing Equations 4.61 and 4.53 as:

$$\log s = \log \left(\frac{Q}{4\pi T} \right) + \log W(u) \quad (4.65)$$

$$\log \frac{t}{r^2} = \log \left(\frac{S}{4T} \right) + \log \frac{1}{u} \quad (4.66)$$

Because $Q/4\pi T$ and $S/4T$ are constants, the relation between $\log(s)$ and $\log(t/r^2)$ must be similar to the relation between $\log W(u)$ and $\log 1/u$. Therefore, drawdown measurements derived from pumping tests are plotted on double-logarithmic paper and $W(u)$ against $1/u$ on the same double-logarithmic paper; the two plotted curves have the same shape, but they are offset by the constants $(Q/4\pi T)$ and $(S/4T)$, vertically and horizontally, respectively, with parallel coordinate axes. Therefore, plot each curve on a separate sheet, place one graph on top of the other one, and move it horizontally and vertically until the curves are matched. When superimposed over the type curve, values of $W(u)$, $1/u$, t/r^2 , and s may be selected at any desirable point and substituted in the Theis equation. This is further illustrated in [Figure 4.14](#).

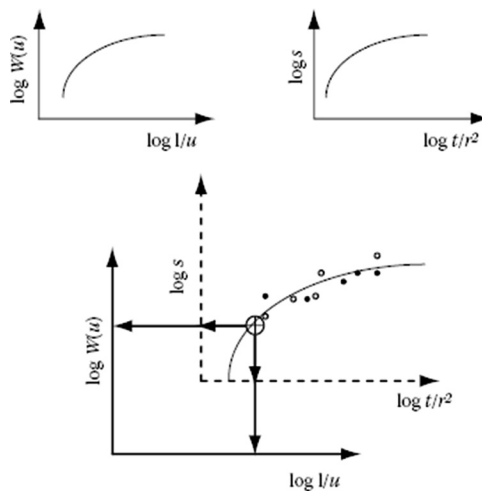


FIGURE 4.14 Graphical procedure to determine t and S from pump test data.

Example 4.11

The drawdown time data recorded at two observation wells situated at a distance of 100 and 200 m from a pumping well are given in [Table 4.2](#). If the well discharge is 1000 m³/day, calculate the transmissibility and storage coefficient of the aquifer.

SOLUTION

The first step is to calculate t/r^2 from the given data. The calculated values are presented in [Table 4.3](#). Then, the measured drawdown versus t/r^2 is plotted on a log paper as shown in [Figure 4.15](#). The data plotted are superimposed on the $W(u)$ versus u plot ([Figure 4.13](#)) as presented in [Figure 4.16](#). An arbitrary match point is selected as:

$$s = 0.167 \text{ m}, \frac{t}{r^2} = 3 \times 10^{-7} \text{ m}^2/\text{day}, \quad W(u) = 2.1, \frac{1}{u} = 12.5$$

From Equations 4.52 and 4.60:

$$T = \frac{1000}{4\pi \times 0.167} \times 2.1 = 1000.7 \text{ m}^2/\text{day},$$

$$S = 4 \times 1000.7 \times 12.5 \times 3 \times 10^{-7} = 0.015 \text{ m}^2/\text{day}$$

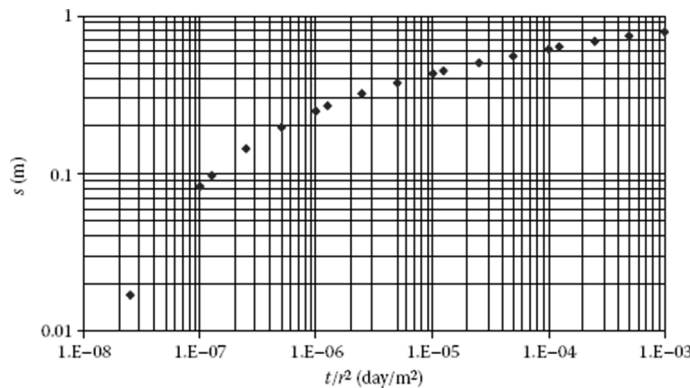
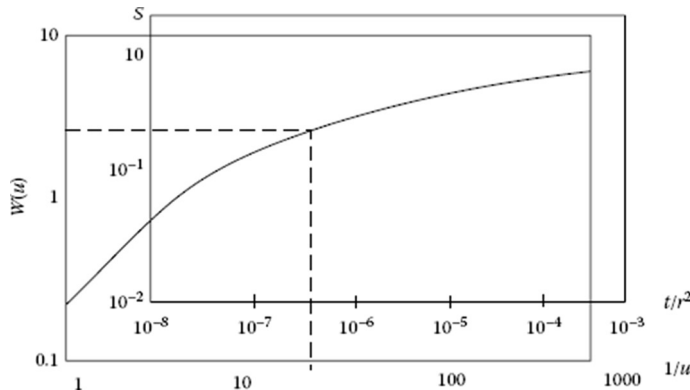
TABLE 4.2

The Drawdown Time Data Recorded at the Distance of 100 and 200 m

| <i>t</i> (Day) | 0.001 | 0.005 | 0.01 | 0.05 | 0.1 | 0.5 | 1 | 5 | 10 |
|---------------------------|--------------|--------------|-------------|-------------|------------|------------|----------|----------|-----------|
| <i>s</i> ₁ (m) | 0.083 | 0.196 | 0.249 | 0.379 | 0.431 | 0.559 | 0.614 | 0.742 | 0.797 |
| <i>s</i> ₂ (m) | 0.017 | 0.097 | 0.145 | 0.267 | 0.322 | 0.449 | 0.504 | 0.632 | 0.687 |

TABLE 4.3**The Drawdown Time Data Recorded at the Distance of 100 and 200 m**

| t (Day) | 0.001 | 0.005 | 0.01 | 0.05 | 0.1 | 0.5 | 1 | 5 | 10 |
|---|--------------------|--------------------|--------------------|--------------------|--------------------|--------------------|--------------------|--------------------|--------------------|
| $t/r^2, d = 100$ m (m^3/day) | 10^{-7} | 5×10^{-7} | 10^{-6} | 5×10^{-6} | 10^{-5} | 5×10^{-5} | 10^{-4} | 5×10^{-5} | 10^{-3} |
| $t/r^2, d = 200$ m (m^3/day) | 0.25×10^7 | 0.13×10^6 | 0.25×10^6 | 0.13×10^5 | 0.25×10^5 | 0.13×10^4 | 0.25×10^4 | 0.13×10^3 | 0.25×10^3 |

**FIGURE 4.15** The drawdown versus t/r^2 for Example 4.11.**FIGURE 4.16** Matching the type curve with drawdown data.

4.4.2.3 Cooper–Jacob Method of Solution

Cooper and Jacob noted that for small values of r and large values of t , the parameter $u = r^2S/4T$ becomes very small and the well function can be approximated by:

$$W(u) = -0.5772 - \ln u \quad (4.67)$$

Thus,

$$s = \frac{Q}{4\pi T} \left(-0.5772 - \ln \left(\frac{r^2 S}{4Tt} \right) \right) \quad (4.68)$$

Rearranging and converting to decimal logs yield:

$$s = \frac{2.3Q}{4\pi T} \log \left(\frac{2.25Tt}{r^2 S} \right) \quad (4.69)$$

A plot of drawdown s versus log of t forms a straight line. A projection of the line back to $s = 0$, where $t = t_0$ yields the following:

$$S = \left(\frac{2.25Tt_0}{r^2} \right) \quad (4.70)$$

$$T = \left(\frac{2.3Q}{4\pi \Delta s} \right) \quad (4.71)$$

where Δs is the slope of the line. The Cooper–Jacob method first solves for T and then for S and is only applicable for small values of $u < 0.01$.

The time t_0 is the time intercept on the zero-drawdown axis. As shown in Figure 4.17, the Cooper–Jacob method is a straight-line approximation on a semi-log paper.

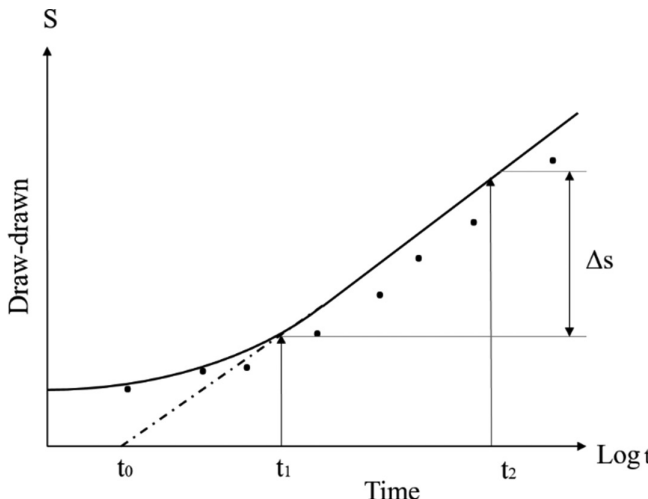


FIGURE 4.17 Illustration of the Cooper–Jacob method showing the straight-line approximation on a semilog paper.

Example 4.12

A well penetrating a confined aquifer is pumped at a rate of $2500 \text{ m}^3/\text{s}$. The drawdown at an observation well at a radial distance of 60 m is presented in [Table 4.4](#). Calculate the transmissibility and storage coefficient of the aquifer.

SOLUTION

The drawdown is plotted against time on a semilog plot ([Figure 4.18](#)). From the fitted line,

$$t_0 = 0.39 \text{ min} = 2.7 \times 10^{-4} \text{ day}$$

$$\Delta s = 0.4 \text{ m}$$

$$T = \left(\frac{2.3Q}{4\pi\Delta s} \right) = \frac{2.3 \times 2500}{4 \times \pi \times 0.4} = 1144.5 \text{ m}^2/\text{day}$$

$$S = \left(\frac{2.25Tt_0}{r^2} \right) = \frac{2.25 \times 1144.5 \times 2.7 \times 10^{-4}}{(60)^2} = 0.000193$$

TABLE 4.4

The Drawdown Time Data Recorded at the Distance of 60 m

| Time (min) | 0 | 1 | 1.5 | 2 | 2.5 | 3 | 4 | 5 | 6 | 8 | 10 | 12 | 14 |
|--------------|------|------|------|------|------|------|------|------|------|------|------|-----|------|
| Drawdown (m) | 0 | 0.2 | 0.27 | 0.3 | 0.34 | 0.37 | 0.41 | 0.45 | 0.48 | 0.53 | 0.57 | 0.6 | 0.63 |
| Time (min) | 18 | 24 | 30 | 40 | 50 | 60 | 80 | 100 | 120 | 150 | 180 | 210 | 240 |
| Drawdown (m) | 0.67 | 0.72 | 0.76 | 0.81 | 0.85 | 0.9 | 0.93 | 0.96 | 1 | 1.04 | 1.07 | 1.1 | 1.12 |

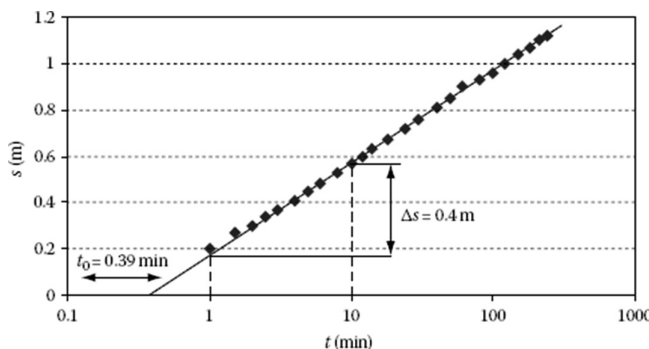


FIGURE 4.18 Time-drawdown plot for Example 4.12.

Example 4.13

A well was pumped at a rate of 200 gal/min. Drawdown as shown was measured in an observation well 250 ft away from the pumping well (Table 4.5).

(A) Plot the time drawdown data on a four-cycle semilogarithmic paper. Use the Cooper–Jacob straight-line method to find the aquifer transmissivity and storativity.

SOLUTION

The drawdown is plotted against time on a semilog plot (Figure 4.19). From the fitted line,

$$t_0 = 0.337 \text{ min} \times \frac{1}{1440} \text{ day/min} = 0.23 \times 10^{-3} \text{ day}$$

$$Q = 200 \text{ gal/min} \times \frac{1}{7.48} \text{ ft}^3/\text{gal} \times 1440 \text{ min/day} = 38502.7 \text{ ft}^3/\text{day}$$

$$\Delta(h_0 - h) = 1.3 \text{ ft}$$

$$T = \left(\frac{2.3Q}{4\pi\Delta(h_0 - h)} \right) = \frac{2.3 \times 38,502.7}{4 \times 3.14 \times 1.3} = 5423.6 \text{ ft}^2/\text{day}$$

TABLE 4.5

The Drawdown Time Data Recorded at the Distance of 250 ft

| Time (min) | 0 | 1 | 1.5 | 2 | 2.5 | 3 | 4 | 5 | 6 | 8 | 10 | 12 | 14 |
|---------------|-----|------|------|------|------|------|------|------|------|------|------|------|------|
| Drawdown (ft) | 0 | 0.66 | 0.87 | 0.99 | 1.11 | 1.21 | 1.36 | 1.49 | 1.59 | 1.75 | 1.86 | 1.97 | 2.08 |
| Time (min) | 18 | 24 | 30 | 40 | 50 | 60 | 80 | 100 | 120 | 150 | 180 | 210 | 240 |
| Drawdown (ft) | 2.2 | 2.36 | 2.49 | 2.65 | 2.78 | 2.88 | 3.04 | 3.16 | 3.28 | 3.42 | 3.51 | 3.61 | 3.67 |

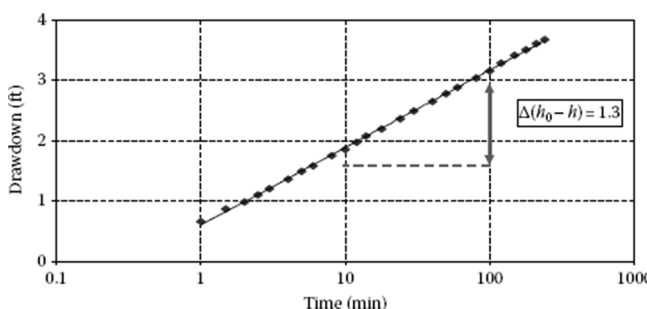


FIGURE 4.19 Time-drawdown plot for Example 4.13.

$$r = 250 \text{ ft}$$

$$S = \frac{2.25Tt_0}{r^2} = \frac{2.25 \times 5423.6 \times 0.23 \times 10^{-3}}{(250)^2} = 0.044 \times 10^{-6}$$

4.4.2.4 Variable Pumping Test

In the previous section, a pumping test was discussed for a well pumped at a constant rate. In this case, the aquifer parameters were estimated using the Theis nonequilibrium equation or the Cooper–Jacob method. However, a constant discharge during pumping is often difficult to achieve in an actual field (Kruseman and de Ridder, 1991). In such a situation, the discharge may decrease with the decline of head in the well, with the sharpest decrease occurring soon after pumping starts. Birsoy and Summers (1980) found an analytical solution considering variable-discharge rates. Applying the principle of superposition to the Cooper–Jacob method, the drawdown in a confined aquifer at time t during the n th pumping period is calculated as follows:

$$s_n = \frac{2.3Q_n}{4\pi T} \log \left\{ \left(\frac{2.25T}{r^2 S} \right) \beta_{t(n)} (t - t_n) \right\} \quad (4.72)$$

In case of intermittent pumping, the adjusted time can be calculated as follows (Figure 4.20):

$$\beta_{t(n)} (t - t_n) = \prod_{i=1}^n \left(\frac{t - t_i}{t - t'_i} \right)^{\frac{\Delta Q_i}{Q_n}} \quad (4.73)$$

where:

s_n : is the drawdown at time t during the n th pumping period

$\beta_{t(n)} (t - t_n)$: is the adjusted time at time t during the n th pumping period

t_i : is the time at which the i th pumping period started

t'_i : is the time at which the i th pumping period ended

$t - t_i$: is the time since the i th pumping period started

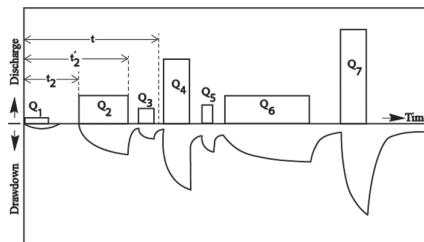


FIGURE 4.20 Drawdown responses corresponding to intermittent discharge of varying duration and different pumping rates.

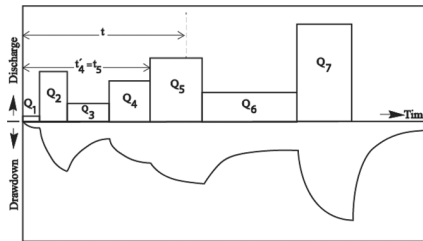


FIGURE 4.21 Drawdown responses associated with uninterrupted discharge of varying duration and different pumping rates.

$t - t_i'$: is the time since the i th pumping period ended

Q_i : is the constant well discharge during the i th pumping period

$\Delta Q_i = Q_i - Q_{i-1}$: is the discharge increment beginning at time t_i .

When a well is continuously pumped at varying rates, the discharge curve can be divided into equal time intervals. The average discharge for each interval can then be used to calculate the drawdowns.

In case of uninterrupted pumping, the adjusted time can be calculated as follows (Figure 4.21):

$$\beta_{t(n)}(t - t_n) = \prod_{i=1}^n (t - t_i) \frac{\Delta Q_i}{Q_n} \quad (4.74)$$

Plotting s_n/Q_n versus adjusted time of pumping on a semilogarithmic paper should fall on the same straight line with a slope s' and horizontal axis intercept point t_0 . Therefore, Equation 4.70 can be applied to calculate storage coefficient S , and Equation 4.71 is modified to calculate transmissivity as follows:

$$T = \frac{2.3}{4\pi\Delta s} \quad (4.75)$$

Example 4.14

A well penetrating a confined aquifer is pumped for 30 minutes at a rate of 2500, 2200, and 2000 m^3/s at 10-minute intervals. The transmissivity and storage coefficient are 1100 m^2/day and 0.0002, respectively. Calculate the drawdown at an observation well at a radial distance of 30 m soon after pumping ends.

SOLUTION:

$$t = 30 \text{ min} \rightarrow n = 3$$

The adjusted time of 30-minute pumping can be calculated as follows:

$$\begin{aligned}\beta_{t(3)}(30-t_3) &= \prod_{i=1}^3 (30-t_i)^{\frac{\Delta Q_i}{Q_i}} = (30-0)^{\frac{2500}{2000}} \times (30-10)^{\frac{-300}{2000}} \times (30-20)^{\frac{-200}{2000}} \\ &= 35.56 \text{ min} = 0.025 \text{ day} \\ s &= \frac{2.3 \times 2000}{4\pi \times 1100} \log \left\{ \left(\frac{2.25 \times 1100}{30^2 \times 0.0002} \right) \times 0.025 \right\} = 1.38 \text{ m}\end{aligned}$$

Example 4.15

A well penetrating a confined aquifer is pumped at a rate of $0.008 \text{ m}^3/\text{min}$. After 30 minutes of pumping, the discharge is increased to $0.055 \text{ m}^3/\text{min}$ and continues for another 30-minute period. Finally, during the next 30-minute step, water is discharged at a rate of $0.122 \text{ m}^3/\text{min}$. The drawdown data of an observation well located at the distance of 60 m were recorded 30 minutes after pumping through the end. The recorded drawdowns are presented in [Table 4.6](#). Determine the transmissivity and storage coefficient of the aquifer.

SOLUTION

The adjusted time of pumping is calculated for each pumping time according to Equation 4.74. To illustrate, the adjusted time for 30.5 minutes after pumping is calculated as follows:

$$t = 30.5 \text{ min} \rightarrow n = 2$$

TABLE 4.6
Drawdown Data Recorded at the Distance of 60 m from the Well

| | | | | | | | | | |
|--------------|------|------|------|------|------|------|------|------|------|
| Time (min) | 30 | 30.5 | 31 | 31.5 | 32 | 32.5 | 33 | 33.5 | 34 |
| Drawdown (m) | 0.32 | 0.62 | 0.77 | 0.87 | 0.94 | 1.00 | 1.05 | 1.09 | 1.13 |
| Time (min) | 34.5 | 35 | 35.5 | 36 | 36.5 | 37 | 37.5 | 38 | 38.5 |
| Drawdown (m) | 1.16 | 1.19 | 1.22 | 1.25 | 1.27 | 1.30 | 1.32 | 1.34 | 1.36 |
| Time (min) | 39 | 39.5 | 40 | 41 | 42 | 43 | 44 | 45 | 46 |
| Drawdown (m) | 1.37 | 1.39 | 1.41 | 1.44 | 1.47 | 1.5 | 1.53 | 1.56 | 1.58 |
| Time (min) | 47 | 48 | 49 | 50 | 52 | 54 | 56 | 58 | 60 |
| Drawdown (m) | 1.61 | 1.63 | 1.66 | 1.68 | 1.72 | 1.76 | 1.80 | 1.84 | 1.88 |
| Time (min) | 60.5 | 61 | 62 | 62.5 | 63 | 63.5 | 64 | 64.5 | 65 |
| Drawdown (m) | 2.33 | 2.56 | 2.83 | 2.93 | 3.02 | 3.10 | 3.15 | 3.21 | 3.26 |
| Time (min) | 65.5 | 66 | 66.5 | 67 | 67.5 | 68 | 68.5 | 69 | 69.5 |
| Drawdown (m) | 3.31 | 3.35 | 3.39 | 3.42 | 3.46 | 3.50 | 3.53 | 3.56 | 3.59 |
| Time (min) | 70 | 71 | 72 | 73 | 74 | 75 | 76 | 77 | 78 |
| Drawdown (m) | 3.62 | 3.68 | 3.73 | 3.78 | 3.83 | 4 | 3.92 | 3.96 | 4.00 |
| Time (min) | 79 | 80 | 82 | 84 | 86 | 88 | 90 | | |
| Drawdown (m) | 4.04 | 4.08 | 4.15 | 4.22 | 4.27 | 4.33 | 4.39 | | |

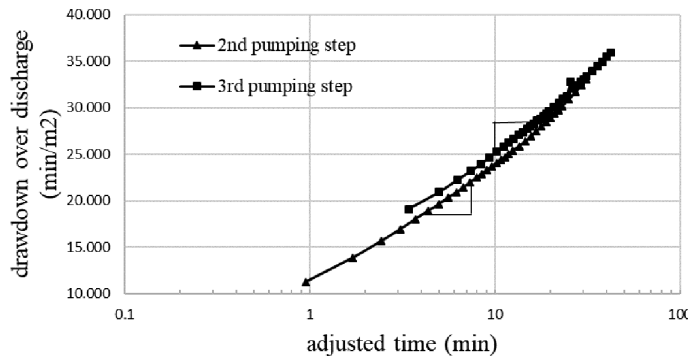


FIGURE 4.22 Time-drawdown plot for Example 4.15.

$$\beta_{t(2)}(30.5 - t_2) = \prod_{i=1}^2 (t - t_i)^{\frac{\Delta Q_i}{Q_n}} = (30.5 - 0)^{\frac{0.008 - 0}{0.055}} \times (30.5 - 30)^{\frac{0.055 - 0.008}{0.055}} \\ = 1.65 \times 0.56 = 0.92 \text{ min}$$

Plotting s_n/Q_n versus adjusted time of pumping on semilogarithmic paper, the transmissivity is estimated by the average slope of the two lines in [Figure 4.22](#).

$$\Delta s = \frac{0.25 + 0.29}{2} = 0.27$$

$$T = \frac{2.3}{4\pi\Delta s} = \frac{2.3}{4 \times 3.14 \times 0.27} = 0.678 \text{ m}^2/\text{min}$$

The x-axis interception of the second and third stage pumping line is 1.07 and 1.15, respectively. Hence, t_0 is:

$$t_0 = \frac{1.07 + 1.15}{2} = 1.11$$

Using Equation 4.70, the storage coefficient of the aquifer can be calculated as follows:

$$S = \frac{2.25 \times 0.678 \times 1.11}{60^2} = 0.00047$$

The details of the computation are presented in [Table 4.7](#).

4.4.3 UNSTEADY STATE FOR UNCONFINED AQUIFER

When water is being pumped from an unconfined aquifer, it is derived from the storage by gravity drainage of tile interstices above the cone of depression. In the nonequilibrium solution, the effects of gravity drainage are not considered. Gravity

TABLE 4.7
Drawdown, Adjusted Time, and Drawdown Over Discharge
Data at the Distance of 60 m from the Well

| Time (min) | Drawdown (m) | Adjusted Time (min) | Drawdown Over Discharge min/m ² |
|------------|--------------|---------------------|--|
| 30 | 0.32 | — | 5.70 |
| 30.5 | 0.62 | 0.92 | 11.23 |
| 31 | 0.77 | 1.67 | 13.86 |
| 31.5 | 0.87 | 2.42 | 15.61 |
| 32 | 0.94 | 3.09 | 16.93 |
| 32.5 | 1.00 | 3.73 | 18.02 |
| 33 | 1.05 | 4.37 | 18.90 |
| 33.5 | 1.09 | 4.98 | 19.61 |
| 34 | 1.13 | 5.59 | 20.32 |
| 34.5 | 1.16 | 6.19 | 20.87 |
| 35 | 1.19 | 6.78 | 21.42 |
| 35.5 | 1.22 | 7.36 | 21.97 |
| 36 | 1.25 | 7.94 | 22.46 |
| 36.5 | 1.27 | 8.51 | 22.90 |
| 37 | 1.30 | 9.08 | 23.28 |
| 37.5 | 1.32 | 9.65 | 23.67 |
| 38 | 1.34 | 10.21 | 24.05 |
| 38.5 | 1.36 | 10.77 | 24.43 |
| 39 | 1.37 | 11.32 | 24.71 |
| 39.5 | 1.39 | 11.87 | 24.98 |
| 40 | 1.41 | 12.42 | 25.36 |
| 41 | 1.44 | 13.51 | 25.86 |
| 42 | 1.47 | 14.6 | 26.40 |
| 43 | 1.50 | 15.68 | 26.95 |
| 44 | 1.53 | 16.75 | 27.45 |
| 45 | 1.56 | 17.81 | 27.99 |
| 46 | 1.58 | 18.87 | 28.43 |
| 47 | 1.61 | 19.93 | 28.87 |
| 48 | 1.63 | 20.99 | 29.31 |
| 49 | 1.66 | 22.04 | 29.75 |
| 50 | 1.68 | 23.08 | 30.18 |
| 52 | 1.72 | 25.17 | 30.90 |
| 54 | 1.76 | 27.25 | 31.72 |
| 56 | 1.80 | 29.32 | 32.38 |
| 58 | 1.84 | 31.38 | 33.09 |
| 60 | 1.88 | — | 15.36 |
| 60.5 | 2.33 | 3.41 | 19.10 |
| 61 | 2.56 | 5.01 | 20.94 |
| 61.5 | 2.72 | 6.29 | 22.26 |
| 62 | 2.83 | 7.4 | 23.19 |

(Continued)

TABLE 4.7 (Continued)
Drawdown, Adjusted Time, and Drawdown Over Discharge
Data at the Distance of 60 m from the Well

| Time (min) | Drawdown (m) | Adjusted Time (min) | Drawdown Over Discharge min/m ² |
|------------|--------------|---------------------|--|
| 62.5 | 2.93 | 8.42 | 23.98 |
| 63 | 3.02 | 9.36 | 24.68 |
| 63.5 | 3.10 | 10.24 | 25.33 |
| 64 | 3.15 | 11.08 | 25.80 |
| 64.5 | 3.21 | 11.89 | 26.25 |
| 65 | 3.26 | 12.67 | 26.68 |
| 65.5 | 3.31 | 13.42 | 27.08 |
| 66 | 3.35 | 14.16 | 27.40 |
| 66.5 | 3.39 | 14.88 | 27.70 |
| 67 | 3.42 | 15.58 | 28.00 |
| 67.5 | 3.46 | 16.27 | 28.30 |
| 68 | 3.50 | 16.95 | 28.60 |
| 68.5 | 3.53 | 17.61 | 28.85 |
| 69 | 3.56 | 18.27 | 29.12 |
| 69.5 | 3.59 | 18.92 | 29.37 |
| 70 | 3.62 | 19.56 | 29.62 |
| 71 | 3.68 | 20.82 | 30.09 |
| 72 | 3.73 | 22.05 | 30.52 |
| 73 | 3.78 | 23.27 | 30.94 |
| 74 | 3.83 | 24.46 | 31.29 |
| 75 | 4.00 | 25.65 | 32.73 |
| 76 | 3.92 | 26.81 | 32.06 |
| 77 | 3.96 | 27.97 | 32.41 |
| 78 | 4.00 | 29.12 | 32.73 |
| 79 | 4.04 | 30.25 | 33.06 |
| 80 | 4.08 | 31.38 | 33.38 |
| 82 | 4.15 | 33.61 | 33.96 |
| 84 | 4.22 | 35.82 | 34.50 |
| 86 | 4.27 | 38.01 | 34.95 |
| 88 | 4.33 | 40.18 | 35.45 |
| 90 | 4.39 | 42.33 | 35.93 |

drainage is not immediate and, for unsteady flow of water toward a well for unconfined conditions, is characterized by the slow drainage of interstices. A graphical method for the analysis of an aquifer test in an unconfined aquifer was developed by Neuman (1975).

Figure 4.23 shows three distinct segments of the time-drawdown curve for water table conditions, and it does not require the definition of any empirical constants.

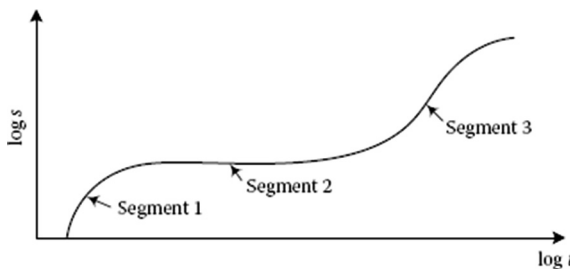


FIGURE 4.23 Three segments of a time-drawdown curve for water table conditions.

The first segment occurs for early drawdown data, when instantaneous release of water from storage occurs in the same manner as an artesian aquifer. It is possible to determine the coefficient of transmissibility under certain conditions by applying the nonequilibrium solution to the time-drawdown curve data. The gravity drainage is not immediate, and the water is released instantaneously from the storage. As time elapses, the effects of gravity drainage and vertical flow cause deviation from the nonequilibrium-type curve. The coefficient of storage is computed by using the early time-drawdown, it is in the artesian range, and cannot be used to predict long-term drawdown.

The second segment represents an intermediate stage of the decline of the water level due to the slow expansion of the cone of depression, and it is replenished by the gravity drainage. Recharge is reflected as the slope of the time-drawdown curve decreases. Pump test data deviate significantly from the nonequilibrium theory during the second segment.

The third segment is used for late drawdown data, when the effects of gravity drainage become smaller. This segment occurs at later times. After the effects of delayed gravity drainage cease to influence the drawdown in observation wells, the time-drawdown field data conform closely to the nonequilibrium solution as illustrated above. By applying the nonequilibrium solution to the third segment of the time-drawdown data, the coefficient of transmissibility of an aquifer can be determined. The coefficient of storage is in the unconfined range and can be used to predict long-term effects.

The solution of Neuman (1975) also reproduced three segments of the time-drawdown curve, and it does not require the definition of any empirical constants. The proposed equation for drawdown in an unconfined aquifer with fully penetrating wells and a constant discharge condition Q was presented:

$$s = h_0 - h = \frac{Q}{4\pi T} W(u_a, u_y, \eta) \quad (4.76)$$

where $W(u_a, u_y, \eta)$ is the well function for water table aquifer, and:

$$u_a = \frac{r^2 S}{4\pi T} \left(\text{for small values of } t \right) \quad (4.77)$$

$$u_y = \frac{r^2 S_y}{T t} \quad (\text{for large values of } t) \quad (4.78)$$

$$\eta = \frac{r^2 K_v}{b^2 K_h} \quad (4.79)$$

where:

$s = h_0 - h$ is the drawdown (L)

Q is the pumping rate (L^3/T)

T is the transmissivity

r is the radial distance from the pumping well

S is the storativity

S_y is the specific yield

t is the time

K_v is the vertical hydraulic conductivity

K_h is the horizontal hydraulic conductivity

b is the initial saturated thickness of the aquifer.

Figure 4.23 is a plot of this function for various values of η with two sets of type curves. Type-A curves that grow out of the left-hand side of the Theis curve in Figure 4.24 are good for early drawdown data. Type-B curves that are asymptotic to the right-hand side of the Theis curve in Figure 4.24 are followed at a later time. The Type-B curves end on a Theis curve, and the distance-drawdown data can be analyzed using the nonequilibrium solution technique.

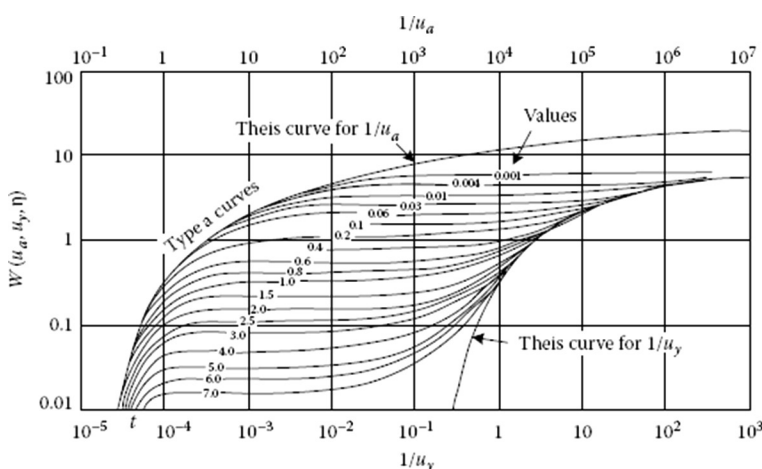


FIGURE 4.24 Theoretical curves of $W(u)$ versus $1/u_a$, for an unconfined aquifer. (From Neuman, S.P., *Water Resources. Res.*, 11, 329, 1975.)

Example 4.16

A well in an unconfined aquifer was pumped at a rate of $873 \text{ m}^3/\text{day}$. Drawdown was measured in a fully penetrating observation well located 90 m away (Figure 4.25). The following data were obtained (Kruseman and de Ridder, 1991). Find the transmissivity, storativity, and specific yield of the aquifer.

SOLUTION

The best match for Type-A curve and the early drawdown data is with the $\eta = 0.01$ curve. At the match point $1/u_a = 10$, $W(u_a, \eta) = 1$, $h_0 - h = 4.8 \times 10^{-2} \text{ m}$, and $t = 10.5 \text{ min} (7.3 \times 10^{-3} \text{ day})$. Substitute these values in Equations 4.71 and 4.72.

$$T = \frac{Q}{4\pi(h_0 - h)} W(u_a, \eta), \text{ given } Q = 873 \text{ m}^2/\text{day}$$

$$T = \frac{873 \text{ m}^2/\text{day} \times 1.0}{4\pi \times 4.8 \times 10^{-2}} = 1400 \text{ m}^2/\text{day}$$

$$S = \frac{4Tut}{r^2}, \text{ given } r = 90 \text{ m}$$

$$1/u_A = 10, u_A = 0.1$$

$$S = \frac{4 \times 1400 \text{ m}^2/\text{day} \times 7.3 \times 10^{-3} \text{ day}}{90 \times 90 \text{ m}} \times 0.1 = 0.0005$$

The Type-B curve for $\eta = 0.01$ is matched to the late drawdown data. The match point values are $1/u_y = 10^2$, $W(u_y, \eta) = 1$, and $t = 880 \text{ min} (6.1 \times 10^{-1} \text{ day})$.

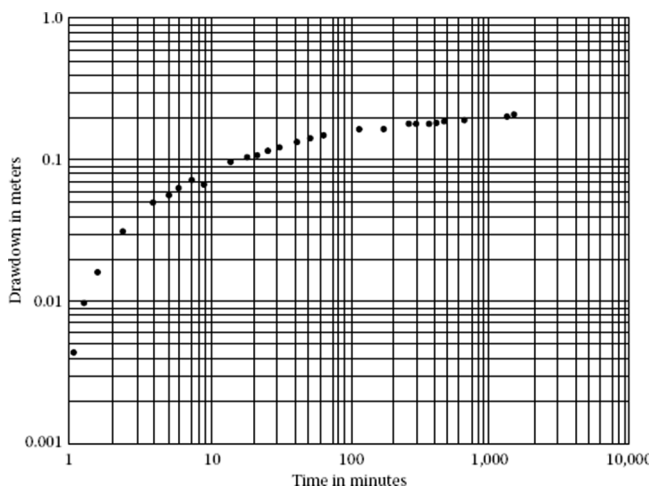


FIGURE 4.25 Drawdown in the unconfined aquifer as a function of time.

$$T = \frac{873 \text{ m}^2 / \text{day} \times 1.0}{4\pi \times 4.3 \times 10^{-2}} = 1600 \text{ m}^2 / \text{day}$$

$$S_y = \frac{4 \times 1600 \text{ m}^2 / \text{day} \times 6.1 \times 10^{-1} \text{ day} \times 0.01}{90 \times 90 \text{ m}} = 0.0005$$

4.5 MULTIPLE-WELL SYSTEMS

The drawdown in hydraulic head at any point of the aquifer with more than one well is equal to the summation of the drawdowns that occur from each of the wells independently. The total drawdown of n wells pumping at rates $Q_1, Q_2 \dots Q_n$ can be found from the superposition of well response individually. Where pumping is from a confined aquifer,

$$H_e - h = \sum_{i=1}^n \frac{Q}{2\pi K b} \ln \left(\frac{r_{ei}}{r_i} \right) \quad (4.80)$$

where:

$H_e - h$ is the drawdown at any given point in the area of influence

r_{ei} is the distance from the i th well to a point at which the drawdown becomes negligible

r_i is the distance from the i th well to the given point.

For an unconfined aquifer the total drawdown is calculated as:

$$H_e^2 - h^2 = \sum_{i=1}^n \frac{Q}{\pi K} \ln \left(\frac{r_{ei}}{r_i} \right) \quad (4.81)$$

For example, for an unconfined aquifer with unsteady-state pumping, the drawdown at a point that its radial distance from each well given by $r_1, r_2 \dots r_n$ is the arithmetic summation of the Theis solutions as follows:

$$h_0 - h = \frac{Q_1}{4\pi T} W(u_1) + \frac{Q_2}{4\pi T} W(u_2) + \dots + \frac{Q_n}{4\pi T} W(u_n) \quad (4.82)$$

where:

$$u_i = \frac{r_i^2 S}{4T t_i}, \quad i = 1, 2, 3, \dots, n$$

t_i is the time since pumping started at the well with the discharge of Q_i .

Example 4.17

A building is located on an island. The water table under the building needs to be decreased to the allowable depth. Therefore, four wells as shown in Figure 4.26 are utilized to withdraw the water. Determine the discharge from each well to

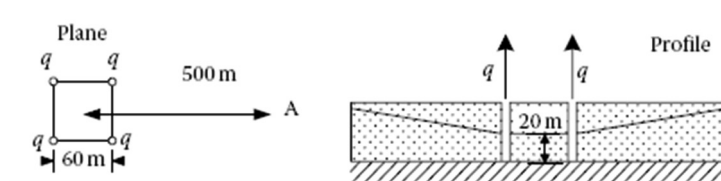


FIGURE 4.26 Plane and profile views of Example 4.17.

decrease the water table in the building center to 20 m, assuming the water table before pumping is at 50 m, the drawdown effect is predicted to be 500 m (Point A) and $K = 10^{-3}$ m/s.

SOLUTION

The drawdown in the building center is equal to the sum of the drawdowns that would arise from each of the wells independently. r_{ei} is the distance between the well i and the negligible drawdown point. r_i is the distance between the well i and the central point.

$$H_e^2 - h^2 = \sum_{i=1}^n \frac{Q}{\pi K} \ln\left(\frac{r_{ei}}{r_i}\right)$$

$$50^2 - 20^2 = \frac{Q}{\pi \times 10^{-3}} \left[2 \ln\left(\frac{\sqrt{530^2 + 30^2}}{\sqrt{30^2 + 30^2}}\right) + 2 \ln\left(\frac{\sqrt{470^2 + 30^2}}{\sqrt{30^2 + 30^2}}\right) \right]$$

$$Q = 0.67 \text{ m}^3/\text{s}$$

4.6 EFFECTIVE CONDITIONS ON TIME-DRAWDOWN DATA

In order to apply the Theis equation, basic assumptions are made in developing the equations for groundwater flow. However, geologic or hydrologic conditions do not conform fully in actual aquifers. One of these assumptions is that aquifers have an infinite areal extent and clearly it is necessary in order to solve many groundwater problems. It is obvious that this type of aquifer cannot exist in reality and the aquifers have some boundaries. A hydrologic boundary could be the edge of the aquifer, a region of recharge to a fully confined artesian aquifer, or the source of recharge such as a stream or lake (Fetter, 2001). The boundary conditions can be divided into two categories: recharge boundaries and impermeable boundaries. Another assumption for applying the developed formula is the fully penetrated well that leads to change in the flow pattern.

4.6.1 RECHARGE BOUNDARY

Equilibrium conditions that stabilize the cone of depression around a pumping well may develop in several general situations. One of these is when an aquifer

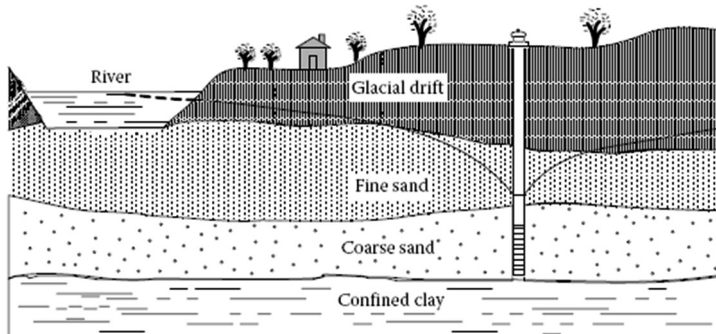


FIGURE 4.27 Cone of depression between the aquifer and river. (From Driscoll, F.G., *Groundwater and Wells*, 2nd edn., Johnson Division, St. Paul, MN, 1986.)

is recharged from a river or lake. A recharge boundary is a region in which the aquifer is replenished. [Figure 4.27](#) shows a recharge boundary after equilibrium has been reached.

The drawdown data due to water pumping show that the cone of depression does not extend to the river and no recharge is evident. By keeping on pumping, the water table in the well decreases. A hydraulic gradient develops between groundwater in the aquifer and water in the river when the cone of depression intersects a river channel. If the stream bed is hydraulically connected with the aquifer, river water will percolate downward through the pervious streambed under the influence of the hydraulic gradient. Thus, the river recharges the aquifer at an increasing rate as the cone of depression enlarges. When the rate of recharge to the aquifer equals the rate of discharge from the well, the cone of depression and the pumping level become stable (Driscoll, 1986).

In order to predict aquifer behavior in the presence of boundaries, introduce imaginary wells such that the response at the boundary is made true. The image-well method is widely used in heat-flow theory and has been adapted for application in the groundwater milieu, in order to predict the decreased drawdowns that occur in a confined aquifer in the vicinity of a constant-head boundary, such as what would be produced by the slightly unrealistic case of a fully penetrating stream ([Figure 4.28a](#)). For this case, the imaginary infinite stream ([Figure 4.28b](#)) is introduced in order to set up a hydraulic flow system which will be equivalent to the effects of a known physical boundary. The recharge boundary can be simulated by a recharging image well duplicated in an equal and opposite side from the real well ([Figure 4.28c](#)).

The summation of the cone of depression from the pumping well and the cone of impression from the recharge well lead to an expression for the drawdown in an aquifer bounded by a constant-head boundary:

$$h_0 - h = \frac{Q}{4\pi T} [W(u_r) - W(u_i)] \quad (4.83)$$

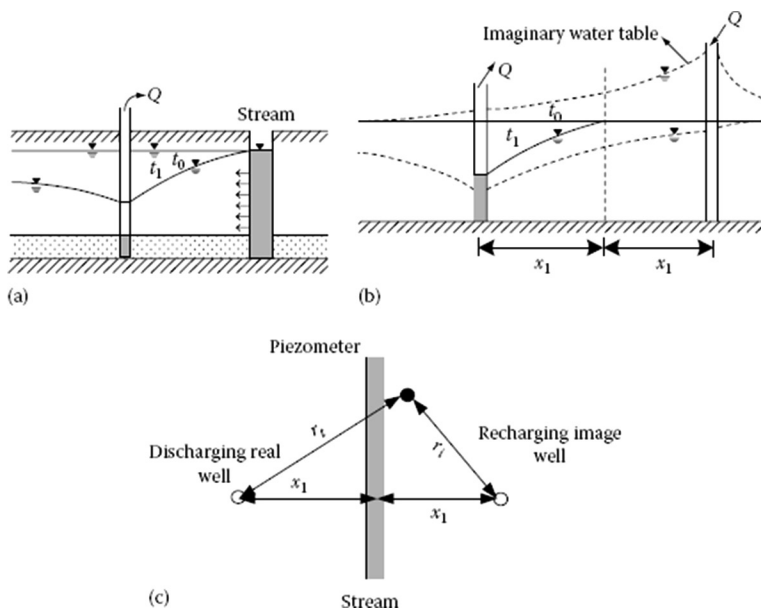


FIGURE 4.28 Drawdown in an aquifer bounded on one side by a stream. (a) A fully penetrating stream, (b) an imaginary infinite stream, and (c) a recharging image well.

$$u_r = \frac{r_r^2 S}{4 T t} \text{ and } u_i = \frac{r_i^2 S}{4 T t} \quad (4.84)$$

4.6.2 IMPERMEABLE BOUNDARY

In many localities, definite geologic and hydraulic boundaries limit aquifers to certain areas. An impermeable boundary is an edge of the aquifer, where it terminates by thinning or abutting a low-permeability formation (Fetter, 2001). Assuming that there is no groundwater flow across this layer, it is called a zero-flux boundary. The effects of an impermeable boundary on the time-drawdown data are opposite to the effects of recharge boundary. When an aquifer is bounded on one side by a straight-line impermeable boundary, drawdowns due to pumping will be greater near the boundary (Figure 4.29a). The effect of the impermeable boundary to flow in some regions of the aquifer is to accelerate the drawdown (Figure 4.29b). In order to simulate an impermeable boundary, a discharging image well is duplicated in an equal and opposite side from the real well (Figure 4.29c). The summation of the cone of depression from the pumping well and the cone of impression from the discharge well lead to an expression of the drawdown in an aquifer bounded by a constant-head boundary:

$$h_0 - h = \frac{Q}{4 \pi T} \left[W(u_r) + W(u_i) \right] \quad (4.85)$$

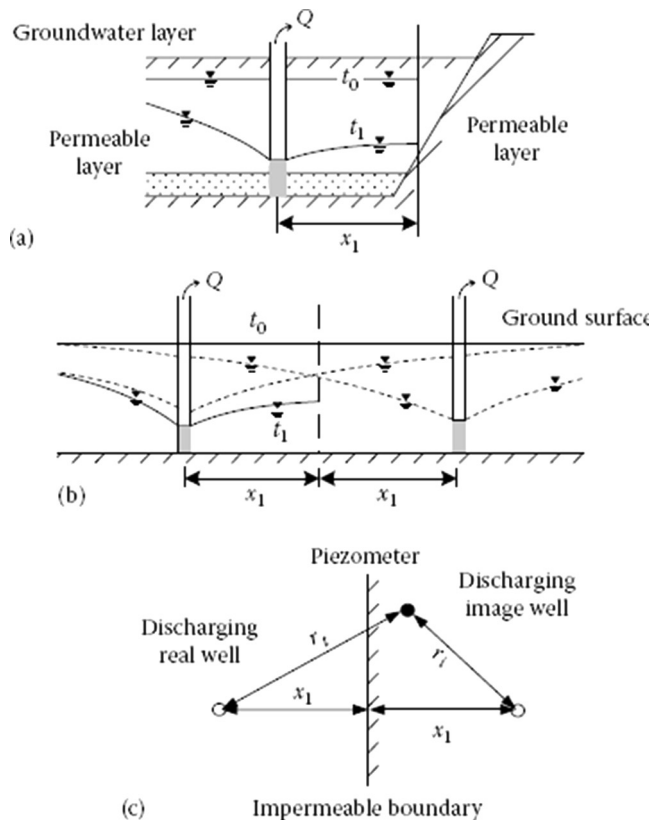


FIGURE 4.29 Drawdown in an aquifer bounded on one side by an impermeable boundary. (a) One sided impermeable aquifer, (b) effect on water table, and (c) a discharging image well.

u_r and u_i are as defined in connection with Equation 4.84. It is possible to use the image-well approach to provide predictions of drawdown in systems with more than one boundary.

Example 4.18

A well is being pumped at a rate of $0.03 \text{ m}^3/\text{s}$ near an impermeable boundary (Figure 4.30). The transmissivity of the aquifer is 6.4×10^{-3} , and its storativity is 3×10^{-5} . Calculate the drawdown in the observation well after 36,000 s of continuous pumping.

SOLUTION

An image well is placed across the boundary at the same distance from the boundary as the pumping well. The drawdown in the observation well is from the actual well and the imaginary well.

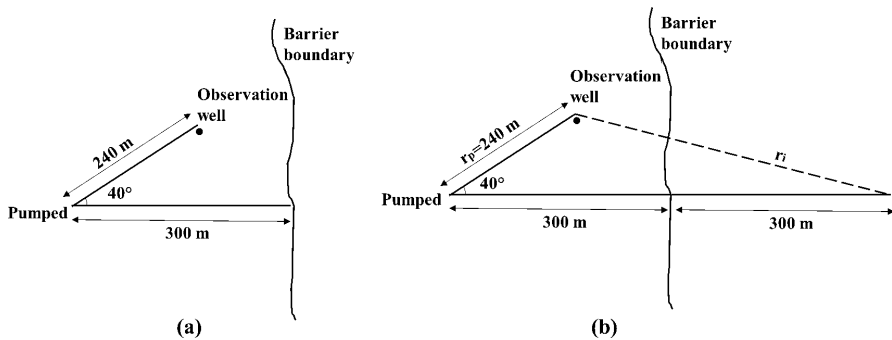


FIGURE 4.30 (a) Well locations and (b) image well location.

$$s = h_0 - h = \frac{Q}{4\pi T} [W(u_r) + W(u_i)]$$

$$u_r = \frac{r_r^2 S}{4Tt} = \frac{(240)^2 (3 \times 10^{-5})}{4(20)(3.2 \times 10^{-4})(36,000)} = 1.88 \times 10^{-3}$$

The distance from the observation well to the image well:

$$r_i^2 = 600^2 + 240^2 - 2(600)(300)\cos 40^\circ = 196,979 \text{ m}^2$$

$$r_i = 443 \text{ m}$$

$$u_i = \frac{r_i^2 S}{4Tt} = \frac{(196,979)(3 \times 10^{-5})}{4(20)(3.2 \times 10^{-4})(36,000)} = 6.41 \times 10^{-3}$$

$$W(u_r) = 1.88 \times 10^{-1}$$

$$W(u_i) = 4.17$$

$$s = 3.86 \text{ m}$$

The drawdown attributable to the barrier boundary is computed as:

$$s_i = \frac{Q}{4\pi T} [W(u_i)] = \frac{0.03}{4\pi(20)(3.2 \times 10^{-4})} (4.17) = 1.55 \text{ m}$$

4.6.3 PARTIALLY PENETRATING WELLS

In practice and well construction, it happens that water enters the well bore over a length which is less than the aquifer thickness. This is called a partially

penetrating well. The flow pattern will differ from the radial flow which is thought to exist around wells which fully penetrate. Flow toward a partially penetrating well experiences convergence that is in addition to the convergence in flow toward a fully penetrating well. By changing the flow pattern, the presented equations cannot be used to estimate the drawdowns because flow is not strictly radial.

Partial penetration causes the flow to have a vertical component in the vicinity of the well as shown in Figure 4.31. Some typical flow lines or paths of water particles are presented by the arrows as they move through the formation toward the intake portion of the well. Water in the lower part of the aquifer moves upward along the curved lines to reach the well screen. Therefore, the path that water must take is longer than radial flow lines. Also, the flow must converge through a smaller cross-sectional area while approaching the short screen. The result of the longer flow paths and the smaller cross-sectional area is an increase in head loss. For a given yield, therefore, the drawdown in a pumping well is greater if the aquifer thickness is only partially screened. For a given drawdown, the yield from a well partially penetrating the aquifer is less than the yield from one completely penetrating the aquifer (Driscoll, 1986).

It is assumed that for distances from the well that exceed about $1.5b\sqrt{K_h / K_v}$, the vertical components of flow are negligible and developed equations can be applied for the partially penetrating case, provided that $r > 1.5b\sqrt{K_h / K_v}$. $\sqrt{K_h / K_v}$ are the horizontal and vertical conductivity, respectively, in an anisotropic aquifer. In case of $r < 1.5b\sqrt{K_h / K_v}$, the discharge per unit of drawdown is smaller than if the well is fully penetrating. One of the basic equations for the partially penetrating case utilizes a continuous superposition of sinks to represent the partially penetrating well to derive an approximate relationship between the discharge of a partially penetrating well and that for a fully penetrating well (Musket, 1946). The discharge per unit drawdown is called specific capacity and is widely used to characterize the discharge capacity of pumped wells.

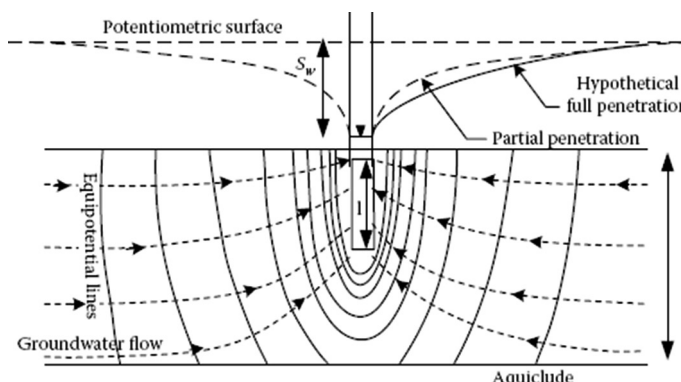


FIGURE 4.31 Flow lines toward a partially penetrating well.

$$\left(\frac{Q}{S_w}\right)_p = \left(\frac{Q}{S_w}\right) \left[\frac{l}{b} \left\{ 1 + 7 \left(\frac{r_w}{2l} \right)^{1/2} \cos \frac{\pi l}{2b} \right\} \right] \quad (4.86)$$

where:

l is the length of well bore over which water enters the well
subscript p denotes the partially penetrating case.

Example 4.19

A well with an effective well radius of 0.15 m exhibits a specific capacity of 0.032 m²/s in an aquifer with a 35 m thickness. The length of screened well bore is 10 m. If the length of well screen is increased to 20 m, estimate the increase in specific capacity.

SOLUTION

By applying Equation 4.86 for a partially penetrating case, the specific capacity for full penetration is:

$$\left(\frac{Q}{S_w}\right) = \frac{(Q/S_w)_p}{\left[(l/b) \left\{ 1 + 7 \left(r_w / 2l \right)^{1/2} \cos \pi l / 2b \right\} \right]}$$

$$\left(\frac{Q}{S_w}\right) = \frac{0.032}{\left[10/35 \left\{ 1 + 7 \left(0.15/20 \right)^{1/2} \cos 10\pi/70 \right\} \right]} = 0.072 \text{ m}^2/\text{s}$$

The specific capacity with $l = 20$ m is:

$$\left(\frac{Q}{S_w}\right)_p = 0.072 \left[20/35 \left\{ 1 + 7 \left(0.15/40 \right)^{1/2} \cos 20\pi/70 \right\} \right] = 0.052 \text{ m}^2/\text{s}$$

Increasing the length of well screen to 20 m will change the specific capacity from 0.032 to 0.052 m²/s, an increase of 63%.

4.7 DESIGN OF WELLS

A well is an intake structure dug in the ground to remove water from groundwater resources. Exploitation wells are drilled for the supply of municipal, industrial, and irrigation water demands, and for water table control for drainage purposes. The wells can be made as open, dug wells, or tube wells; tapping an unconfined aquifer; or penetrating the ground to tap a confined aquifer. The design of tube wells, a typical installation, is given in [Figure 4.32](#).

The design of a well is the process of selecting appropriate dimensions of various components and determining the physical materials for a well construction. Dimensional factors, strength requirements, and construction/maintenance cost

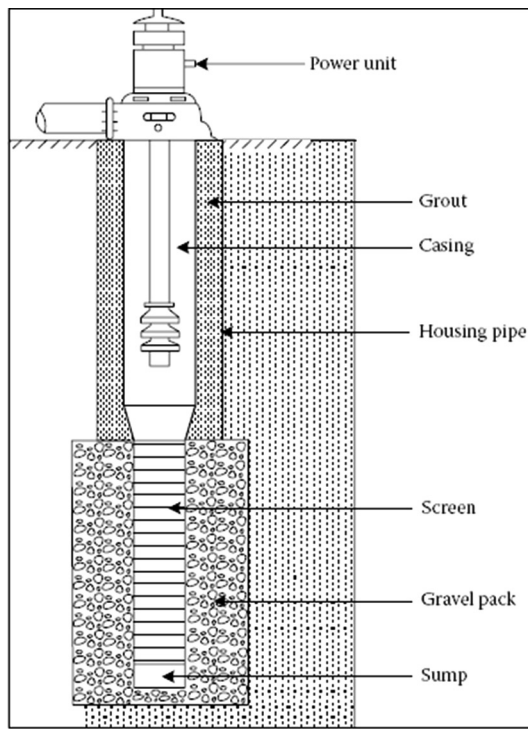


FIGURE 4.32 Typical installation of tube wells.

play an important role in establishing the design parameters. A good design of a well minimizes economic costs, including capital and maintenance costs as well as the possibility of collapse of service in large water-supply developments, and also increases the life of the well.

A well is composed of two main elements, which include the casing and the screen.

Casing is used to maintain an open access in the earth and to avoid any entrance or leakage into the well. Housing for the pumping equipment and a vertical conduit for water flowing upward from the aquifer to the pump intake is accommodated in the casing. The pump housing is the upper section of blind casing which supports the well against collapse. The pump housing diameter should be such that the pump could be placed with enough clearance for installation. It is recommended that the casing diameter be two pipe sizes larger than the nominal diameter of the pump. The length of the pump housing should be tall enough so that the pump remains below the water level in the well during the lifetime of the well. Thus, the maximum expected drawdown determines the length of the pump casing for a water-supply well and the water table should be used instead for drainage purposes. The casing material is chosen based on water quality, well depth, diameter, drilling procedure, construction cost, and well regulations. The most popular materials used for casing are black steel, galvanized steel, *PVC* pipe, and concrete pipe. The space around the

outside of the well is filled by grout to prevent the intrusion of contaminants. A mix of cement, bentonite, or concrete can be used as grout.

The intake portion of wells is generally screened to prevent sand and fine material from entering the well during pumping and to minimize the head loss and entrance velocity. The screen keeps sand and gravel out of the well while allowing groundwater and water from formations to enter into the well. The wall of the well is supported from the loose formation material and the aquifer materials in many consolidated formations, especially sandstone and limestone, are established, and chemical and physical corrosion by the pumped water is resisted.

The optimum length of the well screen is based on the thickness of the aquifer and the total cost for water discharge or drainage. The total cost includes capital cost and pumping cost. In thick aquifers, while a fully penetrating well has high construction cost, it reduces the pumping cost since it reduces head loss. For confined aquifers, about 80%–90% of the depth at the center of the aquifer is advised to be screened. For unconfined aquifers, it is recommended to provide screen in the lower one-third thickness. The screen length can be chosen to keep the actual screen entrance velocity in the allowable ranges. The minimum length of the well screen can be calculated using the relationship between different screen parameters (AWWA, 1998):

$$l_{\min} = \frac{Q}{86,400 A_e V_e} \quad (4.87)$$

where:

l_{\min} is the minimum screen length (m)

Q is the discharge of the well (m³/day)

A_e is the effective open area per meter screen length (m²/m)

V_e is the screen entrance velocity (m/s).

The entrance velocity near the well screen does not exceed 0.03 m/s (Walton, 1962).

The size of screen slot openings depends on the grain-size-distribution curve for the aquifer materials. The size is selected to limit the moving of the finer formation materials near the borehole into the screen and pumped from the well during development. The typical approach to determine the size of slot openings for nonhomogeneous sediments is to select a slot through which 60% of the material will pass and 40% will be retained. With corrosive water, the 50%-retained size should be chosen, because even a small enlargement of the slot openings due to corrosion could cause sand to be pumped (Driscoll, 1986).

The screen materials' strength should withstand the physical forces acting upon them during and following their installation, and during their use, including forces due to suspension in the borehole, grouting, development, purging, pumping, and sampling, as well as forces exerted on them by the surrounding geologic materials (Wilson and Strock, 1995). Screens are available in many materials, the most popular being stainless steel and slotted PVC pipe.

They should be resistant to incrustation and corrosion and should maintain their structural integrity and durability in the environment in which they are used over

their operating life. The quality of groundwater, diameter and depth of the well, and type of strata are important factors in selecting screen material.

In order to minimize the passage of formation materials into the well and to stabilize the well assembly, the annular space between the borehole wall and the screen or slotted casing should be filled. To make the zones around the well screen more permeable, some formation materials around the well are removed and replaced with graded material. A filter pack is selected to retain about 90% of the gravel pack after development. A filter pack is appropriate when the natural formation is a uniform fine sand, silt, or clay.

4.8 WELL CONSTRUCTION

Well construction usually includes drilling, installing the casing, placing a well screen and filter pack, grouting, and developing the well. There are various well drilling and installation methods depending on the size of the tube well, depth and formation to be drilled, and available facility and technical proficiency.

The cable-tool and rotary drilling methods are the most common methods for drilling deep wells.

4.8.1 CABLE-TOOL DRILLING

Cable-tool drilling machines or percussion rigs operate by repeatedly lifting and dropping a heavy string of drilling tools into the borehole (Delleur, 1999). The consolidated rock is crushed into small fragments by impacts of the drill bit on the lower end with a relatively sharp tool. The cutting tool for breaking the rock is suspended from a cable and by the up-and-down movement of the sharp tool, the drilling is accomplished. During the drilling, water is injected to the well, and the slurry is made after mixing with crushed or loosened particles. Water use increases as drilling proceeds. The slurry is removed from the borehole by a sand pump when the penetration rate decreases.

A rig consists of a mast, lines of hoist for operating the drilling tool, and a sand pump as shown in [Figure 4.33](#). A full string of a drilling tool as shown in the figure consists of a drill bit, drill stem, drilling jars, and rope socket. The drill stem is a long steel bar that adds weight and length to the drill so it will cut rapidly, and vertically fixed above the bit, it provides additional tools in order to maintain a straight line. The drilling jars consist of a pair of linked steel bars and can be moved in a vertical direction relative to each other. Their purpose is only to loosen the tools should they stick in the hole. The rope socket connects the string of tools to the cable (Todd and Mays, 2008).

4.8.2 ROTARY DRILLING METHOD

In this method, a rotating bit drills the hole and circulation of a drilling fluid removes the crushed or loosened particles. Drilling mud, which consists of a suspension of water, bentonite, clay, and various organic additives, is entered into the hollow to loosen and to lubricate the rotating bit hole. Then, the mud is removed from the hole. In this method, the walls of the well are sealed and the holes of the walls are filled.

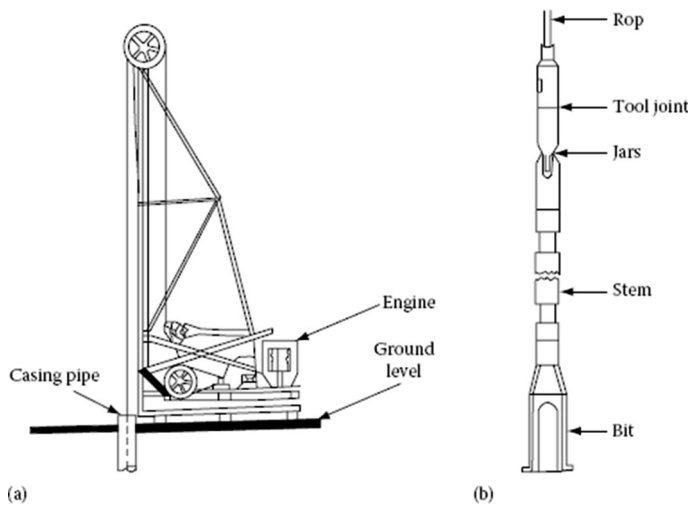


FIGURE 4.33 Cable-tool percussion drilling: (a) drilling rig and (b) drilling tools.

The method operates continuously with a hollow rotating bit through which a mixture of clay and water, or drilling mud, is forced. Material loosened by the bit is carried upward in the hole by the rising mud. No casing is ordinarily required during drilling because the mud forms a clay lining, or mud cake, on the wall of the well by filtration. This seals the walls, thereby preventing caving, entry of groundwater, and loss of drilling mud. For the rotary method of drilling without casing, screens are lowered into place as drilling mud is diluted and again are sealed by a lead packer to an upper permanent casing.

Direct rotary and reverse rotary methods are two primary types of rotary drilling methods. In the direct rotary method, the drilling mud is picked up from the annular space between the hole and drill pipe and brought to the ground surface by the pump. The fluid is cleaned in a settling pit and stored in a storage pit from where it is pumped back into the hole and recirculated. The schematic of the direct rotary is shown in [Figure 4.34](#). The major difference between the two methods as shown in this figure is in the direction of the flowing fluid.

4.8.2.1 Well Development

During well construction, unconsolidated aquifer materials and packed artificial gravel are placed around the well screens and the permeability around the borehole is reduced. Well development is used to increase well-specific capacity, prevent sanding, and maximize economical well life. Well development also removes smaller grains initially present in the formation immediately surrounding the well screen to create a more permeable and stable zone adjacent to the well screen.

The development procedures are varied and include pumping, surging, use of compressed air, hydraulic jetting, addition of chemicals, and use of explosives. The simplest method of removing finer material from the borehole is pumping at a higher rate than the well will be pumped during exploitation or over pumping.

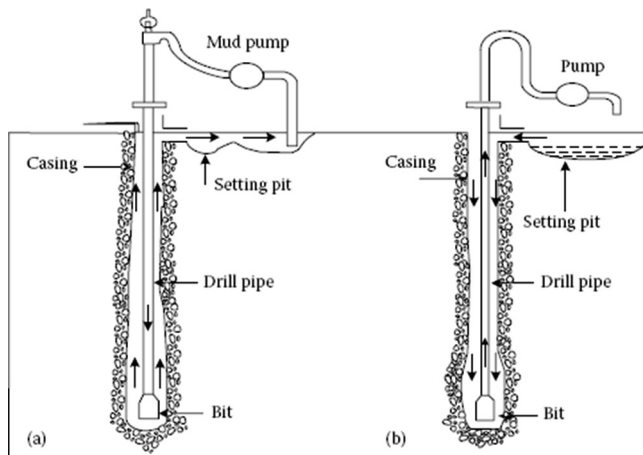


FIGURE 4.34 Rotary drilling: (a) direct rotary and (b) reverse rotary.

PROBLEMS

- 4.1** Consider two strata of the same soil material that lie between two channels. The first stratum is confined, and the second one is unconfined, and the water surface elevations in the channels are 30 and 15 m above the bottom of the unconfined aquifer. What is the thickness of the confined aquifer for which,
- The discharge through both strata are equal?
 - The discharge through the confined aquifer is half as compared to the unconfined aquifer?
- 4.2** Two parallel rivers *A* and *B* are separated by a land mass as shown in [Figure 4.35](#). Estimate the seepage from river *A* to river *B* per unit length of the river.
- 4.3** Two parallel rivers *A* and *B* are separated by a land mass as shown in [Figure 4.36](#). Estimate the seepage from river *A* to river *B* per unit length of the river.

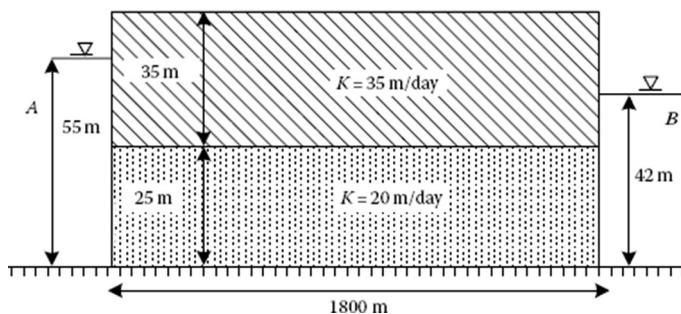


FIGURE 4.35 Cross section of parallel rivers as described in Problem 4.2.

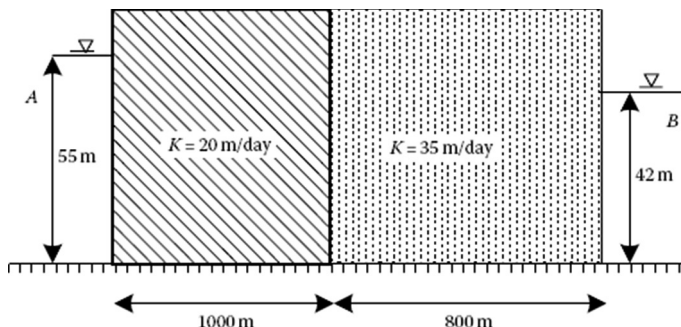


FIGURE 4.36 Cross section of parallel rivers as described in Problem 4.3.

- 4.4** For the unconfined aquifer shown in Example 4.6, determine the steady-state head distribution. Assume the aquifer is homogeneous and isotropic and has a uniform recharge rate, R , with a different water table in two sides of the aquifer (h_1, h_2).
- 4.5** A well fully penetrates a 30-m thick confined aquifer. After a long period of pumping at a constant rate of $0.07 \text{ m}^3/\text{s}$, the drawdowns at distances of 40 and 120 m from the well were observed to be 3 and 1.5 m, respectively. Determine the hydraulic conductivity and the transmissibility. What type of unconsolidated deposit would you expect this to be?
- 4.6** A well penetrates an unconfined aquifer. Prior to pumping, the water level (head) is $h_0 = 30 \text{ m}$. After a long period of pumping at a constant rate of $0.07 \text{ (m}^3/\text{s)}$, the drawdowns at distances of 40 and 120 m from the well were observed to be 3 and 1.5 m, respectively. Determine the hydraulic conductivity. What type of deposit would the aquifer material probably be?
- 4.7** An unconfined aquifer ($K = 5 \text{ m/day}$) situated on the top of a horizontal impervious layer connects two parallel water bodies M and N which are 1200 m apart. The water surface elevations of M and N , measured above the horizontal impervious bed, are 10 and 8 m, respectively. If a uniform recharge at the rate of $0.002 \text{ m}^3/\text{day/m}^2$ of horizontal area occurs on the ground surface, estimate:
- The water table profile
 - The location and elevation of the water table divide
 - The seepage discharges into the lakes
- 4.8** Two wells, A and B , are located 200 m apart and pump from an aquifer for which $T = 1.1 \text{ (m}^2/\text{min)}$ and $S = 0.11$. The wells begin pumping simultaneously at rate $Q_A = 2 \text{ (m}^3/\text{min)}$ and $Q_B = 3 \text{ (m}^3/\text{min)}$. Compute the drawdown in an observation well located at a distance of 50 m from well A and 200 m from well B after 7 days of continuous pumping from both wells.
- 4.9** Three monitoring wells are used to determine the direction of groundwater flow in a confined aquifer (as shown in Figure 4.37). The piezometric heads in the wells are found to be 45 m in well 1, 40 m in well 2, and 42 m in well 3. Determine the magnitude and the direction of the hydraulic gradient.

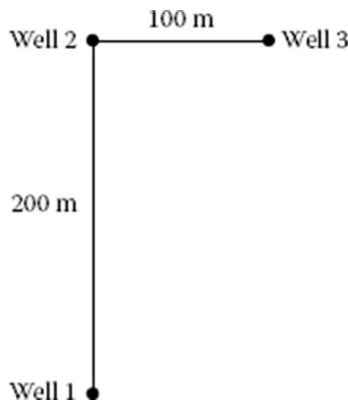


FIGURE 4.37 Location of the wells, Problem 4.9.

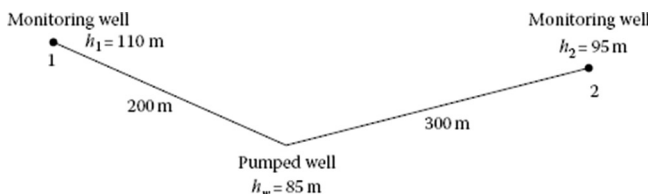


FIGURE 4.38 Location of the wells, Problem 4.10.

- 4.10** A 40-cm diameter well fully penetrates vertically through a confined aquifer 15 m thick. When the well is pumped at $0.035 \text{ m}^3/\text{s}$, the heads in the pumped well and the two other observation wells were found to be as shown in Figure 4.38. Does this test suggest that the aquifer material is fairly homogeneous in the directions of the observation wells?
- 4.11** Three pumping wells along a straight line are spaced 150 m apart. What should be the steady-state pumping rate from each well so that the drawdown in each well will not exceed 1.5 m? The transmissibility of the confined aquifer at which all the wells penetrate fully is $2500 \text{ m}^2/\text{day}$ and all wells are 30 cm in diameter. Take the thickness of the aquifer $b = 50 \text{ m}$ and the radius of influence of each well to be 1000 m.
- 4.12** The following data were collected during a test of a confined aquifer in a monitoring well located 305 m away from a pumping well. This well fully penetrated the aquifer and the observation wells were constructed so that the observed drawdown are average values over the entire saturated thickness ($Q = 1200 \text{ m}^3/\text{day}$). Calculate the aquifer properties using a Theis type curve (Table 4.8).
- 4.13** Table 4.9 lists drawdown versus time data in an unconfined aquifer. Data are collected at an observation well 50 m away from a well being pumped at $2 \text{ m}^3/\text{min}$. Both the pumping and observation wells are fully penetrating.

TABLE 4.8
Test of Confined Aquifer Data, Problem 4.12

| | | | | | | | |
|------------|----------|----------|----------|----------|----------|---------|----------|
| Time (day) | 1.30E-04 | 3.47E-04 | 6.94E-04 | 1.39E-03 | 3.47E-03 | 6.94E-3 | 1.39E-02 |
| s (m) | 0 | 0 | 0.006 | 0.043 | 0.168 | 0.302 | 0.445 |
| Time (day) | 3.47E-02 | 6.94E-02 | 1.39E-01 | 3.47E-01 | 6.94E-01 | 2.3 | |
| s (m) | 0.594 | 0.634 | 0.637 | 0.637 | 0.64 | 0.643 | |

TABLE 4.9
Drawdown Versus Time Data in an Unconfined Aquifer, Problem 4.13

| Time (min) | S (m) | Time (min) | S (m) |
|------------|-------|------------|-------|
| 0.1 | 0 | 19.36 | 1.06 |
| 0.13 | 0 | 25.19 | 1.06 |
| 0.17 | 0.01 | 32.78 | 1.06 |
| 0.22 | 0.02 | 42.65 | 1.06 |
| 0.29 | 0.06 | 55.49 | 1.07 |
| 0.37 | 0.11 | 72.21 | 1.07 |
| 0.49 | 0.18 | 93.96 | 1.08 |
| 0.63 | 0.28 | 122.26 | 1.08 |
| 0.82 | 0.39 | 159.08 | 1.09 |
| 1.07 | 0.51 | 206.99 | 1.1 |
| 1.39 | 0.64 | 269.34 | 1.12 |
| 1.81 | 0.75 | 350.47 | 1.14 |
| 2.36 | 0.85 | 456.03 | 1.16 |
| 3.07 | 0.93 | 593.38 | 1.19 |
| 3.99 | 0.99 | 772.1 | 1.24 |
| 5.19 | 1.04 | 1004.66 | 1.29 |
| 6.75 | 1.05 | 1307 | 1.36 |
| 8.79 | 1.05 | 1701.01 | 1.44 |
| 11.43 | 1.06 | 2213.34 | 1.55 |
| 14.88 | 1.06 | 2280 | 1.68 |

The original saturated thickness of the aquifer is 50 meters. Calculate the hydraulic parameters of the aquifer using the type-curve method. Please use the type curves provided at the end of this assignment.

- 4.14** A well with an effective well radius of 0.3 m exhibits a specific capacity of 0.032 m³/s in an aquifer with 28 m thickness. Estimate the specific capacity for full penetration when the length of a screened well bore is 15 m.
- 4.15** Find the minimum screen length of a well with the designed discharge of 3.6 m³/min, a well screen with an open area of 30%, and a diameter of 0.25 m.

REFERENCES

- AWWA (American Water Works Association). 1998. AWWA standard for water wells; American National Standard. ANSI/AWWA A100-97, AWWA, Denver, CO.
- Birsoy, Y.K. and Summers, W.K. 1980. Determination of aquifer parameters from step tests and intermittent pumping data. *Groundwater*, 18(2), 137–146.
- Delleur, J.W. 1999. *The Handbook of Groundwater Engineering*. CRC Press/Springer-Verlag, Boca Raton, FL.
- Driscoll, F.G. 1986. *Groundwater and Wells*, 2nd edn. Johnson Division, St. Paul, MN.
- Fetter, C.V. 2001. *Applied Hydrogeology*, 4th edn. Prentice Hall, Englewood Cliffs, NJ.
- Hantush, M.S. and Jacob, C.E. 1955. Non-steady radial flow in an infinite leaky aquifer. *Transactions, American Geophysical Union*, 36(1), 95–100.
- Karamouz, M., Szidarovszky, F., and Zahraie, B. 2003. *Water Resources Systems Analysis*. Lewis Publishers, Boca Raton, FL.
- Kruseman, G.P. and de Ridder, N.A. 1991. *Analysis and Evaluation of Pumping Test Data*, 2nd edn. International Institute for Land Reclamation and Improvement, Wageningen, the Netherlands.
- Marino, M.A. and Luthin, J.N. 1982. *Seepage and Groundwater: Developments in Water Science*. Elsevier Scientific Publishing Co, Amsterdam, the Netherlands, 489p.
- Musket, M. 1946. *The Flow of Homogeneous Fluids through Porous Media*. J.W. Edwards, Ann Arbor, MI.
- Neuman, S.P. 1975. Analysis of pumping test data from anisotropic unconfined aquifers considering delayed gravity response. *Water Resources Research*, 11, 329–342.
- Theim, G. 1906. *Hydrologische Methoden*. Gebhardt, Leipzig, Germany, 56pp.
- Theis, C.V. 1935. The lowering of the piezometer surface and the rate and discharge of a well using groundwater storage. *Transactions, American Geophysical Union*, 16, 519–524.
- Todd, D.K. and Mays, L.W. 2008. *Groundwater Hydrology*, 3rd edn. John Wiley & Sons, New York.
- U.S. Bureau of Reclamation. 1981. *Groundwater Manual*. U.S. Government Printing Office, Denver, CO.
- Walton, W.C. 1962. Selected analytical methods for well and aquifer evaluation. *Illinois State Water Survey Bulletin*, 49, 81.
- Willis, R. and Yeh, W.W.-G. 1987. *Groundwater Systems Planning and Management*. Prentice Hall, Englewood Cliffs, NJ.
- Wilson, P. and Strock, J. 1995. *Monitoring Well Design and Construction for Hydrogeologic Characterization*. Guidance Manual for Ground Water Investigations. The California Environmental Protection Agency, CA.



Taylor & Francis

Taylor & Francis Group

<http://taylorandfrancis.com>

5 Groundwater Quality

5.1 INTRODUCTION

Societal dependency on water and the shortage of adequate surface water have increased the use of groundwater. Since groundwater is used to supply the industrial, agricultural, and domestic needs, quality aspects are very important. A number of factors can contribute to changes in the quality of groundwater, including changes in atmospheric composition, changes in soil chemistry, and human activities that directly alter the physical or chemical conditions of soil layers.

There are many parameters that affect groundwater solubility, such as pH, sorption to solids, ionic strength, temperature, and microbiological factors.

Many activities are responsible for the pollution of groundwater, including leaching from municipal and chemical landfills and abandoned dump sites, accidental spills of chemicals or waste materials, improper underground injection of liquid wastes, and placement of septic tank systems in hydrologically and geologically unsuitable locations.

These substances may be introduced to the aquifer system either through the hydraulic interaction with polluted surface waters or directly through injection wells and/or spreading basins or through seepage from waste disposal sites. Hydraulic and mass transport equations are used to describe how the groundwater quality system is affected by waste contaminants.

In this chapter, groundwater constituents and contaminants are introduced. Then, a description of water quality standards and factors affecting groundwater solubility is provided. Finally, sources of groundwater contamination as well as contaminant transport in the saturated and unsaturated zones are evaluated.

5.2 GROUNDWATER CONSTITUENTS AND CONTAMINANTS

Groundwater contains various constituents and contaminants such as inorganics, organics, dissolved gasses, and particles, which are explained in the following subsections.

5.2.1 INORGANIC CONTAMINANTS

Nitrogen: Nitrogen is mostly from agricultural activities and the disposal of sewage on or beneath the land surface. The main form of nitrogen that exists in groundwater is NO_3^- . However, dissolved nitrogen can also be found in the form of ammonium (NH_4^+). Other forms of nitrogen that might be found in groundwater are ammonia (NH_3), nitrite (NO_2^-), nitrogen (N_2), nitrous oxide (N_2O), and organic nitrogen.

Metals: The mobility of metals in groundwater has received considerable attention due to increasing industrial activities. The metals for which maximum permissible or recommended limits have been set in drinking water standards include silver (Ag), cadmium (Cd), chromium (Cr), copper (Cu), mercury (Hg), iron (Fe), manganese (Mn), and zinc (Zn). Most of the above metals are known as heavy metals. The occurrence and mobility of the heavy metals in groundwater environments can be influenced by adsorption processes.

Nonmetals: The most common nonmetals that have been assessed in groundwater studies include carbon, chlorine, sulfur, nitrogen, fluorine, arsenic, selenium, phosphorus, and boron. Carbon, chlorine, and sulfur may exist in high concentrations in dissolved forms in most natural and contaminated groundwater systems. Arsenic and its compounds have been used as insecticides and herbicides for a long time and can be found in groundwater systems influenced by agricultural activities. Selenium may exist in high concentrations in some rocks, such as shale, as well as in coal, uranium, and some soil particles. Fluoride is used as a municipal water-supply additive in many cities due to its beneficial effects on dental health. It is also a natural constituent of groundwater. Phosphorus causes accelerated growth of algae and aquatic vegetation, and, in consequence, eutrophication in ponds, lakes, reservoirs, and streams. However, it is not a harmful constituent in drinking water. The main sources of phosphorus are the widespread use of fertilizers and the disposal of sewage on land.

5.2.2 ORGANIC CONTAMINANTS

Carbon is the key element in organic compounds. Generally, organic compounds have carbon and usually hydrogen and oxygen as the main elements in their chemical structure. Dissolved organic carbon is most commonly in concentrations of 0.1–10 mg/L in groundwater. However, in some areas, values might be as high as several tens of milligrams per liter. The compositions H_2CO_3 , CO_2 , HCO_3^- , and CO_3^{2-} are some exceptions that are not considered as organic components. These compositions are important constituents in all groundwater systems, though.

The prevalent organic constituents in uncontaminated groundwater systems are humic substances that are from decay in plant and animal matter. Fulvic acid, humic acid, and humin are three classes of humic substances. Among these classes, only fulvic acid is soluble in groundwater. Many organic substances have extremely low solubility in water.

Pesticides are one of the major contributors to groundwater contamination in areas with dominated agricultural land use or from urban landscapes. [Table 5.1](#) presents the maximum permissible concentrations and solubilities of some of the most commonly used pesticides.

5.2.3 DISSOLVED GASSES

The natural gases involved in the geochemical cycle of groundwater are carbon dioxide (CO_2), oxygen (O_2), and nitrogen (N_2). These gases mostly originate from the atmosphere. Additionally, some biochemical processes produce dissolved gases

TABLE 5.1
Typical Limits on Drinking Water and the Solubilities of Four Commonly Used Pesticides

| Pesticide | Maximum Permissible Concentration (mg/L) | Solubility in Water (mg/L) |
|-----------------|--|----------------------------|
| Methoxychlor | 0.1 | 0.1 |
| Toxaphene | 0.005 | 3 |
| 2,4-D | 0.1 | 620 |
| 2,4,5-TP Silvex | 0.01 | — |

Source: Oregon State University, *Disposal of Environmentally Hazardous Wastes*, Oregon State University, Corvallis, OR, 210, 1974.

TABLE 5.2
Typical Gas-Phase Compositions in Atmosphere

| Gas | Percentage by Volume |
|------------------|----------------------------|
| N ₂ | 78.1 |
| O ₂ | 20.9 |
| Ar | 0.93 |
| H ₂ O | 0.1–2.8 |
| CO ₂ | 0.03 |
| Ne | 1.8×10^{-3} |
| He | 5.2×10^{-4} |
| CH ₄ | 1.5×10^{-1} |
| Kr | 1.1×10^{-4} |
| CO | $(0.6-1) \times 10^{-4}$ |
| SO ₂ | 1×10^{-4} |
| N ₂ O | 5×10^{-5} |
| H ₂ | 5×10^{-5} |
| O ₃ | $(0.1-1.0) \times 10^{-5}$ |
| Xe | 8.7×10^{-6} |
| NO ₂ | $(0.05-2) \times 10^{-5}$ |

Source: Mirtov, B.A., *Gaseous Composition of the Atmosphere and its Analysis*, U.S. Department of Commerce, Office of Technical Services, Washington DC, 209, 1961.

in groundwater. These include the flammable gases methane (CH₄) and hydrogen sulfide (H₂S). The typical compositions of different gases in the atmosphere are presented in Table 5.2. Some of these constituents have significant roles in determining the chemistry of rain and snow, and, in consequence, the chemistry of the water resource could be influenced by the quality of rain and snow.

Some important atmospheric gases which affect the quality of groundwater are defined in the following:

CO_2 dissolves in water and forms carbonic acid. This acid can be dissociated from bicarbonate (HCO_3^-) and carbonate (CO_3^{2-}) ions. The carbonate system is a key component, which plays an important role in groundwater composition through precipitation reactions (explained in [Chapter 9](#)). Besides, the carbonic acid cycle influences the determination of the pH and buffering capacity of precipitation. Water at equilibrium with atmospheric CO_2 will have a pH of approximately 5.7, which can be used as a benchmark in evaluation of the effects of atmospheric constituents.

O_2 plays an important role in microbiological activities depending on aerobic, anoxic, or anaerobic conditions. The common concentrations in the liquid phase are approximately 8–10 mg/L, depending on the altitude and temperature.

Nitrogen and sulfur oxides (NO_x and SO_x) may cause the production of strong acids, such as HNO_3 and H_2SO_4 . Many natural processes, such as volcanic and microbiological activity release NO_x and SO_x into the atmosphere.

H_2S rarely accumulates to dangerous proportions and has a distinctive rotten egg odor.

CH_4 is produced by the decomposition of buried plant and animal matter in unconsolidated and geologically young deposits. It is a colorless, tasteless, and odorless gas, which can cause serious problems. For example, if there is as little as 1–2 mg/L of methane in water, an explosion in a poorly ventilated air space can take place.

5.2.4 PARTICLES

Constituents that exist in the solid phase either within or apart from the groundwater are referred to as particulate matters. Generally, constituents with a size of 10 nm or greater are considered as particles in groundwater systems. A graphical representation of the spectrum of particle sizes is depicted in [Figure 5.1](#).

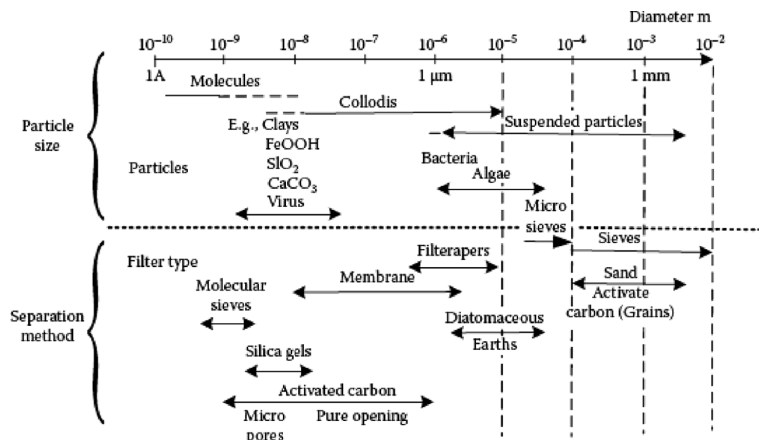


FIGURE 5.1 Spectrum of particle sizes to be seen in natural waters, including groundwater and physical processes for separation of particles. (From Stumm, W., *Environ. Sci. Technol.*, 11, 1070, 1977.)

Microorganisms are also important particulate contaminants in groundwater systems. Microbial contaminants in groundwater can be categorized into viruses, bacteria, and protozoan cysts. All these microorganisms move in groundwater systems, and the larger microorganisms generally move slower than viruses. Protozoan cysts are more difficult to inactivate than either bacteria or viruses. They might be found in higher concentrations in groundwater supplies that are under the direct influence of surface waters. Therefore, more rigorous disinfection requirements are recommended for potabilization in case protozoan cysts exist in the groundwater system.

5.3 WATER QUALITY STANDARDS

To evaluate the suitability of a water resource for specific uses, chemical properties of the water need to be compared with water quality standards assigned for that specific use. Therefore, standards are defined to serve as a basis for water quality evaluations. Drinking water standards (Table 5.3) are the most important of these standards.

TABLE 5.3
Summary of EPA's National Primary Drinking Water Standards (MCLG, MCL)

| Contaminant | MCLG (mg/L) | MCL (mg/L) |
|--------------------------------------|--------------------|-----------------|
| Inorganics | | |
| Antimony | 0.006 | 0.006 |
| Asbestos (>10 nm) | 7 MFL ^a | 7 MFL |
| Barium | 2 | 2 |
| Beryllium | 0.004 | 0.004 |
| Cadmium | 0.005 | 0.005 |
| Chromium (total) | 0.1 | 0.1 |
| Copper | 1.3 | TT ^b |
| Cyanide | 0.2 | 0.2 |
| Fluoride | 4 | 4 |
| Lead | 0 | TT |
| Mercury (inorganic) | 0.002 | 0.002 |
| Nitrate | 10 | 10 |
| Nitrite | 1 | 1 |
| Selenium | 0.05 | 0.05 |
| Thallium | 0.0005 | 0.002 |
| Coliform and surface water treatment | | |
| Giardia lamblia | 0 detected | TT |
| Legionella | 0 detected | TT |
| Standard plate count | N/A | TT |
| Total coliform | 0 detected | c |
| Turbidity | N/A | TT |
| Viruses | 0 detected | TT |

(Continued)

TABLE 5.3 (Continued)**Summary of EPA's National Primary Drinking Water Standards (MCLG, MCL)**

| Contaminant | MCLG (mg/L) | MCL (mg/L) |
|-------------------------------|-------------|-------------|
| Adionuclides | | |
| Radium 226 + radium 228 | 0 | 5 pCi/L |
| Gross alpha particle activity | 0 | 15 pCi/L |
| Beta particle + photon | 0 | 4 mrem/year |
| Radioactivity | | |

Source: Delleur, J.W., *The Handbook of Groundwater Engineering*, CRC Press/Springer-Verlag, Boca Raton, FL, 992, 1999.

^a MFL, million fibers per liter.

^b TT, treatment techniques in lieu of a numerical standard.

^c No more than 5% of samples can be total coliform positive.

In 2006, the World Health Organization recommended values for chemicals that are of health significance in drinking water. These values are presented in [Table 5.4](#).

In many regions, the most important uses of groundwater are for agriculture. In these situations, it is appropriate to appraise the quality of groundwater relative to criteria or guidelines established for livestock or irrigation. Recommended concentration limits for these uses are listed in [Table 5.5](#). The list of constituents and the concentration limits are not as stringent as for drinking water. The serious

TABLE 5.4**Selected Guideline Values for Chemicals of Health Significant Concerns in Drinking Water**

| Chemical | Guideline Value (mg/L) |
|----------------------|------------------------|
| Arsenic | 0.01 (P) |
| Barium | 0.7 |
| Benzene | 0.1 |
| Boron | 0.5 (T) |
| Cadmium | 0.003 |
| Carbon tetrachloride | 0.004 |
| Chlorate | 0.7 (D) |
| Chlordane | 0.0002 |
| Chlorine | 5 (C) |
| Chlorite | 0.7 (D) |
| Chloroform | 0.3 |

(Continued)

TABLE 5.4 (Continued)
Selected Guideline Values for Chemicals of Health Significant Concerns in Drinking Water

| Chemical | Guideline Value (mg/L) |
|--------------------------------------|--|
| Chlorotuluron | 0.03 |
| Chlorpyrifos | 0.03 |
| Chromium | 0.05 (P) |
| Copper | 2 |
| Cyanazine | 0.0006 |
| Cyanide | 0.07 |
| Cyanogen chloride | 0.07 |
| 2,4-D(2,4-dichlorophenoxyaceticacid) | 0.03 |
| 2,4-DB | 0.09 |
| DDT and metabolites | 0.001 |
| Dibromochloromethane | 0.1 |
| Dichlorobenzene, 1,2- | 1 (C) |
| Dichlorobenzene, 1,4 | 0.3 (C) |
| Dichloroethene, 1,2 | 0.05 |
| Dichloromethane | 0.02 |
| Fluoride | 1.5 |
| Nickel | 0.07 |
| Nitrate (as NO ₃) | 50 |
| Nitritolnacetic acid (NTA) | 0.2 |
| Nitrite (as NO ₂) | 0.2 (P) |
| Tetrachloroethene | 0.04 |
| Toluene | 0.7 (C) |
| Trichloroacetate | 0.2 |
| Trichbracetene | 0.02 (P) |
| Trichlorophend,2,4,6- | 0.2 (C) |
| Trihalomethanes | |
| Uranium | 0.015 (P) [only chemical aspects of uranium addressed] |
| Vinyl chloride | 0.0003 |
| Xylenes | 0.5 (C) |

Source: WHO, *Guidelines for Drinking-Water Quality*, First Addendum to 3rd edn., Vol. 1 Recommendations, 2006.

Notes: P, provisional guideline value, as there is evidence of a hazard, but the available information on health effects is limited; T, provisional guideline value because the calculated guideline value is below the level that can be achieved through practical treatment methods, source protection, etc.; D, provisional guideline value because disinfection is likely to result in the guideline value being exceeded; C, concentrations of the substance at or below the health-based guideline value may affect the appearance, taste, and odor of the water leading to consumer complaints.

TABLE 5.5**Recommended Concentration Limits for Water Used for Livestock and Irrigation Crop Production**

| | Livestock: Recommended Limits (mg/L) | Irrigation Crops: Recommended Limits (mg/L) |
|------------------------|---|--|
| Total dissolved solids | | |
| Small animals | 3000 | 700 |
| Poultry | 5000 | |
| Other animals | 7000 | |
| Nitrate | 45 | — |
| Arsenic | 0.2 | 0.1 |
| Boron | 5 | 0.75 |
| Cadmium | 0.05 | 0.01 |
| Chromium | 1 | 0.1 |
| Fluoride | 2 | 1 |
| Lead | 0.1 | 5 |
| Mercury | 0.01 | — |
| Selenium | 0.05 | 0.02 |

Source: U.S. Environmental Protection Agency, *Water Quality Criteria 1972*. EPA R373033, Government Printing Office, Washington, DC, 1973.

degradation of groundwater quality could be due to man's activity that forces the concentration of a variety of constituents to increase.

In 2006, the state of Wisconsin established numerical groundwater quality standards for substances of public health or welfare concern. These standards are listed in **Table 5.6**.

It should be stated that *standards* may not have a scientific basis, but must be regarded as a law or regulation. *Criteria* have a scientific basis, but may not be regarded as a law or regulation. McKee (1960) illustrated the difference between standards and criteria as:

The term *standard* applies to any definite rule, principle, or measure established by authority. The fact that it has been established by an authority makes a standard somewhat rigid, official, or quasi-legal, but this fact does not necessarily mean that the standard is fair, equitable, or based on sound scientific knowledge, for it may have been established somewhat arbitrary on the basis of inadequate technical data tempered by a caution factor of safety. Where health is involved and where scientific sparse, such arbitrary standards may be justified. A *criterion* designates a mean by which anything is tried in forming a correct judgment concerning it. Unlike a standard, it carries no connotation of authority other than of fairness and equity nor does it imply an ideal condition. Where scientific data are being accumulated to serve as yardsticks of water quality, without regard for legal authority, the term *criterion* is most applicable.

TABLE 5.6
Public Health Groundwater Quality Standards

| Substance | Enforcement Standard (µg/L) | Preventive Action Limit (µg/L) |
|--------------------------------------|-----------------------------|--------------------------------|
| Acetone | 1000 | 200 |
| Alachlor | 2 | 0.2 |
| Aldicarb | 10 | 2 |
| Antimony | 6 | 1.2 |
| Anthracene | 3000 | 600 |
| Arsenic | 10 | 1 |
| Atrazine, total chlorinated residues | 3 | 0.3 |
| Bacteria, total coliform | 0 | 0 |
| Barium | 2 mg/L | 0.4 mg/L |
| Bentazon | 300 | 60 |
| Benzene | 5 | 0.5 |
| Benzo(b)flouranthene | 0.2 | 0.02 |
| Benzo(a)pyrene | 0.2 | 0.02 |
| Beryllium | 4 | 0.4 |
| Boron | 960 | 190 |
| Bromodichloromethane | 0.6 | 0.06 |
| Bromoform | 4.4 | 0.44 |
| Bromomethane | 10 | 1 |
| Butylate | 67 | 6.7 |
| Cadmium | 5 | 0.5 |
| Carbaryl | 960 | 192 |
| Carbofuran | 40 | 8 |
| Carbon disulfide | 1000 | 200 |
| Carbon tetrachloride | 5 | 0.5 |
| Chloramben | 150 | 30 |
| Chlordane | 2 | 0.2 |
| Chloroethane | 400 | 80 |
| Chloroform | 6 | 0.6 |
| Chloromethane | 3 | 0.3 |
| Chromium | 100 | 10 |
| Chrysene | 0.2 | 0.02 |
| Cobalt | 40 | 8 |
| Capper | 1300 | 130 |
| Cyanazine | 1 | 0.1 |
| Cyanide | 200 | 40 |
| Dacthal | 4 mg/L | 0.8 mg/L |
| 1,2-Dibromoethane (EDB) | 0.05 | 0.005 |
| Dibromochloromethane | 60 | 6 |
| 1,2-Dibromo-3-chloropropane (BDCP) | 0.2 | 0.02 |
| Dybutyl phthalate | 100 | 20 |

(Continued)

TABLE 5.6 (Continued)
Public Health Groundwater Quality Standards

| Substance | Enforcement Standard (µg/L) | Preventive Action Limit (µg/L) |
|--|-----------------------------|--------------------------------|
| Dicamba | 300 | 60 |
| 1,2-Dichlorobenzene | 600 | 60 |
| 1,3-Dichlorobenzene | 1250 | 125 |
| 1,4-Dichlorobenzene | 75 | 15 |
| Dichlorodifluoromethane | 1000 | 200 |
| 1,1-Dichloroethane | 850 | 85 |
| 1,2-Dichloroethane | 5 | 0.5 |
| 1,1-Dichloroethylene | 7 | 0.7 |
| 1,2-Dichloroethylene(<i>cis</i>) | 70 | 7 |
| 1,2-Dichloroethylene(<i>trans</i>) | 100 | 20 |
| 2,4-Dichlorophenoxy acetic acid (2,4-D) | 70 | 7 |
| 1,2-Dichloropropane | 5 | 0.5 |
| 1,3-Dichloropropane(<i>cis/trans</i>) | 0.2 | 0.02 |
| Di(2-ethylhexyl)phthalate | 6 | 0.6 |
| Dimethoate | 2 | 0.4 |
| 2,4-Dinitrotoluene | 0.05 | 0.005 |
| 2,6-Dinitrotoluene | 0.05 | 0.005 |
| Dinoseb | 7 | 1.4 |
| Dioxin (2,3,7,8-TCDD) | 0.00003 | 0.000003 |
| Endrin | 2 | 0.4 |
| EPTC | 250 | 50 |
| Ethylbenzene | 700 | 140 |
| Ethylene glycol | 7 mg/L | 0.7 mg/L |
| Fluoranthene | 400 | 80 |
| Fluorene | 400 | 80 |
| Fluoride | 4 mg/L | 0.8 mg/L |
| Fluorotrichloromethane | 3490 | 698 |
| Formaldehyde | 1000 | 100 |
| Heptachlor | 0.4 | 0.04 |
| Heptachlor epoxide | 0.2 | 0.02 |
| Hexachlorobenzene | 1 | 0.1 |
| N-hexane | 600 | 120 |
| Hydrogen sulfide | 30 | 6 |
| Lead | 15 | 1.5 |
| Lindane | 0.2 | 0.02 |
| Mercury | 2 | 0.2 |
| Methanol | 5000 | 1000 |
| Methoxychlor | 40 | 4 |
| Methylene chloride | 5 | 0.5 |
| Methyl ethyl ketone (MEK) | 460 | 90 |
| Methyl isobutyl ketone (MIBK) | 500 | 50 |

(Continued)

TABLE 5.6 (Continued)
Public Health Groundwater Quality Standards

| Substance | Enforcement Standard (µg/L) | Preventive Action Limit (µg/L) |
|--|-----------------------------|--------------------------------|
| Methyl <i>tert</i> -butyl ether (MTBE) | 60 | 12 |
| Metolachlor | 15 | 1.5 |
| Metribuzin | 250 | 50 |
| Monochlorobenzene | 100 | 20 |
| Naphthalene | 40 | 8 |
| Nickel | 100 | 20 |
| Nitrate (as N) | 10 mg/L | 2 mg/L |
| Nitrate + nitrite (as N) | 11 mg/L | 2 mg/L |
| Nitrite (as N) | 1 mg/L | 0.2 mg/L |
| N-Nitrosodiphenylamine | 7 | 0.7 |
| Pentachlorophenol (PCP) | 1 | 0.1 |
| Phenol | 6 mg/L | 1.2 mg/L |
| Picloram | 500 | 100 |
| Toxaphene | 3 | 0.3 |
| 1,2,4-Trichlorobenzene | 70 | 14 |
| 1,1,1-Trichloroethane | 200 | 40 |
| 1,1,2-Trichloroethane | 5 | 0.5 |
| Trichloroethylene (TCE) | 5 | 0.5 |
| 2,4,5-Trichlorophenoxy-propionic acid (2,4,5-TP) | 50 | 5 |
| 1,2,3-Trichloropropane | 60 | 12 |
| Trifluralin | 7.5 | 0.75 |
| Trimethylbenzenes (1,2,4- and 1,3,5-combined) | 480 | 96 |
| Vanadium | 30 | 6 |
| Vinyl chloride | 0.2 | 0.02 |
| Xylene | 10 mg/L | 1 mg/L |

5.4 GROUNDWATER SOLUBILITY

The solubility of a contaminant compound will determine the transport, fate, and toxicology of that compound in a groundwater system. The main characteristics of a system, which may affect solubility are pH, sorption to solids, and temperature.

For a chemical process, concentrations of reacting components and reaction products play the role of a driving force for the entire reaction process. Most chemical reactions are, to some extent, reversible, which means that they proceed in both directions at once. In a generalized reversible reaction, consider the constituents *A* and *B* reacting to produce the products *C* and *D*,



where a , b , c , and d are the coefficients corresponding to the number of moles of the chemical constituents A , B , C , and D , respectively. The double arrow designation indicates that the reaction proceeds in both directions at the same time, i.e., it is a reversible reaction.

When the reaction reaches an equilibrium, the law of mass action expresses the relation between the reactants and products as:

$$K = \frac{[C]^c [D]^d}{[A]^a [B]^b} \quad (5.2)$$

where K is the thermodynamic equilibrium constant or the stability constant.

The brackets represent the concentration of substances at equilibrium, expressed in moles per liter.

Based on Equation 5.2, for any initial condition, the corresponding reaction (Equation 5.1) will proceed until both the reactants and products reach their equilibrium condition. Initial activities cause the reaction to proceed to the left or to the right until the equilibrium condition is reached. It should also be emphasized that Equation 5.2 is valid only when a chemical equilibrium is established, if ever. However, the law of mass action does not express the rate at which the reaction proceeds and does not indicate the kinetics of the chemical process.

A disturbance in the system, e.g., an addition of reactants, causes the system to continue to proceed toward a new equilibrium condition. Changes in the temperature or pressure can also result in a move toward a new equilibrium.

If auto-ionization occurs in water, H^+ and OH^- will be produced.



The notation H^+ is a representation for the hydrated proton. For this reaction, the corresponding equilibrium expression is:

$$\frac{[H^+][OH^-]}{[H_2O]} = K \quad (5.3b)$$

$[H_2O]$ can be included in the equilibrium constant because it is essentially a constant, as water is only slightly dissociated. Hence,

$$[H^+][OH^-] = K_w = 1 \times 10^{-14} \quad \text{at } 25^\circ\text{C} \quad (5.3c)$$

where K_w is the dissociation constant for water. Equation 5.3c is always one of the equations to be satisfied, regardless of the source of H^+ or OH^- , when analyzing the problems of chemical equilibrium in water.

H^+ is used to determine the pH of water as:

$$pH = -\log_{10}(H^+) \quad (5.4)$$

where (H^+) is the activity of the hydrogen ion.

TABLE 5.7
Acid Dissociation Constants for Common Ionizable Groundwater Constituents at 25°C

| Compound (Formula) | Conjugate Base (Formula) | pK_a |
|---|---|--------|
| Hydrochloric acid (HCl) | Chloride (Cl ⁻) | -3 |
| Sulfuric acid (H ₂ SO ₄) | Bisulfate (HSO ₄ ⁻) | -3 |
| Nitric acid (HNO ₃) | Nitrate (NO ₃ ⁻) | -1 |
| Bisulfate (HSO ₄ ⁻) | Sulfate (SO ₄ ²⁻) | 1.9 |
| Phosphoric acid (H ₃ PO ₄) | Dihydrogen phosphate (H ₂ PO ₄ ⁻) | 2.1 |
| Acetic acid (CH ₃ COOH) | Acetate (CH ₃ COO ⁻) | 4.7 |
| Hydrogen sulfide (H ₂ S) | Bisulfide (HS ⁻) | 7.1 |
| Dihydrogen phosphate (H ₂ PO ₄ ⁻) | Hydrogen phosphate (HPO ₄ ²⁻) | 7.2 |
| Hydrogen cyanide (HCN) | Cyanide (CN ⁻) | 9.2 |
| Ammonium (NH ₄ ⁺) | Ammonia (NH ₃) | 9.3 |
| Orthosilicic acid (Si(OH) ₄) | Silicate (SiO(OH) ₃ ⁻) | 9.5 |
| Silicate (SiO(OH) ₃ ⁻) | (SiO ₂ (OH) ₂ ²⁻) | 12.6 |
| Bisulfide (HS ⁻) | Sulfide (S ²⁻) | 17 |

Source: Stumm, W. and Morgan, J.J., *Aquatic Chemistry*, 3rd edn., John Wiley & Sons, New York, 1022, 1996.

The speciation of all acids and bases in a solution can be specified by the pH level of the solution. Table 5.7 lists some important acid-base pairs. These constants indicate the importance of pH in determining the characteristics of the acid-base behavior of groundwater.

Another term commonly used for describing the activity of a constituent is pC, which is defined as the negative \log_{10} of the activity of the constituent. pC–pH diagrams are used to illustrate acid-base behavior over a broad range of conditions.

These diagrams also demonstrate the equilibrium relationships and the total concentration of the compounds.

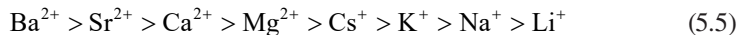
Some important conditions in evaluating the rates and equilibrium of chemical reactions and processes are discussed in the following:

Sorption to solids: There are two types of associations among aqueous and solid phases: (1) the accumulation of materials at a water-solid interface, which is called adsorption and (2) the intermingling of solute molecules with the molecules of the solid phase, which is termed absorption. In other words, absorption is the dissolution of a liquid material in a solid solvent. It is usually hard, or sometimes even impossible, to distinguish between the two processes. The term sorption can be used for both these processes.

In general, there are three types of sorptions for groundwater systems. In all these three types, bonds are formed between the constituent and the solid phase. These types are

- *Physisorption*: Relatively weak physical bonds, such as van der Waal's forces, are formed in this type.
- *Chemisorption*: Under certain conditions, a chemical bond is formed between the solute and a solid surface.
- *Ion exchange*: Ion exchange occurs due to an electrostatic interaction between the solute and a solid surface.

In physisorption and ion exchange processes, the forces responsible for the attraction of a solute to the solid are relatively weak. Therefore, these processes tend to be readily reversible. The selectivity order in ion exchange for some common cations is:



Ions will replace those ions on their right in the selectivity order. As an example, Mg^{2+} will replace Na^+ . However, based on the circumstances, the specific selectivity order may vary from that defined in Equation 5.5.

Temperature: The rates and equilibria of chemical reactions are highly dependent on thermodynamic conditions. In higher temperatures, more thermal energy is available, and in consequence, reaction rates increase. If a given reaction consumes energy (an endothermic reaction), an increase in temperature promotes the forward reaction, and the equilibrium will be shifted to the right (more product formation). For example, heat may affect groundwater contaminants as it: (1) changes the equilibria and kinetics of precipitation and the dissolution of minerals and (2) changes the rates of biological transformation processes.

In groundwater systems, temperature is usually assumed to be at a value of 1°C – 2°C greater than the annual average ambient air temperature for the region (Freeze and Cherry, 1979). In higher depths, greater than approximately 10 m, diurnal and seasonal variations of air temperature have minimal effects on groundwater; therefore, groundwater temperature at these depths is often assumed to be approximately 13°C .

Microbiological factors: In groundwater, bacteria are the most important microorganisms in redox processes. Algae, fungi, yeasts, and protozoans are important in other aqueous environments. The size of bacteria generally ranges from about 0.5 to 3 μm . The main effect of microorganisms on groundwater contaminants is that they catalyze the important redox reactions in groundwater.

5.5 DISEQUILIBRIUM AND SATURATION INDEX

In a condition of disequilibrium, if the reaction expressed in Equation 5.1 is considered, the relation between the reactants and products can be shown as:

$$Q = \frac{[A]^a [B]^b}{[C]^c [D]^d} \quad (5.6)$$

where Q is the reaction quotient and the other parameters are as expressed in Equation 5.2. In thermodynamic equilibrium conditions, the following ratio can be used to compare the status of a mineral; the dissolution–precipitation reaction at a particular time or space:

$$S_t = \frac{Q}{K_{eq}} \quad (5.7)$$

where S_t is the *saturation index*. For example, the saturation index for calcite is defined as:

$$S_t = \frac{[\text{Ca}^{2+}][\text{CO}_3^{2-}]}{K_{cal}} \quad (5.8)$$

The ion activities for Ca^{2+} and CO_3^{2-} are obtained by analyzing groundwater samples, and the equilibrium constant, K_{cal} , is obtained from equilibrium constant tabulations. Some equilibrium constants, in particular temperature and pressure conditions, are presented in **Table 5.8**.

$S_t > 1$ shows that the ionic constituents exceed the normal conditions. Therefore, the reaction proceeds to the left, and, in consequence, mineral precipitation occurs. If $S_t < 1$, the reaction proceeds to the right and results in the dissolution of the mineral. $S_t = 1$ shows that the reaction is at equilibrium, and the water is saturated by the mineral. The saturation index helps to compare the status of water samples with the computed equilibrium conditions.

TABLE 5.8
Equilibrium Constants for Calcite, Dolomite, and Major Aqueous Carbonate Species in Pure Water, 0°C–30°C, and 1 Bar Total Pressure

| Temperature (°C) | $\text{p}K_{\text{CO}_2}^{\text{a}}$ | $\text{p}K_{\text{H}_2\text{CO}_3}$ | $\text{p}K_{\text{HCO}_3^-}$ | $\text{p}K_{\text{cal}}$ | $\text{p}K_{\text{dol}}$ |
|------------------|--------------------------------------|-------------------------------------|------------------------------|--------------------------|--------------------------|
| 0 | 1.12 | 6.58 | 10.62 | 8.34 | 16.56 |
| 5 | 1.2 | 6.52 | 10.56 | 8.345 | 16.63 |
| 10 | 1.27 | 6.47 | 10.49 | 8.355 | 16.71 |
| 15 | 1.34 | 6.42 | 10.43 | 8.37 | 16.79 |
| 20 | 1.41 | 6.38 | 10.38 | 8.385 | 16.89 |
| 25 | 1.47 | 6.35 | 10.33 | 8.4 | 17 |
| 30 | 1.67 | 6.33 | 10.29 | 8.51 | 17.9 |

Source: Freeze, R. and Cherry, J., *Groundwater*, Prentice-Hall, Englewood Cliffs, NJ, 1979, 604.

^a $\text{p}K = -\log K$.

5.6 SOURCES OF GROUNDWATER CONTAMINATION

Water in the hydrologic cycle is subject to quality changes due to physical, chemical, and biological characteristics of the environment. The changes can be natural or man-made. For example, the quality of groundwater is widely affected by waste disposal, underground storage of waste materials, and seepage from agricultural fertilizers and pesticides as well as leakage from underground tanks.

5.6.1 DISPOSAL OF SOLID WASTES

A considerable number of examinations on the infiltration of water through refuses in Europe have shown that this penetration is ascribed to the water table below the landfill. As a result of this event, leachate descends from the landfill into groundwater as shown in [Figure 5.2](#). Under this condition, the seepage of the leachate source at the perimeter of the landfill into surface-water bodies will be probable. If the leachate does not pass through the aquifers including potable water, its downward movement will not endanger and pollute groundwater resources.

5.6.2 UNDERGROUND PETROLEUM TANK LEAKAGE

In industrial countries and urban areas, numerous storage tanks are buried at gas stations and in residential, commercial, and industrial compounds to produce thermal and other kinds of energy. Petroleum products are carried by underground pipelines passing through continents. Also, a small amount of oils and gases are carried by tanker trucks that are continuously on the move. Therefore, groundwater quality will be increasingly menaced by seepages and penetrations from these sources. A strict testing of the buried storage tanks is required, but it is only gradually being performed in most countries. As a result, leakage problems due to rust on the tanks, especially those that are located in regions with high water tables and frequent infiltration, are common. As oils and gasoline are not mixable in water, they migrate into the unsaturated zone, form leakages, and stay on the water table. Some dense chemical products such as heavy metals and other materials move downward to deeper parts of the aquifer and threaten deep-water supply wells.

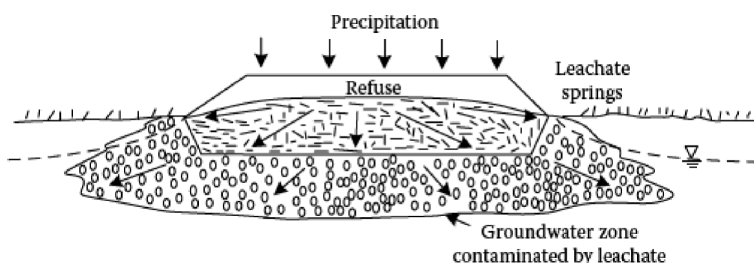


FIGURE 5.2 Water table plume under a landfill, causing leachate springs and migration of contaminants deeper into the groundwater zone.

5.6.3 DISPOSAL OF LIQUID WASTES

In many areas, liquid waste injection has been widely used to practice waste disposal. Its main purpose is to isolate hazardous substances from the biosphere (Freeze and Cherry, 1979). Strict regulations have been implemented to prevent the discharge of contaminants to rivers and lakes and to protect surface water from pollution. Therefore, in waste management, using the deep permeable zones for liquid waste disposal is a desired option for many industries.

Figure 5.3 shows the impact of an injection well in a hypothetical horizontal aquifer on the hydrodynamic conditions in a regional flow. The injection well leads to an increase in the potentiometric surface. The mound enlarges in the flow direction asymmetrically. On continuing with the injection, the mound expands over an ever-increasing area.

In regions with injection wells close to each other, the potentiometric mounds merge similarly to the drawdown interface in fields of pumping wells. The front of the mound spreads very quickly in comparison with the spread of the zone of injected waste. The pressure translation leads to a spread in front of the potentiometric mound, which occurs as a volume displacement. There is a direct relation between the affected area and the injected cumulative volume of waste. The dispersion also progressively decreases the interface between the water and waste.

5.6.4 SEWAGE DISPOSAL ON LAND

Sewage is reaching subsurface flow in a variety of ways. Widespread use of septic tanks and drains in rural, recreational, urban, and suburban areas contributes filtered or unfiltered sewage effluent directly to the ground. Septic tanks and cesspools are

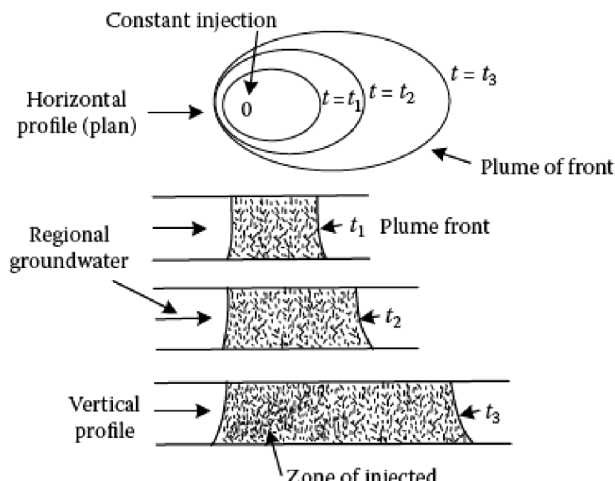


FIGURE 5.3 Potentiometric mound caused by waste disposal injection and the expansion of the affected zone occupied at times t_1 , t_2 , and t_3 .

the largest of all contributors of wastewater to the ground. Sewage disposal on land can cause the transportation of many kinds of contaminants to groundwater such as nitrogen and phosphorus, detergents, pathogenic bacteria and viruses, etc. There are absorption wells in many cities, even some megacities, such as Tehran/Iran with three million absorption wells.

5.6.5 AGRICULTURAL ACTIVITIES

Of all the man-made activities that influence the quality of groundwater, the use of chemicals in agriculture is probably the most important factor. Among the main agricultural activities that can cause a degradation of groundwater quality is the use of fertilizers and pesticides and the storage or disposal of livestock wastes on land. The most widespread effects result from the use of fertilizers. In developed and developing countries, most fertilizers are produced with chemicals. These fertilizers are known as inorganic fertilizers. In less developed countries, animal or human wastes are widely used as organic fertilizers.

5.6.6 OTHER SOURCES OF CONTAMINATION

There are many other sources that contribute to the contamination of groundwater, including:

- Large quantities of salts that are spread on the roads to ease ice conditions during winter
- Activities of the mining industry
- Seepage from industrial waste lagoons
- Urbanization and urban surface runoff spreading into the recharge areas of major aquifers

Table 5.9 and Figure 5.4 show groundwater contamination in different categories.

TABLE 5.9

Sources of Groundwater Quality Degradation

Groundwater Quality Problems That Originate on the Land Surface

- Infiltration of polluted surface water
- Land disposal of either solid or liquid wastes dumps
- Disposal of sewage and water-treatment plant sludge
- Deicing salt usage and storage
- Animal feedlots
- Fertilizers and pesticides
- Accidental spills
- Particulate matter from airborne sources

Groundwater Quality Problems That Originate in the Ground above the Water Table

- Septic tanks, cesspools, and privies

- Holding ponds and lagoons

(Continued)

TABLE 5.9 (Continued)
Sources of Groundwater Quality Degradation

Sanitary landfills
 Waste disposal in excavations
 Leakage from underground storage tanks
 Leakage from underground pipelines
 Artificial recharge

Groundwater Quality Problems That Originate in the Ground below the Water Table

Waste disposal in well excavations
 Drainage wells and canals
 Well disposal of wastes
 Underground storage
 Exploratory wells
 Groundwater development

Source: U.S. Environmental Protection Agency, *Protection of Public Water Supplies from Ground-Water Contamination, Center for Environmental Research Information*, U.S. Environmental Protection Agency, Washington, DC, 2005.

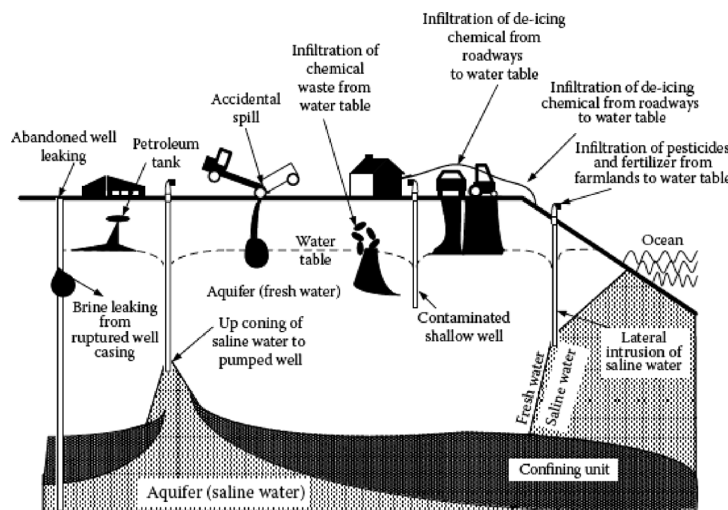


FIGURE 5.4 Sources of groundwater contamination. (From Delleur, J.W., *The Handbook of Groundwater Engineering*, CRC Press/Springer-Verlag, Boca Raton, FL, 992, 1999.)

5.7 MASS TRANSPORT OF DISSOLVED CONTAMINANTS

In groundwater contamination studies, the basic theories and processes behind the movement of contaminants are required to be understood. In the subsurface area, complex processes occur that operate the movement of substances through porous media. These processes can be expressed mathematically. The main processes for

the transportation of dissolved contaminants are advection, dispersion, and diffusion. In the advection process, moving groundwater carries dissolved solutes. Along with advection, the dispersion process occurs that dilutes the solute. In the diffusion process, ionic and molecular species dissolved in water move from areas of higher concentration to areas of lower concentration. There are also chemical and physical processes that cause the retardation of the solute movement so that it may not move as fast as the advection rate would indicate.

5.7.1 DIFFUSION

Diffusion is a net transport of molecules from a region of higher concentration to one of lower concentration by random molecular motion. The diffusion of a contaminant through water in 1D condition is described by Fick's laws. Under steady-state conditions, Fick's first law describes the flux of a solute as:

$$F_{dif} = \frac{-DdC}{dx} \quad (5.9)$$

where:

F_{dif} is the mass flux of the solute per unit area per unit time

D is the diffusion coefficient (area/time)

C is the solute concentration (mass/volume)

dC/dx is the concentration gradient (mass/volume/distance).

The above equation is set for surface water. To apply this equation for groundwater, the porosity of the media must be taken into account. The negative sign indicates that the movement is from greater to lower concentrations. Values of the diffuse coefficient, D , for some ions in water, are presented in [Table 5.10](#).

TABLE 5.10
Diffusion Coefficients in Water for Certain Ions at 25°C

| Cation | D (10 ⁻⁶ cm ² /s) | Anion | D (10 ⁻⁶ cm ² /s) |
|------------------|---|-------------------------------|---|
| H ⁺ | 93.1 | OH ⁻ | 52.7 |
| Na ⁺ | 13.3 | F ⁻ | 14.6 |
| K ⁺ | 19.6 | Cl ⁻ | 20.3 |
| Rb ⁺ | 20.6 | Br ⁻ | 20.1 |
| Cs ⁺ | 20.7 | HS ⁻ | 17.3 |
| Mg ²⁺ | 7.05 | HCO ₃ ⁻ | 11.8 |
| Ca ²⁺ | 7.93 | CO ₃ ²⁻ | 9.55 |
| Sr ²⁺ | 7.94 | SO ₄ ²⁻ | 10.7 |
| Ba ²⁺ | 8.48 | PO ₄ ³⁻ | 6.12 |
| Ra ²⁺ | 8.89 | | |
| Mn ²⁺ | 6.88 | | |
| Fe ²⁺ | 7.19 | | |
| Cr ³⁺ | 5.94 | | |
| Fe ³⁺ | 6.07 | | |

If the concentrations of contaminants in water change with time, Fick's second law may be applied:

$$\frac{\partial C}{\partial t} = \frac{\partial^2 C}{\partial x^2} \quad (5.10)$$

where $\partial C/\partial t$ indicates the change in concentration with time.

Example 5.1

A site has been contaminated by dieldrin. The porosity of the soil is 0.35 in this site. If the gradient of dieldrin concentration is 0.0003 mg/L/m , calculate the difusive flux. The diffusion coefficient of dieldrin is $4.74 \times 10^{-6} \text{ cm}^2/\text{s}$.

SOLUTION

$$\begin{aligned} F_{\text{dif}} &= nDdC/dx \\ &= 0.35 \times 4.74 \times 10^{-6} \text{ cm}^2/\text{s} \times 10^{-6} \text{ m}^2/\text{cm}^2 \times 0.0003 \text{ mg/L/m} \\ &= 5.00 \times 10^{-16} \text{ mg/m}^2/\text{s} = 4.32 \times 10^{-11} \text{ mg/m}^2/\text{day} \end{aligned}$$

In porous media, the ions must follow longer pathways as they travel around mineral grains. Therefore, the diffusion process in groundwater is slower than in surface water. An effective diffusion coefficient, D^* , is used to take this decrease in velocity into account. This coefficient is calculated as:

$$D^* = \tau D \quad (5.11)$$

where τ is an empirical coefficient determined by laboratory experiments. It ranges from 0.5 to 0.01 for species that are not adsorbed onto the mineral surface (Freeze and Cherry, 1979).

Even in the absence of groundwater movement, contaminants existing in the aquifer tend to diffuse in all directions, which cause a blurring of the boundary between contaminated groundwater and the surrounding groundwater. So, if the groundwater is not flowing, contaminants may still move through the porous medium by diffusion, i.e., even in the condition of a zero hydraulic gradient, a contaminant could still move. Diffusion is dominant especially in rocks and soil with very low permeability that the water may be moving very slow.

If a solid waste is placed on a soil liner and both are saturated with water, contaminant ions from the solid waste (where the concentration is greater) will diffuse into the soil liner even if there is no water flow. Assume that the concentrations of the contaminant in the solid waste and soil liner are C_0 and C_i , respectively. C_i at distance d and time t is calculated as (Crank, 1956):

$$C_i(d, t) = C_0 \operatorname{erfc} \frac{d}{2(D^* t)^{0.5}} \quad (5.12)$$

Example 5.2

A landfill holds a solid waste that has chloride ions in its leachate. This landfill has a clay liner. The concentration of chloride in the leachate is 150 mg/L. What is the concentration of chloride 7 m away from the interface of the landfill and the liner after 80 years? The diffuse coefficient is $1.8 \times 10^{-8} \text{ m}^2/\text{s}$ and τ is 0.5.

SOLUTION

$$D^* = \tau D = 0.5 \times 1.8 \times 10^{-8} = 9.0 \times 10^{-9} \text{ m}^2/\text{s}$$

$$t = 80 \text{ years} \times 365 \text{ day/year} \times 86400 \text{ s/day} = 2.52 \times 10^9 \text{ s}$$

$$C_i = 150 \text{ mg/L} \times \operatorname{erfc} \frac{7}{2 \times (9 \times 10^{-9} \text{ m}^2 \text{ s} \times 2.52 \times 10^9)^{0.5}}$$

$$C_i = 150 \text{ mg/L} \times \operatorname{erfc}(0.735) = 44.8 \text{ mg/L}$$

5.7.2 ADVECTION

As explained in [Chapter 3](#), the rate of groundwater flow is determined from Darcy's law (Equation 3.1). Contaminant transport by the movement of a bulk of water is called advection. The rate of transport is then the same rate as the average linear velocity of the groundwater.

Example 5.3

Assume that a bulk of dissolved contaminants reaches an unconfined aquifer that has a hydraulic conductivity of $5 \times 10^{-5} \text{ m/s}$ and a porosity of 0.4. If the hydraulic gradient in this aquifer is 0.08, how far might this contaminant move in 3 years?

SOLUTION

Since it is assumed that the contaminant is being transported only by complete mixing, it has the same velocity as the groundwater. Therefore,

$$v = \frac{Ki}{n} = \frac{5 \times 10^{-5} \times 0.08}{0.4} = 1.0 \times 10^{-5} \text{ m/s}$$

$$= 10^{-5} \text{ m/s} \times 86,400 \text{ s/day} \times 365 \text{ day/year} = 31.54 \text{ m/year}$$

So, the distance that the contaminant moves in 3 years is:

$$d = 31.54 \text{ m/year} \times 3 \text{ years} = 94.62 \text{ m}$$

The 1D mass flux, F_x , due to advection can be calculated as:

$$F_x = v_x n C \quad (5.13)$$

where:

v_x is the velocity of groundwater in x direction

n is the porosity

C is the concentration of dissolved contaminants.

Example 5.4

A stream is being recharged by an unconfined aquifer which is 2.2 m thick and 98 m wide. The porosity of the aquifer is 0.23, and groundwater is flowing in this aquifer with the velocity of 0.3 m/day. Assuming that the concentration of nitrate is 22 mg/L in the groundwater, what is the mass flux of nitrate being discharged into the stream?

SOLUTION

$$\begin{aligned}
 F_x &= v_x n C \\
 &= 0.3 \text{ m/day} \times 0.23 \times 22 \text{ mg/L} \times 0.001 \text{ g/mg} \times 1000 \text{ L/m}^3 \\
 &= 1.52 \text{ g/m}^2 \text{ - day}
 \end{aligned}$$

Therefore, the total flux discharged to the stream is:

$$\begin{aligned}
 F_T &= 1.52 \text{ g/m}^2 \text{ - day} \times 2.2 \text{ m} \times 98 \text{ m} \\
 &= 327.7 \text{ g/day}
 \end{aligned}$$

5.7.3 MECHANICAL DISPERSION

Another process that causes a contaminant plume to be spread out is dispersion. A contaminant plume follows irregular pathways as it moves. In other words, a portion of the contaminant plume may find large pore spaces in which it can move quickly, while other portions have to force their way through more confining voids. Therefore, there will be a difference in speed of an advancing plume that tends to cause the plume to be spread out. So, dispersion can be defined as the dilution of contaminants because of being mixed with noncontaminated water. If the mixing occurs along the streamline of fluid flow, it is called longitudinal dispersion. Transverse dispersion occurs perpendicular to the main direction of flow. Since contamination spreads out as it moves, it does not arrive all at once at a given location down-gradient. This effect is easily demonstrated in the laboratory by establishing a steady-state flow regime in a column packed with a homogeneous granular material and then introducing a continuous stream of a nonreactive tracer, as shown in [Figure 5.5a](#). If the tracer had no dispersion, a plot of concentration versus the time that it takes to leave the column would show a sharp jump (dashed line in [Figure 5.5b](#)). Instead, the front is smeared out by dispersion and lagged by retardation, as shown in [Figure 5.5b](#).

When the contaminants move through an aquifer, some contaminants are absorbed by solids along the way and other contaminants are adhered to the surface of particles (is called adsorbed). The general term sorption applies to both processes.

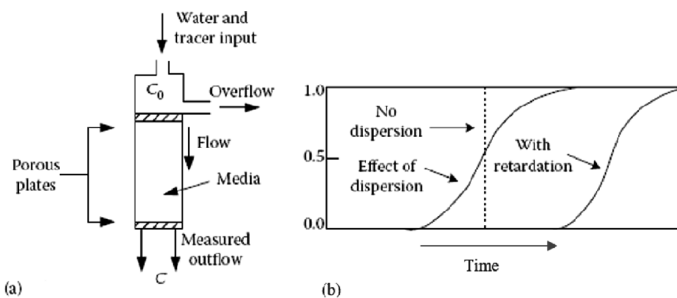


FIGURE 5.5 Dispersion and retardation as a continuous feed of tracer passes through a column. With no dispersion, the tracer emerges all at once. With retardation and dispersion, the tracer smears out and emerges with some delay (a) laboratory setup and (b) emerging tracer. (From Masters, G.M. and Ela, W.P., *Introduction to Environmental Engineering and Science*, Prentice Hall, Simon and Schuster, Englewood Cliffs, NJ, 576, 2008.)

Retardation processes (which will be discussed in [Chapter 9](#)) remove contaminants from the groundwater during transport. Thus, the contaminant concentration arriving at a certain point at a certain time is less than it would have been for a nonretarded contaminant. The ratio of total contaminant in a unit volume of aquifer to the contaminant dissolved in groundwater is called the retardation factor. For example, retardation factor for chloride ions is 1, that means all of it is dissolved in groundwater:

$$R = \frac{v'}{v} \geq 1 \quad (5.14)$$

where:

- v' is the average groundwater velocity
- v is the velocity of the sorbed materials.

While the column experiment described in [Figure 5.5](#) illustrates longitudinal dispersion, there is also some dispersion normal to the main flow. [Figure 5.6](#) shows what might be expected if an instantaneous (pulse) source of contaminant is injected into a flow field, such as what might occur with an accidental spill that contaminates groundwater. As the plume moves down-gradient, dispersion causes the plume to spread in the longitudinal as well as orthogonal directions.

Longitudinal dispersion occurs based on the following reasons:

1. Fluid moves faster through the center of the pore than along the edges.
2. Some portions of the fluid travel in longer pathways than other portions.
3. The movement of fluid through larger pores travels faster than that in smaller pores.
4. Heterogeneity of the aquifer causes the groundwater to move faster in some layers and slower in some others.

[Figure 5.7](#) shows the fluid movement through soil particles.

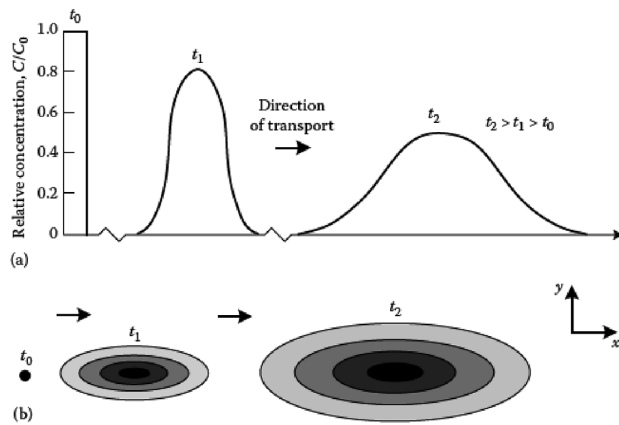


FIGURE 5.6 An instantaneous (pulse) source in a flow field creates a plume that spreads as it moves down-gradient: (a) in 1D and (b) in 2Ds (darker colors mean higher concentrations). (From Bedient, P.B. et al., *Ground Water Contamination: Transport and Remediation*, Prentice-Hall Publishing, Englewood Cliffs, NJ, 560, 1994.)

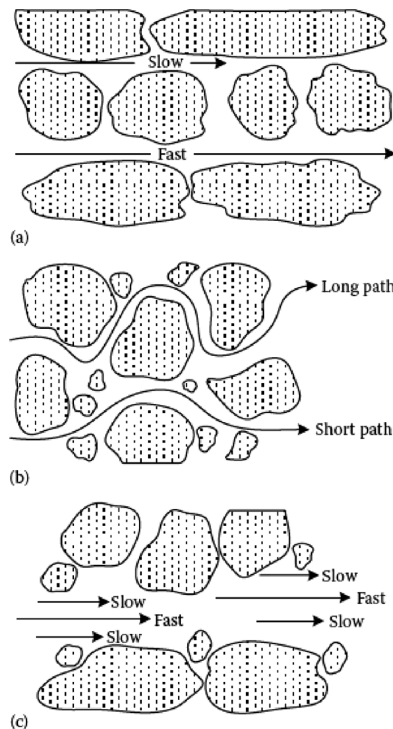


FIGURE 5.7 Main factors that cause longitudinal dispersion in subsurface area. (a) Larger pores let fluid move faster, (b) travel time through longer paths is more than shorter ones, and (c) fluid moves faster through the center of the pore.

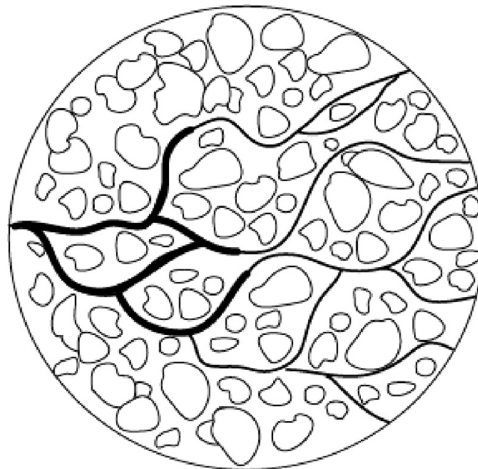


FIGURE 5.8 Flow paths in the porous medium causing transverse dispersion.

The main reason for the occurrence of the transverse dispersion is that flow paths branch out to the sides while passing through a porous medium (Figure 5.8).

For uniform flow fields, the mechanical dispersion is equal to the product of the dynamic dispersivity (α_L) and the average linear velocity:

$$D_m = \alpha_L \times v_i \quad (5.15)$$

where:

D_m is the mechanical dispersion

v_i is the linear velocity in the i direction.

Xu and Eckstein (1995) found a relationship between the apparent longitudinal dynamic dispersivity and flow length. This relationship is expressed as:

$$\alpha_L = 0.83(\log L)^{2.414} \quad (5.16)$$

where:

α_L is the apparent longitudinal dynamic dispersivity

L is the length of the flow path.

5.7.4 HYDRODYNAMIC DISPERSION

Since molecular diffusion and mechanical dispersion usually take place coincidentally in groundwater movement, and they both tend to smear the edges of the plume, they are sometimes linked together and are simply referred to as *hydrodynamic dispersion*.

To take into account both the mechanical dispersion and diffusion, the coefficient of the hydrodynamic dispersion, D_L , is introduced. For a 1D flow, this coefficient can be represented as:

$$D_L = \alpha_L v_i + D^* \quad (5.17)$$

where:

D_L is the longitudinal coefficient of the hydrodynamic dispersion

α_L is the dynamic dispersivity

v_i is the average linear groundwater velocity

D^* is the effective diffusion coefficient.

For calculating the transverse coefficient of dispersion, Equation 5.16 is rewritten as:

$$D_T = \alpha_T v_i + D^* \quad (5.18)$$

where α_T is the transverse dynamic dispersivity.

5.7.5 DERIVATION OF THE ADVECTION–DISPERSION EQUATION

Imagine a representative elementary volume of the porous media (Figure 5.9). To derive the advection–dispersion equation, the conservation of the mass of contaminant flux into and out of this volume is considered.

Assuming a homogeneous aquifer, the contaminant transport in the i direction based on advection and hydrodynamic dispersion can be calculated as:

$$T_a = v_i n C dA \quad (5.19)$$

$$T_d = n D_i \frac{\partial C}{\partial i} dA \quad (5.20)$$

where:

T_a and T_d are the advective and dispersive transport, respectively

dA is the cross-sectional area of the element.

The total mass of contaminant per unit cross-sectional area transported in the i direction per unit time, F_i , can be computed as the sum of the advective and the dispersive transport:

$$F_i = v_i n C - n D_i \frac{\partial C}{\partial i} \quad (5.21)$$

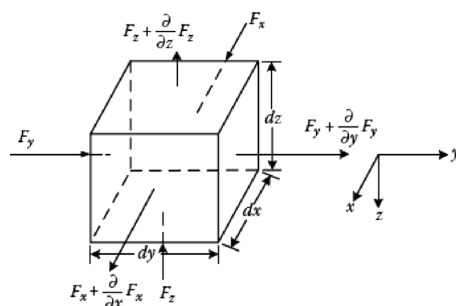


FIGURE 5.9 Representative elementary volume for groundwater flow.

Since the dispersive flux is from areas of greater to areas of lesser concentration, the second term has a negative sign.

The total amount of contaminant entering the representative elementary volume is $F_x d_z d_y + F_y d_z d_x + F_z d_x d_y$. The amount of contaminant leaving the representative elementary volume is:

$$\left(F_x + \frac{\partial F_x}{\partial x} dx \right) dz dy + \left(F_y + \frac{\partial F_y}{\partial x} dy \right) dz dx + \left(F_z + \frac{\partial F_z}{\partial x} dz \right) dx dy \quad (5.22)$$

On the other hand, the rate of mass change in the representative elementary volume is:

$$n \frac{\partial C}{\partial t} dx dy dz \quad (5.23)$$

This rate of mass change in the representative elementary volume must be equal to the difference in the mass of the solute entering and the mass leaving. Therefore,

$$\frac{\partial F_x}{\partial x} + \frac{\partial F_y}{\partial y} + \frac{\partial F_z}{\partial z} = -n \frac{\partial C}{\partial t} \quad (5.24)$$

Values of F_x , F_y , and F_z can be found and substituted using Equation 5.18. The resulting equation will be the 3D equation of mass transport for a conservative contaminant.

The general equation for 1D transportation in a homogeneous, isotropic porous media is:

$$D_L \frac{\partial^2 C}{\partial x^2} - v_x \frac{\partial C}{\partial x} = \frac{\partial C}{\partial t} \quad (5.25)$$

The solution of this equation depends on boundary and initial conditions.

Contamination problems in aquifers can be because of the instantaneous injection or continuous release of contaminants. In both cases, the concentration of the contaminant decreases with time and distance (Figure 5.10).

If there are stepwise changes in concentration of the contaminant (instantaneous injection), Equation 5.25 is solved as (Ogata and Banks, 1961):

$$C = \frac{C_0}{2} \left[erfc \left(\frac{L - v_x t}{2\sqrt{D_L t}} \right) + \exp \left(\frac{v_x L}{D_L} \right) erfc \left(\frac{L + v_x t}{2\sqrt{D_L t}} \right) \right] \quad (5.26)$$

In Table 5.11, values of the error function, $erf(\psi)$, and the complementary error function, $erfc(\psi)$, for different numbers are presented.

$$erf(\psi) = \frac{2}{\pi} \int_0^{\beta} e^{-\varepsilon^2} d\varepsilon \quad (5.27)$$

$$erf(-\psi) = -erf(\psi) \quad (5.28)$$

$$erfc(\psi) = 1 - erf(\psi) \quad (5.29)$$

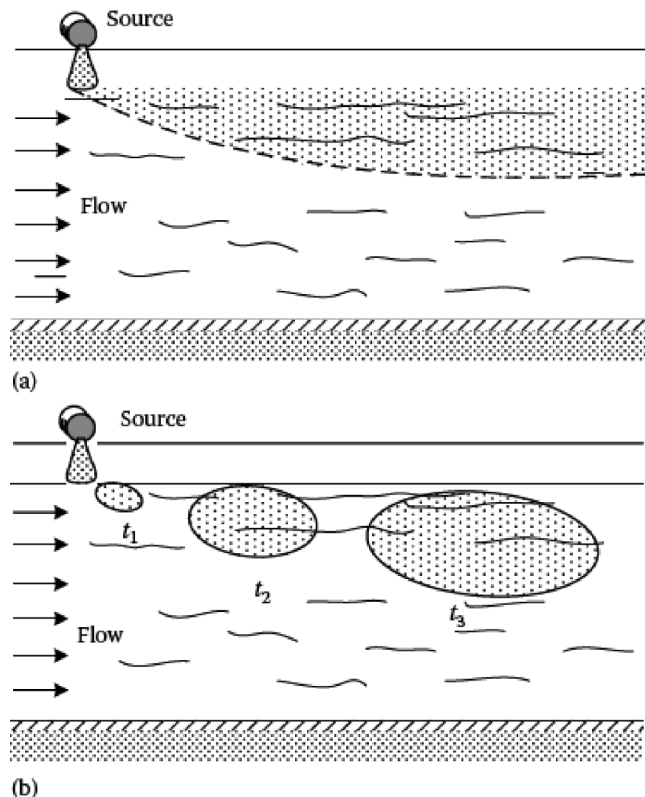


FIGURE 5.10 (a) Continuous release (leaching). (b) Instantaneous injection (spill) of contaminant from a point source into an aquifer with isotropic sand in a 2D uniform field.

TABLE 5.11
Values of Complementary Error Function for
Different Numbers

| ψ | $erf(\psi)$ | $erfc(\psi)$ |
|--------|-------------|--------------|
| 0.00 | 0.00 | 1.00 |
| 0.05 | 0.056372 | 0.943628 |
| 0.10 | 0.112463 | 0.887537 |
| 0.15 | 0.167996 | 0.832004 |
| 0.20 | 0.222703 | 0.777297 |
| 0.25 | 0.276326 | 0.723674 |
| 0.30 | 0.328627 | 0.671373 |
| 0.35 | 0.379382 | 0.620618 |
| 0.40 | 0.428392 | 0.571608 |
| 0.45 | 0.475482 | 0.524518 |
| 0.50 | 0.5205 | 0.4795 |

(Continued)

TABLE 5.11 (Continued)
Values of Complementary Error Function for
Different Numbers

| ψ | $erf(\psi)$ | $erfc(\psi)$ |
|--------|-------------|--------------|
| 0.55 | 0.563323 | 0.436677 |
| 0.60 | 0.603856 | 0.396144 |
| 0.65 | 0.642029 | 0.357971 |
| 0.70 | 0.677801 | 0.322199 |
| 0.75 | 0.711156 | 0.288844 |
| 0.80 | 0.742101 | 0.257899 |
| 0.85 | 0.770668 | 0.229332 |
| 0.90 | 0.796908 | 0.203092 |
| 0.95 | 0.820891 | 0.179109 |
| 1.00 | 0.842701 | 0.157299 |
| 1.10 | 0.880205 | 0.119795 |
| 1.20 | 0.910314 | 0.089686 |
| 1.30 | 0.934008 | 0.065992 |
| 1.40 | 0.952285 | 0.047715 |
| 1.50 | 0.966105 | 0.033895 |
| 1.60 | 0.976348 | 0.023652 |
| 1.70 | 0.98379 | 0.01621 |
| 1.80 | 0.989091 | 0.010909 |
| 1.90 | 0.99279 | 0.00721 |
| 2.00 | 0.995322 | 0.004678 |
| 2.10 | 0.997021 | 0.002979 |
| 2.20 | 0.998137 | 0.001863 |
| 2.30 | 0.998857 | 0.001143 |
| 2.40 | 0.999311 | 0.000689 |
| 2.50 | 0.999593 | 0.000407 |
| 2.60 | 0.999764 | 0.000236 |
| 2.70 | 0.999866 | 0.000134 |
| 2.80 | 0.999925 | 0.000075 |
| 2.90 | 0.999959 | 0.000041 |
| 3.00 | 0.999978 | 0.000022 |

If there is a continuous change in concentration of the contaminant (continuous release), the equation is solved as (Sauty, 1978):

$$C = \frac{C_0}{2} \left[erfc \left(\frac{L - v_x t}{2\sqrt{D_L t}} \right) - \exp \left(\frac{v_x L}{D_L} \right) erfc \left(\frac{L + v_x t}{2\sqrt{D_L t}} \right) \right] \quad (5.30)$$

As can be seen in Equations 5.26 and 5.30, the only difference is that the second term is subtracted in the case of continuous injection rather than being added if the contaminant is applied to the field at once. In continuous injection, concentration at the

source point continuously increases to reach its maximum level, while in instantaneous injection, it has its maximum level at the beginning. Therefore, in Equation 5.26 there is a positive sign between error function terms and in Equation 5.30 there is a negative sign.

When the distance or time is large, the second term on the right-hand side of Equations 5.26 and 5.30 can be neglected. Therefore,

$$C = \frac{C_0}{2} \left[\operatorname{erfc} \left(\frac{L - v_x t}{2\sqrt{D_L t}} \right) \right] \quad (5.31)$$

Example 5.5

Nitrobenzene is being released from a point source to an aquifer. The hydraulic conductivity of this aquifer is 4.5×10^{-5} m/s, and its porosity is 0.35. The hydraulic gradient in this aquifer is 0.0015 m/m. Assuming that the concentration of nitrobenzene is 670 mg/L at the source, compute the concentration after 2 years at 50 m away from the source. The effective diffusion coefficient for nitrobenzene is assumed to be equal to 1.12×10^{-8} m²/s.

SOLUTION

To calculate the value of the longitudinal dispersion coefficient, first, the velocity of groundwater and the apparent longitudinal dynamic dispersivity must be computed. Therefore,

$$V_x = \frac{Ki}{n} = \frac{4.5 \times 10^{-5} \text{ m/s} \times 0.0015}{0.35} = 1.9 \times 10^{-7} \text{ m/s}$$

$$\alpha_L = 0.83 (\log L)^{2.414} = 0.83 (\log 50 \text{ m})^{2.414} = 2.98$$

D_L is calculated as:

$$D_L = \alpha_L \times v_x + D^* = (2.98 \text{ m} \times 1.9 \times 10^{-7} \text{ m/s}) + 1.12 \times 10^{-8} \text{ m}^2/\text{s}$$

$$= 5.77 \times 10^{-7} \text{ m}^2/\text{s}$$

$$t = 2 \text{ years} \times 86,400 \text{ s/day} \times 365 \text{ days/year} = 6.3 \times 10^7 \text{ s}$$

Now, the concentration of nitrobenzene after 2 years at 50 m away from the source is calculated as:

$$C = \frac{C_0}{2} \left[\operatorname{erfc} \left(\frac{L - v_x t}{2\sqrt{D_L t}} \right) + \exp \left(\frac{v_x L}{D_L} \right) \operatorname{erfc} \left(\frac{L + v_x t}{2\sqrt{D_L t}} \right) \right]$$

$$= \frac{670 \text{ mg/L}}{2} \left\{ \operatorname{erfc} \left(\frac{50 - (1.9 \times 10^{-7} \text{ m/s} \times 6.3 \times 10^7 \text{ s})}{2\sqrt{5.77 \times 10^{-7} \text{ m}^2/\text{s} \times 6.3 \times 10^7 \text{ s}}} \right) \right\}$$

$$\begin{aligned}
 & + \exp\left(\frac{1.9 \times 10^{-7} \text{ m/s} \times 50 \text{ m}}{5.77 \times 10^{-7} \text{ m}^2/\text{s}}\right) \operatorname{erfc}\left(\frac{50 \text{ m} + (1.9 \times 10^{-7} \text{ m/s} \times 6.3 \times 10^7 \text{ s})}{2\sqrt{5.77 \times 10^{-7} \text{ m}^2/\text{s} \times 6.3 \times 10^7 \text{ s}}}\right) \Big\} \\
 C &= 335 \text{ mg/L} \left[\operatorname{erfc}\left(\frac{50 \text{ m} - 11.97 \text{ m}}{12.06 \text{ m}}\right) + \exp(16.46) \operatorname{erfc}\left(\frac{50 \text{ m} + 11.97 \text{ m}}{12.06 \text{ m}}\right) \right] \\
 &= 335 \text{ mg/L} [\operatorname{erfc}(3.15) + \exp(16.46) \times \operatorname{erfc}(5.14)] \\
 &= 335 \text{ mg/L} \times 1.35 \times 10^{-5} \\
 &= 4.5 \times 10^{-3} \text{ mg/L} = 4.5 \text{ µg/L}
 \end{aligned}$$

Example 5.6

An underground tank leaches benzene continuously into an aquifer. The hydraulic conductivity of the aquifer is 1.90 m/day, the effective porosity is 0.15, and the hydraulic gradient is 0.06 m/m. Assuming that the coefficient of the hydraulic depression is 0.55 m²/s, find the time it takes for the contaminant concentration to reach 10% of the initial concentration at $L = 600$ m in a 1D movement. Neglect any other degradation processes.

SOLUTION

Using Darcy's Law, the seepage velocity V_x is first calculated:

$$v_x = \frac{Ki}{n} = \frac{1.9 \times 0.06}{0.15} = 0.76 \text{ m/day}$$

$$\frac{C}{C_0} = \frac{1}{2} \operatorname{erfc}\left(\frac{L - v_x t}{2\sqrt{D_l t}}\right)$$

$$0.1 = \frac{1}{2} \operatorname{erfc}\left(\frac{600 - 0.76t}{2\sqrt{0.55t}}\right)$$

By trial and error or using solver in Microsoft Excel:

$$t = 741 \text{ days}$$

Therefore, it takes more than 2 years for the contaminant to reach 10% of its initial concentration.

Example 5.7

An unconfined aquifer has the hydraulic conductivity of 1.5×10^{-4} m/s and porosity of 0.35. If a dissolved contaminant with the initial contamination of 470 mg/L reaches this aquifer, (a) how far could this contaminant move in 1 year, and what will be the concentration of the contaminant at that distance? (b) How long would

it take the contamination to reach 15 percent of its initial concentration at this distance? Assume that the hydraulic gradient in this aquifer is 0.05 and effective diffusion coefficient diffusion of the contaminant is $2.34 \times 10^{-8} \text{ m}^2/\text{s}$.

SOLUTION

$$\text{a. } V_x = \frac{K \cdot i}{n} = \frac{1.5 \times 10^{-4} \times 0.05}{0.35} = 2.14 \times 10^{-5} \text{ m/s}$$

$$L = 2.14 \times 10^{-5} \times 86400 \times 365 = 675.7 \text{ (m)}$$

$$\alpha_L = 0.83(\log L)^{2.414} = 0.83 \times (\log 675.7)^{2.414} = 10.22$$

$$D_L = \alpha_L \times V_x + D^* = 10.22 \times 2.14 \times 10^{-5} + 2.34 \times 10^{-8} = 2.19 \times 10^{-4} \left(\text{m}^2/\text{s} \right)$$

$$C = C_0 / 2 \left[\operatorname{erfc} \left(\frac{L - V_x t}{2\sqrt{D_L t}} \right) - \exp \left(\frac{V_x L}{D_L} \right) \operatorname{erfc} \left(\frac{L + V_x t}{2\sqrt{D_L t}} \right) \right]$$

b. The concentration of the contaminant after a year at 675.7 m away from the source is calculated as follows:

$$\alpha_L = 0.83(\log L)^{2.414} = 0.83 \times (\log 675.7)^{2.414} = 10.22$$

$$D_L = \alpha_L \times V_x + D^* = 10.22 \times 2.14 \times 10^{-5} + 2.34 \times 10^{-8} = 2.19 \times 10^{-4} \left(\text{m}^2/\text{s} \right)$$

$$\begin{aligned} C &= C_0 / 2 \left[\operatorname{erfc} \left(\frac{L - V_x t}{2\sqrt{D_L t}} \right) - \exp \left(\frac{V_x L}{D_L} \right) \operatorname{erfc} \left(\frac{L + V_x t}{2\sqrt{D_L t}} \right) \right] \\ &= \frac{470}{2} \left[\operatorname{erfc} \left(\frac{675.7 - 2.14 \times 10^{-5} \times 365 \times 86400}{2\sqrt{2.19 \times 10^{-4} \times 365 \times 86400}} \right) - \exp \left(\frac{2.14 \times 10^{-5} \times 675.7}{2.19 \times 10^{-4}} \right) \right. \\ &\quad \left. \operatorname{erfc} \left(\frac{675.7 + 2.14 \times 10^{-5} \times 365 \times 86400}{2\sqrt{2.19 \times 10^{-4} \times 365 \times 86400}} \right) \right] \\ &= 203 \frac{\text{mg}}{\text{lit}} \end{aligned}$$

c. Since the distance is large, we can use the simplified equation (Equation 5.30) as follows:

$$C = \frac{C_0}{2} \operatorname{erfc} \left(\frac{L - V_x t}{2\sqrt{D_L t}} \right)$$

$$0.15C_0 = \frac{C_0}{2} \operatorname{erfc} \left(\frac{675.7 - 2.14 \times 10^{-5} \times t \times 365 \times 24 \times 3600}{2\sqrt{2.19 \times 10^{-4} \times t \times 365 \times 24 \times 3600}} \right) \rightarrow$$

$$0.3 = erfc \left(\frac{675.7 - 2.14 \times 10^{-5} \times t \times 365 \times 24 \times 3600}{2\sqrt{2.19 \times 10^{-4} \times t \times 365 \times 24 \times 3600}} \right) \rightarrow$$

$$0.73 = \frac{675.7 - 2.14 \times 10^{-5} \times t \times 365 \times 24 \times 3600}{2\sqrt{2.19 \times 10^{-4} \times t \times 365 \times 24 \times 3600}} \rightarrow \text{trial and error } t \geq 0.84 \text{ year} \approx 10 \text{th month}$$

The variations of concentration over time and distance from the contaminant are illustrated in [Figures 5.11](#) and [5.12](#), respectively.

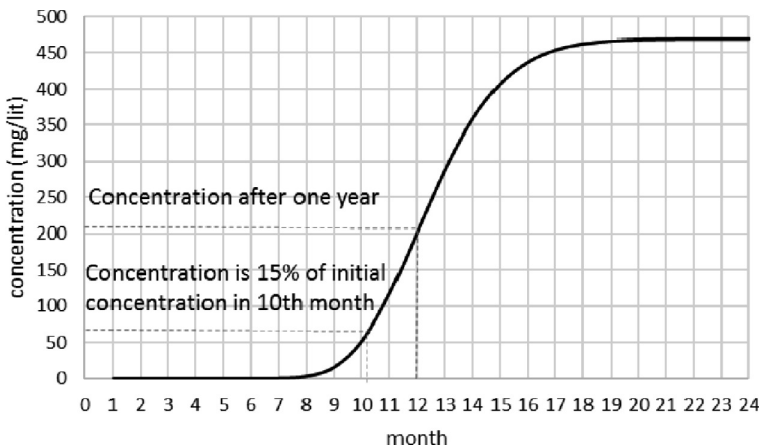


FIGURE 5.11 Variation of concentration at the distance of 675.7 m from pollutant over time.

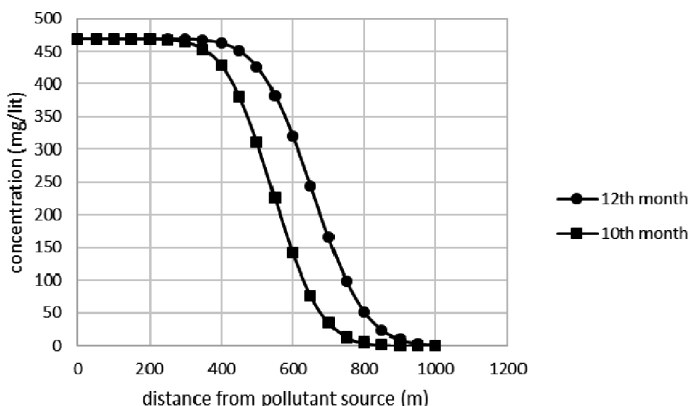


FIGURE 5.12 Variation of concentration over distance from pollutant after 10th and 12th months.

5.7.6 SOLUTE TRANSPORT EQUATION

Within a control volume in an aquifer, there are several processes that act as sources and sinks for a solute. These processes include sorption/desorption, chemical or biological reactions, and decay. In the sorption/desorption process, the net rate of reaction, r , can be expressed as:

$$r = \theta \frac{\partial C}{\partial t} = -\rho_b \frac{\partial \bar{C}}{\partial t} \quad (5.32)$$

where:

θ is the volumetric water content of the porous media

ρ_b is the bulk density of the porous media

C is the concentration of the dissolved contaminants

\bar{C} is the concentration of the sorbed contaminants.

\bar{C} can be calculated as the mass of solute divided by the volume of groundwater, and C can be obtained by dividing the mass of solute by the mass of dry porous media. If the reaction is in equilibrium, the concentration of the sorbed contaminants is:

$$\bar{C} = K_d C \quad (5.33)$$

where K_d is the equilibrium distribution coefficient (L^3/M). Combining Equations 5.32 and 5.33:

$$\left(\frac{\partial(\theta C)}{\partial t} \right)_{\text{sorption}} = -\rho_b K_d \frac{\partial C}{\partial t} \quad (5.34)$$

Equation 5.34 gives the net rate of solute production based on a sorption/desorption reaction between a solute and the porous media within a control volume.

In case biological degradation or decay is imposed on the solute, the net rate of solute production is expressed as:

$$\left(\frac{\partial(\theta C)}{\partial t} \right)_{\text{decay}} = -\lambda(\theta C + \rho_b K_d C) \quad (5.35)$$

where λ is the decay rate constant for the solute.

On the other hand, the net rate of solute inflow can be expressed as:

$$\text{Net rate of solute inflow} = -\frac{\partial}{\partial x}(v_x C) + D_x \frac{\partial^2}{\partial x^2}(\theta C) + D_y \frac{\partial^2}{\partial y^2}(\theta C) + D_z \frac{\partial^2}{\partial z^2}(\theta C) \quad (5.36)$$

Based on the law of conservation of mass for solute transport, the rate of change of solute mass within a control volume is equal to the summation of the net rate of solute inflow and the net rate of solute production. Substituting Equations 5.34 through 5.36 into the law of conservation of mass for solute transport, the solute transport equation will be obtained as:

$$\frac{\partial(\theta C)}{\partial t} = D_x \frac{\partial^2}{\partial x^2}(\theta C) + D_y \frac{\partial^2}{\partial y^2}(\theta C) + D_z \frac{\partial^2}{\partial z^2}(\theta C) - \frac{\partial}{\partial x}(v_x C) - \frac{\partial}{\partial t}(\rho_b K_d C) - \lambda(\theta C + \rho_b K_d C) \quad (5.37)$$

In this equation, the rate of change of solute transport in the control volume has been shown as $\partial(\theta C)/\partial t$. The solution of this equation will be explained in [Chapter 6](#).

5.7.7 CAPTURE-ZONE CURVES

Installing extraction wells has become the most common way for beginning the cleanup of contaminated groundwater. In this process, the contaminated groundwater is pumped out through the extraction well. Then, it is cleaned in an aboveground treatment facility and may be returned to the aquifer. The process is referred to as *pump-and-treat* technology and will be discussed in [Chapter 9](#).

In [Figure 5.13](#), an extraction well is located in a region with a uniform and steady regional groundwater flow. This well is parallel to and in the reverse direction of the x -axis. As demonstrated in this figure, the natural streamlines are bent toward the well as water is extracted through the well. The outer envelope of the streamlines

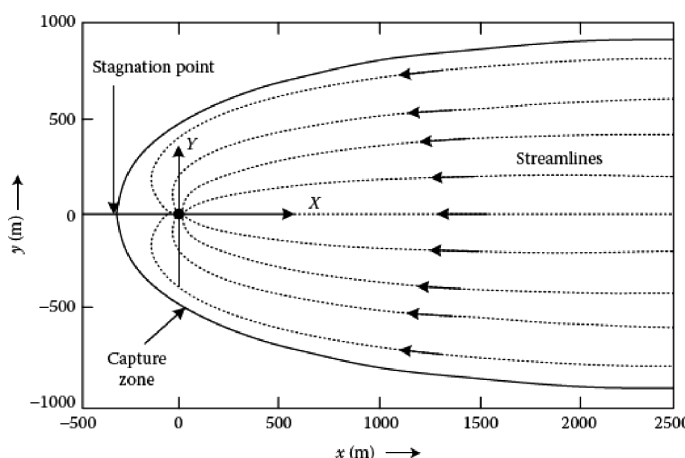


FIGURE 5.13 Single extraction well located at $x = 0$, $y = 0$, in an aquifer with a regional flow along the x -axis. The capture zone is the region in which all flow lines converge on the extraction well. Drawn for $(Q/Bv) = 2000$. (From Javandel, I. and Tsang, C.F., *Ground Water*, 24(5), 616, 1986.)

that converge on the well is called the *capture-zone* curve. Only that portion of groundwater, which is inside the capture zone, is extracted. There is no extraction of groundwater outside the capture zone. Although the flow lines outside of the capture zone curve toward the well, there is no extraction though those flow lines. The reason is that the regional flow associated with the natural hydraulic gradient is so strong that it carries groundwater past the well (Masters and Ela, 2008).

Javandel and Tsang (1986) assumed an ideal aquifer that is homogeneous, isotropic, uniform in cross section, and infinite in width and developed the use of capture-zone type curves. These curves can be used for the design of extraction well fields for aquifer cleanup. These curves are appropriate for confined or unconfined aquifers with an insignificant drawdown relative to the total thickness of the aquifer. In their analysis, they considered that the extraction wells extend downward through the entire thickness of the aquifer, and they assumed that the wells are screened to extract uniformly from every level. Although these assumptions are so strict and never happen in actual conditions, acceptable insight into the main factors for even more complex models can be obtained by this analysis.

Consider the extraction well located at the origin of the coordinate system shown in [Figure 5.13](#). The following relationship between the x and y coordinates of the envelope surrounding the capture zone was derived by Javandel and Tsang (1986):

$$y = \pm \frac{Q}{2Bv} - \frac{Q}{2\pi Bv} \tan^{-1} \frac{y}{x} \quad (5.38)$$

where:

B is the aquifer thickness (m)

v is the Darcy velocity (conductivity \times gradient (m/day))

Q is the pumping rate from the well (m^3/day).

Equation 5.38 is then rewritten to consider an angle ϕ (in radians), which is drawn from the origin of the coordinate system to the coordinate of interest on the capture-zone curve ([Figure 5.14](#)):

$$\tan \phi = \frac{y}{x} \quad (5.39)$$

For $0 \leq \phi \leq 2\pi$,

$$y = \frac{Q}{2Bv} \left(1 - \frac{\phi}{\pi} \right) \quad (5.40)$$

In Equation 5.40, if x approaches infinity, $\phi = 0$ and $y = Q/(2Bv)$. Therefore, the maximum total width of the capture zone will be $2[Q/(2Bv)] = Q/Bv$. If $\phi = \pi/2$, then $x = 0$, and y will be equal to $Q/(4Bv)$. Thus, the width of the capture zone along the y -axis is $Q/(2Bv)$, which is half of its width at an infinite distance. [Figure 5.14](#) illustrates these relationships.

Pumping rate, Q , has a direct impact on the width of the capture zone, while the product of the Darcy flow velocity, v , and the aquifer thickness, B , inversely affect the

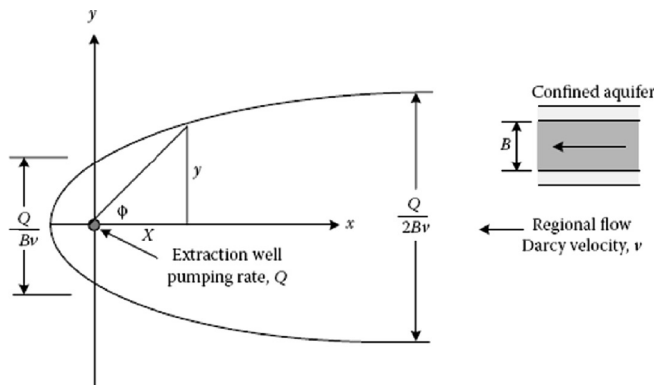


FIGURE 5.14 Capture-zone curve for a single extraction well located at the origin in an aquifer with regional flow velocity v , thickness B , and pumping rate Q . (From Masters, G.M. and Ela, W.P., *Introduction to Environmental Engineering and Science*, Prentice Hall, Simon and Schuster, Englewood Cliffs, NJ, 576, 2008.)

width of this zone. Therefore, to capture the same area at higher regional flow velocities, higher pumping rates are required. However, there are some limitations for maximum pumping rates that restrict the size of the capture zone (Masters and Ela, 2008).

In capture-zone type curve analysis, the curve corresponding to the maximum acceptable pumping rate is first drawn. Then, the plume is superimposed onto the capture-zone curve. By evaluating this superposition, it can be determined whether or not the well of interest is sufficient to extract the entire plume. It can also be used to specify the location of the well. It should be noted that both the capture-zone type curve and the plume need to be drawn to the same scale. [Figure 5.15](#) illustrates this analysis (Masters and Ela, 2008).

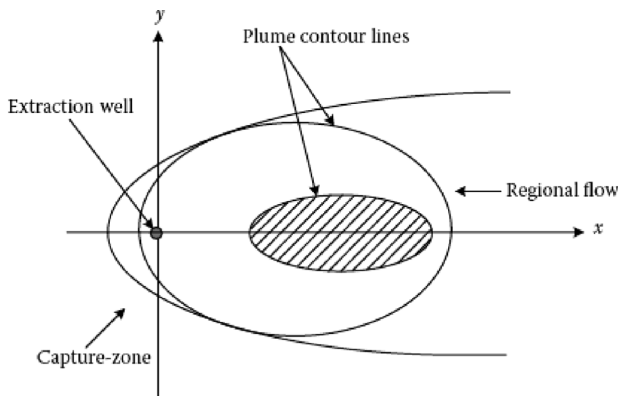


FIGURE 5.15 Superimposing the plume onto a capture-zone type curve for a single extraction well. (From Masters, G.M. and Ela, W. P., *Introduction to Environmental Engineering and Science*, Prentice Hall, Simon and Schuster, Englewood Cliffs, NJ, 576, 2008.)

Example 5.8

A confined aquifer has been contaminated, and a rectangular (for simplicity) plume has been created in this aquifer. To clean up this aquifer, it is decided to pump out the groundwater and treat it at the aboveground facilities. Determine the location of a single well that can totally extract the plume. The characteristics of the aquifer are as follows:

- Thickness of the aquifer = 25 m
- Hydraulic conductivity = 1.5×10^{-3} m/s
- Regional hydraulic gradient = 0.001
- Maximum pumping rate = 0.003 m³/s
- Width of the plume = 60 m

SOLUTION

First, the regional Darcy velocity is calculated as:

$$V = K \frac{dh}{dx} = 1.5 \times 10^{-3} \text{ m/s} \times 0.001 = 1.5 \times 10^{-6} \text{ m/s}$$

The width of the capture zone along the y-axis is:

$$\frac{Q}{2Bv} = \frac{0.003 \text{ m}^3/\text{s}}{2 \times 25 \text{ m} \times 1.5 \times 10^{-6} \text{ m/s}} = 40 \text{ m}$$

As discussed earlier in this section, at an infinite distance up-gradient, this width becomes twice:

$$\frac{Q}{Bv} = 80 \text{ m}$$

Therefore, if the well is located some distance downgrading from the front edge, the capture zone encompasses the 60 m wide plume (Figure 5.16). Considering $y = 30$ m,

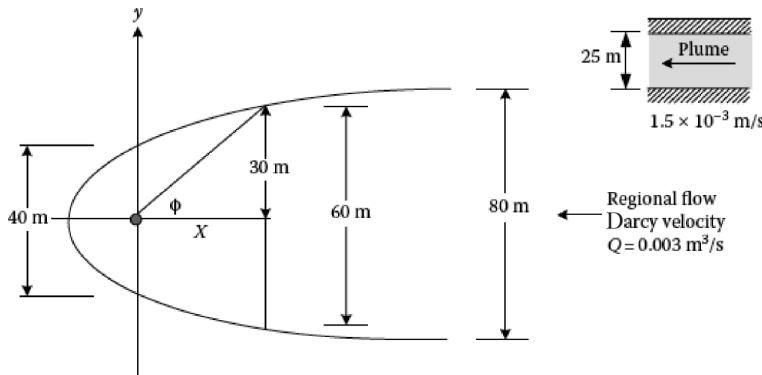


FIGURE 5.16 Problem with extraction well in Example 5.8.

$$y = \frac{Q}{2Bv} \left(1 - \frac{\phi}{\pi} \right) = 30 = 40 \left(1 - \frac{\phi}{\pi} \right)$$

From Figure 5.16,

$$x = \frac{y}{\tan \phi} = \frac{30}{\tan(0.25\pi)} = 30 \text{ m}$$

Therefore, the extraction well should be placed in line with the oncoming plume and 30 m ahead of it.

The main issue in Example 5.8 is that the extraction well will be located far down-gradient from the plume, which results in the extraction of a large volume of clean groundwater before the contaminated plume reaches the well. This situation imposes significant pumping costs. To solve this situation, more extraction wells must be installed closer to the head of the plume.

Capture-zone type curves for a series of n optimally placed wells were also derived by Javandel and Tsang (1986). They assumed each well is pumping at the same rate, Q , and the wells are lined up along the y -axis. In this analysis, the maximum spacing between wells is optimized while the wells prevent any flow from passing between them. Therefore, the optimized distance between two wells is $Q/(\pi Bv)$. Locating wells with this distance apart from each other provides the possibility of capturing a plume as wide as $Q/(Bv)$ along the y -axis and as wide as $2Q/(Bv)$ along the x -axis, i.e., far up-gradient from the wells (Figure 5.17a). Figure 5.17b also depicts correspondent parameters for the case of three optimally spaced wells.

A general form for the positive half of the capture-zone type curve for n optimally spaced wells is:

$$y = \frac{Q}{2Bv} \left(n - \frac{1}{\pi} \sum_{i=1}^n \phi_i \right) \quad (5.41)$$

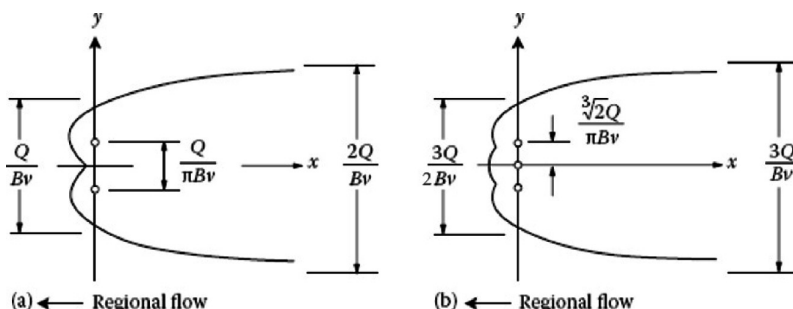


FIGURE 5.17 Capture-zone type curves for optimally spaced wells along the y -axis, each pumping at the rate Q : (a) two wells and (b) three wells. (From Masters, G.M. and Ela, W.P., *Introduction to Environmental Engineering and Science*, Prentice Hall, Simon and Schuster, Englewood Cliffs, NJ, 576, 2008.)

where ϕ_i is the angle between a horizontal line through the i th well and a spot on the capture-zone curve. It is assumed in this equation that the wells have been arranged symmetrically along the y -axis.

Example 5.9

Recalculate Example 5.8 for the case of two wells. What minimum pumping rate, Q , is required to capture the plume completely? Assume the two optimally spaced wells are aligned along the leading edge of the plume. What is the optimum space between the wells?

Imagine the length of the plume is 750 m, how long would it take to pump out all of the contaminated groundwater? The aquifer porosity is 0.45.

SOLUTION

The plume width along the y -axis (also the leading edge of the plume) is 60 m, so from [Figure 5.18](#),

$$\frac{Q}{Bv} = \frac{Q}{25 \text{ m} \times 1.5 \times 10^{-6} \text{ m/s}} = 60 \text{ m}$$

$$Q = 0.00225 \text{ m}^3/\text{s}$$

Therefore, each well has the pumping rate of $0.00225 \text{ m}^3/\text{s}$. From [Figure 5.18](#), optimal spacing between the wells = $\frac{Q}{\pi Bv}$

$$= \frac{0.00225 \text{ m}^3/\text{s}}{\pi \times 25 \times 1.5 \times 10^{-6} \text{ m/s}} = 19.1 \text{ m}$$

The porosity times the plume volume gives the volume of contaminated water in the plume:

$$V = 0.45 \times 60 \times 25 \times 750 \text{ m} = 506,250 \text{ m}^3$$

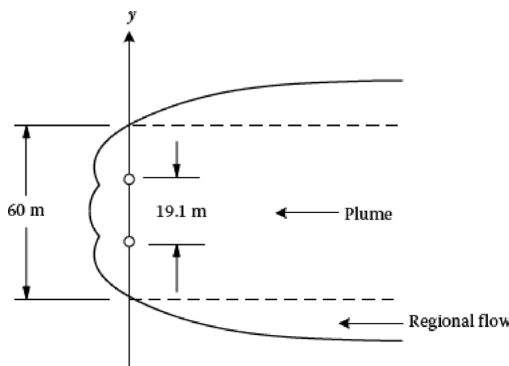


FIGURE 5.18 Problem with two extraction wells in Example 5.9.

The total pumping rate is $2 \times 0.00225 \text{ m}^3/\text{s} = 0.0045 \text{ m}^3/\text{s}$. Therefore, the time to pump out the total contaminated groundwater is:

$$t = \frac{506,250 \text{ m}^3}{0.0045 \text{ m}^3/\text{s} \times 3,600 \text{ s/h} \times 24 \text{ h/day} \times 365 \text{ day/year}} = 3.57 \text{ year}$$

However, it should be noted that it would take much longer to pump out the whole plume due to retardation (which will be discussed in [Chapter 9](#)), and there will also be some uncontaminated groundwater removed with the plume.

Details about designing more complicated well fields can be found in Gupta (1989) and Bedient et al. (1994).

5.8 MODELING CONTAMINANT RELEASE

Analytical solutions of the advection–dispersion equation can be used for many applications, such as assessing the potential impacts of releases of contaminants to groundwater, estimating the potential exposure concentrations at different locations, and providing tools for parameter estimation. Analytical models can also be used for establishing the soil cleanup level. In this regard, critical exposure locations are identified, and exposure concentrations are determined at these locations. Then, the models can be used “backwards” to calculate the concentration at the source that would result in this critical exposure. This procedure can be performed to establish the minimum cleanup standard levels.

5.8.1 MODELING INSTANTANEOUS RELEASE OF CONTAMINANTS

A few models of chemical spills are briefly discussed in this section. Generally, in these models, the initial distribution of chemical concentrations is given, and the models determine how concentration changes through time and space.

To simplify calculations, flow is usually considered 1D, despite the fact that dispersion transport can occur in 3Ds. Depending on the number of dimensions considered and the different initial distributions of contaminants, the models may vary.

5.8.1.1 Fourier Analysis in Solute Transport

The problem of transport of a solute in a uniform flow field in the x -direction, with mixing in all three directions for an arbitrary initial distribution of contaminants can be expressed as:

$$\frac{\partial c}{\partial t} + v' \frac{\partial c}{\partial x} + \lambda c = D'_{xx} \frac{\partial^2 c}{\partial x^2} + D'_{yy} \frac{\partial^2 c}{\partial y^2} + D'_{zz} \frac{\partial^2 c}{\partial z^2} \quad (5.42)$$

where

$v' = v/R$ is the retarded velocity

$D'_{xx} = D_{xx}/R$ is the retarded x -dispersion coefficient.

Fourier methods can be used to solve this equation. Based on these methods, the solution to Equation 5.42 for a 1D case is:

$$c(x, y) = \int_{-\infty}^{\infty} c(\xi, 0) G(x, t|\xi, 0) d\xi e^{-\lambda t} \quad (5.43)$$

where

$$G(x, t|\xi, 0) \equiv \frac{1}{\sqrt{4\pi D't}} \exp\left(-\frac{(x - \xi - v't)^2}{4D't}\right) \quad (5.44)$$

The function from Equation 5.44 plays the part of an impulse response function for the partial differential Equation 5.41. It is called Green's function. This function gives the contribution to the solution at point x and time t due to the initial unit mass at point $x = \xi$. The contaminant decays with the rate λ . The solution with decay is equal to the solution without decay times the exponential decay term.

5.8.1.2 Point Spill Model

Imagine a contaminant with concentration c_0 is being released with the volume V_0 at point $x = 0$. If the time period of release is so small that we can consider the release instantaneous, the mass, M , released from the source is equal to $c_0 V_0$. Then, the concentration of the contaminant at point x and time t is:

$$c(\tilde{x}, t) = \frac{V_0 c_0 \exp\left(-\frac{(x - v't)^2}{4D'_{xx}t} - \frac{y^2}{4D'_{yy}t} - \frac{z^2}{4D'_{zz}t}\right)}{nR\sqrt{64x^3 D'_{xx} D'_{yy} D'_{zz} t^3}} e^{-\lambda t} \quad (5.45)$$

where R is the retardation factor. Also, the maximum concentration at any time is:

$$c_{\max}(t) = \frac{V_0 c_0}{nR\sqrt{64x^3 D'_{xx} D'_{yy} D'_{zz} t^3}} e^{-\lambda t}; \quad \tilde{x} = (x, y, z) = (v't, 0, 0) \quad (5.46)$$

5.8.1.3 Vertically Mixed Spill Model

If the release is mixed over the thickness of the aquifer; i.e., if the release occurs through a fully penetrating and screened well, the transport equation is the same as Equation 5.44, except that there are no vertical gradients and the term involving z does not appear:

$$c(\tilde{x}, t) = \frac{V_0 c_0 \exp\left(-\frac{(x - v't)^2}{4D'_{xx}t} - \frac{y^2}{4D'_{yy}t}\right)}{4\pi n b t \sqrt{D_{xx} D_{yy}}} e^{-\lambda t} \quad (5.47)$$

where:

- b is the aquifer thickness and the retarded dispersion coefficient
- R is no longer being used.

5.8.1.4 Vertical Mixing Region

If the point release of a contaminant is at the top of the aquifer, near the source, the spreading is in 3Ds. In this case, Equation 5.45 is not applicable anymore and the correct solution near the source is twice that of Equation 5.45. This is because it has half of the mass spreading above the water table. The solution is then:

$$c(\tilde{x}, t) = \frac{V_0 c_0 \exp\left(-\frac{(x - v't)^2}{4D'_{xx}t} - \frac{y^2}{4D'_{yy}t} - \frac{z^2}{4D'_{zz}t}\right)}{4nR\sqrt{\pi^3 D'_{xx} D'_{yy} D'_{zz} t^3}} e^{-\lambda t} \quad (5.48)$$

Far from the source, the contaminant is spread over the thickness of the aquifer and is only spread in the two lateral directions. That is because the base of the aquifer prevents further vertical migration (Figure 5.19). Therefore, Equation 5.48 cannot be applied anymore, and Equation 5.46 is used. Now, it must be determined at what horizontal distance the 3D solution ceased to be valid.

Equation 5.48 is appropriate both for the near-field and far-field solutions. However, it is inconvenient to use the infinite system of images. Therefore, it must be identified when the simple 3D and 2D solutions can be applied in place of Equation 5.48.

$$c(x, y, z, t) = \frac{V_0 c_0 \exp\left(-\frac{(x - v't)^2}{4D'_{xx}t} - \frac{y^2}{4D'_{yy}t}\right)}{4nR\sqrt{\pi^3 D'_{xx} D'_{yy} D'_{zz} t^3}} e^{-\lambda t} \sum_{j=-\infty}^{\infty} \exp\left(-\frac{(z + 2jb)^2}{4D'_{zz}t}\right) \quad (5.49)$$

Charbeneau (2000) shows that the 2D solution can be used when:

$$t > \frac{Rb^2}{D_{zz}} \quad (5.50)$$

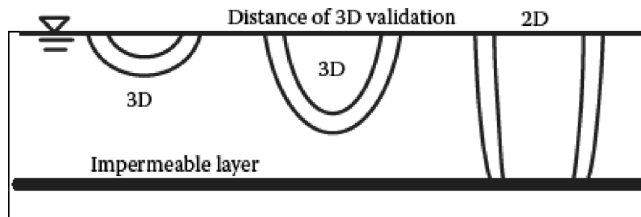


FIGURE 5.19 Schematic spreading of a point release.

By this time, the center of the spill would have moved a distance:

$$x = \frac{vt}{R} > \frac{vb^2}{D_{zz}} \quad (5.51)$$

If mechanical dispersion dominates the mixing process, the 2D solution is valid after:

$$x > \frac{b^2}{a_v} \quad (5.52)$$

where a_v is the vertical dispersivity. Likewise, the 3D solution is valid up to the distance:

$$x < \frac{0.2vb^2}{D_{zz}} \quad (5.53)$$

Therefore, the general solution of Equation 5.48 is used when:

$$\frac{0.2vb^2}{D_{zz}} < x < \frac{vb^2}{D_{zz}} \quad (5.54)$$

For shorter and longer distances, the single source 3D and 2D solutions are used, respectively.

Example 5.10

An industrial facility releases its wastewater on the adjacent ground surface at the top of an aquifer. The wastewater infiltrates into the underlying soil and reaches the aquifer. If the velocity of groundwater in the aquifer is 1.5 m/day and the thickness of the aquifer is 5 m, calculate the extent to which a 3D solution of the contaminant distribution is applicable. Also, determine from what distance the 2D solution can be used. Assume that dynamic dispersivity is 6 m.

SOLUTION

$$D_{zz} = a_L v = 6 \text{ m} \times 1.5 \text{ m/day} = 9 \text{ m}^2/\text{day}$$

The 3D solution can be applied up to:

$$x < \frac{0.2vb^2}{D_{zz}} = \frac{0.2 \times 1.5 \times 5^2}{9} = 0.83 \text{ m}$$

And the 2D solution can be used from:

$$x > \frac{vb^2}{D_{zz}} = \frac{1.5 \times 5^2}{9} = 4.17 \text{ m}$$

5.8.2 MODELING CONTINUOUS RELEASE OF CONTAMINANTS

If the source release continues at a constant rate, the contaminant distribution appears as a plume that initially grows in length and width and eventually reaches a steady-state distribution. The general mathematical framework from which plume models can be developed as well as the steady-state concentration distribution near a source of releasing mass at a constant rate for a long time period are discussed in this section.

5.8.2.1 Development of Contaminant Plume Models

The simplest way to develop a contaminant plume model is to consider the plume as being derived from a continuing series of spills.

Assume that $c_s^*(x, y, z, t)$ represents the mathematical model for a chemical spill of unit mass, $M = 1$. Then, the solution for a plume that develops from a source with a time-variable mass release rate $\dot{m}(t)$ is given by:

$$c_p(x, y, z, t) = \int \dot{m}(\tau) c_s^*(x, y, z, t - \tau) d\tau \quad (5.55)$$

This equation gives the plume concentration distribution at time t . If the mass release rate is constant \dot{m} , the concentration distribution is obtained by:

$$c_p(x, y, z, t) = \dot{m} \int_0^t c_s^*(x, y, z, \tau) d\tau \quad (5.56)$$

Assume that $\chi(\xi)$ represents an indicator variable for the source region. $\chi(\xi)$ is equal to 1, $\chi(\xi) = 1$, if the point spill is within the initial source zone of the spill. Otherwise, $\chi(\xi) = 0$. Also, if the volume of the source region is represented by $V(\Omega)$, the formal solution for a contaminant plume model, when the source strength is variable through time, can be obtained by:

$$c_p(\tilde{x}, t) = \frac{1}{V(\Omega)} \int_0^t \dot{m}(\tau) \int_{\Omega} \chi(\tilde{\xi}) G(\tilde{x}, t - \tau | \tilde{\xi}, 0) d\tilde{\xi} \cdot e^{-\lambda(t-\tau)} d\tau \quad (5.57)$$

5.8.2.2 Simple Plume Model

Imagine that a constant mass release rate \dot{m} occurs at the point $(x, y) = (0, 0)$. Considering only advection and transverse dispersion, and assuming that longitudinal dispersion is negligible, the steady-state transport equation is expressed as:

$$v \frac{\partial c}{\partial x} - D_{yy} \frac{\partial^2 c}{\partial y^2} + \lambda R c = 0 \quad (5.58)$$

and the solution of this equation is:

$$c(x, y) = \frac{\dot{m}}{qb} \frac{1}{\sqrt{4\pi \frac{D_{yy}}{v} x}} \exp\left(-\frac{y^2}{4 \frac{D_{yy}}{v} x}\right) \exp\left(-\frac{\lambda Rx}{v}\right) \quad (5.59)$$

5.8.2.3 Point-Source Plume Model

If the longitudinal dispersion is also supposed to be considered in a point-source model, the transient period of development of the plume as well as the steady-state plume solution is expressed as:

$$c_p(x, y, t \rightarrow \infty) = \frac{\dot{m} \exp(vx / 2D_{xx})}{2\pi nb \sqrt{D_{xx} D_{yy}}} K_0\left(\frac{r}{B}\right) \quad (5.60)$$

where $K_0()$ is the modified Vessel function of the second kind of order zero. Also, the steady-state (maximum) concentration along the x -axis is obtained by:

$$c_p(x, y=0, t \rightarrow \infty) = \frac{\dot{m} \exp\left(\frac{vx}{2D_{xx}} \left(1 - \sqrt{1 + \frac{4\lambda RD_{xx}}{v^2}}\right)\right)}{nb \sqrt{4\pi D_{yy} vx \sqrt{1 + \frac{4\lambda RD_{xx}}{v^2}}}} \quad (5.61)$$

If $\lambda = 0$, Equations 5.59 and 5.61 become identical for the solution along the x -axis. [Figure 5.20](#) depicts the configuration for the point-source plume model.

5.8.2.4 Gaussian-Source Plume Model

The point-source plume model explained previously predicts infinite concentrations at the source, which is required to introduce a finite mass flux to the aquifer through

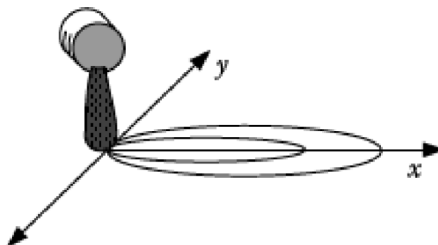


FIGURE 5.20 Configuration of the point source plume model.

a single point. If it is supposed to predict concentrations near the source as well as in the far field, then a source of finite size must be considered. The Gaussian-source plume model can be considered for this purpose.

In the Gaussian-source plume model, it is assumed that the leachate from a surface source migrates through the unsaturated zone and mixes with groundwater flowing underneath the source (Figure 5.21). Assume that the source has the length L and width W with respect to the mean flow direction, and the total penetration depth of leachate at the down-gradient end of the source is H . Both the vertical dispersion and the vertical advection of water as it moves beneath the source cause penetration. The depth of penetration of the contaminant into the aquifer beneath the source is calculated as:

$$H = H_{adv} + H_{dis} = b \left(1 - \exp \left(\frac{i_f L}{q_x b} \right) \right) + \sqrt{2a_v L} \quad (5.62)$$

where:

- i_f is the infiltration through the contaminant source
- a_v is the vertical dispersivity.

If the value of H calculated with Equation 5.61 exceeds b , $H > b$, H is considered equal to b , $H = b$.

If $H < b$, recharge forces the plume deeper into the aquifer and H remains constant. In the case $H = b$, the recharge serves to dilute the plume and acts as an equivalent decay term. In this latter case, the transport equation is:

$$\frac{\partial c}{\partial t} + v' \frac{\partial c}{\partial x} + \left(\lambda + \frac{i_r}{nRH} \right) c = D'_{xx} \frac{\partial^2 c}{\partial x^2} + D'_{yy} \frac{\partial^2 c}{\partial y^2} \quad (5.63)$$

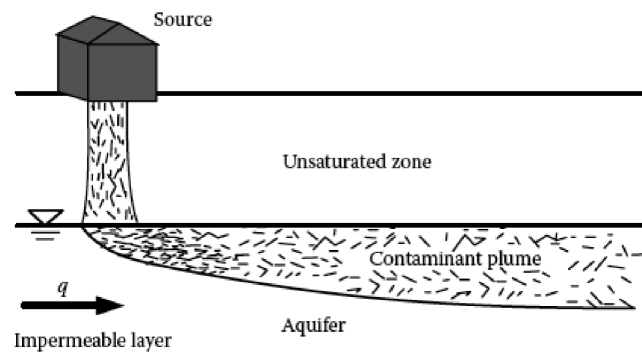


FIGURE 5.21 Set up of Gaussian source plume model.

where i_r is the diffuse recharge rate outside of the source. This equation assumes that the flow is steady and the velocity remains uniform in the x -direction. The solution for this steady-state problem can be developed using Fourier transforms. Smith and Charbeneau (1990) proposed:

$$c(x, y, t \rightarrow \infty) = \frac{c_0 \exp\left(A - \frac{y^2}{B}\right)}{C} \quad (5.64)$$

In this equation,

$$A = \frac{vx}{2D_{xx}} \left(1 - \sqrt{1 + \frac{4\lambda^* RD_{xx}}{v^2}} \right)$$

$$B = 2\sigma^2 \left(1 + \frac{2xD_{yy}}{\sigma^2 v \sqrt{1 + \frac{4\lambda^* RD_{xx}}{v^2}}} \right)$$

$$C = \sqrt{1 + \frac{2xD_{yy}}{\sigma^2 v \sqrt{1 + \frac{4\lambda^* RD_{xx}}{v^2}}}}$$

where σ is a measure of the width of the source, and $\lambda^* = \lambda + \frac{i_r}{nRH}$.

More details about these models can be found in Charbeneau (2000). He compared the results obtained from the simple plume model, the point source model, and the Gaussian-source plume model for a hypothetical aquifer in steady-state conditions. [Figure 5.22](#) shows the concentration contours for these models. The most significant feature is the similarity between the contours suggesting equivalence in solution. In this figure, the smaller contours represent the higher concentrations. As demonstrated in this figure, there is a significant similarity between the contours that show the equivalence in solutions. Longitudinal dispersion has minor importance in determining steady-state plume concentration distributions.

Charbeneau concluded that based on this comparison, if the source is small and maximum concentrations from a continual source are supposed to be determined, then the simple plume model is adequate. For small sources, if transient effects are important, then the point-source plume model is preferred because the calculations are simple. The Gaussian-source model is used when the size of the source is important.

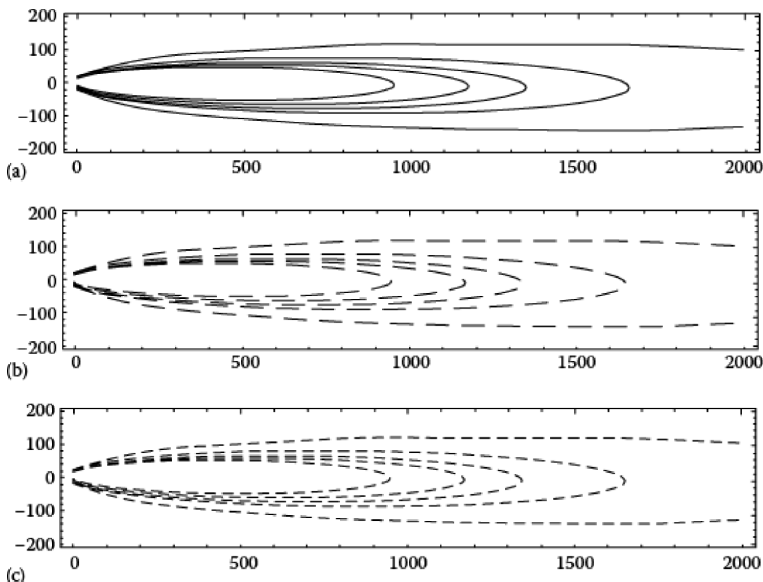


FIGURE 5.22 Steady-state plume model concentration contours for (a) simple plume model, (b) point-source plume model, and (c) Gaussian source plume model. (From Charbeneau, R.J., *Groundwater Hydraulics and Pollutant Transport*, Waveland Press, Long Grove, IL, 593, 2000.)

PROBLEMS

- 5.1** Groundwater deep in a sedimentary basin has an electrical conductance of 300 micro-siemens. Make a rough estimate of the total dissolved solids of this water (in mg/L).
- 5.2** A dissolved contaminant is being leached from a point source with the concentration of 114 mg/L. There is a stream 7.5 m away from the point source. What concentration of the contaminant reached the stream after 5 years? Diffuse coefficient and τ are 2.15×10^{-8} and 0.48, respectively.
- 5.3** A landfill is located on a 6-m thick dense clay overlying an aquifer, which is the primary source of drinking water to a small town. Leachate-contaminated groundwater has accumulated at the base of the landfill. The hydraulic gradient in the aquifer is 0.9, the hydraulic conductivity of the clay is approximately 1.8×10^{-10} m/s, and the porosity is 22%. How long will it take for the nonreactive contaminants to move through the clay into the aquifer.
- 5.4** The hydrogeologic cross section in Figure 5.23 illustrates the pattern of groundwater flow along a local flow system. Assuming that the contamination is transported from the source only by the advection process, estimate at what time in the future the plume will reach the stream.
- 5.5** Groundwater flows through the left face of a cube of sandstone (2 m on a side) and out of the right face with a linear groundwater velocity of 3×10^{-5} m/s. The porosity of the sandstone is 0.12 and the diffusion

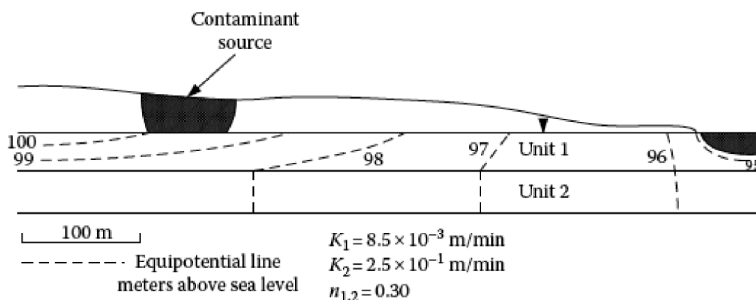


FIGURE 5.23 The hydrogeologic cross section of the area in Problem 5.4.

coefficient is $9 \times 10^{-9} \text{ m}^2/\text{s}$. Assume that a tracer has concentrations of 1.25 and $0.75 \times 10^4 \text{ mg/m}^3$ at the inflow and the outflow faces, respectively. Calculate the mass flux at the outflow due to advection and diffusion.

- 5.6** An unconfined aquifer has the hydraulic conductivity of $1.5 \times 10^{-4} \text{ m/s}$ and porosity of 0.35 . If a dissolved contaminant with the initial contamination of 470 mg/L reaches this aquifer, how far may this contaminant move in 1 year ? Assume that the hydraulic gradient in this aquifer is 0.05 and the effective diffusion coefficient of the contaminant is $2.34 \times 10^{-8} \text{ m}^2/\text{s}$.

- 5.7** A contaminated site has the porosity of 0.28 . If the gradient of the contaminant concentration is 0.0018 mg/L/m , calculate the diffusive flux. The diffusion coefficient of the contaminant is $5.86 \times 10^{-6} \text{ cm}^2/\text{s}$.

- 5.8** A contaminant is being released from a point source to an aquifer. This aquifer is being discharged to a stream 40 m away from the contaminant source. Compute the concentration of the contaminant that reaches the stream through the aquifer after 3 years .

Hydraulic conductivity = $2.5 \times 10^{-6} \text{ m/s}$

Porosity = 0.25

Hydraulic gradient = 0.035 m/m

Concentration of nitrobenzene at the source = 520 mg/L

Effective diffusion coefficient diffusion for nitrobenzene = $1.93 \times 10^{-8} \text{ m}^2/\text{s}$.

- 5.9** Nitrate is being leaked from an industrial facility with the concentration of 22 mg/L . If the diffuse coefficient is $1.95 \times 10^{-7} \text{ m}^2/\text{s}$ and τ is 0.35 , what is the concentration of nitrate 500 m away from the facility in 20 years ? The velocity of groundwater is $4.74 \times 10^{-7} \text{ m/s}$.

- 5.10** An unconfined aquifer with porosity of 0.3 is being discharged to a stream flow. The groundwater flow velocity is 0.25 m/day , and the thickness and width of the aquifer are 1.5 m and 75 m , respectively. What mass flux of bicarbonate may be discharged into the stream by advection if the concentration of bicarbonate in groundwater is 18 mg/L in the groundwater.

- 5.11** How long does it take for a contaminant to reach 20 percent of its initial concentration 500 m away from the source. Assume one-dimensional movement. The hydraulic conductivity of the aquifer is 2.50 m/day , effective porosity is 0.35 , and hydraulic gradient is 0.08 m/m . The longitudinal coefficient of hydraulic depression is $0.62 \text{ m}^2/\text{s}$.

REFERENCES

- Bedient, P.B., Rifai, H.S., and Newell, C.J. 1994. *Ground Water Contamination: Transport and Remediation*. Prentice-Hall Publishing, Englewood Cliffs, NJ, 560p.
- Charbeneau, R.J. 2000. *Groundwater Hydraulics and Pollutant Transport*. Waveland Press, Long Grove, IL, 593p.
- Crank, J. 1956. *The Mathematics of Diffusion*. Oxford University Press, New York, 424p.
- Delleur, J.W. 1999. *The Handbook of Groundwater Engineering*. CRC Press/Springer-Verlag, Boca Raton, FL, 992p.
- Freeze, R. and Cherry, J. 1979. *Groundwater*, Prentice-Hall, Englewood Cliffs, NJ, 604p.
- Gupta, R.S. 1989. *Hydrology and Hydraulic Systems*. Prentice-Hall, Englewood Cliffs, NJ.
- Javandel, I. and Tsang, C.F. 1986. Capture-zone type curves: A tool for aquifer cleanup. *Ground Water*, 24(5), 616–625.
- Masters, G.M. and Ela, W.P. 2008. *Introduction to Environmental Engineering and Science*. Prentice Hall Inc., Simon and Schuster, Englewood Cliffs, NJ, 576p.
- McKee, J.E. 1960. The need for water quality criteria, *Conference of the Physiological Aspects of Water Quality*, 1960, Division of Water Supply and Pollution Control, U.S. Public Health Service, Washington, DC.
- Mirtov, B.A. 1961. *Gaseous Composition of the Atmosphere and Its Analysis*. Akad. Nauk SSSR, Inst. Prikl. Geofiz. Moskva (translated by the Israel Program for Scientific Translations). U.S. Department of Commerce, Office of Technical Services, Washington, DC, 209p.
- Ogata, A. and Banks, R.B. 1961. *A Solution of the Differential Equation of Longitudinal Dispersion in Porous Media*. U.S. Geological Survey Professional Paper 411-A.
- Oregon State University. 1974. *Disposal of Environmentally Hazardous Wastes*. Task Force Report, Environment Health Science Center, Oregon State University, Corvallis, OR, 210p.
- Sauty, J.P. 1978. Identification des paramètres du transport hydrodispersif dans les aquifères par interprétation de tracages en écoulement cyclique ou divergent. *Journal of Hydrology*, 39(1), 145–158.
- Smith, V.J. and Charbeneau, R.J. 1990. Probabilistic soil contamination exposure assessment procedures. *Journal of Environmental Engineering*, 116(6), 1143–1163.
- Stumm, W. 1977. Chemical interaction in particle separation, *Environmental Science and Technology*, 11, 1070.
- Stumm, W. and Morgan, J.J. 1996. *Aquatic Chemistry*, 3rd edn. John Wiley & Sons, New York, 1022p.
- U.S. Environmental Protection Agency. 1973. *Water Quality Criteria 1972*. EPA R3 73033. Government Printing Office, Washington, DC.
- U.S. Environmental Protection Agency. 2005. *Protection of Public Water Supplies from Ground-Water Contamination*, Center for Environmental Research Information, U.S. Environmental Protection Agency, Washington, DC.
- WHO. 2006. *Guidelines for Drinking-Water Quality*, First Addendum to 3rd edn. Vol. 1 - Recommendations.
- Xu, M. and Eckstein, Y. 1995. Use of weighted least squares method in evaluation of the relationship between dispersivity and field scale. *Ground Water*, 33(6), 905–908.

6 Groundwater Modeling

6.1 INTRODUCTION

A mathematical groundwater model can be used to simulate and describe real-world groundwater flow. The mathematical model is developed by translating a conceptual model in the form of governing equations, with associated boundary and initial conditions. This model can then be solved using a numerical model, which is developed through the implementation of computer programs (codes). A groundwater simulation model is a nonunique model due to different sets of assumptions used for simplifying the mathematical description of groundwater flow. It can be less burdened by approximating the investigated groundwater system and taking simplifying assumptions such as homogeneity, isotropy, direction of flow, geometry of the aquifer, mechanisms of contaminant transport, and its reaction. Models can simulate more complicated problems with higher accuracy, utilizing more inputs, system parameters, and boundary conditions. A successful model can result from a complete site investigation and field data. Thus, the model selection is a trade-off among different computational burdens including boundary conditions, grid discretization, time steps, the model accuracy, and ways to avoid truncation errors and numerical oscillations.

The performance and efficiency of a model depend on how accurate the mathematical equations approximate the physical system being modeled. However, it should be noted that the developed model is just an approximation and not an exact simulation of the actual groundwater flow.

The first step in groundwater system modeling is the conceptualization of the model, which includes a set of assumptions for the system's components, the media properties, and the transport processes in the system. A mathematical model contains the same information as the conceptual one, but it is transformed to a numerical model by the fundamental laws of hydraulics.

Numerous numerical methods such as the finite-difference method (FDM), finite element method (FEM), and finite volume method (FVM) have been developed to solve and simulate the numerical models of groundwater flow system in porous media. These models and their functions are explained in this chapter.

6.2 PROCESS OF MODELING

The process of aquifer modeling consists of the following activities (Thangarajan, 2007):

- The parameters characterizing the physical framework of the aquifer and the system conditions are identified.
- The hydrogeological parameters are estimated using field data in specific points.

- The spatial distribution of parameters is estimated utilizing interpolation/extrapolation methods.
- All of the estimated parameters and field data are utilized to structure the conceptual model.
- A mathematical model is developed to describe the conceptual model by expressing the system condition using the groundwater flow equations.
- The mathematical model is transformed to a numerical model to find the aquifer response including hydraulic head or pollutants concentrations.
- The generated model is solved by numerical methods of solution.
- Sensitivity analysis is done to identify key model coefficients that need to be adjusted to calibrate the model.
- The model is calibrated to more accurately predict the behavior of the groundwater system using the available field data.
- The model is verified to eliminate errors resulting from numerical approximations.
- Effects of implementation of defined management strategies on aquifer restoration and optimal utilization of the groundwater system are assessed using the model.

The model accuracy depends upon the level of conceptualization and understanding of the groundwater system as well as the assumptions embedded in the derivation of the mathematical equations.

6.3 MATHEMATICAL MODELING

Prediction of subsurface flow, water table level, solute transport, and simulation of natural or human-induced stresses are necessary for groundwater management (Karamouz et al., 2003). Such predictions can be used in planning and decision-making processes for the groundwater resource. Groundwater simulation models have been widely used for such predictions and simulations in groundwater system analysis and management. These models generally require the solution of partial differential equations.

Mathematical models may be deterministic, stochastic (statistical), or a combination of both. In stochastic models, a range of predictions, based on probabilities of occurrence, is provided to the model. Stochastic models can help to evaluate the uncertainties of a system.

Deterministic models, widely used for solving regional groundwater problems, are based on a cause-and-effect relationship of known systems and processes. Deterministic models can be further classified as analytical and numerical.

Analytical modeling is an easy method to evaluate the physical characteristics of an aquifer. This method of solution provides a rapid preliminary analysis of the groundwater system utilizing a number of simplifying assumptions. These models cannot be used for solving the problems with the irregularity of the domain's shape, the heterogeneity of the domain, and complex boundary conditions. For such situations, numerical models are implemented using computer programs to address more complicated problems.

The exact solutions for some simple or idealized problems can be found by numerical models. These models can yield approximate solutions by discretization of time and space. Numerical models can be further classified as the FDM, FEM, and FVM.

In the FDM, the first derivative in partial differential equations is approximated by the difference between values of independent variables at adjacent nodes considering the distance between the nodes and considering the duration of time step increment at two successive times. In the FEM, functions of dependent variables and parameters are used to evaluate equivalent integral formulation of partial differential equations (PDEs) (Delleur, 1999). Although each approach has some advantages and disadvantages, FDMs are generally easier to program because of their conceptual and mathematical simplicity.

There are two ways of solving the PDEs in the aforementioned methods to obtain the grid-point values of the dependent variable. One way, used in the FEM, is that the head variable consists of the grid-point values, and the shape function is employed to interpolate between the grid points. In the other way, used in the FDM, neglecting the head variations between the grids, the equations include the grid-point values of the head. These values are obtained at some discrete locations without any statement about the variation between these locations similar to a laboratory experiment.

The flexibility of the FEM in close spatial approximation of irregular aquifer boundaries and parameters of zones within the aquifer is a major advantage of this method. However, mesh generation and specification and construction of input data-sets for an irregular finite element grid are much more difficult in comparison with a regular rectangular finite-difference grid.

The FVM is a method for representing and evaluating PDEs as algebraic equations. Similar to the FDM, values are calculated at discrete places on a meshed geometry. Finite volume refers to the small volume surrounding each node point on a mesh.

One advantage of the FVM over the FDM is that it does not require a structured mesh. The FVM is also preferable to other methods because of the fact that boundary conditions can be applied noninvasively. This is true because the values of the conserved variables are located within the volume element, and not at nodes or the surface. FVMs are especially powerful on coarse nonuniform grids and in calculations where the mesh moves to track interfaces or shocks.

6.3.1 ANALYTICAL MODELING

An analytical model provides a solution for a mathematical description of a physical process. In this structure, groundwater flow equations require several simplifying assumptions including the domain's shape, boundary, and initial conditions.

Because of the simplifications inherent with analytical models, it is not possible to account for field conditions that change with time or space (Mandle, 2002). Thus, the system under study may vary from actual conditions. Analytical models have mostly been in use for particular sets of conditions and involve manually solving equations, such as Darcy's law and the Theis equation, generating solutions utilizing curve-matching techniques, inverse solutions for interpretation of flow tests, and verification of numerical models.

The earliest work on analytical solutions for groundwater flow can be found in Carslaw and Jaeger (1959). Other examples of finding analytical solutions for groundwater flow include Bear (1979), van Genuchten and Alves (1982), Walton (1989), and Strack (1989). In most of the analytical methods for solution of two-dimensional (2D) groundwater problems, a suitable function is first determined to transform the problem from a geometrical domain into a domain with a more straightforward solution algorithm (Karamouz et al., 2003). A transformation that possesses the property of preserving angles of intersections and the approximate image of small shapes is conformal mapping. Harr (1962) presented various functions and discussed a way in which these functions transform geometric figures from one complex plan to another. Toth (1962, 1963) developed two analytical solutions for the boundary value problem with steady-state flow in a 2D, saturated, homogeneous, isotropic flow field bounded on top by a water table and on the other three sides by impermeable boundaries.

6.3.2 NUMERICAL MODELING

Numerical modeling is used to solve the PDEs that represent the groundwater flow. It gives an approximate solution, which may vary with respect to the assumptions. There are several types of numerical models depending on the numerical techniques employed. These models include finite-difference, finite element, integrated finite-difference, boundary element, and particle tracking. The main features of the various numerical models are (Bear and Verruijt, 1992):

1. The models are solved only at specified points in the space and time domains defined for the problem (discrete values). These points are considered as discontinuous state variables for the entire domain.
2. The PDEs that describe the groundwater flow are transformed by a set of mathematical equations in certain points as discrete values of the state variables.
3. The solution is for a specified set of numerical values of the various model coefficients rather than a general relationship in terms of these coefficients.
4. A computer program is employed to solve the large number of equations that must be solved simultaneously.

6.4 FINITE-DIFFERENCE METHOD

The FDM consists of transforming the partial derivatives in difference equations over a small interval by algebraic expressions written in terms of aquifer characteristics and conditions. The problem domain is divided into a connected series of discrete points called nodes. This method replaces a continuous media by a discrete set of points and assigns various hydrogeological parameters to each node (Thangarajan, 2007). The FDM can be used to discretize both time and space. The partial derivatives are replaced utilizing the difference operators that define the spatial-temporal relationships between some parameters. The developed model is solved in each node by obtaining the solution for a set of algebraic equations in that node. There are various

methods to solve the simplified equations. Some of the prevalent iterative numerical methods are: (1) successive over relaxation method (Aziz and Settari, 1972; Watts, 1971, 1973); (2) alternating direction implicit (ADI) procedure (Bredehoeft and Pinder, 1970; Peaceman and Rachford, 1955; Remson et al., 1971; Rushton, 1974); (3) modified iterative ADI method (Prickett and Lonnquist, 1971); and (4) strongly implicit procedure (Stone, 1968; Trescott et al., 1976; Weinstein et al., 1970, etc.).

The advantage of the FDM is the ease of following a complex system including complicated loading path and highly nonlinear behavior, since it is easy to understand and to prepare the program. Thus, it is an economic method for solving large nonlinear groundwater flow problems. The use of the FDM is difficult for an irregular geometrical domain. Generally, the conventional FDM with regular grid systems suffers from the shortcomings in irregular shape domain, complex boundary conditions, and material heterogeneity.

The continuous media is expressed in Equation 6.1. It is replaced by a finite set of discrete points in space, and time is discretized:

$$\frac{\partial}{\partial x} \left(K_x \frac{\partial h}{\partial x} \right) + \frac{\partial}{\partial y} \left(K_y \frac{\partial h}{\partial y} \right) + \frac{\partial}{\partial z} \left(K_z \frac{\partial h}{\partial z} \right) = S_s \frac{\partial h}{\partial t} \quad (6.1)$$

The partial derivatives are replaced by terms calculated from the differences in head values at each node. Simultaneous linear algebraic difference equations are achieved through the derivatives of variables. Their solutions lead to the head values at nodes and time by solving the linear algebraic equations. The solutions obtained by this method are just approximations. [Figure 6.1](#) shows a three-dimensional (3D) discretized aquifer. In this aquifer, i , j , and k address the location of each node in the mesh, representing rows, columns, and layers, respectively.

The head in each node is a function of both space and time, and it is required to discretize the continuous media into discrete nodes and times. The equation is solved for the nodes that are located within each cell. There are many schemes for locating nodes in cells, such as a mesh-centered node or block-centered node as shown in [Figure 6.2](#).

Finite-difference approximations for the first- and second-order derivatives of the groundwater flow and mass transport equations can be developed directly from the

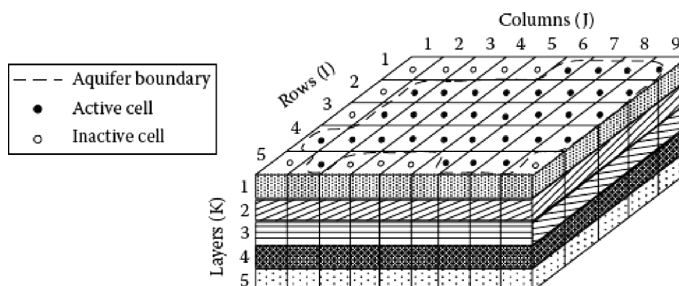


FIGURE 6.1 Illustration of discretization of continuous media into finite-difference cells.

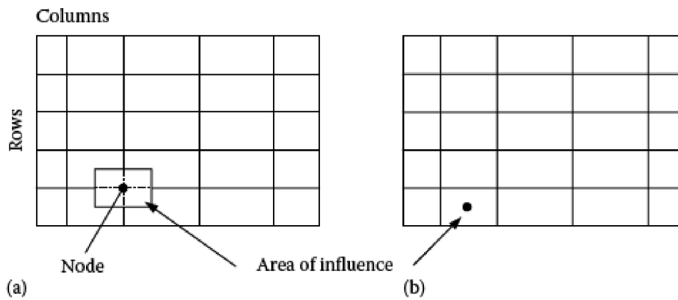


FIGURE 6.2 Illustration of 2D space discretization methods: (a) mesh-centered and (b) block-centered.

Taylor series approximations of the temporal and spatial derivatives. In the discrete groundwater model, the head or mass concentration at the nodal points $x + \Delta x$ or $x - \Delta x$ is expressed in terms of the state variables, and all the derivatives are evaluated at an adjacent nodal point, x ,

$$h(x - \Delta x) = h(x) - \frac{\partial h}{\partial x} \Big|_x \Delta x + \frac{\partial^2 h}{\partial x^2} \Big|_x \frac{\Delta x^2}{2!} - \frac{\partial^3 h}{\partial x^3} \Big|_x \frac{\Delta x^3}{3!} + \dots \quad (6.2)$$

By rearranging Equation 6.2,

$$\frac{\partial h}{\partial x} \Big|_x = \frac{h(x + \Delta x) - h(x)}{\Delta x} - \frac{\Delta x}{2!} \frac{\partial^2 h}{\partial x^2} \Big|_x - \frac{\Delta x^2}{3!} \frac{\partial^3 h}{\partial x^3} \Big|_x - \dots \quad (6.3)$$

The forward and backward first differences are obtained as:

$$\frac{\partial h}{\partial x} \Big|_x = \frac{h(x + \Delta x) - h(x)}{\Delta x} + O(\Delta x) \quad (6.4)$$

$$\frac{\partial h}{\partial x} \Big|_x = \frac{h(x) - h(x + \Delta x)}{\Delta x} + O(\Delta x) \quad (6.5)$$

respectively.

Differencing Equations 6.2 and 6.3, and isolating the first-order derivative, give a central difference approximation to the first derivative:

$$\frac{\partial h}{\partial x} \Big|_x = \frac{h(x + \Delta x) - h(x)}{\Delta x} + O(\Delta x^2) \quad (6.6)$$

The error, \bar{E} , is on the order of Δx , which means a positive constant δ exists, which is independent of Δx , and $|\bar{E}| \leq \delta |\Delta x|$ for all sufficiently small Δx s. The errors of these approximations are called truncation errors. The truncation error of the central difference approximation is:

$$\bar{E} = -\frac{\Delta x^2}{3!} \frac{\partial^3 h}{\partial x^3} \Big| = O(\Delta x^2) \quad (6.7)$$

It is decreased by decreasing the values of Δx and Δt . An approximation to the second derivative can be obtained by Equation 6.2:

$$\frac{\partial^2 h}{\partial x^2} \Big|_x \approx \frac{h(x + \Delta x) - 2h(x) + h(x - \Delta x)}{\Delta x^2} \quad (6.8)$$

The truncation error of the second-order approximation is:

$$\bar{E} = \frac{\Delta x^2}{12} \frac{\partial^4 h}{\partial x^4} \Big|_{\xi} = O(\Delta x^2) \quad (6.9)$$

Higher-order derivative approximations can be developed using linear difference operators.

Similar discretization could be used for time intervals. Therefore, the approximations of $\partial h / \partial t$ using forward and backward differences are as follows:

$$\frac{\partial h}{\partial x} \Big|_t = \frac{h^{t+1} - h^t}{\Delta t} \quad (6.10)$$

$$\frac{\partial h}{\partial x} \Big|_t = \frac{h^t - h^{t-1}}{\Delta t} \quad (6.11)$$

respectively.

Figure 6.3 shows time and space discretization at node (i, j) in a 2D finite-difference grid and illustrates the application of some simple finite-difference methods for solving groundwater flow equation. These methods are explained later in this section.

6.4.1 FORWARD DIFFERENCE EQUATION

The head at point (i, j) at time step $(n + 1)$ can be obtained utilizing the value of h at time step n and the forward difference time derivative. Therefore, there is a finite-difference equation for each node at time step $n + 1$ with only one unknown variable. As shown in Figure 6.3a, all values of head h are known at all spatial nodes at time n . This method is called forward difference or explicit method.

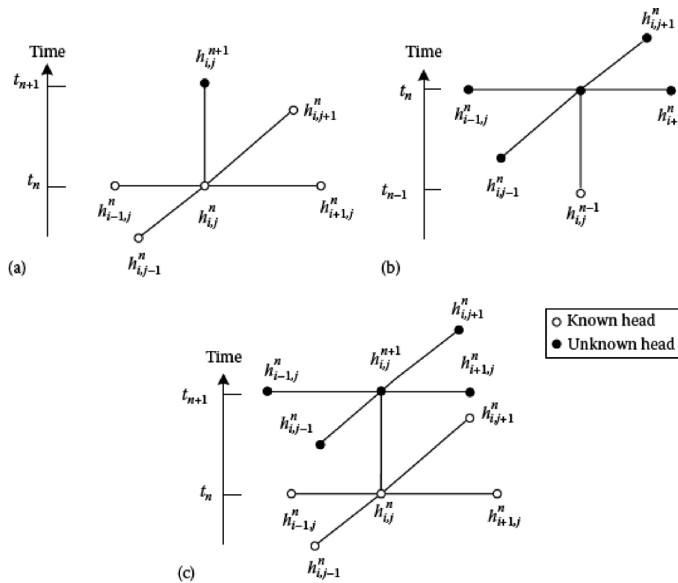


FIGURE 6.3 (a) The forward difference, (b) backward difference, and (c) Crank–Nicholson method in a 2D finite-difference grid.

In a 2D groundwater flow equation for a heterogeneous, anisotropic aquifer, Equation 6.1 can be written as:

$$\begin{aligned}
 S_s \left(\frac{h_{i,j}^{n+1} - h_{i,j}^n}{\Delta t} \right) = & K_{x(i-1/2,j)} \left(\frac{h_{i-1,j}^n - h_{i,j}^n}{(\Delta x)^2} \right) + K_{x(i+1/2,j)} \left(\frac{h_{i+1,j}^n - h_{i,j}^n}{(\Delta x)^2} \right) \\
 & + K_{y(i,j-1/2)} \left(\frac{h_{i,j-1}^n - h_{i,j}^n}{(\Delta y)^2} \right) + K_{y(i,j+1/2)} \left(\frac{h_{i,j+1}^n - h_{i,j}^n}{(\Delta y)^2} \right) \quad (6.12)
 \end{aligned}$$

In this equation, only $h_{i,j}^{n+1}$ is unknown. Equation 6.12 can be solved explicitly at each grid for the head at the new time level. Since the solution is dependent only upon known values of heads in the adjacent grids at the beginning of the time periods, the computation for $h_{i,j}^{n+1}$ in any grid can be made in any order without regard to values of $h_{i,j}^{n+1}$ for any other grid (Karamouz et al., 2003).

For example, in a one-dimensional (1D) groundwater flow equation for a heterogeneous, isotropic, and confined aquifer, Equation 6.12 can be written as:

$$S \left(\frac{h_i^{n+1} - h_i^n}{\Delta t} \right) = Kb \left(\frac{h_{i-1}^n - h_i^n}{(\Delta x)^2} \right) + Kb \left(\frac{h_{i+1}^n - h_i^n}{(\Delta x)^2} \right) \quad (6.13)$$

or

$$h_i^{n+1} = \frac{T\Delta t}{S(\Delta x)^2} (h_{i-1}^n + h_{i+1}^n) + h_i^n \left(1 - \frac{2T\Delta t}{S(\Delta x)^2} \right) \quad (6.14)$$

Explicit finite-difference equations are simple to solve, but when time increments are too large, small numerical errors can propagate into larger errors in the next computational stages. A stable solution is ensured in a 1D heterogeneous case if:

$$\frac{T\Delta t}{S(\Delta x)^2} < \frac{1}{2} \quad (6.15)$$

Consequently, the time increment cannot be selected independently of the space increment.

Example 6.1

Consider a nonsteady, 1D flow in a confined aquifer shown in [Figure 6.4](#). Let $\Delta x = 3 \text{ m}$, $b = 3 \text{ m}$, $h_1 = 5 \text{ m}$, $h_5 = 1 \text{ m}$ for $t > 0$, $K = 0.5 \text{ m/day}$, $S = 0.03$. The initial conditions are $h_1 = h_2 = h_3 = h_4 = h_5 = 5 \text{ m}$. Determine the spatial variation of piezometric head.

SOLUTION

To satisfy the stability requirement of Equation 6.15, the maximum time step Δt is computed as:

$$h_i^{n+1} = \frac{T\Delta t}{S(\Delta x)^2} (h_{i-1}^n + h_{i+1}^n) + h_i^n \left(1 - \frac{2T\Delta t}{S(\Delta x)^2} \right)$$

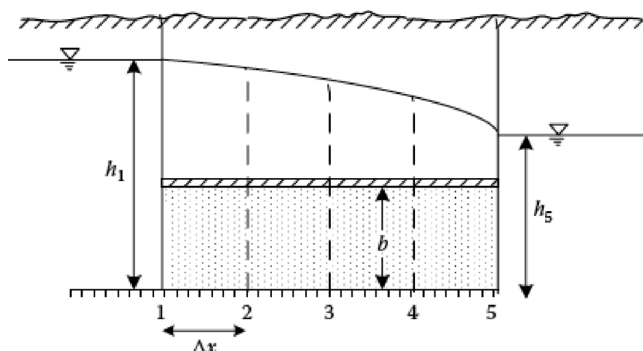


FIGURE 6.4 The confined aquifer in Example 6.1.

$$\Delta t < \frac{S(\Delta x)^2}{2T} = \frac{1}{2} \frac{(0.03)(3)^2}{0.5 \times 3} = 0.09 \text{ day}$$

Therefore, the time increment is selected as 0.08 days. With assumption of: $h_1 = h_2 = h_3 = h_4 = h_5 = 5 \text{ m}$, $h_1^{0.08} = h_2^{0.08} = h_3^{0.08} = h_4^{0.08} = h_5^{0.08} = 1 \text{ m}$. For the first time, step grid (4) is affected and Equation 6.14 becomes:

$$\begin{aligned} h_4^{2 \times 0.08} &= \frac{T \Delta t}{S(\Delta x)^2} (h_3^{0.08} + h_5^{0.08}) + h_4^{0.08} \left(1 - \frac{2T \Delta t}{S(\Delta x)^2} \right) \\ &= \frac{1.5 \times 0.08}{0.03(3)^2} (5 + 1) + 5 \times \left(1 - \frac{2 \times 1.5 \times 0.08}{0.03(3)^2} \right) = 3.22 \text{ m} \end{aligned}$$

$$h_2^{2 \times 0.08} = h_3^{2 \times 0.08} = 5 \text{ m}$$

For the second time step $t = 3 \times 0.08$ for grid (4):

$$h_2^{3 \times 0.08} = 5 \text{ m}, h_3^{3 \times 0.08} = 4.21 \text{ m}, h_4^{3 \times 0.08} = 3.02 \text{ m}$$

The above process is repeated until the head at each grid is calculated at the desired time. To illustrate the stability problem, a set of calculations was made in which Δt was selected to be 0.12 days so that the expression for stability results in:

$$\frac{T \Delta t}{S(\Delta x)^2} = \frac{1.5 \times 0.12}{0.03(3)^2} > \frac{1}{2}$$

The calculated head in grid (4) as a function of time is shown in Figure 6.5. The computed values fluctuate with each time step for $\Delta t = 0.12$, giving completely erroneous results. Also, the amplitude of the fluctuation increases with increasing time.

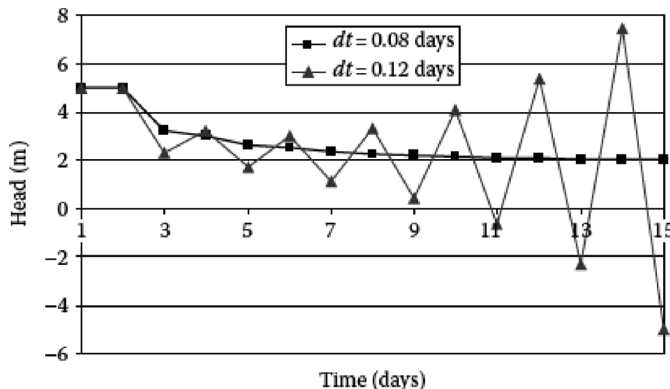


FIGURE 6.5 Calculated piezometric head in grid (4), using the forward difference equation.

6.4.2 BACKWARD DIFFERENCE EQUATION

Figure 6.3b shows the time derivative as a backward difference from the heads at time level, $n - 1$, which are the known heads. Therefore, the difference equation of each node will have five unknown variables. For a grid with N nodes, there is a system of N equations containing N unknown variables. This system of equations can be solved simultaneously considering the boundary conditions. This method is called backward difference or implicit method. The implicit finite-differential form of 2D groundwater equation, (Equation 6.1), can be expressed as follows:

$$S_s \left(\frac{h_{i,j}^n - h_{i,j}^{n-1}}{\Delta t} \right) = k_{x(i-1/2,j)} \left(\frac{h_{i-1,j}^n - h_{i,j}^n}{(\Delta x)^2} \right) + k_{x(i+1/2,j)} \left(\frac{h_{i+1,j}^n - h_{i,j}^n}{(\Delta x)^2} \right) \\ + k_{y(i,j-1/2)} \left(\frac{h_{i,j-1}^n - h_{i,j}^n}{(\Delta y)^2} \right) + k_{y(i,j+1/2)} \left(\frac{h_{i,j+1}^n - h_{i,j}^n}{(\Delta y)^2} \right) \quad (6.16)$$

For example, in a 1D groundwater flow equation for a heterogeneous, isotropic, and confined aquifer, Equation 6.16 can be written as:

$$S \left(\frac{h_i^n - h_i^{n-1}}{\Delta t} \right) = Kb \left(\frac{h_{i-1}^n - h_i^n}{(\Delta x)^2} \right) + Kb \left(\frac{h_{i+1}^n - h_i^n}{(\Delta x)^2} \right) \quad (6.17)$$

Rearranging Equation 6.17 so that all of the known values are on the right-hand side of the equal sign results in:

$$h_{i-1}^n - h_i^n \left(2 + \frac{S(\Delta x)^2}{T\Delta t} \right) + h_{i+1}^n = -\frac{S(\Delta x)^2}{T\Delta t} h_i^{n-1} \quad (6.18)$$

The head in grid (i) depends upon the value of the head at time n in the adjacent grids, ($i + 1$) and ($i - 1$). Thus, Equation 6.18 represents a set of algebraic equations that must be solved simultaneously.

Example 6.2

Solve Example 6.1 using the backward difference equation.

SOLUTION

Equation 6.18 is used for determining the three interior grids (2), (3), and (4). Grids (1) and (5) are boundary grids and values of head at these grids are specified as 5 and 1 m, respectively. With assumption of $h_1 = h_2 = h_3 = h_4 = h_5 = 5$ m and

$h_1^{0.08} = h_2^{0.08} = h_3^{0.08} = h_4^{0.08} = h_5^{0.08} = 5 \text{ m}$ and $h_5^{0.08} = 1 \text{ m}$, for the second time step $\Delta t = 0.08 \text{ days}$, the following equations for grids (2), (3), and (4) are obtained:

$$5 - 4.25h_2^{0.16} + h_3^{0.16} = -11.25$$

$$h_2^{0.16} - 4.25h_3^{0.16} + h_4^{0.16} = -11.25$$

$$h_3^{0.16} - 4.25h_4^{0.16} + 1 = -11.25$$

Rearranging the above equations so that all known values are placed on the right-hand side and summing them up, we get:

$$h_2^{0.16} = 4.9451, \quad h_3^{0.16} = 4.7665, \quad h_4^{0.16} = 4.0627 \text{ m}$$

Example 6.3

Develop the finite-difference approximation (FDA) of flow equation for a 2D semi-confined, inhomogeneous, and anisotropic aquifer.

SOLUTION

The FDA of a flow equation in a semi-confined aquifer equation in an inhomogeneous and isotropic aquifer is as follows:

$$\begin{aligned} \frac{1}{\Delta x^2} \{ T_x^{i+1/2,j} (h_{i+1,j} - h_{i,j}) - T_x^{i-1/2,j} (h_{i,j} - h_{i-1,j}) \} + \frac{1}{\Delta y^2} \{ T_y^{i,j+1/2} (h_{i,j+1} - h_{i,j}) \} \\ - T_y^{i,j-1/2} (h_{i,j} - h_{i,j-1}) \pm \frac{Q_{w,i,j}}{\Delta x \Delta y} + \frac{K_{a,i,j} (h_{a,i,j} - h_{i,j})}{b_a} = S_{i,j} h_{i,j} \end{aligned} \quad (6.19)$$

By rewriting Equation 6.19 for all internal nodes ($i, j; i = 1, \dots, m$ and $j = 1, \dots, m$) of the domain, a set of linear equations can be expressed in the following form:

$$A\mathbf{h} + B\mathbf{h} + \mathbf{g} = 0 \quad (6.20)$$

In these equations, which are called *dynamic response equations*, \mathbf{h} is a column vector of unknown heads, $\mathbf{h} = (h_{11}, \dots, h_{1m}, \dots, h_{n1}, \dots, h_{nm})^T$. Vector \mathbf{g} contains the rate of pumping and injections that can be the decision variables in the ground-water planning models. The coefficient matrices A and B depend on the flow and hydraulic properties of porous media. Dynamic response equations can easily provide the hydraulic head at the nodes as a linear function of initial condition and the pumping/injection rate of well sites.

6.4.3 ALTERNATING DIRECTION IMPLICIT METHOD

Considering that the space derivative of head is calculated at time $(n + 1)$, the ground-water flow Equation (6.1) can be rewritten as follows:

$$\frac{h_{i+1,j}^{n+1} - 2h_{i,j}^{n+1} + h_{i-1,j}^{n+1}}{(\Delta x)^2} + \frac{h_{i,j+1}^{n+1} - 2h_{i,j}^{n+1} + h_{i,j-1}^{n+1}}{(\Delta y)^2} + \frac{Q_{i,j}}{T \Delta x \Delta y} = \frac{S}{T} \left[\frac{h_{i,j}^{n+1} - h_{i,j}^n}{\Delta t} \right] \quad (6.21)$$

where $Q_{i,j}$ is negative if it represents discharge and positive if it represents recharge at row j and column i .

Solving this equation requires solving a pentadiagonal matrix which is a time-consuming process. For solving this issue, the ADI method is proposed. This method is comprised of two sets of tridiagonal simultaneous equations. In this procedure, equations are first solved for all rows and then solved for each column. Ultimately, an iteration is considered complete (Hoffmann and Chiang, 1989). If we assume $q_{i,j} = \frac{Q_{i,j}}{\Delta x \Delta y}$, the finite-difference equations in the ADI formulation are:

$$\frac{h_{i+1,j}^{n+\frac{1}{2}} - 2h_{i,j}^{n+\frac{1}{2}} + h_{i-1,j}^{n+\frac{1}{2}}}{(\Delta x)^2} + \frac{h_{i,j+1}^n - 2h_{i,j}^n + h_{i,j-1}^n}{(\Delta y)^2} + \frac{q_{i,j}}{T} = \frac{S}{T} \left[\frac{h_{i,j}^{n+\frac{1}{2}} - h_{i,j}^n}{\frac{\Delta t}{2}} \right] \quad (6.22)$$

$$\frac{h_{i+1,j}^{n+\frac{1}{2}} - 2h_{i,j}^{n+\frac{1}{2}} + h_{i-1,j}^{n+\frac{1}{2}}}{(\Delta x)^2} + \frac{h_{i,j+1}^{n+1} - 2h_{i,j}^{n+1} + h_{i,j-1}^{n+1}}{(\Delta y)^2} + \frac{q_{i,j}}{T} = \frac{S}{T} \left[\frac{h_{i,j}^{n+1} - h_{i,j}^{n+\frac{1}{2}}}{\frac{\Delta t}{2}} \right] \quad (6.23)$$

First, Equation 6.22 is solved implicitly for the unknowns in the x -direction (y -direction), and then Equation 6.23 is solved implicitly in the y -direction (x -direction). Each full step is divided into two half steps. That is the reason for considering $n + \frac{1}{2}$ in the x -direction.

Equation 6.22 can be rewritten as:

$$h_{i-1,j}^{n+\frac{1}{2}} + B_i h_{i,j}^{n+\frac{1}{2}} + h_{i+1,j}^{n+\frac{1}{2}} = D_i \quad (6.24)$$

where B_i and D_i are constants and can be calculated in x -direction as:

$$B_i = - \left(2 + \frac{2S\Delta x^2}{T\Delta t} \right) \quad (6.25)$$

$$D_i = - \frac{\Delta x^2}{\Delta y^2} h_{i,j-1}^n - \left(\frac{2S\Delta x^2}{T\Delta t} - \frac{2\Delta x^2}{\Delta y^2} \right) h_{i,j}^n - \frac{\Delta x^2}{\Delta y^2} h_{i,j+1}^n - \frac{q_{i,j}\Delta x^2}{T} \quad (6.26)$$

For the y -direction, Equation 6.23 can be rewritten as:

$$h_{i,j-1}^{n+1} + B_j h_{i,j}^{n+1} + h_{i,j+1}^{n+1} = D_j \quad (6.27)$$

where:

$$B_j = -\left(2 + \frac{2S\Delta y^2}{T\Delta t} \right) \quad (6.28)$$

$$D_j = -\frac{\Delta y^2}{\Delta x^2} h_{i-1,j}^{n+\frac{1}{2}} - \left(\frac{2S\Delta y^2}{T\Delta t} - \frac{2\Delta y^2}{\Delta x^2} \right) h_{i,j}^{n+\frac{1}{2}} - \frac{\Delta y^2}{\Delta x^2} h_{i+1,j}^{n+\frac{1}{2}} - \frac{q_{i,j}\Delta y^2}{T} \quad (6.29)$$

Equations 6.24 through 6.26 are solved for all rows in half time steps ($n + \frac{1}{2}$), and then Equations 6.27 through 6.29 are solved for each column in a full time step ($n + 1$).

Example 6.4

Two fully penetrating wells in a confined aquifer system are shown in Figure 6.6, wells 1 and 2 pump at the rates of 90 and 60 L/s, respectively. The aquifer is bounded by a stream on one side and has impermeable boundaries on two sides. The initial piezometric head is horizontal, in level with the stream. Determine the spatial variation of the piezometric head after one day of pumping.

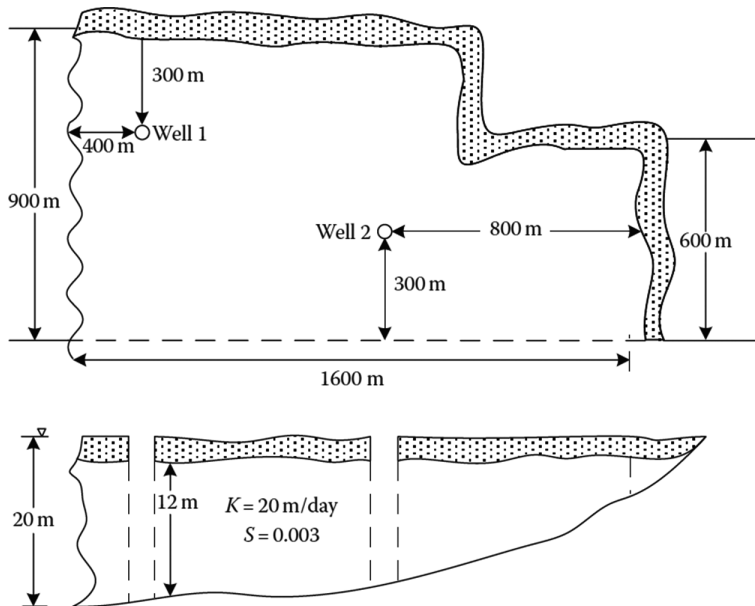


FIGURE 6.6 Plan and cross section of confined aquifer. (From Gupta, R.S., *Hydrology and Hydraulic Systems*, Prentice-Hall, Englewood Cliffs, NJ, 1989.)

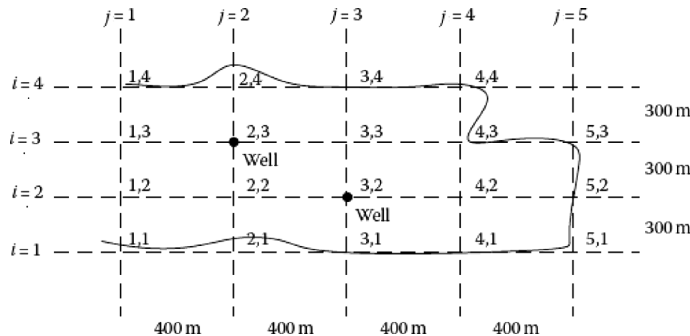


FIGURE 6.7 Finite-difference grid and its coordinates.

SOLUTION:

The grid layout is shown in Figure 6.7. As the initial condition, the heads of all nodes are 20 m at $t = 0$ and boundary conditions are as follows:

Recharge boundary:

$$h_{1,1} = h_{1,2} = h_{1,3} = h_{1,4} = 20$$

Impermeable boundaries:

$$h_{5,1} = h_{4,1} \quad h_{2,4} = h_{2,3}$$

$$h_{5,2} = h_{4,2} \quad h_{4,4} = h_{3,4}$$

$$h_{3,4} = h_{3,3} \quad h_{4,3} = h_{3,3}$$

$$h_{4,4} = h_{4,3} \quad h_{4,2} = h_{5,2}$$

$$T = Kb = 20 \times 12 = 240 \frac{\text{m}^2}{\text{day}}$$

The solution procedure starts with the tridiagonal system. The formulation is implicit in the x -direction and explicit in the y -direction; thus, the solution at this stage is referred to as the x sweep. The time step is broken into two half time steps, one half time step in the x -direction and the other half time step in the y -direction.

Sweeping in the x -direction:

A time step Δt of 1 day is selected as the time interval. Since there is no pumping on the first row, piezometric heads in this row will not change in the first time step. For row 2, $i = 2$, we have:

$$B_i = -\left(2 + \frac{2S\Delta x^2}{T\Delta t}\right)$$

$$B_2 = -\left(2 + \frac{2 \times 0.003 \times 400^2}{240 \times 1}\right) = -6$$

$$B_2 = B_3 = B_4 = -6$$

and

$$D_2 = -\frac{400^2}{300^2} \times 20 - \left(\frac{2 \times 0.003 \times 400^2}{240 \times 1} - \frac{2 \times 400^2}{300^2} \right) \times 20 - \frac{400^2}{300^2} \times 20 - 0 = -80$$

Since:

$$q = \frac{Q}{\Delta x \Delta y} = \frac{-60 \times 86.4}{300 \times 400} = -0.0432 \frac{\text{m}}{\text{day}}$$

hence,

$$D_3 = -80 - \left(\frac{-0.0432 \times 400^2}{240} \right) = -51.2$$

$$D_4 = D_2$$

Substituting the B , D , initial, and boundary conditions,
For node $i = 2$ & $j = 2$:

$$20 - 6h_{2,2}^{\frac{1}{2}} + h_{3,2}^{\frac{1}{2}} = -80$$

For node $i = 2$ & $j = 3$:

$$h_{2,2}^{\frac{1}{2}} - 6h_{2,3}^{\frac{1}{2}} + h_{2,4}^{\frac{1}{2}} = -51.2$$

For node $i = 2$ & $j = 4$:

$$h_{2,3}^{\frac{1}{2}} - 6h_{2,4}^{\frac{1}{2}} + h_{2,4}^{\frac{1}{2}} = -80$$

or

$$\begin{bmatrix} -6 & 1 & 0 \\ 1 & -6 & 1 \\ 0 & 1 & -5 \end{bmatrix} \begin{bmatrix} h_{2,2}^{\frac{1}{2}} \\ h_{2,3}^{\frac{1}{2}} \\ h_{2,4}^{\frac{1}{2}} \end{bmatrix} = \begin{bmatrix} -100 \\ -51.2 \\ -80 \end{bmatrix}$$

Solving gives:

$$\begin{bmatrix} h_{2,2}^{\frac{1}{2}} \\ h_{2,3}^{\frac{1}{2}} \\ h_{2,4}^{\frac{1}{2}} \end{bmatrix} = \begin{bmatrix} 19.15 \\ 14.89 \\ 18.97 \end{bmatrix}$$

The values of heads at row 3's nodes are obtained by a similar procedure.

$$B_2 = B_3 = -\left(2 + \frac{2 \times 0.003 \times 400^2}{240 \times 1}\right) = -6$$

$$q = \frac{Q}{\Delta x \Delta y} = \frac{-0.09}{300 \times 400} = -0.0648 \frac{\text{m}}{\text{day}}$$

$$D_2 = -\frac{400^2}{300^2} \times 20 - \left(\frac{2 \times 0.003 \times 400^2}{240 \times 1} - \frac{2 \times 400^2}{300^2} \right) \times 20 - \frac{400^2}{300^2} \times 20$$

$$- \frac{-0.0648 \times 400^2}{240} = -36.9$$

Now, we have two unknown variables and a set of two equations:

$$\begin{bmatrix} -6 & 1 \\ 1 & -5 \end{bmatrix} \begin{bmatrix} h_{3,2}^{\frac{1}{2}} \\ h_{3,3}^{\frac{1}{2}} \end{bmatrix} = \begin{bmatrix} -56.9 \\ -80 \end{bmatrix}$$

$$\begin{bmatrix} h_{3,2}^{\frac{1}{2}} \\ h_{3,3}^{\frac{1}{2}} \end{bmatrix} = \begin{bmatrix} 12.55 \\ 18.51 \end{bmatrix}$$

Since row 4 is an impermeable boundary, the values of heads at this row will have the same value as the heads in row 3. The values of nodal heads after sweeping in the x-direction are shown in [Figure 6.8](#).

The results of sweeping in the x-direction provide the necessary data for sweeping in the y-direction.

Sweeping in the y-direction:

The results of the first step are the initial heads of the second step. In this step, computations are made by column. Therefore, for column 2 ($j = 2$), we have:

$$B_1 = -\left(2 + \frac{2 \times 0.003 \times 300^2}{240 \times 1}\right) = -4.25$$

$$B_1 = B_2 = B_3 = -4.25$$

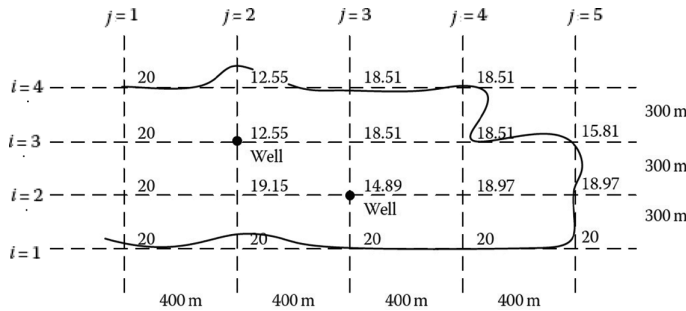


FIGURE 6.8 The results of sweeping in the x -direction.

As the aquifer in this direction extends beyond the grid boundary, the head outside of the boundary is included and assumed to be equal to the initial head of 20 m.

And:

$$D_1 = -\frac{300^2}{400^2} \times 20 - \left(\frac{2 \times 0.003 \times 300^2}{240 \times 1} - \frac{2 \times 300^2}{400^2} \right) \times 20 - \frac{300^2}{400^2} \times 20 - \frac{0 \times 300^2}{240} = -45$$

$$D_2 = -\frac{300^2}{400^2} \times 20 - \left(\frac{2 \times 0.003 \times 300^2}{240 \times 1} - \frac{2 \times 300^2}{400^2} \right) \times 19.15 - \frac{300^2}{400^2} \times 14.89 - \frac{0 \times 300^2}{240} = -41.17$$

$$D_3 = -\frac{300^2}{400^2} \times 20 - \left(\frac{2 \times 0.003 \times 300^2}{240 \times 1} - \frac{2 \times 300^2}{400^2} \right) \times 12.55 - \frac{300^2}{400^2} \times 18.51 - \frac{-0.0648 \times 300^2}{240} = -11.48$$

For node $j = 2$ & $i = 1$:

$$20 - 4.25h_{1,2}^1 + h_{2,2}^1 = -45$$

For node $j = 2$ & $i = 2$:

$$h_{1,2}^1 - 4.25h_{2,2}^1 + h_{3,2}^1 = -41.17$$

For node $j = 2$ & $i = 3$:

$$h_{2,2}^1 - 4.25h_{3,2}^1 + h_{4,2}^1 = -11.48$$

Now, we have three unknown variables and a set of three equations:

$$\begin{bmatrix} -4.25 & 1 & 0 \\ 1 & -4.25 & 1 \\ 0 & 1 & -3.25 \end{bmatrix} \begin{bmatrix} h_{1,2}^1 \\ h_{2,2}^1 \\ h_{3,2}^1 \end{bmatrix} = \begin{bmatrix} -65 \\ -41.17 \\ -11.48 \end{bmatrix}$$

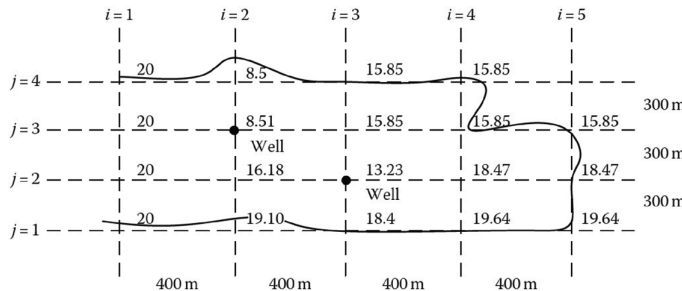


FIGURE 6.9 Heads at the end of day one.

$$\begin{bmatrix} h_{1,2}^1 \\ h_{2,2}^1 \\ h_{3,2}^1 \end{bmatrix} = \begin{bmatrix} 19.10 \\ 16.18 \\ 8.51 \end{bmatrix}$$

Again, the heads at all nodes in the columns are obtained by a similar procedure. The values of nodal heads at the end of day one (after $t = 1$ day) are shown in Figure 6.9. As illustrated in this figure, the values of heads in row 4 are the same as in row 3, which is because of the impermeable boundaries.

Example 6.5: Tutorial

This tutorial presents a model to simulate groundwater level variations using the ADI method, as explained in Section 6.4.3, after illustrating how to locate a suitable site for artificial recharge. The studied aquifer is located in Ghorveh Dehghan, in the western part of Iran. There has been a considerable decrease in the level of groundwater table in this alluvial aquifer due to overexploitation. This modeling effort implements artificial recharge strategies to raise groundwater level.

First, appropriate areas for artificial recharge are identified using geographic information system (GIS) analysis on recharge and groundwater characteristics. The Soil and Water Assessment Tool (SWAT), developed by the USDA Agricultural Research Service and Texas A&M AgriLife Research Lab, is used to obtain actual penetration rates before and after artificial recharge in the region.

In order to develop GIS maps that show appropriate locations for artificial recharge, certain parameters must be defined as listed below and a GIS layer should be created for each of these parameters. To develop raster layers, point data are collected for each parameter and an interpolation method (kriging) is used to generate regional layers from the collected point data.

In this study, seven raster layers have been developed for the parameters of surface slope, soil permeability, alluvium thickness, transmissivity, drainage density, land use, and electrical conductivity. Then, multicriteria decision-making systems and the Analytical Hierarchy Process method are used to assign specific weights to each layer, based on the importance of the corresponding parameter. The Analytical Hierarchy Process is a comprehensive system designed for multicriteria decision-making and relies on three principles: analysis, comparative judgments, and combination of priorities (Saaty, 1980). This process allows

a sensitivity analysis of criteria and subcriteria. Other important advantages of this technique include clarification of consistency, and inconsistency of decisions, as well as identification and prioritization of the decision-making elements. In order to overlay the weighted layers and prepare final maps, Boolean (Machiwal and Singh, 2015) and fuzzy logic (Shadid et al., 2000) as well as GIS analyses are used. The Boolean algorithm classifies all events such as land use and naturally and artificially created events into proper and improper events to locate a suitable site for artificial recharge. In the fuzzy logic method, all parameters and components of a layer are given a membership function between 0 and 1. According to this division, each of them is valued, and the layer with the highest cumulative value is selected for the site.

Analyzing the generated maps, two regions showed higher potential for artificial recharge, regions A and B in [Figure 6.10](#).

Following the identification of suitable areas for artificial recharge, the SWAT model is developed for the area to investigate variations in soil water penetration. Main input data include soil maps, land use, daily rainfall, daily temperature, and average monthly discharge. The average monthly data for the hydrometric stations are available from 1988 to 2015. After constructing the model, effective parameters are identified through a sensitivity analysis. The Sequential Uncertainty Fitting algorithm has been linked to the SWAT (Abbaspour et al., 2007). The Sequential Uncertainty Fitting-2 algorithm is used for model calibration and uncertainty analysis of parameters of a SWAT model.

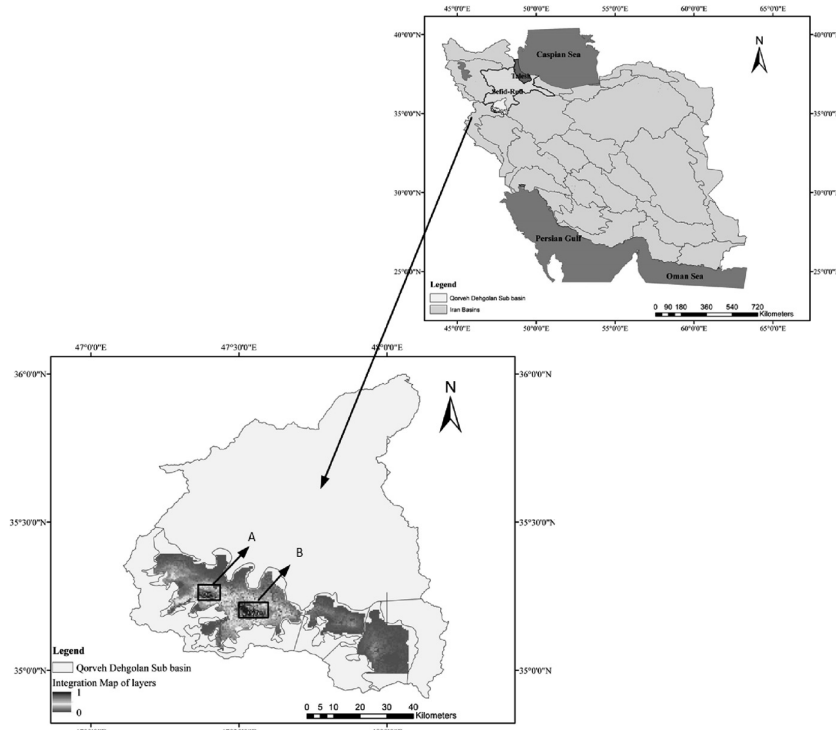


FIGURE 6.10 Watershed area and locations of regions A and B.

In order to investigate the amount of infiltrated water into regions A and B, four reservoirs are assumed to be located in these areas (Figure 6.11). The calibrated SWAT model is then run for two scenarios, before and after artificial recharge through the reservoirs, and the difference in water penetration between the two scenarios is evaluated as shown in Figures 6.12 and 6.13.

In order to simulate groundwater level variations, an ADI method-based model, called the Teymoor model, is used. This model has been developed in MATLAB to simulate the aquifer state before artificial groundwater recharge.

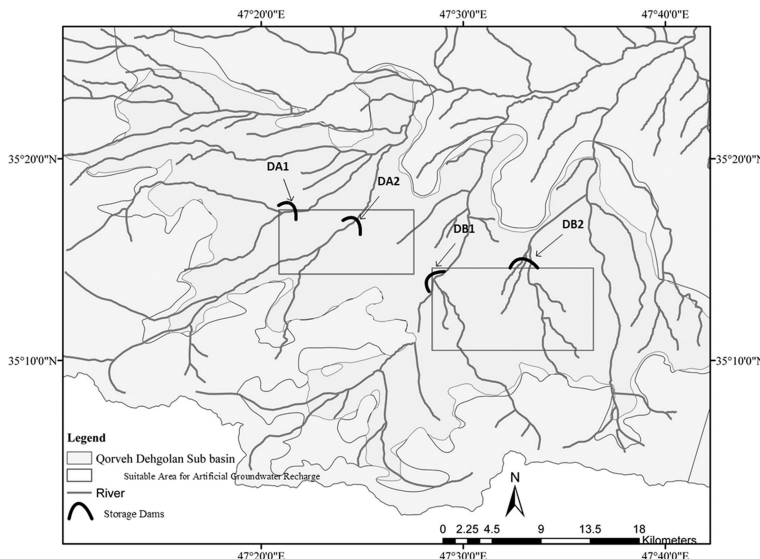


FIGURE 6.11 Water storage tanks locations in selected areas for artificial recharge.

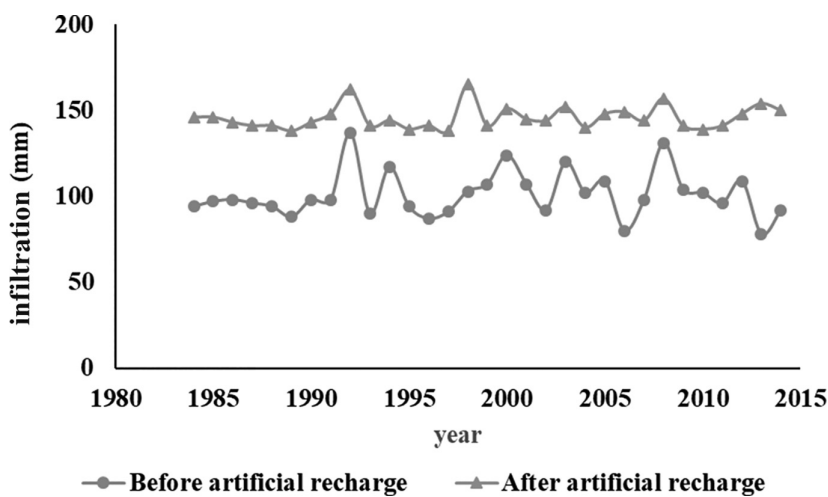


FIGURE 6.12 Average penetrated water (mm) in region A before and after artificial recharge.

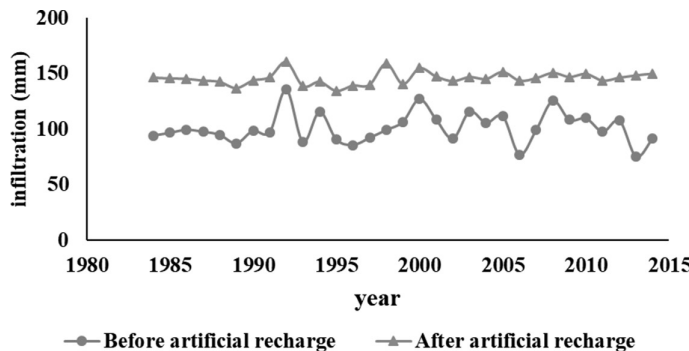


FIGURE 6.13 Average penetrated water (mm) in region B before and after artificial recharge.

- Specification of regions A and B in the Teymoor model:
Region A includes 240 square grids of 500 * 500 meters, with a total area of 6000 hectares and four observation wells. Region B consists of 608 squared grids with similar sizes with a total area of 15,200 hectares and nine observation wells. There are 260 wells with an annual discharge of 25 million cubic meters (MCM) in region A and 450 wells with an annual discharge of 69 MCM in region B.
- Model inputs:
Aquifer thickness matrix (b), initial hydraulic conductivity matrix (k), and hydraulic head (h), each included in a separate excel file.
Aquifer transmissivity (T) is obtained by multiplying aquifer thickness by its hydraulic conductivity ($b * k$).
The aquifer storage coefficient for both regions is the same and equal to 0.011.
- Initial conditions:
The initial condition is the groundwater level at the beginning of the first year (1988).
- Boundary conditions:
 - Without flow: In this type of boundary condition, the head and flow rate changes in the boundaries are considered zero.
 - With flow: In this case, the aquifer is bounded by a stream on the left and right sides, so a column of grids is considered outside the region on these sides. The top and bottom of the region is impermeable.
 In order to calibrate the model and obtain K and S values based on the range of variations provided for each parameter, the model is executed and the best values of K and S , which have the highest R^2 coefficient and the lowest Root Mean Square Error (RMSE) in the observed wells are selected.
- Model Calibration
In order to calibrate the model, hydraulic head (h) is considered constant and aquifer storage coefficient (S) and hydraulic conductivity (K) are adjusted. Using observation wells data, initial values for storage coefficient and hydraulic conductivity values are identified. These values are then adjusted to obtain the lowest error rate between the observed and simulated aquifer levels.

%The code of Teymoor Model Before AGR includes the calibration code and the implementation of the model before artificial recharge, and simulates the current aquifer state for obtaining calibrated hydraulic conductivity and storage coefficient values.

```
clearvars -except hc  
close all  
clc;
```

% This part of the code includes entering some basic information to run the model such as initial aquifer level for the years of implementation from 1988 to 2015 named in the form of a matrix called the hinit.

Because the groundwater level has been measured from the sea level, the bedrock level should be reduced

%from the groundwater level to measure the level of water from the bedrock.

```
load hinit  
load bastarA%bedrock level
```

%Grid Size

```
DeltaX=500; %length of the flow network  
DeltaY=500; % length and width of the flow network
```

```
A=DeltaX*DeltaY;
```

%Initial storage coefficient

```
S=0.011;
DeltaT=0.5;
for i=1:28
hinit(:,:,i)=hinit(:,:,i)-bastarA;
end
```

```
load b %Aquifer thickness  
load k %Initial hydraulic conductivity matrix
```

```
K=mean2(k);
TA = b.*K; % Transmissivity matrix
```

```

TA= b.*K; %Transmissivity matrix
h0=hinit(:, :, 1); %initial aquifer level for the years of implementation from
1988 to 2015

```

N_{rows} (b0, 1) : % Number of rows

M_size = (b, 2); % Number of columns

% recharge and decharge

load netdechargeA %natural discharge
load netrechargeA %natural recharge

```
load netrechargeGA %natural recharge  
welldechargeA=4.08; %amount of withdrawn from the groundwater  
precipitationA=1.5896; %amount of infiltration in the aquifer
```

pre
p-1

%-amount of artificial recharge

ACRA = 0; %3.96*10^-4 (After artificial recharge for this case study)

dechargeA-net dechargeA-ntkwell dechargeA-

rechargeA-netrechargeA+precipitationAtones (28.1)

```

for i=1:length(rechargeA)
    recharge(:,:,i)= rechargeA(i)*ones(N,M) ;
    decharge(:,:,i)= dechargeA(i)*ones(N,M) ;
    AGR(:,:,i)= AGRA*ones(N,M) ;
end
%The final value of the withdrawal from the aquifer, which is the difference
%between inputs and outputs to the aquifer, for each year, is indicated by
%a matrix called q1 with unit liters per sec. And multiplied by 86.4 to
%convert this amount to per cubic meter per year and denoted by q.
q1 = decharge(:,:,1)- recharge(:,:,1)-AGR(:,:,1); %for 1st year
q=q1*86.4;

htotal(:,:,1)=h0(2:N-1,2:M-1);

nwell=4;
%%%%%%%%%%%%%ADI method
%In order to solve the pentadiagonal system of equations ADI method has been used.
%The algorithm produces two sets of tridiagonal simultaneous equations to be solved in
sequence.
%This tridiagonal matrix can be solved by tridig function it in MATLAB.
%%%%%%%%%%%%%
T=TA(2:N-1,2:M-1);
N=N-2;
M=M-2;

%Number of year for calibration
calib=20;
K=linspace(1,20,20);
%For the aquifer storage coefficient,
%it is considered that the model is implemented for all values in this range
SS=linspace(0.0003,0.0030,20);
%Sweep over rows
for r=1:length(SS)
S=SS(r);
for s=1:length(K)
    TA=b.*K(s);
    T=TA(2:N+1,2:M+1);
%To calculate B and D, it is necessary to determine the discharge or recharge values
%again in the form of a matrix called q, as well as the initial equilibrium value
%for each node with the matrices h0 and h00.
    for t=1:27
        h0=hinit(:,:,t);
        h00=htotal(:,:,t);
        q1 = decharge(:,:,t)- recharge(:,:,t)+AGR(:,:,t);
        q=q1*86.4;
        for j=1:N
            D1(1)=h0(1,1);
            B1(1)=1;
            if j==1
                for i=1:M
                    B1(i)=-(2+S/T(j,i)*DeltaX^2/DeltaT);

```

(Continued)

```

D1(i)=-h00(j,i)*(DeltaX/DeltaY)^2-h00(j,i)* ...
(S/T(j,i)*DeltaX^2/DeltaT-2*(DeltaX/
DeltaY)^2) - ...
h00(j+1,i)*(DeltaX/DeltaY)^2+q(j,i)/
A*(DeltaX^2/T(j,i));
end
elseif j==N
for i=1:M
B1(i)=- (2+S/T(j,i)*DeltaX^2/DeltaT);
D1(i)=-h00(j,i)*(DeltaX/DeltaY)^2-h00(j,i)* ...
(S/T(j,i)*DeltaX^2/DeltaT-2*(DeltaX/
DeltaY)^2) - ...
h00(j,i)*(DeltaX/DeltaY)^2+q(j,i)/
A*(DeltaX^2/T(j,i));
end
else
for i=1:M
B1(i)=- (2+S/T(j,i)*DeltaX^2/DeltaT);
D1(i)=-h00(j-1,i)*(DeltaX/DeltaY)^2-h00(j,i)* ...
(S/T(j,i)*DeltaX^2/DeltaT-2*(DeltaX/
DeltaY)^2) - ...
h00(j+1,i)*(DeltaX/DeltaY)^2+q(j,i)/
A*(DeltaX^2/T(j,i));
end
end
aa(1)=1;
aa(2:M-1)=B1(2:M-1);
aa(M)=1;
bb(1)=0;
bb(M)=0;
bb(2:M-1)=1;
cc=bb;
ff(1)=h0(j+1,1);
ff(2:M)=D1(2:M);
ff(M)=h0(j+1,M+1);
hstar1(j,:)=tridiag(aa,bb,cc,ff);
end
h1=hstar1;
hstar1(1,:)=hstar1(2,:);
hstar1(N,:)=hstar1(N-1,:);
h1=hstar1;
%sweep over columns
for i=1:M
if i==1
h1(:,i)=h0(2:N+1,1);
continue
elseif i==M
h1(:,i)=h0(2:N+1,i+2);
continue
else
for j=1:N

```

(Continued)

```

B2(j)=- (2+S/T(j,i))*DeltaY^2/DeltaT);
D2(j)=-hstar1(j,i-1)*(DeltaY/DeltaX)^2-hstar1
(j,i)* ...
(S/T(j,i)*DeltaY^2/DeltaT-2*(DeltaY/
DeltaX)^2)- ...
hstar1(j,i+1)*(DeltaY/DeltaX)^2+q(j,i)/
A*(DeltaY^2/T(j,i));
end
aa2(1:N-1)=B2(1:N-1);
aa2(N)=1+B2(N);
bb2(1)=0;
bb2(2:N)=1;
cc2(1)=2;
cc2(2:N-1)=1;
cc2(N)=0;
ff2(1:N)=D2;
tridiag(aa2,bb2,cc2, ff2);
h1(:,1)=tridiag(aa2,bb2,cc2, ff2);
h1(1,:)=h1(2,:);
h1(N,:)=h1(N-1,:);
end
RMSE=(1/nwell*((h1(8,1)-h00(8,1))^2+(h1(3,3)-h00(3,3))^2+ ...
(h1(9,7)-h00(9,7))^2+(h1(6,19)-h00(6,19))^2))^0.5;
htotal(:, :, t+1) = h1;
end
well1sim(:)=htotal(8,1,1:calib);
well1obs(:)=hinit(9,2,1:calib);

R2well1=sum((well1obs(:)-mean(well1obs(:))).* ...
((well1sim(:)-mean(well1sim(:))))^2/(sum((well1obs(:)- ...
mean(well1obs(:))).^2)*sum((well1sim(:)-mean ...
(well1sim(:))).^2)))

well2sim(:)=htotal(3,3,1:calib);
well2obs(:)=hinit(4,4,1:calib);
R2well2=sum((well2obs(:)-mean(well2obs(:))).* ...
((well2sim(:)-mean(well2sim(:))))^2/(sum((well2obs(:)- ...
mean(well2obs(:))).^2)*sum((well2sim(:)-mean ...
(well2sim(:))).^2)))

well3sim(:)=htotal(9,7,1:calib);
well3obs(:)=hinit(10,8,1:calib);
R2well3=sum((well3obs(:)-mean(well3obs(:))).* ...
((well3sim(:)-mean(well3sim(:))))^2/(sum((well3obs(:)- ...
mean(well3obs(:))).^2)*sum((well3sim(:)-mean ...
(well3sim(:))).^2)))

well4sim(:)=htotal(6,19,1:calib);
well4obs(:)=hinit(7,20,1:calib);
R2well4=sum((well4obs(:)-mean(well4obs(:))).* ...
((well4sim(:)-mean(well4sim(:))))^2/(sum((well4obs(:)- ...
mean(well4obs(:))).^2)*sum((well4sim(:)-mean ...
(well4sim(:))).^2)))

```

(Continued)

```

mean(well4obs(:))) .^2)*sum((well4sim(:)-mean
(well4sim(:))) .^2))

R2selective(r,s)=mean([R2well1,R2well2,R2well3,R2well4])

end
end
% Calibration
[row, col] = find(ismember(R2selective, max(R2selective(:)))) )
R2selective(row,col);
Sselective=SS(row); %Selected S
Kselective=K(col); %Selected K
%Considering the calibrated values for K and S, values B and D are obtained again, and
the model is first
%performed in a row and then in a column.
TA=b.*Kselective;
T=TA(2:N+1,2:M+1);
S=Sselective
valid=28;

for t=1:27
h0=hinit(:,:,t);
h00=htotal(:,:,t);
for j=1:N
D1(1)=h0(1,1);
B1(1)=1;
if j==1
for i=1:M
B1(i)=- (2+S/T(j,i)*DeltaX^2/DeltaT);
D1(i)=-h00(j,i)*(DeltaX/DeltaY)^2-h00(j,i)* ...
(S/T(j,i)*DeltaX^2/DeltaT-2*(DeltaX/
DeltaY)^2)- ...
h00(j+1,i)*(DeltaX/DeltaY)^2+q(j,i)/A* ...
(DeltaX^2/T(j,i));
end
elseif j==N
for i=1:M
B1(i)=- (2+S/T(j,i)*DeltaX^2/DeltaT);
D1(i)=-h00(j,i)*(DeltaX/DeltaY)^2-h00(j,i)* ...
(S/T(j,i)*DeltaX^2/DeltaT-2*(DeltaX/DeltaY)^2)- ...
h00(j,i)*(DeltaX/DeltaY)^2+q(j,i)/A* ...
(DeltaX^2/T(j,i));
end
else
for i=1:M
B1(i)=- (2+S/T(j,i)*DeltaX^2/DeltaT);
D1(i)=-h00(j-1,i)*(DeltaX/DeltaY)^2-h00(j,i)* ...
(S/T(j,i)*DeltaX^2/DeltaT-2*(DeltaX/
DeltaY)^2)- ...
h00(j+1,i)*(DeltaX/DeltaY)^2+q(j,i)/A* ...
(DeltaX^2/T(j,i));
end
end
end

```

(Continued)

```

aa(1)=1;
aa(2:M-1)=B1(2:M-1);
aa(M)=1;
bb(1)=0;
bb(M)=0;
bb(2:M-1)=1;
cc=bb;
ff(1)=h0(j+1,1);
ff(2:M)=D1(2:M);
ff(M)=h0(j+1,M+1);
hstar1(j,:)=tridiag(aa,bb,cc,ff);
end
h1=hstar1;
hstar1(1,:)=hstar1(2,:);
hstar1(N,:)=hstar1(N-1,:);
h1=hstar1;
%sweep over columns
for i=1:M
    if i==1
        h1(:,i)=h0(2:N+1,1);
        continue
    elseif i==M
        h1(:,i)=h0(2:N+1,i+2);
        continue
    else
        for j=1:N
            B2(j)=- (2+S/T(j,i)*DeltaY^2/DeltaT);
            D2(j)=-hstar1(j,i-1)*(DeltaY/
                DeltaX)^2-hstar1(j,i)* ....
                (S/T(j,i)*DeltaY^2/DeltaT-2*(DeltaY/
                DeltaX)^2) - ....
                hstar1(j,i+1)*(DeltaY/DeltaX)^2+q(j,i)/
                A*(DeltaY^2/T(j,i));
        end
    end
    aa2(1:N-1)=B2(1:N-1);
    aa2(N)=1+B2(N);
    bb2(1)=0;
    bb2(2:N)=1;
    cc2(1)=2;
    cc2(2:N-1)=1;
    cc2(N)=0;
    ff2(1:N)=D2;
    tridiag(aa2,bb2,cc2, ff2);
    h1(:,i)=tridiag(aa2,bb2,cc2, ff2);
    h1(1,:)=h1(2,:);
    h1(N,:)=h1(N-1,:);
end
%%%%%%%%%%%%%
%Based on the calibrated values for K and S, the RMSE error rate, as well as the
%correlation coefficient R^2, are calculated for the observation wells in the region and the
%lowest error is obtained.
%%%%%%%%%%%%%

```

(Continued)

```

RMSE=(1/nwell*((h1(8,1)-h00(8,1))^2+(h1(3,3)-h00(3,3))^2+...
...+(h1(9,7)-h00(9,7))^2+(h1(6,19)-h00(6,19))^2))^0.5;
htotal(:,:,t+1)= h1;
end
clear well1sim well1obs well2sim well2obs well3sim well3obs
well4sim well4obs
well1sim(:)=htotal(8,1,1:valid);
well1obs(:)=hinit(9,2,1:valid);
R2well1=sum((well1obs(:)-mean(well1obs(:))).* ...
((well1sim(:)-mean(well1sim(:))))^2/(sum((well1obs
(:)- ...
mean(well1obs(:))).^2)*sum((well1sim(:)-mean(well1sim
(:))).^2))

well2sim(:)=htotal(3,3,1:valid);
well2obs(:)=hinit(4,4,1:valid);
R2well2=sum((well2obs(:)-mean(well2obs(:))).* ...
((well2sim(:)-mean(well2sim(:))))^2/
(sum((well2obs(:)- ...
mean(well2obs(:))).^2)*sum((well2
sim(:)-mean(well2sim(:))).^2))

well3sim(:)=htotal(9,7,1:valid);
well3obs(:)=hinit(10,8,1:valid);
R2well3=sum((well3obs(:)-mean(well3obs(:))).* ...
((well3sim(:)-mean(well3sim(:))))^2/(sum((well3obs
(:)- ...
mean(well3obs(:))).^2)*sum((well3sim(:)-mean(well3sim
(:))).^2))

well4sim(:)=htotal(6,19,1:valid);
well4obs(:)=hinit(7,20,1:valid);
R2well4=sum((well4obs(:)-mean(well4obs(:))).* ...
((well4sim(:)-mean(well4sim(:))))^2/(sum((well4obs
(:)- ...
mean(well4obs(:))).^2)*sum((well4sim(:)-mean(well4sim
(:))).^2))

```

- Model Verification

Based on the coefficients obtained during the calibration period, validation has been done for 8 years. The results are shown in [Figures 6.14](#) and [6.15](#).

- Outputs:

By implementing the model, simulated groundwater levels and groundwater levels after artificial recharge are obtained. Graphs of simulated groundwater level before and after artificial recharge for observation wells are plotted.

The output of the model for one of the wells is presented in [Figure 6.16](#), which shows groundwater level has increased after artificial recharge.

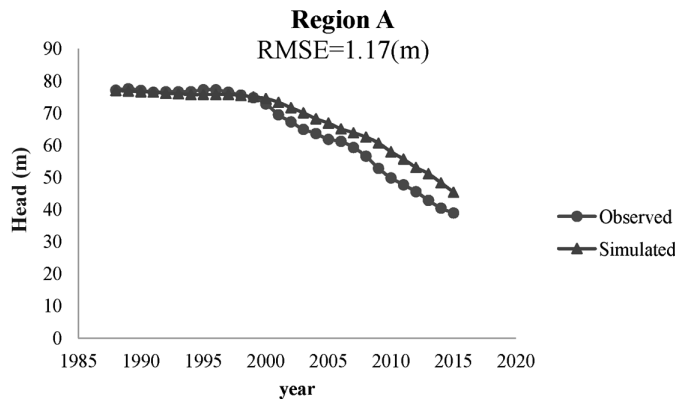


FIGURE 6.14 Observed and simulated groundwater levels in region A.

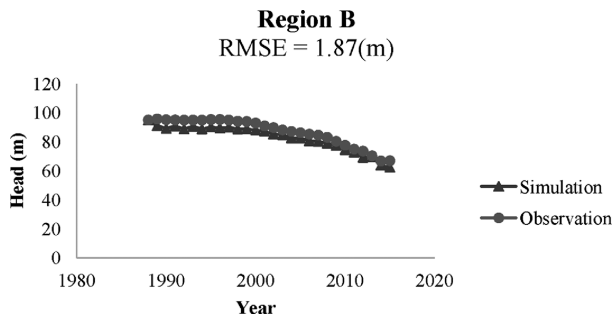


FIGURE 6.15 Observed and simulated groundwater levels in region B.

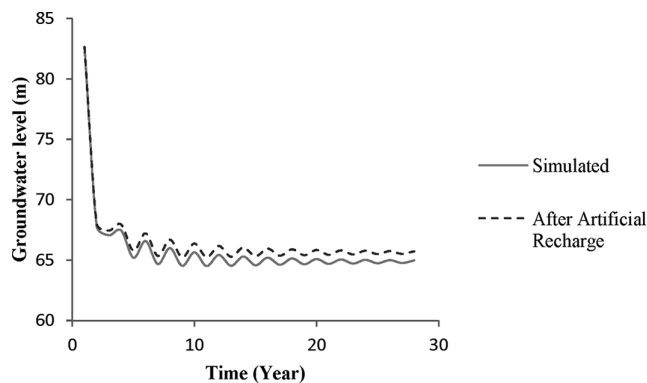


FIGURE 6.16 Groundwater level variation before and after artificial recharge.

6.4.4 CRANK–NICOLSON DIFFERENCE EQUATION

The Crank–Nicolson method is based on a central difference in space. It is the average of forward Euler and backward Euler in time. For example, in one dimension, if the partial differential equation is

$$\frac{\partial u}{\partial t} = F\left(u, x, t, \frac{\partial h}{\partial x}, \frac{\partial^2 h}{\partial x^2}\right) \quad (6.30)$$

then, letting $h(i\Delta x, n\Delta t) = h_i^n$, the Crank–Nicolson method is the average of the forward Euler method at n and the backward Euler method at $n + 1$. The forward difference equation can be expressed as:

$$\frac{u_i^{n+1} - u_i^n}{\Delta t} = F_i^n\left(u, x, t, \frac{\partial h}{\partial x}, \frac{\partial^2 h}{\partial x^2}\right) \quad (6.31)$$

The backward difference equation can be shown as:

$$\frac{u_i^{n+1} - u_i^n}{\Delta t} = F_i^{n+1}\left(u, x, t, \frac{\partial h}{\partial x}, \frac{\partial^2 h}{\partial x^2}\right) \quad (6.32)$$

The Crank–Nicolson difference equation is formulated as:

$$\frac{u_i^{n+1} - u_i^n}{\Delta t} = \frac{1}{2}\left(F_i^n\left(u, x, t, \frac{\partial h}{\partial x}, \frac{\partial^2 h}{\partial x^2}\right) + F_i^{n+1}\left(u, x, t, \frac{\partial h}{\partial x}, \frac{\partial^2 h}{\partial x^2}\right)\right) \quad (6.33)$$

The function F must be discretized spatially with a central difference. The discretization will also be nonlinear if the PDE is nonlinear. Thus, advancing in time will involve the solution of a system of nonlinear algebraic equations, although linearization is possible.

In groundwater modeling, the heads at all nodes are changed between time steps (n) and $(n + 1)$. Using head values at time (n) to approximate the space derivatives is valid only if relatively small time steps are considered. The approximation is improved by evaluating the space derivatives between $t = n\Delta t$ and $t = (n + 1)\Delta t$. It can be improved using a weighted average of the approximations at (n) and $(n + 1)$ as shown in [Figure 6.3c](#). The weighting parameter is represented by α , and it lies between 0 and 1. If time step $(n + 1)$ is weighted by α and time step (n) is weighted by $(1 - \alpha)$, then:

$$\frac{\partial^2 h}{\partial x^2} \cong \alpha \frac{h_{i-1,j}^{n+1} - 2h_{i,j}^{n+1} + h_{i+1,j}^{n+1}}{\Delta x^2} + (1 - \alpha) \frac{h_{i-1,j}^n - 2h_{i,j}^n + h_{i+1,j}^n}{\Delta x^2} \quad (6.34)$$

The parameter α is selected by the model. For $\alpha = 1$, the space derivatives are approximated solely at the advanced time level $(n + 1)$, and the finite-difference scheme is said to be fully implicit. Use of the fully implicit scheme implies that the value of the space derivatives at the future time is the best approximation. Use of the explicit scheme $\alpha = 0$ implies that the value of the space derivatives at the old time level is the best approximation. When $\alpha = 1/2$, the best value lies halfway between time levels (n) and $(n + 1)$. The FDA associated with a choice of $\alpha = 1/2$ is called the Crank–Nicolson method (Wang and Anderson, 1995).

Example 6.6

A plan view of an unconfined aquifer is shown in Figure 6.17. A mesh-centered grid system has been overlaid such that $\Delta x = \Delta y = 100$ m. The shaded area in the figure represents a gravel pit including 12 wells along its boundary for water pumping. Each well is to be pumped at a rate of 3500 m³/day. The hydraulic conductivity of the aquifer is 50 m/day and $S = 0.2$. The boundary conditions are also given. The heads are relative to a datum at the base of the aquifer. Compute the drawdowns in the gravel pit after 200 days of pumping. For initial conditions, use the steady-state head configuration without pumping. Write the mass balance calculation and incorporate it into your program (Wang and Anderson, 1995).

SOLUTION

The groundwater flow equation can be written as follows:

$$\frac{\partial}{\partial x} \left(K_x h \frac{\partial h}{\partial x} \right) + \frac{\partial}{\partial y} \left(K_y h \frac{\partial h}{\partial y} \right) = S \frac{\partial h}{\partial t} - R(x, y, t)$$

If $K_x = K_y = K$, then:

$$\frac{\partial}{\partial x} \left(\frac{K}{2} \frac{\partial h^2}{\partial x} \right) + \frac{\partial}{\partial y} \left(\frac{K}{2} \frac{\partial h^2}{\partial y} \right) = S \frac{\partial h}{\partial t} - R(x, y, t)$$

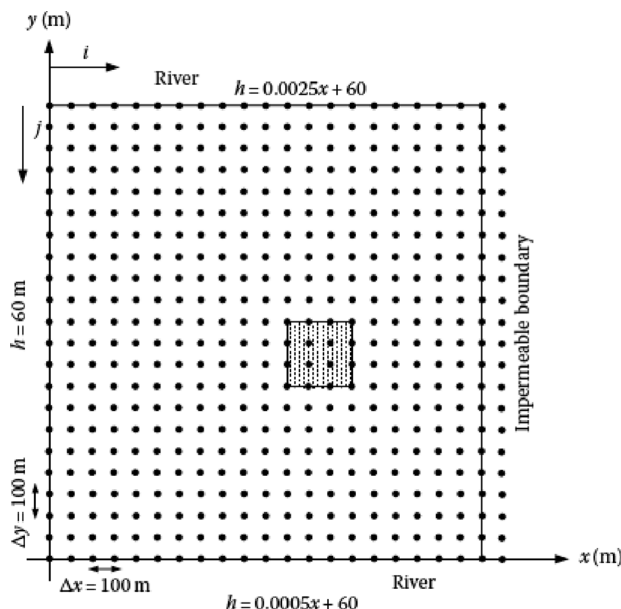


FIGURE 6.17 Discretization and boundary conditions of unconfined aquifer in Example 6.6.

or

$$\frac{K}{2} \left[\frac{\partial^2 h^2}{\partial x^2} + \frac{\partial^2 h^2}{\partial y^2} \right] = S \frac{\partial h}{\partial t} - R(x, y, t)$$

With assumption $V = h^2$, we have:

$$\frac{K}{2} \left[\frac{\partial^2 V}{\partial x^2} + \frac{\partial^2 V}{\partial y^2} \right] = S \frac{\partial h}{\partial t} - R(x, y, t)$$

Substituting Equation 6.34 using the Crank–Nicolson method, the transition flow equation can be approximated by:

$$\begin{aligned} \alpha \left(\tilde{V}_{i,j}^{n+1} - V_{i,j}^{n+1} \right) + (1 - \alpha) \left(\tilde{V}_{i,j}^n - V_{i,j}^n \right) &= \frac{a^2 S}{2} \frac{\sqrt{V_{i,j}^{n+1}} - \sqrt{V_{i,j}^n}}{K \Delta t} - \frac{a^2 R_{i,j}^n}{2K} \\ \tilde{V}_{i,j}^n &= \frac{V_{i-1,j}^n + V_{i+1,j}^n + V_{i,j-1}^n + V_{i,j+1}^n}{4} \end{aligned}$$

where $\Delta x = \Delta y = a$. All the unknowns are put on the left-hand side and all the known parameters on the right-hand side and multiply each side by -1 :

$$\left(\frac{a^2 S}{4K \Delta t \sqrt{V_{i,j}^{n+1}}} + \alpha \right) V_{i,j}^{n+1} - \alpha \tilde{V}_{i,j}^{n+1} = \frac{a^2 S}{4K \Delta t \sqrt{V_{i,j}^{n+1}}} V_{i,j}^n + (1 - \alpha) \left(\tilde{V}_{i,j}^n - V_{i,j}^n \right) + \frac{a^2 R_{i,j}^n}{2K}$$

The above equation represents a system of linear equations for $V_{i,j}$ at time level $(n + 1)$. As expressed in Figure 6.10, in the mesh-centered grid, $\Delta x = \Delta y = 100$ m. The right boundary is approximated as a symmetry boundary. In the computer model, the lower, upper, and left boundaries are also considered to be known boundaries. The groundwater flow equation for initial conditions, the steady-state flow without pumping, can be written as follows:

$$\frac{\partial}{\partial x} \left(K_x h \frac{\partial h}{\partial x} \right) + \frac{\partial}{\partial y} \left(K_y h \frac{\partial h}{\partial y} \right) = 0$$

If $K_x = K_y = K$, then:

$$\frac{K}{2} \left[\frac{\partial^2 h^2}{\partial x^2} + \frac{\partial^2 h^2}{\partial y^2} \right] = 0$$

With assumption $V = h^2$, we have:

$$\frac{K}{2} \left[\frac{\partial^2 V}{\partial x^2} + \frac{\partial^2 V}{\partial y^2} \right] = 0$$

Substituting Equation 6.34 using the Crank–Nicolson method, the transition flow equation can be approximated by:

$$\alpha \left(\tilde{V}_{i,j}^{n+1} - V_{i,j}^{n+1} \right) + (1 - \alpha) \left(\tilde{V}_{i,j}^n - V_{i,j}^n \right) = 0$$

$$\tilde{V}_{i,j}^n = \frac{V_{i-1,j}^n + V_{i+1,j}^n + V_{i,j-1}^n + V_{i,j+1}^n}{4}$$

This system can be solved directly using matrix methods or by iteration the same way as what is used to solve the system of linear equations for the steady-state Laplace's or Poisson's equation. The difference is that, for the transient flow problem, a new system of equations must be solved at each time step. A FORTRAN code is developed to solve this problem, which is shown in [Figure 6.18](#). It calculates the volume of water removed by pumping in the 12 nodes, the volume of water removed from storage over the entire aquifer, and the volume of water flowing across the boundaries. [Figures 6.19](#) and [6.20](#) show the computed water head at the initial condition and 200 days after pumping, respectively.

6.5 FINITE ELEMENT METHOD

Another numerical technique for the solution of groundwater flow and contaminant mass transport problems is the FEM. For many groundwater problems, the FEM is superior to classical finite-difference models. Groundwater problems with an irregular shape domain, complex boundary conditions, and material heterogeneity can be modeled using the FEM, while the FDM implies the complicated interpolation schemes to approximate complex boundary conditions.

In the FEM, the irregular shape domain can be divided into a set of elements with different sizes or shapes. In order to reflect variation of state variables or parameter values, the element sizes can be changed. The PDEs for the elements are approximated utilizing several approaches such as the direct approach, the weighted residual approach, and the variational approach to obtain a set of algebraic equations. The piecewise continuous representation of the dependent variables and, possibly, the parameters of the groundwater system can increase the accuracy of the numerical approximations (Karamouz et al., 2003).

6.5.1 DISCRETIZE THE PROBLEM DOMAIN

The problem domain is divided into some nonoverlapping elements as the first step in solving a groundwater flow or solute transport problem by the FEM. In this regard, the problem domain is replaced with a series of nodes and discrete elements or finite element mesh. The elements are generated by connecting two or more nodes together

```

14      CONTINUE
13      CONTINUE
TIME=-0.01
!START TIME STEPS
!AT EACH TIME STEP SOLVE SYSTEM OF EQUATIONS BY ITERATION
NEND=53
DO 5 N=1,NEND
TIME=TIME+DT
NUMIT=0
10      AMAX=0.
NUMIT=NUMIT+1
IF (NUMIT.GT.500) GO TO 50
IF (TIME.EQ.0.0) THEN
DO 45 J=2,22
VNEW(22,J)=VNEW(20,J)
45      CONTINUE
DO 15 I=2,21
DO 16 J=2,21
! FOR T=0 : R=0, H=H0, INDEPENDENT OF TIME
OLDVAL=VNEW(I,J)
VNEW(I,J)=(VNEW(I-1,J)+VNEW(I+1,J)+VNEW(I,J-1) +
VNEW(I,J+1)+2.*R(I,J)*DX* DX/K)/4.
VNEW(I,J)=OMEGA*VNEW(I,J)+(1.-OMEGA)*OLDVAL
ERR=ABS(VNEW(I,J)-OLDVAL)
IF (ERR.GT.AMAX) AMAX=ERR
16      CONTINUE
15      CONTINUE
ELSE
DO 87 I=2,21
DO 88 J=2,21
OLDVAL=VNEW(I,J)
V1=(VOLD(I,J+1)+VOLD(I,J-1)+VOLD(I+1,J)+VOLD(I-1,J))/4.
V2=(VNEW(I,J+1)+VNEW(I,J-1)+VNEW(I+1,J)+VNEW(I-1,J))/4.
F1=(DX*DX*S/(4*K*SQRT(VOLD(I,J))*DT)+ALPHA)
VNEW(I,J)=(ALPHA*V2+(F1-ALPHA)*VOLD(I,J) +
&(1-ALPHA)*(V1-VOLD(I,J))+DX*DX*R(I,J)/2/K)/F1
ERR=ABS(VNEW(I,J)-OLDVAL)
IF (ERR.GT.AMAX) AMAX=ERR
88      CONTINUE
87      CONTINUE
!BOUNDARY CONDITION ON RIGHT
DO 17 J=2,22
VNEW(22,J)=VNEW(20,J)
17      CONTINUE
END IF
IF (AMAX.GT.0.001) GO TO 10
50      DO 47 I=1,22
DO 48 J=1,22
IF (VNEW(I,J).LT.0)VNEW(I,J)=0.

```

FIGURE 6.18 FORTRAN program for solving Example 6.6.

(Continued)

```

drawdown example-unconfined aquifer- transient conditions
      DIMENSION HNEW(22,22),HOLD(22,22),R(22,22),DD(22,22),
      &H0(22,22),VNEW(22,22),VOLD(22,22)
      !DEFINE INPUT PARAMETERS
      S=0.2
      K=50.
      !H0 IS INITIAL HEAD
      P=60.
      DX=100.
      DT=.01
      SUML=0.
      SUMB=0.
      SUMT=0.
      Drawd1=0.
      Drawd2=0.
      SUMR=0.
      !USE CRANK-NICOLSON APPROXIMATION
      ALPHA=0.5
      !SET RELAXATION FACTOR
      OMEGA=1.8
      !INITIALIZE ARRAYS
      !HOLD IS HEAD AT THE TIME STEP N
      !HNEW IS HEAD AT THE TIME STEP N+1
      DO 3 I=1,21
      DO 4 J=1,22
      HNEW(I,J)=P
      HOLD(I,J)=P
      R(I,J)=0.
  4    CONTINUE
  3    CONTINUE
      DO 33 J=1,22
      HNEW(1,J)=60.
      HOLD(1,J)=60.
  33    CONTINUE
      DO 30 I=2,21
      HNEW(I,1)=.0025*(I-1)*100.+60.
      HOLD(I,1)=.0025*(I-1)*100.+60.
      HNEW(I,22)=.0005*(I-1)*100.+60.
      HOLD(I,22)=.0005*(I-1)*100.+60.
  30    CONTINUE
      DO 36 J=1,22
      HNEW(22,J)=HNEW(20,J)
      HOLD(22,J)=HOLD(20,J)
  36    CONTINUE
      !DEFINE PUMPING RATE AS RECHARGE TO CELL AT ORIGIN
      R0=-3500./DX/DX
      DO 13 I=1,22
      DO 14 J=1,22
      VNEW(I,J)=HNEW(I,J)*HNEW(I,J)
      VOLD(I,J)=HOLD(I,J)*HOLD(I,J)
      R(I,J)=0.

```

FIGURE 6.18 (Continued) FORTRAN program for solving Example 6.6.

```

HNEW(I,J)=SQRT(VNEW(I,J))
VOLD(I,J)=VNEW(I,J)
HOLD(I,J)=HNEW(I,J)
48  CONTINUE
47  CONTINUE
    ! PREPARE FOR NEXT TIME STEP
    ! PUT HNEW VALUES INTO HOLD ARRAY
    IF (TIME.EQ.0.) THEN
    DO 27 I=1,22
    DO 28 J=1,22
    H0(I,J)=HNEW(I,J)
28  CONTINUE
27  CONTINUE
    WRITE (50,74)
74  FORMAT(10X,"HEAD AT TIME=0 ",/7X,"*****")
    WRITE (50,31) ((HNEW(I,J),I=1,21),J=1,22)
    WRITE(50,75)
75  FORMAT(//10X,"HEAD IN STEADY STATE SOLUTION",/)
    ELSE
    DT=DT*1.5
    IF(DT.GT.5.0) DT=5.0
    END IF
    R(12,11)=R0
    R(13,11)=R0
    R(14,11)=R0
    R(15,11)=R0
    R(12,14)=R0
    R(13,14)=R0
    R(14,14)=R0
    R(15,14)=R0
    R(12,12)=R0
    R(12,13)=R0
    R(15,12)=R0
    R(15,13)=R0
    ! COMPUTE DRAWDOWN
    DO 25 I=1,22
    DO 26 J=1,22
    DD(I,J)=H0(I,J)-HNEW(I,J)
26  CONTINUE
25  CONTINUE
    DO 64 J=1,22
    SUML=SUML+K/2*(HNEW(1,J)**2-HNEW(2,J)**2)*DT
64  CONTINUE
    DO 65 I=1,22
    SUMT=SUMT+K/2*(HNEW(I,1)**2-HNEW(I,2)**2)*DT
    SUMB=SUMB+K/2*(HNEW(I,22)**2-HNEW(I,21)**2)*DT
65  CONTINUE
    ! PRINT RESULTS
    WRITE(50,29) TIME,DT,NUMIT

```

FIGURE 6.18 (Continued) FORTRAN program for solving Example 6.6.

```

29      FORMAT(1X,"TIME=",F9.2,5X,"DT=",F9.2,5X,"NUMIT=",I8,/)
30      WRITE(50,32)((DD(I,J),I=1,21),J=1,22)
31      FORMAT(1X,21F6.2)
32      FORMAT(21F4.2)
33      CONTINUE
34      DO 81 I=1,20
35      DO 82 J=1,22
36      Drawd1=Drawd1+DD(I,J)
37      CONTINUE
38      CONTINUE
39      DO 83 J=1,22
40      Drawd2=Drawd2+DD(21,J)
41      CONTINUE
42      Drawd1=.2*DX*DX*Drawd1
43      Drawd2=Drawd1+.1*DX*DX*Drawd2
44      SUMTOTAL=SUML+SUMB+SUMT
45      ERROR=1000*(SUMTOTAL+Drawd2-3500*12*200)/3500/200/12
46      WRITE(50,66) SUML,SUMT,SUMB,SUMTOTAL,Drawd2,ERROR
47      FORMAT(//5X,"SUML=",F10.1," SUMT=",F10.1,",
48      &SUMB=",F10.1," SUMTOTAL=",F11.1,/10X, "Drawdown=",
49      &F14.3,/5X,"ERROR=",F7.3,"%")
50      WRITE(50,85)
51      FORMAT(//10X,"FINAL HEAD"/,10X,"*****")
52      WRITE(50,31)((HNEW(I,J),I=1,21),J=1,22)
53      STOP
54      END

```

FIGURE 6.18 (Continued) FORTRAN program for solving Example 6.6.

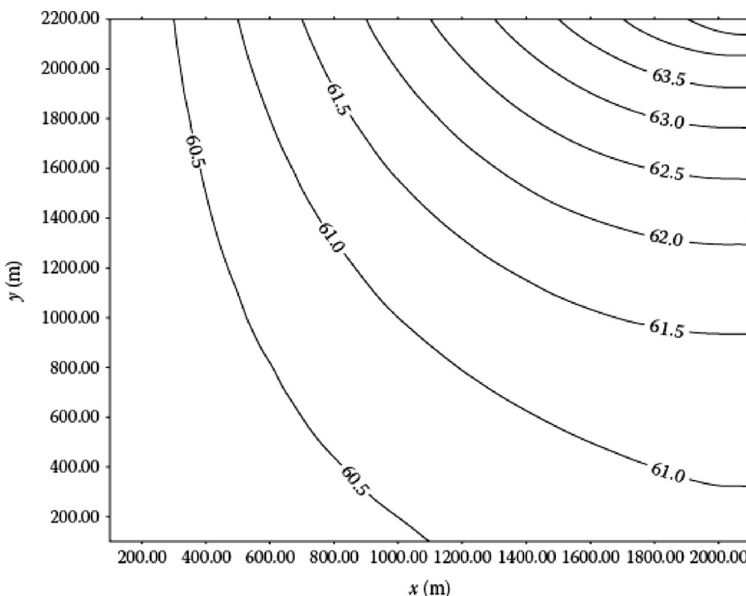


FIGURE 6.19 Water heads at initial condition (Example 6.6).

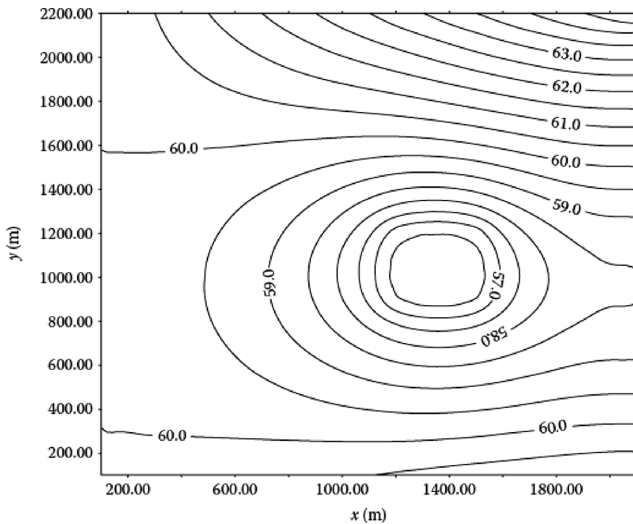


FIGURE 6.20 Water table contour after 200 days of pumping (Example 6.6).

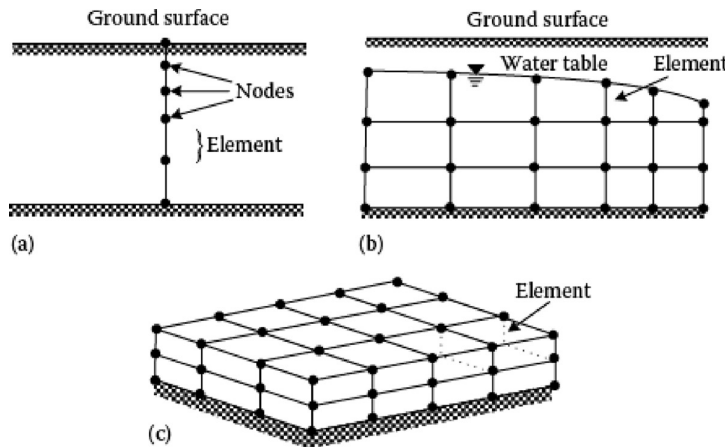


FIGURE 6.21 Discretization of (a) 1D, (b) 2D, and (c) 3D problem domains.

utilizing the lines as shown in Figure 6.21. Then, a node number is assigned to each node and an element number is assigned to each element. However, there is much computer software that creates this mesh. Elements can have one, two, or three dimensions with any size. Figure 6.22 shows different element types. In each element, the groundwater flow characteristics should be specified.

Drawing the mesh with the knowledge of the groundwater flow and solute transport process is a helpful way to achieve a groundwater system solution with a reasonable cost for computational burden and acceptable precision. This could be done with respect to flow or transport process visualization and flownets. The problem

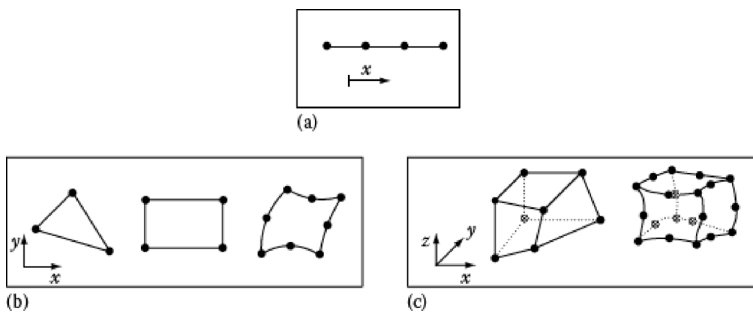


FIGURE 6.22 Some types of finite elements: (a) 1D, (b) 2D, and (c) 3D.

could be modeled using different finite element mesh types and the results could be similar. Thus, there is no unique choice of mesh type and size for modeling.

The finite element modeling with a fine mesh yields a more precise solution than a coarse mesh, which leads to a lower precision. A fine mesh has more nodes and requires more computational effort to obtain a solution, thus, it is a trade-off between the computational burden and the precision of modeling. The mesh size can be determined by repeating the calculations with a finer mesh and see how significantly the results change. In the first repetition of modeling, the coarse finite element mesh can be generated with a few nodes. Therefore, a solution can be derived with little computational effort. In the repetition of modeling, a finer finite element mesh can be prepared, which needs more computational effort and leads to a more precise solution. The modeling results of two repetitions are compared to investigate the improving results. If the change in the results is more than the tolerance modeling parameter, which is a predetermined parameter, and it is defined based on the acceptable level of precision, more mesh refinement is needed. Otherwise, the modeling process is stopped because no significant change in the computed values is achieved (Istok, 1989).

6.5.2 DERIVE THE APPROXIMATING EQUATIONS

After preparing the finite element mesh, the next step of groundwater modeling is to evaluate the integral formulation for the governing groundwater flow or solute transport equation. A system of algebraic equations is generated by implementation of the integral formulation over the domain. By solving the algebraic equations, the groundwater flow is simulated and the values of the field variable such as hydraulic head, pressure head, or solute concentration can be determined at each node in the mesh. Numerical integration methods are extensively employed to derive the integral formulation for a PDE that presents the groundwater flow and solute transport. The method of weighted residuals is the most common approach that is widely used in groundwater modeling.

In the method of weighted residuals, an approximate solution is developed and by replacing the approximate solution into the governing equation, the residual at each node is determined. The weighted average of the residuals for each point is supposed

to be equal to zero. In this method, the trial solution to the system's equations is expressed in terms of the differential operator L , as:

$$L(h - F) = 0 \quad (6.35)$$

where:

h is the field variable

F is a known function.

The approximate solution can be written as follows:

$$h \approx \hat{h}(x, t) = \sum_{i=1}^n N_i(x) \tilde{h}_i(t) \quad (6.36)$$

where:

\hat{h} is the approximate solution

$N_i(x)$ are the basis or shape functions of node i , defined over the entire domain,

n is the number of linearly independent shape functions

$\tilde{h}_i(t)$ are the unknown variables (heads) that are determined for each node of the finite element grid.

Regarding spatial variation of the state variables in the domain, shape function for each node can be defined, which are interpolation functions (Karamouz et al., 2003).

For example, the approximate solution for a 1D element with two nodes i and j , as shown in [Figure 6.23](#), can be formulated as follows:

$$\hat{h}^{(e)}(x) = N_i^{(e)}(x) h_i + N_j^{(e)}(x) h_j \quad (6.37)$$

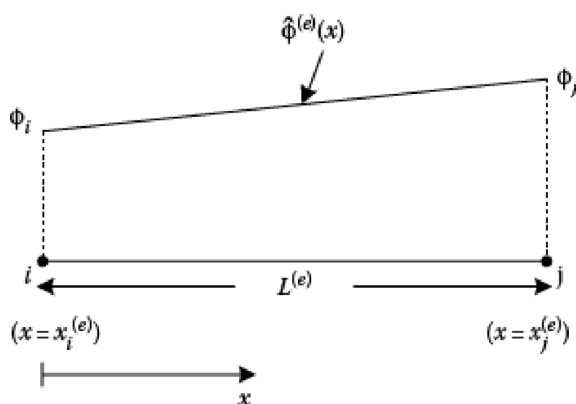


FIGURE 6.23 Approximate solution for an element.

or in the matrix form:

$$\hat{h}^{(e)}(x) = \left[N^{(e)} \right] \{h\} \quad (6.38)$$

where:

$$\left[N^{(e)} \right] = \left[N_i^{(e)}(x) \ N_j^{(e)}(x) \right] \quad (6.39)$$

$$\{h\} = \begin{cases} h_i(t) \\ h_j(t) \end{cases} \quad (6.40)$$

The interpolation functions are equal to one at each node and decrease linearly to zero at the node in the other side. The interpolation functions can be written as:

$$N_i^{(e)}(x) = \frac{x_j^{(e)} - x}{x_j^{(e)} - x_i^{(e)}} = \frac{x_j^{(e)} - x}{L^{(e)}} \quad (6.41)$$

$$N_j^{(e)}(x) = \frac{x - x_i^{(e)}}{x_j^{(e)} - x_i^{(e)}} = \frac{x - x_i^{(e)}}{L^{(e)}} \quad (6.42)$$

where $L^{(e)}$ is the element length. These interpolation functions are shown in Figure 6.24. The value of $\hat{h}(x, t)$ is h_i at node i and decreases linearly to h_j at node j , and at the midpoint of the element $x = (x_j + x_i)/2$ and $\hat{h}(x, t)$ is $h = (h_j + h_i)/2$.

Although many types of interpolation functions have been defined to develop an approximate solution for $\hat{h}(x, t)$, the linear interpolation functions are the most commonly used. Because the approximate solution does not satisfy Equation 6.35,

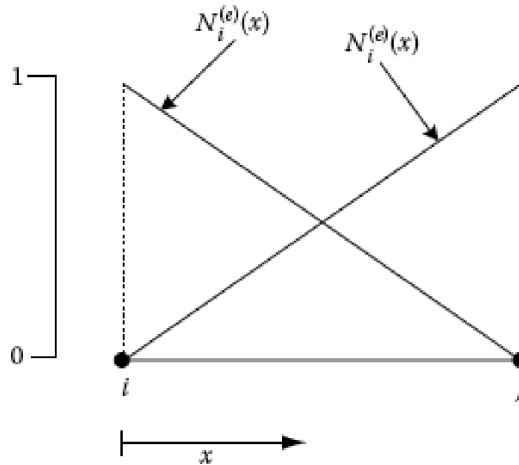


FIGURE 6.24 Linear interpolation functions for an element.

the residual or error R can be estimated by substituting the approximate solution \hat{h} into Equation 6.35 as follows:

$$R = L(\hat{h} - F) \neq 0 \quad (6.43)$$

In order to determine the unknown coefficients \tilde{h}_i , the residual of approximate solution is minimized. The estimation error may be different in each point in the calculation domain. Hence, the residual cannot be zero at certain specified points. The residual might have low value in some points, while it has large value in the other points. Thus, minimizing the errors is achieved by integrating the weighted average of the error over the domain (D) and setting it equal to zero as follows:

$$\int_D W_k R dD = \int_D W_k L(\hat{h}) dD = 0, k = 1, 2, \dots, n \quad (6.44)$$

where:

W_k is the weighting function in node i

D is a length in the 1D mesh or an area in the 2D mesh or a volume in the 3D mesh.

To determine the n state variables at nodal points, the weighting function should be specified and the integral equation can be calculated by breaking it into n simple equations.

The form of the weighting function W in Equation 6.44 must also be specified. The type of weighted residual method is selected by choosing the n weighting functions. Although several weighted residual methods such as the subdomain method, collocation method, and Galerkin method have been applied in water resource engineering, the Galerkin method is commonly used to represent the hydraulic and mass transport response equations of the aquifer system.

In the Galerkin method, the weighting function for a node is considered similar to the interpolation function used in the definition of the approximate solution for $\hat{h}(x, t)$. The modified integral equation (Equation 6.44) is then given by:

$$\int_D N_k L(\hat{h}) dD = 0, k = 1, 2, \dots, n \quad (6.45)$$

The modified integral equation is straightforward to solve and can be converted to n simultaneous algebraic equations of the form:

$$[K]\{h\} = \{F\} \quad (6.46)$$

where $[K]$ is the global conductance matrix. In order to develop this matrix, the conductance matrix is computed for all nodes, and then the global conductance matrix is

obtained for the finite element mesh. In Equation 6.46, $\{F\}$ addresses specified flow rates at boundary conditions. The system of algebraic equations is revised based on the known variables on the boundary condition, and unknown values are obtained by solving the equations.

Example 6.7

Solve the differential equation $d^2h/dx^2 - h = 0$ using the Galerkin method. Consider the following conditions:

$$0 \leq x \leq 5$$

$$h = 0 \text{ m where } x = 0$$

$$h = 8 \text{ m where } x = 5$$

SOLUTION

As shown in Figure 6.25, the problem domain is divided into four nodes/three elements, and for each node, a partially linear shape function $N_i(x)$ is considered. Therefore, the approximate function $\hat{h}(x, t)$, at node i , is defined as follows:

$$h \approx \hat{h}(x, t) = \sum_{i=1}^w N_i(x) \hat{h}_i(t), \quad 0 \leq x \leq 5$$

Considering the unknown variables h_1, h_2, \dots, h_4 , Equation 6.44 can be rewritten as follows:

$$\int_0^5 W_i \left(\frac{d^2 \hat{h}}{dx^2} - \hat{h} \right) dx = 0, \quad i = 1, 2, \dots, 4$$

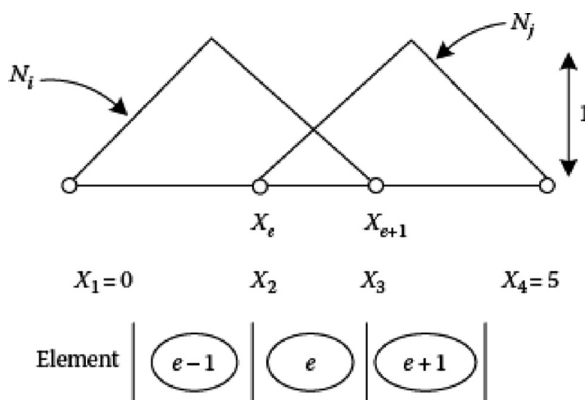


FIGURE 6.25 General numbering of nodes and elements of Example 6.7.

or

$$\int_0^5 \left(\frac{dW_i}{dx} \frac{d\hat{h}}{dx} + W_i \hat{h} \right) dx + \left[W_i \frac{d\hat{h}}{dx} \right]_0^5 = 0, \quad i = 1, 2, \dots, 4$$

This equation can then be rewritten as follows using the Galerkin method ($W_i = N_i$):

$$Kh = F$$

$$K_{ij} = \int_0^5 \left(\frac{dN_i}{dx} \frac{dN_j}{dx} + N_i N_j \right) dx, \quad 1 \leq i, j \leq 4$$

$$F_i = \left[N_i \frac{dh}{dx} \right]_0^5, \quad 1 \leq i \leq 4$$

If the above equation is used for each element (e) between nodes m and n , the coefficients of the equation can be calculated using Equations 6.41 and 6.42. Assuming $X = x - x_m$, the shape functions are as follows:

$$N_m = N_m^e = \frac{X}{L^e}$$

$$N_n = N_n^e = \frac{L^e - X}{L^e}$$

where $L^e = x_n - x_m$. Therefore, the components of matrix A are calculated as follows:

$$K_{mn}^e = K_{nm}^e = \int_0^{L^e} \left[\frac{dN_m^e}{dx} \frac{dN_n^e}{dx} + N_m^e N_n^e \right] dx = \frac{-1}{L^e} + \frac{L^e}{6}$$

$$K_{mm}^e = K_{nn}^e = \int_0^{L^e} \left[\left(\frac{dN_m^e}{dx} \right)^2 + (N_n^e)^2 \right] dx = \frac{1}{L^e} + \frac{L^e}{3}$$

The matrix K is calculated from submatrices K^e , considering the position of the element in [Figure 6.25](#). Assuming $L_1 = 2$ m, $L_2 = 1$ m, $L_3 = 2$ m, the matrices K^e and matrix K can be calculated as:

$$K^1 = \begin{bmatrix} \frac{1}{L_1} + \frac{L_1}{3} & \frac{-1}{L_1} + \frac{L_1}{6} & 0 & 0 \\ \frac{-1}{L_1} + \frac{L_1}{6} & \frac{1}{L_1} + \frac{L_1}{3} & 0 & 0 \\ 0 & 0 & 0 & 0 \\ 0 & 0 & 0 & 0 \end{bmatrix}$$

$$K^2 = \begin{bmatrix} 0 & 0 & 0 & 0 \\ 0 & \frac{1}{L_2} + \frac{L_2}{3} & \frac{-1}{L_2} + \frac{L_2}{6} & 0 \\ 0 & \frac{-1}{L_2} + \frac{L_2}{6} & \frac{1}{L_2} + \frac{L_2}{3} & 0 \\ 0 & 0 & 0 & 0 \end{bmatrix}$$

$$K^3 = \begin{bmatrix} 0 & 0 & 0 & 0 \\ 0 & 0 & 0 & 0 \\ 0 & 0 & \frac{1}{L_3} + \frac{L_3}{3} & \frac{-1}{L_3} + \frac{L_3}{6} \\ 0 & 0 & \frac{-1}{L_3} + \frac{L_3}{6} & \frac{1}{L_3} + \frac{L_3}{3} \end{bmatrix}$$

$$K = \begin{bmatrix} \frac{1}{L_1} + \frac{L_1}{3} & \frac{-1}{L_1} + \frac{L_1}{6} & 0 & 0 \\ \frac{-1}{L_1} + \frac{L_1}{6} & \left(\frac{1}{L_1} + \frac{L_1}{3}\right) + \left(\frac{1}{L_2} + \frac{L_2}{3}\right) & \frac{-1}{L_2} + \frac{L_2}{6} & 0 \\ 0 & \frac{-1}{L_2} + \frac{L_2}{6} & \left(\frac{1}{L_2} + \frac{L_2}{3}\right) + \left(\frac{1}{L_3} + \frac{L_3}{3}\right) & \frac{-1}{L_3} + \frac{L_3}{6} \\ 0 & 0 & \frac{-1}{L_3} + \frac{L_3}{6} & \frac{1}{L_3} + \frac{L_3}{3} \end{bmatrix}$$

Considering $Kh = F$, we have:

$$K \begin{bmatrix} h_1 \\ h_2 \\ h_3 \\ h_4 \end{bmatrix} = \begin{bmatrix} -\frac{d\hat{h}}{dx} \Big|_{x=0} \\ 0 \\ 0 \\ -\frac{d\hat{h}}{dx} \Big|_{x=5} \end{bmatrix}$$

h_1 and h_4 are known, therefore from the above equation set, we have:

$$\left(\frac{1}{L_1} + \frac{L_1}{3} + \frac{1}{L_2} + \frac{L_2}{3}\right)h_2 + \left(-\frac{1}{h_2} + \frac{L_2}{6}\right)h_3 = 0$$

$$\left(-\frac{1}{h_2} + \frac{L_2}{6}\right)h_2 + \left(\frac{1}{L_2} + \frac{L_2}{3} + \frac{1}{L_3} + \frac{L_3}{3}\right)h_3 = -8\left(-\frac{1}{h_3} + \frac{L_3}{6}\right)$$

if $L_1 = 2$ m, $L_2 = 1$ m, $L_3 = 2$ m, the results are as follows:
 $h_2 = 0.2$ m and $h_3 = 0.6$ m.

Example 6.8

Two parallel rivers A and B are separated by a confined aquifer as shown in [Figure 6.26](#). Consider the aquifer is multilayered and the lengths of layers are $L_1 = 2$ m, $L_2 = 3$ m, $L_3 = 4$ m with $K_1 = 2$, $K_2 = 4$, and $K_3 = 1$. Determine the spatial variation of piezometric head using the FEM.

SOLUTION

In order to solve the problem, the problem domain is divided into a mesh with five nodes and four different elements. The governing differential equation is the 1D form of the steady state, saturated groundwater flow equation:

$$\frac{\partial}{\partial x} \left(K_x \frac{\partial h}{\partial x} \right) = 0$$

where:

K_x is the saturated hydraulic conductivity in the x-direction
 h is the hydraulic head.

Using the method of weighted residuals, an approximate solution of h is defined. If this approximate solution is substituted into the above equation, the differential equation is not satisfied exactly:

$$\frac{\partial}{\partial x} \left(K_x \frac{\partial h}{\partial x} \right) = R(x) \neq 0$$

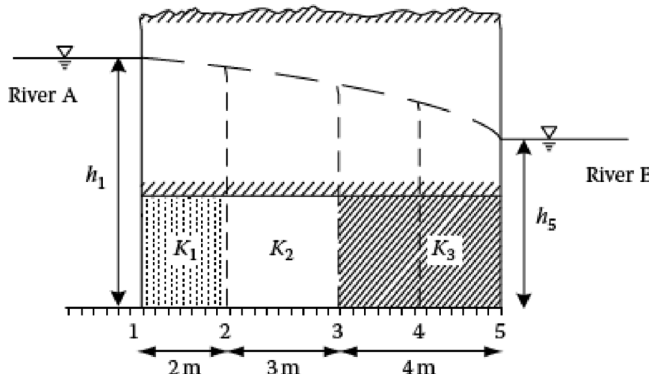


FIGURE 6.26 Two parallel rivers and a confined aquifer of Example 6.8.

where R is the error of the estimation of the residual in each node that varies from point-to-point within the problem domain. For the residual at any node i , R represents the error between the exact value of hydraulic head and the approximate solution of h at that node:

$$\{R\} = \begin{bmatrix} R(x=0) \\ R(x=2) \\ R(x=5) \\ R(x=7) \\ R(x=9) \end{bmatrix} = \begin{bmatrix} R_1 \\ R_2 \\ R_3 \\ R_4 \\ R_5 \end{bmatrix}$$

where R_i is the value of the residual at node i ($i = 1, \dots, 5$). The approximate solution at a node is estimated utilizing the values of hydraulic head at the nodes in all elements and assembling the contributed element to node i . As shown in [Figure 6.27](#), elements 1 and 2 are joined to node 2. Thus, the values of hydraulic head for the other nodes in these elements contribute to the residual at node 2. This can be written as:

$$R_2 = R_2^{(1)} + R_2^{(2)}$$

where the first term in the left-hand side of the equation is the contribution of element 1 to the residual at node 2 and the second term is the contribution of element 2 to the residual at node 2. Thus, the residual at each node is (Istok, 1989):

$$R_i = \sum_{e=1} R_i^{(e)}$$

where e is the number of elements that are joined to node i . The contribution of element e to the residual at node i can be obtained from the integral formulation for that node.

For the 1D elements in this example, we have:

$$R_i^{(e)} = - \int_{x_i^{(e)}}^{x_i^{(e)}} N_i^{(e)} \left[K_x^{(e)} \frac{\partial^2 \hat{h}^{(e)}}{\partial x^2} \right] dx$$

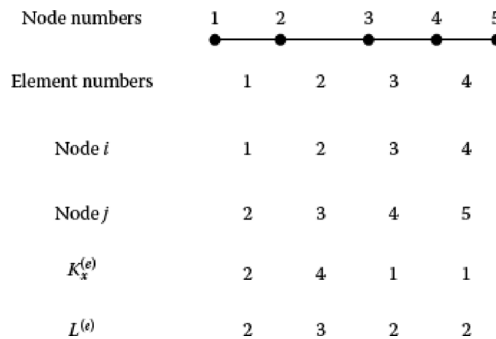


FIGURE 6.27 Assigning node numbers and element numbers j .

A similar equation can be written for the contribution of element e to the residual at any other node j joined to the element:

$$R_j^{(e)} = - \int_{x_i^{(e)}}^{x_j^{(e)}} N_j^{(e)} \left[K_x^{(e)} \frac{\partial^2 \hat{h}^{(e)}}{\partial x^2} \right] dx$$

where:

$x_i^{(e)}$ and $x_j^{(e)}$ are the coordinates of the nodes at each end of the element
 $N_i^{(e)}$ is the weighting function for node i in element e (which is identical to the interpolation function for node i in element e because the Galerkin method is used)

$K_x^{(e)}$ is the saturated hydraulic conductivity for element e

$K_x^{(e)}$ is assumed to be constant within an element, but can vary from one element to another. The equation was multiplied by -1 for later convenience.

Using Equations 6.37, 6.41, and 6.42, the approximate solution \hat{h} in each element can be written as follows based on the interpolation functions and the unknown element:

$$\hat{h}^{(e)}(x) = N_i^{(e)}h_i + N_j^{(e)}h_j = \left(\frac{x_j^{(e)} - x}{L^{(e)}} \right) h_i + \left(\frac{x - x_i^{(e)}}{L^{(e)}} \right) h_j$$

Because the approximate solution is a linear function of x , $\partial^2 h / \partial x^2$ is not defined. The approximate solution does have a continuous first derivative, however, we can evaluate $R_i^{(e)}$ if $\partial^2 h / \partial x^2$ is rewritten in the other form:

$$\int_{x_i^{(e)}}^{x_j^{(e)}} N_i^{(e)} \left[K_x^{(e)} \frac{\partial^2 \hat{h}^{(e)}}{\partial x^2} \right] dx = - \int_{x_i^{(e)}}^{x_j^{(e)}} K_x^{(e)} \frac{\partial N_i^{(e)}}{\partial x} \frac{\partial \hat{h}^{(e)}}{\partial x} dx + \left[N_i^{(e)} K_x^{(e)} \frac{\partial \hat{h}^{(e)}}{\partial x} \right]_{x_i^{(e)}}^{x_j^{(e)}}$$

$$F_i^{(e)} = \left[N_i^{(e)} K_x^{(e)} \frac{\partial \hat{h}^{(e)}}{\partial x} \right]_{x_i^{(e)}}^{x_j^{(e)}}$$

$F_i^{(e)}$ shows the inflow/outflow from the element. It is positive for inflow to the element. If the flow is not specified or at impermeable aquifer boundaries, $F_i^{(e)}$ will be zero. For elements on the interior of the mesh, the term $F_i^{(e)}$ for adjacent elements with opposite signs will be zero, and their contribution in $F^{(e)}$ is not considered:

$$R_i^{(e)} = - \int_{x_i^{(e)}}^{x_j^{(e)}} N_i^{(e)} \left[K_x^{(e)} \frac{\partial^2 \hat{h}^{(e)}}{\partial x^2} \right] dx = \int_{x_i^{(e)}}^{x_j^{(e)}} K_x^{(e)} \frac{\partial N_i^{(e)}}{\partial x} \frac{\partial \hat{h}^{(e)}}{\partial x} dx - \left[N_i^{(e)} K_x^{(e)} \frac{\partial \hat{h}^{(e)}}{\partial x} \right]_{x_i^{(e)}}^{x_j^{(e)}}$$

$$= \int_{x_i^{(e)}}^{x_j^{(e)}} K_x^{(e)} \frac{\partial N_i^{(e)}}{\partial x} \frac{\partial \hat{h}^{(e)}}{\partial x} dx$$

From the definition for h in Equation 6.37 and definitions of the interpolation functions, we have:

$$\frac{\partial N_i^{(e)}}{\partial x} = \frac{\partial}{\partial x} \left(\frac{x_j^{(e)} - x}{L^{(e)}} \right) = -\frac{1}{L^{(e)}}$$

$$\frac{\partial N_j^{(e)}}{\partial x} = \frac{\partial}{\partial x} \left(\frac{x - x_j^{(e)}}{L^{(e)}} \right) = \frac{1}{L^{(e)}}$$

So:

$$\frac{\partial \hat{h}^{(e)}}{\partial x} = -\frac{1}{L^{(e)}} h_i + \frac{1}{L^{(e)}} h_j = \frac{1}{L^{(e)}} (-h_i + h_j)$$

$$R_i^{(e)} = \int_{x_i^{(e)}}^{x_j^{(e)}} K_x^{(e)} \left(-\frac{1}{L^{(e)}} \right) \left(\frac{1}{L^{(e)}} \right) (-h_i + h_j) dx = -\frac{K_x^{(e)}}{L^{(e)2}} (x_j^{(e)} - x_i^{(e)}) (-h_i + h_j)$$

But:

$$x_j^{(e)} - x_i^{(e)} = L^{(e)}$$

$$R_i^{(e)} = \frac{K_x^{(e)}}{L^{(e)}} (h_i - h_j)$$

Similarly, for the contribution of element e to the residual at node j , we have:

$$R_j^{(e)} = \frac{K_x^{(e)}}{L^{(e)}} (-h_i + h_j)$$

The last two equations can be combined and written in matrix form as follows:

$$\begin{Bmatrix} R_i^{(e)} \\ R_j^{(e)} \end{Bmatrix} = \frac{K_x^{(e)}}{L^{(e)}} \begin{bmatrix} 1 & -1 \\ -1 & 1 \end{bmatrix} \begin{Bmatrix} h_i \\ h_j \end{Bmatrix} = \begin{bmatrix} K_x^{(e)} \\ K_x^{(e)} \end{bmatrix} \begin{Bmatrix} h_i \\ h_j \end{Bmatrix}$$

where:

$$\begin{bmatrix} K_x^{(e)} \\ K_x^{(e)} \end{bmatrix} = \frac{K_x^{(e)}}{L^{(e)}} \begin{bmatrix} 1 & -1 \\ -1 & 1 \end{bmatrix}$$

$K_x^{(e)}$ is the element conductance matrix. This matrix is determined based on the hydraulic conductivity of the aquifer material within the element $K_x^{(e)}$, the size, $L^{(e)}$,

and shape (through the functions for the element) of the element. $[K_x^{(e)}]$ is a square, symmetric matrix with size $n \times n$, where n is the number of nodes in the element. Thus, for a 1D element with two nodes, the size of $[K_x^{(e)}]$ is 2×2 , and for a 2D element with three nodes, the size of $[K_x^{(e)}]$ is 3×3 .

The characteristics of each mesh element are illustrated in [Figure 6.27](#). Node numbers i and j for each element are shown in this figure. Therefore, the element conductance matrices can be derived as follows:

$$[K_x^{(1)}] = \frac{2}{2} \begin{bmatrix} 1 & -1 \\ -1 & 1 \end{bmatrix} = \begin{bmatrix} 1 & -1 \\ -1 & 1 \end{bmatrix}$$

$$[K_x^{(2)}] = \frac{4}{3} \begin{bmatrix} 1 & -1 \\ -1 & 1 \end{bmatrix} = \begin{bmatrix} 4/3 & -4/3 \\ -4/3 & 4/3 \end{bmatrix}$$

$$[K_x^{(3)}] = [K_x^{(4)}] = \frac{1}{2} \begin{bmatrix} 1 & -1 \\ -1 & 1 \end{bmatrix} = \begin{bmatrix} 1/2 & -1/2 \\ -1/2 & 1/2 \end{bmatrix}$$

Consider the aquifer is multilayered $L_1 = 2$ m, $L_2 = 3$ m, $L_3 = 4$ m with $K_1 = 2$, $K_2 = 4$, and $K_3 = 1$. Determine the spatial variation of piezometric head using the FEM.

By assembling the element conductance matrices for all the elements in the mesh, the global conductance matrix can be obtained as follows:

$$[K]_{\text{global}} = \sum_{e=1}^m [K]_{\text{expanded}}$$

where m is the number of elements in the mesh. The element conductance matrices give a system of linear equations of the following form:

$$\{R\} = [K]\{h\} - \{F\} = \{0\}$$

where:

$\{R\}$ is the global residual matrix

$[K]$ is the global conductance matrix

$\{h\}$ is the vector of unknown hydraulic heads

$\{F\}$ is a vector containing the specified fluxes at Neumann nodes.

$\{F\} = \{0\}$, because no fluxes were specified:

$$\{R\}_{5 \times 1} = \begin{bmatrix} R_1 \\ R_2 \\ R_3 \\ R_4 \\ R_5 \end{bmatrix} \quad \{h\}_{5 \times 1} = \begin{bmatrix} h_1 \\ h_2 \\ h_3 \\ h_4 \\ h_5 \end{bmatrix} \quad \{F\}_{5 \times 1} = \begin{bmatrix} 0 \\ 0 \\ 0 \\ 0 \\ 0 \end{bmatrix}$$

The expanded form of the element conductance matrices is as follows:

$$\left[K_x^{(1)} \right] = \frac{2}{2} \begin{bmatrix} 1 & -1 \\ -1 & 1 \end{bmatrix} = \begin{bmatrix} 1 & -1 \\ -1 & 1 \end{bmatrix}$$

$$\left[K_x^{(2)} \right] = \frac{4}{3} \begin{bmatrix} 1 & -1 \\ -1 & 1 \end{bmatrix} = \begin{bmatrix} 4/3 & -4/3 \\ -4/3 & 4/3 \end{bmatrix}$$

$$\left[K_x^{(3)} \right] = \left[K_x^{(4)} \right] = \frac{1}{2} \begin{bmatrix} 1 & -1 \\ -1 & 1 \end{bmatrix} = \begin{bmatrix} 1/2 & -1/2 \\ -1/2 & 1/2 \end{bmatrix}$$

$$\left[K_x^{(1)} \right] = \begin{bmatrix} 1 & -1 & 0 & 0 & 0 \\ -1 & 1 & 0 & 0 & 0 \\ 0 & 0 & 0 & 0 & 0 \\ 0 & 0 & 0 & 0 & 0 \\ 0 & 0 & 0 & 0 & 0 \end{bmatrix} \quad \left[K_x^{(2)} \right] = \begin{bmatrix} 0 & 0 & 0 & 0 & 0 \\ 0 & 4/3 & -4/3 & 0 & 0 \\ 0 & -4/3 & 4/3 & 0 & 0 \\ 0 & 0 & 0 & 0 & 0 \\ 0 & 0 & 0 & 0 & 0 \end{bmatrix}$$

$$\left[K_x^{(3)} \right] = \begin{bmatrix} 0 & 0 & 0 & 0 & 0 \\ 0 & 0 & 0 & 0 & 0 \\ 0 & 0 & 1/2 & -1/2 & 0 \\ 0 & 0 & -1/2 & 1/2 & 0 \\ 0 & 0 & 0 & 0 & 0 \end{bmatrix} \quad \left[K_x^{(4)} \right] = \begin{bmatrix} 0 & 0 & 0 & 0 & 0 \\ 0 & 0 & 0 & 0 & 0 \\ 0 & 0 & 0 & 1/2 & -1/2 \\ 0 & 0 & 0 & -1/2 & 1/2 \\ 0 & 0 & 0 & 0 & 0 \end{bmatrix}$$

and the global conductance matrix is:

$$[K]_{\text{global}} = [K^{(1)}] + [K^{(2)}] + [K^{(3)}] + [K^{(4)}]$$

$$[K_x]_{\text{global}} = \begin{bmatrix} 0 & -1 & 0 & 0 & 0 \\ -1 & 7/3 & -4/3 & 0 & 0 \\ 0 & -4/3 & 11/6 & -1/2 & 0 \\ 0 & 0 & -1/2 & 1 & -1/2 \\ 0 & 0 & 0 & -1/2 & 1/2 \end{bmatrix}$$

The resulting system of equations, when this global conductance matrix is substituted into the system of linear equations, is:

$$\begin{bmatrix} 0 & -1 & 0 & 0 & 0 \\ -1 & 7/3 & -4/3 & 0 & 0 \\ 0 & -4/3 & 11/6 & -1/2 & 0 \\ 0 & 0 & -1/2 & 1 & -1/2 \\ 0 & 0 & 0 & -1/2 & 1/2 \end{bmatrix} \begin{bmatrix} h_1 \\ h_2 \\ h_3 \\ h_4 \\ h_5 \end{bmatrix} = \begin{bmatrix} 0 \\ 0 \\ 0 \\ 0 \\ 0 \end{bmatrix}$$

Considering $h_1 = 12$ and $h_5 = 6$ (nodes 1 and 5 are called Dirichlet nodes) from the boundary conditions, the system of equations can be modified as:

$$\begin{bmatrix} 0 & -1 & 0 & 0 & 0 \\ -1 & 7/3 & -4/3 & 0 & 0 \\ 0 & -4/3 & 11/6 & -1/2 & 0 \\ 0 & 0 & -1/2 & 1 & -1/2 \\ 0 & 0 & 0 & -1/2 & 1/2 \end{bmatrix} \begin{bmatrix} h_1 \\ h_2 \\ h_3 \\ h_4 \\ h_5 \end{bmatrix} = \begin{bmatrix} 0 \\ 0 \\ 0 \\ 0 \\ 0 \end{bmatrix}$$

$$\begin{bmatrix} 7/3 & -4/3 & 0 \\ -4/3 & 11/6 & -1/2 \\ 0 & -1/2 & 1 \end{bmatrix} \begin{bmatrix} h_2 \\ h_3 \\ h_4 \end{bmatrix} = \begin{bmatrix} 12 \\ 0 \\ 3 \end{bmatrix}$$

The results are then given as $h_2 = 10.96$ m, $h_3 = 10.17$ m, and $h_4 = 8.09$ m.

6.5.3 TRANSIENT SATURATED FLOW EQUATION

The 3D form of the equation for transient groundwater flow through saturated porous media is as follows:

$$\frac{\partial}{\partial x} \left(K_x \frac{\partial h}{\partial x} \right) + \frac{\partial}{\partial y} \left(K_y \frac{\partial h}{\partial y} \right) + \frac{\partial}{\partial z} \left(K_z \frac{\partial h}{\partial z} \right) = S_s \frac{\partial h}{\partial t} \quad (6.47)$$

where:

S_s is the specific storage of the porous media

t is the time.

In transient groundwater flow equations, the term $S_s \partial h / \partial t$ implies the steady-state condition. The residual at node i is calculated by replacing the approximate solution for hydraulic head, \hat{h} in Equation 6.47. It can be formulated as:

$$R_i^{(e)} = - \iiint_{V^{(e)}} W_i^{(e)} \left[\frac{\partial}{\partial x} \left(K_x^{(e)} \frac{\partial \hat{h}^{(e)}}{\partial x} \right) + \frac{\partial}{\partial y} \left(K_y^{(e)} \frac{\partial \hat{h}^{(e)}}{\partial y} \right) + \frac{\partial}{\partial z} \left(K_z^{(e)} \frac{\partial \hat{h}^{(e)}}{\partial z} \right) - S_s^{(e)} \frac{\partial \hat{h}^{(e)}}{\partial t} \right] dx dy dz \quad (6.48)$$

where:

$W_i^{(e)}$ is the weighting function for node i of element e , which is similar to $N_i^{(e)}$ in the Galerkin method

$S_s^{(e)}$ is the specific storage for element e .

Assuming that the values of $K_x^{(e)}$, $K_y^{(e)}$, $K_z^{(e)}$, and $S_s^{(e)}$ are constant within an element, Equation 6.48 can be rearranged as:

$$\begin{aligned}
 R_i^{(e)} &= - \iiint_{V^{(e)}} N_i^{(e)} \left[K_i^{(e)} \frac{\partial^2 h^{(e)}}{\partial x^2} + K_y^{(e)} \frac{\partial^2 h^{(e)}}{\partial y^2} + K_z^{(e)} \frac{\partial^2 h^{(e)}}{\partial z^2} - S_s^{(e)} \frac{\partial h^{(e)}}{\partial t} \right] dx dy dz \\
 &= \iiint_{V^{(e)}} N_i^{(e)} \left[K_x^{(e)} \frac{\partial^2 h^{(e)}}{\partial x^2} + K_y^{(e)} \frac{\partial^2 \hat{h}^{(e)}}{\partial y^2} + K_z^{(e)} \frac{\partial \hat{h}^{(e)}}{\partial z^2} \right] dx dy dz \\
 &\quad + \iiint_{V^{(e)}} N_i^{(e)} S_s^{(e)} \frac{\partial \hat{h}^{(e)}}{\partial t} dx dy dz
 \end{aligned} \tag{6.49}$$

Based on the approximated solution as a function of the interpolation function and unknown hydraulic head at the element's nodes, the above integral can be summarized in the matrix form as:

$$\begin{Bmatrix} R_1^{(e)} \\ \vdots \\ R_n^{(e)} \end{Bmatrix}_K = \begin{bmatrix} K^{(e)} \end{bmatrix} \begin{Bmatrix} h_1 \\ \vdots \\ h_n \end{Bmatrix} + \begin{bmatrix} C^{(e)} \end{bmatrix} \begin{Bmatrix} \frac{h_1}{\partial t} \\ \vdots \\ \frac{h_n}{\partial t} \end{Bmatrix} \tag{6.50}$$

where:

$[K^{(e)}]$ is the element conductance matrix

$[C^{(e)}]$ is the element capacitance matrix (Istok, 1989):

$$\begin{bmatrix} K^{(e)} \end{bmatrix} = - \iiint_{V^{(e)}} \begin{bmatrix} \frac{\partial N_1^{(e)}}{\partial x} & \frac{\partial N_1^{(e)}}{\partial y} & \frac{\partial N_1^{(e)}}{\partial z} \\ \vdots & \vdots & \vdots \\ \frac{\partial N_n^{(e)}}{\partial x} & \frac{\partial N_n^{(e)}}{\partial y} & \frac{\partial N_n^{(e)}}{\partial z} \end{bmatrix} \begin{bmatrix} K_x^{(e)} & 0 & 0 \\ 0 & K_y^{(e)} & 0 \\ 0 & 0 & K_z^{(e)} \end{bmatrix} \begin{bmatrix} \frac{\partial N_1^{(e)}}{\partial x} & \dots & \frac{\partial N_n^{(e)}}{\partial x} \\ \frac{\partial N_1^{(e)}}{\partial y} & \dots & \frac{\partial N_n^{(e)}}{\partial y} \\ \frac{\partial N_1^{(e)}}{\partial z} & \dots & \frac{\partial N_n^{(e)}}{\partial z} \end{bmatrix} dx dy dz \tag{6.51}$$

$$\begin{bmatrix} C^{(e)} \end{bmatrix} = - \iiint_{V^{(e)}} \begin{bmatrix} N_1^{(e)} \\ \vdots \\ N_n^{(e)} \end{bmatrix} \begin{bmatrix} S_s^{(e)} \end{bmatrix} \begin{bmatrix} N_1^{(e)} & \dots & N_n^{(e)} \end{bmatrix} dx dy dz \tag{6.52}$$

or

$$\left[C^{(e)} \right] = S_s^{(e)} \begin{bmatrix} N_1^{(e)} N_1^{(e)} & \dots & N_1^{(e)} N_n^{(e)} \\ \vdots & \dots & \vdots \\ N_n^{(e)} N_1^{(e)} & \dots & N_n^{(e)} N_n^{(e)} \end{bmatrix} - \iiint_{V^{(e)}} dx dy dz \quad (6.53)$$

If the lumped element formulation is used, the element capacitance matrix is:

$$\left[C^{(e)} \right] = S_s^{(e)} \frac{V^{(e)}}{n} \begin{bmatrix} 1 & & 0 \\ & \ddots & \\ 0 & & 1 \end{bmatrix} \quad (6.54)$$

Thus, the time derivative of the approximate solution should be defined over the element domain for estimating the errors. For this purpose, the interpolation functions and the values of the time derivative at the nodes are required.

The global conductance matrix and global capacitance matrix are obtained by assembling the element matrices for all the elements in the finite mesh. These are square and symmetric matrices with size $p \times p$, where p is the number of nodes in the mesh. Thus, Equation 6.50 can be written as:

$$\left[C \right] \begin{Bmatrix} \frac{\partial h_1}{\partial t} \\ \vdots \\ \frac{\partial h_p}{\partial t} \end{Bmatrix} + \left[K \right] \begin{Bmatrix} h_1 \\ \vdots \\ h_p \end{Bmatrix} = \left[F \right] \quad (6.55)$$

or

$$\left[C \right] \overset{\circ}{\begin{Bmatrix} h \end{Bmatrix}} + \left[K \right] \{h\} = \{F\} \quad (6.56)$$

global global global

where:

$$\overset{\circ}{\{h\}} = \begin{Bmatrix} \frac{\partial h_1}{\partial t} \\ \vdots \\ \frac{\partial h_p}{\partial t} \end{Bmatrix} \quad \{h\} = \begin{Bmatrix} h_1 \\ \vdots \\ h_p \end{Bmatrix} \quad (6.57)$$

The solution of the system of algebraic equations determines the head and the head time derivative values at each node in the mesh. Among various methods for

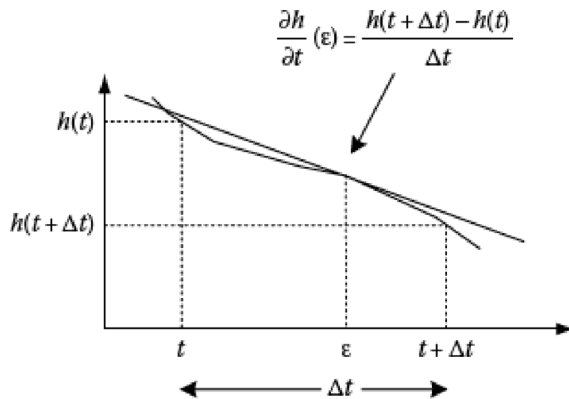


FIGURE 6.28 The time derivative approximation using the FDM.

modeling the time derivative value, the FDM is commonly used. In this method, the head time derivative value is computed based on the difference between the head values of the two end points of the interval FDA to the time derivative for hydraulic head as shown in [Figure 6.28](#). The variation of hydraulic head is considered linear between given time intervals.

For the point with the position of ε in the interval t to $t + \Delta t$, the unknown hydraulic head can be calculated based on the FDM. Thus, the time derivative for hydraulic head is expressed as follows:

$$\frac{\partial h}{\partial t}(\varepsilon) = \frac{h(t + \Delta t) - h(t)}{\Delta t} \quad (6.58)$$

or

$$h(\varepsilon) = h(t) + (\varepsilon - t) \frac{\partial h}{\partial t}(\varepsilon) \quad (6.59)$$

A variable α is defined as:

$$\alpha = \frac{\varepsilon - t}{\Delta t} \quad (6.60)$$

Thus, Equation 6.59 can be written as:

$$h(\varepsilon) = (1 - \alpha)h(t) + \alpha h(t + \Delta t) \quad (6.61)$$

Therefore, based on the Equation 6.61, unknown hydraulic heads $\{h\}$ vector and $\{F\}$ vector can be written as:

$$\{h\} = (1 - \alpha)\{h\}_t + \alpha\{h\}_{t+\Delta t} \quad (6.62)$$

$$\{F\} = (1 - \omega) \alpha \{F\}_t + \alpha \{F\}_{t+\Delta t} \quad (6.63)$$

By substituting Equations 6.62, 6.63, and 6.58 into Equation 6.56, the finite-difference formulation for the transient, saturated flow equation is derived as follows:

$$\begin{matrix} [C] & \overset{\circ}{[K]} & \{h\} \\ \text{global} & \text{global} & \text{global} \end{matrix} = \{F\} \quad (6.64)$$

$$\begin{aligned} ([C] + \alpha \Delta t [K]) \{h\}_{t+\Delta t} &= ([C] - (1 - \alpha) \Delta t [K]) \{h\}_t \\ &\quad + \Delta t ((1 - \alpha) \{F\}_t + \alpha \{F\}_{t+\Delta t}) \end{aligned} \quad (6.65)$$

For solving the developed set of equations, the initial value of $\{h\}_{t_0}$ is required. This value is specified at time $t = t_0 = 0$ as the initial condition. Then, the system of linear equations is solved to obtain values of $\{h\}$ at the end of the first time step, $\{h\}_{t_0+\Delta t}$. This process is repeated for each time step (Istok, 1989). Similar to the FDM, there are several ways to formulate the time derivative equations by selecting the value of α . If α is considered equal to zero, the method is called the forward difference method and is expressed as:

$$[C] \{h\}_{t+\Delta t} = ([C] - \Delta t [K]) \{h\}_t + \Delta t \{F\}_t \quad (6.66)$$

If α is considered equal to 0.5, the method is called the Crank–Nicolson difference method and is shown as:

$$\left([C] \frac{\Delta t}{2} [K] \right) \{h\}_{t+\Delta t} = \left([C] - \frac{\Delta t}{2} [K] \right) \{h\}_t + \frac{\Delta t}{2} (\{F\}_t + \{F\}_{t+\Delta t}) \quad (6.67)$$

when α is equal to one, it is called the backward difference method, given as:

$$([C] + \Delta t [K]) \{h\}_{t+\Delta t} = [C] \{h\}_t + \Delta t \{F\}_{t+\Delta t} \quad (6.68)$$

Example 6.9

Consider the confined aquifer shown in Example 6.8. Initially, the aquifer is in a steady-state, saturated condition with a distribution of hydraulic head computed from the previous example (Figure 6.29). At time $t = 0$, the water level in river A increases (at the upper boundary, node 1) from 12 to 18 m. Assume $S_s^{(2)} = 0.04$ and $S_s^{(3)} = S_s^{(1)} = 0.02$ for the mesh elements. Find the value of hydraulic head at each node at time $t = 1$ s.

SOLUTION

The governing differential equation is a 1D form of groundwater flow:

$$\frac{\partial}{\partial z} \left(K_x \frac{\partial h}{\partial x} \right) = S_s \frac{\partial h}{\partial t}$$

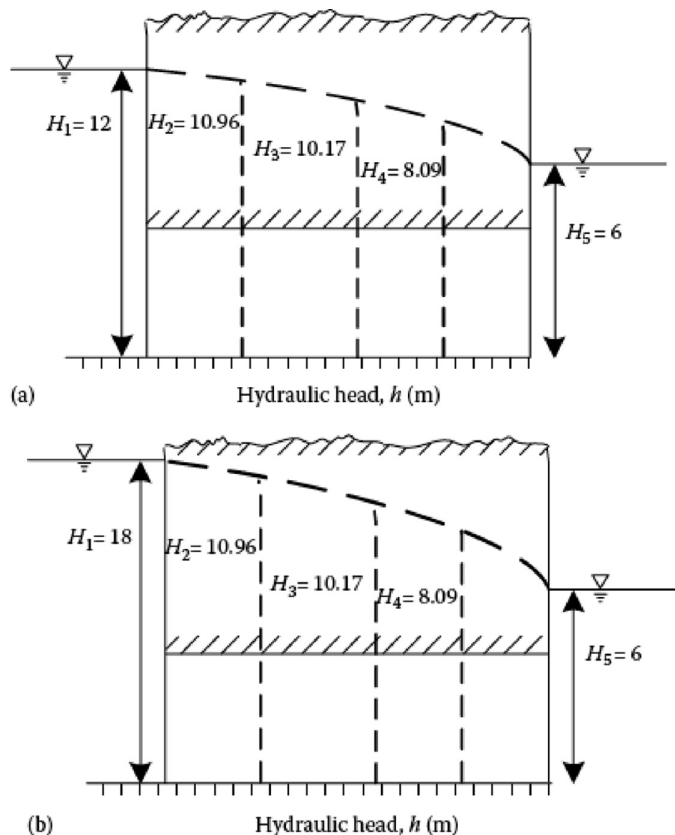


FIGURE 6.29 Flow problem in Example 6.9: (a) steady-state solution and (b) initial conditions.

where K_x is the saturated hydraulic conductivity in the direction of flow (the x-axis is directed vertically downward in this case). For a 1D element with two nodes, the element capacitance matrices are given as:

$$[C^{(1)}] = \frac{S_s^{(1)} L^{(1)}}{2} \begin{bmatrix} 1 & 0 \\ 0 & 1 \end{bmatrix} = \frac{(0.02)(2)}{2} \begin{bmatrix} 1 & 0 \\ 0 & 1 \end{bmatrix} = \begin{bmatrix} 0.02 & 0 \\ 0 & 0.02 \end{bmatrix}$$

$$[C^{(2)}] = \frac{S_s^{(2)} L^{(2)}}{2} \begin{bmatrix} 1 & 0 \\ 0 & 1 \end{bmatrix} = \frac{(0.04)(3)}{2} \begin{bmatrix} 1 & 0 \\ 0 & 1 \end{bmatrix} = \begin{bmatrix} 0.06 & 0 \\ 0 & 0.06 \end{bmatrix}$$

$$[C^{(3)}] = [C^{(4)}] = \frac{S_s^{(3)} L^{(3)}}{2} \begin{bmatrix} 1 & 0 \\ 0 & 1 \end{bmatrix} = \frac{(0.02)(2)}{2} \begin{bmatrix} 1 & 0 \\ 0 & 1 \end{bmatrix} = \begin{bmatrix} 0.02 & 0 \\ 0 & 0.02 \end{bmatrix}$$

The global capacitance matrix is obtained by adding the expanded form of the element capacitance matrices:

$$\begin{aligned}
 [C] &= \begin{bmatrix} 0.02 & 0 & 0 & 0 & 0 \\ 0 & 0.02 + 0.06 & 0 & 0 & 0 \\ 0 & 0 & 0.06 + 0.02 & 0 & 0 \\ 0 & 0 & 0 & 0.02 + 0.02 & 0 \\ 0 & 0 & 0 & 0 & 0.02 \end{bmatrix} \\
 &= \begin{bmatrix} 0.02 & 0 & 0 & 0 & 0 \\ 0 & 0.08 & 0 & 0 & 0 \\ 0 & 0 & 0.08 & 0 & 0 \\ 0 & 0 & 0 & 0.04 & 0 \\ 0 & 0 & 0 & 0 & 0.02 \end{bmatrix}
 \end{aligned}$$

From the previous example, the global conductance matrix is given as:

$$[K_x]_{global} = \begin{bmatrix} 1 & -1 & 0 & 0 & 0 \\ -1 & 7/3 & -4/3 & 0 & 0 \\ 0 & -4/3 & 11/6 & -1/2 & 0 \\ 0 & 0 & -1/2 & 1 & -1/2 \\ 0 & 0 & 0 & -1/2 & 1/2 \end{bmatrix}$$

The initial values of hydraulic head at the nodes are:

$$\{h\}_{t=0} = \begin{Bmatrix} h_1 \\ h_2 \\ h_3 \\ h_4 \\ h_5 \end{Bmatrix}_{t=0} = \begin{Bmatrix} 18 \\ 10.96 \\ 10.17 \\ 8.09 \\ 6 \end{Bmatrix}$$

The backward difference formulation is used with a time step $\Delta t = 1$ s. By setting $\{F\} = 0$ (no specified flow rates), the system of equations at the end of the first time step becomes as follows:

$$([C] + \Delta t [K]) \{h\}_{t=1} = [C] \{h\}_{t=0} + \Delta t \{F\}_{t=1}^0$$

Substituting equations in the above equation gives:

$$[K_x]_{global} = \begin{bmatrix} 1 & -1 & 0 & 0 & 0 \\ -1 & 7/3 & -4/3 & 0 & 0 \\ 0 & -4/3 & 11/6 & -1/2 & 0 \\ 0 & 0 & -1/2 & 1 & -1/2 \\ 0 & 0 & 0 & -1/2 & 1/2 \end{bmatrix}$$

$$\begin{bmatrix} 0.02 & 0 & 0 & 0 & 0 \\ 0 & 0.08 & 0 & 0 & 0 \\ 0 & 0 & 0.08 & 0 & 0 \\ 0 & 0 & 0 & 0.04 & 0 \\ 0 & 0 & 0 & 0 & 0.02 \end{bmatrix}$$

$$+ (1) \begin{bmatrix} 1 & -1 & 0 & 0 & 0 \\ -1 & 7/3 & -4/3 & 0 & 0 \\ 0 & -4/3 & 11/6 & -1/2 & 0 \\ 0 & 0 & -1/2 & 1 & -1/2 \\ 0 & 0 & 0 & -1/2 & 1/2 \end{bmatrix} \begin{Bmatrix} h_1 \\ h_2 \\ h_3 \\ h_4 \\ h_5 \end{Bmatrix}_{t=1}$$

which can be simplified to:

$$\begin{bmatrix} 1.02 & -1 & 0 & 0 & 0 \\ -1 & 2.41 & -1.33 & 0 & 0 \\ 0 & -1.33 & 1.91 & -0.5 & 0 \\ 0 & 0 & -0.5 & 1.04 & -0.5 \\ 0 & 0 & 0 & -0.5 & 0.52 \end{bmatrix} \begin{Bmatrix} h_1 \\ h_2 \\ h_3 \\ h_4 \\ h_5 \end{Bmatrix}_{t=1} = \begin{Bmatrix} 0.36 \\ 0.88 \\ 0.81 \\ 0.32 \\ 0.12 \end{Bmatrix}$$

The hydraulic heads at the upper and lower boundary conditions are $h_1 = 18$ and $h_5 = 6$, respectively, for all values of t . Modifying the last equation for these known values, we have:

$$\begin{bmatrix} 2.41 & -1.33 & 0 \\ -1.33 & 1.91 & -0.5 \\ 0 & -0.5 & 1.04 \end{bmatrix} \begin{Bmatrix} h_2 \\ h_3 \\ h_4 \end{Bmatrix}_{t=1} = \begin{Bmatrix} 18.88 \\ 0.81 \\ 3.32 \end{Bmatrix}$$

This equation can be solved to obtain the values of hydraulic head at the end of the time step as follows:

$$\begin{Bmatrix} h_1 \\ h_2 \\ h_3 \\ h_4 \\ h_5 \end{Bmatrix}_{t=1} = \begin{Bmatrix} 18.00 \\ 15.40 \\ 13.71 \\ 9.78 \\ 6.00 \end{Bmatrix}$$

6.5.4 SOLUTE TRANSPORT EQUATION

The 3D form of the solute transport equation for uniform groundwater flow in the x -direction is:

$$\begin{aligned} \frac{\partial(\theta C)}{\partial t} = & D_x \frac{\partial^2}{\partial x^2}(\theta C) + D_y \frac{\partial^2}{\partial y^2}(\theta C) + D_z \frac{\partial^2}{\partial z^2}(\theta C) - \frac{\partial}{\partial x}(v_x C) \\ & - \frac{\partial}{\partial t}(\rho_b K_d C) - \lambda(\theta C + \rho_b K_d C) \end{aligned} \quad (6.69)$$

where:

C is the solute concentration

θ is the volumetric water content of the porous media

D_x , D_y , D_z are the dispersion coefficients of the porous media in the x -, y -, and z -directions

v_x is the apparent groundwater velocity in the x -direction

ρ_b is the density of the porous media

K_d is the distribution coefficient

λ is the solute decay constant.

The unknown concentration at each node is determined by solving the solute transport equation. Similar to applying the FEM for solving groundwater flow, an approximate solution for an unknown concentration, C , within element e is considered as \hat{C} :

$$\hat{C}^{(e)}(x, y, z) = \sum_{i=1}^n N_i^{(e)} C_i \quad (6.70)$$

where:

$N_i^{(e)}$ is the interpolation function for node i within element e

C_i is the unknown solute concentration in this node.

By substituting the approximate solution into Equation 6.69, the error or residual due to the difference of the exact solution and the approximate solution at each node occurs. The residual can be expressed as:

$$R_i^{(e)} = - \iiint_{V^{(e)}} W_i^{(e)}(x, y, z) \left[D_x \frac{\partial^2}{\partial x^2} \left(\theta \hat{C}_i^{(e)} \right) + D_y \frac{\partial^2}{\partial y^2} \left(\theta \hat{C}_i^{(e)} \right) + D_z \frac{\partial^2}{\partial z^2} \left(\theta \hat{C}_i^{(e)} \right) \right. \\ \left. - \frac{\partial}{\partial x} \left(v_x \hat{C}_i^{(e)} \right) - \frac{\partial}{\partial t} \left(\rho_b K_d \hat{C}_i^{(e)} \right) - \lambda \left(\theta \hat{C}_i^{(e)} + \rho_b K_d \hat{C}_i^{(e)} \right) - \frac{\partial}{\partial t} \left(\theta \hat{C}_i^{(e)} \right) \right] \quad (6.71)$$

where $W_i^{(e)}$ is the element's weighting function for node i . The weighting function for each node in the element is considered to be equal to the element's interpolation function for that node in the Galerkin method ($W_i^{(e)} = N_i^{(e)}$):

$$R_i^{(e)} = - \iiint_{V^{(e)}} N_i^{(e)}(x, y, z) \left[D_x^{(e)} \theta^{(e)} \frac{\partial^2 \hat{C}^{(e)}}{\partial x^2} + D_y^{(e)} \theta^{(e)} \frac{\partial^2 \hat{C}^{(e)}}{\partial y^2} \right. \\ \left. + D_z^{(e)} \theta^{(e)} \frac{\partial^2 \hat{C}^{(e)}}{\partial z^2} - v_x^{(e)} \frac{\partial \hat{C}^{(e)}}{\partial x} - \rho_b^{(e)} K_d^{(e)} \frac{\partial \hat{C}^{(e)}}{\partial t} \right. \\ \left. - \lambda \left(\theta^{(e)} \hat{C}^{(e)} + \rho_b^{(e)} K_d^{(e)} \hat{C}^{(e)} \right) - \theta^{(e)} \frac{\partial \hat{C}^{(e)}}{\partial t} \right] dx dy dz \quad (6.72)$$

Extending Equation 6.72, we have:

$$R_i^{(e)} = - \iiint_{V^{(e)}} N_i^{(e)} \left[D_x^{(e)} \theta^{(e)} \frac{\partial^2 \hat{C}^{(e)}}{\partial x^2} + D_y^{(e)} \theta^{(e)} \frac{\partial^2 \hat{C}^{(e)}}{\partial y^2} + D_z^{(e)} \theta^{(e)} \frac{\partial^2 \hat{C}^{(e)}}{\partial z^2} \right] dx dy dz \\ + \iiint_{V^{(e)}} N_i^{(e)} \left[v_x^{(e)} \frac{\partial \hat{C}^{(e)}}{\partial x} \right] dx dy dz + \iiint_{V^{(e)}} N_i^{(e)} \left[\lambda \left(\theta^{(e)} \hat{C}^{(e)} + \rho_b^{(e)} K_d^{(e)} \hat{C}^{(e)} \right) \right] dx dy dz \\ + \iiint_{V^{(e)}} N_i^{(e)} \left[\rho_b^{(e)} K_d^{(e)} \frac{\partial \hat{C}^{(e)}}{\partial t} \right] dx dy dz + \iiint_{V^{(e)}} N_i^{(e)} \left[\theta^{(e)} \frac{\partial \hat{C}^{(e)}}{\partial t} \right] dx dy dz \quad (6.73)$$

Equation 6.73 can be presented in matrix form as:

$$\begin{bmatrix} R_1^{(e)} \\ \vdots \\ R_n^{(e)} \end{bmatrix} = \begin{bmatrix} D^{(e)} \end{bmatrix} \begin{bmatrix} C_1 \\ \vdots \\ C_n \end{bmatrix} + \begin{bmatrix} A^{(e)} \end{bmatrix} \begin{bmatrix} \frac{\partial C_1}{\partial t} \\ \vdots \\ \frac{\partial C_n}{\partial t} \end{bmatrix} \quad (6.74)$$

where:

$[D^{(e)}$ is the advection-dispersion matrix of the element

$[A^{(e)}$ is the sorption matrix of the element.

The advection-dispersion matrix of the element is defined as:

$$\begin{aligned} & \left[D^{(e)} \right] \\ &= \iiint_{V^{(e)}} \begin{bmatrix} \frac{\partial N_1^{(e)}}{\partial x} & \frac{\partial N_1^{(e)}}{\partial y} & \frac{\partial N_1^{(e)}}{\partial z} \\ \vdots & \vdots & \vdots \\ \frac{\partial N_n^{(e)}}{\partial x} & \frac{\partial N_n^{(e)}}{\partial y} & \frac{\partial N_n^{(e)}}{\partial z} \end{bmatrix} \begin{bmatrix} D_x^{(e)} \theta^{(e)} & 0 & 0 \\ 0 & D_y^{(e)} \theta^{(e)} & 0 \\ 0 & 0 & D_z^{(e)} \theta^{(e)} \end{bmatrix} \begin{bmatrix} \frac{\partial N_1^{(e)}}{\partial x} \dots \frac{\partial N_n^{(e)}}{\partial x} \\ \frac{\partial N_1^{(e)}}{\partial y} \dots \frac{\partial N_n^{(e)}}{\partial y} \\ \frac{\partial N_1^{(e)}}{\partial z} \dots \frac{\partial N_n^{(e)}}{\partial z} \end{bmatrix} dx dy dz \\ & \quad n \times n \quad n \times 3 \quad 3 \times 3 \quad 3 \times n \\ &+ \iiint_{V^{(e)}} \begin{bmatrix} N_1^{(e)} \\ \vdots \\ N_n^{(e)} \end{bmatrix} V_x^{(e)} \begin{bmatrix} \frac{\partial N_1^{(e)}}{\partial x} & \dots & \frac{\partial N_n^{(e)}}{\partial x} \end{bmatrix} dx dy dz \\ & \quad n \times 1 \quad 1 \times 1 \quad 1 \times n \\ &+ \iiint_{V^{(e)}} \begin{bmatrix} N_1^{(e)} \\ \vdots \\ N_n^{(e)} \end{bmatrix} \left[\lambda \theta^{(e)} + \rho_b^{(e)} K_d^{(e)} \right] \begin{bmatrix} \partial N_1^{(e)} \dots \partial N_n^{(e)} \end{bmatrix} dx dy dz \\ & \quad n \times n \quad 1 \times 1 \quad 1 \times n \end{aligned} \quad (6.75)$$

where $V^{(e)}$ is the volume of element e . The sorption matrix of the element is defined as:

$$\begin{bmatrix} A^{(e)} \end{bmatrix} = \iiint_{V^{(e)}} \begin{bmatrix} N_1^{(e)} \\ \vdots \\ N_n^{(e)} \end{bmatrix} \left[\rho_b^{(e)} K_d^{(e)} + \theta^{(e)} \right] \begin{bmatrix} N_1^{(e)} \dots N_n^{(e)} \end{bmatrix} dx dy dz$$

$$n \times 1 \quad 1 \times 1 \quad 1 \times n \quad (6.76)$$

or

$$\begin{bmatrix} A^{(e)} \end{bmatrix} = \left(\rho_b^{(e)} K_d^{(e)} + \theta^{(e)} \right) \left(\frac{V^{(e)}}{n} \right) \begin{bmatrix} 1 & & 0 \\ & \ddots & \\ 0 & & 1 \end{bmatrix}$$

$$n \times n \quad (6.77)$$

The finite-difference is used to estimate the time derivative of the approximate solution, $\partial \hat{C} / \partial t$. By summing up the advection-dispersion matrix $[D]$ of all elements in the mesh and their sorption matrix $[A]$, the global matrices can be obtained as follows:

$$\begin{bmatrix} D \end{bmatrix}_{\text{global}} = \sum_{e=1}^m \begin{bmatrix} D^{(e)} \end{bmatrix}$$

$$p \times p \quad n \times n \quad (6.78)$$

$$\begin{bmatrix} A \end{bmatrix}_{\text{global}} = \sum_{e=1}^m \begin{bmatrix} A^{(e)} \end{bmatrix}$$

$$p \times p \quad n \times n \quad (6.79)$$

where,

m is the number of elements

p is the number of nodes in the mesh.

The weighted residual formulation for the solute transport equation becomes:

$$\begin{bmatrix} D \end{bmatrix} \begin{Bmatrix} C_1 \\ \vdots \\ C_p \end{Bmatrix} + \begin{bmatrix} A \end{bmatrix} \begin{Bmatrix} \frac{\partial C_1}{\partial t} \\ \vdots \\ \frac{\partial C_p}{\partial t} \end{Bmatrix} = \{F\}$$

$$\text{global} \quad \text{global} \quad \text{global} \quad (6.80)$$

Two vectors $\{C\}$ and $\{\dot{C}\}$ are defined as:

$$\{C\} = \begin{Bmatrix} C_1 \\ \vdots \\ C_p \end{Bmatrix} \quad \{\dot{C}\} = \begin{Bmatrix} \frac{\partial C_1}{\partial t} \\ \vdots \\ \frac{\partial C_p}{\partial t} \end{Bmatrix} \quad (6.81)$$

Equation 6.80 can be written as:

$$\begin{matrix} [A] & \{\dot{C}\} & + [D] & \{C\} & = \{F\} \\ \text{global} & & \text{global} & & \end{matrix} \quad (6.82)$$

The solution of the system of algebraic equations determines the concentration and the concentration time derivative values at each node in the mesh. The finite-difference formulation for Equation 6.82 can be expressed as:

$$\begin{aligned} ([A] + \alpha \Delta t [D]) \{C\}_{t+\Delta t} &= ([A] - (1-\alpha) \Delta t [D]) \{C\}_t \\ &+ \Delta t ((1-\alpha) \{F\}_t + \alpha \{F\}_{t+\Delta t}) \end{aligned} \quad (6.83)$$

Example 6.10

Consider the confined aquifer shown in Figure 6.30. Steady-state, saturated ground-water flow is occurring in this aquifer. Initially, the solute concentration is constant in the aquifer at 5 mg/L. At time $t = 0$, the solute concentration in river A increases to 25 mg/L and remains constant thereafter and the solute concentration in the river B remains constant at 5 mg/L. Find the solute concentration in the aquifer after 5 days.

$$V_x^{(e)} = 0.12 \text{ m/day}, D_x^{(e)} = 1.0 \text{ m}^2/\text{day}, \theta^{(e)} = n^{(e)} = 0.3$$

$$L_1^{(e)} = 2 \text{ m}, L_2^{(e)} = 3 \text{ m}, L_3^{(e)} = 2 \text{ m}, L_4^{(e)} = 2 \text{ m}$$

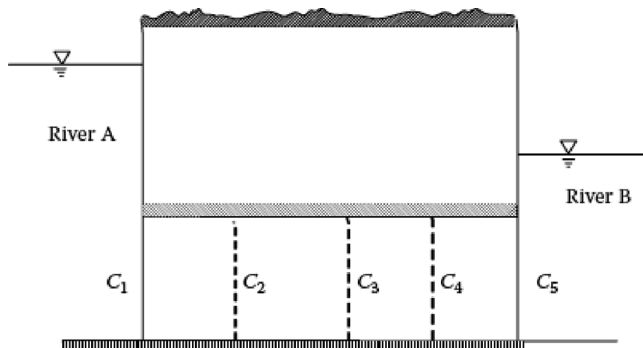


FIGURE 6.30 Confined aquifer with solute transportation for Example 6.10.

SOLUTION

The problem domain is discretized into a mesh with four elements and five nodes. The dispersion-advection matrix for each element is considered 1D, i.e., each element has two nodes:

$$\begin{aligned}
 \left[D^{(e)} \right] = & \int_{x_i^{(e)}}^{x_j^{(e)}} \left[\begin{array}{c} \frac{\partial N_1^{(e)}}{\partial x} \\ \frac{\partial N_2^{(e)}}{\partial x} \end{array} \right] \left[\begin{array}{c} D_x^{(e)} \theta^{(e)} \\ D_x^{(e)} \end{array} \right] \left[\begin{array}{c} \frac{\partial N_1^{(e)}}{\partial x} \frac{\partial N_2^{(e)}}{\partial x} \\ N_1^{(e)} N_2^{(e)} \end{array} \right] dx + \int_{x_i^{(e)}}^{x_j^{(e)}} \left[\begin{array}{c} N_1^{(e)} \\ N_2^{(e)} \end{array} \right] \left[\begin{array}{c} V_x^{(e)} \\ \frac{\partial N_1^{(e)}}{\partial x} \frac{\partial N_2^{(e)}}{\partial x} \end{array} \right] dx \\
 & 2 \times 2 \quad 2 \times 1 \quad 1 \times 1 \quad 1 \times 2 \quad 2 \times 1 \quad 1 \times 1 \quad 1 \times 2 \\
 & + \int_{x_i^{(e)}}^{x_j^{(e)}} \left[\begin{array}{c} N_1^{(e)} \\ N_2^{(e)} \end{array} \right] \left[\begin{array}{c} \lambda \theta^{(e)} + \rho_b^{(e)} K_d^{(e)} \\ N_1^{(e)} \dots N_n^{(e)} \end{array} \right] dx \\
 & 2 \times 1 \quad 1 \times 1 \quad 1 \times 2
 \end{aligned} \tag{6.84}$$

Based on the Galerkin method, the interpolation functions for all of the elements in the mesh are:

$$\begin{aligned}
 N_1^e &= \frac{x_j^{(e)} - x}{L^{(e)}}, \frac{\partial N_1^e}{\partial x} = \frac{-1}{L^{(e)}} \\
 N_2^e &= \frac{x - x_i^{(e)}}{L^{(e)}}, \frac{\partial N_2^e}{\partial x} = \frac{1}{L^{(e)}}
 \end{aligned}$$

Since the solute does not react with the porous media and does not decay, $K_d^{(e)} = 0$ and $\lambda = 0$. In addition, because the porous media is saturated, $\theta^{(e)} = n^{(e)}$. Therefore,

$$\begin{aligned}
 \left[D^{(e)} \right] &= \int_{x_i^{(e)}}^{x_j^{(e)}} \left[\begin{array}{c} -1 \\ \frac{1}{L^{(e)}} \end{array} \right] \left[\begin{array}{c} D_x^{(e)} \\ \frac{1}{L^{(e)}} \end{array} \right] \left[\begin{array}{c} -1 \quad 1 \\ L \quad L \end{array} \right] dx + \int_{x_i^{(e)}}^{x_j^{(e)}} \left[\begin{array}{c} \frac{x_j^{(e)} - x}{L^{(e)}} \\ \frac{x - x_i^{(e)}}{L^{(e)}} \end{array} \right] \left[\begin{array}{c} V_x^{(e)} \\ \frac{-1}{L^{(e)}} \frac{1}{L^{(e)}} \end{array} \right] dx \\
 & 2 \times 2 \\
 & = \frac{D_x^{(e)}}{L^{(e)}} \begin{bmatrix} 1 & -1 \\ -1 & 1 \end{bmatrix} + \begin{bmatrix} V_x^{(e)} \\ \frac{-1}{2\theta^{(e)}} \end{bmatrix} \begin{bmatrix} 1 & -1 \\ -1 & 1 \end{bmatrix}
 \end{aligned}$$

For the elements in [Figure 6.30](#), these matrices are given as:

$$\begin{aligned}
 \left[D^{(1)} \right] &= \frac{1}{2} \begin{bmatrix} 1 & -1 \\ -1 & 1 \end{bmatrix} + \frac{0.12}{2(0.3)} \begin{bmatrix} -1 & 1 \\ -1 & 1 \end{bmatrix} = \begin{bmatrix} 0.3 & -0.3 \\ -0.7 & 0.7 \end{bmatrix} \\
 \left[D^{(2)} \right] &= \frac{1}{3} \begin{bmatrix} 1 & -1 \\ -1 & 1 \end{bmatrix} + \frac{0.12}{2(0.3)} \begin{bmatrix} -1 & 1 \\ -1 & 1 \end{bmatrix} = \begin{bmatrix} 0.13 & -0.13 \\ -0.53 & 0.53 \end{bmatrix} \\
 \left[D^{(3)} \right] &= \left[D^{(1)} \right]
 \end{aligned}$$

Using Equation 6.77, the sorption matrix of the element is simplified as:

$$[A^{(e)}] = \left(\frac{p_b^{(e)} K_b^{(e)}}{n^{(e)}} + 1 \right) \frac{L^{(e)}}{2} \begin{bmatrix} 1 & 0 \\ 0 & 1 \end{bmatrix} = \frac{L^{(e)}}{2} \begin{bmatrix} 1 & 0 \\ 0 & 1 \end{bmatrix}$$

For the elements in [Figure 6.30](#), these matrices are given as:

$$[A^{(1)}] = \frac{2}{2} \begin{bmatrix} 1 & 0 \\ 0 & 1 \end{bmatrix} = \begin{bmatrix} 1 & 0 \\ 0 & 1 \end{bmatrix}$$

$$[A^{(1)}] = [A^{(3)}] = [A^{(4)}]$$

$$[A^{(2)}] = \frac{3}{2} \begin{bmatrix} 1 & 0 \\ 0 & 1 \end{bmatrix}$$

The global matrices $[D]$ and $[A]$ are obtained by combining the matrices $[D]$ and $[A]$ of all elements:

$$[D] = \begin{bmatrix} 0.3 & -0.3 & 0 & 0 & 0 \\ -0.7 & 0.7 + 0.13 & -0.13 & 0 & 0 \\ 0 & -0.53 & 0.53 + 0.3 & 0 & 0 \\ 0 & 0 & -0.7 & 0.7 + 0.3 & -0.3 \\ 0 & 0 & 0 & -0.7 & 0.7 \end{bmatrix}$$

$$= \begin{bmatrix} 0.3 & -0.3 & 0 & 0 & 0 \\ -0.7 & 0.83 & -0.13 & 0 & 0 \\ 0 & -0.53 & 0.83 & -0.3 & 0 \\ 0 & 0 & -0.7 & 1 & -0.3 \\ 0 & 0 & 0 & -0.7 & 0.7 \end{bmatrix}$$

$$[A] = \begin{bmatrix} 1 & 0 & 0 & 0 & 0 \\ 0 & 1+1.5 & 0 & 0 & 0 \\ 0 & 0 & 1.5+1 & 0 & 0 \\ 0 & 0 & 0 & 1+1 & 0 \\ 0 & 0 & 0 & 0 & 1 \end{bmatrix}$$

$$= \begin{bmatrix} 1 & 0 & 0 & 0 & 0 \\ 0 & 2.5 & 0 & 0 & 0 \\ 0 & 0 & 2.5 & 0 & 0 \\ 0 & 0 & 0 & 2 & 0 \\ 0 & 0 & 0 & 0 & 1 \end{bmatrix}$$

The backward difference method is used, thus,

$$([A] + \Delta t [D]) \{C\}_{t+\Delta t} = [A \{C\}]_t + \Delta t \{F\}_{t+\Delta t}$$

The solute concentrations at the nodes at time $t = 0$ are given as:

$$\{C\}_{t=0} = \begin{bmatrix} C_1 \\ C_2 \\ C_3 \\ C_4 \\ C_5 \end{bmatrix}_{t=0} = \begin{bmatrix} 5 \\ 5 \\ 5 \\ 5 \\ 5 \end{bmatrix}$$

The equation can be solved to obtain the concentrations at the end of the time step ($\Delta t = 5$):

$$([A] = 5[D]) \{C\}_{t=5} = [A] \{C\}_{t=0}$$

$$\begin{aligned} &= \begin{bmatrix} 2.5 & -1.5 & 0 & 0 & 0 \\ -3.5 & 6.65 & -0.65 & 0 & 0 \\ 0 & -2.65 & 6.65 & -1.5 & 0 \\ 0 & 0 & -3.5 & 7 & -1.5 \\ 0 & 0 & 0 & -3.5 & 4.5 \end{bmatrix} \begin{bmatrix} C_1 \\ C_2 \\ C_3 \\ C_4 \\ C_5 \end{bmatrix}_{t=5} \\ &= \begin{bmatrix} 1 & 0 & 0 & 0 & 0 \\ 0 & 2.5 & 0 & 0 & 0 \\ 0 & 0 & 2.5 & 0 & 0 \\ 0 & 0 & 0 & 2 & 0 \\ 0 & 0 & 0 & 0 & 1 \end{bmatrix} \begin{bmatrix} 5 \\ 5 \\ 5 \\ 5 \\ 5 \end{bmatrix} = \begin{bmatrix} 2 \\ 12.5 \\ 12.5 \\ 10 \\ 5 \end{bmatrix} \end{aligned}$$

This system of equations must be modified because of the boundary conditions, $C_{A, t=5} = 25$ and $C_{B, t=5} = 5$. Modifying this system of equations gives:

$$\begin{bmatrix} 6.65 & -0.65 & 0 \\ -2.65 & 6.65 & -1.5 \\ 0 & -3.5 & 7 \end{bmatrix} \begin{bmatrix} C_2 \\ C_3 \\ C_4 \end{bmatrix}_{t=5} = \begin{bmatrix} 100 \\ 12.5 \\ 17.5 \end{bmatrix}$$

This equation is solved to obtain the values of C_2 – C_4 at the end of the time step. The solution is:

$$= \begin{Bmatrix} C_1 \\ C_2 \\ C_3 \\ C_4 \\ C_5 \end{Bmatrix}_{t=5} = \begin{Bmatrix} 25 \\ 16.01 \\ 9.95 \\ 7.47 \\ 5 \end{Bmatrix}$$

This solution is then substituted into the right-hand side of Equation 6.98, and the procedure is repeated for the next time step if more time steps are supposed to be considered.

6.6 FINITE VOLUME METHOD

In the FVM, a number of weighted residual equations are generated by dividing the calculation function to be control volumes, and setting the weighting function to be unitized over the control volume. In a control volume, the integral of the residual must become equal to zero (Patankar, 1980).

The basic idea of the control volume formulation is easy to understand and helps to direct physical interpretation. The problem domain is divided into a number of control volumes with no overlap. The differential equation is integrated over one control volume that surrounds each grid point. The piecewise continuousness represents the variation of h between the grid points and is used to evaluate the integrals. The result is the discretization equation containing the values of h for a group of grid points. The conservation principle for h for the finite control volume is obtained in the discretization equation. The integral conservation of quantities such as mass, momentum, and energy is exactly satisfied over any group of control volumes and over the entire problem domain. This is the most attractive feature of the control volume formulation for any number of grid points; even the coarse grid solution shows the exact integral balances.

In the FVM, a structured mesh is not needed, and it is an advantage of the FVM over FDMs. The values of the conserved variables are located within the volume element, and not at nodes; hence, the FVM is preferable to other methods as a result of the fact that boundary conditions can be applied noninvasively.

6.6.1 STEADY-STATE ONE-DIMENSIONAL FLOW EQUATION

Consider the steady-state, 1D heat conduction equation as follows:

$$\frac{d}{dx} \left(K \frac{dh}{dx} \right) + R = 0 \quad (6.85)$$

To derive the discretization equation, the grid-point cluster is employed as shown in [Figure 6.31](#). Consider the grid point P that has the grid points E and W as its neighbors. (E denotes the east side, i.e., the positive x -direction, while W stands for west or

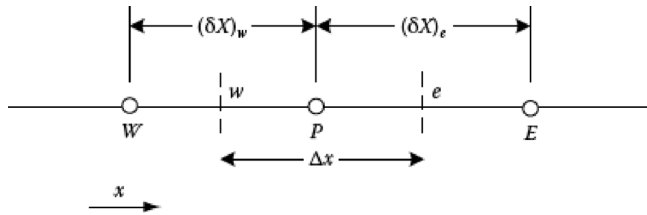


FIGURE 6.31 A grid-point cluster for a 1D problem.

the negative x -direction.) The dashed lines show the faces of the control volume; their exact locations are unimportant at first. The letters e and w denote these faces. For a 1D problem, a unit thickness in the y - and z -directions is assumed. Thus, the volume of the control volume is $\Delta x \times 1 \times 1$. If Equation 6.85 is integrated over the control volume:

$$\left(K \frac{dh}{dx} \right)_e - \left(K \frac{dh}{dx} \right)_w + \int_w^e R dx = 0 \quad (6.86)$$

To make further progress, a profile assumption or an interpolation formula is required. Two simple profile assumptions are shown in Figure 6.32. The simplest possibility is to assume that the value of h at a grid point is the same as the value of h over the entire control volume. This gives the stepwise profile sketched in Figure 6.32a.

For this profile, the slope dh/dx is not defined at the control volume faces (i.e., at w or e). As shown in Figure 6.32b, the linear interpolation functions are used between the grid points. Therefore, in this profile, the slope dh/dx is defined for the control volume faces.

Evaluating the derivatives dh/dx in Equation 6.86 for the piecewise-linear profile, the resulting equation will be as follows:

$$\frac{K_e (h_E - h_p)}{(\delta x)_e} - \frac{K_w (h_p - h_w)}{(\delta x)_w} + \bar{R} \Delta x = 0 \quad (6.87)$$

where \bar{q}_e is the average value of q_e over the control volume. It is assumed that the simplest profile is used to evaluate dh/dx . Several interpolation functions could be used for other

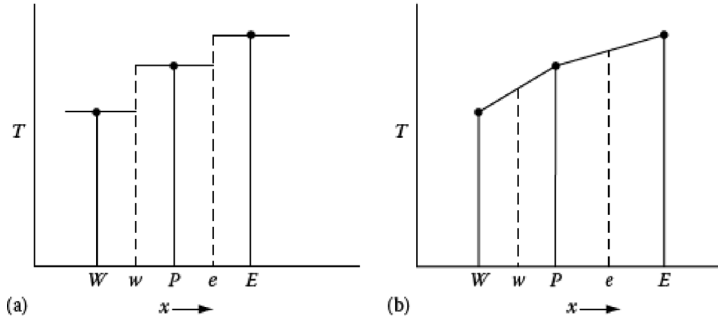


FIGURE 6.32 Two simple profile assumptions: (a) stepwise profile and (b) piecewise linear profile.

variables. For example, \bar{R} needs not to be calculated by a linear variation of R between the grid points. It is useful to modify the discretization Equation (6.87) to the following form:

$$a_p h_p = a_E h_E + a_w h_w + b \quad (6.88)$$

$$a_e = \frac{k_e}{(\Delta x)_e} \quad (6.89a)$$

$$a_w = \frac{k_w}{(\Delta x)_w} \quad (6.89b)$$

$$a_p = a_E + a_w \quad (6.89c)$$

$$b = \bar{R} \Delta x \quad (6.89d)$$

Equation 6.88 represents the standard form of the discretization equations. h_p in the left side of this equation shows the hydraulic head at the central grid point.

By increasing the dimension of the problem, the number of neighbors increases. Generally, Equation 6.89 can be written as follows for more than 1D problems:

$$a_p h_p = \sum a_{nb} h_{nb} + b \quad (6.90)$$

where the subscript nb denotes a neighbor and the summation is to be taken over all the neighbors.

Example 6.11

Consider a steady-state 1D flow in a confined aquifer between two rivers as shown in Figure 6.33. Assume $L = 50$ m, $h_A = 10$ m, $h_B = 50$ m. Determine the spatial variation of piezometric head.

SOLUTION

The groundwater flow equation for 1D flow in a confined aquifer can be written as follows:

$$\frac{d}{dx} \left(K \frac{dh}{dx} \right) = 0$$

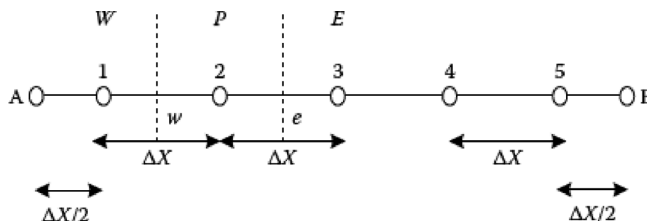


FIGURE 6.33 Elements of the confined aquifer between rivers A and B in Example 6.11.

As shown in Figure 6.31, for the grid point P , points E and W are its x -direction neighbors. For the control volume around P (when P is set at nodes 2, 3, 4), we have:

$$\int_{C.V.} \frac{d}{dx} \left(K \frac{dh}{dx} \right) A dx = 0$$

or

$$AK \frac{dh}{dx} \Big|_w^e = 0$$

$$AK \frac{dh}{dx} \Big|_e - AK \frac{dh}{dx} \Big|_w = 0$$

$$A_e K_e \frac{h_E - h_p}{(\Delta x)_e} - A_w K_w \frac{h_p - h_w}{(\Delta x)_w} = 0$$

$$\left(A_e \frac{K_e}{(\Delta x)_e} + A_w \frac{K_w}{(\Delta x)_w} \right) h_p = \left(A_w \frac{K_w}{(\Delta x)_w} \right) h_w + \left(A_e \frac{K_e}{(\Delta x)_e} \right) h_E$$

If $A_e = A_w$, $K_e = K_w$ and $(\Delta x)_e = (\Delta x)_w = \Delta x$, then $h_p = (h_w + h_E)/2$. For the control volume around P , when it is set at node 1, $(\Delta x)_e = \Delta x$ and $(\Delta x)_w = \Delta x/2$. Thus,

$$A_e K_e \frac{h_E - h_p}{\Delta x} - A_w K_w \frac{h_p - h_A}{\Delta x/2} = 0$$

$$\frac{h_E - h_p}{\Delta x} - \frac{h_p - h_A}{\Delta x/2} = 0$$

$$3h_p = h_E + 2h_A$$

When P is set at node 5, $(\Delta x)_e = \Delta x/2$ and $(\Delta x)_w = \Delta x$. So,

$$A_e K_e \frac{h_B - h_p}{\Delta x/2} - A_w K_w \frac{h_p - h_w}{\Delta x} = 0$$

$$3h_p = h_w + 2h_B$$

Therefore, the following matrix for grids 1 through 5 is obtained:

$$\begin{bmatrix} 3 & -1 & 0 & 0 & 0 \\ -1 & 2 & -1 & 0 & 0 \\ 0 & -1 & 2 & -1 & 0 \\ 0 & 0 & -1 & 2 & -1 \\ 0 & 0 & 0 & -1 & 3 \end{bmatrix} \begin{bmatrix} h_1 \\ h_2 \\ h_3 \\ h_4 \\ h_5 \end{bmatrix} = \begin{bmatrix} 2h_A \\ 0 \\ 0 \\ 0 \\ 2h_B \end{bmatrix}$$

Solving this matrix, the values of heads are obtained as follows:

$$h_1 = 14, \quad h_2 = 22, \quad h_3 = 30, \quad h_4 = 38, \quad h_5 = 46.$$

6.6.2 UNSTEADY-STATE, ONE-DIMENSIONAL FLOW EQUATION

In this section, the solution for the unsteady-state, 1D groundwater equation is sought. The general form of this equation can be expressed as follows:

$$\frac{S}{b} \frac{\partial h}{\partial t} = \frac{d}{dx} \left(K \frac{dh}{dx} \right) \quad (6.91)$$

In this equation, it is assumed that S/b is constant. Since time is a one-way coordinate, the solution is obtained by marching in time from a given initial distribution of temperature. In a typical time step, given the grid-point values of T at time t , the values of T at time $t + \Delta t$ are determined. The given values of T at the grid points will be specified by h_P^0, h_E^0, h_W^0 , and the unknown values at time $t + \Delta t$ by h_P^1, h_E^1, h_W^1 .

The discretization equation can now be derived by integrating Equation 6.91 over the control volume shown in Figure 6.24 and over the time interval from t to $t + \Delta t$:

$$\frac{S}{b} \int_w^e \int_t^{t+\Delta t} \frac{\partial h}{\partial t} dt dx = \int_w^e \int_t^{t+\Delta t} \frac{\partial}{\partial} \left(K \frac{\partial h}{\partial x} \right) dt dx \quad (6.92)$$

where the order of the integration is chosen according to the nature of the term. For the representation of the term $\partial h / \partial t$, it is assumed that the grid-point value of h prevails throughout the control volume. Then,

$$\frac{S}{b} \int_w^e \int_t^{t+\Delta t} \frac{\partial h}{\partial t} dt dx = \frac{S}{b} = \Delta x (h_P^1 - h_P^0) \quad (6.93)$$

Following the steady-state practice for $\partial h / \partial t$, we have:

$$\frac{S}{b} \Delta x (h_P^1 - h_P^0) = \int_t^{t+\Delta t} \left[\frac{K_e (h_E - h_P)}{(\delta x)_e} - \frac{K_w (h_P - h_W)}{(\delta x)_w} \right] dt \quad (6.94)$$

At this point, an assumption about how h_P , h_E , h_W vary with time from t to $t + \Delta t$ is made. Some assumptions can be generalized by proposing the following:

$$\int_t^{t+\Delta t} h_P dt = [\alpha h_P^1 + (1-\alpha) h_P^0] \Delta t \quad (6.95)$$

where α is a weighting factor, which ranges from 0 to 1. Using similar formulas for the integrals of h_E , h_W , Equation 6.94 can be rewritten as:

$$\begin{aligned} \frac{S}{b} \Delta x (h_P^1 - h_P^0) &= \int_t^{t+\Delta t} \alpha \left[\frac{K_e (h_E^1 - h_P^1)}{(\delta x)_e} - \frac{K_w (h_P^1 - h_W^1)}{(\delta x)_w} \right] \\ &\quad + (1-\alpha) \left[\frac{K_e (h_E^0 - h_P^0)}{(\delta x)_e} - \frac{K_w (h_P^0 - h_W^0)}{(\delta x)_w} \right] \end{aligned} \quad (6.96)$$

By rearranging the equation and considering that h_P , h_E , h_W henceforth stand for the new values of h at time $t + \Delta t$, we have (Patankar, 1980):

$$\begin{aligned} a_P h_P &= a_E [\alpha h_E + (1-\alpha) h_E^0] + a_W [\alpha h_W + (1-\alpha) h_W^0] \\ &\quad + [a_P^0 - (1-\alpha) a_E + (1-\alpha) a_W] h_P^0 \end{aligned} \quad (6.97)$$

where,

$$a_E = \frac{K_e}{(\delta x)_e} \quad (6.98a)$$

$$a_W = \frac{K_w}{(\delta x)_w} \quad (6.98b)$$

$$a_P^0 = \frac{S \Delta x}{b \Delta t} \quad (6.98c)$$

$$a_P = \alpha a_E + \alpha a_W + a_P^0 \quad (6.98d)$$

6.6.3 TWO-DIMENSIONAL FLOW EQUATION

A portion of a 2D mesh is shown in [Figure 6.34](#). In this figure, grid points E and W are neighbors of point P in x -direction and points N and S (denoting north and south) are the neighbors in y -direction. The hatched area around P shows the control volume. Its thickness in the z -direction is assumed to be unity. It is usually preferred to set the control volume faces exactly *midway* between the neighboring grid points.

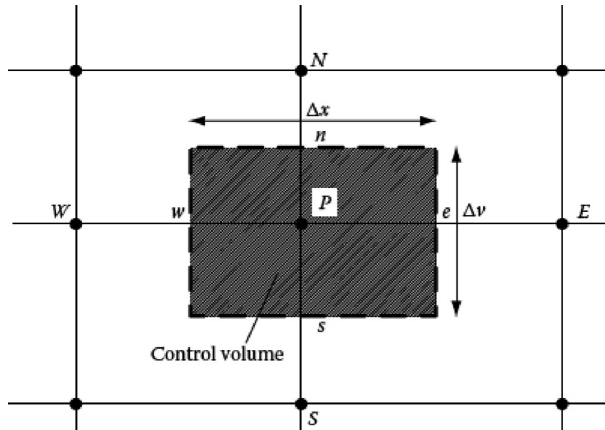


FIGURE 6.34 A control volume for a 2D mesh.

However, other practices can also be employed (Patankar, 1980). The general form of the 2D flow equation can be written as:

$$\frac{S}{b} \frac{\partial h}{\partial t} = \frac{d}{dx} \left(K \frac{dh}{dx} \right) + \frac{d}{dy} \left(K \frac{dh}{dy} \right) + R \quad (6.99)$$

Similar to the 1D form, the differential equation can be discretized as:

$$a_p h_p = a_E h_E + a_W h_W + a_N h_N + a_S h_S + b \quad (6.100)$$

where

$$a_E = \frac{K_e \Delta y}{(\delta x)_e} \quad (6.101a)$$

$$a_W = \frac{K_w \Delta y}{(\delta x)_w} \quad (6.101b)$$

$$a_N = \frac{K_n \Delta x}{(\delta x)_n} \quad (6.101c)$$

$$a_S = \frac{K_s \Delta x}{(\delta x)_s} \quad (6.101d)$$

$$a_p^0 = \frac{S \Delta x \Delta y}{b \Delta t} \quad (6.101e)$$

$$b = S_c \Delta x \Delta y + a_p^0 h_p^0 \quad (6.101f)$$

$$a_P = a_E + a_W + a_N + a_S + a_P^0 - S_P \Delta x \Delta y \quad (6.101g)$$

Since the thickness in the z -direction is unity, the product of $\Delta x \Delta y$ gives the volume of the control volume.

Example 6.12

Estimate the net flow for seepage under the sheet piling shown in Figure 6.35 for $K = 10^{-4}$ m/s, $L = 300$ m, and $\Delta x = \Delta y = 10$ m with steady-state condition.

SOLUTION

The governing differential equation is a 2D equation for a confined aquifer:

$$\frac{\partial^2 h}{\partial x^2} + \frac{\partial^2 h}{\partial y^2} = 0$$

$$\iint_{sw}^e \frac{\partial}{\partial x} \left(\frac{\partial h}{\partial x} \right) dx dy + \iint_{ws}^e \frac{\partial}{\partial y} \left(\frac{\partial h}{\partial y} \right) dx dy = 0$$

$$\int_s^n \frac{\partial h}{\partial x} \Big|_w^e dy + \int_w^n \frac{\partial h}{\partial y} \Big|_s^n dx = 0$$

$$\int_s^n \left[\left(\frac{\partial h}{\partial x} \right)_e - \left(\frac{\partial h}{\partial x} \right)_w \right] dy + \int_w^n \left[\left(\frac{\partial h}{\partial y} \right)_n - \left(\frac{\partial h}{\partial y} \right)_s \right] dx = 0$$

$$\left[\left(\frac{\partial h}{\partial x} \right)_e - \left(\frac{\partial h}{\partial x} \right)_w \right] \Delta y + \left[\left(\frac{\partial h}{\partial y} \right)_n - \left(\frac{\partial h}{\partial y} \right)_s \right] \Delta x = 0$$

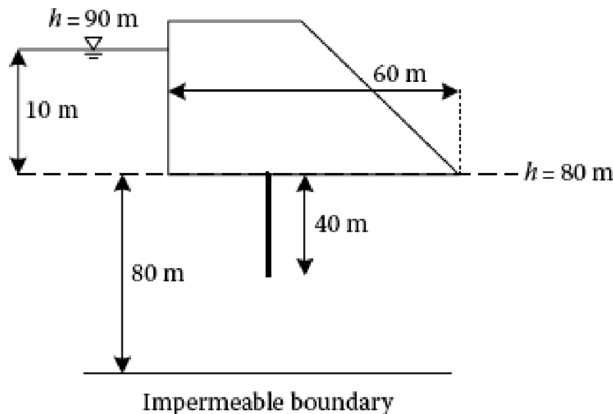


FIGURE 6.35 A dam with the sheet piling for Example 6.12.

$$\left(\frac{h_E - h_P}{(\delta x)_e} \right) \Delta y - \left(\frac{h_P - h_W}{(\delta x)_w} \right) \Delta y + \left(\frac{h_N - h_P}{(\delta y)_n} \right) \Delta x - \left(\frac{h_P - h_S}{(\delta y)_s} \right) \Delta x = 0$$

$$h_P \left(\frac{\Delta y}{(\delta x)_e} + \frac{\Delta y}{(\delta x)_w} + \frac{\Delta x}{(\delta y)_n} + \frac{\Delta x}{(\delta y)_s} \right) = h_E \frac{\Delta y}{(\delta x)_e} + h_W \frac{\Delta y}{(\delta x)_w} + h_N \frac{\Delta x}{(\delta y)_n} + h_S \frac{\Delta x}{(\delta y)_s}$$

If $\delta x = \Delta x$, $\delta y = \Delta y$, then,

$$h_P = \frac{(h_E + h_W)(\Delta y / \Delta x) + (h_N + h_S)(\Delta x / \Delta y)}{2(\Delta y / \Delta x + \Delta x / \Delta y)}$$

If $\Delta x = \Delta y$, then,

$$h_P = \frac{h_E + h_W + h_N + h_S}{4}$$

The boundary condition at the bottom of the aquifer is an impervious layer that has no inflow (Figure 6.36a):

$$\left(\frac{h_E - h_P}{(\delta x)_e} \right) \frac{\Delta y}{2} - \left(\frac{h_P - h_W}{(\delta x)_w} \right) \frac{\Delta y}{2} + \left(\frac{h_N - h_P}{(\delta y)_n} \right) \Delta x = 0$$

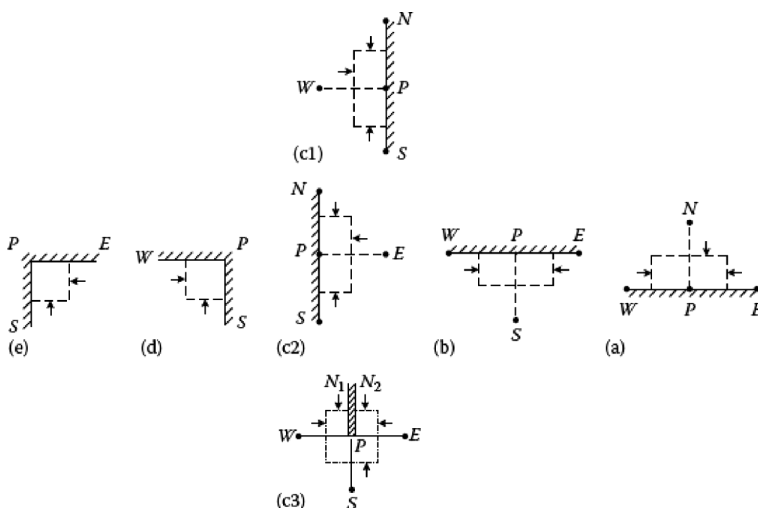


FIGURE 6.36 The boundary conditions for Example 6.12. (a) bottom of the aquifer, (b) base of the dam, (c1) right side of the sheet piling, (c2) left side of the sheet piling, (c3) bottom edge of the sheet piling, (d) left edge of the sheet piling and (e) right edge of the sheet piling.

If $\delta x = \Delta x$ and $\delta y = \Delta y$, then,

$$h_p = \frac{h_E(\Delta y/2\Delta x) + h_W(\Delta y/2\Delta x) + h_N(\Delta x/\Delta y)}{(\Delta y/\Delta x + \Delta x/\Delta y)}$$

In the left and right boundaries (condition 2), it is assumed that $\partial h/\partial x = 0$. The finite volume problem domain is expanded by two additional columns to the left and right, which are called imaginary or fictitious nodes. The value of head along the fictitious column must reflect across the boundary.

For the base of the dam (condition 3), the control volume can be considered as shown in [Figure 6.36b](#):

$$\left(\frac{h_E - h_p}{(\delta x)_e} \right) \frac{\Delta y}{2} - \left(\frac{h_p - h_W}{(\delta x)_w} \right) \frac{\Delta y}{2} - \left(\frac{h_p - h_S}{(\delta y)_s} \right) \Delta x = 0$$

If $\delta x = \Delta x$ and $\delta y = \Delta y$, then:

$$h_p = \frac{h_E(\Delta y/2\Delta x) + h_W(\Delta y/2\Delta x) + h_S(\Delta x/\Delta y)}{(\Delta y/\Delta x + \Delta x/\Delta y)}$$

At the sheet piling (condition 4):

1. For the right side of the sheet piling, the control volume has been shown in [Figure 6.36c1](#):

$$h_p = \frac{h_W(\Delta y/\Delta x) + h_N(\Delta x/2\Delta y) + h_S(\Delta x/2\Delta y)}{(\Delta y/\Delta x + \Delta x/\Delta y)}$$

2. For the left side of the sheet piling, the control volume has been shown in [Figure 6.36c2](#):

$$h_p = \frac{h_E(\Delta y/\Delta x) + h_N(\Delta x/2\Delta y) + h_S(\Delta x/2\Delta y)}{(\Delta y/\Delta x + \Delta x/\Delta y)}$$

3. For the bottom edge of the sheet piling, the control volume has been shown in [Figure 6.36c3](#):

$$\left(\frac{h_E - h_p}{(\delta x)_e} \right) \Delta y - \left(\frac{h_p - h_W}{(\delta x)_w} \right) \Delta y - \left(\frac{h_p - h_S}{(\delta y)_s} \right) \Delta x + \left(\frac{h_{N1} - h_p}{(\delta y)_s} \right) \frac{\Delta x}{2} + \left(\frac{h_{N2} - h_p}{(\delta y)_s} \right) \frac{\Delta x}{2} = 0$$

$$h_p = \frac{h_E(\Delta y/\Delta x) + h_W(\Delta y/\Delta x) + h_S(\Delta x/\Delta y) + h_{N1}(\Delta x/2\Delta y) + h_{N2}(\Delta x/2\Delta y)}{2(\Delta y/\Delta x + \Delta x/\Delta y)}$$

4. For the left edge of the sheet piling, where it is connected to the dam, the control volume has been shown in [Figure 6.36d](#):

$$-\left(\frac{h_p - h_W}{(\delta x)_w} \right) \frac{\Delta y}{2} - \left(\frac{h_p - h_S}{(\delta y)_s} \right) \Delta x = 0$$

$$h_p = \frac{h_w(\Delta y/2\Delta x) + h_s(\Delta x/2\Delta y)}{1/2(\Delta y/\Delta x + \Delta x/\Delta y)}$$

5. For the right edge of the sheet piling, where it is connected to the dam, the control volume has been shown in Figure 6.36e:

$$h_p = \frac{h_E(\Delta y/2\Delta x) + h_S(\Delta x/2\Delta y)}{1/2(\Delta y/\Delta x + \Delta x/\Delta y)}$$

A FORTRAN code has been developed to solve this problem. This code is presented in Figure 6.37. The results of this code determine the equipotential lines.

```

***** Condition 2
DO J=1,5
  P1(32,J)=F1(31,J)
END DO
***** Condition 3
J=9
DO I=28,30
  P1(I,J)=((F(I+1,J)+F(I-1,J))*DY/(2*DX)+F(I,J-1)*DX/DY)/A
END DO
DO I=33,35
  P1(I,J)=((F(I+1,J)+F(I-1,J))*DY/(2*DX)+F(I,J-1)*DX/DY)/A
  P1(I,J)=P1(I,J-1)
END DO
***** Condition 4
* Condition 4-1
DO J=6,JMAX-1
  P1(31,J)=(F(30,J)*DY/DX+(F(31,J+1)+F(31,J-1))*DX/(2*DY))/A
END DO
* Condition 4-2
DO J=6,JMAX-1
  P1(32,J)=(F(33,J)*DY/DX+(F(32,J+1)+F(32,J-1))*DX/(2*DY))/A
END DO
* Condition 4-3
I=31
J=5
  P1(I,J)=((F(I+2,J)+F(I-1,J))*DY/DX+(F(I,J-1)+&F(I,J+1)/2+F(I+1,J+1)/2)*DX/DY)/2/A
* Condition 4-4
J=9
I=32
  P1(I,J)=(F(I+1,J)*DY/DX+F(I,J-1)*DX/DY)/A
* Condition 4-5
I=31
  P1(I,J)=(F(I-1,J)*DY/DX+F(I,J-1)*DX/DY)/A
DO I=1,62
DO J=1,JMAX
  DIF=ABS(F(I,J)-P1(I,J))
  F(I,J)=P1(I,J)
  IF(DIF.GT.DIFMX) DIFMX=DIF
END DO
END DO
  WRITE(*,*) "ITER=",ITER
  WRITE(1,11)(I,I=1,IMAX)
11  FORMAT(62I10)
  DO J=JMAX,1,-1
    WRITE(1,10)(F(I,J)+80,I=1,IMAX)
10  FORMAT(62F10.4)
  ENDDO
  IF(DIFMX.GT.0.00001) GOTO 5
END

```

FIGURE 6.37 FORTRAN program for solving Example 6.12.

(Continued)

```

***** Condition 2
DO J=1,5
F1(32,J)=F1(31,J)
END DO
***** Condition 3
J=9
DO I=28,30
F1(I,J)=((F(I+1,J)+F(I-1,J))*DY/(2*DX)+F(I,J-1)*DX/DY)/A
END DO
DO I=33,35
F1(I,J)=((F(I+1,J)+F(I-1,J))*DY/(2*DX)+F(I,J-1)*DX/DY)/A
F1(I,J)=F1(I,J-1)
END DO
***** Condition 4
* Condition 4-1
DO J=6,JMAX-1
F1(31,J)=(F(30,J)*DY/DX+(F(31,J+1)+F(31,J-1))*DX/(2*DY))/A
END DO
* Condition 4-2
DO J=6,JMAX-1
F1(32,J)=(F(33,J)*DY/DX+(F(32,J+1)+F(32,J-1))*DX/(2*DY))/A
END DO
* Condition 4-3
I=31
J=5
F1(I,J)=((F(I+2,J)+F(I-1,J))*DY/DX+(F(I,J-1)+&F(I,J+1))/2+F(I+1,J+1)/2)*DX/DY)/2/A
* Condition 4-4
J=9
I=32
F1(I,J)=(F(I+1,J)*DY/DX+F(I,J-1)*DX/DY)/A
* Condition 4-5
I=31
F1(I,J)=(F(I-1,J)*DY/DX+F(I,J-1)*DX/DY)/A
DO I=1,62
DO J=1,JMAX
DIF=ABS(F(I,J)-F1(I,J))
F(I,J)=F1(I,J)
IF(DIF.GT.DIFMX) DIFMX=DIF
END DO
END DO
WRITE(*,*) "ITER=",ITER
WRITE(1,11)(I,I=1,IMAX)
11 FORMAT(62I10)
DO J=JMAX,1,-1
WRITE(1,10)(F(I,J)+80,I=1,IMAX)
10 FORMAT(62F10.4)
ENDDO
IF(DIFMX.GT.0.00001) GOTO 5
END

```

FIGURE 6.37 (Continued) FORTRAN program for solving Example 6.12.

Example 6.13

A building is supposed to be built on an island. For construction purposes, the water table needs to be lowered to a certain depth. For this purpose, the groundwater is pumped out from four wells as shown in [Figure 6.38](#). Determine the discharge from each well in steady-state condition.

SOLUTION

The governing differential equation is a 2D equation for an unconfined aquifer:

$$-q + \frac{\partial}{\partial x} \left(K_x h \frac{\partial h}{\partial x} \right) + \frac{\partial}{\partial y} \left(K_y h \frac{\partial h}{\partial y} \right) = 0$$

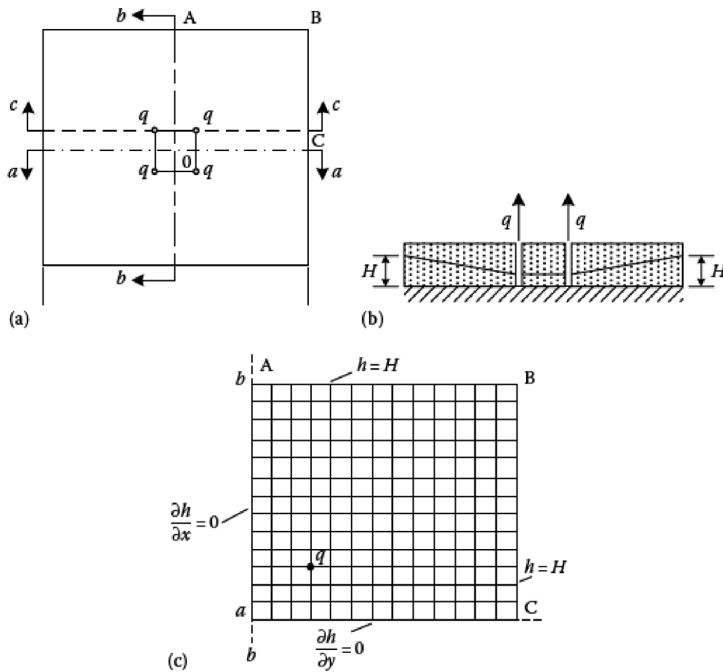


FIGURE 6.38 The definition sketch for Example 6.13: (a) plan view, (b) section view, and (c) one quarter of the plan.

Assuming $K_x = K_y$, we have:

$$-q + \frac{\partial}{\partial x} \left(\frac{K}{2} \frac{\partial h^2}{\partial x} \right) + \frac{\partial}{\partial y} \left(\frac{K}{2} \frac{\partial h^2}{\partial y} \right) = 0$$

$$-q + \frac{K}{2} \left(\frac{\partial^2 h^2}{\partial x^2} + \frac{\partial^2 h^2}{\partial y^2} \right) = 0$$

$$\iint_S \frac{K}{2} \frac{\partial^2 h^2}{\partial x^2} dx dy + \iint_W \frac{K}{2} \frac{\partial^2 h^2}{\partial y^2} dx dy - \iint_W q dx dy = 0$$

$$\int_S^n \left. \frac{K}{2} \frac{\partial h^2}{\partial x} \right|_W^e dy + \int_W^e \left. \frac{K}{2} \frac{\partial h^2}{\partial y} \right|_S^n dx - q \Delta x \Delta y = 0$$

$$\int_S^n \left[\frac{K_e}{2} \left(\frac{\partial h^2}{\partial x} \right)_e - \frac{K_w}{2} \left(\frac{\partial h^2}{\partial x} \right)_w \right] dy + \int_W^e \left[\frac{K_n}{2} \left(\frac{\partial h^2}{\partial y} \right)_n - \frac{K_s}{2} \left(\frac{\partial h^2}{\partial y} \right)_s \right] dx - q \Delta x \Delta y = 0$$

$$\left[\frac{K_e}{2} \left(\frac{\partial h^2}{\partial x} \right)_e - \frac{K_w}{2} \left(\frac{\partial h^2}{\partial x} \right)_w \right] \Delta y + \left[\frac{K_n}{2} \left(\frac{\partial h^2}{\partial y} \right)_n - \frac{K_s}{2} \left(\frac{\partial h^2}{\partial y} \right)_s \right] \Delta x - q \Delta x \Delta y = 0$$

$$\frac{K_e}{2} \left(\frac{h_E^2 - h_P^2}{(\delta x)_e} \right) \Delta y - \frac{K_w}{2} \left(\frac{h_P^2 - h_W^2}{(\delta x)_w} \right) \Delta y + \frac{K_n}{2} \left(\frac{h_N^2 - h_P^2}{(\delta y)_n} \right) \Delta x - \frac{K_s}{2} \left(\frac{h_P^2 - h_S^2}{(\delta y)_s} \right) \Delta x - q \Delta x \Delta y = 0$$

Assuming $H = h^2$, we have:

$$K_e \frac{h_E + h_P}{2} \left(\frac{h_E - h_P}{(\delta x)_e} \right) \Delta y + K_w \frac{h_P + h_W}{2} \left(\frac{h_W - h_P}{(\delta x)_w} \right) \Delta y + K_n \frac{h_N + h_P}{2} \left(\frac{h_N - h_P}{(\delta y)_n} \right) \Delta x$$

$$- K_s \frac{h_P + h_S}{2} \left(\frac{h_S - h_P}{(\delta y)_s} \right) \Delta x - q \Delta x \Delta y = 0$$

We have $h_e = (h_E + h_P)/2$, $h_w = (h_W + h_P)/2$, $h_n = (h_N + h_P)/2$, $h_s = (h_S + h_P)/2$, thus,

$$K_e h_e \left(\frac{h_E - h_P}{(\delta x)_e} \right) \Delta y + K_w h_w \left(\frac{h_W - h_P}{(\delta x)_w} \right) \Delta y + K_n h_n \left(\frac{h_N - h_P}{(\delta y)_n} \right) \Delta x$$

$$- K_s h_s \left(\frac{h_S - h_P}{(\delta y)_s} \right) \Delta x - q \Delta x \Delta y = 0$$

These equations can be solved for one quarter of the plan. It is assumed that $\partial h^2 / \partial x = 0$ and $\partial h^2 / \partial y = 0$ are the borders of each quarter.

The boundary conditions are shown in Figure 6.39. The mathematical forms of these boundary conditions are presented in the following.

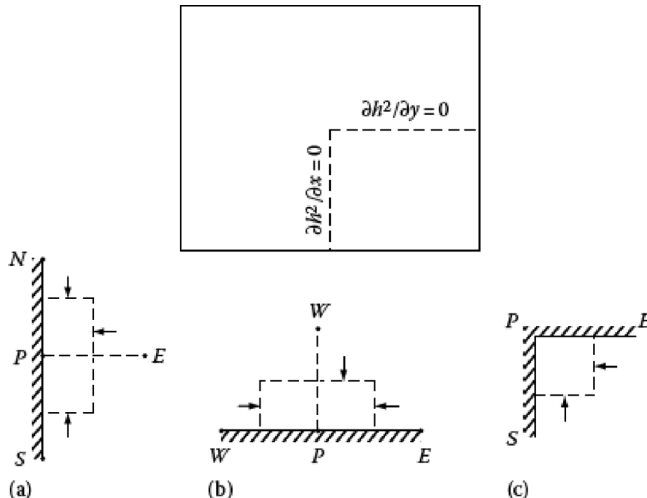


FIGURE 6.39 Boundary conditions of Example 6.13. (a) left boundary, (b) bottom boundary and (c) corner boundary.

For the left boundary, the equation for the control volume shown in Figure 6.39a is

$$\frac{K_e}{2} \left(\frac{h_E^2 - h_P^2}{(\delta x)_e} \right) \Delta y + \frac{K_n}{2} \left(\frac{h_N^2 - h_P^2}{(\delta x)_n} \right) \frac{\Delta x}{2} - \frac{K_s}{2} \left(\frac{h_P^2 - h_S^2}{(\delta x)_s} \right) \frac{\Delta x}{2} - q \Delta x \Delta y = 0$$

If $\Delta x = \Delta y$ and $K_x = K_y = K$, then:

$$h_P = \left(\frac{h_E^2}{2} + \frac{h_N^2}{4} + \frac{h_S^2}{4} - \frac{q \Delta x \Delta y}{K} \right)^{1/2}$$

For the bottom boundary, the equation for the control volume shown in Figure 6.39b is:

$$\frac{K_e}{2} \left(\frac{h_E^2 - h_P^2}{(\delta x)_e} \right) \Delta y - \frac{K_w}{2} \left(\frac{h_P^2 - h_W^2}{(\delta x)_w} \right) \Delta y - \frac{K_n}{2} \left(\frac{h_N^2 - h_P^2}{(\delta x)_n} \right) \Delta x - q \Delta x \Delta y = 0$$

If $\Delta x = \Delta y$ and $K_x = K_y = K$, then:

$$h_P = \left(\frac{h_E^2}{4} + \frac{h_W^2}{4} + \frac{h_N^2}{2} - \frac{q \Delta x \Delta y}{K} \right)^{1/2}$$

For the corner boundary, the equation for the control volume shown in Figure 6.39c is:

$$\frac{K_e}{2} \left(\frac{h_E^2 - h_P^2}{(\delta x)_e} \right) \Delta y + \frac{K_s}{2} \left(\frac{h_S^2 - h_P^2}{(\delta x)_s} \right) \frac{\Delta x}{2} - q \Delta x \Delta y = 0$$

If $\Delta x = \Delta y$ and $K_x = K_y = K$, then:

$$h_P = \left(\frac{h_E^2}{2} + \frac{h_S^2}{2} + \frac{q \Delta x \Delta y}{K} \right)^{1/2}$$

The discharge from each well is determined with trial and error. The piezometric heads are calculated with some discharge values from wells to set the water table at the given depth.

6.6.4 ORTHOGONALS COORDINATE SYSTEM

The discretization equations in orthogonal coordinate systems are formulated by using a grid in the Cartesian coordinate system. However, the presented method is not limited to Cartesian grids, and the equations can be developed with a grid in any orthogonal coordinate system. In order to illustrate the derivation of the

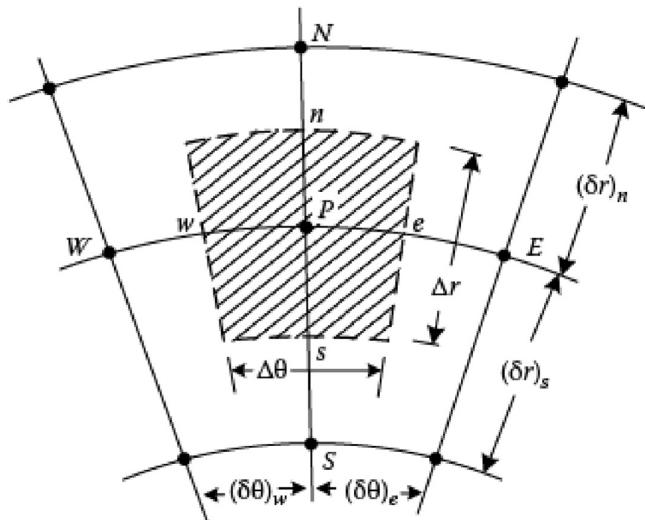


FIGURE 6.40 Control volume in polar coordinates.

discretization equation in Cartesian coordinate systems, a 2D situation is considered in polar coordinates, r and θ . The $r\theta$ counterpart is:

$$\frac{1}{r} \frac{d}{dr} \left(rK \frac{dh}{dr} \right) + \frac{1}{r} \frac{\partial}{\partial \theta} \left(\frac{K}{r} \frac{\partial h}{\partial \theta} \right) = \frac{s}{b} \frac{\partial h}{\partial t} \quad (6.102)$$

The grid and the control volume in $r\theta$ coordinates are shown in Figure 6.40. The z -direction, thickness of the control volume, is assumed to be unity.

The discretization equation is obtained by multiplying Equation 6.102 by r and integrating with respect to r and θ over the control volume. (This operation gives the volume integral, since $rdrd\theta$ represents a volume element of unit thickness) Discretization equations in orthogonal coordinate systems are then derived similar to the Cartesian coordinate.

Example 6.14

Develop the finite volume approximation of flow equation for a 2D confined aquifer in the orthogonal coordinate system.

SOLUTION

Since flow is symmetric, the governing equation can be written as:

$$\frac{1}{r} \frac{d}{dr} \left(r \frac{dh}{dr} \right) = \frac{S}{T} \frac{\partial h}{\partial t}$$

For the grid and the control volume in $r\theta$ coordinates, as shown in Figure 6.33, we have:

$$\int_t^{t+\Delta t} \int_w^n \int_s^n \frac{1}{r} \frac{\partial h}{\partial r} \left(r \frac{\partial h}{\partial r} \right) dr (rd\theta) dt = \int_s^n \int_w^n \int_t^{t+\Delta t} \frac{S}{T} \frac{\partial h}{\partial t} dt (rd\theta) dr$$

The left side of the equation is:

$$\begin{aligned} \int_t^{t+\Delta t} \int_w^n r \frac{\partial h}{\partial r} \Big|_s^n dr \theta dt &= \int_t^{t+\Delta t} \int_w^n \left[r_n \frac{\partial h}{\partial r} \Big|_n - r_s \frac{\partial h}{\partial r} \Big|_s \right] dr \theta dt \\ \int_t^{t+\Delta t} \int_w^n r \frac{\partial h}{\partial r} \Big|_s^n dr \theta dt &= \int_t^{t+\Delta t} r_n \frac{h_N - h_P}{(\delta r)_n} - r_s \frac{h_P - h_S}{(\delta r)_s} \Delta \theta dt \\ \int_t^{t+\Delta t} \int_w^n r \frac{\partial h}{\partial r} \Big|_s^n dr \theta dt &= \left[r_n \frac{h_N^{m+1} - h_P^{m+1}}{(\delta r)_n} - r_s \frac{h_P^{m+1} - h_S^{m+1}}{(\delta r)_s} \right] \Delta \theta \Delta t \end{aligned}$$

And the right side of the equation is:

$$\begin{aligned} \int_s^n \int_w^n \int_t^{t+\Delta t} \frac{S}{T} \frac{\partial h}{\partial t} dt (rd\theta) dr &= \int_s^n \int_w^n \frac{S}{T} [h_P]_t^{t+\Delta t} (rd\theta) dr \\ \int_s^n \int_w^n \int_t^{t+\Delta t} \frac{S}{T} \frac{\partial h}{\partial t} dt (rd\theta) dr &= \int_s^n \int_w^n \frac{S}{T} (h_P^{m+1} - h_P^m) (rd\theta) dr \\ \int_s^n \int_w^n \int_t^{t+\Delta t} \frac{S}{T} \frac{\partial h}{\partial t} dt (rd\theta) dr &= \int_s^n \int_w^n \frac{S}{T} (h_P^{m+1} - h_P^m) (rd\theta) dr \\ \int_s^n \int_w^n \int_t^{t+\Delta t} \frac{S}{T} \frac{\partial h}{\partial t} dt (rd\theta) dr &= \int_s^n \frac{S}{T} (h_P^{m+1} - h_P^m) r \Delta \theta dr \\ \int_s^n \int_w^n \int_t^{t+\Delta t} \frac{S}{T} \frac{\partial h}{\partial t} dt (rd\theta) dr &= \frac{S}{T} (h_P^{m+1} - h_P^m) r \Delta \theta \int_s^n r dr \\ \int_s^n \int_w^n \int_t^{t+\Delta t} \frac{S}{T} \frac{\partial h}{\partial t} dt (rd\theta) dr &= \frac{S}{T} (h_P^{m+1} - h_P^m) r \Delta \theta \left(\frac{r_n^2 - r_s^2}{2} \right) \end{aligned}$$

Therefore,

$$\left[r_n \frac{h_N^{m+1} - h_P^{m+1}}{(\delta r)_n} - r_s \frac{h_P^{m+1} - h_S^{m+1}}{(\delta r)_s} \right] \Delta \theta \Delta t = \frac{S}{T} (h_P^{m+1} - h_P^m) r \Delta \theta \left(\frac{r_n^2 - r_s^2}{2} \right)$$

The continuity equation is obtained by rearranging the equation:

$$K \left[\frac{h_N^{m+1} - h_p^{m+1}}{(\delta r)_n} (b r_n \Delta \theta) + \frac{h_s^{m+1} - h_p^{m+1}}{(\delta r)_s} (b r_s \Delta \theta) \right] = \frac{S}{T} \frac{(h_p^{m+1} - h_p^m)}{\Delta t} \Delta r \left(\Delta \theta \frac{r_n + r_s}{2} \right)$$

This equation shows that the volume of water flowing across the boundaries (the left side of the equation) is equal to the volume of water removed from storage over the entire control volume (the right side of the equation).

6.7 SIMULATION OF GROUNDWATER FLOW USING THE DISCRETE KERNEL APPROACH

The finite-difference method, discussed in [Section 6.4](#), can be used to solve the partial differential equation of groundwater flow. This method uses the initial conditions at the beginning of the time step as well as the aquifer pumping or recharging rates occurred during the time step to calculate unknown heads at the end of the time step. Therefore, a large number of equations need to be solved simultaneously at each time step, which makes this simulation technique very time consuming for groundwater planning and management objectives that usually require long-term simulation of large aquifers.

The discrete kernel approach uses a simple discrete convolution, the solution of the grid system for a few time steps to simulate the entire aquifer during the long-term period. Considering an aquifer pumped at well p anywhere in the aquifer, the drawdown at a given point, w , can be expressed as follows (Morel-Seytoux and Daly, 1975; Illangasekare et al., 1984):

$$s_w(n) = \sum_{p=1}^P \sum_{v=1}^n \delta_{wp}(n-v+1) Q_p(v) \quad (6.103)$$

where $s_w(n)$ represents the drawdown at the end of the n th week, P is the number of pumping wells, n is the number of weeks, δ_{wp} is the kernel function (aquifer response to a unit volume of water withdrawn from well p on a weekly basis), and $Q_p(v)$ is the pumping volume of the p th well during the v th week.

For an infinite and homogenous aquifer, the kernel function can be derived analytically as follows (Morel-Seytoux and Daly, 1975):

$$\delta_{wp}(v) = \frac{1}{4\pi T} \int_0^1 \exp\left(-\frac{Sr_{wp}^2}{4T(v-\tau)}\right) \frac{d\tau}{v-\tau} \quad (6.104)$$

where S is the storativity coefficient, T is the transmissivity, r_{wp} is the distance between the pumping well p and the point of interest, w , where the response is required, and τ is the time. For a more realistic condition, where the aquifer is finite and heterogeneous, simulation based on finite-difference or finite element method can be used to derive the response (drawdown) of the aquifer to pumping (see [Sections 6.4](#) and [6.5](#)).

Example 6.15

The position of three pumping wells on an infinite and homogenous confined aquifer is illustrated in Figure 6.41. During the first week, 10,000, 15,000, and 10,000 cubic meters of water are pumped out, during the second week, 5000, 10,000, 15,000 cubic meters, and during the third week, 15,000, 5000, and 10,000 cubic meters of water are withdrawn from wells 1 through 3, respectively, as shown in Figure 6.42. Using the discrete kernel approach, calculate the drawdown in an observation well (OW) located 350, 1050, and 1400 m away from the pumping wells 1 through 3, respectively, over 15 weeks. The storativity coefficient and transmissivity of the aquifer are 0.2 and $10,000 \frac{m^2}{week}$, respectively.

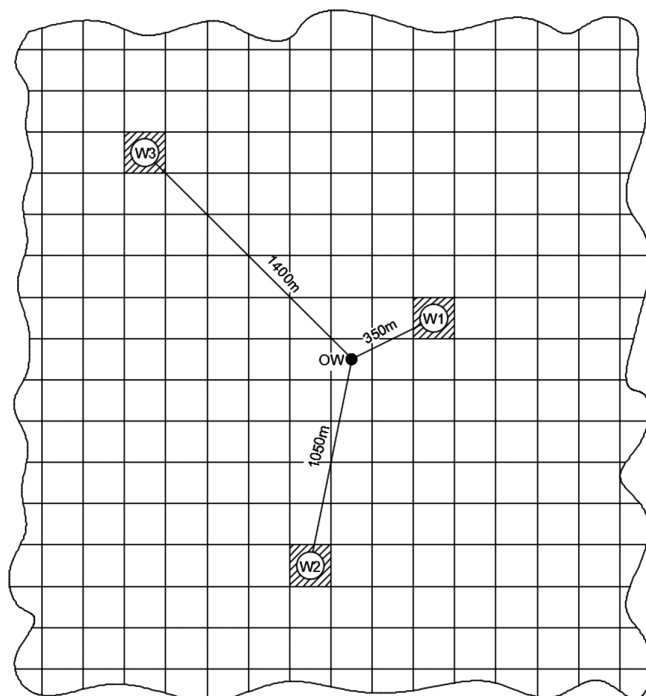


FIGURE 6.41 The position of the observation and pumping wells.

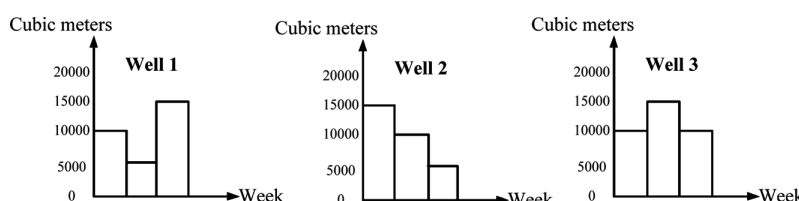


FIGURE 6.42 A three-week schedule of pumping.

SOLUTION:

Given the infinity and homogeneity of the aquifer, the response of the observation well to the wells' unit withdrawal of water per week, or the kernel coefficients, is analytically derived from Equation (6.104). This integral can be solved using any mathematical software including Maple, Mathematica, MATLAB, etc. **Table 6.1** presents solutions to this integral for weeks 1 through 15 at each pumping well. These values are the response (drawdown) of the observation well to one cubic meter of withdrawal per week from each pumping well. The kernel functions are illustrated in [Figures 6.43](#) through [6.45](#) for the three pumping wells.

TABLE 6.1
Kernel Coefficients at Different Distances from the Observation Well

| Week | 350 m from OW | 1050 m from OW | 1400 m from OW |
|------|---------------|----------------|----------------|
| 1 | 0.353E-05 | 0.503E-08 | 0.412E-10 |
| 2 | 0.360E-05 | 0.137E-06 | 0.102E-07 |
| 3 | 0.251E-05 | 0.346E-06 | 0.639E-07 |
| 4 | 0.192E-05 | 0.468E-06 | 0.132E-06 |
| 5 | 0.155E-05 | 0.512E-06 | 0.200E-06 |
| 6 | 0.130E-05 | 0.530E-06 | 0.243E-06 |
| 7 | 0.112E-05 | 0.524E-06 | 0.271E-06 |
| 8 | 0.979E-06 | 0.509E-06 | 0.287E-06 |
| 9 | 0.872E-06 | 0.489E-06 | 0.295E-06 |
| 10 | 0.786E-06 | 0.469E-06 | 0.298E-06 |
| 11 | 0.715E-06 | 0.448E-06 | 0.298E-06 |
| 12 | 0.656E-06 | 0.429E-06 | 0.295E-06 |
| 13 | 0.606E-06 | 0.410E-06 | 0.291E-06 |
| 14 | 0.564E-06 | 0.392E-06 | 0.285E-06 |
| 15 | 0.526E-06 | 0.375E-06 | 0.279E-06 |

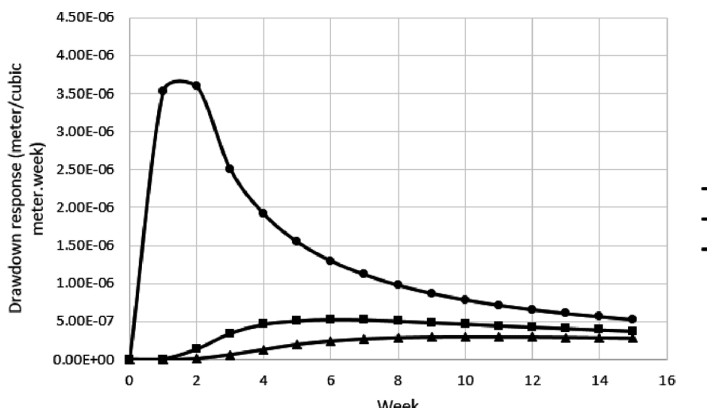


FIGURE 6.43 Observation well's response (drawdown) to one cubic meter of withdrawal per week from wells 1, 2, and 3.

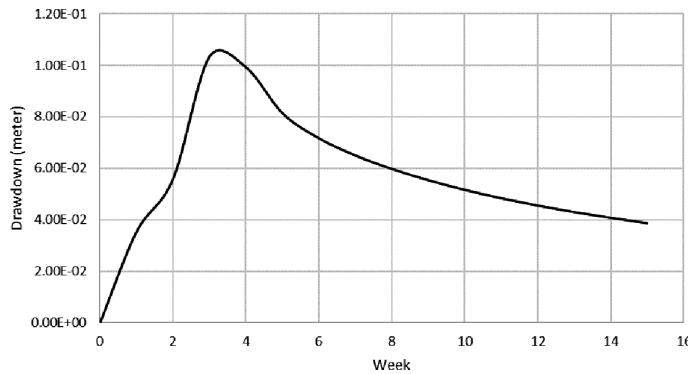


FIGURE 6.44 Total drawdowns at the location of the observation well over 15 weeks.

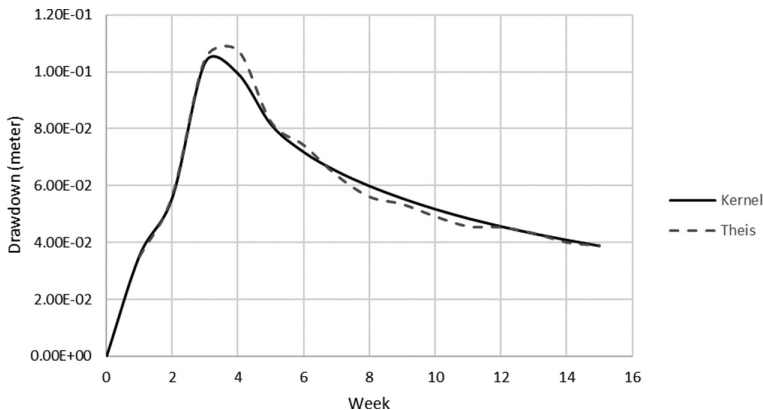


FIGURE 6.45 Total drawdowns at the location of the observation well over 15 weeks calculated by the discrete Kernel approach and Theis equation.

The total drawdown in the observation well at the end of the first week can be calculated according to Equation 6.103 as follows:

$$\begin{aligned}
 s_w(1) &= \sum_{p=1}^3 \sum_{v=1}^1 \delta_{wp}(1) Q_p(1) = \delta_{w1}(1) Q_1(1) + \delta_{w2}(1) Q_2(1) + \delta_{w3}(1) Q_3(1) \\
 &= 0.353 \times 10^{-5} \times 10000 + 0.503 \times 10^{-8} \times 15000 + 0.412 \times 10^{-10} \times 10000 \\
 &= 0.0354 \text{ m}
 \end{aligned}$$

The same procedure can be followed to calculate the total drawdown at the location of the observation well at the end of each week. The results are presented in [Table 6.2](#) and illustrated in [Figure 6.46](#).

THE THEIS SOLUTION

Using Equation 4.59, total drawdowns at the location of the observation well can also be calculated using the Theis equation.

TABLE 6.2
Total Drawdown at the Observation Well at the End of Each Week Calculated Using the Kernel Method

| Week | Total Drawdown at the OW (m) |
|------|------------------------------|
| 1 | 0.0354 |
| 2 | 0.0558 |
| 3 | 0.1034 |
| 4 | 0.0992 |
| 5 | 0.0814 |
| 6 | 0.0717 |
| 7 | 0.0650 |
| 8 | 0.0597 |
| 9 | 0.0554 |
| 10 | 0.0516 |
| 11 | 0.0483 |
| 12 | 0.0455 |
| 13 | 0.0430 |
| 14 | 0.0408 |
| 15 | 0.0387 |

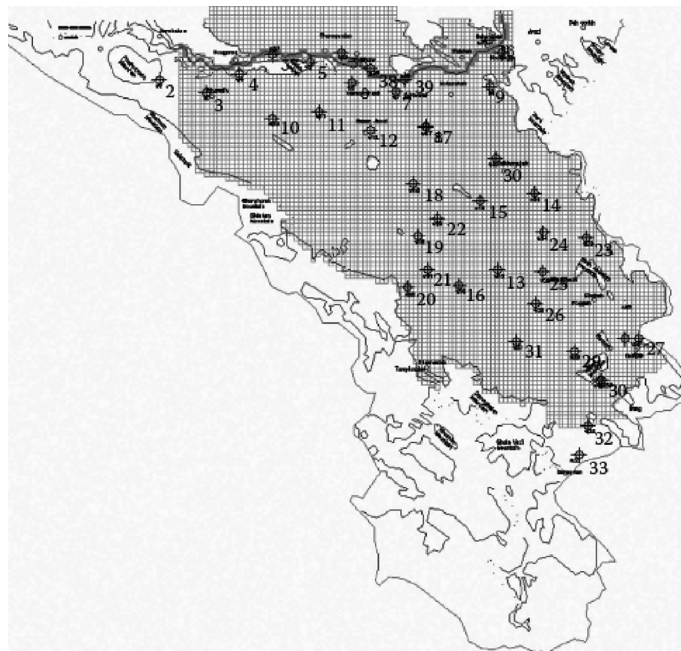


FIGURE 6.46 Study area, showing the location of the river and piezometric wells in the region.

TABLE 6.3
Values of u for Each of the Pumping Wells

| Week | u (350) | u (1050) | u (1400) |
|------|-----------|------------|------------|
| 1 | 0.6125 | 5.5100 | 9.8000 |
| 2 | 0.3062 | 2.7562 | 4.900 |
| 3 | 0.2042 | 1.8366 | 3.2667 |
| 4 | 0.1531 | 1.3775 | 2.4500 |
| 5 | 0.1225 | 1.1020 | 1.9600 |
| 6 | 0.1021 | 0.9183 | 1.6333 |
| 7 | 0.0875 | 0.7870 | 1.4000 |
| 8 | 0.0765 | 0.6887 | 1.2250 |
| 9 | 0.0681 | 0.6122 | 1.0888 |
| 10 | 0.0612 | 0.5510 | 0.9800 |
| 11 | 0.0557 | 0.5009 | 0.8909 |
| 12 | 0.0510 | 0.4592 | 0.8166 |
| 13 | 0.0471 | 0.4238 | 0.7538 |
| 14 | 0.0437 | 0.3936 | 0.7000 |
| 15 | 0.0408 | 0.3673 | 0.6533 |

The calculated values of u for different weeks at each of the pumping wells are presented in [Table 6.3](#).

Using [Table 6.4](#), $W(u)$ are obtained for different weeks and presented in Table 4.

1st week:

$$s_{w1}(1) = \frac{Q_{w1}(1)}{4\pi T} W\left(\frac{r_{w1}^2 S}{4Tt}\right) = \frac{10000}{4 \times \pi \times 10000} W\left(\frac{350^2 \times 0.2}{4 \times 10000 \times 1}\right) \\ = 0.0796 \times W(0.6125) = 0.0796 \times 0.4400 = 0.035 \text{ m}$$

$$s_{w2}(1) = \frac{Q_{w2}}{4\pi T} W\left(\frac{r_{w2}^2 S}{4Tt}\right) = \frac{15000}{4 \times \pi \times 10000} W\left(\frac{1050^2 \times 0.2}{4 \times 10000 \times 1}\right) \\ = 0.1194 \times W(5.5100) = 0.1194 \times 7.226 \times 10^{-4} = 8.6 \times 10^{-5} \text{ m}$$

$$s_{w3}(1) = \frac{Q_{w3}}{4\pi T} W\left(\frac{r_{w3}^2 S}{4Tt}\right) = \frac{10000}{4 \times \pi \times 10000} W\left(\frac{1400^2 \times 0.2}{4 \times 10000 \times 1}\right) = 0.0796 \times W(9.8) \approx 0$$

$$s_w(1) = s_{w1}(1) + s_{w2}(1) + s_{w3}(1) = 0.035 + 0.000086 + 0 = 0.0351 \text{ m}$$

TABLE 6.4
 $W(u)$ Values for Each of the Pumping Wells

| Week | $W(u) (350)$ | $W(u) 1050$ | $W(u) 1400$ |
|------|--------------|-------------|-------------|
| 1 | 0.4400 | 0.0007 | 0 |
| 2 | 0.8970 | 0.0218 | 0.0014 |
| 3 | 1.2070 | 0.0768 | 0.0105 |
| 4 | 1.5014 | 0.1548 | 0.0292 |
| 5 | 1.6850 | 0.2017 | 0.0558 |
| 6 | 1.8074 | 0.2525 | 0.1113 |
| 7 | 1.9475 | 0.3178 | 0.1510 |
| 8 | 2.0720 | 0.3790 | 0.1807 |
| 9 | 2.1785 | 0.4402 | 0.2039 |
| 10 | 2.2820 | 0.5039 | 0.2272 |
| 11 | 2.3731 | 0.5590 | 0.2637 |
| 12 | 2.4530 | 0.6171 | 0.3017 |
| 13 | 2.5309 | 0.6667 | 0.3377 |
| 14 | 2.6023 | 0.7134 | 0.3700 |
| 15 | 2.6632 | 0.7687 | 0.4074 |

2nd week:

$$\begin{aligned}
 s_{w1}(2) &= \frac{Q_{w1}(1)}{4\pi T} W\left(\frac{r_{w1}^2 S}{4T t_2}\right) + \left(\frac{Q_{w1}(2) - Q_{w1}(1)}{4\pi T}\right) W\left(\frac{r_{w1}^2 S}{4T(t_2 - t_1)}\right) \\
 &= \frac{10000}{4 \times \pi \times 10000} W\left(\frac{350^2 \times 0.2}{4 \times 10000 \times 2}\right) \\
 &\quad + \frac{5000 - 10000}{4 \times \pi \times 10000} W\left(\frac{350^2 \times 0.2}{4 \times 10000 \times (2-1)}\right) \\
 &= 0.0796 \times W(0.3062) - 0.0398 \times W(0.6125) \\
 &= 0.0796 \times 0.8970 - 0.0398 \times 0.4400 = 0.0714 - 0.0175 = 0.0539 \text{ m}
 \end{aligned}$$

$$\begin{aligned}
 s_{w2}(2) &= \frac{Q_{w2}(1)}{4\pi T} W\left(\frac{r_{w2}^2 S}{4T t_2}\right) + \left(\frac{Q_{w2}(2) - Q_{w2}(1)}{4\pi T}\right) W\left(\frac{r_{w2}^2 S}{4T(t_2 - t_1)}\right) \\
 &= \frac{15000}{4 \times \pi \times 10000} W\left(\frac{1050^2 \times 0.2}{4 \times 10000 \times 2}\right) \\
 &\quad + \frac{10000 - 15000}{4 \times \pi \times 10000} W\left(\frac{1050^2 \times 0.2}{4 \times 10000 \times (2-1)}\right) \\
 &= 0.1194 \times W(2.7562) - 0.0398 \times W(5.5100) \\
 &= 0.1194 \times 0.0218 - 0.0398 \times 7.226 \times 10^{-4} = 0.0026 - 0.000029 = 0.0026 \text{ m}
 \end{aligned}$$

$$\begin{aligned}
s_{w3}(2) &= \frac{Q_{w3}(1)}{4\pi T} W\left(\frac{r_{w3}^2 S}{4T t_2}\right) + \left(\frac{Q_{w3}(2) - Q_{w3}(1)}{4\pi T}\right) W\left(\frac{r_{w3}^2 S}{4T(t_2 - t_1)}\right) \\
&= \frac{10000}{4 \times \pi \times 10000} W\left(\frac{1400^2 \times 0.2}{4 \times 10000 \times 2}\right) + \frac{15000 - 10000}{4 \times \pi \times 10000} W\left(\frac{1050^2 \times 0.2}{4 \times 10000 \times (2-1)}\right) \\
&= 0.0796 \times W(4.9) + 0.0398 \times W(9.8) = 0.0796 \times 0.0014 + 0.0398 \times 0 = 0.0001 \text{ m}
\end{aligned}$$

Superimposing the drawdowns, the total drawdown can be computed as follows:

$$s_w(2) = s_{w1}(2) + s_{w2}(2) + s_{w3}(2) = 0.0539 + 0.0026 + 0.0001 = 0.0566 \text{ m}$$

3rd week:

$$\begin{aligned}
s_{w1}(3) &= \frac{Q_{w1}(1)}{4\pi T} W\left(\frac{r_{w1}^2 S}{4T t_3}\right) + \left(\frac{Q_{w1}(2) - Q_{w1}(1)}{4\pi T}\right) W\left(\frac{r_{w1}^2 S}{4T(t_3 - t_1)}\right) \\
&\quad + \left(\frac{Q_{w1}(3) - Q_{w1}(2)}{4\pi T}\right) W\left(\frac{r_{w1}^2 S}{4T(t_3 - t_2)}\right) \\
&= \frac{10000}{4 \times \pi \times 10000} W\left(\frac{350^2 \times 0.2}{4 \times 10000 \times 3}\right) \\
&\quad + \frac{5000 - 10000}{4 \times \pi \times 10000} W\left(\frac{350^2 \times 0.2}{4 \times 10000 \times (3-1)}\right) \\
&\quad + \frac{15000 - 5000}{4 \times \pi \times 10000} W\left(\frac{350^2 \times 0.2}{4 \times 10000 \times (3-2)}\right) \\
&= 0.0796 \times W(0.2042) - 0.0398 \times W(0.3062) + 0.0796 \times W(0.6125) \\
&= 0.0796 \times 1.2070 - 0.0398 \times 0.8970 + 0.0796 \times 0.4400 \\
&= 0.0961 - 0.0357 + 0.0350 = 0.0954 \text{ m}
\end{aligned}$$

$$\begin{aligned}
s_{w2}(3) &= \frac{Q_{w2}(1)}{4\pi T} W\left(\frac{r_{w2}^2 S}{4T t_3}\right) + \left(\frac{Q_{w2}(2) - Q_{w2}(1)}{4\pi T}\right) W\left(\frac{r_{w2}^2 S}{4T(t_3 - t_1)}\right) \\
&\quad + \left(\frac{Q_{w2}(3) - Q_{w2}(2)}{4\pi T}\right) W\left(\frac{r_{w2}^2 S}{4T(t_3 - t_2)}\right) \\
&= \frac{15000}{4 \times \pi \times 10000} W\left(\frac{1050^2 \times 0.2}{4 \times 10000 \times 3}\right) \\
&\quad + \frac{10000 - 15000}{4 \times \pi \times 10000} W\left(\frac{1050^2 \times 0.2}{4 \times 10000 \times (3-1)}\right) \\
&\quad + \frac{5000 - 10000}{4 \times \pi \times 10000} W\left(\frac{1050^2 \times 0.2}{4 \times 10000 \times (3-2)}\right) \\
&= 0.1194 \times W(1.8366) - 0.0398 \times W(2.7562) - 0.0398 \times W(5.5100) \\
&= 0.1194 \times 0.0768 - 0.0398 \times 0.0218 - 0.0398 \times 0.0007 \\
&= 0.0092 - 0.0009 - 0 = 0.0083 \text{ m}
\end{aligned}$$

$$\begin{aligned}
s_{w3}(3) &= \frac{Q_{w3}(1)}{4\pi T} W\left(\frac{r_{w3}^2 S}{4T t_3}\right) + \left(\frac{Q_{w3}(2) - Q_{w3}(1)}{4\pi T}\right) W\left(\frac{r_{w3}^2 S}{4T(t_3 - t_1)}\right) \\
&\quad + \left(\frac{Q_{w3}(3) - Q_{w3}(2)}{4\pi T}\right) W\left(\frac{r_{w3}^2 S}{4T(t_3 - t_2)}\right) \\
&= \frac{10000}{4 \times \pi \times 10000} W\left(\frac{1400^2 \times 0.2}{4 \times 10000 \times 3}\right) \\
&\quad + \frac{15000 - 10000}{4 \times \pi \times 10000} W\left(\frac{1050^2 \times 0.2}{4 \times 10000 \times (3-1)}\right) \\
&\quad + \frac{10000 - 15000}{4 \times \pi \times 10000} W\left(\frac{1050^2 \times 0.2}{4 \times 10000 \times (3-2)}\right) \\
&= 0.0796 \times W(3.2667) + 0.0398 \times W(4.9) - 0.0398 \times W(9.8) \\
&= 0.0796 \times 0.0105 + 0.0398 \times 0.0014 - 0 \\
&= 0.0008 + 0.0001 = 0.0009 \text{ m}
\end{aligned}$$

$$s_w(3) = s_{w1}(3) + s_{w2}(3) + s_{w3}(3) = 0.0954 + 0.0083 + 0.0009 = 0.1046 \text{ m}$$

4th week:

$$\begin{aligned}
s_{w1}(4) &= \frac{Q_{w1}(1)}{4\pi T} W\left(\frac{r_{w1}^2 S}{4T t_4}\right) + \left(\frac{Q_{w1}(2) - Q_{w1}(1)}{4\pi T}\right) W\left(\frac{r_{w1}^2 S}{4T(t_4 - t_1)}\right) \\
&\quad + \left(\frac{Q_{w1}(3) - Q_{w1}(2)}{4\pi T}\right) W\left(\frac{r_{w1}^2 S}{4T(t_4 - t_2)}\right) \\
&\quad + \left(\frac{Q_{w1}(4) - Q_{w1}(3)}{4\pi T}\right) W\left(\frac{r_{w1}^2 S}{4T(t_4 - t_3)}\right) \\
&= \frac{10000}{4 \times \pi \times 10000} W\left(\frac{350^2 \times 0.2}{4 \times 10000 \times 4}\right) \\
&\quad + \frac{5000 - 10000}{4 \times \pi \times 10000} W\left(\frac{350^2 \times 0.2}{4 \times 10000 \times (4-1)}\right) \\
&\quad + \frac{15000 - 5000}{4 \times \pi \times 10000} W\left(\frac{350^2 \times 0.2}{4 \times 10000 \times (4-2)}\right) \\
&\quad + \frac{0 - 15000}{4 \times \pi \times 10000} W\left(\frac{350^2 \times 0.2}{4 \times 10000 \times (4-3)}\right) \\
&= 0.0796 \times W(0.1531) - 0.0398 \times W(0.2042) + 0.0796 \times W(0.3062) \\
&\quad - 0.1194 \times W(0.6125) \\
&= 0.0796 \times 1.5014 - 0.0398 \times 1.2070 + 0.0796 \times 0.8970 - 0.1194 \\
&\quad \times 0.4400 = 0.1195 - 0.048 + 0.0714 - 0.0525 = 0.0904 \text{ m}
\end{aligned}$$

$$\begin{aligned}
s_{w2}(4) &= \frac{Q_{w2}(1)}{4\pi T} W\left(\frac{r_{w2}^2 S}{4T t_4}\right) + \left(\frac{Q_{w2}(2) - Q_{w2}(1)}{4\pi T}\right) W\left(\frac{r_{w2}^2 S}{4T(t_4 - t_1)}\right) \\
&\quad + \left(\frac{Q_{w2}(3) - Q_{w2}(2)}{4\pi T}\right) W\left(\frac{r_{w2}^2 S}{4T(t_4 - t_2)}\right) \\
&\quad + \left(\frac{Q_{w2}(4) - Q_{w2}(3)}{4\pi T}\right) W\left(\frac{r_{w2}^2 S}{4T(t_4 - t_1)}\right) \\
&= \frac{15000}{4 \times \pi \times 10000} W\left(\frac{1050^2 \times 0.2}{4 \times 10000 \times 4}\right) \\
&\quad + \frac{10000 - 15000}{4 \times \pi \times 10000} W\left(\frac{1050^2 \times 0.2}{4 \times 10000 \times (4-1)}\right) \\
&\quad + \frac{5000 - 10000}{4 \times \pi \times 10000} W\left(\frac{1050^2 \times 0.2}{4 \times 10000 \times (4-2)}\right) \\
&\quad + \frac{0 - 5000}{4 \times \pi \times 10000} W\left(\frac{1050^2 \times 0.2}{4 \times 10000 \times (4-3)}\right) \\
&= 0.1194 \times W(1.3775) - 0.0398 \times W(1.8366) - 0.0398 \times W(2.7562) \\
&\quad - 0.0398 \times W(5.5100) \\
&= 0.1194 \times 0.1548 - 0.0398 \times 0.0768 - 0.0398 \times 0.0218 - 0.0398 \\
&\quad \times 0.0007 = 0.0185 - 0.0031 - 0.0009 - 0 = 0.0145 \text{ m}
\end{aligned}$$

$$\begin{aligned}
s_{w3}(4) &= \frac{Q_{w3}(1)}{4\pi T} W\left(\frac{r_{w3}^2 S}{4T t_4}\right) + \left(\frac{Q_{w3}(2) - Q_{w3}(1)}{4\pi T}\right) W\left(\frac{r_{w3}^2 S}{4T(t_4 - t_1)}\right) \\
&\quad + \left(\frac{Q_{w3}(3) - Q_{w3}(2)}{4\pi T}\right) W\left(\frac{r_{w3}^2 S}{4T(t_4 - t_2)}\right) \\
&\quad + \left(\frac{Q_{w3}(3) - Q_{w3}(2)}{4\pi T}\right) W\left(\frac{r_{w3}^2 S}{4T(t_4 - t_1)}\right) \\
&= \frac{10000}{4 \times \pi \times 10000} W\left(\frac{1400^2 \times 0.2}{4 \times 10000 \times 4}\right) \\
&\quad + \frac{15000 - 10000}{4 \times \pi \times 10000} W\left(\frac{1050^2 \times 0.2}{4 \times 10000 \times (4-1)}\right) \\
&\quad + \frac{10000 - 15000}{4 \times \pi \times 10000} W\left(\frac{1050^2 \times 0.2}{4 \times 10000 \times (4-2)}\right) \\
&\quad + \frac{0 - 10000}{4 \times \pi \times 10000} W\left(\frac{1050^2 \times 0.2}{4 \times 10000 \times (4-3)}\right) \\
&= 0.0796 \times W(2.4500) + 0.0398 \times W(3.2667) - 0.0398 \times W(4.9) - 0.0796 \\
&\quad \times W(9.8) = 0.0796 \times 0.0292 + 0.0398 \times 0.0105 - 0.0398 \times 0.0014 \\
&= 0.0023 + 0.0004 - 0.0001 = 0.0026 \text{ m}
\end{aligned}$$

TABLE 6.5
Total Drawdowns at the Location of the
Observation Well Using the Theis Equation

| Week | Total Drawdown at the OW |
|------|--------------------------|
| 1 | 0.0351 |
| 2 | 0.0566 |
| 3 | 0.1046 |
| 4 | 0.1075 |
| 5 | 0.0824 |
| 6 | 0.0742 |
| 7 | 0.0636 |
| 8 | 0.0561 |
| 9 | 0.0535 |
| 10 | 0.0492 |
| 11 | 0.0457 |
| 12 | 0.0454 |
| 13 | 0.0433 |
| 14 | 0.0401 |
| 15 | 0.0390 |

$$s_w(4) = s_{w1}(4) + s_{w2}(4) + s_{w3}(4) = 0.0904 + 0.0145 + 0.0026 = 0.1075 \text{ m}$$

For the remaining weeks (5th–15th), the drawdowns can be calculated as follows using MATLAB (Table 6.5):

```
for t=5:15
s1(t)=0.0796 * W1(t) - 0.0398 * W1(t - 1) + 0.0796 * W1(t - 2) - 0.1194 * W1(t - 3);
s2(t)=0.1194 * W2(t) - 0.0398 * W2(t - 1) - 0.0398 * W2(t - 2) - 0.0398 * W2(t - 3);
s3(t)=0.0796 * W3(t) + 0.0398 * W3(t - 1) - 0.0398 * W3(t - 2) - 0.0796 * W3(t - 3);
sw(t)=s1(t) + s2(t) + s3(t);
end
```

Figure 6.45 illustrates that the solutions based on the kernel approach and Theis equation are consistent. However, in the kernel approach, kernel coefficients are derived based on finite-difference modeling, which enables the approach to be applied to a wide range of boundary conditions and aquifer responses.

6.8 SATURATED-UNSATURATED TRANSPORT (SUTRA) CODE

SUTRA is a computer program that simulates fluid movement and the transport of either energy or dissolved substances in a subsurface environment. The original version of SUTRA was released by Voss in 1984. SUTRA version 2.2

(Voss and Provost, 2002) enables the previous version to specify time-dependent sources and boundary conditions (without programming) and to output information pertaining to source and boundary condition nodes in a convenient format. SUTRA may be utilized for areal and cross-sectional modeling of saturated groundwater flow systems, and for cross-sectional modeling of unsaturated zone flow. Solute transport simulation using SUTRA may be employed to model natural or man-induced chemical species transport including processes of solute sorption, production, and decay, and may be applied to analyze groundwater contaminant transport problems and aquifer restoration designs.

The fluid mass balance and the solute mass balance equations (Equations 6.105 and 6.106, respectively) in SUTRA are solved simultaneously to characterize variable-density flow associated with saltwater intrusion. The fluid mass balance equation demonstrates the single-phase flow in saturated and unsaturated porous media, and the solute mass balance equation describes the solute transport including advection and dispersion mechanisms (Voss and Provost, 2010).

$$\left(S_w \rho S_{OP} + \varepsilon \rho \frac{dS_w}{dP} \right) \frac{\partial P}{\partial t} + \varepsilon \frac{\partial P}{\partial c} \frac{\partial c}{\partial t} - \nabla \left[\frac{k k_r \rho}{\mu} (\nabla P - \rho g) \right] = Q_P \quad (6.105)$$

$$\frac{\partial (\varepsilon S_w \rho c)}{\partial t} + \nabla (\varepsilon S_w \rho v c) - \nabla (\varepsilon S_w \rho (D_m I + D) \nabla c) = Q_P c^* \quad (6.106)$$

where:

S_w (–) is the saturation degree

ρ (ML^{-3}) is the fluid density

S_{OP} ($\text{LT}^2 \text{M}^{-1}$) is the specific pressure storativity

P ($\text{ML}^{-1} \text{T}^{-2}$) is the fluid pressure

t (T) is the time

ε (–) is the aquifer volumetric porosity

c ($\text{M}_s \text{M}^{-1}$) is the solute concentration

k (L^2) is the solid matrix intrinsic permeability

k_r is the relative permeability with respect to the water phase

μ ($\text{ML}^{-1} \text{T}^{-1}$) is the fluid dynamic viscosity

g ($\text{L}^2 \text{T}^{-1}$) is the gravitational acceleration

Q_P ($\text{ML}^{-3} \text{T}^{-1}$) is the fluid mass sink or source

v (LT^{-1}) is the average fluid velocity

D_m ($\text{L}^2 \text{T}^{-1}$) is the molecular diffusion

I is the identity tensor

D ($\text{L}^2 \text{T}^{-1}$) is the mechanical dispersion tensor

c^* ($\text{M}_s \text{M}^{-1}$) is the solute concentration as a mass fraction of fluid sources.

6.9 MODFLOW

MODFLOW is a 3D, finite-difference groundwater model that was first released in 1984. It is a modular finite-difference groundwater flow model developed by the U.S. Geological Survey (McDonald and Harbaugh, 1988). This program is designed

to simplify model development and data input for groundwater modeling to develop maps, diagrams, and text files. It is one of the most widely used groundwater simulation models. This model can be found and downloaded from the U.S. Geological Survey Website. Many new capabilities have been added to the original model in recent versions.

MODFLOW-2000 simulates steady and unsteady flow in an irregularly shaped flow system in which aquifer layers can be confined, unconfined, or a combination of confined and unconfined. Flow from external stresses, such as flow to wells, surface recharge, evapotranspiration, flow to drains, and flow through riverbeds, can be simulated. Hydraulic conductivities or transmissivities for any layer may differ spatially and be anisotropic (restricted to having the principal directions aligned with the grid axes), and the storage coefficient may be heterogeneous. Specified head and flux boundaries can be simulated by this model. It is also capable of modeling head-dependent flux across the outer boundary of the model, which allows water to be supplied to a boundary block in the modeled area at a rate proportional to the current head difference between a source of water outside the modeled area and the boundary block.

In addition to simulating groundwater flow, the scope of MODFLOW-2000 has been expanded to incorporate capabilities such as solute transport and parameter estimation. In this model, the groundwater flow equation is solved using the FDA. The flow region is subdivided into blocks in which the medium properties are assumed to be uniform. In the plan view, blocks are made from a grid of mutually perpendicular lines that may be variably spaced. Model layers can have varying thicknesses. A flow equation is written for each block, or cell. Several methods are provided for solving the resulting matrix problem; the user can choose the best one for a particular problem. Flow rate and cumulative volume, which are balanced from each type of inflow and outflow, are computed for each time step.

MODFLOW-2005 is similar in design to MODFLOW-2000. The primary change in MODFLOW-2005 is the incorporation of a different approach for managing internal data. FORTRAN modules are used to declare data that can be shared among subroutines. This allows data to be shared without using subroutine arguments. As a result of using these FORTRAN modules, a change in terminology for MODFLOW has been made.

Processing MODFLOW for Windows (PMWIN) is a simulation system for modeling groundwater flow and transport processes with the modular 3D, finite-difference groundwater model MODFLOW. PMWIN also supports the calculation of elastic and inelastic compaction of an aquifer due to changes of hydraulic heads (Chiang and Kinzelbach, 2005).

The groundwater modeling system is a powerful graphical tool for model creation and visualization of results. Models can be built using digital maps and elevation models as reference and source data. One of the greatest strengths of the groundwater modeling system has traditionally been the conceptual model approach. This approach makes it possible to build a conceptual model in the groundwater modeling system map module using GIS feature objects. The conceptual model defines the boundary conditions, sources/sinks, and material property zones for a model. The model data can then be automatically discretized to the model grid or mesh. The conceptual model approach makes it possible to deal with large complex

models in a simple and efficient manner. An example solved with MODFLOW is presented in the following section.

The first step toward creating a model is the development of a grid system, then layers are added and parameters of hydraulic conductivity, initial head, storage coefficient, top elevation, and bottom elevation are specified for each cell. The number of stress periods over which the model will run and the time of their operation should be set.

Results could be analyzed through contour plots, if desired. Superimposing a grid over a graphic image or digitized line drawing is one of the most powerful features of a graphic groundwater. These images are generally 2D plan views representing the area that is going to be modeled.

Example 6.16

This tutorial presents a model to simulate the groundwater of the Lenjanat aquifer and Zayandeh-Rud River in central Iran.

In this area, 750 and 220 MCM per year of groundwater are supplied for agricultural and industrial uses, respectively. Meanwhile, more than 800 MCM per year is supplied from the Zayandeh-Rud River. This river has an average of 1300 MCM discharge per year. The return flows from agricultural and industrial sectors to groundwater are, respectively, 15% and 10% of the supplied water. The transmissivity in the Lenjanat unconfined aquifer varies from 300 to 2400 m²/day. The average coefficient of hydraulic conductivity is about 3 m/day.

There are about 40 piezometric wells to record the water table in this aquifer. The Lenjanat aquifer is mainly recharged by precipitation, infiltration from the riverbed, inflow from neighboring aquifers, and return flows from industrial and agricultural sectors. The discharge from the aquifer occurs through water extraction from wells, springs, and qanats, as well as groundwater outflow and evapotranspiration.

The industrial and agricultural return flows are the most important sources of water pollution in the region. The recharged water from the aquifer to the river is also the cause of increasing water salinity. The total dissolved solids (TDSs) variation is a good index for assessing these pollutants ([Figure 6.46](#)).

The problem consists of creating a mathematical model to simulate the Lenjanat aquifer using the PMWIN software. The goal is to define the monthly average groundwater table variations in the agriculture zones, which are functions of discharge, recharge, water head in the river, inflow, and outflow at the boundaries as well as physical characteristics of the aquifer.

SOLUTION

Step 1: Grid creation

The model is created from the file menu. Next, the mesh size including the number of layers, columns, and rows is entered in the model dimension box according to [Figure 6.47](#). Then, the grid is generated as shown in [Figure 6.48](#).

Step 2: Layer properties

Using the layer options from the grid menu, the type of layers is assigned. In this case, the unconfined type is chosen for the aquifer ([Figure 6.49](#)).

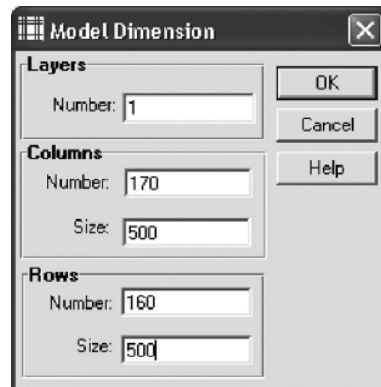


FIGURE 6.47 Model dimension input box.

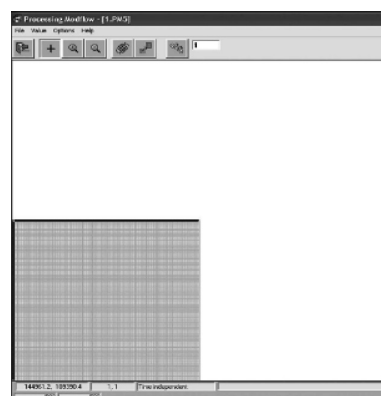


FIGURE 6.48 Generated model grid.

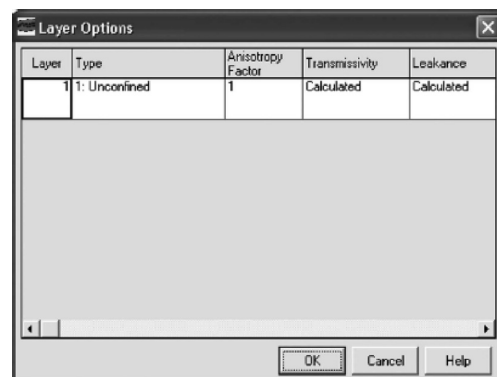


FIGURE 6.49 The Layer Options dialog box and the layer type drop-down list.

Step 3: Using background maps

In this step, using the maps options, up to five background DXF maps (DXF format is a file format for vector drawings) can be displayed. The study area map can be imported as shown in [Figure 6.50](#).

Step 4: Coordinates properties

The grid coordinates and worksheet size are determined by entering the sizes in the “Environment Options” window as shown in [Figure 6.51](#).

Step 5: Boundary conditions

In order to define boundary conditions, the boundary condition is selected from the menu and the value 1 is entered as shown in [Figure 6.52](#). The number of active grid cells is 6210.

Step 6: Layer elevations

The top and bottom elevations of each aquifer are specified in the Top of Layer and Bottom of Layer menu. The values are entered based on the

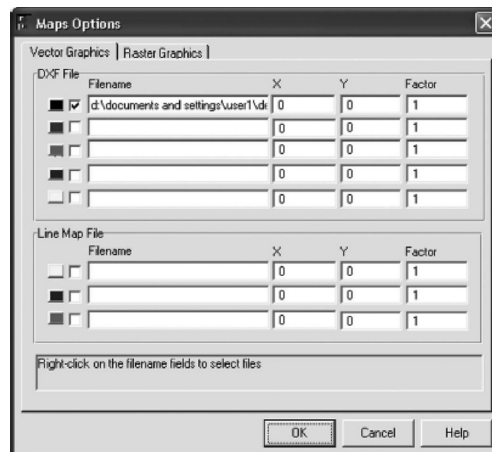


FIGURE 6.50 Map Options window.

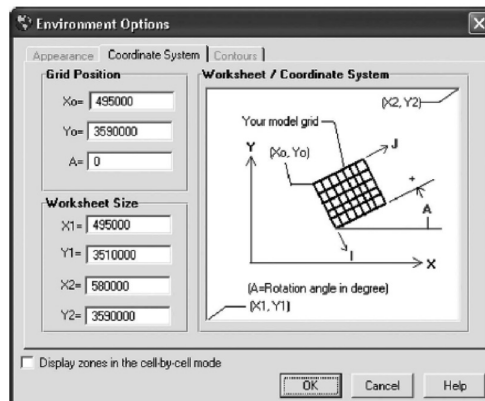


FIGURE 6.51 Environment Options window.

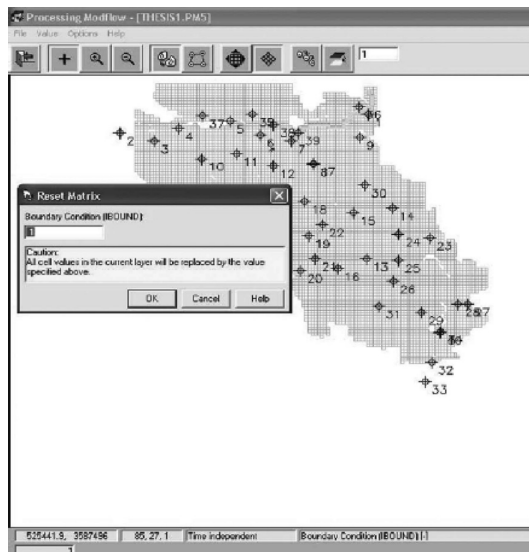


FIGURE 6.52 Boundary condition window.

topographic map and geophysical studies in the study area. The top and the bottom elevations are 1865.01 and 1515.18 (meters above sea level), respectively.

Step 7: Simulation time properties

After determining the aquifer elevation, the time parameters are indicated by choosing the time menu. The simulation time unit is changed to "days," and the flow type is chosen to be transient for this example as shown in [Figure 6.53](#).

Step 8: Initial conditions

The initial hydraulic heads are loaded in the browse matrix box. Its value in this study is considered to be 1874.484 m ([Figure 6.54](#)).

Also, the horizontal hydraulic conductivity, effective porosity, and specific yield are chosen from the parameter menu, and their values are entered in the reset matrix box from the value menu. These parameter values in the study area are 3 m/day, 25%, and 0.58, respectively. The related boxes are shown in [Figures 6.55](#) through [6.57](#).

In addition, the recharge rate with the value of 1.9778×10^{-4} m/day as a necessary model input is entered using the recharge box from the model menu ([Figure 6.58](#)). In order to edit the model data for a specific stress period, a period from the Temporal Data window is selected, and then the "Edit Data" option is chosen ([Figure 6.59](#)).

In the next step, the river data for each cell are entered. To do this, the river package from the MODFLOW model is chosen. Then, the river hydraulic conductivity, head, and elevation of the riverbed bottom saved in three ASCII matrix files are imported. These files are loaded in the reset matrix box from the value menu as shown in [Figure 6.60](#).

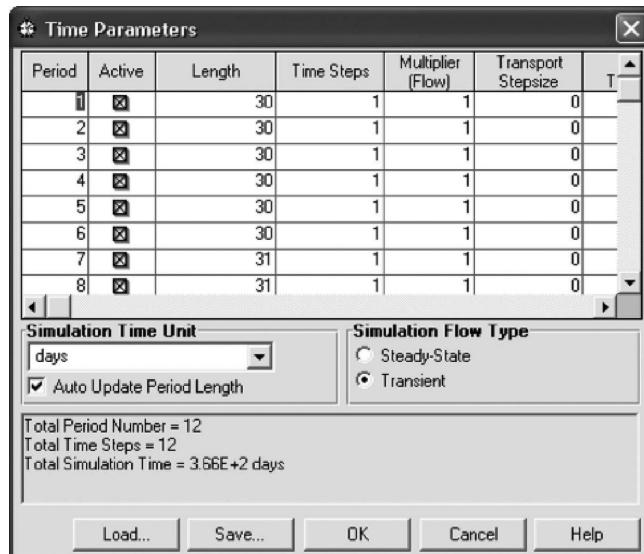


FIGURE 6.53 Time Parameters window.

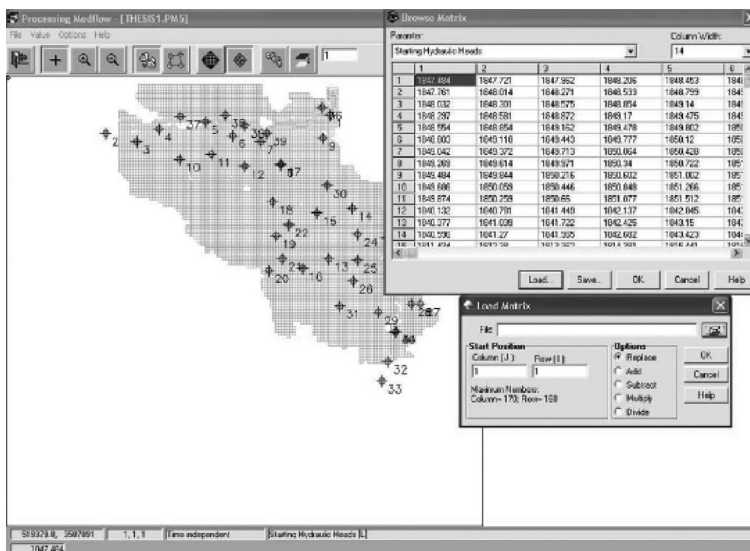


FIGURE 6.54 Browse Matrix window.

Then, the well data should be introduced to the model. To enter the recharge rate of the well, which is $-38.77 \text{ m}^3/\text{day}$ in this example, the well package is selected from the MODFLOW model. Then, by choosing the reset matrix menu, the cell value box, as shown in Figure 6.61, is appeared. The value is entered into the box and this step is repeated for all wells in this example.

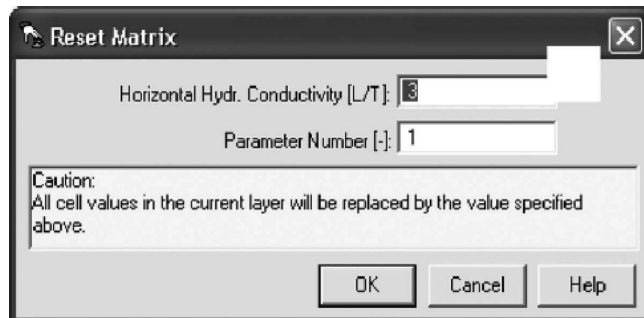


FIGURE 6.55 Horizontal Hydraulic Conductivity window.

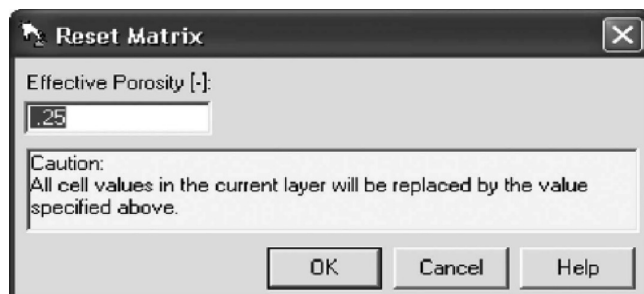


FIGURE 6.56 Effective Porosity window.

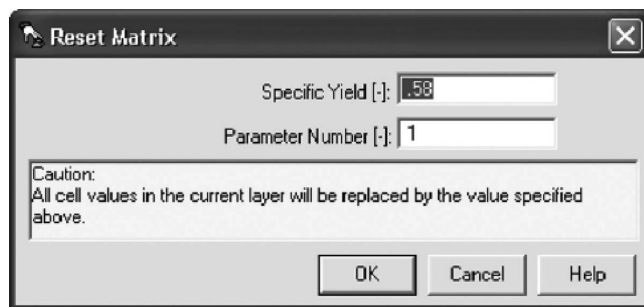


FIGURE 6.57 Specific Yield window.

Step 9: Output control

After entering all parameters of initial conditions, the user should control the output of these unformatted files. This can be done by choosing the output control from the MODFLOW menu. The related box is shown in Figure 6.62. The output terms can be seen in this figure. The pre-defined values of nonflow cells and dry cells are -999.99 and $1E + 30$, respectively.

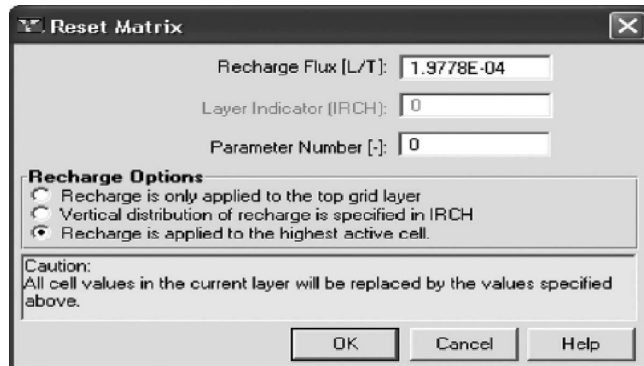


FIGURE 6.58 Recharge Rate window.

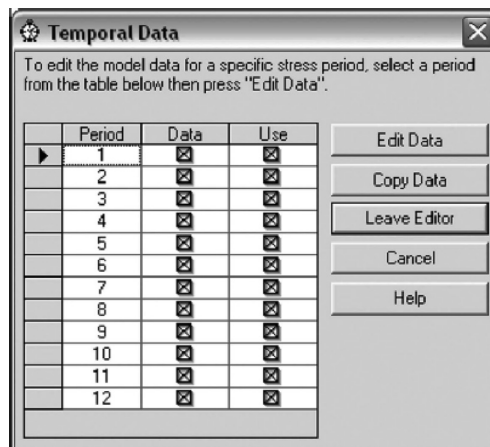


FIGURE 6.59 Temporal Data window.

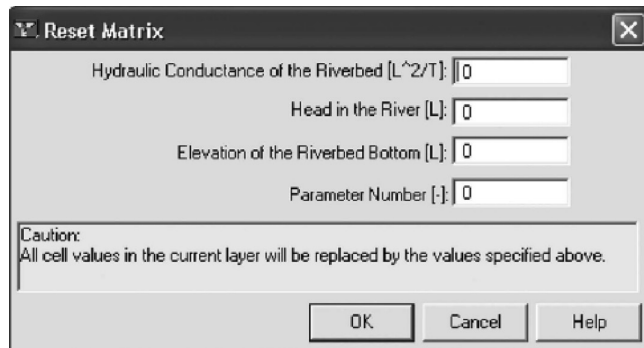


FIGURE 6.60 Reset Matrix window for the river package.

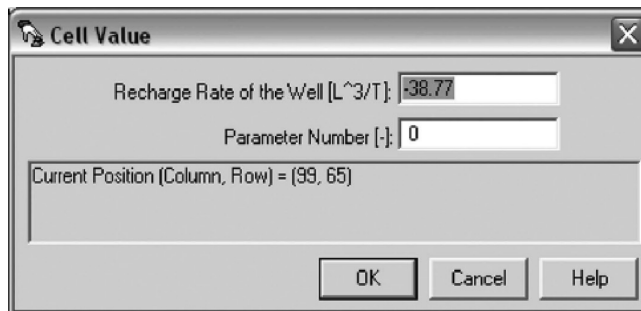


FIGURE 6.61 Cell Value window.

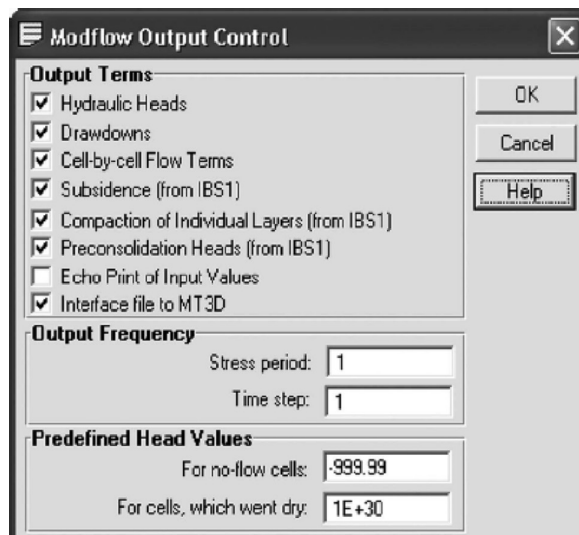


FIGURE 6.62 MODFLOW Output control window.

Step 10: Run MODFLOW

In this step, the run option from the MODFLOW menu is selected to generate the required data files and to run the model. As shown in [Figure 6.63](#), the modflow2v.exe file (c:\program files\pmwin\modflw96\lkmt2\modflow2v.exe) from the MODFLOW program is chosen to run the model ([Figure 6.64](#)).

Step 11: Modular 3-Dimensional Transport model data preparation

To evaluate groundwater quality in the aquifer, the salinity concentrations need to be imported to the model. By selecting the matrix option from the value menu and choosing the Modular 3-Dimensional Transport model (MT3D) option, the initial concentration values are entered and loaded ([Figure 6.65](#)).

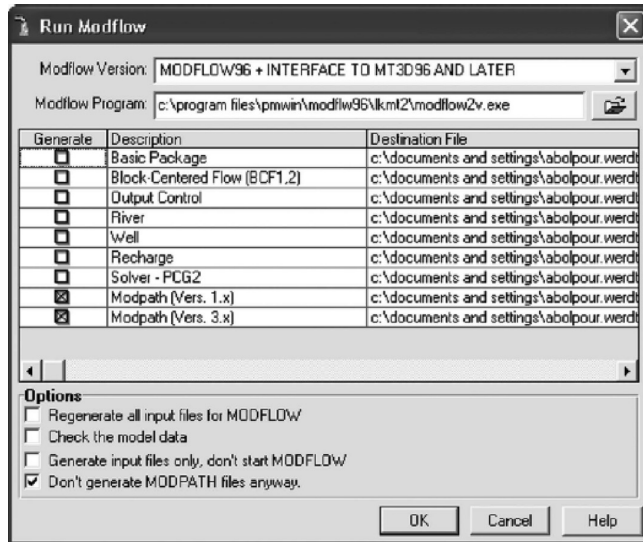


FIGURE 6.63 Configuration to run MODFLOW.

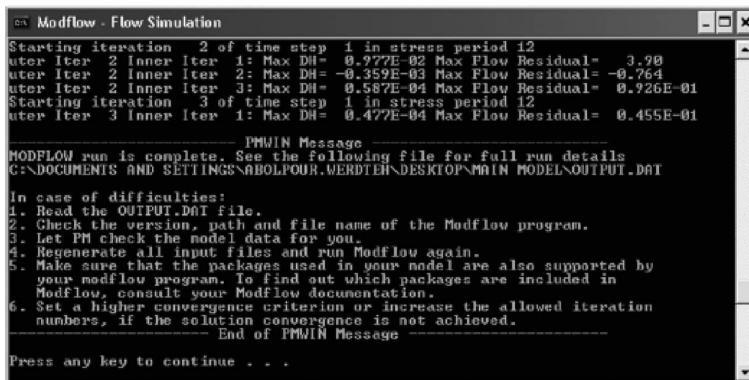


FIGURE 6.64 Completion of the flow simulation in a MS-DOS environment.

The MT3D option can also be used to import transport parameters to the advection package. In the advection package box, as shown in Figure 6.66, the methods of characteristics for the solution scheme and first-order Euler for the particle tracking algorithm are selected.

In the next step, the MT3D option under the dispersion package is chosen to enter the ratio of transverse dispersivity to longitudinal dispersivity as shown in Figure 6.67. The diffusion molecular coefficient (DMCOEF) value is considered to be 0.000004 m²/day for this example. This parameter is the effective molecular diffusion coefficient.

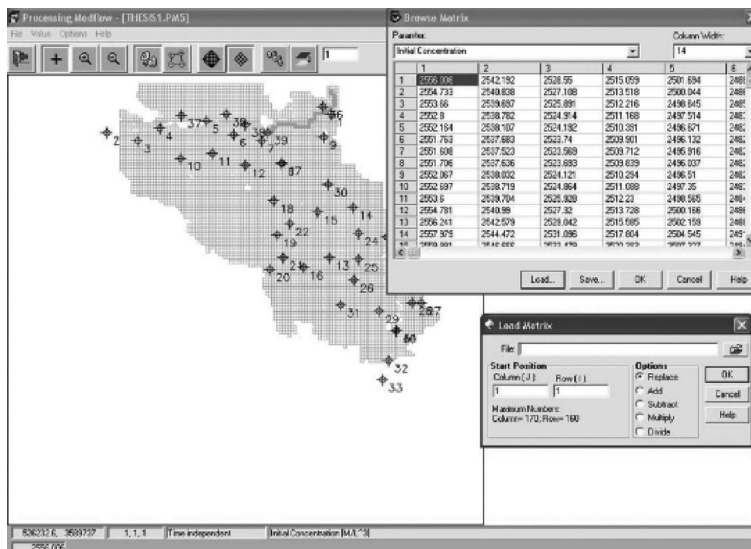


FIGURE 6.65 The Browse Matrix window.

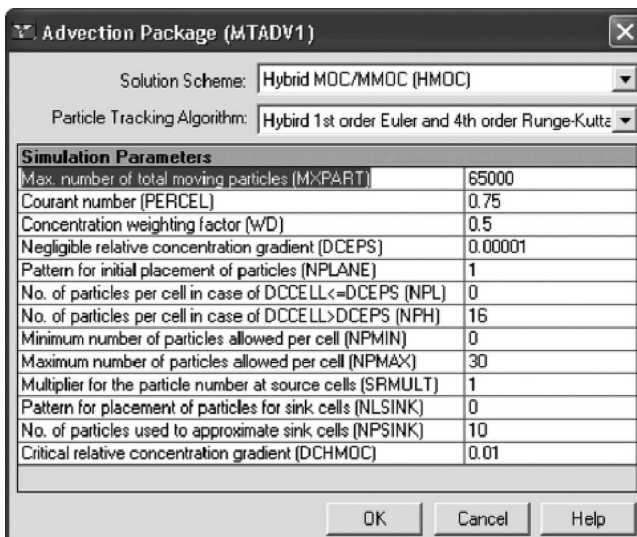


FIGURE 6.66 The Advection Package window.

Moreover, to specify the output times, the parameters, which should be controlled, are selected. To specify the output times, the Output Times tab within the Output Control window from the model menu is chosen (Figure 6.68). For this example, intervals of 30 are introduced.

To perform the transport simulation, the Run from the MT3D program is selected. The MT3D program is then identified as c:\program

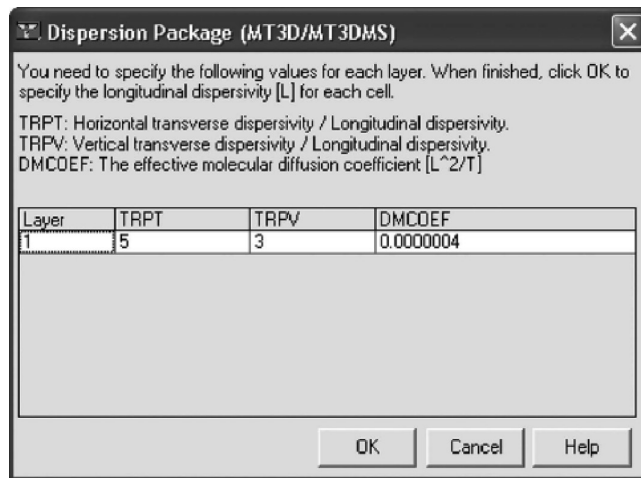


FIGURE 6.67 The Advection Package (MTADV1) dialog box.

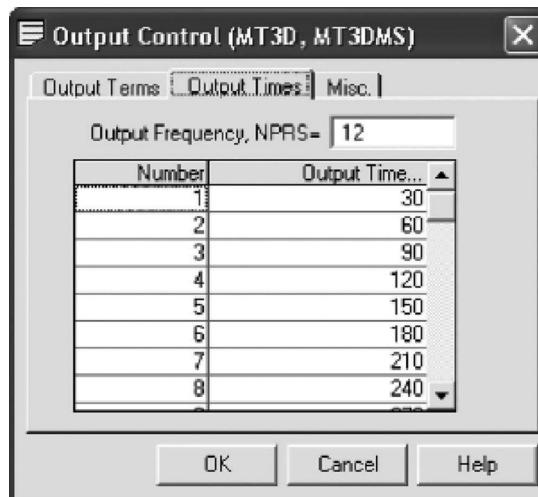


FIGURE 6.68 The Output Control dialog box.

files\pmwin\mt3d\mt3dv.exe to run the model. Prior to running MT3D, PMWIN will use user-specified data to generate input files for MT3D (Figure 6.69).

Step 12: Output evaluation

Graphs of observed and calculated heads can be compared using the tools menu. As shown in Figure 6.70, the head-time curves are created. Their scatter diagram is shown in Figure 6.71. These two figures show the results in all existing wells.

For comparison, the calculated head values (y-axis) are plotted against the observed values (x-axis).

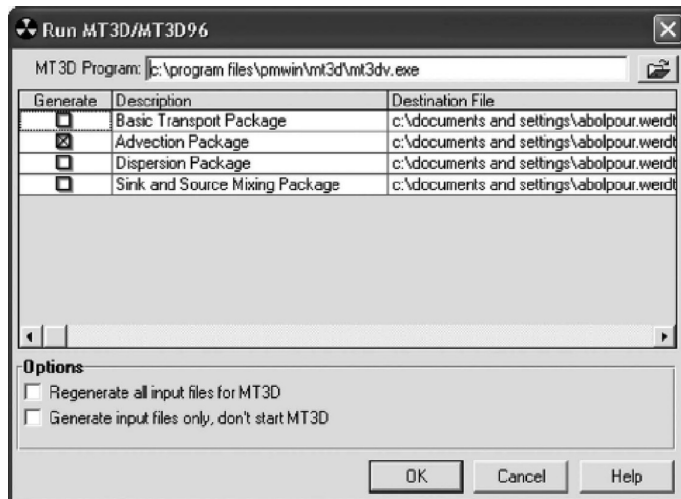


FIGURE 6.69 The Run MT3D/MT3D96 window.

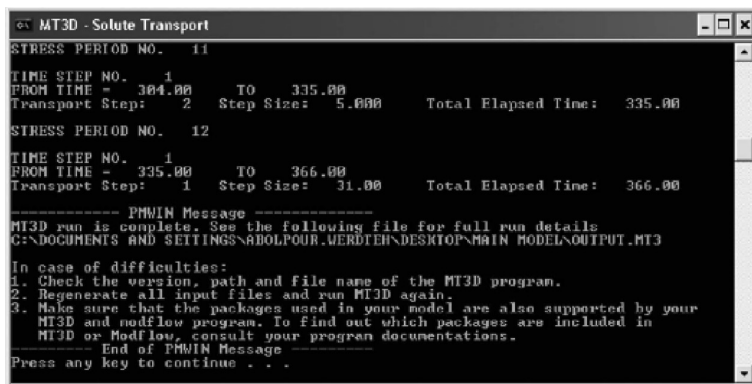


FIGURE 6.70 Running the solute transport in a MS-DOS environment.

The model is used to simulate for one year. The time step is monthly, and the measurement unit is in days. The flow type is unsteady.

In Figures 6.72 through 6.74, the drawdown-time curve for well 34 and concentration-time curve for well 39 are shown.

The contour maps of head variations and TDSs concentrations are shown in Figures 6.75 and 6.76.

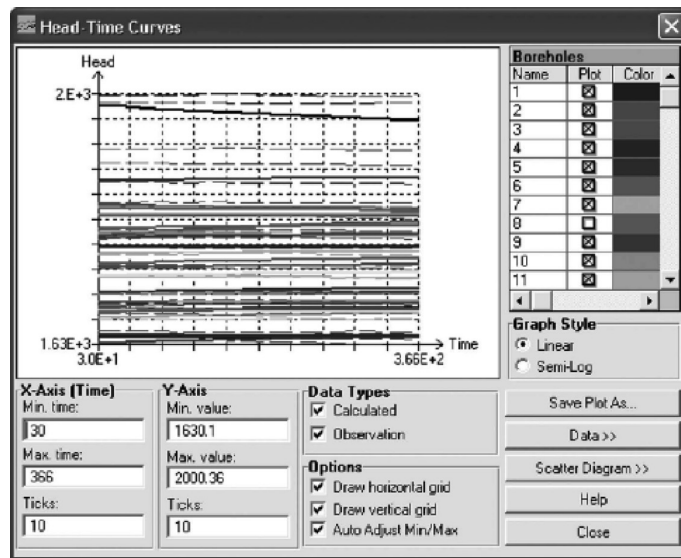


FIGURE 6.71 Head-Time Curves window.

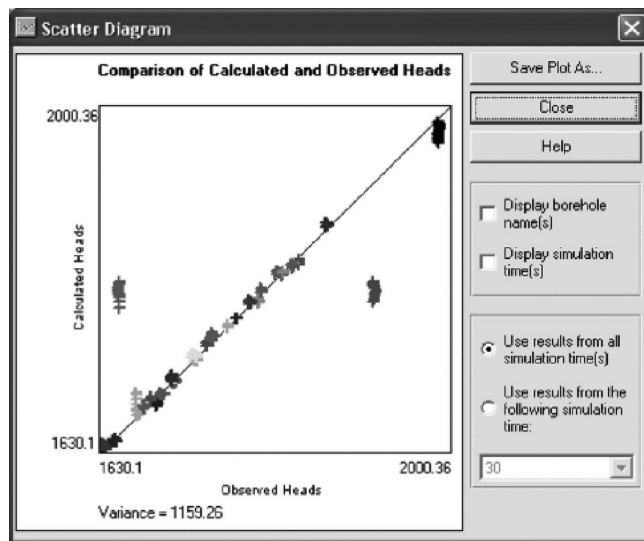


FIGURE 6.72 Scatter Diagram window.

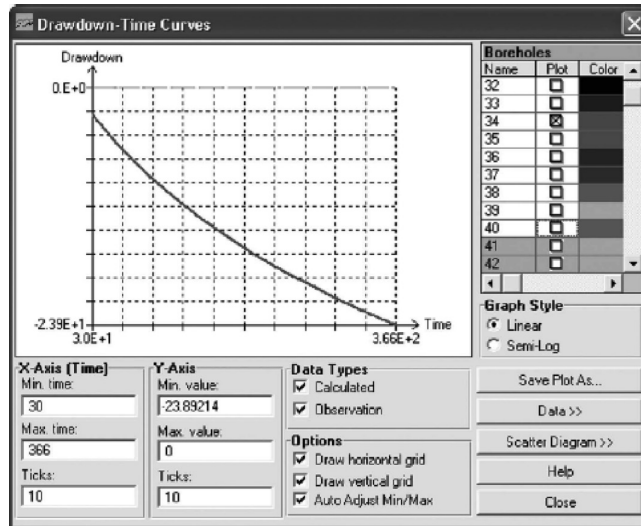


FIGURE 6.73 Drawdown-Time Curves window.

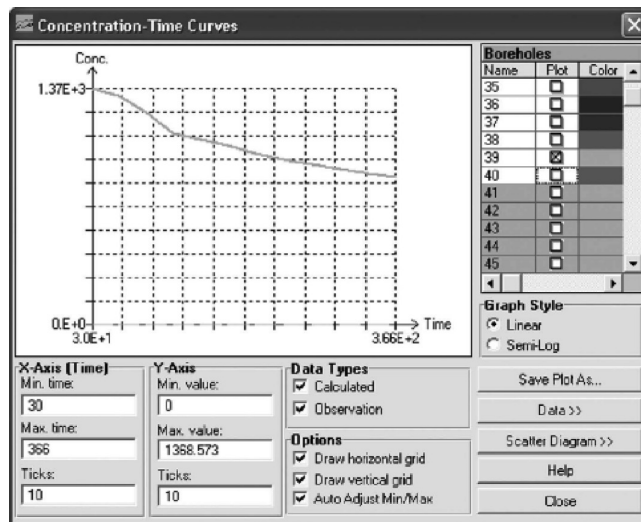


FIGURE 6.74 Concentration-Time Curves window.

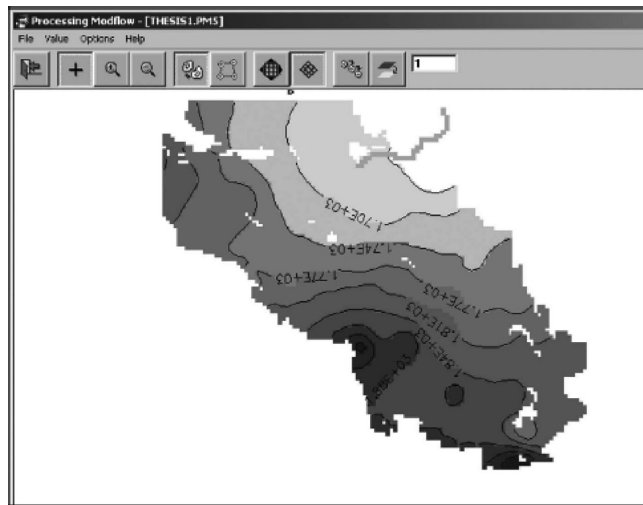


FIGURE 6.75 Water table elevation in the study area.

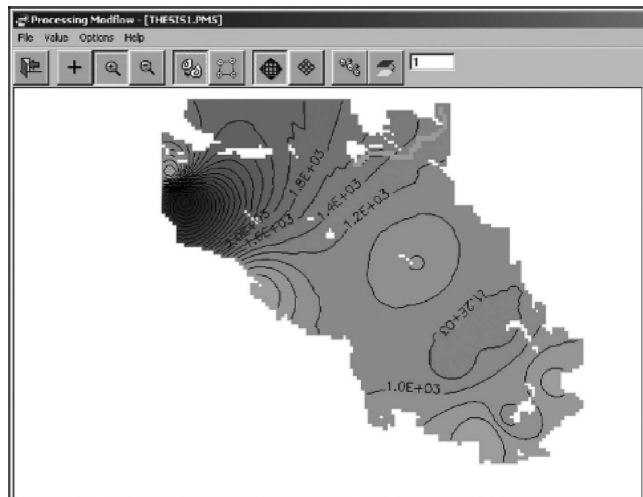


FIGURE 6.76 TDS concentration contours in the study area.

PROBLEMS

- 6.1** Consider the plan view of the confined aquifer shown in [Figure 6.17](#). A mesh-centered grid system has been overlaid such that $\Delta x = \Delta y = 100$ m. Boundary conditions are given. The heads are relative to a datum at the base of the aquifer. The shaded area in the figure represents a gravel pit which must be dewatered by pumping from 12 wells along the boundary of the pit. Each well must be pumped at a rate of $1200 \text{ m}^3 \text{ day}^{-1}$, $T = 300 \text{ m}^2 \text{ day}^{-1}$, and $S = 0.002$. Compute the drawdowns after 200 days of pumping. For initial conditions, use the steady-state head configuration without pumping.
- 6.2** Solve the differential equation of $d^2h/dx^2 = 0$ using the Galerkin method and considering: $0 \leq x \leq 3$
- $h = 0 \text{ m}$, where $x = 0$
- $h = 10 \text{ m}$, where $x = 3$.
- 6.3** In the confined aquifer system shown in [Figure 6.6](#), the pumping rates in wells 1 and 2 are 0.02 and $0.03 \text{ m}^3/\text{s}$, respectively. The initial piezometric head is 20 m everywhere. Applying the alternate-direction implicit procedure, determine the head distribution after one day of pumping.
- 6.4** The column of soil shown in [Figure 6.77](#) is saturated and water is flowing vertically downwards at a constant rate Q . Hydraulic head is held constant at the upper and lower ends of the column. Calculate the values of head at points A and B. Compute the hydraulic head along the column.
- 6.5** Consider the column of soil shown in [Figure 6.77](#). Initially, the column is in steady-state saturated flow conditions with a distribution of hydraulic head computed from the previous example. At time $t = 0$, the value of

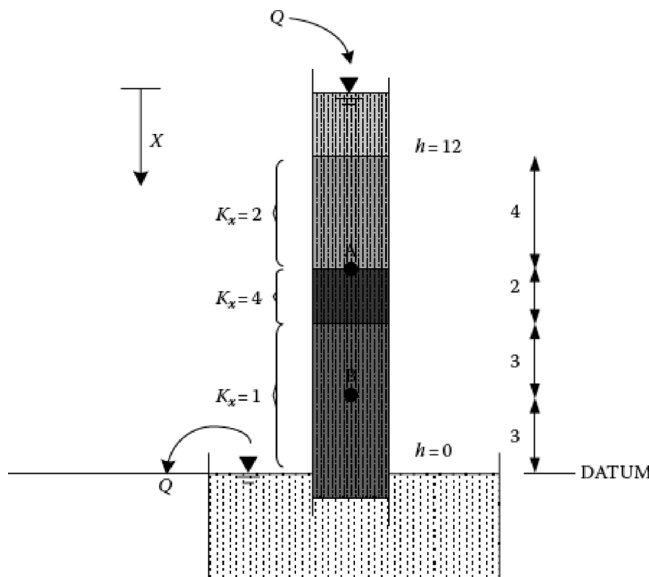


FIGURE 6.77 A soil column of Problem 6.4.

hydraulic head increases at the upper boundary (node 1) from 12 to 25 cm. Find the value of hydraulic head at each node at times $t = 1, 2, \dots$ seconds. $S_S^{(1)} = 0.02$, $S_S^{(2)} = 0.04$, $S_S^{(3)} = S_S^{(4)} = 0.02$.

- 6.6** Consider a steady-state, saturated groundwater flow is occurring in a confined aquifer. Initially, no solute is present. At time zero, the solute concentration along the left boundary of the aquifer is increased to 10 mg/L and remains constant thereafter. Assuming $V_x^{(e)} = 0.03 \text{ m/d}$, $D_x^{(e)} = 1 \text{ m}^2/\text{d}$, $L^{(e)} = 10 \text{ m}$, $\theta^{(e)} = n^{(e)} = 0.3 \text{ m}$, compute the hydraulic head in five elements with equal condition of the aquifer.
- 6.7** Consider a one-dimensional flow in a confined aquifer as shown in Figure 6.78. Let $\Delta x = 3 \text{ m}$, $b = 6 \text{ m}$, $h_1 = 15 \text{ m}$, $h_5 = 8 \text{ m}$, $K = 0.5 \text{ m/day}$. Determine the spatial variation of the piezometric head using the finite volume method.
- 6.8** Estimate the net flow for seepage under the sheet piling shown in Figure 6.79 for $K_1 = 10^{-4} \text{ m/s}$, $K_2 = 2 \times 10^{-4} \text{ m/s}$, $L = 400 \text{ m}$, and $\Delta x = \Delta y = 10 \text{ m}$ with a steady-state condition using the finite volume method.

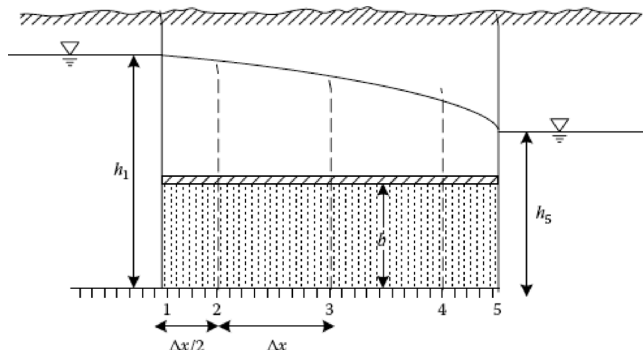


FIGURE 6.78 A confined aquifer between rivers A and B.

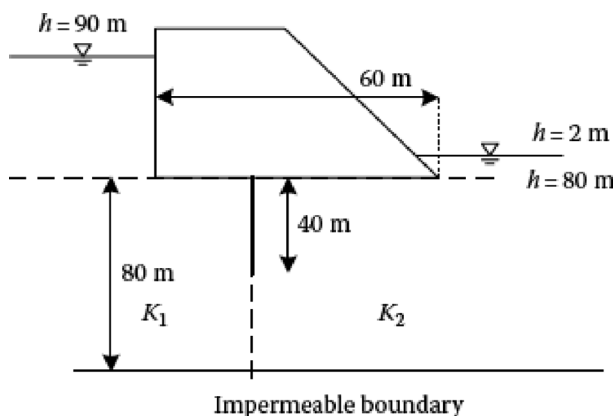


FIGURE 6.79 A dam with a sheet pile in a soil with non-homogenous conductivity.

REFERENCES

- Abbaspour, K. C., Yang, J., Maximov, I., Siber, R., Bogner, K., Mieleitner, J., Zobrist, J., and Srinivasan, R. 2007. Modelling hydrology and water quality in the prealpine/alpine Thur watershed using SWAT. *Journal of Hydrology*, 333, 413–430.
- Aziz, K. and Settari, A. 1972. A new interactive method for solving reservoir simulation equations. *Journal Canadian Technology*, 11, 62–68.
- Bear, J. 1979. *Hydraulics of Groundwater*. McGraw-Hill, New York, 38p.
- Bear, J. and Verruijt, A. 1992. *Modeling Groundwater Flow and Pollution with Computer Programs for Sample Cases*. Redial Publishing Company, Dordrecht, the Netherlands, 414p.
- Bredehoeft, J. D. and Pinder, G. F. 1970. Digital analysis of areal flow in multiaquifer groundwater systems: A quasi three-dimensional model. *Water Resources Research*, 6(3), 883–888.
- Carslaw, H. S. and Jaeger, J.C. 1959. *Conduction of Heat in Solids*. Oxford University Press, New York, 510p.
- Chiang, W. H. and Kinzelbach, W. 2005. *3D-Groundwater Modeling with PMWIN: A Stimulation System for Modeling Groundwater Flow and Transport Processes*. Springer-Verlag, Berlin, Germany.
- Delleur, J. W., ed. 1999. *The Handbook of Groundwater Engineering*. CRC Press/Springer-Verlag, Boca Raton, FL, 518p.
- Gupta, R. S. 1989. *Hydrology and Hydraulic Systems*. Prentice-Hall, Englewood Cliffs, NJ.
- Harr, M. E. 1962. *Groundwater and Seepage*. McGraw-Hill, New York, 309p.
- Hoffmann, K. A. and Chiang, S. T. 1989. *Computational Fluid Dynamics Volume I*. Engineering Education System, Wichita, KS.
- Illangasekare, T. H., Morel-Seytoux, H. J., and Verdin, K. L. 1984. A technique of reinitialization for efficient simulation of large aquifers using the discrete kernel approach. *Water Resources Research*, 20(11), 1733–1742.
- Istok, J. D. 1989. *Groundwater Modeling by the Finite Element Method*. American Geophysical Union, Washington, DC, 415p.
- Karamouz, M., Szidarovszky, F., and Zahraie, B. 2003. *Water Resources Systems Analysis*. Lewis Publishers, Boca Raton, FL, 608p.
- Machiwal, D. and Singh, P. K. 2015. Comparing GIS-based multi-criteria decision-making and Boolean logic modelling approaches for delineating groundwater recharge zones. *Arabian Journal of Geosciences*, 8(12), 10675–10691. doi:10.1007/s12517-015-2002-5.
- Mandle, R. J. 2002. *Groundwater Modeling Guidance*. Groundwater Modeling Program, Michigan Department of Environmental Quality, Lansing, MI, 55p.
- McDonald, M. G. and Harbaugh, A. W. 1988. *A Modular Three-Dimensional Finite-Difference Ground-Water Flow Model: Techniques of Water-Resources Investigations of the United States Geological Survey*, Book 6, Chap. A1, U.S. Geological Survey, Washington, DC, 586p.
- Morel-Seytoux, H. J. and Daly, C. J., 1975. A discrete kernel generator for stream-aquifer studies. *Water Resources Research*, 11(2), 253–260.
- Patankar, S. V. 1980. Numerical heat transfer and fluid flow. Series in *Computational Methods in Mechanics and Thermal Sciences*, W. J. Minkowycz and E. M. Sparrow, eds., McGraw-Hill, New York, 214p.
- Peaceman, D. and Rachford, M. 1955. The numerical solution of parabolic and elliptic differential equations. *Journal of SIAM*, 3, 28–41.
- Prickett, T. A. and Lonnquist, C. G. 1971. Selected digital computer for groundwater resource evaluation. III. *State Water Survey Bulletin*, 55, 62.
- Remson, I., Hormberger, G. M., and Molz, F. J. 1971. *Numerical Methods in Subsurface Hydrology With an Introduction to the Finite Element*. John Wiley & Sons, New York, 416p.

- Rushton, K. R. 1974. Aquifer analysis using backward difference methods. *Journal of Hydrology*, 22, 253–369.
- Saaty, T. L. 1980. *The Analytical Hierarchy Process*. McGraw-Hill, New York, 350p.
- Shadid, S., Nath, S. K., and Roy, J. 2000. Groundwater potential modeling in a soft rock area using a GIS. *International Journal of Remote Sensing*, 21(9), 1919–1924.
- Stone, H. L. 1968. Iterative solution of implicit approximations of multidimensional partial differential equations. *SIAM Journal of Numerical Analysis*, 5, 530–558.
- Strack, O. D. L. 1989. *Groundwater Mechanics*. Prentice Hall, Englewood Cliffs, NJ, 732p.
- Thangarajan, M. 2007. *Groundwater: Resource Evaluation, Augmentation, Contamination, Restoration, Modeling and Management*. Springer, the Netherlands, 362p.
- Toth, J. 1963. A theoretical analysis of groundwater flow in small drainage basins. *Journal of Geophysical Research*, 68, 4795–4812.
- Toth, J. 1962. A theory of groundwater motion in small drainage basins in Central Alberta, Canada. *Journal of Geophysical Research*, 67(11), 4375–4387.
- Trescott, P. C., Pinder, G. F., and Larson, S. P. 1976. *Finite-Difference Model for Aquifer Simulation in Two-Dimensions with Results of Numerical Experiments. Techniques of Water-resources Investigations of the United States Geological Survey*, U.S. Geological Survey, Washington, DC, 116p.
- Voss, C. I. and Provost, A. M. 2002. SUTRA: A Model for 2D or 3D Saturated–Unsaturated, Variable Density Groundwater Flow with Solute or Energy Transport. USGS Water-Resources Investigations Report, 02-4231, U.S. Geological Survey, Reston, VA.
- Voss, C. I. and Provost, A. M. 2010. SUTRA: A Model for Saturated–Unsaturated, Variable Density Groundwater Flow with Solute or Energy Transport. USGS Water-Resources Investigations Report, 02-4231, U.S. Geological Survey, Reston, VA.
- van Genuchten, M. T. and Alves, W. J. 1982. *Analytical Solutions of the One-Dimensional Convective-Dispersive Solute Transport Equation*. U.S. Department of Agriculture, Washington, DC, 151p.
- Walton, W. 1989. *Analytical Ground Water Modeling*. Lewis Publishers, Chelsea, MI, 173p.
- Wang, H. F. and Anderson, M. P. 1995. *Introduction to Groundwater Modeling: Finite Difference and Finite Element Methods*. Academic Press, New York, 237p.
- Watts, J. W. 1971. An interactive matrix solution method suitable for anisotropic problems. *Society of Petroleum Engineers Journal*, 11, 47–51.
- Watts, J. W. 1973. A method for improving line successive over-relaxation in anisotropic problems: A theoretical analysis. *Society of Petroleum Engineers Journal*, 13, 105–118.
- Weinstein, H. G., Stone, H. L., and Kwan, T. V. 1970. Simultaneous solution of multiphase reservoir flow equations. *Society of Petroleum Engineers Journal*, 10(2), 99–110.



Taylor & Francis

Taylor & Francis Group

<http://taylorandfrancis.com>

7 Groundwater Planning and Management

7.1 INTRODUCTION

Development of the groundwater resources involves planning for the entire aquifer. The increasing demand for water throughout the world makes the aquifers vast underground reservoirs, and their proper management has become a matter of considerable interest. Groundwater development is characterized by unrestricted land use, growth of agriculture, and use of shallow aquifers, which allows human settlement in large areas including the semiarid regions with scarce surface water resources (Kresic, 2009). A program for the subsurface water development considering the objectives of social, economic, and environmental issues is developed through the management of the groundwater. The management objectives include providing an economic and continuous water supply to meet a continuous growing demand from an underground water resource.

The management objectives for developing and operating the aquifer consider geologic and hydrologic, economic, legal, political, and financial aspects. The integrated approach that coordinates the use of both the surface water and groundwater resources should be considered in selecting the objective functions. The total water resources and water demands are evaluated in the region, and then the optimal water development strategies in an area can be obtained considering the alternative management plans. One scenario could obtain the quantity of water to meet the water demands with the acceptable water quality considering the objective functions. Finally, action plans can be taken by the appropriate public bodies or agencies.

The general perception is that the groundwater is an unlimited, reliable, and safe drinking water source. This could only occur if there is a balance between the water recharged to the aquifer and the water removed from wells. The rapid groundwater development causes overexploitation, which leads to the lowering of the water table and the widespread shallow groundwater contamination. The continued development without a management plan could have more obvious consequences such as the water table depletion and land subsidence.

Several technical tools and techniques that are classified as simulation, optimization, and economic analysis are utilized for the groundwater planning and management. The engineering applications primarily use the analysis and design techniques. Simulation models have been used to test the performance of the groundwater systems and answer the development questions under different design and operation alternatives in a physical-mathematical fashion. The simulation models are the overlay between the engineering and management tools, and they may require substantial data and detailed modeling. In the analysis of the groundwater systems, three classes

of management problems can be considered: the estimation of model parameters, the prediction of system responses, and knowing the set of inputs to the system. The simulation models need to be calibrated and verified utilizing the collected and recorded data. One of the simulation techniques that has received a great deal of attention is the system dynamics utilizing object-oriented programming. In this chapter, some simulation models are presented. The agent-based modeling takes the social aspects into account, considering stakeholders behavior.

Considering the economic, social, and environmental issues and conflicting objectives in the groundwater management leads to a multi-objective planning and conflict resolution problem. Therefore, the analysis of the system is a trade-off between different objective functions. The optimal pumping schedules (well locations and pumping rates) to satisfy the given water demand, the optimal injection schedules (well locations and injection rates) necessary to satisfy a waste load demand, and the optimal allocation schedule from the groundwater and surface water resources in a region to meet the different water demands are some examples in the groundwater management. In this chapter, different optimization models and methods to solve them are introduced. The conventional and evolutionary optimization techniques are then presented. Economic analyses in the groundwater systems are described. There are certain inserts from the Karamouz et al. (2003, 2010) books that are adapters for the groundwater management. Some case studies on the groundwater planning and management using simulation and optimization techniques are presented.

7.2 DATA COLLECTION

The groundwater simulation models require considerable data to define all the nodal parameters. The accuracy of simulation depends on the reliability of the estimated parameters as well as the accuracy of model and boundary conditions (Karamouz et al., 2003). Recently, the computer-based models were used to expedite the modeling. In the model calibration and verification stages, extensive field data are needed to set the variable parameters. Considerable technical skill is required as well. The computer models can extend the data collected and enhance the findings. They can be utilized to generate the management scenarios and run them to get the response of the system to different plans and find the best management practices scenarios.

The following data should be collected for the groundwater management according to Todd (1980):

- *Topographic data:* They are used for locating and identifying the wells, measuring the groundwater tables, and plotting the areal data.
- *Geologic data:* They are utilized for modeling the surface and the subsurface water interactions based on the geologic maps.
- *Hydrologic data:* They are used to model the hydrologic cycle elements. They can be the precipitation, soil moisture, evaporation and transpiration, temperature, land use, water demand, surface storage, groundwater storage, and surface and subsurface inflow and outflow data. The primary purpose of the hydrologic data collection is the evaluation of the hydrologic conservation equation in an aquifer.

Nowadays, many simulation models utilize the geographic information system (GIS) for the data input and the presentation of results. The GIS can also be used to evaluate and find the patterns of recharge within a region utilizing the available information of the observed groundwater table at the specified locations. In the groundwater studies, in order to study the distributions of the nonpoint source contamination of the groundwater, spatial statistics can be used. It could be utilized to determine the spatial correlation of the nonpoint source pollution and to eliminate the detections from the point sources of pollution in a water quality database. The spatial variation of the hydrogeologic factors affecting the solute transport including the hydraulic conductivity of the aquifer, slope, and the groundwater properties can then be assessed.

DRASTIC (D: depth to groundwater; R: net recharge; A: aquifer media; S: soil media; T: general topography or slope; I: vadose zone; C: hydraulic conductivity) and SEEPAGE are simple techniques that can be used for developing the regional-scale groundwater vulnerability maps. The capabilities of the GIS in the spatial statistics and grid design can improve the modeling effort. Linking the GIS with the modular three-dimensional finite-difference groundwater flow model (MODFLOW) is another example of a groundwater numerical model interfaced with a GIS.

7.3 SIMULATION TECHNIQUES

A groundwater simulation model is used for the mathematical formulations. Generally, the simulation model structure addresses a detailed and realistic representation of the complex physical, economic, and social characteristics of a water resources system utilizing the mathematical formulations.

The simulation model represents a process or concept by means of a number of variables which are defined to represent the inputs, outputs, and internal states of the process, and it utilizes a set of equations and inequalities describing the interaction of these variables. The simulation techniques are used for analyzing the groundwater systems and evaluating the systems performance under a given set of inputs and operating policies. The simulation models may deal with steady-state or transient conditions. The pumping test in the aquifers could be done in both of the states.

One of the differences between the simulation and optimization models is that the simulation model is not used for the optimal decision determination in comparison with the optimization model. Since the groundwater planning models with the highly nonlinear relationships and constraints cannot be handled by the constrained optimization procedures, the simulation method is used in the optimization process. The optimal scenarios are usually selected based on the simulation results of the system and the evaluation of the system performance under different groundwater development projects. Therefore, linking the simulation and optimization models for the estimation of the groundwater system performance for different scenarios is required.

Thus, a simulation model is an input–output relation in a certain sense, when the input is the set of model parameters and our actions, and the output is the consequence of our actions. In [Chapter 6](#), some numerical models for the simulation of the groundwater systems are presented. Sometimes, running the numerical simulation models is time consuming, and it has a high computational burden. Also, in analyzing complex systems, the physical model and the mathematical description are so

complicated that no solution algorithm can be developed. In many of these cases, no mathematical model is even available. The only choice we have then is the conceptual simulation of the model. In this chapter, some conceptual models recently used for the groundwater simulation are introduced.

7.3.1 MODEL CALIBRATION

As the parameters of the groundwater models cannot be measured directly, they can be estimated from the historical data using an inverse parameter estimation procedure (ReVelle and McGarity, 1997).

The simulation models are categorized in two groups, namely, deterministic and stochastic. If the system is subject to random input events, or generates them internally, the model is called stochastic. The model is deterministic if no random components are involved.

In the deterministic groundwater simulation models, the difference between the observed data of the aquifer responses (such as water table variation) and the corresponding values calculated by the model considered as the objective function are minimized in the calibration procedure. The comparison between the observed and calculated values is usually subjective, and it should be considered that a good match does not necessarily show the validity of the model (Karamouz et al., 2003).

The model calibration is done through a trial-and-error procedure to modify the model parameters by evaluating the model output, using the changing of the aquifer properties. It could consist of model sensitivity analysis by changing the aquifer recharges and discharges, aquifer properties, and initial and boundary conditions and considering the uncertainties in the sources, sinks, and initial and boundary conditions, as well as the uncertainties in the aquifer properties. The model calibration procedure is usually time-consuming. Therefore, the experience and engineering judgment of the modeler and the considerable technical skill and commitment from the personnel are important factors in the efficient calibration of the model.

The automated parameter estimation techniques, extended as the simulation model software, based on the least square deviation as a criterion to obtain the estimate of the system parameters can be used for expediting the model calibration.

7.3.2 MODEL VERIFICATION

The calibrated model should be verified before using it for the groundwater simulation. For this purpose, the calibrated model is used to simulate the groundwater system under the observed input data that have not been used in the model calibration process. Then, the simulated results are compared with the observed aquifer responses and the reliability and accuracy of the model simulation is evaluated. If the model has a good reliability in the verification procedure, it is selected as the simulation model.

One of the limitations in the groundwater model verification is the data deficiency. In this case, the unverified model should be applied only if the sensitivity analyses for both the model calibration and prediction are performed (ReVelle and McGarity, 1997).

There are several performance functions that may be used to evaluate the simulation model performance, such as percent bias (PBIAS), relative error (RE), root mean squared error (RMSE), mean bias error (MBE), mean absolute error (MAE),

coefficient of determination (R^2), and Nash-Sutcliffe efficiency (NSE). These performance functions are formulated in the following equations:

$$\text{PBIAS} = \frac{\sum_{t=1}^n (\hat{y}_t - y_t)}{\sum_{t=1}^n y_t} \times 100 \quad (7.1)$$

$$\text{RE} = \frac{\bar{y} - \bar{\hat{y}}_t}{\bar{y}_t} \times 100 \quad (7.2)$$

$$\text{RMSE} = \sqrt{\frac{\sum_{t=1}^n (y_t - \hat{y}_t)^2}{n}} \quad (7.3)$$

$$\text{MBE} = \frac{\sum_{t=1}^n (\hat{y}_t - y_t)}{n} \quad (7.4)$$

$$\text{MAE} = \frac{\sum_{t=1}^n |\hat{y}_t - y_t|}{n} \quad (7.5)$$

$$R^2 = \left\{ \frac{\sum_{t=1}^n (y_t - \bar{y}_t)(\hat{y}_t - \bar{\hat{y}})}{\sqrt{\sum_{t=1}^n (y_t - \bar{y}_t)^2 * \sum_{t=1}^n (\hat{y}_t - \bar{\hat{y}})^2}} \right\}^2 \quad (7.6)$$

$$\text{NSE} = \frac{\sum_{t=1}^n (\hat{y}_t - y_t)^2}{\sum_{t=1}^n (y_t - \bar{y}_t)^2} \quad (7.7)$$

where:

y_t is the observed data

\hat{y}_t is the simulated data

\bar{y}_t is the mean of observed data

$\bar{\hat{y}}_t$ is the mean of simulated data

n is the total number of data.

7.3.3 MODEL PREDICTIONS

A calibrated model should have a good performance in the model predictions. The uncertainties of the model parameters and variables as well as boundary conditions are the main sources of the prediction errors. For example, if the aquifer boundary conditions such as the imposed stresses have been changed during the prediction

horizon, the model cannot simulate the future condition of a groundwater system with the calibrated model. Therefore, if a model is continuously used for the prediction of future conditions of a groundwater system, the model should be periodically post-audited, or calibrated using the field monitoring data (Delleur, 1999).

7.3.3.1 Artificial Neural Networks

The artificial neural networks (ANNs) model is significantly used to simulate a groundwater system with a large number of the observed data, but no known mathematical model exists. These models are used in the different groundwater systems such as the simulation of the water quality in monitoring wells or the simulation of the water table fluctuation. This model is utilized to simplify an excessively complex model by a typical ANN formulation. The ANNs are global nonlinear function approximates and are powerful and easy to use (StatSoft, 2013).

An ANN is a computational model that tries to emulate the structure or functional aspects of the biological neural networks. It can be trained to recognize patterns and can learn from their interaction with the environment. The objective of the neural network is to transform the inputs into meaningful outputs. The ANN structure is based on a biological neural system in which a network of cells, known as neurons, is proceeded using the powerful functions. An ANN imitates this structure by distributing the computation to small and simple processing units, called artificial neurons or nodes.

Thus, an ANN is composed of many artificial neurons that are linked together according to the specific network architecture. Each network basically contains three types of layers including neurons with similar characteristics. The first layer is called the input layer which connects the input neurons to the next layer. The second layer, or the hidden layer, is between the input and output layers and not connected externally. The third layer is the output layer which includes the output variables/neurons. Thus, generally, each neuron receives a number of the inputs from either the original data or other neurons. The hidden layer can be more than one. Generally, connections are allowed from the input layer to the first hidden layer, from the first hidden layer to the second, and from the last hidden layer to the output layer. The strength of the connection between an input and a neuron is noted by the value of the weight. The negative weight values reflect the inhibitory connections, while the positive values designate the excitatory connections. The neural network model can be considered as a simple subroutine of the input–output computations in any descriptive or optimization procedure, because the input–output relation is easy to compute.

7.3.3.1.1 *The Multi-player Perception Network*

Figure 7.1 shows a simple neural network with three types of layers where the input variables are in the neurons of the input layer and the output variables are in the neurons of the output layer. The number of the input and output variables are R and K , respectively. In order to provide a high level of flexibility in the model formulation, the hidden layers are defined in the middle; its neurons correspond to the hidden or artificial variables. The weights on all the links specified by the rule set and the biases on the units (b_i) corresponding to the consequents are set so that the network responds in exactly the same manner as the rules upon which it is based.

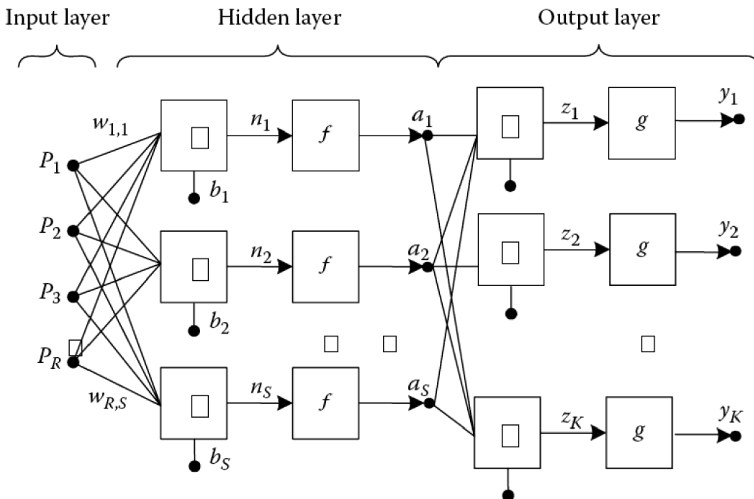


FIGURE 7.1 Illustration of a simple neural network.

Let a_j denote the artificial variables corresponding to the j th neuron of the hidden layer. This variable is calculated as follows:

$$a_j = f \left(\sum_{i=1}^R w_{ij} P_i + b_j \right) \quad (7.8)$$

where:

R is the number of input variables

f is a transfer function.

The coefficients W_{ij} are the constants estimated by the training process and specified by the rule set.

The model output is calculated as follows:

$$y_j = g \left(\sum_{i=1}^S w_{ij} a_i + b'_j \right) \quad (7.9)$$

where S is the number of the hidden variables. The coefficients w_{jk} are also estimated by the training process. There are many transfer functions used in developing the neural networks, but here, the three most popular ones are introduced. The hard-limit transfer function shown in Figure 7.2a limits the output of the neuron to either 0, if the net input argument n is less than 0; or 1, if n is greater than or equal to 0. This function is used to create the neurons that make classification decisions (Demuth and Beale, 2002).

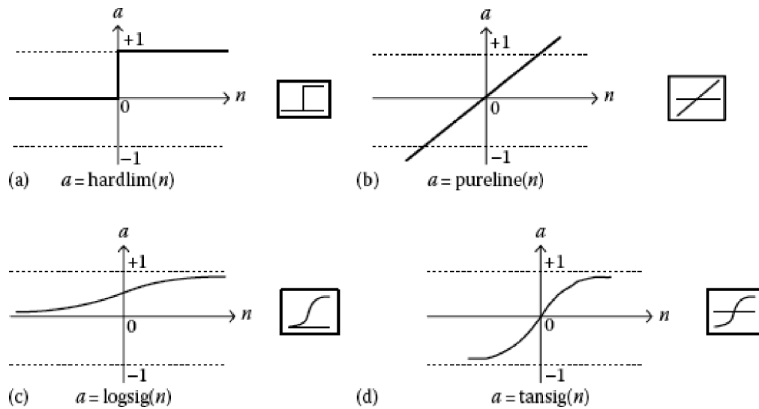


FIGURE 7.2 Transfer function types: (a) hard limit, (b) linear, (c) log sigmoid, and (d) tangent sigmoid.

The linear transfer function is shown in Figure 7.2b. The neurons of this type are used as a linear approximation and also employed in the output layer. The sigmoid transfer function depicted in Figure 7.2c takes the input, which may have any value between plus and minus infinity, and squashes the output into the range of 0–1. Also, the tangent sigmoid transfer function is shown in Figure 7.2d. The sigmoid transfer function can be formulated as:

$$a = \frac{1}{1 + e^{-cn}}, \quad c > 0 \quad (7.10)$$

This transfer function is commonly used in the back propagation networks, in part, because it is differentiable (Demuth and Beale, 2002).

A multi-layer perceptron (MLP) network, which is usually called the feed-forward network, has one or more hidden layers. In this network, the information moves in only one direction, forward, from the input nodes through the hidden nodes to the output nodes. There are no cycles or loops in the network as illustrated in Figure 7.1. Once the network weights are fixed, the states of the units are totally determined by the inputs, independent of initial and past states of the units. Thus, the MLP is a static network in which information is transmitted through the connections between its neurons only in the forward direction, and the network has no feedback over its initial and past states. The MLP can be trained with the standard back propagation algorithm.

The ANN models need the estimation of the model parameters including the bias value in each neuron of the hidden layer (b_j) and the outputs layer (b'_j) and also the weights on all the links W_{ij} and \tilde{w}_{ij} . The most frequently applied methodology is training the network, which is an iteration procedure that successively improves the parameter values. The weights between the output layer and the hidden layer could be modified as:

$$\bar{w}_{jk}(t+1) = \bar{w}_{jk}(t) + \beta E_k(t) y_k(t) \quad (7.11)$$

where:

β is the learning rate

$y_k(t)$ is the actual output

$E_k(t) = d_k(t) - y_k(t)$ is the error of estimation and is calculated using the difference between the desired and actual outputs.

Since the hidden variables are unknown, the weights between the input and hidden layers can be modified by:

$$w_{ij}(t+1) = w_{ij}(t) + \beta a_j(t) \sum_k \bar{w}_{jk}(t) E_k(t) \quad (7.12)$$

This updating process is used iteratively for a large number of input–output pairs until the error terms $E_k(t)$ become sufficiently small.

The back propagation algorithm is a common method of teaching the ANNs during the supervised learning for the nonlinear multi-layer networks. In this method of model training, the gradient of the error function is estimated using the chain rule of differentiation. In this algorithm, the network weights are moved along the negative of the gradient of the performance function. The weights in the training process are updated through each iteration (which is usually called epoch) in the steepest descent direction based on the simulation error of the outputs.

Example 7.1

Assume that the groundwater table variation is a function of two variables including the volumes of aquifer recharge and aquifer discharge. The monthly data of the groundwater table variation and the volumes of aquifer recharge and aquifer discharge for 12 years are given in Tables 7.1 through 7.3, respectively. The studies have also demonstrated that the relation of the water table variation with these parameters is complicated and could not be formulated in the regular

TABLE 7.1
Monthly Recharge to the Aquifer (MCM) of Example 7.1

| Year | 1995 | 1996 | 1997 | 1998 | 1999 | 2000 | 2001 | 2002 | 2003 | 2004 | 2005 | 2006 |
|----------|-------|-------|-------|-------|-------|-------|-------|-------|-------|-------|-------|-------|
| January | 5.13 | 3.16 | 8.05 | 3.79 | 3.19 | 3.39 | 2.77 | 2.76 | 2.45 | 2.7 | 3.74 | 6.29 |
| February | 5.16 | 4.07 | 6.83 | 5.78 | 5.86 | 4.89 | 6.16 | 4.1 | 4.13 | 4.69 | 4.35 | 6.29 |
| March | 4.36 | 4.47 | 8.04 | 5.59 | 5.6 | 5.46 | 5.16 | 5.33 | 4.48 | 4.07 | 5.68 | 8.08 |
| April | 4.23 | 4.87 | 7.26 | 4.84 | 4.59 | 5.54 | 4.38 | 6.69 | 4.71 | 4.45 | 6.15 | 8.13 |
| May | 4.99 | 6.1 | 9.47 | 5.61 | 5.7 | 7.98 | 5.77 | 6.06 | 4.08 | 5.71 | 7.45 | 10.02 |
| June | 26.21 | 9.73 | 11.02 | 7.39 | 15.09 | 10.32 | 9.74 | 7.14 | 7.36 | 6.93 | 13.51 | 12.73 |
| July | 24.27 | 23.27 | 29.6 | 18.22 | 23.94 | 14.68 | 32.43 | 17.52 | 18.52 | 42.41 | 38.67 | 17.22 |

(Continued)

TABLE 7.1 (Continued)**Monthly Recharge to the Aquifer (MCM) of Example 7.1**

| Year | 1995 | 1996 | 1997 | 1998 | 1999 | 2000 | 2001 | 2002 | 2003 | 2004 | 2005 | 2006 |
|-----------|-------|-------|------|------|-------|------|-------|------|-------|-------|-------|-------|
| August | 14.19 | 13.99 | 18.2 | 14.5 | 25.23 | 2.75 | 24.99 | 5.45 | 24.43 | 39.81 | 30.05 | 11.33 |
| September | 2.02 | 4.83 | 9.6 | 1.15 | 12.74 | 0.66 | 1.95 | 4.18 | 8.16 | 15.53 | 10.23 | 5.96 |
| October | 0.33 | 1.48 | 2.17 | 0.06 | 4.15 | 0.15 | 0.07 | 1.87 | 2.1 | 2.48 | 3.66 | 2.81 |
| November | 0.03 | 0.42 | 0.15 | 0.4 | 3.41 | 0.1 | 0 | 0.08 | 0.38 | 1.35 | 1.36 | 0.21 |
| December | 2.57 | 0.84 | 1.56 | 0.95 | 2.63 | 0.6 | 2.02 | 1.15 | 0.68 | 1.47 | 2.37 | 2.53 |

TABLE 7.2**Monthly Discharge of the Aquifer (MCM) of Example 7.1**

| Year | 1995 | 1996 | 1997 | 1998 | 1999 | 2000 | 2001 | 2002 | 2003 | 2004 | 2005 | 2006 |
|-----------|-------|-------|-------|-------|-------|-------|-------|-------|-------|-------|-------|-------|
| January | 6.79 | 2.73 | 3.09 | 2.73 | 2.73 | 2.73 | 2.73 | 2.73 | 2.73 | 2.73 | 2.73 | 7.15 |
| February | 2.73 | 2.73 | 3.09 | 3.09 | 3.09 | 2.73 | 3.09 | 2.73 | 2.73 | 2.73 | 2.73 | 3.09 |
| March | 2.73 | 2.73 | 3.09 | 3.09 | 3.09 | 3.09 | 2.73 | 3.09 | 2.73 | 2.73 | 3.09 | 3.09 |
| April | 2.73 | 2.73 | 3.09 | 2.73 | 2.73 | 3.09 | 2.73 | 3.09 | 2.73 | 2.73 | 3.09 | 3.09 |
| May | 2.73 | 3.09 | 3.09 | 3.09 | 3.09 | 3.09 | 3.09 | 3.09 | 2.73 | 3.09 | 3.09 | 3.09 |
| June | 4.3 | 3.09 | 1.42 | 3.09 | 1.42 | 3.09 | 3.09 | 3.09 | 3.09 | 3.09 | 1.42 | 1.42 |
| July | 4.3 | 4.3 | 5.44 | 1.6 | 4.3 | 1.42 | 1.52 | 1.6 | 1.6 | 4.52 | 4.52 | 1.6 |
| August | 13.61 | 9.55 | 9.72 | 9.55 | 8.36 | 6.79 | 8.36 | 7.15 | 8.36 | 12.65 | 13.57 | 9.55 |
| September | 18.98 | 10.86 | 15.27 | 10.86 | 13.61 | 10.86 | 10.86 | 10.86 | 11.21 | 17.67 | 19.34 | 15.27 |
| October | 23.04 | 14.92 | 23.04 | 14.92 | 23.04 | 14.92 | 18.98 | 14.92 | 14.92 | 27.11 | 27.11 | 18.98 |
| November | 23.04 | 14.92 | 23.04 | 14.92 | 23.04 | 14.92 | 18.98 | 14.92 | 14.92 | 27.11 | 27.11 | 23.04 |
| December | 10.86 | 10.86 | 10.86 | 10.86 | 10.86 | 6.79 | 10.86 | 6.79 | 6.79 | 10.86 | 14.92 | 10.86 |

TABLE 7.3**Monthly Groundwater Table Variation of the Aquifer (cm) of Example 7.1**

| Year | 1995 | 1996 | 1997 | 1998 | 1999 | 2000 | 2001 | 2002 | 2003 | 2004 | 2005 | 2006 |
|-----------|--------|-------|--------|-------|-------|-------|-------|-------|-------|--------|--------|--------|
| January | 71.5 | 49.13 | 43.85 | 51.56 | 39.33 | 52.09 | 35.09 | 43.51 | 31.79 | 38.72 | 53.3 | 57.81 |
| February | 69.84 | 49.55 | 48.82 | 52.62 | 39.78 | 52.75 | 35.13 | 43.54 | 31.51 | 38.69 | 54.31 | 56.95 |
| March | 72.26 | 50.89 | 52.56 | 55.31 | 42.56 | 54.9 | 38.2 | 44.91 | 32.91 | 40.64 | 55.93 | 60.15 |
| April | 73.89 | 52.63 | 57.51 | 57.81 | 45.07 | 57.28 | 40.63 | 47.15 | 34.66 | 41.98 | 58.52 | 65.15 |
| May | 75.39 | 54.77 | 61.68 | 59.92 | 46.93 | 59.73 | 42.27 | 50.75 | 36.63 | 43.7 | 61.58 | 70.19 |
| June | 77.65 | 57.78 | 68.07 | 62.44 | 49.54 | 64.62 | 44.96 | 53.73 | 37.98 | 46.32 | 65.95 | 77.12 |
| July | 99.56 | 64.42 | 77.67 | 66.75 | 63.21 | 71.86 | 51.61 | 57.78 | 42.25 | 50.16 | 78.03 | 88.43 |
| August | 119.53 | 83.39 | 101.82 | 83.37 | 82.85 | 85.11 | 82.52 | 73.7 | 59.18 | 88.05 | 112.18 | 104.05 |
| September | 120.11 | 87.84 | 110.3 | 88.32 | 99.72 | 81.07 | 99.15 | 72 | 75.24 | 115.22 | 128.66 | 105.84 |
| October | 103.14 | 81.81 | 104.62 | 78.61 | 98.85 | 70.87 | 90.24 | 65.33 | 72.19 | 113.07 | 119.56 | 96.52 |
| November | 80.43 | 68.37 | 83.75 | 63.75 | 79.95 | 56.1 | 71.33 | 52.28 | 59.37 | 88.45 | 96.11 | 80.35 |
| December | 57.41 | 53.87 | 60.85 | 49.23 | 60.32 | 41.28 | 52.35 | 37.44 | 44.83 | 62.69 | 70.36 | 57.52 |

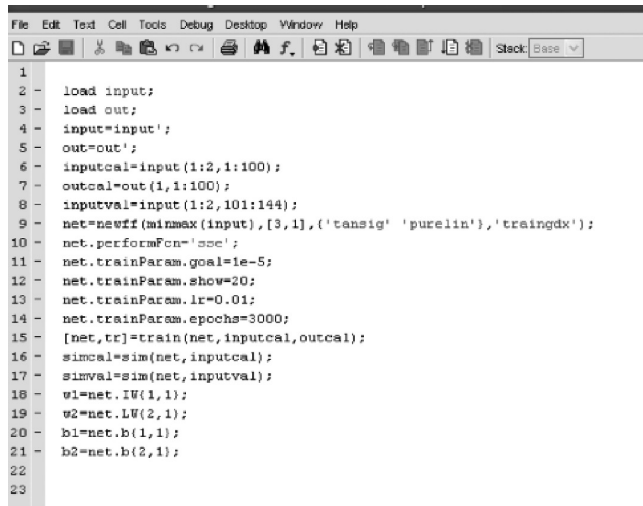
form. Develop an MLP model to simulate the monthly groundwater table variation of this aquifer as a function of the monthly volumes of aquifer recharge and aquifer discharge.

SOLUTION

The water table and the volumes of aquifer recharge and aquifer discharge data are standardized by subtracting the average of the data and then dividing to its standard division. It should be noted that for using the log sigmoid function, the data should be between zero and one. In this example, a network with three layers and six neurons in a hidden layer is developed. The log sigmoid and the linear functions in the hidden and output layers are used as the transfer functions. The number of data for developing the network is 144. As shown in [Figure 7.3](#), 100 series of data are used for the model calibration (inputcal and outcal), and the remaining is considered for the model validation (inputval and outval). The model is trained in 3500 steps (epochs), and the model goal is to achieve an error of less than 0.00001. The simulated and recorded monthly groundwater table variation data are compared in [Figure 7.4](#). As shown in this figure, about 30% of the data have been simulated with less than 5% error and 60% of the data have been simulated with an error of less than 10%.

7.3.3.1.2 Temporal Neural Networks

The temporal neural networks are an alternative neural network architecture whose primary purpose is to work on the continuous data. The advantage of this architecture is to adapt to the network online and, hence, is helpful in many real-time applications. In many cases such as the hydrological modeling, the input pattern comprises one or more temporal signals such as the time series prediction. The temporal perceptual learning relies on finding the temporal relationships in the sensory



```

1
2 - load input;
3 - load out;
4 - input=input';
5 - out=out';
6 - inputcal=input(1:2,1:100);
7 - outcal=out(1,1:100);
8 - inputval=input(1:2,101:144);
9 - net=newff(minmax(input),[3,1],{'tansig','purelin'},'traingdx');
10 - net.performFcn='sse';
11 - net.trainParam.goal=1e-5;
12 - net.trainParam.show=20;
13 - net.trainParam.lr=0.01;
14 - net.trainParam.epochs=3000;
15 - [net,tr]=train(net,inputcal,outcal);
16 - simcal=sim(net,inputcal);
17 - simval=sim(net,inputval);
18 - w1=net.IW(1,1);
19 - w2=net.LW(2,1);
20 - b1=net.b(1,1);
21 - b2=net.b(2,1);
22
23

```

FIGURE 7.3 Structure of a developed MLP model for the simulation of the monthly groundwater table.

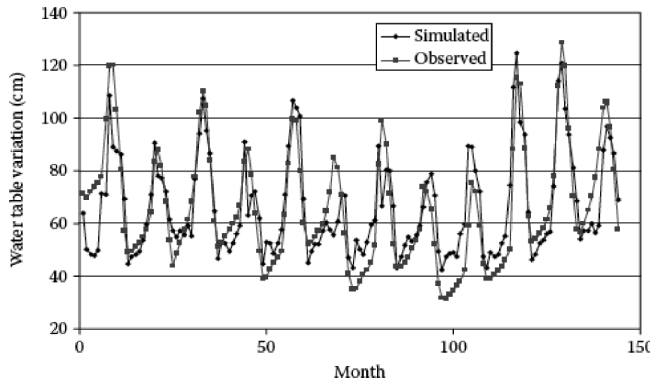


FIGURE 7.4 Comparison between the simulated groundwater table variation with the MLP and the observed data.

signal inputs. In an environment, the statistically salient temporal correlations can be found by monitoring the arrival times of the sensory signals.

The time delay operators, recurrent connections, and the hybrid method are different approaches, which are used to design the temporal neural networks. The different types of temporal neural networks are introduced in the following subsection based on Karamouz et al. (2007).

7.3.3.1.3 Tapped Delay Line

The tapped delay line (TDL) is based on a combination of the time delay operators in a sequential order. The architecture of the TDL corresponds to a buffer containing the N most recent inputs generated by a delay unit operator D . Given an input variable $p(t)$, D operating on $p(t)$ yields its past values $p(t - 1), p(t - 2), \dots, p(t - N)$, where N is the tapped delay line memory length. Thus, the output of the TDL is an $(N + 1)$ -dimensional vector, made up of the input signal at the current time and the previous input signals. The architecture of the TDL is illustrated in [Figure 7.5](#). The TDLs help networks to process dynamically through the flexibility in considering a sequential input.

Using MATLAB toolbox:

A two-layer feed-forward network with the sigmoid hidden neurons and linear output neurons is used to fit the multi-dimensional mapping problems arbitrarily well, given consistent data and enough neurons in its hidden layer.

The network will be trained with the Levenberg-Marquardt backpropagation algorithm unless there is not enough memory, in which case the scaled conjugate gradient backpropagation will be used.

The input data consist of the discharge and recharge that are represented in two rows of the input table. The output data are the groundwater table and will be stored in the V-T (V: monthly groundwater variation; T: target) table, which is constructed during the calculations.

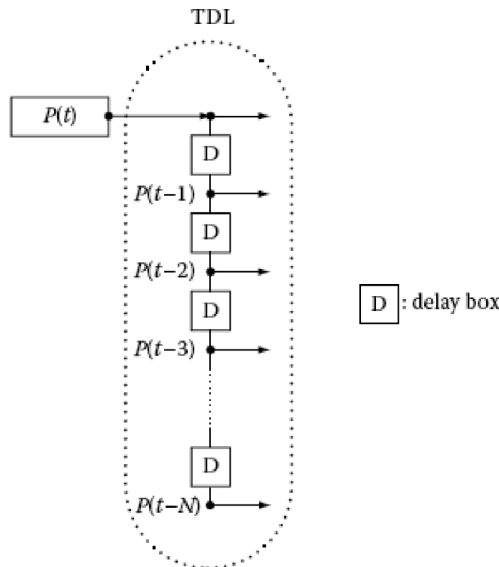


FIGURE 7.5 Tapped delay line in a temporal neural networks model.

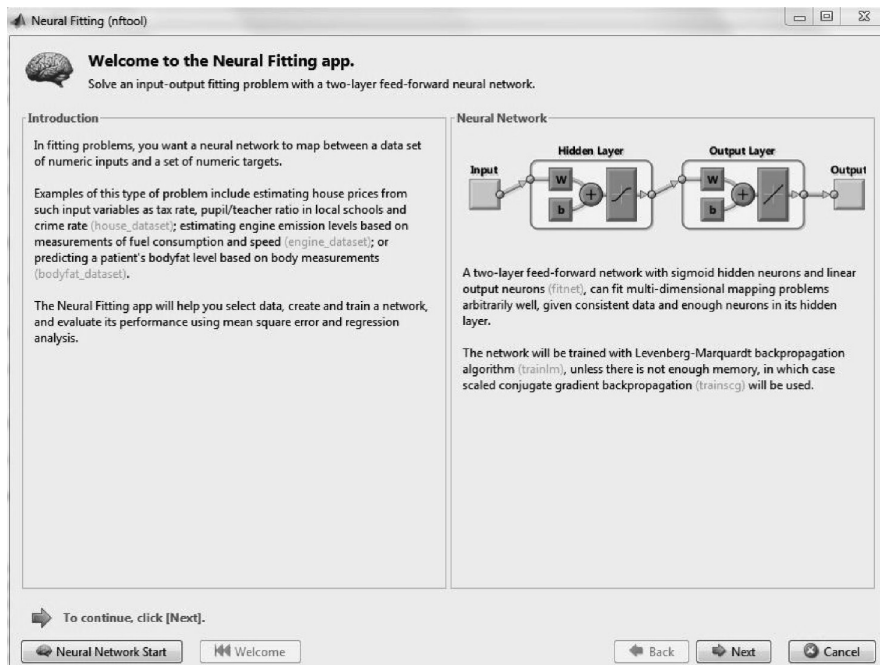


FIGURE 7.6 ANN toolbox in MATLAB.

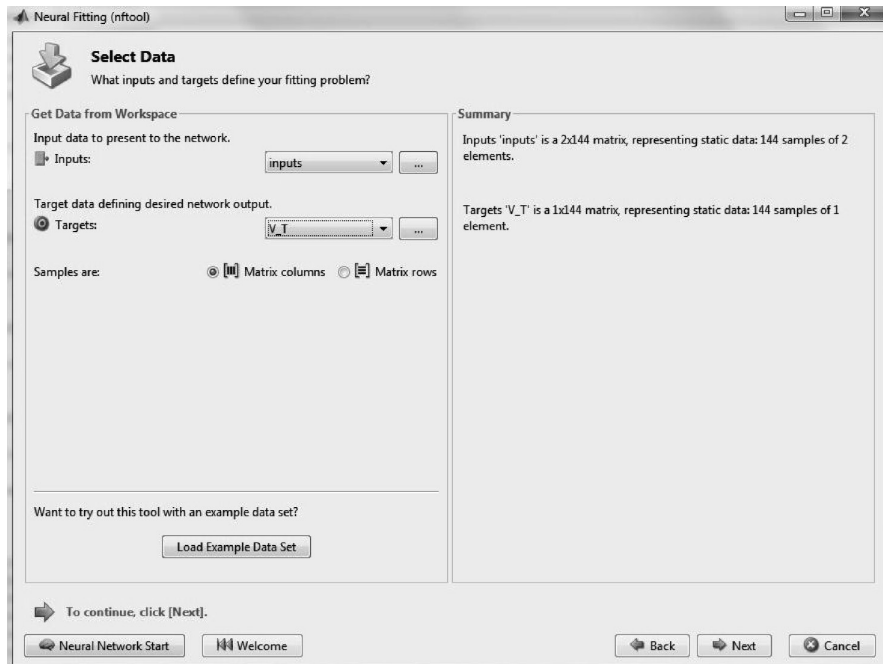


FIGURE 7.7 Defining inputs and targets in an ANN.

By selecting the neural net fitting in the applications window in the MATLAB toolbar, the tables of input and targets, which are shown in [Figures 7.6](#) and [7.7](#), should be selected.

Much of the data are devoted to the training, which are presented to the network during the training, and the network is adjusted according to its error. Some of the data are used to measure the network generalization, and the other data are for testing, which have no effect on the training and the performance measurement during and after the training processes. The data allocation to these three parts is arbitrary. Usually 70% of the data are allocated for training, 15% for validation, and 15% for testing. These values are shown on [Figure 7.8](#).

The process of selecting the number of neurons is a trial and error process. For example, by selecting ten hidden neurons, as shown in [Figure 7.9](#), the network does not perform well. So after training, the user can return to this panel and change the number of neurons.

Then, the Levenberg-Marquardt algorithm can be selected ([Figure 7.10](#)). This algorithm typically requires more memory, but less time.

Finally, by selecting the plot regression, the plots ([Figure 7.11](#)) and the neural network training error histogram ([Figure 7.12](#)) can be shown.

7.3.3.1.4 Adaptive Linear Filter

The Adaptive Linear (ADALINE) network is similar to the perceptron, but its activation function is linear. The linear activation function allows the ADALINE networks to take on any output value, thus solving the linearly separable problems.

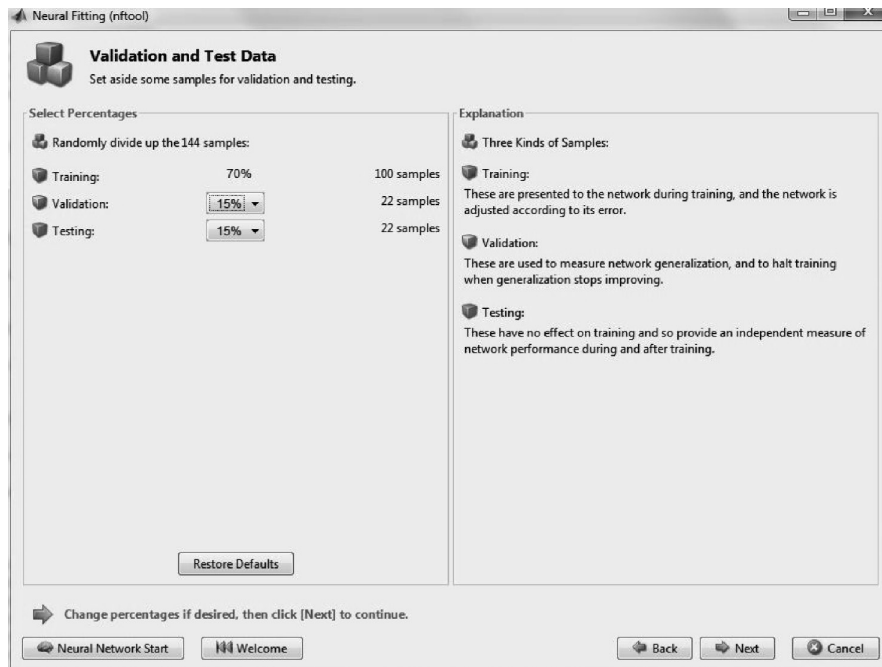


FIGURE 7.8 Define validation and testing samples.

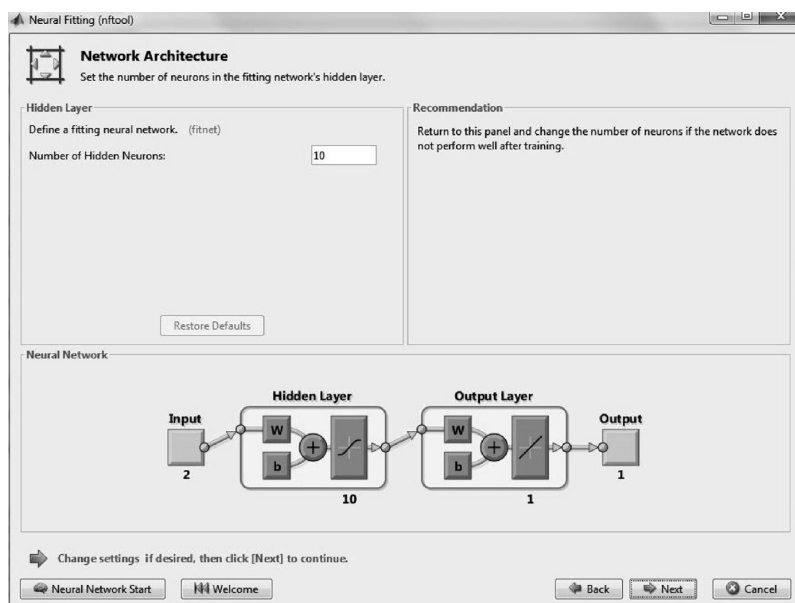


FIGURE 7.9 Number of neurons in an ANN.

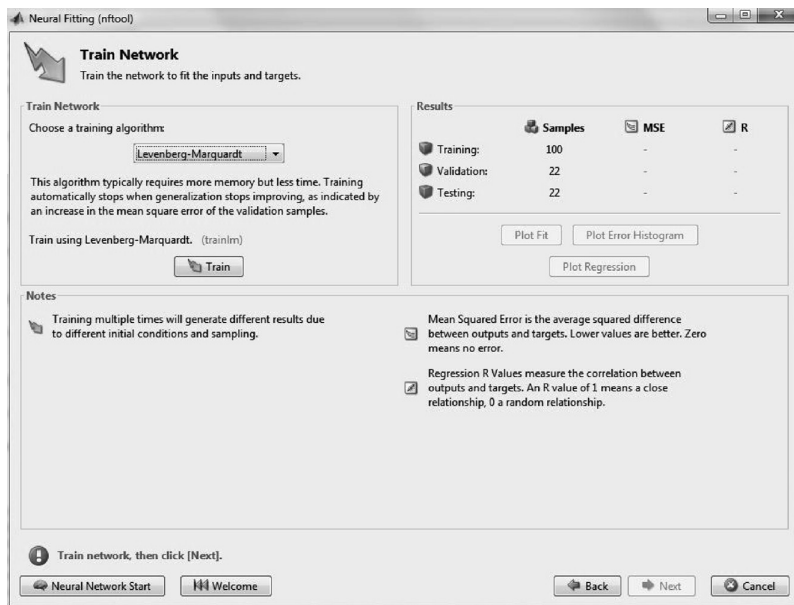


FIGURE 7.10 The Train Network in an ANN.

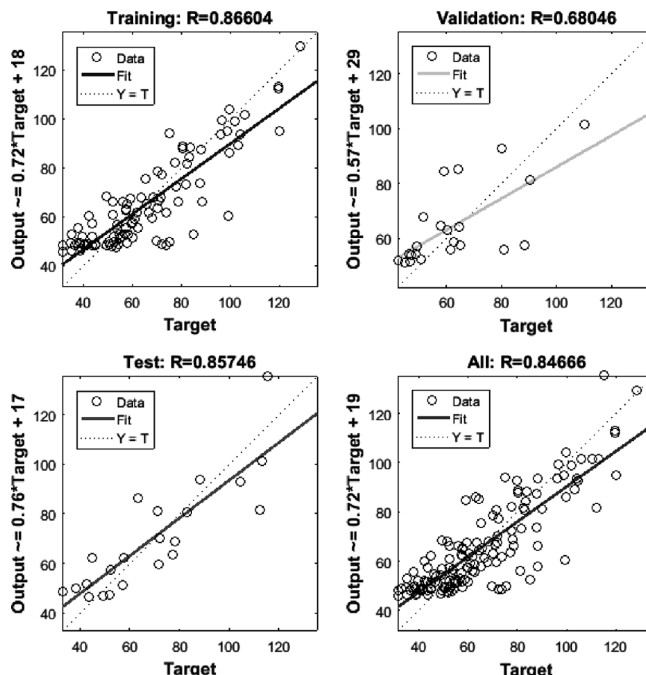


FIGURE 7.11 Linear regression in an ANN toolbox.

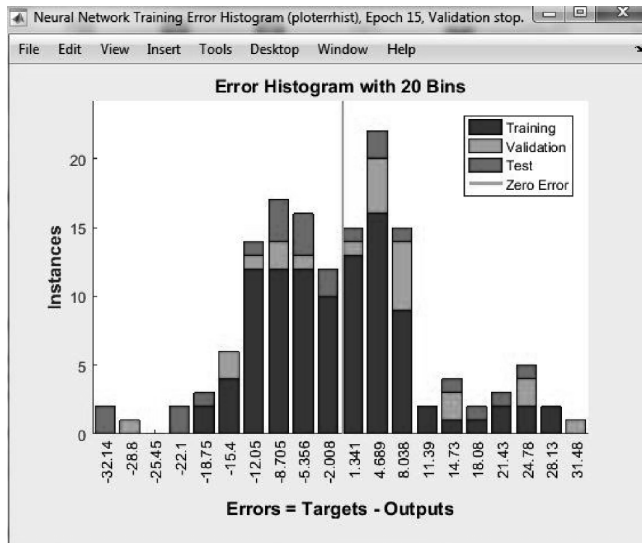


FIGURE 7.12 Neural network training error histogram.

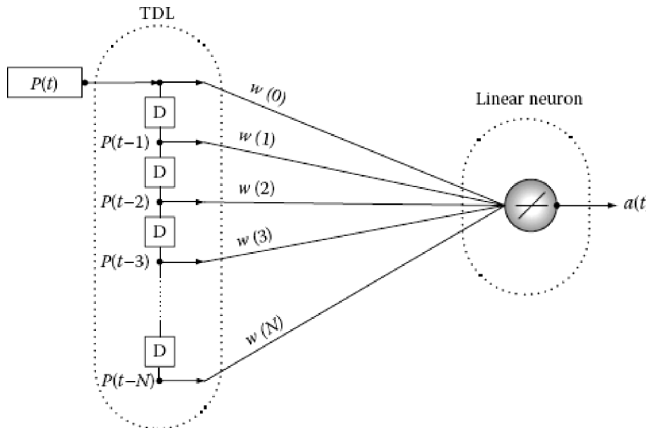


FIGURE 7.13 The architecture of the adaptive ADALINE.

The architecture of the ADALINE is shown in Figure 7.13. The ADALINE has a counterpart in statistical modeling, in this case, least square regression. The ADALINE network is a widely used ANN found in the practical applications, especially in adaptive filtering. In the ADALINE, the learning rule is based on the least mean squares method, which minimizes the mean square error. The adaptive filter is produced by combining a tapped delay line and an ADALINE network. At each time step, this filter is adjusted and finds the weights and biases that minimize the network's sum

squared error for the recent input and target vectors. In the ADALINE network, the output, $a(t)$ is obtained as follows:

$$a(t) = \sum_{k=0}^N w(k) P(t-k) + b \quad (7.13)$$

where:

$w(k)$ is the k th member of weight vector

b is the bias of the linear neuron

t denotes a discrete time

P is the input matrix.

7.3.3.1.5 Recurrent Neural Network

The recurrent neural networks (RNNs) have feedback elements that enable the signals from one layer to feedback to a previous layer. The recurrent scheme differs from the MLP in the way that its outputs recur either from the output layer or the hidden layer back to its input layer. So a context unit consists of several time delay operators and represents the time implicitly by its effects on the processing, in contrast to a TDL component, which explicitly considers the temporal processing. Attaching the recurrent connections (context unit) to a MLP network results in an RNN. Thus, in a recurrent network, the weight matrix for each layer contains the input weights from all other neurons in the network, not just the neurons from the previous layer. The architecture of the RNNs is illustrated in Figure 7.14. There are three general models of a RNN, depending on the architecture of the recurrent connections: the Jordan RNN (Jordan, 1986), which has feedback connections from the output layer to the input layer; the Elman RNN (Elman, 1990), which has feedback connections from the hidden layer to the input layer; and the local RNN (Fransconi et al., 1992), which uses only local feedback.

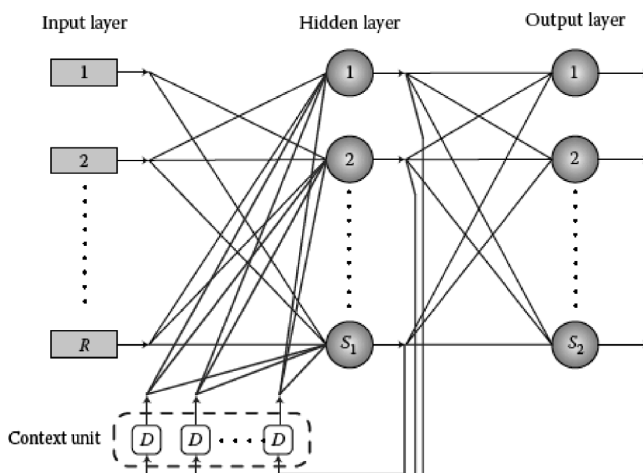


FIGURE 7.14 A typical architecture of an Elman RNN. (From Karamouz, M. et al., *J. Am. Water Resourc. Assoc.*, 37, 1301, 2001.)

The network employs its output signals from the hidden layer to train the networks. The input layer is divided into two parts: the true input units and the context unit, which are a tapped delay line memory of S_1 neurons from the hidden layer. The Elman RNN is formulated by the following equations:

$$a_j^1(t) = F \left(\sum_{i=1}^R w_{j,i}^1 P_i(t) + \sum_{c=1}^{S_1} w_{j,c}^C a_c^1(t-1) + b_j^1 \right), \quad 1 \leq j \leq S_1 \quad (7.14)$$

$$a_k^2(t) = G \left(\sum_{j=1}^{S_1} w_{k,j}^2 a_j^1(t) + b_k^2 \right), \quad 1 \leq k \leq S_2 \quad (7.15)$$

where:

t denotes a discrete time

R is the number of input signals

S_1 and S_2 are the numbers of the hidden neurons and the output neurons, respectively
 w^1 and w^C are the weight matrices of the hidden layer for the real inputs and the context unit

w^2 is the output layer weight matrix

b^1 and b^2 are the bias vectors of the hidden and output layers, respectively

P is the input matrix

a^1 and a^2 are the hidden and output layers' output vectors, respectively

F and G are the hidden and output layers' activation functions, respectively.

It is noteworthy that the modifiable connections are all feed-forward, and the weights from the context units can be trained in exactly the same manner as the weights from the input units to the hidden units by the conventional back propagation method (Fauset, 1994).

7.3.3.1.6 Input-Delayed Neural Network

The input-delayed neural network (IDNN) can be used to design the temporal neural networks as a capable alternative. The IDNN consists of two parts: the first part is a memory structure that saves the latest information, and the second part is a nonlinear associator that processes the information and predicts the future. The memory structure is a time delay line that corresponds to a buffer containing the recent inputs generated by the delay unit operator D , while the associator is the conventional feed-forward network with one hidden layer and one output layer (Coulibaly et al., 2001).

The IDNN is a time delay neural network, where only the input layer owns the memory, and this makes it different from the general time delay neural network. The structure of a typical IDNN with recurrent connection is shown in [Figure 7.15](#) that each input variable is delayed several time steps and fully connected to the hidden layer. The output of the IDNN is given by:

$$a_j^1(t) = F \left(\sum_{d=0}^D \sum_{i=1}^R w_{j,i,d}^1 p_{i,d+1}(t) + b_j^1 \right), \quad 1 \leq j \leq S_1 \quad (7.16)$$

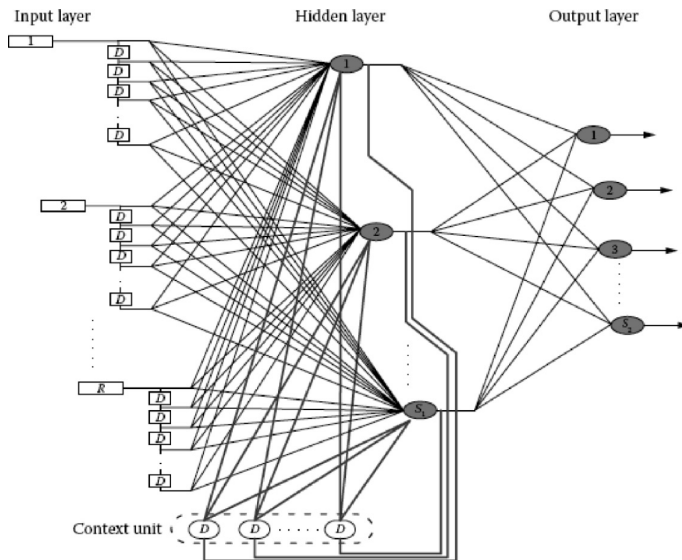


FIGURE 7.15 A typical architecture of an IDNN (with recurrent connection) (IDRNN).

$$a_k^2(t) = G \left(\sum_{j=1}^{S_1} w_{k,j}^2 a_j^1(t) + b_k^2 \right), \quad 1 \leq k \leq S_2 \quad (7.17)$$

where:

t denotes a discrete time

D is the time delay memory order

R is the number of input signals

S_1 and S_2 are the numbers of the hidden neurons and the output neurons, respectively

w^1 and w^2 are the weight matrices of the hidden and output layers

b^1 and b^2 are the bias vectors of the hidden and output layers

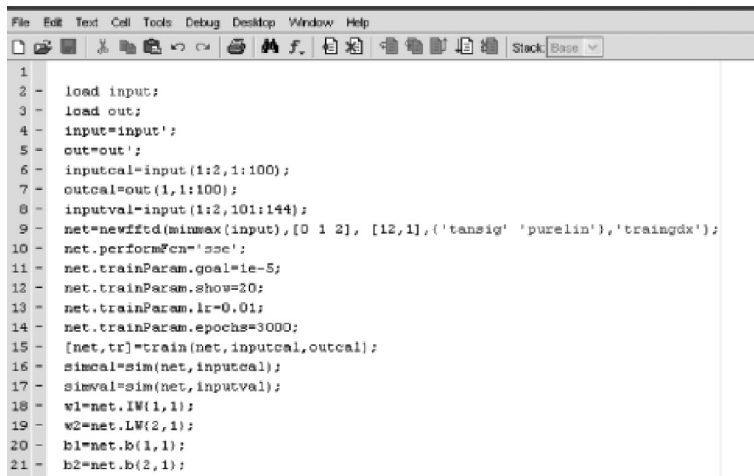
p is the input matrix and a^1 and a^2 are the hidden and output layers' output vectors

F and G are the hidden and output layers' activation functions, respectively.

A time-delay recurrent neural network (TDRNN) is presented using both the mentioned components in the architecture of a neural network in order to perform dynamically. A major feature of this architecture is that the nonlinear hidden layer receives the contents of both the input time delays and the context unit, which makes it suitable for complex sequential input learning.

Example 7.2

For the aquifer of Example 7.1, simulate the groundwater table variation using the IDNN model.



```

1
2 - load input;
3 - load out;
4 - input=input';
5 - out=out';
6 - inputcal=input(1:2,1:100);
7 - outcal=out(1,1:100);
8 - inputval=input(1:2,101:144);
9 - net=newffd([minmax(input),[0 1 2], [12,1],{'tansig' 'purelin'},'traingdx']);
10 - net.performFcn='sse';
11 - net.trainParam.goal=1e-5;
12 - net.trainParam.show=20;
13 - net.trainParam.lr=0.01;
14 - net.trainParam.epochs=3000;
15 - [net,tr]=train(net,inputcal,outcal);
16 - simcal=sim(net,inputval);
17 - simval=sim(net,inputval);
18 - w1=net.IW(1,1);
19 - w2=net.LW(2,1);
20 - b1=net.b(1,1);
21 - b2=net.b(2,1);

```

FIGURE 7.16 Developed IDNN model for simulation of the groundwater table variation.

SOLUTION

The same procedure as the previous example is followed for preparing the input data of the IDNN model. The developed structure of the IDNN model is shown in Figure 7.16. The tapped delay line memory of the developed model is 2 and there are 12 neurons in its hidden layer. The transfer functions of the hidden and output layers are the tangent sigmoid and the linear, respectively. The model is trained in 3000 steps (epochs), and the model goal is achieving an error less than 0.00001. The simulated and recorded monthly groundwater table variation data are compared in Figure 7.17. About 26% of the data has been simulated with less than 5% error, and 62% of the data has been simulated with an error of less than 10%.

7.3.3.2 Fuzzy Sets and Parameter Imprecision

Two approaches of randomization or fuzzification are used for evaluating the parameter uncertainty in the water resources and the hydrologic modeling. The fuzzy rules could be developed to incorporate the uncertainty of the variables, and it could be utilized as a simulation model or as a model to develop the operation policy in the real-time operation of the groundwater systems. In this section, the fundamentals of the fuzzy sets and the fuzzy decisions are introduced.

Let X be the set of certain objects. A *fuzzy set* A in X is a set of ordered pairs as follows:

$$A = \{(x, \mu_A(x))\}, x \in X \quad (7.18)$$

where:

$\mu_A: X \mapsto [0,1]$ is called the membership function
 $\mu_A(x)$ is the grade of the membership of x in A .

In the classical set theory, $\mu_A(x)$ equals 1 or 0, because x either belongs to A or does not.

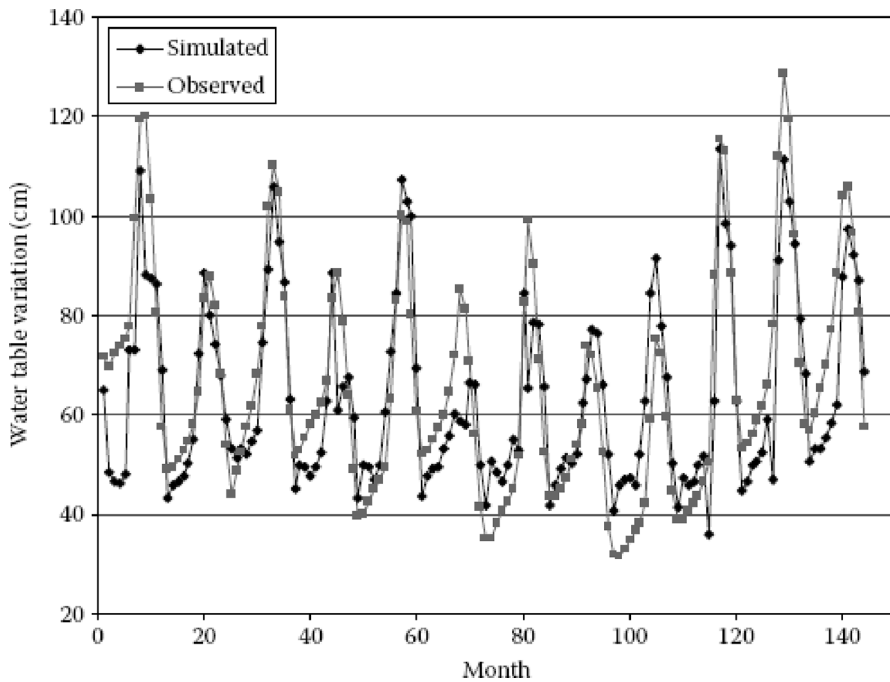


FIGURE 7.17 Comparison between the simulated groundwater table variation with an IDNN and the observed data.

The basic concepts of the fuzzy sets are as follows:

A fuzzy set A is *empty*, if $\mu_A(x) = 0$ for all $x \in X$.

A fuzzy set A is called *normal*, if:

$$\sup_x \mu_A(x) = 1 \quad (7.19)$$

For normalizing a nonempty fuzzy set, the normalized membership function is computed as follows:

$$\bar{\mu}_A(x) = \frac{\mu_A(x)}{\sup_x \mu_A(x)} \quad (7.20)$$

The *support* of a fuzzy set A is defined as:

$$S(A) = \{x | x \in X, \mu_A(x) > 0\} \quad (7.21)$$

The fuzzy sets A and B are equal, if for all $x \in X$:

$$\mu_A(x) = \mu_B(x) \quad (7.22)$$

A fuzzy set A is a *subset* of B ($A \subseteq B$), if for all $x \in X$,

$$\mu_A(x) \leq \mu_B(x) \quad (7.23)$$

A' is the *complement* of A , if for all $x \in X$,

$$\mu_{A'}(x) = 1 - \mu_A(x) \quad (7.24)$$

The *intersection* of the fuzzy sets A and B is defined as:

$$\mu_{A \cap B}(x) = \min\{\mu_A(x); \mu_B(x)\} \quad (\text{for all } x \in X) \quad (7.25)$$

Notice that (v) and (vii) imply that $A \subseteq B$ if and only if $A \cap B = A$.

The *union* of the fuzzy sets A and B is given as:

$$\mu_{A \cup B}(x) = \max\{\mu_A(x); \mu_B(x)\} \quad (\text{for all } x \in X) \quad (7.26)$$

The *algebraic product* of the fuzzy sets A and B is denoted by AB and is defined by the following relation:

$$\mu_{AB}(x) = \mu_A(x)\mu_B(x) \quad (\text{for all } x \in X) \quad (7.27)$$

The *algebraic sum* of the fuzzy sets A and B is denoted by $A + B$ and has the membership function:

$$\mu_{A+B}(x) = \mu_A(x) + \mu_B(x) - \mu_A(x)\mu_B(x) \quad (\text{for all } x \in X) \quad (7.28)$$

A fuzzy set A is *convex*, if for all $x, y \in X$ and $\lambda \in [0,1]$,

$$\mu_A(\lambda x + (1-\lambda)y) \geq \min\{\mu_A(x); \mu_A(y)\} \quad (7.29)$$

If A and B are convex, then it can be demonstrated that $A \cap B$ is also convex.

A fuzzy set A is *concave*, if A' is convex. In the case that A and B are concave, the $A \cup B$ will also be concave.

Consider $f: X \mapsto Y$ a mapping from the set X to the set Y and A a fuzzy set in X . The fuzzy set B *induced* by mapping f is defined in Y with the following membership function:

$$\mu_B(y) = \sup_{x \in f^{-1}(y)} \mu_A(x) \quad (7.30)$$

where:

$$f^{-1}(y) = \{x | x \in X, f(x) = y\}.$$

Example 7.3

Fuzzy sets A and B are defined in $X = [-\infty, \infty]$, by the membership functions as follows (Figure 7.18):

$$\mu_A(x) = \begin{cases} x - 1 & \text{if } 1 \leq x \leq 2 \\ 1 & \text{if } 2 < x \leq 3 \\ -x + 4 & \text{if } 3 < x \leq 4 \\ 0 & \text{otherwise} \end{cases}$$

$$\mu_B(x) = \begin{cases} x - 3 & \text{if } 3 \leq x \leq 4 \\ 1 & \text{if } 4 \leq x \leq 5 \\ -x + 6 & \text{if } 5 \leq x \leq 6 \\ 0 & \text{otherwise} \end{cases}$$

Determine the membership functions of the $A \cap B$, $A \cup B$, AB , and $A + B$ fuzzy sets.

SOLUTION

$\mu_{A \cap B}(x)$ is $\min \{\mu_A(x); \mu_B(x)\}$, therefore $A \cap B$ is:

$$\mu_{A \cap B}(x) = \begin{cases} x - 3 & \text{if } 3 \leq x \leq 3.5 \\ -x + 4 & \text{if } 3.5 < x \leq 4 \\ 0 & \text{otherwise} \end{cases}$$

and $\mu_{A \cup B}(x) = \max \{\mu_A(x); \mu_B(x)\}$, thus $A \cup B$ is as follows:

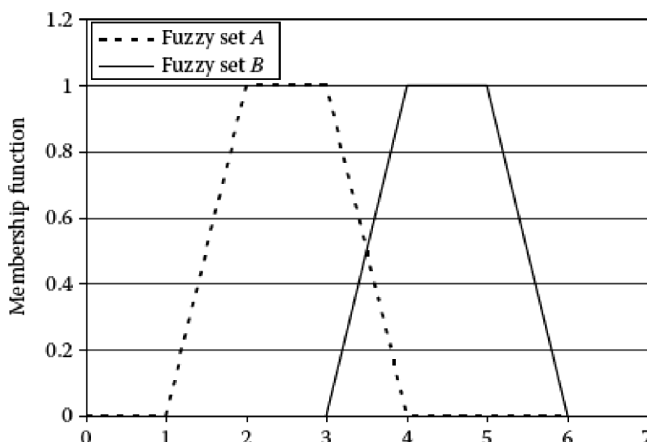


FIGURE 7.18 Membership function of A and B .

$$\mu_{A \cup B}(x) = \begin{cases} x-1 & \text{if } 1 \leq x \leq 2 \\ 1 & \text{if } 2 \leq x \leq 3 \\ -x+4 & \text{if } 3 \leq x \leq 3.5 \\ x-3 & \text{if } 3.5 \leq x \leq 4 \\ 1 & \text{if } 4 \leq x \leq 5 \\ -x+6 & \text{if } 5 < x \leq 6 \\ 0 & \text{otherwise} \end{cases}$$

The product of A and B is determined as follows:

$$\mu_{AB}(x) = \begin{cases} (x-3)(-x+4) & \text{if } 3 \leq x \leq 4 \\ 0 & \text{otherwise} \end{cases}$$

Finally, the summation of the fuzzy sets is determined as follows:

$$\mu_{A+B}(x) = \begin{cases} x-1 & \text{if } 1 \leq x \leq 2 \\ 1 & \text{if } 2 \leq x \leq 3 \\ 1+(x-3)(x-4) & \text{if } 3 \leq x \leq 4 \\ 1 & \text{if } 4 \leq x \leq 5 \\ -x+6 & \text{if } 5 < x \leq 6 \\ 0 & \text{otherwise} \end{cases}$$

The membership functions of the $A \cap B$, $A \cup B$, AB , and $A + B$ fuzzy sets are illustrated in [Figure 7.19](#).

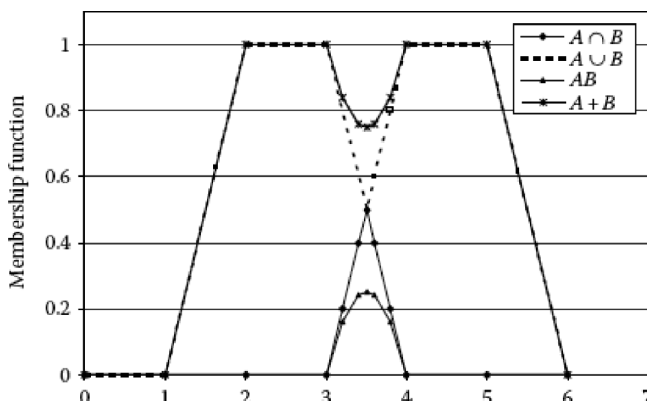


FIGURE 7.19 Operations of fuzzy sets $A \cap B$, $A \cup B$, AB , $A + B$.

Let X be the set of decision alternatives. A fuzzy constraint is defined by a fuzzy set C in X , and the membership function value $\mu_c(x)$ shows the degree an alternative satisfies the constraint C . Similarly, any objective function can be identified by a fuzzy set G , and $\mu_G(x)$ shows the degree an alternative represents an attainment of the goal represented by this objective function. Any multi-criteria decision-making problem can be defined in a fuzzy environment as the set of the fuzzy goals G_1, \dots, G_M and the fuzzy constraints C_1, \dots, C_N . The solution of the problem is the decision alternative that satisfies the constraints C_j in as high a level as possible and gives the best attainment of the goals possible. In other words, the intersection of the fuzzy sets G_1, \dots, G_M and C_1, \dots, C_N must have its highest membership value. Therefore, we consider and find the alternative x that maximizes this membership function. The interested reader may be referred to Bellman and Zadeh (1970) or to the section of the fuzzy decision in Szidarovszky et al. (1986).

$$\mu_D(x) = \min \{\mu_{G_1}(x), \dots, \mu_{G_M}(x); \mu_{C_1}(x), \dots, \mu_{C_N}(x)\} \quad (7.31)$$

Example 7.4

Assume that there are five alternatives to select from for improving a groundwater system; there are three constraints including the groundwater table fluctuation and supplying the minimum water demand with the acceptable water quality. Two objective functions are considered including maximizing the annual groundwater yield and minimizing the costs. The membership values for all the alternatives with respect to the constraints and objectives are given in [Table 7.4](#).

SOLUTION

The last row gives the values of μ_D by selecting the smallest numbers of all columns. The largest value of μ_D appears in the third column, so the second alternative is the best.

TABLE 7.4
Membership Values in Fuzzy Decision

| | | Alternatives | | |
|--|-------------|--------------|------|------|
| | | 1 | 2 | 3 |
| | μ_{G_1} | 0.85 | 0.95 | 0.80 |
| | μ_{G_2} | 0.90 | 0.90 | 0.75 |
| | μ_{C_1} | 0.89 | 0.87 | 0.83 |
| | μ_{C_2} | 0.82 | 0.90 | 0.74 |
| | μ_{C_3} | 0.73 | 0.87 | 0.78 |
| | μ_D | 0.73 | 0.87 | 0.74 |
| | | | | 0.85 |
| | | | | 0.73 |
| | | | | 0.95 |
| | | | | 0.63 |
| | | | | 0.66 |
| | | | | 0.81 |
| | | | | 0.63 |

7.3.3.3 System Dynamics

A system includes a collection of elements which continually interact over time to form a unified body. These interactions among the elements of a system are called the structure of the system. The system dynamics (SDs) approach gives users a better understanding of the complex interrelationships among the different elements within a system. The SD provides insight into the feedback process for simulating the system behavior. The simulation of the model over time is considered essential to understand the dynamics of the system. The development of an SD simulation model includes major steps such as understanding the system and its boundaries, identifying the key variables, representation of the physical processes or variables through mathematical relationships, mapping the model structure, and simulating the model for understanding its behavior. The SD approach is based on the theory of the feedback process using the system thinking paradigm. Feedback systems can be classified into two different classes (Ahmad and Simonovic, 2000):

Negative feedback, which seeks a goal and responds as a consequence of failing to achieve the goal.

Positive feedback, which generates the growth processes where an action builds a result that generates a greater action.

The feedback loop indicates how a system might behave because of its internal feedback loops and the effects that positive and negative feedback loops have on a system.

It was originally rooted in the management and engineering sciences in the 1960s, but has gradually been expanded to other fields. The advantages of this approach are the ease of constructing “what if” scenarios and tackling the physics of big, messy, real-world problems mathematically. In addition, the general principles of the SD simulation tools could be applied to social, economic, and ecological and biological systems for the system development (Karamouz et al., 2006, 2010, 2011).

In the system dynamics approach, we use several diagramming tools to capture the structure of systems, including causal loop diagrams and stock and flow maps. The causal loop diagrams (CLDs) are an important tool for representing the feedback structure of the systems. A causal diagram consists of the variables connected by arrows denoting the causal influences among the variables. The important feedback loops are also identified in the diagram (Sterman, 2000).

Figure 7.20 shows the basic elements of the SD simulation modeling. It is similar to a reservoir system. As shown in this figure, the interactions among the inflow, storage, outflow, and other site-specific issues such as the release values form the structure of the reservoir system. The stock represents the accumulations and can be used as a source, for example, the water stored in the reservoir. The accumulation needs the flow (inflow to the reservoir), which is modeled by the flow. The flow and stock are inseparable and make the minimum set of elements needed to describe the dynamics. The converters convert the input to outputs. They can represent the information or material quantities. The connectors link stocks to converters, the stocks to flow regulators, and the converters to other converters. It, representing the relationship between other objects, conveys the information from one variable to the others.

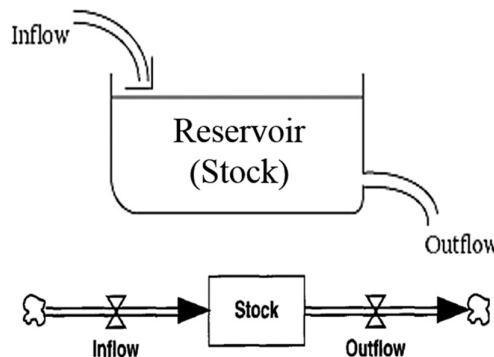


FIGURE 7.20 A schematic of an urban storage tank in system dynamic modeling.

The stocks, flows, converters, and connectors tools are used for the object-oriented programming.

The behavior and response of the system is simulated over time considering the dynamics of the system. In the reservoir example, the behavior is described by the dynamics of the reservoir storage filling and draining. This behavior is due to the influences of the inflow, outflow, losses, and environment, which are the elements of the system. The SD can also be used to analyze how the structural changes in one part of a system might affect the behavior of the system as a whole. The visual effects of SD mapping help the decision-makers to clearly evaluate the impacts of the different scenarios. The model results are functionally transparent to all parties involved in the water management.

The modeling process is a cycling process arrived at by cycling back through the entire sequence several times while working on the model. There are some steps for defining the system including clearly stating the purpose of the model, developing a base behavior pattern, and developing a system diagram (Table 7.5).

In the first step, the purposes of the modeling are clarified utilizing some tools such as reference behavior pattern. The reference behavior pattern is a graph over time for one or more variables which best captures the dynamic phenomenon the decision-makers are seeking to understand and focuses the efforts for the behavioral dimensions. In the second step of the modeling process, the hypotheses responsible for generating the behavior pattern are represented. Using a framework including the dynamic organizing principles, based on the stock/flow, the feedback loop is developed as the core of the model. Once the flows associated with the hypotheses have been characterized, the next step in mapping is to close the loops. A system diagram is composed of the essential actors or sectors. The model will help to focus the effort on the structural dimension.

There are many tools used for implementing the object-oriented modeling approach. Computer software tools such as systems thinking, experimental learning laboratory with animation (STELLA) developed by High Performance Systems Inc., VENSIM developed by Ventana System Inc., and POWERSIM developed by POWERSIM Software help the execution of these processes.

TABLE 7.5
Steps of System Dynamics Modeling Process

1. **Problem Articulation (Boundary Selection)**
 - **Theme selection:** What is the problem?
 - **Key variables:** What are the key variables that must be considered?
 - **Time horizon:**
 - **Dynamic problem definition:** What is the historical behavior of the key variables?
2. **Formulation of Dynamic Hypothesis**
 - **Initial hypothesis generation:** What are the current theories of the behavior?
 - **Endogenous focus:** Formulate a dynamic hypothesis.
 - **Mapping:** Develop maps of causal structure based on initial hypotheses, key variables, reference modes, and other available data, using tools such as
 - Model boundary diagrams
 - Subsystem diagrams, CLDs, Stock & flow maps, Policy structure diagrams
3. **Simulation Model Formulation**
 - **Specification** of structure and decision rules. **Estimation** of parameters, behavioral relationships, and initial conditions, **Tests** for consistency with the purpose and boundary.
4. **Testing**
 - **Comparison to reference modes**
 - **Robustness under extreme conditions**
 - **Sensitivity:**
5. **Policy Design and Evaluation**
 - **Scenario specification:** What environmental conditions might arise?
 - **Policy design:** What new decision rules, strategies, and structures might be tried in the real world?
 - **“What if...” analysis**
 - **Sensitivity analysis:** How robust are the policy recommendations under different scenarios and given uncertainties?
 - **Interactions of policies:** Do the policies interact?

Source: Sterman, J.D., *Business Dynamics: Systems Thinking and Modeling for a Complex World*. McGraw-Hill, Boston, MA, 2000.

Example 7.5

In a region, the water authority board considers a law to reduce the rate of the groundwater and river withdrawals. It would be given the authority to set an initial charge price for the consumed water. The water consumers are initially charged \$0.1/m³, and then it is based on the quantity of the produced wastewater. A group of researchers collected and analyzed the data about the monthly effects that resulted from this regulation. For this period the following relationships are developed:

$$A_t = 10 - 4.2 \times P_{st} \quad (7.32)$$

$$B_t = 0.9(0.3 + 2P_{rt})A_t \quad (7.33)$$

$$C_t = 0.38(A_t - B_t) \quad (7.34)$$

$$D_t = A_t - B_t - C_t \quad (7.35)$$

$$E_t = A_t - B_t \quad (7.36)$$

$$P_{s,t+1} = 0.88 - \frac{0.006B_t}{A_t} + P_t \quad (7.37)$$

$$P_{n,t+1} = 0.4 - 0.03E_t \quad (7.38)$$

where:

A_t is the quantity of the consumed water per month t (1000 m³/month)

B_t is the quantity of the treated wastewater per month t (1000 m³/month)

C_t is the quantity of the water loss without any usage per month t (1000 m³/month)

D_t is the quantity of the wastewater discharged to the groundwater through the absorption wells and septic tanks per month t (1000 m³/month)

E_t is the quantity of the supplied water per month t (1000 m³/month)

$P_{s,t}$ is the sale price of 1 m³ of the supplied water

$P_{n,t}$ is the cost of the supplying of 1 m³ of water

$P_{r,t}$ is the initial charge for 1 m³ water usage.

Based on the above information, explain the expected changes in the water usage and the wastewater production and the corresponding economic impacts through answering the following questions.

Explain the above equations in the system structure. Draw a system graph, which is primarily designed to support the statements about the water flow in the city. Represent the water supply system of the city within a system boundary, SB, using three components called: (1) the water treatment plants, (2) the water distribution system, and (3) the wastewater treatment system. Relate these three components of the system to three systems in its environment including: (1) water loss, (2) groundwater, and (3) surface water resources. Then show what components are associated with each of the above described prices. Finally, show in your graph two cash flows, namely, NB_t = monthly water supply budget (10³ \$/month) and R_t = monthly water supplying revenue (10³ \$/month).

Solve the problem with initial values of $A_0 = 9.1$, $B_0 = 3.7$, $C_0 = 0.9$, $D_0 = 5.08$, $E_0 = 8.36$, and $P_{r0} = 0.05$. Repeat the calculation with $P_{r1} = 0.1$, 0.2 , 0.3 . Draw the variation of the treated water and the discharged water to the groundwater as a function of P_{r1} .

Plot the diagram of the effect of different P_{r1} on the monthly revenue of the water authority board and the water supplying budget.

SOLUTION

1. a. $A_t = 10 - 4.2 \times P_{s,t}$: As the sale price of the water increases, the quantity of the water consumption decreases proportionally from some consumption limitation and employing water conservation strategies. The maximum of the quantity of water consumption is equal to 10 (for $P_{s,t} = 0$).
- b. $B_t = 0.9(0.3 + 2P_{r1})A_t$: The treated wastewater is a portion of the consumed water, and its quantity increases by the increase in the initial charge of consumers.

- c. $C_t = 0.38(A_t - B_t)$: 38% of the nontreated water is lost because of the problems in the water supply and the distribution system.
 - d. $D_t = A_t - B_t - C_t$: The quantity of the discharged wastewater to the groundwater and the river is obtained by the mass continuity equation knowing the quantity of the consumed, the treated, and the lost water quantities in the water supply system.
 - e. $E_t = A_t - B_t$: The required water supply of the month is obtained by using the continuity equation considering the water consumption and the treated wastewater.
 - f. $P_{s,t+1} = 0.88 - 0.006B_t/A_t + P_{rt}$: The water sale cost will decrease with the percentage of the wastewater treated the month before, and will increase with the initial charge.
 - g. $P_{n,t+1} = 0.4 - 0.03E_t$: The price of the water production in a month will decrease with an increase of the quantity of the water supply in the preceding month.
2. The system graph and associated costs are illustrated in [Figure 7.21](#). Also, $NB_t = P_{n,t}E_t$ and $R_t = P_{st}A_t$
3. The results are tabulated in [Tables 7.6](#) through [7.9](#).

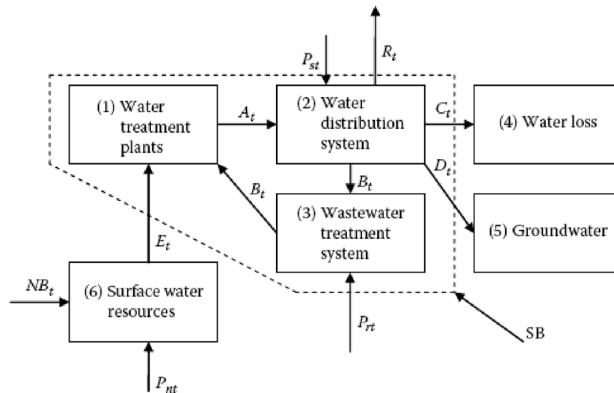


FIGURE 7.21 The diagram of the water flow in the water supply and the distribution system.

TABLE 7.6
Variation of Water Quantity and Price for $P_{rt} = 0.05$

| T | A_t | | B_t | | C_t | | D_t | | E_t | | P_{rt} | P_{st} | P_{nt} | NB | R |
|-------|--------------------|--------------------|--------------------|--------------------|--------------------|--------------------|--------------------|--------------------|--------------------|--------------------|----------------|----------------|----------------|-----------|-----------|
| | 10^3 m^3 | \$ | \$ | \$ | $10^3 \$$ | $10^3 \$$ |
| Month | Month | Month | Month | Month | Month | Month | Month | Month | Month | Month | m ³ | m ³ | m ³ | Month | Month |
| 0 | 9.100 | 3.700 | 0.900 | 5.080 | 8.360 | 0.050 | — | — | — | — | — | — | — | — | — |
| 1 | 6.104 | 2.198 | 1.485 | 2.422 | 3.907 | 0.050 | 0.928 | 0.149 | 0.583 | 5.662 | | | | | |
| 2 | 6.103 | 2.197 | 1.484 | 2.422 | 3.906 | 0.050 | 0.928 | 0.283 | 1.105 | 5.663 | | | | | |
| 3 | 6.103 | 2.197 | 1.484 | 2.422 | 3.906 | 0.050 | 0.928 | 0.283 | 1.105 | 5.663 | | | | | |
| 4 | 6.103 | 2.197 | 1.484 | 2.422 | 3.906 | 0.050 | 0.928 | 0.283 | 1.105 | 5.663 | | | | | |
| 5 | 6.103 | 2.197 | 1.484 | 2.422 | 3.906 | 0.050 | 0.928 | 0.283 | 1.105 | 5.663 | | | | | |

TABLE 7.7**Variation of Water Quantity and Price for P_{rt} Equal to 0.1**

| T | A_t | | B_t | | C_t | | D_t | | E_t | | P_{rt} | P_{st} | P_{nt} | NB | R | |
|-------|--------------------|--------------------|--------------------|--------------------|--------------------|--------------------|--------------------|--------------------|--------------------|--------------------|----------|--------------|--------------|--------------|-----------|-----------|
| | 10^3 m^3 | \$ | m^3 | m^3 | m^3 | $10^3 \$$ | $10^3 \$$ |
| Month | Month | Month | Month | Month | Month | Month | Month | Month | Month | Month | Month | Month | Month | Month | Month | Month |
| 0 | 9.100 | 3.700 | 0.900 | 5.080 | 8.360 | 0.100 | — | — | — | — | — | — | — | — | — | — |
| 1 | 5.894 | 2.652 | 1.232 | 2.010 | 3.242 | 0.100 | 0.978 | 0.149 | 0.484 | 0.484 | 0.484 | 0.484 | 0.484 | 0.484 | 5.762 | 5.762 |
| 2 | 5.895 | 2.653 | 1.232 | 2.010 | 3.242 | 0.100 | 0.977 | 0.303 | 0.982 | 0.982 | 0.982 | 0.982 | 0.982 | 0.982 | 5.762 | 5.762 |
| 3 | 5.895 | 2.653 | 1.232 | 2.010 | 3.242 | 0.100 | 0.977 | 0.303 | 0.982 | 0.982 | 0.982 | 0.982 | 0.982 | 0.982 | 5.762 | 5.762 |
| 4 | 5.895 | 2.653 | 1.232 | 2.010 | 3.242 | 0.100 | 0.977 | 0.303 | 0.982 | 0.982 | 0.982 | 0.982 | 0.982 | 0.982 | 5.762 | 5.762 |
| 5 | 5.895 | 2.653 | 1.232 | 2.010 | 3.242 | 0.100 | 0.977 | 0.303 | 0.982 | 0.982 | 0.982 | 0.982 | 0.982 | 0.982 | 5.762 | 5.762 |

TABLE 7.8**Variation of Water Quantity and Price for P_{rt} Equal to 0.15**

| T | A_t | | B_t | | C_t | | D_t | | E_t | | P_{rt} | P_{st} | P_{nt} | NB | R | |
|-------|--------------------|--------------------|--------------------|--------------------|--------------------|--------------------|--------------------|--------------------|--------------------|--------------------|----------|--------------|--------------|--------------|-----------|-----------|
| | 10^3 m^3 | \$ | m^3 | m^3 | m^3 | $10^3 \$$ | $10^3 \$$ |
| Month | Month | Month | Month | Month | Month | Month | Month | Month | Month | Month | Month | Month | Month | Month | Month | Month |
| 0 | 9.100 | 3.700 | 0.900 | 5.080 | 8.360 | 0.200 | — | — | — | — | — | — | — | — | — | — |
| 1 | 5.474 | 3.449 | 0.770 | 1.256 | 2.025 | 0.200 | 1.078 | 0.149 | 0.302 | 0.302 | 0.302 | 0.302 | 0.302 | 0.302 | 5.899 | 5.899 |
| 2 | 5.480 | 3.452 | 0.770 | 1.257 | 2.028 | 0.200 | 1.076 | 0.339 | 0.688 | 0.688 | 0.688 | 0.688 | 0.688 | 0.688 | 5.898 | 5.898 |
| 3 | 5.480 | 3.452 | 0.770 | 1.257 | 2.028 | 0.200 | 1.076 | 0.339 | 0.688 | 0.688 | 0.688 | 0.688 | 0.688 | 0.688 | 5.898 | 5.898 |
| 4 | 5.480 | 3.452 | 0.770 | 1.257 | 2.028 | 0.200 | 1.076 | 0.339 | 0.688 | 0.688 | 0.688 | 0.688 | 0.688 | 0.688 | 5.898 | 5.898 |
| 5 | 5.480 | 3.452 | 0.770 | 1.257 | 2.028 | 0.200 | 1.076 | 0.339 | 0.688 | 0.688 | 0.688 | 0.688 | 0.688 | 0.688 | 5.898 | 5.898 |

TABLE 7.9**Variation of Water Quantity and Price for P_{rt} Equal to 0.25**

| T | A_t | | B_t | | C_t | | D_t | | E_t | | P_{rt} | P_{st} | P_{nt} | NB | R | |
|-------|--------------------|--------------------|--------------------|--------------------|--------------------|--------------------|--------------------|--------------------|--------------------|--------------------|----------|--------------|--------------|--------------|-----------|-----------|
| | 10^3 m^3 | \$ | m^3 | m^3 | m^3 | $10^3 \$$ | $10^3 \$$ |
| Month | Month | Month | Month | Month | Month | Month | Month | Month | Month | Month | Month | Month | Month | Month | Month | Month |
| 0 | 9.100 | 3.700 | 0.900 | 5.080 | 8.360 | 0.300 | — | — | — | — | — | — | — | — | — | — |
| 1 | 5.054 | 4.094 | 0.365 | 0.595 | 0.960 | 0.300 | 1.178 | 0.149 | 0.143 | 0.143 | 0.143 | 0.143 | 0.143 | 0.143 | 5.952 | 5.952 |
| 2 | 5.064 | 4.102 | 0.366 | 0.597 | 0.962 | 0.300 | 1.175 | 0.371 | 0.357 | 0.357 | 0.357 | 0.357 | 0.357 | 0.357 | 5.951 | 5.951 |
| 3 | 5.064 | 4.102 | 0.366 | 0.597 | 0.962 | 0.300 | 1.175 | 0.371 | 0.357 | 0.357 | 0.357 | 0.357 | 0.357 | 0.357 | 5.951 | 5.951 |
| 4 | 5.064 | 4.102 | 0.366 | 0.597 | 0.962 | 0.300 | 1.175 | 0.371 | 0.357 | 0.357 | 0.357 | 0.357 | 0.357 | 0.357 | 5.951 | 5.951 |
| 5 | 5.064 | 4.102 | 0.366 | 0.597 | 0.962 | 0.300 | 1.175 | 0.371 | 0.357 | 0.357 | 0.357 | 0.357 | 0.357 | 0.357 | 5.951 | 5.951 |

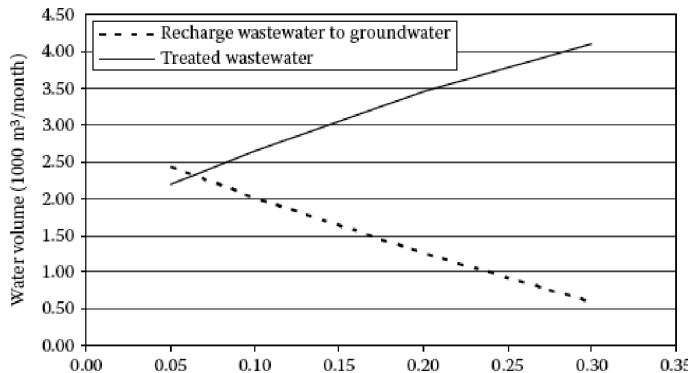


FIGURE 7.22 Variation of treated water and recharged water to groundwater with P_{rt}

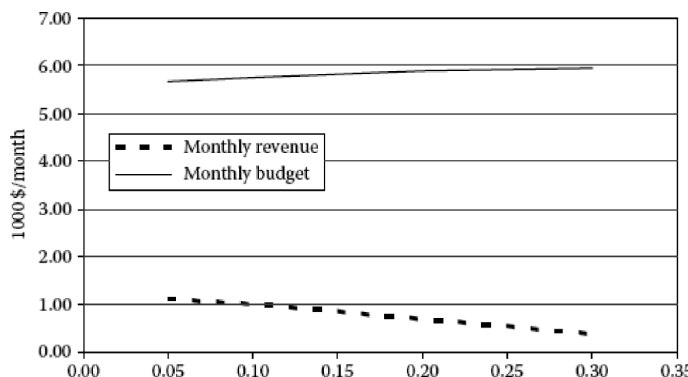


FIGURE 7.23 The effect of different P_{rt} on the monthly revenue and the water supply budget.

4. The variation of the treated water and the recharged water to the groundwater with P_{rt} is plotted in [Figure 7.22](#). By increasing the P_{rt} , the treated water quantity considerably increases and the recharged wastewater to groundwater decreases.
5. The diagram of the effect of the different P_{rt} on the monthly revenue and the water supplying budget is illustrated in [Figure 7.23](#). The figure shows the monthly revenue increases and the monthly water supplying budget decreases due to increasing P_{rt} . It is increasing the treated water that leads to decreasing the water consumption.

To describe the steps of [Table 7.5](#) for this example,

1. **Problem Articulation (Boundary Selection):** Water authority board
 - **Theme selection:** The problem is the withdrawal increase.
 - **Key variables:**
 - A_t is the quantity of the consumed water per month t (1000 m³/month)
 - B_t is the quantity of the treated wastewater per month t (1000 m³/month)

C_t is the quantity of the water loss without any usage per month t (1000 m³/month)

D_t is the quantity of the wastewater discharged to the groundwater through the absorption wells and septic tanks per month t (1000 m³/month)

E_t is the quantity of the supplied water per month t (1000 m³/month)

P_{st} is the sale price of 1 m³ of supplied water

P_{nt} is the cost of supplying 1 m³ of water

P_{rt} is the initial charge for 1 m³ water usage.

- **Time horizon:** One month
- **Dynamic problem definition (reference modes):** A group of researchers collected and analyzed the data about the monthly effects that resulted from this regulation.

2. Formulation of Dynamic Hypothesis:

The goal is to reduce the rate of the groundwater and river withdrawals. It would be given the authority to set an initial charge price for the consumed water.

3. Formulation of a Simulation Model:

The simulation model is presented in [Figure 7.24](#).

4. Testing:

- **Comparison to reference modes:** It is observed from the diagrams.

5. Policy Design and Evaluation:

The water consumers are initially charged \$0.1/m³ and then it is based on the quantity of the produced wastewater.

Example 7.6

Assume that the relationships between the population, the water demands, and the groundwater resources for the water supply in a region are as follows:

$$P_{t+1} = P_t + 0.8 \left(\frac{D_t}{P_t} - 0.5 \right) \times 10^{10} \quad (7.39)$$

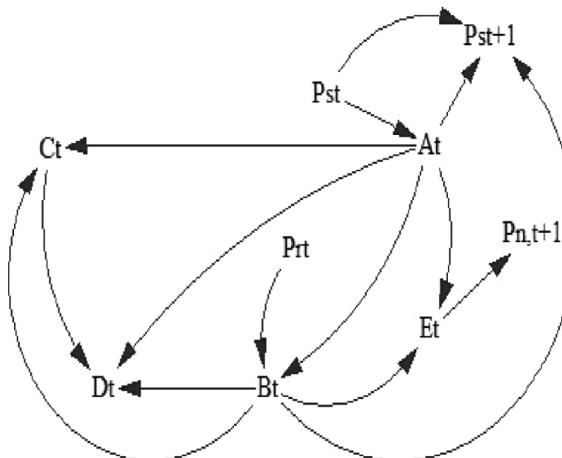


FIGURE 7.24 Simulation model (CLD) for Example 7.5.

$$D_t = \frac{R_t P_t}{2 \times 10^9} \quad (7.40)$$

$$R_t = 10^9 + 0.2P_t - 0.02P_t^{1.168} \quad (7.41)$$

where:

P_t is the population in the region at year t

D_t is the water demand (MCM) at year t

R_t is the groundwater resources (MCM) at year t .

Assuming that the city population in the first year is equal to 0.5×10^5 , determine the maximum possible population of the region.

SOLUTION

For determining the maximum possible population of the region, Equation 7.41 is replaced in Equation 7.40, and then it is replaced in Equation 7.39. It is solved based on the population factor.

$$D_t = \frac{(10^9 + 0.2P_t - 0.02P_t^{1.168})P_t}{2 \times 10^9} \quad (7.42)$$

Finally, the obtained relation is substituted in the population relation.

$$P_{t+1} = P_t + 0.8 \left(\frac{(10^9 + 0.2P_t - 0.02P_t^{1.168})P_t / 2 \times 10^9}{P_t} - 0.5 \right) \times 10^{10} \quad (7.43)$$

The population of each year is more than the previous year $P_{t+1} > P_t$, so that the expression in the brackets should be more than zero.

$$\begin{aligned} 0.8 \left(\frac{(10^9 + 0.2P_t - 0.02P_t^{1.168})P_t / 2 \times 10^9}{P_t} - 0.5 \right) &> 0 \\ \Rightarrow \frac{(10^9 + 0.2P_t - 0.02P_t^{1.168})}{2 \times 10^9} &> 0.5 \end{aligned} \quad (7.44)$$

$$10^9 + 0.2P_t - 0.02P_t^{1.168} > 10^9 \Rightarrow 0.2P_t - 0.02P_t^{1.168} > 0$$

$$\Rightarrow P_t > 0.1P_t^{1.168} 10 > P_t^{0.168} \Rightarrow P_t < 9 \times 10^5 \quad (7.45)$$

Therefore, the population cannot exceed 9×10^5 persons because of the limitations of the water resources. Once the population reaches this value, it will fluctuate around it. The variations of P_t , R_t , and D_t are shown in Figures 7.25 through 7.27, respectively. As it is shown in these figures, after about 70 years, the curves converge to straight lines, reaching their limits.

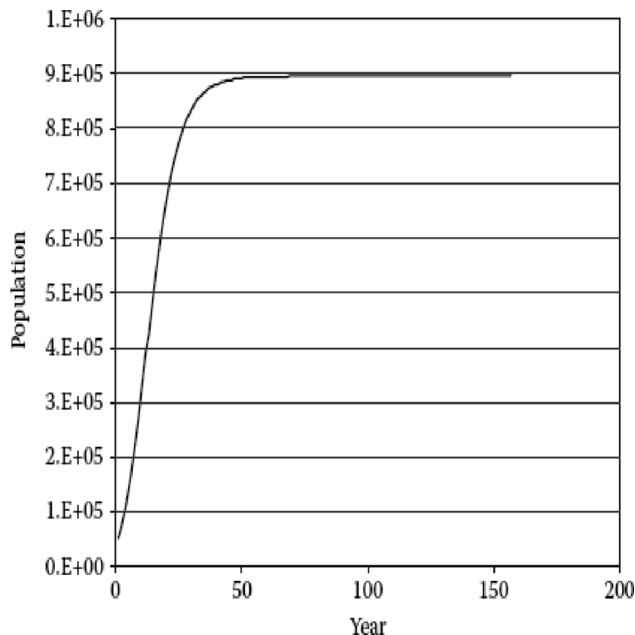


FIGURE 7.25 Variations of the population over time.

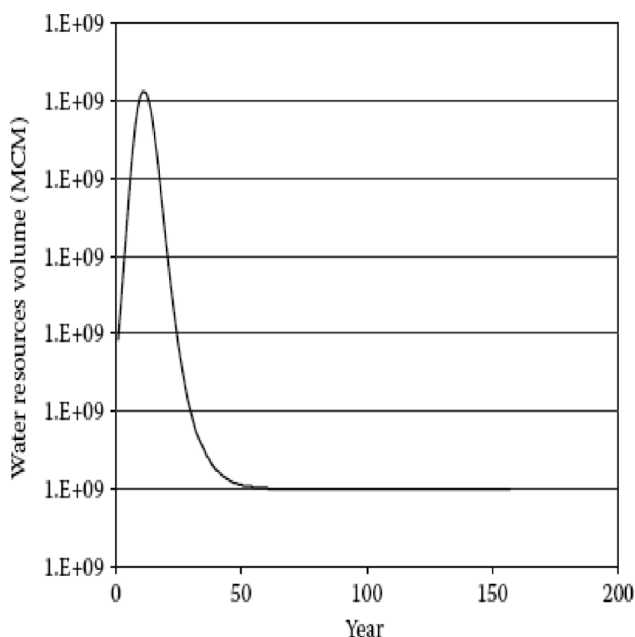


FIGURE 7.26 Variations of the available water resources over time.

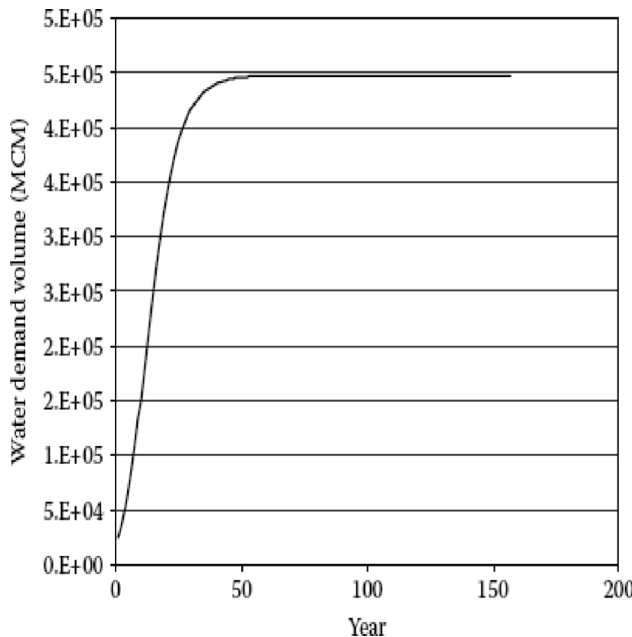


FIGURE 7.27 Variations of the water demand over time.

7.3.3.4 Agent-Based Modeling

Agent-based modeling is a relatively new tool developed and used to model complex systems such as water resources (Bandini et al., 2009). This modeling tool is utilized for the simulation of human social life and the reciprocating interactions of different agents/units (Macy and Willer, 2002). Agents in such models are considered as independent institutions or units that cooperate and work together in a common environment. Each agent is capable of establishing relations with the other agents through the surrounding environment. The models illustrate the way each agent affects the others and its interactions with the environment to simulate and represent the human decision-making process.

In agent-based models, each agent is defined as an individual, group, stakeholder, institution, or organization with different levels of decision-making authority. The agent has unique characteristics and powers, which are utilized in decision-making. The agent characteristics include experience, attributes, expertise knowledge, adaptability, independence, memory, updatability, and the ability to interact with others. Each of these characteristics may be taken into account in the model on a case-by-case basis. Important heterogeneities in the agent attributes and decision rules can then be modeled. The interactions occur as a result of the relations among agents, during which messages are communicated, which impact the behavior of each agent involved. The success and affectability of the agents' communications depend on the specific characteristics of each agent. Obviously, no reciprocal changes can be expected between the agents if no relations exist and no interactions occur in the system (Berglund, 2015).

Additionally, each agent's understanding and relations with the others and the environment are based on the feedback that it receives from that environment and its components. Therefore, the development of the agent-based models relies on the identification of the key agents, the definition of the environment in which the agents interact with each other, the agents' behavioral characteristics, and the formulation of the interactions between agents and the surrounding environment (Berglund, 2015).

The effects of the interactions of an agent are influenced by the other agents' characteristics and environmental conditions (Berglund, 2015). [Figure 7.28](#) shows the general influence of the surrounding environment and the agents on each other in a hypothetical system with three key agents: state or regulatory agencies, environmental sector, and agricultural sector that diverts water. In water resources systems, because the environmental conditions determine the water availabilities and limitations of the system, the perceptions of the agents are strongly influenced by the environment. The environmental sector's perception is only influenced by the environment. Both the agricultural water users (diversions) and the environmental sector influence the perception of the state agent by informing it about their concerns and water demands, and justifying the importance of their goals. In addition, the state affects the perception of the agricultural water users by informing them about the new policies, regulations, educational plans, assigned penalties, incentives, etc.

Kelly et al. (2013) reviewed five common modeling approaches for integrated environmental assessment and management including systems dynamics, Bayesian networks, coupled component models, agent-based models, and knowledge-based models. They summarized that agent-based models simulate the dynamics of the individuals or the groups of humans or animals. These agents usually have their own goals, use the environment to achieve these goals, share resources, and communicate with each other. They react to changes based on the “perceived” changes in the environment according to the pre-defined rules. [Figure 7.29](#) shows their guiding framework for selecting the most appropriate modeling approach in the form

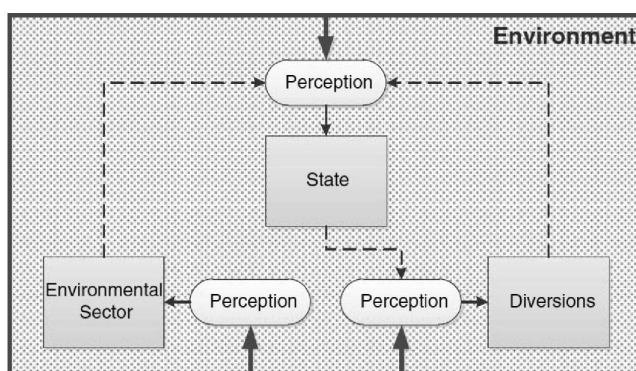


FIGURE 7.28 Influence of the environment and other agents on each agent. (From Akhbari, M. and Grigg, N.S., *J. Water Res. Manag.*, 27(11), 4039–4052, 2013. doi: 10.1007/s11269-013-0394-0.)

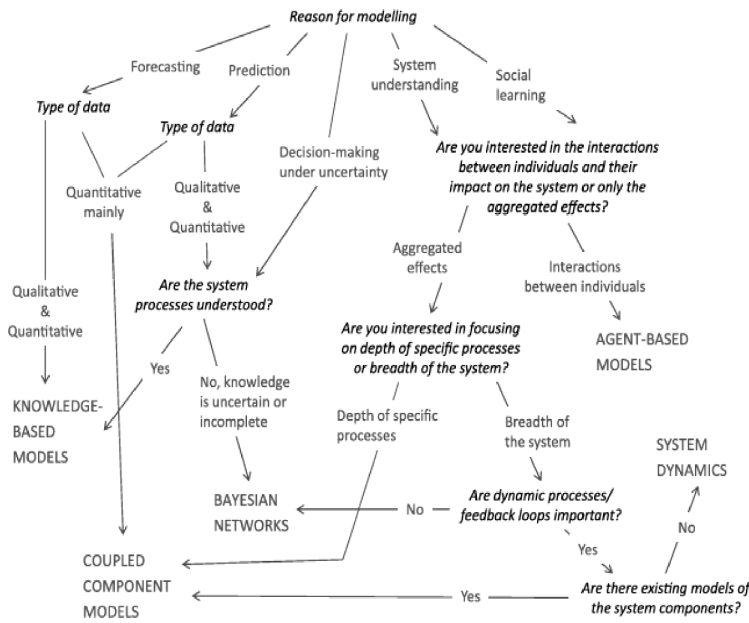


FIGURE 7.29 Decision tree for selecting the most appropriate integrated modeling approach under standard application. (From Kelly, R.A. et al., *Environ. Model. Software*, 47, 159–181, 2013.)

of a decision tree. They concluded that the agents-based modeling helps develop a framework of techniques that promotes thinking about the elementary system structures and their interactions. These models are suitable for theory-testing and useful for developing a shared system understanding when working with the diverse stakeholder groups. The model purpose is usually social learning, and the types of data available for this modeling are mainly qualitative in model conceptualization and quantitative for model calibration and testing. There are different simulation methods for the agent-based modeling, ranging from the simple cellular automata to the detailed, disaggregated system dynamics models.

7.3.3.4.1 Agent-Based Modeling for Groundwater Management

A typical agent-based model has three major elements: (1) key agents, their characteristics, and distinct behaviors; (2) the environment within which the agents interact with each other and the surrounding environment; and (3) the agents' relationships and methods of interactions with each other and with the environment, which in this context can be defined as the aquifer or basin of interest.

Figure 7.30 presents a conceptual framework for a shared aquifer to define the different levels of decision-making and interactions in an agent-based model. The first level contains the government agencies, environmental sector, and regulators which are the institutional agents. In the second level, there are agent groups such as water user associations, groundwater management districts, or water markets.

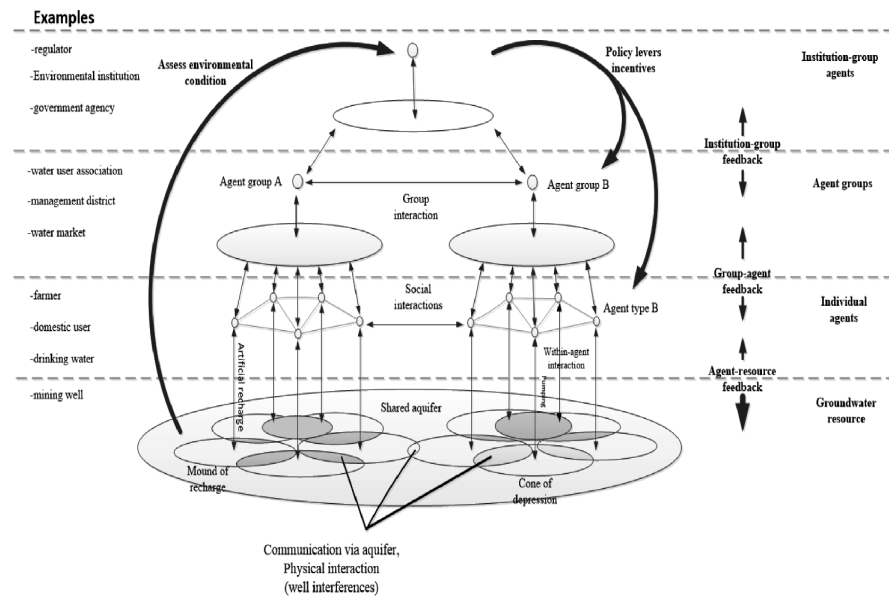


FIGURE 7.30 Scales of decision-making and modes of interaction in the social simulator. (Castilla-Rho, J.C. et al., *Environ. Model. Software*, 73, 305–323, 2015.)

The individual agents or stakeholders such as farmers, domestic users, and drinking water wells are in the third level, while the users are withdrawing water from the shared groundwater resources.

7.3.3.4.2 Agents and Their Characteristics

Examples of agents normally involved in water decisions include: the agricultural, industrial, urban/domestic, environmental, and regulatory sectors. They can be characterized based on their attributes, behavioral rules, memory, decision-making sophistication (the amount of information an agent requires to make decisions), and resources/flows (Macal and North, 2006). The decision-making sophistication can be classified as simple, medium, and high. In water resources management, the world of perception about the water also influences agents' characteristics and their interactions with the others. Wolf (2008) defined four worlds of perception: the physical, emotional, knowing/intellectual, and spiritual. For example, a glass of water is recognizable on a physical plane (physical perception). A thirsty person perceives it emotionally (emotional perception), and it can be intellectualized considering its components and the interaction of water with our body, or considering how its use could be translated into economic gain; e.g., through agricultural production and sale (intellectual perception). It becomes a source of spiritual nourishment in some religions as the followers must perform specific ritual practices in water (spiritual perception) (Wolf, 2008). In a conflict resolution process, consideration and understanding the agents' perceptions become meaningful because different sides of a conflict have different perceptions about the water, e.g., one side may have an intellectual perception and the other side an emotional perception. Agents with

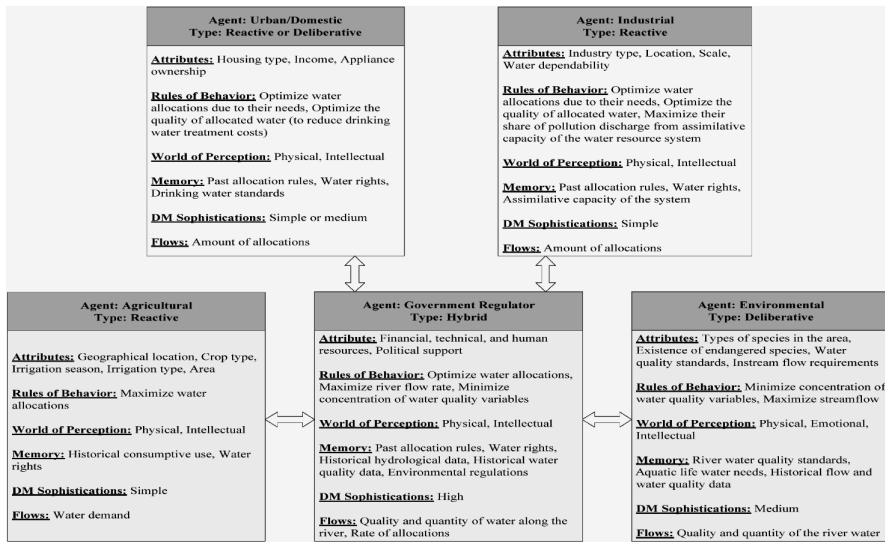


FIGURE 7.31 Proposed characteristics for some agents typically involved in water resources systems (arrows show interactions). (Adapted from Akhbari, M. and Grigg, N.S., *Water Res. Manag.*, 29(14), 5201–5216, 2015.)

physical or intellectual perceptions are more likely to relax their demand through negotiations, incentives, etc. However, the agents with spiritual or emotional perceptions are expected to be stricter and it may be harder to change their water demand.

Characterizing agents is case-specific; however, Figure 7.31 suggests an overall framework to characterize some types of agents typically involved in the water resources systems. All agents except regulators demand water. The decision-making sophistication level is relatively simple for the agricultural and industrial agents as there is a simple relationship between their water demands and the potential benefits through production opportunities. Depending on the complexity and the number of parameters in a case, decision-making sophistication might be simple or medium for urban/domestic agents where the source water quality, size, finance, and other key factors affect the level of sophistication.

7.4 OPTIMIZATION MODELS FOR GROUNDWATER MANAGEMENT

Nowadays, due to the increasing water demands and water pollution, a significant challenge is to determine the optimal amount of water withdrawal from the aquifer to supply the water demands and sustain the native peoples and ecosystems. The optimal water supply to the municipal, industrial, and agricultural water demands considering the physical, socio-economic, and environmental constraints is the major objective of the groundwater planning and management. The following planning problems are associated with the groundwater supply management (Yeh, 1992):

1. The determination of an optimal pumping pattern such as the location of pumping wells and their pumping rate to satisfy water demands
2. The timing and staging of the well system development (capacity expansion) considering the future water demands
3. The design of the water transfer facilities for the optimal allocation and distribution of the water to the demand points in the basin

In this section, some typical optimization models for the groundwater operation management, capacity expansion, and conjunctive use of the surface and groundwater resources are presented.

7.4.1 OPTIMIZATION MODEL FOR GROUNDWATER OPERATION

Optimal policies for the groundwater operation such as the optimal extraction, allocation, and optimal recharge of the aquifer can be determined using the groundwater operation model considering the physical, environmental, and socio-economic constraints. The objective function of the optimization model could be to minimize the total discounted operational costs as follows:

$$\text{Min } Z = \sum_{t=1}^T \left(\frac{1}{1+\alpha} \right)^t \sum_{w \in W} C_w(Q_w^t, h_w^t) \quad (7.46)$$

where:

T is the number of time steps in the planning horizon

α is the interest rate

W is the set of the well sites

$C_w(Q_w^t, h_w^t)$ is the water extraction cost from the well site w , which is a nonlinear function of the discharge Q_w^t and the head h_w^t at each time step t .

The water head at each time step can be determined using the groundwater response equations, and it can be considered as a system's constraint. The response equations for each planning period in a linear, distributed parameter groundwater system can be expressed as follows (Willis and Yeh, 1987):

$$h^t - A_1 h^{t-1} A_2 \mathbf{g}(Q^{t-1}) = 0 \quad \forall t \quad (7.47)$$

where:

h^t and h^{t-a} are vectors of the groundwater head at time steps t and $t - 1$

A_1 and A_2 are the coefficient matrices vector

Q^{t-a} is defined as follows:

$$Q^{t-1} = (Q_1^{t-1}, Q_2^{t-1}, \dots, Q_w^{t-1})^T \quad \forall t, w \in W \quad (7.48)$$

The following constraints can be considered in a groundwater operation optimization model:

- Supplying demands:

$$\sum_{w \in W} Q_w^t \geq D^t \quad \forall t \quad (7.49)$$

where D^t is the total water demand at time step t .

- The discharge capacity for each well:

$$0 \leq Q_w^t \leq Q_w^{max} \quad \forall t, w \in W \quad (7.50)$$

where Q_w^{max} is the discharge capacity of well w .

- The lower bound constraints on the head levels (h_w) are considered to ensure that the excessive depletion of the aquifer does not occur:

$$h_w^t \geq h_w^{min} \quad \forall t, w \in W \quad (7.51)$$

where h_w^{min} is the minimum groundwater head at well site w .

- The nonnegativity of the decision variables is considered as:

$$h^t, Q_w^t \geq 0 \quad \forall t, w \in W \quad (7.52)$$

The above planning model is the basic framework for the groundwater systems planning and management.

Example 7.7

The groundwater pumping schedules include determining the discharges from well sites and the lengths of the planning periods. The pumping schedule for three planning periods is shown in [Figure 7.32](#). Develop a management model to minimize the drawdown for determining the optimal pumping pattern in the basin for the pumping schedule.

SOLUTION

The objective function of the management model is expressed as:

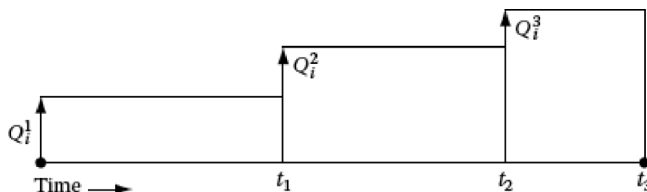


FIGURE 7.32 The pumping schedule during planning horizon.

$$\min z = \sum_k \sum_{w \in \pi} s_w^k \quad (7.53)$$

where s_w^k is the drawdown at well w at the end of period k .

The hydraulic response equations could be developed from the Theis equation. The drawdown $s(r, t)$ occurring during the first planning period can be calculated as:

$$s(r, t) = \sum_{w \in \pi} \frac{Q_w^1}{4\pi T} W\left(\frac{r_w^{-2} S}{4Tt}\right), \quad 0 \leq t \leq t_1 \quad (7.54)$$

where:

Q_w^k is the discharge from the well site i in period k

t, t_1 is the length of the planning period

π is number of wells

r_w is the distance from the w th well to any point r in the aquifer

S and T are the storage and transmissivity parameters, respectively.

In the second time period, the drawdown is given as:

$$s(r, t) = \sum_{w \in \pi} \frac{Q_w^1}{4\pi T} W\left(\frac{r_w^{-2} S}{4Tt}\right) + \sum_{w \in \pi} \left(\frac{Q_w^2 - Q_w^1}{4\pi T} \right) W\left(\frac{r_w^{-2} S}{4T(t-t_1)}\right), \quad t_1 \leq t \leq t_2 \quad (7.55)$$

Similarly, for the third period,

$$s(r, t) = \sum_{w \in \pi} \frac{Q_w^1}{4\pi T} W\left(\frac{r_w^{-2} S}{4Tt}\right) + \sum_{w \in \pi} \left(\frac{Q_w^2 - Q_w^1}{4\pi T} \right) W\left(\frac{r_w^{-2} S}{4T(t-t_1)}\right) + \sum_{w \in \pi} \left(\frac{Q_w^3 - Q_w^2}{4\pi T} \right) W\left(\frac{r_w^{-2} S}{4T(t-t_2)}\right), \quad t \geq t_3 \quad (7.56)$$

The water withdrawal target for each period can be considered as a model constraint:

$$\sum_{w \in \pi} Q_w^k \geq D^k \quad \forall k \quad (7.57)$$

where D^k is the demand in period k .

The drawdown should be less than the maximum allowable drawdown at certain control locations in the aquifer:

$$s_a^k \leq s^*, \quad a \in \Delta \quad (7.58)$$

where $a \in \Delta$ are the control locations.

7.4.2 OPTIMIZATION MODEL FOR CAPACITY EXPANSION

A full-scale network system is initially installed to use the groundwater resources. However, the system capacity may exceed the water demand in the early stages because the water demand generally increases with time. Therefore, a capacity expansion planning capable of determining an optimal schedule is needed to expand the system capacity according to the increasing water demand. The target of the capacity expansion is to increase the reliability of the water supply by structural methods. The capacity expansion model provides information about how to expand the water supply system so that it meets the increasing demand over time. This involves deciding the expansion size (sizing), expansion time (timing), and expansion capacity types. The construction of a new dam, increasing the height of an existing reservoir, well field development, and construction of tunnels or channels for interbasin water transfers are some common examples of expansion capacity types; however, they are somewhat limited by site-related, geophysical, geographic, economic, and institutional factors.

The capacity expansion or timing and staging of the well field development are usual problems in the groundwater systems planning. In these problems, it is assumed that in the conventional design, the well sites have been developed and the operation policies are developed for the existing conditions. Therefore, the capital cost can be neglected in developing the operation policies and should be considered in the capacity expansion models. The objective function of the capacity expansion model, which is the minimization of the total discounted capital and operational costs, is as follows:

$$\text{Min } Z = \sum_{t=1}^T \left(\frac{1}{1+\alpha} \right)^t \sum_{w \in W} \left(KC(Q_w^{\max}) X_w^t + C_w(Q_w^t, h_w^t) Y_w^t \right) \quad (7.59)$$

where:

T is the number of time steps in the planning horizon

α is the interest rate

W is the set of the well sites

$KC(Q_w^{\max})$ is the capital cost of the well site w , which is considered as a function of the well capacity, (Q_w^{\max})

$C_w(Q_w^t, h_w^t)$ are the water extraction costs from the well site w , which is a nonlinear function of the discharge Q_w^t and the head h_w^t at each time step t

X_w^t and Y_w^t are the 0–1 integer variables

X_w^t indicates whether or not the well site w is developed in the period t

X_w^t is equal to 1, if the well site w is developed in the time period t and equal to zero otherwise.

Similarly, Y_w^t is equal to 1 if the well site w is in operation and equal to zero otherwise.

This objective function should be minimized considering the groundwater response equations and the system's constraints.

- The response equation for each planning period is:

$$\mathbf{h}^t - A_1 \mathbf{h}^{t-1} - A_2 \mathbf{g}(\mathbf{Q}^{t-1}) = 0 \quad \forall t \quad (7.60)$$

- Supplying demands:

$$\sum_{w \in W} Y_w^t Q_w^t \geq D^t \quad \forall t \quad (7.61)$$

where D^t is the total water demand in the time step t .

- The constraint of the well capacity for each well site w is:

$$0 \leq Q_w^t \leq Q_w^{max} \quad \forall t, w \in W \quad (7.62)$$

where Q_w^{max} is the discharge capacity of the well w .

- The lower bound constraints on the head levels (h_w) are considered to ensure that the excessive depletion of the aquifer does not occur:

$$h_w^t \geq h_w^{min} \quad \forall t, w \in W \quad (7.63)$$

where h_w^{min} is the minimum groundwater head at the well site w .

- The 0–1 integer variables are defined as follows:

$$X_w^t, Y_w^t = [0,1] \quad (7.64)$$

- The maximum number of the developed wells over the planning horizon is one, therefore,

$$\sum_{t=1}^T X_w^t \leq 1 \quad w \in W \quad (7.65)$$

- The limitation on the total capital and operational cost at each planning period can be considered as follows:

$$\sum_{w \in W} \left(KC(Q_w^{max}) X_w^t + C_w(Q_w^t, h_w^t) Y_w^t \right) \leq C_{total,t} \quad \forall t \quad (7.66)$$

where $C_{total,t}$ is the total capital and operational cost in the planning period t .

- The nonnegativity of the decision variables:

$$h^t, Q_w^t \geq 0 \quad \forall t, w \in W \quad (7.67)$$

Because of the uncertainties in the future operational and capital cost functions, and projected water demands, the developed optimal policies should be revised when more information becomes available.

Example 7.8

The water demand of a city is supplied from the groundwater resources, and it increases over time due to the population growth as shown in [Figure 7.33](#). Four well field development projects are studied for supplying the future demands of this city in a 30-year planning time horizon. The current capacity of the water supply system is 100 MCM. Assume that the construction cost stays constant. The capacity and capital costs of these projects are shown in [Table 7.10](#). The interest rate is considered to be 5%. Find the optimal sequence of implementing the projects.

SOLUTION

[Table 7.11](#) shows the present value of the initial investment of the projects, which are estimated using $P = F/(1 + i)^t$ in the different years that the water demand has increased. In order to find the best timing for the construction of the well field development projects, the minimization of the present value of the cost is considered as the objective function of a linear programming model as follows:

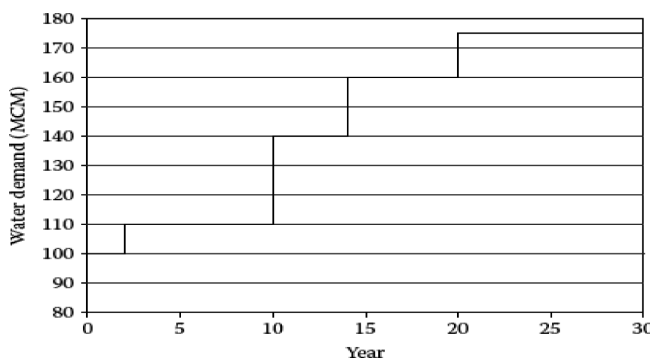


FIGURE 7.33 Water demand of a city over a 30-year period.

TABLE 7.10
Initial Investment and Capacity of Well Field Development

| Well Field Development Project | Capital Costs (\$10 ⁶) | Capacity (MCM) |
|--------------------------------|------------------------------------|----------------|
| A | 2 | 15 |
| B | 2.5 | 20 |
| C | 1.8 | 10 |
| D | 4 | 30 |

TABLE 7.11
Present Value of Capital Costs for Well Field Development
Projects (\$10⁶)

| Project | $t = 2$ Years | $t = 10$ Years | $t = 14$ Years | $t = 20$ Years |
|---------|---------------|----------------|----------------|----------------|
| A | 1.81 | 1.23 | 1.01 | 0.75 |
| B | 2.27 | 1.53 | 1.26 | 0.94 |
| C | 1.63 | 1.11 | 0.91 | 0.68 |
| D | 3.63 | 2.46 | 2.02 | 1.51 |

$$\begin{aligned}
 \text{Minimize } C = & 1.81X_{11} + 1.23X_{12} + 1.01X_{13} + 0.75X_{14} \\
 & + 2.27X_{21} + 1.53X_{22} + 1.26X_{23} + 0.94X_{24} \\
 & + 1.63X_{31} + 1.11X_{32} + 0.91X_{33} + 0.68X_{34} \\
 & + 3.63X_{41} + 2.46X_{42} + 2.02X_{43} + 1.51X_{44}
 \end{aligned}$$

Subject to

$$15X_{11} + 20X_{21} + 10X_{31} + 30X_{41} \geq 10$$

$$15X_{11} + 20X_{21} + 10X_{31} + 30X_{41} + 15X_{12} + 20X_{22} + 10X_{32} + 30X_{42} \geq 40$$

$$15X_{11} + 20X_{21} + 10X_{31} + 30X_{41} + 15X_{12} + 20X_{22} + 10X_{32} + 30X_{42}$$

$$+ 15X_{13} + 20X_{23} + 10X_{33} + 30X_{43} \geq 60$$

$$15X_{11} + 20X_{21} + 10X_{31} + 30X_{41} + 15X_{12} + 20X_{22} + 10X_{32} + 30X_{42}$$

$$+ 15X_{13} + 20X_{23} + 10X_{33} + 30X_{43} + 15X_{14} + 20X_{24} + 10X_{34} + 30X_{44} \geq 75$$

$$X_{11} + X_{12} + X_{13} + X_{14} \leq 1$$

$$X_{21} + X_{22} + X_{23} + X_{24} \leq 1$$

$$X_{31} + X_{32} + X_{33} + X_{34} \leq 1$$

$$X_{41} + X_{42} + X_{43} + X_{44} \leq 1$$

$$X_{ij} = \begin{cases} 1 & \text{if project } i \text{ constructed in the } j\text{th time period} \\ 0 & \text{otherwise} \end{cases}$$

In this problem, the constraints are defined to satisfy the additional demand in the different years. They also assure that each project can only be constructed once. The developed program in Lingo 8 is shown in [Figure 7.34](#). The optimal timing

FIGURE 7.34 Solution for Example 7.8 (Lingo 8 source code).

of the implementation of the projects is found to be as projects *C* at year 2, *D* at year 10, *B* at year 14, and *A* at year 20. The present value of the costs of the construction of the projects is also estimated to be $\$6.1 \times 10^6$.

7.4.3 OPTIMIZATION MODEL FOR WATER ALLOCATION

The policy instruments for the groundwater allocation such as the tradable extraction rights and the groundwater extraction charges determine both the economic efficiency of the groundwater use and the distribution of the groundwater among users. The groundwater allocation problem provides the optimal water distributed to the different users such as the agricultural, industrial, and municipal demands in a river basin, with a minimal effect on the environment and water users. The objective function of this model maximizes the net discounted benefit of the water supply as follows:

$$Max Z = \sum_{t=1}^T \left(\frac{1}{1+\alpha} \right)^t \sum_i \left\{ \int_0^{\mathcal{Q}_i^t} D_i(\mathcal{Q}_i^t) d\mathcal{Q} - \sum_{w \in W} C_w(\mathcal{Q}_w^t, h_w^t) \right\} \quad (7.68)$$

where:

T is the number of the time steps in the planning horizon

α is the interest rate

W is the set of the well sites

$D_i Q_i^t$ is the groundwater demand function of the subregion i , which depends on Q_i^t

Q_i^t is the water pumped from the subregion I

$C_w(Q_w^t, h_w^t)$ is the extraction cost from the well site w , which is a nonlinear function of the discharge Q_w^t and the head h_w^t at each time step t .

This objective function should be maximized considering the groundwater response equations and the system's constraints:

- The response equation for each planning period is:

$$h^t - A_1 h^{t-1} - A_2 g(Q^{t-1}) = 0 \quad \forall t \quad (7.69)$$

- The constraint of the water balance in each subregion is:

$$Q_i^t = \sum_{w \in W} Q_w^t \quad (7.70)$$

- The constraint of the well capacity for each well site w is:

$$0 \leq Q_w^t \leq Q_w^{\max} \quad \forall t, w \in W \quad (7.71)$$

where Q_w^{\max} is the discharge capacity of the well w .

- The nonnegativity of the decision variables:

$$h^t, Q_w^t, Q_i^t \geq 0, \forall t, w \in W \quad \forall i \quad (7.72)$$

The water allocation model can provide a schedule for the optimal groundwater extraction.

Example 7.9

Develop a stochastic planning model to determine the optimal, temporal allocation of the groundwater supply of a confined aquifer. Assume (1) the dynamics of the groundwater system can be represented by the model:

$$S_{t-1} = S_t - P_t + R_t \quad (7.73)$$

where:

S_t is the quantity of the water in the groundwater storage at the end of the time period t , where t is numbered backward with respect to real time

P_t and R_t are the groundwater pumping and recharge occurring during the period t and (2) the groundwater recharge is a random variable described by the probability density function, $h(R_t)dR_t$, which is independently distributed over time.

SOLUTION

The stochastic planning problem can be formulated as a dynamic programming problem. More details about the dynamic programming are presented in the special methods for optimization techniques in this chapter. The stages of the model correspond to the time; the state variable is the groundwater storage. Defining $B_t(S_t, P_t)$ as the net benefit resulting from the pumping P_t , then $f_t(S)$, the optimal return with the t stages remaining, is given by the recursive equation (Burt, 1964):

$$f_t(S) = \max_{R_t \leq S} \left\{ B_t(S_t, P_t) + \left(\frac{1}{1+\rho} \right) E[f_{t-1}(S_t + R_t - P_t)] \right\} \quad (7.74)$$

$$f_t(S) = \max_{P_t \leq S} \left\{ B_t(S_t, P_t) + \left(\frac{1}{1+\rho} \right) \int_0^{\infty} f_{t-1}(S_t + R_t - P_t) h(R_t) dR_t \right\} \quad (7.75)$$

where:

- E is the mathematical expectation operator
- ρ is the discount rate.

The functional equation can be interpreted as the maximization with respect to the water consumption at the stage t of the immediate net benefit plus the expected return in the $t - 1$ remaining stages, given that an optimal policy will be used during the remaining $t - 1$ stages.

The solution of the dynamic programming model is usually accomplished by discretizing the groundwater storage, recharge, and pumping. The dynamic programming model then becomes a finite Markovian decision process. Defining N discrete levels for the groundwater storage ($j = 1, \dots, N$), m values for R_t , and n values for P_t ($k = 1, \dots, n$), the functional equation can be expressed for a particular groundwater storage level, S_i , as:

$$f_t(S_i) = \max_k \left\{ B_t(S_{ti}, P_{tk}) + \left(\frac{1}{1+\rho} \right) \sum_{j=1}^N f_{t-1}(S_{ti} + R_{tj} - P_{tk}) \cdot P(R_t = R_t^j) \right\}, \quad p_{tk} \leq S_i \quad (7.76)$$

For each groundwater storage level, S_{ti} , we can also define a probability, P_{ij}^k , for each P_{tk} as the probability of going to S_{ti} , given that the groundwater storage was S_{ti} at the beginning of the period and the P_{tk} is the withdrawal. The recursive equation can then be expressed in terms of these conditional probabilities as:

$$f_t(S_i) = \max_k \left\{ B_t^k(S_i) + \left(\frac{1}{1+\rho} \right) \sum_{j=1}^n P_{ij}^k f_{t-1}(S_i) \right\}, \quad t = 0, 1, 2, B_t^k(S_i) = B_t(S_{ti}, P_{tk}) \quad (7.77)$$

An interesting property of the dynamic programming model occurs when the system benefit function is constant over the planning horizon. The solution of the programming model will then converge to an optimal policy that is independent

of the stage when the number of stages becomes very large. The optimal policies are found from the solution of the equation:

$$(I - \beta P)x = b \quad (7.78)$$

where:

I is the identity matrix, $\beta = (1 + \rho)^{-1}$

P is an $n \times n$ matrix containing p_{ij}^k , $b = [B_i^k(S_i), \dots, B_i^k(S_i)]^T$
 $x = [f_1, f_2, \dots, f_n]^T$ the optimal return vector.

7.4.4 OPTIMIZATION MODEL FOR CONJUNCTIVE WATER USE

The conjunctive water use model provides an optimal allocation schedule from the groundwater and surface water resources in a region to meet the different water demands. The objective function maximizes the net discounted economic benefit as follows:

$$\text{Max } Z = \sum_{t=1}^T \left(\frac{1}{1+\alpha} \right)^t \left\{ \sum_l \left[\int_0^{Q_l^t} D_l(Q_l^t) dQ - \sum_m g_{ml}^t(G_{ml}^t) - \sum_n s_{nl}^t(S_{nl}^t) \right] \right\} \quad (7.79)$$

where:

$l/m/n$ are the indexes that define the different demands, groundwater resources, surface water resources in the region

$D_l(Q_l^t)$ is the demand function, which depends on the water allocated to the demand, Q_l^t

$g_{ml}^t(G_{ml}^t)$ is the cost function of the groundwater allocation from the resource m , which depends on the amount of the groundwater allocated to that demand, G_{ml}^t

$s_{nl}^t(S_{nl}^t)$ is the cost function of the surface water allocation from the resource n , which depends on the amount of the surface water allocated to that demand, S_{nl}^t .

The model is constrained to the response equations and physical limitations.

- The response equations for each groundwater resource is:

$$h_g^t - A_l^m h_g^{t-1} - A_2^m g \left(\sum_m G_{ml}^{t-1} \right) = 0 \quad (7.80)$$

- The surface water balance equation is:

$$\bar{S}_n^t = \bar{S}_n^{t-1} + R_j^t - \sum_l S_{nl}^t \quad (7.81)$$

- The related groundwater allocation and pumping schedule is:

$$\sum_l G_{ml} = \sum_{w \in W} Q_{w,m}^t \quad \forall m \quad (7.82)$$

where:

$Q_{w,m}^t$ is the pumping rate from the well w in the resource m
 W defines the well site of the region.

- The well capacity limitation:

$$Q_{w,m}^t \leq Q_{w,m}^{max} \quad \forall m \quad (7.83)$$

- The lower bound constraints on the head levels (h_w) are considered to ensure the excessive depletion of the aquifer does not occur:

$$h_w^t \geq h_w^{min} \quad \forall t, w \in W \quad (7.84)$$

- The nonnegativity of the decision variables:

$$h_l^t, Q_w^t, Q_l^t, G_{ml}^t, S_{nl}^t \geq 0 \quad \forall t, w \in W, \forall l, m, n \quad (7.85)$$

This optimization problem can be solved using the different methods such as the nonlinear, dynamic programming, and genetic algorithm. For more details and examples of this management model, refer to [Chapter 8](#).

7.4.5 OPTIMAL GROUNDWATER QUALITY MANAGEMENT MODEL

The management of the groundwater with the water quality issue in the aquifer systems is a multi-objective planning problem, which is solved with trade-offs between different objectives. The wastewater can be injected to control the seawater intrusion, decrease the land subsidence, and increase the groundwater level. In the groundwater quality management model, the objective function is to minimize the possible contamination of the aquifer or the cost of the surface waste treatment and/or waste storage. The decision variables of the optimization model are the well location and the pumping/injection rates to satisfy the water demand and the maximum waste input concentration to satisfy the groundwater quality requirements. The objective function of the optimization model defined as the weighted sum of the water quantity and quality objectives such as the minimization of the possible contamination of the aquifer or the cost of surface waste treatment can be expressed as follows.

If we consider a dynamic model and assume: (1) a single waste constituent and (2) that the planning horizon consists of the T^* discrete time periods, or:

$$Max z = \sum_{k=1}^{T^*} \sum_1 \lambda_1 f_1(h^k, c_s^k, Q_w^k, Q_r^k) \quad (7.86)$$

f_1 is the f th objective of the planning problem, and we have assumed that a particular objective is a function of the state variables (the head and mass concentrations in planning period k) and the pumping (Q_w^k) and injection (Q_r^k) policies. The λ_1 represents the preferences or weights associated with the planning objective.

The constraints of the model are meeting the water demand and the waste load disposal target, expressed as follows:

$$\sum_{W \in \pi} Q_w^k \geq D^k \quad \forall k \quad (7.87)$$

$$\sum_{r \in \Psi} Q_r^k \geq WL^k \quad \forall k \quad (7.88)$$

where:

Q_w^k is the pumping rate

Q_r^k is the injection rate

D_k is the water demand

WL_k is the magnitude of the waste load in the planning period k .

The index sets π and ψ define the feasible pumping and the injection sites in the basin.

Others constraints are on the maximum pumping and the injection rates as well, as follows:

$$Q_w^k \leq Q_w^*, \quad w \in \pi \quad \forall k \quad (7.89)$$

$$Q_r^k \leq Q_r^*, \quad r \in \Psi \quad \forall k \quad (7.90)$$

Also there are constraints on the concentrations of the water withdrawal for demand supplying and injection as follows:

$$c_{s,w}^k \leq \bar{c}_{s,w}^*, \quad w \in \pi \quad \forall k \quad (7.91)$$

$$c_{s,r}^k \leq \bar{c}_{s,w}^*, \quad r \in \Psi \quad \forall k \quad (7.92)$$

The simulation model can be utilized for the estimation of the concentration and the water head as the state variables. It can be linked with the optimization model for developing the control policies. The decision variables are the waste injection concentrations and the pumping and injection rates.

7.4.6 OPTIMIZATION MODEL FOR PARAMETERS OF GROUNDWATER MODEL

The system parameters in the groundwater flow and the transport simulation are estimated for precise modeling. These parameters are the transmissivity, storage coefficient, conductivity, dispersivity, retardation factor, and reaction rate. The techniques

based on trial and error and graphical matching are the traditional methods. The parameters values of the groundwater modeling are estimated from the observations of the system response through the inverse problem. In this method, the parameters are determined to match the observations through a systematic adjustment in the spatial and time domains. In the inverse problem, an optimization model is developed to determine the system's hydraulic and mass transport parameters.

Yeh (1986) classified the solution algorithms of the parameter identification in the groundwater systems as being part of either the *output error criterion method* or the *equation error criterion method*. In the equation error criterion method, the unknown parameters are determined based on the analytical solutions of the governing equations of the aquifer system, such as the finite-element or finite-difference approximation. In this method, an optimization model is developed to minimize the sum of squares of errors for the equation to obtain the unknown parameters. The error is estimated using the observed or interpolated data at each node of the domain. In the output error criterion method, an optimization model is developed to minimize a given output error criterion in the identification of the flow model parameters. The parameter estimates are required to satisfy the aquifer system's hydraulic or water duality equations and the possible upper or lower bounds (Willis and Yeh, 1987).

7.5 OPTIMIZATION TECHNIQUES

Decision-making is the science of choice. In a particular problem, we might have a single person who is in charge of deciding what to do, or there are several people or organizations which are involved in the decision-making process who are termed as the *decision makers*. The options from which the selection is made are called the *alternatives*, and the set of all possible alternatives is called the *decision space*. If the decision space is finite, then the decision-making problem is called *discrete*, and if the decision alternatives are characterized by the continuous variables, then the problem is called *continuous*.

All decision-making problems are faced with the limitations which result from financial constraints, technological, social, and environmental restrictions, among others. These limitations are called the *constraints* of the problem. The alternatives satisfying all the constraints are called *feasible*, and the set of all feasible alternatives is called the *feasible decision space*.

The goodness of any alternative can be characterized by several ways, which are called the *attributes*. Most of them can be described verbally such as "how clean the water is," or "how does it satisfy the customers." In mathematical modeling, we need the measurable quantities describing the goodness of each alternative with respect to the attributes. Such measures are called the *criteria*. For example, the water quality can be measured by the pollutants' concentration, consumer satisfaction by supplies, and so on.

If there is only one criterion, the problem is called the *single-criterion* optimization problem. In the presence of more than one criterion, we have a *multiple-criteria* decision problem. In the case of multiple decision-makers, we might consider the problem as multiple-criteria decision-making when the criteria of all decision-makers are considered as the criteria of the problem (Karamouz et al., 2003).

A set of constraints considering the technical, economic, legal, or political limitations of the project should be considered in evaluating the optimal solution. There may also be some constraints in the form of either the equalities or inequalities on the decision and state variables.

The optimization problem can be solved through a manual trial-and-error adjustment or using a formal optimization technique. Although the trial-and-error method is simple, it is tedious and also does not guarantee reaching the optimal solution. On the contrary, an optimization technique can be used to identify the optimal solution which is feasible in terms of satisfying all the constraints.

The commonly used optimization techniques are:

1. Linear programming (LP) (e.g., Lefkoff and Gorelick, 1987)
2. Nonlinear programming (NLP) (e.g., Ahlfeld et al., 1988; Wagner and Gorelick, 1987)
3. Mixed integer linear programming (e.g., Willis, 1976, 1979)
4. Mixed integer nonlinear programming (e.g., McKinney and Lin, 1995)
5. Differential dynamic programming (DDP) (e.g., Chang et al., 1992; Culver and Shoemaker, 1992; Sun and Zheng, 1999)

These methods are considered as the “gradient” methods because the gradients of the objective function regarding the variables to be optimized are repetitively calculated in the process of finding the optimal solution. Beside the computational efficiency of these techniques, there are some significant limitations. First, when the objective function is highly complex and nonlinear, with multiple optimal points, a gradient method may be trapped in one of the local optimal solutions and cannot reach the globally optimal solution. Second, sometimes the numerical difficulties in the gradient methods result in instability and convergence problems.

More recently, the evolutionary optimization methods such as the simulated annealing (SA), genetic algorithms (GA), and tabu search which are based on heuristic search techniques have been introduced. These methods imitate natural systems, such as biological evolution in the case of the genetic algorithms, to identify the optimal solution, instead of using the gradients of the objective function. The evolutionary methods generally require intensive computational efforts; however, they are increasingly being used because of their ability to identify the global optimum, their efficiency in handling the discrete decision variables, and their easy application in the different simulation models.

7.5.1 SINGLE-CRITERION OPTIMIZATION

Let X denote the feasible decision space, and let be any feasible alternative. If X is a finite set, then the value of X can be any one of the numbers $1, 2, \dots, N$, when N is the number of the elements of X . If X is a continuous set characterized by the continuous decision variables, then x is a vector, $x = (x_1, \dots, x_n)$, where n is the number of the decision variables and x_1, x_2, \dots, x_n are the decision variables. If f denotes the single criterion, then we assume that f is defined on X and for all $x \in X$, $f(x)$ is a real number. This condition is usually defined as $f: X \rightarrow \mathbb{R}$. Since f is real valued, all the possible values of $f(x)$ can be represented on the real line, and the set:

$$H = \{f(x) \mid x \in X\} \quad (7.93)$$

is called the *criterion space*. Notice that the elements of X show the decision choices and the elements of H give the consequences of the choices in terms of the values of the evaluation criterion. We can simply say that X shows what we can do and H shows what we can get.

If X is finite and the number of its elements is small, then by comparing the $f(x)$ values, the best alternative can be easily identified. If the number of elements of X is large or even infinite, but X is a discrete set (e.g., when it is defined by the decision variables with integer values), then the methods of the discrete and combinatorial optimization are used. This methodology can be found in any textbook of advanced optimization techniques.

The most simple single-criterion optimization problem with continuous variables is the *linear programming*. In order to give a general formulation, let n be the number of the decision variables and x_1, x_2, \dots, x_n the decision variables. It is assumed that the criterion and all constraints are linear. The criterion is sometimes also called *the objective function*, and it is assumed to have the form:

$$f(x) = c_1x_1 + c_2x_2 + \dots + c_nx_n = \underline{c}^T \underline{x} \quad (7.94)$$

where c_1, c_2, \dots, c_n are real numbers, $c = (c_1, c_2, \dots, c_n)$, and

$$\underline{x} = \begin{bmatrix} x_1 \\ x_2 \\ \vdots \\ x_n \end{bmatrix} \quad (7.95)$$

The linear constraints are equalities or inequalities. The equality constraints have the general form:

$$a_{i1}x_1 + a_{i2}x_2 + \dots + a_{in}x_n = b_i \quad (7.96)$$

and the inequality constraints can be written as:

$$\begin{aligned} & a_{i1}x_1 + a_{i2}x_2 + \dots + a_{in}x_n \quad \text{or} \quad b_i \\ & \geq \\ & \leq \end{aligned} \quad (7.97)$$

By repeating the above procedure to all the variables and constraints, if necessary, the resulting problem will have only the nonnegative variables and the \leq type inequalities in the constraints. Hence, any linear programming problem can be rewritten in this way into its *primal form*:

$$\text{Maximize } c_1x_1 + c_2x_2 + \dots + c_nx_n$$

Subject to:

$$\begin{aligned}
 & x_1, x_2, \dots, x_n \geq 0 \\
 & a_{11}x_1 + a_{12}x_2 + \dots + a_{1n}x_n \leq b_1 \\
 & a_{21}x_1 + a_{22}x_2 + \dots + a_{2n}x_n \leq b_2 \\
 & \vdots \\
 & a_{m1}x_1 + a_{m2}x_2 + \dots + a_{mn}x_n \leq b_m
 \end{aligned} \tag{7.98}$$

Note that the objective function may represent the cost, contained pollutant amount, and so on, when the smaller objective values represent better choices. In such cases, the objective function is minimized. In the above formulation, we assume the maximization, since the minimization problems can be rewritten into the maximization problems by multiplying the objective function by (-1) .

In the very simple case of two decision variables, Equation 7.98 can be solved by the graphical approach. As an illustration, consider the following example. The most common procedure to solve this kind of problems is the *simplex method*. For more details, please see Karamouz et al. (2003).

7.5.2 MULTI-CRITERIA OPTIMIZATION

As in the previous session, let X denote the feasible decision space, and let f_1, \dots, f_I be the criteria. Set X shows which decisions can be made; however, in the presence of the multiple criteria, we need to represent the set of all possible outcomes. The set:

$$H = \left\{ (f_1(x), \dots, f_I(x)) \mid x \in X \right\} \tag{7.99}$$

is called the *criteria space* that shows what we can get by selecting the different alternatives.

Example 7.10

Assume that the selection has to be made from four available technologies to perform a certain groundwater cleaning restoration task. These technologies are evaluated by their costs and convenience of usage. The cost data are given in \$1000 units, and the convenience of usage is measured in a subjective scale between 0 and 100, where 100 is the best possible measure. The data are given in [Table 7.12](#). Which technique is the acceptable solution?

SOLUTION

The cost data are multiplied by (-1) in order to maximize both the criteria. Similarly to the single-criterion case, the criteria are sometimes called the *objective function*. The criteria space has four isolated points in this case as shown in

TABLE 7.12
Costs and Convenience Numbers of Four Projects

| Technology | Cost | Convenience |
|------------|------|-------------|
| 1 | -25 | 85 |
| 2 | -18 | 65 |
| 3 | -27 | 93 |
| 4 | -15 | 50 |

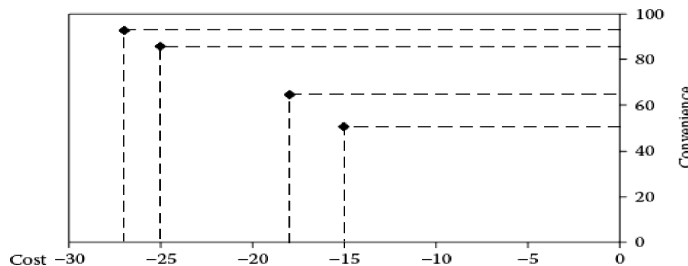


FIGURE 7.35 Criteria space in the discrete case.

Figure 7.35. It is clear that none of the points dominates any other point, since the lower cost is always accompanied by the lower convenience, that is, increasing any objective should result in decreasing the other one. Therefore, any one of the four technologies could be accepted as the solution.

7.5.2.1 Sequential Optimization

This method is based on the ordinal preference order of the objectives. Assume that the objectives are numbered so that f_1 is the most important, f_2 is the second most important, and so on, and f_i is the least important. In applying the method, first, f_1 is optimized. If the optimal solution is unique, then the procedure terminates regardless of the values of the less important other objectives. Otherwise, f_1 is kept on its optimal level and f_2 is optimized if there is a unique optimal solution, then it is selected as the solution of the problem, otherwise both f_1 and f_2 are kept optimal and f_3 is optimized, and so on, until there is a unique optimal solution or f_1 is already optimized.

7.5.2.2 The ϵ -Constraint Method

In the case of the sequential optimization, the procedure often terminates before all the objectives are optimized. Therefore, the less important objectives may have very unfavorable values. In order to avoid such possibilities, the following method can be suggested. Assume that the most important objective is specified, and the minimal

acceptable levels are given for all the other objectives. If f_1 is the most important objective, and $\varepsilon_2, \varepsilon_3, \dots, \varepsilon_I$ are the minimum acceptable levels, then the solution is obtained by solving the following single-objective optimization problem:

$$\text{Maximize } f_1(x)$$

$$\text{Subject } x \in X$$

$$f_2(x) \geq \varepsilon_2$$

$$\vdots$$

$$f_I(x) \geq \varepsilon_I \quad (7.100)$$

Example 7.11

Assume that in Example 7.10, the cost is more important than the convenience, but we want to have at least 82 in the convenience. Which technique is the acceptable solution?

SOLUTION

This condition makes technology variants 2 and 4 infeasible. Both alternatives 1 and 3 satisfy these minimal requirements. The less expensive among these two remaining alternatives is variant 1, so it is the choice.

7.5.2.3 The Weighting Method

In the application of this method, all the objectives are taken into account by the importance weights supplied by the decision-makers. Assume that c_1, c_2, \dots, c_I are the relative importance factors of the objectives, which are specified by the decision-makers on some subjective basis, or are obtained by some rigorous methods such as pair-wise comparisons. It is always assumed that $c_i > 0$ for all i , and $\sum_{i=1}^I c_i = 1$. In applying the weighting method, the composite objective is a weighted average of all the objectives, where the weights are the relative importance factors c_1, \dots, c_I . Hence, the single-objective optimization problem:

$$\text{Maximize } c_1 f_1(x) + c_2 f_2(x) + \dots + c_I f_I(x)$$

$$\text{Subject to } x \in X \quad (7.101)$$

is solved. A transformation called the *normalizing* procedure is needed that is a simple linear transformation. The procedure is outlined as follows:

Let f_i denote an objective function. Let m_i and M_i denote its possible smallest and largest values, respectively. These values may be computed by simply minimizing and maximizing f_i over the feasible decision space X or their values also can be supplied by the decision-makers based on the subjective judgments. Then the normalized objective function is obtained as:

$$\bar{f}_i(x) = \frac{f_i(x) - m_i}{M_i - m_i} \quad (7.102)$$

In many practical cases, the decision-makers are able to provide a utility function to each objective that shows his/her satisfaction level for the different values of that objective. Such a function is illustrated in [Figure 7.36](#), where m_i gives the least 0 satisfaction level and M_i gives the largest 1 (=100%) satisfaction level. Then the objective f_i is replaced by the corresponding utility value:

$$\bar{f}_i(x) = u_i(f_i(x)) \quad (7.103)$$

Notice that Equation 7.102 corresponds to the linear utility function:

$$u_i(f_i) = \frac{(f_i - m_i)}{(M_i - m_i)} \quad (7.104)$$

We always require that the lowest possible utility value is 0 and the largest is 1, so $\bar{f}_i(x) \in [0,1]$ for all $x \in X$. Then Equation 7.101 is modified as:

$$\text{Maximize } c_1 \bar{f}_1(x) + c_2 \bar{f}_2(x) + \dots + c_I \bar{f}_I(x)$$

Subject to

$$x \in X \quad (7.105)$$

In this new composite objective, only the dimensionless values are added, and the linear combination of the normalized objectives can be interpreted as an average satisfaction level based on all the objectives.

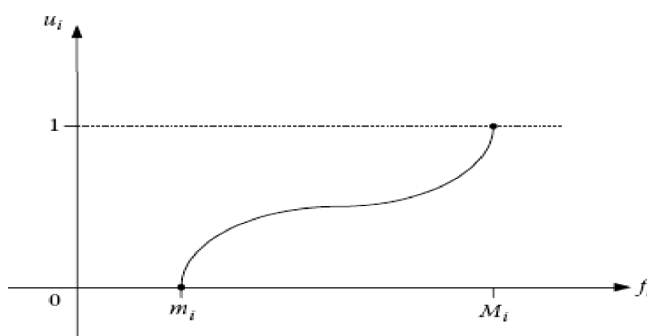


FIGURE 7.36 Utility function of the objective f_i .

Example 7.12

Assume that in Example 7.10, the decision-makers consider \$30,000 as the worst possible cost, and they believe that a cost of \$15,000 would give them 100% satisfaction.

SOLUTION

So, $m_1 = -30$ and $M_1 = -15$, and if the linear utility function is assumed between these values, then the linearization is based on the linear transformation as: $f_1 = (f_1 + 30)/(-15 + 30)$, so the cost values in [Table 7.12](#) have to be modified accordingly. The convenience data are already given in the satisfaction levels (in %), so these numbers are divided by 100 in order to transform them into the unit interval [0,1]. The normalized values are shown in [Table 7.13](#).

Assume that equal importance is given to the objectives, that is, $c_1 = 0.3$ and $c_2 = 0.7$. The composite objective values for the four technology variants are as follows:

$$0.3(0.33) + 0.7(0.85) = 0.694$$

$$0.3(0.8) + 0.7(0.65) = 0.695$$

$$0.3(0.2) + 0.7(0.93) = 0.71$$

$$0.3(1) + 0.7(0.5) = 0.65$$

Therefore, the third alternative is the choice.

7.5.2.4 Interactive Fuzzy Approach

The fuzzy application became possible when Bellman and Zadeh (1970) and, a few years later, Zimmermann (1978) introduced the fuzzy sets into the field of the multiple criteria analysis. In recent years, an interactive approach in the fuzzy environment was used as one of the most effective approaches for solving the multi-objective optimization problems. For the fuzzy multi-objective optimization, the concept of the membership-Pareto optimal solutions, which is defined in terms of the membership

TABLE 7.13
Normalized Objectives of Four Projects

| Technology | Cost | Convenience |
|------------|------|-------------|
| 1 | 0.33 | 0.85 |
| 2 | 0.8 | 0.65 |
| 3 | 0.2 | 0.93 |
| 4 | 1 | 0.50 |

functions instead of the objective functions, was introduced. The decision-maker must specify the reference membership levels to express the preferences for the objective functions and to generate a candidate for the satisfying solution (also called the membership-Pareto optimal solution). For the decision-maker's reference membership levels, $\bar{\mu}_i^r$, the corresponding optimal solution which is the nearest to the requirements in the mini-max sense or better than that if the reference membership levels are attainable is obtained by solving the following problem:

$$\underset{x \in X}{\text{Min Max}} \left[\bar{\mu}_i^r - \mu_i(Z_i(x)) \right] \quad (7.106)$$

or equivalently

$$\begin{aligned} & \text{Min} \lambda \\ & \text{s.t.} \bar{\mu}_i^r - \mu_i(Z_i(x)) \leq \lambda, i = 1, \dots, p \\ & \quad x \in X \end{aligned} \quad (7.107)$$

where $\mu_i(Z_i(x))$ is the membership function for each of the objective functions $Z_i(x)$, $i = 1, \dots, p$. This method for obtaining the trade-off information between the p objectives can be summarized as follows:

1. Solve the p individual optimization problems to find the optimal solution for each of the individual p objectives.
2. Compute the value of each of the objectives and determine the individual minimum Z_i^{\min} and individual maximum Z_i^{\max} of each objective function under the given constraints.
3. Derive a membership function for each of the objectives and the associated extreme values. The membership function $\mu_i(Z_i(x))$ for the fuzzy-max objective function $Z_i(x)$ can be defined as:

$$\mu_i(Z_i(x)) = \begin{cases} 0 & Z_i(x) \leq Z_i^{\min} \\ \frac{(Z_i(x) - Z_i^{\min})}{(Z_i^{\max} - Z_i^{\min})} & Z_i^{\min} < Z_i(x) \leq Z_i^{\max} \\ 1 & Z_i(x) > Z_i^{\max} \end{cases} \quad (7.108)$$

4. Set the initial reference membership levels to 1 for incorporating the initial opinion of the decision-maker.
5. Solve the min-max problem, then the optimal solution and the membership functions are determined based on the results.
6. The reference membership levels and the membership functions of the objectives can be revised considering the results of the trade-off between the objectives and repeat from step 5.

7.5.3 SPECIAL METHODS FOR GROUNDWATER OPTIMIZATION

Some special methodologies, which are useful in the application in the groundwater optimization, are presented in this section.

7.5.3.1 Dynamic Programming

In the water resources planning, the dynamism of the system is a major concern, which has to be taken into account in the modeling and optimization. The DP is the most popular tool in optimizing dynamic systems. The DP is used extensively in the optimization of the groundwater resource systems (Buras, 1966). The popularity and success of this technique can be attributed in part to its efficiency in incorporating the nonlinear constraints and the objectives and the stochastic or random variables in the DP formulation of the management or planning problem. In this method, highly complex problems with a large number of the decision variables are decomposed into a series of subproblems that can be solved recursively (Willis and Yeh, 1987). In the DP formulation of the planning or operational model, the optimization model is described or characterized by the state variables of the system, the system stages, and the control or decision variables. In the groundwater systems, the state variables may represent the hydraulic head or the mass concentrations, or the amount of the groundwater in storage at any time. The decision variables control, in any time period, the pumping, recharge, or waste injection schedules. The time clement of the planning problem defines the stages of the DP model.

An important element of any DP model is the state transition equations of the system. The response or transfer equations, which can be developed using finite-difference or finite-element methods, define how the system state variables change over the successive stages or time periods. Consider the linear groundwater system which is homogeneous and isotropic. The stage-to-stage transformation is then described by the continuity equation, which for a lumped parameter, the linear system can be expressed as:

$$S_{t+1} - S_t + R_t = I_t - E_t \quad (7.109)$$

where:

S_t is the storage at the beginning of the time period or stage t

R_t is the groundwater extraction during the stage t

I_t is the groundwater recharge

E_t is the subsurface outflow, leakage, or evaporation that occurs during the stage t .

Assuming that the system objective, $f(R_t, S_t)$ is a function of the state variable, the groundwater storage, and the pumping occurring in any stage or time period,

$$\text{Min } Z = \sum_{t=1}^T f(R_t, S_t) \quad (7.110)$$

where T is the time horizon. Additional constraints of the model include the maximum and minimum storage bounds to limit the groundwater extractions or to prevent possible flooding of the land surface, or:

$$S_t^{\max} \geq S_t \geq S_t^{\min}, t = 1, \dots, T \quad (7.111)$$

$$R_t^{\max} \geq R_t \geq R_t^{\min}, t = 1, \dots, T \quad (7.112)$$

$$|S_{t+1} - S_t| \leq SC_s, t = 1, \dots, T \quad (7.113)$$

where SC_s is the maximum allowable change in the storage of the reservoir s within each month considering the dam stability and the safety conditions. Because of the many decision variables and constraints, finding the direct solution is computationally difficult. Through the DP procedure, this unique optimization problem is changed to solve many smaller-sized problems in the form of a recursive function. The DP recursive equation can be expressed as:

$$V_t(S_t) = \min \left\{ f_t(R_t, S_t) + V_{t+1}(f_{t+1}(R_{t+1}, S_{t+1})) \right\} \quad (7.114)$$

In most applications, the optimization Equation 7.114 cannot be solved analytically, and the recursive functions are determined only numerically. In such cases, the discrete DP (DDP) is used, where the state and decision spaces are discretized. The main problem of using this method is known as the “curse of dimensionality.” This is because the number of points that should be considered in the evaluation of the different possible situations drastically increases by the number of discretizations. Therefore, the DDP is used only up to four or five decision and state variables.

The different successive approximation algorithms such as the differential dynamic programming, discrete differential dynamic programming, and state incremental dynamic programming were developed to overcome this problem. In applying any of these methods, the user should provide an initial estimation of the optimal policy. This estimation is improved in each step until the convergence occurs. However, the limit might be only a local optimum. The survey paper by Yakowitz (1982) gives a summary of the different versions of the DP with applications to the water resources planning and management.

Example 7.13

Assume an aquifer supplies part of the water demand for a city. The monthly water demand (D_t) is about 25 million cubic meters. The maximum storage bond of the aquifer is 30 million cubic meters. Let S_t (aquifer storage at the beginning of month t) take the discrete values, 0, 10, 20, and 30. The cost of operation is estimated as the total sum of the squared deviations from the storage (ST_t) and release target (D_t) as follows:

$$C_t(S_t, R_t) = (S_t - ST_t)^2 - (R_t - D_t)^2 \quad (7.115)$$

Formulate a forward-moving deterministic DP model for finding the optimal release in the next 3 months.

Formulate a backward-moving deterministic DP model for finding the optimal release in the next 3 months.

Solve the DP model developed in part (a), assuming that the inflows to the aquifer in the next 3 months ($t = 1, 2, 3$) are forecasted to be 10, 30, and 20, respectively. The aquifer storage at the current month is 20 million cubic meters.

SOLUTION

a. The forward deterministic DP model is formulated as follows:

$$f_t(S_{t+1}) = \min(C_t(S_t, R_t) + f_{t-1}(S_t)) \quad t = 1, 2, 3, \quad S_t \in \Omega_t$$

$$S_t \leq S_{max}, \quad S_{max} = 30 \text{ MCM}$$

$$C_t(S_t, R_t) = (S_t - ST_t)^2 - (R_t - D_t)^2 \quad (7.116)$$

$$S_{t+1} = S_t + I_t - R_t$$

where:

Ω_t is the set of the discrete storage volumes (states) that will be considered for the beginning of the month t at the site s

S_{t+1} is the storage at the beginning of the month $t + 1$.

b. The backward deterministic DP model is formulated as follows:

$$f_t(S_t) = \min(C_t(S_t, R_t) + f_{t+1}(S_{t+1})) \quad t = 1, 2, 3 \quad (7.117)$$

The constraints are as mentioned above.

c. The loss is calculated using the forward formulation for 3 months.

The results are shown in [Table 7.14](#).

Therefore, the optimal water withdrawals from the aquifer are $R_1^* = 20$, $R_2^* = 20$, and $R_3^* = 20, 30$.

7.5.3.2 Genetic Algorithm

The genetic algorithms are the stochastic search methods that imitate the process of natural selection and the mechanism of population genetics. They were first introduced by Holland (1975) and later further developed and popularized by Goldberg (1989). The genetic algorithms are used in a number of different application areas ranging from the function optimization to solving the large combinatorial optimization problems. The GA begins with the creation of a set of solutions referred to as a population of individuals. Each individual in a population consists of a set of parameter values that completely describes a solution. A solution is encoded in a string called a chromosome, which consists of genes that can take a number of values. A general form of three genes (which are the string elements, for example, bits) in one chromosome with 4-bit representation is shown in [Figure 7.37](#). Initially, the collection of the solutions (population) is generated randomly, and at each iteration (also called generation), a new generation of the solutions is formed by applying the genetic operators including selection, crossover, and mutation, analogous to the ones

TABLE 7.14
DP Model Solution for Example 7.13

| t | I_t | S_t | R_t | 10 | 20 | 30 | 40 | $f_t(S_t, R_t)$ | R_t^* |
|---------|-------|-------|-----------|-----------|-----------|-----------|-----|-----------------|---------|
| $t = 3$ | 20 | 0 | 625 | 425 | 425 | 625 | 425 | 425 | 20 |
| | | 10 | 325 | 125 | 125 | 325 | 125 | 125 | 20,30 |
| | | 20 | 225 | 25 | 25 | 225 | 25 | 25 | 20,30 |
| | | 30 | 325 | 125 | 125 | 325 | 125 | 125 | 20,30 |
| $t = 2$ | 30 | 0 | 625 + 25 | 425 + 125 | 425 + 425 | — | — | 550 | 20 |
| | | 10 | 325 + 125 | 125 + 25 | 125 + 125 | 325 + 425 | 150 | 150 | 20 |
| | | 20 | — | 25 + 125 | 25 + 25 | 225 + 125 | 50 | 50 | 30 |
| | | 30 | — | — | 125 + 125 | 325 + 25 | 25 | 25 | 30 |
| $t = 1$ | 10 | 20 | 225 + 50 | 25 + 150 | 25 + 550 | — | — | 175 | 20 |

R_t^* is the optimal policy at each month.

$\frac{\mathbf{1} \mathbf{0} \mathbf{1} \mathbf{1} \mathbf{0} \mathbf{0}}{\mathbf{H1}}$ $\frac{\mathbf{1} \mathbf{0} \mathbf{0} \mathbf{1} \mathbf{1} \mathbf{1}}{\mathbf{H2}}$ $\frac{\mathbf{0} \mathbf{0} \mathbf{1} \mathbf{0} \mathbf{0} \mathbf{0}}{\mathbf{H3} \dots \dots}$...

FIGURE 7.37 A general framework of a chromosome including genes.

from natural evolution. Each solution is evaluated using an objective function (called a fitness function), and this process is repeated until some form of the convergence in fitness is achieved. The objective of the optimization process is to minimize or maximize the fitness.

In creating the chromosomes, we have to map the decision space into a set of the encoded strings. The encoding mechanism depends on the problem being solved. One possible way is to use the binary representation of the decision variables. We have to decide also on the size of the breeding pool, that is, on the number of the chromosomes being involved in the process. A larger number of chromosomes increases diversity, but the algorithm becomes slower. First, an initial population is selected randomly.

The *fitness* of each string is often evaluated based on the objective functions, the constraints, and the encoding mechanism. A usual way is to add a penalty term to the objective function if any chromosome becomes infeasible by violating one or more constraints (Figure 7.38).

A: 0 1 0 1 0 1 0 1 0 1 1 | 1 1 0 0 0 C: 0 1 0 1 0 1 0 1 0 1 1 | 0 1 1 0 1
 B: 1 0 1 0 1 0 1 0 1 0 0 | 0 1 1 0 1 D: 1 0 1 0 1 0 1 0 1 0 0 | 1 1 0 0 0

FIGURE 7.38 An example of using crossover in the generation of chromosomes C and D from chromosomes A and B.

The pairs of chromosomes are formed randomly, and they are then subjected to certain genetic manipulations. They modify the genes in the parent chromosomes. A typical procedure is called *crossover*, which swaps a part of the genetic information contained in the two chromosomes. Usually a substring portion is selected randomly in the chromosomes, and the genes within that substring are exchanged. By this way, new offspring are created to replace the parent chromosomes. An example of using crossover in the generation-two chromosomes is shown in [Figure 7.39](#). The particular structure of the crossover mechanism is usually problem-specific and has to result in meaningful and feasible solutions.

There is no guarantee that the new pairs of chromosomes will be better than the parent chromosomes. To overcome this difficulty, *mutations* are allowed to occur, which reverse one or more of the genes in a chromosome. This simple step may reintroduce certain genes into the solution that may be essential for the optimal solution, having been lost from the breeding population in previous stages. An example of using mutations in the generation-two chromosomes is shown in [Figure 7.40](#). Using mutations more frequently makes the search more broadly random, resulting in the slower convergence of the algorithm.

By repeating the above steps, we sequentially replace either the entire previous population or only the less fit members of it. The cycle of the creation, evaluation, selection, and manipulation is iterated until an optimal or an acceptable solution is reached.

The GA again raises a couple of important features. First, it is a stochastic algorithm; randomness has an essential role in the genetic algorithms. Both the selection and reproduction need random procedures. A second very important point is that the genetic algorithms always consider a population of solutions. Keeping in memory more than a single solution at each iteration offers a lot of advantages. The algorithm can recombine different solutions to get better answers, and so it can use the benefits of the assortment. The robustness of the algorithm should also be mentioned as something essential for the algorithm success. The robustness refers to the ability to perform consistently well on a broad range of problem types.

Example 7.14

In an area, the cost function of the aquifer restoration is the function of the treatment and pumping operation. Find the maximum point of function $f(x) = -x^2 + x + 1$ in the $[0,1]$ interval using the genetic algorithm where $f(x)$ is the cost function, and x is the injection concentrations (oxygen and nutrient).

A: 010101010101111000 C: 000100110111011001
 B: 101010101010001101 D: 111011001000101100

FIGURE 7.39 An example of using a mutation in the generation of chromosomes C and D from chromosomes A and B.

SOLUTION

First, the decision space is discretized, and each is encoded. For illustration purposes, we have 4-bit representations (musk). The population in musk and the corresponding value is provided in [Table 7.15](#). Next, the initial population is selected. We have chosen six chromosomes; they are in [Table 7.16](#), where their actual values and the objective function values are also presented.

The best objective function values are obtained at 0101 and 0100. Assume the mutation probability, P_m , is 0.01 and the crossover probability is considered as 1. Also assume that four random numbers are generated to compare with the mutation probability for each bit as [0.213, 0.008, 0.853, 0.462] of the chromosome 0001. A simple crossover procedure is performed by interchanging the two middle bits to obtain 0000 and 0100. The new population is presented in [Table 7.17](#). The next populations are generated and presented in [Tables 7.18](#) and [7.19](#).

The results show how the best objective function evolves from population to population. Starting from the initial table, the value of 1.224 increased to 1.249, then remained the same. Since this value is the global optimum, it will not increase in further steps. In the practical application, we stop the procedure if no, or very small, improvement occurs after a certain (user-specified) number of iterations.

TABLE 7.15
Population of Chromosomes

| Musk | X | Musk | X |
|------|------|------|------|
| 1001 | 0.6 | 0000 | 0 |
| 1010 | 0.67 | 0001 | 0.07 |
| 0101 | 0.34 | 0010 | 0.13 |
| 0111 | 0.47 | 0100 | 0.27 |
| 1110 | 0.93 | 1000 | 0.53 |
| 1101 | 0.87 | 0011 | 0.2 |
| 1011 | 0.73 | 0110 | 0.4 |
| 1111 | 1 | 1100 | 0.8 |

TABLE 7.16
Initial Population in GA Solution

| Chromosomes | Value | Objective Function |
|-------------|-------|--------------------|
| 0000 | 0 | 1 |
| 0101 | 0.34 | 1.224 |
| 0100 | 0.27 | 1.197 |
| 1101 | 0.87 | 1.113 |
| 1111 | 1 | 1 |
| 0010 | 0.13 | 1.113 |

TABLE 7.17
Second Population in GA Solution

| Chromosomes | Value | Objective Function |
|-------------|-------|--------------------|
| 0000 | 0 | 1 |
| 0101 | 0.34 | 1.224 |
| 0100 | 0.27 | 1.197 |
| 1101 | 0.87 | 1.113 |
| 1111 | 1 | 1 |
| 0010 | 0.13 | 1.113 |

TABLE 7.18
Third Population in GA Solution

| Chromosomes | Value | Objective Function |
|-------------|-------|--------------------|
| 1010 | 0.67 | 1.221 |
| 0111 | 0.47 | 1.249 |
| 0110 | 0.4 | 1.240 |
| 1111 | 1 | 1 |
| 0101 | 0.34 | 1.224 |
| 1000 | 0.53 | 1.249 |

TABLE 7.19
Fourth Population in GA Solution

| Chromosomes | Value | Objective Function |
|-------------|-------|--------------------|
| 1001 | 0.6 | 1.24 |
| 0111 | 0.47 | 1.249 |
| 0000 | 0 | 1 |
| 0011 | 0.2 | 1.16 |
| 1100 | 0.8 | 1.16 |
| 1000 | 0.53 | 1.249 |

7.5.3.3 Simulation Annealing

The SA developed based on the analogy between the physical annealing process of solids and the optimization problems. In the SA, one can simulate the behavior of a system of particles in thermal equilibrium using a stochastic relaxation technique developed by Metropolis et al. (1953). This stochastic relaxation technique helps the SA procedure escape from the local minimum. The SA starts at a feasible solution, q_0 (a real-valued vector representing all the decision variables), and the objective function, $J_0 = J(q_0)$. A new solution q_1 is randomly selected from the neighbors of the

initial solution, and the objective function, $J_1 = J(q_1)$, is evaluated. If the new solution has a smaller objective function value, $J_1 < J_0$ (in minimization problems), the new solution is definitely better than the old one, and therefore it is accepted and the search moves to q_1 and continues from there. On the other hand, if the new solution is not better than the current one, $J_1 < J_0$, the new solution may be accepted, depending on the acceptance probability defined as:

$$P_r(\text{accept}) = \exp\left\{\frac{-(J_1 - J_0)}{T}\right\} \quad (7.118)$$

where T is a positive number that will be discussed later.

For a given value of T , the acceptance probability is high when the difference between the objective function values is small. To decide whether or not to move to the new solution q_1 or stay with the old solution q_0 , the SA generates a random number U between 0 and 1. If $U < P_r(\text{accept})$, the SA moves to q_1 and resumes the search. Otherwise, the SA stays with q_0 and selects another neighboring solution. At this step, one iteration has been completed.

The control parameter T plays an important role in reaching the optimal solution through the SA because the acceptance probability is strongly influenced by the choice of T . When the T is high, the acceptance probability calculated is close to 1, and the new solution will very likely be accepted, even if its objective function value is considerably worse than that of the old solution. On the other hand, if T is low, approaching zero, then the acceptance probability is also low, approaching zero. This effectively precludes the selection of the new solution even if its objective function value is only slightly worse than that of the old solution. Therefore, there is no new solution for which $J_1 > J_0$, is likely to be selected. Rather, only “downhill” points ($J_1 < J_0$) are accepted; therefore, a low value of T leads to a descending search.

The successful performance of the SA method requires that T be assigned a high initial value, and that it be reduced gradually throughout the sequence of the calculation by the reduction factor λ . The number of iterations under each constant T should be sufficiently large. But the higher the initial T and the larger the number of iterations mean a longer simulation time and may severely limit computational efficiency. The SA stops either when it has completed all the iterations or when the termination criterion (a specific value of the objective function) is reached.

As a rule of thumb to balance the computational efficiency and quality of the SA method, the initial T should be chosen in such a way that the acceptance ratio is somewhere between 70% and 80%. It is recommended that a number of simulation runs should be executed first to estimate the acceptance ratio. Second, the number of iterations under a constant T is about ten times the size of the decision variables. In literature, the amount of 0.9 is suggested as a reasonable number for λ , the reduction factor (Egels, 1990).

The SA has many advantages including easy implementation, not requiring much computer memory and coding, and providing a guarantee for the identification of an optimal solution if an appropriate schedule is selected. The last point becomes much more important in the cases when the solution space is large and the objective

function has several local minima or changes dramatically with the small changes in the parameter values. Examples of the SA application in the hydrologic literature include Dougherty and Marryott (1991) and Wang and Zheng (1998).

7.6 CONFLICT RESOLUTION

The operation of the groundwater systems is mostly a multi-objective problem, and there are some economic, hydraulic, water quality, or environmental objectives that are usually in conflict, for example:

- There are several demand points, and the water which is supplied to one of these demand points, cannot be used by others. Therefore, the major conflict issue in the groundwater operation happens when the groundwater storage is not capable of supplying all of the demands.
- Extra discharge of the aquifer or a high variation of the groundwater table can cause some problems such as the settlement of buildings and the ground surface.
- Recharge of the aquifer with polluted water such as the infiltration of agricultural return flows, disposal of sewage or water treatment plant sludge, and sanitary landfills can produce some environmental problems.

This topic is discussed by Karamouz et al. (2003). There are many interbasin issues that could be treated in the same fashion.

The optimal operation policies of the groundwater systems can be developed using the conflict resolution models considering the groundwater systems hydraulic, water quality response equation, possible well capacity, hydraulic gradient, and water demand requirements. The common conflict issue in the groundwater systems planning and operation happens when the aquifer should supply the water to the different demand points for the different purposes and there are some constraints on the groundwater table variations and the groundwater quality. Consider an aquifer system which supplies the following demands:

- Domestic water demand
- Agricultural water demand
- Industrial water demand

The utility function for each of these agencies should be considered when formulating the conflict resolution problems.

There are several alternative ways to solve the conflict situations. One might consider the problem as a multi-objective optimization problem with the objectives of the different decision-makers. The conflict situations can also be modeled as social choice problems in which the rankings of the decision-makers are taken into account in the final decision. A third way of resolving conflicts was offered by Nash, who considered a certain set of conditions that the solution has to satisfy, and proved that exactly one solution satisfies his “fairness” requirements. In this section, the Nash bargaining solution will be outlined:

Assume that these are the I decision-makers. Let X be the decision space and $f_i: X \rightarrow R$ the objective function of the decision-maker i . The criteria space is defined as:

$$H = \left\{ \underline{u} \mid \underline{u} \in R^I, \underline{u} = (u_i), u_i = f_i(x) \text{ with some } x \in X \right\} \quad (7.119)$$

It is also assumed that in the case when decision-makers are unable to reach an agreement, all the decision-makers will get low objective function values. Let d_i denote this value for the decision-maker i , and let $\underline{d} = (d_1, d_2, \dots, d_I)$. Therefore, the conflict is completely defined by the pair (H, \underline{d}) , here H shows the set of all possible outcomes and \underline{d} shows the outcomes if no agreement is reached. Therefore, any solution of the conflict depends on both H and \underline{d} . Let the solution be therefore denoted as a function of H and \underline{d} : $\phi(H, \underline{d})$. It is assumed that the solution function satisfies the following conditions:

1. The solution has to be feasible: $\phi(H, \underline{d}) \in H$.
2. The solution has to at least provide the disagreement outcome to all decision-makers, $\phi(H, \underline{d}) \geq \underline{d}$.
3. The solution has to be nondominated. That is, there is no $f \in H$ such that $f \neq \phi(H, \underline{d})$ and $f \geq \phi(H, \underline{d})$.
4. The solution must not depend on unfavorable alternatives. That is, if $H_1 \subset H$ is a subset of H such that $\phi(H, \underline{d}) \in H_1$ then $\phi(H, \underline{d}) = \phi(H_1, \underline{d})$.
5. Increasing the linear transformation should not alter the solution. Let T be a linear transformation on H such that $T(f) = (\alpha_1 f_1 + \beta_1, \dots, \alpha_I f_I + \beta_I)$ with $\alpha_i > 0$ for all i , then $\phi(T(H), T(\underline{d})) = T(\phi(H, \underline{d}))$.
6. If two decision-makers have equal positions in the definition of the conflict, then they must get equal objective values at the solution. Decision-makers i and j have an equal position if $d_i = d_j$ and any vector $f = (f_1, \dots, f_I) \in H$ if and only if $(\bar{f}_1, \dots, \bar{f}_I) \in H$ with $\bar{f}_i = f_i, \bar{f}_i = f_j, \bar{f}_l = f_l$ for $l \neq i, j$. Then we require that $\phi_i(H, \underline{d}) = \phi_j(H, \underline{d})$.

Therefore, all of the conflict issues and the responsible agencies should be recognized in the first step in the conflict resolution studies. The utility function typically consists of a range of full satisfaction (utility = 1.0) and point(s) of no satisfaction (utility = 0).

Before showing the method to find the solution satisfying these properties, some conditions must be followed. The feasibility condition requires that the decision-makers cannot get more than the amount available. No decision-maker would agree in an outcome that is worse than the amount he/she would get anyway without the agreement. This property is given in condition 2. The requirement that the solution is nondominated shows that there is no better possibility available for all. The fourth requirement states that if certain possibilities become infeasible, but the solution remains feasible, then the solution must not change. If any of the decision-makers changes the unit of his/her objective, then a linear transformation is performed on H . The fifth property requires that the solution must remain the same. The last requirement shows a certain kind of fairness stating that if two decision-makers have the

same outcome possibilities and the same disagreement outcome, then there is no reason to distinguish among them in the final solution.

If H is convex, closed, and bounded, and there is at least one $f \in H$ such that $f > d$, then there is a unique solution $f^* = \varphi(H, d)$, which can be obtained as the unique solution of the following optimization problem:

$$\text{Maximize } (f_1 - d_1)(f_2 - d_2) \dots (f_I - d_I)$$

Subject to

$$f_i \geq d_i \quad (i = 1, 2, \dots, I)$$

$$\underline{f} = (f_1, \dots, f_I) \in H \quad (7.120)$$

The objective function is called the *Nash product*. Notice that this method can be considered as a special distance-based method, when the geometric distance is maximized from the disagreement point d .

Example 7.15

Consider Example 7.10 again. Assume that the cost and the convenience are the objectives of two different-decision makers. Assume that the disagreement point for the cost and convenience is $d = (-30, 50)$. Choose the best technology using the Nash product.

SOLUTION

Assume that $d = (-30, 40)$, when -30 is considered as a worst possibility of the cost and 50 as the same for the convenience. The values of the Nash product for the four alternatives are as follows:

$$(-25 + 30)(85 - 40) = 225$$

$$(-18 + 30)(65 - 40) = 300$$

$$(-27 + 30)(93 - 40) = 159$$

$$(-15 + 30)(50 - 40) = 150$$

Since the second alternative gives the largest value, the second technology variant is considered as the solution.

Example 7.16

In an unconfined aquifer system, the following agencies are affected by the decisions made to discharge from the aquifer to supply the water demands:

Agency 1: Department of Water Supply

Agency 2: Department of Agriculture

Agency 3: Industries

Agency 4: Department of Environmental Protection

Agency 5: Department of Domestic Water Use

The Department of Water Supply has a twofold role, namely, to allocate the water to different purposes and control the groundwater table variations. The decision-makers in the different agencies are asked to set their utility functions, which are shown in [Figures 7.40](#) through [7.42](#).

The analyst should set the weights shown in [Table 7.20](#) on the role and the authority of the different agencies in the political climate of that region.

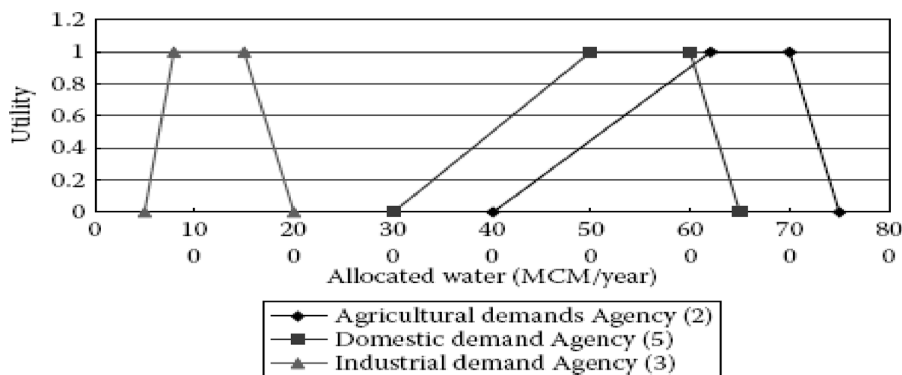


FIGURE 7.40 The utility function of different agencies for the water allocated to different demands.

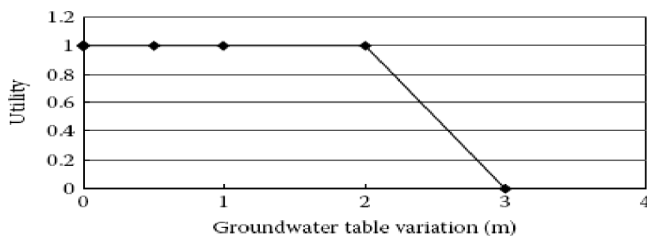


FIGURE 7.41 The utility function of agency 1 for the average groundwater variation.

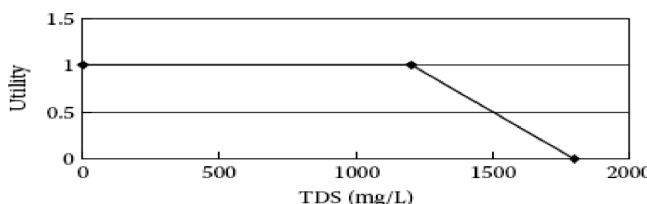


FIGURE 7.42 The utility function of agency 4 for the TDS concentration.

TABLE 7.20
Relative Weights or Relative Authority of Agencies

| Agencies | Relative Weight (Case 1) | Relative Weight (Case 2) |
|--|--------------------------|--------------------------|
| Department of agriculture | 0.133 | 0.17 |
| Department of domestic water | 0.33 | 0.2 |
| Department of water supply | 0.2 | 0.23 |
| Industries | 0.133 | 0.1 |
| Department of environmental protection | 0.2 | 0.3 |

The initial surface, volume, and total dissolved solids (TDSs) concentration of the water content of the aquifer are 600 km², 1140 million cubic meters, and 1250 mg/L, respectively. The net underground inflow is 1100 million cubic meters per year with a TDS concentration equal to 1250 mg/L. Assume that 60% of the allocated water returns to the aquifer as return flow and the average TDSs concentration of the return flow is 2000 mg/L, and the average storage coefficient of the aquifer is 0.06. Find the most appropriate water allocation scheme for this year using the Nash's bargaining theory.

SOLUTION

The nonsymmetric Nash solution of the problem is the unique optimal solution of the following problem:

$$\text{Maximize} \prod_{i=1}^5 (f_i - d_i)^{w_i} \quad (7.121)$$

Subject to:

$$d_i \leq f_i \leq f_i^* \quad \forall i \quad (7.122)$$

where:

w_i is the relative weight

f_i is the utility function

d_i is the disagreement point

f_i^* is the ideal point of the player (agency) i .

This objective function should be maximized considering the constraints of the groundwater surface variation and the groundwater quality that are as follows:

- The average groundwater table variation:

$$\Delta I \approx (q_1 + q_2 + q_3 - I_N) \times \left(\frac{1}{S} \right) \times \left(\frac{1}{A} \right) \quad (7.123)$$

where:

q_1, q_2, q_3 are the annual agricultural, domestic, and industrial groundwater withdrawal (MCM)

IN is the net annual underground inflow (MCM)

S is the storage coefficient

A is the area of the aquifer (km^2).

Therefore,

$$\Delta I \approx \frac{(q_1 + q_2 + q_3 - 1100)}{0.06 \times 600} \quad (7.124)$$

The average groundwater quality:

Considering the TDSs as the indicator water quality variable, the average TDSs concentration of the groundwater at the end of the year can be estimated as follows:

$$C_{new} = \frac{(V_{in.} \times C_{in.} + IN \times C_{IN} + \alpha_1 \times C_1 \times q_1 + \alpha_2 \times C_2 \times q_2 + \alpha_3 \times C_3 \times q_3 - C_{mean})(q_1 + q_2 + q_3)}{(V_{in.} + IN + (\alpha_1 - 1) \times q_1 + (\alpha_2 - 1) \times q_2 + (\alpha_3 - 1) \times q_3)} \quad (7.125)$$

and,

$$C_{mean} = \frac{(C_{in.} + C_{new})}{2} \quad (7.126)$$

where:

$V_{in.}/C_n$ is the initial volume and the TDSs concentration of the water content of the aquifer

C_{IN} is the TDSs concentration of the net groundwater inflow

$\alpha_1/\alpha_2/\alpha_3$ is the return flow percent of the annual agricultural, domestic, and industrial groundwater withdrawal

$C_1/C_2/C_3$ is the average TDSs concentration of the agricultural, domestic, and industrial groundwater withdrawal

C_{mean} is the average TDSs concentration of the groundwater

C_{new} is the TDSs concentration of the aquifer at the end of the year

Therefore,

$$C_{new} = \frac{(1440 \times 1250 + 1100 \times 1250 + 0.6 \times 2000 \times q_1 + 0.6 \times 2000 \times q_2 + 0.6 \times 2000 \times q_3 - C_{mean}(q_1 + q_2 + q_3))}{1440 + 1100 + (0.6 - 1)(q_1 + q_2 + q_3)}$$

and,

$$C_{mean} = \frac{(1250 + C_{new})}{2}$$

This nonlinear optimization can be solved using different NLP solvers. The allocated water considering the different relative weights for the agencies is presented in [Table 7.21](#).

TABLE 7.21
Results of Conflict Resolution Method

| Variable | Result (Case 1) | Result (Case 1) |
|--|-----------------|-----------------|
| Allocated water to agricultural demands (MCM) | 492 | 533 |
| Allocated water to domestic demands (MCM) | 500 | 460 |
| Allocated water to industries (MCM) | 80 | 80 |
| Groundwater table drawdown (m) | 2.64 | 2 |
| The final average TDS concentration of groundwater | 1440 | 1439 |

As it can be seen in [Table 7.21](#) in case 1, the domestic demands that have the highest priority and the industrial demands that have less volume have been completely supplied, but the utilities of the other agencies are less than 1. The comparison between cases 1 and 2 shows the effect of the relative weights on the allocated water. Increasing the relative weights of the Department of Water Supply, the Department of Environmental Protection, and the Department of Agriculture has improved the allocated water to the agricultural demands and the groundwater table variation, but it does not have any significant effect on the TDSs concentration of the groundwater.

7.6.1 STAKEHOLDER INVOLVEMENT

As the water scarcity concerns become more and more prevalent, creating a dynamic dialogue among the stakeholders with conflicting interests to find practical solutions for the sustainable water resources management becomes increasingly desired. The stakeholders in this context could be individuals, agencies, or organizations with stakes regarding the outcome of the decisions related to the water or the assimilative capacity sharing, because they are either directly affected by the decisions or have the power to influence or block the decisions (Wolf, 2002). However, due to the high economic and social stakes in risk, the dialogues over the water resources issues are usually intense, time consuming, emotional, and a consensus could not easily or quickly be achieved.

Professional facilitators could help foster the discussions among the diverse water resources stakeholders and the interests on the conflicting issues, such as the timing and magnitude of the groundwater use reductions in support of the sustainable management of a groundwater basin. A facilitator is an individual who organizes the group activities to support and encourage the participation of *all* the members to attain the group's goals and objectives. The outcomes of such meetings could be quantified to be introduced as the inputs to the groundwater simulation models (e.g., revised aquifer withdrawal rates), optimization models (as constraints), or behavioral simulation models (such as agent-based models discussed in Section 7.3.4). This section will have two main focuses: (1) how to effectively facilitate among the stakeholders involved in a dialogue and (2) how to quantify meeting outcomes.

7.6.1.1 Effective Meeting Facilitation

The most fundamental keys to facilitation include relationship-building, creating, and maintaining trust. Once a facilitator loses trust from the stakeholders, persuading their participation will most likely become impossible. Prior to a meeting, the facilitator should become familiar with all the participants, their goals, interests, and concerns. It is recommended that the facilitator creates a timed meeting agenda, which states the purpose and the desired outcomes for the meeting and includes the type of action needed and the type of output expected from each major topic in the agenda. Providing a time window for each major topic allows the sufficient time for a discussion and will help things stay on time. The agenda must also include an explanation of the meeting objectives and the ground rules. Examples of the ground rules include: allow everyone to participate; listen with an open mind; stay on point and on time; attack the problem, not the participants, etc.

During the meeting, the facilitator should constantly stay engaged, and avoid having biased ideas or using words that would trigger any of the participants. The facilitator should also assure that all participants are engaged and have an equal voice. This would effectively support building a collective intelligence, defined as the general ability of a group to perform a wide variety of tasks (Woolley et al., 2010). In two studies with 699 people, working in groups of two to five, Woolley et al. (2010) found converging evidence of a general collective intelligence factor. The first study contained 40 three-person groups that worked together for up to 5 hours on a diverse set of simple group tasks and a complex criterion task. The second study used 152 groups ranging from two to five members. While they did not find strong correlation between the group's collective intelligence and the average or maximum intelligence of the group members, they concluded that the group's collective intelligence was strongly correlated with the following:

1. Social sensitivity, measured by the "Reading the Mind in the Eyes" test (Baron-Cohen et al., 1997).
2. Equality in the distribution of conversational turn-taking. They found less collective intelligence in the groups where a few members dominated the conversation than those with a more equal distribution of conversational turn-taking.
3. Proportion of females in the group, mainly due to the higher social sensitivity of women in their sample.

This study had considered many other factors such as the group cohesion, motivation, and satisfaction. However, these factors were not significantly correlate with the collective intelligence factor. As the facilitator cannot control the social sensitivity of the group members and most probably the proportion of the different genders in the participants, its main role would be to assure that there is an equal distribution of conversational turn-taking and all the participants have an equal voice.

7.6.1.2 Conflict Handling

If handled appropriately, the conflicts are healthy, positive elements of a problem, forcing people to think out of the box, gauge their positions, understand others, and support the well-being and evolution of the system. However, not everyone is capable

of handling conflicts effectively. The facilitator could play an important role in the conflicting situations. Some recommended facilitation actions during a conflict include (Delaware Department of Human Resources, 2018):

- Listen effectively to clearly notice what each side is stating
- Think before reacting
- Attack the problem not each other
- Encourage people to build on the others' ideas
- Accept responsibility; i.e., do not attempt to place blame, which creates resentment and anger
- Use direct communication: I-Message; e.g., "I need feedback on my suggestion" vs. "YOU didn't give me feedback," or "I need more information" vs. "YOU don't give me enough information."
- Look for common interests as the foundation and build on those
- Focus on the future and what is desired to be different in the future

In a consensus-oriented process, people work together to reach as much agreement as possible. A unanimous consent, however, refers to the outcome of a vote when all the members agree on a solution, strategy, or opinion (Hartnett, 2018). In the water-related conflicts, unanimity could be unlikely and the negotiation processes are usually consensus-oriented. Therefore, in addition to the aforementioned actions, agreeing on the merits of the disagreements is often unavoidable.

7.6.1.3 Quantifying Meeting Outcomes

As mentioned earlier, the meeting outcomes could be quantified to be used in models. For example, the utility functions of different stakeholders could be negotiated during the meetings and developed using the meeting outcomes. [Figure 7.43](#) presents the typical form of the utility functions of the different stakeholders (Karamouz et al., 2011). In [Figure 7.43a](#), which shows the most generic form of a utility function, points *b* and *c* are the lower and upper bounds of the range with the utility of 1, which corresponds to 100% satisfaction of the stakeholder. Point *a* is the minimum and point *d* is the maximum values of an objective with a utility value more than zero. The objective shown on the *x*-axis of [Figure 7.43a](#) could be the groundwater allocation rates. The values corresponding to the parameters *a*, *b*, *c*, and *d* could be negotiated during a meeting to come up with the most practical form of the utility function, which has the consensus of all the stakeholders.

[Figures 7.43b](#) and [c](#) show more specific types of the utility function. For example, [Figure 7.43b](#) shows a typical utility function for the quality of the allocated groundwater or for the groundwater table elevations. Point *d'* is the maximum allowable concentration of the water quality variable of interest or the maximum allowable reduction in the water table elevation. [Figure 7.43c](#) expresses a typical form of the utility function for the stakeholders whose discharges permeate into the ground and reach an aquifer, which would degrade the groundwater quality in the aquifer. Parameter *a''* is the minimum quality of the effluent that the stakeholder is willing to discharge to reduce the treatment costs. Example 7.16 shows how these utility functions could be used in a real-world problem.

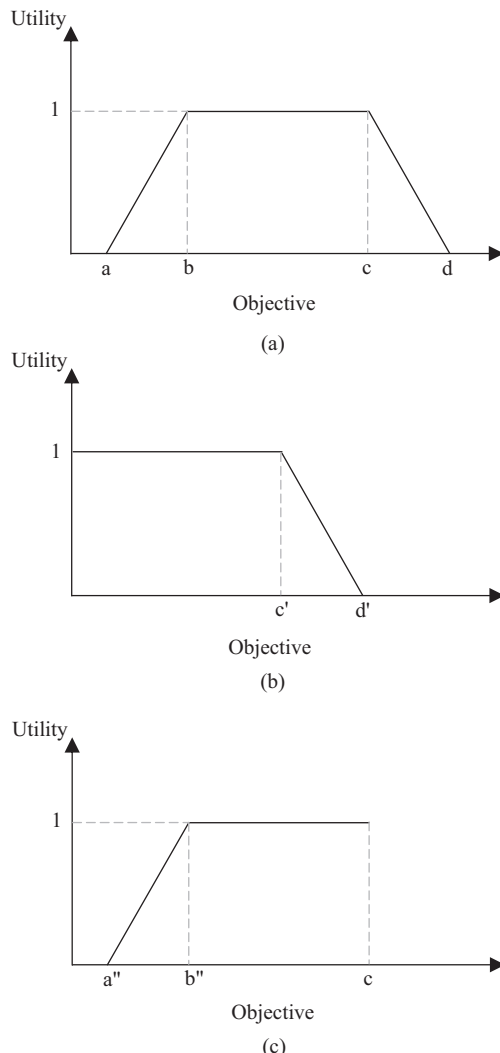


FIGURE 7.43 Typical forms of utility functions for the different stakeholders (a) A generic utility function (b) A utility function for groundwater quality or groundwater table elevations (c) A utility function for discharges permeate into the groundwater.

7.6.2 APPLICATION OF GAME THEORY IN MULTI-OBJECTIVE GROUNDWATER MANAGEMENT

In order to find the solutions for the multi-objective groundwater problems, a cooperative or noncooperative approach might be considered. In a cooperative management approach, it is assumed that all the stakeholders collaborate within a grand coalition. But as a common-pool resource, the groundwater is often overexploited

with the growing management pressures. The difficulty of monitoring and managing the stakeholders' use of water could lead to noncooperative decision-making, which suggests the ineffectiveness of a cooperative approach. The noncooperative approach can be expected to be more practical, as it introduces more realism into the modeling of the stakeholders' decision-making processes.

Given the nature of the groundwater as a common-pool resource, assume that there are two groups of beneficiaries with different objectives and preferences, namely, the government and farmers. The optimization model for such a scenario consists of two objectives. The objective function for the farmers is to maximize their total profit during the modeling period, Z_1 (Equation 7.127), and the objective function for the government sector is to minimize the mean groundwater level drawdown, Z_2 , as shown in Equation 7.128. The monthly allocation of the groundwater to each crop and its corresponding cultivated area (CA) during the planning period are the decision variables in this model (Nazari and Ahmadi, 2019).

$$\text{Maximize } Z_1 = \sum_{d=1}^D (B_d - C_d) \quad (7.127)$$

$$\text{Minimize } Z_2 = \frac{\sum_{d=1}^D \Delta h_d}{D} \quad (7.128)$$

where:

D is the number of zones in the study area

B_d is the profit of the crop cultivation during the planning horizon in the zone d (US dollar)

C_d is the cost of the cultivation in the zone d (US dollar)

Δh_d is the groundwater level drawdown in the zone d during the planning horizon.

The farmers' net benefit is the difference between their revenue and the costs in each zone. The revenue is calculated using Equation 7.129. Their revenue is proportional to the crop yields, cultivated area, and the sale price of products as expressed in Equation 7.130.

$$B_d = \sum_{t=1}^T \sum_{p=1}^P (Y a_{dtp} \times T_{tp} \times A_{dp}) \quad (7.129)$$

$$Y a_{dtp} = Y m_p \times \prod_{m=1}^M \left(1 - K y_{pm} \left(1 - \left(\frac{V g_{dipm}}{\text{Demand}_{dipm}} \right) \right) \right) \quad (7.130)$$

where:

T is the total number of years in the plan horizon

M is the total number of months in one year

$Y a_{dtp}$ is the actual crop production for the crop p in the year t and the zone d (kg/ha)

T_{tp} is the price of the crop p in the year t (US dollar/kg)

A_{dp} is the production area of the crop p in the zone d (ha)

Y_{mp} is the maximum yield of the crop p in the month m (kg/ha)

Ky_{pm} shows the sensitivity coefficient for the crop p in the month m (dimensionless)

Vg_{dtpm} is the groundwater allocation to the crop p in the zone d , the month m , the year t (m^3/ha)

$Demand_{dtpm}$ is the water demand of the crop p in the zone d , the year t , the month m (m^3/ha).

The model also considers the salinity effects of the water on the crop yield. The higher water salinity could reduce the yield of products.

Cultivation costs, C_d , include fixed cultivation costs and the pumping cost, calculated by Equation 7.131:

$$W_{P_d} = \frac{9.8 \times 10^6}{3600 \times \eta} \times \sum_{t=1}^T \sum_{m=1}^M (G_{dpm} \times \Delta h_{dpm} \times Pr_t) \quad (7.131)$$

$$C_d = W_{P_d} + \sum_{t=1}^T \sum_{p=1}^P FC_{tp} \times A_{dp} \quad (7.132)$$

where:

W_{P_d} is the pumping cost for the groundwater extraction (US dollar)

FC_{tp} is the cultivation cost of the crop p in the year t (US dollar/ha)

η is the pumping efficiency (%)

G_{dpm} is the volume of the groundwater extraction from the wells in the zone d , the month m , the year t (m^3)

Δh_{dpm} is the groundwater level drawdown in the zone d , the year t , the month m (m)

Pr_t is the price of the electricity needed for the groundwater pumping (US dollar/kwh).

The constraints of the optimization model include the cultivated area limitations expressed as follows:

$$\sum_{p=1}^P A_{dp} \leq MaxA_d \quad (7.133)$$

where $MaxA_d$ is the total cultivated area in the zone d (ha).

Finally, the cultivated area must be in the allowable cultivated area ranges in each zone as follows:

$$A_{dp, min} \leq A_{dp} \leq A_{dp, max} \quad (7.134)$$

where:

$A_{dp, min}$ represents the minimum cultivated area for the product p in the zone d (ha)

$A_{dp, max}$ is the maximum CA for this product in the same zone.

The Pareto solutions are obtained using the multi-objective optimization techniques.

7.6.2.1 Non-cooperative Stability Definitions

There are several types of stability definitions in the noncooperative games, namely, Nash, general meta-rationality (GMR), symmetric meta-rationality (SMR), and sequential stability (SEQ). The types of stability can be categorized based on three criteria: (i) the foresight that indicates the number of the examined movements in a model, (ii) willingness to disimprovement, which represents a player's willingness to choose a strategy that hurts their own payoff in order to hurt others, and (iii) the decision-maker's awareness about the other individuals' priorities (Fang et al., 1989; Selbirkak, 1994).

The Nash theory is the most widely used theory for determining a stable response in noncooperative games. In fact, this theory models the behavior of risk-averse decision-makers. Assuming the players' complete rationality and the lack of foresight in this theory, the strategy is determined by each decision-maker to maximize their payoff.

In fact, the Nash solution is created when the decision-maker i cannot make any improvement in the outcome by changing the strategy; and if the answer j is the Nash response for all the players, the Nash solution will be the solution of the entire game. The basic problem with the Nash solution concept is the player's lack of knowledge about the opponents' selected strategies; hence, the Nash solution usually fails to identify the exact output of the game. Therefore, other theories have been developed in noncooperative games in order to reinforce the Nash theory and apply the opponents' reactions to the decision-making.

The GMR is another stable definition in a noncooperative game. According to the decision-makers, a state is the GMR stable if any unilateral move, which improves the payoff, is limited by the other opponents. As another stable definition, the SMR provides a more limited definition than the GMR. For each decision-maker, the SMR refers to a definition in which the strategy change from x to z is limited by the opponent, but no y choice exists with a higher payoff than x for the first player. The SEQ is defined like the GMR, but the players only do moves that improve their payoff, and they are not intended to reduce the opponent payoff. In fact, players are conservative and also the risk taker. Further information about types of stability definitions is provided by Madani and Hipel (2011).

7.7 GROUNDWATER SYSTEMS ECONOMICS

Economics includes analytical tools that are used to determine the allocations of scarce resources by balancing the competing objectives. Different, important, and complex decisions should be made in the process of the planning, design, construction, operation, and maintenance of the groundwater resources systems. Economic considerations beside the technological and environmental concerns play an important role in decision-making about the groundwater resources planning and management.

The economic analysis of the groundwater development projects reveals two sides. They create value, and they also encounter costs. The preferences of

individuals for goods and services are considered in the value side of the analysis. The value of goods or services is related to the willingness to pay. The costs of economic activities are classified as fixed and variable costs. The range of operation or activity level does not affect the fixed costs such as the general management and administrative salaries and taxes on facilities, but the variable costs are determined based on the quantity of the output or other measures of the activity level.

The costs are also classified as the private costs and the social costs. The private costs are directly experienced by the decision-makers, but all the costs of an action are considered in the social costs without considering who is affected by them (Field, 1997). The difference between the social and private costs is called external costs or usually environmental costs. Since the firms or agencies do not normally consider these costs in decision-making, they are called “external.” However, it should be noted that these costs may be real costs for some members of society. The open access resources such as the reservoirs in the urban areas are the main source of the external or environmental costs.

Example 7.17

There are two choices, A and B alternative, for the well development in a region; \$25,000 and \$20,000 per week should be paid to provide the needed materials for the project application, respectively. The other costs of two trenchless replacement methods are summarized in [Table 7.22](#). Compare the two methods in terms of their fixed, variable, and total costs when 20 km of mains should be replaced. For the selected method, how many meters of the mains should be replaced before starting to make a profit, if there is a payment of \$30/m of main replacement?

SOLUTION

Choice A

As it is depicted in the [Table 7.23](#), the plant setup is a fixed cost, whereas the payment for the traffic jams and the rent are variable costs.

TABLE 7.22
Costs of Choices A and B for Trenchless Replacement

| Cost | Method A | Method B |
|------------------------------------|-------------|-------------|
| Distance from construction site | 12 week | 8 week |
| Weekly rental of site | \$6,500 | \$1,500 |
| Cost to setup and remove equipment | \$175,000 | \$225,000 |
| Transferring expenses | \$25,000/km | \$20,000/km |

TABLE 7.23
Analysis of Costs of Two Choices for Main Replacement

| Cost | Fixed | Variable | Choice A | Choice B |
|--------------|-------|----------|------------------------|-----------------------|
| Rent | | ✓ | \$78,000 | \$12,000 |
| Plant setup | ✓ | | \$1,750,000 | \$225,000 |
| Transferring | | ✓ | 12(\$25,000) = 300,000 | 8(\$20,000) = 160,000 |
| Sum | | | \$553,000 | \$505,000 |

Choice B

As can be seen in [Table 7.23](#), although choice B has the higher fixed costs, it has less total cost than choice A. The project will make a profit at the point where the total revenue equals the total cost of the kilometers of the mains replaced. For choice B, the variable cost per meter of replacement is calculated as follows:

$$\frac{(\$12,000 + \$160,000)}{20,000} = \$8.6$$

Total cost = Total revenue when the project starts to make a benefit. Considering the meters of the mains that should be replaced before starting to make a profit as X , we will, therefore, have:

$$\$225,000 + \$8.6 X \text{ and } X \text{ is determined as } 10,514 \text{ m}$$

Therefore, if choice B is selected, the project will begin to make a profit after replacing 10,514 m of the mains.

Similarly, external benefits are defined. An external benefit is a benefit that is experienced by somebody outside the decision about consuming the resources or using the services. For example, consider that a private power company constructed a dam for producing hydropower. The benefits experienced by the people downstream such as mitigating both floods and low flows are classified as external benefits.

Many values of an action cannot be measured in the commensurable monetary units as is desired for the economists. For example, the effects on human beings physically (through loss of health or life), emotionally (through loss of national prestige or personal integrity), and psychologically (through environmental changes) cannot be measured by the monetary units. These sorts of values are called intangible or irreducible (James and Lee, 1971).

In most engineering activities, the capital investment is committed for a long period; therefore, the effects of time should be considered in the economic analysis. This is because of the different values of the same amount of money spent or received at the different times. The future value of a present amount of money will be larger than the existing amount due to the opportunities that are available for

TABLE 7.24
Relations Between General Cash Flow Elements Using Discrete Compounding Interest Factors

| To Find: | Given: | Factor by Which to Multiply “Given” | Factor Name | Factor Function Symbol |
|----------|--------|---|--------------------------------|------------------------------------|
| F | P | $(1+i)^N$ | Single-payment compound amount | $\left(\frac{F}{P}, i\%, N\right)$ |
| P | F | $\frac{1}{(1+i)^N}$ | Single-payment present worth | $\left(\frac{P}{F}, i\%, N\right)$ |
| F | A | $\frac{(1+i)^N - 1}{i}$ | Uniform series compound amount | $\left(\frac{F}{A}, i\%, N\right)$ |
| P | A | $\frac{(1+i)^N - 1}{i(1+i)^N}$ | Uniform series present worth | $\left(\frac{P}{A}, i\%, N\right)$ |
| A | F | $\frac{i}{(1+i)^N - 1}$ | Sinking fund | $\left(\frac{A}{F}, i\%, N\right)$ |
| A | P | $\frac{i(1+i)^N}{(1+i)^N - 1}$ | Capital recovery | $\left(\frac{A}{P}, i\%, N\right)$ |
| P | G | $\frac{i(1+i)^N - 1 - Ni}{i^2(1+i)^N}$ | Discount gradient | $\left(\frac{P}{G}, i\%, N\right)$ |
| A | G | $\frac{(1+i)^N - 1 - Ni}{i(1+i)^N - i}$ | Uniform series gradient | $\left(\frac{A}{G}, i\%, N\right)$ |

Source: DeGarmo, E. P. et al., *Engineering Economy*, Prentice-Hall, Upper Saddle River, NJ, 647 p., 1997.

investment in various enterprises to produce a return over a period. The interest rate is the rate at which the value of the money increases from the present to the future. In contrast, the discount rate is the rate by which the value of money is discounted from the future to the present.

A summary of relations between general cash flow elements using the discrete compounding interest factors is presented in [Table 7.24](#) using the following notation:

i : interest rate

N : number of periods (years)

P : present value of the money

F : future value of the money

A : end of the cash flow period in a uniform series that continues for a specific number of periods

G : End-of-period uniform gradient cash flows.

More details about the time-dependent interest rates and the interest formulas for continuous compounding are given in DeGarmo et al. (1997) and Au and Au (1983).

Example 7.18

A well development for pumping water to supply the agricultural demand in a region produces benefits, as expressed in Figure 7.44: \$125,000 benefit in year 1 is increased in 10 years on a uniform gradient to \$1,250,000. Then it reaches \$1,640,000 in year 25 with a uniform gradient of \$26,000/year, and then it remains constant at \$1,640,000 each year until year 40, the end of the project life-span. Assume an interest rate of 5%. What is the present worth of this project?

SOLUTION

First, the present value of the project benefits in years 1 through 10 is calculated as follows:

$$125,000 \left(\frac{P}{G}, 5\%, 10 \right) + 125,000 \left(\frac{P}{A}, 5\%, 10 \right) = \$4,921,723$$

The same procedure is repeated in years 11 through 25:

$$1,276,000 \left(\frac{P}{A}, 5\%, 15 \right) \left(\frac{P}{F}, 5\%, 10 \right) + 26,000 \left(\frac{P}{G}, 5\%, 15 \right) \left(\frac{P}{F}, 5\%, 10 \right) \\ = 1,276,000 \times 10.379 \times 0.613 + 26,000 \times 63.28 \times 0.613 = 6,126,886$$

The present value of the benefits in years 26 through 40:

$$1,640,000 \left(\frac{P}{A}, 5\%, 15 \right) \left(\frac{P}{F}, 5\%, 25 \right) = 1,640,000 \times 10.379 \times 0.295 = 5,021,360$$

The total present worth is equal to \$19,069,969, the summation of the above three values.

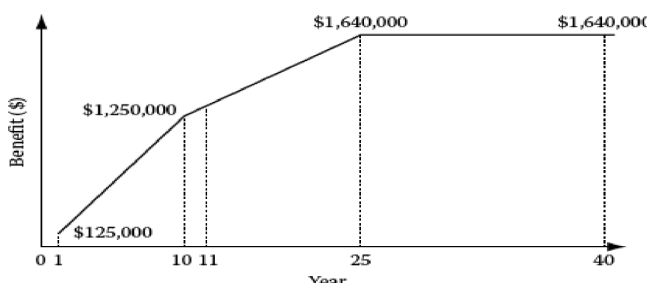


FIGURE 7.44 Cash flow diagram.

7.7.1 ECONOMIC ANALYSIS OF MULTIPLE ALTERNATIVES

Through economic analysis, it is determined whether a capital investment and the cost associated with the project within the project lifetime can be recovered by revenues or not. It should also be determined how attractive the savings are regarding the involved risks and the potential alternative uses. The five most common methods including the present worth, the future worth, the annual worth, the internal rate of return, and the external rate of return methods are briefly explained in this section. The life-span of the different projects should be incorporated in the economic analysis through a repeatability assumption.

In the present worth method, the alternative with the maximum present worth (PW) of the discounted sum of benefits minus costs over the project life-span, Equation 7.135, is selected.

$$PW = \sum_{t=1}^N (B_t - C_t) \left(\frac{P}{F}, i\%, t \right) \quad (7.135)$$

where:

C_t is the cost of the alternative at the year t

B_t is the benefit of the alternative at the year t

N is the study period

i is the interest rate.

In the case of cost alternatives, the one with the least negative equivalent worth is selected. Cost alternatives are all negative cash flows except for a possible positive cash flow element from the disposal of assets at the end of the projects useful life (DeGarmo et al., 1997).

In the future worth method, all the benefits and costs of the alternatives are converted into their future worth, and then the alternative with the greatest future worth or the least negative future worth is selected. Two choices are available for selecting the study period including the repeatability assumption and the co-terminated assumption. Based on the last assumption, for the alternatives with a life-span shorter than the study period, the estimated annual cost of the activities is used during the remaining years. The same for the alternatives with a life-span longer than the study period, a re-estimated market value is normally used as a terminal cash flow at the end of the project's co-terminated life as stated by DeGarmo et al. (1997).

In the annual worth method, the costs and benefits of all the alternatives are considered in the annual uniform, and similar to the other methods, the alternative with the greatest annual worth or the least negative worth is selected. As in this method, the worth of the alternatives is evaluated annually, the projects with different economic lives are compared without any change in the study period.

The internal rate of return (IRR) method is commonly used in the economic analysis of the different alternatives. The IRR is defined as the discount rate that when considered, the net present value or the net future value of the cash flow profile will be equal to zero. The PW and annual worth methods are usually used for finding

the IRR. In this method, the minimum attractive rate of return is defined and the projects with an IRR less than the considered threshold are rejected.

The main assumption of this method is that the recovered funds, which are not consumed in each time, are reinvested in the IRR. In such cases that it is not possible to reinvest the money in the IRR, rather than the minimum attractive rate of return, the external rate of return method should be used. The interest rate, external to a project at which net cash flows produced by the project over its life-span can be reinvested, is considered in this method.

Example 7.19

Two different types of pumps (A, B) can be used in a pumping station for removing the water from an aquifer. The costs and benefits of each of the pumps are displayed in [Table 7.25](#). Compare the two pumps economically using the minimum attractive rate of return = 10% and considering the time of the study equal to 12 years.

SOLUTION

The study period is considered 12 years. By using the repeatability assumption, it can be written that:

$$\begin{aligned} \text{PW of costs of A} &= \$200 + (\$200 - \$50)(P/F, 10\%, 6) - \$50 (P/F, 10\%, 12) = \$269 \\ \text{PW of benefits of A} &= \$95 (P/A, 10\%, 12) = \$647 \\ \text{PW of costs of B} &= \$700 - \$150 (P/F, 10\%, 12) = \$652 \\ \text{PW of benefits of B} &= \$120 (P/A, 10\%, 12) = \$818. \end{aligned}$$

For selecting the economically best alternative, the graphical method is employed in this example. The location of the projects on a graph showing the present value of the benefits versus the present value of the costs is determined as points A and B, and then the slope of the line connecting the points is estimated and compared with a 45° slope line where the points on it have equal present value of the costs and benefits ([Figure 7.45](#)). When the slope of the line, connecting two projects, is less (more) than 45°, the project with less (more) initial cost would be selected. As shown in [Figure 7.45](#), pump A, which has less initial cost, should be selected.

TABLE 7.25
Different Characteristics of Pumps

| Economic Characteristics | Pump A | Pump B |
|--------------------------|--------|--------|
| Initial investment | \$200 | \$700 |
| Annual benefits | \$95 | \$120 |
| Salvage value | \$50 | \$150 |
| Useful life | 6 | 12 |

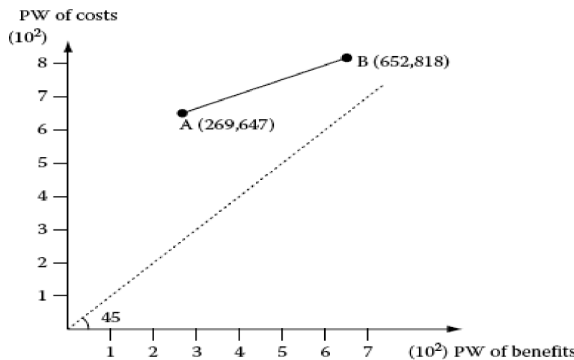


FIGURE 7.45 Comparing two pumps in Example 7.19 by the rate-of-return method.

7.7.2 ECONOMIC EVALUATION OF PROJECTS USING BENEFIT-COST RATIO METHOD

The benefit-cost ratio method which considers the ratio of the benefits to the costs has been widely used in the economic analysis of the water resources projects. The ratio is estimated based on the equivalent worth of the discounted benefits and costs in the form of annual worth, present worth, and/or future worth, to consider the time value of money. Equations 7.136 and 7.137 are the basic formulations of the benefit-cost ratio method.

$$\frac{B}{C} = \frac{B}{I + C} \quad (7.136)$$

$$\frac{B}{C} = \frac{B - C}{I} \quad (7.137)$$

where:

B is the net equivalent benefits

C is the net equivalent annual cost including the operation and maintenance costs

I is the initial investment.

If the benefit-cost ratio of a project is less or equal to 1, it is not considered. Through the following equation, the associated salvage value of the investment is considered in the benefit-cost method:

$$\frac{B}{C} = \frac{B - C}{I - S} \quad (7.138)$$

where S is the salvage value of investment.

Example 7.20

Assume that the annual costs of operation and maintenance of pumps A and B are equal to \$5500 and \$7000, respectively. Compare the two pumps from an economic aspect, using the benefit-cost ratio method.

SOLUTION

For considering the salvage value of the pumps, Equation 7.138 is employed. Because of the different life-spans of the pumps, the annual worth method is employed for more simplicity as follows:

Pump A:

$$\frac{B}{C} = \frac{12,000 - 5500}{30,000(A/P, 8\%, 7) - 6000(A/F, 8\%, 7)} = 1.1358$$

Pump B:

$$\frac{B}{C} = \frac{14,000 - 7000}{75,000(A/P, 8\%, 12) - 12,000(A/F, 8\%, 12)} = 0.711$$

As can be seen, the benefit-cost ratio for pump B is less than 1. Therefore, it is rejected and pump A is selected.

7.8 CASE STUDIES

In this section, the application of mythologies is discussed as two practical case studies conducted by Karamouz et al. (2001, 2004, 2007). The first case includes the application of object-oriented programming based on the conflict resolution methods for the water resource planning in the study area. The second case includes a water pollution control model based on Nash bargaining theory to resolve the existing conflicts for the aquifer restoration.

7.8.1 CASE 1: DEVELOPMENT OF A SYSTEM DYNAMICS MODEL FOR WATER TRANSFER

In this case, a system approach to the water transfer from the southeast to southwest of Tehran, the capital of Iran, is discussed. By the construction of this channel, up to 7 m³/s of mostly urban drainage water can be transferred from the east to the west in the region to overcome the negative impacts of the water rise in the east and to utilize the urban water drainage in the cultivated lands and for other municipal applications in the west. The channel intercepts several local rivers and drainage channels and could partially collect water from these outlets. In order to simulate the state of the system under the different water transfer scenarios and the water allocation schemes, an object-oriented simulation model has been developed. Using different objects, the user can change the allocation schemes for any give demand points. An economic model based on the conflict resolution methods is developed for the resource planning in the study area.

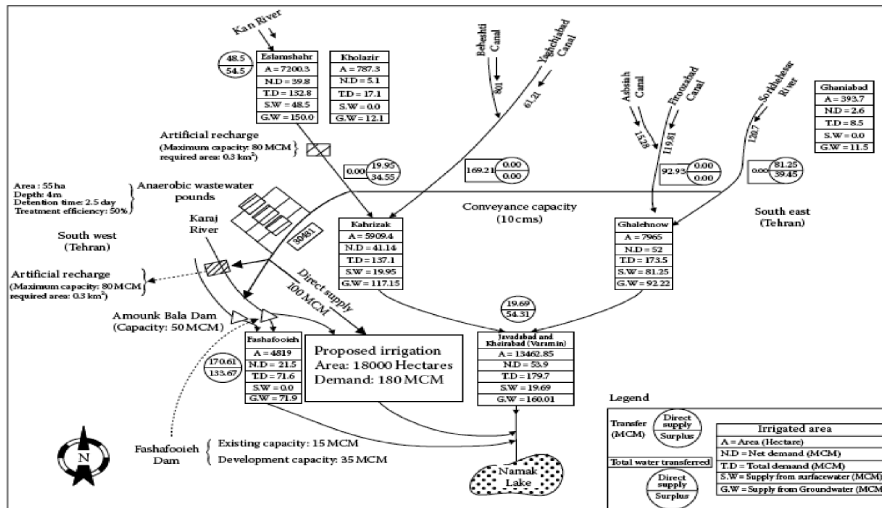


FIGURE 7.46 Schematic map of the Tehran metropolitan area water supply and demand in the study area. (From Karamouz, M. et al., *J. Am. Water Resour. Assoc.*, 37, 1301, 2001.)

7.8.1.1 Area Characteristics

The distribution of land with different capabilities for agricultural development may significantly affect the water supply planning in the southern part of Tehran. Figure 7.46 shows a system of local rivers which includes the Sorkheh-Hesar River, Absiah, and Firouz-abad drainage channels in the east and Beheshti and Yakhchih-abad drainage channels and the Kan River in the west. This collection of rivers and channels drains the sanitary and industrial wastewater as well as urban surface water of the different parts of the region and supplies the water for irrigation zones in the southern part of Tehran. As shown in this figure, there are five agricultural water supply zones which are Fashfooyeh, Kahrizak, Varamin, Eslamshahr and Khalazir, and Ghalehshahr and are named zone 1 through zone 5, respectively.

Because of a shortage of water and having the more suitable and cultivated lands in the western part in comparison with the eastern part, a water transfer channel from the east to the west is proposed by Karamouz et al. (2005). This channel crosses all the local rivers and wastewater channels from the east to the west in the study area before reaching the irrigation lands.

7.8.1.2 Conflict Resolution Model for Land Resources Allocation in Each Zone

For each irrigated area, an SD model of the water sharing conflict has been developed. The dynamic hypothesis of this model is shown in Figure 7.47. In this model, it is assumed that each irrigated area has only three different types of crops including wheat, barley, and tomato. Knowing the area and the water demand of each crop, the first estimate of its water allocation has been made.

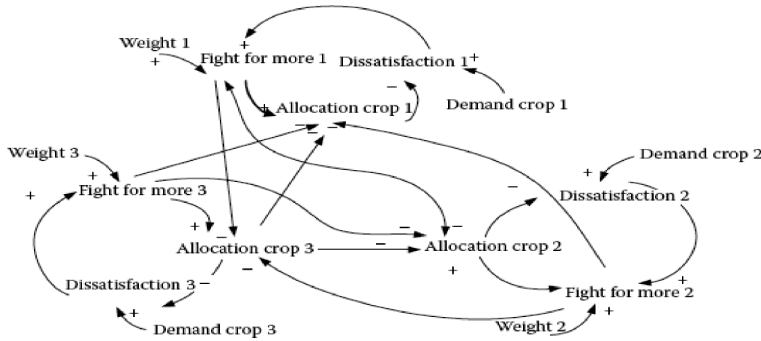


FIGURE 7.47 Dynamic hypothesis of the land resources allocations in each zone.

The weight of each crop is defined based on their usage and price. According to the demand and price of each crop, the weight of wheat, barley, and tomato is considered as 3, 1, and 2, respectively. [Figure 7.48](#) shows the schematic diagram for finding the land resources allocations in each zone, based on [Figure 7.47](#) of the dynamic hypothesis.

Finally, when the allocation of all the crops is determined, the area where each crop can be planted with regard to its water demand is determined in the converters area crop 1, 2, and 3. The converter available land refers to the total lands that can be planted in a specific plain. The ultimate estimate of each crop area is made based on the total available lands and the crop area that has been determined before. The converter benefit represents the total benefit of the plain due to its land resources allocations.

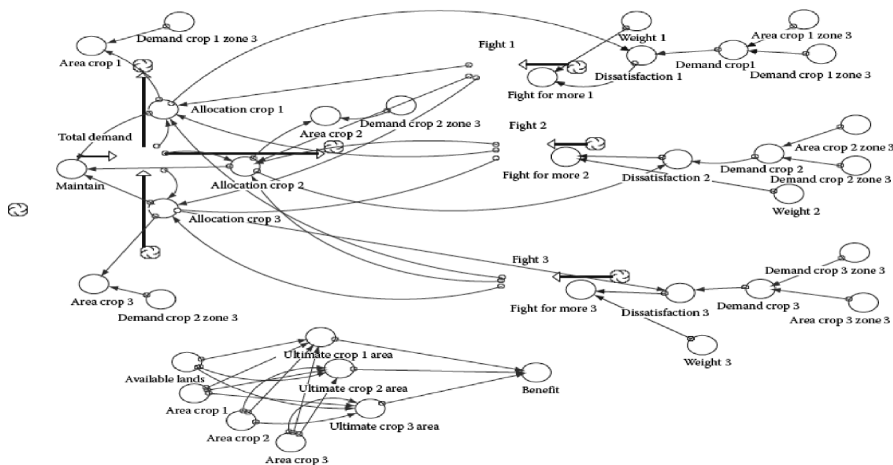


FIGURE 7.48 Schematic diagram of a developed model.

The formulation of the above descriptions is as follows:

$$Ds_i = As_i - Al_i \quad (7.139)$$

$$F_i = \sqrt{Ds_i} \times w_i \quad (7.140)$$

$$Al_i = f \left(\frac{\sum_t F}{\sum_i \sum_t F} \right) \quad (7.141)$$

where:

Ds_i is the dissatisfaction of the stakeholder i

As_i is the aspiration of the stakeholder i

Al_i is the water allocation to the stakeholder i

F_i is the fight for more water of the stakeholder i

w_i is the weight of the stakeholder i .

7.8.1.3 Results of the Conflict Resolution Model

As the groundwater withdrawal is expensive in the study area, all the residents prefer to use the surface water for the water supply. The surface water allocated to each zone and the lands associated with each zone are presented in [Table 7.26](#). The allocated water is calculated, based on each zone's demand. The relative weight of each zone is also related to the condition of the groundwater table in that zone. The land resource allocation in each zone is calculated from its weight and water demand. The relative weight of each crop is considered, based on its price.

TABLE 7.26
Resource Allocation to Each Zone

| Zone | Water Demand (MCM) | Allocated Water (MCM) | Area Allocated (ha) | Income (10^6 \$) |
|--------|--------------------|-----------------------|---------------------|---------------------|
| Zone 1 | 53.8 | 40.3 | 1754.1 | 1.6 |
| | | | 2113.3 | |
| | | | 951.6 | |
| | | | 2200.9 | |
| Zone 2 | 102.9 | 75.8 | 1297.8 | 2.6 |
| | | | 2410.7 | |
| | | | 6299.8 | |
| Zone 3 | 135.0 | 102.6 | 3198.8 | 5.4 |
| | | | 3964.3 | |
| | | | 2745.5 | |
| Zone 4 | 112.3 | 79.3 | 3624.9 | 2.6 |
| | | | 1619.6 | |
| | | | 6296.4 | |
| Zone 5 | 130.0 | 101.7 | 1280.6 | 2.7 |
| | | | 379.0 | |

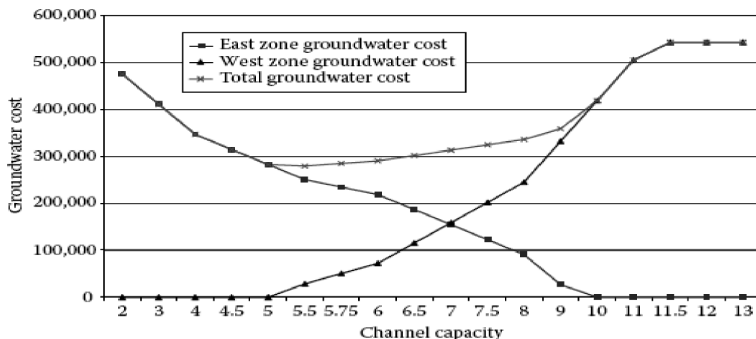


FIGURE 7.49 Variation of the groundwater withdrawal cost at the western and eastern plains due to different water transfer channel capacity.

7.8.1.4 Optimal Groundwater Withdrawal in Each Zone

Due to the shortage of the surface water in the study area, the remaining water demand of each zone is allocated from the groundwater storage. Figure 7.49 shows the variation of the groundwater withdrawal cost in the eastern and western plains. The cost of the groundwater withdrawal is calculated by:

$$\text{Cost} = \frac{h \times R}{\eta \times E} \quad (7.142)$$

where:

R is the cost of the KW/h power used for the water purpose that is equal to 0.004\$
 h is the depth of the groundwater

E is the pumping efficiency that is assumed as 90%
 η is equal to 0.102.

As the groundwater table is down in the western plains, it is economical that more surface water is allocated to the western plains because of their high cost of the groundwater withdrawal. The groundwater depth in different zones is shown in Table 7.27.

7.8.1.5 Sizing Channel Capacity

As discussed before, the groundwater withdrawal is economical in the eastern plains, because of the higher groundwater table in these zones than the western plains. So,

TABLE 7.27
Groundwater Depth in Different Zones

| Zone | Zone 1 | Zone 2 | Zone 3 | Zone 4 | Zone 5 |
|-----------------------|--------|--------|--------|--------|--------|
| Groundwater depth (m) | 50 | 14.5 | 21 | 20 | 8.6 |

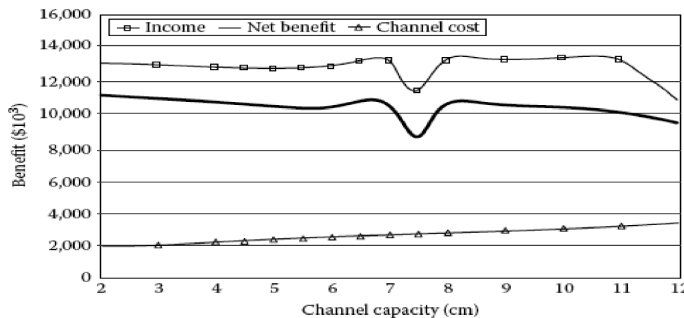


FIGURE 7.50 Variation of the agricultural income and conveying capacity of the channel.

the construction of a transfer channel, 15 km long from the east to the west of the study area, will be economical. For finding the optimal channel capacity, the different scenarios are considered and each scenario's net benefit of the agricultural land is calculated.

The net benefit of each zone is the equal benefit resulting from the optimal land resource allocation benefit less the groundwater withdrawal cost. Figure 7.50 shows the variation of the agricultural income and channel cost in the study area. As presented in Figure 7.50, the channel should be designed to carry 7 m³ of water per second.

7.8.1.6 Conclusion—Making Technologies Work

Many communities around the world are searching for the solutions for the water problems. Their ability to solve them is limited by the scarce resources and data and, in some instances, the undefined/unsettled water governance and by their planning schemes affected by the politics and subjective decisions.

As a result, the regions and municipalities are looking for quick results and planning schemes for the period of a decision-maker's term in his or her office. In the developing countries, there is a misrepresentation that developed countries have access to better techniques and hardware/software, and therefore utilizing the technologies from those countries will bring them the tools that could make magic. They ended up with black boxes with little or no adaptation capability and without the environment and the experts which could utilize them. So the reliance will be shifted to in-house models.

Again some of the in-house models soon become obsolete because of the many assumptions and simplifications that were necessary to make in order to build the models with the scarce data and also with substandard software support systems. So the new challenge in planning, more than the development of models and tool boxes, is geared toward making transparent data and algorithms that are adaptable to the regional and native characteristics and could be used to bring the different decision-makers and stakeholders together and create a consensus. A shared vision planning is needed to make the selected techniques and allocation schemes useable, adaptable, and expandable. Participatory planning is the key to the sound water

management. The SD and conflict resolution techniques can be used to formulate the problems with the intention of bringing the stakeholders into the decision-making process.

7.8.2 CASE 2: CONFLICT RESOLUTION IN WATER POLLUTION CONTROL FOR AN AQUIFER

In this case, a conflict resolution approach to the water pollution control in the Tehran metropolitan area, with its complex system of water supply, demand, and water pollution, is discussed. Tehran's annual domestic consumption is close to one billion cubic meters. Water resources in this region include the water storage in three reservoirs, the Tehran aquifer, as well as local rivers and channels which are mainly supplied by urban runoff and wastewater. The sewer system mainly consists of the traditional absorption wells. Therefore, the return flow from the domestic consumption has been one of the main sources of the groundwater recharge and pollution. Some parts of this sewage are drained into the local rivers and drainage channels and partially contaminate the surface runoff and local flows. These polluted surface waters are used in conjunction with the groundwater for irrigation purposes in the southern part of Tehran. Different decision-makers and stakeholders are involved in the water pollution control in the study area, which usually has conflicting interests. In this study, the Nash bargaining theory is used to resolve the existing conflicts and provide the surface and groundwater pollution control policies considering the different scenarios for the development projects. The results show how significant an integrated approach is for the water pollution control of the surface and groundwater resources in the Tehran region.

7.8.2.1 Water Resources Characteristics in the Study Area

The Tehran Plain lies between 35° and $36^{\circ} 35'$ northern latitude and $50^{\circ} 20'$ and $51^{\circ} 51'$ eastern longitude, in the south of the Alborz mountain ranges. About 800 million cubic meters of water per year is provided for the domestic consumption by over eight million inhabitants. More than 60% of the water consumption in Tehran returns to the Tehran aquifer via the traditional absorption wells. Some of the sewage is also drained into the local rivers and is used for irrigation in the southern part of Tehran (Karamouz et al., 2001).

The groundwater in the Tehran aquifer, which is used as drinking water, is polluted due to the return flow from the domestic absorption wells. In order to overcome the current problems, several development plans are being investigated and implemented. These projects will change the current balance of the recharge and water use in the region (Karamouz et al., 2004).

Table 7.28 presents the forecasted Tehran aquifer recharge due to the return flow from the domestic water use (without considering the effects of the TWCP) and the corresponding nitrate load as a water quality indicator. The Tehran wastewater collection project (TWCP) is the most important ongoing project for solving the current quantity and quality problems of the sewage disposal in the study area. The initial study of the TWCP was performed with the aid of the World Health Organization and the United Nations. Table 7.29 and Figure 7.51 present the main characteristics of the Tehran's wastewater collection system.

TABLE 7.28
Forecasted Water Demand, Wastewater, and Aquifer Pollution Load—Case Study 1

| Year | Population | Water Demand (MCM) | Wastewater (MCM) | Recharge to the Groundwater (MCM) | Aquifer Pollution Load (Nitrate) (kg/year) |
|------|------------|-----------------------|---------------------|---|--|
| 2006 | 8,120,402 | 889.184 | 693.564 | 522.744 | 40,251,288 |
| 2011 | 9,042,420 | 990.145 | 772.313 | 601.493 | 46,314,961 |
| 2016 | 9,956,493 | 1090.236 | 85.384 | 67.528 | 52,323,656 |
| 2021 | 10,786,922 | 1181.168 | 921.311 | 750.491 | 57,787,807 |

TABLE 7.29
Main Characteristics of Tehran Wastewater Collection Project

| Project Phase | Population Covered by TWCP | Construction Cost (Cumulative) (US dollars) | Nitrate Load Reduction (kg/year) | Reduction in Discharged Wastewater (m ³ /year) |
|---------------|----------------------------------|---|--|--|
| 1 | 2,100,000 | 13,650,000 | 13,810,797 | 179,361,000 |
| 2 | 4,200,000 | 27,300,000 | 27,621,594 | 358,722,000 |
| 3 | 6,300,000 | 40,950,000 | 41,432,391 | 538,083,000 |
| 4 | 8,400,000 | 54,600,000 | 55,243,188 | 717,444,000 |
| Total | 10,500,000 | 68,250,000 | 69,053,985 | 896,805,000 |

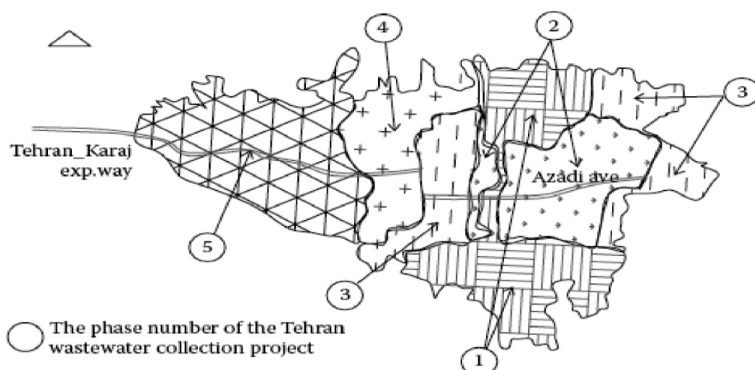


FIGURE 7.51 Area covered by different phases of the Tehran Wastewater Collection Project.

Another completed project is a network of drainage wells to lower the groundwater table in the southern part of the city. In this project, more than 100 drainage wells have been constructed. The pumped water is discharged to the local streams and channels and contributes to the surface water in the southern part of the city. For more detailed information about surface water resources in the study area, see Karamouz et al. (2004).

In this study, the optimal operating policies for the drainage wells as well as the optimal coverage of the TWCP are developed for the different scenarios in the development stages considering the objectives and utility functions of the decision-makers and the stakeholders of the system.

7.8.2.2 Conflict Resolution Model

Based on the available data and the results of some brainstorming sessions, the main decision-makers and the stakeholders of the system and their utilities are as follows:

Department of Environment: Water quality in the Tehran aquifer is the main concern of this department. The available data show that the concentration of some water quality variables such as nitrate, TDS, and coliform bacteria deviate from the groundwater and drinking water quality standards. Nitrate is considered as the representative water quality variable in this study. As the suggested nitrate concentration for the groundwater is usually between 25 and 50 mg/L, the utility function of this department (f_{env}) is formulated as follows:

$$f_{env.} = \begin{cases} 1 & \text{if } c < 25 \text{ mg/L} \\ 1 - 0.04(c - 25) & \text{if } 25 \leq c < 50 \text{ mg/L} \\ 0 & \text{if } c \geq 50 \text{ mg/L} \end{cases} \quad (7.143)$$

where c is the average nitrate concentration in the Tehran aquifer.

Tehran Water and Wastewater Company: The main objective of this company is the water supply to the domestic demands and the wastewater collection and disposal. Considering the importance of the water supply reliability in the urban areas, its most favorite range in the study area is more than 94%. Therefore, the utility function of the decision-makers in this company for reliability of the water supply is assumed as:

$$f_{wws.} = \begin{cases} 1 & \text{if } s > 94 \\ 1 - 0.0156(s - 30) & \text{if } 30 < s < 94 \\ 0 & \text{if } 0 < s \leq 30 \end{cases} \quad (7.144)$$

where:

$f_{wws.}$ is the utility function related to the water supply reliability
 s is the percentage of the supplied domestic water demand.

As the construction cost of different phases of the TWCP is different, the utility function of the Tehran Water and Wastewater Company is assumed to be as follows:

$$f_{wwx} = \begin{cases} 1 & \text{if } x \leq 13.65 \\ 0.95 - 0.00366(x - 13.65) & \text{if } 13.65 < x \leq 27.3 \\ 0.85 - 0.00366(x - 27.3) & \text{if } 27.3 < x \leq 54.6 \\ 0.75 - 0.00366(x - 40.95) & \text{if } 40.95 < x \leq 54.6 \\ 0.65 - 0.00366(x - 54.6) & \text{if } 54.6 < x \leq 68.25 \end{cases} \quad (7.145)$$

where:

f_{wwx} is the construction cost of the TWCP

x is the total allocated budget to the TWCP (million \$).

The utility function of the construction cost of the TWCP is evaluated based on the estimated cost of the different phases of the TWCP.

Tehran Health Department: The main objective of this department is to make sure that the water supplied to the domestic sector meets the drinking water quality standards. As the recommended nitrate concentration in the allocated water is less than 10 mg/L, the utility function of the decision-makers of this department (f_{hd}) is assumed to be as follows:

$$f_{hd} = \begin{cases} 1 & \text{if } c \leq 10 \text{ mg / L} \\ 1 - 0.02(c - 10) & \text{if } 10 < c \leq 25 \text{ mg / L} \\ 0.7 - 0.028(c - 25) & \text{if } 25 < c \leq 50 \text{ mg / L} \\ 0 & \text{if } c > 50 \text{ mg / L} \end{cases} \quad (7.146)$$

where c is the average nitrate concentration in the Tehran aquifer.

Water Supply Authority (Water and Wastewater Company): The main objective of this organization is to supply water in order to meet the different water demands in the study area. Controlling the variations of the groundwater table elevation in the Tehran aquifer and reducing the pumping costs of the drainage wells, which are used to drawdown the rising groundwater table, are the main utilities of this company. The most favorite range of the average groundwater table level variation in the Tehran aquifer is about 2 cm due to its impacts on the subsidence of the building foundations, especially in the southern part of the city which has experienced considerable groundwater table variations. The utility function of the Tehran Water Supply Authority for the groundwater table variations is assumed to be as follows:

$$f_{wsl} = \begin{cases} 1 & \text{if } 0 \leq l < 2 \text{ cm} \\ 1 - 0.0556(l - 2) & \text{if } 2 \leq l < 20 \text{ cm} \\ 0 & \text{if } l \geq 20 \text{ cm} \end{cases} \quad (7.147)$$

where:

f_{wsl} is the utility function related to the variation of the groundwater table level

l is the average annual variation of the groundwater table in the Tehran aquifer.

The existing pumping capacity of the drainage wells located in the southern part of Tehran is about 100 million cubic meters. The utility function of the Tehran Water Supply Authority for the total pumping capacity of drainage wells is as follows:

$$f_{wsd.} = \begin{cases} 1 & \text{if } 0 \leq d < 100 \text{ MCM} \\ 1 - 0.033(d - 100) & \text{if } 100 \leq d < 400 \text{ MCM} \\ 0 & \text{if } d \geq 400 \text{ MCM} \end{cases} \quad (7.148)$$

$f_{wsd.}$ is the utility function related to the discharge volume from the drainage wells, respectively

d is the total annual discharge from the drainage wells located in the southern part of Tehran (million cubic meters).

Considering the Nash product as the objective function, the following model is formulated for the water pollution control in the study area:

$$\begin{aligned} MaxZ = & (f_{env.} - d_{env.})^{w_1} \cdot (f_{wws.} - d_{wws.})^{w_2} \cdot (f_{wwx.} - d_{wwx.})^{w_3} \cdot \\ & (f_{hd.} - d_{env.})^{w_4} \cdot (f_{wsl.} - d_{wsl.})^{w_5} \cdot (f_{wsd.} - d_{wsd.})^{w_6} \end{aligned} \quad (7.149)$$

Subject to:

$$\Delta V_A = (R + 1) - (s + d) \quad (7.150)$$

$$L = \frac{S_A}{A_A} \Delta V_A \quad (7.151)$$

$$c = \frac{c_R R + c_0 V_A}{V_A + R + I} \quad (7.152)$$

$$x = f(A) \quad (7.153)$$

$$R = f(A, P) \quad (7.154)$$

where:

$d_{env.}/d_{wws.}/d_{wwx.}/d_{hd.}/d_{wsd.}/d_{wsd.}$ are the disagreement points of each decision-maker/agency in the study area

S_A is the storage coefficient

A_A is the aquifer area

ΔV_A is the variation in the aquifer water storage

I is the aquifer recharge due to the infiltration from the precipitation, the infiltration from streams, canals, as well as underground inflow at the boundaries

R is the infiltration from the absorption wells

- c_R is the concentration of the water quality variables in the discharging flow
 c_0 is the initial average concentration of the water quality variable in the Tehran aquifer
 A is the area covered by the TWCP
 L is the variation in the water table elevation
 d is the discharge from the drainage wells
 s is the allocated groundwater to the domestic demand
 P is the population
 x is the TWCP construction cost
 w_i is the relative weight/authority of the decision-maker/stakeholder i
 d_j is the disagreement point of the decision-makers/stakeholders corresponding to the utility function j .

The results of applying this model for the water pollution control in the Tehran aquifer are presented in the next section.

7.8.2.3 Results and Discussion

The conflict resolution model presented in this study is applied for determining the optimal area that should be covered by the TWCP as well as the pumping discharge of the drainage wells in the development stages of the project. In the water balance of the Tehran aquifer, it is assumed that only the domestic water supply, the return flows from the absorption wells, and the water discharge from drainage wells are variables, and the other terms in the water balance equation are constant. The discharges from the drainage wells usually control the annual groundwater table variation.

As mentioned before, the aquifer is polluted mainly due to the wastewater discharge through the absorption wells. Based on the available data, nitrate can be considered as the water quality indicator. The average concentration of nitrate and the total nitrogen in the raw domestic sewage are 90 and 5 mg/L, respectively. Close to 86% of the total nitrogen can be converted to nitrate through a nitrification process. Therefore, it is assumed that the ultimate nitrate concentration in the wastewater discharged to the Tehran aquifer is equal to 77 mg/L. As presented in [Table 7.30](#), the per capita water use and the corresponding wastewater have been estimated. Therefore, the aquifer pollution load can be estimated considering different scenarios for Tehran's population and the subregions covered by the TWCP.

The relative authority of the utility functions w_1, w_2, \dots, w_6 are assumed as 0.18, 0.27, 0.13, 0.2, 0.13, and 0.09, respectively. Based on the form of the utility function, the disagreement points of all the decision-makers are set to zero. The results of the proposed model for the different planning horizons are presented in [Table 7.30](#). As seen in this table, the population covered by the TWCP will reach 7.4 million people in the year 2006. In this year, the nitrate concentration will be less than the drinking water standard (10 mg/L). The results show that the discharge capacity of the drainage wells should be maintained as 50 million cubic meters per year. Based on the derived operating policies, the quality of the groundwater and also the groundwater table variation can be effectively controlled during the planning horizon.

TABLE 7.30
Results of the Conflict Resolution Model for Water and Wastewater Management—Case Study 1

| Decision Variables | Year | | | |
|--|-------------|-------------|-------------|-------------|
| | 2006 | 2011 | 2016 | 2021 |
| Average nitrate concentration (mg/L) | 9.65 | 9.68 | 12.21 | 9.5 |
| Reliability of domestic water supply | 94.7 | 95.9 | 94.6 | 95.3 |
| Average rising in groundwater table level (m) | 0.077 | 0.072 | 0.0696 | 0.0652 |
| Average discharge from drainage wells (MCM) | 50 | 50 | 50 | 50 |
| Total cost of TWCP (million \$) | 48.1 | 53.3 | 54.6 | 62.4 |
| Population covered by TWCP (million persons) | 7.4 | 8.2 | 8.4 | 9.6 |
| Population covered by TWCP based on the Timetable of the project (million persons) | 2.5 | 4.6 | 6.7 | 8.8 |

7.8.3 CASE 3: AN AGENT-BASED MODELING APPLICATION IN GROUNDWATER

7.8.3.1 Case Study Characteristics

The study region is the Lenjanat sub-basin located in the Zayandehrood basin, Iran. The groundwater in the region is extracted through 543 qanats and 3760 water wells, while 2355 wells are legal and the rest are illegal water wells. The total volume of the groundwater abstraction in the region is about 244.1 MCM. The annual volume of the water used by the agricultural sector in Lenjanat amounts to 387.2 MCM through the conjunctive use of the groundwater and surface water resources. The over exploitation of the Lenjanat aquifer leads to an annual drop of 0.27 m in its water table and a total drop of 5.9 m over the period from 1991 to 2016. The fluctuations in the water table are presented in [Figure 7.52](#).

Around 38% of the wells in the region are illegal and the regional water authority tries to control and surveil the water wells to plug the illegal wells into the monitoring network. A large portion of the time and energy in this area is devoted to the recognition of illegal wells.

In this case, the regional water authority monitors the consumption rates and the water balance in the aquifer to protect the groundwater resources and restore them. Also they have established some regulations for the public prosecutors to deal with the excessive withdrawals. Based on the field investigations, the key agents with the direct impact on the environment are the water users, the regional water authority, and the public prosecutor's office. The interactions among the agents (water users, regional water authority, and public prosecutor's office) and the environment (i.e., groundwater resources) are modeled. While the water users are exploiting the water from the resources, the regional water authority is continuously monitoring the water abstracting from the wells. In times of water deficiency, the regulations are more

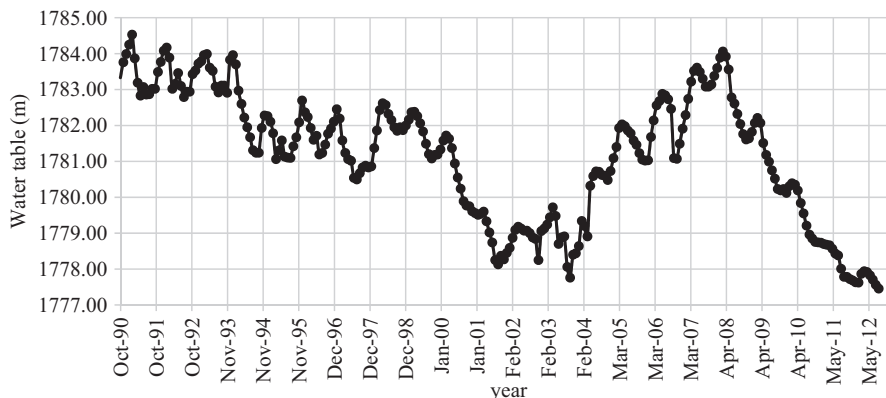


FIGURE 7.52 Water table elevations in the Lenjanat aquifer over a 22-year period.

restricted, and the relations and interactions become more pronounced. However, in these times, some violations such as the unauthorized well drilling and the water abstraction in excess of an aquifer's safe yield widely occur, which impose the water table drawdown. A great portion of the time and resources of the groundwater regulators are devoted to control these violations and enforce the regulations. When a water user violates the limitations imposed by the regulations, the public prosecutor may get involved. These interactions among the agents and the environment are considered in the model development.

7.8.3.2 Model Characteristics

In this model, the main components of the system include the water resources, the water users, the regional water authority, and the public prosecutor's office.

a. Water Users

This group includes the agents who generate the profitable products using the water. The farmers are included in this category as they need water for the improved farm productivity. The main goal of these agents is the enhanced productivity. They interact with the regional water authority and are affected by its decisions. In the times that the farmers continue violating their assigned groundwater usage rates, they will face the reactions from the public prosecutor's office. For the purposes of this study, examples of the farmer water users, who faced indictments of unauthorized well drilling and water abstraction in excess of the aquifer capacity were reviewed.

b. Regional water authorities (RWA)

This agent group is responsible for supplying the water to users and is in charge of surveillance and control of the water withdrawals by the users and the aquifer restoration. This agent monitors the water users based on the prevalent regulations to prevent their violation in the water withdrawals. Thus, this group is mandated to preserve and protect the water resources and to maintain the balance between the aquifer's safe yield and

the groundwater withdrawals. The regional water authorities are mandated to communicate in writing with those users who break the regulations. This agent submits the report of the water users' violations and a lawsuit to the public prosecutor's office. The water users must take the proper actions (i.e., well plugging) after the confirmation by the public prosecutor's office.

c. Public prosecutor's office

In cases where the law is violated by the water users, after submitting the report and filling the lawsuit by the regional water authority, the public prosecutor's office will come into play as an agent. The decisions and the verdicts by the public prosecutor's office are deemed binding for both the regional water authority and the water user.

In order to develop the model, the agent's behaviors are extracted from the empirical data based on the actual data including the archive of the lawsuits. Each lawsuit on each illegal water well is reviewed, and the behavior of the agents involved including well plugging, and the interactions among the agents are extracted. The interactions among the agents are presented in [Figure 7.53](#).

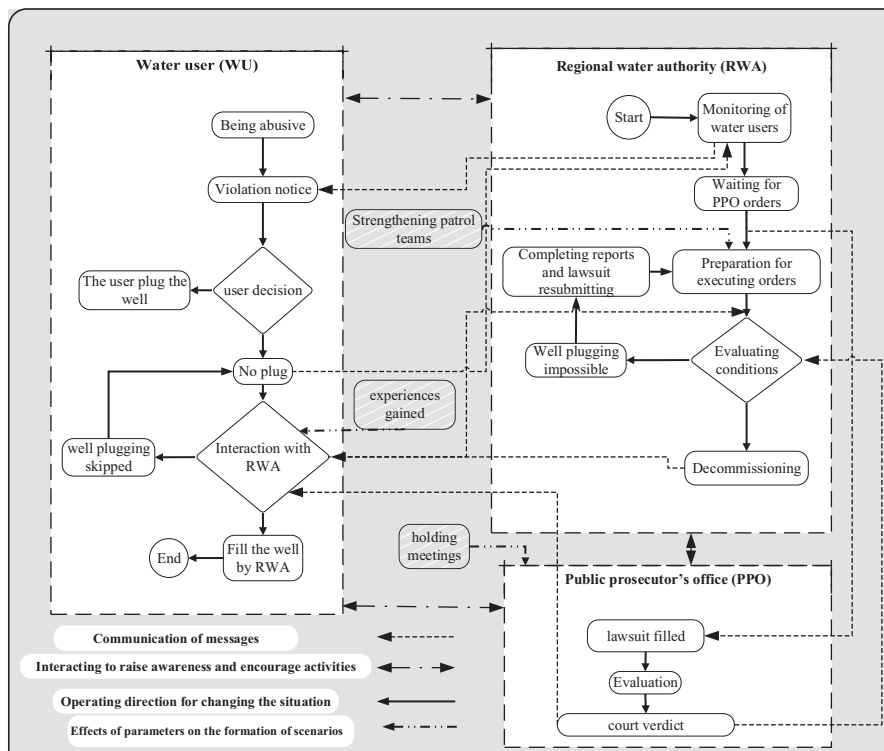


FIGURE 7.53 Interactions among the agents in an aquifer environment. (Adapted from Ohab Yazi, S.A and Ahmadi, A., *Simul. Model. Pract. Theor.*, 87, 274–292, 2018.)

7.8.3.3 Model Calibration and Verification

The agent-based model was developed using the AnyLogic software to simulate the interactions among the agents. The processes employed in the model are based on the observed groundwater level data, the reports from the regional water authority, and the information extracted from the water-related lawsuits and interviews with experts. The modeling time period is from 2006 to 2009 (36 months). The data from the first 28 months are used for the model calibration and the remaining 8 months for the model verification. The results of the model calibration and verification are presented in [Figure 7.54](#).

7.8.3.4 Results of Agent-Based Modeling

Based on the real conditions in the study area, it is assumed the decision-makers and the public organizations take keeping the water users' satisfaction more seriously than their responsibility in controlling and surveilling the groundwater usage, which has led to the decline of the RWA's authority and power and their failure to protect the resources. Therefore, the water resources have been left in derelict, the laws and regulations have been neglected, the water users have learned to ignore notices, and they have even shown resistance against the official laws and regulations such as well plugging. The response to the violations of the regulations begins with filing a report, receiving orders from the central office, and the submission of a lawsuit to the public prosecutor's office.

[Figure 7.55](#) shows the simulation model results over a period of 60 months (2011–2016). This figure shows that the water tables levels have on average decreased about 1.5 meters over a period of 60 months. The numbers of the violation reports, the court decisions issued, and the illegal wells decommissioned and plugged are shown in this figure utilizing the simulation model. According to [Figure 7.55](#), 403 violation reports were confirmed and 166 of which had court decisions issued, 142 illegal wells were decommissioned and plugged by the RWA, and 24 wells remained unplugged.

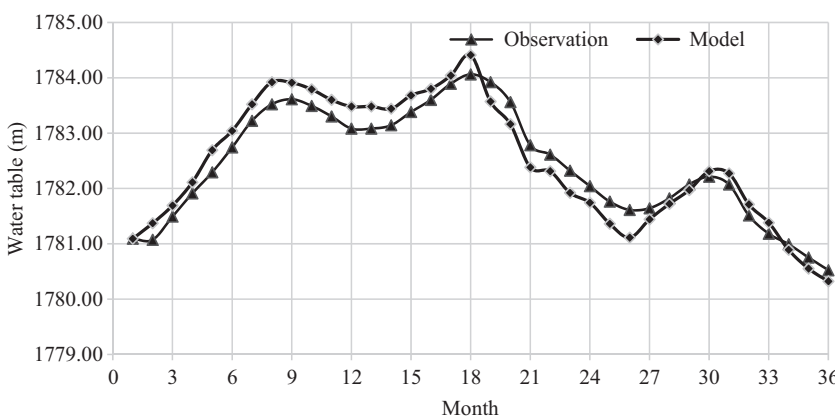


FIGURE 7.54 Results of model calibration and validation. (From Ohab Yazi, S.A and Ahmadi, A., *Simul. Model. Pract. Theor.*, 87, 274–292, 2018.)

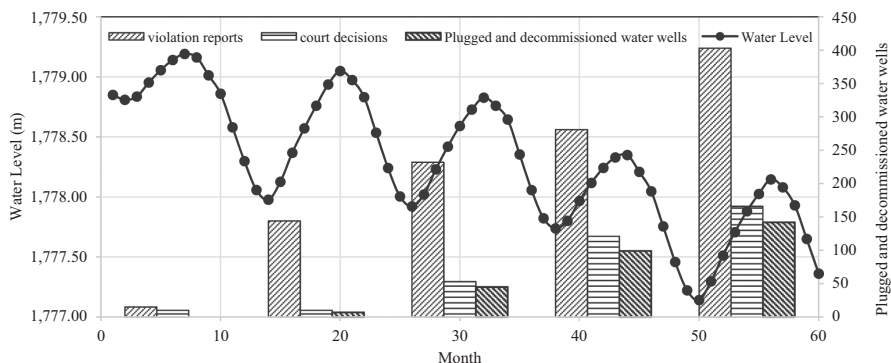


FIGURE 7.55 Results obtained from the agent-based model. (From Ohab Yazi, S.A and Ahmadi, A., *Simul. Model. Pract. Theor.*, 87, 274–292, 2018.)

The results show that 41 percent of the cases were completely addressed and about 6% of the total violation reports led to no final decisions. It is because of the inefficiency of the RWA staff performance, the water users' strong resistance, and the failure of the public prosecutor to issue final decisions.

The lack of the strong law that provides the sufficient enforcement authority to the RWA, the long waiting time for the court decisions at the public prosecutor's office, the poor understanding and awareness of the water regulations among the relevant public organizations, and not taking the violations from the regulations pertaining to the water resources seriously enough are among the factors responsible for the difficulty and the long and slow process of handling violations.

7.8.4 CASE 4: DEVELOPMENT OF A NONCOOPERATIVE GAME IN GROUNDWATER MANAGEMENT

In this case study, the game theory with a noncooperative approach is utilized to investigate the conflicts among the groundwater users. The following case study and methodology is applied from Nazari and Ahmadi (2019). Developing a noncooperative simulation model empowers the user to examine the decision-making processes of the stakeholders who are unwilling to cooperate, to assess the impact of the stakeholders' foresight on their decision-making, and to investigate the possibility of reaching a cooperative solution in the absence of the stakeholders' cooperation behavior.

7.8.4.1 Area Characteristics

The Bad-Khaledabad region is located within the Siahkouh basin in central Iran. The Bad-Khaledabad region has an area of 1851.4 km². There are 173 wells, 9 qanats, and 1 spring within this region with a total annual discharge of 86.86 MCM, of which, 79.2 MCM is from the wells. The location of the study area in Iran and the location of the aquifer are presented in Figure 7.56.

Based on the observed well data from 1996 to 2016, the study area is divided into three zones: zone 1 covers the north area with the increasing water levels in recent

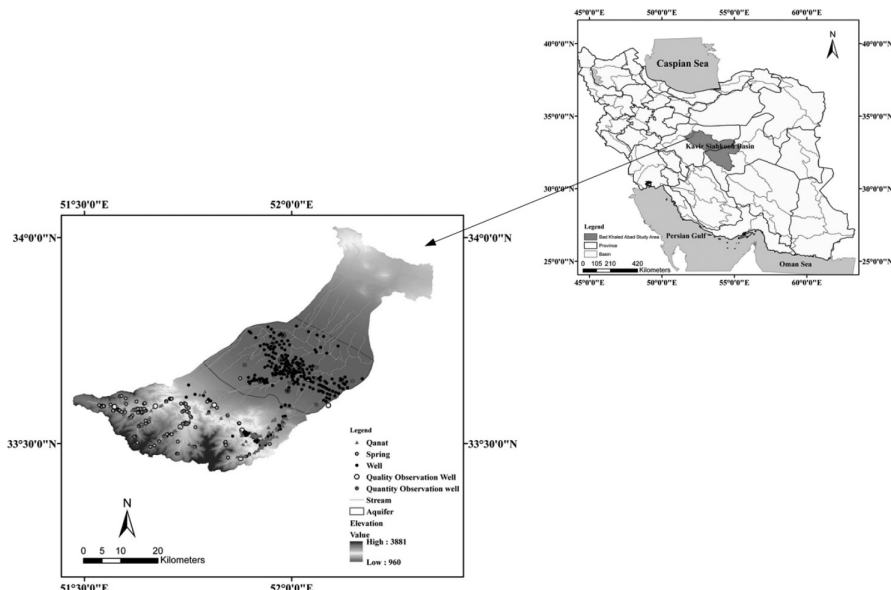


FIGURE 7.56 The Bad-Khaledabad study area.

years; zone 2 in the middle area has the highest cultivation density and the largest decline in the water level during the 5-year period of simulation (2010–2015); and zone 3 covers the southern area with continuous water fluctuations.

The monthly water allocations are optimized for a 5-year period in each zone. The cultivated areas are attributed by their dominant crops, which include barley, alfalfa, wheat, corn, onions, and cantaloupe. Hence, in the optimization model, there are a total of 1098 decision variables ($5 \text{ years} \times 12 \text{ months} \times 6 \text{ CAs} \times 3 \text{ zones} + 18$).

The groundwater flow was simulated using the groundwater modeling system software. The water table and the groundwater quality were simulated using MODFLOW and modular transport, 3-dimensional, multi-species model (MT3DMS), respectively. First, a conceptual model was developed by defining the position and specification of the study area, and the aquifer area was divided into a network of 1000×1000 grids. The groundwater simulation model was calibrated for the Bad-Khaledabad region using the data from June 22, 2011, to September 22, 2013. A part of this period is used for modeling the steady flow, and the rest are used for the transient flow in 24 monthly steps. Salinity as a water quality variable is simulated, and its impacts on the crop yields are considered.

7.8.4.2 Simulation-Multi-objective Optimization Model

The linked simulation, multi-objective optimization model (SMO) was developed to determine the groundwater allocation rates to the farmers. These values are introduced as the groundwater exploitation values to the simulation model (MODFLOW and MT3DMS), which determines the water and salinity levels in the study area.

These values are re-introduced back to the optimization model to calculate the second objective (minimizing the water level drawdown) subject to the salinity control constraint. These steps are repeated until the maximum number of iterations, as the termination condition, is met.

The implications of the following three strategies are tested using the SMO model in order to examine how the beneficiaries (government and farmers) may choose possible strategies.

1. The current conditions continue, including the cultivated area of each crop will be equal to the mean cultivated area in the historical period, and the water level variation was simulated using the MODFLOW model.
2. The crop pattern changes to the optimal cropping pattern: The SMO model determines the cultivated area of the six products in three zones according to Equations 7.127 to 7.134. The optimal cropping pattern is determined considering the current conditions. In Equation 7.134, $A_{dp,min} = 0.8 \times A_{dp,mean}$ and $A_{dp,max} = 1.2 \times A_{dp,mean}$, where, $A_{dp,mean}$ is equal to the mean area of the crop p in the zone d during 1996–2016.
3. Cropping pattern shift: the cultivated area is changed from the water-intensive and less profitable products to more valuable products with relatively lower water consumption. This strategy is aimed to examine the effect of a shift in the cropping pattern toward more profitable products with lower water requirements. For this strategy, in Equation 7.134 $0.4A_{dp,mean} \leq A_{dp} \leq 0.8A_{dp,mean}$ was considered to change the cultivated area of barley, alfalfa, and cantaloupe; and $0.8A_{dp,mean} \leq A_{dp} \leq 1.5A_{dp,mean}$ was used to change the cultivated area of onion, corn, and wheat.

[Figure 7.57a](#) and [b](#) represents the net benefit from the crops in the three strategies and the total yield resulted from the three strategies in each zone. [Figure 7.57c](#) shows the mean groundwater level fluctuations in the study area. Among the examined strategies, the “optimal cropping pattern based on the current conditions” strategy leads to the lowest groundwater withdrawal, and the lowest water allocation to the crop patterns for farmers. In this strategy, the benefit is also the lowest. If the farmers change the crop pattern to the more profitable patterns (the cropping pattern shift strategy), the highest value of the net benefit is achieved among the strategies.

7.8.4.2.1 Results of the Noncooperative Decision-Making

This game was developed to simulate the farmers and the government decision-making procedure for the irrigation efficiency improvement. In this game, it is assumed that the cultivated area is similar to the historical values and the cropping areas are limited to 0.8 to 1.2 times of the mean cultivated area in the present conditions. The irrigation efficiency is considered to be 55 percent. As the irrigation efficiency increases, the recharge to the groundwater from the irrigation decreases.

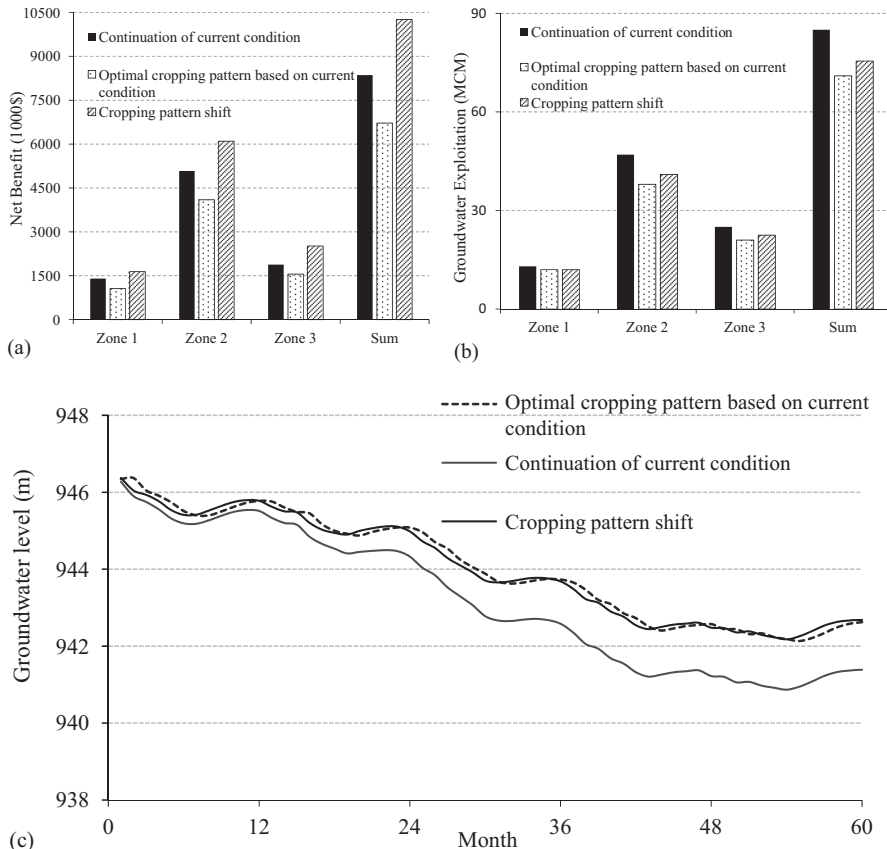


FIGURE 7.57 (a) The net benefit from each strategy in each zone, (b) the annual groundwater withdrawal during the 5-year simulation, and (c) the mean of the monthly groundwater level fluctuations for the three strategies. (From Nazari, S. and Ahmadi, A., *J. Hydrol.*, 578, 124075, 2019.)

The states of the two players including the government and the farmers are presented in Table 7.31. The government can invest in the efficiency improvements by the cost reimbursements; i.e., payments, or continue the current state without payments. The farmers also have two alternatives: either to accept the optimal cropping pattern with the improved efficiencies (Accept) or refuse it (Don't Accept). Figure 7.58 shows a strategic matrix of the efficiency improvement game between the government and the farmers. In this figure, the values in parenthesis (a, b) show player payoffs: a indicates the government's payoff and b indicates the farmers' payoff.

Table 7.32 presents how the different states including Nash, GMR, SMR, and SEQ help stabilize a solution between the two players. The state (Don't Pay, Accept)

| | | |
|------------|--------------|--------|
| | Farmers | |
| | Don't Accept | Accept |
| Government | | |
| Pay | (1,4) | (3,3) |
| Don't Pay | (2,1) | (4,2) |

FIGURE 7.58 The matrix form of the efficiency improvement game.

TABLE 7.31
The Government and Farmers Strategies in the Efficiency Improvement Game

| States | Government | Farmers | Feature |
|---------------------------|--|---|--|
| (Pay, Don't Accept) | The government will pay all the costs of irrigation efficiency improvement | Farmers will develop the cultivation area | Recharge from irrigation will decrease, and the water table level will drawdown more than the current condition due to increased pumping |
| (Pay, Accept) | The government will pay all the cost of irrigation efficiency improvement | Farmers accept the optimal cropping pattern of efficiency improvement condition (obtained by SMO model) | Indicating cooperative relation between the farmers and government |
| (Don't Pay, Don't Accept) | The government will continue the current condition | Farmers will develop the cultivation area | The current condition and trend will continue |
| (Don't Pay, Accept) | The government will continue the current condition | Farmers accept the optimal cropping pattern of efficiency improvement condition (obtained by SMO model) | This state will not occur in reality |

Source: Nazari, S. and Ahmadi, A., *J. Hydrol.*, 578, 124075, 2019.

TABLE 7.32
Different Types of Stabilities for the Farmers and Government in the Efficiency Improvement Game

| Stability Definition | Nash | | GMR | | SMR | | SEQ | |
|---------------------------|------------|---------|------------|---------|------------|---------|------------|---------|
| | Government | Farmers | Government | Farmers | Government | Farmers | Government | Farmers |
| (Pay, Don't Accept) | ✓ | | | ✓ | ✓ | ✓ | ✓ | ✓ |
| (Pay, Accept) | | ✓ | ✓ | | ✓ | ✓ | ✓ | ✓ |
| (Don't Pay, Don't Accept) | ✓ | | | ✓ | | ✓ | | ✓ |
| (Don't Pay, Accept) | ✓ | ✓ | ✓ | ✓ | ✓ | ✓ | ✓ | ✓ |

Source: Nazari, S. and Ahmadi, A., *J. Hydrol.*, 578, 124075, 2019.

represents the scenario in which the government does not take any action, but the farmers still choose the optimal cropping pattern. Since the farmers have no desire to change their cropping patterns without any government support, this scenario will not come to reality.

On the other hand, the state (Pay, Accept) is a stable solution in all the stability definitions except for Nash. This state can be achieved by the cooperation between the government and the farmers. This is not a stable state from the Nash definition. Based on the results of the optimization model, the groundwater exploitation in this state is 66.5 MCM.

PROBLEMS

- 7.1** The studies in an aquifer have shown that the groundwater TDSs concentration of the aquifer is a function of the TDSs concentration and the volume of the aquifer recharge. The monthly data of the groundwater TDSs concentration and the volume of the aquifer recharge are given in [Tables 7.33](#) through [7.35](#), respectively. Develop the MLP and IDNN models to simulate the monthly TDSs concentration of this aquifer as a function of the monthly TDSs concentration and the volume of the aquifer recharge.
- 7.2** The variation of the annual water demand from the groundwater over a 30-year planning time horizon is exhibited in [Table 7.36](#). The current capacity of the water supply system is 100 MCM. It is assumed that the aquifer will

TABLE 7.33
TDS Concentration of the Aquifer (mg/L)

| Year | 1998 | 1999 | 2000 | 2001 | 2002 | 2003 | 2004 | 2005 |
|-----------|------|------|------|------|------|------|------|------|
| January | 355 | 275 | 391 | 387 | 470 | 347 | 428 | 622 |
| February | 255 | 402 | 297 | 303 | 353 | 472 | 414 | 382 |
| March | 357 | 490 | 498 | 451 | 445 | 613 | 424 | 508 |
| April | 301 | 346 | 325 | 118 | 390 | 405 | 467 | 252 |
| May | 405 | 354 | 293 | 317 | 439 | 425 | 426 | 497 |
| June | 285 | 522 | 328 | 103 | 371 | 411 | 488 | 331 |
| July | 439 | 361 | 338 | 461 | 517 | 449 | 351 | 312 |
| August | 380 | 650 | 429 | 779 | 414 | 734 | 343 | 787 |
| September | 269 | 326 | 284 | 364 | 383 | 447 | 427 | 670 |
| October | 341 | 308 | 457 | 239 | 490 | 396 | 443 | 352 |
| November | 301 | 381 | 283 | 257 | 382 | 499 | 402 | 233 |
| December | 303 | 339 | 405 | 785 | 392 | 430 | 759 | 555 |

TABLE 7.34
Recharged Water Volume to the Aquifer (MCM)

| Year | 1998 | 1999 | 2000 | 2001 | 2002 | 2003 | 2004 | 2005 |
|-----------|------|------|------|------|------|------|------|------|
| January | 36 | 27 | 40 | 27 | 10 | 8 | 10 | 12 |
| February | 25 | 41 | 30 | 4 | 8 | 10 | 9 | 5 |
| March | 36 | 48 | 48 | 46 | 10 | 13 | 10 | 10 |
| April | 30 | 35 | 33 | 0 | 9 | 9 | 10 | 7 |
| May | 41 | 36 | 29 | 16 | 10 | 10 | 10 | 16 |
| June | 28 | 50 | 33 | 5 | 9 | 9 | 11 | 7 |
| July | 44 | 37 | 34 | 21 | 11 | 10 | 8 | 9 |
| August | 39 | 56 | 43 | 95 | 9 | 15 | 8 | 60 |
| September | 26 | 33 | 28 | 83 | 9 | 10 | 10 | 103 |
| October | 35 | 31 | 45 | 29 | 11 | 9 | 10 | 51 |
| November | 30 | 39 | 19 | 9 | 9 | 11 | 9 | 7 |
| December | 30 | 34 | 19 | 15 | 9 | 10 | 9 | 17 |

TABLE 7.35
TDS Concentration of Recharging Water to the Aquifer (mg/L)

| Year | 1998 | 1999 | 2000 | 2001 | 2002 | 2003 | 2004 | 2005 |
|-----------|------|------|------|------|------|------|------|------|
| January | 853 | 685 | 921 | 680 | 1006 | 782 | 929 | 1105 |
| February | 637 | 940 | 735 | 518 | 793 | 1009 | 903 | 680 |
| March | 858 | 1075 | 1085 | 973 | 959 | 1266 | 922 | 1070 |
| April | 743 | 836 | 793 | 102 | 859 | 887 | 1001 | 548 |
| May | 946 | 852 | 724 | 933 | 950 | 924 | 925 | 1311 |
| June | 707 | 1116 | 800 | 303 | 826 | 899 | 1039 | 654 |
| July | 1002 | 866 | 820 | 912 | 1091 | 967 | 788 | 675 |
| August | 901 | 1235 | 985 | 1490 | 904 | 1487 | 773 | 1583 |
| September | 670 | 795 | 704 | 1122 | 847 | 964 | 927 | 1444 |
| October | 825 | 758 | 1029 | 423 | 1042 | 870 | 957 | 643 |
| November | 743 | 903 | 530 | 1274 | 846 | 1059 | 906 | 1301 |
| December | 747 | 822 | 522 | 1093 | 864 | 932 | 869 | 1025 |

TABLE 7.36
Annual Water Demand for Planning Horizon

| | Year | | | |
|--------------------|-------|-------|-------|-------|
| | 2020 | 2025 | 2035 | 2040 |
| Water Demand (MCM) | 137.5 | 156.3 | 181.3 | 212.5 |

TABLE 7.37
Initial Investment and Capacity of Well Field Development

| Well Field Development Project | Capital Costs (\$10 ⁶) | Capacity (MCM) |
|--------------------------------|------------------------------------|----------------|
| A | 2 | 15 |
| B | 3 | 20 |
| C | 1.5 | 10 |
| D | 5 | 25 |

supply 80% of the water demand in each year. Three projects are studied in order to supply the demands of this area. Considering the cost of each project given in [Table 7.37](#) and the 6% rate of return, find the optimal sequence of implementing the groundwater projects using linear programming.

- 7.3 Assume that there are six alternatives to select from for improving a groundwater system, there are two constraints including the groundwater table fluctuation and supplying the minimum water demand. Two objective functions are considered including maximizing the annual groundwater yield and minimizing the costs. The membership values for all the alternatives with respect to the constraints and objectives are given in [Table 7.38](#).
- 7.4 Assume that a central authority in an irrigation district has the authority to allocate the groundwater so as to maximize the net return from the agricultural production. The district is also responsible for determining the optimal cropping pattern for the region, the amount of acreage devoted to the various

TABLE 7.38
Membership Values in Fuzzy Decision

| | Alternatives | | | | | |
|-------------|--------------|------|------|------|-----|------|
| | 1 | 2 | 3 | 4 | 5 | 6 |
| μ_{G_1} | 0.8 | 0.65 | 0.7 | 0.9 | 0.9 | 0.85 |
| μ_{G_2} | 0.75 | 0.72 | 0.69 | 0.8 | 0.8 | 0.9 |
| μ_{C_1} | 0.7 | 0.68 | 0.65 | 0.75 | 0.8 | 0.8 |
| μ_{C_2} | 0.81 | 0.8 | 0.6 | 0.85 | 0.6 | 0.95 |

crops in the area. Develop an optimization model to determine the optimal groundwater extraction pattern and the economic trade-offs associated with increasing the pumping capacity or reducing the head lower restriction.

- 7.5 Consider an aquifer with subsidence due to the overextraction of the groundwater. Develop an optimization model for the subsidence control at the critical points.
- 7.6 Consider an aquifer with the excessive groundwater pumping as shown in [Figure 7.59](#). Develop an optimization model to generate the pumping strategies that reverse the intrusion of saltwater while continuing to meet the demands for fresh water.
- 7.7 Consider an aquifer that discharges to a river under steady flow conditions. Two water supply wells are to be operated in a way to maximize the total rate of the water withdrawal under steady conditions and minimize the amount of water that is drawn from the river. Develop an optimization model to find the pumping strategies.
- 7.8 Assume the net benefits of the withdrawal from three wells are $f_1 = 6x_1 - x_1^2$, $f_2 = 7x_2 - 1.5x_2^2$, and $f_3 = 8x_3 - 0.5x_3^2$, respectively. If the allowed total withdrawal from the aquifer is subject to 8 MCM, and at least 2 MCM needs to be removed for the environmental water requirement, find the optimal withdrawal from each well to maximize the net benefits using dynamic programming.
- 7.9 The annual water demand of 50 MCM needs to be supplied. In a region, the water is withdrawn from a river and a well. The cost of removing the water from the well is \$0.5 per MCM per meter of lift, and the cost for the water allocation from the river is \$35 per MCM. The minimum depth to the water in the well is 50 m, and the well depth is such that it is not possible to extract water below a depth of 90 m. The recharge to the aquifer is 10 MCM, and due to 1 MCM of storage removal, the water level decreases one meter. If the interest rate is 6 percent, develop an optimization model to minimize the costs during 3 years of the planning horizon. Solve it using dynamic programming.
- 7.10 Find the maximum net benefit of the water withdraw from an aquifer as a function of $f(x) = 2x - x^2$ in the $[0,2]$ interval using the genetic algorithm.

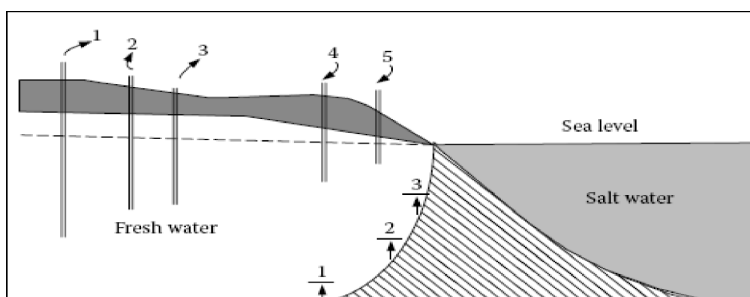


FIGURE 7.59 The salt water intrusion in Problem 7.6.

TABLE 7.39
The Costs of Considered Three Projects

| Costs | Timing | Project A | Project B | Project C |
|---------------------------------|-------------|-------------|-------------|-------------|
| Initial investment | Year 0 | \$2,000,000 | \$1,000,000 | \$1,500,000 |
| | Year 10 | 0 | \$1,000,000 | \$1,200,000 |
| | Year 20 | 0 | \$1,000,000 | 0 |
| Operation and Maintenance costs | Years 1–10 | \$7,000 | \$4,000 | \$6,000 |
| | Years 10–20 | \$8,000 | \$7,000 | \$8,000 |
| | Years 20–25 | \$9,000 | \$9,000 | \$9,000 |

TABLE 7.40
The Characteristics of Considered Projects

| | Project A | Project B |
|---------------------|-----------|-----------|
| Capital investment | \$160,000 | \$240,000 |
| Annual revenues | \$80,000 | \$112,000 |
| Annual expenses | \$35,200 | \$68,800 |
| Useful life (years) | 8 | 12 |

- 7.11** The three alternatives described above are available for supplying a community water supply for the next 25 years when the economic lives and the period of analysis terminates. Using the costs presented in Table 7.39 and a 5 percent discount rate, compare the three projects with the present worth method.
- 7.12** The two alternatives including improving the irrigation efficiency and the well development in a region are available for supplying a community water supply for the next 15 years. Using the costs presented in Table 7.40, compare the three projects with the present worth method.

REFERENCES

- Ahlfeld, D.P., Mulvey, J.M., Pinder, G.F., and Wood, E.F. 1988. Contaminated groundwater remediation design using simulation, optimization and sensitivity theory, 1. Model development. *Water Resources Research*, 24(5), 431–441.
- Ahmad, S. and Simonovic, S.P. 2000. Modeling reservoir operations using system dynamics. *Journal of Computing in Civil Engineering*, 14(3), 190–198.
- Akhbari, M. and Grigg, N.S. 2013. A framework for an agent-based model to manage water resources conflicts. *Journal of Water Resources Management*, 27(11), 4039–4052. doi: 10.1007/s11269-013-0394-0.
- Akhbari, M. and Grigg, N.S. 2015. Managing water resources conflicts: Modelling behavior in a decision tool. *Water Resources Management*, 29(14), 5201–5216. doi: 10.1007/s11269-015-1113-9.

- Au, T. and Au, T.P. 1983. *Engineering Economics for Capital Investment Analysis*, Allyn and Bacon, Boston, MA, 540 p.
- Bandini, S., Manzoni, S., and Vizzari, G. 2009. Agent based modeling and simulation: An informatics perspective. *The Journal of Artificial Societies and Social Simulation*, 12(4), <http://jasss.soc.surrey.ac.uk/12/4/4.html>.
- Baron-Cohen, S., Jolliffe, T., Mortimore, C., and Robertson., M. 1997. Another advanced test of theory of mind: Evidence from very high functioning adults with autism or Asperger syndrome. *Journal of Child Psychology and Psychiatry, and Allied Disciplines*, 38(7), 813–822.
- Bellman, R.E. and Zadeh, L.A. 1970. Decision making in a fuzzy environment. *Journal of Management Science*, 17, 141–164.
- Berglund, E.Z. 2015. Using agent-based modeling for water resources planning and management. *Journal of Water Resources Planning and Management*, 141(11), [https://doi.org/10.1061/\(ASCE\)WR.1943-5452.0000544](https://doi.org/10.1061/(ASCE)WR.1943-5452.0000544).
- Buras, N. 1966. Dynamic programming in water resources development. *Journal of Advances in Hydroscience*, 3, 367–412.
- Burt, O.R. 1964. The economics of conjunctive use of groundwater and surface water. *Hilgardia*, 3, 31–111.
- Castilla-Rho, J.C., Mariethoz, G., Rojas, R., Andersen, M.S., and Kelly, B.F.J. 2015. An agent-based platform for simulating complex human: Aquifer interactions in managed groundwater systems. *Environmental Modelling & Software*, 73, 305–323.
- Chang, L.C., Shoemaker, C.A., and Liu, P.L.-F. 1992. Optimal time-varying pumping rates for groundwater remediation: Application of a constrained optimal control theory. *Water Resources Research*, 28(12), 3157–3174.
- Coulibaly, P., Anctil, F., and Bobe, E.B. 2001. Multivariate reservoir inflow forecasting using temporal neural networks. *Journal of Hydrologic Engineering ASCE*, 6(5), 367–376.
- Culver, T.B. and Shoemaker, C.A. 1992. Dynamic optimal control for groundwater remediation with flexible management periods. *Water Resources Research*, 28(3), 629–641.
- DeGarmo, E.P., Sullivan, W.G., Bontadelli, J.A., and Wicks, E.M. 1997. *Engineering Economy*, Prentice-Hall, Upper Saddle River, NJ, 647 p.
- Delaware Department of Human Resources. 2018. *Preparing for the Conflict Resolution Process What to Expect*. <https://dhr.delaware.gov/training/conflict/documents/conflict-resolution-process.pdf>.
- Delleur, J.W. 1999. *The Handbook of Groundwater Engineering*, CRC Press/Springer-Verlag, Boca Raton, FL, 992 p.
- Demuth, H. and Beale, M. 2002. *Neural Network Toolbox for MATLAB, User's Guide*. <http://www.mathworks.com/>.
- Dougherty, D.E. and Marryott, R.A. 1991. Optimal groundwater management 1. Simulated annealing. *Water Resources Research*, 27(10), 2493–2508.
- Egles, R.W. 1990. Simulated annealing: A tool for operational research. *European Journal of Operational Research*, 46, 271–281.
- Elman, J.L. 1990. Finding structure in time. *Cognitive Science*, 14, 179–211.
- Fang, L., Hipel, K.W., and Kilgour, D.M. 1989. Conflict models in graph form: Solution concepts and their interrelationships. *European Journal of Operational Research*, 41(1), 86–100.
- Fauset, L.V. 1994. *Fundamentals of Neural Networks, Architecture, Algorithms, and Application*, Prentice Hall, Upper Saddle River, NJ, 461 p.
- Field, B.C. 1997. *Environmental Economics: An Introduction*, McGraw-Hill, New York.
- Fransconi, P., Gori, M., and Soda, G. 1992. Local feedback multilayered networks. *Neural Computation*, 4, 120–130.
- Goldberg, D.E. 1989. *Genetic Algorithms in Search, Optimization, and Machine Learning*, Addison-Wesley, Reading, MA, 412 p.

- Hartnett, T. 2018. *Consensus Facilitation: Generating Widespread Agreement: Consensus & Unanimity*. <http://groupfacilitation.net/Articles for Facilitators/Consensus & Unanimity.html> (December 19, 2018).
- Holland, J. 1975. *Adaptation in Natural and Artificial Systems*, The University of Michigan Press, Ann Arbor, MI, 228 p.
- James, L.D. and Lee, R.R. 1971. *Economics of Water Resources Planning*, McGraw-Hill, New York, 640 p.
- Jordan, M.I. 1986. Attractor dynamics and parallelism in a connectionist sequential machine. *8th Annual Conference*, August 15–17, Cognitive Science Society, MIT Press, Amherst, MA, pp. 531–546.
- Karamouz, M., Kerachian, R., and Moridi, M. 2004. Conflict resolution in water pollution control in urban areas: A case study. In *Proceeding of the 4th International Conference on Decision Making in Urban and Civil Engineering*, Porto, Portugal, October 28–30, 2004.
- Karamouz, M., Akhbari, M., and Moridi, A. 2011. Resolving disputes over reservoir-river operation. *Journal of Irrigation and Drainage Engineering*, ASCE, 137(5), 327–339. doi: 10.1061/(ASCE)IR.1943-4774.0000292.
- Karamouz, M., Akhbari, M., Kerachian, R., and Moridi, A. 2006. A system dynamics-based conflict resolution model for river water quality management. *Iranian Journal of Environmental Health Science and Engineering*, 3(3), 147–160.
- Karamouz, M., Moridi, A., and Nazif, S. 2005. Development of an object oriented programming model for water transfer in Tehran metropolitan area, in *Proceedings of the 10th International Conference on Urban Drainage*, Copenhagen, Denmark, June 10–13.
- Karamouz, M., Moridi, M., and Nazif, N. 2010. *Urban Water Engineering and Management*, CRC Press, Boca Raton, FL, 602 p.
- Karamouz, M., Razavi, S., and Araghinejad, S.H. 2007. Long-lead seasonal rainfall forecasting using time-delay recurrent neural networks: A case study. *Journal of Hydrological Processes*, 22(2), 229–238.
- Karamouz, M., Szidarovszky, F., and Zahraie, B. 2003. *Water Resources Systems Analysis*, Lewis Publishers, Boca Raton, FL, 590 p.
- Kelly, R.A. et al. 2013. Selecting among five common modelling approaches for integrated environmental assessment and management. *Environmental Modelling & Software*, 47, 159–181.
- Kresic, N. 2009. *Groundwater Resources: Sustainability, Management, and Restoration*, McGraw-Hill, New York, 852 p.
- Lefkoff, L.J. and Gorelick, S.M. 1987. AQMAN: Linear and quadratic programming matrix generator using two-dimensional groundwater flow simulation for aquifer Management Modeling. *U.S. Geological Survey Water Resources Investigations Report*, 87(4061), 7–94.
- Macal, C.M. and North, M.J. 2006. Tutorial on agent-based modeling and simulation part 2: How to model with agents. *Proceedings of the 2006 Winter Simulation Conference*, Vols. 1–5, pp. 73–83. doi:10.1109/Wsc.2006.323040.
- Macy, M.W. and Willer, R. 2002. From factors to actors: Computational sociology and agent-based modeling. *Annual Review of Sociology*, 28(2002), 143–166.
- Madani, K. and Hipel, K.W. 2011. Non-cooperative stability definitions for strategic analysis of generic water resources conflicts. *Water Resources Management*, 25(8), 1949–1977.
- McKinney, D.C. and Lin, M.D. 1995. Approximate mixed-integer nonlinear programming methods for optimal aquifer remediation design. *Water Resources Research*, 31(3), 731–740.
- Metropolis, N., Rosenbluth, A., Rosenbluth, M., Teller, A., and Teller, E. 1953. Equation of state calculations by fast computing machines. *Journal of Chemical Physics*, 21, 1087–1092.

- Nazari, S., Ahmadi, A. 2019. Non-cooperative stability assessments of groundwater resources management based on the tradeoff between the economy and the environment. *Journal of Hydrology*, 578, 124075.
- Ohab Yazi, S.A. and Ahmadi, A. 2018. Using the agent-based model to simulate and evaluate the interaction effects of agent behaviors on groundwater resources, a case study of a sub-basin in the Zayandehroud River basin. *Simulation Modelling Practice and Theory*, 87, 274–292.
- ReVelle, C. and McGarity, A.E. eds., 1997. *Design and Operation of Civil and Environmental Engineering Systems*, John Wiley & Sons, New York, 752 p.
- Selbirkak, T. 1994. Some concepts of non-myopic equilibria in games with finite strategy sets and their properties. *Annals of Operations Research*, 51(2), 73–82.
- StatSoft has freely provided the *Electronic Statistics Textbook* as a public service since 1995.
- Sterman, J.D. 2000. *Business Dynamics: Systems Thinking and Modeling for a Complex World*, McGraw-Hill, Boston, MA.
- Sun, M. and Zheng, C. 1999. Long-term groundwater management by a MODFLOW based dynamic groundwater optimization tool. *Journal of AWRA*, 35(1), 99–111.
- Szidarovszky, F., Gershon, M., and Duckstein, L. 1986. *Techniques of Multi-Objective Decision Making in Systems Management*, Elsevier, Amsterdam, the Netherlands.
- Todd, D.K. 1980. *Groundwater Hydrology*, John Wiley & Sons, New York, 535 p.
- Wagner, B.J. and Gorelick, S.M. 1987. Optimal groundwater quality management under parameter uncertainty. *Water Resources Research*, 23(7), 1162–1174.
- Wang, M. and Zheng, C. 1998. Application of genetic algorithms and simulated annealing in groundwater management: Formulation and comparison *Journal of American Water Resources Association*, 34(3), 519–530.
- Willis, R. and Yeh, W.W.-G. 1987. *Groundwater Systems Planning and Management*, Prentice Hall, Englewood Cliffs, NJ, 416 p.
- Willis, R.L. 1976. Optimal groundwater quality management, well injection of waste waters. *Water Resources Research*, 12, 47–53.
- Willis, R.L. 1979. A planning model for the management of groundwater quality. *Water Resources Research*, 15, 1305–1313.
- Wolf, A.T. 2008. Healing the enlightenment rift: Rationality, spirituality and shared waters. *Journal of International Affairs*, 6, 51–73. doi:10.1007/s11069-006-9094-x.
- Wolf, A.T. 2002. *Conflict Prevention and Resolution in Water Systems*, Edward Elgar Publishing Limited, Cheltenham, UK.
- Woolley, A.W. et al. 2010. Evidence for a collective intelligence factor in the performance of human groups. *Science*, 330(6004), 686–688.
- Yakowitz, S. 1982. Dynamic programming applications in water resources. *Water Resources Research*, 18, 673–696.
- Yeh, W.W.-G. 1986. Review of parameter identification procedures in groundwater hydrology: The inverse problem. *Water Resources Research*, 22(1), 95–108.
- Yeh, W.W.-G. 1992. System analysis in groundwater planning and management. *Journal of Water Resources Planning and Management*, 118(3), 224–237.
- Zimmermann, H.J. 1978. Fuzzy programming and linear programming with several objective functions. *Journal of Fuzzy Sets and System*, 1, 45–55.



Taylor & Francis

Taylor & Francis Group

<http://taylorandfrancis.com>

8 Surface Water and Groundwater Interaction

8.1 INTRODUCTION

Surface and groundwater systems are in continuous dynamic interaction. They are the two components of a hydrological cycle that are not isolated from the interaction. Surface water and groundwater resources are traditionally managed as independent systems. This can lead to over-allocation of resources and adverse environmental impacts. Development of land and water resources affects the quantity and quality; therefore, understanding the connectivity between surface water and groundwater systems is required to plan and manage surface water and groundwater resources accordingly.

Effective policies and management practices should be proposed based on a foundation that recognizes that surface water and groundwater are simply two components of a single integrated resource. The river basin can be considered as a unit for analyzing the interactions and interrelations between the various components of the hydrologic system and for practicing the water management policy. Due to increasing concerns over water resources and the environment, considering groundwater and surface water as a single resource has become important.

Watershed planners formulate and practice water management strategies to integrate important issues such as water resource conservation, economical, social, environmental, water resource allocation, and water demand management. Issues related to water supply, water quality, and degradation of aquatic environments can be practiced.

One of the strategies of water supply management is the conjunctive use of surface and groundwater. It is applied to optimize the water resources development, management, and conservation within a watershed. The conjunctive use is the application of programming techniques for optimum utilization of water resources on a regional scale. The artificial recharge of aquifers is also used effectively for water resources development.

In this chapter, for a better understanding of the river-aquifer systems, the interaction of surface and groundwater, followed by the conjunctive water use, and, finally, conjunctive use modeling with some examples and case studies are explained.

8.2 INTERACTION BETWEEN SURFACE AND GROUNDWATER

The water that flows directly on top of the ground is called surface water such as streams, lakes, springs, and reservoirs. The overland flow can be generated when the rate of rainfall exceeds the infiltration capacity of the soil.

Most of this water returns to the stream at the sharp steps to sustain flows during extended dry periods. In the following, the infiltration is discussed as the process for groundwater and surface water.

8.2.1 INFILTRATION

The source of surface water for groundwater recharge is infiltration of precipitation through the unsaturated zone. Rainwater chemistry, soil chemistry, vegetated land, soil moisture, and hydraulic conductivity are effective in soil infiltration. The unsaturated zone consists of soil, air, and water that control the infiltration rates. Groundwater flow quantifying in this zone is more complicated than in the saturated zone. Water seeps from the surface into the subsurface depending upon the gravity and moisture potential, which are called hydraulic and pressure heads, respectively. Moisture potential varies with the moisture content and pore size of the medium. The total potential h in unsaturated flow is the summation of moisture potential $\psi(\theta)$ and gravity potential Z .

Any change in the infiltration rate requires a change in moisture content θ . Regarding the infiltration in the unsaturated zone, which is controlled by moisture potential $\psi(\theta)$ as well as hydraulic conductivity $K(\theta_v)$, Richards equation is used to describe the 1D flow in the unsaturated zone:

$$\frac{\partial}{\partial z} \left[K(\theta_v) \left(\frac{\partial h}{\partial z} \right) \right] = \frac{\partial \theta}{\partial t} \quad (8.1)$$

$$\frac{\partial}{\partial z} \left[K(\theta_v) \left(\frac{\partial \psi}{\partial z} + \frac{\partial z}{\partial z} \right) \right] = \frac{\partial \theta}{\partial t} \quad (8.2)$$

Based on Richard equation, a decrease in the moisture potential decreases cumulative infiltration. When the moisture potential approaches zero, the infiltration rate decreases to a rate equivalent to saturated vertical hydraulic conductivity, K_v . The infiltration rate is shown in [Figure 8.1](#). The moisture content of the soil controls the initial infiltration capacity f_0 . The saturated vertical hydraulic conductivity of the soil K_v controls the final infiltration capacity.

8.2.2 CONCEPTS OF INTERACTION BETWEEN SURFACE WATER AND GROUNDWATER

The interaction between streams and groundwater and the direction of flow are controlled based on the seasonal conditions. Groundwater discharges to the stream when the hydraulic gradient of the aquifer is toward the stream and the stream is a gaining or effluent stream. [Figure 8.2](#) shows the gaining streams receive water from the groundwater system.

A stream loses water to groundwater by outflow through the streambed when the hydraulic gradient of the aquifer is away from the stream and the stream is losing or

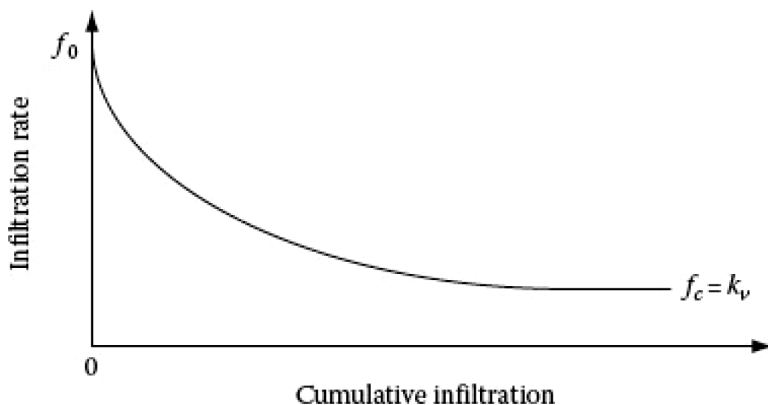


FIGURE 8.1 Infiltration capacity curve. (From U.S. Army Corps of Engineers, *Engineering and Design, Groundwater Hydrology*, Department of the Army, Washington, DC, 1999.)

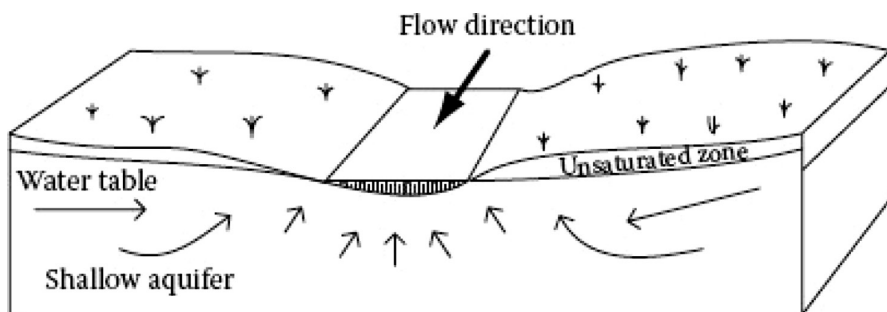


FIGURE 8.2 Groundwater discharges to the stream. (From Winter et al., *Ground Water and Surface Water: A Single Resource*, USGS (U.S. Geological Survey), Denver, CO, 1998.)

influent. The depth of water and the hydraulic gradient are the effective factors on the interaction flow. [Figure 8.3](#) shows the losing streams lose water to the groundwater system.

In some conditions, the flow direction can vary on two sides of a stream—one side receives groundwater, while the other side loses water to groundwater. In some environments, the flow direction can vary along a stream; some reaches receive groundwater or lose water to groundwater, or the reach loses or gains water at different times of the year.

Losing streams can be connected to groundwater by a continuous saturated zone directly, as shown in [Figure 8.3](#), or it may be disconnected from the groundwater system by an unsaturated zone. In this case, the water seeps through a streambed of streams to a deep water table, as illustrated in [Figure 8.4](#).

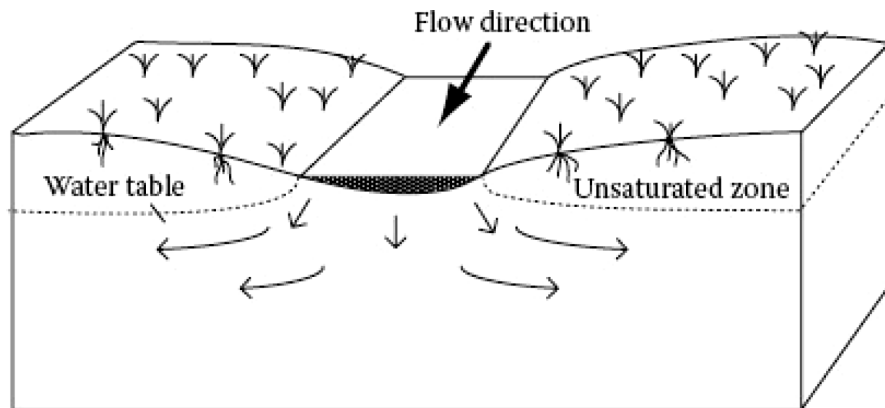


FIGURE 8.3 Stream loses water to groundwater. (From Winter et al., *Ground Water and Surface Water: A Single Resource*, USGS (U.S. Geological Survey), Denver, CO, 1998.)

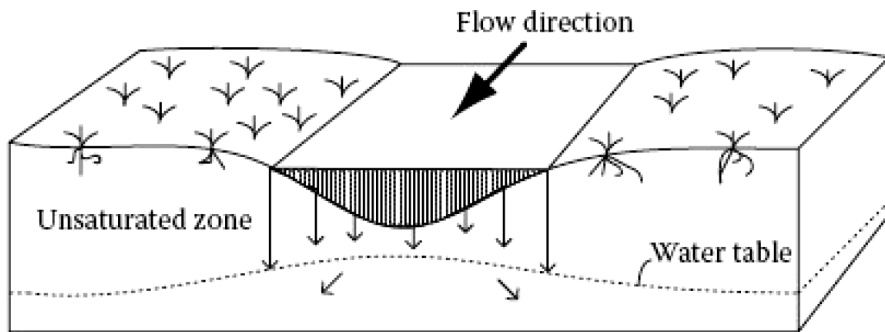


FIGURE 8.4 Disconnected streams. (From Winter et al., *Ground Water and Surface Water: A Single Resource*, USGS (U.S. Geological Survey), Denver, CO, 1998.)

In order to assess the interaction between a stream and the groundwater, it is assumed that water moves vertically through the streambed. The rate of flow between the stream and the aquifer can be estimated based on Darcy's equation:

$$q = -KLWi \quad (8.3)$$

where:

K is the vertical hydraulic conductivity of the streambed

L is the length of the stream reach over which seepage is assessed

W is the average width of the stream over the reach

i is the hydraulic gradient between the stream and the groundwater, which can be defined as:

$$i = \frac{h_{\text{aquifer}} - h_{\text{stream}}}{M} \quad (8.4)$$

where:

- h_{aquifer} is the elevation of the groundwater
- h_{stream} is the elevation of the stream water surface
- M is the thickness of the streambed.

8.2.3 BANK STORAGE AND BASEFLOW RECESSION

A rapid rise in stream stage in nearly all streams generates another type of interaction between groundwater and streams. A period of high flows, such as floods, release from a dam, storm precipitation, and rapid snowmelt may cause tremendous amounts of water to flow from the stream into the streambanks (see [Figure 8.5](#)). This flow will contribute seepage through the streambed to the underlying water table, thus saturating the depleted stream-side deposits. It may require a few days or weeks of high flow to replenish the groundwater reservoirs and for the streambanks to return to the stream.

The rising and recession limbs of a hydrograph are generated in a rapid rise in stream stage. Discharge during this decay period is due to the groundwater contributions as the stream drains water from the declining groundwater reservoir. The baseflow recession is the lower part of the falling limb. Since the baseflow is principally groundwater effluent, the baseflow recession curves represent a withdrawal from groundwater storage. This baseflow recession for a drainage basin is the function of the overall topography, drainage patterns, soils, and geology of the watershed.

The term hydrograph separation refers to the process of separating the time distribution of baseflow from the total runoff hydrograph. The baseflow recession equation is:

$$Q = Q_0 e^{-at} \quad (8.5)$$

where:

- Q is the flow at time t in recession limbs of a hydrograph
- Q_0 is the flow at the start of the recession (m^3/s)
- a is the recession constant for the watershed
- t is the time from the start of the recession.

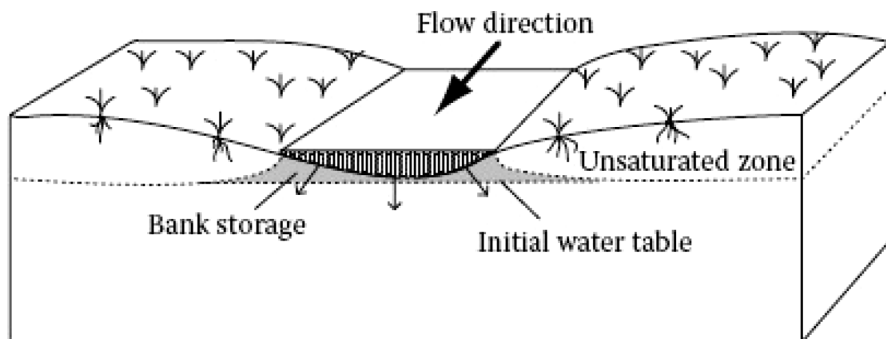


FIGURE 8.5 Movement of water into stream banks as bank storage. (From Winter et al., *Ground Water and Surface Water: A Single Resource*, USGS (U.S. Geological Survey), Denver, CO, 1998.)

Initially, the rate of bank storage discharge is high because of the steep water-level gradient, but as the gradient decreases, so does the groundwater runoff. The recession segment of the stream hydrograph gradually tapers off into what is called a depletion curve. There are some methods for hydrograph separation such as the master-depletion curve method, constant-discharge baseflow separation, constant-slope baseflow separation, and concave-baseflow separation. This method needs some hydrographs for different events in the watershed. If adequate data are not available, then other separating hydrograph methods are used.

8.2.3.1 Master-Depletion Curve Method

Depletion curves are plotted as a combination of several arcs of recession limbs of hydrographs with overlapping in their lower parts. In order to plot the master-depletion curve, a hydrograph is plotted on a tracing paper, which is a semilog paper. Then, another hydrograph is plotted on the tracing paper, which is moved horizontally until the arc coincides in its lower part with the arc already traced. The process is continued until all the available arcs are plotted.

Example 8.1

The lower parts of five hydrographs are presented in [Table 8.1](#). Find the master-depletion curve for the watershed.

SOLUTION

Using semilog paper, $\log Q$ versus time, the recession curves are plotted as shown in [Figure 8.6](#). In plotting the figure, the recession curve for the smaller storm is plotted, and then the recession curve for the next event with a larger magnitude of Q is plotted; hence, the master-depletion curve appears to extend along a line coincident with the recession curve of the first event.

TABLE 8.1
The Lowering Parts of Five Hydrographs

| Time | Storm 1 | Storm 2 | Storm 3 | Storm 4 | Storm 5 |
|------|---------|---------|---------|---------|---------|
| 1 | 36.7 | 27.92 | 83 | 14.25 | 8.93 |
| 2 | 29 | 23.6 | 15.34 | 8.6 | 5.43 |
| 3 | 23.7 | 19.32 | 10.28 | 6.69 | 4.24 |
| 4 | 20.7 | 16.67 | 8.49 | 5.68 | 3.91 |
| 5 | 17.7 | 14.29 | 7 | 4.94 | 3.46 |
| 6 | 14.38 | 12.16 | 5.9 | 4.32 | 2.86 |
| 7 | 12.88 | 10.71 | 5.43 | 3.82 | 2.52 |
| 8 | 11.64 | 9.33 | 5 | 3.38 | 2.3 |
| 9 | 10.52 | 8.22 | 4.8 | 3 | 2.1 |
| 10 | 10 | 6.95 | 4.6 | 2.9 | 2.05 |
| 11 | 9 | 6.3 | 4.5 | 2.8 | 2 |
| 12 | 8.7 | 6.1 | 4.46 | 2.7 | |
| 13 | 8.5 | 6 | 4.35 | | |

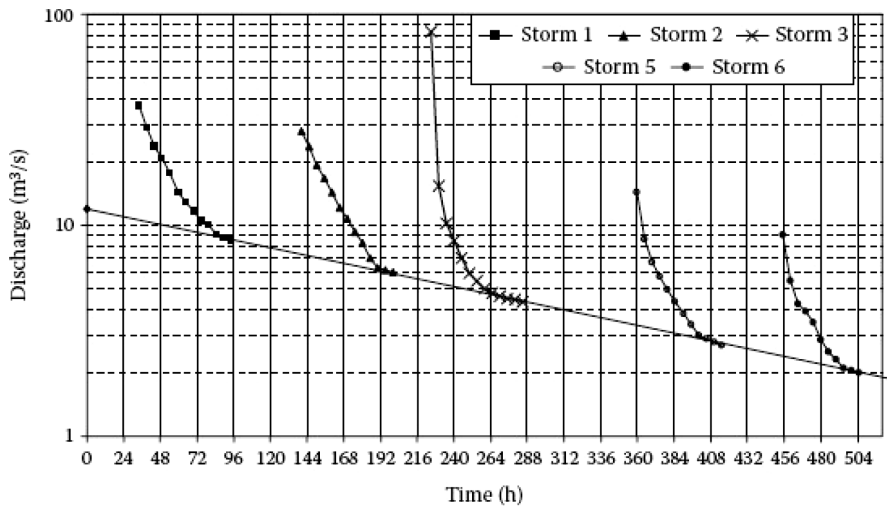


FIGURE 8.6 Master-depletion curve using recessions of five storms events.

The master-depletion curve is constructed in such a way that it extends through the recessions of the observed events. This curve is presented by the form of Equation 8.5 using any two points. With points $t = 0$, $Q_0 = 12$, and $t = 528$, $Q_t = 1.85$, the recession constant for the watershed is calculated using Equation 8.5 as follows:

$$1.85 = 12e^{-a(528-0)}; \quad a = 0.00354$$

So, the form of a master-depletion curve for the watershed is:

$$Q = 12e^{-0.00354t}$$

8.2.3.2 Seasonal Recession Method (Meyboom Method)

The Meyboom method is an easy way to estimate groundwater recharge in a basin, which incorporates stream hydrographs of two or more consecutive years. In this method, the groundwater recharge between two consecutive baseflow recessions is equal to the difference between the total potential groundwater discharge at the beginning and the remaining of the recession. Throughout a complete groundwater recession, the total potential groundwater discharge is defined as the volume of water that would be discharged, which can be calculated from (Fetter, 2001; Meyboom, 1961):

$$V_{tp} = \frac{Q_0 t_1}{2.3026} \quad (8.6)$$

where

V_{tp} is the volume of the total potential groundwater discharge, m^3

Q_0 is the baseflow at the start of the recession, m^3/s

t_1 is the time that it takes the baseflow to go from Q_0 to $0.1Q_0$, s

After some time, t (s), from the start of a baseflow recession, the amount of remaining potential baseflow, V_t (m^3), is as follows:

$$V_t = \frac{V_{tp}}{10^{(t/t_1)}} \quad (8.7)$$

Example 8.2

Consider two consecutive baseflow recessions. For the first recession, Q_0 is 1000 m^3 and it lasts 8 months. As for the second recession, Q_0 is 850 m^3 . Determine the amount of groundwater recharge between the two recessions assuming that it takes 6 months for both of them to reach $0.1Q_0$.

SOLUTION

For the first recession,

$$V_{tp} = \frac{Q_0 t_1}{2.3026} = \frac{1000 \times 6 \times 30 \times 24 \times 60 \times 60}{2.3026} = 6.8 \times 10^9 \text{ m}^3$$

and

$$V_t = \frac{V_{tp}}{10^{(t/t_1)}} = \frac{6.8 \times 10^9}{10^{(8/6)}} = 3.2 \times 10^8 \text{ m}^3$$

For the second recession,

$$V_{tp} = \frac{850 \times 6 \times 30 \times 24 \times 60 \times 60}{2.3026} = 5.7 \times 10^9 \text{ m}^3$$

Hence,

$$\text{Recharge} = 5.7 \times 10^9 - 3.2 \times 10^8 = 5.4 \times 10^8 \text{ m}^3$$

8.2.3.3 Constant-Discharge Baseflow Separation

In this method, the line separating baseflow and direct runoff begins from a minimum value immediately prior to the beginning of storm hydrograph (A) to a constant-discharge rate until it intersects the recession limb of the hydrograph (B). This method is illustrated in [Figure 8.7](#), which is easy to apply.

8.2.3.4 Constant-Slope Baseflow Separation

This method allows the estimation of baseflow recession in streams with limited continuous data. The constant-slope method connects the start of the rising limb (A) to a point directly under the hydrograph peak with the same slope of the hydrograph starting line (C), and then extends to the point of end-of-surface runoff (D). Point D can be estimated by the following empirical equation:

$$N = 0.83A^{0.2} \quad (8.8)$$

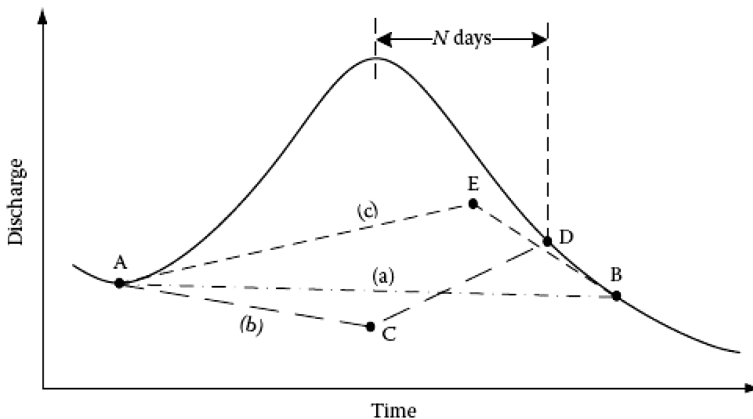


FIGURE 8.7 Graphics methods for separating the baseflow from direct runoff: (a) constant-discharge baseflow method, (b) constant-slope baseflow method, and (c) concave-baseflow method.

where:

N is the number of days after a peak when surface runoff ends

A is the watershed area (km^2).

In this method, it is assumed that the baseflow decreases in the rising limb due to the movement of water into streambanks as bank storage, and then increases in the recession limb.

8.2.3.5 Concave-Baseflow Separation

The concave method connects the start of the rising limb (A) to a point directly under the turning point of the hydrograph recession limb (E), and then extends to the point of end-of-surface runoff (B). Point E is derived by intersecting the vertical line from the turning point of the hydrograph recession limb and the extended backline of the recession curve.

Example 8.3

The observed discharges in a watershed outlet during a rainfall event are presented in [Table 8.2](#). The area of the watershed is about $20,000 \text{ km}^2$. Separate the baseflow from the direct runoff.

SOLUTION

Points A, B, C, D, and E are determined using graphical methods, which include the constant-discharge, constant-slope, and concave-baseflow separation methods as shown in [Figure 8.8](#). The number of days after a peak

TABLE 8.2
Watershed Flows During a Rainfall Event (m³/s)

| Time (Day) | 1 | 2 | 3 | 4 | 5 | 6 | 7 | 8 | 9 |
|--------------------------|------|------|------|------|------|------|------|------|------|
| Flow (m ³ /s) | 1200 | 1150 | 1350 | 1720 | 2200 | 2620 | 3200 | 2920 | 2510 |
| Time (Day) | 10 | 11 | 12 | 13 | 14 | 15 | 16 | 17 | |
| Flow (m ³ /s) | 2200 | 1850 | 1500 | 1320 | 1160 | 1060 | 1040 | 1030 | |

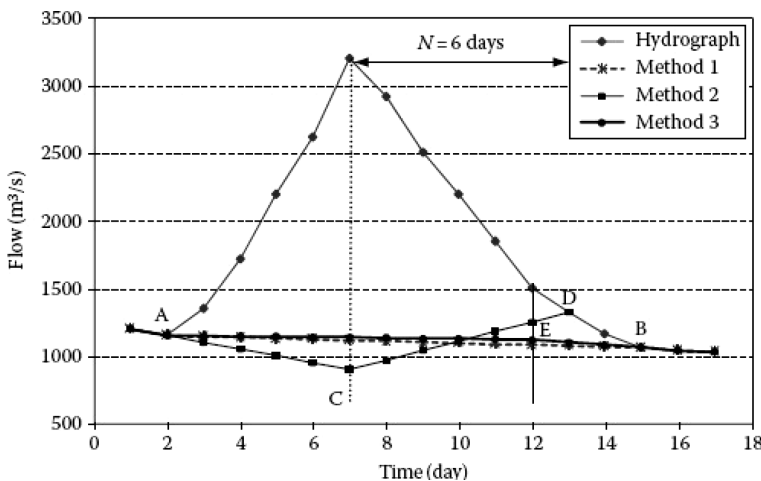


FIGURE 8.8 Illustration of base flow separation using three methods.

when surface runoff ends in the constant-slope method is calculated using Equation 8.8 as follows:

$$N = 0.83 \times 2000^{0.2} \approx 4 \text{ days}$$

The baseflow and the direct runoff in each method are presented in [Table 8.3](#).

8.2.4 GROUNDWATER AND LAKES

Groundwater interacts with lakes the same way as it interacts with streams. Lakes interact with the groundwater with a much larger surface water and bed area than streams. Due to sediments on the lake floor, the permeability of the lake bed is lower than that of streams. Lakes can receive groundwater inflow throughout their bed and have seepage loss throughout the lake bed, or they receive groundwater inflow in some parts of the bed and lose groundwater inflow in other parts. [Figure 8.9](#) shows the basic ways of groundwater and lakes interaction.

TABLE 8.3
The Direct Runoff Obtained from Three Methods (m³/s)

| Time (Days) | Method 1 | Method 2 | Method 3 |
|-------------|----------|----------|----------|
| 1 | 0 | 0 | 0 |
| 2 | 0 | 0 | 0 |
| 3 | 207 | 250 | 203 |
| 4 | 584 | 670 | 576 |
| 5 | 1071 | 1200 | 1059 |
| 6 | 1498 | 1670 | 1482 |
| 7 | 2085 | 2300 | 2065 |
| 8 | 1812 | 1950 | 1788 |
| 9 | 1408 | 1470 | 1381 |
| 10 | 1105 | 1090 | 1074 |
| 11 | 762 | 670 | 727 |
| 12 | 419 | 250 | 380 |
| 13 | 246 | 0 | 220 |
| 14 | 93 | 0 | 80 |
| 15 | 0 | 0 | 0 |
| 16 | 0 | 0 | 0 |
| 17 | 0 | 0 | 0 |

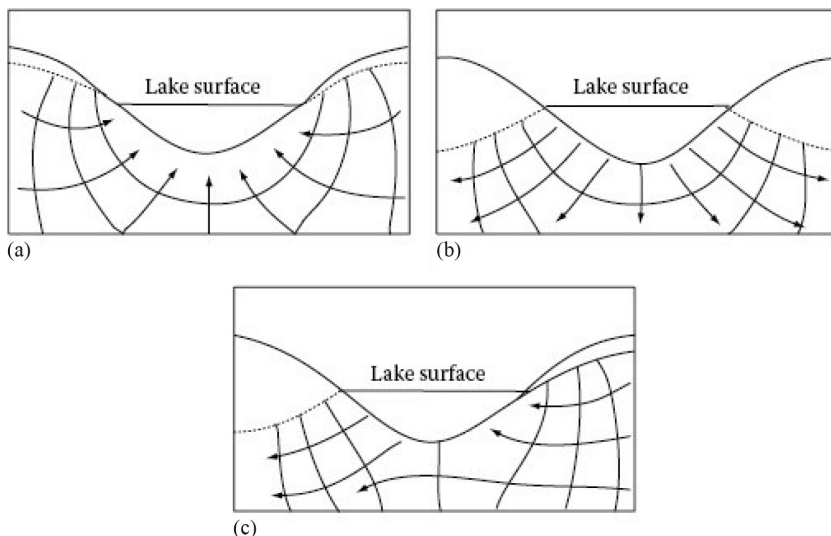


FIGURE 8.9 (a) Lakes receiving groundwater inflow; (b) lakes losing water as seepage to groundwater; or (c) both at the same time. (From Winter et al., *Ground Water and Surface Water: A Single Resource*, USGS (U.S. Geological Survey), Denver, CO, 1998.)

In order to estimate the effects of lakes, wetlands, or any surface water feature on groundwater, the same approach of the stream interaction can be applied.

8.3 CONJUNCTIVE USE OF SURFACE AND GROUNDWATER

In most climates around the world, precipitation and peak river discharge occur during particular months of the year, whereas crop irrigation water requirements are at their highest level during periods of low rainfall. This is when unregulated stream flows are significantly low, which would place more reliance on groundwater. Irrigation water supply is aligned with crop water requirements and is provided through the construction and management of dams which capture water during periods of high flow, enabling regulated releases to meet crop water requirements. However, the construction and operation of dams, and distribution of water from them, are inherently costly. Furthermore, dams and the associated distribution systems are commonly subject to high system losses through evaporation and leakage (though it is debatable whether the latter is actually detrimental given that it often contributes substantially to groundwater recharge), and they have social and ecological impacts on communities and the environments within which they are built. Conversely, under natural recharge regimes, aquifers serve as a natural distribution system, and groundwater storage requires no infrastructure. Under a sustainable extraction regime, groundwater of a suitable quality can provide a reliable source of water either as a sole supply of water or to supplement alternative sources. Commonly, a large storage to annual use ratio for regional aquifers means that the reliability of supply from groundwater is less affected by seasonal variations in surface water supplies and may indeed provide significant buffering against droughts. However, most intensively used groundwater systems (within the context of irrigation) exist in the semiarid parts of the world and are characterized by relatively low annual recharge. The ratio of annual use to long-term annual recharge becomes the predominant measure of sustainability for these systems, independent of aquifer storage. While being capable of providing a large storage and natural distribution system, aquifers are generally unable to capture a significant portion of runoff arising from large rainfall events. Aquifers, therefore, do not annually harvest water on a scale that justifies the construction and operation of centralized water delivery systems based on groundwater resources alone.

Water resources of surface water and groundwater are managed separately. However, surface water including streams, lakes, reservoirs, and wetlands interact with groundwater. Withdrawal of water from streams can deplete groundwater or, conversely, water in streams, lakes, or wetlands can be depleted by the pumping of groundwater. Also, pollution of surface water can cause degradation of groundwater quality and vice versa. Considering quantity and quality effects of development of one on the other and using an integrated water resources management approach for sustainable development, the surface water and groundwater should be managed simultaneously.

The conjunctive use of surface and groundwater consists of harmoniously combining the use of both sources of water in order to minimize the undesirable physical, environmental, and economical effects of each solution and to optimize the water

demand/supply balance. Surface water and groundwater are used simultaneously for planning the usage of water. It is applied to supply water demands and to the quality management of water resources for obtaining the sustainable development.

Surface water operations require reservoirs for water storage in suitable locations. But groundwater can be stored naturally in an aquifer without the need of storage construction. With the conjunctive use planning, water can be temporarily stored in the aquifers and water demand can be supplied from surface water. During water scarcity, water can be withdrawn to meet water demands. The characteristics and extent of the interactions of groundwater and surface water affect the success of such planning of the conjunctive use of surface and groundwater resources.

8.3.1 ADVANTAGES OF CONJUNCTIVE USE

The conjunctive use of surface and groundwater resources increases the management efficiency for supplying water by storing the existing water resources to supply future water demands. Groundwater resources can be considered as a reliable resource for supplying water demands. Usually, the periods of lowest streamflow and recharge coincide with the largest demand, or vice versa. Conjunctive water management could reduce the agricultural damages in dry periods. During wet periods, surface water can be utilized to supply the water demands and to recharge the aquifers. Generally, it could be a reliable alternative for water supply in the basin during all seasons. Also, using the groundwater resources for supplying the water demand can decrease the allocation streamflow volume that leads to the reduction in the construction costs of large-scale canals.

On the other hand, groundwater exploitation as a single water resource leads to groundwater depletion and inordinate fluctuations of the groundwater level. So, the conjunctive use can replenish aquifers in terms of quality and quantity. Conjunctive water management is utilized in many areas to assure the sustainable availability of water, particularly for the agricultural sector.

The justification of conjunctive use plans can be based on benefit/cost analysis. For this purpose, water balance and the hydrologic conditions in the plain are evaluated. The data for evaluation consist of land use, crop pattern, water demand, meteorological, and hydrologic conditions. Based on the analysis, surface and groundwater availability and water demand are determined. In order to evaluate the management plans in the case study, some scenarios are generated based on conjunctive use planning, and their impacts on water demand and supply are assessed. For this purpose, a watershed model is needed to simulate the scenarios in different hydrologic conditions, and then optimal policies for utilization of groundwater to conjunct with surface waters are developed. The optimal conjunctive water management strategies can be developed using simulation/optimization models. These models can help determine the best spatially distributed balance between using surface and underground water. They can be used for planning, management, and operations perspectives. Finally, benefits and costs of applying the generated scenarios are determined, and the best scenario for executive conjunctive use planning is selected based on benefits/costs analysis.

However, the best conjunctive water management involves satisfying hydrogeologic, technical, sociologic, ecologic, economic, and institutional constraints. Water laws and regulations can help conjunctive water management.

8.3.2 IMPEDIMENTS OF CONJUNCTIVE USE

Despite the many advantages of conjunctive use as explained in the final section, there are some drawbacks in its full development for urban water supply, especially in developing countries (World Bank, 2010):

- Frequent split responsibility for surface water and groundwater management (and development) between local (provincial or state) government, municipal authorities, and sometimes even involving the national government, resulting in failure to identify and to engineer opportunities for planned conjunctive use
- Lack of sound and intelligible information about conjunctive use opportunities, which can be provided to policymakers and the general public, because of the absence of an “Information and Communication Unit” at the level relevant to local water resource agencies
- Urban water engineers often tend to count only on operationally simple set-ups, such as a major surface water source and large treatment works, rather than more secure and robust conjunctive use solutions, and do not adequately appreciate the benefits which rational development of groundwater resources offer
- Urban water service utilities are often politically or institutionally constrained from proposing the development and protection of urban well fields in favorable areas (where high yields and good quality can be obtained), located outside the city’s municipal boundaries
- Inadequate understanding of the extent of private in-situ self-supply with groundwater from shallow aquifers, its benefits and hazards. The following paragraphs describe an example of irrigation with the conjunctive use of groundwater and surface water resources

8.3.3 CASE STUDY 1: CONJUNCTIVE USE OF SURFACE AND GROUNDWATER IN LAKHAOTI CANAL UTTAR PRADESH, INDIA

Foster et al. (2010) described the setting for the conjunctive use in Uttar Pradesh State in India, which is categorized as a humid, but drought-prone middle alluvial plain. The alluvial plains of the Ganges Valley (the Indo-Gangetic Plain) in Uttar Pradesh, India, are underlain by an extensive aquifer system holding groundwater that represents as much as 70% of overall irrigation water supply. This is one of the largest groundwater storage reserves in the world. Its use as a water resource has primarily increased in response to a reduction in surface water supply and unreliable operation of the irrigation canal systems. The aquifers are directly recharged from infiltrating monsoon rainfall, but also indirectly from canal leakage and low irrigation efficiency (i.e., excess rates of field application); a common source of aquifer

recharge in such hydrogeological settings. Increasing groundwater abstraction has resulted in a declining water table, especially in high intensity “groundwater exploitation zones,” whereas in other areas (in some cases within 10–20 km), flood irrigation and canal leakage have maintained shallow water tables. The decline in water tables in some areas is correlated with evidence of irrigation tube well dewatering, yield reduction, and heart failure, together with hand-pump failure in rural water-supply wells. On the other hand, threats arising from shallow water tables elsewhere are evident in around 20% of the land, and the area is subject to shallow or rising groundwater levels, with soil saturation and salinization leading to crop losses and even land abandonment (Foster et al., 2010).

Protocols for operation of the distributary canal system exist, but they have not been strictly adhered to in the past, and this has contributed to an imbalance in surface water delivery through the system. In light of the challenges posed by rising water tables in some areas, and declines elsewhere, in the Jaunpur Branch canal-command field in central Pradesh, a “more planned conjunctive-use approach” is being implemented. The adopted approach utilizes extensive datasets and associated analysis to understand the hydrogeological, agronomic, and socio-economic situation. Strategies include attempts to reduce leakage through the maintenance of bank sealing in major irrigation canals, enforcing current operational codes, promotion of tube well use in noncommand and high water table areas, investment into research and specialist extension in soil salinity mitigation, as well as sodic land reclamation.

Figure 8.10 depicts the maps of the Lakhota Branch Canal in Utter Pradesh, India. The darker areas show where groundwater levels are close to the surface. These natural

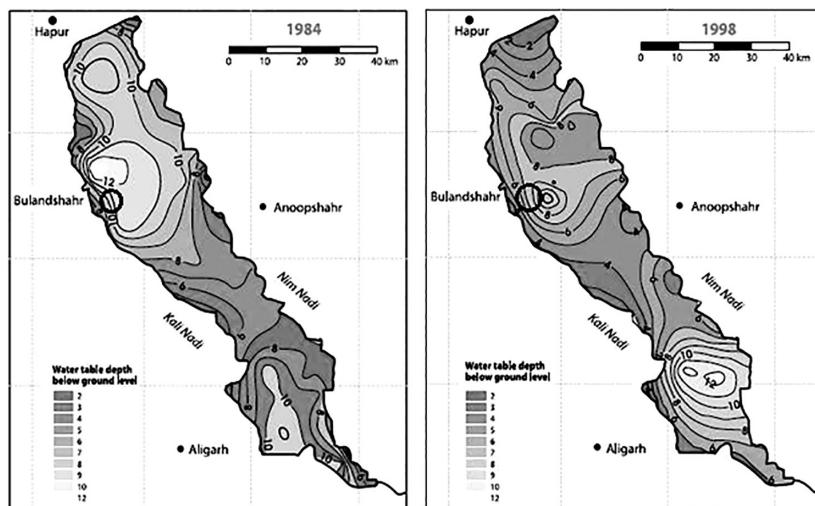


FIGURE 8.10 Comparison of water table depth before (1984) and after (1998) recharge, Lakhota Canal, Uttar Pradesh. (From IWMI, *IWMI-Tata Water Policy Briefing*, No. 1. Gujarat, India, 2002).

processes are being aligned with the pursuit of an appropriate management plan for which the land surface has been subdivided on the basis of hydrogeological and agroeconomic criteria into “micro-planning and management zones.” For each zone, a canal reach (e.g., head, mid, or tail) is designated with an indication of current irrigation canal flow and water table. The irrigation water service station, groundwater resource status, and groundwater management needs are then keyed out. This zoning approach allows targeted management actions that include encouragement of groundwater use in the head end of the irrigation systems where shallow groundwater levels prevail, focusing upon higher value crops in some fields, and improving canal water availability for those at the lower ends of the system. Jointly, these mechanisms are intended to provide a more balanced approach across the canal command (and beyond) and contribute to a sustainable future for agriculture in the region (Foster et al., 2010). [Figure 8.10](#) shows the beneficial changes in water table depth for one such targeted area. International Water Management Institute (IWMI, 2002) distinguished the situation for the western Indo-Gangetic Plain, where although rainfall ranges between 650 and 1000 mm annually, only 200 mm naturally percolates through soil layers to recharge underlying aquifers. In this area, like many others in India, groundwater pumping by farmers exceeds recharge (from rainfall, leakage from surface waters, e.g., canals and rivers, and application excess). Farmers are at the mercy of monsoon rains which can fail to provide water when and where it is required. The high concentration of rainfall, over a three-month period, means the majority of water runs off the already saturated soil. During the dry season, a lack of canal water means a reliance on pumping from groundwater storages which are not totally replenished from the previous year, resulting in further depletion of the aquifer system. A pilot project (the Madhya Ganga Canal Project) implemented in this area has demonstrated a low-cost way of utilizing the excess surface water during monsoon season to maintain and rejuvenate falling groundwater reserves. The project involved diversion of 234 m³/s of monsoon waters in the River Ganga to the Madhya Ganga Canal, which runs through both the Upper Ganga Canal system and the Lakhota Branch Canal system. Through systems of unlined (unsealed) earthen canals, water is delivered to farmers for irrigation of water-intensive monsoon crops such as paddy rice and sugarcane. The unlined nature of the canal systems and infiltration of excess irrigated water facilitates the recharge of underlying aquifers in which the water table was elevated from an average of 12 m below ground to an average of 6.5 m below ground. Simulations showed that without such a conjunctive management approach, levels would have proceeded to decline to an average depth of 18.5 m below ground over the course of the study.

The conjunctive management of surface water and groundwater has proved productive in terms of the average net income increasing by 26% through reductions in pumping costs and improved cropping systems. It has demonstrated a more sustainable organization through improved cropping patterns and more reliable and sometimes new (e.g., providing water in previously existing dry pockets) sources of water for irrigation and other uses, such as domestic or industrial supplies. During the dry season, drawdown from groundwater pumping prevents saturation and maximizes storage space for recharge during the next year’s monsoon. Unused (often lined) drainage canals constructed in the 1950s to control saturation and floods are also being targeted as a means for diverting monsoon waters across India either for irrigation, storage and later use, or recharge to underlying aquifers. Adjustment of

previously lined canals can aid their transformation into temporary reservoirs, where “check structures” at suitable intervals slow down water flow and increase the aquifer recharge capacity (IWMI, 2002).

In combination with the use of earthen irrigation canals, the use of old drainage networks can maximize water use and storage for a very low cost compared to establishing new infrastructure such as dams (IWMI, 2002).

8.3.4 SURFACE AND GROUNDWATER CONJUNCTIVE USE MODELING

The conjunctive water use model provides an optimal allocation schedule for surface and groundwater resources in a region to meet different water demands. Conjunctive water use planning should increase the efficiency, reliability, and cost-effectiveness of water use. The conjunctive water use can be simulated by coupled stream-aquifer models. In order to develop optimal policies, the conjunctive use planning can be formulated as an optimization model of the water resources system. The decision variables of the model are water allocations of the groundwater and surface in each planning period. The objective functions of the optimization model are to maximize the objectives of the water resource system while satisfying the hydraulic response equations of the surface and groundwater systems, and any constraints limiting the head variations and the surface water availability (Willis and Yeh, 1987).

The economic-based objective function of the optimization model can be considered as maximizing the net benefit of water use. The economic benefit can be achieved by the sale of the water to different sectors and sale of the agricultural and industrial productions due to water allocation. The costs include capital, operation, and maintenance to extract and convey the allocated water.

The objective function of conjunctive use planning can be as follows:

$$\text{Max } Z = \sum_{t=1}^T B_t - C_t \quad (8.9)$$

where:

$$B_t = f_{b_t}(GW_t, SW_t, D_t) \quad (8.10)$$

$$C_t = f_{c_t}(GW_t, SW_t) \quad (8.11)$$

where:

B_t is the total benefits of surface water (SW_t) and groundwater (GW_t) allocations generated through the revenue of water sale and benefit fraction from water productions, which is function (f_{b_t}) of surface water, groundwater, and water demands D_t in time t .

C_t is the total costs of surface water and groundwater allocations based on the costs of capital, operation, and maintenance, which is function (f_{c_t}) of surface water and groundwater volumes in time t .

The optimization model can be constrained by the continuity equation, the hydraulic response equations, possible limitations on river runoff, pumping discharge volume from groundwater, allocated water discharge volume from surface water, groundwater table fluctuations, and appropriate well pumping rates at each planning period. In order to prevent excessive groundwater overdraft or water logging of the agricultural areas of the basin, constraints can be introduced to limit the head variation in each aquifer system. The hydraulic head in the aquifers can be obtained utilizing the hydraulic response equations described in [Chapters 4](#) and [6](#). For a groundwater system, the response equations can be expressed functionally as:

$$h_t = f(h_{t-1}, GW_t, SW_t) \quad (8.12)$$

where h is hydraulic heads in a groundwater system at the period t . In recent years, more complex and user-friendly simulation packages have been used to develop and calibrate the groundwater response equations considering the principle of superposition.

The optimization model can be linked with the water head simulation model to obtain the optimal water allocation policies. Also, the water quality simulation model for a groundwater system can be utilized to evaluate the water allocation policies on the objective function. The structure of the optimization model, which is a nonlinear programming problem, can be developed based on target objective functions and the possible constraints in the study region.

Example 8.4

Develop a conjunctive use model to determine the optimal allocation of surface and groundwater in the river basin as shown in [Figure 8.11](#). There are two agricultural plains above unconfined aquifers A and B.

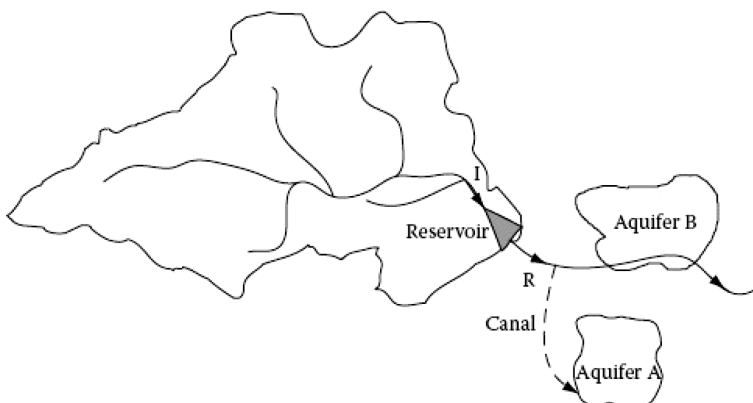


FIGURE 8.11 Schematic map of the problem river basin.

SOLUTION

Assuming that the system objective is to minimize the costs of surface water and groundwater allocation, the objective function optimization model is expressed by:

$$\begin{aligned} \text{Min } Z = & \sum_{t=1}^T f_{C_1}(GW_{At}) + f_{C_2}(GW_{Bt}) + f_{C_3}(SW_{At}) + f_{C_4}(GW_{At}, WD_{At}) \\ & + f_{C_5}(GW_{At}, WD_{At}) + f_{C_6}(\mathfrak{R}_t, ED_t) \end{aligned}$$

where:

GW_{At} , GW_{Bt} are groundwater extractions from aquifers A and B

SW_{At} is diversion water from the river to the aquifer A at each time period

f_{C_1} and f_{C_2} are the cost functions related to well pumping of aquifers A and B

f_{C_3} is the cost function associated with canal diversion construction

WD_{At} , WD_{Bt} are water demands of agricultural zones A and B

f_{C_4} and f_{C_5} are the cost functions related to agricultural damages due to water scarcity

ED_t is the environmental water demand and RE_t is the instream flow in the downstream of the river

f_{C_6} is the cost function related to unsupplying the environmental water demand.

This problem is constrained by the continuity equation for the reservoir as follows:

$$S_t = S_{t-1} + I_t - E_t - R_t$$

where:

S_t is the reservoir storage

I_t is inflow to the reservoir

E_t is the evaporation loss

R_t is the reservoir release at time t .

The reservoir storage should be in a feasible range, between the minimum and maximum storage volumes S_{min} and S_{max} as follows:

$$S_{min} \leq S_t \leq S_{max}$$

Writing water balance in the river leads to the following equation:

$$R_t - SW_{At} - SW_{Bt} = \mathfrak{R}_t$$

There are limitations on the capacity of a diversion canal:

$$SW_{At} \leq Cap_A$$

where Cap_A is the capacity of the canal for water convey.

For an unconfined aquifer A, the hydraulic head can be calculated using groundwater flow equations as follows:

$$\frac{\partial}{\partial x} \left(T \frac{\partial h}{\partial x} \right) + \frac{\partial}{\partial y} \left(T \frac{\partial h}{\partial y} \right) + RW_{At} - GW_{At} = S_y \frac{\partial h}{\partial t}$$

where:

- h is the hydraulic head
- RW_{At} is the groundwater recharge
- S_s is the specific storage
- T is transmissivity for the aquifer.

The hydraulic heads are obtained by solving the differential equations utilizing numerical methods introduced in [Chapter 6](#).

A constraint can be applied for limiting the maximum and minimum groundwater levels.

(h_{min} and h_{max}) in each planning period as follows:

$$h_{min} \leq h_t \leq h_{max}$$

The optimization model can be solved using the optimization techniques introduced in [Chapter 7](#).

Example 8.5

Determine the average monthly allocated groundwater and surface water to four agricultural zones shown in [Figure 8.12](#). As it can be seen in this figure, a channel can transfer surface water to zone 4. The monthly discharge of rivers and the volume of discharge by precipitation during the last 2 years and gross water demands of the agricultural zones are presented in [Tables 8.4](#) and [8.5](#), respectively. The equations of the average groundwater table fluctuations, based on the discharge from agricultural wells and recharge from precipitation, are presented in [Table 8.6](#). In this table, $G(i)$ is the groundwater discharge from agricultural zone i (MCM), $Q(3)$ is the transferred surface water to zone (4), and P is the groundwater recharge from precipitation (MCM). The effects of other parameters such as recharge of precipitation and underground inflow and outflow are considered to be a monthly constant. The acceptable (without any cost) range for cumulative groundwater table variation in each zone is ± 4 m. The maximum capacity of the water transfer channel is 4 m³/s, and it is assumed that 90% of the transferred water is supplied by river 1. The initial groundwater table depth in zones 1, 2, 3, and 4 are considered to be 17, 8.1, 12.6, and 67 m, respectively.

The objectives of the developed model are water supply to agricultural lands, minimizing the pumping cost, and controlling the average groundwater table fluctuations in agricultural zones.

SOLUTION

The pumping cost can be considered as a linear function of pumping power (P_{pump}) as follows:

$$P_{pump} = \frac{\gamma GH}{75 * \eta}$$

where:

- γ is the specific gravity of water (kg/m³)
- G is the pumping discharge (m³/s)
- H is the groundwater table depth (m)
- η is the pumping efficiency.

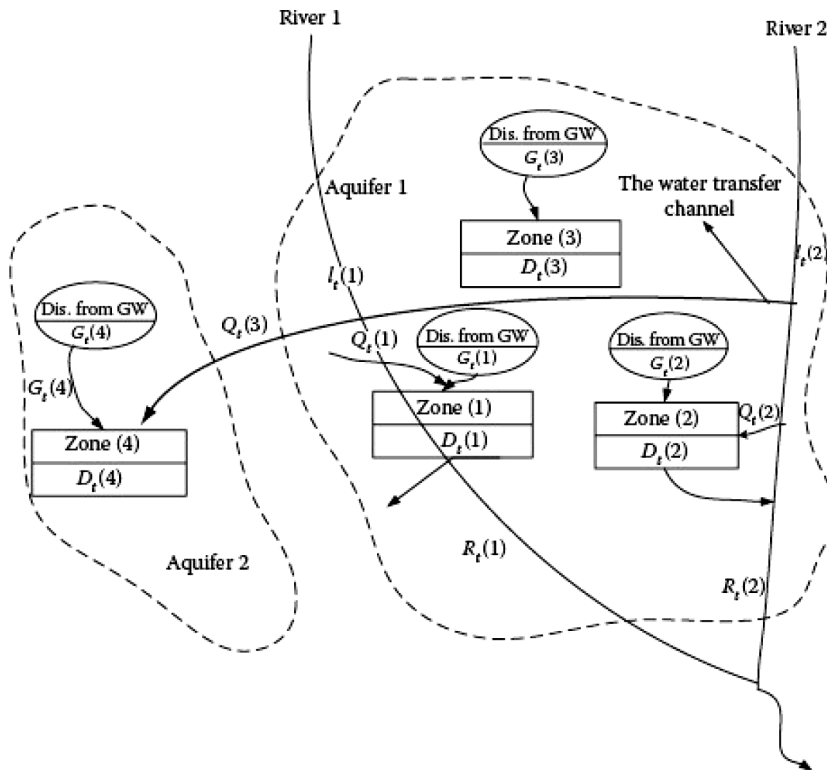


FIGURE 8.12 $I_t(1)$: the inflow surface water to zone (1) in month t , (MCM), $I_t(2)$: the inflow surface water to zone (2) in month t , (MCM), $R_t(2)$: the outflow surface water from zone (1) in month t , (MCM), $R_t(1)$: the outflow surface water from zone (2) in month t , (MCM), $G_t(i)$: the extracted groundwater from zone (i) in month t , (MCM), $Q_t(i)$: allocated surface water to zone (i) in month t , (MCM), and $D_t(i)$: agricultural water demand in zone (i) in month t . Components of surface and groundwater resources for Example 8.5.

TABLE 8.4
The Values of Monthly River Discharge and Precipitation

| Water Year | Month | Discharge from River (1) (MCM) | Discharge from River (2) (MCM) | Recharge of Aquifer (1) by Precipitation (MCM) | Recharge of Aquifer (2) by Precipitation (MCM) |
|------------|----------|--------------------------------|--------------------------------|--|--|
| 1 | October | 13.48 | 15.49 | 0.7 | 0.05 |
| 1 | November | 6.16 | 16.51 | 1.2 | 0.2 |
| 1 | December | 9.38 | 22.78 | 2 | 0.18 |
| 1 | January | 14.34 | 20.19 | 2.5 | 0.19 |
| 1 | February | 15.9 | 27.18 | 3 | 0.3 |
| 1 | March | 18.17 | 26.25 | 3 | 0.31 |
| 1 | April | 10.08 | 26.99 | 2.5 | 0.3 |

(Continued)

TABLE 8.4 (Continued)**The Values of Monthly River Discharge and Precipitation**

| Water Year | Month | Discharge from River (1) (MCM) | Discharge from River (2) (MCM) | Recharge of Aquifer (1) by Precipitation (MCM) | Recharge of Aquifer (2) by Precipitation (MCM) |
|------------|-----------|--------------------------------|--------------------------------|--|--|
| 1 | May | 7.11 | 26.16 | 2 | 0.15 |
| 1 | June | 5.3 | 23.14 | 0.5 | 0.04 |
| 1 | July | 3.76 | 20.29 | 0 | 0.01 |
| 1 | August | 3.23 | 19.65 | 0 | 0.2 |
| 1 | September | 2.85 | 17.43 | 0.5 | 0.05 |
| 2 | October | 18.83 | 30.18 | 0.6 | 0.06 |
| 2 | November | 7.44 | 26.23 | 1.2 | 0.2 |
| 2 | December | 8.58 | 26.64 | 2.2 | 2.2 |
| 2 | January | 10.89 | 26.45 | 2.3 | 2.3 |
| 2 | February | 14.72 | 25.61 | 3.2 | 3.2 |
| 2 | March | 25.79 | 20.22 | 2.9 | 2.9 |
| 2 | April | 35.17 | 48.29 | 2.6 | 2.6 |
| 2 | May | 15.07 | 35.09 | 2 | 2 |
| 2 | June | 9.47 | 28.07 | 0.56 | 0.56 |
| 2 | July | 19.08 | 23.16 | 0.2 | 0.2 |
| 2 | August | 37.51 | 19.16 | 0 | 0 |
| 2 | September | 30.25 | 16.47 | 0.51 | 0.51 |

TABLE 8.5**Monthly Agricultural Water Demands and Downstream Water Right (MCM)**

| Month | Zone (1) | Zone (2) | Zone (3) | Zone (4) | Downstream Water Right |
|-----------|----------|----------|----------|----------|------------------------|
| October | 8.536 | 10.07 | 0.64 | 3.01 | 1.86 |
| November | 8.494 | 8.59 | 0.48 | 3.82 | 3.43 |
| December | 3.45 | 2.57 | 0.2 | 1.41 | 1.045 |
| January | 2.448 | 2.03 | 0.153 | 1.24 | 0.965 |
| February | 2.371 | 1.79 | 0.133 | 0.81 | 0.37 |
| March | 4.5 | 3.33 | 0.353 | 1.32 | 0.54 |
| April | 11.44 | 9.75 | 1.176 | 6.15 | 6.92 |
| May | 34.64 | 31.76 | 3.44 | 20.58 | 28.57 |
| June | 36.6 | 35.22 | 4.02 | 19.12 | 27.6 |
| July | 19.45 | 18.83 | 2.53 | 4.93 | 8.92 |
| August | 23.9 | 25.86 | 2.66 | 4.97 | 5.78 |
| September | 21.31 | 23.49 | 1.68 | 4.26 | 3.76 |

TABLE 8.6**The Equations of Average Groundwater Table Fluctuation (m)**

| | |
|----------|--|
| Zone (1) | $\Delta L_1 = 1.9 \times 10^{-4} G(1) + 1.2e^{-3} G(2) - 2e^{-5} G(3)^2 + 7.8e^{-4} G(3) - 0.02P - 0.03$ |
| Zone (2) | $\Delta L_2 = 1 \times 10^{-6} G(1) + 3.7e^{-3} G(2) - 4e^{-5} G(3)^2 + 1.9e^{-4} G(3) - 0.018P - 0.07$ |
| Zone (3) | $\Delta L_3 = 1 \times 10^{-7} G(1) + 1.1e^{-3} G(2) - 4.1e^{-4} G(3) - 0.01P - 0.02$ |
| Zone (4) | $\Delta L_4 = -0.0149G(4)^2 + 0.41G(4) - 7e^{-5} Q(3)^2 - 0.028Q(3) - 0.02$ |

Note: The positive values show the groundwater table drawdown.

Since the objective function and the constraints are nonlinear, the dynamic programming method can be effectively used in this study. The recursive function of the dynamic programming model is developed as follows:

$$f_t(G_t(i), Q_t(i)) = \text{Min} \{C_t(G_t(i), Q_t(i)) + f_t(G_{t-1}(i), Q_{t-1}(i))\}$$

where:

i is the index of zone $i = 1, \dots, 4$

$G_t(i)$ is the amount of groundwater extracted from zone i , in month t (MCM)

$Q_t(i)$ is the allocated surface water to zone i , in month t (MCM)

$C_t(G_t(i), Q_t(i))$ is the cost of operation during time period t

$f_t(G_{t-1}(i), Q_{t-1}(i))$ is the minimum of the total operational cost till the end of time period $t - 1$.

The cost of operation in each period is estimated as follows:

$$C_t(G_t(i), Q_t(i)) = \sum_{i=1}^4 \text{Loss}_t(i)$$

$$\text{Loss}_t(i) = \alpha (D_t(i) - Q_t(i) - G_t(i))^2 + \beta (G_t(i), H_t(i)) + \gamma (|L_t(i)| - L_{max}(i))^2$$

$$\alpha = 0 \text{ if } D_t(i) \leq (Q_t(i) + G_t(i))$$

$$\gamma = 0 \text{ if } |L_t(i)| \leq L_{max}(i)$$

where:

$D_t(i)$ is the agricultural water demand in zone i and time period t

$L_t(i)$ is the total variation of the water table level until the end of time period t

$L_{max}(i)$ is the maximum allowable cumulative groundwater table fluctuation in agricultural zone i

$H_t(i)$ is the depth of the groundwater table in agricultural zone i at the end of month t . α, β, γ are weights of objectives (constant).

The constraints of the model are as follows:

Control of groundwater level fluctuations:

$$H_t(i) = H_0(i) + \sum_{t=1}^T \Delta L_t(i), \quad i = 1, \dots, 4$$

$$L_t(i) = \sum_{t=1}^T \Delta L_t(i), \quad i = 1, \dots, 4$$

$$\Delta L_t(i) = f_i(G_t(i), Q_t(i), I, O)$$

where:

- $H_0(i)$ is the initial depth of the groundwater table in the agricultural zone i
- $\Delta L_t(i)$ is the variation of the water table level in time period t in agricultural zone i (drawdown is considered to be positive)
- $f_i(G_t(i), Q_t(i), I, O)$ is the groundwater table fluctuation in agricultural zone i and time period t , which is the function of total discharge (O), and the total recharge (I) of the aquifers.

Estimation of the surface water outflow from the agricultural zones 1 and 2 ($R_t(i)$):

$$R_t(i) = I_t(i) - Q_t(i) - \left(1 - \frac{\psi}{100}\right) Q_t(3), \quad i = 1, 2$$

where:

- ψ is the percentage of transferred water to zone 4 from the surface water resources of zone 2

$I_t(i)$ is the surface water inflow to zone i in the time period t (MCM).

Minimum instream flow requirements downstream of agricultural zones:

$$\sum_{i=1}^2 R_t(i) \geq R_{t,min}$$

where:

$R_{t,min}$ is the minimum instream flow required in the downstream in time period t

$R_t(i)$ is the surface water outflow from zone i in time period t in MCM.

Maximum capacity of canal:

$$Q_t(4) \leq Q_{t,max}$$

As the problem is multi-objective, the coefficients α , β , and γ are the relative weights of the objectives, which should be determined in order to make these objectives comparable. The allocated water to different agricultural zones in July (a dry month) for $\alpha = 1$, $\beta = 0.005$, and $\gamma = 120$ and the corresponding cumulative groundwater table are presented in [Table 8.7](#) and [Figure 8.13](#) (Karamouz et al., 2002).

TABLE 8.7
Average Allocated Surface and Groundwater to
Different Zones in July (MCM)

| Source | Zone (1) | Zone (2) | Zone (3) | Zone (4) |
|-------------------|----------|----------|----------|----------|
| Surface water | 5.8 | 15.6 | — | — |
| Groundwater | 21.2 | 3.0 | 3.0 | 1.0 |
| Transferred water | — | — | — | 3 |

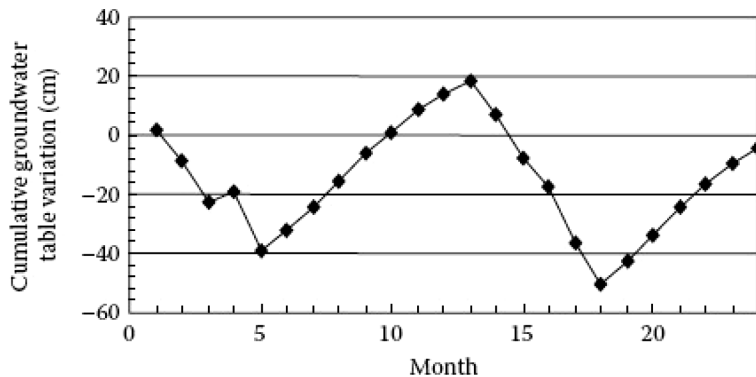


FIGURE 8.13 Cumulative groundwater table variation in zone 1 for Example 8.5.

8.3.5 MULTI-OBJECTIVE CONJUNCTIVE USE OPTIMIZATION

In a basin system, the components of water resources and water users have interaction with others that lead to a complex system. The basin could include the reservoir, stream, river, aquifer, irrigated area, water demands, pumping wells, and a diversion canal. [Figure 8.14](#) illustrates different components of a basin. There are interactions between groundwater and a water storage reservoir, irrigated field, and lakes. Also, return flows from the allocated water to different sectors for supplying the agricultural, municipal, and industrial water demands recharge the aquifers. Water can be delivered to users through pipes and canals.

The major objective function for the optimization of models can be considered to maximize water provided from wells plus surface water diversions to supply water demands. Other objective functions could be considered to minimize the total cost or improve the quality of allocated water. The multi-objective optimization model can be solved by the techniques introduced in [Chapter 7](#).

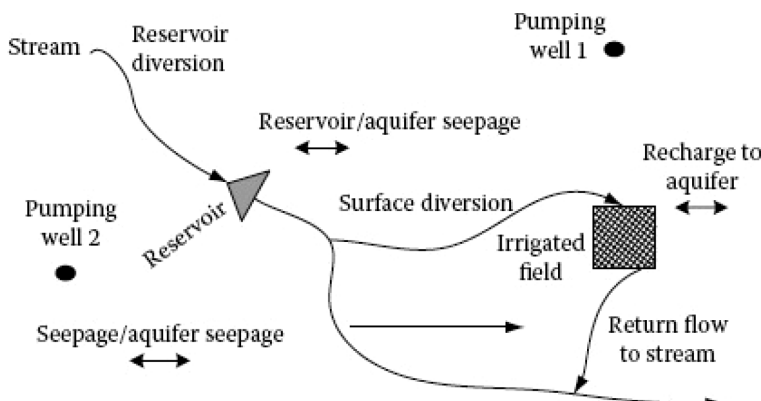


FIGURE 8.14 Different components of an aquifer-stream system.

8.3.5.1 Groundwater Resource Sustainability Limits

The excessive use of groundwater has led to questions regarding its sustainability. To what extent can groundwater be exploited without unduly compromising the principle of sustainable development? The sustainability of groundwater utilization must be evaluated from an interdisciplinary point of view, where hydrology, environmental science, geomorphology, and climatology play an important role. Shallow groundwater flow systems should be separated from deep groundwater flow systems; the former interact with surface water, while the latter do not.

- The potential for (and dynamics of) the conjunctive use in agricultural irrigation varies considerably with the “hydrogeological setting,” including such factors as average rainfall and geomorphological position. Bearing in mind that we are principally concerned with alluvial plains, some generalizations on water resource availability and constraints for irrigated agriculture can be given.
- In some instances, spontaneous conjunctive use encounters the problem of increasing groundwater salinity, which, if not adequately diagnosed and controlled will result in a serious subsequent decline in agricultural productivity and also becomes a menace to the security of drinking-water supplies. Groundwater salinity threats arise by one of a number of completely distinct mechanisms:
 - Rising water table due to excessive canal seepage and/or field application in head water areas leading to soil saturation and salinization, or sometimes naturally saline unconfined groundwater becoming mobilized especially in land-surface depressions.
 - Leaching of soil salinity to groundwater throughout irrigation areas due to first habitation of arid soils and/or fractionation of salts during “efficient” irrigation, with subsequent accumulation at the water table and around the tail end sections of irrigation canal commands if no groundwater discharge/drainage occurs.
 - More classical intrusion and encroachment of saline groundwater due to excessive abstraction of fresh groundwater, both in arid inland basins and coastal regions.
 - Additionally, there are hyper-arid areas in which virtually all groundwater is naturally saline, except where some infiltration occurs from surface water courses and irrigation canals to form “freshwater lenses,” requiring very careful management as a dependable source of drinking-water supply. It is also for supplementary irrigation to avoid on the one hand saline up-coning and on the other excessive infiltration and water table rise accompanied by salinization.
- The lining of primary and secondary irrigation canals will be a high priority:
 - on arid alluvial plains where the unconfined aquifer is naturally saline (with fresh groundwater confined at greater depth), because canal seepage will often represent a nonrecoverable resource loss contributing to a rising water table, soil saturation, and salinization

- on humid alluvial plains with a rising water table in a shallow fresh groundwater system, because excessive canal seepage will be contributing to soil saturation and associated secondary salinization.
- On the contrary, on highly permeable alluvial terraces (especially in more arid areas), the secondary and tertiary canal systems are often found to carry water for relatively few days each year, and the majority of irrigation users depend entirely on water wells. Nevertheless, this is still regarded as the conjunctive use since canal seepage is responsible for the greater part of aquifer recharge. An important result is that any attempt to line these canals to “save water” for use in other areas can be very detrimental to existing conjunctive use because canal seepage provides an important component of aquifer recharge—and careful water resource impact assessment is needed to avoid counterproductive “double accounting” (World Bank, 2010).

8.3.6 CASE STUDY 2: APPLICATION OF GENETIC ALGORITHMS AND ARTIFICIAL NEURAL NETWORKS IN CONJUNCTIVE USE OF SURFACE AND GROUNDWATER RESOURCES

The proposed model is applied to the conjunctive use of the surface and groundwater resources in the southern part of Tehran. The Tehran Plain is bounded by the Kan River in the west and the Sorkhe Hesar River in the east. About one billion cubic meters of water per year is provided for domestic consumption of over 8 million people. [Figure 8.15](#) shows a map of the surface water resources of Tehran Plain.

More than 60% of the water consumption in Tehran returns to the Tehran aquifer via traditional absorption wells. Three major agricultural zones, namely, Eslamshahr-Kahrizak (zone 1), Ghaleno (zone 2), and Khalazir (zone 3) are the main users of surface and groundwater resources in the study area (see [Figure 8.15](#)). The Tehran aquifer is mainly recharged by inflow at the boundaries, precipitation, local rivers, and return flows from the domestic, industrial, and agricultural sectors. The discharge from the aquifer is through water extraction from wells, springs, groundwater outflow, and evapotranspiration.

8.3.6.1 Simulation Model

To simulate the groundwater table elevation in this study area, the processing MODFLOW for windows (PMWIN) model is used. The Tehran aquifer is considered as a single-layered aquifer, and therefore, only the horizontal hydraulic conductivity is estimated. [Figure 8.16](#) shows the generated grid as well as the boundary conditions in the PMWIN model. [Figure 8.17](#) presents the comparison between computed and historical groundwater table elevation in the study area. This figure shows how closely the model can reproduce the monthly water table variations.

The response functions in the optimization model show the monthly groundwater table variations in the Tehran aquifer. They are functions of discharge, recharge, inflow, and outflow at the boundaries as well as physical characteristics of the aquifer. Based on the available water quality data, NO_3 that usually deviates from the standards is selected as an indicator water quality variable in the simulation model.

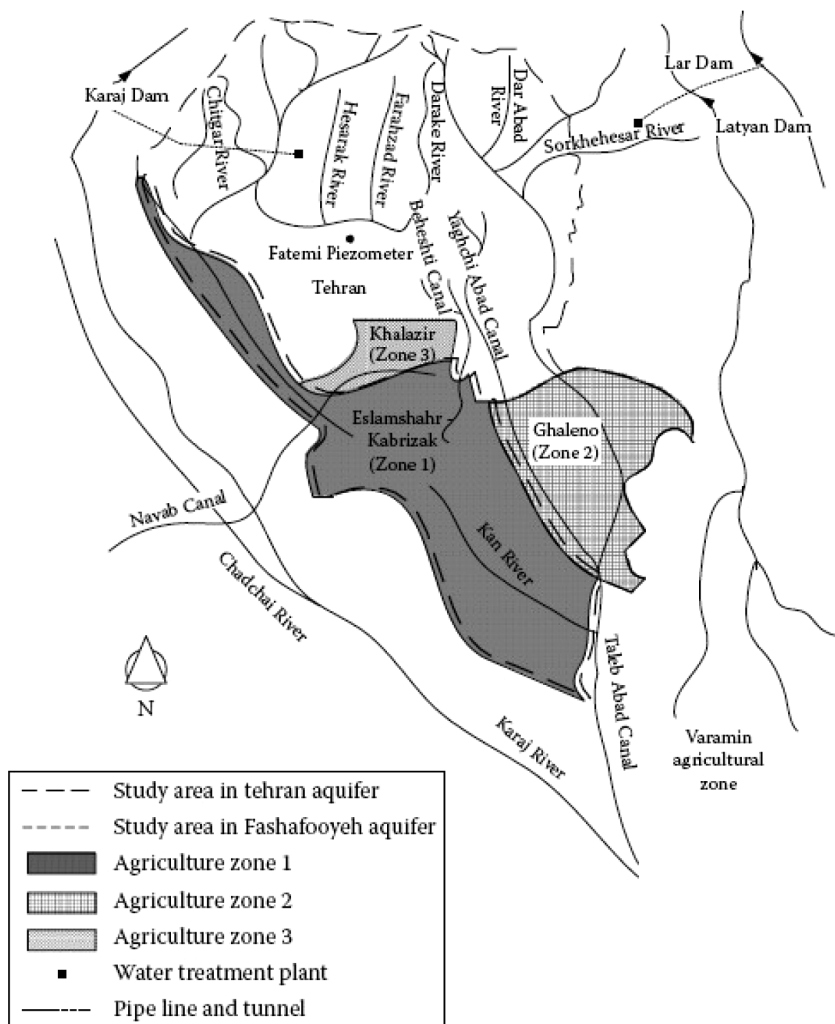


FIGURE 8.15 Surface water resources and the agricultural zones in the study.

The linkage of the optimization and simulation models will significantly increase the computational problems and also the time needed to achieve the optimal solution of the model. In the proposed methodology, the results of the (Processing MODFLOW) groundwater simulation model are used to train the artificial neural networks (ANN)-based simulation model.

The results of the frequent execution of the groundwater simulation model (PMWIN) for different sets of recharge-discharge values, and by considering the principle of superposition, the selected ANN is trained for estimating monthly water table variations that have been obtained for each agricultural zone. The suitable variables, which significantly affect the groundwater table variations, have been selected

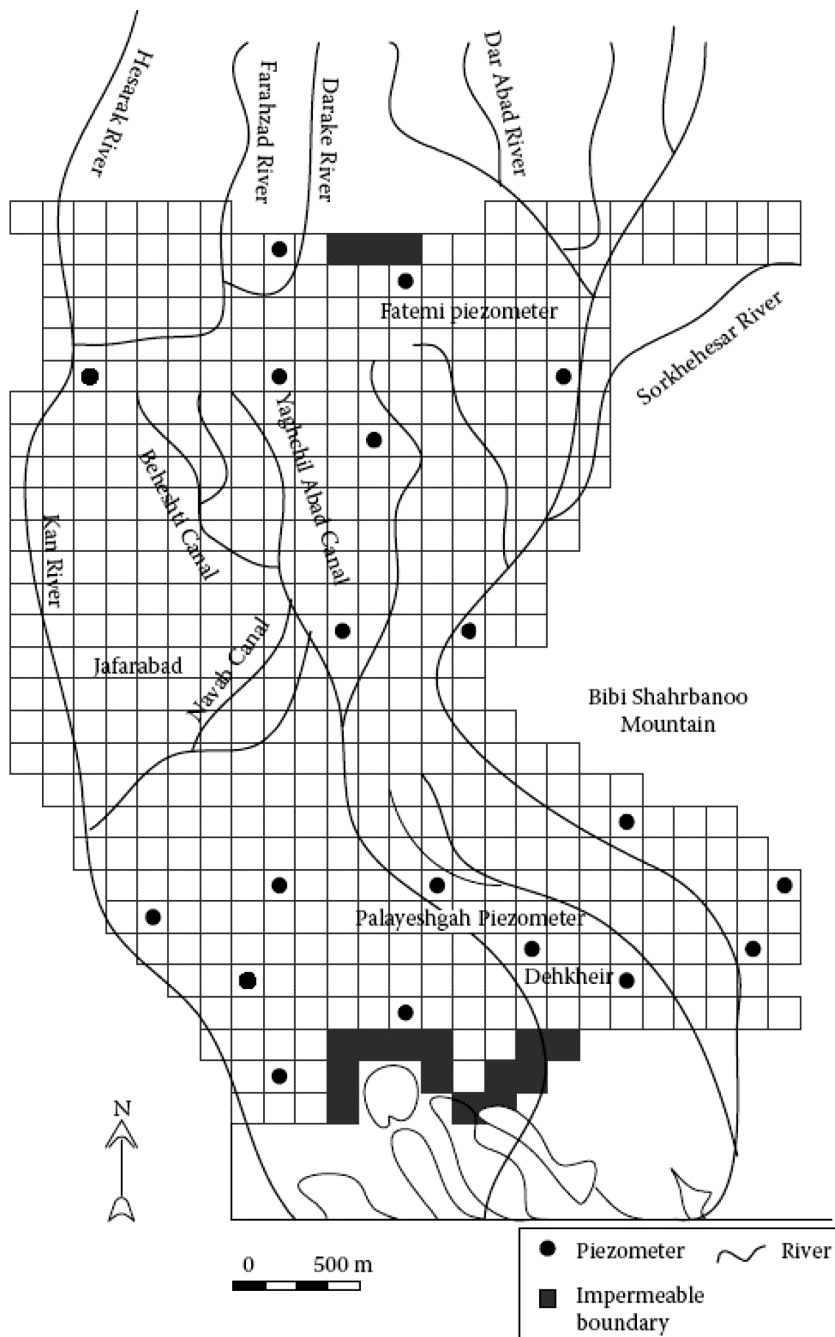


FIGURE 8.16 The generated grid and boundary condition in the PMWIN model.

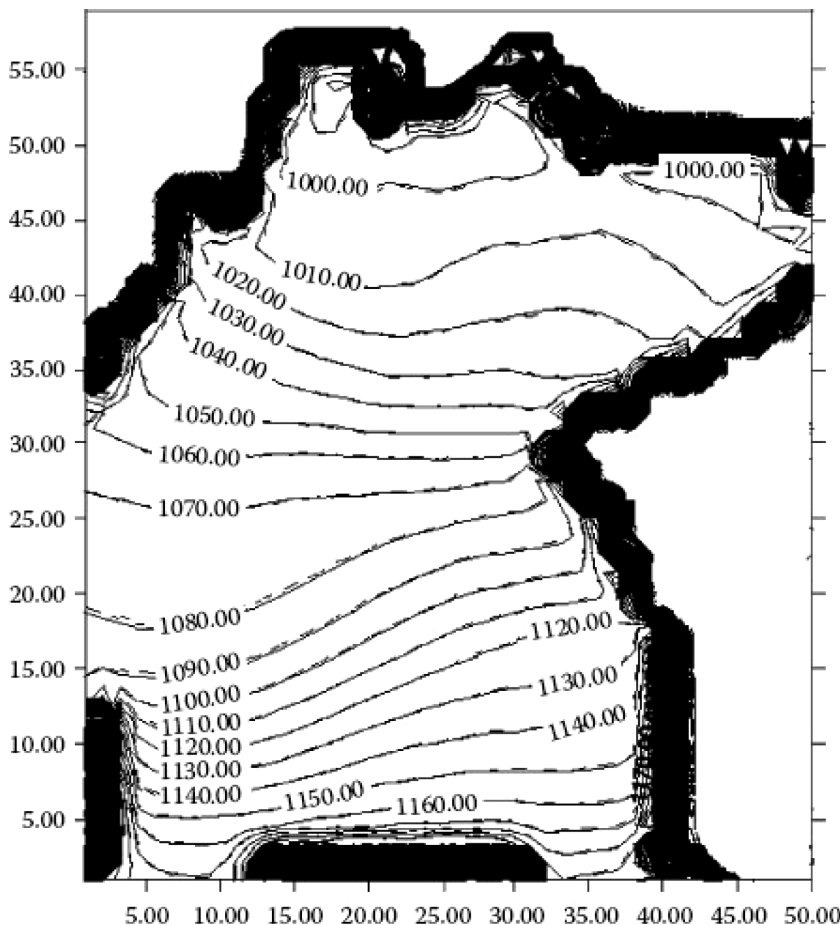


FIGURE 8.17 Comparison between observed and simulated groundwater table levels.

using a trial and error process. Finally, the total monthly groundwater discharge and the average groundwater table level in the aquifer at the beginning of the month have been considered as variables; and the other factors that have a negligible effect on the groundwater table variations are assumed to be constant for each month. The general form of the response function of the average groundwater table variation in month t in each zone is estimated as follows:

$$\Delta H_t = \text{purelin}\left(w'_{2t} \times \text{tansig}\left((w_{1t} \times h_t) + b_{1t}\right) + b_{2t}\right) \quad (8.13)$$

where:

ΔH_t is the vector of the groundwater table variations in month t (m) in agriculture zones (negative values refer to water table drawdown)

w'_{2t} is the weight parameter in the second layer of the ANN developed for month t

- w_{1t} is the weight parameter in the first layer of the ANN developed for month t
 h_t is the input matrix, which consists of the average groundwater table level at the beginning of each month and discharge average from agriculture zones
 b_{1t} is the bias parameter in the first layer of the ANN developed for month t
 b_{2t} is the bias parameter in the second layer of the ANN developed for month t .

8.3.6.2 Optimization Model Framework

A methodology for the conjunctive use of surface and groundwater resources is developed using the combination of the genetic algorithms (GAs) and the ANNs. Water supply, reduction of pumping costs, and controlling the groundwater table fluctuations are considered as the objective functions of the model. The main objectives of the conjunctive use models are usually as follows:

- Water supply to the agricultural demands
- Improving the quality of allocated water
- Minimizing the pumping costs
- Controlling the groundwater table fluctuations

Considering the abovementioned objectives, the formulation of the proposed model is as follows:

$$\text{Minimize} \sum_{i=1}^4 \alpha_i Z_i$$

Subject to:

$$Z_1 = \begin{cases} 0 & \text{if } D_{imy} \leq Q_{imy} + G_{imy} \quad i = 1, \dots, n, \quad y = 1, \dots, 15, \quad m = 1, \dots, 12 \\ \sum_{i=1}^n \sum_{y=1}^{15} \sum_{m=1}^{12} ((D_{imy} - Q_{imy} - G_{imy}) / D_{imy}) / (n \times 15 \times 12), & \text{otherwise} \end{cases}$$

$$Z_2 = \sum_{i=1}^n \sum_{y=1}^{15} \sum_{m=1}^{12} (G_{imy} H_{imy} / (G_3 H_3)_{max}) / (n \times 15 \times 12)$$

$$Z_3 = \left(\sum_{i=1}^n \left(\sum_{y=1}^{15} \sum_{m=1}^{12} \Delta L_{imy} \right) / \Delta L_{max} \right) / n \quad (8.14)$$

$$Z_4 = \left(\sum_{i=1}^n \left(\sum_{y=1}^{15} \sum_{m=1}^{12} C_{imy} \right) / C_{max} \right) / n \quad (8.14)$$

$$\Delta L_{imy} \leq \Delta L_{max}, \quad y = 1, \dots, 15, \quad m = 1, \dots, 12 \quad (8.15)$$

$$RD_{imy} = R_{imy} - Q_{imy} \quad (8.16)$$

$$\sum_{i=1}^2 RD_{imy} \geq E_{my,min} \quad (8.17)$$

$$\sum_{i=1}^4 \alpha_i = 1 \quad (8.18)$$

$$Q_{imy} \leq R_{imy}, \quad i = 1, \dots, n, \quad y = 1, \dots, 15, \quad m = 1, \dots, 12 \quad (8.19)$$

$$\Delta L_{imy} = f(\tilde{G}_{my}, \tilde{O}_{my}, \tilde{M}_{my}) \quad (8.20)$$

$$\Delta C_{imy} = f'(\tilde{G}_{my}, \tilde{O}_{my}, \tilde{M}_{my}, c_{my}) \quad (8.21)$$

where:

G_{imy} is the volume of groundwater extracted in the agriculture zone i in month m of year y (m^3/day)

Q_{imy} is the volume of surface water allocated to agriculture zone i in month m of year y (m^3/day)

C_{imy} is the average concentration of the water quality indicator in the allocated water to agriculture zone i in month m of year y (mg/L)

c_{my} is the average concentration of the water quality indicator in the return flow to agriculture zone i in month m of year y (m^3/day)

D_{imy} is the agricultural water demand in zone i in month m of year y (m^3/day)

ΔL_{imy} is the variation of the groundwater table level in month m of year y in the agriculture zone i (m) (drawdown is considered to be negative)

ΔL_{max} is the maximum allowable cumulative groundwater table fluctuation (m)

C_{max} is the maximum allowable concentration of water quality variable in allocated water (mg/L)

C_{im} is the volume of groundwater extracted in agriculture zone i in month m (m^3/day)

H_{imy} is the groundwater table level in agriculture zone i in month m in year y

$(C_{im} \times G_{im})_{max}$ is the maximum value of $(C_{im} \times G_{im})$ in different years

R_{imy} is the surface water flow rate in zone i in month m of year y

$E_{im,max}$ is the environmental water demand in month m of year y

RD_{imy} is the unused surface water in zone i in month m of year y

Z_1 is the loss function of water allocation

Z_2 is the loss function of pumping cost

Z_3 is the loss function of groundwater table fluctuation

Z_4 is the loss function of the quality of allocated water

α_i is the relative weight of the objective function i

m is the number of months in the planning horizon

n is the number of agricultural zones in the study area

y is the number of years in the planning horizon

The objective functions Z_1-Z_4 should be normalized between 0 and 1. For this purpose, the relative weight α_i can be assigned much easier based on the relative importance of the objectives. Based on the Equation 8.15, the monthly variation of the water table level is limited to a maximum level. Equation 8.20, which is called the response function, presents the monthly groundwater table variations in each zone, which is a function of the set of the volumes of the groundwater extracted in month m of year y in the agricultural zones (\tilde{G}_{my}), the outflow at the boundaries, the groundwater discharge through springs and Qantas in month m of year y (\tilde{Q}_{my}), recharge by direct precipitation, allocated surface water, and also recharge by absorption wells (\tilde{M}_{my}). This equation should be formulated using a comprehensive groundwater simulation model (Karamouz et al., 2007).

8.3.6.3 Results and Discussion

The cumulative groundwater table variations in each zone, which has experienced a total fluctuation of more than ± 20 m in the last 20 years, are limited to ± 5 m over the planning horizon (15 years). The relative weight of Z_1 to Z_4 are considered to be 30, 10, 35, and 25, respectively. [Table 8.8](#) presents the reliability of the water supply to the agricultural water demands and the share of ground and surface water resources allocation. Based on the results presented in [Table 8.8](#), only 79% of the total water demand can be allocated and more than 64% of the allocated demand is supplied by the groundwater resources. [Figure 8.18](#) shows the cumulative variation of groundwater table in the agricultural zones based on the optimal operating policies. In zone 2, less groundwater is extracted because of a lower concentration of water quality variable in the surface water of this zone (see [Figures 8.19](#) through [8.21](#)). It can be seen in [Figure 8.20](#), most of the allocated water to zone 2 is supplied from surface water resources due to the availability of the surface water and best water quality in this zone, as well as to reduce the pumping cost. [Figure 8.22](#) presents the total allocated water to zone 1. The peak value shown in [Figure 8.22](#) is due to the over-allocating of the groundwater to zone 1 to control the groundwater table in this zone. Based on the conjunctive use policies, the groundwater is allocated to zone 3 to control the increasing level of the groundwater table in this agricultural zone. Results of this study show that the proposed model can be effectively used for the conjunctive use of surface and groundwater resources considering the water quality issues.

TABLE 8.8

The Share of Surface and Groundwater Resources in Water Allocation to Different Zones

| Zone | Percent of Demand Supplied by Groundwater | Percent of Demand Supplied by Surface Water | Reliability of Water Supply (without Quality) | Reliability of Water Supply (with Quality) |
|------|---|---|---|--|
| 1 | 79 | 21 | 99 | 95 |
| 2 | 14 | 86 | 85 | 77 |
| 3 | 100 | 0 | 75 | 65 |

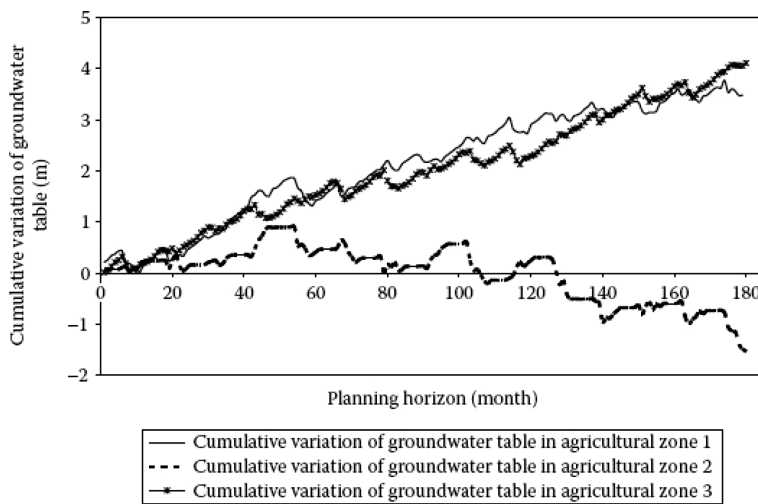


FIGURE 8.18 Cumulative variation of the groundwater water table level in the agricultural zones.

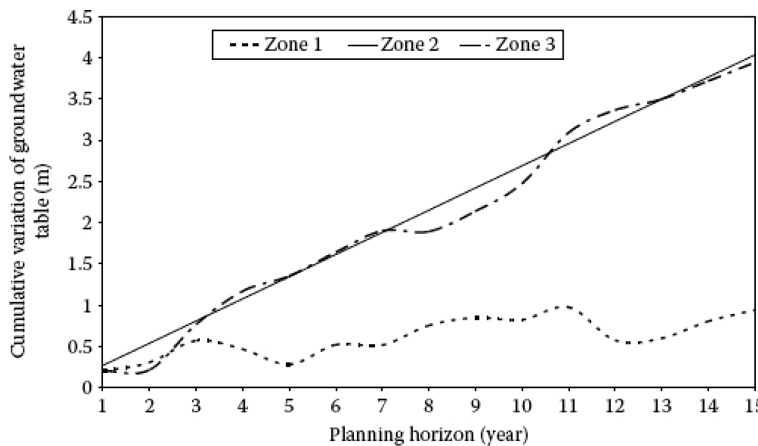


FIGURE 8.19 Cumulative variation of the groundwater level in the agricultural zones.

8.3.7 CASE STUDY 3: WATER ALLOCATION FROM THE AQUIFER-RIVER SYSTEM USING A CONFLICT RESOLUTION MODEL

The proposed optimization model is applied to the Lenjanat aquifer and Zayandeh-Rud River in central Iran, as shown in Figure 8.23. About 750 million cubic meters of water per year is provided for agricultural consumption and 220 million cubic meters of water per year is provided for industrial consumption. A water demand of more than 800 million cubic meters is supplied from the Zayandeh-Rud River.

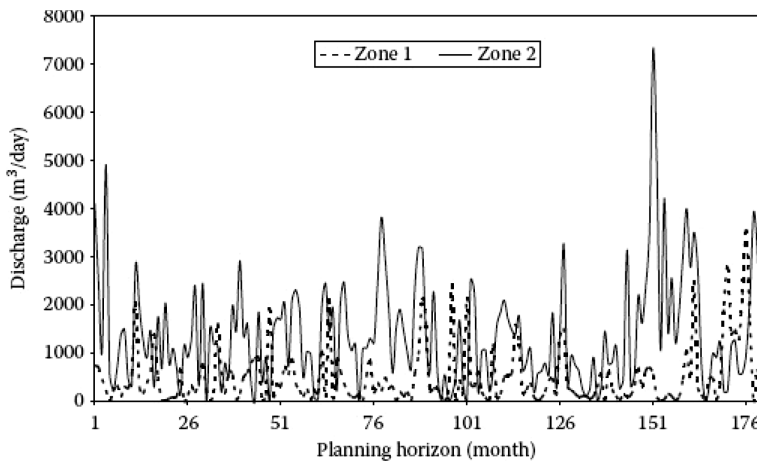


FIGURE 8.20 Monthly allocated surface water to agricultural zones 1 and 2.

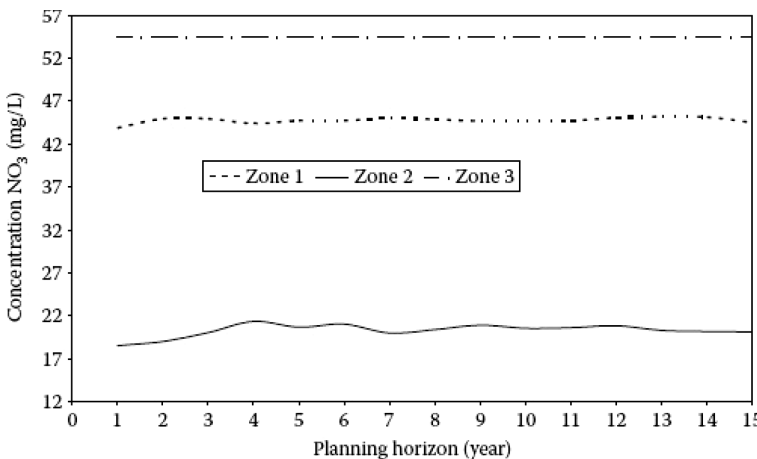


FIGURE 8.21 Average annual NO_3 concentration of the allocated water to the agricultural zones.

The area is located in the Gavkhouni Basin in central Iran. The return flows from the agricultural and industrial sectors are 15% and 10% of the allocated water, respectively. The transmissivity in the Lenjanat unconfined aquifer varies from 300 to 2400 m^2/day . The average coefficient of hydraulic conductivity in this aquifer is about 7 m/day . There are about 40 piezometric wells in this aquifer.

The Lenjanat aquifer is mainly recharged by inflow at the boundaries, precipitation, infiltration from the bed of the river, and return flows from the industrial and agricultural sectors. The discharge from the aquifer is through water extraction from wells, springs, and Qanats, as well as groundwater outflow and evapotranspiration.

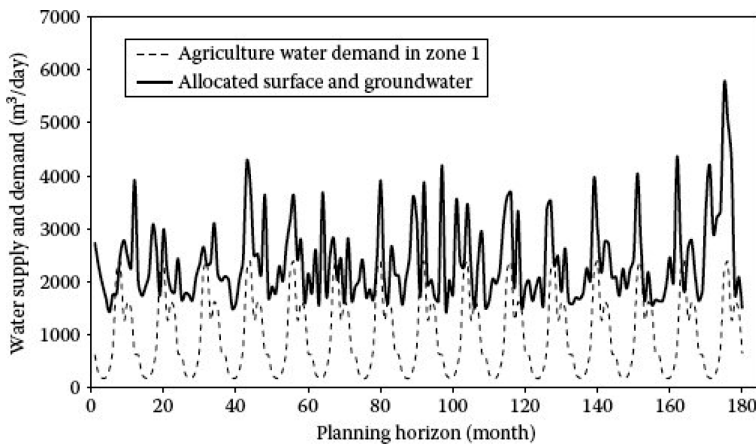


FIGURE 8.22 Monthly allocated water to agricultural zone 1.

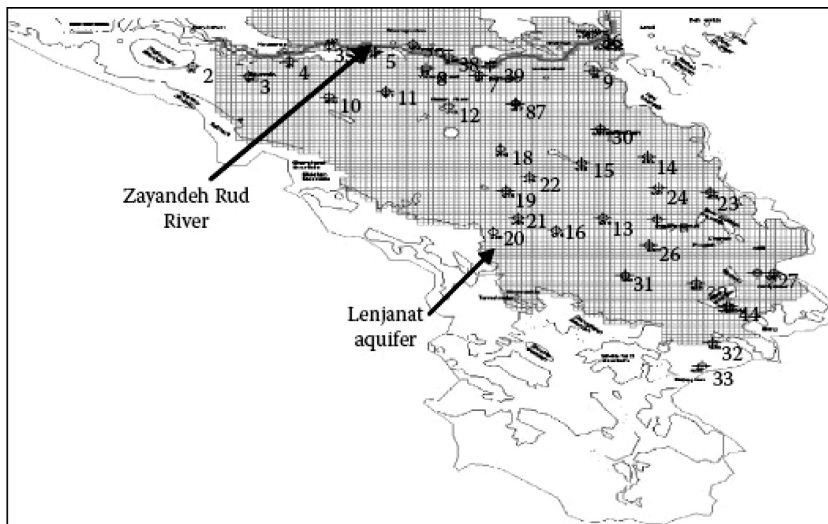


FIGURE 8.23 Studied area and the location of river and piezometric wells in the region.

The Zayandeh-Rud River has an average of 1300 million cubic meters of discharge per year. The industrial and agricultural return flows are the most important sources of water pollution in the region. The recharged water from the aquifer to the river is also the cause of increasing water salinity. The total dissolved solids (TDS) variation could be a good index for assessing these pollutants, and therefore it was used in this study. The PMWIN model is used to simulate the aquifer, and then based on the simulation results, two seasonal ANN models are developed. The input variables to the selected ANN model are the number of the month, average groundwater table level at the beginning of the month, discharge from wells in the aquifer, and recharges through

to the aquifer including agricultural drainage as well as recharge due to precipitation, head water in the river, concentration of water quality at the beginning of the month, and TDS concentration of the river and recharge (Karamouz et al., 2006).

In this study, the Nash bargaining theory is used to incorporate the conflicting interests of the decision-makers. A typical utility function in the Nash bargaining theory is illustrated in Figure 8.24. The utility function for different sectors is determined based on the available data and the results of some brainstorming sessions with the main decision-makers and stakeholders of the system.

Environmental sector: The quality and quantity of water in the Lenjanat aquifer and Zayandeh-Rud River are the main concerns for this sector. The utility function related to water quality is determined based on the river ecosystems needs and instream flow requirements. The utility function of water quality ($f_{r,c,m}$) and quantity ($f_{r,q,m}$) in the river in month m are described, respectively, as follows:

$$f_{r,c,m}(C_{d,m}) = \begin{cases} 0 & \text{if } C_{d,m} \geq 2500 \text{ mg/L} \\ 1 & \text{if } C_{d,m} \leq 1200 \text{ mg/L} \end{cases} \quad (8.22)$$

$$f_{r,q,m}(Q_{d,m}) = \begin{cases} 1 & \text{if } Q_{g,m} \geq 30 \text{ MCM} \\ 0 & \text{if } Q_{g,m} < 10 \text{ MCM} \end{cases} \quad (8.23)$$

where $C_{d,m}$ and $Q_{d,m}$ are the concentration of water quality indicator and discharge in the river in month m .

The utility function of water quality in the aquifer and water table fluctuations in month m are described, respectively, as follows:

$$f_{G,c,m}(C_{G,m}) = \begin{cases} 1 & \text{if } C_{G,c,m} < 1200 \text{ mg/L} \\ 0 & \text{if } C_{G,c,m} \geq 2500 \text{ mg/L} \end{cases} \quad (8.24)$$

$$f_{G,l,m}(l_m) = \begin{cases} 1 & \text{if } 0 \leq l_m < 3 \text{ cm} \\ 0 & \text{if } l_m \geq 5 \text{ cm} \end{cases} \quad (8.25)$$

where $C_{G,m}$ and l_m are the concentration of water quality indicator in the aquifer and the water table fluctuation in month m .

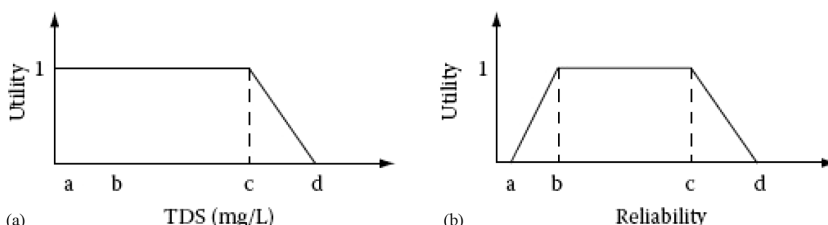


FIGURE 8.24 Utility functions of (a) allocated water quality indicator, TDS and (b) reliability of water supply.

Industrial sector: The industry sector is one of the most important water consumers in the study area, and the quantity and quality of allocated water to this sector is one of the most important issues of the water policy in the region. The utility function of the industrial sector is considered a function of reliability of water supply (I_m) as follows:

$$f_{I,m}(I_m) = \begin{cases} 1 & \text{if } I_m > 85 \\ 1 & \text{if } 0 < I_m \leq 30 \\ 0 & \text{if } I_m < 0 \end{cases} \quad (8.26)$$

The utility function of water quality for this sector is considered as follows:

$$f_{I,c,m}(C_{I,m}) = \begin{cases} 1 & \text{if } C_{I,m} \leq 1500 \\ 1 & \text{if } C_{I,m} > 3000 \\ 0 & \text{if } 0 < C_{I,m} \leq 3000 \end{cases} \quad (8.27)$$

where $C_{G,m}$ and I_m are the concentration of water quality indicator and reliability of the demand supply for the industrial sector.

Agricultural sector: The main objectives of this sector are water supply, water with an acceptable quality to agricultural demands, and reduction of waste removal cost. The utility of this sector related to the water supply is based on the water supply reliability. Also, the utility functions related to water quality and quantity of the agricultural sector are expressed as follows:

$$f_{A,m}(A_m) = \begin{cases} 1 & \text{if } A_m > 80 \\ 1 & \text{if } 0 < A_m \leq 20 \\ 0 & \text{if } A_m < 0 \end{cases} \quad (8.28)$$

$$f_{A,c,m}(C_{A,m}) = \begin{cases} 1 & \text{if } C_{A,m} \leq 1500 \\ 1 & \text{if } C_{A,m} \geq 3000 \\ 0 & \text{if } 0 < C_{A,m} \leq 3000 \end{cases} \quad (8.29)$$

where $C_{A,m}$ and A_m are the concentration of water quality indicator and reliability of the demand supply for the agricultural sector.

8.3.7.1 Optimization Model Framework

Based on the Nash bargaining theory, the utilities and the objectives of the decision-makers of the system as well as their relative authorities should be considered in the water allocation to different sectors. The Nash bargaining-based objective function in the optimization model is considered as:

$$\begin{aligned} \text{Maximize: } Z = & \prod_{m=1}^{12 \times \text{year}} (f_{A,m}(A_m) - d_{A,m})^{w_A} (f_{A,c,m}(C_{A,m}) - d_{A,c,m})^{w_{Ac}} (f_{r,c,m}(C_{d,m}) - d_{r,c,m})^{w_{rc}} \\ & \times (f_{r,q,m}(Q_{d,m}) - d_{r,q,m})^{w_{rq}} (f_{G,I,m}(I_m) - d_{G,I,m})^{w_{GI}} (f_{G,c,m}(C_{G,m}) - d_{G,c,m})^{w_{Gc}} \\ & \times (f_{I,m}(I_m) - d_{I,m})^{w_I} (f_{I,c,m}(C_{I,m}) - d_{I,c,m})^{w_{Ic}} \end{aligned} \quad (8.30)$$

Subject to:

$$\begin{aligned} Q_{I,m} &= Q_{I,r,m} + Q_{I,G,m} \quad m = 1, 2, \dots, 10 \times \text{year} \\ Q_{A,m} &= Q_{A,r,m} + Q_{A,G,m} \end{aligned} \quad (8.31)$$

$$\begin{aligned} I_m &= \frac{Q_{I,m}}{D_{I,m}} \\ A_m &= \frac{Q_{A,m}}{D_{A,m}} \end{aligned} \quad (8.32)$$

$$\begin{aligned} C_{I,m} &= \frac{(Q_{I,r,m} \times C_{r,m} + Q_{I,G,m} \times C_{G,m})}{Q_{I,m}} \\ C_{A,m} &= \frac{(Q_{A,r,m} \times C_{r,m} + Q_{A,G,m} \times C_{G,m})}{Q_{A,m}} \end{aligned} \quad (8.33)$$

$$C_{d,m} = \frac{C_{r,m} (Q_{u,m} - Q_{r,m} - IN_{G,m}) + C_{I,w,m} Q_{I,w,r,m} + C_{A,w,m} Q_{A,w,r,m} + IN_{r,m} C_{G,m}}{Q_{u,m} - Q_{r,m} + Q_{I,w,r,m} + Q_{A,w,r,m} R_{r,m}} \quad (8.34)$$

$$\begin{aligned} Q_{d,m} &= Q_{u,m} + Q_{I,w,r,m} + Q_{A,w,r,m} - Q_{r,m} - IN_{G,m} + IN_{r,m} \\ IN_{R,m} &= f(Q_{G,m}, h_{r,m}, R_{G,m}) \\ IN_{G,m} &= f(Q_{G,m}, h_{r,m}, R_{G,m}) \end{aligned} \quad (8.35)$$

$$\begin{aligned} C_{G,m} &= f(Q_{G,m}, R_m, C_{w,G,m}, h_{r,m}, C_{r,m}) \\ l_m &= f(Q_{G,m}, h_{r,m}, R_{G,m}) \end{aligned} \quad (8.37)$$

where:

$Q_{I,r,m}$, $Q_{I,G,m}$ is the allocated water to the industrial sector from surface and groundwater resources in month m

$Q_{A,r,m}$, $Q_{A,G,m}$ is the allocated water to the agricultural sector from surface and groundwater resources in month m

$D_{I,m}$, $D_{A,m}$ are the water demands of the industrial and agricultural sectors in month m , respectively

$C_{r,m}$, $C_{G,m}$ are the water qualities of river and aquifers in month m

$C_{w,G,m}$ is the concentration of return flow to the aquifer in month m

l_m is the water table fluctuation in month m

$R_{G,m}$ is the volume of recharge to the aquifer in month m

$Q_{d,m}$, $Q_{u,m}$ are the discharges in the downstream and upstream of the river in month m , respectively

$C_{I,w,m}$, $C_{A,w,m}$ are the concentrations of the industrial and agricultural return flow in month m

$Q_{I,w,c,m}$, $Q_{A,w,G,m}$ are the discharge volumes of the industrial and agricultural return flow to the aquifer in month m

$h_{R,m}$ is the water depth in the river in month m

$Q_{e,G,m}$ is the discharge to the aquifer due to precipitation in month m

$IN_{R,m}$ is the discharge to the aquifer due to river interaction in month m

$IN_{G,m}$ is the discharge to the river due to aquifer interaction in month m .

In the formulation, the objective function is the multiplication of each of the utility functions subtracted from their point of disagreement for every sector (agricultural, industrial, and domestic), river and aquifer interaction, and groundwater variation in the aquifer for a specific target. The model constraints include the continuity equation, mass balance, upper and lower limits, water quality, and water table simulation models, which are linked to the optimization model.

The water quality variations in an aquifer and river can be implicitly obtained using a groundwater quality simulation model and a river water quality. Variations of the groundwater table and water quality in each month are functions of the time series of recharges to the groundwater, water withdrawal from wells, and interaction between river and aquifer that can be implicitly obtained using a comprehensive groundwater simulation model. River water quality at control points in each month is a function of the return flows quality and quantity and time series of upstream water quantity and quality that can be implicitly obtained using a river water quality simulation model.

8.3.7.2 Results and Discussion

In this study, 10 years of monthly streamflow quality and quantity data (1990–2000) are used to allocate water from the Zayandeh-Rud River and Lenjanat aquifer, considering quantity and quality issues. In this study, GA is used to solve the optimization model. In this model, the gene values are the monthly allocated surface water and groundwater to the agricultural and industrial sectors.

Figure 8.25 shows the time series of allocated water to the agricultural sector and industrial sectors, respectively. The results show that 86% and 90% of water demand

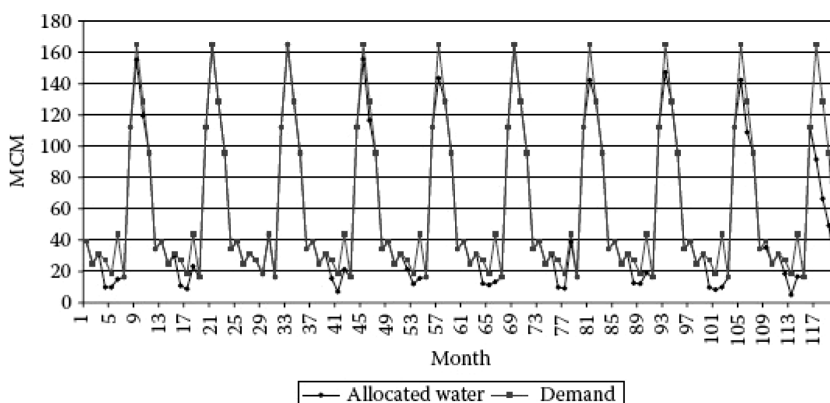


FIGURE 8.25 Allocated water to agricultural sector during the operating period.

in the agricultural sector and the industrial sector have been provided during the 10 years operating period.

Figure 8.26 shows the TDS concentration in allocated water to the different sectors. As shown in Figure 8.26, the utility function related to this restriction has been satisfied. This is the result of the TDS concentration in the water resources of the studied area which is above.

Figure 8.27 shows the TDS concentration in the river in both upstream and downstream of the studied area aquifer. The agricultural and industrial

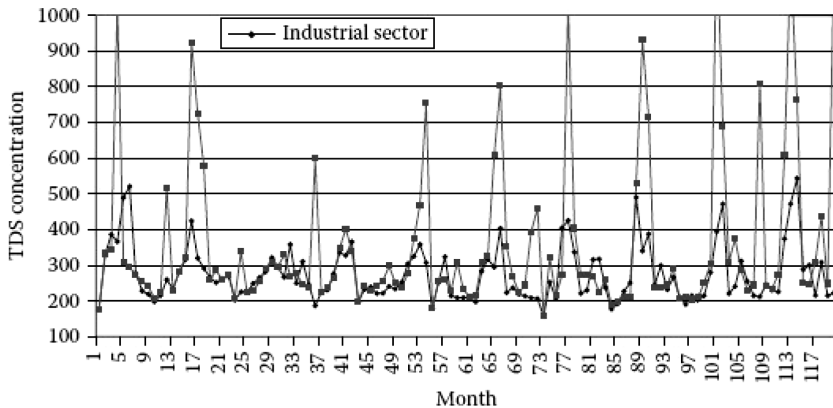


FIGURE 8.26 TDS concentration in allocated water to the agricultural zones.

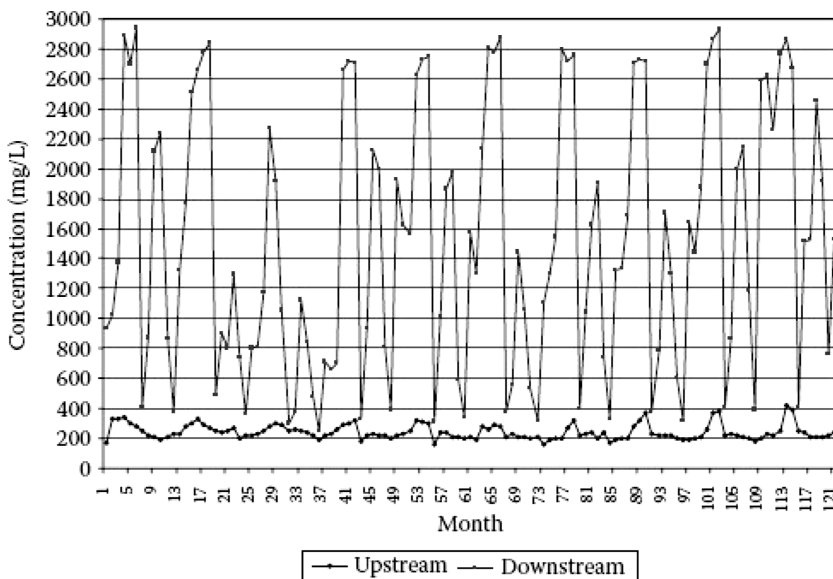


FIGURE 8.27 TDS concentration in the upstream and downstream of the studied area and industrial sectors.

wastewater and water seepage from the aquifer to the river is the cause of the increase in TDS concentration downstream. The cumulative groundwater table variation in the studied aquifer, which has experienced a total fluctuation of more than 2.5 m in the last 10 years, could be kept under 1.1 m over the planning horizon using this model.

8.3.8 CASE STUDY 4: CONJUNCTIVE USE AND CROP PATTERN MANAGEMENT

The proposed model is applied to the plains, surrounding Tehran, the capital city of Iran. The Tehran Plains are located between $34^{\circ}52'$ and $36^{\circ}2'T'$ of northern latitude and between $50^{\circ}10'$ and $53^{\circ}9'$ of eastern longitude. The area is bounded by four major watersheds, namely, Kavir, Mazandaran, Sefidrood, and Hamedan-Markazy, respectively, as shown in Figure 8.28.

In the study area, the weather is assumed to be affected by Mediterranean systems in the winter and warm Arabian systems in the summer. The average amount of precipitation in the Varamin Plain is about 131.4 mm/year and the temperature varies from -14.4°C to 45.5°C . The minimum and maximum relative humidity rates are 15% and 75% in the summer and winter, respectively.

The surface water resources of Varamin are limited to the Jajroud and Shour Rivers in the west and north of the plain, respectively (see Figure 8.29). The effluents of Tehran wastewater treatment plant no. 6 are also transferred to this plain by a canal to be used for irrigation. Table 8.9 shows the average monthly discharge of Jajroud and Shour Rivers upstream of the Varamin Plain.

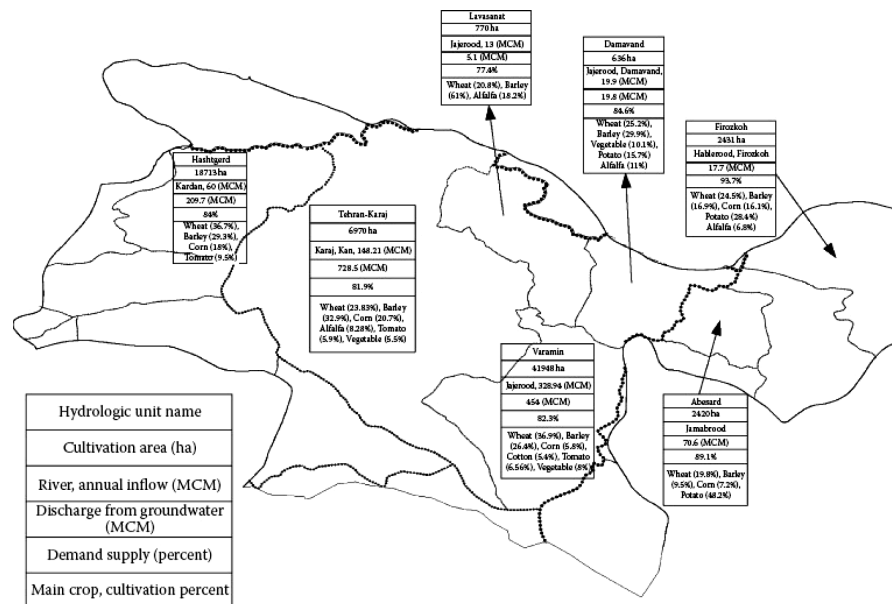


FIGURE 8.28 Characteristics of hydrologic units of the Tehran province.

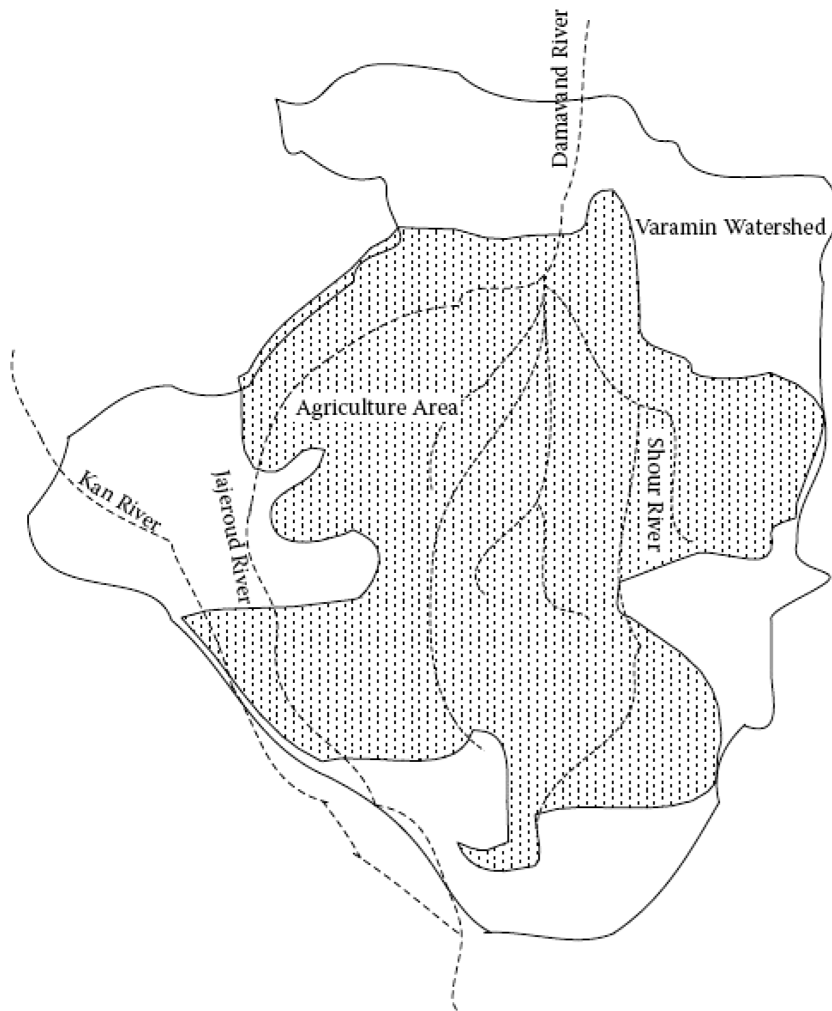


FIGURE 8.29 Rivers located in the Varamin Plain.

TABLE 8.9

Average Monthly Discharge of Jajroud and Shour Rivers in Upstream of the Varamin Plain

Average Monthly Discharge (MCM)

| River Name | October | November | December | January | February | March | April | May | June | July | August | September |
|------------|---------|----------|----------|---------|----------|-------|-------|-------|-------|------|--------|-----------|
| Jajroud | 6.1 | 11.45 | 12.91 | 11.25 | 14.89 | 29.58 | 58.79 | 56.47 | 21.65 | 4.78 | 4.55 | 2.16 |
| Shour | 8.27 | 20.68 | 28.56 | 22.26 | 24.53 | 23.92 | 22.99 | 21.22 | 5.93 | 3.69 | 0.74 | 1.42 |

8.3.8.1 Optimization Model Structure

In this study, a genetic algorithm model is developed to optimize the crop pattern of agricultural lands considering the water allocation priorities and surface and ground water availability. The objective function of this model is to maximize the net benefits of the agricultural products considering the allowable water table fluctuations, the pumping costs, as well as the impacts of a water supply deficit in crop production. The model is formulated in a way that both crop pattern and water allocation from surface or ground-water resources are simultaneously optimized (Karamouz et al., 2008). The main objective of the proposed model is to maximize the difference between the gross benefit of crop production and the pumping costs. The main constraints of this model are:

- Maximum incremental and cumulative allowable water table fluctuations
- Total area of agricultural lands
- Availability of surface water
- Instream flow requirements in the rivers

Considering the above objectives and constraints, the formulation of the problem is as follows:

$$\text{Maximize } Z = B - C \quad (8.38)$$

Subject to:

$$B = \sum_{j=1}^y \sum_{i=1}^n \sum_{p=1}^c (Y a_{pj} \times T_p \times \alpha_{pj} \times A_j) \quad (8.39)$$

$$C = \sum_{j=1}^n \sum_{f=1}^y \sum_{k=1}^m \left(\frac{G_{jfk} \times H_{jfk} \times h_{jfk} \times Pr}{\eta \times 0.102} \right) + \left(\frac{S_{jfk} \times H'_{jfk} \times h'_{jfk} \times Pr'}{\eta \times 0.102} \right) \quad (8.40)$$

$$D_{jfk} = \sum_{p=1}^c (\alpha_{pj} \times A_j \times d_{pjfk}), \quad j = 1, \dots, n, \quad k = 1, \dots, m, \quad f = 1, \dots, y \quad (8.41)$$

$$\sum_{p=1}^c \alpha_{pj} = 1, \quad j = 1, 2, \dots, n \quad (8.42)$$

$$S_{jfk} \leq 0.7 \times I_{jfk}, \quad j = 1, \dots, n, \quad k = 1, \dots, m, \quad f = 1, \dots, y \quad (8.43)$$

$$\Delta L_{jfk} = \frac{\left(Ch_{jfk} + \alpha \times \left(\sum_{j=1}^n (S_{jfk} + G_{jfk}) \right) - \sum_{j=1}^n G_{jfk} - GD_{jfk} \right)}{(Ss_j \times A_j)} \quad (8.44)$$

$$j = 1, \dots, n, \quad k = 1, \dots, m, \quad f = 1, \dots, y$$

$$Ya_{pjf} = Ym_p \times \prod_{k=1}^m \left(1 - Ky_{pk} \left(1 - \left(\frac{ETa_{pjfk}}{ETm_{pjfk}} \right) \right) \right), \quad p = 1, \dots, c, \quad j = 1, \dots, n, \quad f = 1, \dots, y \quad (8.45)$$

$$\mathfrak{R}_{jfk} = 0.3 \times (S_{jfk} + G_{jfk}), \quad j = 1, \dots, n, \quad k = 1, \dots, m, \quad f = 1, \dots, y \quad (8.46)$$

$$|\Delta L_{jfk}| \leq \Delta L_{max_j}, \quad j = 1, \dots, n, \quad k = 1, \dots, m, \quad f = 1, \dots, y \quad (8.47)$$

$$S_{jfk} + G_{jfk} \geq D_{jfk}, \quad j = 1, \dots, n, \quad k = 1, \dots, m, \quad f = 1, \dots, y \quad (8.48)$$

$$\sum_{f=1}^y \sum_{k=1}^m \Delta L_{jfk} < 5, \quad j = 1, 2, \dots, n \quad (8.49)$$

where:

Z is the net benefit of the crop cultivation

B is the gross benefit of crop cultivation in the planning horizon

C is the pumping cost of surface and groundwater in the planning horizon

G_{jfk} is the volume of groundwater withdrawal from wells in zone j of month k and year f (MCM)

S_{jfk} is the volume of surface water withdrawal from rivers in zone j of month k and year f (MCM)

D_{jfk} is the monthly crop water demand in zone j of month k and year f (MCM)

ΔL_{jfk} is the water table fluctuations in zone j of month k and year f (m)

ΔL_{max_j} is the maximum monthly allowable fluctuation of the water table in zone j (m)

ETa_{pjfk} is the water allocation to crop p of zone j of month k and year f

ETm_{pjfk} is the water demand of crop p of zone j of month k and year f

Ss_j is the storage coefficient of the aquifer in zone j

Ch_{jfk} is the aquifer recharge in zone j of month k and year f (MCM)

GD_{jfk} is the aquifer discharge through drainage in zone j of month k and year f (MCM)

A_j is the agricultural area in zone j (ha)

α_{pj} is the area allocated percent for crop p in zone j (%)

d_{pjfk} is the monthly crop water demand for crop p in zone j of month k and year f (m)

I_{jfk} is the discharge of the river in zone j of month k and year f (MCM)

Ya_{pjf} is the actual yield for crop p in zone j and year f (kg/ha)

Ym_p is the maximum yield for crop p (kg/ha)

Ky_{pk} is the sensitive coefficient for crop p in the month k

T_p is the price of crop p (Rial/kg)

RF_{jfk} is the volume of recharged water to the groundwater from the total water used for irrigation in zone j of month k and year f (MCM)

$(G_{jfk} \times H_{jfk} \times hr_{jfk}) / (\eta \times 0.102)$ is the power needed for groundwater pumping (kWh)

$(S_{jfk} \times H'_{jfk} \times hr'_{jfk}) / (\eta \times 0.102)$ is the power needed for surface water pumping (kWh)

H_{jfk} is the depth of the water table in zone j of month k and year f (m)

H'_{jfk} is the head of water derived from the river in zone j of month k and year f (m)

Pr is the price of electricity needed for water pumping from the groundwater

Pr' is the price of electricity needed for water pumping from the surface water, η is the pumping efficiency (%)

hr_{jfk} is the total number of hours of pumping from the groundwater in zone j of month k and year f (h)

H'_{jfk} is the total number of hours of pumping from the surface water in zone j of month k and year f (h)

c is the number of crops in zone j

n is the number of zones

m is the number of months

y is the number of years in planning horizon

Constraint (8.39) is used for estimating the total income based on actual crop production and the selling price of different crops. Constraint (8.40) is formulated for estimating the cost of water pumping. Constraint (8.41) calculates the monthly water demand according to the area allocated to each crop and the monthly net demands estimated based on the regional conditions. Constraints (8.42) and (8.43) are used for considering the total area and surface water availability in the region. Constraint (8.44) shows the relation of water table fluctuations with different characteristics of the aquifer. To calculate the amount of crop production, a production function developed by Dorenbos and Kassam (1979), which is a function of actual and potential evapotranspiration extended by Ghahraman and Sepaskhah (2004) as well as allocated water and crop water demand supply, is used in this study. The amount of water returns to groundwater and the maximum allowable water table fluctuation are considered in Constraints (8.46) and (8.47), respectively. Constraints (8.48) and (8.49) show the allocated water resources for irrigation demands and the maximum cumulative fluctuation of allowable groundwater level.

Due to the large number of decision variables and nonlinearity of the problem, GA is used to find the optimal solution. The schematic of one chromosome used in the GA model in the proposed optimization model is shown in [Figure 8.30](#). The number of genes in a chromosome for a y year planning horizon with P dominant crops is equal to $P + 2 \times m \times y$. The first set of P genes presents the percentage of each crop in the plain. The remaining genes are filled with the amount of allocated water from surface and groundwater resources for m months of y years. One of the main advantages of the proposed model is to consider the time series of monthly crop water demand, which allows the incorporation of demand uncertainty in the development of optimal operation policies. A production function has also been used to estimate the production rate with respect to the amount of water allocation and water supply deficits (Karamouz et al., 2009).

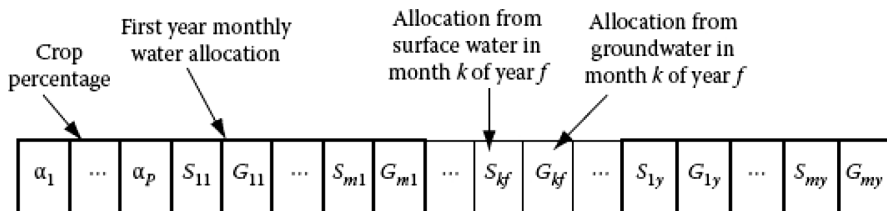


FIGURE 8.30 Schematic of a chromosome used in the proposed GA model.

8.3.8.2 Results and Discussion

The obtained optimal crop pattern is presented in [Table 8.10](#). In this scenario, the coverage area of barley and cucumber, which have a high yield with a low water demand, has increased to improve the region income. Components of the objective function including the benefit and cost corresponding to the optimal crop pattern are presented in [Table 8.11](#). The maximum fraction of cost is obtained through wheat

TABLE 8.10
Components of Objective Function in Scenario A

| Crops | Percent (%) | Benefit (Million Dollars) | Cost (Million Dollars) |
|----------|-------------|---------------------------|------------------------|
| Wheat | 12 | 16.6 | 7.99 |
| Barley | 47 | 554 | 93.5 |
| Cucumber | 39 | 45.3 | 16.6 |
| Tomato | 2 | 2.53 | 1.36 |
| Maize | 0 | 0 | 0 |
| Total | 100 | 618.1 | 119.45 |

TABLE 8.11
Crop Pattern, Net Benefit, and Allocated Surface and Groundwater in Observed Condition and Optimal Results

| | Actual Observed | Optimal Allocated Area |
|-------------------------------|-----------------|------------------------|
| Crop pattern (%) | | |
| Wheat | 38 | 12 |
| Barley | 29 | 47 |
| Cucumber | 4.5 | 39 |
| Tomato | 6.5 | 2 |
| Maize | 22 | 0 |
| Net benefit (million dollar) | 79 | 440 |
| Allocated surface water (MCM) | 399 | 228 |
| Allocated groundwater (MCM) | 454 | 217 |

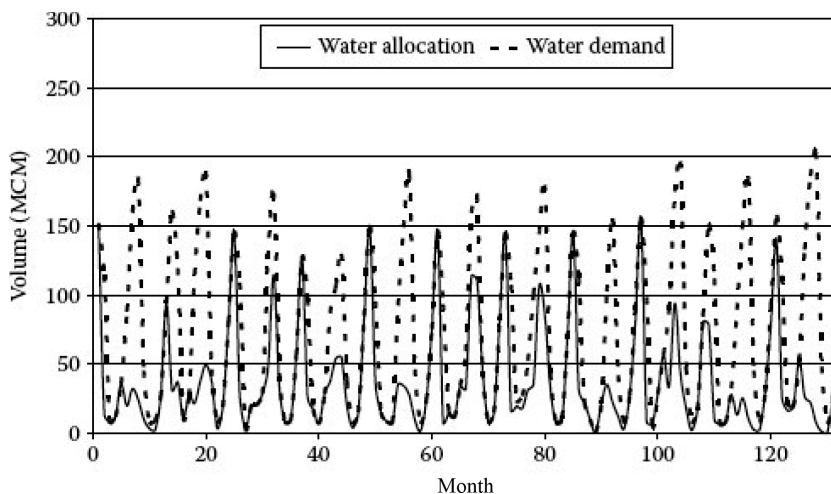


FIGURE 8.31 Comparison of water demand and allocation.

cultivation out of the optimal crop pattern. As shown in [Table 8.11](#), cucumber is the most beneficial crop, although its cultivation has considerable cost. The total benefit of the optimal option is about (million U.S.\$) 440, while the benefit of the existing condition is about (million U.S.\$) 79.

Investigation of the optimal water allocation scheme in comparison with water demand variation during the 11 years of the study period ([Figure 8.31](#)) shows that in certain months when the surface water is more than the water demand, the preference option in water allocation is surface water. However, in some months with less of a demand for avoiding the water table increasing beyond the desired level, the total allocated water exceeds demand. The reliability, resiliency, and vulnerability of supplying the water demand are calculated as 50.0%, 36.4%, 24.1% MCM/month, respectively.

8.4 OPERATION OF GROUNDWATER RESOURCES IN SEMIARID REGION

In arid and semiarid regions, water demand is supplied by storing water in holes as the only water source for domestic use and small-scale irrigation. Even today, people in some regions use water holes in sand rivers. Coarse sand and gravel in sand rivers can store the water in the voids between the solids of sand, and then it can be extracted from the holes.

However, flooding water is usually stored for a short period. In order to prevent pulling water downstream in a sand river, the underground dykes can be created. As it is shown in [Figure 8.32](#), creating sand dams increase the volume of sand and water by forcing flash floods to deposit coarse sand.

Sand dams are one type of groundwater dam. It is a weir of suitable size constructed across the streambed that leads to the deposit of the sand carried by heavy

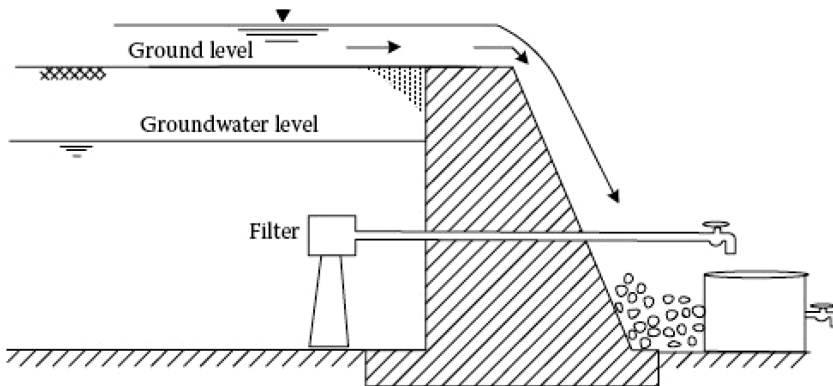


FIGURE 8.32 Typical sand storage dam.

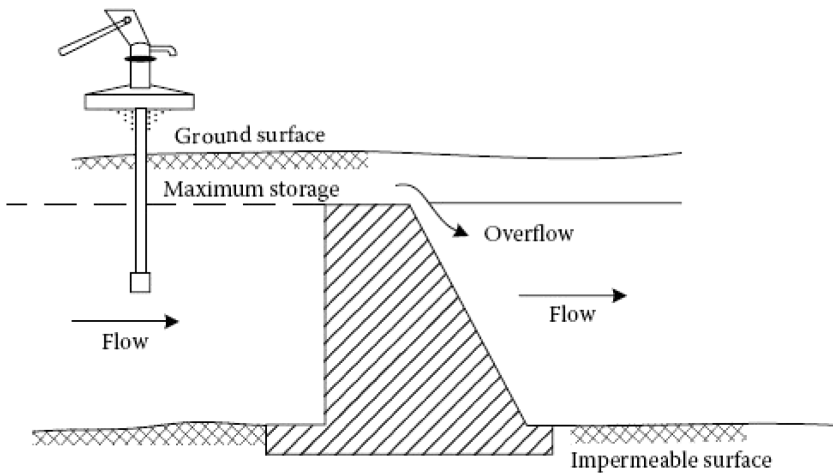


FIGURE 8.33 Typical subsurface dam.

flows during the rain. Thus, a reservoir is made that is filled up with sand (Onder and Yilmaz, 2005; Wipplinger, 1958).

Another type of groundwater dam is a subsurface dam, which is built underground to store underground water and to interrupt the natural flow of groundwater as shown in [Figure 8.33](#). The underground reservoirs have certain advantages compared to surface reservoirs as follows: (1) water is stored underground, and hence, the land above the underground dam can be utilized, (2) the evaporation losses are much less for water stored underground, (3) risk of contamination of the stored water from the surface is reduced because the ground layer can filter the contamination, and (4) disaster caused by the cut-off wall failure is prevented.

However, a groundwater dam has some disadvantages: (1) construction of a cut-off wall needs to have careful controls and (2) the operation and maintenance of the intake facilities are expensive.

Groundwater dams are effective in parts of the world which have a large variance of groundwater during the rainy and dry seasons with sufficient groundwater inflow to the underground area and the negligible contribution of land use in groundwater contamination. It should have high effective porosity, sufficient thickness needs, and an impermeable bedrock layer under the aquifer. The dam is built in an underground valley to reduce the construction costs.

PROBLEMS

- 8.1** Groundwater pumping and canal diversion schedules are to be determined for the water resources system shown in [Figure 8.34](#) (Longenbaugh, 1970). The groundwater basin is an unconfined aquifer; seepage and percolation of precipitation and irrigation water account for the majority of groundwater recharge. Develop an optimization model to determine the optimal groundwater and surface water allocation. Assume that the system objective is to minimize the total cost of meeting the forecasted agricultural water demand, and that the stream can be represented by a constant head boundary condition.
- 8.2** The data presented in [Table 8.12](#) are for a storm at a stream gage station. The area of the watershed is about 9000 km^2 . Compute the direct runoff

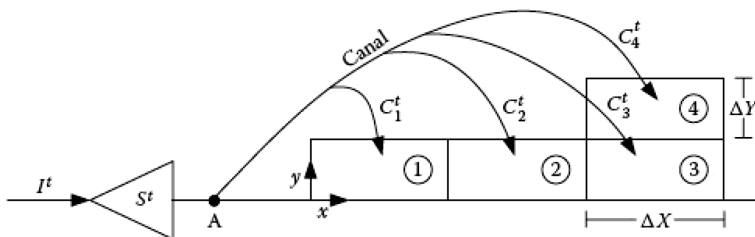


FIGURE 8.34 Water resources system in Problem 8.1.

TABLE 8.12
Recorded Discharge at a Stream Gage Station

| Time | $q \text{ (m}^3/\text{s)}$ | Time | $q \text{ (m}^3/\text{s)}$ | Time | $q \text{ (m}^3/\text{s)}$ |
|------|----------------------------|------|----------------------------|------|----------------------------|
| 1 | 580 | 6 | 2670 | 11 | 1930 |
| 2 | 531 | 7 | 3900 | 12 | 1240 |
| 3 | 705 | 8 | 4300 | 13 | 920 |
| 4 | 1012 | 9 | 3800 | 14 | 815 |
| 5 | 1700 | 10 | 2940 | 15 | 765 |

TABLE 8.13
Recorded Discharge for Six Storms

| Storm 1 | Storm 2 | Storm 3 | Storm 4 | Storm 5 | Storm 6 |
|---------|---------|---------|---------|---------|---------|
| 2100 | 440 | 1310 | 250 | 1040 | 900 |
| 1890 | 410 | 1210 | 220 | 920 | 780 |
| 1710 | 375 | 1120 | 196 | 810 | 700 |
| 1570 | 355 | 1040 | 181 | 760 | 630 |
| 1460 | 330 | 975 | 170 | 680 | 580 |
| 1460 | 312 | 925 | 159 | 640 | 550 |
| 1400 | 298 | 880 | 150 | 610 | 525 |
| 1330 | 286 | 840 | 144 | 580 | 505 |
| 1210 | 273 | 800 | 138 | 560 | 485 |
| 1160 | | 770 | 130 | 535 | 460 |
| | | 740 | 126 | | 440 |
| | | | | | 425 |

and base flow distribution and the volume of direct runoff for each of the following: (a) the constant-discharge method assuming direct runoff and (b) the constant-slope method.

- 8.3** The daily discharge rates from recession curves for six storms are presented in **Table 8.13**. Estimate the parameters of fitting the depletion curve in this region.

REFERENCES

- Dorenbos, H. and Kassam, A.H. 1979. Yield response to water. *Irrigation and Drainage Paper, FAO*, 33, 193.
- Fetter, C.V. 2001. *Applied Hydrogeology*, 4th edn. Prentice Hall, Englewood Cliffs, NJ. ISBN 0-13-066239-9.
- Foster, S., van Steenbergen, F., Zuleta, J., and Garduño, H., 2010. *Conjunctive Use of Groundwater and Surface Water: From Spontaneous Coping Strategy to Adaptive Resource Management*. GW-MATE Strategic Overview Series 2, World Bank, Washington, DC. www.worldbank.org/gwmate
- Ghahraman, B. and Sepaskhah, A.R. 2004. Linear and non-linear optimization models for allocation of a limited water supply. *Journal of Irrigation and Drainage Engineering*, 124(5), 138–149.
- IWMI. 2002. Innovations in groundwater recharge. *IWMI-Tata Water Policy Briefing*, No. 1. <http://www.iwmi.cgiar.org/gwmate>.
- Karamouz, M., Ahmadi, A., and Nazif, S. 2009. Development of management schemes in irrigation planning: Economic parameters and crop pattern consideration. *International Journal of Science & Technology, Scientia Iranica*, 16(6), 457–466.
- Karamouz, M., Hashemi Olya, R., Moridi, A., and Ahmadi, A. 2006. Water allocation from river system considering the interaction between River and aquifer. *ASCE Environmental and Water Resources Institute Conference*, Delhi, India, December, 2006.

- Karamouz, M., Kerachian, R., Zahraie, Ba., and Zahraie, Be. 2002. Conjunctive use of surface and groundwater resources, in *Proceedings of ASCE Environmental and Water Resources Institute Conference*, Roanoke, VA, May 19–22, 2002.
- Karamouz, M., Tabari, M.M., and Kerachian, R. 2007. Application of artificial neural networks and generic algorithms in conjunctive use of surface and groundwater resources. *Water International, IWRA*, 32(1), 163–167.
- Karamouz, M., Zahraie, B., Kerachian, R., and Eslami, A. 2008. Cropping pattern and conjunctive use management: A case study. *Irrigation and Drainage*, 57, 1–13.
- Longenbaugh, R.A. 1970. Determining optimum operational policies for conjunctive use of ground and surface water using linear programming. *ASCE, 18th Annual Specialty Conference*, Minneapolis, MN.
- Meyboom, P. 1961. Estimating ground-water recharge from stream hydrographs. *Journal of Geophysical Research*, 66(4), 1203–1214.
- Onder, H. and Yilmaz, M. 2005. Underground dams, A tool of sustainable development and management of groundwater resources. *European Water*, 11/12, 35–45.
- U.S. Army Corps of Engineers. 1999. *Engineering and Design, Groundwater Hydrology*. EM 1110-2-1421, Department of the Army, Washington, DC.
- Willis, R. and Yeh, W.W.-G. 1987. *Groundwater Systems Planning and Management*. Prentice-Hall, Englewood Cliffs, NJ, pp. 165–342.
- Winter, T.C., Harvey, J.W., Franke, O.L., and Alley, W.M. 1998. *Ground Water and Surface Water: A Single Resource*, USGS (U.S. Geological Survey), 1139, Denver, CO, 79 p.
- Wipplinger, O. 1958. *The Storage of Water in Sand*, South West Africa Administration, Windhoek, South West Africa, 107 p.
- World Bank. 2010. *Conjunctive Use of Groundwater and Surface Water from Spontaneous Coping Strategy to Adaptive Resource Management*, Strategic Overview Series, Washington, DC, No. 2.

9 Aquifer Restoration and Monitoring

9.1 INTRODUCTION

The pollution of groundwater can result from many activities, including leaching from municipal and chemical landfills, accidental leaking of chemicals or waste materials, and improper underground injection of liquid wastes from septic tank systems. On the other hand, population increase and failure in economically developing surface water supplies have increased the demand for groundwater usage. Until recently, the primary reason to deal with polluted aquifers was that once an aquifer becomes polluted, its water usage must be limited. However, due to the increase in water demand, this approach is not reasonable anymore. Therefore, the development of appropriate methodologies for both aquifer recharge as well as its cleanup and restoration have been considered as new approaches to meet the supplying needs.

When a contaminant is applied to a field, depending on the type of the contaminant, a portion of it can be adsorbed by layers of soil, a portion might be volatilized, a portion might be degraded by microorganisms, a portion might be taken by plants uptake, and the rest of that may reach the underlying aquifers. Therefore, due to the type of the contaminant applied to a field, the amount that reaches the underlying aquifer might be significantly less than the initial amount. But this diluted amount of contaminant can still cause quality problems for the underlying aquifer. Some toxics and chemicals as well as some dissolved contaminants are not even degraded or adsorbed and almost all of what is applied to the field will reach the aquifer. Aquifers suspected to be polluted or the ones likely to become contaminated must be monitored. As soon as some concentrations of a pollutant are observed in the aquifer or unsaturated zone, restoration programs or reformatory actions may be set to protect the aquifer against contamination.

On the other hand, in order to increase the security of groundwater resources, Managed Aquifer Recharge (MAR) programs need to be developed, especially in aquifers that are overdrafted or those that are anticipated to be overdrafted in the future due to the increasing demand on water resources as well as negative effects of climate change. In arid and semiarid climates, well designed MAR projects could play a crucial role in increasing groundwater security and social and economic sustainability of the community relying on the groundwater resource. Through MAR projects, excessive surface water (such as stormwater), highly treated wastewater, or recycled water is stored in aquifers for future use to balance supply and demand fluctuations.

In this chapter, the partitioning process of the contaminants is explained in order to determine the amount of the applied pollutions to a field that might reach the underlying aquifer. This is followed by a description of natural ways that may reduce the concentration of some contaminants. The potential ways for groundwater pollution control as well as groundwater treatment methods are also explained as the most important elements of groundwater restoration. The methods and processes of monitoring the quality status of water in unsaturated zones and groundwater are explained in the last part of this chapter. The last section of this chapter focuses on principal considerations for developing MAR projects, describes different MAR methods, and explains how MAR projects could support groundwater sustainability in urban, agricultural, and coastal settings.

9.2 PARTITIONING PROCESS

Since contaminants move through soil layers to reach groundwater, it is important to know how much of the pollutant is adsorbed to the soil particles and how much is in solution or can potentially be dissolved into pore water. In the dissolved phase, the pollutants can be transported to aquifers and surface waters.

The term partitioning is used to divide the total pollutant mass between the particulate (adsorbed on particulate matter) and dissolved fractions.

Adsorption of the contaminant into the particulate form immobilizes contaminants and makes them biologically unavailable in most cases. Dissolved or dissociated (ionized) contaminants are mobile with soil pore water. The master variables that affect the interactions between the soluble and particulate fractions of the contaminant are the pH, the anion-cation composition of the soil-pore-water solution, and the particulate and dissolved organic carbon (Salomons and Stol, 1995).

Hydrophilic or water-soluble compounds have higher bioavailability and leach more easily into groundwater. On the other hand, hydrophobic or water-insoluble compounds are immobile, and they accumulate in soils.

The mobility of an organic chemical in soils is related to the octanol–water partitioning coefficient, K_{OW} . For nonionic chemicals and some other chemicals, the partitioning can be correlated to the octane partitioning coefficient. Rao and Davidson (1982) presented the values of K_{OW} for different pesticides.

For describing the proportion between the dissolved (ionized) and adsorbed (precipitated) particulate fractions, among several proposed mathematical formulations of adsorption equilibrium (isotherms), the Langmuir, Freundlich, and linear isotherms are most widely accepted.

The Langmuir adsorption model is expressed as:

$$r = \frac{Q^0 b C_d}{1 + b C_d} \quad (9.1)$$

where:

r is the adsorbed concentration of the contaminant ($\mu\text{g/g}$)

C_d is the dissolved concentration of the contaminant in water or pore water of soil ($\mu\text{g/L}$)

Q^0 is the adsorption maximum at the fixed temperature ($\mu\text{g/g}$)

b is a constant related to the energy of net enthalpy of adsorption ($\text{L}/\mu\text{g}$).

The general form of the Freundlich isotherm is:

$$r = KC_d^{1/n} \quad (9.2)$$

where K and n are constants.

If bC_d in the Langmuir isotherm is much less than 1 or the exponent in the Freundlich equation is close to 1, the isotherm becomes linear. This isotherm is expressed as:

$$r = \Pi C_d \quad (9.3)$$

where $\Pi = bQ^0$ is the partition coefficient and has units of L/g if r is in $\mu\text{g/g}$ and C_d is in $\mu\text{g/L}$.

The total concentration of a pollutant in the soil is then a sum of the dissolved and adsorbed particulate concentrations:

$$C_T = \theta C_d + r \rho_{bd} \quad (9.4)$$

where:

C_T is the total concentration of the pollutant in the soil ($\mu\text{g/L}$)

θ is the water content of the soil

ρ_{bd} is the bulk density of solids (g/L) and is calculated as $\rho_{bd} = 2.65 (1 - n)$.

In this relation, $2.65 (\text{g/cm}^3)$ is the density of soil particles and n is the porosity.

The relation of the dissolved (pore water) concentration of a chemical and the total concentration in the soil is obtained from the following equation:

$$C_d = \frac{1}{\theta + \Pi \rho_{bd}} C_T \quad (9.5)$$

Example 9.1

Phosphorus 9 is applied and distributed uniformly to a field through the first 25 cm of the soil's depth at a rate of 105 kg/ha. The soil's maximum adsorption of phosphorus is $310 \mu\text{g/g}$. The porosity of the soil and the specific density of the soil sample are 45% and 1460 kg/m^3 ($=\text{g/L}$), respectively. Estimate the approximate groundwater contamination by phosphorus during a long period of rain (the soil is saturated). Assume that the constant b is equal to $0.0018 \text{ L}/\mu\text{g}$.

SOLUTION

The total inorganic P content of the soil is:

$$C_T = \frac{105 \text{ kg/ha} \times 10^9 \mu\text{g/kg}}{0.25 \text{ m} \times 10^4 \text{ m}^2/\text{ha} \times 1,000 \text{ L/m}^3} = 42,000 \mu\text{g/L}$$

This concentration is distributed between adsorbed and dissolved fractions as:

$$C_T = r\rho_{bd} + C_d\theta = \frac{Q^0 b C_d}{1 + b C_d} \rho_{bd} + C_d\theta$$

Since the soil is saturated, θ = porosity. Therefore:

$$42,000 \text{ }\mu\text{g/L} = \frac{310 \text{ }\mu\text{g/L} \times 0.0018 \text{ L}/\mu\text{g} \times C_d}{1 + 0.0018 \text{ L}/\mu\text{g} \times C_d} \times 1,460 \text{ g/L} + C_d \times 0.45$$

Solving this equation, the groundwater contamination by phosphorus from the application of this fertilizer is 56.8 $\mu\text{g/L}$.

9.3 RETARDATION

In subsurface zones, organic chemicals move more slowly than dissolved contaminants since they are retarded by adsorption. To incorporate adsorption to groundwater contaminant transport calculations, a retardation factor is introduced. A retardation factor is an empirical term derived from a partitioning coefficient and is the ratio of total chemicals to dissolved chemicals:

$$R = \frac{\text{Total chemicals}}{\text{Dissolved chemicals}} = \frac{\theta C_d + r\rho_{bd}}{\theta C_d} \quad (9.6)$$

where R is the retardation factor. In the above equation, r can be substituted by its corresponding value (ΠC_d), and we have:

$$R = 1 + \frac{\rho_{bd}\Pi}{\theta} \quad (9.7)$$

The chemical solute moves only in the dissolved phase and the adsorbed phase is not moving. Therefore, the ratio of the velocity of water to the velocity of the solute can also be determined by R :

$$V_{\text{Solute}} = \frac{V_{\text{Water}}}{R} \quad (9.8)$$

The downward velocity of water/or dissolved phase is equal to the infiltration rate divided by the soil water content.

So far, we determined how fast a solute moves downward in the unsaturated zone. It is also important to determine how far the solute goes downward. Imagine a depth of water per unit time, d , is added to the soil at a constant water content, θ . The depth to which the water moves down, D , is computed as:

$$D = \frac{d}{\theta} \quad (9.9)$$

If this water contains a chemical with the concentration C_d , and assuming this concentration remains constant, the chemical moves downward to the depth:

$$D' = \frac{D}{R} = \frac{d}{\theta R} \quad (9.10)$$

Example 9.2

A pesticide is applied to an agricultural field with 1.2 cm/day net water through the irrigation system. The soil water content and bulk density are 0.30 and 1600 kg/m³, respectively. Assuming the partitioning coefficient is 1.25 L/kg, what fraction of the total chemical may reach the groundwater? How far can the dissolved portion go downward in a day? Imagine the water table depth is 1.8 m, how long does it take for the chemical to reach the water table? Assume the soil water content remains constant.

SOLUTION

$$\rho_{bd} = 1600 \text{ kg/m}^3 = 1.6 \text{ kg/L}$$

$$R = 1 + \frac{\rho_{bd}\Pi}{\theta} = 1 + \frac{1.6 \text{ kg/L} \times 1.25 \text{ L/kg}}{0.30} = 7.67$$

$$\text{Dissolved fraction} = \frac{1}{R} = \frac{1}{7.67} = 0.13 = 13\%$$

The depth to which the chemical reaches:

$$D' = \frac{d}{\theta R} = \frac{1.2}{0.3 \times 7.67} = 0.52 \text{ cm/day}$$

$$t = \frac{180}{0.52} = 346 \text{ days}$$

Therefore, the chemical reaches the water table after 346 days.

9.4 NATURAL LOSSES OF CONTAMINANTS

Generally, not all of the contaminants applied to a field reach the underlying aquifer. There are different paths that the pollutants may be removed from soil before reaching aquifers. These paths include volatilization, biological degradation, and plant uptake, which are explained in the following section.

9.4.1 VOLATILIZATION

Volatilization is the loss of chemicals in vapor form from soil or water surfaces to the atmosphere. The potential of volatilization is mainly related to the saturated vapor pressure of the chemical in the air above the interface. It should be noted that volatilization does not occur from submerged aquatic sediments.

The relation between the vapor density and the corresponding concentration of the chemical in water solution can be computed by Henry's law:

$$C_d = K_H C_g \quad (9.11)$$

where:

K_H is Henry's constant for the chemical and is considered dimensionless

C_g is the vapor density of the chemical ($\mu\text{g/L}$).

To include the vapor phase of a chemical in the partitioning equation, Equation 9.11 is expanded as:

$$C_d = \frac{1}{\theta + \Pi \rho_{bd} + (n - \theta) / K_H} C_T \quad (9.12)$$

9.4.2 BIOLOGICAL DEGRADATION

The breakdown of a chemical by microorganisms to more simple compounds is interpreted as biological degradation. In this process, the chemical is ultimately transformed to carbon dioxide, water, methane, ammonium, and other simple by-products. Decomposition of the compound into mineral products is called mineralization. On the other hand, transformation is a change to another form, which may or may not be less environmentally hazardous. Chemicals that are not biodegradable are called persistent in the environment. The removal of persistent chemicals is only by transferring to another medium (from soil to water or air) or by burial. Some microorganisms or fungi can also cause biotransformation of chemicals. These organisms require energy and an organic carbon source as well as nutrients for their growth.

In general, the degradation rate of chemicals can be calculated using the first-order reaction as the most accepted model:

$$C_t = C_0 e^{-k_d t} \quad (9.13)$$

where:

C_t and C_0 are the chemical masses at time t and 0, respectively

k_d is the overall degradation coefficient (day^{-1})

t is the time (day).

Given the values of C_t and C_0 from the experiment, the value of k_d can be calculated using the above relation. Then the half-life of the organic chemicals, which is the

mean time required for 50% degradation of the original chemical in the soil, or their persistence in the soil is computed as:

$$t_{1/2} = -\frac{\ln(0.5)}{k_d} = \frac{0.69}{k_d} \quad (9.14)$$

9.4.3 PLANT UPTAKE

Plants uptake nutrients and some chemicals and immobilize them. The nutrient and chemical uptake process is a part of the overall transpiration process of plants. Nutrients and chemicals are transported into plant tissues from the dissolved or ionic pool of chemicals in pore water. Therefore, chemicals and nutrients adsorbed on soil particles or precipitated in soils are not removed from the system by plant uptake. These adsorbed pollutants must first be transferred into the pore water by disruption or dissolution.

Example 9.3

A pesticide, atrazine, is applied to an agricultural field at a rate of 1.5 kg/ha. This field is irrigated at a rate of 2 cm/day, and the crop water use is 0.45 cm/day. Assuming the soil water content remains constant at 0.35, the partitioning coefficient is 0.97, the soil bulk density is 1.5 g/cm³, and the water table depth is 2.5 m. Determine the load of dissolved atrazine that reaches to the water table. The decay factor for atrazine is 0.042 (day⁻¹).

SOLUTION

First, the fraction of adsorbed and dissolved atrazine is calculated:

$$R = 1 + \frac{\rho_{bd}\Pi}{\theta} = 1 + \frac{1.5 \times 0.97}{0.35} = 5.16$$

$$\text{Dissolved fraction} = \frac{1}{R} = \frac{1}{5.16} = 0.194 = 19.4\%$$

$$\text{Adsorbed fraction} = 100 - 19.4 = 80.6\%$$

Out of 2 cm/day water that is applied to the field, 0.45 cm/day is used by the crop. Therefore, the depth to which water reaches in a day is:

$$D = \frac{d}{\theta} = \frac{2 - 0.45}{0.35} = 4.4 \text{ cm}$$

The depth to which atrazine reaches in a day is:

$$D' = \frac{D}{R} = \frac{4.4}{5.16} = 0.85 \text{ cm}$$

The time needed for atrazine to reach the water table at the depth of 2.5 m is:

$$t = \frac{250 \text{ cm}}{0.85 \text{ cm}} = 294 \text{ days}$$

Using the first-order reaction equation and given the value of the decay factor, the concentration of dissolved atrazine that will remain in the water when it reaches the water table is computed:

$$C_t = C_0 e^{-k_d t} = 1.5 \text{ kg/ha} \times e^{-(0.042 \times 294)} = 6.5 \times 10^{-6} \text{ kg/ha}$$

9.5 GROUNDWATER POLLUTION CONTROL

To be able to perform any aquifer restoration activities, it is important to have information about the best available technologies. In other words, what technology can be applied to prevent, abate, or clean up polluted groundwater? In this section, the information on institutional measures and source control strategies for preventing or minimizing the groundwater pollution is provided. The information involves physical control measures such as well and interceptor systems, surface capping and liners, and physical containment barriers such as sheet piling, grouting, and slurry walls.

9.5.1 INSTITUTIONAL TOOLS

The main purpose of using institutional tools is to protect groundwater resources. Institutional tools include regional groundwater management, land zoning, effluent charges/credits, guidelines, aquifer standards, and criteria.

9.5.1.1 Regional Groundwater Management

Regional management of groundwater can be an effective approach in the prevention of long-term quality and quantity polluting activities. Public education and some regulatory enforcement are some possible functions of this approach.

Public education could include proper use of agricultural fertilizers, pesticides, herbicides, chemicals, waste disposal guidelines, and lists of reputable groundwater professionals such as well drillers. Minimal enforcement capabilities could help prevent such polluting activities as overuse or abuse of chemicals, excessive groundwater withdrawal, etc.

9.5.1.2 Land Zoning

Land zoning is related to optimum site selection and disallows industrial or waste disposal activities in groundwater recharge areas.

9.5.1.3 Effluent Charges/Credits

Economic incentives are important tools to protect groundwater resources. On the other hand, by applying charges to polluting effluents applied to or disposed of on the soil, the quality of effluent from certain facilities may be improved, and in consequence, less pollution load is transferred to groundwater resources. Concurrently,

credits can be applied to those facilities that move to improve the groundwater resources such as those employing artificial recharge measures.

9.5.1.4 Guidelines

Establishing guidelines or standards for construction and operation of groundwater polluting activities is one of the most effective tools to protect aquifers. Many states are now adopting standards for the construction of waste disposal facilities, and this can be expanded to include oil well drilling, mining and minerals extraction, on-site sewage disposal, and other activities.

9.5.1.5 Aquifer Standards and Criteria

Other effective institutional tools to protect aquifers from pollution is the establishment and application of groundwater quality standards and criteria for aquifers and modification of current surface water beneficial use standards to be able to apply them for groundwater resources.

9.5.2 SOURCE CONTROL STRATEGIES

The best solution to pollution is prevention (Novotny 2003). Source control strategies represent attempts to minimize or prevent groundwater pollution before a potential polluting activity is initiated. These strategies can be considered as another institutional tool. By applying source control strategies, the volume of wastewater or the pollution load from an effluent can be reduced.

Source control strategies are applied to the design of new facilities as a component of one or more groundwater pollution prevention steps. However, some of the strategies can be used as pollution reduction tools for existing facilities.

Knox et al. (1986) summarized some common types of source control strategies that can be applied to prevent groundwater pollution at waste disposal facilities. These strategies are as follows:

1. Volume reduction strategies
 - a. Recycling
 - b. Resource recovery
 - i. Materials recovery
 - ii. Waste-to-energy conversion
 - c. Centrifugation
 - d. Filtration
 - e. Sand drying beds
2. Physical/chemical alteration strategies
 - a. Chemical fixation
 - i. Neutralization
 - ii. Precipitation
 - iii. Chelation
 - iv. Cementation
 - v. Oxidation-reduction
 - vi. Biodegradation

- b. Detoxification
 - i. Thermal
 - ii. Chemical—ion-exchange, pyrolysis, etc.
 - iii. Biological—activated sludge, aerated lagoons, etc.
- c. Degradation
 - i. Hydrolysis
 - ii. Dechlorination
 - iii. Photolysis
 - iv. Oxidation
- d. Encapsulation
- e. Waste segregation
- f. Co-disposal
- g. Leachate recirculation

The only criterion applicable to these strategies is that they all require extensive monitoring and recordation. The advantages of source control strategies include the following:

- 1. Enhancing groundwater quality by reducing the pollution load applied to the aquifer
- 2. Reducing the stabilization time of waste disposal facilities
- 3. Decreasing the cost of aquifer restoration and groundwater treatment

The disadvantages of source control strategies are the following:

- 1. It is hard to convince industries to apply these strategies because of the lack of public knowledge about the environmental hazards
- 2. Installation and maintenance costs
- 3. Monitoring and skilled operator requirements

9.5.3 STABILIZATION/SOLIDIFICATION STRATEGIES

By structurally isolating the waste material in a solid matrix prior to landfilling, the threat to groundwater from the land disposal of waste materials can be reduced. This process, known as stabilization/solidification, is becoming significantly popular for hazardous and radioactive waste disposal. In this process, the waste in a solid matrix is chemically fixed. This reduces the exposed surface area and minimizes leaching of toxic constituents. In the immobilization process, toxic components chemically react to form compounds immobile in the environment and/or the toxic material in an inert stable solid entrapp. Thus, stabilization and solidification have different meanings, although the terms are often used interchangeably. From a definitional perspective, stabilization refers to immobilization by a chemical reaction or entrapping, while solidification means the production of a solid, monolithic mass with enough integrity to be easily transported. These processes may overlap or take place within one operation. An example is cementation, where the process

both stabilizes by producing insoluble heavy metal compounds and solidifies into a formed mass while entrapping the pollutants.

When a material is chemically stabilized, a substance which is more resistant to leaching and also more amenable to the solidification process is provided. By chemically fixing the hazardous waste constituents, their release will be minimized in the event of a breakdown of the solid matrix. pH adjustment is the simplest stabilization process. In most industrial sludge, toxic metals are precipitated as amorphous hydroxides that are insoluble at an elevated pH. By carefully selecting a stabilization system of suitable pH, the solubility of any metal hydroxide can be minimized. Certain metals can also be stabilized by forming insoluble carbonates or sulfides. It should still be taken into account that there is a probability for these metals to be remobilized because of changes in pH or redox conditions after they have been introduced into the environment.

By microencapsulation or macro-encapsulation, stabilized wastes can be solidified into a solid mass. Microencapsulation refers to the dispersion and chemical reaction of the toxic materials within a solid matrix. Therefore, any breakdown of the solid material only exposes the material located at the surface to potential release to the environment. Macro-encapsulation is the sealing of the waste in a thick, relatively impermeable coating layer. Plastic and asphalt coatings, or secured landfilling, are considered to be macro-encapsulation methods. Breakdown of the protective layer with macro-encapsulation could result in a significant release of toxic material to the environment.

By stabilization/solidification processes, a material is produced which does not pose a threat to the land on which it is disposed. The resultant stabilized/solidified material is impervious, having a good dimensional stability and load-bearing characteristics. It should have satisfactory wet-dry and freeze-thaw weathering resistance. These properties plus optimum size and shape will make the material easily transportable.

Because of their chemical and toxic components, most of stabilized industrial wastes cannot be used on agricultural land; however, they might be suitable for building subfoundations or as subgrade materials under roads or runways. There is no optimum stabilization/solidification process applicable to every type of hazardous waste. Each individual waste must be characterized and bench tests and pilot studies performed to determine the suitability of a given process.

Some common solidification/stabilization systems, suggested by Knox et al. (1986) are as follows:

1. Solidification through cement addition
2. Solidification through the addition of lime and other pozzolanic materials
3. Techniques involving embedding wastes in thermoplastic materials such as bitumen, paraffin, or polyethylene
4. Solidification by the addition of an organic polymer
5. Encapsulation of wastes in an inactive coating
6. Treatment of the wastes to produce a cementitious product with major additions of other constituents
7. Formation of a glass by the fusion of wastes with silica

9.5.4 WELL SYSTEMS

For groundwater pollution control purposes, the subsurface hydraulic gradient is manipulated through injection or withdrawal of water. In well systems, the movement of the water phase is controlled directly and the concentration of pollutants in the subsurface water is controlled indirectly. This approach is often referred to as plume management. There are three main classes of well systems. These three classes are well point systems, deep well systems, and pressure ridge systems. There is injection of water in the latter one and water withdrawal in the other ones. All of these three systems require the installation of several wells at selected sites. These wells are then pumped (or injected) at specified rates so as to promote the movement of the water phase and associated pollutants.

The use of well systems is the most common method of groundwater pollution control. Well systems represent the most assured means of controlling subsurface flows contaminants. These systems can be installed readily, can sometimes include the recharge of the aquifer, and have high design flexibility. In addition, construction costs for these systems can be lower than artificial barriers. However, operation and maintenance costs are high and well systems require continued monitoring after installation. Besides, clean water may also be removed along with polluted water in withdrawal systems, and these systems may require surface treatment prior to discharge.

9.5.5 INTERCEPTOR SYSTEMS

In interceptor systems, a trench is excavated below the water table and a pipe is placed in the trench. The function of these drains or trenches is similar to an infinite line of extraction wells; that is, they affect a continuous zone of depression, which runs the length of the drainage trench (Kufs et al., 1983). [Figure 9.1](#) shows an interceptor trench. Usually the trench receives perforated pipe and coarse backfill

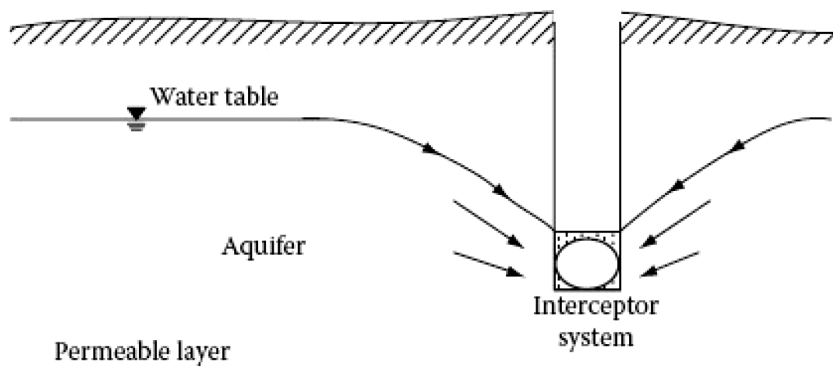


FIGURE 9.1 Hydraulic gradient toward interceptor system.

material for efficiency of collecting incoming water and transporting it. Interceptor systems are classified as preventive measures (leachate collection systems) or abatement measures (interceptor drains).

Interceptor systems provide a means of collecting leachate without the use of impervious liners and since flow to underdrains is by gravity, operation costs are relatively cheap. Design of underdrains is flexible and construction methods are simple. However, these systems are not recommended for poorly permeable soils, and it is not feasible to situate underdrains beneath an existing site. In addition, interceptor systems require continuous and careful monitoring to assure adequate leachate collection. The following disadvantages can also be considered for interceptor systems:

1. When dissolved constituents are involved, it may be necessary to monitor groundwater down-gradient of the recovery line (Quince and Gardner, 1982).
2. Open systems require safety precautions to prevent fires or explosions.
3. Interceptor trenches are less efficient than well-point systems.
4. Not useful for deep disposal sites (U.S. Environmental Protection Agency, 1979).

9.5.6 SURFACE WATER CONTROL, CAPPING, AND LINERS

Surface water control, capping, and liners are three different technologies that are usually used in conjunction with each other. The three technologies serve different purposes in preventing groundwater pollution. Using surface water control tools, the amount of surface water flowing onto a site is minimized, which results in reducing the amount of potential infiltration. By the capping of a site, the infiltration of any surface water or direct precipitation coming onto a site is reduced. Impermeable liners provide groundwater protection by inhibiting the downward flow of leachate and other pollutants by adsorption processes. These technologies are preventive measures, although surface water control and capping have also been used successfully to abate groundwater pollution problems (Emrich et al., 1980). One of the approaches for placement of liners after a polluting activity has been initiated is the use of grouts. Grouting will be discussed in a subsequent section.

Surface water control measures are a relatively inexpensive means of minimizing future groundwater pollution problems. Surface water flow in streams and channels is easily minimized by using structural techniques such as diversion dams and drainage ditches (Smith, 1983). The design of a site utilizing surface caps or impermeable liners, or both, is based on a water balance for the site.

There are four combinations of capping and liners that could be used (in conjunction with surface water control measures) at a waste site. [Figure 9.2](#) depicts these combinations. In this figure, Q_C is the rate of water collected by the system and Q_R is the rate of water released from the system. Type (a) is called a natural attenuation site and neither capping nor lining is utilized in this type. It relies entirely on the pollutant-attenuating capacity of the native soil. Type (b) utilizes an engineered liner (impermeable liner) to maximize the amount of leachate collected and minimize the amount escaping. The engineered cover (impermeable cap) sites are designed to minimize infiltration

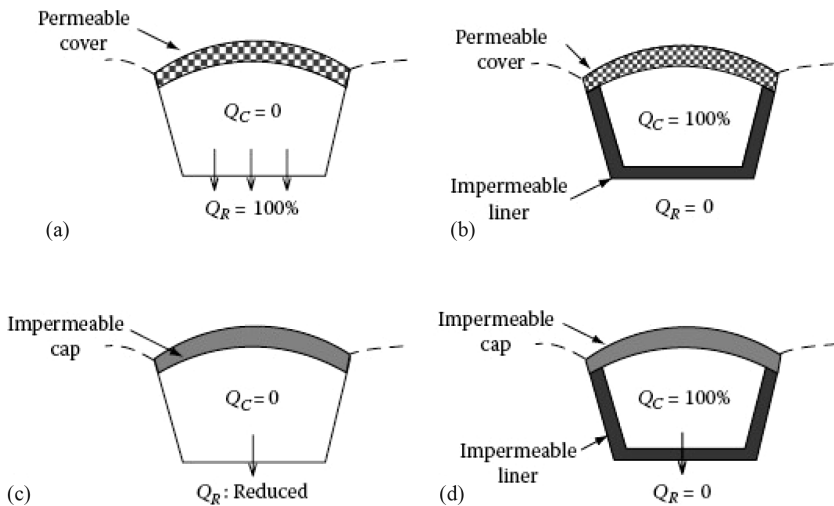


FIGURE 9.2 Four combinations of capping and lining systems. (a) a natural attenuation site and neither capping nor lining, (b) an engineered liner (impermeable liner) (c) a engineered cover (impermeable cap) sites and (d) a combination of engineered cover and liner (total containment).

into the waste source by maximizing surface runoff and evapotranspiration (type (c)). The sites that have the combination of engineered cover and liner (total containment) are designed to minimize infiltration and maximize the collected leachate (type (d)).

Natural attenuation systems do not have leachate collection, transport, and treatment costs; but they require a unique hydrogeologic setting, and it is difficult to obtain regulatory acceptance in these systems. Engineered liner systems decrease hydrogeologic impact and stabilize waste quickly. However, the construction costs are higher and surface discharge is likely in these systems. Engineered cover systems decrease hydrogeologic impact after closure. The construction costs relative to liners are reduced in these systems, but closure costs are increased. There is no leachate control during site operations, and these systems need long-term monitoring. Engineered cover systems have lesser environmental impacts, and they are more acceptable socially and politically. They also minimize post-closure leachate collection, transport, and treatment costs. However, they have higher engineering and construction costs and need high-quality clay or synthetic material. In addition, these systems need more time for waste stabilization.

9.5.7 SHEET PILING

In sheet piling, a thin impermeable permanent barrier for flow is created by driving lengths of steel that connect together into the ground. Timber and concrete can also be used if the groundwater is not polluted. Pile driving requires a relatively uniform, loose, boulder-free soil for ease of construction. Steel sheet piles are also effective and economical for groundwater control. As the size of a project increases, the application of sheet piling becomes uneconomical.

Construction of sheet piles can be economical and is not difficult, since excavation is not necessary. There is no maintenance required after construction. However, driving piles through ground that contains boulders is difficult. In addition, for steel sheet piles, certain chemicals may attack the steel and the steel sheet piling is not initially watertight.

9.5.8 GROUTING

The grouting technology is used to increase soil-bearing capacity or to decrease the permeability of soils. This technology has been used in the construction industry for years. In the grouting process, a liquid, slurry, or emulsion is injected under pressure into the soil. This fluid occupies the available pore spaces. It then solidifies, resulting in a decrease in the original soil permeability and an increase in the soil-bearing capacity. Grouts are usually applied in two types: particulate and chemical. Particulate grouts consist of water plus particulate material that solidifies within the soil matrix. Chemical grouts consist of two or more liquids that form a gel when they are combined together. Particulate grouts have higher viscosities than chemical grouts and are therefore better suited for larger pore spaces, whereas chemical grouts are better suited for smaller pore spaces (USEPA, 1998).

Grouts have been used for over 100 years in construction and soil stabilization projects. They can be used successfully for groundwater pollution control. There are many kinds of grouts available that suit a wide range of soil types. However, grouting is limited to granular types of soils that have a pore size large enough to accept grout fluids under a pressure which is small enough to prevent significant pollutant migration before the implementation of the grout program. Highly layered soil profiles are not suitable for grouting since they may result in incomplete formation of a grout envelope. In addition, the presence of a high water table and rapidly flowing groundwater limits groutability.

9.5.9 SLURRY WALLS

Slurry walls encapsulate an area to prevent groundwater pollution and restrict the movement of contaminated groundwater. In this method, a trench is first excavated around an area. This trench is then filled with an impermeable material. This technology is regarded as an effective method of isolating hazardous waste and preventing the migration of pollutants (Pearlman 1999). Slurry walls can either be placed up-gradient from a waste site (Figure 9.3) to prevent the flow of groundwater into the site, or placed around a site (Figure 9.4) to prevent movement of polluted groundwater away from a site.

Slurry walls have been applied to the Rocky Mountain Arsenal in Colorado and the Gilson Road Hazardous Waste Dump in New Hampshire (Knox et al., 1986).

The construction methods for slurry walls are simple and adjacent areas are not usually affected by groundwater drawdown. Slurry walls have low maintenance requirements. They eliminate risks due to pump breakdowns or power failure. If bentonite is used in the slurry wall, it will not deteriorate with age. The most widely used technique for containment is the soil-bentonite slurry wall. It is typically the

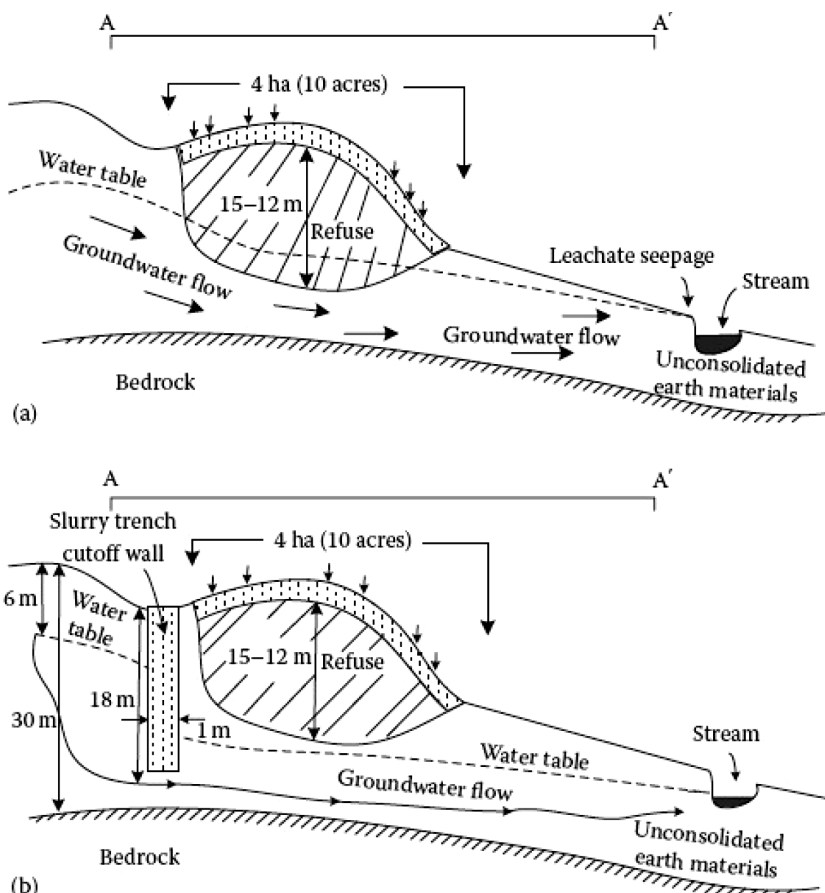


FIGURE 9.3 Cross section of landfill (a) before and (b) after the installation of slurry trench cutoff wall. (From Tolman, et al., *Guidance Manual for Minimizing Pollution from Waste Disposal Sites*, EPA-600/2-78-142, August, U.S. Environmental Protection Agency, Cincinnati, OH, 1978.)

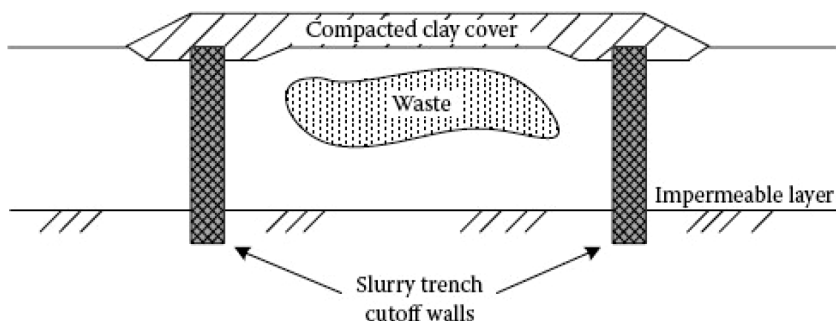


FIGURE 9.4 Isolation of existing buried waste.

most economical, utilizes low-permeability backfill, and usually allows reuse of all or most of the material excavated during trenching (Kresic, 2009).

However, bentonite deteriorates when exposed to high ionic strength leachates. Since bentonite is available mostly in the West, in applying bentonite slurry walls in other areas, the shipping cost must also be taken into consideration. In addition, some construction procedures for slurry walls are patented and will require a license.

9.6 TREATMENT OF GROUNDWATER

The type of treatment required for site-specific contaminated groundwaters depends on the contaminants being removed. Due to the number of chemicals that potentially exist in groundwater as contaminants; the treatment can be simple or extremely complex. Some treatment processes such as air stripping, activated carbon, biological treatment for organics in groundwater, and chemical precipitation for inorganics in groundwater will be explained in this section.

9.6.1 AIR SPARGING

In situ air sparging (IAS) is primarily used to remove volatile organic carbons (VOCs) from the saturated subsurface. The removal process is done through stripping. The basic IAS system strips VOCs by injecting air into the saturated zone to promote contaminant partitioning from the liquid to the vapor phase. [Figure 9.5](#) depicts a typical IAS system. Since injected air, oxygen, can induce the activity of indigenous microbes, IAS can be effective in increasing the rate of natural aerobic biodegradation. In addition, by injecting a nonoxygenated gaseous carbon source, anaerobic

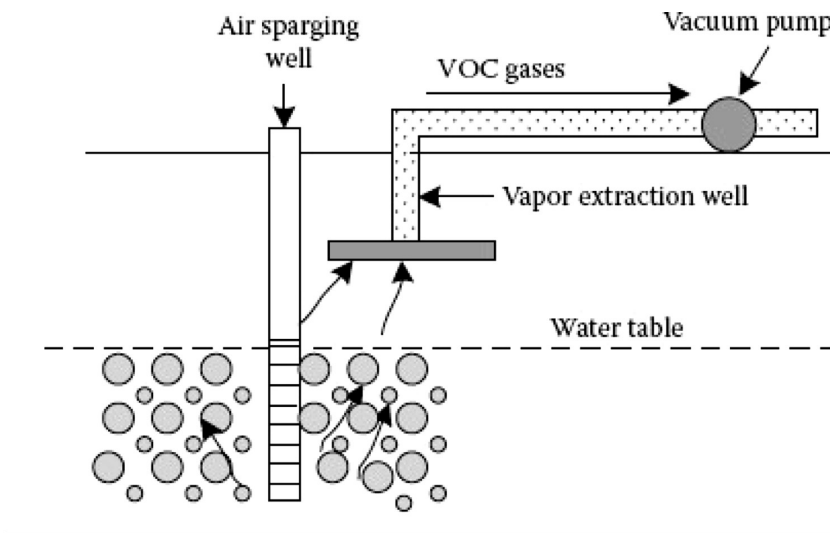


FIGURE 9.5 Typical in situ air sparging system.

environments can be created to provide denitrification conditions for nitrate removal from the groundwater. Enhanced degradation of organic compounds, such as chlorinated VOCs, to daughter products would result in increased volatility, which could improve the effectiveness of stripping and phase transfer during IAS (USACE, 2008).

IAS is relatively easy to implement and the equipment necessary for IAS is inexpensive and easily obtained. It is a well known process to regulatory agencies. Therefore, IAS is one of the most practiced engineered technologies for in situ groundwater remediation (Kresic, 2009). However, the presence and distribution of preferential airflow pathways, the degree of groundwater mixing, and potential precipitation and clogging of the soil formation by inorganic compounds are important aspects to be taken into consideration in designing an IAS system.

In air stripping, a substance is transferred from the solution in water to the solution in a gas, and then it is transferred to the atmosphere. The rate of mass transfer can be calculated, using the following equation:

$$M = K_L A (C_L - C_g) \quad (9.15)$$

where:

M is the mass of substance transferred per unit time and volume ($\text{g}/\text{h}/\text{m}^3$)

K_L is the coefficient of mass transfer (m/h)

A is the effective area (m^2/m^3)

C_L is the concentration in liquid phase (g/m^3)

C_g is the concentration in gas phase (g/m^3)

$(C_L - C_g)$ is the driving force.

The driving force is the difference between actual conditions in the air stripping unit and conditions associated with equilibrium between the gas and liquid phases. If equilibrium exists at the air-liquid interface, the liquid phase concentration is related to the gas phase concentration by Henry's law:

$$C_{g\text{-}eq} = K_H C_{l\text{-}eq} \quad (9.16)$$

where:

$C_{g\text{-}eq}$ is the equilibrium concentration in the gas phase (g/m^3)

$C_{l\text{-}eq}$ is the equilibrium concentration in the liquid phase (g/m^3)

K_H is the Henry's law constant.

If a compound has a high Henry's law constant, it is stripped from water easier than the one with a lower Henry's law constant.

9.6.2 CARBON ADSORPTION

An organic molecule can be held on the surface of activated carbon by physical and/or chemical forces. Due to the balance between the forces that keep the compound in solution and the forces that attract the compound to the carbon surface, the quantity of a compound that can be adsorbed by activated carbon is determined. The following factors can affect this balance:

1. There is an inverse relation between adsorptivity and solubility.
2. The pH has a significant impact on the adsorptive capacity. For example, organic acids adsorb better under acidic conditions, while amino compounds prefer alkaline conditions.
3. Aromatic and halogenated compounds adsorb better than aliphatic compounds.
4. Adsorption capacity (but not the rate of adsorption) and temperature have an inverse relationship.

When activated carbon begins adsorbing organic chemicals, their concentration will decrease from an initial concentration, C_0 , to an equilibrium concentration, C_e .

Using Freundlich and Langmuir isotherms, the approximate capacity of the carbon for the application can be estimated and a rough estimate of the carbon dosage required can be provided. Activated carbon adsorption is a successful way for removing organics from contaminated groundwater.

9.6.3 ADDING CHEMICALS AND IN SITU CHEMICAL OXIDATION

Adding chemicals to contaminated aquifers is one the effective ways for the removal of inorganic compounds. The carbonate system, the hydroxide system, and the sulfide system are three common basic types of chemical addition systems. Among these chemicals, the sulfide system removes the most inorganics, with the exception of arsenic (because of the low solubility of sulfide compounds). But the side effect is that sulfide sludge might be oxidized to sulfate when exposed to air, resulting in resolubilization of the metals. In the carbonate system, soda ash is used to adjust the pH to 8.2 and 8.5. This system is difficult to control in actual condition. The hydroxide system has almost the best performance for the removal of inorganics and metals. The system uses either lime (CaOH) or sodium hydroxide (NaOH) as the chemical to adjust the pH upwards.

In the in situ chemical oxidation method, groundwater or soil contaminants are transformed into less harmful chemical species by the introduction of a chemical oxidant into the subsurface. In the remediation of contaminated groundwater using in situ chemical oxidation, oxidants and potential amendments are directly injected into the source zone and down-gradient plume. The oxidant chemicals react with the contaminants and produce harmless substances such as carbon dioxide, water, etc. In situ chemical oxidation is a suitable method for removing BTEX (benzene; toluene; ethylbenzene; and o-xylenes, m-xylenes, and p-xylenes), methyl tert-butyl ether (MTBE), total petroleum hydrocarbons (TPH), chlorinated solvents (ethenes and ethanes), polycyclic aromatic hydrocarbons (PAHs), polychlorinated biphenyls (PCBs), chlorinated benzenes, phenols, and organic pesticides. The most commonly used oxidants for remediation purposes are as follows:

- Permanganate (MnO_4^-)
- Hydrogen peroxide (H_2O_2) and iron (Fe) (Fenton-driven or H_2O_2 -derived oxidation)
- Persulfate ($\text{S}_2\text{O}_8^{2-}$)
- Ozone (O_3)

The persistence of the oxidant in the subsurface is important, since this affects the contact time for advective and diffusive transport and ultimately the delivery of the oxidant to targeted zones in the subsurface (Huling and Pivetz, 2006). For example, permanganate persists for long periods of time, but H_2O_2 can persist in soil and aquifer material for minutes to hours. Therefore, the diffusive and advective transport distances may be relatively limited for H_2O_2 . The rates of oxidation reactions are dependent on many variables that must be considered simultaneously, including temperature, pH, concentration of the reactants, catalysts, reaction by-products, and system impurities such as natural organic matter and oxidant scavengers (ITRC, 2005).

9.6.4 THERMAL TECHNOLOGIES

In situ thermal heating methods are generally used for enhanced oil recovery. These methods include hot water injection, steam injection, hot air injection, and electric resistive heating. Soil and groundwater zones contaminated by chlorinated solvents can be remediated by these methods. Volatile and semi-VOCs (SVOCs), such as PCBs, PAHs, pesticides, and various fuels, oils, and lubricants can also be treated by in situ thermal technologies.

A thermal heating system typically consists of a series of injection and extraction wells. The injection wells are usually placed in clean areas around the source zone, if possible, to minimize the risk of contaminant spreading. Figure 9.6 expresses a schematic of a thermal heating system. In this figure, hot water, steam, or hot air is injected into the subsurface to dissolve, vaporize, and mobilize contaminants that are then recovered. Then, mobilized contaminants are extracted from the subsurface using vapor and liquid extraction equipment. Extracted vapors and liquids are then treated using conventional aboveground treatment technologies.

In all thermal technologies, the viscosity of nonaqueous phase liquids are lowered and the vapor pressure and solubility of VOCs or SVOCs are increased. In consequence,

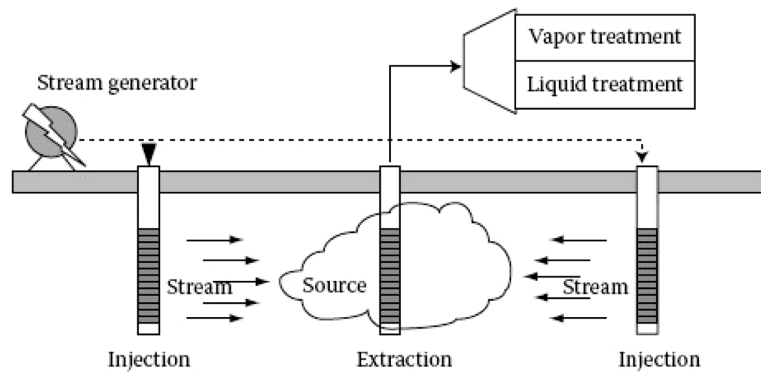


FIGURE 9.6 Schematic of thermal heating systems. (From USEPA, *In Situ Thermal Treatment of Chlorinated Solvent; Fundamentals and Field Applications*, EPA 542/R-04/010, Office of Solid Waste and Emergency Response, U.S. Environmental Protection Agency, Washington, DC, 2004.)

the removal of nonaqueous phase liquids is enhanced. For the removal and treatment of mobilized contaminants, a vapor extraction or liquid extraction system, in case of steam injection, must be integrated with other thermal technologies.

9.6.5 BIOREMEDIAL TECHNIQUES

In [Section 9.4.2](#), the biological treatment of contaminants was explained as a natural way for contaminant removal. Bioremediation can also be enhanced by adding some materials or microorganisms artificially to remove organic chemicals. In the application of biological means for the in situ treatment of organic chemicals in the saturated zone, growth and reproduction of microorganisms, which are capable of degrading the chemicals, the enhanced VOCs are the most frequently occurring type of contaminant in soil and groundwater at hazardous waste sites in the United States. In situ enhanced bioremediation of halogenated VOCs, and in particular of chlorinated aliphatic hydrocarbons, is the most rapidly growing technology for groundwater remediation (Kresic, 2009). Bioremediation technologies have been developed and implemented to reduce the cost and time required to clean up those sites. These technologies are usually less expensive than the other available alternatives, they do not require waste extraction or excavation, and are more publicly acceptable since they rely on natural processes to treat contaminants (USEPA, 2000).

In bioremediation technology, the concentration of electron acceptors, electron donors, and nutrients in groundwater are adjusted to stimulate biodegradation of contaminants by indigenous microorganisms. An electron acceptor is a compound capable of accepting electrons during oxidation-reduction reactions. Microorganisms obtain energy by transferring electrons from electron donors to an electron acceptor. Bioremediation also includes the addition of microbes or exogenous microorganisms into the subsurface to degrade specific contaminants. In-site characteristics that control aquifer bioremediation are (Testa and Winegardner, 2000) as follows:

- Hydraulic conductivity
- Soil structure and stratification
- Groundwater mineral content
- Groundwater pH
- Groundwater temperature
- Microbial presence

In designing an aquifer bioremediation system, the following issues must be taken into account:

- Electron acceptor and nutrient requirements must be estimated.
- Location of injection, extraction, and monitoring wells must be selected carefully.
- The rate of electron acceptor and nutrient addition must be specified.
- The site must be equipped with failure control and alarm systems for safety and operational concerns.
- After setting up the system, it must be monitored at least weekly. In the monitoring process, some information such as groundwater electron

acceptor concentration, nutrient concentration, pH, conductivity, and groundwater levels must be recorded. By monitoring groundwater and aquifer media samples, the remedial progress is controlled.

9.6.6 DISSOLVED PHASE (PLUME) REMEDIATION

Many contaminated sites have multiple point sources of groundwater contamination. These sources may form individual plumes of individual contaminants, individual plumes of mixed contaminants from identifiable sources, or merged plumes of various contaminants from multiple sources, which might be identifiable. Developing an effective prescription to remediate these complex contaminated sites is sometimes impossible. Therefore, some strategies such as pump and treat or the application of permeable reactive barriers might be selected to deal with these contaminated sites.

9.6.6.1 Pump and Treat

Pump and treat is the most widely used groundwater remediation technology today and is an important component of groundwater remediation efforts (USEPA, 2007). This technology is only criticized because of its inability to reduce contaminants to levels required by health-based standards in 5–10 years. However, since the complete aquifer restoration is an unrealistic goal for many contaminated sites, pump and treat systems can be considered as effective practices for aquifer remediation. It should still be taken into account that pump and treat systems, especially when combined with in situ restoration technologies, can also result in the full restoration at some sites with relatively simple characteristics.

Pump and treat systems are primarily used to: (1) control the movement of contaminated groundwater and prevent the continued expansion of the contaminated zone (hydraulic containment) and (2) reduce the dissolved contaminant concentrations in groundwater to a degree that complies with cleanup standards (treatment) (USEPA, 1996).

[Figure 9.7](#) shows the zone of hydraulic containment, capture zone, which is the three-dimensional region that contributes the groundwater extracted by a well. This zone is different from the radius of well influence. The capture zone embraces the volume of porous media from which groundwater flows toward the well(s). This zone is eventually extracted by the well(s). The radius of well influence is the zone in which the hydraulic head is lowered as a result of the well(s) operation. However, the groundwater flow direction in this zone is not reversed from the pre-pumping direction. In the well capture zone, enough monitoring wells must be installed to show the actual gradient reversal in all three dimensions.

9.6.6.2 Permeable Reactive Barriers

Permeable reactive barriers are not barriers to the water; they are barriers to the contaminant. In this method, reactive materials are placed in the subsurface across the path of a plume of contaminated groundwater to create a passive treatment system. When the polluted groundwater passes through these materials, treated water comes out the other side. [Figure 9.8](#) sketches a plume being treated by a permeable reactive barrier.

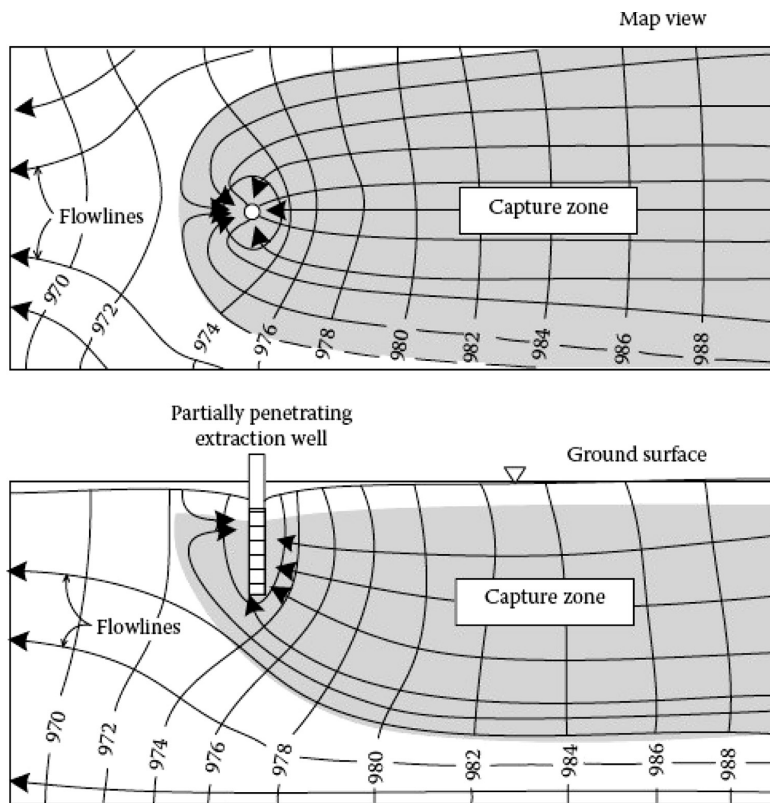


FIGURE 9.7 Illustration of capture zone in map view (top) and cross-sectional view (bottom) for a pump-and-treat system. (From USEPA, *A Systematic Approach for Evaluation of Capture Zones at Pump and Treat Systems: Final Project Report*, EPA/600/R-08/003, U.S. Environmental Protection Agency, Office of Research and Development, Washington, DC, p. 38.)

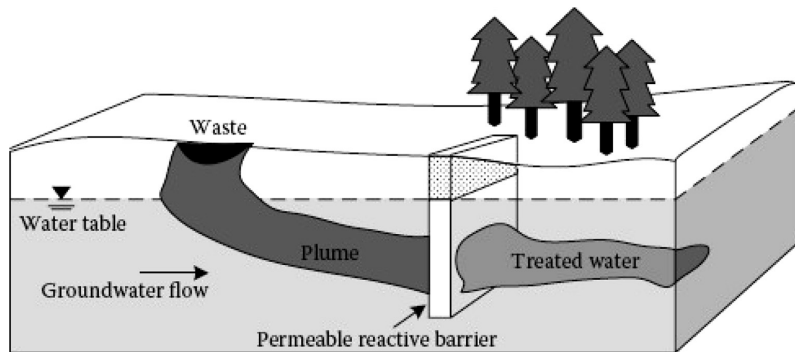


FIGURE 9.8 Plume being treated by a permeable reactive barrier. (From USEPA, *Evaluation of Subsurface Engineered Barriers at Waste Sites*, EPA 542-R-98005, Office of Solid Waste and Emergency Response, U.S. Environmental Protection Agency, Washington, DC, 1998.)

Permeable reactive barriers may be installed using trenches or by injecting reactive materials into the subsurface via boreholes. These barriers may contain metal-based catalysts for degrading volatile organics, nutrients, and oxygen for microorganisms to enhance biodegradation or other agents.

The barrier can be a precipitation wall or a sorption wall. The former reacts with the contaminants to form insoluble products, which may remain in the wall and the latter adsorbs contaminants to the wall surface.

Granular iron has been the most widely used reactive media in full-scale barriers. This material abiotically degrades a variety of chlorinated solvent compounds such as perchloroethylene and trichloroethylene (Wilkin and Puls, 2003). The process induces substitution of chlorine atoms by hydrogen in the structure of chlorinated hydrocarbons.

9.7 AQUIFER RESTORATION—OVERDRAFT ISSUES

In many regions around the world with water scarcity issues, groundwater resources have considerably been depleted, occasionally to a point of no return. Farmers in areas with profitable agricultural productions such as pistachio, saffron, and rice in the central and northeastern parts of Iran, and many other developing countries, are often using groundwater in excess of regulatory requirements. Industrial water needs for petrochemical and oil refinery activities are among other examples of the severe lowering of groundwater tables that has caused land subsidence and other environmental predicaments.

Other issues that have exacerbated the trend of groundwater over-exploitation are:

- Lack of effective governance in groundwater management
- Construction of large dams in watersheds, which would reduce direct interaction between surface and groundwater downstream of the dams.
- Limited regulatory and enforcement instruments due to financial, social, and political constraints.
- Lack of serious and effective attention to the formation and strengthening of water user groups for better coordination and better stewardship of water use.
- Approval of the agricultural development plans without enough water resources in the past several years.
- Increased use of water for agricultural crop production beyond the aquifers' safe yield.
- Low irrigation and water conveyance efficiencies

The activities and projects that could remedy the situation and restore the vitality of groundwater aquifers include the following activities that are mostly based on what have been anticipated in the national agenda of certain developing countries such as Iran.

1. Data collection and analysis, including preparation and installation of piezometric wells with instrumentation, as well as development of database systems.
2. Projects for sound operation of groundwater resources and capacity building.
3. Projects for control of groundwater table depletion and implementation of recharge facilities.

In the following case study, more details of a national project in the Middle East are described.

9.7.1 CASE STUDY: THE NATIONAL RESTORATION AND REMEDIATION OF GROUNDWATER RESOURCES IN IRAN

Iran is considered as an arid and semiarid region, with groundwater being the most important source of water with high quality and reliability. But the fast development being disproportional to the natural capacities of nonrenewable water resources has caused irreparable damage to the aquifers. In other words, the process of resource management and water use has led to over-exploitation of groundwater resources in most of the country's aquifers.

9.7.1.1 General Purpose

In the rehabilitation program of groundwater resources, it has been emphasized to compensate and recharge 110 billion cubic meters of water that has been excessively withdrawn from groundwater resources over the last 20 years.

9.7.1.2 Projects

The Ministry of Energy has implemented a resource balancing plan in its agenda to control the loss of groundwater reservoirs. Projects of restoration and balancing include seven types of national projects in the field of “Assessment, supervision/Inspection, and strengthening the decision making process,” and six types of projects in the field of “Actual Implementation,” as well as two projects in the field of “development and growth of social institutions.” These projects have been implemented in all major aquifers in the country. A general breakdown of these projects are as follows:

First Category: Projects for data collection and retrieval, scrutiny of information, water usage, and the status of aquifers.

1. Installing piezometric and exploratory wells
2. Instrumenting piezometric wells with measuring instruments
3. Providing balance sheets and updating the area's database

Second Category: Projects to control and supervise the exploitation of groundwater resources and capacity building. The Ministry of Energy is in charge of these projects unless another agency is listed in the parenthesis.

4. Strengthening and deploying compliance agents and inspection groups
5. Organizing drilling contractors
6. Establishing water markets
7. Establishing water organizations and conducting technical and financial support for the operations (Ministry of Agriculture)
8. Updating the National Water Statute/Bylaw (Ministry of Agricultural)
9. Subsidence studies in different plains overlying the aquifers (Geological Survey and mineral exploration of Iran)
10. Public awareness and engagement

Third Category: Projects to Control Groundwater Table Depletion and Aquifer Recharge Facilities.

11. Buying and dismantling unauthorized agricultural wells.
12. Replacement of effluent with agricultural wells in declared illegal groundwater operation plains.
13. Providing and installing bulk volume and smart meters on wells
14. Implementation of artificial recharge and flood propagation projects
15. Study and implementation of watershed management plans (Ministry of Agriculture)

9.7.1.3 Operational Program (Action Plans)

Each of the 26 water authority boards in the country have been commissioned to implement all 15 projects in every major aquifer within their territories. The following actions have been taken:

- Establish a collaborative approach between consulting firms, the ministries, the national Water Resources Management Company, and the academia to oversee the projects.
- Separation of projects that directly contribute to the balancing of groundwater (main projects) and projects that support infrastructure and monitor the performance of major projects. Special attention will be paid to the effective artificial recharge programs.
- Creating an interactive program to determine the relationship and provide the necessary support (hardware and software) and prioritize projects. The program identifies whether these projects are complementing each other, as well as whether the subprojects and the planned facilities are sufficient. Measures to strengthen and correct, if necessary, are recommended.
- Evaluation of details of 15 projects and how they can be promoted.
- Determination of the driver, pressure, state, impact, response framework of the Organization for Economic Co-operation and Development proposed for accurate identification of effective factors in the current groundwater dilemma and the plan integration. Solutions to identify the causes and effect of possible problems will be presented.
- Providing a road map for identifying appropriate options and strategies, screening the most important solutions, and defining time sensitive priorities.
- Coordination among project supervisors and determination of the critical path for implementation of the project and management of noncompliance in executive activities and compensatory actions.
- To create balance and coordinate subprojects among the ministries and the Geological Survey Organization.
- Survey of stakeholders participation in different projects by considering social, economic, and environmental factors and providing the framework of their participation in different projects of local markets.
- Investigation of strategies for adjustment of socio-economic stress of stakeholders and providing a framework for the projects in a 5-year horizon.

- Preparation of doable procedures to monitor the progress of the project and dealing with possible delays through prevention or compensation.
- Determination of the effective framework based on the developed monitoring program of the work/field environment by consultants in which changes in groundwater level are continuously recorded and monitored. Providing a framework for validation of the activities/measures of the Office of Basic Data/Studies, considering the time delay between activities and performance evaluation.
- Preparation of annual report of interaction based on the interactive evaluation of projects and analysis of reasons for the lack of achieving annual collective goals.

9.7.1.4 Time Table

This project was planned to be implemented in a 6-year period in the country (during the six- and part of the seven-year development plan), with 500 million cubic meters recovery of the deficit in the first year and the rest of the plan objectives during the rest of the six-year period ending in about 2023. Due to the high cost of the project, perhaps a 10-year time horizon seems more realistic. The national Water Resources Management Company and Regional Water Authority Boards have had some progress to curb the ongoing over-exploitation of groundwater. The national restoration and remediation of groundwater resources in Iran is a major effort with many social, environmental, and economical challenges, but it could certainly bring some order into the use of this vital resource in an arid and semiarid region in the Middle East.

9.8 MONITORING SUBSURFACE WATER

The purpose of water quality monitoring is to obtain quantitative information about the qualitative characteristics of water using statistical sampling. In other words, the purpose of water quality monitoring is to define the physical, chemical, and biological characteristics of water.

The growing concern for the quality of surface and groundwater has put significant demands on the optimal design of monitoring networks and extraction of suitable information from the collected data. Monitoring is one of the most important steps of water quality management since the process of decision-making is based on available information related to water quality characteristics. Houlihan and Lucia (1999) categorized the purposes of water quality monitoring as follows:

- Detection monitoring programs that are used to detect an impact to surface and groundwater quality.
- Assessment monitoring programs that are used to assess the nature and extent of detected contaminants and to collect data that may be needed for remediation of contaminants.
- Corrective action monitoring programs that are used to assess the impact of remediation or pollution control programs of contaminant concentrations.
- Performance monitoring programs that are used to evaluate the effectiveness of an element on remediation systems in meeting its design criteria.

9.8.1 VADOSE-ZONE MONITORING

So far, it was understood that restoration of contaminated groundwater is so complex and costly. Therefore, it is always desirable to prevent groundwater against becoming contaminated. In this regard, it must be determined if groundwater contamination is likely to occur in the future so that reformatory action could be taken early enough to prevent contamination from reaching the water table. For example, a groundwater monitoring system might be installed to detect leaks from the facilities when a landfill or a lagoon is constructed.

The main purpose of monitoring a vadose zone is to detect leaks from overlying facilities prior to the time that the contaminant reaches the water table. This way, reformatory actions could be accomplished to avoid contamination of the groundwater. Examples of these reformatory actions are draining a lagoon and repairing the liner.

Contaminants in the vadose/unsaturated zone move in both the liquid and vapor phases. Depending on their relative density and air-pressure gradients, vapors may move in any direction. But liquids generally move only downward. Vadose-zone monitoring systems for liquids are usually installed beneath the facility to be monitored due to the direction the liquid would be seeping. It is difficult to install monitoring devices after constructing facilities. Hence, these devices are usually installed prior to the time that the facility is constructed. Since vapors can migrate laterally, gas-monitoring wells can be placed to the side of active facilities. Therefore, it is easier to install gas-monitoring devices than liquid-monitoring devices in the vadose zone. Gas-monitoring wells can also be located beneath a landfill or lagoon if they are installed before construction. But after construction, they can be placed to the side of an active facility.

Gas monitoring wells terminate in the unsaturated zone. [Figure 9.9](#) shows a typical gas monitoring well. These wells are usually used to detect the movement of methane from municipal landfills. Gas-monitoring wells can also detect the vapors of volatile organic chemicals in the vadose zone. Most of the volatile organic chemicals are suspected carcinogens, and they move rapidly in groundwater.

There are also some indirect means to monitor a vadose zone. For example, by monitoring the changes in soil moisture in a lagoon that has aqueous liquid, it can be determined if there is a potential leak. If the lagoon holds a brine, changes in the electrical conductivity in the soil beneath the landfill could mean a leak. Temperature changes in the vadose zone could also indicate a leak.

The vadose zone can also be sampled by direct sampling of the soil. The moisture content as well as chemical composition of the moisture extracted from the sample is tested. Soil samples can also be leached with a standard leaching solution and the leachate is tested. If the soil sample is placed in a vial, a good indication of the organics in the soil can be obtained by testing the volatile organic in the headspace in the vial.

Generally, the devices that are placed in the vadose zone to collect a sample of the liquid in the pores fall into two categories:

1. *Suction lysimeters*: These devices apply tension to a porous ceramic cup to induce the pore water that is under negative pressure to enter the porous cup, and then it will be transported to the surface. The suction lysimeter has been used for many years in agricultural applications and landfills to

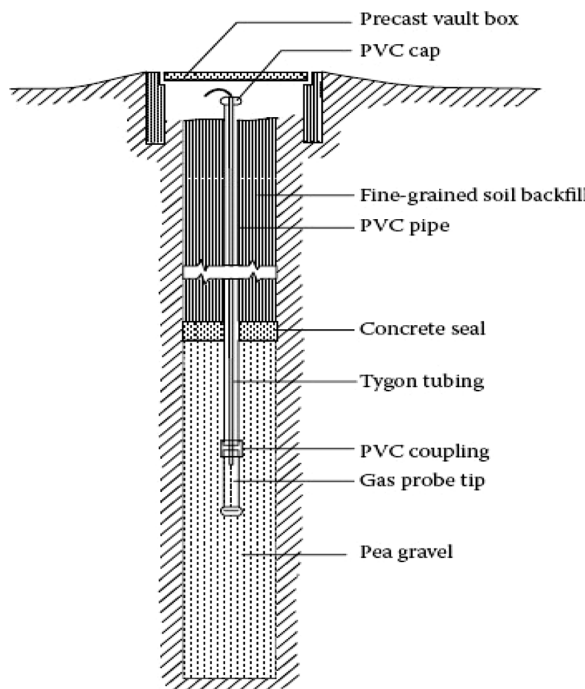


FIGURE 9.9 Gas monitoring well in vadose zone. (From Wilson, L.S., *Ground Water Monit. Rev.*, 3, 155, 1983.)

monitor for leachate. The vacuum that can be applied is limited to 0.5–0.8 bar. This limitation in the vacuum causes the failure of collecting liquids in some applications because the lysimeter becomes clogged. Furthermore, if the suction lysimeter is not located under a leak, that leak may not be detected.

2. *Collection lysimeters*: These devices have a membrane liner buried in the vadose zone, and the liquid is collected on the liner until the soil above it becomes saturated, forcing the liquid to flow to a wet well. The liquid is then sampled in this well. Collection lysimeters fail less than the other type. They can be made any size and can be placed under spots where failure of a system component is more likely.

9.8.2 GROUNDWATER MONITORING

Sanders et al. (1987) proposed general guidelines for the establishment of a monitoring system (Table 9.1). As shown in this table, network design is one of the five steps. Identifying the information to be obtained and statistical methods for converting the data to the useful information are considered in the first two steps, and the third step deals with monitoring network design. Monitoring operation plans are specified in the fourth step. In the fifth step, the information related to original monitoring objectives is determined.

TABLE 9.1
Major Steps in the Design of a Water Quality Monitoring System

| | |
|--------|---|
| Step 1 | Evaluate information expectations Water quality concerns Information goals Monitoring objectives |
| Step 2 | Establish statistical design criteria Development of hypotheses Selection of statistical methods |
| Step 3 | Design monitoring network Where to sample What to measure How frequently to sample |
| Step 4 | Develop operation plans and procedures Sampling procedures Laboratory analysis procedures Quality control procedures Data storage and retrieval |
| Step 5 | Develop information reporting procedures Types and timing of reports Reporting formats Distribution of information Monitoring program evaluation (Are information expectations being met?) |

Source: Sanders, T.G. et al., *Design of Networks for Monitoring Water Quality*, Water Resources Publications, Littleton, CO, 1987.

9.8.3 WATER QUALITY VARIABLE SELECTION

Selection of the water quality variables is one of the most important steps in design and operation of water quality-monitoring networks. The quality of the water body is usually characterized by interrelated sets of physical, chemical, and biological variables. Therefore, the relationships between the water quality and quantity variables are often complex. Many variables are needed to completely describe the quality of the water body, and it is economically unfeasible to measure all of them. Therefore, the variables should be ranked, and a minimum number of water quality variables should be selected for sampling. The variables can be scored and ranked based on the multi-criterion decision-making methods. The variables should be selected in both time and space. One problem in the economical selection of water variables is that the water quality variables are time-space stochastic processes that cannot be recorded continuously by an instrument at a site.

TABLE 9.2**Hierarchical Ranking of Water Quantity, Water Quality Random Variables for Purposes of Information Procurement on Water Quality Processes**

| Primary, Basic Variables | Water Quantity Carrier Variables | First Level Variables |
|--|---|------------------------|
| Quantity discharge, water level, small volume in a body of water | | |
| Secondary associated Examples | Quality variables of aggregated effects Temperature, pH, turbidity, biological oxygen demand (BOD), dissolved oxygen (DO), cations anions, conductivity, chlorides, radioactivity | Second level variables |
| Aggregate-producing quality variables | Quality variables that produce aggregated effects | Third level variables |
| Example 1 | Radioactivity-producing variables: strontium, cesium, tritium, etc. | |
| Example 2 | Turbidity-producing variables: suspended matter, colloids, biota groups, dissolved minerals, etc. | |
| Or species producing effects in aggregation | Specific compounds most detailed classification of quality variables | Fourth level variables |
| Examples | Minerals affecting turbidity: iron oxides, manganese compounds, alumina, etc. | |

Source: Sanders, T.G. et al., *Design of Networks for Monitoring Water Quality*, Water Resources Publications, Littleton, CO, 1987.

Establishing the relationship between the water quality and quantity variables and analyzing the dependencies between water quality variables are necessary to select representative variables. These correlations can be used to produce information for variables that are not regularly monitored.

Sanders et al. (1987) proposed a hierarchical ranking of the water quantity and quality variables that can be efficiently used in variable selection for monitoring a network (Table 9.2). In the hierarchical classification of variables, the optimal cutoff point to select suitable variables is determined considering the objectives of monitoring, sample collection laboratory analysis costs, and the correlation structure between variables.

9.8.4 GEOSTATISTICAL TOOLS FOR WATER QUALITY-MONITORING NETWORKS

Geostatistics is referred to as the study of a phenomenon that fluctuates in space and/or time. Geostatistics offers a collection of deterministic and statistical tools for modeling spatial and/or temporal variability. The basic concept of geostatistics is to determine any unknown value Z as a random variable Z , with a probability distribution, which models the uncertainty of Z . The random variable is a variable that can take a variety of values according to a probability distribution. One of the most famous methods of geostatistics is kriging, which is used widely in the field of environment, mining, surveying, and water resources engineering studies. The ability of regionalizing a spatiotemporal process has made these methods efficient tools for

designing a water quality-monitoring network. It suggests the most suitable points for locating monitoring stations, by considering the kriging estimation errors (estimation variances) for the regionalized components of the concentration of an indicator water quality variable.

9.8.4.1 Kriging

Kriging is a collection of generalized linear regression techniques for minimizing the estimation variance, defined from a prior model for covariance. It is of importance to have an area-wide distribution of drought information before applying a drought-control measure to the entire basin. Kriging could be used in its spatial form to determine the drought-affected areas in a region or for future installation of new gage stations in an ungaged area. Kriging methods may be used to study the temporal variation of a process. In this case, a temporal domain, time variogram, and covariance function could be used to predict variables of unobserved data. Regionalization data resulting from dynamic processes in space/time use variograms and covariance functions, allowing prediction through space and time.

Kriging in the simplest form applies first-order analysis based on the following intrinsic hypotheses (Bogardi et al., 1985):

The expectation of $Z(x)$, a single realization of the parameter Z , exists and is independent of the point x :

$$E[Z(x)] = m \quad (9.17)$$

Or if there is a known function $m(x)$ in which,

$$E[Z(x)] = m(x) \quad (9.18)$$

A variable such as $Y(x)$ could be used as:

$$Y(x) = Z(x) - m(x) \quad (9.19)$$

and

$$E[Y(x)] = 0, \text{ for all } x \quad (9.20)$$

For all vectors h , the increment $[Z(x + h) - Z(x)]$ has a finite variance independent of x :

$$\text{Var}[Z(x + h) - Z(x)] = 2\gamma(h) \quad (9.21)$$

The γ function is called the variogram. Variograms are obtained from the following three parameters:

1. “Nugget” effect, which can partly be explained by the measurement error (C_0)
2. “Sill,” which is the total variance of the data beyond a certain distance or “range” (C)
3. “Range” or zone of influence (R) (see [Figure 9.10](#)).

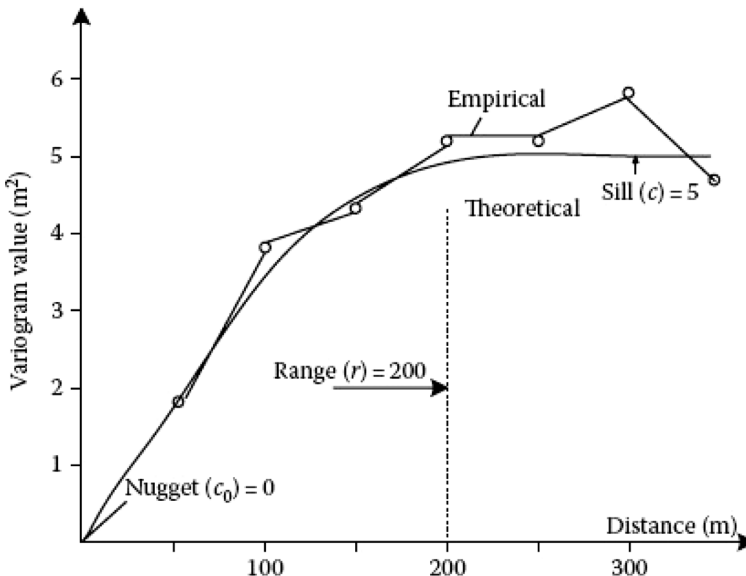


FIGURE 9.10 A pair of empirical and theoretical variograms.

The first step in the kriging analysis is to estimate a semivariogram.

In all applications, the purpose is to analyze the correlation between neighboring measurements of a property, and thereby derive the spatial variability of such a property. The functional description of this spatial structure, if it exists, is called the semivariogram in geostatistics. The computational form of a semivariogram is:

$$\gamma(h) = \frac{1}{2n} \sum \left[(z(x_i) - z(x_i + h))^2 \right] \quad (9.22)$$

where:

$\gamma(h)$ is the semivariogram value for the distance h

$z(x_i)$ is the measurement of location x_i

$z(x_i + h)$ is the measurement at location $x_i + h$

n is the number of measurement pairs separated by a vectorial distance, h .

The empirical variogram could be replaced by a theoretical variogram model to be used in a kriging problem. A theoretical semivariogram model consists of an isotropic nugget effect and any positive linear combination of the following standard semivariogram models:

Spherical model:

$$\gamma(h) = c \cdot Sph\left(\frac{h}{a}\right) = \begin{cases} c \cdot \left[1.5 \frac{h}{a} - 0.5 \left(\frac{h}{a} \right)^3 \right], & \text{if } (h \leq a) \\ c, & \text{if } (h > a) \end{cases} \quad (9.23)$$

where:

a is an actual range

c is the positive variance contribution or sill.

Exponential model:

$$\gamma(h) = c \cdot \text{Exp}\left(\frac{h}{a}\right) = c \cdot \left[1 - \exp\left(-\frac{3h}{a}\right)\right] \quad (9.24)$$

Gaussian model:

$$\gamma(h) = c \left[1 - \exp\left(-\frac{(3h)^2}{a^2}\right)\right] \quad (9.25)$$

Power model:

$$\gamma(h) = ch^\omega \quad (9.26)$$

where ω is a constant between 0 and 2. Hole effect model:

$$\gamma(h) = c \left[1.0 - \cos\left(\frac{h}{a}\pi\right)\right] \quad (9.27)$$

Consider the estimate of an unknown (unsampled) value $z(u)$ from neighboring data values $z(u_\alpha)$, $\alpha = 1, \dots, n$. The random function model $z(u)$ is stationary with mean m and covariance $C(h)$. In its simplest form, also known as simple kriging, the algorithm considers the following linear estimator:

$$Z_{SK}^*(u) = \sum_{\alpha=1}^n \lambda_\alpha(u) Z(u_\alpha) + \left(1 - \sum \lambda_\alpha(u)\right) m \quad (9.28)$$

where:

Z_{SK}^* is the simple kriging estimator

$\lambda_\alpha(u)$ are the weights to minimize the error variance, also called “estimation variance.”

The minimization of the error variance in a set of normal equations results:

$$\sum_{\beta=1}^n \lambda_\beta(u) C(u_\beta - u_\alpha) = C(u - u_\alpha), \quad \forall \alpha = 1, \dots, n \quad (9.29)$$

where:

C is the stationary covariance

$C(0)$ is the stationary variance of $Z(u)$.

The corresponding minimum estimated variance, or kriging variance, is:

$$\sigma_{SK}^2(u) = C(0) - \sum_{\alpha=1}^n \lambda_\alpha(u) C(u - u_\alpha) \geq 0 \quad (9.30)$$

Ordinary kriging is the most commonly used method of kriging, whereby the sum of weights $\sum_{\alpha=1}^n \lambda_\alpha(u)$ is limited to 1. This allows building an estimator $Z_{OK}^*(u)$ that does not require prior knowledge of the stationary mean m and remains unbiased in the sense that:

$$E\{Z_{OK}^*(u)\} = E\{Z(u)\} \quad (9.31)$$

There is a relationship between the weights λ and the semivariograms introduced earlier. This relationship could be represented in a matrix form as follows:

$$\begin{pmatrix} 0 & \gamma_{12} & \gamma_{13} & \cdots \gamma_{1n} & 1 \\ \gamma_{21} & 0 & \gamma_{23} & \cdots \gamma_{2n} & 1 \\ \vdots & \vdots & \vdots & \ddots & \vdots \\ \gamma_{n1} & \gamma_{n2} & \gamma_{n3} & \cdots & 0 & 1 \\ 1 & 1 & 1 & \cdots & 1 & 0 \end{pmatrix} \begin{pmatrix} \lambda_0^1 \\ \lambda_0^2 \\ \vdots \\ \lambda_0^n \\ \dots \end{pmatrix} = \begin{pmatrix} \gamma_{10} \\ \gamma_{20} \\ \vdots \\ \gamma_{n0} \\ 1 \dots \end{pmatrix} \quad (9.32)$$

where:

λ_0^i represents the weight of station i

0 is for the origin station.

In the following section, a water quality-monitoring network in a case study is presented.

9.8.5 LOCATION OF WATER QUALITY MONITORING STATIONS

The location of a permanent monitoring station is very important because when the collected samples are not representative of the water body, the other activities in the water quality monitoring system can be inconsequential. The factors that can affect the location of a water quality monitoring station are different in ground and surface water resources because length is the dominant space coordinate in rivers, while depth and width have the same role in groundwater.

Groundwater monitoring objectives should be defined before monitoring because they can affect the needed procedures, techniques, and analyses. The main objectives of groundwater monitoring are as follows:

- Ambient trend monitoring
- Source monitoring

Ambient trend monitoring is used to discover the spatial and temporal trends of groundwater quality variables. The cost of ambient trend monitoring is highly related to the number of sampling stations and the sampling frequency.

Source monitoring determines the qualitative characteristics and the rate of pollutant movement. The flow rate can be determined using flownet. The pollutant's mass flow rate can be determined as:

$$R_{total} = \sum_{i=1}^n q_i c_i \quad (9.33)$$

where:

R_{total} is the total mass flow rate

n is the total number of sections

q_i is the flow rate in section i

c_i is the water quality variable concentration in section i .

A suitable groundwater-monitoring network should provide the spatial and temporal characteristics of the groundwater resources pollution from the sources of pollution such as plumes.

Hudak and Loaiciga (1993) proposed a quantitative, analytically based hydrologic approach for monitoring network design (sampling location) in a multi-layered groundwater flow system. In this method, which is described below, the susceptibility to contamination of points in the model domain is quantified using weight values. This network design methodology consists of three steps as follows:

1. Domain definition and discretization
2. Determination of relative weights for candidate monitoring sites
3. Selection of an optimal configuration for monitoring network.

9.8.5.1 Definition and Discretization of the Model Domain

The model domain includes the contaminant source and a surrounding area, which could be affected by the pollutant sources and within which monitoring wells are selected. Zones that encompass the pathways of contaminant migration are defined by advection envelopes. Advection envelopes are extended from hydrogeologic outlets of pollutant sources based upon the known or inferred variation of hydraulic head (Figure 9.11). The two flow lines that originate from the separate ends of the hydrogeological outlet can be considered as boundaries of the advection envelopes. Monitoring well sites can be classified as "background" and "detection" monitoring sites. Detection monitoring wells are constructed for the early detection of contamination by the pollutant source, but background monitoring sites determine the background water quality and are located in the up-gradient zone of the model domain.

The background monitoring wells should not be located adjacent to the contaminant source and advection envelope. They also should not be intersected by an outward normal line extended from an advection envelope (Hudak and Loaiciga, 1993).

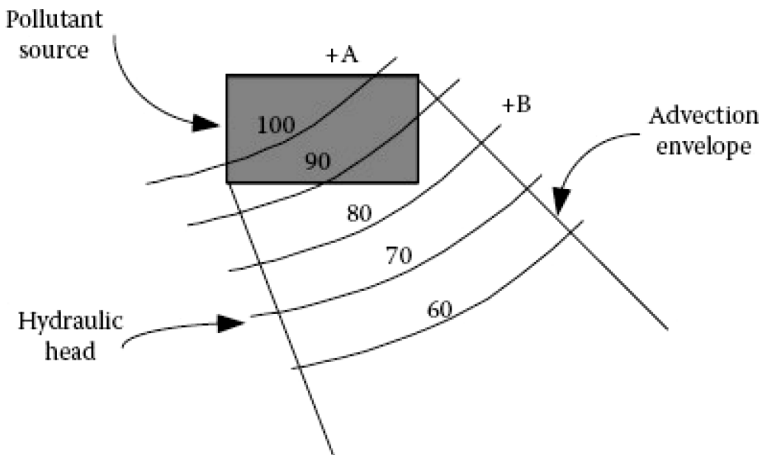


FIGURE 9.11 Advection envelope extended from hypothetical contaminant. (From Hudak, P.F. and Loaiciga, H.A., *Water Resour. Res.*, 29, 2835, 1993.)

9.8.5.2 Calculation of Weights for Candidate Monitoring Sites

The relative weight of each monitoring site should be calculated based on the location of the site relative to the pollutant source and advection envelope. The proposed model can be used for designing a monitoring network for an uncontaminated aquifer (before pollutant is released from the pollutant source). Therefore, the existing contamination concentrations are not used in the monitoring wells configuration.

The relative weight of each candidate monitoring well in a multi-layer aquifer is determined as (Hudak and Loaiciga, 1993):

$$W_{jk} = \frac{1}{D(s)_{jk} D(e)_{jk}} \quad (9.34)$$

where:

j is a real index of the potential well site, k : HSI (hydrostratigraphic interval) index; a HSI is defined as a layer, which has relatively uniform hydraulic conductivity

$D(s)_{jk}$ is the horizontal distance from the contaminant source boundary to the node j in HSI k

$D(e)_{jk}$ is the perpendicular distance from node j in HSI k to the closest boundary of the advection envelope boundary (equal to $D(e)_{jk}$ if node j cannot be intersected by a perpendicular distance from an advection envelope)

$D(e)_{jk}$ is the maximum value of $D(e)_{jk}$ among nodes for which the quantity can be measured.

Based on the above equation, nodes located close to an area with a higher probability of contamination have higher weights. To reduce the computational efforts, the boundaries of the pollutant source and advection envelopes are approximated by

nodes within a grid of candidate groundwater monitoring wells. The value of $D(e)_{jk}$ is calculated only for nodes that are susceptible to contamination from plume spreading, which are intersected by an outward normal line extended from an advection envelope. Other nodes, which are not intersected by an outward perpendicular line from an advection envelope, are assigned the maximum value of $D(e)_{jk}$ calculated for all other nodes. On the other hand, the nodes located within the advection envelope are assigned the minimum value of $D(e)_{jk}$. For example, in Figure 9.11, nodes A and B have an equal distance from the advection envelope, although node B has a greater probability to be contaminated because node A is located in an upgradient area and should be assigned the maximum of $D(e)_{jk}$ ($D(e)(\max)$).

9.8.5.3 Optimal Configuration of a Monitoring Well Network

The optimal configuration of monitoring sites can be obtained using a mathematical model. The objective function of this model is a preferential location of monitoring wells at points with a high probability of contamination. The model formulation can be as follows (Hudak and Loaiciga, 1993):

$$\text{Max } Z = \sum_{k \in K} \sum_{j \in J_{k-u_k}} W_{jk} x_{jk} - \sum_{k \in K} \sum_{j \in J_{u_k}} W_{jk} x_{jk} \quad (9.35)$$

Subject to:

$$\sum_{j \in J_k} x_{jk} \geq P_k (\min), \text{ for each } k \in K \quad (9.36)$$

$$\sum_{j \in J_{u_k}} x_{jk} = P_{u_k}, \text{ for each } k \in K \quad (9.37)$$

$$\sum_{k \in K} \sum_{j \in J_k} x_{jk} = P \quad (9.38)$$

$$x_{jk} = \begin{cases} 0, & \text{otherwise} \\ 1, & \text{if a well is installed at node } j \text{ in HSI } k \end{cases} \quad \text{for each } j \in J_k, k \in K \quad (9.39)$$

where:

j is the area 1 index of a potential well site, J_k is the set of potential well sites in HSI k

J_{k-u_k} is the set of potential well sites, excluding sites in an up-gradient zone, in HSI k

J_{u_k} is the set of potential well sites in an up-gradient zone in HSI k

k is the HSI index

K is the set of HSIs

W_{jk} is the weight for node j in HSI k

$P_k(\min)$ is the minimum number of wells to be located in HSI k

P_{uk} is the number of wells allocated to an up-gradient zone in HSI k

P is the total number of wells to be located.

The second term of Equation 9.35 ensures that the nodes with the lowest weight will be selected for background monitoring in an up-gradient zone. Equations 9.36 and 9.37 constraint the minimum and total number of wells in an up-gradient zone in each HSI. Constraint 9.38 ensures that all the wells are located throughout the model domain and Constraint 9.39 shows that variable x_{jk} is a binary integer.

The total number of monitoring wells in each layer could be determined by budgetary constraints or regulatory requirements. A budget constraint can be written as:

$$\sum_{k \in K} \sum_{j \in J_k} C_{jk} x_{jk} \leq R \quad (9.40)$$

where:

C_{jk} is the construction cost of a well at monitoring site j in HSI k

R is the total available budget.

The proposed formulation can be solved using integer programming techniques. This model can define the location of the P monitoring wells including P_{uk} up-gradient wells. For more details, the reader is referred to Hudak and Loaiciga (1993).

9.8.5.4 Kriging Method in Designing an Optimal Monitoring Well Network

The following steps can be performed to find the optimal locations of a monitoring network (Karamouz et al., 2009):

First the water quality indicators are selected considering the characteristics of pollution loads and water uses as well as the existing spatial and temporal variations of the water quality variables of the system. Then, the spatial distribution of the existing water quality-monitoring stations is investigated. After that, the data of the selected water quality variables are standardized, and the time series are plotted in order to determine a pattern (monthly, seasonal, etc.) for their temporal variations.

Among the mathematical or statistical time series models, a model which best fits the time series of the water quality data is selected to represent the temporal trend of the concentration of the water quality variables. Then, the parameters of this model will be regionalized using the kriging method and the experimental variograms of the regional parameters are plotted, and the best theoretical variograms are fitted to them. A sample of these variograms is shown in Figure 9.12. For example, if the trend of the variables has sine and cosine cycles, the Fourier series is fitted to the series. Therefore, the trend component is determined as:

$$Z(t) = a \cos\left(\frac{2\pi t}{T}\right) + b \sin\left(\frac{2\pi t}{T}\right) \quad (9.41)$$

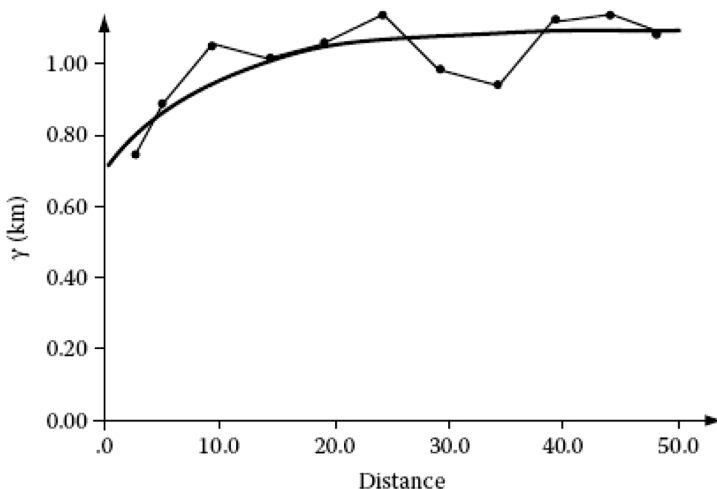


FIGURE 9.12 The experimental and theoretical variograms for the stochastic (residual) component of the chemical oxygen demand (COD) time series at a water quality monitoring station in Karoon River. (From Karamouz, M. et al., *J. Environ. Model. Assess.*, 14, 705–714, 2009.)

In this equation, a and b are the coefficients of the Fourier series and T is the number of periods (e.g., 12 for monthly data). The regional parameters, which have to be regionalized using the kriging analysis, will then be as follows:

- The cosine coefficient (a) of the trend component
- The sine coefficient (b) of the trend component
- The parameters of the theoretical variograms of the residuals (range and nugget effect)

After regionalizing the parameters, the kriging analysis is done for the regional parameters using the theoretical variograms in order to calculate the values of estimations and estimation variances. Figure 9.13 depicts the typical results of the kriging estimation and estimation variance for regionalized parameters as two-dimensional color pixel plots.

Ultimately, a set of potential points for the monitoring stations is proposed considering the spatial variations of the kriging estimation variances for the regionalized parameters, accessibility of stations, locations of the main point loads, locations of the main water withdrawals, locations of the main tributaries, locations of the development projects, and locations of existing stations and the length of their water quality and quantity data.

9.8.5.5 Genetic Algorithms in Designing an Optimal Monitoring Well Network

To design the monitoring network using a genetic algorithms (GAs) optimization model, a water quality simulation model is usually linked to the optimization. The simulation model acts as a tool to check the performance and results obtained

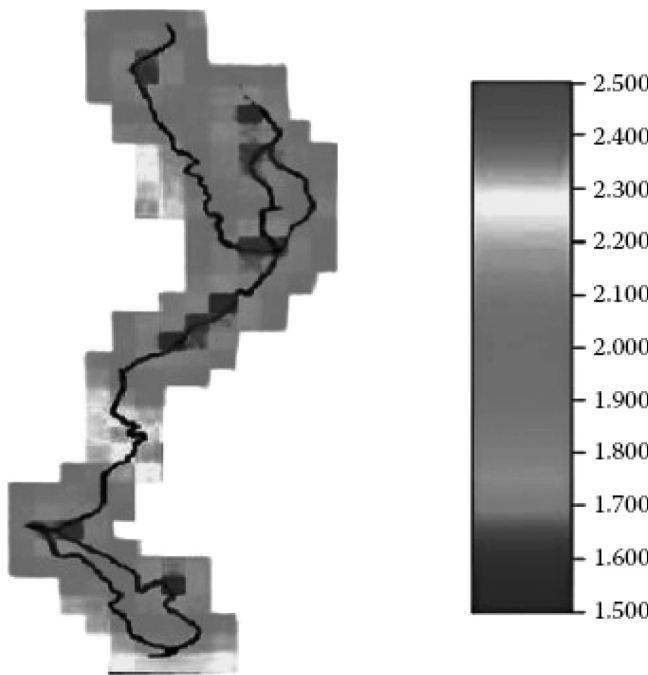


FIGURE 9.13 Two-dimensional kriging estimation variance plots for the cosine coefficient (a) in the deterministic (trend) component of the COD time series. (From Karamouz, M. et al., *J. Environ. Model. Assess.*, 14, 705–714, 2009.)

from the GA optimization model. As discussed in [Chapter 7](#), GA is a method to identify the optimal solutions. This method can be used to evaluate if the existing monitoring wells are performing reasonably well. In this regard, the historical data from the existing monitoring wells are considered. Besides the existing monitoring wells, some data may also be collected from piezometric and operation wells, which are likely to be useful for the purpose of monitoring. These wells are selected based on the engineering judgment.

The simulation water quality model is calibrated based on the observed data. Then, the stations are determined using GAs. The simulated water quality variables should be best fitted to the historical spatial and temporal variations of the selected water quality variables. Therefore, the main objective of the model is to minimize the absolute difference between the observed and the simulated concentration of the selected water quality variables. Karamouz et al. (2009) proposed the following objective function for an optimization model to design a river water quality-monitoring network:

$$\text{Minimize: } Z = \sum_{p=1}^{n_p} \sum_{t=1}^T \sum_{s=1}^{n_s} w_p \frac{|C_{t,s,p} - C'_{t,s,p}|}{C_{t,s,p}} \quad (9.42)$$

where:

- p is the index of water quality variables selected for water quality monitoring
- n_p is the total number of selected water quality variables
- t is the time step (month)
- T is the total number of time steps in the planning horizon
- s is the river section
- n_s is the total number of potential sampling stations
- $C_{t,s,p}$ is the observed or simulated concentration of water quality variable p in river section s in time step t ; simulated values are based on the real values of point load quality and quantity
- $C'_{t,s,p}$ is the concentration of p th water quality variable in station s at time step t .

It is obtained from a water quality simulation model using the monthly average values of point loads quality and quantity, and w_p is the relative weight of the p th water quality variables.

This objective function minimizes the difference between the observed and simulated values of the considered water quality variable concentration. It can be solved using GAs.

9.8.6 SAMPLING FREQUENCY

Sampling frequency shows how often water quality samples should be gathered. The detection of stream standard violations and the determination of temporal water quality variation are main criteria for sampling frequency analysis. The selection of sampling frequency requires some background information on the behavior of the random variables, which are important in water quality. The analyst may face three situations:

- There is water quality data from the stream, which is under study.
- There is only water quality data from a stream in a region, which has similar characteristics to the study area.
- There is no existing data from the stream under consideration and similar streams.

When there is no data available, a two-stage monitoring program should be utilized. In this case, design data, collected in the first stage, can be used for a suitable design of a monitoring network and to estimate the sampling frequency. When the water quality data are available only for the similar rivers in the region, the water quality data should be generated for the stream which is under study. In this case, the similarity between their geological and hydrologic characteristics, distribution of pollutant sources, and pollutant characteristics are usually considered for water quality data generation.

9.8.6.1 Methods of Selecting Sampling Frequencies

The sampling frequency design can vary from a single station, single water quality variable to multiple stations, multiple water quality variables. Sanders et al. (1987) proposed statistical methods for each case that is presented in the next sections.

9.8.6.2 Single Station and Single Water Quality Variable

In this case, the selected sampling frequency for a specified water quality variable at a station should provide the desired confidence interval around the annual mean. If the collected samples can be assumed independent, the variance of sample mean is given as:

$$\text{Var}(\bar{x}) = \frac{\sigma^2}{n} \quad (9.43)$$

where:

σ^2 is the population variance

n is the number of samples.

The confidence interval for the population mean, μ , is as follows:

$$\bar{x} - Z_{\alpha/2} \left(\frac{\sigma^2}{n} \right)^{1/2} \leq \mu \leq \bar{x} + Z_{\alpha/2} \left(\frac{\sigma^2}{n} \right)^{1/2} \quad (9.44)$$

where $Z_{\alpha/2}$ is the standard normal deviate corresponding to the probability of $\alpha/2$. With rearranging terms, the number of samples required, n , to estimate the mean with a known confidence level, α , is as follows:

$$n \geq \left[\frac{Z_{\alpha/2} \sigma}{\mu - \bar{x}} \right]^2 \quad (9.45)$$

When sample standard deviation is used instead of σ , the $Z_{\alpha/2}$ is replaced with Student's t statistic, $t_{\alpha/2}$:

$$n \geq \left[\frac{t_{\alpha/2} s}{\mu - \bar{x}} \right]^2 \quad (9.46)$$

In this case, the computation of n becomes an iterative problem because when t distribution is used, the number of degrees of freedom, which is $n - 1$, must be known, but it is not known. Therefore, for solving the problem, an initial value for n is estimated and degrees of freedom are determined, and a new estimation of n is obtained using Equation 9.46. By repeating this procedure, the values of n converge to a desired value. When the number of samples is large (more than 30), σ can be estimated with s , without any significant error in determining the sampling frequency.

Example 9.4

Select the sampling frequency for a monitoring well, which monitors BOD concentration. The annual mean and variance of BOD concentration based on historical data are 6.01 mg/L and 8.1 (mg/L)². The desired confidence interval width is assumed to be 3 mg/L with a 95% confidence level.

SOLUTION

$$\text{The confidence interval width} = 2 \times 1.96 \times \frac{\sigma}{\sqrt{n}}$$

$$2 \times 1.96 \times \frac{\sigma}{\sqrt{n}} = 3$$

$$n = \left[\frac{2 \times 1.96}{3} \right]^2 \sigma^2 = \left[\frac{2 \times 1.96}{3} \right]^2 \times 8.1$$

$$n = 13.8 \approx 14 \text{ samples/year}$$

9.8.6.3 Single Station and Multiple Water Quality Variables

If the problem of sampling frequency selection includes more than one water quality variable, a compromise programming should be used to obtain the most acceptable confidence interval considering all water quality variables.

One of the simple ways of doing this is to compute a weighted average of confidence interval widths for several water quality variables over a variety of sampling frequencies being considered and then choosing the sampling frequency that provides the most satisfactory results. The relative weights of water quality variables can be selected by engineering judgment so that the contributions of all water quality variables are comparable. If not, the impact of a single variable that occurs at very low concentrations would be marginal in the sum.

Example 9.5

Select the sampling frequency for a monitoring well, which has four water quality variables. Assume that the average 95% confidence interval width about the mean will be equal to one fourth of average of means. The historical population statistics of variables are presented in [Table 9.3](#).

SOLUTION

The width of the 95% confidence interval should be one fourth of the average of the means. Thus,

$$\frac{R_1 + R_2 + R_3 + R_4}{4} = \frac{1}{4} \left[\frac{\mu_1 + \mu_2 + \mu_3 + \mu_4}{4} \right]$$

TABLE 9.3
Mean and Variance of Four Water Quality Variables

| Variable | Mean (mg/L) | Variance (mg/L) ² |
|------------------------------|-------------|------------------------------|
| BOD | 41 | 286 |
| TN | 10 | 18.1 |
| Ca ⁺ ² | 40 | 38 |
| Mg ⁺ ² | 34 | 60 |

where R is the width of confidence interval in the station i that can be computed using the following equation:

$$R_i = 2(1.96) \frac{\sigma_i}{\sqrt{n}}, \quad i=1,2,3,4$$

$$\frac{1}{4}(\mu_1 + \mu_2 + \mu_3 + \mu_4) = \frac{2 \times 1.96}{\sqrt{n}}(\sigma_1 + \sigma_2 + \sigma_3 + \sigma_4)$$

$$n = \left[4 \times 2 \times 1.96 \frac{(16.91 + 4.25 + 6.16 + 7.75)}{(41 + 10 + 40 + 34)} \right]^2 = 19.35 \approx 20 \text{ samples/year}$$

Note that in this example the relative weights are equal.

9.8.6.4 Multiple Stations and a Single Water Quality Variable

As the designer usually wants to obtain equal information from each sampling station of the monitoring network, it can be a basis for the selection of the sampling frequency. If based on historical data, the means of concentrations in the stations are approximately equal, the sampling frequencies should be selected so that they provide equal confidence intervals about the means in different stations. In a simple procedure, which was proposed by Ward et al. (1979), the total numbers of samples, (N), are allocated to stations based upon their relative weights, using the following equation:

$$n_i = w_i N \quad (9.47)$$

where:

n is the allocated samples to station i

w_i is the relative weight of station i

N is the total number of samples.

The relative weights show the relative importance (priority) of stations and can be estimated based on historical data. For example, relative weights based on the historical mean or historical variance can be computed using following equations:

$$w_i = \frac{\mu_i}{\sum_{i=1}^{N_s} \mu_i} \quad (9.48)$$

$$w_i = \frac{\sigma_i^2}{\sum_{i=1}^{N_s} \sigma_i^2} \quad (9.49)$$

where:

μ_i and σ_i^2 are the historical mean and variance of the water quality variable at station i

N_s is the total number of stations in the water quality-monitoring network.

9.8.6.5 Multiple Stations and Multiple Water Quality Variables

The design problem encountered most frequently in practice involves more than one water quality variable, as well as more than one sampling station. In this case, a separate sampling frequency should be selected for each water quality variable at each station and a weighted average of them can be considered as the station's sampling frequency. Sanders et al. (1987) expressed that a weighted average variance over the water quality variables can be computed for each station and used in Equation 9.49. In the case of multiple variables, it is not possible to obtain equal confidence interval; widths for water quality variables in all station if all variables at a given station are sampled by the same frequency.

Example 9.6

The historical means and variances for three water quality variables in four stations have been calculated and shown in [Table 9.4](#). Select the sampling frequency for each station using the weighting factors that are based on historical variances. The total number of samples per year is considered to be equal to 40.

SOLUTION

The total number of samples should be allocated to each station for each water quality variable using weighting factors. The relative weight of each station for each variable is as follows:

$$w_i = \frac{\sigma_i^2}{\sum_{i=1}^4 \sigma_i^2}, \quad i = 1, 2, 3, 4 \quad (9.50)$$

The weighting factors for different water quality variables based on the variances have been presented in [Table 9.5](#). [Table 9.6](#) shows the average number of samples estimated for each station.

9.8.7 ENTROPY THEORY IN A WATER QUALITY-MONITORING NETWORK

Water quality monitoring systems are designed to obtain quantitative information about temporal and spatial distribution of water quality variables and thus on the physical, chemical, and biological characteristics of water resources. Due

TABLE 9.4
Means and Variance for Three Water Quality Variables

| Station | TN | | BOD | | TP | |
|---------|-------------|----------|-------------|----------|-------------|----------|
| | Mean (mg/L) | Variance | Mean (mg/L) | Variance | Mean (mg/L) | Variance |
| 1 | 2.4 | 0.50 | 4.51 | 3.41 | 0.21 | 0.01 |
| 2 | 3.3 | 0.90 | 5.01 | 8.04 | 0.22 | 0.01 |
| 3 | 5.4 | 1.31 | 3.50 | 1.52 | 1.28 | 0.01 |
| 4 | 3.8 | 1.20 | 4.41 | 3.66 | 0.23 | 0.02 |

TABLE 9.5
Relative Weights of Stations in Example 9.6

| Station | TN | BOD | TP |
|---------|------|------|-----|
| 1 | 0.13 | 0.21 | 0.2 |
| 2 | 0.23 | 0.48 | 0.2 |
| 3 | 0.33 | 0.09 | 0.2 |
| 4 | 0.31 | 0.22 | 0.4 |

TABLE 9.6
Allocation of Samples via Proportional Sampling Based on Variances

| Station Number | Number of Samples Allocated | | | Average (TN, BOD, and TP) |
|----------------|-----------------------------|-----|----|---------------------------|
| | TN | BOD | TP | |
| 1 | 5 | 8 | 8 | 7 |
| 2 | 9 | 19 | 8 | 12 |
| 3 | 13 | 4 | 8 | 8 |
| 4 | 13 | 9 | 16 | 13 |

to the important role of rivers for supplying water demands and also the considerable capital and operational costs of sampling and monitoring systems, the design of an optimal monitoring network should be considered an optimal as well as economic constraint. The entropy theory could be used to eliminate the stations with redundant information in designing the water quality-monitoring network.

9.8.7.1 Entropy Theory

The entropy (or information) theory, developed by Shannon (1948), recently has been applied in many different fields. The entropy theory has also been applied in hydrology and water resources for measuring the information content of random variables and models, evaluating information transfer between hydrological processes, evaluating data acquisition systems, and designing water quality-monitoring networks.

The idea behind information theory is that it is more informative to know that an unexpected event has happened than to learn that a probable event happened. There are four basic information measures based on entropy: marginal, joint, and conditional entropies, and transinformation. Shannon and Weaver (1949) were the first to define the marginal entropy, $H(X)$, of a discrete random variable X as:

$$H(X) = \sum_{i=1}^n p(x_i) \log p(x_i) \quad (9.51)$$

Here, N represents the number of elementary events with probabilities $p(x_i)$ ($i = 1, \dots, N$). The lowest entropy is for a situation in which there is a single event with a probability of 1 (i.e., a certainty). As for the highest entropy (i.e., maximum uncertainty), it happens when all events have equal probabilities since it is hard to anticipate the outcome. The total entropy of two independent random variables X and Y is equal to the sum of their marginal entropies.

$$H(X, Y) = H(X) + H(Y) \quad (9.52)$$

where X and Y are stochastically dependent, their joint entropy is less than the total entropy of the two. The conditional entropy of X given Y represents the uncertainty remaining in X when Y is known, and vice versa.

$$H(X|Y) = H(X, Y) - H(Y) \quad (9.53)$$

Transinformation is another entropy measure that measures the redundant or mutual information between X and Y . It is described as the difference between the total entropy and the joint entropy of dependent X and Y .

$$T(X, Y) = H(X) + H(Y) - H(X, Y) \quad (9.54)$$

or

$$T(X, Y) = H(X) - H(X|Y) = H(Y) - H(Y|X) \quad (9.55)$$

The above expression can be extended to the multivariate case with M variables (Harmancioglu and Alpaslan, 1992). The total entropy of independent variables X_m ($m = 1, \dots, M$) equals:

$$H(X_1, X_2, \dots, X_m) = \sum_{m=1}^M H(X_m) \quad (9.56)$$

If the variables are dependent, their joint entropy can be expressed as:

$$H(X_1, X_2, \dots, X_m) = H(X_1) + \sum_{m=2}^M H(X_m | X_1, X_2, \dots, X_{m-1}) \quad (9.57)$$

It is sufficient to compute the joint entropy of the variables to estimate the conditional entropies of Equation 9.57, as the latter can be obtained as the difference between two joint entropies; for example:

$$H(X_m | X_1, X_2, \dots, X_{m-1}) = H(X_1, X_2, \dots, X_m) - H(X_1, X_2, \dots, X_{m-1}) \quad (9.58)$$

Finally, when the multivariate normal distribution is assumed for $f(X_1, X_2, \dots, X_M)$, the joint entropy of X , with X being the vector of M variables, can be expressed as:

$$H(X_1, X_2, \dots, X_M) = \left(\frac{M}{2}\right) \ln 2\Pi + \left(\frac{1}{2}\right) \ln |C| + \frac{M}{2} - M \ln(\Delta x) \quad (9.59)$$

where:

$|C|$ is the determinant of the covariance matrix C

Δx is the class interval size assumed to be the same for all M variables.

The design of water quality-monitoring networks is still a controversial issue, for there are difficulties in the selection of temporal and spatial sampling frequencies, the variables to be monitored, the sampling duration, and the objectives of sampling (Harmancioglu et al., 1999). The entropy theory can be used in the optimal design of water quality monitoring systems. By adding new stations and gathering new information, the uncertainty (entropy) in the quality of the water is reduced. In other words, transinformation can show the redundant information obtained from a monitoring system which is due to spatial and temporal correlation among the values of water quality variables. Therefore, this index can be effectively used for optimal location of the monitoring stations as well as determining the sampling frequencies.

9.9 MANAGED AQUIFER RECHARGE

Managed Aquifer Recharge (MAR) programs have been developed to intentionally harvest and infiltrate water to recharge depleted aquifer storage to increase the security of groundwater resources (Figure 9.14). Limited natural recharge potential in arid and semiarid climates has led to the development and implementation of MAR programs around the globe to increase the security of groundwater resources.

The predicted increase in aridity and the occurrence of droughts due to climate change could exacerbate the groundwater overdraft (Seager et al., 2007) and around the globe. Climate change may increase the precipitation frequency and magnitude, which could result in more extreme flood events during wet years and greater surface runoff from precipitation in excess of infiltration, which will reduce the groundwater recharge (Dettinger, 2011; Pierce et al., 2013). Therefore, well designed MAR projects could play a crucial role in increasing the groundwater security. Such projects must be carefully tailored to the local needs and constraints (Dahlke et al., 2018). MAR projects are applicable where there is no suitable surface storage site available and could be considered as part of an integrated water management strategy to store water in aquifers for future use, balance supply/demand fluctuations, stabilize or raise groundwater levels in overdrafted regions, decrease losses via evaporation and runoff, prevent storm runoff and soil erosion, improve water quality, sustain environmental flows in streams and rivers, prevent intrusion of saline water in coastal areas, protect against land subsidence, and help dispose or reuse wastewater and stormwater (Gale, 2005).

9.9.1 PRINCIPAL CONSIDERATION

The success of MAR projects in increasing the security and quality of water supplies in water-scarce areas depends on how well they have been planned, designed, and operated. Such projects should be an integral part of watershed management strategies. A 2002 meeting of representative organizations at UNESCO in Paris concurred to produce coherent plans and activities in support of MAR projects in semiarid

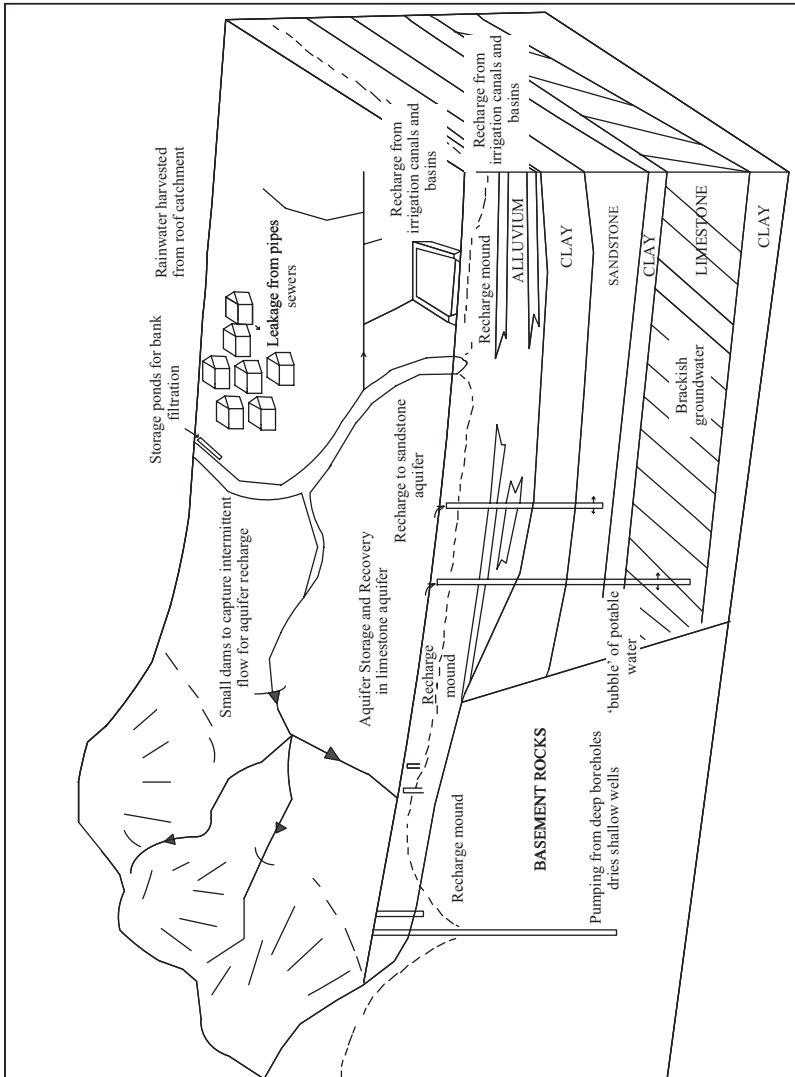


FIGURE 9.14 Managed Aquifer Recharge methods. (From Gale, J., Strategies for Managed Aquifer Recharge (MAR) in Semi-Arid Areas, UNESCO IHP, Landais, France, <https://recharge.jah.org/files/2017/01/Gale-Strategies-for-MAR-in-semiarid-areas.pdf>, 2005.)

regions. As part of this initiative, the International Association of Hydrogeologists Commission on MAR with the support of the UNESCO International Hydrology Programme and the British Department for International Development compiled a document that draws together experiences of the applications of MAR in semi-arid regions as guidance and examples of good practice throughout the world (Gale, 2005). This section provides a summary of this report.

Aquifers could be recharged through spreading, infiltration ponds, inter-dune ponds, streambed modification, open wells, shafts and trenches, borehole recharge, induced bank filtration, and soakaways from rooftop catchments. To plan for MAR projects, institutional and management aspects that must be considered include: water rights, land ownership, legal and regulatory issues, source of funding, project beneficiaries, entity(ies) responsible for managing, integrated management (users/NGOs/governments), conjunctive use, and demand management. The benefits of MAR projects could be assessed using metrics such as: stabilized or escalating piezometric levels, increased base flow, decreased saline intrusion, declined land subsidence, sustained groundwater source, sustained irrigated area, stabilized soil erosion, positive cost/benefit analysis, and improved livelihoods.

To assess a site for MAR projects, first a hydrogeological conceptual model should be developed to understand the system and its hydrology. Storage space in the aquifer for additional water should be estimated and the components of the water balance need to be quantified. Water quality in the aquifer and source water should also be evaluated. Numerical models could be used to assess scheme. Additionally, the impacts downstream of the structure should also be determined.

9.9.1.1 Sources of Recharge Water and Its Quality Considerations

The main requirement for Managed Aquifer Recharge is the availability of a source of water in sufficient quantity with suitable quality. It is also important to understand the baseline water quality, the impacts of anthropogenic activities, and the geochemical processes involved. Groundwater abstraction, recharge enhancement, irrigation, land use changes, agriculture and forestry, urbanization, mining, and liquid and solid waste disposal are common anthropogenic activities altering groundwater quality, especially in unconfined aquifers.

High quality water could be introduced to an aquifer to improve its quality by recharging with surplus runoff through surface infiltration structures. Such an approach enhances water quality through dilution, or it can provide a hydraulic barrier to lateral saline intrusion. The source water could be surface water, runoff water, imported water, treated effluent, or potable supply water:

Surface Water: Water diverted from perennial rivers, recharge facilities or induced-bank filtration directly from rivers are common sources of surface water. Since considerable quantities of silt and sediments are usually carried by rivers, settling ponds should be used before the water enters infiltration ponds. If the source water is from lakes, where water is not flowing significantly and has little or no suspended material, the settling ponds could be omitted.

Storm-Water Runoff: Urban stormwater runoff is highly variable in quantity with peak discharges happening after heavy rainfalls. In urban areas, runoff from rooftops has the best quality. To obtain supply consistency, it is recommended to use measures such as infiltration and stormwater retention ponds, grassed areas, porous pavements, and wetlands (Murray and Tredoux, 1998). Intense rainfall in rural areas generates surface runoff from agricultural fields and uncultivated land. Stormwater runoff significantly varies in quality. The first flush usually contains the highest contamination load and is recommended to be discarded. In general, the contamination load could include atmospheric deposition on watershed surfaces, road surface accumulation, loads from construction fields, industrial runoff, animal wastes, litter, decaying vegetation, fertilizers and pesticides, septic tank seepage, and fecal matter from livestock and humans.

Reclaimed Water: Reclaimed or recycled water as a source water for aquifer recharge usually has a predictable volume with a fairly uniform flow rate and constant, but inferior quality (Murray and Tredoux, 1998). Wastewater goes through significant treatment processes to reach the acceptable quality for aquifer recharge that do not degrade the groundwater quality. Gaining public acceptance and the associated costs for pipelines, pumping stations, and other features of the water conveyance system from the wastewater treatment plant to where it is needed are the most challenging constraints on using reclaimed wastewater. A less cost-intensive approach is to use spreading basins to improve the wastewater quality through Soil Aquifer Treatment and dilute it with natural groundwater (Bouwer, 2002).

Potable Water: As a major source of recharge water, potable water is used in Aquifer Storage and Recovery projects, where a bubble of potable water is created in the aquifer by injecting treated, high-quality water into confined aquifers through wells.

9.9.1.2 Hydrogeological Settings and Controls on Recharge

Local hydrogeological conditions include whether the recharge water could percolate through the unsaturated zone and the aquifer has the storage capacity. The main factors to consider include:

- Degree of confinement and hydraulic boundaries of the aquifer
- Hydrogeological characteristics of the aquifer and overlying formations
- Aquifer hydraulic gradient
- Aquifer depth and its piezometric surface
- Quality of groundwater
- Mineralogy of the aquifer

When spreading techniques are employed, the water moves downward through the unsaturated zone to reach the aquifer, and the percolation rate depends on the

vertical permeability of the soil and unsaturated zone. In these circumstances, the hydrogeological characteristics at the surface and in the unsaturated zone are most important. The aquifer extent, its thickness and hydraulic characteristics, such as transmissivity and storativity, play the primary roles in identifying storage capacity once the recharge water reaches the water table. High hydraulic conductivities cause rapid dispersal of the recharge water, resulting in the storage of only limited quantities of water, which is acceptable only if the recharge project aims to supplement groundwater and base flow to streams on a regional basis. The wide variety of hydrogeological environments could be grouped into four general categories:

Alluvium: Alluvium may contain fluvial, marine, and lacustrine deposits that range in thickness from a few tens of meters to several kilometers. In terms of permeability, the sediments range from highly permeable coarse gravel to fine-grained impermeable silt and mud. Considerable deposits could usually be found in the lower reaches of river basins, which form flood plains.

Fractured Hard Rock: Fractured bedrock are usually comprised of igneous, metamorphic, or volcanic rocks and are found over large areas in semiarid regions. Such aquifers have low storativity and transmissivity. Groundwater storage occurs in the weathered zone, where a mechanism for absorbing and storing intermittent rainfall that can then percolate to the underlying aquifer is provided. Therefore, to exploit or recharge these aquifers, the weathered or fractured zones must be located. A borehole injection may be the only option for recharging deep, hard rock aquifers.

Consolidated Sandstone Aquifers: Consolidated sandstone aquifers are porous, fractured aquifers with good storage capacity and transmissive properties. The recharge rate is determined by the composition of the surface layer. The soil developed from the sandstone has a high recharge capacity. However, the recharge capacity could be compromised if the overlying layer is made up of fine-grained alluvial deposits. Very high aquifer permeability may result in quick dissipation loss of the recharged water to base flow in rivers.

Carbonate Aquifers: Carbonate aquifers have similar characteristics to the sandstone aquifers, except that the principal storage and flow are in the solution-enhanced fractures. The proportion of fracture flow to intergranular flow will vary considerably, from low in porous limestones, to high in karstic limestones.

9.9.1.3 MAR Methods

MAR methods range in complexity from simple rainwater harvesting to deep-well injection of water into the aquifer. The appropriate method is selected based on defined local objectives. In most methods, clogging is a major issue that needs to

be addressed to minimize impacts in a cost-effective way. For injection wells, MAR methods could be grouped into the following categories:

Spreading methods, which infiltrate recharged water through permeable surface layers where the unconfined aquifer is at or near to the ground surface. Common spreading methods include:

- *Infiltration ponds and basins:* A land surrounded by a bank or an infiltration basin excavated in the ground retains the recharge water to be percolated through the bottom of the basin (Figure 9.15). Fine-grained aquifer materials result in rapid clogging and require the covering of the bottom and sides with a layer of medium sand. This action helps delay the clogging process and extends the recharge periods (Huisman and Olsthoorn, 1983).
- *Soil Aquifer Treatment:* Systems usually treat effluent from sewage treatment plants to secondary levels and chlorinate it, and then apply it to infiltration ponds (Figure 9.15).
- *Controlled flooding:* When the topography is relatively flat, water may be diverted from a river and spread evenly over a large surface area, forming a thin sheet of water over the soil cover. This method is very cost-effective compared to other spreading methods since it only requires minimum land preparation. However, it needs large land surfaces.
- *Incidental recharge from irrigation:* Where quantified and managed to prevent groundwater quality issues, incidental recharge can become an asset.

In-channel modifications, which include the following techniques:

- *Percolation ponds behind check dams:* The construction of check dams with in situ river alluvium across a streambed can provide an inexpensive way for recharging the underlying aquifer (Figure 9.16).
- *Sand storage dams:* Under arid climatic conditions, where runoff often is a consequence of flash floods, sand storage dams are usually constructed in sandy, ephemeral riverbeds, and a dam wall is constructed on the bedrock

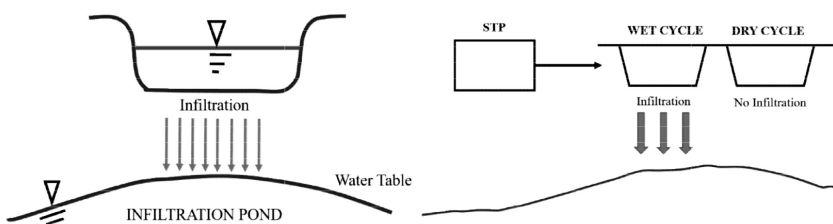


FIGURE 9.15 Schematics of an infiltration pond and soil aquifer treatment system. (From Gale, I., Strategies for Managed Aquifer Recharge (MAR) in Semi-Arid Areas, UNESCO IHP, Landais, France, <https://recharge.iah.org/files/2017/01/Gale-Strategies-for-MAR-in-semiarid-areas.pdf>, 2005.)

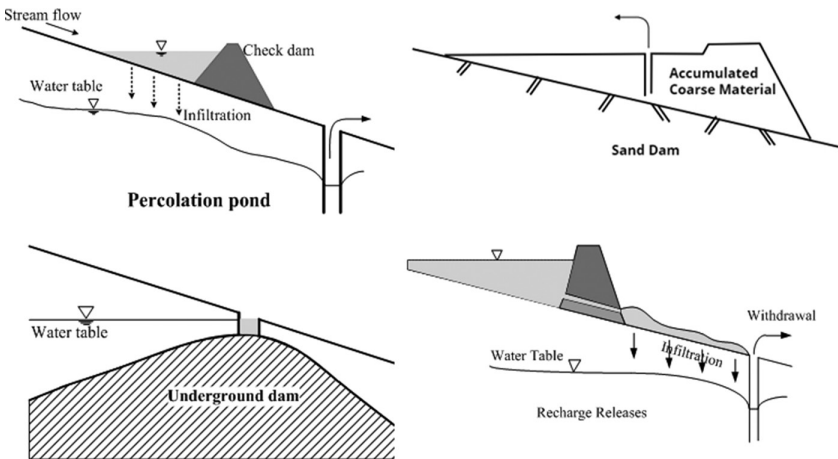


FIGURE 9.16 Schematics of a percolation pond, sand dam, underground dam, and recharge releases. (From Gale, I., Strategies for Managed Aquifer Recharge (MAR) in Semi-Arid Areas, UNESCO IHP, Landais, France, <https://recharge.iah.org/files/2017/01/Gale-Strategies-for-MAR-in-semiarid-areas.pdf>, 2005.)

across the width of the riverbed to slow down flash floods and allow coarser material to accumulate behind the dam wall (Figure 9.16).

- *Subsurface dams:* To help detain water in alluvial aquifers under ephemeral streams, a trench is constructed across the streambed founded on the basement rocks and is backfilled with a low permeability material to constrain groundwater flow (Figure 9.16).
- *Leaky dams and recharge releases:* Constructing dams on ephemeral streams where the flow is very flashy can help prevent losing water downstream before it infiltrates into the aquifer (Figure 9.16).

Well, shaft and borehole recharge, which include the following techniques:

- *Open wells and shafts:* When spreading methods are not effective in the recharge of shallow phreatic aquifers due to the low permeability of surface layers, open wells and shafts are used for recharging purposes. Wells that have become dry due to over-exploitation are increasingly being used for recharge purposes. The presence of suspended solids as well as chemical (nitrates, pesticides, etc.) and bacterial (including fecal) contaminants are common issues associated with this method. While the spreading structures have the advantage of natural infiltration as an extremely effective filtering mechanism, open wells do not have such benefits and may require the treatment of recharge water prior to introducing it to the wells.
- *Drilled wells and boreholes:* These techniques are used to directly recharge water into the aquifers that are overlain by thick, low permeable strata and also where land is scarce. Similar to open wells and shafts, the recharge

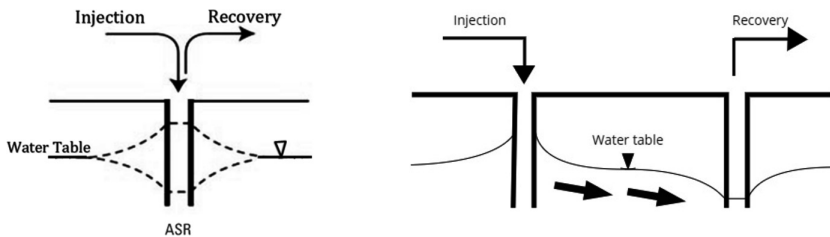


FIGURE 9.17 Schematics of Aquifer Storage Recovery (ASR) and Aquifer Storage Transfer and Recovery (ASTR). (From Gale, I., Strategies for Managed Aquifer Recharge (MAR) in Semi-Arid Areas, UNESCO IHP, Landais, France, <https://recharge.iah.org/files/2017/01/Gale-Strategies-for-MAR-in-semiarid-areas.pdf>, 2005.)

water quality requirements are usually significantly higher for injection into drilled wells and boreholes than for recharge by spreading methods. A detailed description of this method can be found in Pyne (2005). Aquifer Storage Recovery projects (Figure 9.17), where the well/borehole is used for both injection and recovery, have minimized costs and clogging is removed during the recovery cycle. In general, pumping water from an injection well on a daily basis for short periods of time helps mitigate clogging issues (Bouwer, 2002). To increase travel time in order to take advantage of the aquifer water treatment capacity, water can be injected into a borehole and recovered from another one, some distance away. Such projects are called Aquifer Storage Transfer and Recovery (Figure 9.17).

Induced bank infiltration, which include the following techniques:

- *Bank filtration:* In such projects, a gallery or a line of boreholes at a short distance from, and parallel to, the bank of a surface water body are used to pump water out and lower the water table near the river or lake to induce surface water to enter the aquifer system (Figure 9.18). For satisfactory purification of the surface water in the ground, it is recommended that travel time exceeds 30 to 60 days (Huisman and Olsthoorn, 1983), which

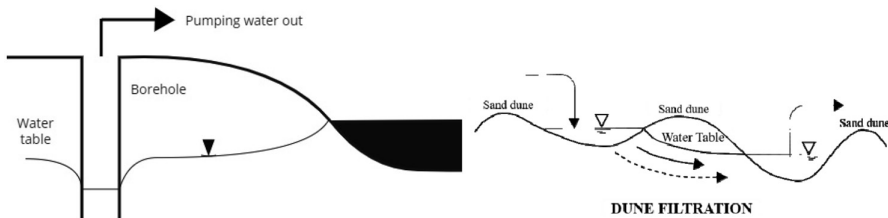


FIGURE 9.18 Schematics of bank filtration and dune filtration. (From Gale, I., Strategies for Managed Aquifer Recharge (MAR) in Semi-Arid Areas, UNESCO IHP, Landais, France, <https://recharge.iah.org/files/2017/01/Gale-Strategies-for-MAR-in-semiarid-areas.pdf>, 2005.)

requires consideration of the corresponding distance for the water to travel when selecting the boreholes.

- *Inter-dune filtration:* The primary objective of this method is to improve the quality of the source water, which could be coastal water, storm, and treated urban wastewater. The valleys between coastal sand dunes are flooded with river water in order to penetrate into the underlying sediments and create a recharge mound (Figure 9.18). This technique has been used along the coast of the Netherlands to prevent saline intrusion using river water as a source of recharge water.

Rainwater harvesting, which include the following techniques:

- *Dry land farming:* In semiarid regions, usually 30%–50% of rainfall is lost to evapotranspiration and 10%–25% goes to runoff. To reduce surface runoff and evaporation, interventions such as field bunds, contour ploughing rock weirs in drainage channels, and floodwater diversions into bunded cropping areas are used to concentrate the water to be stored in the deeper aquifer.
- *Roof-top rainwater harvesting:* In urban areas, rainwater could be collected from rooftops and stored to decrease the demand on the water supply systems and also reduce stormwater runoff and the consequent flooding. In this approach, the outlet pipe from a guttered rooftop is connected to the existing wells, other recharge facilities, or to storage tanks (Figure 9.19). The main sources of contamination are pollution from the air, bird and animal droppings, and insects.

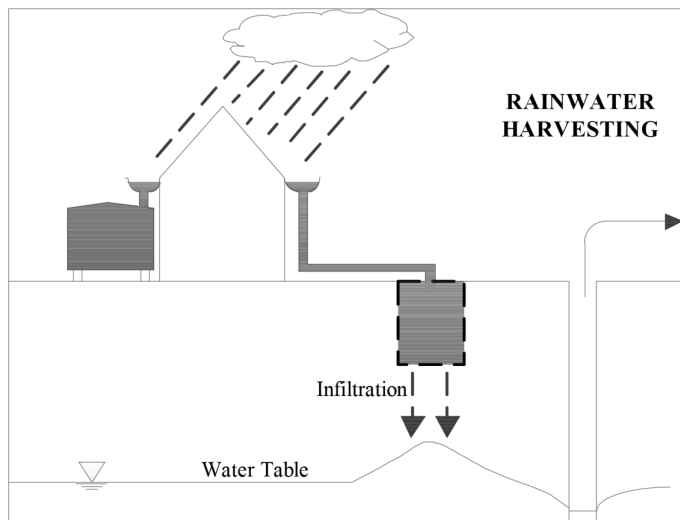


FIGURE 9.19 Schematic of rainwater harvesting. (From Gale, I., Strategies for Managed Aquifer Recharge (MAR) in Semi-Arid Areas, UNESCO IHP, Landais, France, <https://recharge.iah.org/files/2017/01/Gale-Strategies-for-MAR-in-semiarid-areas.pdf>, 2005.)

9.9.2 MAR IN SUPPORT OF GROUNDWATER SUSTAINABILITY

Through a comprehensive effort, Dahlke et al. (2018) overviewed the most common MAR types and applications in urban, agricultural, and coastal areas in semiarid regions, with a special focus on the State of California. This section provides a summary of their study.

9.9.2.1 MAR in Urban Settings

MAR implementation in urban settings could bring diverse benefits, such as stormwater quality management and flood protection. Before the 1980s, centralized MAR projects were common to enhance the water supply in urban settings. These projects usually have a large footprint, which covers an area greater than one hectare (2.47 acres) and has a recharge volume of over 1,000,000 m³/year. Recently, more attention has been given to the implementation of decentralized MAR projects, which have small footprints (less than one hectare and below 10,000 m³/year of recharge volume).

9.9.2.1.1 Centralized MAR Approaches

Infiltration basins and well technologies are the most common centralized MAR approaches in urban settings. While infiltration basins require simple technology with relatively low capital, and annual operation and maintenance costs (Dillon et al., 2010), they need land and facilities constructed exclusively for recharge. A main concern associated with the implementation of infiltration basins is their impact on groundwater quality in settings where groundwater flow velocities are high, which may increase the risk of groundwater contamination with pollutions in the stormwater or surface water (O’Leary et al., 2012). However, depending on the quality of the source of the recharged surface water, it may also have a diluting effect on the groundwater quality. Dry wells and injection wells, on the other hand, are more maintenance-intensive and may have a capital cost factor in areas with high property prices (Dillon et al., 2010).

While soft technologies, such as conjunctive use and in-lieu recharge of groundwater, could be used to enhance recharge management strategies, implementation of these technologies could be dependent on political and institutional factors (Foster et al., 2010). For example, in a collaboration between the San Francisco Public Utilities Commission and its partner agencies, the San Francisco Public Utilities Commission would supply the partner agencies with surface water to assist with in-lieu recharge of their basin (Engineers LSC, 2010), and in return, up to 16 new recovery wells would provide a secure water supply to the city of San Francisco in dry years (Department SFP, 2013).

Recycled water could be a potential water source for MAR projects in urban settings as long as concerns related to potential pathogen presence and disinfection by-products from chlorine treatment are addressed (Leenheer et al., 2001). Pathogen survival and attenuation in aquifers are influenced by the particular species of pathogen and site-specific geochemical factors (Sidhu et al., 2015). Depending on the final intended use, MAR projects using recycled water may require differing levels of pre-treatment.

9.9.2.1.2 Decentralized MAR Approaches

Over the last 100 years, due to limitations associated with the availability of space and economic resources, large-scale centralized infiltration projects have diminished, while decentralized MAR projects have received more attention from urban planners (Parker, 1997; California Department of Water Resources, 2015). Through these projects, smaller volumes of water, usually 10 to 100 m³ per rain event, are usually infiltrated.

Recent studies on decentralized MAR projects in urban settings have mainly concentrated on the implementation of Low Impact Development, which is designed to mitigate the negative effects of urbanization on surface runoff by means such as increasing impervious surfaces (Stephens et al., 2012) through practices that include pervious pavement, vegetated swales, bioretention basins, and small-scale infiltration basins (Dietz, 2007). Dry wells, cisterns, rainwater capture, reuse projects, and rooftop rainwater harvesting and runoff infiltration are other common practices for decentralized MAR projects.

Dry wells are usually susceptible to more direct passage of contaminants to groundwater aquifers, as the recharge water is not infiltrated and filtered through the unsaturated zone (Edwards et al., 2016). On the other hand, bioretention basins and vegetated swales provide water treatment opportunities. Therefore, these measures are usually combined with other decentralized means such as dry wells, cisterns, or infiltration basins (Department of Environmental Resources, 2000). **Figure 9.20** depicts the general design of a dry well combined with a grass swale and sedimentation chamber. They remove high levels of metals and nitrogen, and to

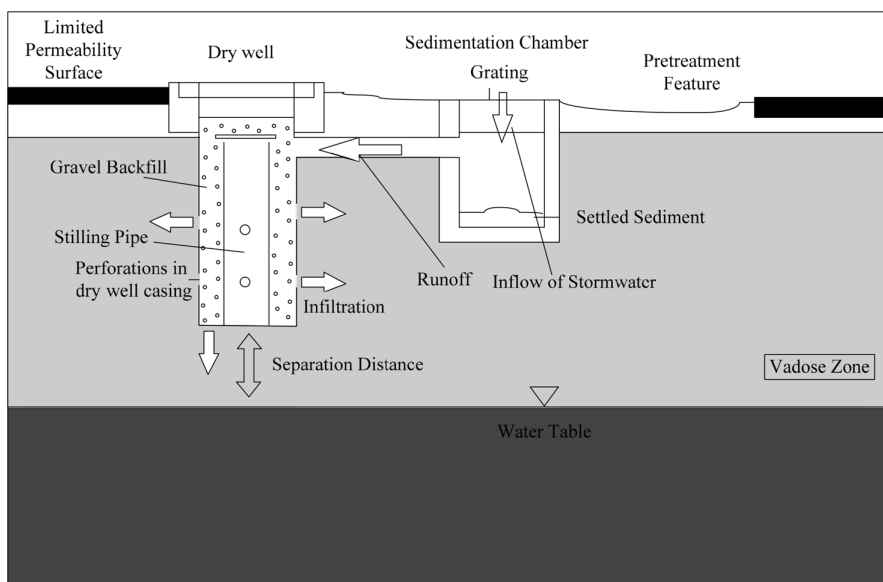


FIGURE 9.20 General design of a drywell, including pre-treatment with a grass swale and sedimentation chamber. (From Edwards, E.C., et al., *J. Hydrol.*, 539, 539–553, 2016. With permission.)

some extent, reduce other contaminants such as suspended solids, phosphorus, salts, and pathogens. Bioretention systems use vegetation, e.g., shrubs or trees, to treat contaminated water by physical, chemical, and biological processes (Dietz, 2007). While being similar to bioretention basins, vegetated swales, also called bioswales, have a smaller capacity to capture stormwater. They have a shallower topographic profile and use grass instead of diverse vegetation. Aside from water treatment potentials, other primary benefits of these measures include: slowing stormwater runoff, removing pollutants, and settling out suspended solids (Dietz and Clausen, 2005).

Capture and reuse or on-site direct use projects are other decentralized MAR approaches. Capture and reuse projects incorporate water storage techniques such as constructed aquifer storage and recovery systems, modular underground storage tanks, and rain barrels to capture precipitation, store it, and reuse or slowly release the stored water over time for irrigation or groundwater recharge (County of San Diego, 2014).

9.9.2.1.3 Water Quality Considerations in Decentralized Urban MAR

Water quality in stormwater runoff is highly variable and depends on the types and variety of land use activities that occur in cities. It may contain sediments, metals accumulated on roads (such as copper, lead, zinc, etc.), construction site runoff, organics (such as animal wastes and decaying vegetation), pesticide and fertilizer runoff from landscaping, and trash (Gale, 2005). Fecal contamination from urban pets (dogs, cats, etc.) is also a common problem in stormwater runoff, which should be addressed to prevent human health impacts when reusing the captured stormwater for landscaping. Groundwater contamination is another common concern that needs to be addressed when designing the recharge projects using urban stormwater runoff (Dahlke et al., 2018). The highest pollutant loads in urban areas are usually observed during the first flush of the wet season, during which, pollutants accumulated on impervious surfaces over the dry season become mobilized and are mixed or dissolved in the stormwater. Such phenomenon is more prevalent in Mediterranean climates with distinctive wet and dry seasons (Lee et al., 2004).

9.9.2.2 MAR in Agricultural Settings

Groundwater overdraft has become one of the most concerning issues in semiarid regions with intensively irrigated agriculture. The long-term sustainability of the agricultural industry is being jeopardized by groundwater overdraft, which has also been exacerbated by changing climate impacts, changing land use, widespread adoption of high-efficiency irrigation systems, and the conversion of rangeland into cropland. A water management approach that helps bring back groundwater basins into sustainability is ag-MAR, which diverts the excess surface water, especially during wet years or seasons, onto agricultural fields to recharge the underlying aquifer for future use during droughts.

Since ag-MAR promotes leveraging agricultural lands for on-farm recharge, it imposes minimal costs compared with other approaches such as infiltration basins or injection wells (Bachand et al., 2014, 2016). Additionally, ag-MAR increases the groundwater elevation without negatively impacting other water users or minimum in-stream flow requirements. Due to concerns about the high levels of sediment transport early in

the wet season, it is recommended to reserve high-magnitude flow events for after the dry periods for channel formation or environmental flows and divert the high-magnitude flows for later in the season for ag-MAR (Kocis and Dahlke, 2017).

There are a number of interconnected and site-specific factors that determine the feasibility of ag-MAR projects. Examples include: water availability, conveyance infrastructure from source waters to fields, costs, local or regional water laws and permits, the soil's physical and biochemical properties, the crop's tolerance to water inundation, the aquifer capacity for water storage and recovery, increased irrigation efficiency, and the effect of the practice on groundwater quality (Figure 9.21). Some of these factors are further explained in the following.

Water Availability: Some of the most common water sources for MAR projects, such as recycled water and desalination water, do not provide the water volumes necessary for supplying ag-MAR projects (Kocis and Dahlke, 2017). High-magnitude flows or flows that occur during large storm events may represent the most accessible and largest source of water available for such projects. Providing these for ag-MAR projects usually does not have an impact on agricultural activities because surface water demand during the winter months, when the majority of these events occur, is relatively low.

Infrastructure: Existing water conveyance structures may not be suitable for transporting high-magnitude flood flows to recharge areas (O'Geen et al., 2015), and their capacity could be a limiting factor for flood flow applications.

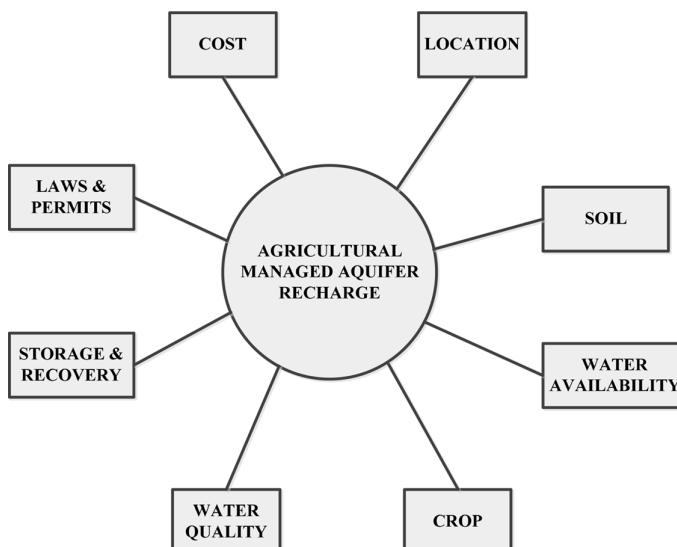


FIGURE 9.21 Factors influencing the feasibility of MAR in agricultural settings. (From Dahlke, et al., *Advances in Chemical Pollution, Environmental Management and Protection*, Academic Press, Elsevier, Cambridge, UK, 2018.)

Field preparation to allow a more rapid infiltration on existing farmland is a cheaper way to capture and store excessive water compared with large-scale surface storage or infiltration basins (Bachand et al., 2014).

Soil Suitability: Critical factors for successful ag-MAR projects across agricultural lands that have been considered in the Soil Agricultural Groundwater Banking Index include (O'Geen et al., 2015):

Deep Percolation, which shows the capability of a site to transmit water through the soil profile. It is estimated by the soil horizon with the lowest saturated hydraulic conductivity. Deep percolation considers the amount of water that will reach the groundwater table.

- **Root zone residence time**, which represents the duration of saturated or near-saturated conditions in the soil profile. It is calculated based on the harmonic mean of saturated hydraulic conductivity of all horizons in the soil profile, classification of soil drainage, and shrink-swell characteristics. Root zone residence time takes into account that prolonged ponding conditions may impact crop health.
- **Chemical limitation**, which considers the salinity and leaching potential of the soil in a site.
- **Topography**, which takes the slope of the field site into account
- **Soil surface condition**, which considers the soil's susceptibility to physical changes, e.g., erosion or compaction.

These factors are weighed based on their relative importance for ag-MAR. However, deep percolation and root zone residence time are ranked as the most important ones.

Crop Tolerance: The crop's ability to tolerate flooding or saturated conditions in the root zone varies by the crop type and local soil properties. Before implementing ag-MAR projects, their effect on root health, especially anoxic conditions in the root zone, must be assessed to avoid lower nutrient uptake, which affects the annual average yields. Applying water during the winter months on highly permeable soils may minimize yield loss in almonds, pistachio trees, alfalfa orchards, or wine grapes (Dahlke et al., 2018; Bachand et al., 2014). On soils with a Soil Agricultural Groundwater Banking Index rating of moderately good or less, flooding the cropland could take place when the land is fallow to minimize the risk of root damage or yield reduction. However, it is recommended to prioritize highly rated soils from the Soil Agricultural Groundwater Banking Index for implementation of ag-MAR projects.

COST: The main sources of costs for ag-MAR projects include: land preparation, farm-scale infrastructure improvements, labor, and fuel (Bachand et al., 2016). Ag-MAR has become a more economically feasible method compared with other water supply strategies such as seawater desalination or surface water storage. For example, ag-MAR costs in California have been estimated to be about \$0.03 per m³, while the cost for seawater desalination is \$1.54–\$2.43 per m³, and for large-scale surface water storage, the

cost is \$1.38–\$2.27 per m³. As water tables drop, the groundwater pumping costs become higher. For example, California experienced an average of a 39% increase in groundwater pumping costs during the 2012–2016 drought (Medellín-Azuara et al., 2016).

Water Quality: Ag-MAR projects could potentially flush contaminants, such as nitrate, salts, and pesticides down toward the groundwater table. The depth to groundwater, soil's hydraulic conductivity, and the region's hydrologic regime are the main factors influencing the time it takes for the nitrate's transportation from the land surface to the groundwater table, which can range from subannual to decadal (Baram et al., 2016). While implementation of ag-MAR projects could potentially create a downward pulse of nitrate from the root zone, successive flooding of the land may cause a dilution effect as the higher quality water is flushed down in the same pathways during later flooding events (Bachand et al., 2011).

Inefficient Irrigation and Canal Seepage: Inefficient irrigation systems can unintentionally infiltrate water, especially when applied in excess of the crop demand, below the root zone, and ultimately to the underlying aquifer. The high-efficiency irrigation systems may sustain water availability for surface water reservoirs. However, they can reduce the groundwater recharge (Niswonger et al., 2014). Leaky surface water conveyance systems, such as unlined canals, ditches, and leaky pipelines, also contribute to the unintentional recharge of groundwater. On average, 20% of the diversion water could be lost through leakage from surface water delivery canals to recharge and 33% of the groundwater inflows could originate from leaky conveyance systems during wet years (Carroll et al., 2010).

Increased Irrigation Efficiency: Irrigation efficiency is defined as the percent of the crop's consumptive use (or the volume of irrigation water stored in the root zone) over the amount of total water applied to the agricultural land for crop production or the volume of irrigation water delivered to the farm (Pfeiffer and Lin, 2014; Irmak et al., 2011). Depending on the type of irrigation water application system, the irrigation efficiency could increase up to 95% (Table 9.7); i.e., total water use could be reduced by up to 95%. Higher irrigation efficiency decreases the water use for a given crop yield, while it may maintain the crop's consumptive use. The portion of the applied water that is not consumed by the crops will either be introduced back to the surface water as agricultural return flow or will recharge the underlying aquifer via percolation. Therefore, while increasing irrigation efficiency could reduce the total agricultural water demand, it may highly reduce groundwater recharge rates from irrigation practices. Additionally, the less irrigation water applied to an agricultural land, the lower capacity it has to wash off fertilizers and pesticides applied to the land. Therefore, pesticides and fertilizers are accumulated until they are washed off by a storm event introducing large loads of pollutants to the surface and groundwater resources.

TABLE 9.7
Irrigation Efficiencies of Different Types of Irrigation
Water Application Systems

| Irrigation System | Irrigation Efficiency (%) |
|-------------------------------------|---------------------------|
| <i>Sprinkler Irrigation Systems</i> | |
| Low energy precision application | 80–95 |
| Linear or lateral move | 75–90 |
| Center pivot | 75–92 |
| <i>Surface Irrigation Systems</i> | |
| Conventional furrow | 45–70 |
| Surge flow | 55–75 |
| Furrow with tailwater reuse | 60–80 |
| <i>Micro-irrigation Systems</i> | |
| Bubbler (low head) | 80–90 |
| Micro-spray | 85–90 |
| Subsurface drip | 90–95 |
| Surface drip | 85–95 |

Source: Irmak, et al., DigitalCommons@University of Nebraska-Lincoln Irrigation Efficiency and Uniformity, and Crop Water Use Efficiency, <https://digitalcommons.unl.edu/biosysengfacpub>, 2011.

9.9.2.3 MAR in Coastal Areas

In coastal regions, the primary goal of MAR projects may be preventing seawater intrusion in addition to the other goals that are also common for agricultural and urban MAR, including: increasing groundwater storage, enhancing water quality, preventing subsidence, or protecting groundwater-dependent ecosystems. Injection wells and infiltration basins are the most common methods for MAR in coastal regions. The main advantage of injection wells over other MAR methods is the higher flexibility in specifying the appropriate locations, allowing them to be sited where they provide the most effective barrier against seawater intrusion.

The main considerations associated with the implementation of infiltration basins include: the cost, challenges of site selection, sediment accumulation, potential nitrate leaching, conveyance of source water, and associated legal and political issues. Infiltration basins have different source water quality considerations compared to injection wells since water receives physical filtration moving through the vadose zone or the geochemical composition of water may be transformed; however, clogging is always a major issue (Bouwer, 2002). The routine scraping of infiltration basins helps remove the accumulated sediments and restore original infiltration rates (Racz et al., 2012).

9.9.3 THE UNITED NATIONS MAR PORTAL

The United Nations International Groundwater Resources Assessment Centre has created a MAR Portal,¹ which intends to promote consideration of MAR as a viable solution for sustainable groundwater resources development and management. This portal facilitates access to international information and knowledge and promotes information sharing.

The United Nation's MAR portal provides detailed information on MAR sites around the globe by compiling and analyzing approximately 1200 case studies from more than 50 countries. The information provided in this inventory include: site name, location, MAR type, operation start time, the source of infiltration water, the final use of stored water, and the main objective of the MAR project. These projects present outstanding best-practice examples that can be used for the planning and implementation of new projects.

The MAR portal also contains regional MAR suitability maps to assist with the selection of suitable locations for MAR projects, as there are many aspects which need to be considered in locating such projects, such as soil and aquifer properties, landscape characteristics, and the availability of the source water. These maps can help decision-makers to successfully implement new MAR projects.

9.10 SUMMARY

Important concepts of aquifer restoration such as institutional tools, groundwater pollution prevention methods, as well as groundwater treatment methods were reviewed in this chapter. Besides these methods, the chapter first explains how to calculate the portion of the total applied contaminant to a field that reaches the groundwater and the retardation rate, caused by adsorption. In addition to adsorption, there are some natural processes that may dilute contaminants before they reach an aquifer. The main natural processes causing the dilution of contaminants, such as volatilization, biological degradation, and plant uptake were discussed in this chapter. On the other hand, since the process of decision-making is based on the available information related to water quality characteristics, unsaturated zone, and groundwater monitoring processes, these were discussed as one of the most important steps of aquifer quality management.

PROBLEMS

- 9.1 What fraction of the total contaminant may reach the underlying unconfined aquifer if the water table is at 1.8 m below the soil surface? Assume that the soil water content and bulk density are 0.35 and 1540 kg/m³, respectively. The partitioning coefficient is 0.98.
- 9.2 In the previous problem, determine how far the dissolved portion can go downward in a day. In addition, compute how long it takes for the contaminant to reach the groundwater? Assume that the irrigation rate is 2 cm/day and the crop water use is 0.45 cm/day.

¹ <https://www.un-igrac.org/ggis/mar-portal>

- 9.3** A chemical is applied to an agricultural field. Determine the load of the dissolved portion of the chemical that reaches groundwater.
- Application rate of the chemical: 3.2 kg/ha.
 - Irrigation rate: 1.5 cm/day
 - Crop water use: 0.38 cm/day
 - Soil water content: 0.40
 - Partitioning coefficient: 0.89
 - Soil bulk density: 1600 kg/m³
 - Depth of water table 2.0 m.
 - Decay factor of the chemical: 0.056 (day⁻¹).
- 9.4** The annual mean and variance of the historical data of the TDS concentrations in a water quality monitoring well are 750 mg/L and 238 (mg/L)², respectively. If the desired confidence interval width is 25 mg/L with a 95% confidence level, what sampling frequency do you suggest for the well?
- 9.5** A fertilizer is applied and uniformly distributed to a field. The characteristics of the underlying soil and the fertilizer are presented below. What is the approximate groundwater contamination by the fertilizer if the soil is saturated?
- Application rate of the fertilizer: 140 kg/h
 - Depth of application: 0.20 m
 - Soil's maximum adsorption: 270 $\mu\text{g}/\text{L}$
 - Soil porosity: 32%
 - Specific density of soil: 1540 kg/m³
 - Constant b : 0.0022 L/ μg
- 9.6** The concentrations of calcium and magnesium are measured at a monitoring well. Select the sampling frequency for this well based on the historical population statistics presented in [Table 9.8](#)
- 9.7** Concentrations of total nitrogen and BOD are being measured in three monitoring wells. Using the weighting factors, based on the historical variances, determine the sampling frequency for each well. Assume that in total, 30 samples are taken per year. The historical means and variances for these water quality variables in the wells are presented in [Table 9.9](#).
- 9.8** A herbicide is applied to a golf course at a rate of 1.5 kg/ha. This field is irrigated at the rate of 2.5 cm/day. If the partitioning coefficient and soil bulk density are 1.2 L/kg and 1670 kg/m³, respectively, determine the fraction of the herbicide that is adsorbed to the soil and the fraction that may reach the groundwater. Assume that the soil is at saturation and its porosity is 40%.

TABLE 9.8**The Concentrations of Calcium and Magnesium in Problem 9.6**

| Variable | Mean (mg/L) | Variance (mg/L) ² | 95 % Confidence Interval Width |
|------------------|-------------|------------------------------|--------------------------------|
| Ca ⁺² | 47 | 62 | 23 |
| Mg ⁺² | 41 | 35 | 22 |

TABLE 9.9
Means and Variances for Water Quality Variables in Problem 9.7

| Station | TN | | BOD | |
|---------|-------------|----------|-------------|----------|
| | Mean (mg/L) | Variance | Mean (mg/L) | Variance |
| 1 | 4.2 | 1.10 | 7.8 | 2.90 |
| 2 | 2.8 | 0.75 | 6.9 | 5.45 |
| 4 | 3.2 | 0.95 | 8.3 | 4.60 |

- 9.9** In the previous problem, determine the amount of herbicide left behind when it reaches the water table at 2.5 m below the soil surface. Assume that the decay constant is 0.018. How long does it take for the herbicide to reach the water table? The crop water use is 0.42 cm/day.

REFERENCES

- Bachand, P.A.M., Roy, S.B., Choperena, J., Cameron, D., and Horwath, W.R. 2014. Implications of using on-farm flood flow capture to recharge groundwater and mitigate flood risks along the Kings River, CA. *Environmental Science & Technology*, 48(23), 13601–13609. <https://doi.org/10.1021/es501115c>.
- Bachand, P.A.M., Horwath, W.R., Roy, S.B., Choperena, J., and Cameron, D. 2011. On-Farm Flood Flow Capture—Addressing Flood Risks and Groundwater Overdraft in the Kings Basin, with Potential Applications throughout the Central Valley. <http://aquaticcommons.org/11289/>.
- Bachand, P.A.M., Roy, S.B., Stern, N., Choperena, J., Cameron, D., and Horwath, W.R. 2016. On-farm flood capture could reduce groundwater overdraft in Kings River Basin. *California Agriculture*, 70(4), 200–207. <https://doi.org/10.3733/ca.2016a0018>.
- Baram, S., Couvreur, V., Harter, T., Read, M., Brown, P.H., Hopmans, J.W., and Smart, D.R. 2016. Assessment of orchard N losses to groundwater with a vadose zone monitoring network. *Agricultural Water Management*, 172, 83–95. <https://doi.org/10.1016/J.AGWAT.2016.04.012>.
- Bogardi, I., Bardossy, A., and Duckstein, L. 1985. Multi-criterion network design using geostatistics. *Water Resources Research*, 21, 199–208.
- Bouwer, H. 2002. Artificial recharge of groundwater: Hydrogeology and engineering. *Hydrogeology Journal*, 10(1), 121–142. <https://doi.org/10.1007/s10040-001-0182-4>.
- California Department of Water Resources. 2015. California's Groundwater Update 2013. Tech. Rep. Update 2013.
- Carroll, R.W.H., Pohll, G., McGraw, D., Garner, C., Knust, A., Boyle, D., Minor, T., Bassett, S., and Pohlmann, K. 2010. Mason Valley Groundwater Model: Linking surface water and groundwater in the Walker River Basin, Nevada. *JAWRA Journal of the American Water Resources Association*, 46(3), 554–573. <https://doi.org/10.1111/j.1752-1688.2010.00434.x>.
- County of San Diego. 2014. *Low Impact Development Handbook: Stormwater Management Strategies*. Department of Public Works, County of San Diego. https://www.sandiegocounty.gov/content/dam/sdc/pds/docs/LID_Handbook_2014.pdf.
- Dahlke, H.E., LaHue, G.T., Mautner, M.R.L., Murphy, N.P., Patterson, N.K., Waterhouse, H., Yang, F., and Foglia, L. 2018. Managed aquifer recharge as a tool to enhance sustainable groundwater management in California: Examples from field and modeling studies, in *Advances in Chemical Pollution, Environmental Management and Protection*, J. Friesen and L. Rodríguez-Sinobas, eds., Academic Press, Elsevier, Cambridge, MA, pp. 215–266.

- Department of Environmental Resources. 2000. *Low-Impact Development: An Integrated Design Approach*. Technical Report Maryland: Prince Georges County.
- Department SFP. 2013. Deir Regional Groundwater Storage and Recovery Project. Technical Report Case No. 2008.1396E. San Francisco Public Utilities Commission.
- Dettinger, M. 2011. Climate change, atmospheric rivers, and floods in California—A multimodel analysis of storm frequency and magnitude changes. *JAWRA Journal of the American Water Resources Association*, 47(3), 514–523. <https://doi.org/10.1111/j.1752-1688.2011.00546.x>.
- Dietz, M.E. and Clausen, J.C. 2005. A field evaluation of rain garden flow and pollutant treatment. *Water, Air, and Soil Pollution*, 167(1–4), 123–138.
- Dietz, M.E. 2007. Low impact development practices: A review of current research and recommendations for future directions. *Water, Air, and Soil Pollution*, 186(1–4), 351–363. <https://doi.org/10.1007/s11270-007-9484-z>.
- Dillon, P., Toze, S., Page, D., Vanderzalm, J., Bekele, E., Sidhu, J., and Rinck-Pfeiffer, S. 2010. Managed aquifer recharge: Rediscovering nature as a leading edge technology. *Water Science and Technology*, 62(10), 2338–2345. <https://doi.org/10.2166/wst.2010.444>.
- Edwards, E.C., Harter, T., Fogg, G.E., Washburn, B., and Hamad, H. 2016. Assessing the effectiveness of drywells as tools for stormwater management and aquifer recharge and their groundwater contamination potential. *Journal of Hydrology*, 539, 539–553. <https://doi.org/10.1016/J.JHYDROL.2016.05.059>.
- Emrich, G.H., Beck, W.W., and Tolman, A.L. 1980. *Top-Sealing to Minimize Leachate Generation: Case Study of the Windham*, Connecticut Landfill, SMC-Martin, King of Prussia, PA.
- Engineers LSC. 2010. Hydrogeologic Setting of the Westside Basin, Technical Report Task 8B Technical Memorandum No. 1. San Francisco Public Utilities Commission.
- Foster, S., van Steenberg, F., Zuleta, J., and Garduo, H. 2010. Conjunctive use of groundwater and surface water. In *GW-Mate, Strategic Overview Series Number 2*, p. 26. <http://documents.worldbank.org/curated/en/874731468315319173/pdf/575560replacem1onjuactive1Use120100.pdf>.
- Gale, I. 2005. Strategies for Managed Aquifer Recharge (MAR) in Semi-Arid Areas. UNESCO IHP, Landais, France. <https://recharge.iah.org/files/2017/01/Gale-Strategies-for-MAR-in-semiarid-areas.pdf>.
- Harmancioglu, N.B. and Alpaslan, N. 1992. Water quality monitoring network design: A problem of multi-objective decision making. *Water Resource Bulletin*, 28(1), 179–192.
- Harmancioglu, N.B., Fistikoglu, O., Ozkul, S.D., Singh, V.P., and Alpaslan, M.N. 1999. *Water Quality Monitoring Network Design*, Kluwer Academic Publishers, Boston, MA.
- Houlihan, M.F. and Lucia, P.C. 1999. *Groundwater Monitoring: The Handbook of Groundwater Engineering*, J.W. Delleur, ed., CRC Press, Boca Raton, FL.
- Hudak, P.F. and Loaiciga, H.A. 1993. An optimization method for monitoring network design in multilayered groundwater flow systems. *Water Resources Research*, 29(8), 2835–2845.
- Huisman, L. and Olsthoorn, T.N. 1983. *Artificial Groundwater Recharge*, Pitman, London, UK.
- Huling, S.G. and Pivetz, B.E. 2006. *In-situ Chemical Oxidation*. Engineering Issue, EPA/600/R-06/072, U.S. Environmental Protection Agency, Office of Research and Development, National Risk Management Research Laboratory, Cincinnati, OH.
- Irmak, S., Odhiambo, L.O., Kranz, W.L., and Eisenhauer, D.E. 2011. DigitalCommons@ University of Nebraska-Lincoln Irrigation Efficiency and Uniformity, and Crop Water Use Efficiency. <https://digitalcommons.unl.edu/biosysengfacpub>.
- ITRC. 2005. *Technical and Regulatory Guidance for In Situ Chemical Oxidation of Contaminated Soil and Groundwater*, 2nd edn. In Situ Chemical Oxidation Team, Interstate Technology & Regulatory Council, Washington, DC.

- Karamouz, M., Kerachian, R., Akhbari, M., and Haafez, B. 2009. Optimal design of river water quality monitoring networks: A case study. *Journal of Environmental Modeling and Assessment*, 14(6), 705–714.
- Knox, R.C., Counter, L.W., Kinconnon, D.F., Stover, E. L., and Ward, C.H. 1986. *Aquifer Restoration: State of the art*, Noyes Publication, Park Ridge, NJ.
- Kocis, T.N. and Dahlke, H.E. 2017. Availability of High-Magnitude Streamflow for Groundwater Banking in the Central Valley, California. *Environmental Research Letters*, 12(8), 084009. <https://doi.org/10.1088/1748-9326/aa7b1b>.
- Kresic, N. 2009. *Groundwater Resources: Sustainability, Management, and Restoration*, McGraw-Hill, New York.
- Kufs, C., Wagner, K., Rogoszewski, P., Kaplan, M., and Repa, E. 1983. Controlling the migration of leachate plumes, in *Ninth Annual Research Symposium*, EPA-600/9-83-018, pp. 87–113.
- Lee, H., Lau, S.-L., Kayhanian, M., and Stenstrom, M.K. 2004. Seasonal first flush phenomenon of urban stormwater discharges. *Water Research*, 38(19), 4153–4163. <https://doi.org/10.1016/J.WATRES.2004.07.012>.
- Leenheer, J.A., Rostad, C.E., Barber, L.B., Schroeder, R.A., Anders, R., and Lee Davisson, M. 2001. Nature and Chlorine Reactivity of Organic Constituents from Reclaimed Water in Groundwater, Los Angeles County, California. <https://doi.org/10.1021/ES001905F>.
- Medellín-Azuara, J., MacEwan, D., Howitt, R.E., Sumner, D.A., Lund, J.R., Scheer, J., Gailey, R. et al. 2016. Economic analysis of the 2016 California drought on agriculture a report for the California department of food and agriculture. https://watershed.ucdavis.edu/files/biblio/DroughtReport_20160812.pdf.
- Murray, E.C. and Tredoux, G. 1998. Artificial Recharge. A Technology for Sustainable Water Resources Development. <http://www.wrc.org.za/wp-content/uploads/mdocs/842-1-98.pdf>.
- Niswonger, R.G., Allander, K.K., and Jeton, A.E. 2014. Collaborative modelling and integrated decision support system analysis of a developed terminal lake basin. *Journal of Hydrology* 517, 521–537. <https://doi.org/10.1016/J.JHYDROL.2014.05.043>.
- Novotny, V. 2003. *Water Quality: Diffuse Pollution and Watershed Management*, John Wiley & Sons, New York.
- O'Geen, A.T., Saal, M., Dahlke, H., Doll, D., Elkins, R., Fulton, A., Fogg, G. et al. 2015. Soil suitability index identifies potential areas for groundwater banking on agricultural lands. *California Agriculture*, 69(2), 75–84. <https://doi.org/10.3733/ca.v069n02p75>.
- O'Leary, D.R., Izbicki, J.A., Moran, J.E., Meeth, T., Nakagawa, B., Metzger, L., Bonds, C., and Singleton, M.J. 2012. Movement of water infiltrated from a recharge basin to wells. *Ground Water* 50(2), 242–55. <https://doi.org/10.1111/j.1745-6584.2011.00838.x>.
- Parker, D.D. 1997. California's water resources and institutions, in *Decentralization and Coordination of Water Resource Management*, pp. 45–54. Springer US, Boston, MA. https://doi.org/10.1007/978-1-4615-6117-0_5.
- Pearlman, L. 1999. Subsurface containment and monitoring systems: Barriers and beyond (Overview Report). U.S. Environmental Protection Agency, Office of Solid Waste and Emergency Response, Technology Innovation Office, Washington, DC.
- Pfeiffer, L. and Cynthia Lin, C.-Y. 2014. Does efficient irrigation technology lead to reduced groundwater extraction? Empirical evidence. *Journal of Environmental Economics and Management*, 67(2), 189–208. <https://doi.org/10.1016/J.JEEM.2013.12.002>.
- Pierce, D.W., Das, T., Cayan, D.R., Maurer, E.P., Miller, N.L., Bao, Y., Kanamitsu, M. et al. 2013. Probabilistic estimates of future changes in California temperature and precipitation using statistical and dynamical downscaling. *Climate Dynamics*, 40(3–4), 839–856. <https://doi.org/10.1007/s00382-012-1337-9>.
- Pyne, R.D.G., 2005. *Aquifer Storage Recovery: A Guide to Groundwater Recharge through Wells*. ASR Systems, Gainesville, FL.

- Quince, J.R. and Gardner, G.L. 1982. Recovery and treatment of contaminated ground water, in *The Second National Symposium on Aquifer Restoration and Ground Water Monitoring*, National water well association, Columbus, OH, pp. 58–68.
- Racz, A.J., Fisher, A.T., Schmidt, C.M., Lockwood, B.S., and Huertos, M.L. 2012. Spatial and temporal infiltration dynamics during managed aquifer recharge. *Groundwater*, 50(4), 562–570. <https://doi.org/10.1111/j.1745-6584.2011.00875.x>.
- Rao, P.S.C. and Davidson, J.M. 1982. Estimation of pesticide retention and transformation parameters required in nonpoint source pollution models, in *Environmental Impact of Nonpoint Source Pollution*. M. R. Overcash and J. M. Davidson eds., Ann Arbor Science, Ann Arbor, MI.
- Salomons, W. and Stol, B. 1995. Soil pollution and its mitigation: Impact of land use changes on soil storage of pollutants, in *Nonpoint Pollution and Urban Stormwater Management*, V. Novotny ed., Technomic Publishing, Lancaster, PA.
- Sanders, T.G., Ward, R.C., Loftis, J.C., Steele, T.D., Ardin, D.D., and Yevjevich, V. 1987. *Design of Networks for Monitoring Water Quality*. Water Resources Publications, Littleton, CO.
- Seager, R., Ting, M., Held, I., Kushnir, Y., Lu, J., Vecchi, G., Huang, H.P. et al. 2007. Model projections of an imminent transition to a more arid climate in southwestern North America. *Science*, 316(5828), 1181–1184. <https://doi.org/10.1126/science.1139601>.
- Shannon, C.E. 1948. A mathematical theory of communication. *Bell System Technical Journal*, 27, 379–423.
- Shannon, C.E. and Weaver, W. 1949. *The Mathematical Theory of Communication*, University of Illinois Press, Urbana, IL.
- Sidhu, J.P.S., Toze, S., Hodgers, L., Barry, K., Page, D., Li, Y. and Dillon, P. 2015. Pathogen decay during managed aquifer recharge at four sites with different geochemical characteristics and recharge water sources. *Journal of Environment Quality*, 44(5), 1402. <https://doi.org/10.2134/jeq2015.03.0118>.
- Smith, M.E. 1983. *Sanitary Landfills, Conference on Reclamation of Difficult Sites*. University of Wisconsin Extension, Madison, WI.
- Stephens, D.B., Miller, M., Moore, S.J., Umstot, T., and Salvato, D.J. 2012. Decentralized groundwater recharge systems using roofwater and stormwater runoff. *JAWRA Journal of the American Water Resources Association*, 48(1), 134–144. <https://doi.org/10.1111/j.1752-1688.2011.00600.x>.
- Testa, S.M. and Wingardner, D.L. 2000. *Restoration of Contaminated Aquifers*, 2nd edn., CRC Press/Lewis Publishers, Boca Raton, FL.
- Tolman, A.L., Ballesteros, A.P., Jr., Beck, W.W. Jr., and Emrich, G.H. 1978. *Guidance Manual for Minimizing Pollution from Waste Disposal Sites*. EPA-600/2-78-142, August, U.S. Environmental Protection Agency, Cincinnati, OH.
- U.S. Environmental Protection Agency. 1979. *Survey of Solidification/Stabilization Technology for Hazardous Industrial Wastes*. EPA-600/2-79-056, U.S. EPA, Cincinnati, OH.
- USACE. 2008. *Engineering and Design: In-situ Air Sparging*. Manual No. 1110-1-4005, Washington, DC. http://140.194.76.129/publications/eng-manuals/em_1110-1-4005/toc.htm
- USEPA. 1996. *Pump-and-Treat Ground-Water Remediation: A Guide for Decision Makers and Practitioners*. EPA/625/R-95/005, Office of Research and Development, U.S. Environmental Protection Agency, Washington, DC.
- USEPA. 1998. *Evaluation of Subsurface Engineered Barriers at Waste Sites*. EPA 542-R-98005, Office of Solid Waste and Emergency Response, U.S. Environmental Protection Agency, Washington, DC.

- USEPA. 2000. *Presenter's Manual for: Superfund Risk Assessment and How You Can Help: A 40-Minute Videotape*. EPA/540/R-99/013, Office of Solid Waste and Emergency Response, U.S. Environmental Protection Agency, Washington, DC.
- USEPA. 2004. *In Situ Thermal Treatment of Chlorinated Solvent; Fundamentals and Field Applications*, EPA. 542/R-04/010 Office of Solid Waste and Mergency Response, U.S. Environmental Protection Agency, Washington, DC.
- USEPA. 2007. *Treatment Technologies for Site Cleanup: Annual Status Report*, 12th edn. EPA-542-R-07-012, U.S. Environmental Protection Agency, Office of Solid Waste and Emergency Response, Washington, DC.
- Ward, R.C., Loftis, J.C., Nielsen, K.S., and Anderson, R.D. 1979. Statistical evaluation of sampling frequencies in monitoring networks. *Journal Water Pollution Control Federation*, 51, 2292–2300.
- Wilkin, R.T. and Puls, R.W. 2003. Capstone report on the application, monitoring, and performance of permeable reactive barriers for groundwater remediation: Volume 1-performance evaluation at two sites. EPA/600/R-03/045a. U.S. Environmental Protection Agency, Washington, DC.
- Wilson, L.S. 1983. Monitoring in the vadose zone: Part III. *Groundwater Monitoring Review*, 3(1), 155–166.



Taylor & Francis

Taylor & Francis Group

<http://taylorandfrancis.com>

10 Groundwater Risk and Disaster Management

10.1 INTRODUCTION

Water is a renewable natural resource that cleanses and redistributes itself through natural cycles. However, its global quantity is finite. Increasing demands for water, the fact that there is no substitute for this essential resource, and decreasing water availability due to overuse, pollution, and inefficient water management lead to worldwide water disaster.

Besides the increasing demand for water, water shortages, water pollution, flood disasters, and aging water infrastructures are becoming more serious. Therefore, the need for disaster planning and management is growing fast. These problems are especially more significant in developing countries. The developed societies are also becoming more vulnerable since they are highly dependent on water. The rapid expansion of water sectors and inadequate institutional and infrastructural setups are worsening these problems.

Water-related problems grew significantly in the 1980s due to rapid urban and industrial growth. More concerns about water-related problems were created in the 1990s that grabbed the attention of researchers to global issues. Efforts by governments and international organizations have resulted in action plans being put into practice to remedy the problems. In this maze of complexity, groundwater is a target for both threats and hazards aimed at more widespread vulnerabilities, but it is more stable when the region is facing contained and noninvasive threats. Surface water resources and storage facilities have more vulnerability to direct structural threats.

In the previous chapters, water-related problems due to human activities and the strategies to decrease the negative influences of these activities on water resources were discussed. However, it should be noted that natural causes are the source of many disasters. The problem is more devastating in developing countries, where the social infrastructure is not sufficient. Devastating floods, droughts, and hurricanes have always caused regional disasters. Nonetheless, the complexity of societies and urban settings as well as means of transportation and communication have caused greater vulnerability for water disaster. Climate change also intensifies flood and drought impacts all around the world with adverse effect on water resources, supplies, and public water services and utilities.

In this chapter, risk as an overlay of hazard and vulnerability is discussed. Disasters are described as the realization of risk. Both natural and man-made hazards and vulnerabilities are changing as well as our adaptive capacity due to climate change and our more interconnected complex world. These are presented in this context in the following sections and in [Chapter 11](#).

10.2 GROUNDWATER RISK ASSESSMENT

Risk assessment includes a wide variety of disciplines and the perspectives of engineers, hydrogeologists, environmental scientists, chemists, microbiologists, geologists, geographers, and public administrators. Furthermore, it includes the impact of groundwater pollution on human health. Some elements of risk analysis and assessment are briefly discussed in this section.

10.2.1 ELEMENTS OF RISK ASSESSMENT

There are two basic elements associated with risk assessment. These elements are risk quantification or estimation and risk evaluation (Lee and Nair, 1979). In risk quantification, the hazard is defined, and the initiating events that would cause the hazard are identified. Furthermore, the response and consequences to the receptor system are evaluated and probabilities of occurrence are determined.

[Figure 10.1](#) shows hypothetically the extent of probable hazards and vulnerabilities. Risk is the overlay and intersection of the two sets. Other components such as social and climate sensitivities can form another layer that should be considered for an assessment of risk. The adaptive capacity of a system such as a groundwater supply system or the entire aquifer to face different threats and hazards is directly related to the measures that can be taken to reduce future vulnerabilities. [Figure 10.2](#) shows the need to consider the impact of social and climate change in assessing future vulnerabilities.

Risk assessment can be used as a tool in evaluating the potential impacts on public health of hazardous materials in remote or disposal facilities. See Masters and Ela (2008) for more details. As an example, McTernan and Kaplan (1990) assessed the potential impacts of a hypothetical release from a landfill/disposal site to groundwater and its subsequent impact on public health. In evaluating the potential exposure of contaminations to groundwater, it is important to define the characteristics of the aquifer and the extent of physical space and chemical content to be evaluated. The U.S. Environmental Protection Agency's (EPA) groundwater strategy (USEPA, 1986) sets the guideline for assessing the risks associated with potential water supplies.

The National Research Council (1983), when dealing with health hazards, divided risk assessment into the following four steps: hazard identification, dose-response assessment, exposure assessment, and risk characterization. Risk assessment process steps are shown in [Figure 10.3](#).

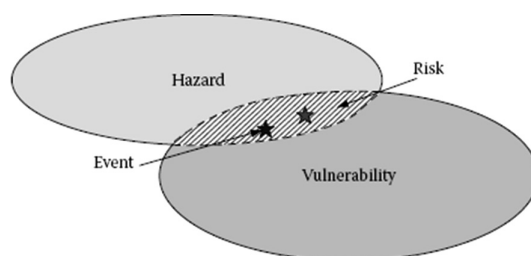


FIGURE 10.1 Risk as an overlay of hazard and vulnerability.

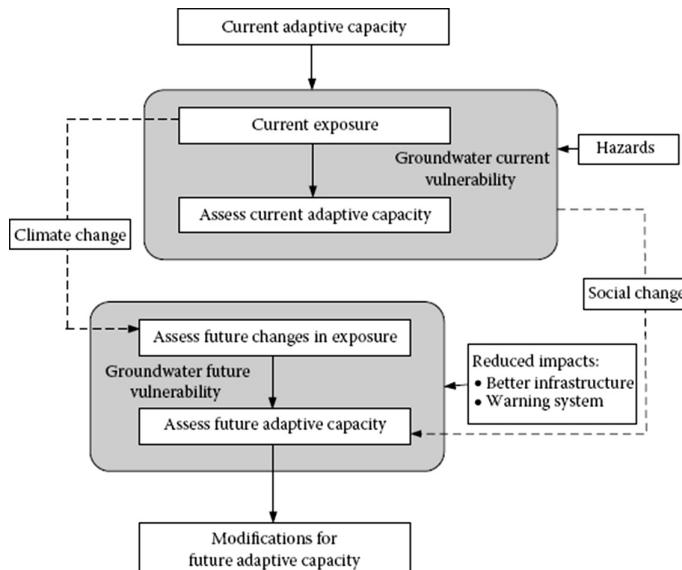


FIGURE 10.2 Main steps in groundwater vulnerability and the adaptive capacity and action approach.

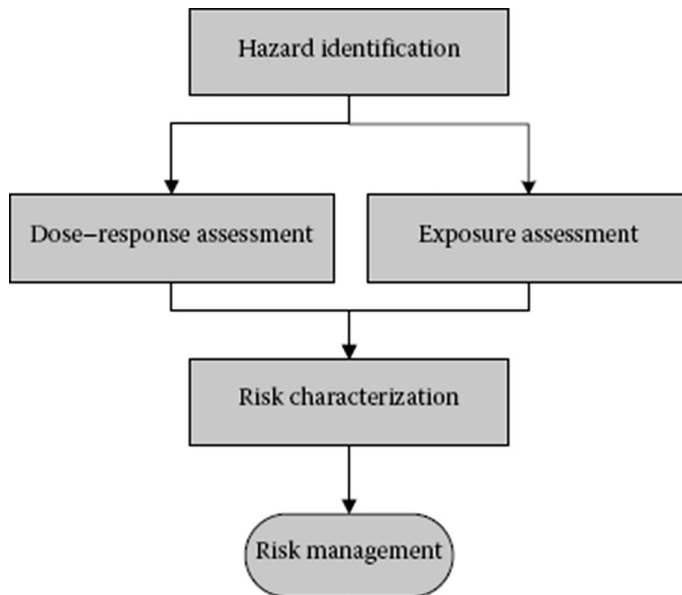


FIGURE 10.3 Risk assessment process steps. (From Masters, G.M. and Ela, W.R., *Introduction to Environmental Engineering and Science*, Prentice Hall, Simon and Schuster, Englewood Cliffs, NJ, 576 p, 2008.)

- *Hazard identification* determines the linkage between a particular chemical to particular health effects, such as cancer or birth defects. As the availability of human data is so often scarce, this step focuses on the toxicity of a chemical in animals or other test organisms.
- *Dose-response assessment* describes the relationship between the dose of an administered or received agent and the occurrence of an adverse health effect. Some conditions such as the response characteristics of being carcinogenic or not and the experimental condition of being a one-time acute test or a long-term chronic test lead to a diversity of response relationships for any given agent. In this assessment, a method of extrapolating animal data to humans is included.
- *Exposure assessment* determines the size of the population exposed to the toxicant under consideration, the duration of the exposure, and the concentration of the toxicant. Factors such as the age and health of the subjected population, the likelihood that members of the population might be pregnant, and whether or not synergistic effects might occur due to exposure to multiple toxicants should be considered.
- *Risk characterization* contains the preceding three steps that estimate the magnitude of the public-health problem. In this step, the data collected in the previous steps are combined to generate a statement of risk. The final statement of risk can be qualitative or quantitative.

One of the most controversial and sensitive issues dealing with groundwater contamination is the hazard of gradual exposure to the fumes and vapors released through the unsaturated zone. Volatile hydrocarbons have a tendency to evaporate from the surface of a water table. In many industrial zones or landfills converted to residential areas, occupants have experienced health hazards, some with carcinogenic potential. As a result of gradual exposure, some people have developed reproductive damage, neurological, and/or birth defects. Due to these problems, the development of risk assessment criteria has been launched by the USEPA. Risk assessment is a process to measure and estimate the probable adverse effects of past, existing, and/or future hazards to human and ecological entities.

Another aspect of the risk could entail the hazard of the intentional contamination of a well or a well fluid system. Even though the hazard of groundwater contamination by terrorist acts could be low compared to surface water, the vulnerability could be higher due to the invisible notation of groundwater and the widespread movement of the contaminants. It is a much slower process, but, once contaminated, it will be very difficult to capture, monitor, and remediate the long lasting effects.

10.2.2 ASSESSMENT OF DOSE-RESPONSE

In dose-response assessment, a mathematical relationship between the toxic materials that humans are subject to and the risk of an unhealthy response to that dose is obtained. In dose-response curves, the severe toxicity amount is measured in milligrams per kilogram of body weight. These curves are obtained due to the chronic toxicity that explains the organism's prolonged exposure over a substantial fraction

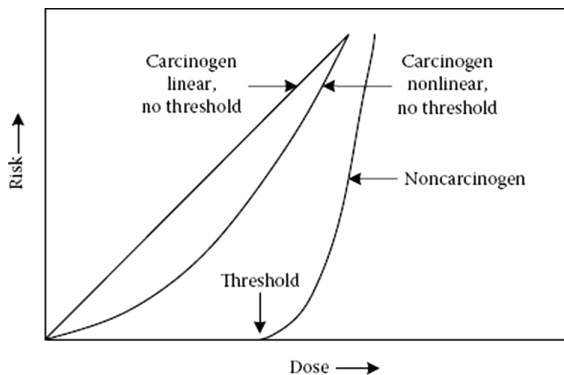


FIGURE 10.4 Hypothetical dose-response curves.

of its life. The horizontal axis in these curves is a dose with the unit of the average milligrams of content per kilogram of body weight per day (mg/kg-day). The average exposure of a dose is over a whole lifetime. For instance, the human exposure time could be 70 years, the life expectancy period. The vertical axis is the response (risk) that is the probability of the occurrence of adverse health effects.

For a carcinogenic response, there is always a routine practice to assume that exposure to any amount of the carcinogen will cause the probable occurrence of cancer. For noncarcinogenic responses, a threshold dose is assumed below which there will be no response. From these two assumptions, and as is shown in Figure 10.4, it can be concluded that the application of the dose-response curves and the methods for carcinogenic and noncarcinogenic effects are different. Dose-response curves for carcinogens are assumed to have no threshold; that is, any exposure produces some chance of causing cancer. It should be noted that the same chemical may cause both kinds of response.

A scaling factor is presented through which the dose-response data obtained from animal bioassays can be extrapolated for humans as well. Sometimes, if the dose amounts for human and animal per unit of body weight are the same, the scaling factor will be assumed equal. The resulting human dose-response curve is described by the standard mg/kg-day units for dose. Also, for differences in the rates of chemical absorption, animal and human responses have to be adjusted. In most cases, due to insufficient data, the absorption rate is assumed to be same.

10.2.3 RISK ASSESSMENT METHODS AND TOOLS

The method of extrapolating from the high doses to the low doses is the most debatable aspect of dose-response curves for carcinogens. The high doses are implemented to test animals, and, for human exposure, the low dose is considered.

To extrapolate the low doses, different mathematical models have been proposed, but it is not possible to test the accuracy of these models because no model can be validated without actual data on humans. Then, the model selection is strictly

a policy decision. The one-hit model is a commonly used model that expresses the relationship between the dose (d) and the lifetime risk (probability) of cancer, $P(d)$ (Crump, 1984).

$$P(d) = 1 - e^{-(q_0 + q_1 d)} \quad (10.1)$$

where q_0 and q_1 are parameters picked to fit the data. This model is based on the assumption that a single chemical exposure (hit) could produce a cancer tumor.

By substituting $d = 0$ into Equation 10.1 and using the following mathematical expansion for an exponential,

$$e^x = 1 + x + \frac{x^2}{2!} + \dots + \frac{x^n}{n!} \cong 1 + x \quad (\text{for small } x) \quad (10.2)$$

P can be obtained assuming that the background cancer causing rate is small:

$$P(0) = 1 - e^{q_0} \cong 1 - [1 + (-q_0)] = q_0 \quad (10.3)$$

Using the exponential expansion again, the lifetime probability of cancer for small dose rates can be expressed as:

$$P(d) \cong 1 - [1 - (q_0 + q_1 d)] = q_0 + q_1 d = P(0) + q_1 d \quad (10.4)$$

For low doses, the added risk of cancer is:

$$\text{Added risk} = A(d) = P(d) - P(0) = q_1 d \quad (10.5)$$

In order to protect public health, the EPA chooses a modified multistage model. It is a linearized model at low doses with the constant of proportionality picked to result in 95% probability of overestimating the risk. See Masters and Ela (2008) for more details.

10.2.3.1 Potency Factor for Cancer-Causing Substances

To study chronic toxicity, a low dose is implemented over a primary part of one's lifetime. At low doses, where the dose-response curve is linear, the curve slope is referred to as the potency factor (PF):

$$PF = \frac{Risk}{CDI} \quad (10.6)$$

where:

Risk is the incremental lifetime risk

CDI is the average milligrams of toxicant absorbed per kilogram of body weight per day in mg/kg-day.

Risk is expressed as a probability and has no units; therefore, the potency factor unit is the inverse of the CDI unit.

By knowing the chronic daily intake (CDI) (based on exposure data), PF (from [Table 10.1](#)), the lifetime, the incremental cancer risk can be found as follows:

$$\text{Risk} = \text{CDI} \times \text{PF} \quad (10.7)$$

According to the USEPA, this value should be less than 10^{-6} or one person in a million. The potency factors in Equation 10.7 are obtained from an EPA database on toxic substances referred to as the Integrated Risk Information System. A short list of the PF for some of these chemicals (for both oral and inhalation exposure) is shown in [Table 10.1](#).

TABLE 10.1
Toxicity Data for Selected Potential Carcinogens

| Chemical | Category | Potency Factor Oral Route (mg/kg-day) ⁻¹ | Potency Factor Inhalation Route (mg/kg-day) ⁻¹ |
|-----------------------------------|----------|--|--|
| Arsenic | A | 1.75 | 50 |
| Benzene | A | 2.9×10^{-2} | 2.9×10^{-2} |
| Benzol(a)pyrene | B2 | 11.5 | 6.11 |
| Cadmium | B1 | — | 6.1 |
| Carbon tetrachloride | B2 | 0.13 | — |
| Chloroform | B2 | 6.1×10^{-3} | 8.1×10^{-2} |
| Chromium VI | A | — | 41 |
| DDT | B2 | 0.34 | — |
| 1,1-Dichloroethylene | C | 0.58 | 1.16 |
| Dieldrin | B2 | 30 | — |
| Heptachlor | B2 | 3.4 | — |
| Hexachloroethane | C | 1.4×10^{-2} | — |
| Methylene chloride | B2 | 7.5×10^{-3} | 1.4×10^{-2} |
| Nickel and compounds | A | — | 1.19 |
| Polychlorinated biphenyls (PCBs) | B2 | 7.7 | — |
| 2,3,7,8-TCDD (dioxin) | B2 | 1.56×10^5 | — |
| Tetrachloroethylene | B2 | 5.1×10^{-2} | $1.0-3.3 \times 10^{-3}$ |
| 1,1,1-Trichloroethane (1,1,1-TCA) | D | — | — |
| Trichloroethylene (TCE) | B2 | 1.1×10^{-2} | 1.3×10^{-2} |
| Vinyl chloride | A | 2.3 | 0.295 |

To calculate the CDI, the following expression is used:

$$\text{CDI}(\text{mg/kg-day}) = \frac{\text{ADD}}{W} \quad (10.8)$$

where:

ADD is the average daily dose in (mg/day) over an assumed 70 year lifetime

W is the body weight in kg.

Example 10.1

An underground storage tank has been leaking benzene to the groundwater of a city that only makes basic treatment. A 70 kg person is exposed in different ways including drinking 1.8 L of water with a benzene concentration of 0.007 mg/L every day for 7 years. Assume the standard 70 year lifetime. Find the upper-bound cancer risk for this individual.

SOLUTION

From [Table 10.1](#), we see that benzene is a probable human carcinogen with a potency factor of $2.9 \times 10^{-2} (\text{mg/kg-day})^{-1}$ for both oral and inhalation exposure. Using Equation 10.8, the chronic daily intake is:

$$\begin{aligned} \text{CDI}(\text{mg/kg-day}) &= \frac{\text{ADD}}{W} \\ &= \frac{0.007 \text{ mg/L} \times 1.8 \text{ L/day} \times 7 \text{ year}}{70 \text{ kg} \times 70 \text{ year}} = 0.000018 \text{ mg/kg-day} \end{aligned}$$

Using Equation 10.7, the incremental lifetime cancer risk is:

$$\text{Risk} = \text{CDI} \times \text{PF}$$

$$= 0.000018 \text{ mg/kg-day} \times 2.9 \times 10^{-2} (\text{mg/kg-day})^{-1} = 0.52 \times 10^{-6}$$

So, over a 70 year period, the upper-bound estimate of the probability that a person will be affected by adverse health from this drinking water is about 0.52 in 1 million, which is less than the EPA acceptable limit of 10^{-6} .

An event tree is another tool that provides a structure for risk quantification. Event trees provide a structured approach for risk quantification, as shown in [Figure 10.5](#). In this figure, assume that the initiating event is the placement of hazardous materials at a site with two liners. Systems 1 and 2 represent the primary (top) liner and the secondary (bottom) liner, respectively. If system 1 fails and system 2 works, there is no damage. But, if both systems fail, there is the possible release of the hazardous materials to the subsurface environment. [Figure 10.5](#) shows how the probabilities of each branch of the event tree can be calculated.

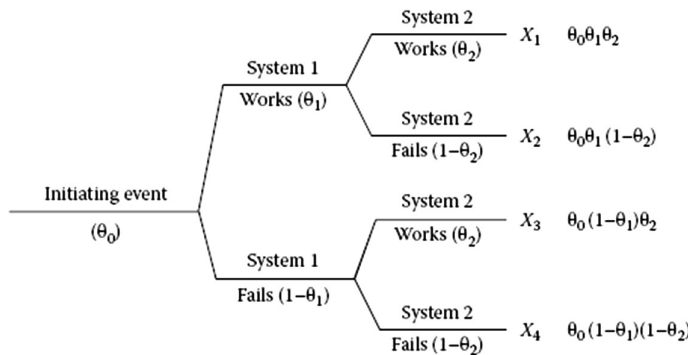


FIGURE 10.5 Risk quantification using an event tree. (From Lee, W. W. and Nair, K., Risk quantification and risk evaluation, in *Proceedings of National Conference on Hazardous Material Risk Assessment, Disposal and Management*, Information Transfer, Silver Spring, MD, pp. 44–48, 1979.)

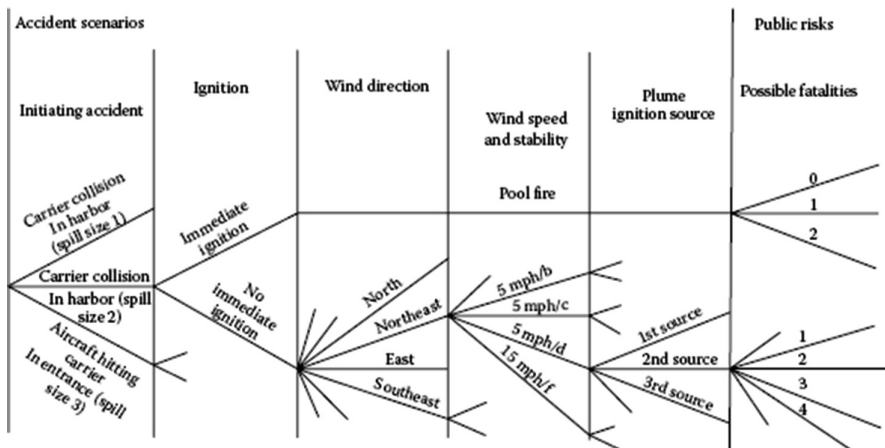


FIGURE 10.6 Event tree analysis of liquified natural gas spills. (From Lee, W. W. and Nair, K., Risk quantification and risk evaluation, in *Proceedings of National Conference on Hazardous Material Risk Assessment, Disposal and Management*, Information Transfer, Silver Spring, MD, pp 44–48, 1979.)

Figure 10.6 shows an actual event tree provided by Lee and Nair (1979) for a risk assessment of liquified natural gas spills in a coastal harbor. Decision trees can also be developed as a part of a risk quantification process.

In risk evaluation, socially acceptable risks are determined. One approach for risk evaluation is to compare the quantified risk with various possible existing risks in everyday life. This evaluation approach is called the “revealed societal preferences” approach. Risk evaluation is a difficult and controversial task in risk assessment.

10.2.4 ENVIRONMENTAL RISK ANALYSIS

There are four major approaches suggested by Conway (1982) for environmental risk analysis. These approaches are:

1. The stochastic/statistical approach: In this approach, large amounts of data are obtained under a variety of conditions. Then, the correlations between the input of a certain material and its observed concentrations and effects are determined in various environmental compartments.
2. The model ecosystem approach: In this approach, which is also called the “microcosm” approach, a physical model of a given environmental situation is constructed. A chemical is then applied to the model. The fate and effects of the chemical are observed through the model.
3. The “deterministic” approach: A simple mathematical model is used in this approach to describe the rates of individual transformations and the transport of the chemical in the environment. [Figure 10.7](#) depicts a sample of this approach.
4. The “baseline chemical” approach: In this approach, transformations, transports, and effects are measured as in the deterministic approach. Then, the results are compared with data on chemicals of known degrees of risk.

Cornaby et al. (1982) suggested an approach for the risk analysis of environmental pathways from a waste site, like the one depicted in [Figure 10.8](#). This approach integrates human and ecological aspects of environmental concerns. [Figure 10.9](#) shows the overall steps in this approach.

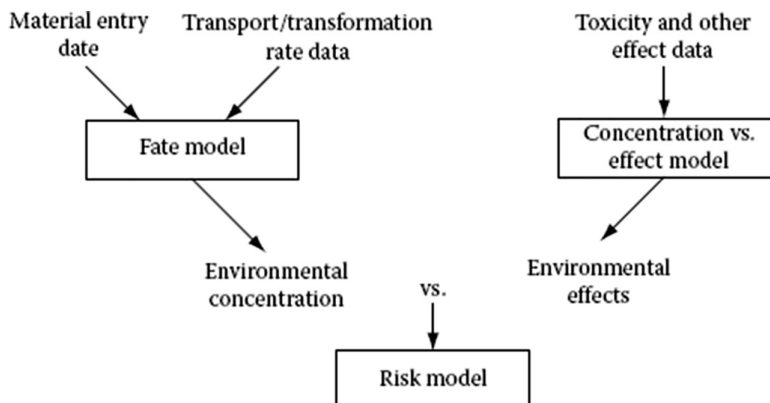


FIGURE 10.7 Sample of the deterministic approach to environmental risk analysis. (From Conway, R.A., Introduction to environmental risk analysis, [Chapter 1](#), in *Environmental Risk Analysis for Chemicals*, R.A. Conway, ed., Van Nostrand Reinhold Company, New York, pp. 1–30, 1982.)

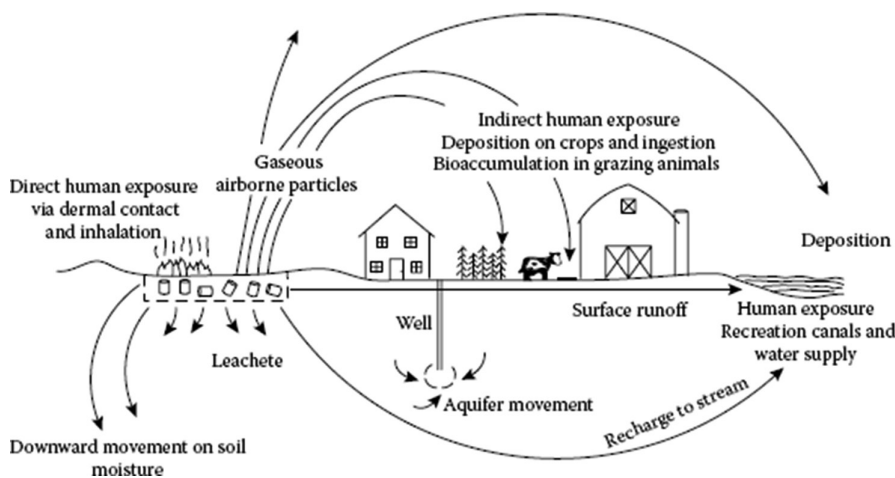


FIGURE 10.8 Environmental pathways from a waste site. (From Schweitzer, G. E., Risk assessment near uncontrolled hazardous waste sites: Role of monitoring data, in *Proceedings of the National Conference on Management of Uncontrolled Hazardous Waste Sites*, Hazardous Materials Control Research Institute, Silver Spring, MD, pp. 238–247, 1981.)

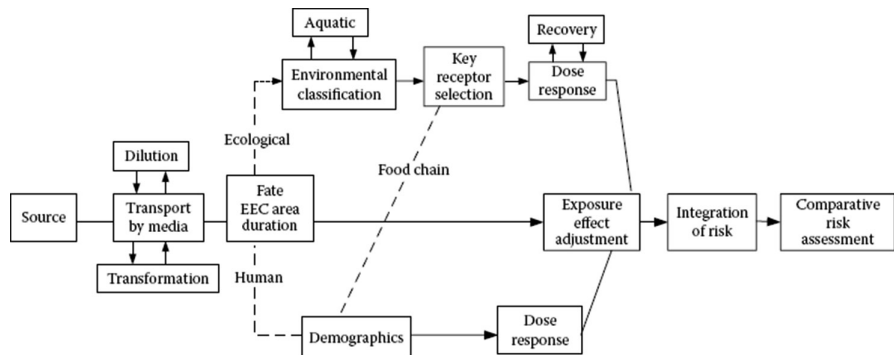


FIGURE 10.9 Overall environmental risk assessment scheme. (From Cornaby, B. W. et al., Application of environmental risk techniques to uncontrolled hazardous waste sites, in *Proceedings of the National Conference on Management of Uncontrolled Hazardous Waste Sites*, Hazardous Materials Control Research Institute, Silver Spring, MD, pp. 380–384, 1982.)

10.3 GROUNDWATER RISK MANAGEMENT

A set of policies, procedures, and practices applied to minimize disaster risks at all levels and locations is called risk management. The aim of risk management is to increase awareness, assessment, analysis, evaluation, and management measures. The framework of risk management includes legal provisions defining the

responsibilities for disaster damage and long-term social impacts and losses (Sine, 2004a). In risk management, administrative decisions, technical measures, and the participation of the public should protect water-supply and sanitation facilities from natural disasters. The following actions are required to be performed for risk assessment and disaster formulation (Sine, 2004b):

- Risk awareness and assessment including hazard analysis and vulnerability/capacity analysis
- Knowledge development (education, training, research, and information)
- Institutional frameworks (organizational, policy, legislation, and community action)
- Application of measures such as environmental management, land use and urban planning, protection of critical facilities, application of science and technology, partnership and networking, and financial instruments
- Using early warning systems including forecasting, public notification of warnings, and preparation measures.

In other words, risk management includes preventive, organizational, and technical activities with the aim of preparing the society for disasters and decreasing their consequences. Jeggle (2005) stated, “The most important aspects of effective disaster management are precisely those activities that are undertaken and pursued at the times when there is no disaster.”

When planning the location and construction of wells, some hydrological data are needed. These data include water level, stream discharge, recurrence of floods, extent of the flooded area, and the morphology of the flood plain. This is especially important when deciding about urban planning in flood plains. The water management authorities should know in advance the measures that are required to be applied for protecting the wells and springs in case of floods or other disasters. In addition, it is important to inform the administration authorities, civil defense, fire brigades, and volunteer organizations (Red Cross and Red Crescent) in time about an expected flood. Then they can coordinate their activities and inform and protect the population.

In case of a disaster, newer wells in low vulnerable aquifers should be proposed, drilled, and tested to serve as emergency water resources, and the public should be aware of the location of the emergency drinking water resources. If emergency water resources are not available, a system of water supply by mobile cisterns can be established, and drinking water can be distributed by vehicles.

In general, in groundwater risk management, the preventive control and protection of drinking water supplies and the relevant technical devices (e.g., pumping stations) are taken into account with the aim of reducing the impact of disasters on the water supply and distribution systems as much as possible.

10.3.1 GROUNDWATER RISK MITIGATION

Risk mitigation can be structural and nonstructural measures used to limit the adverse impacts of natural and technological hazards as well as environmental degradation (Sine, 2004b). These measures include:

- Switch off polluted wells to avoid infectious diseases
- Activate emergency water resources, such as deep wells, springs, etc.
- Provide water in mobile tanks in case of no local emergency water resources
- Make people aware of the location of emergency water resources
- Ration water in case of water scarcity threats
- Take immediate actions for the restoration of the affected water supply systems after the hazard.

10.4 GROUNDWATER DISASTER

Disaster is the realization of the risk. Groundwater is less vulnerable to short-term natural disasters such as floods, but it is more vulnerable toward long-term man-induced disasters such as overexploitation, gradual drawdown, and widespread contamination. Many regional problems are the direct result of regional climates, geography, and hydrology. Others are as a result of human activities and mismanagement. Traditionally, natural water disasters are referred to as droughts and floods. A drought is the deficit of water that is required to meet basic demands. A drought also causes inadequate recharge of groundwater. Water supplies in urban areas are frailler during drought events because of limited storage facilities and high water demand variability. Floods are the result of excess runoff.

Besides the quantity of water, its quality could also be the cause of a water disaster. The contamination of water mains and water supply reservoirs by accidental or intentional acts in both developed and developing countries has been taken into consideration by many investigators, which has created a new awareness about water security among public and private agencies dealing with water.

10.4.1 REQUIREMENTS FOR INSTITUTIONAL AND TECHNICAL CAPACITIES

For developing and implementing disaster mitigation and management plans, all the dimensions of a country's institutional and technical capacity building, and whether such capacities are applied in a consistent manner need to be considered. To effectively address disaster prevention, preparedness, emergency response, recovery and mitigation, and national and local institutional and technical capacity building are required.

Institutional capacity building includes governmental authorities, the legal framework, control mechanisms, the availability of human resources and public participation, awareness, and education. Generally, institutional capacity building has the following aspects:

- Governmental authorities are responsible for the coordination of water governance activities, the implementation of water risk management, and disaster mitigation plans. The coordination is carried out among policy and decision-makers, civil society institutions, water managers and stakeholders, the scientific community, and the general public. Multi-sectorial national disaster risk mitigation mechanisms have been effective approaches implemented by many countries for disaster reduction and the management of post-disaster rescue activities (Vrba, 2006).

- In disaster management, a legal framework and regulatory status are required to be established to support disaster reduction. This framework is considered the implementation of effective environmental and water protection management and policy. Preventive protection measures of water resources like water supply protection zones and the operation of early warning monitoring systems, as well as the public right to information can also be included within this framework.
- Control mechanisms are also required to be established by environmental and water governmental authorities for the protection of water resources against natural and man-made hazards. These mechanisms such as monitoring and warning systems, provide data on natural and anthropogenic hazards.
- Some other important disaster mitigation policies involve public participation, information, and education, which are very effective in the prevention and mitigation of natural and man-induced impacts on water resources.
- Groundwater systems analysis, the identification of potential and existing pollution sources and natural hazards, the establishment of early warning monitoring systems, and, in general, technical and scientific capacity building, which need interdisciplinary research and the transfer of knowledge and expertise.

10.4.2 PREVENTION AND MITIGATION OF NATURAL AND MAN-INDUCED DISASTERS

There are five phases in a disaster event. These phases include anticipatory, warning, impact, relief, and rehabilitation (Dooge, 2004). Within each phase of disaster prevention and mitigation, the following activities related to public and domestic drinking water supplies can be implemented:

Anticipatory phase: Identification and assessment of the potential risk and vulnerability of existing public and domestic water supply systems, as well as the identification, investigation, delineation, and evaluation of the groundwater resources resistant to natural hazards.

The warning phase: The activities of this phase are strongly related to the activities in the previous phase. The main activities of the warning phase are the establishment and operation of early warning monitoring systems, geological monitoring systems, and integrated hydro-climatological monitoring systems. The important elements of the warning phase are the formulation of suitable indicators of disaster risk and vulnerability as well as relevant groundwater indicators.

The impact and relief phases: These phases focus on rescue efforts during and after disasters, as well as on immediate external help. These efforts include the distribution of drinking water, which requires identification, development, and setting aside rescue activities for the immediate emergency. In many regions affected by natural disasters, water supplies depend on the transport of water by tankers from somewhere outside of the area or on the import of bottled water.

The rehabilitation phase: This is a long-term phase and involves the reconstruction of the water supply systems and the water distribution infrastructure, the remediation of polluted water, and the intensive pumping of existing deep wells or developing deeper aquifers of low vulnerability in areas with known properties. Other effective activities are well cleaning, rehabilitation of both well and pumping mechanisms and well dewatering and disinfection, and well deepening (in case of a drought). Post-evaluation of all phases of the rescue process, the preparation of plans for rehabilitation, including water management plans, and an assessment of emergency costs can help the situation.

10.4.3 DISASTER MANAGEMENT PHASES

Disaster management includes all activities, programs, and measures that can be attended to before, during, and after a disaster with the main purposes of avoiding a disaster, reducing its impacts, and recovering from its losses. There are three phases in disaster management as shown in Figure 10.10:

1. *Before a disaster (pre-disaster):* Initiatives are taken to reduce human and property losses caused by a potential disaster. For example, conducting awareness campaigns, strengthening the existing weak structures,

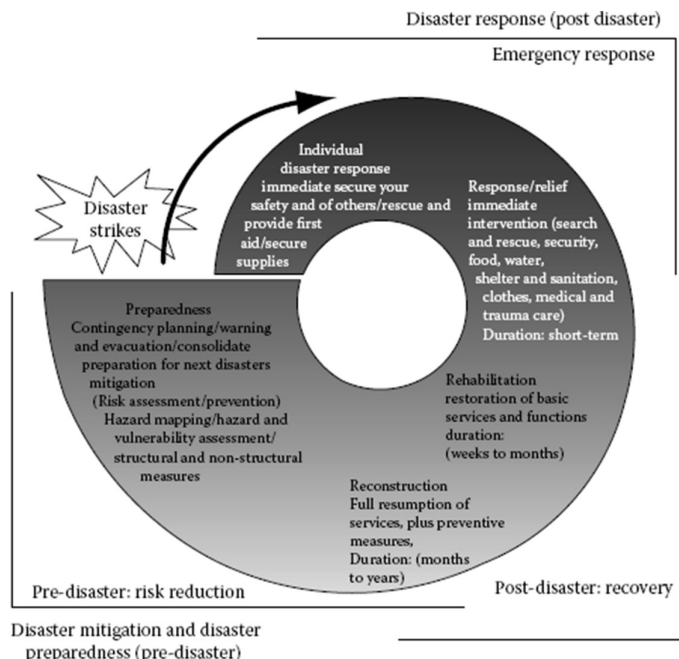


FIGURE 10.10 Disaster mitigation, preparedness, response, and recovery. (From Toshimaru, N., Are you prepared? Learning from the Great Hanshin-Awaji earthquake disaster, *Handbook for Disaster Reduction and Volunteer Activities*, Hyogo University, Kokogawa, Hyogo, Japan 1998.)

providing disaster management plans at the household and community level, etc. These risk reduction measures are called “mitigation and preparedness activities.”

2. *During a disaster (disaster occurrence):* Activities are undertaken to ensure that the needs of victims are met and the impacts are minimized. Activities in this stage are called “emergency response activities.”
3. *After a disaster (post-disaster):* Activities are immediately undertaken right after a disaster for the recovery and rehabilitation of affected communities. These activities are termed as “response and recovery activities.”

10.5 DISASTER INDICES

Indicators of the water supply security can be used to measure the relative level of water disaster. The most common indicators are reliability, resiliency, and vulnerability. A weighted combination of the reliability of supply and resources, the resiliency of the system to return to a satisfactory state of operation, and the vulnerability of the system to a high impact on the available safe water supply determine the state of the systems’ readiness for a disaster (Karamouz et al., 2010).

Therefore, relative levels of disaster can be quantified by disaster indices. These criteria can be economic, environmental, ecological, and social. There are different ways to define these indicators. For this purpose, the overall set of criteria is first identified. Then the range of satisfactory values is specified for each indicator. These decisions for identifying the set of criteria and the ranges are subjective and based on human judgments or social goals, not scientific theories. Most criteria are not predefined. However, for many criteria, the duration and magnitude of individual or cumulative failures are important.

10.5.1 RELIABILITY

System performance indices identify optimal situations. If the performance of a system is undesired, the condition is called failure. For example, if a system cannot deliver water with the desired pressure and the demanded quantity and quality, the condition is considered as a failure. To assess the performance of a system, the mean and standard deviation of the outputs of the system are evaluated. However, it is not sufficient. [Figure 10.11](#) shows two systems with totally different performances that have the same mean and standard deviation. There are two failure events in [Figure 10.11b](#), but there is no failure situation in [Figure 10.11a](#). Therefore, the probability, severity, and frequency of a system failure cannot be defined by only mean and standard deviation indices.

To evaluate the probability of failure and system performance, reliability is one of the reasonable indices that can be used. In determining the reliability of a system, the random variable of X_t is the system’s output. The output can be a failure output or a success output. The probability that X_t belongs to the success output group is the reliability of the system (Hashimoto et al., 1982). The reliability of a system is calculated as:

$$\alpha = \text{Prob}[X_t \in S] \forall t \quad (10.9)$$

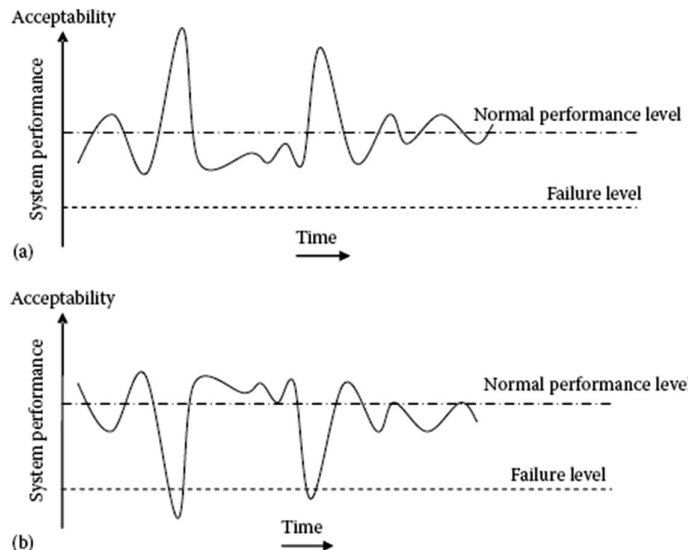


FIGURE 10.11 Comparison of two different functions (a and b) with the same mean and standard deviation. (From Hashimoto, T. et al., *J. Water Resour. Res.*, 18, 14, 1982.)

where S is the set of all satisfactory outputs. Therefore, reliability is the opposite of risk, which is the probability of a system failure. However, reliability is conceptually related to the probability of a system failure. There are several different ways to measure reliability. These ways depend on the needs and relevance of a particular situation. For instance, the expected length of time between consecutive failures may be characterized, such as a 100 year flood event, an event that is expected to occur on average once in 100 years. Reliability can also be considered in qualitative rather than quantitative terms. Therefore, there is no one definition and a measurement approach is applicable in all aspects of influence and applications.

Reliability depends on the complexity of interactions between water-related rights, regulations, laws, and rules. Hence, in order to define water supply reliability, these interactions need to be specified.

For reliability estimation, two different methods can be used.

1. Statistical analysis of recorded data of failures of similar systems
2. Indirect analysis by combination of significant parameter impacts on reliability.

In the reliability theory, lifetime (the time between two successive system failures) is usually modeled by the Weibull distribution. The cumulative probability function of the system failures is:

$$F(t) = 1 - e^{-\alpha t^\beta}, \quad (t > 0) \quad (10.10)$$

where $\alpha, \beta > 0$ are parameters of the distribution that must be estimated. Another definition of reliability is the probability that no failure will occur within the planning horizon (Karamouz et al., 2003). This can be formulated as:

$$R(t) = 1 - F(t) = e^{-\alpha t^\beta} \quad (10.11)$$

The density function of the time of failure occurrences is obtained by a simple differentiation of Equation 10.10:

$$f(t) = \alpha \beta t^{\beta-1} e^{-\alpha t^\beta}, (t > 0) \quad (10.12)$$

It should be noted that in the special case of $\beta = 1$, $f(t) = \alpha e^{-\alpha t}$, which is the density function of the exponential distribution. Because of the forgetfulness property of the exponential distribution, this distribution is rarely used in reliability studies. If X is a exponential variable indicating the time when the system fails, then for all $t, \tau > 0$:

$$P(X > t + \tau | X > \tau) = P(X > t) \quad (10.13)$$

This equation illustrates that the probability of the working condition in any time length t is independent of the time length that the system has been working. Equation 10.13 can be rewritten as:

$$P(X > t + \tau | X > \tau) = \frac{P(X > t + \tau)}{P(X > \tau)} = \frac{R(t + \tau)}{R(\tau)} = \frac{e^{-\alpha(t+\tau)}}{e^{-\alpha\tau}} = e^{-\alpha\tau} = R(t) = P(X > t) \quad (10.14)$$

In most practical cases, the breakdown probability increases by the aging of the system. Hence, the exponential variable is inappropriate in such cases.

In case of a failure, the hazard rate can be computed as the ratio of the density function of time between failure occurrences and the reliability function (Karamouz et al., 2003):

$$\rho(t) = \lim_{\Delta t \rightarrow 0} \frac{P(t \leq X \leq t + \Delta t | t \leq X)}{\Delta t} \quad (10.15)$$

Therefore,

$$\rho(t) = \lim_{\Delta t \rightarrow 0} \frac{P(t \leq X \leq t + \Delta t)}{P(t \leq X) \Delta t} = \lim_{\Delta t \rightarrow 0} \frac{F(t + \Delta t) - F(t)}{\Delta t} \frac{1}{R(t)} = \frac{f(t)}{R(t)} \quad (10.16)$$

Example 10.2

Assume the time between drought events in an aquifer system follows the Weibull distribution. Formulate the reliability and hazard rate for this system.

SOLUTION

The reliability is:

$$R(t) = 1 - F(t) = e^{-\alpha t^\beta}$$

The hazard rate is calculated using Equation 10.16:

$$\rho(t) = \frac{\alpha \beta t^{\beta-1} e^{-\alpha t^\beta}}{e^{-\alpha t^\beta}} = \alpha \beta t^{\beta-1}$$

It shows that the hazard rate follows an increasing polynomial of t , which means failure will occur more frequently as time goes by (i.e., for larger values of t). In the special case of $\beta = 1$, $\rho(t) = \alpha$, which means that the hazard rate remains constant.

If the hazard rate is given, $F(t)$ or the reliability function can be recalculated (Karamouz et al., 2003). For this purpose, first,

$$\rho(t) = \frac{f(t)}{1 - F(t)} = \frac{(F(t))'}{1 - F(t)} = -\frac{(1 - F(t))'}{1 - F(t)} \quad (10.17)$$

Integrating both sides in the interval $[0, t]$:

$$\int_0^t \rho(\tau) d\tau = \left[-\ln(1 - F(\tau)) \right]_{\tau=0}^t = -\ln(1 - F(t)) + \ln(1 - F(0)) \quad (10.18)$$

Since $F(0) = 0$, the second term in the right-hand side of the equation is equal to zero, so:

$$\ln(1 - F(t)) = - \int_0^t \rho(\tau) d\tau \quad (10.19)$$

Therefore,

$$1 - F(t) = \exp \left(- \int_0^t \rho(\tau) d\tau \right) \quad (10.20)$$

Finally,

$$F(t) = 1 - \exp \left(- \int_0^t \rho(\tau) d\tau \right) \quad (10.21)$$

Example 10.3

Construct the cumulative distribution function (CDF) of failure events for the following situations:

1. The hazard rate is constant, $\rho(t) = \alpha$
2. $\rho(t) = \alpha\beta t^{\beta-1}$.

SOLUTION

Using Equation 10.21 for $\rho(t) = \alpha$:

$$F(t) = 1 - \exp\left(-\int_0^t \rho(\tau) d\tau\right) = 1 - \exp\left(-\int_0^t \alpha d\tau\right) = 1 - e^{-\alpha t}$$

If $\rho(t) = \alpha\beta t^{\beta-1}$,

$$F(t) = 1 - \exp\left(-\int_0^t \alpha\beta\tau^{\beta-1} d\tau\right) = 1 - \exp\left(-[\alpha\tau^\beta]_0^t\right) = 1 - e^{-\alpha t^\beta}$$

which demonstrates that the distribution is Weibull.

In contrast with $F(t)$ which is increasing, $F(0) = 0$ and $\lim_{t \rightarrow \infty} F(t) = 1$, $R(t)$ is decreasing, $R(0) = 1$, and $\lim_{t \rightarrow \infty} R(t) = 0$. In the Weibull distribution,

- If $\beta > 2$, then $\rho(0) = 0$, $\lim_{t \rightarrow \infty} \rho(t) = \infty$, and $\rho(t)$ is a strictly increasing and strictly convex function.
- If $\beta = 2$, then $\rho(t)$ is linear.
- If $1 < \beta < 2$, then $\rho(t)$ is strictly increasing and strictly concave.
- If $\beta = 1$, then $\rho(t)$ is constant.
- If $\beta < 1$, the hazard rate is decreasing in t , in which case defective systems tend to fail early.

$$\rho'(t) = \frac{f'(t)(1-F(t)) + f(t)^2}{(1-F(t))^2} \quad (10.22)$$

which is positive if the numerator is positive.

$$f'(t) > -\frac{f(t)^2}{1-F(t)} = -f(t)\rho(t) \quad (10.23)$$

If the inequality of Equation 10.23 is satisfied, $\rho(t)$ locally increases; otherwise $\rho(t)$ decreases.

The above discussions about reliability are applicable to a simple system with one component. The actual natural systems have several components, and the reliability in these systems depends on the configuration of the components in the entire system. The combination of components of systems can be "series," "parallel," or



FIGURE 10.12 Series combination of system components.

“combined.” In a series system, the failure of any component results in a system failure, but, in a parallel system, failure occurs only if all components fail simultaneously.

Figure 10.12 depicts a typical series combination. In this system, $R_i(t)$ denotes the reliability function of component i ($i = 1, 2, \dots, n$). The reliability function of the entire system could be estimated as:

$$R(t) = P(X > t) = P((X_1 > t) \cap (X_2 > t) \cap \dots \cap (X_n > t)) \quad (10.24)$$

where:

X is the time of the system failure

X_1, \dots , and X_n are the times of failure for the components.

If it is assumed that the failures of the different components occur independently of each other,

$$R(t) = P(X_1 > t) = P(X_2 > t) \dots P(X_n > t) = \prod_{i=1}^n R_i(t) \quad (10.25)$$

Inclusion of a new component into the system may result in a smaller reliability function because it is multiplied by the new factor $R_n + 1(t)$, which is below 1.

Figure 10.13 shows a parallel system. As mentioned before, the system fails if all components fail. The system failure probability can then be calculated as:

$$P(X \leq t) = P((X_1 \leq t) \cap (X_2 \leq t) \cap \dots \cap (X_n \leq t)) \quad (10.26)$$

If the components fail independently of each other,

$$\begin{aligned} R(t) &= 1 - F(t) = 1 - P(X \leq t) = 1 - \prod_{i=1}^n P(X_i \leq t) = 1 - \prod_{i=1}^n F_i(t) \\ &= 1 - \prod_{i=1}^n (1 - R_i(t)) \end{aligned} \quad (10.27)$$

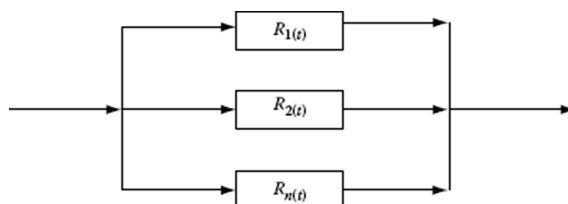


FIGURE 10.13 Parallel combination of system components.

where F and F_i are the cumulative distributions up to the first failure of the system and component i , respectively. In parallel systems, the reliability of the system increases by inclusion of a new component in the system.

In practical cases, usually a combined series and a parallel combination between systems components is considered. In the combined case, Equations 10.26 and 10.27 need to be combined appropriately.

10.5.2 RESILIENCY

Once failure occurs in a system, the time taken for the system to recover from the failure is described by resiliency. We may measure the duration of an unsatisfactory condition. In general form, the resiliency of a system can be calculated as (Karamouz et al., 2003):

$$\beta = \text{Prob} \left[X_{t+1} \in S \mid X_t \in F \right] \quad (10.28)$$

where S and F are the sets of all satisfactory and unsatisfactory outputs, respectively.

Resiliency originates from ecology. Holling (1973) defined resiliency as “a measure of the persistence of systems and of their ability to absorb changes and disturbances and still maintain the same relationships between populations and state variables.” Pimm (1991) defined resiliency as “the speed with which a system disturbed from equilibrium recovers some proportion of its equilibrium.” In general, resiliency can be considered as a tendency to stability and a resistance to perturbation. However, there is no general and overall accepted definition for resiliency.

Depending on the field of application, the definition and formulation of resiliency may vary and be specialized. For example, resilient flood risk management is a management approach that aims at giving room to the floods while minimizing the impacts (De Bruijn and Klijn, 2001). In a hazard event, if the less valuable parts are damaged prior to the more valuable parts, the system as a whole is resilient.

10.5.3 VULNERABILITY

The distance of the failed state from the desired condition in a historical time series describes the vulnerability of the corresponding system. Vulnerability can be considered as the maximum distance from the desired situation, the expected value of system failure cases, or the probability of failure occurrence. However, the approach that considers vulnerability as the expected value of a system failure is more common. Hence, the vulnerability of a system can be defined as:

$$\text{Vulnerability} = \frac{\sum_{X_T > X_t} \text{No. of situations with positive } (X_T - X_t)}{\text{No. of times } X_T > X_t} \quad (10.29)$$

where:

X_T is the desired situation

X_t is the system situation.

Using the probability of failure occurrence, the vulnerability of a system can be calculated by:

$$v = \sum_{j \in F} S_j e_j \quad (10.30)$$

where e_j is the probability that X_j corresponds to S_j .

10.6 GROUNDWATER VULNERABILITY

The vulnerability of groundwater in general and natural terms depends on the geological setting of the groundwater system. The deeper the hydrogeological structure and the older the groundwater, the lower its vulnerability. Therefore, the deeply confined aquifers have a lower vulnerability than unconfined aquifers (Figure 10.14).

Hydrogeological investigation and knowledge of the geological setting of the region are the requirements for the development of groundwater resources in deep aquifers. Wells must be located beyond alluvial plains and the mouth of the well shaft. The casing should be above the level of the expected flood. The main types of aquifers vulnerable to natural hazards and human impacts are (Vrba, 2006):

- Shallow uppermost unconfined aquifers located in unconsolidated fluvial and glacial deposits that are overlain by a permeable unsaturated zone of low thickness (less than 10 m). These aquifers can be characterized by young groundwater with an interface with surface water.

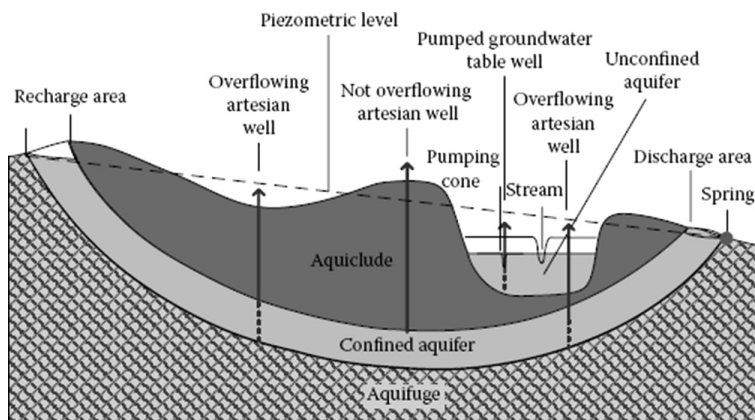


FIGURE 10.14 Example of an unconfined vulnerable aquifer over a confined aquifer in a floodplain. (From Keshari, A.K. et al., Impact of the 26-12-2004 tsunami on Indian coastal groundwater and emergency remediation strategy, in *Groundwater for Emergency Situations*, IHP-VI, Series on Groundwater (12), J. Vrba and B.T. Verhagen, eds., UNESCO, Paris, pp. 80–85, 2006.)

- Deeper unconfined aquifers located in consolidated rocks, such as sandstones of regional extent, overlain by a permeable unsaturated zone consist of a number of laterally and vertically interconnected groundwater flow systems.
- Karstic aquifers located in carbonate rocks with groundwater flow in conduits; typically with high groundwater flow velocities; springs are important phenomena of the groundwater karstic regime.
- Coastal aquifers—tidal fluctuations, streamflow changes, the gradient and volume of the groundwater flow toward the seashore, and the geological environment control seawater intrusion into coastal aquifers. In these aquifers, groundwater pumping has a significant impact on the groundwater-seawater interface.
- Recharge areas of all types of aquifers.

The aquifers resistant to natural hazards and human impacts are:

- Deep confined aquifers, which are aquifer systems mostly in sedimentary rocks overlain by a thick low permeable or impermeable unsaturated zone.
- Deep mostly confined aquifers, which are aquifer systems overlain by a thick low permeable or impermeable unsaturated zone. Low intensity of groundwater circulation, very limited aquifer replenishment, and very large aquifer storage are typical characteristics of these systems. The average annual aquifer renewal in these systems is less than 0.1% of the aquifer storage. Hence, the average renewal period would be at least 1000 years (Margat et al., 2006).
- Water entrapped in the sediments of low permeability at the time of their deposition.

10.6.1 DROUGHT

In the case of water disasters, cyclones, hurricanes, storms, and floods always come to mind first, with less attention to droughts, which could be a disaster with the longest effects and intense social and environmental impacts. A drought is referred to as a sustained and extensive occurrence of low flow thresholds on natural water availability.

Meteorological drought, agricultural drought, hydrologic drought, and socio-economic drought are different types of droughts. These droughts are defined as follows:

- Meteorological or climatic drought is a period of well below-average or normal rainfall that lasts from a few months to several years.
- Agricultural drought is a period when soil moisture is inadequate to meet the demands for crops to initiate and sustain plant growth.

- Hydrologic drought is a period of below-average streamflow that sometimes causes rivers to dry up completely and remain dry for a very long period and there is significant depletion of water in aquifers.
- Socio-economic drought refers to the situation where a physical water shortage affects people and their welfare.

Groundwater is normally the last water resource within the hydrological cycle that reacts to a drought situation, unless surface water is mainly fed by groundwater. In deep aquifers, only major meteorological droughts will cause groundwater droughts. The lag between a meteorological and a groundwater drought can be months or even years, while the lag between a meteorological and a streamflow drought varies from days to months (Tallaksen and van Lanen, 2004). The following factors have influence on the impact of a meteorological drought on groundwater:

- *Severity and duration of the drought:* In cases that the groundwater responds slowly to rainfall deficit, it generally also recovers more slowly after a drought. It results in complex and unrelated linkages between rainfall and the impact on groundwater resources
- *Design and location of the groundwater well or borehole:* Shallow wells may be expected to be more sensitive to recharge variations than deeper boreholes
- *Hydraulic characteristics of the aquifer:* This refers to the connectivity and linkage of the aquifer to recharge sources and the storage characteristics of the aquifer itself
- *Excessive demand and source failure:* Decrease of the water table level and depletion of the aquifer during drought events may cause failure of the pump, and in consequence, increase of demand on a neighboring source, which results in increasing stress and probability of failure
- *Long-term increases in demand:* Long-term increases in demand due to population growth, economic change, and the introduction of irrigation or other water-intensive activities can eventually mean that demand will exceed supply
- *Long-term changes in climate:* Climate change affects recharge processes that put both high- and low-yielding sources at risk. An increase in the erosion of the soil cover as well as vegetation removal because of climate change may increase runoff and reduce recharge that may result in an inadequate recharge for groundwater recovery.

In many parts of the world, the groundwater is increasingly exploited as a resource to supply domestic, industrial, and agricultural demands. Hence, the response of the groundwater systems to drought events and their performance under drought conditions is important. When a drought affects groundwater systems, first groundwater recharge and later groundwater levels, and eventually groundwater discharge, decreases. These droughts are called groundwater droughts, and their time scale is generally months to years (Van Lanen and Peters, 2000). The characteristics of the

droughts, such as duration, severity, and frequency, are changed by the groundwater system. Therefore, droughts have different impacts on the groundwater levels and discharge rather than groundwater recharge.

The effect of a drought on public water supplies necessitates cooperation among all stakeholders, such as water users and local, regional, and national public officials.

For drought management, strategies focus on reducing the impact of droughts by regional analysis and determining the most vulnerable parts of a region. [Figure 10.15](#) shows the vulnerable areas of the Lorestan Province in Iran for a drought with a 10 year return period. The hatched parts show vulnerable areas that require more attention in the case of a 10 year return period drought. In drought planning and management, these issues must be taken into account—the risk of potential economic and social (psychological) damages resulting from a drought, the ecological and economical costs, and the benefits of exercising alternative options such as aquifer recharge and capacity (physical) building (filling the reservoir) schemes. Besides, it must be determined how these options can reduce potential damages and provide an opportunity to face future droughts (Karamouz, 2002).

Developing a national or regional drought policy and an emergency response program is essential for reducing societal vulnerability and disaster, thereby also reducing water disaster impacts. Resiliency in the context of drought management has recently received attention (Karamouz et al., 2004).

Drought contingency plans provide a structured response that minimizes the damaging effects caused by water shortage conditions. A common feature of drought contingency plans is a structure that allows rigorous drought response measures to be implemented in successive stages as the water supply diminishes or increases. The termination of each implementation stage should be defined by specific “triggering” criteria. Triggering criteria ensure that: (1) timely action is taken in response to a developing situation and (2) the response is appropriate for the level of severity of the situation.

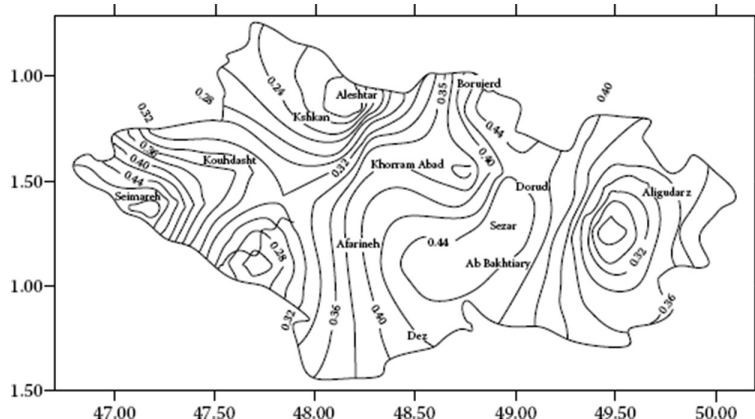


FIGURE 10.15 Vulnerable areas of the Lorestan Province in Iran for a drought with a 10 year return period.

10.6.1.1 Drought Indicators

Effective drought management depends on drought indicators and triggers. Drought indicators can be defined as variables for detecting and characterizing drought conditions. They describe the magnitude, duration, severity, and spatial extent of a drought. Typical indicators are based on meteorological and hydrological variables, such as precipitation, streamflows, soil moisture, reservoir storage, and groundwater levels. When several indicators are synthesized into a single indicator on a quantitative scale, the result is called a drought index. In creating drought indices, how each indicator is combined and weighted in the index, and how an arbitrary index value relates to geophysical and statistical characteristics of a drought are some challenging issues. Indicator thresholds to define and activate levels of drought responses are called drought triggers. Determining indicators and triggers, and using them in a drought management plan, becomes more challenging due to the complexity of a drought.

Atmospheric condition, such as days without measurable rainfall, is a basic factor in the regions that have groundwater as their primary or only source of supply to identify drought conditions. Palmer Drought Severity, Standard Precipitation, and Keetch-Byram are some commonly used drought indices. These indices can be used to determine local drought conditions and appropriate responses.

10.6.1.2 Drought Triggers

Threshold values of an indicator that identify a drought level are called drought triggers. They determine when management actions should begin and end. Triggers specify the indicator value, the time period, the spatial scale, and the drought level. Drought levels (phases, stages) are categorized as mild, moderate, and severe, extreme drought, or stage 1, stage 2, and stage 3 droughts corresponding, respectively, to the local conditions of a drought “watch,” “warning,” or “emergency.”

Drought indicators and triggers can be used for the following purposes (Steinemann et al., 2005):

- To detect and monitor drought conditions
- To determine the timing and level of drought responses
- To characterize and compare drought events.

Drought response triggers are based on an assessment of the water user’s vulnerability, and they are specific to each water supplier. The groundwater drought triggers can be based on the levels of demand, the capabilities of a water treatment plant or delivery system, and the water levels in monitoring wells that have a record of historical measurements. Trigger criteria are defined on well established relationships between the benchmark and historical experience. If historical observations are not available, then common sense must prevail until such time that more specific data can be presented.

The groundwater triggers are not identified as easily as factors related to surface water systems. The reason is the rapid response of stream discharge and reservoir storage to (even short-term) changes in climatic conditions and the slower response of the groundwater systems to recharge processes. Wet climatic conditions could have a significant impact on the availability of surface water even over a period of

1 year. But, the underlying aquifers might not show such a response as surface waters for much longer periods of time. The response of these aquifers depends on infiltration rates, size and location of the recharge areas, the distribution of precipitation, and the extent to which aquifers are developed and exploited.

Aquifers that do not receive sufficient recharge to maintain a balance between the recharge and natural discharge or pumping may have groundwater be depleted over time. In such aquifers, the level of the water table may decrease over a long period of time, and eventually reaches a point at which the cost of pumping water becomes uneconomical. Therefore, in these situations, the water levels alone may not be a satisfactory drought trigger. Thus, the average annual rate of the water level of the aquifer, and increased well pumping costs due to the water level's drop, may be considered as drought triggers.

If historical water level measurements are available, water levels in observation wells in municipal well fields may be considered as drought triggers for municipalities. Water levels below specified elevations for a given period of time might be viewed as rational groundwater indicators of drought conditions.

When a measuring device is installed, the staged pumping level triggers are set for the well. These staged triggers must be above the critical pumping level, which is defined as the lowest pumping level that can be tolerated in a well without deterioration or damage to the well or the pump.

After determining the critical pumping level, two or three staged triggers are established above the critical pumping level to trigger a local drought watch, drought warning, and drought emergency conditions, and the appropriate emergency response measures. These triggers must be set in a way that sufficient warning for an adequate emergency response is given by them. However, it must be noted that these levels should not trigger response actions so frequently or prematurely that the public loses trust and does not respond. Since drawdowns to the critical pumping level may cause damage to the well or pump, all trigger levels must be above the critical pumping level. The annual fluctuation of the groundwater pumping levels is depicted schematically in [Figure 10.16](#). In this figure, the pumping level triggers are

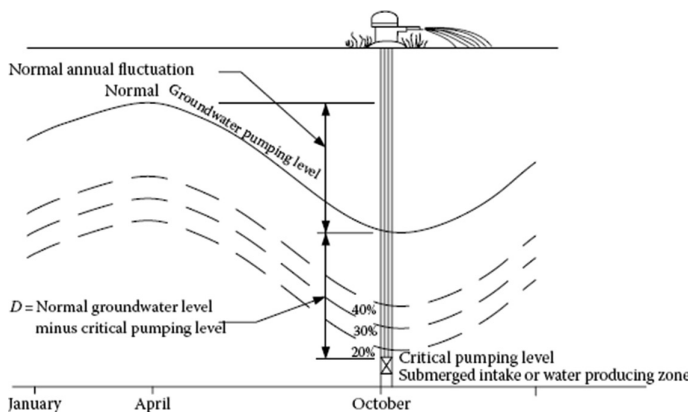


FIGURE 10.16 Groundwater pumping levels and drought triggers in a well.

set at 40%, 30%, and 20% of the distance between the normal pumping levels and the critical pumping level for each month of the year. At 40% of the distance between a normal pumping level and the critical level, a drought watch would trigger; at 30%, a warning would trigger; and at 20%, an emergency would trigger. These percentage triggers can be considered as initial settings until a more precise set of triggers are developed.

10.6.1.3 Drought Management Strategy Plan

Drought contingency plans must be developed and submitted by local water utilities to the water district to grant well permits and groundwater transfer permits. Actions that must be taken by local utilities to conserve water under given demand scenarios are specified by these plans. These actions include customer awareness, voluntary water conservation, mandatory water use restrictions, and critical water use restrictions.

The groundwater availability is influenced by a drought in two ways: (1) recharge from precipitation on the aquifer outcrop and infiltration of surface water are reduced and (2) the groundwater pumping is increased to make up for surface water supplies that are more susceptible to drought conditions. To manage district groundwater resources in droughts, the district's vulnerability to a drought is evaluated and triggering criteria for specific management zones are defined. Then, drought response goals and measures are determined.

After the installation of water level measures in the water district, data of rainfall and water levels in monitoring wells are measured for several years. These data are then evaluated to establish a basis for revising the initial drought management strategy plan. The drought vulnerability assessment is specific to the groundwater management zones. It reflects the differences in aquifer depths, local and regional use patterns, recharge areas in the district, and other factors.

Due to the water demands, the following are recommended as the district's response goals or trigger levels:

- *Response level 1:* Public awareness and notification of drought conditions. This level could also be triggered by occurrence of when a moderate drought occurs. A moderate drought could be defined as a Palmer Drought Severity Index of -2.0.
- *Response level 2:* Water rate incentives or penalties, i.e., surcharges for excess use when an extreme drought over a planning period in the water district occurs, this level is triggered. An extreme drought is defined as a Palmer Drought Severity Index of -4.0.
- *Response level 3:* Imposition of water rationing. Permits for high capacity new wells should incorporate provisions for water rate incentives and water rationing.

10.6.1.4 Drought Vulnerability Maps

Drought vulnerability maps are central to the optimum use of groundwater during a drought. Regions that are more vulnerable to groundwater drought are pointed out by these maps. They include a variety of decisive factors. Some of these factors are

aquifer type, depth of the saturated zone, well and borehole yields, and the amount and variability of rainfall. It should be noted that some regions are more vulnerable to groundwater droughts than others. Some examples of these regions are where there is low water supply coverage and high population density, and dependencies on traditional sources.

In vulnerability maps, different layers are incorporated and superimposed. Two important layers in vulnerability maps are:

- A socio-geological dataset that determines the distribution of demands
- A physical dataset that identifies the availability and accessibility of resources

Using these maps eases the identification of vulnerable regions and helps to target them to plan some preparations such as the design of wells and boreholes in pre-drought periods

10.6.1.5 Drought Early Warning Systems

In comparison with drought vulnerability mapping, early warning systems are based on longer-term meteorological forecasting. The groundwater drought early warning is usually accomplished at two levels: global and regional levels. The global level is in international meteorological scales and considers climate and climate variation, including long-term changes. At the regional level, which is in government, donor, and NGO scales, watershed/aquifer scale signals of the groundwater drought and possible consequences are considered (Verhagen, 2006).

Reliable data and long-term observed and antecedent meteorological and hydrological time series, such as water levels and yields, are required for developing a meaningful groundwater drought early warning system. These data are then compiled and analyzed and user needs are determined. Finally, an early warning system is developed to identify drought management areas.

10.6.1.6 Case Study

The province of Yazd with an area of 131,000 km² is located in the central plateau of Iran, which possesses an arid climate. It is located on the desert belt of the northern hemisphere, with a relatively low elevation, far away from surface water bodies. Dry anticyclones, topographical conditions coupled with intensive sunlight make this region dry and arid. The province of Yazd is 1568 m above sea level on average, and the highest spot in the region (Shirkooch Mountain) is 4075 m and the lowest point (the northeastern desert) is about 670 m above sea level. The average annual rainfall amounts to 109.4 mm in the province and 59.1 mm in Yazd City, the capital of the province. In this region, the annual average evaporation is 3193 mm, annual average temperature is 17°C, and annual relative humidity does not exceed 43%. These conditions account for the absence of any permanent surface stream in this area, in fact, there is no permanent river, but some seasonal rivers originating from Shirkooch Mountain, located in the central part of the province, for a few months in case of a wet year. Therefore, only the groundwater supplies limited discharge for the agricultural, industrial, and domestic sectors.

In 2001, the province of Yazd faced a problematic decline in the amount of precipitation, this aggravated the ongoing drought and resulted in a considerable depletion of the aquifer water table. During the spring, the total rainfall received was less than 5 mm. Therefore, a considerable part of the vegetation was dried out. So the villagers, who had to buy forage for the cattle to flock instead of grazing, could no longer afford the installments of the existing loans. The farmers witnessed no yield on their crops due to the water scarcity in the region. Furthermore, the orchards dried up despite long-time investment and hard work.

Considering the hydrological conditions of the province as well as the fact that 91% of the available groundwater was being consumed by the agricultural sector, the following groundwater protection activities were performed by governmental agencies to alleviate the depletion of groundwater reserves (Yazdi and Khaneiki, 2006):

1. Rehabilitation and repair of qanats
2. Construction of artificial recharge dams
3. Implementation of cloud seeding projects
4. Intensifying legal penalties in case of overpumping without an official permit
5. Reducing withdrawal from the aquifer by means of modifying and limiting the existing permits
6. Replacing diesel pumps with electric ones to make it possible to control the amount of water by measuring the electricity consumption
7. Installing bulk meters on the wells

10.6.1.7 Qanats

Qanats were first developed in Iran, but their use spread to India, Arabia, Egypt, North Africa, Spain, and even to the New World. They are referred to by different names in different areas. In Afghanistan and Pakistan, they are known as karez, in North Africa, as foggers, and in the United Arab Emirates, as falaj. In Iran, traditional irrigation has an inherent mechanism to adapt the existing water to environmental conditions. One of the critical concerns of Iran is the evaporation and acute transpiration of surface water under solar radiation. In different regions of Iran, the groundwater plays a key role in all forms of development. To make use of the limited amounts of water in arid regions, the Iranians developed man-made underground water channels called qanats.

A qanat is a traditional delivery system with over 3000 years of history used to provide a reliable supply of water for irrigation in hot, arid, and semiarid climates. The qanat system consists of underground channels that convey water from the groundwater aquifers in high lands to the surfaces at a lower level by gravity. Qanats are constructed as a series of wells connected by gently sloping tunnels. In qanat systems, a large quantity of water is delivered to the surface without the need for pumping. The water drains rely on gravity, with the destination lower than the source, which is typically an upland aquifer. Qanats allow water to be transported over long distances in hot dry climates without losing a large proportion of the water due to seepage or evaporation. [Figure 10.17](#) shows a schematic cross section of a qanat.

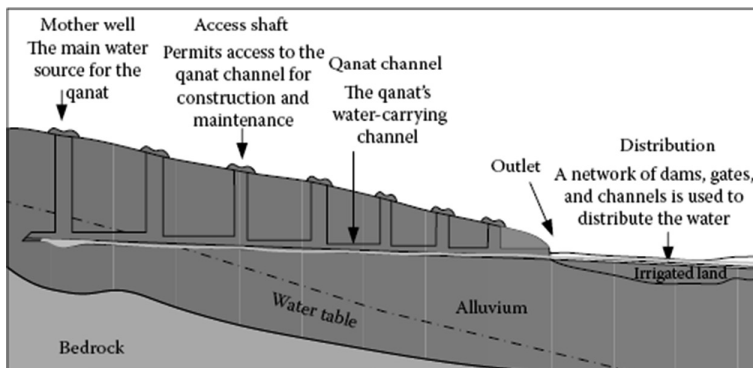


FIGURE 10.17 Schematic cross section of a qanat.

This mechanism works through technical factors as well as water management. In case of a drought, the users of qanats have two choices to cope with this situation technically. These choices are to extend the gallery of the qanat by digging it up through the aquifer and adjusting the area of farmlands to the available water. The farmlands are divided into two parts for trees and vegetables. A special ratio should be considered between the areas of orchards and farms so that the maximum amount of the available water would meet the agricultural needs for the total area. The area of the cultivated lands and the cropping pattern is adjusted to match the existing discharge and to avoid placing pressure on the groundwater sources and in consequence facing a drought.

Traditional water management is very flexible to environmental conditions. It is necessary to mention that a qanat may belong to hundreds of farmers who have an assigned share of water from the qanats to irrigate their lands. This water-sharing system can match all likely changes in the volume of water during a year, while satisfying agricultural needs. For example, if the volume of water decreases due to a drought, each farmer receives two times more water than his normal share, but once every two periods. By doing so, this amount of water can reach every corner of his farm.

Qanats are renewable water supply systems that have sustained agricultural settlement on the Iranian plateau for a millennia. The great advantages of qanats are, no evaporation during transit, little seepage, no raising of the water table, and no pollution in the area surrounding the conduits. The sustainable management of underground reservoirs should be based on a reasonable and economical exploitation of such natural resources. The agricultural sector is the greatest consumer of the groundwater. Therefore, existing agricultural methods need to be modified so that more valuable crops are gained with a minimum consumption of water. In the study area, if the methods of irrigation are optimized to reach a 5% decrease in water consumption, the water demand for the present industries, mines, towns, and villages can be supplied.

10.6.2 FLOOD

Floods continue to be the most destructive natural hazard in terms of short-term damages and economic losses to a region. According to the United States Federal Emergency Management Agency, floods are the second most common and widespread of all natural disasters (drought is the first globally). Each year, an average of 225 people are killed and more than \$3.5 billion in property damage is experienced by heavy rains and flooding across the United States (FEMA, 2008).

Floods are most frequently caused by a coincidence of meteorological and hydrological circumstances. However, the flooding of lands has geological or anthropogenic (caused by humans) reasons, especially in urban areas that have more impermeable surfaces. The main impacts of floods on groundwater systems can be summarized as:

- Infiltration of flood water directly into the aquifer
- Infiltration of overland flow into sewer systems and from the sewer system into the groundwater
- Increasing inflow from the recharge areas
- Transferring contaminants from the ground surface to the underlying aquifers

However, increasing urbanization causes decreasing infiltration capacities, and as a consequence, the rate of recharge to aquifers is reduced. On the other hand, flood runoff is accumulated in rivers that cause greater interaction with and recharge of the aquifers.

Flash floods occur even in arid regions where they can cause damage to the communities and where groundwater resources are located in dry streambeds. These floods may cause the water supply and polluted wells to collapse the groundwater. However, it should be noted that the floods of a longer duration caused by regional rains are different from the flash floods. In some climatic zones, floods are a common phenomenon linked with regular precipitation. The most vulnerable groundwater resources are those in direct contact with the earth's surface where the groundwater recharge occurs, such as in sediment deposits of the flood plain, in outcrops of permeable rocks (e.g., sandstone), or in karstified areas.

Flood plains provide a large volume of groundwater recharge, but, due to a high suspended load, their infiltration capacity is low. Nonetheless, since the aquifers recharged by floods are vulnerable to pollution, they are not recommended as substitutions for drinking water sources. The groundwater in the coastal aquifers could be polluted by marine water from the surface due to coastal floods/tsunamis. This groundwater should be carefully utilized without disturbing the underlying brackish water as shown in [Figure 10.18](#).

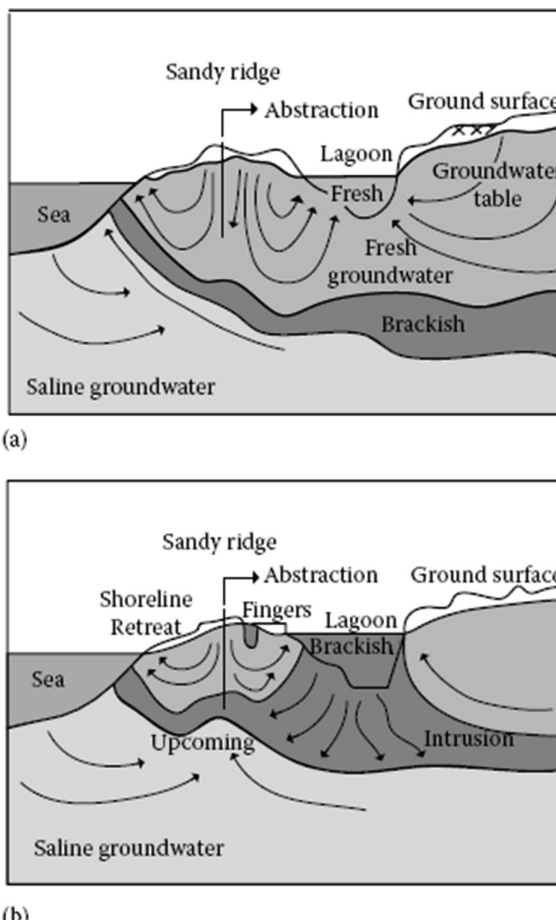


FIGURE 10.18 Schematic presentation of a mechanism of tsunami events affecting a coastal groundwater system (a) before and (b) after a tsunami. (From Keshari, A. K. et al., Impact of the 26-12-2004 tsunami on Indian coastal groundwater and emergency remediation strategy, in *Groundwater for Emergency Situations*, IHP-VI, Series on Groundwater (12), J. Vrba and B.T. Verhagen, eds., UNESCO, Paris, France, pp. 80–85, 2006.)

10.6.2.1 Maps of Groundwater Flood Hazard

Groundwater flooding can cause many problems. Structural damage, sewer system backups, and damaged appliances are three of the most inconvenient consequences. The aim of groundwater flood hazard maps is to indicate areas with need of protection for underground structures against groundwater floods. After regionalizing the subsurface hazard potential, it is possible to create maps of groundwater flood hazard (Sommer, 2006). [Figure 10.19](#) depicts an example of hazard potential maps (Sommer and Ullrich, 2005). Flood control and flood prevention strategies can be configured as a pyramid of measures. [Figure 10.20](#) illustrates this pyramid.

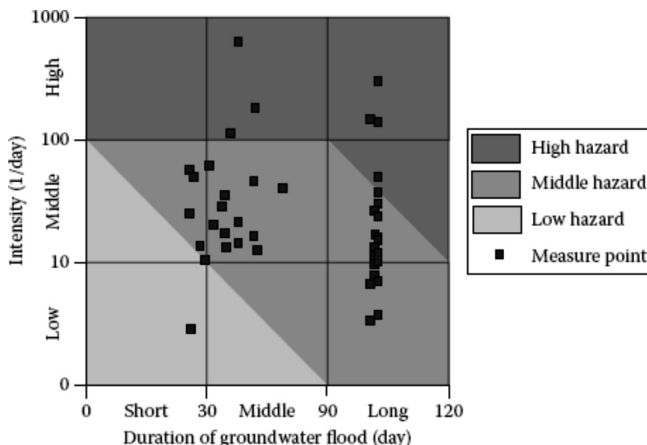


FIGURE 10.19 Example of hazard potential maps.

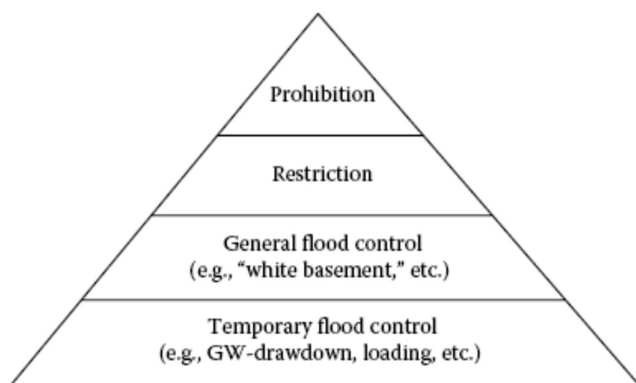


FIGURE 10.20 Control measures against groundwater flood. (From Sommer, T. H. and Ullrich, K., Influence of flood event 2002 on groundwater. Research Report (in German). Environmental Office, City of Dresden, 68 p, 2005.)

Temporary flood control means measures during a flood against damages caused by the rising groundwater, e.g., groundwater drawdown as well as loading or basement flooding. General flood control refers to preventive measures concerning buildings with basements or buildings without basements. Temporary flood control measures are recommended in areas with a long duration of groundwater floods. General flood control measures are recommended in areas with a high intensity of groundwater floods. While the building owner is responsible for temporary and general flood control measures, the communal authority should decree restrictions for buildings or prohibition of underground structures by urban land-use planning for areas with a high hazard potential.

10.6.3 LAND SUBSIDENCE

Gradual settling or sudden sinking of the earth's surface due to the movement of earth materials is called land subsidence. There are three main processes causing land subsidence:

1. Compression (compaction or consolidation) of the interbedded layers of clay and silt within the aquifer system
2. Drainage and oxidation of organic soils
3. Dissolution and collapse of susceptible rocks

The sudden collapse of the ground to form a depression and also the slow subsidence or compaction of the near-surface sediments and soils are considered subsidence hazards. In comparison with earthquake, volcanic, or landslide events, sudden collapse events are rarely major regional disasters. However, the slow subsidence of areas can cause significant economic damage during a longer period of time, even if the types of hazards associated with subsidence are different from those caused by sudden and catastrophic natural events (e.g., floods and earthquakes), because surface sinking is a slow event, extensive damage can occur.

Overextraction of the groundwater from aquifers is the major cause of subsidence (Bell, 1997). When large amounts of water are pumped, the aquifer may be compacted due to the reduction of the size and number of open pore spaces that are used to hold water. In consequence, the total storage capacity of the aquifer may be reduced permanently.

For example, if an aquifer has beds of clay or silt, the reduced water pressure results in a loss of support for the clay and silt beds. Since these beds are compressible, they are compacted and become thinner. Therefore, the land surface is lowered. After land subsidence, recharging the aquifer until the groundwater returns to the original levels would not result in a recovery of the land surface elevation. The main problems caused by land subsidence are:

- Changes in elevation and slope of streams, canals, and drains
- Damage to bridges, roads, railroads, electric power lines, storm drains, sanitary sewers, canals, and levees
- Damage to private and public buildings
- Failure of well casings from forces generated by compaction of fine-grained materials in aquifer systems
- In some coastal areas, subsidence may result in tides moving into low-lying areas that used to be above high-tide levels
- Land subsidence includes loss of levee freeboard, and therefore, reduction in flood protection

To prevent these types of structural damages, it is important to detect land subsidence at very early stages. Because of the rapidly increasing use of groundwater, oil, and gas, major subsidence areas around the world have occurred in the past half century. Most areas of known subsidence are along coasts where the phenomenon becomes more significant when ocean or lake waters start coming further up on the shore.

The accurate monitoring of land subsidence helps to reflect on recommendations for the sustainable use of the underground resources. In case of a land subsidence occurrence, some recommendations include reducing the groundwater use and switching to surface waters where possible, a careful determination of locations for pumping, and artificial recharging. The main objective of artificial recharge is to preserve or enhance the groundwater resources. However, there are many other beneficial purposes, the prevention of land subsidence being one of them.

10.6.3.1 Subsidence Calculation

For a unit area of a horizontal plane at depth Z below the ground surface, and utilizing the pressure equilibrium, the upward fluid pressure P_h , and the granular pressure exerted between the grains of the material is resisted by the total downward pressure P , on the plane due to the weight of the overburden: $P_t = P_h + P_i$. Decreasing the hydrostatic pressure leads to an increase of the granular pressure and a lowering of the water table/piezometric surface. For an aquifer with the thickness of Z and P_{i1} , P_{i2} as the granular pressures before and after decreasing the water table or the piezometric surface, respectively, the vertical subsidence can be estimated as:

$$S_u = Z \frac{P_{i2} - P_{i1}}{E} \quad (10.31)$$

where E is the modulus of elasticity of the soil layer that is presented in [Table 2.5](#) (Delleur, 1999).

Example 10.4

Consider an unconfined and sandy aquifer with a thickness of 50 m and a water table 7 m below the ground surface. Assume that the porosity of the soil is $n = 0.35$, the water content in the unsaturated zone is $\theta = 0.06$, the modulus of elasticity of the sand is $E = 980 \text{ N/cm}^2$, and the specific weight of the solids and water are $\gamma_s = 25.1 \text{ kN/m}^3$ and $\gamma_w = 9.81 \text{ kN/m}^3$, respectively. If the water table drops 15 m, calculate the subsidence.

SOLUTION

The total pressure (granular pressure) at the water table is:

$$P_t = 7 \left[(1 - 0.35) \times 25.1 + 0.06 \times 9.81 \right] = 118.3 \text{ kPa}$$

The total pressure at the bottom of the layer is:

$$P_t = 118.3 + 43 \times \left[(1 - 0.35) \times 25.61 + 0.35 \times 9.81 \right] = 967.5 \text{ kPa}$$

The hydrostatic pressure at the bottom of the layer before decreasing the water table is:

$$P_h = 43 \times 9.81 = 421.8 \text{ kPa}$$

So, the granular pressure is $967.5 - 421.8 = 545.7$ kPa.

After decreasing the water table to 15 m, the depth to the water table would be 22 m. The total pressure at the bottom of the layer is:

$$P_t = 22[(1-0.35) \times 25.1 + 0.06 \times 9.81] + 28[(1-0.35) \times 25.1 + 0.35 \times 9.81] \\ = 924.8 \text{ kPa}$$

The hydrostatic pressure at the bottom of the layer before decreasing the water table is:

$$P_h = 28 \times 9.81 = 274.7 \text{ kPa}$$

So, the granular pressure is $924.8 - 274.7 = 650.2$ kPa.

The granular pressure varies linearly from 0.0 at the 7 m depth to 650.2 kPa at the 22 m depth. The average increment in intergranular pressure is $(0 + 104.5)/2 = 52.25$ kPa, and the settlement in the layer using Equation 10.31 from 7 to 22 m is:

$$S_{u1} = Z \frac{P_{i1} - P_{i2}}{E} = (22 - 7) \frac{(36.45 + 0) / 2}{9800} = 0.028 \text{ m}$$

The subsidence in the layer from 22 to 50 m is:

$$S_{u2} = Z \frac{P_{i1} - P_{i2}}{E} = (50 - 22) \frac{(104.5 + 36.45 / 2)}{9800} = 0.2 \text{ m}$$

The total subsidence is thus $0.028 + 0.2 = 0.228$ m.

10.6.3.2 Monitoring Land Subsidence

For monitoring land subsidence, the most basic approaches use repeated surveys with conventional or GPS leveling. Permanent compaction recorders or vertical extensometers can also be used for monitoring land subsidence.

In these devices, a pipe or a cable is installed inside a well casing. The pipe extends from the ground surface to some depth through compressible sediments. A table at the ground surface holds instruments that monitor changes in distance between the top of the pipe and the table. Actual land subsidence can be measured if the inner pipe and casing go through the entire thickness of compressible sediments. The groundwater levels must also be measured in addition to the measurement of sediments compaction to be able to analyze the data to determine properties that can be used to predict future subsidence.

10.6.3.3 Reducing Future Subsidence

Switching from groundwater to surface water supplies can help to stop land subsidence in some areas where the groundwater pumping has caused subsidence. If surface water is not available, possible measures can be reducing water use and determining locations for pumping and artificial recharge. Optimization models coupled with groundwater flow models can be used to develop such strategies.

10.6.3.4 Examples of Subsidence

There is some evidence in Iran showing subsidence has been caused by the withdrawal of water from aquifers for industrial and other purposes.

1. In the southeast of Iran, near the city of Iranshahr, two residential areas were established 12 years ago. A few years after that, some cracks were observed around the buildings in these residential areas. The buildings, made up of bricks and cement blocks, had cracks appear all around them in all directions with different sizes. Those made with reinforced concrete had cracks right at the joints. All crack-causing factors such as faulting, earth movement, folding, subduction, and subsidence were studied and evaluated. In addition, some instruments such as seismographs were installed and geological studies performed. The studies showed that there were no geological and seismic reasons for these cracks. For a long time, there had been a few small quakes around the area, but they were not of high magnitude. In addition, the study of faults in the area showed no considerable movement during the past few years. Eventually, technical assessments showed that the water level fluctuations due to water withdrawal from the aquifers and the discharge of wastewater into the groundwater, as well as the sensibility of clay, which forms the biggest containment of the soil profile, caused the expansions and shrinking and was the main cause of the cracks and fractures.
2. The Mahyar Plain is located approximately in the central part of Iran. There are almost 200 km² of agricultural planes and several residential zones in this area. The plain is overlain with almost 150–200 m of alluvium consisting of sand, silt, and clay. The bedrock contains 50 m of clay. Over the past 40 years, almost 250 water wells have been pumping out groundwater.

A high rate of groundwater withdrawal from the aquifer without enough recharge has caused a rapid drawdown of the water table, and in consequence, subsidence of the land. Because of the presence of a few meters of clay on the surface of the plain, the subsidence has caused long and wide cracks on the land surface. These types of land surface cracks can also be observed in Houston, Texas, Goose Creek in North Dakota, Santa Clara in California, and in the Kerman Province in Iran. Reducing the drawdown by an injection of water in the aquifers has ceased subsidence and cracking in the area.

10.6.4 WIDESPREAD CONTAMINATION

There are two categories of biological and inorganic groundwater contaminants. Biological forms of microorganisms include viruses and bacteria that can cause various diseases, such as cholera. Harmful microorganisms often enter the groundwater from leaking sewers and latrines. Therefore, latrines should be situated at a down-gradient from supply wells. [Figure 10.21](#) shows different elements of urban life and

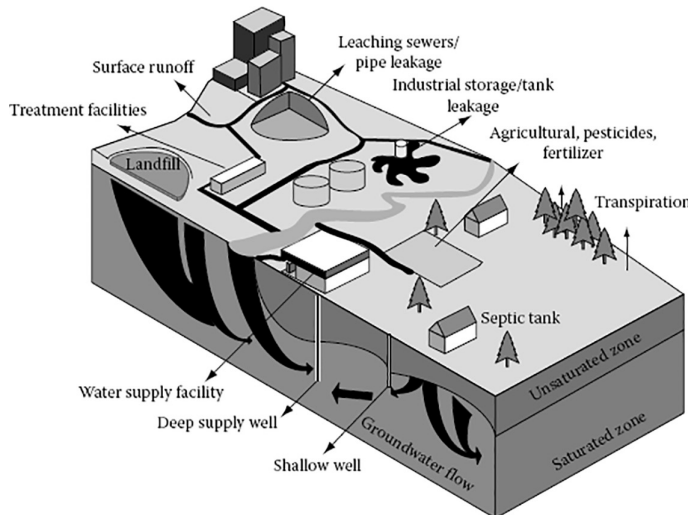


FIGURE 10.21 Threatened hazards of groundwater quality. (From Davies, J. et al., Development of a curriculum and training of supervision teams in borehole construction in Malawi, British Geological Survey Internal Report CR/02/219N, 2002.)

agricultural and industrial activities as they pose potential hazards that threaten the groundwater quality. Groundwater contamination can occur when a source releases contaminants into the environment. The main sources of groundwater pollution with some of their main characteristics are presented in [Table 10.2](#). The source includes:

- The municipal system (urban runoff, sewer leakage, wastewater effluent, septic tanks, sewage sludge, urban runoff, landfill, and latrines)
- Industries (processes, water treatment, industrial effluent, leaking tanks, and pipelines)
- Agriculture (return flows, fertilizers, pesticides, herbalists, and animal wastes)
- Mining (solid wastes and liquid wastes)

Groundwater natural dissolved minerals are primarily expressed as total dissolved solids (TDS) and are derived from soils and rocks. The TDS can be estimated by measuring the electrical conductivity of groundwater. The TDS in mg/L is equivalent to 0.6 times the electrical conductivity in microSiemens per centimeter ($\mu\text{S}/\text{cm}$). As the TDS increases, the water will look more brackish. The natural TDS of groundwater is normally harmless, although some traces of fluoride or arsenic may be present in the groundwater that could be harmful.

TABLE 10.2
Main Sources of Groundwater Pollution with Some of Their Main Characteristics

| Pollution Category | Pollution Source | Main Pollutant | Potential Impact |
|--------------------|---|--|---|
| Municipal | Sewer leakage | Nitrates | Health risk to users, eutrophication of water bodies, odor, and taste |
| | Septic tanks, cesspools, privies | Viruses and bacteria | |
| | Sewage effluent, and sludge | Nitrate, minerals, organic compounds, viruses, and bacteria | |
| | Storm water runoff | Bacteria and viruses | Health risk to users |
| Landfills | | Inorganic minerals, organic compounds, heavy metals, bacteria, and viruses | Health risk to users, eutrophication of water bodies, odor, and taste |
| Cemeteries | | Nitrate, viruses and bacteria | Health risk to users |
| Feedlot wastes | | Nitrate-nitrogen-ammonia, viruses and bacteria | Health risk to users (e.g., methemoglobinemia) |
| Agricultural | Pesticides and herbicides | Organic compounds | Toxic/carcinogenic |
| Fertilizers | | Nitrogen, phosphorous | Eutrophication of water bodies |
| | Leaked salts | Disolved salts | Increased TDS in groundwater |
| Industrial | Process water and plant effluent | Organic compounds heavy metals | Carcinogenic and toxic elements (As, Cn) |
| | Industrial landfills | Inorganic mineral, organic compounds, heavy metals, bacteria, and viruses | Health risk to users, eutrophication of water bodies, odor and taste |
| | Leaking storage tank (e.g., petrol station) | Hydrocarbons, heavy metals | Odor and taste |
| | Chemical transport | Hydrocarbons, chemical | Carcinogens and toxic compounds |
| | Pipelines leaks | | |

(Continued)

TABLE 10.2 (Continued)
Main Sources of Groundwater Pollution with Some of Their Main Characteristics

| Pollution Category | Pollution Source | Main Pollutant | Potential Impact |
|-------------------------|---|--|---|
| Atmospheric deposition | Coal-fired power stations | Acidic precipitation | Acidification of groundwater and toxic leached heavy metals |
| | Vehicles emissions | | |
| Mining | Mine tailings and stockpiles Dewatering of mine shafts | Acidic drainage Salinity, inorganic compounds, metals | May increase concentrations of some compounds to toxic levels |
| Groundwater development | Saltwater intrusion | Inorganic minerals, dissolved salts | Steady water quality deterioration |

Source: Sillito, O. T. N. and Saayman, I. C., Groundwater Vulnerability to Pollution in Urban Catchments, The Water Program Division of Water, Environment and Technology CSIR, University of Cape Town, Cape Town, 2001.

However, the major risk to the groundwater quality is by pollution coming from various anthropogenic activities. Mining or industrial effluents could infiltrate, and pesticides and fertilizers that are spread on the agricultural lands could sink into the ground. The movement of groundwater is usually very slow and has great filtration capacity for pollutants. But this depends on the properties of the aquifer, fractured or intergranular, and the depth of the water table. The pollutant travels more quickly in fractured aquifers. An aquifer is vulnerable when there is a high risk of contamination. The risk will increase as the number of people and other aquifer water users increase. The risk of contamination is especially serious when many people or industries depend on the aquifer for their water.

The vulnerability of an aquifer to different pollutants is related to the hydraulic characteristics of the aquifer and the characteristics of the contaminant attenuation. The groundwater and soil/porous medium and the pollutants determine the vulnerability of a groundwater system to pollution. Land-use planning has a direct impact on the pollution of the groundwater resources with negative impacts. It represents the location of high-risk activities.

Any new development in a general land-use and zoning structure should follow environmental impact assessment legislation to determine the impact of developments on the groundwater resources. A wide range of pollutants including bacteria and other microorganisms, major inorganic ions (NO_3 , Cl , SO_4 , etc.), heavy metals, and a wide range of organic chemicals could contaminate groundwater. The challenges facing engineers to protect groundwater include mechanisms by which pollutants enter groundwater, predictions of the transport of pollutants, and protective measures and legal enforcement issues. In countries such as Sweden (Scharp, 1999), some acts have been exercised to address groundwater protection.

In recognition of the importance of protecting groundwater resources from contamination, scientists and resource managers have sought to develop techniques for predicting which areas are more likely than others to become contaminated as a result of human activities at the land surface. The idea being that once identified, areas prone to contamination could be subjected to certain use restrictions or targeted for greater attention.

10.6.4.1 Vulnerability Assessment in Groundwater Pollution

“Groundwater vulnerability is an amorphous concept not a measurable property” (NRC, 1993). It is a tendency or likelihood that contamination may occur. The vulnerability of the groundwater to pollution depends on:

1. The travel time of infiltrating water carrying contaminants
2. The proportion of contaminants that reaches groundwater
3. The contaminant attenuation capacity of the geological materials through which the contaminated water travels

TABLE 10.3
Example of Different Approaches to Vulnerability Assessment

| Type of Assessment | Scales of Application | Pollution Hazard | Example Identifier | References |
|--------------------|-----------------------|------------------|--------------------|---|
| Empirical | Local | UST- | MATRIX | Oregon DEQ (1991) |
| | Local | Petroleum | LeGrand | Le Grande (1983) |
| | Regional and local | Landfill | DRASTIC | Aller et al. (1987) |
| | Regional | Leakage | GOD | Foster (1987) |
| | Regional/national | Universal | | NRA (1992) |
| | | Universal | | Lorber et al. (1989) |
| | | Aldicarb | | |
| Deterministic | Local/ regional | Specific | | Bachmat and Collin (1987) |
| | Regional | Pollutants | LPI | Meeks and Dean (1990) |
| | | Pesticides | | |
| Combined Empirical | Regional | Pesticides | DRASTIC-CLMS | Ehteshami et al. (1991) Banton and Villeneuve (1989) |
| Deterministic | Regional | Pesticides | DRASTIC-PRZM | |
| Probabilistic | Regional | Pesticides | VULPEST | Villeneuve et al. (1990) |
| | Regional | Pesticides | Discriminate | Teso et al. (1989) |
| Stochastic | Regional possible | Universal | Analysis weight of | New LWRRC project |
| | National | pesticides | evidence models | |

Source: Barber, C. et al., Assessment of the relative vulnerability of groundwater to pollution: A review and background paper for the Conference Workshop on Vulnerability Assessment, AGSO, 14(2/3), pp. 147–154, 1993.

Barber et al. (1993) subdivided the different approaches for predicting groundwater vulnerability into empirical, deterministic, probabilistic, and stochastic methods (Table 10.3). In empirical methods, maps of various physiographic attributes (e.g., geology, soils, depth to water table) of the region are combined and a numerical index or score is assigned to each attribute. This method is based on experiences and professional judgment. The simplest state of this method is that all attributes are assigned equal weights. Empirical methods that attempt to be more quantitative assign different numerical scores and weights to the attributes. The DRASTIC

method (Aller et al., 1987) is the best known example of the experimental method. This method will be explained later in this chapter.

Deterministic approaches use simplified analytical algorithms to arrive at a leaching potential index (LPI). The LPI is expressed in terms of pollutant velocity (V/R , where V is the average vadose zone percolation rate and R is the retardation factor), depth to the groundwater (z), and decay constant (x) such that:

$$\text{LPI} = 1000 \frac{V}{Rxz} \quad (10.32)$$

Probabilistic, numerical/stochastic modeling requires numerical solutions to mathematical equations. In stochastic methods, statistics is used to identify combinations of factors that determine vulnerability. These methods usually incorporate data on given areal contaminant distributions and determine the contaminant potential for a certain area from which data were drawn.

10.6.4.2 DRASTIC Method

All of the existing aquifer vulnerability assessment methods can be grouped into three major categories—overlay and index methods, process-based methods, and statistical methods (Anthony et al., 1998). These developed geographic information system (GIS) maps are useful as preliminary screening tools in setting the groundwater management strategies and for policy and decision-making on a regional scale.

GIS maps were developed on a regional scale by the National Well Water Association in conjunction with the EPA in the 1980s for evaluating the pollution potential of groundwater systems on a regional scale. The DRASTIC model follows the category of overlay and index methods. The aquifer vulnerability DRASTIC model is a standardized system that evaluates the groundwater pollution potential of hydrogeologic settings. DRASTIC is an acronym for the thematic maps required for the model.

The factors considered in DRASTIC are:

- Depth to water table
- Recharge (aquifer)
- Aquifer media
- Soil media
- Topography
- Impact of vadose zone media
- Conductivity (hydraulic) of the aquifer

The DRASTIC model defines ranges and ratings for the classes associated with each of the above thematic maps as well as weights for each thematic map. The significant media types/classes that have bearing on the vulnerability in each map are the ranges, which have associated ratings on a 1–10 scale. The relative importance of each of the above thematic maps on vulnerability is considered as its weight. These ratings and weights are used in obtaining the DRASTIC index, which is calculated as:

$$\text{DRASTIC Index} = D_r D_w + R_r R_w + A_r A_w + S_r S_w + T_r T_w + I_r I_w + C_r C_w \quad (10.33)$$

where:

D_r is the ratings for the depth to water table

D_w is the weight assigned to the depth to water table

R_r is the ratings for ranges of aquifer recharge

R_w is the weight for the aquifer recharge

A_r is the ratings assigned to the aquifer media

A_w is the weight assigned to the aquifer media

S_r is the ratings for the soil media

S_w is the weight for the soil media

T_r is the ratings for topography (slope)

T_w is the weight assigned to topography

I_r is the ratings assigned to the vadose zone

I_w is the weight assigned to the vadose zone

C_r is the ratings for rates of hydraulic conductivity

C_w is the weight given to hydraulic conductivity.

The greater the relative pollution potential, the higher the index that can be calculated. [Table 10.4](#) shows the typical weights for the DRASTIC factors for generic and pesticide models. The DRASTIC index can be converted into qualitative risk categories of low, moderate, high, and very high. GIS maps of the DRASTIC model showing the areas vulnerable to groundwater contamination for a region would have many potential uses, such as the implementation of the groundwater management strategies to prevent the degradation of the groundwater quality and to locate the groundwater monitoring systems (Delleur, 1999).

Example 10.5

This example gives an overview of applying the DRASTIC index to determine the groundwater vulnerability in the Rafsanjan subbasin. It is a part of the Daranjin basin and is located in an arid region in the central part of Iran (see [Figure 10.22](#)).

The annual average maximum and minimum temperatures are 37.6°C and 0.30°C, respectively. The average rainfall is about 87 (mm/year). About 99% of the total demands (agricultural and domestic demands) in the plain are supplied by

TABLE 10.4
Assigned Importance Weights for Factors in Two DRASTIC Models

| Depth to Water Table (D) | Net Recharge (R) | | | Aquifer Media (A) | | | Soil Media (S) | | | Topography (T) | | | Impact of the Vadose-Zone Media (I) | | | Hydraulic Conductivity (C) | | |
|--------------------------|-------------------------|-----------------|---------------|-------------------|-----------------|-----------------|----------------|-----------------|---------------|----------------|-----------------|---------------|-------------------------------------|---------------|-----------------|----------------------------|-----------------|--|
| | Generic Pesticide Model | Pesticide Model | Generic Model | Generic Model | Pesticide Model | Pesticide Model | Generic Model | Pesticide Model | Generic Model | Generic Model | Pesticide Model | Generic Model | Pesticide Model | Generic Model | Pesticide Model | Generic Model | Pesticide Model | |
| 5 | 5 | 4 | 4 | 3 | 3 | 2 | 5 | 5 | 1 | 3 | 5 | 5 | 4 | 3 | 3 | 2 | 2 | |

Source: Aller, L. T. et al., DRASTIC: A standardized system for evaluating groundwater pollution potential using hydrogeologic settings, EPA/600/2-85-018, USEPA, 641 p, 1987.

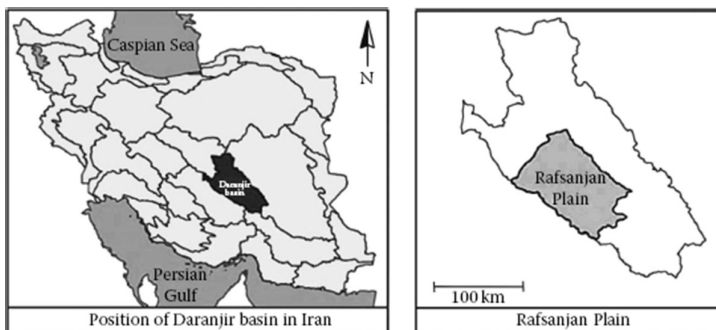


FIGURE 10.22 Position of the Daranjin basin and the Rafsanjan Plain.

TABLE 10.5
Water Supply and Demand Overview of Rafsanjan

| Supplied Water to Sectors | | Water Withdrawal from Resources | | | Groundwater Safe Yield |
|---------------------------|--------------|---------------------------------|---------------|---------|------------------------|
| Agriculture | Domestic | Groundwater | Surface Water | Total | |
| 711 MCM 98% | 14 MCM 2% | 720 MCM 99% | 4 MCM 1% | 725 MCM | 504 MCM |

the groundwater reservoirs (see [Table 10.5](#)). Each year, about 200 MCM of water is discharged, in excess of the aquifers safe yield. An annual average of 0.83 cm water drawdown has been reported over the last 10 years.

With the following data layers on the ArcView software, determine the aquifer sensitivity using the DRASTIC model: depth to aquifer, net recharge, aquifer media, soil media, topography, impact of the vadose zone, and hydraulic conductivity.

SOLUTION

The DRASTIC model for assessing the groundwater vulnerability requires seven criteria—depth to the water table, the recharge rates, aquifer permeability, the soil type, the topography, the impact of the vadose zone, and the conductivity of the vadose zone. DRASTIC evaluates the pollution potential based on a weighted combination of these hydrogeologic settings. Each factor is assigned a weight based on its relative significance in affecting the pollution potential. Each factor is further assigned a rating for different ranges of the values. The assigned importance weights for factors are derived from [Table 10.4](#).

The rating ranges are from 1 to 10, and the weights are from 1 to 5. The DRASTIC index is computed by a summation of the products of rating and weights for each factor (see [Equation 10.33](#)). The results for rating and evaluation of DRASTIC factors are shown in [Table 10.6](#) and [Figure 10.23](#). Each of these parameters is part of a weighted model, resulting in a map of relative sensitivity within the region with a rated scale of 1–10. Areas with a rating of 8, 9, or 10 are highly sensitive to contamination.

TABLE 10.6
Rating and Evaluation of DRASTIC Factors

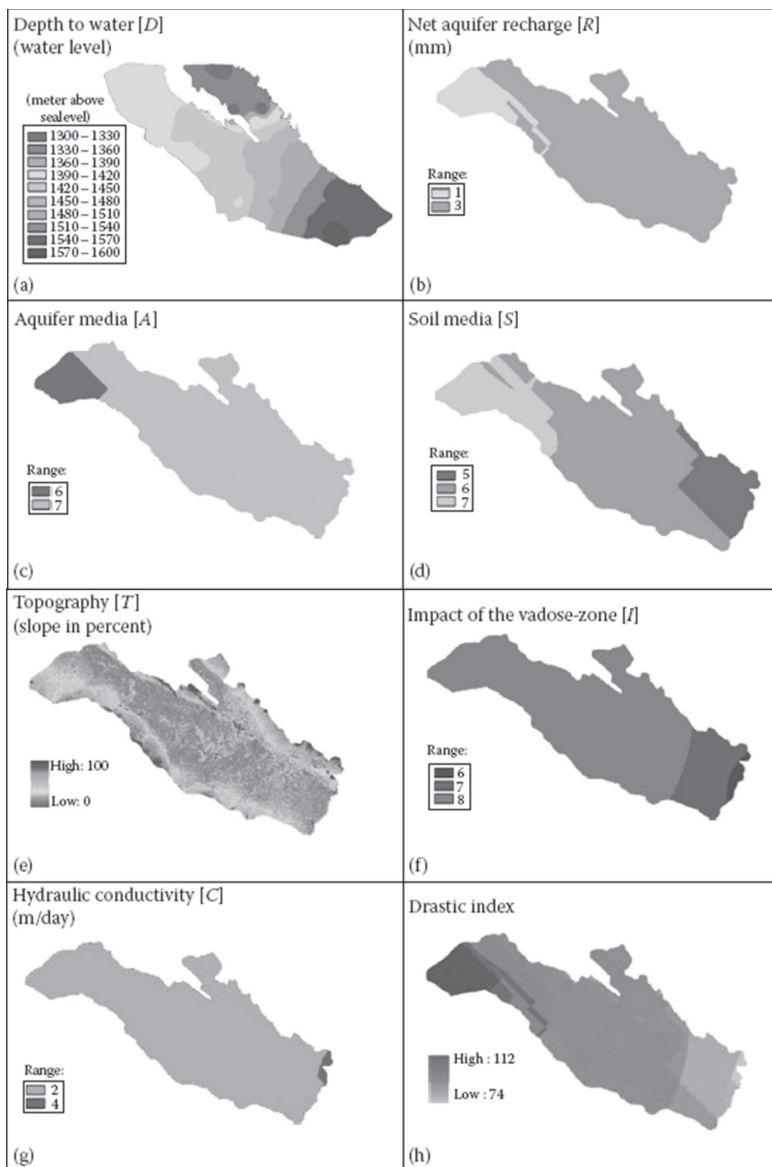


FIGURE 10.23 Variation of (a) depth of water, (b) net aquifer recharge, (c) aquifer media, (d) soil media, (e) topography, (f) impact of the vadose zone, (g) hydraulic conductivity, and (h) drastic index in the Rafsanjan plain.

10.6.5 CASE STUDY: DEVELOPMENT OF VULNERABILITY MAPS FOR A DROUGHT

Vulnerability is an important concept in natural hazards, including a drought (Klein et al., 2003). Vulnerability shows the likelihood of damages from hazards in a certain place by focusing on the system status prior to the disaster (Zhou et al., 2010).

East Azerbaijan Province, which consists of Aras, Sefidrood, and Urmia watersheds, is selected as a case study for a vulnerability assessment. This province consists of 19 counties with a total area of approximately 47,830 km². The data from 16 hydrological stations, including rain gauge stations and a groundwater level station, are used for the evaluation of vulnerability. In this case study, the development of a drought vulnerability map is discussed by extending the methodology utilized by Slejko et al. (2010). His study considers only five parameters: solar radiation, land use, evapotranspiration, soil water holding capacity, and irrigation areas. For the present purposes, ten parameters were selected which cover four important aspects of drought vulnerability. Precipitation, temperature, solar radiation, and potential evapotranspiration are the climate characteristics of the region; slope (topography) and soil type are considered as intrinsic characteristics of the region; surface storage, pumping value, and groundwater level represent the water resource characteristics; and land use is the reflection of the regional policies of human activity. The required data were obtained from Iran Meteorological Organization (<http://www.irimo.ir/far/>), Water Resources Management Company, and Iran Forests, Range, Watershed Management Organization (<http://www.wrm.ir/>). The data duration period for all parameters are from 2001 to 2011. The distribution of synoptic stations is represented in [Figure 10.24](#).

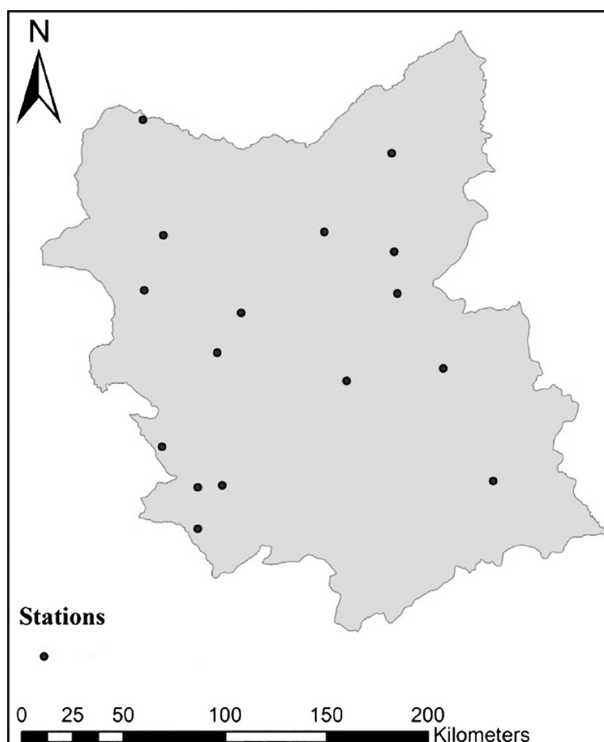


FIGURE 10.24 Distribution of synoptic stations in East Azerbaijan Province.

For each parameter, a category map was created using GIS, which shows the variability of that parameter in the region. This is done by obtaining the average variation of each parameter for 10 years (on a monthly basis), then their range of variation was divided into five classes, where each class was assigned a unique vulnerability value between 0 and 1. Then, a weight was assigned to each category map using an Analytical Hierarchy Process method, and finally all nine category maps were overlaid resulting in a drought vulnerability map. However, there are some drawbacks/limitations in this study that should be investigated further. The first limitation is the use of the average value, which does not show data variability, as a representative of the data. This is particularly important for parameters such as temperature. The second limitation is the way vulnerability values are assigned as a discrete value. Therefore, there will be a jump in vulnerability values just before and after the assigned ranges. This assumption was made to develop the methodology. It is apparent that for actual implementation of this study, this drawback should be rectified.

In [Figure 10.25](#), the variation of each parameter in the vulnerability assessment is shown. These maps were obtained using ArcGIS software. For each map, the variation is classified into five groups.

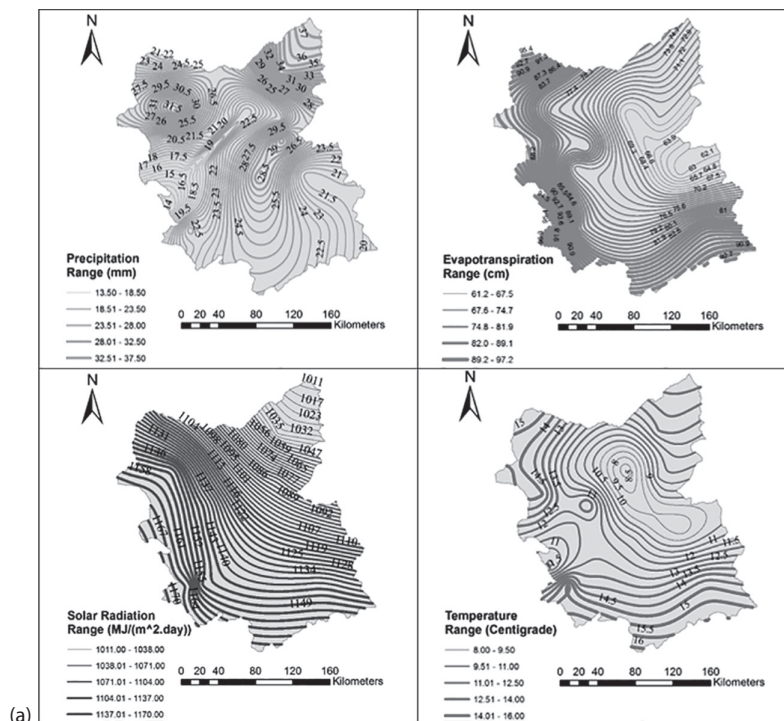


FIGURE 10.25 Variation map of the effective parameters in a drought vulnerability assessment: (a) climate characteristics of the region. *(Continued)*

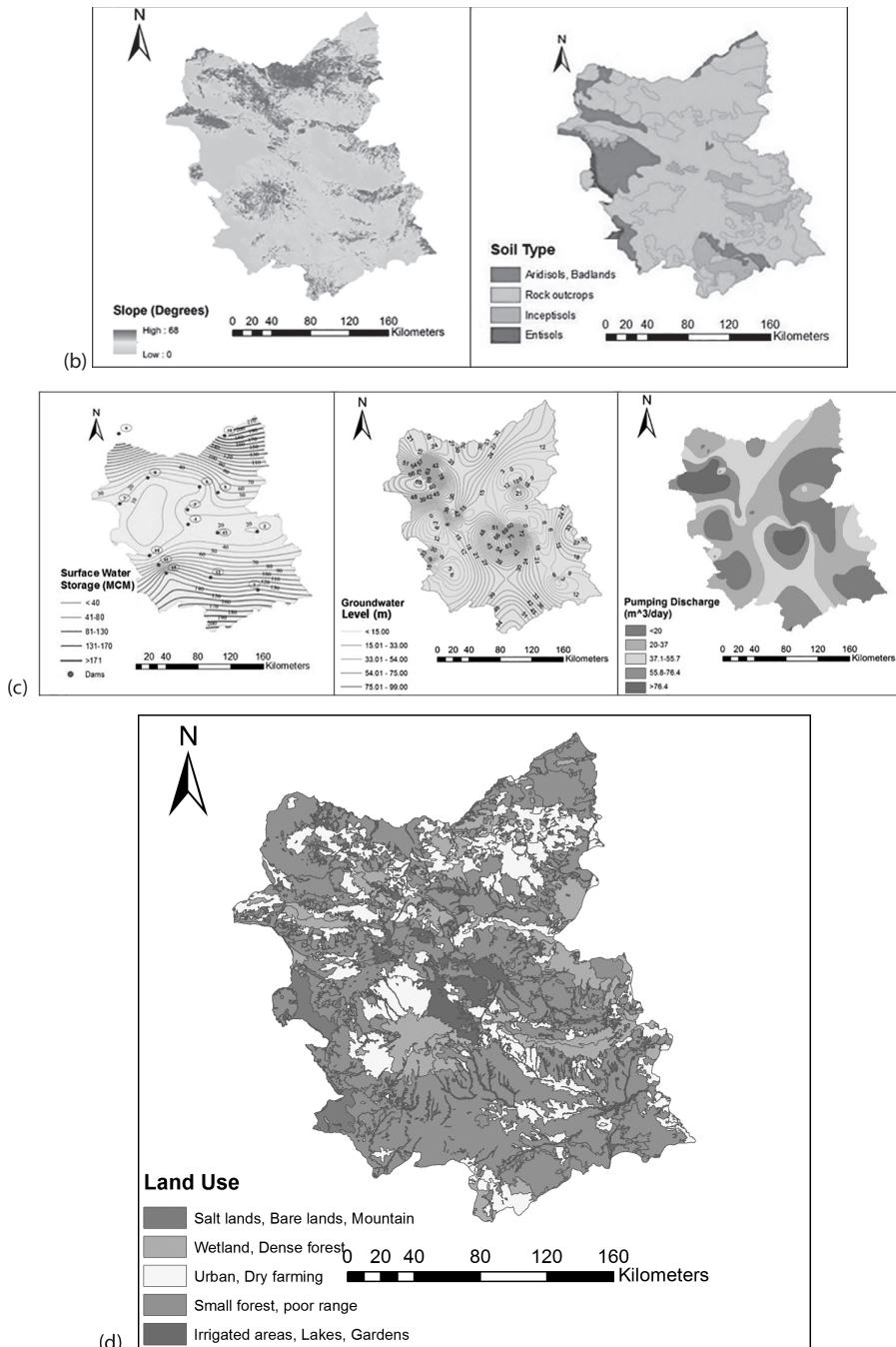


FIGURE 10.25 (Continued) Variation map of the effective parameters in a drought vulnerability assessment: (b) intrinsic characteristics of the region; (c) water resource characteristics; and (d) characteristics reflect the regional policies of human activity.

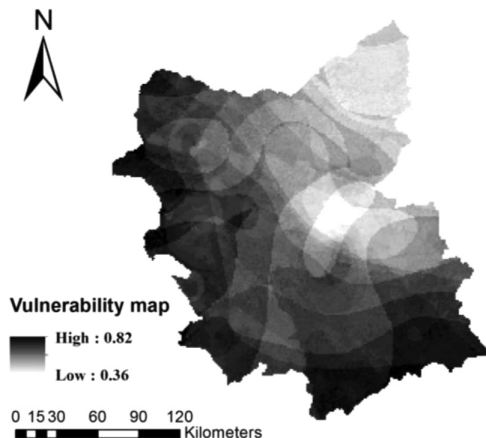


FIGURE 10.26 East Azerbaijan vulnerability map with some strategic points/cities.

Each map was weighted based on the importance of each parameter. The Analytical Hierarchy Process method, which uses experts' opinions, was applied for this task. The category map weights for precipitation, temperature, solar radiation, potential evapotranspiration (PET), slope, soil type, surface water storage, groundwater level, pumping value, and land use were obtained as 0.25, 0.15, 0.1, 0.1, 0.05, 0.05, 0.1, 0.1, 0.05, and 0.05, respectively. Finally, all ten category maps were overlaid to produce a vulnerability map for the region which is shown in [Figure 10.26](#). As can be seen, the vulnerability almost increases gradually from east to west. The western part has the highest vulnerability value (nearly 0.82). This part is next to Urmia Lake, which has lost most of its resources in recent decades from overuse. Therefore, the results seem reasonable as far as showing how the vulnerabilities go. On the other hand, the eastern part of the region shown in [Figure 10.26](#), particularly the northeastern part, has the lowest vulnerability value (0.36). Considering the fact that this region is near the Caspian Sea, with high levels of precipitation, the result seems reasonable.

It should be noted that most of the factors considered in the vulnerability evaluation are closely related to the inherent nature of the region. This means that these features cannot be changed easily. Therefore, a drought is to some extent inevitable. In other words, preventing a drought might not be possible. A good idea in managing this hazard would be to focus on the resiliency of the region, which shows how capable the region is of facing this hazard in a timely manner.

10.6.5.1 Summary

In this study, first a drought vulnerability map was created for East Azerbaijan based on ten parameters: precipitation, temperature, solar radiation, PET, slope, soil type, surface water storage, groundwater elevation, pumping value, and land use. For this purpose, each parameter was classified into five groups and their spatial distributions were mapped in GIS to show the variability of the given parameter. Maps were weighted and then overlaid to provide a drought vulnerability map. The results

showed that the western parts of the region are more vulnerable to drought and so more resources and strategies should be implemented in those parts of the region for drought preparedness. It should be noted that this approach is site-specific, and the vulnerability values should be recalculated for a new location.

PROBLEMS

- 10.1** The concentration of a toxic chemical in an aquifer is 9.8 mg/L. This aquifer is being used as the source of drinking water. Assume that the average weight of adult women in the area is 60 kg and they drink 1.5 L of water per day, determine the total amount of the chemical that an adult woman may intake after 25 years and the chronic daily intake.
- 10.2** Construct the CDF of failure occurrences in two hazard rate situations. (1) $\rho(t) = ta$ and (2) $\rho(t) = e^{t-1}$.
- 10.3** Calculate the reliability of the water supply system shown in [Figure 10.27](#) at $t = 0.5$ using reliability functions of system components.
- 10.4** Calculate the reliability of the water supply system shown in [Figure 10.28](#) at $t = 0.1$ assuming that $R_1(t) = R_4(t) = e^{-2t}$ and $R_2^i(t) = R_3^j(t) = R_5^l(t) = R_6^m(t) = e^{-t}$, $(1 \leq i \leq 2; 1 \leq j \leq 3; 1 \leq l \leq 3; 1 \leq m \leq 2)$.
- 10.5** TDS concentration data of removed water from a well is presented in [Table 10.7](#). The standard value of the TDS concentration in this region is considered as 1400 (mg/L). Calculate the reliability, resiliency, and vulnerability of the water quality requirement.
- 10.6** The monthly water withdrawals from an aquifer and monthly water demand during three years are presented in [Table 10.8](#). Calculate the reliability, resiliency, and vulnerability of this aquifer of water supply.

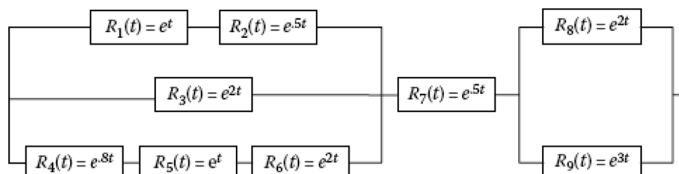


FIGURE 10.27 Water supply system in Problem 10.3.

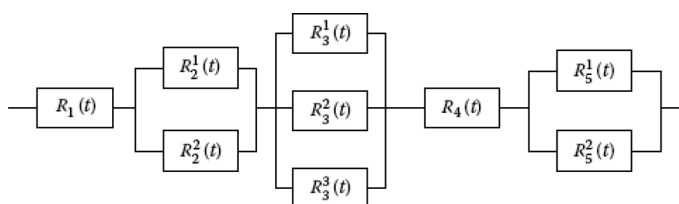


FIGURE 10.28 Water supply system in Problem 10.4.

TABLE 10.7
TDS Concentration of Removed Water from a Well (mg/L)

| | Year 1 | Year 2 | Year 3 | Year 4 |
|-----------|--------|--------|--------|--------|
| January | 1505 | 1422 | 1230 | 1556 |
| February | 1215 | 1498 | 1409 | 1545 |
| March | 1559 | 1410 | 1371 | 1316 |
| April | 1244 | 1526 | 1449 | 1600 |
| May | 1532 | 1210 | 1574 | 1486 |
| Jun | 1260 | 1468 | 1387 | 1549 |
| July | 1480 | 1300 | 1206 | 1317 |
| August | 1228 | 1549 | 1472 | 1275 |
| September | 1312 | 1360 | 1487 | 1300 |
| October | 1574 | 1319 | 1406 | 1539 |
| November | 1309 | 1200 | 1568 | 1491 |
| December | 1468 | 1438 | 1271 | 1506 |

TABLE 10.8
Water Release and Water Demand During Three Years (MCM)

| | Water Release | | Water Demand | |
|-----------|---------------|----|--------------|----|
| January | 8 | 8 | 8 | 10 |
| February | 7 | 6 | 5 | 11 |
| March | 7 | 7 | 6 | 12 |
| April | 8 | 9 | 5 | 12 |
| May | 10 | 10 | 7 | 13 |
| Jun | 11 | 11 | 9 | 12 |
| July | 10 | 9 | 10 | 11 |
| August | 12 | 10 | 12 | 9 |
| September | 13 | 12 | 11 | 7 |
| October | 10 | 8 | 9 | 8 |
| November | 12 | 10 | 11 | 9 |
| December | 11 | 11 | 10 | 9 |

- 10.7** Consider an aquifer with 30 m thickness. The water table in the aquifer is 2 m below the ground surface. After pumping, the water level dropped 5 m in the aquifer. Compute the approximate land subsidence using the following data: $\gamma_s = 25.3 \text{ kN/m}^3$ and $\gamma_w = 9.81 \text{ kN/m}^3$, $n = 0.25$, $E = 980 \text{ N/cm}^2$, and $\theta = 0.04$.
- 10.8** Using GIS data layers of depth to aquifer, net recharge, aquifer media, soil media, topography, impact of vadose zone, and hydraulic conductivity in your region, determine the aquifer vulnerability using the DRASTIC model.

REFERENCES

- Aller, L.T., Bennet, T., Lehr, J.H., and Petty, R.J. 1987. *DRASTIC: A Standardized System for Evaluating Groundwater Pollution Potential Using Hydrogeologic Settings*. EPA/600/2-85-018, USEPA, Washington, DC, 641 p.
- Anthony, J.T., Emily, L.I., and Frank, D.V. 1998. Assessing groundwater vulnerability using logistic regression, in *Proceedings for the Source Water Assessment and Protection 98 Conference*, Dallas, TX, 1998, pp. 157–165.
- Bachmat, Y. and Colin M. 1987. Mapping to assess groundwater vulnerability to pollution, in *Proceeding of the Conference on Vulnerability of Soil and Groundwater to Pollutants*. W. van Duijvenbooden & H. C. T. van Walgeningh eds. National Institute for Public Health and Environmental Hygiene, the Hague, the Netherlands, 1987.
- Banton, O. and Villeneuve, J.-P. 1989. Evaluation of groundwater vulnerability to pesticides: A comparison between the pesticide DRASTIC index and the PRJZM leaching quantities. *Journal of Contaminant Hydrology*, 4, 285–296.
- Barber, C., Bates, L.E., Barren, R., and Allison, H. 1993. Assessment of the relative vulnerability of groundwater to pollution: A review and background paper for the Conference Workshop on Vulnerability Assessment, AGSO, 14(2/3), 147–154.
- Conway, R. A. 1982. Introduction to environmental risk analysis, Chapter 1, in *Environmental Risk Analysis for Chemicals*, R.A. Conway, ed. Van Nostrand Reinhold Company, New York, pp. 1–30.
- Cornaby, B. W. et al. 1982. Application of environmental risk techniques to uncontrolled hazardous waste sites, in *Proceedings of the National Conference on Management of Uncontrolled Hazardous Waste Sites*, Hazardous Materials Control Research Institute, Silver Spring, MD, pp. 380–384.
- Crump, K. S. 1984. A new method for determining allowable daily intakes. *Fundamental and Applied Toxicology*, 4, 854–871.
- Davies, J., Coffing, J., Robins, N. S., Kulubanga, G. H., Mandowa, W., and Hankin, P. 2002. Development of a curriculum and training of supervision teams in borehole construction in Malawi. Nottingham, UK, British Geological Survey Internal Report CR/02/219N.
- De Bruijn, K.M. and Klijn, F. 2001. Resilient flood risk management strategies, in *Proceedings of the IAHR Congress*, Beijing, China, September 16–21, L. Guifen and L. Wenzxue eds., Tsinghua University Press, Beijing, China, pp. 450–457.
- Delleur, J.W. 1999. *The Handbook of Groundwater Engineering*. CRC Press/Springer-Verlag, Boca Raton, FL.
- Dooge, J. 2004. *Ethics of Water Related Disasters*. Series on Water and Ethics, Essay 9. UNESCO, France, Paris.
- Ehteshami, M., Peralta, R.C., Eisele, H., Dear, H., and Tindalt, T. 1991. Assessing groundwater pesticide contamination to groundwater: A rapid approach. *Ground Water*, 29, 862–868.
- Federal Emergency Management Agency (FEMA). 2008. <http://www.fema.gov/library>.
- Foster, S.S.D. 1987. Fundamental concepts in aquifer vulnerability, pollution risk and protection strategy, in *Proceeding of Conference on Vulnerability of Soil and Groundwater to Pollutants*. W. van Duijvenbooden & H. G. van Walgeningh eds., National Institute of Public Health and Environmental Hygiene, the Hague, the Netherlands.
- Hashimoto, T., Stedinger, J.R., and Loucks, D.P. 1982. Reliability, resiliency and vulnerability criteria for water resources performance evaluation. *Journal of Water Resources Research*, 18(1), 14–20.
- Holling, C.S. 1973. Resilience and stability of ecological systems. *Annual Review of Ecology and Systematic*, 4, 1–24.

- Jeggle, T. 2005. Introduction to risk assessment process, in *Disaster Prevention and Reduction*, J. Vrba & A. R. Salamat eds. Czech University of Agriculture, Prague, Czech Republic, CD ROM 9 p.
- Karamouz, M. 2002. Decision support system and drought management in Lorestan Province. Final Report to Lorestan Water Board, Iran.
- Karamouz, M., Szidarovszky, F., and Zahraie, B. 2003. *Water Resources Systems Analysis*. Lewis Publishers, CRC Publishing, Boca Raton, FL.
- Karamouz, M., Torabi, S., and Araghi Nejad, S. 2004. Analysis of hydrologic and agricultural droughts in central part of Iran. *ASCE, Journal of Hydrologic Engineering*, 9(5), 402–414.
- Karamouz, M., Moridi, A., and Nazif, S. 2010. *Urban Water Engineering and Management*, CRC Press, Boca Raton, FL, 628 p.
- Keshari, A.K., Ramanathan, A., and Neupane, B. 2006. Impact of the 26-12-2004 tsunami on Indian coastal groundwater and emergency remediation strategy, in *Groundwater for Emergency Situations*. IHP-VI, Series on Groundwater (12). J. Vrba & B. T. Verhagen, eds., UNESCO, Paris, France, pp. 80–85.
- Klein, R.J., Nicholls, R. J., and Thomalla, F. 2003. Resilience to natural hazards: How useful is this concept? *Global Environ. Change Part B Environ. Hazards*, 5(1), 35–45.
- Le Grande, H. E. 1983. A standardised system for evaluating waste disposal sites, National Water Well Association, Worthington, OH.
- Lee, W.W. and Nair, K. 1979. Risk quantification and risk evaluation, in *Proceedings of National Conference on Hazardous Material Risk Assessment, Disposal and Management*. Information Transfer, Silver Spring, MD, pp. 44–48.
- Lorber, M.N., Cohen, S.Z., Noren, S.E., and De Buchannanne, G.D. 1989. A national evaluation of leaching potential of Aldicarb, Pt 1 An integrated assessment methodology *Groundwater Monitoring Review*, 9(4), 109–125.
- Margat, J., Foster, S., and Loucks, P. 2006. *Non-Renewable Groundwater Resources: A Guidebook on Socially-Sustainable Management for Water Policy-Makers IHP-VI, Series on Groundwater*. UNESCO, Paris, France, p. 10.
- Masters, G.M. and Ela, W. P. 2008. *Introduction to Environmental Engineering and Science*. Prentice Hall, Simon and Schuster, Englewood Cliffs, NJ, 576 p.
- McTernan, W.F. and Kaplan, E. 1990. *Risk Assessment for Groundwater Pollution Control*. Task Committee, Committee on Water Pollution Management, American Society of Civil Engineers, New York, 368 p.
- Meeks, Y.J. and Dean, J.D. 1990. Evaluating groundwater vulnerability to pesticides. *Journal of Water Resources Planning and Management*, 116, 693–707.
- National Research Council (NRC). 1983. *Risk Assessment in the Federal Government: Managing the Process*, National Academy Press, Washington, DC.
- National Research Council (NRC). 1993. *Groundwater Vulnerability Assessment: Predicting Relative Contaminant Potential under Conditions of Uncertainty*, National Academy Press, Washington, DC, 193 p.
- National Rivers Authority (NRA). 1992. *Policy and Practice for the Protection of Groundwater*. HMSO, London, UK, 52 p.
- Oregon Department of Environmental Quality. 1991. UST Clean-up Manual: Clean-up rules for leaking petroleum UST systems and numeric soil clean-up levels for motor fuel and heating oil July 1991, Oregon Department of Environmental Quality, Portland, OR.
- Pimm, S. L. 1991. *The Balance of Nature? Ecological Issues in the Conservation of Species and Communities*, University of Chicago Press, Chicago, IL.
- Scharp, C. 1999. Strategic groundwater protection—A systematic approach. PhD dissertation, Royal Institute of Technology, Stockholm, Sweden, 48 p.

- Schweitzer, G.E. 1981. Risk assessment near uncontrolled hazardous waste sites: Role of monitoring data, in *Proceedings of the National Conference on Management of Uncontrolled Hazardous Waste Sites*. Hazardous Materials Control Research Institute, Silver Spring, MD, pp. 238–247.
- Sililo, O.T.N. and Saayman, I.C. 2001. *Groundwater Vulnerability to Pollution in Urban Catchments*. The Water Program Division of Water, Environment and Technology CSIR, University of Cape Town, Cape Town, South Africa.
- Sine. 2004a. *Water for People Water for Life—The United Nations World Water Development Report, Part IV: Management Challenges: Stewardship and Governance*, 11 Mitigating Risk and Coping with Uncertainty. UNESCO, Paris, France, 290 p.
- Sine. 2004b. *Living with Risk: A Global Review of Disaster Reduction Initiatives*. ISDR, C. D., 2004 version, Geneva, Switzerland, 429 p.
- Slejko, M., Gregoric, G., Bergant, K. and Stanic, S. 2010. Assessing and mapping drought vulnerability in agricultural systems—a case study for Slovenia. *10th European Conference on Applications of Meteorology (ECAM)*, Zürich, Switzerland. <http://meetings.copernicus.org/ems2010/>, id. EMS2010-586.
- Sommer, T.H. 2006. Groundwater management—a part of flood risk management, in *Proceedings of the International Workshop Groundwater for Emergency Situations*, Tehran, Iran, October 29–31.
- Sommer, T.H. and Ullrich, K. 2005. Influence of flood event 2002 on groundwater Research Report (in German). Environmental Office, City of Dresden, Germany, 68 p.
- Steinemann, A., Hayes, M.J., and Cavalcanti, L. 2005. Drought indicators and triggers, in *Drought and Water Crises: Science, Technology, and Management Issues*. D. Wilhite, ed., Marcel Dekker, New York.
- Tallaksen, L.M. and van Lanen, H.A.J. 2004. Hydrological drought, in *Processes and Estimation Methods for Streamflow and Groundwater*, Development in Water Science 48, Elsevier, the Netherlands, 579 p.
- Teso, R.R., Younglove, T., Peterson, M.R., Sheeks, D.L., and Gallavan, R.E. 1989. Soil taxonomy and surveys: Classification of aerial sensitivity to pesticide contamination of groundwater *Journal of Soil and Water Conservation*, 43(4), 1348–1352.
- Toshimaru, N. 1998. Are you prepared? Learning from the Great Hanshin-Awaji earthquake disaster, in *Handbook for Disaster Reduction and Volunteer Activities Hyogo University*, Kakogawa, Hyogo, Japan.
- USEPA. 1986. Quality criteria for water 1986. EPA 440/5-86-001, Washington, DC.
- Van Lanen, H.A.J. and Peters, E. 2000. Definition, effects and assessment of groundwater droughts, in *Drought and Drought Mitigation in Europe*. J. V. Vogt and F. Somma eds., Kluwer Academic Publishers, Dordrecht, the Netherlands, pp. 49–61.
- Verhagen, B.T. 2006. Drought: Identification, investigation, planning and risk management, in *Proceedings of the International Workshop Groundwater for Emergency Situations*, Tehran, Iran, October 29–31.
- Villeneuve, J.-P., Banton, O., and LaFrance, P. 1990. A probabilistic approach for assessing groundwater vulnerability to contamination by pesticides: The VULPEST model. *Ecological Modelling*, 51, 47–58.
- Vrba, J. 2006. Groundwater for emergency situations—UNESCO-IHP VI Project, in *Proceedings of the International Workshop Groundwater for Emergency Situations*, Tehran, Iran, October 29–31.
- Yazdi, A.A.S. and Khaneiki, M.L. 2006. The drought of 2001 and the measures taken by Yazd regional water authority, in *Proceedings of the International Workshop Groundwater for Emergency Situations*, Tehran, Iran, October 29–31.
- Zhou, H., Wan, J., and Jia, H. 2010. Resilience to natural hazards: A geographic perspective. *Nat. Hazards*, 53(1), 21–41.



Taylor & Francis

Taylor & Francis Group

<http://taylorandfrancis.com>

11 Climate Change Impacts on Groundwater

11.1 INTRODUCTION

Increasing water demand for different activities such as agriculture, industry, habitants use, and recreational water leads to a scarcity of clean and safe drinking water in many regions of the world. In addition, human activities play an important role in climate change, affecting global water resources. An increase in the emission of greenhouse gases (GHGs), as well as changes in land cover due to urbanization, desertification, and deforestation, has already affected the earth's climate and, therefore, will have an impact on the hydrologic cycle in the future (IPCC, 2001).

The management of groundwater as an important sustainable development has not been considered properly, and it has resulted in the depletion and degradation of this resource. Without proactive governance, the damaging effects of defective management will surpass the social gains made so far (Mukherji and Shah, 2005). In addition, long-term replenishment of groundwater resources is controlled by long-term climate conditions. Therefore, the proper mitigation and adaptation to the negative impacts of climate change on groundwater are proposed by groundwater management. It is necessary to maintain the particular resilience of larger aquifers as a buffer for climate change and contingency supply capabilities as well as for adequate water quality for human consumption. Studies predicting the climate for different intervals point toward changes in the future climate, which in turn will influence regional hydrological cycles and, consequently, the quantity and quality of regional water resources (Gleick, 1989). These changes should be considered in terms of their impact both directly and indirectly. In fact, variations in major long-term climate variables such as air temperature, precipitation, and evapotranspiration will have a direct impact on changes in groundwater levels, reserves, and quality. For instance, some climate change impacts such as variability of precipitation may add to the existing pressure on groundwater resources to fill eventual gaps in surface water availability. In vulnerable areas, impacts on the groundwater resources may render the only available reserved freshwater unavailable or unsuitable for use in the near future (IPCC, 2007b). Direct interaction of groundwater with surface water resources, such as lakes and rivers, expresses another aspect of the direct relationship between groundwater resources and climate change. Climate change will influence groundwater indirectly through the recharge process with water extracted from aquifers and by impeding recharge capacities in some areas. All these impacts would alter hydrological systems, regional land use, and agricultural practices. Therefore, two important factors, credible prediction of changes in the major climatic variables and precise estimation of groundwater recharge, should be done to cope with potential impacts of climate change on the groundwater.

Groundwater is vulnerable to a number of threats, including climate change and pollution. Protecting it from these threats is vital. A physical approach is required to estimate the impact of changes in climatic parameters on groundwater recharge. Temporal variation and its impact on the hydrologic cycle as well as spatial variation of surface and subsurface properties should be considered.

11.2 CLIMATE CHANGE

Climate is the accumulation of elements such as daily and seasonal weather conditions over a long period of time at a location or in a region. It includes average weather conditions, as well as the variability of elements and includes the occurrence of extreme events (Lutgens and Tarbuck, 1995). Humidity, air temperature and pressure, wind speed and direction, cloud cover and type, and the amount and form of precipitation are all basic elements which influence the atmospheric characteristics of climate and weather. These elements establish the variables by which weather patterns and climatic types are described. The time scale is the main difference between weather and climate. Climate is the trends in weather patterns over an extended period of time, not days, or weeks, or months, but years. Indeed, weather changes create almost diverse weather conditions at any given time and place. As a broad definition, a climate system is an interactive system consisting of five major components: the atmosphere, land surface, hydrosphere, biosphere, and cryosphere, or snow and ice. [Figure 11.1](#) shows the components of a global climate system which includes their process and interaction.

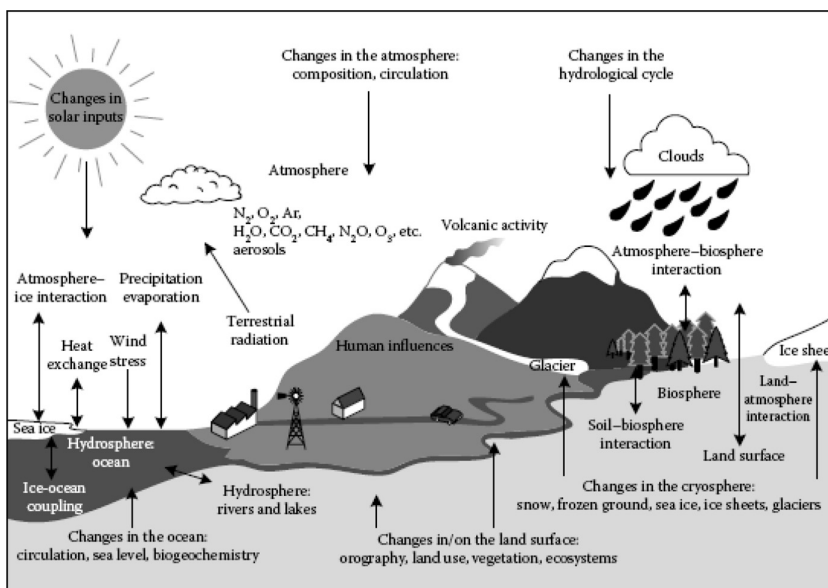


FIGURE 11.1 Components of the global climate system. (From Intergovernmental Panel on Climate Change (IPCC), *Clim. Change*, 2001: The scientific basis, <http://www.ipcc.ch>, 2001.)

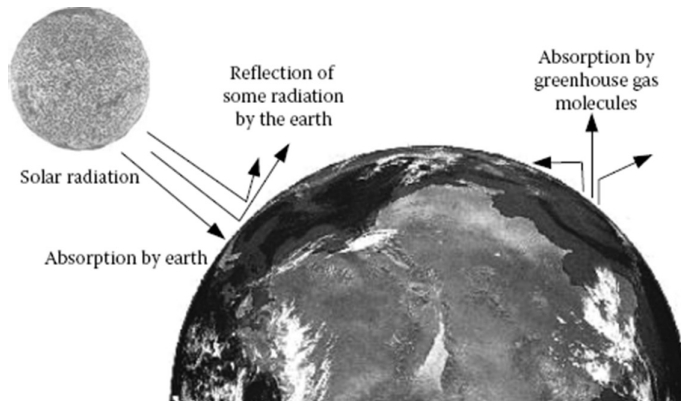


FIGURE 11.2 The greenhouse effect.

These five major components are influenced by changes in various external factors that affect climate such as volcanic eruptions and solar variations. Solar radiation powers the climate system. It passes through the clear atmosphere. Some parts of the sunlight are absorbed by the earth's surface and atmosphere. The other part is reflected back to space, where most of it is absorbed by GHGs (see Figure 11.2). The most important GHGs are water vapor and carbon dioxide. Without the existence of these gases, the earth would be cold. But if the greenhouse effect becomes stronger, it will make the earth warmer than usual. Consequently, in both conditions, living would be impossible.

The greenhouse effect is caused by slow changes in the earth's orbit around the sun or the change in sunlight absorption by the atmosphere due to the increased concentration of GHGs (Mitchell, 1989; Mitchell et al., 1995). The impact of the greenhouse effect depends upon the composition of certain gases in the atmosphere such as water vapor, carbon dioxide, nitrous oxide, and methane. These gases increase global temperature and related climate changes such as evaporation and precipitation (EPA, 2007a). Generally, some other factors which may lead to the greenhouse effect include natural processes within the climate system such as changes in ocean circulation, and human activities such as burning fossil fuels, urbanization, and deforestation, which change the atmosphere's composition and land surface. Generally, all these factors affect the hydrological cycle and, consequently, influence water-storage patterns that exchange among aquifers, streams, rivers, and lakes. Climate change can also have an important impact on the organisms living in surface water aquatic systems and groundwater-dependent ecosystems (see Firth and Fisher, 1992; Fisher and Grime, 1996). As a result, considering climate change as an important factor influencing water resources will be necessary.

11.3 CLIMATE CHANGE IMPACTS ON HYDROLOGICAL CYCLE

The hydrological cycle begins with evaporation from the surface of the ocean or land and continues as air carries the water vapor to locations where it forms clouds and eventually precipitates out. It then continues when the precipitation is either absorbed into the ground or runs off to the ocean, ready to begin the cycle again in an

endless loop. The amount of time needed for the groundwater to recharge can vary with the amount or intensity of precipitation.

Altered precipitation, evapotranspiration, and soil moisture patterns defined as climate change have extreme effects on the hydrological cycle. Since the Industrial Revolution, carbon dioxide concentration in the atmosphere has increased, the continuation of which may meaningfully change global and local temperature and precipitation. Because of the unequal distribution of external precipitation around the globe, a decline in the amount of precipitation in some regions may occur, or the timing of wet and dry seasons may alter significantly. Therefore, information on the local or regional impacts of climate change on hydrological processes and coastal water resources is becoming more important. The key changes to the hydrological cycle associated with greenhouse effects were identified by Prof. Andrew Goudie of Oxford University, which include changes in seasonal patterns and intensity of precipitation under different conditions; changes in snow and rainfall shares of precipitation; an increase in evapotranspiration and decrease in soil moisture; an increase in the extent of saltwater intrusion; changes in land cover due to changes in precipitation and temperature; sea-level rise due to melting glacial ice, a decrease in water density and, consequently, an increase in coastal inundation and wetland loss; an increase in the probability of the occurrence of fire; a decrease in transpiration, and an increase in water-use efficiency due to the impacts of CO₂ on plant physiology. Figure 11.3 presents different aspects of climate change impacts on water resources.

11.3.1 FLOODS AND DROUGHTS

In response to global warming, the average volume of runoff will intensify considerably. Indeed, a rising in temperature due to the greenhouse effects leads to an

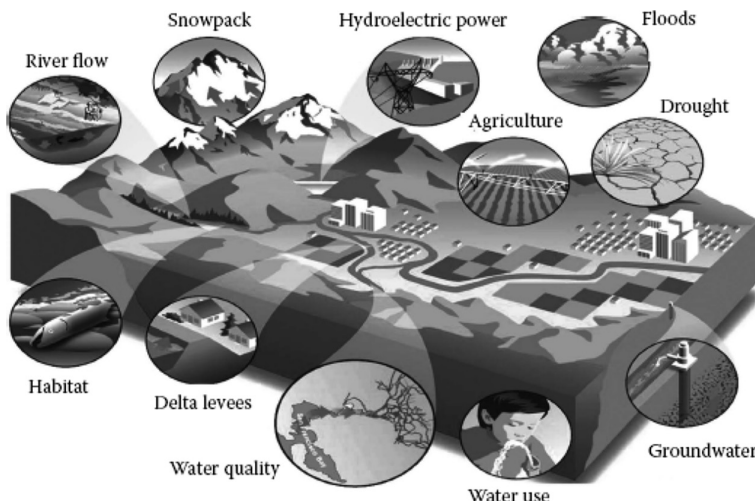


FIGURE 11.3 Different impacts of climate change on hydrological cycle components. (California Department of Water Resource, *Climate Change in California*, CA, <http://www.water.ca.gov/>, 2007.)

increase in evaporation, in the intensity of the water cycling process, and, consequently, causes a high amount of moisture in the air. As a result, the increase in the magnitude and frequency of weather events such as precipitation in tropical storms increases the severity of hydrological extremes such as the variability of streamflows, risk of floods and droughts occurrence, and erosion due to a high velocity of flow. An increase in flood frequencies may increase groundwater recharge in some flood-plains, and also could increase the release of urban and agricultural waste into the groundwater systems, and affect the groundwater quality of aquifers.

On the other hand, in some regions, the precipitation intensity will decrease with the expected climatic changes during the twenty-first century and, therefore, droughts in these regions will grow longer in duration, which could imperil species, put harvests at risk, and decrease food production. Wigley and Jones (1985) used a simple water-balance model to conclude that runoff is the most sensitive to climate changes, and changes in precipitation have more impact on runoff changes than the changes in evaporation. Also, the relative change in runoff is always greater than that in precipitation.

In addition, as a consequence of drought, the level of groundwater development will change unexpectedly and constantly. In fact, use of the groundwater resources to mitigate drought impacts is one of the most effective advance planning strategies for that purpose. Droughts can also have an impact on water levels in aquifers because of the decrease in rainfall intensity, increase in evaporation, and a decline in percolation.

11.3.2 AGRICULTURAL DROUGHTS

One aspect of drought impacts is crop damage, which depends upon the climatic changes, and agriculture is the first economic subdivision affected by droughts. Considering the relationship between the harvest and water shortage is the way to assess agricultural droughts. The lack of moisture to support the average crop yield on a farm results in agricultural droughts. It can also be a result of a long period of low precipitation and/or the type of water usage. Other climatic factors such as high temperature, high wind, and low relative humidity are related to droughts in many regions of the world, and as mentioned before, climate change globally causes these variations and can influence local agriculture. Moreover, agriculture uses a large amount of groundwater in the world. The development of tube wells due to agricultural droughts shows the increasing dependency of agriculture on groundwater. Agricultural development has increased recharge, which has led to higher salinity levels in the groundwater. In addition, soil moisture decline and agricultural drought will impact the groundwater recharge.

11.3.3 WATER USE

Potential changes in climate factors such as temperature and precipitation could affect the water use and water resource availability. Under these impacts, demand management, resource expansion, and changes in resource management play significant roles to satisfy demand. Some aspects of climate change such as changes in the frequency

and severity of flood and drought events, and higher temperatures, increased evaporation, and wildfires reduce water availability for humans and ecosystems. Globally, one-third of the population depends on the groundwater for their drinking water. Therefore, the groundwater, particularly in coastal aquifers, is used to complement available surface water supplies.

11.3.4 WATER QUALITY

Climate change is expected to have significant impacts on the water quality. As mentioned in [Section 11.3.1](#), severe floods due to climatic change transport pollutants into water bodies, overload storm and sewage systems, damnify wastewater treatment devices, and increase the risks of water pollution. In addition, the water quality is influenced by temperature and water amount. Warmer air temperature will result in warmer waters with decreased dissolved oxygen levels, which can endanger aquatic ecosystems. More frequent intensive precipitation events will also release more contaminants and sediments into lakes and rivers and result in declining quality in both surface water and groundwater resources. Global warming also increases the melting rate of snow and contributes to sea-level rise which affects the groundwater quality. This will cause saltwater intrusion, particularly in coastal aquifers, with the amount of intrusion depending upon the local groundwater gradients.

11.3.5 HABITAT

Global warming threatens habitats, and it is difficult for plants and animals to keep up with the rapid changes in their habitats. Some species such as polar bears, trout, and salmon are especially being adversely affected by global warming. It is likely that through direct energy transfer from the atmosphere, climate change will affect lake, reservoir, and stream temperatures. In temperatures higher than their biologic threshold, some species such as salmon and trout will be endangered. Decreased dissolved oxygen that resulted from higher temperatures increase metabolic rates, and result in the decline of the salmon's resistance to pests. In addition, warmer temperatures can increase the infection rate or vulnerability of fish to illness. Changes in temperature regimes also affect ice cover, and result in sea-level rise which leads to the flooding of low-lying areas. This is likely to imperil the riparian habitats and to inundate some agricultural lands on riverbanks. Moreover, groundwater pumping affects the riparian habitat when it causes the water table to drop beyond the reach of riparian plants.

11.3.6 HYDROELECTRIC POWER

The amount of electricity produced by hydroelectric generation and the timing of power production can highly be influenced by climate change. Changes in the magnitude and timing of the river flows, together with a high evaporation from reservoirs will have adverse effects on hydroelectric power production. Hydroelectric

generation is more sensitive to changes in the river flows than other types of water systems. As a consequence, the reduction in hydroelectric generation may significantly be more than the reduction in the river flow.

In addition to the electricity supply, climate change will also affect the electricity demand. In higher temperatures, summer cooling demands will increase. Since the hydroelectric generation is a form of water use, the higher demands for hydroelectric power production will be translated to higher water usage.

11.3.7 SNOWPACK

Climate change results in general changes in snowpack and snow cover. The temperature affects the winter snowfall and, consequently, the magnitude of accumulated snowpack in complex ways. The increasing temperature contributes to a higher moisture availability and total precipitation, and then greater snow accumulation, but if temperatures increase intensely, the snowmelt will increase and, consequently, the snowpack will be reduced.

As a result, the reduced snowpack and earlier spring snowmelt influence other hydrologic variables such as the amount and timing of the runoff, evapotranspiration, and soil moisture (Hamlet et al., 2007; Moore et al., 2007). Additionally, the surface water supplies depending upon the snowmelt will be influenced by changes in the intensity of the precipitation. The precipitation shift from snow to rain, changes in the snow accumulation, and the earlier snow melting will affect the amount and timing of the water supply availability, which will impact the groundwater recharge. During the snowmelt, the soils are frozen, the upland infiltration is reduced, and the snowmelt water mostly runs off. The characteristics of the groundwater basin and soil moisture conditions affect the interaction between the infiltrating snowmelt water and streamflow.

11.3.8 RIVER FLOW

Climate change affects streamflow timing through the changes in snowmelt timing due to the higher temperatures and the changes in the amount of precipitation. Changes in the onset or duration of the rainy seasons can affect the river flow. A lot of hydrological studies have been conducted to assess the impacts of climate change on the streamflow and runoff. Changes in evaporation and precipitation will alter the variation of streamflow. Intensified streamflows and changes in the soil moisture will affect the infiltration rates. This change can influence the groundwater recharge.

11.4 GENERAL CLIMATE CHANGE IMPACTS ON GROUNDWATER

The potential impacts of climate change on the water resources have been recognized for some decades, but there has been little research relating to the groundwater (IPCC, 2001). The groundwater plays a pivotal role in the economy of developing countries, especially in arid and semiarid regions, and restricting access to this source leads to impaired development. In these regions agriculture and industry also depend

on the groundwater, so guidelines of coping with their development must incorporate the impacts of climate change on the groundwater resources. Stuyt (1995) simulated the effect of sea-level rise and climate change on the groundwater salinity and agro-hydrology in a low coastal region of the Netherlands. As a result, simulated crop growth was increased significantly by the temperature and CO₂ increase, without an increase in the demand for irrigation. Jacob et al. (2001) studied the impacts of climate change on the groundwater quality and quantity in the United States. Different aspects including the agricultural chemicals, wastewater treatment, industrial pollution, and saltwater intrusion in coastal aquifers are explained. As a result, effects of climate change on the groundwater influence riparian systems that support a high percentage of the biological diversity. Scanlon (2005) evaluated the impact of land-cover and land-use changes on the groundwater recharge and quality in the southern United States. Based on the strong correlation between these factors and groundwater in this study, it is suggested that managed changes in these factors can be used to control the groundwater recharge and groundwater quality. IGES (2007) assessed the potential impacts of climate change on the groundwater in Asia, and some structural and institutional adaptations were discussed to minimize risk. Ranjan (2007) assessed climatic variability such as the temperature, precipitation, and land-use change and their impacts on saltwater intrusion in coastal aquifers. The results showed that the groundwater recharge increases in arid areas, because deforestation leads to reduced evapotranspiration even though it favors runoff. Hetzel (2008) discussed some challenges and possibilities such as the protection of groundwater, securing soil infiltration, and water saving to use and develop the groundwater under climate change in Africa. Generally, impacts of climate variability on the groundwater resources can be divided into three aspects including changes in the timing and magnitude of recharge, the interaction between the groundwater and surface waters, and water retreats. Using general circulation models to predict the future climate and to quantify these impacts leads to some uncertainties. For example, if the CO₂ concentration level rises, it is predicted that the land surface and soil profile will change due to climate change and water passing through the soil and entering the aquifers; therefore, some regions will encounter a large increase in the rate of groundwater recharge. But, the spatial variability of recharge and other physical properties are significant to assess under climatic changes. Change in the timing of recharge is important to manage both the water use and utilization, and land-use allocation.

Shrestha and Kataoka (2008) have mentioned some direct and indirect impacts of climate change on the groundwater resources. Some direct impacts include a variation in the amount and intensity of precipitation and evapotranspiration, which will change the recharge rates; sea level rising, leading to a saltwater intrusion into the low-lying river deltas; and variation in the atmospheric CO₂ level that may change the rate of dissolved carbonate and karst formation. Some indirect impacts include changes in land cover which may change the recharge rate and the increase of some hydrological events such as floods and droughts, which will decline the surface water reliability and quantity and, consequently, increase the groundwater exploitation. On the other hand, the increase in these events may deteriorate the groundwater quality of alluvial aquifers and change soil properties which may impact the percolation rate above aquifers.

11.4.1 HYDROLOGICAL COMPONENTS AFFECTING THE GROUNDWATER

A variation in temperature, precipitation, and consequently, evaporation, and soil moisture, as hydrological components, affect the groundwater recharge, demand, and other factors related to the groundwater. These impacts and their possible effects on the groundwater could be explained as follows.

11.4.1.1 Temperature and Evaporation

In recent times, several studies around the globe show that climate change is likely to impact significantly upon the freshwater resource availability.

Climate change refers to a significant change in the intensity of climatic factors such as the temperature or precipitation lasting for an expanded period. Most climate change scenarios present the increase in GHG concentrations through 2100, with a continued increase in the average global temperatures (IPCC, 2007, as found in EPA, 2007b). It is expected that global warming has several impacts on the water resources such as a declining snowpack and increasing evaporation, which affects the water supply and its demand rate (Field et al., 2007, p. 619).

The natural resources of the groundwater recharge are the rainfall and snowmelt. In fact, the recharged water is only to be abstracted, otherwise, we run into the trouble of a deficit in the groundwater supply. Changes in the rainfall trend due to climate change will affect the groundwater recharge, and the water scarcity will become a more important problem tomorrow than today. One reason for this problem is a high variation in the rate of evaporation, which depends upon the temperature and relative humidity. This variation impacts the amount of water available to replenish the groundwater supplies. The groundwater reduction can be due to some pivotal impacts of global warming containing more intense rainfall with shorter duration, leading to more runoff and less infiltration, increased evapotranspiration to the atmosphere, and increased irrigation. The second reason is that as the temperature increases, the demand for water will increase, especially in countries like India, Africa, Bangladesh, South America, etc. The increase in the demand leads to more pressure on the groundwater use, and therefore leads to its depletion. Furthermore, the other climate factor that is sensitive to temperature is the spatial and temporal distribution of snow accumulation (Deng et al., 1994). The snowmelt is principally based on the energy balance at the air–snow interface, and on the physical characteristics of the snowcaps (Harms and Chanasyk, 1998). However, the amount and distribution of the infiltrating snowmelt are influenced by the size of the frost layer. The snowmelt or rain may be redistributed by either surface runoff or interflow on top of the frozen soil layer depending on the tile topography (Johnson and Linden, 1991).

11.4.1.2 Precipitation

Climatic factors such as the wind and temperature make the precipitation patterns very dynamic and unbalanced in space and time, leading to huge temporal variability in the water resources, especially in the groundwater recharge. Therefore, determining the precipitation rate is difficult from region to region due to its spatial and temporal variation. For instance, the early snowmelt and diminished late-summer streamflows due to global warming influence the aquifer recharge for underground water supplies. Also, the higher amount of precipitation in the winter could increase the intensity of stormwater runoff instead of a slow recharge.

In the summer, the higher temperature with less rainfall could increase the evaporation and transpiration in surface water and plants, drying the soil. As a consequence, the groundwater levels descend, and, therefore, some wells will go dry. On the other hand, accumulated snowfalls in the winter are made available for infiltration and runoff when a threshold temperature above zero is reached. Thus, estimated recharge is altered due to variations in the groundwater level despite the use of specific yield.

Climate change models predict an increase in the global annual precipitation in the coming century, although changes in its pattern will vary from region to region (IPCC, 2007, as found in EPA, 2007b). However, these projections from climate models are uncertain and not completely reliable.

There are some other impacts of the changing precipitation patterns on groundwater. For example, the increase in rainfall frequency with extending impervious surfaces could increase the urban flood risks, producing more pollution which will affect the groundwater quality degradation. Furthermore, the diversity of the precipitation amounts in different regions impacts on the water-supplying resources such as groundwater to apply for freshwater.

After a rainfall, the infiltration to the lower strata of soil reaches the groundwater recharge. Then, the water level in an observation well in shallow unconfined aquifers rises right away. There are three reasons leading to this rise. First, the infiltrating water around the casing may leak into the well through its perforations unless the well is properly sealed. Second, the rainfall may directly enter the well unless it is capped. And third, the entrapped air pressure within the zone of aeration may injure (Todd, 1980) because the pores near the grimed surface are sealed by the rainwater and the underlying air is compressed by the infiltrating water.

Observation wells usually are capped and sealed near the top, and the perforations are located near their lower ends. Thus, the entrapped air would be the most probable cause for a water-level rise due to the rainfall. As a result, the water rise can be computed by the use of the following equation (Todd, 1980):

$$\Delta h = \frac{d_m}{d_v - d_m} \frac{p_a}{\gamma_w}, \quad (11.1)$$

where:

Δh is the water rise above the water table due to air entrapment

d_m is the depth of the saturated zone of rain infiltration

p_a is the atmosphere pressure $p_a \cong 1000\gamma_w$ ($\gamma_w = 1 \text{ g/cm}^3$)

d_v is the vertical distance between the ground surface and the water table, which is the depth of the vadose zone.

After a short period of time, Δh scatters as a result of the escape of air.

Example 11.1

On a global scale, climate warming results in increased precipitation, and some part of the precipitation absorbs to the ground. The infiltration leads the water

level in an observation well in an unconfined aquifer to rise to 3.33 m after a rainfall. If the depth of the vadose zone is 7.7 m, find the depth of the zone of compressed air above the water table.

SOLUTION

Based on the Equation 11.1, the average zone of compressed air is equal to the difference between d_v and d_m . $\Delta h = 3.33$ m and $d_v = 7.7$ m.

Assume $d_v - d_m = X$. Then $d_m = X - d_v$:

$$p_a \approx 1000\gamma_w$$

$$\Delta h = \frac{d_m}{d_v - d_m} \frac{p_a}{\gamma_w}$$

$$3.33 = \frac{X - d_v}{X} \frac{1000\gamma_w}{\gamma_w}$$

$$d_v - d_m = 7.73 \text{ m}$$

Then, the depth of the zone of compressed air will be 7.73 m.

11.4.1.3 Soil Moisture

The water stored in the soil is basically important to agriculture and is an influence on the rate of actual evaporation, groundwater recharge, and runoff generation. Climate change affects the soil characteristics through changes in waterlogging or cracking, which in turn may affect the soil moisture storage properties. The frequency and intensity of freezing impacts the soil infiltration capacity.

A warmer climate will intensify the hydrologic cycle, changing the rainfall and runoff magnitude and timing. In addition, the higher temperature due to warm air holds more moisture and accelerates the evaporation of surface moisture. Moreover, the increase in temperature and evaporation alters the existent moisture in the soil, which could contribute to longer and more severe droughts. Therefore, change in the climate will affect the soil moisture and groundwater recharge. Especially in unconfined aquifers with water tables near the ground surface, the increase in the temperature leads to fluctuations. Both processes of evaporation and/or transpiration cause a discharge of the groundwater into the atmosphere.

After rainfall occurs, the water table rises, which is the most accurate indication of actual aquifer recharge. The recharge rate can be assumed to be equal to the product of the water-table rise and specific yield (Figure 11.4):

$$R = S_y \Delta h, \quad (11.2)$$

where:

R is the recharge (L)

S_y is the specific yield (dimensionless)

Δh is the water-table rise (L).

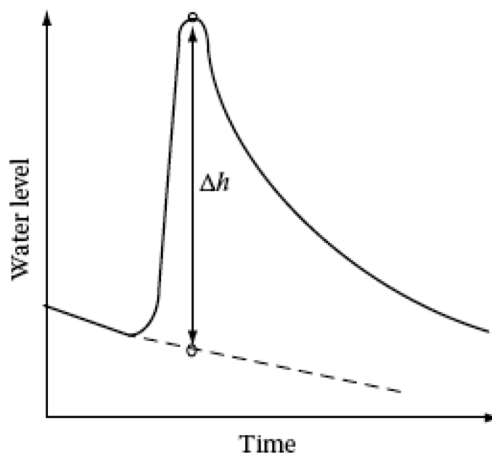


FIGURE 11.4 Principle of the water-table fluctuation method for estimating recharge. (From Kresic, N., *Groundwater Resources: Sustainability, Management, and Restoration*, McGrawHill, New York, 2009.)

This method estimates the groundwater recharge based on the water-level rise. The value of the specific yield in many cases should be assumed, which increases the uncertainty in applying this approach. When the water-table fluctuation method is applied, the frequency of the water-level measurement is considered. Manglik and Rai (2000) applied the finite Fourier sine transform solution and predicted the water-table fluctuation in an unconfined aquifer. Zaidi et al. (2007) calculated the water budget for a semiarid crystalline rock aquifer located in India. They used the double water-table fluctuation method. In this method, the hydrological year is divided into dry and wet seasons influenced by the monsoon characteristics of the rainfall in the area. Then, these two divisions are applied at the following water budget equation twice a year:

$$R + RF + Q_{in} = E + PG + Q_{out} + S_y \Delta h, \quad (11.3)$$

where two parameters, the natural recharge, R , and the specific yield, S_y , are unknown. The water-table fluctuations, Δh , are measured, and the other components of the water budget are independently estimated: RF is the irrigation return flow, Q_{in} and Q_{out} are the horizontal inflows and outflows in the basin, respectively, E is the evaporation, and PG is the groundwater extraction by pumping. As the equation is applied for wet and dry seasons to estimate the recharge and specific yield, the method is referred to as “double water table fluctuation.” This decreases the uncertainties due to the specific yield estimation at a large scale.

11.4.2 DIRECT IMPACTS OF CLIMATE CHANGE ON GROUNDWATER

Global warming influences the hydrological components as mentioned in the previous section. The changes in pattern, intensity, and rate of these components

can affect some items of the groundwater such as recharge and hydraulic conductivity which are explained as follows.

11.4.2.1 Groundwater Recharge

The groundwater recharge is a hydrologic process where soil water infiltrates naturally through the water cycle or anthropologically through the artificial groundwater recharge into the zone of saturation water. This process takes place in the vadose zone. **Figure 11.5** illustrates the main processes. In deeper confined aquifers, the recharge can occur both laterally and vertically through aquitard leakage in the saturated zone (Gerber and Howard, 2000).

To clarify the context of the groundwater recharge, the difference between the infiltration and percolation is given. The infiltration occurs through a unit area of soil surface, whereas the percolation occurs through the slow passage of water through the soil profile in the unsaturated zone. Soil scientists often know the deep-soil water percolation to be the groundwater recharge.

The resource of natural recharge is the precipitation. According to Lerner et al. (1990), the precipitation can recharge the groundwater in three ways: direct recharge is the percolation of precipitation vertically through the unsaturated zone; localized recharge, such as a mediatory recharge, is the depression of the concentrated surface water under the ground; and indirect recharge is the water which flows through the river or lake beds to the water table.

Direct recharge contributes more than the other mentioned recharges to the groundwater system (Knutsson, 1988). In humid climates, the surface water usually works as discharge areas rather than recharge areas, and therefore less is used as the

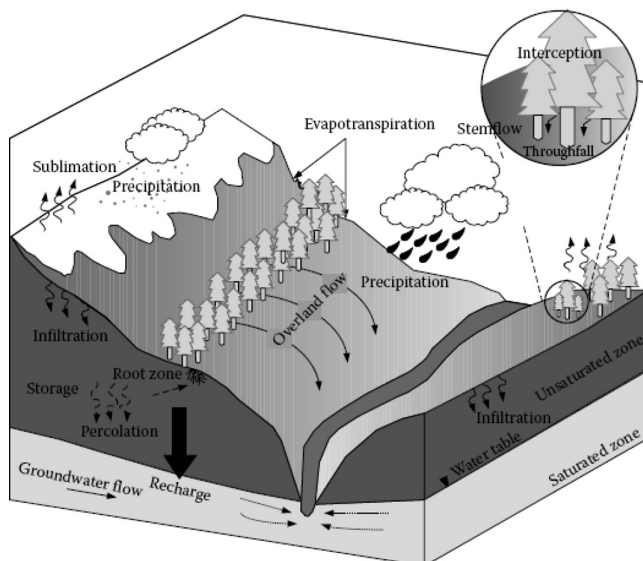


FIGURE 11.5 The hydrologic cycle. (From Delleur, J.W., *The Handbook of Groundwater Engineering*, CRC Press LLC, Boca Raton, FL, 988 p, 2007.)

general production of the groundwater recharge. Climate change can influence the water levels on the surface, recharge and discharge.

As shown in the hydrologic cycle in [Figure 11.5](#), the precipitation is formed either as rain or snow. The rainfall intensity and the land cover lead water to be channeled to the ground via streamflow or to infiltrate through the soils. Then, the infiltrated water penetrates to the lower strata of the soil through the vegetative root zone or evaporative zone roots. Some parts of the infiltrated water will be taken by the roots, and the remaining will percolate deeper to become the groundwater recharge in the saturated zone. Also, the percolated water evaporates from the vadose zone based on the soil moisture content and its amount in different parts of the unsaturated zone. Generally, the variations in the effective rainfall amount will change the recharge duration. Also, the effective rainfall, rivers, and lakes reload aquifers, and the replenishment rate may be high through the fissures or low by infiltrating through soils or rocks.

11.4.2.2 Recharge Estimation Methods

The precipitation recharge is the link between climate change and the groundwater at the land surface and tile recharge and discharge that occur at the surface water bodies. Different studies were done and diverse recharge estimation methods are used. Zhang et al. (1997) prepared a technical report for the recharge estimation in the Liverpool Plains. They used the Agricultural Production System Simulator (McCown et al., 1996). This model combines the plant growth and soil water balance models. Rushton et al. (2005) estimated the groundwater recharge using the daily soil moisture balance in two contrasting case studies, Nigeria and England. These two case studies indicate that the soil moisture balance model is a reliable approach for the recharge estimation in a wide variety of situations. Singhal et al. (2010) estimated the groundwater recharge in India. The water-table fluctuation method is used to estimate the rainfall recharge in the study area during the monsoon season. Also, the specific yield has been calculated using the groundwater equation for the dry season. The difference between the results of the RF infiltration and water-table fluctuation methods is calculated as 40%. Moreover, Lerner et al. (1990) explained five main methods estimating the direct recharge from the precipitation including direct measurement, empirical methods, water budget methods, oracular approaches, and tracers. By comparing the methods, and considering the widespread application of them in different areas, and also, based on the data requirements, the water budget method can be employed. This method is calculated on the basis of the soil moisture balance. All the components of the water balance equation are estimated by the groundwater recharge from the residual terms in the general daily water balance:

$$R = P - ET \pm O \pm \Delta S, \quad (11.4)$$

where:

R is the recharge

P is the precipitation

ET is the actual evapotranspiration

O is the lateral surface runoff in and out of the area

ΔS represents the change in the water storage in the unsaturated zone.

One of the advantages of this method is its application where the precipitation data are available. The climate, soil, and vegetation data are used to explain and direct the water inflow, outflow, and changes in the daily storage. The main disadvantage of this method is that the recharge is estimated as the residual term in a balance equation, but the other budget terms usually are estimated with substantial error. Risser (2008) applied this method to estimate the mean annual recharge for landscapes with various physical characteristics.

11.4.2.3 Aquifers Recharging

Climate change influences the various types of aquifers to be recharged differently. The main two types of aquifers are unconfined and confined. In the unconfined aquifer, the recharge sources are the local rainfall, rivers, and lakes, and the recharge rate will be influenced by the infiltration of overlying rocks and soils. Some samples of the climate change impact on the recharge rate in unconfined aquifers have been studied in France, Kenya, Tanzania, Texas, New York, and the Caribbean islands. Bouraoui et al. (1999) mentioned the considerable decline in the groundwater recharge near Grenoble, France, almost entirely due to the increase in the evaporation rate during the recharge season.

The shallow unconfined aquifers are recharged by the seasonal streamflows and can be reduced directly by the evaporation along the floodplains. Therefore, the recharge changes will be evaluated by the changes in the duration of flow of these streams, and the penetrability of the overlying beds, but by increasing the evaporative demands, the groundwater storage will lower. It is indicated that the unconfined aquifers are sensitive to the local climate change, abstraction, and seawater intrusion. However, determining the recharge amount using the characteristics of the aquifers themselves as well as the overlying rocks and soils is difficult.

On the other hand, a confined aquifer is described by an impermeable overlying bed, and the local rainfall is not considered as an effective factor in the aquifer. This aquifer is recharged from the lakes, rivers, and rainfall with diverse rates from a few days to decades.

Efforts have been made to estimate the recharge rate using carbon-14 isotopes and other modeling techniques. Indeed, these techniques are applicable only for the aquifers that are recharged from short distances and after short durations. However, calculating the recharge rate from long distances and considering the impacts of climate change is complex. Generally, it is necessary to emphasize research on modeling techniques, aquifer attributes, recharge rates, and seawater intrusion, as well as monitoring of the groundwater abstractions. This research will help to better understand and evaluate the impacts of climate change and sea-level rise on the recharge and groundwater resources.

11.4.2.4 Hydraulic Conductivity

Research by scientists and climatologists reveal that the anthropogenic factors such as the changes in land use with overgrazing and burning of forests, and the abnormal spreading of certain gases impact the atmosphere, lead to global warming. The released gases are referred to as GHGs including carbon dioxide (CO_2) and methane (CH_4). The greenhouse entraps the heat from the sun, and then increases the evapotranspiration and precipitation rates in some areas.

Although little research has been done in estimating the climate change impacts on the groundwater, more attention can be expected to estimate the increase or decrease of the recharge rates and amounts. Also, in some studies, the role of the increased pore pressure in the opening of fractures in rocks with the consequent increase in hydraulic conductivity is explained.

It has been known that a slight increase in the fracture width increases the flow rate through a fracture by a power of 3; this is known as the cubic law (Witherspoon et al., 1980) and is given as:

$$Q = \left(\frac{\rho g b^2}{12\mu} \right) (bw) \left(\frac{\partial h}{\partial l} \right), \quad (11.5)$$

where:

Q is the volumetric flow rate

ρ is the density of water

g is the acceleration of gravity

b is the aperture width

μ is the dynamic viscosity of water

w is the fracture width perpendicular to flow direction

h is the hydraulic head

l is the length of the flow path through the fracture.

The fracture is assumed to possess smooth sides, and the laminar flow exists. A consistent set of units must be used. This equation can be significant in determining the relationships between the increased precipitation due to climate change and the water-table rise during a period of increased recharge. Reichard (1995) estimated a significant increase of the recharge rate due to climate change and using this equation determined what the impacts of an increased recharge-induced water-table rise are on the hydraulic conductivity of an aquifer. His studies showed that the increase of the hydraulic conductivity of the fractured aquifers is as much as 15%–30% under such conditions (Delleur, 2007).

11.4.3 INDIRECT IMPACTS OF CLIMATE CHANGE ON GROUNDWATER

Climate change affects different components of the hydrological cycle as mentioned in [Section 11.3](#). The changes in the temperature, precipitation, and evaporation lead to sea-level rise, saltwater intrusion, and land-cover change, which indirectly affect the groundwater recharge. To make it clear, these impacts are explained as follows.

11.4.3.1 Sea-Level Rise

A sea-level rise is one aspect of global warming. Although future sea-level rise estimation will be unreliable, it will, however, be significant and continuous for centuries. Due to the sea-level rise, the low-lying coastal areas will be inundated, and the flooding risks and wind damage from coastal storms will increase. The melting of sea ice will lead to an indirect contribution to the sea level. The water density decreases

as the temperature rises. Due to climate change, the ocean temperatures increase, and consequently, the water will expand, causing a sea-level rise as a result of the thermal expansion.

Based on the Intergovernmental Panel on Climate Change (IPCC) studies, it is indicated that a sea-level rise would have broad effects on the coastal environments and infrastructure. These impacts include saltwater intrusion into the groundwater aquifers, coastal flooding, and coastal erosion. Salinization of the aquifers affects directly the drinking water supplies in the coastal areas. It increases the salinity of both the surface water and groundwater. The intrusion rate depends upon the local groundwater gradients. The shallow coastal aquifers are at the greatest risk. In low-lying islands with a high flooding risk due to the sea-level rise, the groundwater is very sensitive to change. In addition, the coastal erosion and sedimentation will produce pollution and, therefore, will impact the groundwater quality.

11.4.3.2 Saltwater Intrusion in Coastal Aquifers

A saltwater intrusion is one of the major groundwater problems in the coastal regions aquifers. The freshwater in the coastal aquifers is replaced by saltwater as a result of the motion of a saltwater body into the freshwater aquifer. A saltwater intrusion reduces the fresh groundwater availability in the coastal aquifers. Climate change predictions for the current century indicate higher global temperatures and a sea-level rise, which emphasize the risks of the seawater intrusion. Particularly, in the regions where the rate of precipitation becomes less, the groundwater salinity may increase by the more intensive evaporation and anthropogenic pressures. Considering these influencing factors, it is important to study the problem of a saltwater intrusion and estimate the saltwater intrusion due to climate changes and the change in land-use patterns. In the management of coastal groundwater resources, the quantitative understanding of the movement and mixing between freshwater and saltwater is necessary.

In fact, as the coastal aquifers are operational reservoirs in the water-resource systems, the prediction of the aquifer behavior under different conditions will have significant importance. Therefore, useful tools should be developed to facilitate this prediction, especially for identifying the salinity management strategies. [Figure 11.6](#) shows the saltwater–freshwater interface.

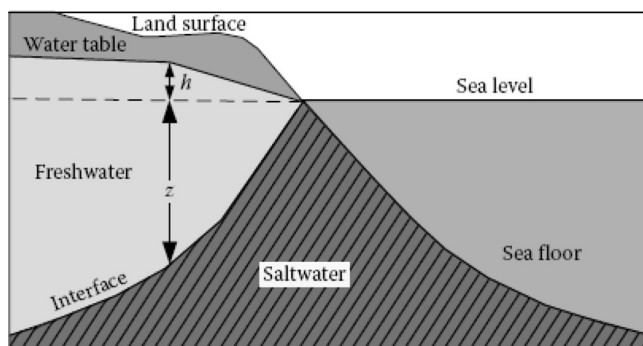


FIGURE 11.6 Saltwater intrusion wedge.

A saltwater intrusion into the freshwater aquifers can be influenced by factors such as: the tidal fluctuations, long-term climate and sea level changes, fractures in coastal rock formations, and seasonal changes in the evaporation and recharge rates, which can be affected in the areas with increased urbanization and thus impervious surfaces. A saltwater intrusion has also occurred in areas because of the water levels being lowered by the construction of drainage canals (Barlow, 2003).

The problem of the aquifer contamination by a saltwater intrusion, together with the extent and seriousness of the problem, are mainly conditioned by three factors: the difference between the respective densities of fresh and saltwater, the hydrodynamic properties of the aquifer, and the flow that the aquifer discharges into the sea. The first two factors are intrinsic to the saltwater intrusion problem regardless of the climate in the region. The flow that the aquifers discharge into the sea is conditioned by the natural conditions or artificial recharge and by pumping. Therefore, the anthropogenic actions can bring about some modifications. The incidents of saltwater intrusion have been detected as early as 1845 in Long Island, New York. The intrusion occurs in the coastal aquifers worldwide and is a growing issue in areas including North Africa, the Middle East, the Mediterranean, China, Mexico, the Atlantic, and Gulf Coasts of the United States. The increased use of the groundwater has also caused the saltwater-freshwater interface to move inland and closer to the ground surface along much of the U.S. Atlantic Coast, as well as Southern California (Howard and Israfilov, 2012).

The intrusion of saltwater into the coastal aquifers is a common problem in the coastal zones of the world, where the increasing water demands and arid climate have resulted in overexploitation of the groundwater systems. The continued exploitation of the limited freshwater resources can also lead to the up-flow of relict marine waters underlying the freshwater zone, compounding the effects of a saltwater intrusion. Overexploitation of the freshwater resources can render the groundwater unfit for the potable or agricultural use without extensive treatment. The sea-level rise reduces the aquifer storativity, which increases the groundwater depletion and causes the subsequent soil subsidence. A saltwater intrusion is currently one of the main causes of the groundwater pollution in about 60% of Spanish coastal aquifers. The most depleted groundwater severely affected by a saltwater intrusion are the Mediterranean and South-Atlantic coastal aquifers as well as Mexico, north of the Pacific and Atlantic coastlines, Chile, Peru, and Australia. The situation is particularly acute in the Yucatan Peninsula in Mexico, the Middle East, southeast and southwest of the United States, the Mediterranean (Gaza, Palestine, Lebanon, etc.), and on many islands with arid to semiarid climates, such as Cyprus, where the freshwater resources are limited in comparison with the large water demands (Sundaram et al., 2008). [Figure 11.7](#) shows the world map of deltaic areas threatened by a saltwater intrusion.

The management of groundwater recharge can reduce this deficit by increasing the recharge areas (or pounding zones) with the artificial replenishment of aquifers during rainfall and by injecting the stormwater/reclaimed water into wells along the coast. For this purpose, even the overflows from the irrigation or treated wastewater derived from the municipal wastewater treatment plants can be used. In Europe, the artificial recharge is recommended by the Water Framework

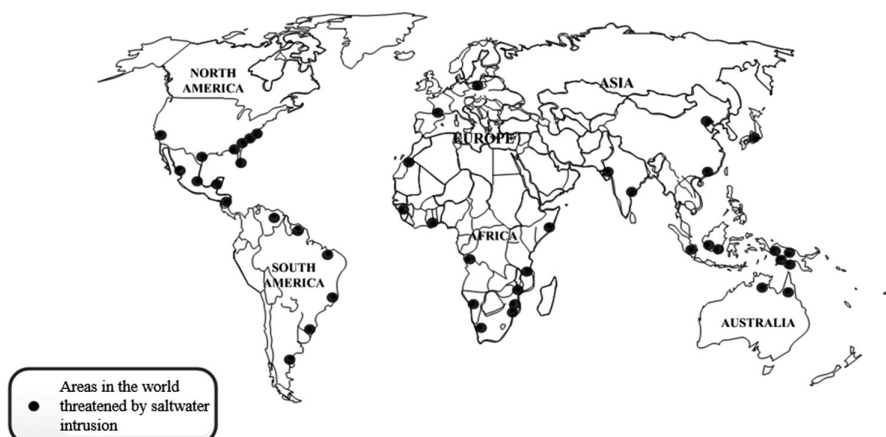


FIGURE 11.7 The world map of deltaic areas threatened by saltwater intrusion. (From Coleman, J.M., *Deltas: Processes of Deposition and Models for Exploration*, Springer Netherlands, Boston, 1981; Oude Essink, G.H.P. et al., 2010, *Water Res. Res.*, 46, 1–16, 2010.)

Directive as a useful measure in preventing and controlling the groundwater pollution. However, technical and health challenges must be carefully evaluated prior to undertakings such as the artificial injection in wells using treated wastewaters (Masciopinto, 2013).

11.4.3.3 Storm Surge and Saltwater Intrusion

A storm surge is a short-term rise in the mean sea level that often accompanies tropical cyclones as a common feature of the coastal regions worldwide (Werner et al., 2013). Many coastal aquifers are expected to experience a saltwater intrusion and be affected by storm surge overwash more severely than a seaward boundary. In the low-lying coastal regions, overwash salinization can be severely increased by a raising in the sea level (Mahmoodzadeh et al., 2014; Passeri et al., 2015). Further, the severity and extent of the salinization due to overwash events depend on the frequency and intensity of the ocean surges which are predicted to increase due to climate change (Yu et al., 2016). A saltwater intrusion into the coastal aquifers due to ocean surge inundation as well as the groundwater salinization recovery should be considered in studies to improve the proper assessment and the management of the coastal fresh groundwater resources (Ketabchi and Ataie-Ashtiani, 2015; Passeri et al., 2015; Yu et al., 2016). Additionally, some important concepts such as the risk assessments, evaluations of vulnerability, and resiliency indicators which have been studied by Karamouz et al. (2016), Karamouz and Zahmatkesh (2016), and Karamouz et al. (2014) can be used for investigations on the fresh groundwater aquifers and saltwater intrusion patterns as critical aspects in the coastal areas.

In the coastal regions, the storm surges can cause saltwater overtopping due to waves running up the face of the coastal protection structures. The damage to the protection structure and the flooding of the land surface behind the protection structure will cause the hazard of overtopping (Mahmoodzadeh and Karamouz, 2019; Yang et al., 2015). The storm surge can also influence the fresh groundwater resources

within islands. In such regions, a low-lying topographic depression can be submerged and completely filled by saltwater during a coastal storm (Chui and Terry, 2012). Based on the Van Biersel et al. (2007) study, in 2005, Hurricane Katrina affected the low-lying coastal regions of the United States Gulf Coast states (Florida, Alabama, Mississippi, Louisiana) and caused severe damages in Louisiana. In 2012, Hurricane Sandy affected 24 states in the United States with New Jersey and New York being affected the most. The storm surge at the Battery in southern Manhattan was 4.3 m above the mean lower low water of the tidal datum, or 3.4 m above the North American Vertical Datum (Blake et al., 2013).

11.4.3.4 Ghyben–Herzberg Relation between Freshwater and Saline Waters

The interface between saline and freshwater occurs at a depth below sea level about 40 times the height of the freshwater head above the sea level. It can be defined as the contact zone between the seawater intruding into rocks of a coastal area and the overlaying fresh groundwater in a coastal aquifer flowing seaward. The location of the interface can be approximated according to the Ghyben–Herzberg model (Drabbe and Badon Ghyben, 1889; Herzberg, 1901). This formula is based on the assumption that the potential lines in the freshwater regime are strictly vertical. The hydrostatic balance between freshwater and saline water can be illustrated by a U-tube. The pressures on each side of the tube must be equal; therefore,

$$\rho_s g z = \rho_f g (z + h_f), \quad (11.6)$$

where, p , z , and h_f are solved for z , which yields to:

$$z = \frac{\rho_f}{\rho_s - \rho_f} h_f, \quad (11.7)$$

which:

z is the depth of the interface below sea level

ρ_s is the density of the saline water

ρ_f is the density of the freshwater

g is the acceleration of gravity

h_f is the elevation of the water table above the saline water body elevation (Todd, 1980)

$$z = 40 h_f. \quad (11.8)$$

Example 11.2

In an unconfined coastal aquifer, the lower true interface is 95 m below the water table. If the densities of the freshwater and saltwater are 1 and 1.03 g/cm³, respectively, find the water-table elevation above sea level at the apex of the saltwater wedge using the Ghyben–Herzberg principle.

SOLUTION

$$Z + h_f = 95 \text{ m}, \rho_s = 1.03 \text{ g/cm}^3, \text{ and } \rho_f = 1.000 \text{ g/cm}^3.$$

$$\text{Using Equation 11.7, } 95 - h_f = \frac{\rho_f}{\rho_s - \rho_f} h_f = \frac{1}{0.03} h_f$$

$$h_f = 2.77/92.23 \text{ m and } z = 92.23 \text{ m.}$$

11.4.3.5 Island Freshwater Lens

On small islands, the fresh groundwater is a distinct part of the water floating on the underlying seawater. The freshwater is the result of the recharge from the precipitation. The climate change impacts on the precipitation amounts will change the recharge rate, affecting the freshwater availability. The thickness of a freshwater body near the center of an island is the largest, which diminishes toward the coast where the freshwater is discharged into the sea. As shown in Figure 11.8, the freshwater accumulation is similar to the shape of a lens (McWhorter and Sunada, 1977).

An equation can be derived to express the relation between the depth of a freshwater lens and the hydraulic conductivity, the island size, and the recharge as shown in the following. This equation is for a circular island, but the approach can be applied for a long island aquifer with a one-dimensional normal flow. As shown in Figure 11.8, the discharge at a distance r from the center of the island is estimated as follows:

$$Q(r) = -2\pi K(z + h)r \frac{dh}{dr} = \pi r^2 W. \quad (11.9)$$

Replacement of h by $(\Delta\rho/\rho)z$, and integration subject to $z = 0$ at $r = R$, yields:

$$z = \left\{ \frac{W(R^2 - r^2)}{2K\Delta\rho(1 + \Delta\rho/\rho)} \right\}^{1/2}. \quad (11.10)$$

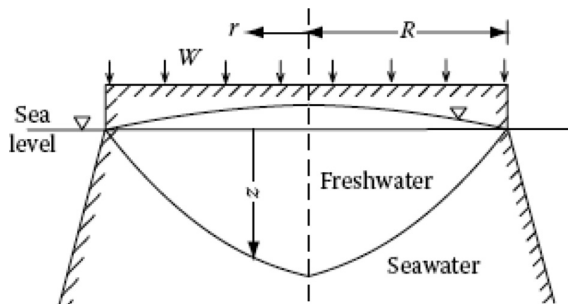


FIGURE 11.8 Freshwater lens on a circular island. (From McWhorter, D.B. and Sunada, D.K., *Ground-Water Hydrology and Hydraulics*, Water Resource Publication, LLC, Highlands Ranch, CO, 290 p, 1977.)

Apparently, considerable freshwater supplies probably are found on large islands, with large recharge rates and small K .

Example 11.3

On many islands, the major source of potable water is the freshwater lens. The extraction systems often consist of a large number of closely spaced shallow wells with very small discharges (on the order of 20 m³/day). In some instances, the shallow trenches are pumped in order to minimize the drawdown per unit discharge. Assume that sea-level rise occurs due to climate change. Consider an approximately circular lens of radius R on which the interface at the center of the lens is 20 m below sea level. Also, considering the sea-level rise impacts on the recharge rates, its value is 45 cm/year. A well field is to be developed near the center of the lens. The plans call for the well field to cover 20% of the lens area. Calculate the withdrawal rate for the well field that will eventually result in a depth to the interface of 5 m at the center of the lens (McWhorter and Sunada, 1977).

SOLUTION

The well field is idealized as a circle of radius R_i . Furthermore, the withdrawal of groundwater by the well field is simulated by a uniform withdrawal at rate W_i . In the well field:

$$Q(r) = \pi r^2 (W - W_i) = -2\pi K (z + h) r \frac{dh}{dr}, \quad r \leq R_i. \quad (11.11)$$

Substituting $h = (\Delta\rho/\rho)z$ into Equation 11.11 and integrating subject to $z = z_0$ at $r = 0$ and $z = z_i$ at $r = R_i$ gives:

$$z_0^2 = \frac{\rho(W - W_i)R_i^2}{2K\Delta\rho(1 + \Delta\rho/\rho)} + z_i^2. \quad (11.12)$$

The next step is to compute z_i^2 . This is accomplished by analyzing the flow for $r \geq R_i$, where the discharge at any r is:

$$Q(r) = (W - W_i)\pi R_i^2 + W\pi(r^2 - R_i^2) = -2\pi K(Z + h)r \frac{dh}{dr}, \quad r \geq R_i. \quad (11.13)$$

Integration, subject to $z = z_i$ at $r = R_i$ and $z = 0$ at $r = R$, gives:

$$z_i^2 = \frac{\rho}{2K\Delta\rho(1 + \Delta\rho/\rho)} \left\{ W(R^2 - R_i^2) - 2W_iR_i^2 \ln\left(\frac{R}{R_i}\right) \right\}, \quad (11.14)$$

which is combined with Equation 11.12 to yield:

$$z_0^2 = \frac{\rho R^2}{2K\Delta\rho(1+\Delta\rho/\rho)} \left[W - W_i \left(\frac{R_i}{R} \right)^2 \left\{ 1 + \ln \left(\frac{R}{R_i} \right)^2 \right\} \right], \quad (11.15)$$

after some arrangement.

Since the area, A , of the lens and the area, A_i , of the well field are proportional to their respective radii squared, Equation 11.15 can be written as:

$$z_0^2 = \frac{\rho R^2}{2K\Delta\rho(1+\Delta\rho/\rho)} \left[W - W_i \left(\frac{A_i}{A} \right) \left\{ 1 + \ln \left(\frac{A}{A_i} \right) \right\} \right]. \quad (11.16)$$

Before the development of the well field, $A_i = 0$. In the limit as A_i approaches zero, Equation 11.16 is reduced to:

$$z_0^2 = \frac{\rho R^2 W}{2K\Delta\rho(1+\Delta\rho/\rho)}.$$

But, $z_0^2 = (20)^2$ before the development of the well field and $W = 0.3$ m/year. Therefore,

$$\frac{\rho R^2}{2K\Delta\rho(1+\Delta\rho/\rho)} = \frac{(20)^2}{0.45} = 889 \text{ m/year.}$$

Thus, Equation 11.16 becomes:

$$z_0^2 = 889 \left[W - W_i \left(\frac{A_i}{A} \right) \left\{ 1 + \ln \left(\frac{A}{A_i} \right) \right\} \right],$$

which can be solved for W_i :

$$W_i = \frac{W - (z_0^2 / 889)}{A_i / A \left\{ 1 + \ln (A / A_i) \right\}}.$$

Substituting $A_i/A = 0.2$, $W = 0.45$ m/year, and $z_0 = 5$ results in:

$$W_i = \frac{0.45 - (25 / 889)}{0.2 \left\{ 1 + \ln (5) \right\}} = 0.808 \text{ m/year}$$

Thus, the withdrawal rate is 8.08×10^5 m³/year/km². The remaining portion is contributed by the lateral inflow from the land outside of the well field. If the well

field is expanded to cover essentially all of the lens area, the maximum permissible withdrawal rate is reduced to:

$$W_i = 0.45 - \left(\frac{25}{889} \right) = 0.42 \text{ m/year.}$$

11.4.3.6 Land Use and Land Cover

Land-use and land-cover changes can alter the hydrological system. Land-use and land-cover changes have an important effect on the infiltration and, consequently, on the groundwater recharge. They also impact the hydrologic processes through the variation in the evapotranspiration regime and/or the extreme change in the surface runoff. These impacts are influenced by climatic changes. Urbanization also increases the area of impermeable regions by changing the land surface from its natural state. Therefore, it can have a significant impact on the groundwater recharge, while its adverse impact on the groundwater quality is even more significant (Foster, 2001).

Generally, understanding the impact of land-use and land-cover changes on the atmospheric components of the hydrologic cycle is necessary for an optimal management of the natural resources, especially the groundwater. The recharge variations due to the land-cover changes can impact the groundwater quality negatively, because in the semiarid and arid regions, thick unsaturated zones contain the accumulated salts that can permeate into the underlying aquifers.

The recharge quantification and its controls are important for the water-resources evaluation and for analyzing the groundwater sensitivity to contamination. Areas with high recharge rates are particularly most prone to pollution. In arid areas, the combination of the climatic impacts and the land-use changes leads to the increased groundwater recharge due to the deforestation, which reduces the evapotranspiration despite the fact that it favors runoff.

11.5 GROUNDWATER QUANTITY AND QUALITY CONCERNS

The groundwater quality and quantity are depleted and deteriorate by a variety of factors including chemical contamination. Another concerning factor is the salt-water intrusion for groundwater quality, particularly in the coastal areas where the changes in freshwater flows and sea-level rise will both occur. All these factors are influenced by climate change and variability, and because of the importance of the groundwater, especially as the water supply resource, the depletion and deterioration of the groundwater due to climate change impacts are explained separately as follows.

11.5.1 DEPLETION OF GROUNDWATER TABLE

The groundwater volume and quality depend upon the recharge conditions. The groundwater quantity is controlled by the amount of annual precipitation, land-surface characteristics, vegetation type, and soil attributes. The groundwater supplies are less prone to variations in the climate than the surface water, but they are

more influenced by the long-term trends. More regular or prolonged droughts lead to shortages of the surface water supplies, and then, the groundwater serves as a buffer pressure as the groundwater supplies increase. In addition, the declining groundwater levels may affect the seasonal flow intensity and change the temperature regimes that are required to support critical habitat, especially the wetlands. The interactions between the groundwater and surface water are poorly understood in most areas. Variations in the precipitation and temperature regimes may impact the aquifers that are difficult to identify.

11.5.2 DETERIORATION OF GROUNDWATER QUALITY

The groundwater is a vital source of water for the public supply, agriculture, and industry in different countries. Climate change impacts indirectly lead to the degradation of the groundwater quality. The increasing contamination and salinization of the groundwater due to sea-level rise are the most important climate change impacts which worsen the groundwater quality. These two impacts are explained as follows.

11.5.2.1 Increasing Groundwater Contamination

The groundwater quality contamination is related to the public health. The drinking water containing the contamination poses a serious challenge to the water managers. The agricultural chemicals and wastewater treatment by-products such as nitrates also affect the groundwater quality in some areas. The changes in the streamflow, and consequently, the sediment regimes, and the impacts on human health and the ecosystem function are some important water-quality issues. The increase in the precipitation intensity can increase the risk of contamination. As mentioned before, climate change leads to variations in the rainfall regime. This change alters the flow volume, runoff frequency, and timing. For instance, the low flows will decline the contamination dilution capacity, and thus, the higher pollutant concentrations. In areas with overall decreased runoff, the water quality deterioration will be even worse. On the other hand, the extreme streamflows change the sediment and erosion rates on the surface. These sediments may include some pollutant components which can percolate underground. Also, the different extremities of flow rates can affect the land cover and infiltration rate, making the infiltration easier. As a result, the groundwater quality will be at risk of the increasing contamination due to climatic variations. Furthermore, the lower rates of groundwater recharge, flow, and discharge, and the higher aquifer temperatures may increase the levels of the bacterial, pesticide, nutrient, and metal contamination. Correspondingly, the increased flooding could increase the flushing of urban and agricultural waste into the groundwater systems, especially into the unconfined aquifers, and further deteriorate the groundwater quality.

11.5.2.2 Salinization of Groundwater by Sea-Level Rise

As the temperature rises globally, the melting of ice sheets and glaciers will increase and will lead to sea-level rise. When sea-level rising happens, the saltwater will penetrate farther inland and upstream in the low-lying river deltas (IPCC, 1998).

Salinization endangers the surface water, urban water, and groundwater supplies, damaging the ecosystems, and the coastal farmland (IPCC, 1998). Furthermore, the lower rainfall reduces groundwater head and exacerbates the impacts of sea-level rise. The saltwater intrusion into the limestone aquifers is higher than the alluvial aquifers. The saltwater intrusion in the coastal aquifers is another key groundwater quality concern. As the groundwater pumping increases for municipal demand along the coast, the freshwater recharge in the coastal areas declines, and the sea level rises. Thus, the groundwater aquifers are affected by the seawater infiltration. In areas with the low land surface elevations, the relative sea level has been greater. Further increases in the sea level may accelerate the salinity intrusion into the aquifers and affect the coastal ecosystems.

11.6 ADAPTATION TO CLIMATE CHANGE

An effort has been made to mitigate GHG emissions to prevent risky climate change. The other stage of the international effort must cope with the unavoidable impacts. The adaptations to the climate are always made by changing the human settlement and agricultural patterns and other aspects of their economies and lifestyles. Climate change due to human activities gives a complex new dimension to this age-old challenge. In the future, the success of human adaptation to the climate will depend upon producing the greater adaptive capacity with certain patterns of development such as disclosing to people the higher levels of climate risk.

Climate changes have important impacts on the water supplies and the water quality. There is already the widespread acceleration of ice melting and shifting the streamflow from the spring to the winter peaks in many areas. These shifts could affect the water availability for agriculture and other uses. In the coastal aquifers, the sea-level rise will result in a saltwater intrusion, which potentially decreases the water resource availability. The changes in the precipitation regime due to global warming and related climate change are likely to result in frequent hydrological events such as floods and droughts and the increased demand for irrigation water. These events significantly increase the weather-related risks faced by human settlements, and the water and power supply failures. First, it is necessary to evaluate the potential impacts of climate change on the water resources and their management, based on an agreement that global warming is growing and about its regional dynamics and scale.

However, as the current rainfall predictions are indicative and general rather than definitive, climate change predictions are uncertain and unreliable. This uncertainty limits the utility for indicating the type of strategic challenges. This would be consistent with the underlying analysis of the energy flows that underpin the predictions of global warming, and is of great importance for the water managers who necessarily focus on extreme events. Because of the diverse factors which are combined and influence the available water, predicting the impacts of climate change based on them will be difficult. For instance, if the temperature increases, the evaporation rate from the soil and the transpiration rate from the plants will increase, therefore, less water will flow as runoff or infiltrate through the underground aquifers; but if the rainfall intensity increases, a larger amount of water will flow as floods or seep into the deeper layers of soil underground. Although efforts

have been made for predicting the variations of the streamflows and groundwater regimes under climate change scenarios, there is a wide range of possible results.

Some adaptation techniques have been developed and applied in the water sector over decades. For instance, in the coastal aquifers, there is a problem of the seawater intrusion due to climate change in the groundwater. The introduced technique to control the seawater intrusion is to use the recharge well barriers through a line of injection tube wells driven parallel to the coast. This mechanism sets up a pressure ridge which pushes the saline front seawards. [Figure 11.9](#) presents a schematic diagram through a confined aquifer system in the coastal plain areas and injection well barrier measure for the control of seawater intrusion.

Some methods of controlling the seawater intrusion into the aquifers are modification of the groundwater pumping and extraction pattern, artificial recharge, injection barrier, extraction barrier, and subsurface barrier. Each method is described as follows.

11.6.1 ARTIFICIAL RECHARGE

There are a number of methods that can be applied in order to raise the level of the groundwater table. These methods have been developed to recharge the groundwater artificially. For instance, a surface water spreading method should be used in an unconfined groundwater along the coastal plain, whereas the well-recharging method is used for confined aquifers.

11.6.2 MODIFICATION OF GROUNDWATER EXTRACTION PATTERN

The landward migration of the seawater occurs in the pumping pattern of wells. Therefore, changing the situation of the pumping wells will be a necessary factor. Such wells should be dispersed inland to re-establish the groundwater flow gradient toward the sea. At the same time, the volume of the pumped water should decrease from such wells to produce a positive water effect in a freshwater aquifer.

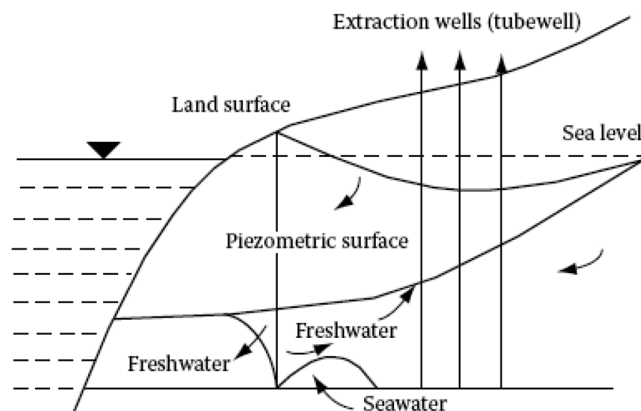


FIGURE 11.9 Schematic diagram of an injection well barrier in a confined aquifer in a coastal plain.

11.6.3 INJECTION BARRIER

The injection well method is applied to recharge confined aquifers where the water is injected into a deep confined aquifer through a line of recharging wells along the coast at a predetermined pressure. The pressure ridge along the coast is formed by the injected water in order to flow the water toward the sea. In this method, a high quality of water is required, which should be available nearby, or it should be imported for the well injection recharge. These kinds of wells are required when a pressure ridge to push the groundwater seaward is needed.

11.6.4 SUBSURFACE BARRIER

The impervious subsurface barrier method is assembled analogous to the coast and through the extent of the freshwater aquifer. This barrier will prevent the flow of the seawater from entering into the aquifer. Materials such as clay, asphalt, cement, and bentonite are utilized to build the barriers.

11.6.5 TIDAL REGULATORS

This method is utilized to control the discharge of the sweet water of a river or stream into the sea. Such structures store the fresh water for injection and prevent the inflow of the saline water into the river. This increases the water table near the structures and also supplies the freshwater along the crest.

Monitoring the groundwater around such recharging, namely, the salinity entering these structures, is an important factor to manage the availability of the freshwater and groundwater.

In this method, the dams and tanks should be checked. Also, information such as the hydrology, runoff, reservoir level, likely submergence area, command area, geology, geography, soil, and drainage network is collected before proposing a suitable design for the tidal regulators.

11.7 IPCC ASSESSMENT REPORT

The United Nations Environment Program and the World Meteorological Organization initiated the IPCC organization in 1988. The purpose of this organization is the evaluation of the scientific, technical, and socio-economic aspects corresponding with the risks, potential impacts, and options for the compatibility and moderation of man-made climate change.

Its main output has been a series of assessment reports, which are based on the peer-reviewed scientific and technical literature. Three types of scenarios were investigated in the first IPCC Report in 1990: (1) equilibrium scenarios with fixed CO₂ concentrations; (2) transient scenarios with increasing CO₂ concentrations by a fixed percentage each year over the duration of the scenario; and (3) four brand-new Scientific Assessment emission scenarios based on the World Bank population projections. These three types of scenarios included a wide variety of time-dependent or transient scenarios which showed the change in population,

energy sources, technology, emissions, atmospheric concentrations, radiative forcing, and/or global temperature.

IPCC initially focused on three areas including science (Working Group 1), impacts and adaptations (Working Group 2), and mitigation (Working group 3). The scenarios that described the possible combination of population, economic growth, and technology drivers that led to the future greenhouse gas emissions were developed in the mitigation group. These emissions scenarios were converted to the regional and global temperatures and climate impacts by the climate modeling community. The information about the scenarios can inform decision-makers about the potential to mitigate these impacts and/or adapting to climate changes.

There were initially four narrative storylines in the Special Report on Emissions Scenarios (SRES) report, they were designated as A1, A2, B1, and B2. In the A storylines, the focus is on the economic growth, while the B storylines have more of an environmental emphasis. The A1 and B1 lines describe more of a homogeneous, globalized future, while the A2 and B2 explain a more fractured world. The A1 line is further designated to be either fossil-fuel intensive (A1-F), a nonfossil fuel, technology emphasis (A1-T), or a more balanced combination of the two (A1-B). These characterizations are listed in [Figure 11.10](#). Even though these scenarios are no longer used as they were defined and utilized in the General Circulation Models (GCMs), their scientific and technical backgrounds remain important for the research communities to define their own scenarios.

The approximations of the greenhouse gas emissions in the proximity of the next 100 years are provided under the SRES scenarios. The climate models use these emissions of greenhouse gases to approximate the future concentration of CO₂, CH₄, N₂O, and other greenhouse gases in the atmosphere. Then, the Global Water Partnership-weighted equivalent CO₂ concentrations can be estimated as these atmospheric concentrations are estimated. See Masters and Ela (2008) for more details.

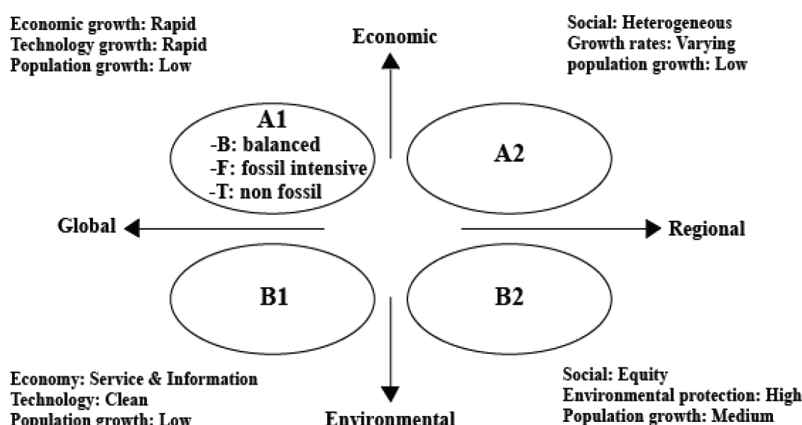


FIGURE 11.10 SRES emission scenarios.

11.8 CLIMATE CHANGE SIMULATION

Quantifying the atmospheric systems has set up processes that occur on a wide range of time and space scales. Some numerical models of these processes are applied for various purposes, such as the predictions of global weather and global climate change. The climate system has dealt with large changes in a geological time scale due to the changes in the atmospheric composition, location of continents, and the earth's orbital parameters. The current focuses are climate changes on time scales of the seasons to centuries. The current research agenda includes the seasonal climate prediction from an observed initial state and the projection of the future climate change. Projecting the climate system in the spatial scales is difficult, both in the atmosphere and on the terrestrial surface.

The high complexities of the earth's climate result in the uncertainty about the changes which will arise from the increase in the carbon dioxide concentrations. To increase the reliability of the predicted climate and to decrease the errors in predictions, more research and refinement of the global circulation models (GCMs) are needed. GCMs describe the atmosphere in terms of a rectangular grid covering the earth with cubes of air above which currently are 2° – 5° grids in latitude and longitude, 6–15 vertical levels, which are assumed the representative of volume elements in the atmosphere as presented in [Figure 11.11](#).

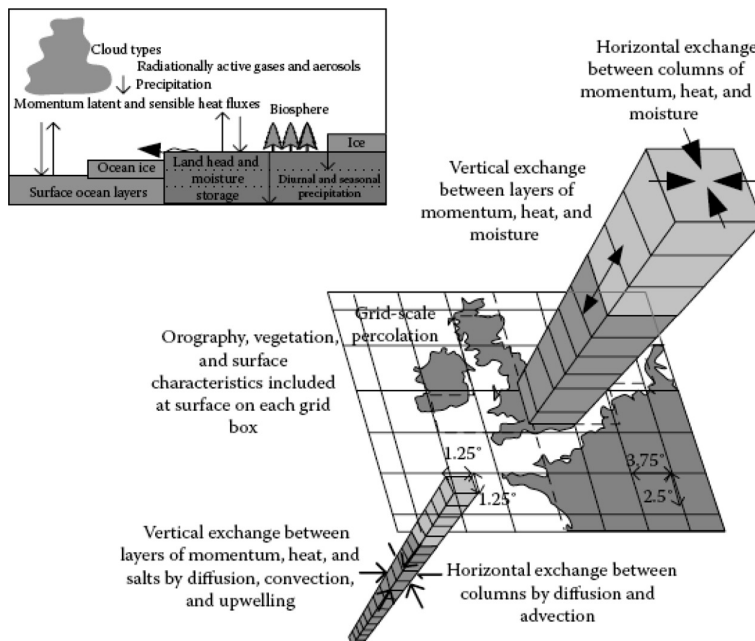


FIGURE 11.11 A schematic discrete of atmosphere for utilizing the GCMs. (From Viner, D. and Hulme, M., Climate change scenarios for impact studies in the UK: General circulation models, scenario construction models and application for impact assessment. Report of Department of Environment, Climatic Research Unit, University of East Anglia, Norwich, UK, 70 p, 1992.)

In the earth's climate simulation by the GCMs, a high number of variables describing the physical and chemical properties of the atmosphere, oceans, and continents are considered. By developing the technology over the past decade, the quality of GCMs has improved vividly. However, some available feebleness should be corrected to improve the GCMs' precision. Much work on these weaknesses needs to be done to simulate the behavior of the earth's oceans in the GCMs more accurately. Moreover, there are some ambiguities such as the physics of clouds, which are poorly understood, that add another measure of uncertainty to the GCMs. In the following sections, the procedure of developing the climate change scenarios, GCM models structure, and the downscaling procedure are introduced.

11.8.1 SPATIAL VARIABILITY

A sufficient number of climate variables on the spatial scales to assess the climate changes are estimated by a number of scenarios. Some scenarios result in a uniform change in climate over an area. Indeed, the diversity of some factors such as the land uses which have completely different responses to climate change impacts are not considered. The regional changes in the climate are defined by the GCM grid boxes, between 250 and 600 km, depending upon a specific GCM model resolution listed in [Table 11.1](#). Due to the lack of accuracy about the regional climates in a GCM model, Von Storch et al. (1993) support the opinion that generally the minimum effective spatial resolution should be defined by at least four GCM grid boxes. The precision of the GCM simulations depends on the spatial autocorrelation of a particular weather variable for an individual grid box.

In the past few years, the hydrological schemes have also been considered in the GCMs with a higher complexity and integration. Nonlinearity in the climate systems leads to difficulty in using a deterministic estimation of the precipitation from the GCMs for hydrological modeling purposes. In this aspect, the methods to transform the output from the GCM to the local weather variables are needed. A weakness of the numerical models of natural systems is their impossibility to validate the described nonclosed systems. However, the need to improve the quality of these models and the benefits in the operational use are pivotal. Although the spatial resolution of the GCMs is increasing, they still simulate the climate at a very coarse spatial scale on the order of 250×250 km, which is not enough for the evaluation of the climate change effects in the urban areas. In the following sections, some methods of improving the spatial precision of the GCM outputs are described.

11.8.1.1 Recent Communities' Scenarios Development

Instead of creating the new scenarios, the IPCC decided to have research communities approve their own development during its 25th session. The IPCC identified a set of benchmark emissions scenarios, called "Representative Concentration Pathways—RCPs." An RCP is a greenhouse gas concentration (not emission) trajectory adopted by the IPCC for its fifth Assessment Report in 2014. The RCPs are used for the climate model simulations that develop the climate scenarios (IPCC, 2013).

TABLE 11.1
The Characteristics of the Available GCM Models for the Globe

| | Acronym | Model | SRES Scenario Runs | | | |
|---|---------------|-------------------------------------|--------------------|--------------|-----|-----|
| | | | A2 | B2 | A2b | A2c |
| Max Planck Institute für Meteorologie Germany | MPIfM | ECHAM4/ OPYC3 | | | | |
| Hadley Centre for Climate Prediction and Research, UK | HCCPR | HadCM3 | A1FI | | A2 | B1 |
| | | | | | A2b | |
| | | | | | A2c | B2b |
| Australia's Commonwealth Scientific and Industrial Research Organisation Australia Important notice concerning the CSIRO data sets | CSIRO | CSIRO-Mk2 | A1 | | A2 | B1 |
| National Center for Atmospheric Research, United States | NCAR | NCAR-CSM | | | A2 | |
| | | | | NCAR- PCM | A1B | A2 |
| Geophysical Fluid Dynamics Laboratory, Untied States | GFDL | R30 | | | A2 | B2 |
| Canadian Center for Climate Modelling and Analysis, Canada | CCCma | CGCM2 | | | A2 | B2 |
| | | | | | A2b | B2b |
| | | | | | | B2c |
| | | | | | A2c | |
| Center for Climate System Research National Institute for Environmental Studies, Japan | CCSR/ NIES | CCSR/NIES AGCM + CCSR OGCM | A1 A1FI | A1T | A2 | B1 |
| | | | | | | B2 |

Source: Intergovernmental Panel on Climate Change (IPCC), Fourth Assessment Report, <http://www.ipcc.ch>, 2007.

As shown in [Table 11.2](#), the RCP8.5 is a high radioactive forcing pathway, reaching more than 8.5 W/m^2 by 2100. The RCP8.5 represents the highest radiative forcing range and approximately the 90th percentile of CO_2 and non- CO_2 GHG emissions scenarios. The RCP3-PD is a low radiative forcing pathway that peaks at a maximum radiative forcing level at about 3 W/m^2 during the twenty-first century. The radiative forcing level declines during the second half of the twenty-first century, and then further declines. The RCP4.5 is an intermediate pathway that does not exceed a stabilization level of approximately 4.5 W/m^2 . There are a large number of published stabilization scenarios at the RCP4.5 level (approximately 650 ppm CO_2 equivalent in year 2100). The RCP6 is a second intermediate pathway that does not exceed a stabilization level of approximately 6 W/m^2 .

TABLE 11.2
Types of Representative Concentration Pathways

| Name | Radiative Forcing | Concentration | Pathway Shape | SRES Temp Anomaly Equity |
|---------|--|---|---------------------------------|--------------------------|
| RCP8.5 | >8.5 W/m ² in 2100 | > ~1370 CO ₂ -eq in 2100 | Rising | A1F1 |
| RCP3-PD | Peak at ~3 W/m ² before 2100 and then decline | Peak at ~490 CO ₂ -eq before 2100 and then decline | Peak and decline | None |
| RCP6 | ~6 W/m ² at stabilization after 2100 | ~850 CO ₂ -eq at stabilization after 2100 | Stabilization without overshoot | B2 |
| RCP4.5 | ~4.5 W/m ² at stabilization after 2100 | ~650 CO ₂ -eq at stabilization after 2100 | Stabilization without overshoot | B1 |

Radiative forcing or climate forcing is the difference between insolation (sunlight) absorbed by the Earth and energy radiated back to space. Changes to Earth's radiative equilibrium, that cause temperatures to rise or fall over decadal periods, are called climate forcing. The current level of radiative forcing, according to the IPCC AR4 IPCC Fourth Assessment Report, is 1.6 W/m² (with a range of uncertainty from 0.6 to 2.4).

11.8.1.2 Downscaling

The GCMs have an unreliability in simulating the climate variables, and the application of a stochastic model in space and time will overcome this. Even the high spatial resolution of the GCMs needs to downscale the results from such models. The downscaling methods are still under development and more work needs to be done to increase the accuracy of such models. It creates a connection between the large-scale circulation defined as the predictors and the local weather variables defined as predictands. But downscaling pertains more to the process of moving from the large-scale predictor to the local predictand. [Figure 11.12](#) shows a schematic of moving from the large scale to the small scale.

The downscaling techniques calculate the subgrid box scale changes in the climate as a function of the larger-scale climate or circulation statistics. The two main approaches to downscaling have used either the regression relationships between large-area and site-specific climates (e.g., Wigley et al., 1990) or the relationships between the atmospheric circulation types and the local weather (e.g., Von Storch et al., 1993). The disadvantage of the downscaling approach is to calibrate the statistical relationship. In doing so, it requires large amounts of the observed data which can be computationally very intensive. Also, as unique relationships need to be derived for each site or region, these methods are very time consuming. A basic assumption in the application of downscaling methods is that the observed statistical relationships will continue to be valid in the future under conditions of climate change. There are a wide range of techniques used for downscaling. The statistical downscaling is usually used for downscaling which is further described in the Section 11.7.2.

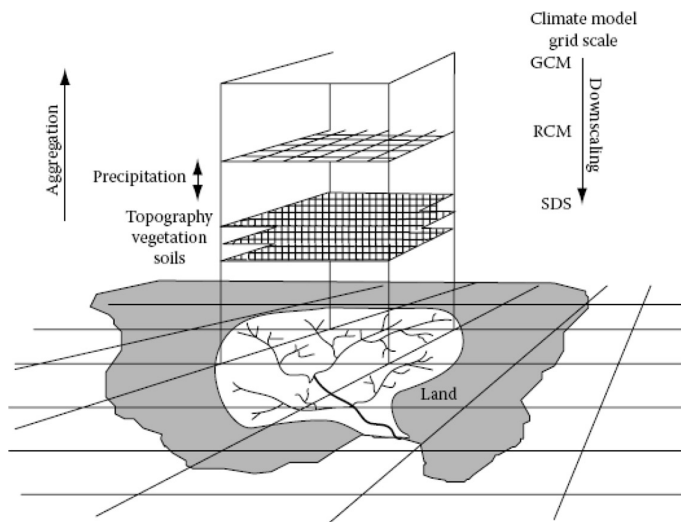


FIGURE 11.12 Schematic drawing of the basic principles of downscaling from the GCM output. (From Wilby, R. L. and Dawson, C.W., *Using SDSM Version 3.1—A Decision Support Tool for the Assessment of Regional Climate Change Impacts*, Climate Change Unit, Environment Agency of England and Wales, Nottingham, U. K. and Department of Computer Science, Loughborough University, Leicestershire, UK, 2004.)

11.8.1.3 Regional Models

To involve the use of the high-resolution regional climate models, an alternative approach is involved. The regional climate models are typically assembled at a much finer resolution than the GCMs (often 50 km) with the domain limitation to continents or subcontinents. In such applications, the detailed information at the spatial scales down to 10–20 km may be established at the temporal scales of hours or less. However, the regional climate models are still compelled at their boundaries by the coarse-scale output from the GCMs. Therefore, in an area, a regional climate model can have the performance similar to that of the driving GCM, and also, their performance in relation to the downscaling techniques has not yet been assessed completely. Indeed, there are some difficulties in creating the interface between the GCM and the regional model. Moreover, the costs of setting these models for a new region and running a climate change experiment are extremely high; therefore, they are not easily accessible. Nevertheless, in the long term, this technique could result in useful results, and their development should be encouraged. Most of the regional models are employed on the northern hemisphere, whereas many of the areas that are most vulnerable to global change lie in the southern hemisphere. Therefore, it remains premature to be used for many regions in the climate impact assessments.

The dynamic downscaling has many advantages particularly around the factors such as the temperature, precipitation, soil moisture, wind direction, and strength which are available in both the GCMs and the nested finer-scale grid. However, supercomputer systems are required in the dynamic downscaling, which are less available

to perform these simulations for all the areas around the world to evaluate the local and or regional impacts and consequences of climate change. Then, increasing the availability of the supercomputer leads to a wide accessibility of dynamic downscaling.

11.8.2 STATISTICAL DOWNSCALING

Developing the statistical downscaling is assuming that an empirical relationship exists between the atmospheric processes at different spatial and temporal scales (Wilby et al., 1998). These relationships can depend on the predictor variables and the broadscale atmospheric variables, such as the mean sea-level pressure and the geopotential height, through a transfer function. The following are some of the criteria that make a downscaling method successful (Hewitson and Crane, 1996):

- Large-scale predictors are sufficiently reproduced by the GCMs.
- For periods outside the calibration period, the relationship between the predictors and the predictands are valid.
- Climate change signals are adequately incorporated in the predictors.

As no predictor meets the three criteria, the predictors which fulfill one or two criteria are selected. The disadvantage is that the degree of freedom in the predictor set is increased, and the results become more difficult to analyze. Hewitson and Crane (1996) outlined the major steps of downscaling, presented as follows:

1. Reduction or processing of the predictor
2. Comparison of the GCM circulation with the observed circulation
3. Spatial analysis and the selection of the predictor and predictand domain
4. Temporal analysis of the predictor and the predictand
5. Temporal manipulation of the predictor, e.g., time-lagging
6. Calibration of the transfer function between the predictor and predictand
7. Evaluating the relationship between the predictor and predictand
8. Application of the developed model to the GCM data

Items 3–7 are repeated until an optimum result is reached for the target objective. During this procedure, the predictor variables and weighting functions are selected, concerning the downscaling method used. It is possible that all these steps are not taken in each method, but they are necessary to be considered to reach the credible results from downscaling. Three statistical downscaling methods are the analog methods, regression methods, and conditional probability approaches. The last one has two main subdivisions containing weather patterns and weather states. These methods are largely used in anticipated hydrological impact studies under climate change scenarios. The main features of statistical downscaling are personal computers which can be used for the calculations, there is no need for a detailed knowledge about the physical processes, and the long and homogeneous time series are needed for fitting and confirming the statistical relationship.

In the second feature, the exact formulation of the processes is not necessarily considered for statistical downscaling. The main advantages of the statistical downscaling approach are easy implementation and cheap computation. In situations where a

low-cost, rapid assessment of highly localized climate change impacts is required, statistical downscaling (currently) represents the more promising option. The integrated feature of the downscaling procedure is that it is calibrated to the local level. Furthermore, with very few parameters, these methods will be attractive for many hydrological applications (Wilby et al., 2000). Precipitation is a nonlinear process, and precipitation fields are characterized by the unusual scaling laws. Also, in assessing the spatial behavior of the precipitation, a dependency to the time scale is shown. The downscaling of the precipitation using the stochastic models helps to better understand the probabilistic structure of the precipitation. These models have long been used to model the hydrologic events, such as runoff. If they are derived from the atmospheric processes that drive the precipitation, they can predict how to govern the precipitation patterns.

Given the wide range of the regional and statistical downscaling techniques, there are a number of model comparisons using the general data sets and model diagnostics. Until recently, these studies just compared the statistical-versus-statistical downscaling models or regional-versus-regional models. However, a growing number of studies have compared the statistical-versus-regional models, and in [Table 11.3](#), their relative strengths and weaknesses are summarized.

In the application of statistical downscaling, the seasonal dependencies are considered an important point. For the regions defined seasonally based on the temperate variations, the driving forces for the precipitation differ over the year, and result in the intra-annual deviations in downscaling. A greater extent of the precipitation during the summer months is driven than during the winter months, which should be considered in developing the classification schemes. A solution for this problem can be dividing the year into four seasons. A crucial example can be the growth season of plants, as there is a nonlinear relationship between the amount of rain and the water-use efficiency of plants.

Furthermore, the downscaling methods must be valid in a troubled climate to be useful in the future studies of climate change. The methods are assumed to estimate the difference between climate situations and must, therefore, work under a situation different from the one under which it was developed. Also, the climate should be stationary and no major shift in the physical processes governing the climate must occur or else it will result in a downscaling scheme outside the calibrated and validated range. To assess the ability of a model to deal with the different climate situations, the model is calibrated on the data from the driest seasons, and then is validated on the wettest seasons in the calibration period and conversely. This is a simple test of the method's sensitivity to the different climate situations. The stability of the model performance in the extreme years is evaluated. The long time series containing many different situations are used in the downscaling. These situations will be more frequent in a perturbed future climate. If the method can model those situations, and if the range of variability of the large-scale variable in a future climate is of the same order as today, the problem will be minimized. There is some difficulty in dealing with the stability and nonstationarity in the downscaling, and one should be careful when applying a model to the output of the GCM simulations. If the climate is nonstationary, the underlying assumptions of the statistical link are unaffected by the climate change for the model validity. The physical laws governing the climate are not likely to change, but the physical processes are parameterized for a specific climate. A multivariate approach is recommended to overcome the problem

TABLE 11.3
Main Strengths and Weaknesses of Statistical Downscaling and Regional Model

| | Statistical Downscaling | Regional Model |
|------------|--|--|
| Strengths | <ul style="list-style-type: none"> • Station-scale climate information from GCM-scale output • Cheap, computationally undemanding, and readily transferable • Ensembles of climate scenarios permit risk/uncertainty analyses • Applicable to “exotic” predictands such as air quality and wave heights | <ul style="list-style-type: none"> • 10–50 km resolution climate information from GCM-scale output • Respond in physically consistent ways to different external forcings • Resolve atmospheric processes such as orographic precipitation • Consistency with GCM |
| Weaknesses | <ul style="list-style-type: none"> • Dependent on the realism of GCM boundary forcing • Choice of domain size and location affects results • Requires high-quality data for model calibration • Predictor–predictand relationships are often nonstationary • Choice of predictor variables affects results • Choice of empirical transfer scheme affects results • Low-frequency climate variability problematic • Always applied off-line, therefore, results do not feedback into the host GCM | <ul style="list-style-type: none"> • Dependent on the realism of GCM boundary forcing • Choice of domain size and location affects results • Requires significant computing resources • Ensembles of climate scenarios seldom produced • Initial boundary conditions affect results • Choice of cloud/convection scheme affects (precipitation) results • Not readily transferred to new regions or domains • Typically applied off-line, therefore results do not always feedback into the host GCM |

Source: Wilby, R.L. and Dawson, C.W., *Using SDSM Version 3.1—A Decision Support Tool for the Assessment of Regional Climate Change Impacts*, Climate Change Unit, Environment Agency of England and Wales, Nottingham, U.K. and Department of Computer Science, Loughborough University, Leicestershire, UK, 2004.

with the nonstationarity of the climate. In this approach, the sufficient data should be available to ensure the statistical integrity of the results. To consider the nonstationarity, a stochastic model is conditioned on the observed inter-annual variability.

The common method for the downscaling is a regression-based method. Wilby and Wigley (1997) defined this method as a model involving the establishing of linear or nonlinear relationships between the subgrid-scale parameters and the coarser-resolution predictor variables. Artificial Neural Networks (Hewitson and Crane, 1996; Olsson et al., 2004) and Canonical Correlation Analysis (Von Storch et al., 1993) are the common regression-based methods in this field. The models and techniques can be different from the simpler multiple regression schemes to the more sophisticated models, such as a method to link the covariances of the atmospheric circulation and of the local weather variables in a bilinear way (Burger, 1996).

These methods can also be classified according to the parameters used in the downscaling procedure. In one approach, the same variable is used for the large-scale predictors as for the local-scale predictands, e.g., temperature, but in most studies, different parameters are used. Four steps are followed in regression methods:

1. Identification of a large-scale parameter G (predictor) as a controller of the local parameter L (predictand). If L is calculated for the climate experiments, then G should be simulated well by the climate models.
2. Developing a statistical relationship between L and G .
3. Validation of the relationship with the independent data.
4. If the relationship is confirmed, then G is derived from the GCM experiments to estimate L .

The idea that the predictor should be well simulated by the GCMs is a key issue in this method. As mentioned before, the statistical downscaling of climate variables is used to determine the impacts of climate change. Although the GCM is still the best tool to predict the future climate, the assumption that the statistical relationships derived will remain fixed in the future is a weak point in this context.

11.9 DOWNSCALING MODELS

In this section, two downscaling models, Statistical Down Scaling Model (SDSM) and the Long Ashton Research Station Weather Generator (LARS-WG), which are widely employed in the climate change studies, are introduced.

11.9.1 STATISTICAL DOWNSCALING MODEL

The SDSM is a statistical downscaling model that enables the construction of the climate change scenarios for the individual sites at the daily time scales, using the grid resolution GCM output. The large-scale predictor variable information has been prepared for a large North American window. Some employed climate variables in the SDSM are listed, which include the mean temperature, mean sea-level pressure, vorticity near surface, specific humidity, etc.

Since the choice of the predictors largely determines the character of the down-scaled climate scenario, this remains one of the most challenging stages in the development of any statistical downscaling model. The decision process is also complicated by the fact that the explanatory power of the individual predictor variables varies both spatially and temporally.

In order to assemble and calibrate the model, the identified large-scale predictor variables are used for determining the multiple linear regression relationships between these variables and the local station data. They also regulate the average and variance of the downscaled daily rainfall considering factors such as the bias, and the variance to confirm the simulated values to the observed one. The first step in the application of the SDSM, to determine that the rainfall should occur daily, is as follows:

$$\omega_i = \alpha_0 + \sum_{j=1}^n \alpha_j \hat{u}_i^{(j)}, \quad (11.17)$$

where:

- ω_i is the candidate in a random process generator that indicates a state of rainfall occurring or not occurring on day i
- \hat{u}_i is the normalized predictor on day i
- α_j is the estimated regression coefficient.

The precipitation on day i occurs if $\omega_i \leq r_i$, where r_i is a stochastic output from a linear random-number generator.

In the second step, the value of the rainfall in each rainy day is estimated using the z -score as follows:

$$Z_i = \beta_0 + \sum_{j=1}^n \beta_j \hat{u}_i^{(j)} + \varepsilon, \quad (11.18)$$

where:

- Z_i is the z -score for day i
- β_j are the estimated regression coefficients for each month
- ε is a normally distributed stochastic error term:

$$y_i = F^{-1}[\phi(Z_i)], \quad (11.19)$$

where:

- ϕ is the normal cumulative distribution function
- F is the empirical function of the y_i daily precipitation amounts.

The standardized predictors used in this method are provided by subtracting the mean and dividing them with the standard deviations over the calibration period.

In the downscaling, a multiple linear regression model is developed between the selected large-scale predictors and local-scale predictands, such as the temperature or precipitation. Based on the correlation analysis, partial correlation, scattered plots, and considering the physical sensitivity between the predictors and predictands, the suitable large-scale predictors are chosen. The higher correlation values imply a higher degree of association, and the lower P -values indicate more chances for the association between variables. It is important to know that the P -values lesser than 0.05 as the threshold do not necessarily mean that the result can be statistically significant. On the other hand, the high P -value would indicate that the predictor–predictand correlation could be chance related (Wilby and Dawson, 2004).

Example 11.4

A rain gage of an area called station A is located at $60^\circ 34'$ longitude and $26^\circ 12'$ latitude. The precipitation data for 10 years from 1994 to 1999 are available in this rain gage. The monthly data are given in [Table 11.4](#). Produce the precipitation data of station A under the Hadley Centre Coupled Model, version 3 (HadCM3), B2 scenario outputs from 2010 to 2014 using the SDSM.

TABLE 11.4
Monthly Observed Precipitation for Station A for Period of 1992–2001

| | January | February | March | April | May | June | July | August | September | October | November | December |
|------|---------|----------|-------|-------|------|------|------|--------|-----------|---------|----------|----------|
| 1994 | 1.20 | 0.00 | 0.08 | 0.20 | 0.00 | 0.00 | 0.77 | 1.50 | 0.00 | 0.05 | 0.00 | 0.69 |
| 1995 | 0.00 | 0.24 | 0.00 | 0.61 | 0.00 | 0.24 | 2.51 | 0.20 | 0.27 | 0.36 | 0.05 | 3.01 |
| 1996 | 2.35 | 0.63 | 0.87 | 0.00 | 0.45 | 0.15 | 0.00 | 0.00 | 0.00 | 0.08 | 0.53 | 0.00 |
| 1997 | 0.86 | 0.00 | 3.26 | 0.10 | 0.00 | 1.42 | 0.00 | 0.00 | 0.00 | 3.52 | 0.64 | 2.45 |
| 1998 | 1.60 | 0.13 | 3.85 | 0.00 | 0.00 | 0.00 | 0.00 | 0.10 | 0.00 | 0.00 | 0.00 | 0.00 |
| 1999 | 0.00 | 0.75 | 1.30 | 0.00 | 0.00 | 0.00 | 1.32 | 0.00 | 0.00 | 0.00 | 0.00 | 0.00 |

SOLUTION

The downscaling procedure at station A is described step by step as follows:

Step 1: The input file is prepared, the daily precipitation data are sorted, based on the time in two columns, first the date and second the precipitation amount (the monthly data are interpolated to develop the daily data needed as input of SDSM).

Step 2: Then the process of the quality control is run to test the format of the prepared input file.

Step 3: In this step, the 16 available weather variables are screened to find the variables that could be used as precipitation predictand. For station A, the data start from January 1, 1994 and end at December 31, 1999. The analysis is done in an annual period under an unconditional process.

At the end of this analysis, the results of the explained variance and the correlation matrix between the precipitation and the selected weather variables are given (Figures 11.13 and 11.14).

Two variables are selected for the precipitation simulation as follows:

The relative humidity at 850 hPa height

The near the surface specific humidity

The related correlation analysis of these variables is given in Figures 11.13 and 11.14. The *P*-value is low and the partial correlations are high, which show the accuracy of the downscaling process.

Step 4: The model is calibrated using the observed data and the selected signals. At the end of this step, the *R*-squared and the standard error are reported (Figures 11.15 and 11.16).

Step 5: The weather generator. In this step, the data for the considered period and the selected climate change scenario (here HadCM3B2) are developed (see Table 11.5). The start date of the data generating and the amount of data to generate according to the considered years will be entered. In this step, you can choose the production of one or more ensembles, wherein the one ensemble is selected.

Step 6: In this step, the statistical analysis of the observed and the developed data through the tables and graphs are given (Figure 11.17).

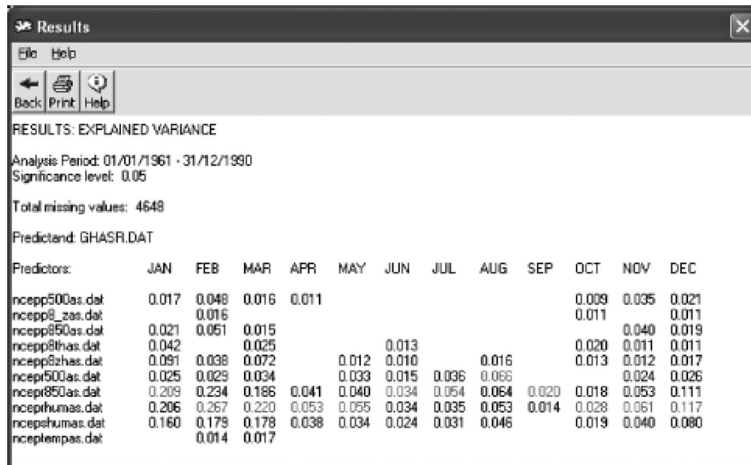


FIGURE 11.13 Results of correlation analysis between the predictors and daily precipitation.

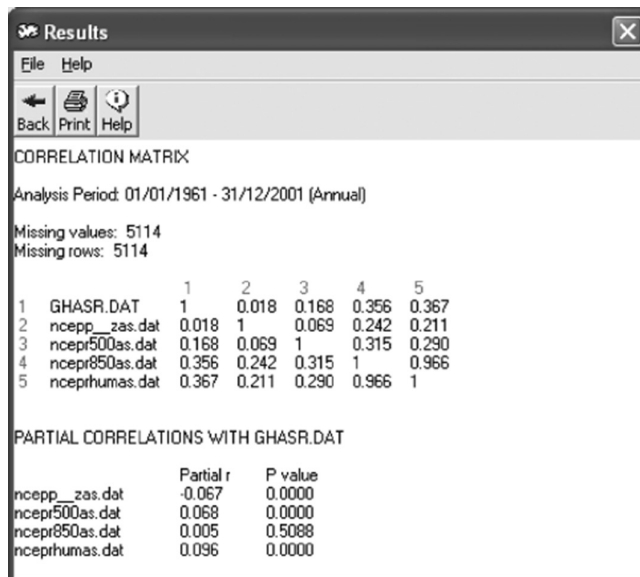


FIGURE 11.14 Matrix of the correlation between predictors and predictands.

11.9.2 LARS-WG MODEL

One of the most important downscaling models is the LARS-WG. The input data of this model are the daily time series of climate variables such as the precipitation, solar radiation, and maximum and minimum temperatures. This model is a stochastic

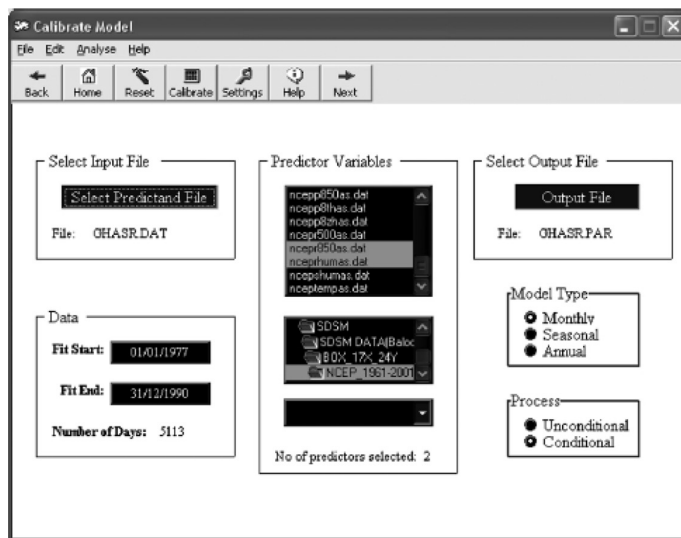


FIGURE 11.15 Model calibration window.

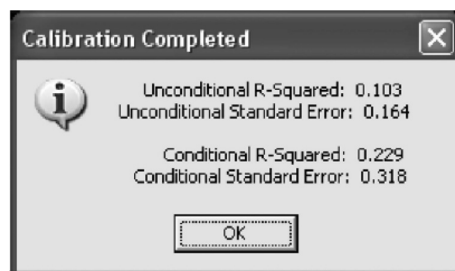


FIGURE 11.16 Model calibration results.

TABLE 11.5
Average Monthly Simulated Precipitation (mm) at Station A HadCM3B2 Scenario for the Period 2010–2014

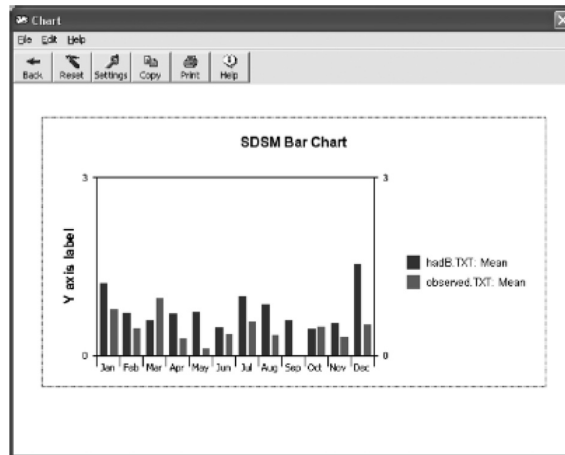


FIGURE 11.17 Comparison of the HadCM3B2 scenario results and the observed precipitation.

weather generator that simulates the weather data at a single site under both the current and future climate conditions (Racska et al., 1991; Semenov and Brooks, 1999; Semenov et al., 1998).

The two main purposes of the development of the stochastic weather generator are:

1. To prepare a means of simulating the synthetic weather time series with the statistical characteristics analogous to the observed statistics at a site, and long enough for the assessment of the risk in the hydrological or agricultural applications
2. To simulate the weather time series to the unobserved locations, through the interpolation of the weather generator parameters obtained from running the models at neighboring sites.

The stochastic weather generator cannot be used in weather forecasting as a predictive tool, but it can generate an identical time series of the synthetic weather to the observations.

The semiempirical distributions are used for the lengths of the wet and dry day series, daily precipitation, and daily solar radiation. The semiempirical distribution $\text{Emp} = \{a_0, a_i; h_i, i = 1, \dots, 10\}$ is a histogram having ten intervals, $[a_{i-1}, a_i]$, where $a_{i-1} < a_i$, and h_i denotes the number of the events from the observed data in the i th interval. The random values are chosen by first selecting the intervals, and then selecting a value within that interval from the uniform distribution. This kind of distribution is flexible and can approximate a wide variety of shapes by adjusting the intervals $[a_{i-1}, a_i]$. However, this flexibility leads to specifying 21 parameters, 11 values indicating the interval bounds and 10 values indicating the number of the events within each interval, in comparison with, for instance, 3 parameters for the mixed-exponential distribution used in an earlier version of the model to define the dry and wet series (Racska et al., 1991).

Based on the expected properties of the weather variables, the intervals $[a_{i-1}, a_i]$ are selected. For the solar radiation, the intervals $[a_{i-1}, a_i]$ are divided into the minimum and maximum values of the monthly observed data, whereas for the period of the dry and wet series and for the precipitation, the interval size regularly increases as i increases. In the last two cases, there are typically many small values and a few very large ones, and the use of a very coarse resolution for small values is prevented by this choice of the interval structure.

The simulation of the precipitation occurrence is modeled as the alternate wet and dry series. A day with the precipitation >0.0 mm is identified as a wet day. The random length of each series is selected from the wet or dry semiempirical distribution when the series starts in a month. To determine the distribution, the observed series are allocated to the month. The precipitation value for a wet day is generated using the semiempirical precipitation distribution for the particular month, which does not depend on the length of the wet series or the amount of the precipitation in the previous days.

The daily minimum and maximum temperatures are considered as the stochastic processes with the daily means and the daily standard deviations conditioned on the wet or dry status of the day. The technique used to simulate the process is very similar to that presented in Racsko et al. (1991). The seasonal cycles of the means and standard deviations are modeled by a finite Fourier series of order 3, and the residuals are approximated by a normal distribution. The Fourier series for the mean is fitted to the observed mean values for each month. To give an estimated average daily standard deviation, the observed standard deviations for each month are adjusted before fitting the standard deviation Fourier series. To do this, the estimated effect of the changes in the mean within the month is removed. Also, the adjustment is calculated using the obtained fitted Fourier series.

The observed residuals analyze a time autocorrelation for the minimum and maximum temperatures, which are obtained by removing the fitted mean value from the observed data. To simplify this procedure, constant amounts throughout the entire year are assumed for both the dry and wet days with the average value from the observed data being used. A preset cross-correlation of 0.6 is considered for the minimum and maximum temperature residuals. In cases with the minimum temperature less than 0.1, the simulated minimum temperature is greater than the simulated maximum temperature. Based on the analysis of the daily solar radiation over many locations, the normal distribution for the daily solar radiation is unsuitable for certain climates (Chia and Hutchinson, 1991). The distribution of the solar radiation also varies significantly on the wet and dry days.

Therefore, in order to describe the solar radiation on the wet and dry days, separate semiempirical distributions were used. An autocorrelation coefficient was also calculated for the solar radiation and was assumed to be constant throughout the year. The solar radiation is modeled independently of the temperature. The sunshine hours are accepted by the LARS-WG as an alternative to the solar radiation data.

The three main parts of the software consist of:

1. *Analysis:* In the first step, the observed station data are analyzed to calculate the weather generator parameters. The LARS-WG observed inputs are the precipitation, maximum and minimum temperature, and sunshine

hours. In this analysis, the semiempirical distributions of the observed data are used for the wet and dry series duration, precipitation amount, and solar radiation. Also, using the Fourier series, the maximum and minimum temperatures are calculated. The resulting parameter file is used in the generation process.

2. *Generator*: In this step, the synthetic weather data are generated from the combination of a scenario file containing information about the changes in the precipitation amount, wet and dry series duration, mean temperature, temperature variability, and solar radiation with the parameter files in step (1). The scenario file will contain the appropriate monthly changes if the LARS-WG is being used to generate the daily data for a particular scenario of climate change.
3. *QTest*: To evaluate the properness of simulating the observed data, the LARS-WG provides the QTest option. In this step, the statistical characteristics of the observed data are compared with those of the synthetic data generated using the parameters derived from the observed station data. Several statistical tests are used to determine whether the distributions, mean values, and standard deviations, of the synthetic data are significantly different from those of the original observed data set.

The main use of the LARS-WG is in the generation of the daily data from the monthly climate change scenario information. The advantage of this software is that a number of different daily time series representing the scenario can be generated by using a different random number to control the stochastic component of the model. Hence, these time series vary on a day-to-day basis, although they have the same statistical characteristics. This permits the risk analyses to be undertaken (Canadian Climate Impacts and Scenarios, 2006).

Example 11.5

A rain gage of an area called station A is located at $47^{\circ} 4'$ longitude and $38^{\circ} 26'$ latitude. The precipitation data for 10 years from 1986 to 2007 are available in this rain gage. Produce the precipitation data of station B under the HadCM3A2 scenario outputs from 2011 to 2030, 2046 to 2065, and 2080 to 2099 using the LARS model. Show the result of 2011–2020 in a table.

SOLUTION

Step 1: For applying the LARS model, two input files should be developed as follows:

Station A.st file: This file includes the site name, latitude, longitude, and altitude of the station A rain gage, the directory path location and the name of the file containing the observed weather data for the station A, and the format of the observed weather data in the file, which here is the year (YEAR), Julian day (JDAY, i.e., from 1 to 365), minimum temperature (MIN; °C), maximum temperature (MAX; °C), precipitation (RAIN; mm), and solar radiation (RAD; MJm-2day-1) or sun shine hours (SUN). Note that if you have SUN as an input variable, the LARS-WG automatically converts it to global radiation ([Figure 11.18](#)).

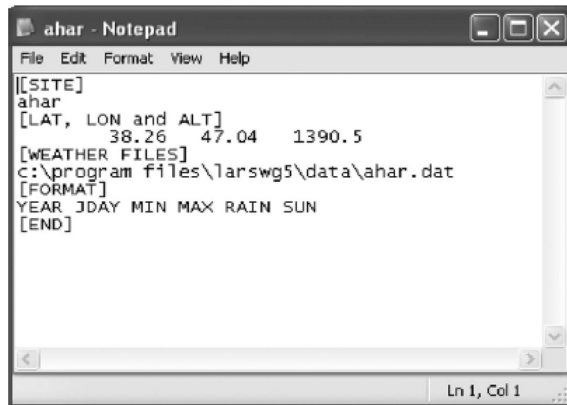


FIGURE 11.18 A layout of the basic characteristics of station A (station A. st file).

| Untitled - Notepad | | | | | |
|--------------------|------|--------|------|------|------|
| File | Edit | Format | View | Help | |
| 1987 | 259 | 9 | 26.4 | 0 | 10.7 |
| 1987 | 260 | 10.2 | 22.6 | 0 | 10.2 |
| 1987 | 261 | 8.2 | 21.6 | 0 | 0 |
| 1987 | 262 | 7.6 | 13 | 0 | 5.2 |
| 1987 | 263 | 7.4 | 17 | 0 | 6.8 |
| 1987 | 264 | 5 | 27.8 | 0 | 10.7 |
| 1987 | 265 | 5.2 | 27 | 0 | 10.6 |
| 1987 | 266 | 5.2 | 26.8 | 0.1 | 2.2 |
| 1987 | 267 | 4 | 18.8 | 0 | 10.4 |
| 1987 | 268 | 5 | 27.4 | 0 | 8.7 |
| 1987 | 269 | 10 | 30.4 | 0 | 9.5 |
| 1987 | 270 | 12 | 30.2 | 0 | 5.3 |
| 1987 | 271 | 8.4 | 22 | 0 | 5.7 |
| 1987 | 272 | 7.4 | 24.5 | 0 | 10 |
| 1987 | 273 | 8 | 27 | 0 | 9.8 |
| 1987 | 274 | 10.8 | 28.6 | 0 | 9.7 |
| 1987 | 275 | 13.6 | 29 | 0 | 10 |
| 1987 | 276 | 11.8 | 28.8 | 0 | 6.7 |
| 1987 | 277 | 3.4 | 11.8 | 1 | 0 |
| 1987 | 278 | 0.2 | 2.6 | 14 | 0 |
| 1987 | 279 | 0.2 | 1.4 | 14 | 0 |
| 1987 | 280 | 1 | 6.5 | 1 | 0 |
| 1987 | 281 | 4 | 6 | 3.6 | 0 |
| 1987 | 282 | 3.6 | 8 | 0 | 1.5 |
| 1987 | 283 | 2.2 | 9.7 | 0 | 8 |
| 1987 | 284 | 0.4 | 10 | 0 | 8.2 |
| 1987 | 285 | -0.6 | 9.8 | 0 | 10.2 |
| 1987 | 286 | 1 | 15.6 | 0 | 8.2 |
| 1987 | 287 | 0.6 | 12.4 | 0 | 9.2 |
| 1987 | 288 | 5.2 | 11.8 | 0 | 2.4 |
| 1987 | 289 | 8.4 | 12.5 | 0 | 4.4 |
| 1987 | 290 | 7.6 | 13.2 | 0 | 5.4 |

FIGURE 11.19 The input data of station A for the LARS model (station A.sr).

(Station A.sr) file: Contains the daily data of rainfall, maximum temperature, minimum temperature, and solar radiation at the station A in the order mentioned at the station A.st file (Figure 11.19).

Step 2: After preparing the mentioned files for calibrating the model, the SITE ANALYSIS option is selected and the station A.st is addressed to the model. Two files called station A.sta and station A.wg are created. These

| [SERIES seasonal distributions: WET and DRY] | | | | | | | | | | | | | |
|---|---|--|--|--|--|--|--|--|--|--|--|--|--|
| [DJF] | | | | | | | | | | | | | |
| 554 23 2.18 1.29 2.22 1.32 | | | | | | | | | | | | | |
| 0.000 0.048 0.095 0.143 0.180 0.238 0.286 0.333 0.381 0.429 0.476 0.524 0.571 0.571 | 1.00 1.00 1.00 1.00 1.00 1.00 1.00 1.00 1.00 1.00 1.00 1.00 1.00 2.00 | | | | | | | | | | | | |
| 547 23 5.67 5.43 5.78 5.52 | | | | | | | | | | | | | |
| 0.000 0.048 0.095 0.143 0.190 0.238 0.286 0.333 0.381 0.429 0.476 0.524 0.571 0.571 | 1.00 1.00 1.00 1.00 1.00 1.00 2.00 2.00 2.00 2.00 2.00 2.00 2.00 5.00 | | | | | | | | | | | | |
| [MAM] | | | | | | | | | | | | | |
| 680 23 2.71 1.27 2.75 1.31 | | | | | | | | | | | | | |
| 0.000 0.048 0.095 0.143 0.190 0.238 0.286 0.333 0.381 0.429 0.476 0.524 0.571 0.571 | 1.00 1.00 1.00 1.00 1.00 1.00 2.00 2.00 2.00 2.00 2.00 2.00 2.00 3.00 | | | | | | | | | | | | |
| 677 23 4.13 4.42 4.32 4.99 | | | | | | | | | | | | | |
| 0.000 0.048 0.095 0.143 0.190 0.238 0.286 0.333 0.381 0.429 0.476 0.524 0.571 0.571 | 1.00 1.00 1.00 1.00 1.00 1.00 2.00 2.00 2.00 2.00 2.00 2.00 2.00 3.00 | | | | | | | | | | | | |
| [JJA] | | | | | | | | | | | | | |
| 336 23 2.08 1.01 2.05 0.95 | | | | | | | | | | | | | |
| 0.000 0.048 0.095 0.143 0.190 0.238 0.286 0.333 0.381 0.429 0.476 0.524 0.571 0.571 | 1.00 1.00 1.00 1.00 1.00 1.00 2.00 2.00 2.00 2.00 2.00 2.00 2.00 2.00 | | | | | | | | | | | | |
| 334 23 1.79 1.31 1.23 1.07 | | | | | | | | | | | | | |
| 0.000 0.048 0.095 0.143 0.190 0.238 0.286 0.333 0.381 0.429 0.476 0.524 0.571 0.571 | 1.00 1.00 1.00 1.00 1.00 1.00 2.00 2.00 2.00 2.00 2.00 2.00 2.00 8.00 | | | | | | | | | | | | |
| [SON] | | | | | | | | | | | | | |
| 387 23 3.34 1.21 2.20 1.17 | | | | | | | | | | | | | |
| 0.000 0.048 0.095 0.142 0.180 0.238 0.286 0.333 0.381 0.429 0.476 0.524 0.571 0.571 | 1.00 1.00 1.00 1.00 1.00 1.00 2.00 2.00 2.00 2.00 2.00 2.00 2.00 2.00 | | | | | | | | | | | | |
| 378 23 9.42 7.65 8.42 7.72 | | | | | | | | | | | | | |
| 0.000 0.048 0.095 0.143 0.190 0.238 0.286 0.333 0.381 0.429 0.476 0.524 0.571 0.571 | 1.00 1.00 1.00 1.00 1.00 1.00 2.00 2.00 2.00 2.00 2.00 2.00 2.00 8.00 | | | | | | | | | | | | |
| [SERIES statistics: max, N of observations, mean and std for WET and DRY] | | | | | | | | | | | | | |
| 7.00 7.00 7.00 9.00 7.00 4.00 4.00 4.00 4.00 6.00 8.00 7.00 | | | | | | | | | | | | | |
| 212 170 213 238 228 175 199 68 93 141 148 172 | 2.40 2.40 2.40 2.54 2.54 2.54 2.79 1.79 1.42 2.42 2.48 2.56 | | | | | | | | | | | | |
| 1.39 1.15 1.00 1.11 1.48 0.97 0.89 0.73 0.72 0.62 0.94 2.38 1.96 | 26.00 22.00 16.00 15.00 50.00 65.00 103.00 62.00 40.00 39.00 38.00 31.00 | | | | | | | | | | | | |
| 212 170 210 232 235 184 103 75 85 139 146 165 | 5.41 5.53 4.49 3.72 4.66 7.20 18.61 17.45 10.55 7.87 7.99 6.21 | | | | | | | | | | | | |
| 5.84 4.50 3.29 2.86 6.15 10.07 20.15 14.93 10.01 0.62 7.13 6.32 | 0.000 0.253 0.463 0.493 0.522 0.552 0.582 0.612 0.642 0.672 0.702 0.731 0.761 | | | | | | | | | | | | |
| [RAIN distributions] | | | | | | | | | | | | | |
| 413 23 2.63 2.77 2.87 2.95 | | | | | | | | | | | | | |
| 0.000 0.107 0.144 0.180 0.217 0.253 0.490 0.526 0.562 0.599 0.635 0.672 0.708 | 1.00 1.00 1.00 1.10 1.10 1.10 1.40 1.60 1.90 2.10 2.30 2.80 3.10 | | | | | | | | | | | | |
| 430 23 2.37 2.86 2.47 2.90 | | | | | | | | | | | | | |
| 0.000 0.253 0.463 0.493 0.522 0.552 0.582 0.612 0.642 0.672 0.702 0.731 0.761 | 1.00 1.00 1.00 1.00 1.00 1.00 2.00 2.00 2.00 2.00 2.00 2.00 2.00 | | | | | | | | | | | | |

FIGURE 11.20 The summary statistics produced through LARS for station A at a seasonal scale.

two files provide the statistical characteristics of the data and the parameter information which will be used by the LARS-WG to synthesize the artificial weather data in the GENERATOR process.

In the station A.sta file (Figure 11.20), the first few lines give the site name and the location information. This is followed by the statistical characteristics of the observed weather data.

First, the empirical distribution characteristics for the length of the wet and dry series of days in the observed data are obtained. This information is given in four lines by the season (i.e., winter [DJF], spring [MAM], summer [JJA], and autumn [SON]), where the first two lines of each section correspond to the wet series and the last two lines represent the dry series. The wet and dry series are modeled based on the histograms constructed from the observed data. The histograms in this case consist of ten intervals and the cut-off points for each interval are given in the first line and the number of the events in the observed data falling into each interval is given in the second line.

So, using station A.sta, it can be seen that the wet series intervals (h_i) are $0 \leq h_1 < 1, 1 \leq h_2 < 2, 2 \leq h_3 < 3, 3 \leq h_4 < 4, 4 \leq h_5 < 5, 5 \leq h_6 < 6, 6 \leq h_7 < 7, 7 \leq h_8 < 8, 8 \leq h_9 < 9$, and $9 \leq h_{10} < 10$, with the corresponding frequencies of the occurrence of 236, 161, 44, 16, 8, 3, 0, 2, 0, and 0, respectively (Figure 11.21). The same data are given for the precipitation. The summary statistics (min, max, mean, standard deviation) of the wet and dry day, precipitation, minimum and maximum temperature, and solar radiation in the monthly and daily scales are also given in this file.

| aharWG - Notepad | | | | | | | | | | | | | | |
|----------------------------|-------|-------|-------|-------|-------|-------|-------|-------|-------|-------|-------|-------|-------|------|
| File Edit Format View Help | | | | | | | | | | | | | | |
| [NAME] aharwg | | | | | | | | | | | | | | |
| [LAT, LON and ALT] | | | | | | | | | | | | | | |
| 39.26 47.04 1390.50 | | | | | | | | | | | | | | |
| [YEARS] 1 50 | | | | | | | | | | | | | | |
| [SERIES WET] | | | | | | | | | | | | | | |
| 1 | 23 | 2.05 | 1.30 | 2.06 | 1.20 | 0.00 | 0.286 | 0.333 | 0.381 | 0.429 | 0.476 | 0.524 | 0.571 | |
| 0.000 | 0.048 | 0.095 | 0.143 | 0.190 | 0.238 | 0.286 | 0.333 | 0.381 | 0.429 | 0.476 | 0.524 | 0.571 | | |
| 1.00 | 1.00 | 1.00 | 1.00 | 1.00 | 1.00 | 1.00 | 1.00 | 1.00 | 1.00 | 1.00 | 1.00 | 1.00 | 1.00 | 2.00 |
| 1.70 | 23 | 2.49 | 1.25 | 2.52 | 1.28 | 2.00 | 0.286 | 0.333 | 0.381 | 0.429 | 0.476 | 0.524 | 0.571 | |
| 1.00 | 1.00 | 1.00 | 1.00 | 1.00 | 1.00 | 1.00 | 1.00 | 1.00 | 1.00 | 1.00 | 1.00 | 1.00 | 1.00 | 2.00 |
| 213 | 23 | 2.85 | 1.10 | 2.80 | 1.10 | 2.00 | 0.286 | 0.333 | 0.381 | 0.429 | 0.476 | 0.524 | 0.571 | |
| 1.00 | 2.00 | 2.00 | 2.00 | 2.00 | 2.00 | 2.00 | 2.00 | 2.00 | 2.00 | 2.00 | 2.00 | 2.00 | 2.00 | 3.00 |
| 238 | 23 | 2.14 | 1.19 | 2.19 | 1.19 | 2.00 | 0.286 | 0.333 | 0.381 | 0.429 | 0.476 | 0.524 | 0.571 | |
| 0.000 | 0.048 | 0.095 | 0.143 | 0.190 | 0.238 | 0.286 | 0.333 | 0.381 | 0.429 | 0.476 | 0.524 | 0.571 | | |
| 1.00 | 1.00 | 1.00 | 1.00 | 1.00 | 1.00 | 1.00 | 1.00 | 1.00 | 1.00 | 1.00 | 1.00 | 1.00 | 1.00 | 2.00 |
| 228 | 23 | 2.77 | 1.48 | 2.80 | 1.46 | 2.00 | 0.286 | 0.333 | 0.381 | 0.429 | 0.476 | 0.524 | 0.571 | |
| 0.000 | 0.048 | 0.095 | 0.143 | 0.190 | 0.238 | 0.286 | 0.333 | 0.381 | 0.429 | 0.476 | 0.524 | 0.571 | | |
| 1.00 | 1.00 | 1.00 | 1.00 | 1.00 | 1.00 | 1.00 | 1.00 | 1.00 | 1.00 | 1.00 | 1.00 | 1.00 | 1.00 | 2.00 |
| 1.00 | 1.00 | 1.00 | 1.00 | 1.00 | 1.00 | 1.00 | 1.00 | 1.00 | 1.00 | 1.00 | 1.00 | 1.00 | 1.00 | 2.00 |
| 175 | 23 | 2.50 | 0.97 | 2.50 | 1.01 | 2.00 | 0.286 | 0.333 | 0.381 | 0.429 | 0.476 | 0.524 | 0.571 | |
| 0.000 | 0.048 | 0.095 | 0.143 | 0.190 | 0.238 | 0.286 | 0.333 | 0.381 | 0.429 | 0.476 | 0.524 | 0.571 | | |
| 1.00 | 1.00 | 1.00 | 1.00 | 1.00 | 1.00 | 1.00 | 1.00 | 1.00 | 1.00 | 1.00 | 1.00 | 1.00 | 1.00 | 2.00 |
| 99 | 23 | 1.19 | 0.89 | 1.84 | 0.92 | 2.00 | 0.286 | 0.333 | 0.381 | 0.429 | 0.476 | 0.524 | 0.571 | |
| 0.000 | 0.048 | 0.095 | 0.143 | 0.190 | 0.238 | 0.286 | 0.333 | 0.381 | 0.429 | 0.476 | 0.524 | 0.571 | | |
| 1.00 | 1.00 | 1.00 | 1.00 | 1.00 | 1.00 | 1.00 | 1.00 | 1.00 | 1.00 | 1.00 | 1.00 | 1.00 | 1.00 | 2.00 |
| 69 | 23 | 1.00 | 1.00 | 1.00 | 1.00 | 1.00 | 0.286 | 0.333 | 0.381 | 0.429 | 0.476 | 0.524 | 0.571 | |
| 0.000 | 0.048 | 0.095 | 0.143 | 0.190 | 0.238 | 0.286 | 0.333 | 0.381 | 0.429 | 0.476 | 0.524 | 0.571 | | |
| 1.00 | 1.00 | 1.00 | 1.00 | 1.00 | 1.00 | 1.00 | 1.00 | 1.00 | 1.00 | 1.00 | 1.00 | 1.00 | 1.00 | 1.00 |
| 93 | 23 | 1.43 | 0.72 | 1.44 | 0.75 | 2.00 | 0.286 | 0.333 | 0.381 | 0.429 | 0.476 | 0.524 | 0.571 | |
| 0.000 | 0.048 | 0.095 | 0.143 | 0.190 | 0.238 | 0.286 | 0.333 | 0.381 | 0.429 | 0.476 | 0.524 | 0.571 | | |
| 1.00 | 1.00 | 1.00 | 1.00 | 1.00 | 1.00 | 1.00 | 1.00 | 1.00 | 1.00 | 1.00 | 1.00 | 1.00 | 1.00 | 1.00 |
| 141 | 23 | 2.35 | 0.94 | 2.41 | 0.95 | 2.00 | 0.286 | 0.333 | 0.381 | 0.429 | 0.476 | 0.524 | 0.571 | |
| 0.000 | 0.048 | 0.095 | 0.143 | 0.190 | 0.238 | 0.286 | 0.333 | 0.381 | 0.429 | 0.476 | 0.524 | 0.571 | | |
| 1.00 | 1.00 | 1.00 | 1.00 | 1.00 | 1.00 | 1.00 | 1.00 | 1.00 | 1.00 | 1.00 | 1.00 | 1.00 | 1.00 | 2.00 |
| 148 | 23 | 2.10 | 1.36 | 2.12 | 1.38 | 2.00 | 0.286 | 0.333 | 0.381 | 0.429 | 0.476 | 0.524 | 0.571 | |
| 0.000 | 0.048 | 0.095 | 0.143 | 0.190 | 0.238 | 0.286 | 0.333 | 0.381 | 0.429 | 0.476 | 0.524 | 0.571 | | |
| 1.00 | 1.00 | 1.00 | 1.00 | 1.00 | 1.00 | 1.00 | 1.00 | 1.00 | 1.00 | 1.00 | 1.00 | 1.00 | 1.00 | 2.00 |
| 177 | 23 | 2.09 | 1.24 | 2.06 | 1.23 | 2.00 | 0.286 | 0.333 | 0.381 | 0.429 | 0.476 | 0.524 | 0.571 | |
| 0.000 | 0.048 | 0.095 | 0.143 | 0.190 | 0.238 | 0.286 | 0.333 | 0.381 | 0.429 | 0.476 | 0.524 | 0.571 | | |
| 1.00 | 1.00 | 1.00 | 1.00 | 1.00 | 1.00 | 1.00 | 1.00 | 1.00 | 1.00 | 1.00 | 1.00 | 1.00 | 1.00 | 2.00 |
| [SERIES DRY] | | | | | | | | | | | | | | |
| 212 | 23 | 5.41 | 4.84 | 5.11 | 4.78 | 2.00 | 0.286 | 0.333 | 0.381 | 0.429 | 0.476 | 0.524 | 0.571 | |
| 0.000 | 0.048 | 0.095 | 0.143 | 0.190 | 0.238 | 0.286 | 0.333 | 0.381 | 0.429 | 0.476 | 0.524 | 0.571 | | |
| 1.00 | 1.00 | 1.00 | 1.00 | 1.00 | 1.00 | 2.00 | 0.286 | 0.333 | 0.381 | 0.429 | 0.476 | 0.524 | 0.571 | |
| 171 | 23 | 5.13 | 4.90 | 5.33 | 4.86 | 2.00 | 0.286 | 0.333 | 0.381 | 0.429 | 0.476 | 0.524 | 0.571 | |
| 0.000 | 0.048 | 0.095 | 0.143 | 0.190 | 0.238 | 0.286 | 0.333 | 0.381 | 0.429 | 0.476 | 0.524 | 0.571 | | |
| 1.00 | 1.00 | 1.00 | 1.00 | 1.00 | 1.00 | 2.00 | 0.286 | 0.333 | 0.381 | 0.429 | 0.476 | 0.524 | 0.571 | |

FIGURE 11.21 The summary statistics produced through LARS for station A at a monthly scale.

File station A.wg contains the monthly histogram intervals and the frequency of the events in these intervals for the wet and dry and the rainfall series in four lines similar to station A.sta, four Fourier coefficients, $a[i]$ and $b[i]$, $i = 1, \dots, 4$, for the means and standard deviations of the different combinations of the minimum and maximum temperature and the solar radiation on the wet and dry days (Figure 11.21).

Step 3: For the model validation, the Test option is selected from the QTest module in the LARS model. The QTest option carries out a statistical comparison of the synthetic weather data generated using the LARS with the parameters derived from the observed weather data in the calibrated model. Selecting the Test option, first, the name of station A would be selected, then the simulation period (20 years), and the random segment related to the stochastic predicting model will be selected (Figure 11.20). The performance of the model in simulating the observed precipitation pattern in the calibration period is evaluated in Figure 11.22. The model output matches closely the observed values (scenario A2).

Step 4: The Generator option in the LARS model is used to simulate the synthetic weather data. This option is used to generate the synthetic data which have the same statistical characteristics as the observed weather data, or to generate the synthetic weather data corresponding to a scenario of climate change.

First, the scenario related to the considered area would be determined. Here, scenarios obtained according to the GCM climatic model,

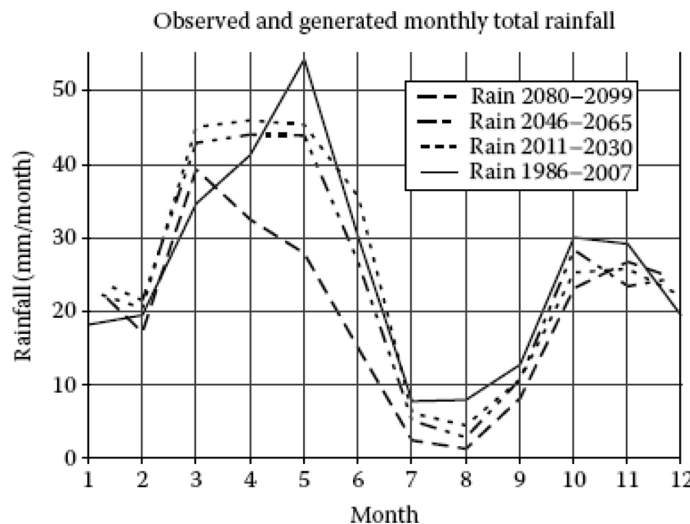


FIGURE 11.22 Generated and observed monthly total rainfall in different intervals.

namely, ECHO-G A1 for grid 17–31, are used. The initial inputs of this stage are the name and the address of the GCM scenario.

After selecting the site and setting up the appropriate scenario files, there are three further options to be completed. The first is the Scaling factor. This factor can be used if a climate change scenario is implemented for a particular future time period, say 2100, to obtain the data for an earlier time period without having to create a scenario file for this earlier time period. The Scaling factor allows this by assuming that the changes in the climate over time are linear. Here, the Scaling factor has been considered equal to 1 and the model is simulated in 20 years with a random seed of 877. The simulated monthly data for the period of year 2011 to year 2020 are given in [Table 11.6](#).

TABLE 11.6
Generated Precipitation (Scenario A1B for 2011–2020 Period) for 10 Years

| Year | Monthly Total Precipitation (mm) | | | | | | | | | | | |
|------|----------------------------------|----------|-------|-------|-------|-------|-------|--------|-----------|---------|----------|----------|
| | January | February | March | April | May | June | July | August | September | October | November | December |
| 1 | 23.90 | 27.60 | 59.80 | 11.80 | 46.60 | 52.80 | 14.80 | 4.90 | 0.50 | 3.40 | 16.50 | 44.50 |
| 2 | 49.90 | 18.50 | 9.30 | 55.90 | 75.20 | 35.70 | 3.60 | 0.00 | 3.60 | 22.90 | 22.30 | 44.70 |
| 3 | 22.90 | 0.90 | 23.30 | 60.20 | 95.00 | 68.30 | 5.00 | 14.60 | 0.00 | 17.20 | 11.60 | 23.20 |
| 4 | 1.40 | 23.60 | 40.50 | 61.00 | 26.20 | 8.70 | 5.80 | 0.00 | 0.00 | 9.70 | 0.00 | 16.00 |
| 5 | 29.10 | 42.10 | 27.20 | 75.50 | 57.30 | 44.70 | 1.70 | 4.00 | 8.20 | 8.30 | 55.20 | 21.80 |
| 6 | 19.90 | 15.10 | 56.50 | 50.10 | 67.20 | 42.30 | 0.30 | 9.20 | 0.00 | 46.80 | 14.60 | 14.80 |
| 7 | 40.90 | 32.30 | 71.20 | 43.50 | 60.40 | 31.70 | 3.50 | 3.20 | 0.00 | 27.10 | 24.50 | 53.10 |
| 8 | 18.10 | 2.00 | 55.40 | 40.00 | 67.10 | 0.00 | 13.90 | 0.00 | 7.70 | 30.90 | 21.60 | 10.90 |
| 9 | 6.40 | 38.30 | 46.80 | 32.90 | 26.50 | 26.40 | 1.70 | 11.10 | 10.90 | 54.50 | 8.20 | 28.00 |
| 10 | 25.50 | 3.10 | 57.80 | 32.80 | 35.70 | 60.80 | 1.30 | 0.00 | 30.30 | 41.10 | 25.10 | 68.40 |

11.10 NEW INSIGHTS—RISKS AND VULNERABILITIES

Our world is threatened by multiple stressors including climate change, climate variability, land-use change, degradation of ecosystems, poverty and inequality, and cultural factors which bring many possible future scenarios with differing levels of resilience and risk. These factors oppose each other in many instances, while a lower risk results in a higher resiliency and vice versa. In a decision space, a lower risk and higher resilience can be achieved by adaptation and adaptive learning, increased scientific knowledge, and mitigation measures. The water availability plays a major role in the climate stressors, and the higher imbalances between the groundwater and surface water supply and demand will intuitively increase the risk elements and reduce the resiliencies. Iterative risk management is a useful framework for decision-making in the upcoming climate change-induced situations with complex uncertainties. The elements of this decision-making context are: (1) scope risks, objectives, and decision criteria, (2) problem definition and solution-based scenarios, modeling analysis, and evaluating options, (3) monitoring plans and knowledge exchange platforms, and (4) test cases, progress against goals, revisited scenarios, and revised options. In many water resources-related activities including conjunctive use of groundwater and surface water, all the elements of this context are being challenged.

Other elements that must be considered when planning with respect to climate change include vulnerability and exposure reduction; low regret strategies and actions; addressing multidimensional inequalities; risk perception; risk assessment, iterative risk management; and mitigating anthropogenic effects. This second set of elements, as they relate to the groundwater, are the attributes dealing with the slow dynamics of the groundwater resources facing a fast pace of changes in climate and social behaviors.

Cultural change, livelihood, migration and mobility, and conflicts have interactions with each other, which could increase or decrease the climate stresses. For example, regarding cultural change and livelihood, educating women could enhance the food security, which reduces the climate stresses. As another example regarding livelihood, migration, and mobility, the increased climate stresses will lead to the involuntary abandonment of the settlements.

Based on the investigation about the climate change effects on the crop types, there would be a huge decrease in the wheat and maize yield impact, but there would not be a lot of changes in the soy yield impact. The crop yield variations are perhaps the result of many factors including the temporal and spatial variation of the groundwater and surface water availability that should be investigated (see Revi et al., 2014; Pachauri et al., 2014; Field, 2014 for more info).

The engineered and technological climate change controlling options are commonly implemented as the adaptive responses. For example, the strategies such as the subnational development planning, early warning systems, integrated water resources management, agroforestry, and coastal reforestation of mangroves are taken into action in Asia, or the incremental adaptation assessment and planning is practiced by the governments in North America.

Climate change is influenced by the water, food, and energy cycle. For example, the water is used for producing energy by cooling the thermal power plants, hydro-power generation, and irrigation of bioenergy crops. On the other hand, the energy

is used for the withdrawal and transportation of the water or for the water treatment. The water is also used for producing food by irrigation, for supplying livestock water demand, and for processing food. The inter-linkages between the supply and demand, the quality and quantity of water, and the energy and food with the changing climatic conditions have implications for both the adaptation and mitigation strategies. There is a trade-off between the mitigation and adaptation with a sustainable win-win situation that illustrates the synergies in which the actions enable the achievement of both the adaptation and mitigation goals.

Many of the groundwater quality issues explained in [Chapter 5](#), planning issues in [Chapter 7](#), and conjunctive use and risk assessment platforms in [Chapters 8](#) and [9](#) should be revisited as the impacts of climate change are becoming more apparent.

11.11 CLIMATE CHANGE IMPACTS ON WATER AVAILABILITY IN AN AQUIFER

The impacts of climate change on the water suppliers may involve many cause-and-effect relationships, which are more remote and uncertain in terms of both the chain of events and the timing. For the appropriate planning of the water systems, a working knowledge about the cause-and-effect relationships that produce the impacts is needed. The groundwater is an important part of the water-supply resources, which is influenced by climate change in different aspects. In the following, an example is presented demonstrating how to combine a groundwater model (MODFLOW) with the decision support system (DSS) tool (water evaluation and planning [WEAP]). This method could be applied in similar studies to examine the effects of climate change, land-use management, and demand management on the groundwater.

Example 11.6

A main river basin located in a semiarid climate, with the precipitation only in the winter months, encompasses 783 km². Most of this precipitation is lost through evapotranspiration. The aquifer consists of fractured crystalline bedrock and alluvial fills in the valleys, and its saturated thickness varies between 35 m in the south to about 53 m in the north. Determine the impacts of climate change on the runoff, groundwater recharge, and cell head changes in this watershed.

SOLUTION

The following sections intend to introduce you to the built-up model.

Step 1: The installation and running of the software:

You need a regular personal computer (PC) with Microsoft Windows XP, Vista, or 7 installed as the operating system. These steps are required to install and run the model:

1. Run "WEAP 2.2054.exe" and follow the installation wizard. Do not change the installation target (C:Program FilesWEAP21). The installed software is a trial version of WEAP. In order to get the product license, refer to <http://www.weap21.org>.

2. Now you need to create the project into the software directory. To do so, extract "WEAP_MODFLOW.zip" and copy the whole extracted folder named WEAP_MODFLOW to C:Program FilesWEAP21.
3. Run WEAP, go to AreaOpenWEAP_MODFLOW.

Step 2: MODFLOW model:

An existing MODFLOW groundwater model for the main river basin was taken originally from the GMS Tutorial and modified to the current model. The groundwater flow is toward the spring, the main river, and its two tributaries. The spring represents the headflow of the main river, with an average monthly discharge of about 320,000 m³. In the north, outside the model area, the main river finally drains into a reservoir lake with a constant water level of 304.8 meter above sea level (m.a.s.l.). The topography gradually decreases from the south (353 m.a.s.l.) to the north (335 m.a.s.l.) (see [Figure 11.23](#)).

Mathematical model:

Grid: The model consists of one layer (one unconfined aquifer, 60–80 m layer thickness, 35–50 m saturated thickness) with 88 × 70 cells.

The cell sizes vary in the width and the height between 200 and 1200 m ([Figure 11.24](#)).

Boundary conditions: A specified-head boundary in the north (reservoir lake level). All other boundaries are the no-flow boundaries ([Figure 11.24](#)).

Hydraulic conductivity: The four hydraulic conductivity zones for the model are shown in the figure below. The hydraulic conductivity of the aquifer varies between 100 (m/day) along the river valley to 40 (m/day) toward the basin boundary.

Recharge: Five different recharge zones have been defined. The values in the zones range from 0 to 0.0015 m/day ([Figure 11.25](#)).

Additional package: The spring was modeled as two DRAIN-cells and the rivers as RIVER-cells (black in [Figure 11.25](#)).

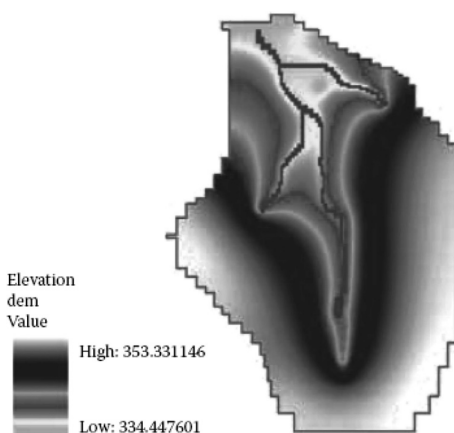


FIGURE 11.23 Topography maps. (From Huber, M. et al., *WEAP-MODFLOW Tutorial*, Version 01/2009, http://www.acsad-bgr.org/DSS-Tutorial/WEAP_MODFLOW_Tutorial.zip, 2009.)

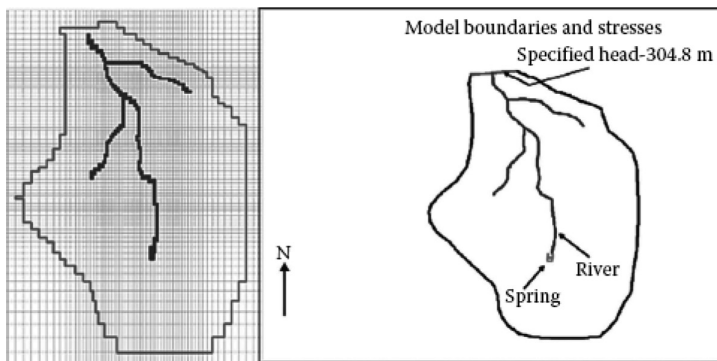


FIGURE 11.24 Model boundaries and stresses. (From Huber, M. et al., *WEAP-MODFLOW Tutorial*, Version 01/2009, http://www.acsad-bgr.org/DSS-Tutorial/WEAP_MODFLOW_Tutorial.zip, 2009.)

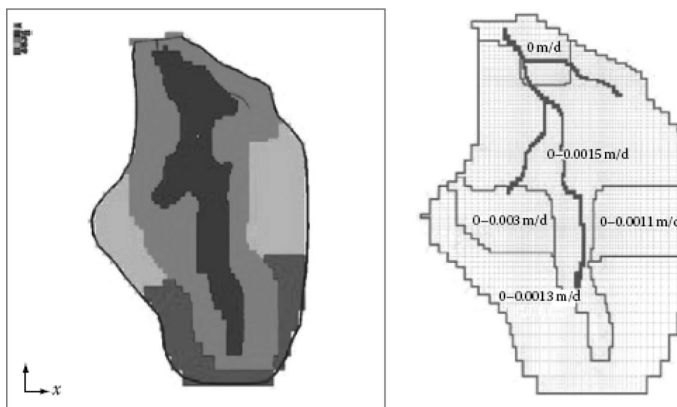


FIGURE 11.25 Model hydraulic conductivity and recharge. (From Huber, M. et al., *WEAP-MODFLOW Tutorial*, Version 01/2009. http://www.acsad-bgr.org/DSS-Tutorial/WEAP_MODFLOW_Tutorial.zip, 2009.)

Initial head: The initial head ranges from 306 to 327 m.a.s.l., resulting in a depth to the water table of 25–36 m (see [Figure 11.26](#)).

The model has been built and run on the transient state in order to cover 2 years of the recharge variation. It consists of 24 monthly stress periods, which contain three equal time steps each. The final balance (see [Figure 11.27](#)—units in m^3 or m^3/day) shows that the model is almost balanced or close to steady state, with the recharge as the main inflow and the river leakage as the main outflow fraction.

Step 3: Extracting data from a MODFLOW model:

Building up a WEAP-model using the “hard data approach,” requires reading out the data which are stored in the native MODFLOW2000 model files, like the natural recharge rate, well abstraction, or riverbed conductance. The number and type of information depend upon the model’s characteristics and the MODFLOW packages that are defined for the chosen model.

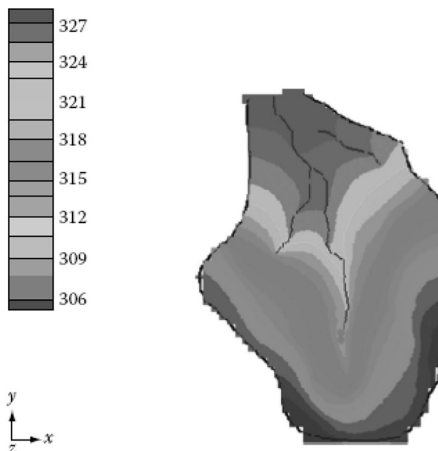


FIGURE 11.26 Initial head. (From Huber, M. et al., *WEAP-MODFLOW Tutorial*, Version 01/2009, http://www.acsad-bgr.org/DSS-Tutorial/WEAP_MODFLOW_Tutorial.zip, 2009.)

| VOLUMETRIC BUDGET FOR ENTIRE MODEL AT END OF TIME STEP 3 IN STRESS PERIOD 24 | | | |
|--|----------------|--------------------------|-------------|
| CUMULATIVE VOLUMES | | RATES FOR THIS TIME STEP | |
| | | L**3/T | |
| IN: | | IN: | |
| --- | | --- | |
| STORAGE = | 158684992.0000 | STORAGE = | 25869.2949 |
| CONSTANT HEAD = | 0.0000 | CONSTANT HEAD = | 0.0000 |
| DRAINS = | 0.0000 | DRAINS = | 0.0000 |
| RIVER LEAKAGE = | 0.0000 | RIVER LEAKAGE = | 0.0000 |
| RECHARGE = | 357105632.0000 | RECHARGE = | 635431.5625 |
| TOTAL IN = | 515790624.0000 | TOTAL IN = | 661300.8750 |
| OUT: | | OUT: | |
| --- | | --- | |
| STORAGE = | 160023184.0000 | STORAGE = | 248629.9062 |
| CONSTANT HEAD = | 5145124.0000 | CONSTANT HEAD = | 6988.5078 |
| DRAINS = | 7527779.5000 | DRAINS = | 10904.8906 |
| RIVER LEAKAGE = | 343096672.0000 | RIVER LEAKAGE = | 394787.0938 |
| RECHARGE = | 0.0000 | RECHARGE = | 0.0000 |
| TOTAL OUT = | 515792768.0000 | TOTAL OUT = | 661310.3750 |
| IN - OUT = | -2144.0000 | IN - OUT = | -9.5000 |
| PERCENT DISCREPANCY = | 0.00 | PERCENT DISCREPANCY = | 0.00 |

FIGURE 11.27 Volumetric budget for the entire model. (From Huber, M. et al., *WEAP-MODFLOW Tutorial*, Version 01/2009, http://www.acsad-bgr.org/DSS-Tutorial/WEAP_MODFLOW_Tutorial.zip, 2009.)

As the native MODFLOW files are somewhat confusing in their file structure and complicated to read data from, a tool called Modflow2Weap has been developed to do this job. Modflow2Weap is a slim tool which reads out values from the native MODFLOW2000 files and transcribes these values to a spreadsheet-format (*.dbf) output file. Additionally, it is capable to create a shape-file which can be used as the basis for the linkage-file between the WEAP and the MODFLOW.

Using Modflow2Weap to create the linkage consists of four steps: selecting the MODFLOW name-file, selecting the MODFLOW packages

for extraction, the output options, and the running the process. For more information about this tool please refer to Huber et al. (2009).

Step 4: Building a WEAP model:

A schematic model of the catchment was created in WEAP, as a basis for assigning the respective data in the following section (see [Figure 11.28](#)).

A new area is created, and the working area boundaries are set. Then, the background layers are loaded and the four rivers are digitized. Finally, the five catchments and the five groundwater nodes are added and named.

WEAP's internal Food and Agriculture Organization (FAO)-Rainfall-Runoff model was utilized to calculate the groundwater recharge. The FAO-Rainfall-Runoff model is a simple water balance model, which does not consider any soil parameters, based on the following equations. This runoff volume can be fractioned to a surface runoff and a groundwater recharge fraction under the Supply and Resources Runoff and the Infiltration from the catchment Inflow and Outflow Runoff Fraction; here, it was assigned 40% surface runoff and 60% groundwater recharge. If the evapotranspiration amount is more than the precipitation, the irrigation demand is obtained by subtracting these two values. Also, the actual evapotranspiration is calculated by multiplying the reference evapotranspiration (ET_{ref}) and crop coefficient (K_c).

The calibration target for the Rainfall-Runoff model was to get the same recharge values like in the initial stand-alone MODFLOW model. To achieve this, monthly precipitation, evapotranspiration, and crop coefficients have been entered to the model.

The required data for WEAP to run the simulation are the Demand Site Area, Crop Coefficients, Monthly Precipitation, Monthly Evapotranspiration, Runoff Fraction, and River Head flows.

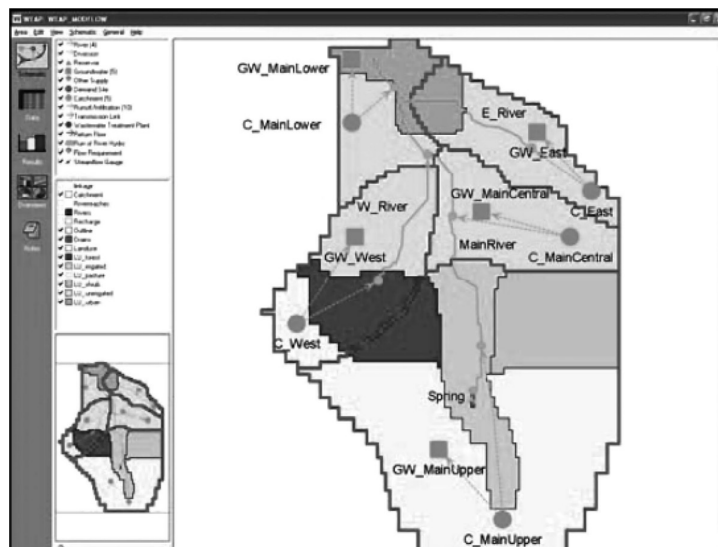


FIGURE 11.28 The schematic of respective data. (From Huber, M. et al., *WEAP-MODFLOW Tutorial*, Version 01/2009, http://www.acsad-bgr.org/DSS-Tutorial/WEAP_MODFLOW_Tutorial.zip, 2009.)

Step 5: WEAP scenarios:

Initially the main river basin was a natural system without any human interference; however, through time, various measures can take place to utilize the water resources of the basin or changes of the climate and the land use may occur. The strength of WEAP is to model the scenarios, historic or future ones, so that the user can see the respective impacts and choose the best option for planning in accordance with the decision-makers.

In this section, some changes are introduced as respective scenarios showing the changes and impacts happening from the “natural” Current Account year (2000) to the future (year 2001–2020). As a reference, the scenario “Reference” is kept for comparison (repetition of the Current Account Year) and is at the same time the basis for all other scenarios.

In the “Climate Change” scenario, we will evaluate the impact of climate change on the surface runoff, groundwater levels, and spring flow. The declining precipitation accompanied with the increasing temperatures is expected in the hypothetical model. The higher temperature will increase the evapotranspiration and decrease the infiltration and the surface runoff. We compare the respective impacts by creating a Climate Change scenario based on the scenario Reference.

The “Climate Change” scenario describes a linear trend in the monthly precipitation and evapotranspiration, which will be applied simultaneously, during the future 20 years.

Step 6: Results:

Water balance: The result shows the decline of the surface runoff ([Figure 11.29](#)). The groundwater levels for each scenario are shown ([Figure 11.30](#)). [Figure 11.31](#) shows the groundwater storage volumes.

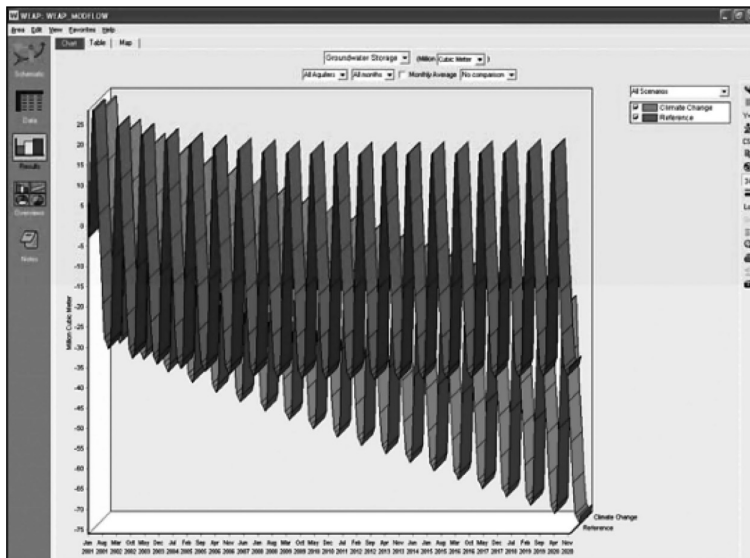


FIGURE 11.29 Runoff from precipitation changes during 2001–2020.

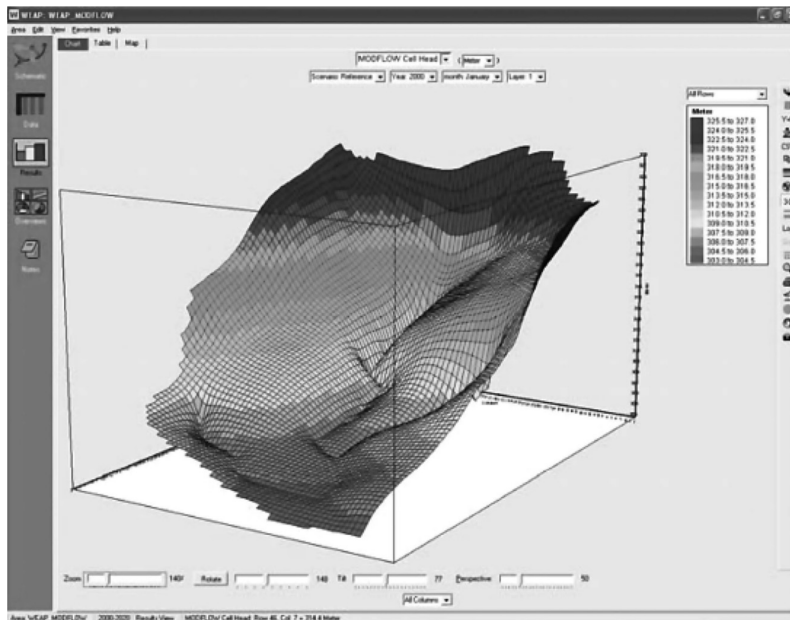


FIGURE 11.30 Groundwater cell head changes.

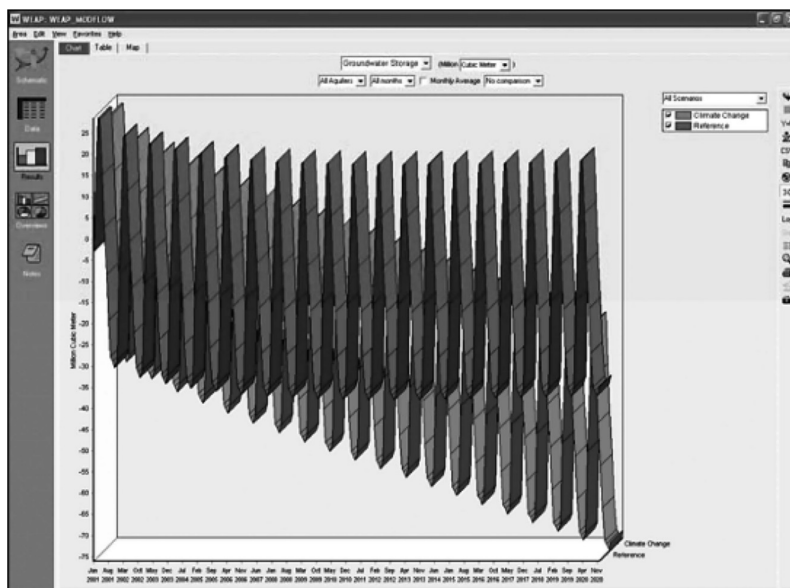


FIGURE 11.31 Monthly groundwater storage of each scenario during 2001–2020.

11.12 CONCLUSION

Climate change can directly affect the water balance of a surface water system; the impact on the groundwater system is indirect and is influenced through the spatially and temporally varying recharge and discharge boundary conditions that link the groundwater system to the surface water system. The groundwater is an irreplaceable resource for livelihoods and agriculture. The adverse impacts of climate change on the groundwater resources are expected, including the changes in recharge rates, saline intrusion in the coastal aquifers, and decreased long-term groundwater storage. The groundwater may increase in importance and help to ameliorate the worst effects of climate change on the water resources and the sustainable development. However, once seriously damaged, recovering the groundwater resources requires vast amounts of funds and time. The role and demand for the groundwater will increase as the water resources in general become scarcer and less predictable with climate change and the other global changes, such as the population growth, urbanization, and increasing living standards. The groundwater provides a strategic resource with relatively good and stable properties, in terms of the quality and quantity. In arid areas, it may be the primary water source, and in semiarid and less arid areas, it may serve to bridge the dry periods and supplement the dwindling, poor quality, or mismanaged surface water resources. The groundwater often provides a relatively easily accessible resource, both from a physical/technical point of view, but also from a socio-economic and equity point of view. Generally, the groundwater recharge, discharge, and storage are influenced by climate change. The recharge can occur as a result of the precipitation events, while both the recharge and discharge can occur at the surface water bodies. The variations in the recharge include change in the diffuse recharge due to the change in rainfall and the land-use change, and the change in river recharge due to the change in the river stage. Climate change leads to some changes in the discharge as the increase in the demand for extraction, and due to the changes in the river stage. Moreover, some changes in the storage are due to the change in recharge, in extraction, and sea-level rise, which could lead to a saltwater intrusion in the coastal areas.

It is obvious that the projected climate change resulting in warming, the sea-level rise, and the melting of glaciers will adversely affect the water balance in different parts of the world, and the quality of the groundwater and its recharge rate along the coastal plains. Based on these impacts, and also because of the importance of the groundwater as a source for the water supply, more studies should be assessed and evaluated to predict and adapt to climate change.

PROBLEMS

- 11.1** Based on the available GCM data of rainfall, compare the results of scenarios B1 and B2 from the HADCM3 model for grid 46×35 in the period of 2010–2049. Discuss the possible reasons for the observed differences. Use both the 10 and 1 ensembles and compare the differences between the results. Which should be considered more for planning a water resources development project in a city located in this grid?

- 11.2 Using the precipitation data of a station in your own city, evaluate the changes in the mean, maximum, and minimum monthly rainfall and the wet and dry spells under scenarios HadCM3 B2 and A2. Discuss the changes which occurred in each scenario and the intensity of the climate change effects. How should the water resources planning changes be planned in response to these changes?
- 11.3 During a long wet season, the water table raised 10 m (average). The water was increased due to the rainfall. Assuming the specific yield is 0.2, what is the change in the recharge rate due to the rainfall?
- 11.4 Describe the difference between the infiltration and the percolation, and then, explain how climate change leads to the change in the infiltration rate which influences the groundwater.
- 11.5 Explain the sea level rise impacts on the groundwater quality, and mention why these changes would be concerning.
- 11.6 Mention some adaptation methods to climate change, and explain one related to the groundwater.
- 11.7 Utilize the rainfall, minimum temperature, and maximum temperature data of a station in a city in the LARS model and downscale it. Define different scenarios and evaluate the effect of climate change on the statistics of the considered variables.
- 11.8 Develop a multilayer perceptron (MLP) model to simulate the monthly water demand of an aquifer in the city mentioned in Problem 11.9 as a function of the rainfall, minimum, and maximum temperatures.
- 11.9 Formulate a simple model based on the dynamic hypothesis of climate change impacts on the water balance in a region; in this model, consider the following causal loops and their interactions. For simplicity, separate the primary and secondary impacts considering their interactions and feedbacks.
- 11.10 Simulate the climate change impacts on the groundwater in a catchment located in your country having an area of at least 500 km². The input data include the monthly precipitation 2001–2010. Use the WEAP-MODFLOW model, and show the recharge changes during the interval 2010–2030.
- 11.11 Considering the model simulated in Problem 11.12, generate the storage volume and cell head changes using the climate change scenario in years 2040, 2045, and 2050.
- 11.12 Use the daily temperature data 1980–2000 of station B located at 56° 01' longitude and 30° 24' latitude and with the elevation 1469 m. Generate the data of station B under HadCM3A2 and B1 scenario outputs from 2020 to 2025, using both the SDSM and LARS models, and compare the difference between the results. Judge which will be more accurate.
- 11.13 Solve Example 11.4 considering 50 ensembles and use the Brier's skill score to choose the best ensemble, and then use Levene's test and the Wilcoxon rank sum test to determine the best scenario between HADA and HADB. Give the results including the *P*-value for each month in a table.

REFERENCES

- Barlow, P. M. 2003. *Groundwater in Freshwater-Saltwater Environments of the Atlantic Coast*. U.S. Geological Survey Circular, Reston, VA, 1262.
- Blake, E.S., Kimberlain, T.B., Berg, R.J., Cangialosi, J.P., and Beven II, J.L. 2013. Tropical cyclone report: Hurricane sandy (AL182012). National Hurricane Center, Miami, FL.
- Bouraoui, F., Vachaud, G., Li, L.Z.X., LeTreut, H., and Chen, T. 1999. Evaluation of the impact of climate changes on water storage and groundwater recharge at the watershed scale. *Climate Dynamics*, 15, 153–161.
- Burger, G. 1996. Expanded downscaling for generating local weather scenarios. *Climate Research*, 7, 111–128.
- California Department of Water Resource. 2007. *Climate Change in California*, CA. <http://www.water.ca.gov/>.
- Canadian Climate Impacts and Scenarios. 2006. *Canadian Institute for Climate Studies*. University of Victoria, Victoria, BC.
- Chia, E. and Hutchinson, M.F. 1991. The beta distribution as a probability model for daily cloud duration. *Agricultural and Forest Meteorology Elsevier*, 56, 195–208.
- Chui, T.F.M. and Terry, J.P. 2012. Modeling freshwater lens damage and recovery on atoll islands after storm-wave washover. *Groundwater*, 50, 412–420.
- Coleman, J.M. 1981. *Deltas: Processes of Deposition and Models for Exploration*. 1st ed. Springer Netherlands, Boston.
- Delleur, J.W. 2007. *The Handbook of Groundwater Engineering*. CRC Press LLC, Boca Raton, FL, 988 p.
- Deng, Y., Flerchinger, G.N., and Cooley, K.R. 1994. Impacts of spatially and temporally varying snowmelt on subsurface flow in a mountainous watershed: 2. Subsurface processes. *Hydrological Sciences Journal/Journal des Sciences Hydrologiques*, 39, 521–534.
- Drabbe, J. and Badon Ghyben, W. 1889. *Nota in Verband Met de Voorgenomenputboring Nabij Amssterdam, Tijdschrift van het Koninklijk Instituut van Ingenieurs*. Verhandelingen The Hague, the Netherlands, pp. 8–22.
- EPA. 2007a. Climate change website. Climate change–Science: Temperature changes. <http://www.epa.gov/climatechange/science/recenttc.html>.
- EPA. 2007b. Climate change website. Climate change–Science: Future temperature changes. <http://www.epa.gov/climatechange/science/futuretc.html>.
- Field, C.B. ed., 2014. *Climate Change 2014–Impacts, Adaptation and Vulnerability: Regional Aspects*. Cambridge University Press, Cambridge, UK.
- Field, C.B., Mortsch, L.D., Brklacich, M., Forbes, D.L., Kovacs, P., Patz, J.A., Running, S.W., and Scott, M.J. 2007. North America, in *IPCC. 2007. Climate Change 2007: Impacts, Adaptation and Vulnerability. Contribution of Working Group II to the Fourth Assessment Report of the Intergovernmental Panel on Climate Change*. M.L. Parry, O.F. Canziani, J.P. Palutikof, P.J. van der Linden, and C.E. Hanson, eds. Cambridge University Press, Cambridge, UK and New York. <http://www.ipcc.ch/pdf/assessment-report/ar4/wg2/ar4-wg2-chapter14.pdf>.
- Firth, P. and Fisher, S.G. 1992. *Global Climate Change and Freshwater Ecosystems*. SpringerVerlag, New York, 321 p.
- Fisher, S.G. and Grime, N.B. 1996. Ecological effects of global climate change on freshwater ecosystems with emphasis on streams and rivers, in *Water Resources Handbook*, L.W. Mays, ed., McGraw-Hill, New York, 1568 p.
- Foster, S.S.D. 2001. Interdependence of groundwater and urbanization in rapidly developing cities (Review). *Urban Water*, 3, 185–192.
- Gerber, R.A.F. and Howard, K. 2000. Recharge through a regional till aquitard: Three dimensional flow model water balance approach. *Ground Water*, 38, 411–422.

- Gleick, P.H. 1989. Climate change, hydrology, and water resources. *Reviews of Geophysics*, 27, 329–344.
- Hamlet, A.F., Mote, P.W., Clark, M.P., and Lettenmaier, D.P. 2007. Twentieth-century trends in runoff, evapotranspiration, and soil moisture in the western United States. *Journal of Climate*, 20, 1468–1486.
- Harms, T.E. and Chanasyk, D.S. 1998. Variability of snowmelt runoff and soil moisture recharge. *Nordic Hydrology*, 29, 179–198.
- Herzberg, B. 1901. Die Wasserversorgung einiger Nordseebäder, *Journal of Gasbeleuchtung und Wasserversorgung, Munich*, 44, 815–819, 842–844.
- Hetzell, F., Vaessen, V., Himmelsbach, T., Struckmeier, W., and Villholth, K.G. 2008. *Groundwater and Changes: Challenges and Possibilities*. BGR and GEUS Publications, Hannover, Germany.
- Hewitson, B.C. and Crane, R.G. 1996. Climate downscaling: Techniques and application. *Climate Research*, 7, 85–95.
- Howard, K.W. and Israfilov, R.G. (eds.). 2012. *Current Problems of Hydrogeology in Urban Areas, Urban Agglomerates and Industrial Centres* (Vol. 8). Springer Science & Business Media, Berlin, Germany.
- Huber, M., Wolfer, J., Al-Sibai, M., Al Mahameed, J., Abdallah, A., Al Shihabi, O., and Jnad, I. 2009. *WEAP-MODFLOW Tutorial*, Version 01/2009. http://www.acsad-bgr.org/DSS-Tutorial/WEAP_MODFLOW_Tutorial.zip.
- IGES. 2007. Groundwater and climate change, no longer the hidden resource. IGES (Institute for Global Environmental Strategies) White Paper, Chapter 7. http://enviroscope.iges.or.jp/modules/envirolib/upload/1565/attach/09_chapter7.pdf.
- Intergovernmental Panel on Climate Change (IPCC). 1998. *Regional Impacts of Climate Change: An Assessment of Vulnerability*. Cambridge University Press, New York.
- Intergovernmental Panel on Climate Change (IPCC). 2001. *Climate Change 2001: The scientific basis*. <http://www.ipcc.ch>.
- Intergovernmental Panel on Climate Change (IPCC). 2007a. Expert meeting report, Towards new scenarios for analysis of emission, climate change, impacts, and response strategies, the Netherlands, intergovernmental panel on climate change, Amsterdam, the Netherlands.
- Intergovernmental Panel on Climate Change (IPCC). 2007b. *Fourth Assessment Report*. <http://www.ipcc.ch>.
- International Panel on Climate Change (IPCC). 2013. Climate change 2013: The physical science basis. *Working Group 1 Contribution to the Fifth Assessment Report of the International Panel on Climate Change*. Cambridge, UK.
- Jacobs, K., Adams, D.B., and Gleick, P. 2001. Water resource. Chapter 14, U.S. Global Change Research Program.
- Johnson, H. and Lundin, L. 1991. Surface runoff and soil water percolation as affected by snow and soil frost. *Journal of Hydrology*, 122, 141–159.
- Karamouz, M. and Zahmatkesh, Z. 2016. Quantifying resilience and uncertainty in coastal flooding events: Framework for assessing urban vulnerability. *Journal of Water Resources Planning and Management*, 143(1).
- Karamouz, M., Rasoulnia, E., Zahmatkesh, Z., Olyaei, M.A., and Baghvand, A. 2016. Uncertainty-based flood resiliency evaluation of wastewater treatment plants. *Journal of Hydroinform*, 18(6), 990–1006.
- Karamouz, M., Zahmatkesh, Z., and Nazif, S. 2014. Quantifying resilience to coastal flood events: A case study of New York City. *World Environmental and Water Resources Congress*, pp. 911–923, American Society of Civil Engineers.
- Ketabchi, H. and Ataie-Ashtiani, B. 2015. Review: Coastal groundwater optimization—Advances, challenges, and practical solutions. *Hydrogeology Journal*, 23(6), 1129–1154.

- Knutsson, G. 1988. Humid and arid zone groundwater recharge—A comparative analysis, in *Estimation of Natural Groundwater Recharge*, Simmers, I., ed., NATO ASI Series C, Vol. 222 (*Proceedings of the NATO Advanced Research Workshop, Antalya, Turkey, March*), G. Redial Publication Company, Dordrecht, the Netherlands, pp. 493–504.
- Kresic, N. 2009. *Groundwater Resources: Sustainability, Management, and Restoration*. McGraw-Hill, New York.
- Lerner, D., Issar, A.S., and Simmers, I., eds. 1990. *Groundwater Recharge: A Guide to Understanding and Estimating Natural Recharge*. Heise, Hannover, Germany.
- Lutgens, F.K. and Tarbuck, E.J. 1995. *The Atmosphere*. Prentice-Hall, Englewood Cliffs, NJ, 462 p.
- Mahmoodzadeh, D. and Karamouz, M. 2019. Seawater intrusion in heterogeneous coastal aquifers under flooding events. *Journal of Hydrology*, 568, 1118–1130.
- Mahmoodzadeh, D., Katabchi, H., Ataie-Ashtiani, B., and Simmons, C.T. 2014. Conceptualization of a fresh groundwater lens influenced by climate change: A modeling study of an arid-region island in the Persian Gulf, Iran. *Journal of Hydrology*, 519, 399–413.
- Manglik, A. and Rai, S.N. 2000. Modeling of water table fluctuations in response to time-varying recharge and withdrawal. *Water Resources Management*, 14, 339–347.
- Masciopinto, C. 2013. Management of aquifer recharge in Lebanon by removing saltwater intrusion from coastal aquifers. *Journal of Environmental Management*, 130, 306–312.
- Masters, G.M. and Ela, W.P. 2008. *Introduction to Environmental Engineering and Science*, 3rd edn., Prentice Hall, Englewood Cliffs, NJ.
- McCown, R.L., Hammer, G.L., Hargreaves, J.N.G., Holzworth, D.P., and Freebairn, D.M. 1996. APSIM: A novel software system for model development, model testing, and simulation in agricultural systems research. *Agricultural Systems*, 50, 255–271.
- McWhorter, D.B. and Sunada, D.K. 1977. *Ground-Water Hydrology and Hydraulics*. Water Resource Publication, LLC, Highlands Ranch, CO, 290 p.
- Mitchell, L.F.B. 1989. The greenhouse effect and climate change. *Reviews of Geophysics*, 27, 115–139.
- Mitchell, L.F.B., Johns, T.C., Gregory, L.M., and Teat, S.F.B. 1995. Climate response to increasing levels of greenhouse gases and sulphate aerosols. *Nature*, 376, 501–504.
- Moore, J.N., Harper, J.T., and Greenwood, M.C. 2007. Significance of trends toward earlier snowmelt runoff, Columbia and Missouri Basin headwaters, western United States. *Geophysical Research Letters*, 34(16), L16402, doi:10.1029/2007GL032022.
- Mukherji, A. and Shah, T. 2005. Socio-ecology of groundwater irrigation in South Asia: An overview of issues and evidence, in *Selected Papers of the Symposium on Intensive Use of Groundwater*. Valencia, Spain, December 10–14, 2002, IAH Hydrogeology Selected Papers, Balkema Publishers, Dordrecht, the Netherlands.
- Olsson, J., Uvo, C.B., Jinno, K., Kawamura, A., Nishiyama, K., Koreeda, N., Nakashima, T., and Morita, O. 2004. Neural networks for rainfall forecasting by atmospheric downscaling. *Journal of Hydrologic Engineering*, 9, 1–12.
- Oude Essink, G.H.P., van Baaren, E.S., & de Louw, P.G.B. 2010. Effects of climate change on coastal groundwater systems: A modeling study in the Netherlands. *Water Resources Research*, 46(10), 1–16.
- Pachauri, R.K., Allen, M.R., Barros, V.R., Broome, J., Cramer, W., Christ, R., Church, J. A. et al. 2014. Climate change 2014: Synthesis report. *Contribution of Working Groups I, II and III to the Fifth Assessment Report of the Intergovernmental Panel on Climate Change* (p. 151). IPCC, Geneva, Switzerland.
- Passeri, D.L., Hagen, S.C., Medeiros, S.C., Bilskie, M.V., Alizad, K., and Wang, D. 2015. The dynamic effects of sea level rise on low gradient coastal landscapes: A review. *Earth's Future*, 3(6), 159–181.

- Racsko, P., Szeidl, L., and Semenov, M. 1991. A serial approach to local stochastic weather models. *Ecological Modeling*, 57, 27–41.
- Ranjan, P. 2007. Effect of climate change and land use change on saltwater intrusion. The encyclopedia of earth (EOE) community. http://www.eoearth.org/article/Effect_of_climate_change_and_land_use_change_on_saltwater_intrusion.
- Reichard, J.S. 1995. Modeling the effects of climatic change on groundwater flow and solute transport. PhD, dissertation, Department of Earth and Atmospheric Sciences, Purdue University, West Lafayette, IN.
- Revi, A., Satterthwaite, D., Aragón-Durand, F., Corfee-Morlot, J., Kiensi, R.B., Pelling, M., Roberts, D., Solecki, W., Gajjar, S.P., and Sverdlik, A. 2014. Towards transformative adaptation in cities: The IPCC's Fifth Assessment. *Environment and Urbanization*, 26(1), 11–28.
- Risser, D.W. 2008. Spatial distribution of ground-water recharge estimated with a water-budget method for the Jordan Creek watershed, Lehigh County, Pennsylvania. U.S. Geological Survey Scientific Investigations Report 2008–5041, Reston, VA.
- Rushton, K.R., Eilers, V.H.M., and Carter, R.C. 2005. Improved soil moisture balance methodology for recharge estimation. *Journal of Hydrology*, 318(1–4), 379–399.
- Scanlon, B.R., Reedy, R.C., Stonestrom, D.A., Prudic, D.E., and Dennehy, K.F. 2005. Impact of land use and land cover change on groundwater recharge and quality in the southwestern US. *Global Change Biology*, 11, 1577–1593, doi: 10.1111/j.1365-2486.2005.01026.x.
- Semenov, M.A. and Brooks, R.J. 1999. Spatial interpolation of the LARS-WG stochastic weather generator in Great Britain. *Climate Research*, 11, 137–148.
- Semenov, M.A., Brooks, R.J., Barrow, E.M., and Richardson, C.W. 1998. Comparison of the WGEN and LARS-WG stochastic weather generators in diverse climates. *Climate Research*, 10, 95–107.
- Shrestha, S. and Kataoka, Y. 2008. *Groundwater and Climate Change No Longer the Hidden Resource*. Institute for Global Environmental Strategies (IGES), Hayama, Japan, pp. 159–184.
- Singhal, D.C., Israil, M., Sharma, V.K., and Kumar, B. 2010. Evaluation of groundwater resource and estimation of its potential in Pathri Rao watershed, district Haridwar (Uttarakhand), Special Section: Himalayan Bio-Geo Databases—I. *Current Science*, 98(2), p. 25.
- Stuyt, L.C.P.M., Kabat, P., Postma, J., and Pomper, A.B. 1995. Effect of sea-level rise and climate change on groundwater salinity and agro-hydrology in a low coastal region of the Netherlands. *Studies in Environmental Science*, 65, 943–946.
- Sundaram, V.L.K., Dinesh, G., Ravikumar, G., and Govindarajalu, D. 2008. Vulnerability assessment of saltwater intrusion and effect of artificial recharge in Pondicherry coastal region using GIS. *Indian Journal of Science and Technology*, 1(7), 1–7.
- Todd, D.K. 1980. *Groundwater Hydrology*. John & Wiley Sons, New Delhi, India, 556 p.
- Van Briesen, T.P., Carlson, D.A., and Milner, L.R. 2007. Impact of hurricanes storm surges on the groundwater resources. *Environment Geology*, 53(4), 813–826.
- Viner, D. and Hulme, M. 1992. Climate change scenarios for impact studies in the UK: General circulation models, scenario construction models and application for impact assessment. Report of Department of Environment, Climatic Research Unit, University of East Anglia, Norwich, UK, 70 p.
- Von Storch, H., Zorita, E., and Cubasch, U. 1993. Downscaling of global climate change estimates to regional scales: An application to Iberian rainfall in wintertime. *Journal of Climate*, 6, 1161–1171.

- Werner, A.D., Bakker, M., Post, V.E.A., Vandenbohede, A., Lu, C., Ataie-Ashtiani, B., Simmons, C.T., and Barry, D.A. 2013. Seawater intrusion processes, investigation and management: Recent advances and future challenges. *Advances in Water Resources*, 51(1), 3–26.
- Wigley, T.M.L. and Jones, P.D. 1985. Influence of precipitation changes and direct CO₂ effects on streamflow. *Nature*, 314, 149–151.
- Wigley, T.M.L., Jones, P.D., Briffa, K.R., and Smith, G. 1990. Obtaining sub-grid-scale information from coarse-resolution general circulation model output. *Journal of Geophysical Research*, 95, 1943–1954.
- Wilby, R.L. and Dawson, C.W. 2004. *Using SDSM Version 3.1—A Decision Support Tool for the Assessment of Regional Climate Change Impacts*. Climate Change Unit, Environment Agency of England and Wales, Nottingham, UK and Department of Computer Science, Loughborough University, Leicestershire, UK.
- Wilby, R.L. and Wigley, T.M.L. 1997. Downscaling general circulation model output: A review of methods and limitations. *Progress in Physical Geography*, 21, 530–548.
- Wilby, R.L., Hassan, H., and Hanaki, K. 1998. Statistical downscaling of hydrometeorological variables using general circulation model output. *Journal of Hydrology*, 205, 1–19.
- Wilby, R.L., Hay, L.E., Gutowski, W.J., Arritt, R.W., Takle, E.S., Pan, Z., Leavesley, G.H., and Clark, M.P. 2000. Hydrological responses to dynamically and statistically down-scaled climate model output. *Geophysical Research Letters*, 27, 1199–1202.
- Witherspoon, P.A., Wang, J.S.Y., Iwai, K., and Gale, J.E. 1980. Validity of the cubic law for fluid flow in a deformable rock fracture. *Water Resource Research*, 16(6), 1016–1024.
- Yang, J., Graf, T., and Ptak, I.T. 2015. Sea level rise and storm surge effects in a coastal heterogeneous aquifer: A 2D modelling study in northern Germany. *Grundwasser*, 20(1), 39–51.
- Yu, X., Yang, J., Graf, T., Koneshloo, M., O'Neal, M.A., and Michael, H.A. 2016. Impact of topography on groundwater salinization due to ocean surge inundation. *Water Resources Research*, 52(8), 5794–5812.
- Zaidi, F.K., Ahmed, S., Dewandel, B., and Maréchal, J.-C. 2007. Optimizing a piezometric network in the estimation of the groundwater budget: A case study from a crystalline rock watershed in southern India. *Hydrogeology Journal*, 15, 1131–1145.
- Zhang, L., Stauffacher, M., Walker, G.R., and Dyce, P. 1997. Recharge estimation in the Liverpool Plains (NSW) for input groundwater models, Technical Report. CSIRO Land and Water, Canberra, ACT.

Index

Note: Page numbers in italic and bold refer to figures and tables, respectively.

A

- acid dissociation constants, 211
Adaptive Linear (ADALINE) network, 382, 385, 385–386
ADI method, *see* alternating direction implicit (ADI) method
advection, 220–221
 envelopes, hypothetical contaminant, 578, 579
advection–dispersion equation, 225–232
agent-based modeling, 475–476
 calibration and verification, 475, 475
 characteristics, 405, 408–409, 409
 decision-making and interactions, 407, 408
 defined, 405
 development, 406
 environmental influence, 406, 406
 framework, decision tree, 406–407, 407
 groundwater management, 407–408
 public prosecutor’s office, 474
 RWA, 473–474
 water users, 473
ag-MAR projects
 costs, 604–605
 crop tolerance, 604
 deep percolation, 604
 inefficient irrigation and canal seepage, 605
 infrastructure, 603–604
 irrigation efficiency, 605, 606
 soil suitability, 604
 water availability, 603
 water quality, 605
agricultural droughts, 638, 679
Agricultural Production System Simulator, 688
AIC, *see* Akaike’s information criterion (AIC)
air sparging, 559–560
Akaike’s information criterion (AIC), 117, 127, 128
alluvium, 595
alternating direction implicit (ADI) method, 255, 262–280
ambient trend monitoring, 578
Analytical Hierarchy Process method, 269–270, 666, 668
analytical modeling, 253–254
ANNs, *see* artificial neural networks (ANNs)
aquiclude, 33
aquifer(s), 637–638, 642
 bioremediation, 563
 coastal, 638
 compressibility, 42–43
 confined, 259, 264, 264–269, 637, 637–638
 definition, 33
 karstic, 638
 monthly time series/recharge rates, 124, 125
 observed/forecasted values, recharge rates, 129, 129, 129
 porosity and void ratio, 44–46
 process of, 251–252
 recharging, 689
 safe yield, 52
 specific retention, 47–48
 specific yield, 46
 storage coefficients/specific storage, 48–52
 test application, 165–166
 types, 33–35
 unconfined, 637, 637–638
 vulnerability, 657
aquifer restoration/monitoring
 contaminants, natural losses, 547–550
 groundwater pollution control, 550–559
 overdraft issues, 566–567
 partitioning process, 544–546
 retardation, 546–547
Aquifer Storage Recovery (ASR), 598, 598
Aquifer Storage Transfer and Recovery (ASTR), 598, 598
aquifer-stream system, 515
aquitards, 33–35
ARIMA models, *see* autoregressive integrated moving average (ARIMA) models
ARMA model, *see* autoregressive moving average (ARMA) model
AR models, *see* autoregressive (AR) models
artificial neural networks (ANNs), 517–524, 526, 711
 ADALINE network, 382, 385, 385–386
 IDNN, 387–389, 388, 389, 390
 layers, 374
 MLP, 374–379
 RNNs, 386, 386–387
 TDL, 380–382
 temporal neural networks, 379–380

artificial recharge, 701
 ASR, *see* Aquifer Storage Recovery (ASR)
 ASTR, *see* Aquifer Storage Transfer and Recovery (ASTR)
 autoregressive integrated moving average (ARIMA) models
 ACF graph, 127, 127–128, 128
 AIC values, 127, 128
 characteristics, 123
 forecasting equations, 124
 general form, 123
 monthly time series/recharge rates, aquifer, 124, 125
 normalized and standardized data, 126, 126
 observed/forecasted values, recharge rates, 129, 129, 129
 PACF graph, 127, 127–128, 128
 autoregressive (AR) models, 117–121
 autoregressive moving average (ARMA) model, 122–123

B

back propagation algorithm, 377
 backward difference equation, 258, 261–262
 Bad-Khalebad region, 476–477, 477
 bank filtration, 598, 598–599
 bank storage/baseflow recession, 495, 495–496
 concave method, 499–500
 constant-discharge method, 498, 499
 constant-slope method, 498–499
 master-depletion curve method, 496–497
 Meyboom method, 497–498
 baseline chemical approach, 624
 benefit-cost ratio method, 459–460
 biological degradation, 548–549
 bioremediation techniques, 563–564
 bioswales, 602
 block-centered node, 255, 256
 boreholes, 597–598

C

cable-tool drilling machines, 191, 192
 calibration model, 18, 372, 475, 475, 716
 canal seepage, 605
 cancer-causing substances, PF, 620–623
 Canonical Correlation Analysis, 711
 capacity expansion model, 413–417
 capture-zone curves, extraction well, 237–240
 coordinate system, 235
 pumping rates, 235–236, 236
 regional groundwater flow, 234, 234–235
 superimposing, plume, 236, 236
 carbon adsorption, 560–561
 carbonate system, 561
 carcinogen, 619

CDF, *see* cumulative distribution function (CDF)
 CDI, *see* chronic daily intake (CDI)
 centralized MAR approaches, 600
 chemisorption, 212
 chi-square (χ^2) distribution, 100, 134–135
 chronic daily intake (CDI), 621–622
 Clean Water Act (CWA), 21
 climate change impacts, 1, 676–677
 adaptation, 700–702
 direct, 686–690
 general, 681–682
 hydrological cycle, 677–681, 678
 indirect, 690–698
 simulation, 704–712
 water availability, aquifer, 725
 climatic drought, 638
 clogging, 595–596
 coastal aquifers, 638, 691–693
 coastal areas, MAR projects, 606
 collection lysimeters, 571
 complementary error function, 226, 227–228
 compressibility
 porous medium, 40–42
 values, soil types, 41, 42
 of water, 38
 computer software tools, 396
 concave-baseflow separation method, 499–500
 conceptual model approach, 348
 cone of depression, 153, 155, 161, 175
 aquifer and river, 183
 flow distribution, 154
 radius and depth, 154
 recharge boundary, 182–184
 confined aquifers, 34, 34, 259, 264, 264–269, 689
 impermeable layers, 147
 steady-flow conditions, 145, 145–146
 storage coefficients, 48, 48–49
 unconfined vulnerable aquifer, floodplain, 637, 637–638
 water balance, 36–37
 conflict issues, 10–11
 conflict resolution model
 aquifer system, demands, 440
 criteria space, 441
 decision-makers, 441
 game theory, 449–452
 land resources allocation, 461–463, 462, 463
 Nash product, 442, 444
 relative weights/authority, agencies, 444
 stakeholder involvement, 446–449
 TDSs concentration, 444–445
 TWCP, *see* Tehran wastewater collection project (TWCP)
 utility function, agencies, 443
 conjunctive use, surface/groundwater, 502–503
 advantages, 503–504
 conflict resolution model, 524–532, 526, 530

- and crop pattern management, 532, 532–538, 537
genetic algorithms/ANN, 517–524, 523, 525, 526
impediments of, 504
in Lakhota Canal Uttar Pradesh, India, 504–507, 505
modeling, 507–515
optimization model, 420–421
consolidated sandstone aquifers, 595
constant-discharge baseflow separation method, 498, 499
constant head permeameter, 73, 73
constant-slope baseflow separation method, 498–499, 499
contaminant plume model, 244
contaminant release
 contaminant plume model, 244
 Fourier analysis, solute transport, 240–241
 Gaussian-source plume model, 245–247, 246, 248
 point-source plume model, 245, 245
 point spill model, 241
 simple plume model, 244–245
 vertically mixed spill model, 241–242
 vertical mixing region, 242–243
contaminants, natural losses
 biological degradation, 548–549
 plants uptake nutrients, 549–550
 volatilization, 548
continuity equation, 139–142
control volume, 319
 in polar coordinates, 334, 334
 for 2D mesh, 325
Cooper–Jacob method, 168–172, 169
covered karsts, 56
Crank–Nicolson method, 258, 281–284
crop tolerance, 604
cumulative distribution function (CDF), 96, 634
curse of dimensionality, 433
CWA (Clean Water Act), 21
- D**
- Daranjir basin, 660, 662, 662
Darcy's law, 73, 139, 160
 hypothetical reservoirs, 65
 porosity, 64–65
 potentiometric surface, confined aquifer, 66, 66–67
 pressure distribution/head loss, sand column, 64
 validity of, 68
 velocity, water flowing, 63
- data collection, 370–371
decentralized MAR approaches, 601, 601–602
decision-making process, 423
depletion curve, 496
deterministic approach, 252, 624, 624
diffusion, 218, 218–220
direct recharge, 687
direct rotary method, 192, 193
disaster, 627
 control mechanisms, 628
 institutional/technical capacities, requirements, 627–628
 management phases, 628–630
 mitigation, preparedness, response and recovery, 629
 occurrence, 630
 prevention and mitigation, 628–629
disaster indices, 630
 reliability, 630–636, 631
 resiliency, 636
 vulnerability, 636–637
disaster prevention/mitigation
 anticipatory phase, 628
 impact and relief phases, 628
 rehabilitation phase, 629
 warning phase, 628
disconnected streams, 494
discrete kernel approach, 336–346
discretization method
 continuous media, FDM, 255
 1D, 2D, 3D problem domains, 289
 2D space, 256
disequilibrium condition, 212–213
dispersion
 hydrodynamic, 224–225
 mechanical, 221–224
dissolved gases, 200–202
dissolved phase (plume) remediation, 564–566
dose-response assessment, 616, 617, 618
dose-response curves, 618–619, 619
double water-table fluctuation method, 686
downscaling models, 707, 708, 712
 LARS-WG, 715, 717–723
 SDSM, 712–713
DP, *see* dynamic programming (DP)
DRASTIC method, 658–664, 664
 factors in, 661
 rating and evaluation, 663
drilled wells, 597–598
drinking water
 chemicals/guideline values, health significance, 204, 204–205
 livestock/irrigation crops, 204, 206
 public health groundwater quality standards, 206, 207–209
 standards, 203, 203–204

droughts, 627, 638–640
 agricultural, 638
 characteristics, 639–640
 climatic, 638
 contingency plans, 640
 early warning systems, 644
 groundwater, 639
 hydrologic, 639
 indicators, 641
 Lorestan Province in Iran, 640
 management strategy plan, 643
 meteorological, 638–639
 planning and management, 640
 qanats, 645–646, 646
 socio-economic, 639
 triggers, 641–643, 642
 vulnerability maps, 643–644, 664–668, 666–667
 Yazd province, 644–645
 dry land farming, 599
 Dublin Principles, 11
 dune filtration, 598
 Dupuit–Forchheimer theory, free-surface flow, 81–83
 dye tracers, 58
 dynamic downscaling, 708
 dynamic programming (DP), 432–434, 435, 513
 dynamic response equations, 262

E

East Azerbaijan Province, 665, 665, 668
 economic analysis, 452
 benefit-cost ratio method, 459–460
 cash flow elements, 455, 455
 costs, 453, 453–454, 454
 external benefits, 454
 future worth method, 457
 groundwater use, 12–13
 IRR method, 457–458
 pumps, 458, 458, 459
 water price, 12, 13
 well development, 456
 ecosystem approach, 624
 effective stress, 38–40
 unsaturated zone, 72
 efficiency improvement game, government/
 farmers strategies
 matrix of, 479, 480
 stabilities, 481
 states, 479, 480
 elasticity modules, soils, 49, 50
 electron acceptor, 563
 Elman RNN, 386, 386–387
 emergency response activities, 630
 engineering principles and applications, 7
 entropy theory, 588–591

environmental risk analysis, 624, 624–625, 625
 ϵ -constraint method, 427–428
 equation error criterion method, 423
 equation of motion
 friction and reaction forces, 142–144
 gravity force, 142–143
 groundwater flow equation, 144–153
 pressure force, 142
 equilibrium constants, 213, 213
 evaporation, 683
 explicit method, 257
 exponential model, 576
 exposure assessment, 616, 617, 618

F

falling head permeameter, 73, 73–74
 FDM, *see* finite-difference method (FDM)
 feed-forward network, 376
 FEM, *see* finite element method (FEM)
 fertilizers, 216
 finite-difference method (FDM), 251, 253–257
 ADI method, 262–280
 advantage, 255
 backward difference equation, 258, 261–262
 Crank–Nicolson method, 258, 281–284
 discretization, continuous media, 255
 forward difference equation, 257–260, 258
 time derivative approximation, 306
 finite element method (FEM), 251, 253, 284
 approximating equations, 290–303, 291
 flexibility, 253
 problem domain, 284–290
 solute transport equation, 311–319
 transient saturated flow equation, 303–311
 types, 290
 finite volume method (FVM), 251, 253
 advantage, 253
 conservation principle, 319
 orthogonal coordinate systems, 333–336
 steady-state one-dimensional equation, 319–323
 two-dimensional flow equation, 324–333
 unsteady-state one-dimensional equation, 323–324

flash floods, 647
 floods
 control measures, 648–649, 649
 and droughts, 678–679
 hazard potential maps, 648–649
 impacts of, 647
 plains, 647
 flownets
 anisotropic media, 93, 94
 Darcy's equation, 90–91
 heterogeneous media, 92–93
 seepage under dam, 89, 89–90

- sheet pile, 91–92, 92
strategies and rules, 90
streamlines and equipotential lines, 89–90
two-dimensional flow, 88–89, 89
- fluid mass balance equation, 347
- food security, 20
- FORTRAN program, 284, 285–288, 329, 329–330
- forward difference equation, 257–260, 258
- fractured hard rock, 595
- frequency interval, 102–103
- freshwater lens, 695, 695–698
- Freundlich isotherm, 545, 561
- friction force, 142–144
- fuzzy approach, 430–431
- fuzzy sets, 389–394
- FVM, *see* finite volume method (FVM)
- G**
- gage pressure, 29
- Galerkin method, 293
- GAs, *see* genetic algorithms (GAs)
- gas monitoring wells, 570, 571
- gas-phase compositions, atmosphere, 201
- Gaussian model, 576
- GCMs, *see* global circulation models (GCMs)
- general meta-rationality (GMR), 452
- generation/forecasting, ARMA models, 122–123
- genetic algorithms (GAs), 434–438, 521, 530, 534, 537
- geographic information system (GIS), 269, 371, 659
- geologic data, 370
- GHGs (greenhouse gases), 675, 677
- Ghyben–Herzberg relation, freshwater/saline waters, 694–695
- GIS, *see* geographic information system (GIS)
- global circulation models (GCMs), 704, 704–705, 706
- global climate system, 676
- global warming, 680, 683, 686, 690, 700
- goodness of fit tests
- chi-square (χ^2) test, 113–114, 115
 - skewness coefficient, normality, 115–117, 116
- granular iron, 566
- gravity force, 142–143
- greenhouse effect, 677, 677
- greenhouse gases (GHGs), 675, 677
- Green's function, 241
- grid-point cluster, 320
- groundwater
- availability, 4–5
 - cell head changes, 731
 - droughts, 639
 - extraction pattern, 701
 - levels, 520, 524
 - monitoring, 571, 572, 577
- national restoration/remediation, 567–569
- operation optimization model, 410–412
- pollution control, 550–559
- quantity and quality concerns, 698–700
- recharge, 687–688
- resource sustainability limits, 516–517
- science and engineering, 6–8, 7
- in semiarid region, 538–541
- sustainability, 13–15, 15
- treatment of, 559–566
- groundwater contamination, 654
- agricultural activities, 216
 - liquid waste disposal, 215, 215
 - petroleum tank leakage, 214
 - sewage disposal, 215–216
 - solid waste disposal, 214, 214
 - sources of, 216, 216–217, 217
- groundwater pollution control, 654
- grouting technology, 557
 - institutional tools, 550–551
 - interceptor systems, 554, 554–555
 - sheet piling, 556–557
 - slurry walls, 557, 558, 559
 - source control strategies, 551–552
 - sources and characteristics, 655–656
 - stabilization/solidification strategies, 552–553
 - surface water control/capping/liners, 555–556, 556
 - vulnerability assessment, 657–659, 658
 - well systems, 554
- groundwater quality
- contamination, 699
 - management model, 421–422
 - salinization, sea-level rise, 699–700
- groundwater solubility
- chemical reactions, 209–210
 - microbiological factors, 212
 - pH, 210
 - sorption to solids, 211–212
 - temperature, 212
- groundwater sustainability agencies (GSAs), 23–24
- groundwater sustainability plans (GSPs), 23–24
- groundwater systems
- defined, 6
 - representation, 5, 5
- grouting technology, 557
- GSAs, *see* groundwater sustainability agencies (GSAs)
- GSPs, *see* groundwater sustainability plans (GSPs)
- H**
- habitats, 680
- hazard
- flood, 648–649
 - identification, 616, 617, 618

- hazard (*Continued*)
 potential maps, 649
 threatened, groundwater quality, 654
 and vulnerabilities, 616, 616
- heavy metals, 200
- Henry's law, 548, 560
- heterogeneous systems
 hydraulic conductivity formations, 75, 75
 karst aquifer, 57
- Hole effect model, 576
- holokarst, 56
- hydraulic conductivity, 689–690
 field measurement, 74–75
 laboratory measurement, 72–74, 73
 multilayer structures, 76–80
 and permeability, 71
 and recharge, 727
 in saturated media, 69–70
 in unsaturated media, 70–72
- hydraulic gradient, 139
- hydraulic head, 68, 68–69, 492
- hydrodynamic dispersion, 224–225
- hydroelectric power, 680–681
- hydrograph separation, 495
- hydrologic data, 370
- hydrologic drought, 639
- hydrologic/hydrological cycle
 climate change impacts, 677–681, 678
 groundwater recharge, 687
 schematic representation, 29, 30
- hydrologic time series modeling, 104–105
- hydroxide system, 561
- I**
- IAS, *see* in situ air sparging (IAS)
- IDNN, *see* input-delayed neural network (IDNN)
- implicit method, 261
- induced bank infiltration, 598–599
- inefficient irrigation systems, 605
- infiltration, 492
 capacity curve, 493
vs. percolation, 687
 ponds/basins, 596, 596, 600, 606
- injection well barrier, 606, 701, 702
- inorganic contaminants
 metals/nonmetals, 200
 nitrogen, 199
- input-delayed neural network (IDNN)
 architecture, 387, 388
 groundwater table variation, 388–389, 389, 390
 parts, 387
 TDRNN, 388
- in situ air sparging (IAS), 559, 559–560
- in situ chemical oxidation method, 561–562
- in situ thermal heating methods, 562
- institutional capacity building, 627–628
- institutional tools
 aquifer standards/criteria, 551
 effluent charges/credits, 550–551
 guidelines, 551
 land zoning, 550
 regional groundwater management, 550
- Integrated Risk Information System, 621
- integrated water resources management
 (IWRM), 1, 10
- interactive fuzzy approach, 430–431
- interceptor systems, 554, 554–555
- inter-dune filtration, 598, 599
- Intergovernmental Panel on Climate Change (IPCC), 691
 assessment report, 702–703
- internal rate of return (IRR) method, 457–458
- ion exchange process, 212
- IPCC, *see* Intergovernmental Panel on Climate Change (IPCC)
- irrigation efficiency, 605, 606
- IRR method, *see* internal rate of return (IRR) method
- island freshwater lens, 695, 695–698
- isotropic/anisotropic formations, hydraulic conductivity, 75, 75
- iterative risk management, 724
- K**
- karez, 645
- karst aquifer, 638
 allogenic/autogenic recharge areas, 57, 57
 flood flows, 58
 fluctuation of, 56–57
 terranes, 55–56
 tracing technologies, 58
 types, 56
 water pollution, 59
 water-quality monitoring, 59
 water supply, 58
- kriging method, 574–577
- L**
- lakes, 500, 501, 502
- land subsidence, 650–651
 calculation, 651–652
 examples, 653
 groundwater pumping, 43
 monitoring, 652
 occurrence, 651
 problems, 650
 reducing, 652
- land-use and land-cover, 698
- land zoning, 550
- Languor adsorption model, 544–545

- LARS-WG model, *see Long Ashton Research Station Weather Generator (LARS-WG) model*
leaching potential index (LPI), 659
least square method, 110–111
Lenjanat aquifer and Zayandeh-Rud River, 349–363, 525, 527
 water table elevations, 472, 473
Levenberg-Marquardt algorithm, 380, 382
linear interpolation functions, 292, 292
linear regression, ANN toolbox, 384
liquid waste disposal, 215, 215
liquefied natural gas spills, event tree analysis, 623, 623
L-moment method, 109–110
lognormal distribution, 97–98, 98
Long Ashton Research Station Weather Generator (LARS-WG) model, 715, 717–723
longitudinal dispersion, 221–222, 223
- M**
- macro-encapsulation, 553
Managed Aquifer Recharge (MAR) projects, 543, 591, 592
 agricultural settings, 602–605, 603
 benefits, 593
 coastal areas, 606
 hydrogeological settings/controls, 594–595
 in-channel modifications, 596–597
 induced bank infiltration, 598–599
 principal consideration, 591–593
 rainwater harvesting, 599
 recharge water/quality considerations, 593–594
 spreading methods, 596
 in urban settings, 600–602
 well/shaft/borehole recharge, 597–598
MAR projects, *see Managed Aquifer Recharge (MAR) projects*
mass conservation, 139–141, 140
mathematical models, 252–253
 analytical modeling, 253–254
 groundwater flow, 18
 numerical modeling, 254
MATLAB toolbox, ANNs, 381
 input and targets, 380, 382
 linear regression, 384
 neural network training error histogram, 382, 385
 number of neurons, 382, 383
Train Network, 384
 validation and testing samples, 382, 383
maximum likelihood method, 111–112
mechanical dispersion, 221–224
merokarst, 56
mesh-centered node, 255, 256
meteorological drought, 638–639
Meyboom method, 497–498
microcosm approach, 624
microencapsulation, 553
mineralization, 548
MLP network, *see multi-layer perceptron (MLP) network*
MODFLOW model, 347–363, 727–729
moisture capacity, 55
monitoring subsurface water, 569
 geostatistical tools, 573–577
 groundwater monitoring, 571, 572
 sampling frequency, 584–588
 vadose-zone, 570–571
 water quality monitoring stations, location, 577–584
 water quality variable selection, 572–573, 573
moving average process, 121–122
multi-criteria optimization, 426–431
multi-layer perceptron (MLP) network
 back propagation algorithm, 377
 groundwater table variation, 378, 380
 monthly recharge, aquifer, 377–378
 parameter estimation, 376–377
 simple neural network, 374, 375
 static network, 376
 transfer functions, 375–376, 376
multi-objective conjunctive use optimization, 515–517
multiple-well systems, 181–182
- N**
- Nash bargaining theory, 527–528
National Research Council, 616
nations' vulnerability to water scarcity, 2, 2
natural and man-induced disasters, 628–629
natural attenuation systems, 556
neural network training error histogram, 382, 385
nitrobenzene, 229
nodes, 254
noncarcinogenic response, 619
non-cooperative stability, 452
normal distribution, 95–96, 96, 97, 132–133
numerical modeling, 252–254
- O**
- one-hit model, 620
open wells and shafts, 597
operational program (action plans), 568–569
optimal monitoring well network
 GAs, 582–584
 kriging method, 581–582, 582
 optimal configuration of, 580–581

- optimization models, 508
 capacity expansion, 413–417
 conjunctive water use, 420–421
 groundwater operation, 410–412
 groundwater quality management, 421–422
 parameters, groundwater flow, 422–423
 water allocation, 417–420
- optimization techniques
 decision-making process, 423
 DP, 432–434, 435
 GA, 434–438
 gradient methods, 424
 multi-criteria, 426–431
 SA, 438–440
 single-criterion, 424–426
- organic contaminants, 200
- orthogonal coordinate systems, 333–336
- output error criterion method, 423
- P**
- PACF, *see* partial autocorrelation function (PACF)
- parameter estimation
 least square method, 110–111
 L-moments, 109–110
 maximum likelihood method, 111–112
 method of moments, 108–109
- partial autocorrelation function (PACF), 120, 127, 128, 128
- partial differential equations (PDEs), 253–254
- partially penetrating wells, 186–188, 187
- particle sizes, spectrum of, 202, 202
- partitioning process, aquifers, 544–546
- PDEs (partial differential equations), 253–254
- percentiles, 101–102
- percolation ponds, 596, 597
- permeable reactive barriers, 564–566, 565
- permeameters, hydraulic conductivity, 73, 73–74
- pesticides, 200, 201
- petroleum tank leakage, 214
- PF, *see* potency factor (PF)
- physisorption, 212
- piecewise linear profile, 320, 320
- planning and management
 components, 9–10
 conflict issues, 10–11
 economics of water, 11–13
 groundwater sustainability, 13–15, 15
 IWRM, 10
 management problems, classes, 8
 principles, 9
 water resources, 9
 water supply and demand, 15–17, 16
- plants uptake nutrients, 549–550
- plume management, 554
- PMWIN, *see* Processing MODFLOW for Windows (PMWIN)
- point-source plume model, 245, 245
- point spill model, 241
- porosity, geologic materials, 45, 45
- potable water, 594
- potency factor (PF), 620–621, 621
- power model, 576
- precipitation, 683–685, 688, 710
- prediction models
 agent-based modeling, 405–409
 ANNs, *see* artificial neural networks (ANNs)
 fuzzy sets and parameter imprecision, 389–394
 SDs, 395–405
- pressure force, 142
- pressure head, 70–71, 492
 vertical distribution, 85–86, 87, 87
- primary water supply (PWS), 3–4
- proactive isotopes, 58
- probability interval, 102–103
- Processing MODFLOW for Windows (PMWIN), 348–349, 517, 519
- protection, 21–22
 California's SGMA, 23–24
 CWA, 21
 USEPA Groundwater Rule, 22–23
- protozoan cysts, 203
- public awareness, 19
- public health groundwater quality standards, 206, 207–209
- public prosecutor's office, 474
- pump-and-treat technology, 234, 564, 565
- pumping schedule, 411, 411
- pumping tests, hydraulic conductivity, 74
- PWS (primary water supply), 3–4
- Q**
- qanats, 645–646, 646
- QTest, 719
- quintiles, 101–102
- R**
- radial flow, unconfined aquifer, 159
- radioactive isotopes, 58
- Rafsanjan Plain, 660, 662, 662, 662
- rainwater harvesting, 599
- RCPs, *see* Representative Concentration Pathways (RCPs)
- recharge estimation methods, 688–689
- reclaimed water, 594
- recurrence interval, 102–103
- recurrent neural networks (RNNs), 386, 386–387
- regional groundwater management, 550
- regional models, 708–709, 711

- regional water authorities (RWA), 473–474
regression-based method, downscaling, 711
relative hydraulic conductivity, 55
Representative Concentration Pathways (RCPs), 705–706, 707
response and recovery activities, 630
retardation, 546–547
and dispersion, 221–222, 222
revealed societal preferences approach, 623
reverse rotary method, 192, 193
risk
characterization, 616, 617, 618
evaluation, 623
management, 625–626
mitigation, 626–627
quantification/estimation, 616
and vulnerabilities, 724–725
risk assessment, 616, 618
dose-response assessment, 618–619
elements, 616–618
environmental risk analysis, 624, 624–625, 625
methods and tools, 619–623
process steps, 617
river flow, 681
RNNs, *see* recurrent neural networks (RNNs)
rock, physical properties of, 70
roof-top rainwater harvesting, 599, 599
rotary drilling method, 191–192, 193
RWA (regional water authorities), 473–474
- S**
- SA, *see* simulation annealing (SA)
Safe Drinking Water Act, 22
saltwater intrusion, 691, 691–694, 693
sampling error, 100
sampling frequency, 584
multiple stations/multiple water quality variables, 588
multiple stations/single water quality variable, 587
selecting methods, 584
single station/multiple water quality variables, 586–587
single station/single water quality variable, 585–586
sand storage dams, 538–539, 539, 596–597, 597
saturated hydraulic conductivity, 69–70
saturated-unsaturated transport (SUTRA) code, 346–347
saturation index, 212–213
scaling factor, 619
science framework, groundwater occurrence, 7
SDSM, *see* statistical downscaling model (SDSM)
SDs model, *see* system dynamics (SDs) model
sea-level rise, 690–691
seasonal recession method, 497–498
semiarid region, 538–541
semivariogram, 575
semi-VOCs (SVOCs), 562
sequential optimization, 427
sequential stability (SEQ), 452
sewage disposal, 215–216
SGMA (Sustainable Groundwater Management Act), 23–24
sheet piling, 556–557
simple neural network, 374, 375
simple plume model, 244–245
simulation annealing (SA), 438–440
simulation models, 369–370
calibration, 372
vs. optimization models, 17–19, 371
predictions, *see* prediction models
verification, 372–373
simulation-multi-objective optimization (SMO) model, 477–482
single-criterion optimization, 424–426
slurry walls, 557, 558, 559
smoke and gaseous tracers, 58
SMO model, *see* simulation-multi-objective optimization (SMO) model
snowpack, 681
socio-economic drought, 639
soil
aquifer treatment, 596, 596
moisture, 685–686
physical properties, 70
texture, 85, 85
Soil and Water Assessment Tool (SWAT), 269–270
soil water characteristic curves, 55
Sole Source Aquifer (SSA) program, 22
solid waste disposal, 214, 214
solute transport equation, 233–234, 311–319
source control strategies, 551–552
source monitoring, 578
spatial variability, 705
communities' scenarios development, 705–707
downscaling, 707, 708
regional models, 708–709
Special Report on Emissions Scenarios (SRES), 703, 703
spherical model, 575–576
spreading methods, 596
SRES, *see* Special Report on Emissions Scenarios (SRES)
SSA (Sole Source Aquifer) program, 22
stakeholders, 446
conflict handling, 447–448
effective meeting facilitation, 447
meeting outcomes, 448
utility functions, 449

- standard errors, 100–101
 statistical approach, 624
 statistical downscaling, 709–712, 711
 statistical downscaling model (SDSM), 712–713
 statistical methods, 95–103
 steady-state one-dimensional flow equation, 319–323
 steady-state radial flow, well
 confined aquifer, 155–158
 unconfined aquifer, 158–161
 stepwise profile, 320, 320
 stochastic models, 252, 624
 storage coefficients
 confined/unconfined aquifers, 48, 48–49
 density/specific weight, temperatures, 49, 49
 elasticity modules, soils, 49, 50
 storativity, 48, 595
 storm surge, 693–694
 storm-water runoff, 594
 streamtube, 88
 subsurface barrier method, 702
 subsurface dams, 539, 597, 597
 subsurface water
 capillary zone, 32, 32
 classifications, 29, 31
 development, 369
 intermediate zone, 31–32
 saturated zone, 33
 soil-water zone, 31
 suction lysimeters, 570–571
 sulfide system, 561
 supply and demand side management, 15–17
 surface water, 593
 control/capping/liners, 555–556, 556
 vs. groundwater movement, 8
 resources/agricultural zones, 518
 surface water and groundwater interaction, 491–492
 bank storage/baseflow recession, 495, 495–500
 concepts, 492–495, 493, 494
 infiltration, 492
 lakes, 500, 501, 502
 sustainable development, 1, 13–15, 15
 Sustainable Groundwater Management Act (SGMA), 23–24
 SUTRA (saturated-unsaturated transport) code, 346–347
 SVOCs (semi-VOCs), 562
 SWAT, *see* *Soil and Water Assessment Tool (SWAT)*
 symmetric meta-rationality (SMR), 452
 system dynamics (SDs) model
 behavior and response, 396
 computer software tools, 396
 diagramming tools, 395
 feedback systems, 395
 modeling process, 396, 397
 monthly revenue and water supply budget, 401
 principles, 395
 stocks/flows/converters/connectors tools, 395–396
 treated water and recharged water, 401
 urban storage tank, 396
 water flow, 399
 water quantity and price, 398–399, 399, 400
- T**
- tapped delay line (TDL)
 architecture, 380
 MATLAB toolbox, 380–382
 in temporal neural networks, 381
 TARWR (Total Actual Renewable Water Resources), 2–3
t-distribution, 98–99, 99
 TDL, *see* *tapped delay line (TDL)*
 TDS, *see* *total dissolved solids (TDS)*
 Tehran plain, surface water resources, 517, 518
 Tehran wastewater collection project (TWCP)
 characteristics, 466, 467
 Department of Environment, 468
 phases, 467
 Tehran Health Department, 469
 Tehran Water and Wastewater Company, 468–469
 Tehran Water Supply Authority, 469–471
 wastewater discharge, 471
 water and wastewater management, 472
 temporal neural networks, 379–380
 tapped delay line, 381
 Teymoor model, 271, 273–279
 Theis method, 166–168
 thermal heating system, 562, 562
 thermal technologies, 562–563
 tidal regulators, 702
 time-drawdown curve, water table conditions, 177–178, 178
 time-drawdown data, 167, 167, 168, 170, 171, 176–177
 impermeable boundary, 184–186
 partially penetrating wells, 186–188, 187
 recharge boundary, 182–184
 time series analysis
 AIC, 117
 ARIMA models, 123–129
 ARMA model, 122–123
 AR models, 117–121
 data preparation, 105–108
 goodness of fit tests, 113–117
 hydrologic time series modeling, 104–105
 moving average process, 121–122
 nonstationary hydrologic variables, 103–104
 parameter estimation, 108–112

- tools and techniques, groundwater resources planning, 17, 17–19
topographic data, 370
topography, 604, 726
Total Actual Renewable Water Resources (TARWR), 2–3
total dissolved solids (TDS), 526, 527, 531, 654
tracer tests, 74
Train Network, ANN, 384
transboundary aquifers, groundwater basins, 11, 11
transfer functions, 375–376, 376
transient saturated flow equation, 303–311
transmissivity, 80, 80–81
transverse dispersion, 221, 224, 224
truncation errors, 257
tsunami events, mechanism of, 647, 648
tube well installation, 188–191, 189
TWCP, *see* Tehran wastewater collection project (TWCP)
two-dimensional flow equation, 324–333, 325
two-dimensional horizontal semiconfined/leaky aquifer, 146–147
two-dimensional kriging estimation variance plots, 583
- U**
- unconfined aquifers, 33–34, 34, 637, 637–638
 specific yield, 46
 steady-flow conditions, 149, 149–150
 storage coefficients, 48, 48–49
 uniform recharge rate, 150, 150–153, 151
 water balance, 37
United Nations MAR portal, 607
United States Environmental Protection Agency (USEPA), 21–22, 621
 Groundwater Rule, 22–23
unsaturated hydraulic conductivity, 70–72
unsaturated zone, 29
 effective stress, 72
 groundwater flow, 83–88
 storage in, 52–55
 water balance, 37
unsteady-state one-dimensional flow equation, 323–324
USEPA, *see* United States Environmental Protection Agency (USEPA)
- V**
- vadose-zone monitoring, 570–571
validation process, 18
van Genuchten-Mualem model, 84–85
Varamin plain, 533, 533
variable pumping test, 172–175
variograms, 574
verification model, 372–373, 475, 475
vertically mixed spill model, 241–242
VOCs, *see* volatile organic carbons (VOCs)
volatile hydrocarbons, 618
volatile organic carbons (VOCs), 559, 562–563
volatilization, 548
volumetric budget, 728
volumetric water content, 52–54
vulnerability, 636–638
 adaptive capacity and action approach, 617
 aquifers, 657
 groundwater pollution, 657–659, 658
 and hazard, 616
 maps, droughts, 643–644, 664–668, 666–667
- W**
- water
 allocation model, 417–420
 availability, 2–5, 603
 budget method, 688–689
 level fluctuations, 55
 loss rate, 16
 management approach, 602
 price/value, 12–13, 13
 resources in world, 29, 30
 retention, 55
 saving technologies, 16
 table fluctuation method, 686, 686
 use and climate change, 679–680
water balance
 confined aquifers, 36–37
 general form, 35
 inflow/outflow components, 35
 rainfall seepage, 36
 unconfined aquifers, 37
 unsaturated zone, 37
water demand, 403, 405, 415
 vs. allocation, 538
Water Global Assessment and Prognosis (WaterGAP), 2
water quality, 605, 680
 monitoring stations, 577–584
 simulation model, 582–583
 standards, *see* drinking water
 variable selection, 572–573, 573
water quality-monitoring networks
 entropy theory in, 588–591
 geostatistical tools, 573–577
 in karst, 59
water supply
 and distribution system, 399
 in karst, 58
 population over time, 403, 404
 water demand, 403, 405
 water resources, 403, 404

water transfer, SDs model, 460
 channel capacity, 464–465, 465
 groundwater depth, 464, 464
 groundwater withdrawal, 464
 land resources allocation, 461–463, 462, 463
 planning schemes, 465
 Tehran metropolitan area, 461, 461
weighting method, 428–430
well field development project
 capital costs, 416
 initial investment and capacity, 415

wells, 554
 cable-tool drilling machines, 191, 192
 cone of depression, 153, 154, 155
 confined aquifer, unsteady state, 161–175
 design of, 188–191
 pumping, 153
 rotary drilling method, 191–192, 193
 steady-state flow, 155–161
 unconfined aquifer, unsteady state, 175–181